

DEVELOPMENT OF STEREOSELECTIVE IRIIDIUM-CATALYZED
ALLYLIC ALKYLATION METHODS

Thesis by
Samantha Elizabeth Shockley

In Partial Fulfillment of the Requirements
for the Degree of
Doctor of Philosophy

CALIFORNIA INSTITUTE OF TECHNOLOGY
Pasadena, California

2018
(Defended May 25, 2018)

© 2018

Samantha E. Shockley
ORCID: 0000-0001-5682-8569

All Rights Reserved

To my dad

ACKNOWLEDGEMENTS

First and foremost, I would like to thank my advisor, Professor Brian Stoltz, for his constant support during my graduate education. I know that it is not a given to have an advisor that you respect and like as both a person and a scientist, and I feel very fortunate to have found this in Brian and to have had the opportunity to work in his lab. Brian's ability to simultaneously be there for his students as well as give them latitude to explore and become independent scientists has made him an incredible mentor.

I would also like to sincerely thank the chair of my committee, Professor Sarah Reisman, for all of her help over the past five years with research questions, the Women in Chemistry Committee, and job advice. The Stoltz group is very lucky to have her as a second advisor and her lab as coworkers. In addition, I am deeply appreciative of the insightful questions into my research and the valuable career advice the rest of my thesis committee, Professors Bob Grubbs and Peter Dervan, have given me over my graduate career.

I would not have made it to Caltech without the mentorship and encouragement of my previous advisors. I very grateful for the support of my undergraduate research advisor, Professor Richard Jordan, particularly his patience to go line by line over all my writing and his persistent willingness to meet and discuss chemistry. I am also indebted to my Fulbright grant advisor, Professor Martin Banwell, who gave me the opportunity to join his lab and pursue a project of my choosing.

I need to thank all of the excellent Caltech staff for making my PhD possible. Specifically, Dr. Scott Virgil for all of his help with instrumentation and not laughing me out of his office when I told him I needed to prepHPLC every single compound in

a methods paper. Additionally, Dr. David VanderVelde for hiring me as GLA and helping with many of the structural assignments discussed herein. As well as, Dr. Mike Takase and Larry Henling for their patience and assistance with obtaining X-ray diffraction data, Dr. Mona Shahgholi and Naseem Torian for their tireless work with mass spectrometry data, and Rick Gerhart and Jeff Groseth for repairing everything I broke in graduate school. Finally, I would like to thank Joe Drew, Agnes Tong, Alison Ross, and the rest of the graduate support staff for keeping everything running so well in the CCE department.

During my time at Caltech, I have been extremely lucky to have had excellent project partners. First, I would like to thank Jeff Holder for letting me jump on his project as a first year and putting up with my hysterical panicked calls about breaking instruments. Next, none of the work on iridium-catalyzed allylic alkylation presented in this thesis would have been possible without the early work of Corey Reeves and Boger Liu, who were great mentors in passing the projects down to me. Finally, I have been incredibly lucky to have worked with Caleb Hethcox on many of the projects presented herein. Even when our chemistry was invariably failing, coming to work was always enjoyable. I cannot imagine a better mentor, coworker, or best friend.

I was fortunate to have mentored three students during my time in the Stoltz group. Their fresh enthusiasm for chemistry was often much needed in the depths of my PhD, and for that, I would like to sincerely thank Netgie Laguerre, Bridget Garrity, and Winston Odom for working with me. I look forward to following their, what am sure will be successful, careers in chemistry.

I am very thankful for all of the members, past and present, of the Stoltz lab who have made the group an enjoyable place to come every day. Specifically, I could

not have asked for a better place to work than the Small Office, whose unique culture has always kept things entertaining, especially the Small Office members of Nick O'Connor, Kelly Kim, Christopher Haley, Doug Duquette, Lukas Hilpert, Jared Moore, David Schuman, and Justin Hilf. I am particularly indebted to Nick and Christopher for all of their mentorship when I joined the lab and Kelly for her friendship and willingness to put up with my constant nagging to stop hoarding. Additionally, I would like to thank Beau Pritchett for what can only be described of as being my life coach, but in all seriousness, who I very much respect. Finally, I need to thank my hoodmate of four years, Austin Wright, for tolerating my neurotic cleanliness and persistent need to pick up his half of the hood.

Finally, I would like to thank my friends and family who made my graduate degree possible. Sherrie Xie and Erin Britton for being incredible friends, always being there to talk, and game to travel anywhere. Nik Thompson for his love, unwavering support as my biggest cheerleader, and incredible patience with me, even extending back to the early days of college problem sets. Lastly, my mom, dad, and brother who may not have understood why I would want to be in chemistry graduate school, but were always there to support and help me in any way they could. I am forever appreciative of all of the lunches packed, homework checked, science fair project help, rides to school when I missed the bus for the hundredth time, care packages, trips to cook for me during finals, and cards to celebrate my tiny milestones, amongst everything else you always selflessly did. I would never have made it to or through graduate school without you – I love you!

The work presented in this thesis would not have been possible without the continued support of all these people and many others not specifically mentioned by name. To each of them, I am deeply grateful.

ABSTRACT

The Stoltz group, and moreover the synthetic community at large, has long been interested in the development of methods for the synthesis of enantioenriched all-carbon quaternary stereocenters. Historically, our group's interest has centered on palladium-catalyzed allylic alkylation, though recently effort has moved to include the study of iridium catalysts. This thesis presents four related projects, all unified by the use of enantioselective iridium-catalyzed allylic alkylation to construct highly-congested C–C bonds.

First, the development of the first diastereo-, enantio-, and regioselective iridium-catalyzed allylic alkylation reaction of prochiral enolates to form vicinal tertiary and all-carbon quaternary stereocenters with alkyl-substituted allylic electrophiles is described. Next, the first enantioselective iridium-catalyzed allylic alkylation reaction of a masked acyl cyanide (MAC) nucleophile is presented, representing a rare example of umpolung strategy in iridium-catalyzed allylic alkylation. Additionally, the application of a MAC reagent in the first highly enantioselective iridium-catalyzed allylic alkylation to provide access to products bearing an allylic all-carbon quaternary stereocenter is detailed. The use of the MAC nucleophile enables the one-pot preparation of α -quaternary carboxylic acids, esters, and amides with a high degree of enantioselectivity. Finally, the first enantioselective transition metal-catalyzed allylic alkylation providing access to acyclic products bearing vicinal all-carbon quaternary centers is presented.

PUBLISHED CONTENT AND CONTRIBUTIONS

1. Shockley, S. E.;[‡] Holder, J. C.;[‡] Stoltz, B. M. “A Catalytic, Enantioselective Formal Synthesis of (+)-Dichroanone and (+)-Taiwaniaquinone H.” *Org. Lett.* **2014**, *16*, 6362–6365. DOI: 10.1021/ol5031537.

S.E.S participated in designing second generation synthetic routes, experimental work, data acquisition and analysis, and manuscript preparation.

2. Holder, J. C.; Shockley, S. E.; Wiesenfeldt, M. P.; Shimizu, H.; Stoltz, B. M. “Preparation of (*S*)-*tert*-ButylPyOx ((*S*)-4-(*tert*-butyl)-2-(pyridin-2-yl)-4,5 dihydrooxazole) and Preparation of (*R*)-3-(4-chlorophenyl)-3-methylcyclohexanone.” *Org. Synth.* **2015**, *92*, 247–266. DOI: 10.15227/orgsyn.092.0247.

S.E.S. participated in reaction optimization, experimental work, data acquisition and analysis, and manuscript preparation.

3. Shockley, S. E.; Holder, J. C.; Stoltz, B. M. “Palladium-Catalyzed Asymmetric Conjugate Addition of Arylboronic Acids to α,β -Unsaturated Cyclic Electrophiles.” *Org. Process Res. Dev.* **2015**, *19*, 974–981. DOI: 10.1021/acs.oprd.5b00169.

S.E.S. led the writing of the review manuscript.

4. Hethcox, J. C.;[‡] Shockley, S. E.;[‡] Stoltz, B. M. “Iridium-Catalyzed Diastereo-, Enantio-, and Regioselective Allylic Alkylation with Prochiral Enolates.” *ACS Catal.* **2016**, *6*, 6207–6213. DOI: 10.1021/acscatal.6b01886.

S.E.S. participated in the writing of the review manuscript.

5. Hethcox, J. C.,[‡] Shockley, S. E.,[‡] Stoltz, B. M. "Iridium-Catalyzed Stereoselective Allylic Alkylation Reactions with Crotyl Chloride." *Angew. Chem. Int. Ed.* **2016**, *55*, 16092–16095. (Highlighted in Synfacts **2017**, *13*, 0167). DOI: 10.1002/anie.201609960.

S.E.S. participated in project design, experimental work, data acquisition and analysis, and manuscript preparation.

6. Hethcox, J. C.,[‡] Shockley, S. E.,[‡] Stoltz, B. M. "Enantioselective Iridium-Catalyzed Allylic Alkylation Reactions of Masked Acyl Cyanide Equivalents." *Org. Lett.* **2017**, *19*, 1527–1529. DOI: 10.1021/acs.orglett.7b00449.

S.E.S. participated in project design, experimental work, data acquisition and analysis, and manuscript preparation.

7. Shockley, S. E.,[‡] Hethcox, J. C.,[‡] Stoltz, B. M. "Asymmetric Synthesis of All-Carbon Quaternary Spirocycles via an Enantioselective Allylic Alkylation Strategy." *Tetrahedron Lett.* **2017**, *58*, 3341–3343. DOI: 10.1016/j.tetlet.2017.07.022.

S.E.S. participated in project design, experimental work, data acquisition and analysis, and manuscript preparation.

8. Shockley, S. E.,[‡] Hethcox, J. C.,[‡] Stoltz, B. M. "Enantioselective Synthesis of Acyclic α -Quaternary Carboxylic Acid Derivatives via Iridium-Catalyzed Allylic Alkylation." *Angew. Chem. Int. Ed.* **2017**, *56*, 11545–11548. (Highlighted in Synfacts **2017**, *13*, 1192). DOI: 10.1002/anie.201707015.

S.E.S. participated in project design, experimental work, data acquisition and analysis, and manuscript preparation.

9. Hethcox, J. C.;[‡] Shockley, S. E.;[‡] Stoltz, B. M. “Enantioselective Synthesis of Vicinal All-Carbon Quaternary Centers via Iridium-Catalyzed Allylic Alkylation.” *Angew. Chem. Int. Ed.* **2018**, doi: 10.1002/anie.201804820.

S.E.S. participated in project design, experimental work, data acquisition and analysis, and manuscript preparation.

10. Shockley, S. E.;[‡] Hethcox, J. C.;[‡] Stoltz, B. M. “Stereoselective Iridium-Catalyzed Allylic Alkylation: An Evolutionary Account.” *Manuscript submitted*.

S.E.S. participated in the writing of the review manuscript.

TABLE OF CONTENTS

Dedication	iii
Acknowledgements	iv
Abstract	vii
Published Content and Contributions	viii
Table of Contents	xi
List of Figures	xix
List of Schemes	xxxv
List of Tables	xxxvii
List of Abbreviations	xlili

PROLOGUE **1**

Iridium-Catalyzed Allylic Alkylation

P.1	Introduction	1
P.2	References and Notes	4

CHAPTER 1 **5**

Stereoselective Iridium-Catalyzed Allylic Alkylation Reactions with Crotyl Chloride

1.1	Introduction	5
1.2	Background to Diastereo-, Enantio-, and Regioselective Iridium-Catalyzed Allylic Alkylation with Prochiral Enolates	7
1.2.1	Iridium Catalyst-Controlled Processes	7
1.2.1.1	Acyclic Nucleophiles	7
1.2.1.2	Cyclic Nucleophiles	10
1.2.2	Dual Catalyst-Controlled Processes	15
1.3	Reaction Optimization	19
1.4	Substrate Scope Exploration	21
1.5	Product Transformations	26
1.6	Conclusions	27
1.7	Experimental Section	28
1.7.1	Materials and Methods	28
1.7.1.1	Preparation of Known Compounds	29
1.7.2	Experimental Procedures and Spectroscopic Data	30

1.7.2.1	Experimental Procedures and Spectroscopic Data for the Synthesis of Tetralone Substrates.....	30
1.7.2.2	Additional Optimization of Reaction Parameters	36
1.7.2.3	General Procedure for Optimization Reactions (Table 1.1 & 1.4)	37
1.7.2.4	General Procedure for the Iridium-Catalyzed Allylic Alkylation.....	37
1.7.2.5	Spectroscopic Data for the Iridium-Catalyzed Allylic Alkylation Products	40
1.7.2.6	Experimental Procedures and Spectroscopic Data for the Product Transformations of Allylic Alkylation Products.....	50
1.7.2.7	Determination of Enantiomeric Excess	56
1.8	References and Notes	58

APPENDIX 1 **62**

Spectra Relevant to Chapter 1

APPENDIX 2 **116**

X-Ray Crystallography Reports Relevant to Chapter 1

A2.1	General Experimental	117
A2.1.1	X-Ray Crystal Structure Analysis of Allylic Alkylation Product 58e	117
A2.1.2	X-Ray Crystal Structure Analysis of Triol 63	125
A2.1.3	X-Ray Crystal Structure Analysis of Diol 64	133

CHAPTER 2 **140**

Enantioselective Iridium-Catalyzed Allylic Alkylation Reactions of Masked Acyl Cyanide Equivalents

2.1	Introduction and Background	140
2.2	Reaction Optimization	142
2.3	Substrate Scope Exploration.....	143
2.4	Conclusions.....	146
2.5	Experimental Section	147
2.5.1	Materials and Methods	147
2.5.1.1	Preparation of Known Compounds	148
2.5.2	Experimental Procedures and Spectroscopic Data	149
2.5.2.1	General Procedure for the Synthesis of Electrophiles	149
2.5.2.2	Spectroscopic Data for the Synthesis of Electrophiles.....	150
2.5.2.3	General Procedure for Optimization Reactions (Table 2.1)	151
2.5.2.4	General Procedure for the Iridium-Catalyzed Allylic Alkylation.....	152
2.5.2.5	Procedure for the Preparatory Scale Reaction	153

2.5.2.6	Spectroscopic Data for the Iridium-Catalyzed Allylic Alkylation Products	154
2.5.2.7	Determination of Enantiomeric Excess	162
2.6	References and Notes	164

APPENDIX 3 **168**

Spectra Relevant to Chapter 2

CHAPTER 3 **201**

Enantioselective Synthesis of Acyclic α -Quaternary Carboxylic Acid Derivatives via Iridium-Catalyzed Allylic Alkylation

3.1	Introduction and Background	201
3.2	Reaction Optimization	203
3.3	Mechanistic Insights	204
3.4	Substrate Scope Exploration.....	206
3.5	Product Transformations	210
3.6	Conclusions.....	211
3.7	Experimental Section	212
3.7.1	Materials and Methods	212
3.7.1.1	Preparation of Known Compounds	214
3.7.2	Experimental Procedures and Spectroscopic Data	214
3.7.2.1	Representative Procedures for the Synthesis of Electrophiles	214
3.7.2.1.1	Representative Procedure #1: Oxidative Heck Reaction	214
3.7.2.1.2	Representative Procedure #2: Reduction & Acylation	215
3.7.2.2	Spectroscopic Data for the Synthesis of Electrophiles.....	216
3.7.2.3	General Procedure for Optimization Reactions (Table 3.1)	222
3.7.2.4	General Procedure for the Enantioenriched Carboxylic Acid Synthesis	223
3.7.2.5	Spectroscopic Data for the Enantioenriched Carboxylic Acids	224
3.7.2.6	Experimental Procedures and Spectroscopic Data for the One-pot Syntheses of Carboxylic Acid Derivatives	233
3.7.2.7	Experimental Procedures and Spectroscopic Data for the Product Transformations of α -Quaternary Ester 82	239
3.7.2.8	Determination of Enantiomeric Excess	242
3.8	References and Notes	244

APPENDIX 4 **249**

Spectra Relevant to Chapter 3

APPENDIX 5 **318***X-Ray Crystallography Reports Relevant to Chapter 3*

A5.1	General Experimental	319
A5.1.1	X-Ray Crystal Structure Analysis of Carboxylic Acid 77h	319

CHAPTER 4 **325***Enantioselective Synthesis of Vicinal All-Carbon Quaternary Centers via Iridium-Catalyzed Allylic Alkylation*

4.1	Introduction and Background	325
4.2	Reaction Optimization	327
4.3	Substrate Scope Exploration.....	329
4.4	Product Transformations.....	334
4.5	Conclusions.....	335
4.6	Experimental Section	336
4.6.1	Materials and Methods	336
4.6.1.1	Key Considerations.....	337
4.6.1.2	Preparation of Known Compounds	338
4.6.2	Experimental Procedures and Spectroscopic Data	338
4.6.2.1	General Procedure for the Synthesis of Electrophiles	338
4.6.2.2	Spectroscopic Data for the Synthesis of Electrophiles.....	339
4.6.2.3	General Procedure for Optimization Reactions (Table 4.1)	340
4.6.2.4	General Procedure for the Iridium-Catalyzed Allylic Alkylation	341
4.6.2.5	Spectroscopic Data for the Iridium-Catalyzed Allylic Alkylation Products	342
4.6.2.6	Experimental Procedures and Spectroscopic Data for the Product Transformations of Allylic Alkylation Products.....	355
4.6.2.7	Determination of Enantiomeric Excess	261
4.7	References and Notes	363

APPENDIX 6 **369***Spectra Relevant to Chapter 4***APPENDIX 7** **429***X-Ray Crystallography Reports Relevant to Chapter 4*

A7.1	General Experimental	430
A7.1.1	X-Ray Crystal Structure Analysis of Bis-Nitrile 97c	431

A7.2	References and Notes	440
------	----------------------------	-----

CHAPTER 5 **441**

Stereoselective Iridium-Catalyzed Allylic Alkylation in the Stoltz Laboratory: A Summary

5.1	Introduction.....	441
5.2	Synthesis of Vicinal Tertiary and All-Carbon Quaternary Stereocenters via Enantio- and Diastereoselective Iridium-Catalyzed Allylic Alkylation	445
5.2.1	Cyclic Nucleophiles	445
5.2.2	Acyclic Nucleophiles	449
5.2.3	Alkyl-Substituted Electrophiles.....	450
5.3	Unpoled Iridium-Catalyzed Allylic Alkylation Reactions	454
5.3.1	Tertiary Allylic Stereocenters	455
5.3.2	Quaternary Allylic Stereocenters	457
5.4	Synthesis of Vicinal All-Carbon Quaternary Centers via Enantioselective Iridium-Catalyzed Allylic Alkylation	462
5.5	Conclusions and Future Outlook	464
5.6	References and Notes	466

APPENDIX 8 **471**

A Catalytic, Enantioselective Formal Synthesis of (+)-Dichroanone and (+)-Taiwaniaquinone H

A8.1	Introduction	471
A8.2	Background to the Stoltz Group's Enantioselective Palladium-Catalyzed Conjugate Addition Chemistry	474
A8.2.1	Introduction to Asymmetric Transition Metal-Catalyzed Conjugate Addition Chemistry	474
A8.2.2	Initial Discoveries	475
A8.2.3	Further Reaction Development	479
A8.2.4	Mechanistic Hypothesis.....	483
A8.2.5	Heterocyclic Acceptors	487
A8.3	Retrosynthetic Analysis	488
A8.4	First Generation Route	489
A8.5	Second Generation Route	493
A8.6	Conclusions	498
A8.7	Experimental Section	489
A8.7.1	Materials and Methods	498
A8.7.1.1	Preparation of Known Compounds	499

A8.7.2	Experimental Procedures and Spectroscopic Data	500
A8.7.2.1	General Procedure and Spectroscopic Data for the Synthesis of Resorcinol Pivaloyl Esters	500
A8.7.2.2	General Procedure and Spectroscopic Data for the Synthesis of Borylated Arenes	502
A8.7.2.3	General Procedure and Spectroscopic Data for the Synthesis of Boronic Acid Analogues	505
A8.7.2.4	General Procedure and Spectroscopic Data for the Asymmetric Palladium-Catalyzed Conjugate Addition of Arylboronic Acids	508
A8.7.2.5	Procedures and Spectroscopic Data for Synthetic Intermediates	511
A8.7.2.6	Determination of Enantiomeric Excess	520
A8.7.2.7	Hammett Plot Data	521
A8.8	References and Notes	521

APPENDIX 9 **529**

Spectra Relevant to Appendix 8

APPENDIX 10 **577**

X-Ray Crystallography Reports Relevant to Appendix 8

A10.1	General Experimental	578
A10.1.1	X-Ray Crystal Structure Analysis of Undesired Tricycle 203	578

APPENDIX 11 **589**

*Asymmetric Synthesis of All-Carbon Quaternary Spirocycles via an
Enantioselective Allylic Alkylation Strategy*

A11.1	Introduction and Background	589
A11.2	Reaction Development	591
A11.3	Conclusions	593
A11.4	Experimental Section	594
A11.4.1	Materials and Methods	594
A11.4.1.1	Preparation of Known Compounds	596
A11.4.2	Experimental Procedures and Spectroscopic Data	596
A11.4.2.1	Experimental Procedures and Spectroscopic Data for the Synthesis of Allylic Alkylation Substrates	596
A11.4.2.2	General Procedure for the Asymmetric Palladium-Catalyzed Allylic Alkylation	599

A11.4.2.3	Spectroscopic Data for the Asymmetric Palladium-Catalyzed Allylic Alkylation Products.....	600
A11.4.2.4	General Procedure for Spirocyclic Formation	602
A11.4.2.5	Spectroscopic Data for Spirocyclic Compounds	602
A11.4.2.6	Determination of Enantiomeric Excess	604
A11.5	References and Notes	604

APPENDIX 12 **607**

Spectra Relevant to Appendix 11

APPENDIX 13 **626**

Progress Toward the Synthesis of (+)-Isopalhinine A

A13.1	Introduction and Background	626
A13.2	Iridium-Catalyzed Allylic Alkylation Route	627
A13.3	Palladium-Catalyzed Allylic Alkylation Route with A Masked Stabilized Lactam Enolate	636
A13.4	Piperidone Palladium-Catalyzed Allylic Alkylation Route.....	640
A13.5	Diastereoselective Route	643
A13.6	Future Directions and Proposed Late-Stage Chemistry to Access (+)-Isopalhinine A.....	647
A13.7	Conclusions.....	649
A13.8	Experimental Section	650
A13.8.1	Materials and Methods	650
A13.8.1.1	Preparation of Known Compounds	651
A13.8.2	Experimental Procedures and Spectroscopic Data	652
A13.8.2.1	Experimental Procedures and Spectroscopic Data for the Synthesis of Synthetic Intermediates in Section A13.2	652
A13.8.2.2	Experimental Procedures and Spectroscopic Data for the Synthesis of Synthetic Intermediates in Section A13.3	663
A13.8.2.3	Experimental Procedures and Spectroscopic Data for the Synthesis of Synthetic Intermediates in Section A13.4	671
A13.8.2.4	Experimental Procedures and Spectroscopic Data for the Synthesis of Synthetic Intermediates in Section A13.5	677
A13.8.2.5	Determination of Enantiomeric Excess.....	681
A13.9	References and Notes	683

APPENDIX 14 **687**

Spectra Relevant to Appendix 13

APPENDIX 15**739***Notebook Cross-Reference for New Compounds*

Comprehensive Bibliography	759
Index.....	788
About the Author	791

LIST OF FIGURES

PROLOGUE*Iridium-Catalyzed Allylic Alkylation*

Figure P.1	Challenges of enantio- and diastereoselective iridium-catalyzed allylic alkylation	3
-------------------	------------------------------------------------------------------------------------------	---

CHAPTER 1*Stereoselective Iridium-Catalyzed Allylic Alkylation Reactions with Crotyl Chloride*

Figure 1.1	Enantio-, diastereo-, and regioselective iridium-catalyzed allylic alkylation reactions.....	6
Figure 1.2	Select natural products bearing alkyl-substituted vicinal tertiary and quaternary stereocenters	7
Figure 1.3	Product transformations of allylic alkylation products 54 and 58a	27

APPENDIX 1*Spectra Relevant to Chapter 1*

Figure A1.1	¹ H NMR (400 MHz, CDCl ₃) of compound 54	63
Figure A1.2	Infrared spectrum (Thin Film, NaCl) of compound 54	64
Figure A1.3	¹³ C NMR (101 MHz, CDCl ₃) of compound 54	64
Figure A1.4	¹ H NMR (400 MHz, CDCl ₃) of compound epi-54	65
Figure A1.5	Infrared spectrum (Thin Film, NaCl) of compound epi-54	66
Figure A1.6	¹³ C NMR (101 MHz, CDCl ₃) of compound epi-54	66
Figure A1.7	¹ H NMR (400 MHz, CDCl ₃) of compound 55	67
Figure A1.8	Infrared spectrum (Thin Film, NaCl) of compound 55	68
Figure A1.9	¹³ C NMR (101 MHz, CDCl ₃) of compound 55	68
Figure A1.10	¹ H NMR (400 MHz, CDCl ₃) of compound 56b	69
Figure A1.11	Infrared spectrum (Thin Film, NaCl) of compound 56b	70
Figure A1.12	¹³ C NMR (101 MHz, CDCl ₃) of compound 56b	70
Figure A1.13	¹ H NMR (400 MHz, CDCl ₃) of compound 56c	71
Figure A1.14	Infrared spectrum (Thin Film, NaCl) of compound 56c	72
Figure A1.15	¹³ C NMR (101 MHz, CDCl ₃) of compound 56c	72
Figure A1.16	¹ H NMR (400 MHz, CDCl ₃) of compound 56e	73
Figure A1.17	Infrared spectrum (Thin Film, NaCl) of compound 56e	74
Figure A1.18	¹³ C NMR (101 MHz, CDCl ₃) of compound 56e	74
Figure A1.19	¹ H NMR (400 MHz, CDCl ₃) of compound 56g	75

Figure A1.20	Infrared spectrum (Thin Film, NaCl) of compound 56g	76
Figure A1.21	^{13}C NMR (101 MHz, CDCl_3) of compound 56g	76
Figure A1.22	^1H NMR (400 MHz, CDCl_3) of compound 56h	77
Figure A1.23	Infrared spectrum (Thin Film, NaCl) of compound 56h	78
Figure A1.24	^{13}C NMR (101 MHz, CDCl_3) of compound 56h	78
Figure A1.25	^1H NMR (400 MHz, CDCl_3) of compound 56k	79
Figure A1.26	Infrared spectrum (Thin Film, NaCl) of compound 56k	80
Figure A1.27	^{13}C NMR (101 MHz, CDCl_3) of compound 56k	80
Figure A1.28	^1H NMR (400 MHz, CDCl_3) of compound 58a	81
Figure A1.29	Infrared spectrum (Thin Film, NaCl) of compound 58a	82
Figure A1.30	^{13}C NMR (101 MHz, CDCl_3) of compound 58a	82
Figure A1.31	^1H NMR (400 MHz, CDCl_3) of compound 58b	83
Figure A1.32	Infrared spectrum (Thin Film, NaCl) of compound 58b	84
Figure A1.33	^{13}C NMR (101 MHz, CDCl_3) of compound 58b	84
Figure A1.34	^1H NMR (400 MHz, CDCl_3) of compound 58c	85
Figure A1.35	Infrared spectrum (Thin Film, NaCl) of compound 58c	86
Figure A1.36	^{13}C NMR (101 MHz, CDCl_3) of compound 58c	86
Figure A1.37	^1H NMR (400 MHz, CDCl_3) of compound 58d	87
Figure A1.38	Infrared spectrum (Thin Film, NaCl) of compound 58d	88
Figure A1.39	^{13}C NMR (101 MHz, CDCl_3) of compound 58d	88
Figure A1.40	^1H NMR (400 MHz, CDCl_3) of compound 58e	89
Figure A1.41	Infrared spectrum (Thin Film, NaCl) of compound 58e	90
Figure A1.42	^{13}C NMR (101 MHz, CDCl_3) of compound 58e	90
Figure A1.43	^1H NMR (400 MHz, CDCl_3) of compound 58f	91
Figure A1.44	Infrared spectrum (Thin Film, NaCl) of compound 58f	92
Figure A1.45	^{13}C NMR (101 MHz, CDCl_3) of compound 58f	92
Figure A1.46	^1H NMR (400 MHz, CDCl_3) of compound 58g	93
Figure A1.47	Infrared spectrum (Thin Film, NaCl) of compound 58g	94
Figure A1.48	^{13}C NMR (101 MHz, CDCl_3) of compound 58g	94
Figure A1.49	^1H NMR (400 MHz, CDCl_3) of compound 58h	95
Figure A1.50	Infrared spectrum (Thin Film, NaCl) of compound 58h	96
Figure A1.51	^{13}C NMR (101 MHz, CDCl_3) of compound 58h	96
Figure A1.52	^1H NMR (400 MHz, CDCl_3) of compound 58i	97
Figure A1.53	Infrared spectrum (Thin Film, NaCl) of compound 58i	98
Figure A1.54	^{13}C NMR (101 MHz, CDCl_3) of compound 58i	98
Figure A1.55	^1H NMR (400 MHz, CDCl_3) of compound 58j	99
Figure A1.56	Infrared spectrum (Thin Film, NaCl) of compound 58j	100
Figure A1.57	^{13}C NMR (101 MHz, CDCl_3) of compound 58j	100

Figure A1.58	^1H NMR (400 MHz, CDCl_3) of compound 58k	101
Figure A1.59	Infrared spectrum (Thin Film, NaCl) of compound 58k	102
Figure A1.60	^{13}C NMR (101 MHz, CDCl_3) of compound 58k	102
Figure A1.61	^1H NMR (400 MHz, CDCl_3) of compound 61	103
Figure A1.62	Infrared spectrum (Thin Film, NaCl) of compound 61	104
Figure A1.63	^{13}C NMR (101 MHz, CDCl_3) of compound 61	104
Figure A1.64	^1H NMR (400 MHz, CDCl_3) of compound 62	105
Figure A1.65	Infrared spectrum (Thin Film, NaCl) of compound 62	106
Figure A1.66	^{13}C NMR (101 MHz, CDCl_3) of compound 62	106
Figure A1.67	^1H NMR (400 MHz, CDCl_3) of compound 63	107
Figure A1.68	Infrared spectrum (Thin Film, NaCl) of compound 63	108
Figure A1.69	^{13}C NMR (101 MHz, CDCl_3) of compound 63	108
Figure A1.70	^1H NMR (400 MHz, CDCl_3) of compound 64	109
Figure A1.71	Infrared spectrum (Thin Film, NaCl) of compound 64	110
Figure A1.72	^{13}C NMR (101 MHz, CDCl_3) of compound 64	110
Figure A1.73	^1H NMR (400 MHz, CDCl_3) of compound 65	111
Figure A1.74	Infrared spectrum (Thin Film, NaCl) of compound 65	112
Figure A1.75	^{13}C NMR (101 MHz, CDCl_3) of compound 65	112
Figure A1.76	NOESY (400 MHz, CDCl_3) of compound 65	113
Figure A1.77	^1H NMR (400 MHz, CDCl_3) of compound 66	114
Figure A1.78	Infrared spectrum (Thin Film, NaCl) of compound 66	115
Figure A1.79	^{13}C NMR (101 MHz, CDCl_3) of compound 66	115

APPENDIX 2

X-Ray Crystallography Reports Relevant to Chapter 1

Figure A2.1	X-ray crystal structure of allylic alkylation product 58e	117
Figure A2.2	X-ray crystal structure of triol 63	125
Figure A2.3	X-ray crystal structure of diol 64	133

CHAPTER 2

Enantioselective Iridium-Catalyzed Allylic Alkylation Reactions of Masked Acyl Cyanide Equivalents

Figure 2.1	Iridium-catalyzed allylic alkylation strategies	141
-------------------	-------------------------------------------------------	-----

APPENDIX 3

Spectra Relevant to Chapter 2

Figure A3.1	^1H NMR (400 MHz, CDCl_3) of compound 69c	169
--------------------	---------------------------------------------------------------------------	-----

Figure A3.2	Infrared spectrum (Thin Film, NaCl) of compound 69c	170
Figure A3.3	^{13}C NMR (101 MHz, CDCl_3) of compound 69c	170
Figure A3.4	^1H NMR (400 MHz, CDCl_3) of compound 70e	171
Figure A3.5	Infrared spectrum (Thin Film, NaCl) of compound 70e	172
Figure A3.6	^{13}C NMR (101 MHz, CDCl_3) of compound 70e	172
Figure A3.7	^1H NMR (400 MHz, CDCl_3) of compound 70f	173
Figure A3.8	Infrared spectrum (Thin Film, NaCl) of compound 70f	174
Figure A3.9	^{13}C NMR (101 MHz, CDCl_3) of compound 70f	174
Figure A3.10	^1H NMR (400 MHz, CDCl_3) of compound 70g	175
Figure A3.11	Infrared spectrum (Thin Film, NaCl) of compound 70g	176
Figure A3.12	^{13}C NMR (101 MHz, CDCl_3) of compound 70g	176
Figure A3.13	^1H NMR (400 MHz, CDCl_3) of compound 71a	177
Figure A3.14	Infrared spectrum (Thin Film, NaCl) of compound 71a	178
Figure A3.15	^{13}C NMR (101 MHz, CDCl_3) of compound 71a	178
Figure A3.16	^1H NMR (400 MHz, CDCl_3) of compound 71b	179
Figure A3.17	Infrared spectrum (Thin Film, NaCl) of compound 71b	180
Figure A3.18	^{13}C NMR (101 MHz, CDCl_3) of compound 71b	180
Figure A3.19	^1H NMR (400 MHz, CDCl_3) of compound 71c	181
Figure A3.20	Infrared spectrum (Thin Film, NaCl) of compound 71c	182
Figure A3.21	^{13}C NMR (101 MHz, CDCl_3) of compound 71c	182
Figure A3.22	^1H NMR (400 MHz, CDCl_3) of compound 71d	183
Figure A3.23	Infrared spectrum (Thin Film, NaCl) of compound 71d	184
Figure A3.24	^{13}C NMR (101 MHz, CDCl_3) of compound 71d	184
Figure A3.25	^1H NMR (400 MHz, CDCl_3) of compound 71e	185
Figure A3.26	Infrared spectrum (Thin Film, NaCl) of compound 71e	186
Figure A3.27	^{13}C NMR (101 MHz, CDCl_3) of compound 71e	186
Figure A3.28	^1H NMR (400 MHz, CDCl_3) of compound 71f	187
Figure A3.29	Infrared spectrum (Thin Film, NaCl) of compound 71f	188
Figure A3.30	^{13}C NMR (101 MHz, CDCl_3) of compound 71f	188
Figure A3.31	^1H NMR (400 MHz, CDCl_3) of compound 71g	189
Figure A3.32	Infrared spectrum (Thin Film, NaCl) of compound 71g	190
Figure A3.33	^{13}C NMR (101 MHz, CDCl_3) of compound 71g	190
Figure A3.34	^1H NMR (400 MHz, CDCl_3) of compound 71h	191
Figure A3.35	Infrared spectrum (Thin Film, NaCl) of compound 71h	192
Figure A3.36	^{13}C NMR (101 MHz, CDCl_3) of compound 71h	192
Figure A3.37	^1H NMR (400 MHz, CDCl_3) of compound 71i	193
Figure A3.38	Infrared spectrum (Thin Film, NaCl) of compound 71i	194
Figure A3.39	^{13}C NMR (101 MHz, CDCl_3) of compound 71i	194

Figure A3.40	^1H NMR (400 MHz, CDCl_3) of compound 71j	195
Figure A3.41	Infrared spectrum (Thin Film, NaCl) of compound 71j	196
Figure A3.42	^{13}C NMR (101 MHz, CDCl_3) of compound 71j	196
Figure A3.43	^1H NMR (400 MHz, CDCl_3) of compound 71k	197
Figure A3.44	Infrared spectrum (Thin Film, NaCl) of compound 71k	198
Figure A3.45	^{13}C NMR (101 MHz, CDCl_3) of compound 71k	198
Figure A3.46	^1H NMR (400 MHz, CDCl_3) of compound 71l	199
Figure A3.47	Infrared spectrum (Thin Film, NaCl) of compound 71l	200
Figure A3.48	^{13}C NMR (101 MHz, CDCl_3) of compound 71l	200

CHAPTER 3

Enantioselective Synthesis of Acyclic α -Quaternary Carboxylic Acid Derivatives via Iridium-Catalyzed Allylic Alkylation

Figure 3.1	Synthesis of allylic all-carbon quaternary stereocenters via enantioselective iridium-catalyzed allylic alkylation.....	202
Figure 3.2	One-pot transformations to α -quaternary carboxylic acid derivatives	210
Figure 3.3	Product transformations of α -quaternary ester 82	211

APPENDIX 4

Spectra Relevant to Chapter 3

Figure A4.1	^1H NMR (400 MHz, CDCl_3) of compound 73	250
Figure A4.2	Infrared spectrum (Thin Film, NaCl) of compound 73	251
Figure A4.3	^{13}C NMR (101 MHz, CDCl_3) of compound 73	251
Figure A4.4	^1H NMR (400 MHz, CDCl_3) of compound 74	252
Figure A4.5	Infrared spectrum (Thin Film, NaCl) of compound 74	253
Figure A4.6	^{13}C NMR (101 MHz, CDCl_3) of compound 74	253
Figure A4.7	^1H NMR (400 MHz, CDCl_3) of compound 76c	254
Figure A4.8	Infrared spectrum (Thin Film, NaCl) of compound 76c	255
Figure A4.9	^{13}C NMR (101 MHz, CDCl_3) of compound 76c	255
Figure A4.10	^1H NMR (400 MHz, CDCl_3) of compound 76f	256
Figure A4.11	Infrared spectrum (Thin Film, NaCl) of compound 76f	257
Figure A4.12	^{13}C NMR (101 MHz, CDCl_3) of compound 76f	257
Figure A4.13	^1H NMR (400 MHz, CDCl_3) of compound 76g	258
Figure A4.14	Infrared spectrum (Thin Film, NaCl) of compound 76g	259
Figure A4.15	^{13}C NMR (101 MHz, CDCl_3) of compound 76g	259
Figure A4.16	^1H NMR (400 MHz, CDCl_3) of compound 76h	260
Figure A4.17	Infrared spectrum (Thin Film, NaCl) of compound 76h	261

Figure A4.18	^{13}C NMR (101 MHz, CDCl_3) of compound 76h	261
Figure A4.19	^1H NMR (400 MHz, CDCl_3) of compound 76i	262
Figure A4.20	Infrared spectrum (Thin Film, NaCl) of compound 76i	263
Figure A4.21	^{13}C NMR (101 MHz, CDCl_3) of compound 76i	263
Figure A4.22	^1H NMR (400 MHz, CDCl_3) of compound 76k	264
Figure A4.23	Infrared spectrum (Thin Film, NaCl) of compound 76k	265
Figure A4.24	^{13}C NMR (101 MHz, CDCl_3) of compound 76k	265
Figure A4.25	^1H NMR (400 MHz, CDCl_3) of compound 77b	266
Figure A4.26	Infrared spectrum (Thin Film, NaCl) of compound 77b	267
Figure A4.27	^{13}C NMR (101 MHz, CDCl_3) of compound 77b	267
Figure A4.28	^1H NMR (400 MHz, CDCl_3) of compound 77c	268
Figure A4.29	Infrared spectrum (Thin Film, NaCl) of compound 77c	269
Figure A4.30	^{13}C NMR (101 MHz, CDCl_3) of compound 77c	269
Figure A4.31	^1H NMR (400 MHz, CDCl_3) of compound 77d	270
Figure A4.32	Infrared spectrum (Thin Film, NaCl) of compound 77d	271
Figure A4.33	^{13}C NMR (101 MHz, CDCl_3) of compound 77d	271
Figure A4.34	^1H NMR (400 MHz, CDCl_3) of compound 77e	272
Figure A4.35	Infrared spectrum (Thin Film, NaCl) of compound 77e	273
Figure A4.36	^{13}C NMR (101 MHz, CDCl_3) of compound 77e	273
Figure A4.37	^1H NMR (400 MHz, CDCl_3) of compound 77f	274
Figure A4.38	Infrared spectrum (Thin Film, NaCl) of compound 77f	275
Figure A4.39	^{13}C NMR (101 MHz, CDCl_3) of compound 77f	275
Figure A4.40	^1H NMR (400 MHz, CDCl_3) of compound 77g	276
Figure A4.41	Infrared spectrum (Thin Film, NaCl) of compound 77g	277
Figure A4.42	^{13}C NMR (101 MHz, CDCl_3) of compound 77g	277
Figure A4.43	^1H NMR (400 MHz, CDCl_3) of compound 77h	278
Figure A4.44	Infrared spectrum (Thin Film, NaCl) of compound 77h	279
Figure A4.45	^{13}C NMR (101 MHz, CDCl_3) of compound 77h	279
Figure A4.46	^1H NMR (400 MHz, CDCl_3) of compound 77i	280
Figure A4.47	Infrared spectrum (Thin Film, NaCl) of compound 77i	281
Figure A4.48	^{13}C NMR (101 MHz, CDCl_3) of compound 77i	281
Figure A4.49	^1H NMR (400 MHz, CDCl_3) of compound 77j	282
Figure A4.50	Infrared spectrum (Thin Film, NaCl) of compound 77j	283
Figure A4.51	^{13}C NMR (101 MHz, CDCl_3) of compound 77j	283
Figure A4.52	^1H NMR (400 MHz, CDCl_3) of compound 77k	284
Figure A4.53	Infrared spectrum (Thin Film, NaCl) of compound 77k	285
Figure A4.54	^{13}C NMR (101 MHz, CDCl_3) of compound 77k	285
Figure A4.55	HMBC (400 MHz, CDCl_3) of compound 77k	286

Figure A4.56	^1H NMR (400 MHz, CDCl_3) of compound 78b	287
Figure A4.57	Infrared spectrum (Thin Film, NaCl) of compound 78b	288
Figure A4.58	^{13}C NMR (101 MHz, CDCl_3) of compound 78b	288
Figure A4.59	^1H NMR (400 MHz, CDCl_3) of compound 78c	289
Figure A4.60	Infrared spectrum (Thin Film, NaCl) of compound 78c	290
Figure A4.61	^{13}C NMR (101 MHz, CDCl_3) of compound 78c	290
Figure A4.62	^1H NMR (400 MHz, CDCl_3) of compound 78e	291
Figure A4.63	Infrared spectrum (Thin Film, NaCl) of compound 78e	292
Figure A4.64	^{13}C NMR (101 MHz, CDCl_3) of compound 78e	292
Figure A4.65	^1H NMR (400 MHz, CDCl_3) of compound 79a	293
Figure A4.66	Infrared spectrum (Thin Film, NaCl) of compound 79a	294
Figure A4.67	^{13}C NMR (101 MHz, CDCl_3) of compound 79a	294
Figure A4.68	^1H NMR (400 MHz, CDCl_3) of compound 79b	295
Figure A4.69	Infrared spectrum (Thin Film, NaCl) of compound 79b	296
Figure A4.70	^{13}C NMR (101 MHz, CDCl_3) of compound 79b	296
Figure A4.71	^1H NMR (400 MHz, CDCl_3) of compound 79f	297
Figure A4.72	Infrared spectrum (Thin Film, NaCl) of compound 79f	298
Figure A4.73	^{13}C NMR (101 MHz, CDCl_3) of compound 79f	298
Figure A4.74	HMBC (400 MHz, CDCl_3) of compound 79f	299
Figure A4.75	^1H NMR (400 MHz, CDCl_3) of compound 82	300
Figure A4.76	Infrared spectrum (Thin Film, NaCl) of compound 82	301
Figure A4.77	^{13}C NMR (101 MHz, CDCl_3) of compound 82	301
Figure A4.78	^1H NMR (400 MHz, CDCl_3) of compound 83	302
Figure A4.79	Infrared spectrum (Thin Film, NaCl) of compound 83	303
Figure A4.80	^{13}C NMR (101 MHz, CDCl_3) of compound 83	303
Figure A4.81	^1H NMR (400 MHz, CDCl_3) of compound 84	304
Figure A4.82	Infrared spectrum (Thin Film, NaCl) of compound 84	305
Figure A4.83	^{13}C NMR (101 MHz, CDCl_3) of compound 84	305
Figure A4.84	^1H NMR (400 MHz, CDCl_3) of compound 85	306
Figure A4.85	Infrared spectrum (Thin Film, NaCl) of compound 85	307
Figure A4.86	^{13}C NMR (101 MHz, CDCl_3) of compound 85	307
Figure A4.87	^1H NMR (400 MHz, CDCl_3) of compound 86	308
Figure A4.88	Infrared spectrum (Thin Film, NaCl) of compound 86	309
Figure A4.89	^{13}C NMR (101 MHz, CDCl_3) of compound 86	309
Figure A4.90	^1H NMR (400 MHz, CDCl_3) of compound 88	310
Figure A4.91	Infrared spectrum (Thin Film, NaCl) of compound 88	311
Figure A4.92	^{13}C NMR (101 MHz, CDCl_3) of compound 88	311
Figure A4.93	^1H NMR (400 MHz, CDCl_3) of compound 89	312

Figure A4.94	Infrared spectrum (Thin Film, NaCl) of compound 89	313
Figure A4.95	^{13}C NMR (101 MHz, CDCl_3) of compound 89	313
Figure A4.96	^1H NMR (400 MHz, CDCl_3) of compound 90	314
Figure A4.97	Infrared spectrum (Thin Film, NaCl) of compound 90	315
Figure A4.98	^{13}C NMR (101 MHz, CDCl_3) of compound 90	315
Figure A4.99	^1H NMR (400 MHz, CDCl_3) of compound 91	316
Figure A4.100	Infrared spectrum (Thin Film, NaCl) of compound 91	317
Figure A4.101	^{13}C NMR (101 MHz, CDCl_3) of compound 91	317

APPENDIX 5

X-Ray Crystallography Reports Relevant to Chapter 3

Figure A5.1	X-ray crystal structure of carboxylic acid 77h	319
--------------------	-------------------------------------------------------------	-----

CHAPTER 4

Enantioselective Synthesis of Vicinal All-Carbon Quaternary Centers via Iridium-Catalyzed Allylic Alkylation

Figure 4.1	State-of-the-art in the enantioselective synthesis of vicinal all-carbon quaternary centers via transition metal-catalyzed allylic alkylation	326
Figure 4.2	Product transformations of allylic alkylation products.....	335

APPENDIX 6

Spectra Relevant to Chapter 4

Figure A6.1	^1H NMR (400 MHz, CDCl_3) of compound 93	370
Figure A6.2	Infrared spectrum (Thin Film, NaCl) of compound 93	371
Figure A6.3	^{13}C NMR (101 MHz, CDCl_3) of compound 93	371
Figure A6.4	^1H NMR (400 MHz, CDCl_3) of compound 95a	372
Figure A6.5	Infrared spectrum (Thin Film, NaCl) of compound 95a	373
Figure A6.6	^{13}C NMR (101 MHz, CDCl_3) of compound 95a	373
Figure A6.7	^1H NMR (400 MHz, CDCl_3) of compound 95b	374
Figure A6.8	Infrared spectrum (Thin Film, NaCl) of compound 95b	375
Figure A6.9	^{13}C NMR (101 MHz, CDCl_3) of compound 95b	375
Figure A6.10	^1H NMR (400 MHz, CDCl_3) of compound 95d	376
Figure A6.11	Infrared spectrum (Thin Film, NaCl) of compound 95d	377
Figure A6.12	^{13}C NMR (101 MHz, CDCl_3) of compound 95d	377
Figure A6.13	^1H NMR (400 MHz, CDCl_3) of compound 95e	378
Figure A6.14	Infrared spectrum (Thin Film, NaCl) of compound 95e	379
Figure A6.15	^{13}C NMR (101 MHz, CDCl_3) of compound 95e	379

Figure A6.16	^1H NMR (400 MHz, CDCl_3) of compound 95f	380
Figure A6.17	Infrared spectrum (Thin Film, NaCl) of compound 95f	381
Figure A6.18	^{13}C NMR (101 MHz, CDCl_3) of compound 95f	381
Figure A6.19	^1H NMR (400 MHz, CDCl_3) of compound 95g	382
Figure A6.20	Infrared spectrum (Thin Film, NaCl) of compound 95g	383
Figure A6.21	^{13}C NMR (101 MHz, CDCl_3) of compound 95g	383
Figure A6.22	^1H NMR (400 MHz, CDCl_3) of compound 96b	384
Figure A6.23	Infrared spectrum (Thin Film, NaCl) of compound 96b	385
Figure A6.24	^{13}C NMR (101 MHz, CDCl_3) of compound 96b	385
Figure A6.25	^1H NMR (400 MHz, CDCl_3) of compound 96c	386
Figure A6.26	Infrared spectrum (Thin Film, NaCl) of compound 96c	387
Figure A6.27	^{13}C NMR (101 MHz, CDCl_3) of compound 96c	387
Figure A6.28	^1H NMR (400 MHz, CDCl_3) of compound 96f	388
Figure A6.29	Infrared spectrum (Thin Film, NaCl) of compound 96f	389
Figure A6.30	^{13}C NMR (101 MHz, CDCl_3) of compound 96f	389
Figure A6.31	^1H NMR (400 MHz, CDCl_3) of compound 97a	390
Figure A6.32	Infrared spectrum (Thin Film, NaCl) of compound 97a	391
Figure A6.33	^{13}C NMR (101 MHz, CDCl_3) of compound 97a	391
Figure A6.34	^1H NMR (400 MHz, CDCl_3) of compound 97b	392
Figure A6.35	Infrared spectrum (Thin Film, NaCl) of compound 97b	393
Figure A6.36	^{13}C NMR (101 MHz, CDCl_3) of compound 97b	393
Figure A6.37	^1H NMR (400 MHz, CDCl_3) of compound 97c	394
Figure A6.38	Infrared spectrum (Thin Film, NaCl) of compound 97c	395
Figure A6.39	^{13}C NMR (101 MHz, CDCl_3) of compound 97c	395
Figure A6.40	^1H NMR (400 MHz, CDCl_3) of compound 97d	396
Figure A6.41	Infrared spectrum (Thin Film, NaCl) of compound 97d	397
Figure A6.42	^{13}C NMR (101 MHz, CDCl_3) of compound 97d	397
Figure A6.43	^1H NMR (400 MHz, CDCl_3) of compound 97e	398
Figure A6.44	Infrared spectrum (Thin Film, NaCl) of compound 97e	399
Figure A6.45	^{13}C NMR (101 MHz, CDCl_3) of compound 97e	399
Figure A6.46	^1H NMR (400 MHz, CDCl_3) of compound 97f	400
Figure A6.47	Infrared spectrum (Thin Film, NaCl) of compound 97f	401
Figure A6.48	^{13}C NMR (101 MHz, CDCl_3) of compound 97f	401
Figure A6.49	^1H NMR (400 MHz, CDCl_3) of compound 97g	402
Figure A6.50	Infrared spectrum (Thin Film, NaCl) of compound 97g	403
Figure A6.51	^{13}C NMR (101 MHz, CDCl_3) of compound 97g	403
Figure A6.52	^1H NMR (400 MHz, CDCl_3) of compound 97h	404
Figure A6.53	Infrared spectrum (Thin Film, NaCl) of compound 97h	405

Figure A6.54	^{13}C NMR (101 MHz, CDCl_3) of compound 97h	405
Figure A6.55	^1H NMR (400 MHz, CDCl_3) of compound 97j	406
Figure A6.56	Infrared spectrum (Thin Film, NaCl) of compound 97j	407
Figure A6.57	^{13}C NMR (101 MHz, CDCl_3) of compound 97j	407
Figure A6.58	^1H NMR (400 MHz, CDCl_3) of compound 97k	408
Figure A6.59	Infrared spectrum (Thin Film, NaCl) of compound 97k	409
Figure A6.60	^{13}C NMR (101 MHz, CDCl_3) of compound 97k	409
Figure A6.61	^1H NMR (400 MHz, CDCl_3) of compound 97l	410
Figure A6.62	Infrared spectrum (Thin Film, NaCl) of compound 97l	411
Figure A6.63	^{13}C NMR (101 MHz, CDCl_3) of compound 97l	411
Figure A6.64	^1H NMR (400 MHz, CDCl_3) of compound 101	412
Figure A6.65	Infrared spectrum (Thin Film, NaCl) of compound 101	413
Figure A6.66	^{13}C NMR (101 MHz, CDCl_3) of compound 101	413
Figure A6.67	^1H NMR (400 MHz, CDCl_3) of compound 102	414
Figure A6.68	Infrared spectrum (Thin Film, NaCl) of compound 102	415
Figure A6.69	^{13}C NMR (101 MHz, CDCl_3) of compound 102	415
Figure A6.70	^1H NMR (400 MHz, CDCl_3) of compound 103	416
Figure A6.71	Infrared spectrum (Thin Film, NaCl) of compound 103	417
Figure A6.72	^{13}C NMR (101 MHz, CDCl_3) of compound 103	417
Figure A6.73	HSQC (400 MHz, CDCl_3) of compound 103	418
Figure A6.74	HMBC (400 MHz, CDCl_3) of compound 103	419
Figure A6.75	NOESY (400 MHz, CDCl_3) of compound 103	420
Figure A6.76	^1H NMR (400 MHz, CDCl_3) of compound 104	421
Figure A6.77	Infrared spectrum (Thin Film, NaCl) of compound 104	422
Figure A6.78	^{13}C NMR (101 MHz, CDCl_3) of compound 104	422
Figure A6.79	NOESY (400 MHz, CDCl_3) of compound 104	423
Figure A6.80	^1H NMR (400 MHz, CDCl_3) of compound 105	424
Figure A6.81	Infrared spectrum (Thin Film, NaCl) of compound 105	425
Figure A6.82	^{13}C NMR (101 MHz, CDCl_3) of compound 105	425
Figure A6.83	NOESY (400 MHz, CDCl_3) of compound 105	426
Figure A6.84	^1H NMR (400 MHz, CDCl_3) of compound 106	427
Figure A6.85	Infrared spectrum (Thin Film, NaCl) of compound 106	428
Figure A6.86	^{13}C NMR (101 MHz, CDCl_3) of compound 106	428

APPENDIX 7

X-Ray Crystallography Reports Relevant to Chapter 4

Figure A7.1	X-ray crystal structure of bis-nitrile 97c	431
--------------------	---------------------------------------------------------	-----

CHAPTER 5

Stereoselective Iridium-Catalyzed Allylic Alkylation in the Stoltz Laboratory: A Summary

Figure 5.1	Stoltz group contributions to palladium-catalyzed allylic alkylation methodology and application in natural product total synthesis.....	442
Figure 5.2	Stereodyad-containing natural products as inspiration for the development of novel iridium-catalyzed allylic alkylation technology	443
Figure 5.3	Timeline for the development of iridium-catalyzed allylic alkylation prior to the Stoltz group's entry into the field	444
Figure 5.4	Select examples of diverse product transformations of enantio- and diastereoselective iridium-catalyzed allylic alkylation products 137	454
Figure 5.5	Iridium-catalyzed allylic alkylation strategies.....	455
Figure 5.6	Limitations in enantioselective iridium-catalyzed allylic alkylation prior to 2017	457
Figure 5.7	Enantioselective synthesis of acyclic α -quaternary esters 82 and amides 84	462
Figure 5.8	Product derivatizations of iridium-catalyzed allylic alkylation products 157 bearing vicinal all-carbon quaternary centers	464

APPENDIX 8

A Catalytic, Enantioselective Formal Synthesis of (+)-Dichroanone and (+)-Taiwaniaquinone H

Figure A8.1	Taiwaniaquinoid natural products	472
Figure A8.2	Stoltz group conjugate addition chemistry as inspiration for revised retrosynthetic analysis of (+)-taiwaniaquinone H (158) and (+)-dichroanone (159).....	473
Figure A8.3	Linear relationship of catalyst ee to product ee	484
Figure A8.4	Proposed catalytic cycle for the asymmetric conjugate addition of arylboronic acids to cyclic enones catalyzed by the combination of Pd(OCOCF ₃) ₂ and (<i>S</i>)- <i>t</i> -BuPyOx (L14).....	486
Figure A8.5	Calculated transition states and effect of α' -substituents on enantioselectivity.....	487
Figure A8.6	Planned retrosynthesis of (+)-taiwaniaquinone H (158) and (+)-dichroanone (159).....	489
Figure A8.7	Hammett plot of log ₁₀ (er) vs σ_p for select boronic acids in the palladium-catalyzed conjugate addition reaction	490

APPENDIX 9

Spectra Relevant to Appendix 8

Figure A9.1	^1H NMR (500 MHz, CDCl_3) of compound 169b	530
Figure A9.2	Infrared spectrum (Thin Film, NaCl) of compound 169b	531
Figure A9.3	^{13}C NMR (125 MHz, CDCl_3) of compound 169b	531
Figure A9.4	^1H NMR (500 MHz, CDCl_3) of compound 169c	532
Figure A9.5	Infrared spectrum (Thin Film, NaCl) of compound 169c	533
Figure A9.6	^{13}C NMR (125 MHz, CDCl_3) of compound 169c	533
Figure A9.7	^1H NMR (500 MHz, CDCl_3) of compound 169d	534
Figure A9.8	Infrared spectrum (Thin Film, NaCl) of compound 169d	535
Figure A9.9	^{13}C NMR (125 MHz, CDCl_3) of compound 169d	535
Figure A9.10	^1H NMR (500 MHz, CDCl_3) of compound 169e	536
Figure A9.11	Infrared spectrum (Thin Film, NaCl) of compound 169e	537
Figure A9.12	^{13}C NMR (125 MHz, CDCl_3) of compound 169e	537
Figure A9.13	^1H NMR (500 MHz, CDCl_3) of compound 169f	538
Figure A9.14	Infrared spectrum (Thin Film, NaCl) of compound 169f	539
Figure A9.15	^{13}C NMR (125 MHz, CDCl_3) of compound 169f	539
Figure A9.16	^1H NMR (500 MHz, CDCl_3) of compound 197	540
Figure A9.17	Infrared spectrum (Thin Film, NaCl) of compound 197	541
Figure A9.18	^{13}C NMR (125 MHz, CDCl_3) of compound 197	541
Figure A9.19	^1H NMR (500 MHz, CDCl_3) of compound 198	542
Figure A9.20	Infrared spectrum (Thin Film, NaCl) of compound 198	543
Figure A9.21	^{13}C NMR (125 MHz, CDCl_3) of compound 198	543
Figure A9.22	^1H NMR (500 MHz, CDCl_3) of compound 199	544
Figure A9.23	Infrared spectrum (Thin Film, NaCl) of compound 199	545
Figure A9.24	^{13}C NMR (125 MHz, CDCl_3) of compound 199	545
Figure A9.25	^1H NMR (500 MHz, CDCl_3) of compound 202	546
Figure A9.26	Infrared spectrum (Thin Film, NaCl) of compound 202	547
Figure A9.27	^{13}C NMR (125 MHz, CDCl_3) of compound 202	547
Figure A9.28	^1H NMR (500 MHz, CDCl_3) of compound 203	548
Figure A9.29	Infrared spectrum (Thin Film, NaCl) of compound 203	549
Figure A9.30	^{13}C NMR (125 MHz, CDCl_3) of compound 203	549
Figure A9.31	^1H NMR (500 MHz, CDCl_3) of compound 205	550
Figure A9.32	Infrared spectrum (Thin Film, NaCl) of compound 205	551
Figure A9.33	^{13}C NMR (125 MHz, CDCl_3) of compound 205	551
Figure A9.34	^1H NMR (500 MHz, CDCl_3) of compound 206	552
Figure A9.35	Infrared spectrum (Thin Film, NaCl) of compound 206	553
Figure A9.36	^{13}C NMR (125 MHz, CDCl_3) of compound 206	553

Figure A9.37	^1H NMR (500 MHz, CDCl_3) of compound 207	554
Figure A9.38	Infrared spectrum (Thin Film, NaCl) of compound 207	555
Figure A9.39	^{13}C NMR (125 MHz, CDCl_3) of compound 207	555
Figure A9.40	^1H NMR (500 MHz, CDCl_3) of compound 208	556
Figure A9.41	Infrared spectrum (Thin Film, NaCl) of compound 208	557
Figure A9.42	^{13}C NMR (125 MHz, CDCl_3) of compound 208	557
Figure A9.43	^1H NMR (500 MHz, CDCl_3) of compound 209	558
Figure A9.44	Infrared spectrum (Thin Film, NaCl) of compound 209	559
Figure A9.45	^{13}C NMR (125 MHz, CDCl_3) of compound 209	559
Figure A9.46	^{19}F vs ^{13}C HSQC (376 MHz, CDCl_3) of compound 209	560
Figure A9.47	^1H NMR (500 MHz, CDCl_3) of compound 210	561
Figure A9.48	Infrared spectrum (Thin Film, NaCl) of compound 210	562
Figure A9.49	^{13}C NMR (125 MHz, CDCl_3) of compound 210	562
Figure A9.50	^1H NMR (500 MHz, CDCl_3) of compound 211	563
Figure A9.51	Infrared spectrum (Thin Film, NaCl) of compound 211	564
Figure A9.52	^{13}C NMR (125 MHz, CDCl_3) of compound 211	564
Figure A9.53	^1H NMR (500 MHz, CDCl_3) of compound 212	565
Figure A9.54	Infrared spectrum (Thin Film, NaCl) of compound 212	566
Figure A9.55	^{13}C NMR (125 MHz, CDCl_3) of compound 212	566
Figure A9.56	^1H NMR (500 MHz, CDCl_3) of compound 213	567
Figure A9.57	Infrared spectrum (Thin Film, NaCl) of compound 213	568
Figure A9.58	^{13}C NMR (125 MHz, CDCl_3) of compound 213	568
Figure A9.59	^1H NMR (500 MHz, CDCl_3) of compound 214	569
Figure A9.60	Infrared spectrum (Thin Film, NaCl) of compound 214	570
Figure A9.61	^{13}C NMR (125 MHz, CDCl_3) of compound 214	570
Figure A9.62	^1H NMR (500 MHz, CDCl_3) of compound 215	571
Figure A9.63	Infrared spectrum (Thin Film, NaCl) of compound 215	572
Figure A9.64	^{13}C NMR (125 MHz, CDCl_3) of compound 215	572
Figure A9.65	^1H NMR (500 MHz, CDCl_3) of compound 216	573
Figure A9.66	Infrared spectrum (Thin Film, NaCl) of compound 216	574
Figure A9.67	^{13}C NMR (125 MHz, CDCl_3) of compound 216	574
Figure A9.68	^1H NMR (500 MHz, CDCl_3) of compound 217	575
Figure A9.69	Infrared spectrum (Thin Film, NaCl) of compound 217	576
Figure A9.70	^{13}C NMR (125 MHz, CDCl_3) of compound 217	576

APPENDIX 10

X-Ray Crystallography Reports Relevant to Appendix 8

Figure A10.1	X-ray crystal structure of undesired tricycle 203	578
---------------------	----------------------------------------------------------------	-----

APPENDIX 11*Asymmetric Synthesis of All-Carbon Quaternary Spirocycles via an Enantioselective Allylic Alkylation Strategy*

Figure A11.1	Strategy and inspiration for the catalytic enantioselective synthesis of all-carbon quaternary spirocycles.....	591
---------------------	-----------------------------------------------------------------------------------------------------------------	-----

APPENDIX 12*Spectra Relevant to Appendix 11*

Figure A12.1	¹ H NMR (400 MHz, CDCl ₃) of compound 218a	608
Figure A12.2	Infrared spectrum (Thin Film, NaCl) of compound 218a	609
Figure A12.3	¹³ C NMR (101 MHz, CDCl ₃) of compound 218a	609
Figure A12.4	¹ H NMR (400 MHz, CDCl ₃) of compound 218b	610
Figure A12.5	Infrared spectrum (Thin Film, NaCl) of compound 218b	611
Figure A12.6	¹³ C NMR (101 MHz, CDCl ₃) of compound 218b	611
Figure A12.7	¹ H NMR (400 MHz, CDCl ₃) of compound 218c	612
Figure A12.8	Infrared spectrum (Thin Film, NaCl) of compound 218c	613
Figure A12.9	¹³ C NMR (101 MHz, CDCl ₃) of compound 218c	613
Figure A12.10	¹ H NMR (400 MHz, CDCl ₃) of compound 219a	614
Figure A12.11	Infrared spectrum (Thin Film, NaCl) of compound 219a	615
Figure A12.12	¹³ C NMR (101 MHz, CDCl ₃) of compound 219a	615
Figure A12.13	¹ H NMR (400 MHz, CDCl ₃) of compound 219b	616
Figure A12.14	Infrared spectrum (Thin Film, NaCl) of compound 219b	617
Figure A12.15	¹³ C NMR (101 MHz, CDCl ₃) of compound 219b	617
Figure A12.16	¹ H NMR (400 MHz, CDCl ₃) of compound 219c	618
Figure A12.17	Infrared spectrum (Thin Film, NaCl) of compound 219c	619
Figure A12.18	¹³ C NMR (101 MHz, CDCl ₃) of compound 219c	619
Figure A12.19	¹ H NMR (400 MHz, CDCl ₃) of compound 220a	620
Figure A12.20	Infrared spectrum (Thin Film, NaCl) of compound 220a	621
Figure A12.21	¹³ C NMR (101 MHz, CDCl ₃) of compound 220a	621
Figure A12.22	¹ H NMR (400 MHz, CDCl ₃) of compound 220b	622
Figure A12.23	Infrared spectrum (Thin Film, NaCl) of compound 220b	623
Figure A12.24	¹³ C NMR (101 MHz, CDCl ₃) of compound 220b	623
Figure A12.25	¹ H NMR (400 MHz, CDCl ₃) of compound 220c	624
Figure A12.26	Infrared spectrum (Thin Film, NaCl) of compound 220c	625
Figure A12.27	¹³ C NMR (101 MHz, CDCl ₃) of compound 220c	625

APPENDIX 14*Spectra Relevant to Appendix 13*

Figure A14.1	¹ H NMR (400 MHz, CDCl ₃) of compound 226	688
Figure A14.2	¹ H NMR (400 MHz, CDCl ₃) of compound 233	689
Figure A14.3	¹³ C NMR (101 MHz, CDCl ₃) of compound 233	690
Figure A14.4	¹ H NMR (400 MHz, CDCl ₃) of compound 234	691
Figure A14.5	¹³ C NMR (101 MHz, CDCl ₃) of compound 234	692
Figure A14.6	¹ H NMR (400 MHz, CDCl ₃) of compound 235	693
Figure A14.7	¹³ C NMR (101 MHz, CDCl ₃) of compound 235	694
Figure A14.8	¹ H NMR (400 MHz, CDCl ₃) of compound 238	695
Figure A14.9	¹³ C NMR (101 MHz, CDCl ₃) of compound 238	696
Figure A14.10	¹ H NMR (400 MHz, CDCl ₃) of compound 240 (LG = Cl)	697
Figure A14.11	¹³ C NMR (101 MHz, CDCl ₃) of compound 240 (LG = Cl)	698
Figure A14.12	¹ H NMR (400 MHz, CDCl ₃) of compound 241	699
Figure A14.13	¹³ C NMR (101 MHz, CDCl ₃) of compound 241	700
Figure A14.14	¹ H NMR (400 MHz, CDCl ₃) of compound 243	701
Figure A14.15	¹³ C NMR (101 MHz, CDCl ₃) of compound 243	702
Figure A14.16	¹ H NMR (400 MHz, CDCl ₃) of compound 244	703
Figure A14.17	¹³ C NMR (101 MHz, CDCl ₃) of compound 244	704
Figure A14.18	¹ H NMR (400 MHz, CDCl ₃) of compound 245	705
Figure A14.19	¹³ C NMR (101 MHz, CDCl ₃) of compound 245	706
Figure A14.20	¹ H NMR (400 MHz, CDCl ₃) of compound 247	707
Figure A14.21	¹³ C NMR (101 MHz, CDCl ₃) of compound 247	708
Figure A14.22	¹ H NMR (400 MHz, CDCl ₃) of compound 248	709
Figure A14.23	¹³ C NMR (101 MHz, CDCl ₃) of compound 248	710
Figure A14.24	¹ H NMR (400 MHz, CDCl ₃) of compound 249	711
Figure A14.25	¹³ C NMR (101 MHz, CDCl ₃) of compound 249	712
Figure A14.26	¹ H NMR (400 MHz, CDCl ₃) of compound 256	713
Figure A14.27	¹ H NMR (400 MHz, CDCl ₃) of compound 257	714
Figure A14.28	¹³ C NMR (101 MHz, CDCl ₃) of compound 257	715
Figure A14.29	¹ H NMR (400 MHz, CDCl ₃) of compound 258	716
Figure A14.30	¹³ C NMR (101 MHz, CDCl ₃) of compound 258	717
Figure A14.31	¹ H NMR (400 MHz, CDCl ₃) of compound 259	718
Figure A14.32	¹ H NMR (400 MHz, CDCl ₃) of compound 260	719
Figure A14.33	¹ H NMR (400 MHz, CDCl ₃) of compound 261	720
Figure A14.34	¹³ C NMR (101 MHz, CDCl ₃) of compound 261	721
Figure A14.35	¹ H NMR (400 MHz, CDCl ₃) of compound 262	722
Figure A14.36	¹³ C NMR (101 MHz, CDCl ₃) of compound 262	723

Figure A14.37	^1H NMR (400 MHz, CDCl_3) of compound 263	724
Figure A14.38	^{13}C NMR (101 MHz, CDCl_3) of compound 263	725
Figure A14.39	^1H NMR (400 MHz, CDCl_3) of compound 274	726
Figure A14.40	^1H NMR (400 MHz, CDCl_3) of compound 275	727
Figure A14.41	^{13}C NMR (101 MHz, CDCl_3) of compound 275	728
Figure A14.42	^1H NMR (400 MHz, CDCl_3) of compound 276	729
Figure A14.43	^{13}C NMR (101 MHz, CDCl_3) of compound 276	730
Figure A14.44	^1H NMR (400 MHz, CDCl_3) of compound 277	731
Figure A14.45	^1H NMR (400 MHz, CDCl_3) of compound 280	732
Figure A14.46	^{13}C NMR (101 MHz, CDCl_3) of compound 280	733
Figure A14.47	^1H NMR (400 MHz, CDCl_3) of compound 281	734
Figure A14.48	^{13}C NMR (101 MHz, CDCl_3) of compound 281	735
Figure A14.49	^1H NMR (400 MHz, CDCl_3) of compound 282	736
Figure A14.50	^{13}C NMR (101 MHz, CDCl_3) of compound 282	737
Figure A14.51	^1H NMR (400 MHz, CDCl_3) of compound 291	738
Figure A14.52	^{13}C NMR (101 MHz, CDCl_3) of compound 291	739
Figure A14.53	^1H NMR (400 MHz, CDCl_3) of compound 295	740
Figure A14.54	^{13}C NMR (101 MHz, CDCl_3) of compound 295	741
Figure A14.55	^1H NMR (400 MHz, CDCl_3) of compound 296	742

LIST OF SCHEMES

PROLOGUE*Iridium-Catalyzed Allylic Alkylation*

Scheme P.1	Asymmetric transition metal-catalyzed allylic alkylation.....	2
Scheme P.2	Asymmetric iridium-catalyzed allylic alkylation	2

CHAPTER 1*Stereoselective Iridium-Catalyzed Allylic Alkylation Reactions with Crotyl Chloride*

Scheme 1.1	First report of diastereo- and enantioselective iridium-catalyzed allylic alkylation	8
Scheme 1.2	Allylic alkylation of acyclic β -ketoesters by Stoltz.....	9
Scheme 1.3	Allylic alkylation with acyclic α -alkoxy ketones by Hartwig.....	10
Scheme 1.4	Counterion-assisted iridium-catalyzed allylic alkylation of azlactones by Hartwig	11
Scheme 1.5	Cation control of diastereoselectivity in iridium-catalyzed allylic alkylation of a) 5H-oxazol-4-ones 20 and b) 5H-thiazol-4-ones 24 by Hartwig.....	12
Scheme 1.6	Allylic alkylation of a) bicyclic β -ketoesters 27 and b) monocyclic β -ketoesters 30 by Stoltz	13
Scheme 1.7	Allylic alkylation of extended enolates by Stoltz	14
Scheme 1.8	Allylic alkylation of non-stabilized enolates by Hartwig	15
Scheme 1.9	Dual catalyst-promoted allylic alkylation of aldehydes by Carreira	15
Scheme 1.10	Proline-derived dual catalysis by Carreira	16
Scheme 1.11	Diastereoablative allylic alkylation of 46 by Stoltz.....	17
Scheme 1.12	Bimetallic dual catalytic allylic alkylation by Zhang	18

CHAPTER 2*Enantioselective Iridium-Catalyzed Allylic Alkylation Reactions of Masked Acyl Cyanide Equivalents*

Scheme 2.1	Preparatory scale reaction	146
-------------------	----------------------------------	-----

CHAPTER 5*Stereoselective Iridium-Catalyzed Allylic Alkylation in the Stoltz Laboratory: A Summary*

Scheme 5.1	Enantio- and diastereoselective iridium-catalyzed allylic alkylation of cyclic nucleophiles 128	448
-------------------	--------------------------------------------------------------------------------------------------------------	-----

Scheme 5.2	Iridium-catalyzed allylic alkylation/Cope rearrangement sequence.....	448
Scheme 5.3	Enantio- and diastereoselective iridium-catalyzed allylic alkylation of acyclic nucleophiles 134	449
Scheme 5.4	Enantio- and diastereoselective iridium-catalyzed allylic alkylation with crotyl chloride (57).....	453
Scheme 5.5	First report of MAC reagent 67c in an asymmetric transition-metal catalyzed reaction	457
Scheme 5.6	Enantioselective synthesis of acyclic α -quaternary carboxylic acids 153	461
Scheme 5.7	Synthesis of vicinal all-carbon quaternary centers 157 via enantioselective iridium-catalyzed allylic alkylation.....	463

APPENDIX 8

A Catalytic, Enantioselective Formal Synthesis of (+)-Dichroanone and (+)-Taiwaniaquinone H

Scheme A8.1	Stoltz group retrosynthesis of (+)-dichroanone (159).....	472
Scheme A8.2	Asymmetric transition metal-catalyzed conjugate addition	475
Scheme A8.3	Initial Stoltz group asymmetric palladium-catalyzed conjugate addition with (<i>S</i>)- <i>t</i> -BuPyOx (L14)	476
Scheme A8.4	Necessity of water in developed asymmetric palladium-catalyzed conjugate addition.....	480
Scheme A8.5	Synthesis of acetyl conjugate addition product 169b	491
Scheme A8.6	Unexpected cyclization of phenolic intermediate	492
Scheme A8.7	Synthesis of <i>para</i> -bromo conjugate addition product 169d	495
Scheme A8.8	Isopropenyl cross-coupling.....	496
Scheme A8.9	Synthesis of key intermediate 169f	497

APPENDIX 13

Progress Toward the Synthesis of (+)-Isopalhinine A

Scheme A13.1	Initial retrosynthetic analysis of (+)-isopalhinine A (221) via iridium-catalyzed allylic alkylation of endocyclic 1,3-dicarbonyl nucleophile 225	628
Scheme A13.2	Synthesis of alkyl-substituted electrophile 226	628
Scheme A13.3	Efforts to synthesize endocyclic 1,3-dicarbonyl nucleophiles.....	629
Scheme A13.4	Revised retrosynthetic analysis of (+)-isopalhinine A (221) via iridium-catalyzed allylic alkylation of lactone nucleophile 238	632
Scheme A13.5	Synthesis of lactone nucleophile 238	632
Scheme A13.6	Attempts to advance bicycle 241 to key spirocyclic intermediate 223	635

Scheme A13.7	Retrosynthetic analysis of (+)-isopalhinine A (221) via palladium-catalyzed allylic alkylation of masked stabilized lactam enolate 253	637
Scheme A13.8	Synthesis of spirocyclic intermediate 263 via palladium-catalyzed allylic alkylation	639
Scheme A13.9	Attempted alkylations of spirocyclic enone 263	640
Scheme A13.10	Retrosynthetic analysis of (+)-isopalhinine A (221) via palladium-catalyzed allylic alkylation of piperidone 272	641
Scheme A13.11	Attempts to advance benzyl-protected piperidone 273	642
Scheme A13.12	Attempts to advance Boc-protected piperidone 279	643
Scheme A13.13	Retrosynthetic analysis of (+)-isopalhinine A (221) via diastereoselective alkylation/allylation sequence	644
Scheme A13.14	Attempts at diastereoselective functionalization.....	644
Scheme A13.15	Requisite propyl chain as a nitrogen protecting group	645
Scheme A13.16	Non-strong base route to RCM precursor 298	646
Scheme A13.17	Attempts to advance β -ketolactam 296	646
Scheme A13.18	Proposed route to (+)-isopalhinine A (221) from alkylated spirocycle 223	648
Scheme A13.19	Alternative acyl anion equivalents	649

LIST OF TABLES

CHAPTER 1*Stereoselective Iridium-Catalyzed Allylic Alkylation Reactions with Crotyl Chloride*

Table 1.1	Optimization of reaction parameters	20
Table 1.2	Substrate scope exploration	23
Table 1.3	Substrate scope limitations	25
Table 1.4	Additional optimization of reaction parameters	36
Table 1.5	Determination of enantiomeric excess	57

APPENDIX 2*X-Ray Crystallography Reports Relevant to Chapter 1*

Table A2.1	Crystal data and structure refinement for allylic alkylation product 58e	117
Table A2.2	Atomic coordinates ($\times 10^4$) and equivalent isotropic displacement parameters ($\text{\AA}^2 \times 10^3$) for 58e . $U(\text{eq})$ is defined as one third of the trace of the orthogonalized U_{ij} tensor	118
Table A2.3	Bond lengths [\AA] and angles [$^\circ$] for 58e	119
Table A2.4	Anisotropic displacement parameters ($\text{\AA}^2 \times 10^3$) for 58e . The anisotropic displacement factor exponent takes the form: $-2\pi^2 [h^2 a^{*2} U^{11} + \dots + 2 h k a^* b^* U^{12}]$	123
Table A2.5	Hydrogen coordinates ($\times 10^4$) and isotropic displacement parameters ($\text{\AA}^2 \times 10^3$) for 58e	124
Table A2.6	Crystal data and structure refinement for triol 63	125
Table A2.7	Atomic coordinates ($\times 10^4$) and equivalent isotropic displacement parameters ($\text{\AA}^2 \times 10^3$) for 63 . $U(\text{eq})$ is defined as one third of the trace of the orthogonalized U_{ij} tensor	126
Table A2.8	Bond lengths [\AA] and angles [$^\circ$] for 63	128
Table A2.9	Anisotropic displacement parameters ($\text{\AA}^2 \times 10^3$) for 63 . The anisotropic displacement factor exponent takes the form: $-2\pi^2 [h^2 a^{*2} U^{11} + \dots + 2 h k a^* b^* U^{12}]$	130
Table A2.10	Hydrogen coordinates ($\times 10^4$) and isotropic displacement parameters ($\text{\AA}^2 \times 10^3$) for 63	131
Table A2.11	Crystal data and structure refinement for diol 64	133

Table A2.12	Atomic coordinates ($\times 10^4$) and equivalent isotropic displacement parameters ($\text{\AA}^2 \times 10^3$) for 64 . $U(\text{eq})$ is defined as one third of the trace of the orthogonalized U_{ij} tensor	135
Table A2.13	Bond lengths [\AA] and angles [$^\circ$] for 64	135
Table A2.14	Anisotropic displacement parameters ($\text{\AA}^2 \times 10^3$) for 64 . The anisotropic displacement factor exponent takes the form: $-2\pi^2 [h^2 a^{*2} U^{11} + \dots + 2 h k a^* b^* U^{12}]$	138
Table A2.15	Hydrogen coordinates ($\times 10^4$) and isotropic displacement parameters ($\text{\AA}^2 \times 10^3$) for 64	139

CHAPTER 2

Enantioselective Iridium-Catalyzed Allylic Alkylation Reactions of Masked Acyl Cyanide Equivalents

Table 2.1	Optimization of reaction parameters	143
Table 2.2	Electrophile substrate scope	144
Table 2.3	Electrophile substrate scope limitations	145
Table 2.4	Determination of enantiomeric excess	162

CHAPTER 3

Enantioselective Synthesis of Acyclic α -Quaternary Carboxylic Acid Derivatives via Iridium-Catalyzed Allylic Alkylation

Table 3.1	Optimization of reaction parameters	204
Table 3.2	Electrophile isomers	205
Table 3.3	Aryl substituent substrate scope	207
Table 3.4	Non-aryl substituent substrate scope	208
Table 3.5	Substrate scope limitations	209
Table 3.6	Determination of enantiomeric excess	242

APPENDIX 5

X-Ray Crystallography Reports Relevant to Chapter 3

Table A5.1	Crystal data and structure refinement for carboxylic acid 77h	319
Table A5.2	Atomic coordinates ($\times 10^4$) and equivalent isotropic displacement parameters ($\text{\AA}^2 \times 10^3$) for 77h . $U(\text{eq})$ is defined as one third of the trace of the orthogonalized U_{ij} tensor	321
Table A5.3	Bond lengths [\AA] and angles [$^\circ$] for 77h	321

Table A5.4	Anisotropic displacement parameters ($\text{\AA}^2 \times 10^3$) for 77h . The anisotropic displacement factor exponent takes the form: $-2\pi^2 [h^2 a^{*2} U^{11} + \dots + 2 h k a^* b^* U^{12}]$ 323
Table A5.5	Hydrogen coordinates ($\times 10^4$) and isotropic displacement parameters ($\text{\AA}^2 \times 10^3$) for 77h 323

CHAPTER 4

Enantioselective Synthesis of Vicinal All-Carbon Quaternary Centers via Iridium-Catalyzed Allylic Alkylation

Table 4.1	Optimization of reaction parameters 328
Table 4.2	Nucleophile substrate scope 330
Table 4.3	Electrophile substrate scope 331
Table 4.4	Substrate scope limitations 333
Table 4.5	Determination of enantiomeric excess 361

APPENDIX 7

X-Ray Crystallography Reports Relevant to Chapter 4

Table A7.1	Crystal data and structure refinement for bis-nitrile 97c 432
Table A7.2	Atomic coordinates ($\times 10^4$) and equivalent isotropic displacement parameters ($\text{\AA}^2 \times 10^3$) for 97c . $U(\text{eq})$ is defined as one third of the trace of the orthogonalized U_{ij} tensor 433
Table A7.3	Bond lengths [\AA] and angles [$^\circ$] for 97c 434
Table A7.4	Anisotropic displacement parameters ($\text{\AA}^2 \times 10^3$) for 97c . The anisotropic displacement factor exponent takes the form: $-2\pi^2 [h^2 a^{*2} U^{11} + \dots + 2 h k a^* b^* U^{12}]$ 437
Table A7.5	Hydrogen coordinates ($\times 10^4$) and isotropic displacement parameters ($\text{\AA}^2 \times 10^3$) for 97c 438
Table A7.6	Torsion angles [$^\circ$] for 97c 439

CHAPTER 5

Stereoselective Iridium-Catalyzed Allylic Alkylation in the Stoltz Laboratory: A Summary

Table 5.1	Development of conditions for the iridium-catalyzed allylic alkylation reaction of cyclic nucleophiles forming tertiary and all-carbon quaternary stereocenters 446
------------------	---------------------------------------------------------------------------------------------------------------------------------------------------------------------------

Table 5.2	Optimization of iridium-catalyzed allylic alkylation reaction of alkyl-substituted electrophile 53	451
Table 5.3	Optimization of the enantioselective synthesis of acyclic α -quaternary carboxylic acid derivatives 73	459

APPENDIX 8

A Catalytic, Enantioselective Formal Synthesis of (+)-Dichroanone and (+)-Taiwaniaquinone H

Table A8.1	Scope of arylboronic acid and enone conjugate acceptors	478
Table A8.2	Effect of additives on reaction rate, yield, and enantioselectivity	481
Table A8.3	Expanded substrate scope with improved reaction conditions	483
Table A8.4	Asymmetric conjugate addition of arylboronic acids to heterocyclic conjugate acceptors	488
Table A8.5	Identification of a suitable conjugate addition system	494
Table A8.6	Determination of enantiomeric excess	520
Table A8.7	Data for Hammett analysis of enantioselectivity for select boronic acids	521

APPENDIX 10

X-Ray Crystallography Reports Relevant to Appendix 8

Table A10.1	Crystal data and structure refinement for undesired tricycle 203	578
Table A10.2	Atomic coordinates ($\times 10^4$) and equivalent isotropic displacement parameters ($\text{\AA}^2 \times 10^3$) for 203 . $U(\text{eq})$ is defined as one third of the trace of the orthogonalized U_{ij} tensor	580
Table A10.3	Bond lengths [\AA] and angles [$^\circ$] for 203	581
Table A10.4	Anisotropic displacement parameters ($\text{\AA}^2 \times 10^3$) for 203 . The anisotropic displacement factor exponent takes the form: $-2\pi^2 [h^2 a^{*2} U^{11} + \dots + 2 h k a^* b^* U^{12}]$	584
Table A10.5	Hydrogen coordinates ($\times 10^4$) and isotropic displacement parameters ($\text{\AA}^2 \times 10^3$) for 203	585
Table A10.6	Torsion angles [$^\circ$] for 203	586
Table A10.7	Hydrogen bonds for 203 [\AA and $^\circ$]	588

APPENDIX 11*Asymmetric Synthesis of All-Carbon Quaternary Spirocycles via an Enantioselective Allylic Alkylation Strategy*

Table A11.1	Enantioselective palladium-catalyzed allylic alkylations with substrates bearing a masked methyl vinyl ketone	592
Table A11.2	One-pot synthesis of spirocyclic compounds.....	593
Table A11.3	Determination of enantiomeric excess	604

APPENDIX 13*Progress Toward the Synthesis of (+)-Isopalhinine A*

Table A13.1	Optimization of the iridium-catalyzed allylic alkylation of model endocyclic 1,3-dicarbonyl nucleophile 233	631
Table A13.2	Optimization of the iridium-catalyzed allylic alkylation of lactone 238	634
Table A13.3	Optimization of protecting groups for the palladium-catalyzed allylic alkylation reaction	638
Table A13.4	Determination of enantiomeric excess	681

APPENDIX 15*Notebook Cross-Reference for New Compounds*

Table A15.1	Notebook cross-reference for compounds in Chapter 1	768
Table A15.2	Notebook cross-reference for compounds in Chapter 2	771
Table A15.3	Notebook cross-reference for compounds in Chapter 3	773
Table A15.4	Notebook cross-reference for compounds in Chapter 4	777
Table A15.5	Notebook cross-reference for compounds in Appendix 8	780
Table A15.6	Notebook cross-reference for compounds in Appendix 11	783
Table A15.7	Notebook cross-reference for compounds in Appendix 13	784

LIST OF ABBREVIATIONS

$[\alpha]_D$	specific rotation at wavelength of sodium D line
$^{\circ}\text{C}$	degrees Celsius
Å	Ångstrom
Ac	acetyl
AcOH	acetic acid
APCI	atmospheric pressure chemical ionization
app	apparent
aq	aqueous
Ar	aryl
atm	atmosphere
Bn	benzyl
Boc	<i>tert</i> -butyloxycarbonyl
bp	boiling point
br	broad
Bu	butyl
Bz	benzoyl
c	concentration for specific rotation measurements (g/100 mL)
ca.	about (Latin circa)
calc'd	calculated
cat	catalytic
CBS	Corey–Bakshi–Shibata catalyst
CDI	1,1'-carbonyldiimidazole
cm^{-1}	wavenumber(s)
cod	1,5-cyclooctadiene
Cp	cyclopentadienyl
CSA	camphorsulfonic acid

Cy	cyclohexyl
d	doublet
D	deuterium
DABCO	1,4-diazabicyclo[2.2.2]octane
dba	dibenzylideneacetone
DBDMH	1,3-dibromo-5,5-dimethylhydantoin
DBU	1,8-diazabicyclo[5.4.0]undec-7-ene
DCAA	decarboxylative allylic alkylation
DCE	1,2-dichloroethane
DDQ	2,3-dichloro-5,6-dicyano- <i>p</i> -benzoquinone
DIBAL	diisobutylaluminum hydride
DIPEA	<i>N,N</i> -diisopropylethylamine
DMA	<i>N,N</i> -dimethylacetamide
DMAP	4-dimethylaminopyridine
dmdba	bis(3,5-dimethoxybenzylidene)acetone
DMDO	dimethyldioxirane
DME	1,2-dimethoxyethane
DMF	<i>N,N</i> -dimethylformamide
DMP	Dess–Martin periodinane
DMS	dimethyl sulfide
DMSO	dimethyl sulfoxide
dr	diastereomeric ratio
e.g.	for example (Latin <i>exempli gratia</i>)
EDC	<i>N</i> -(3-dimethylaminopropyl)- <i>N'</i> -ethylcarbodiimide
EDCI	1-ethyl-3-(3-dimethylaminopropyl)carbodiimide
<i>ee</i>	enantiomeric excess
EI+	electron impact
equiv	equivalent(s)
ESI	electrospray ionization

Et	ethyl
EtOAc	ethyl acetate
EWG	electron withdrawing group
FAB	fast atom bombardment
g	gram(s)
GC	gas chromatography
gCOSY	gradient-selected correlation spectroscopy
h	hour(s)
HG-II	Hoveyda-Grubbs catalyst 2 nd generation
HMBC	heteronuclear multiple bond correlation
HMDS	1,1,1,3,3,3-hexamethyldisilazane
HMPA	hexamethylphosphoramide
HPLC	high-performance liquid chromatography
HRMS	high-resolution mass spectroscopy
HSQC	heteronuclear single quantum correlation
Hz	hertz
$h\nu$	light
<i>i</i> -Pr	isopropyl
i.e.	that is (Latin id est)
IBX	2-iodoxybenzoic acid
IPA	isopropanol, 2-propanol
Ipc	diisopinocampheyl
IR	infrared (spectroscopy)
<i>J</i>	coupling constant
K	Kelvin(s) (absolute temperature)
kcal	kilocalorie
KHMDS	potassium hexamethyldisilazide
L	liter; ligand
L*	chiral ligand

LDA	lithium diisopropylamide
LG	leaving group
lit.	literature value
m	multiplet; milli
<i>m</i>	meta
M	metal; molar; molecular ion
<i>m</i> -CPBA	<i>meta</i> -chloroperoxybenzoic acid
<i>m/z</i>	mass to charge ratio
MAC	masked acyl cyanide
Me	methyl
mg	milligram(s)
MHz	megahertz
min	minute(s)
MM	mixed method
mol	mole(s)
MOM	methoxymethyl acetal
mp	melting point
Ms	methanesulfonyl (mesyl)
MS	molecular sieves
n	nano
N	normal
<i>n</i> -Bu	butyl
nbd	norbornadiene
NBS	<i>N</i> -bromosuccinimide
Nf	perfluorobutanesulfonyl fluoride
NMO	<i>N</i> -methylmorpholine <i>N</i> -oxide
NMR	nuclear magnetic resonance
Ns	2-nitrobenzenesulfonyl
Nu	nucleophile

<i>o</i>	ortho
<i>p</i>	para
Pd/C	palladium on carbon
Ph	phenyl
pH	hydrogen ion concentration in aqueous solution
PHOX	phosphinooxazoline ligand
Pin	2,3-dimethylbutane-2,3-diol (pinacol)
Piv	trimethylacetyl, pivaloyl
<i>pK_a</i>	<i>pK</i> for association of an acid
pMBz	4-methoxy-benzoyl
pmdba	bis(4-methoxybenzylidene)acetone
ppm	parts per million
PPTS	pyridinium <i>p</i> -toluenesulfonate
Pr	propyl
Proton sponge	1,8-bis(dimethylamino)naphthalene
Py	pyridine
q	quartet
R	generic for any atom or functional group
RCM	ring-closing metathesis
Red-Al	sodium bis(2-methoxyethoxy)aluminium hydride
Ref.	reference
<i>R_f</i>	retention factor
s	singlet or strong or selectivity factor
sat.	saturated
SFC	supercritical fluid chromatography
t	triplet
<i>t</i> -Bu	<i>tert</i> -butyl
TBAF	tetrabutylammonium fluoride
TBAI	tetrabutylammonium iodide

TBAT	tetrabutylammonium difluorotriphenylsilicate
TBD	1,3,4-triazabicyclo[4.4.0]dec-5-ene
TBDPS	<i>tert</i> -butyldiphenylsilyl
TBHP	<i>tert</i> -butyl hydroperoxide
TBME	<i>tert</i> -butyl methyl ether
TBS	<i>tert</i> -butyldimethylsilyl
TES	triethylsilyl
Tf	trifluoromethanesulfonyl (triflyl)
TFA	trifluoroacetic acid
TFAA	trifluoroacetic anhydride
TFE	2,2,2-trifluoroethanol
THF	tetrahydrofuran
TIPS	triisopropylsilyl
TLC	thin-layer chromatography
TMEDA	<i>N,N,N',N'</i> -tetramethylethylenediamine
TMS	trimethylsilyl
TOF	time-of-flight
Tol	tolyl
t_R	retention time
Ts	<i>p</i> -toluenesulfonyl (tosyl)
UV	ultraviolet
v/v	volume to volume
w	weak
w/v	weight to volume
X	anionic ligand or halide
λ	wavelength
μ	micro

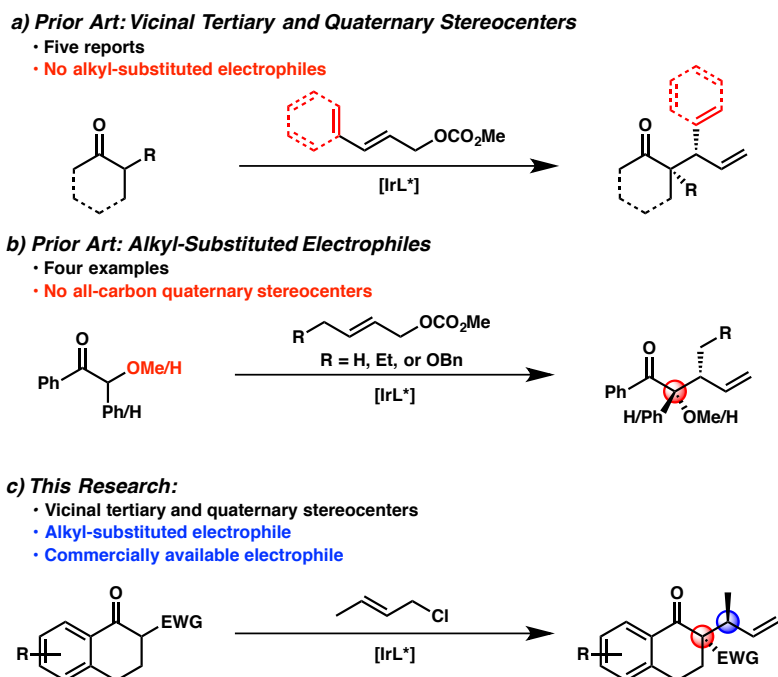
CHAPTER 1

Stereoselective Iridium-Catalyzed Allylic Alkylation Reactions with Crotyl Chloride[†]

1.1 INTRODUCTION

The synthesis of singular all-carbon quaternary stereocenters has been a longstanding challenge in the synthetic community.¹ Significant progress in this area over the past few decades has recently shifted the forefront of investigation toward the more difficult task of constructing vicinal stereodyads bearing at least one quaternary stereocenter. This nascent field is beset with difficulties not only arising from the increased sterics in the bond-forming event, but also the additional requirement of diastereocontrol. Among the available methodologies tailored for this challenge,^{2,3} iridium-catalyzed allylic alkylations represent some of the most selective strategies, yet remain underdeveloped.⁴

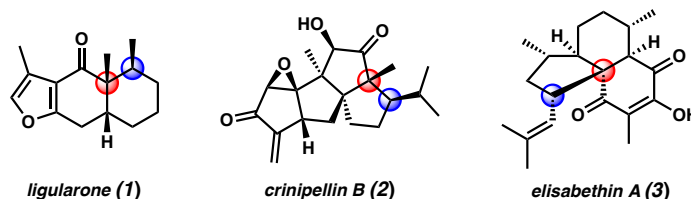
[†] This work was performed in collaboration with Dr. J. Caleb Hethcox. Portions of this chapter have been reproduced with permission from Hethcox, J. C.;[‡] Shockley, S. E.;[‡] Stoltz, B. M. *Angew. Chem. Int. Ed.* **2016**, 55, 16092–16095 © 2016 Wiley-VCH and Hethcox, J. C.;[‡] Shockley, S. E.;[‡] Stoltz, B. M. *ACS Catal.* **2016**, 6, 6207–6213 © 2016 American Chemical Society.

Figure 1.1 Enantio-, diastereo-, and regioselective iridium-catalyzed allylic alkylation reactions

The first diastereo-, enantio-, and regioselective iridium-catalyzed allylic alkylation was disclosed by Takemoto in 2003 and remained the sole report of such a transformation for a decade.⁵ Of the eleven published accounts of enantio- and diastereoselective iridium-catalyzed allylic alkylation since,^{6,7,8} only five reports provide access to vicinal tertiary and *all-carbon quaternary* stereocenters.⁶ However, none of these protocols tolerate the use of *alkyl*-substituted electrophiles (Figure 1.1a). Conversely, the four singular examples employing alkyl-substituted electrophiles in two published papers fail to enable construction of all-carbon quaternary stereocenters (Figure 1.1b).⁷ While these protocols provide access to valuable chiral synthons, a wide variety of synthetic targets require the installation of alkyl-substituted stereodyads between neighboring tertiary and quaternary carbon atoms (Figure 1.2). To the best of our knowledge, no transition metal-catalyzed process allows for the preparation of this

desired motif. Herein, we describe the first method for the iridium-catalyzed synthesis of alkyl-substituted vicinal tertiary and all-carbon quaternary stereocenters via allylic alkylation of prochiral enolates (Figure 1.1c).

Figure 1.2 Select natural products bearing alkyl-substituted vicinal tertiary and quaternary stereocenters.



1.2 BACKGROUND TO DIASTEREO-, ENANTIO-, AND REGIOSELECTIVE IRIIDIUM-CATALYZED ALLYLIC ALKYLATION WITH PROCHIRAL ENOLATES

A more detailed description of the twelve diastereo-, enantio-, and regioselective iridium-catalyzed allylic alkylation methods^{5–8} previously disclosed at the time we began this investigation is discussed *vide infra*.

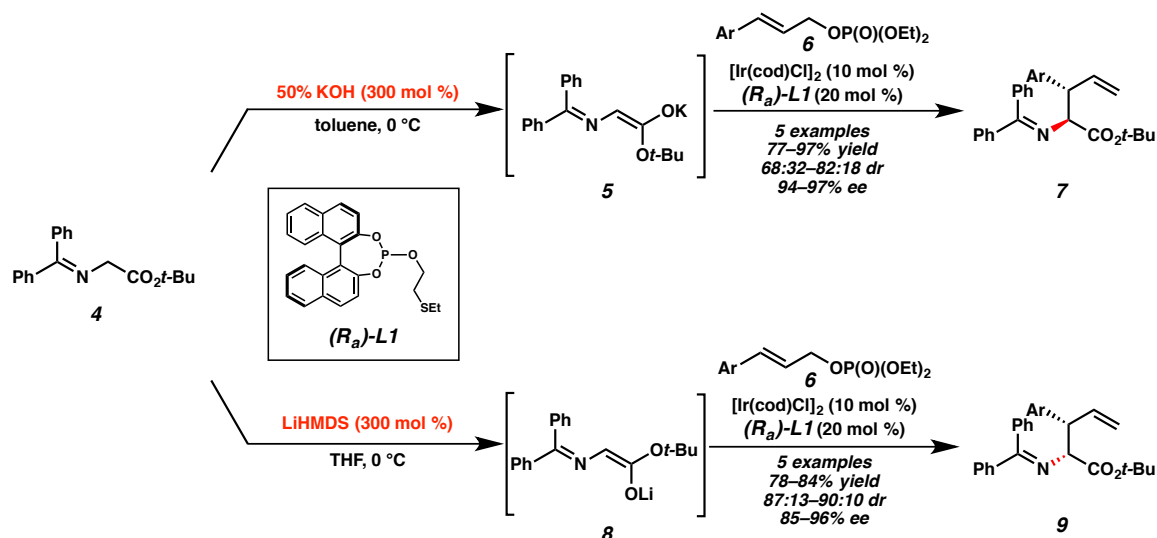
1.2.1 IRIIDIUM CATALYST-CONTROLLED PROCESSES

1.2.1.1 Acyclic Nucleophiles

Takemoto reported the first diastereo-, enantio-, and regioselective iridium-catalyzed allylic alkylation reaction, wherein an iridium complex of bidentate chiral phosphite **L1** and $[\text{Ir}(\text{cod})\text{Cl}]_2$ catalyzes the reaction of glycinate nucleophile **4** and aryl-substituted allylic phosphates **6** (Scheme 1.1).⁵ The corresponding branched products **7**

and **9** bearing vicinal tertiary and trisubstituted stereocenters are afforded in moderate to excellent yields with good to excellent enantioselectivities, albeit with moderate diastereoselectivities. Takemoto also found that simply by employing either KOH or LiHMDS, the diastereomeric ratio can be inverted in order to preferentially access either diastereomer (**7** versus **9**); this synthetically useful phenomenon has yet to be reported again.

Scheme 1.1 First report of diastereo- and enantioselective iridium-catalyzed allylic alkylation

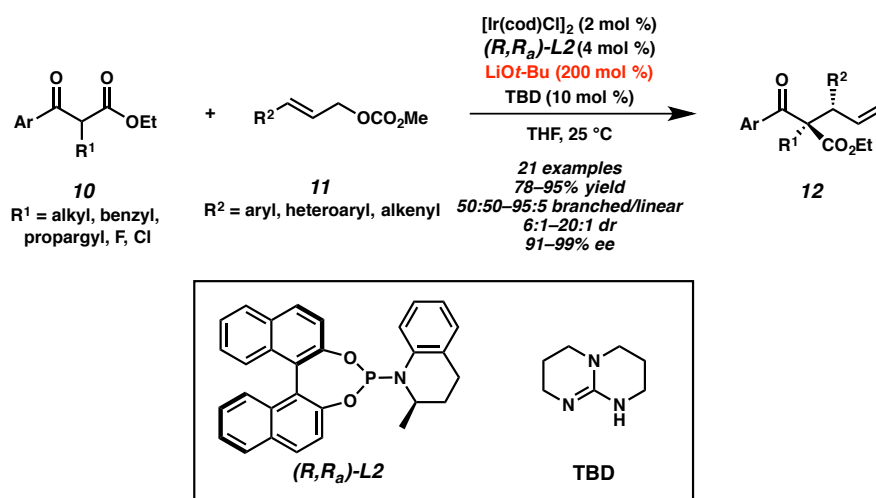


The different behavior of the bases is believed to be the result of contrasting enolate geometry; the hypothesis being that KOH predominately gives the *E*-enolate **5** and LiHMDS instead forms the *Z*-enolate **8**. This observation illuminates the additional challenge that acyclic, prochiral nucleophiles present in contrast to cyclic nucleophiles in diastereo- and enantioselective allylic alkylation chemistry. In acyclic cases, the enolate geometry must be selectively controlled in addition to the facial approach of the

nucleophile. This combination of challenges has resulted in significantly fewer reports of acyclic, prochiral enolate nucleophiles as compared to cyclic, prochiral nucleophiles.

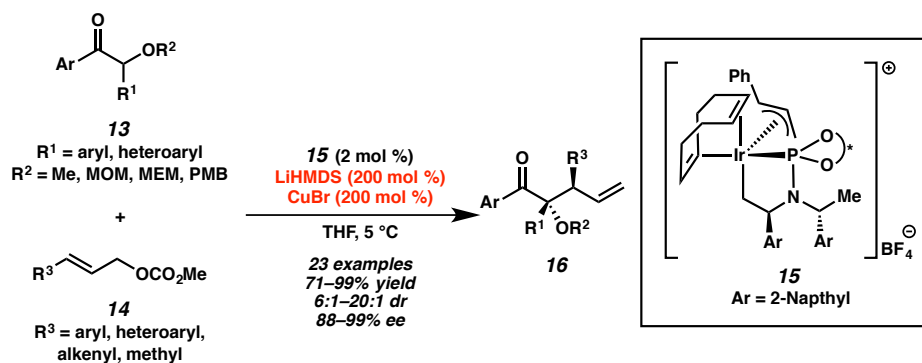
A decade after Takemoto's report, our group disclosed the second report of an iridium-catalyzed allylic alkylation of acyclic enolates in 2013 (Scheme 1.2).^{6a} Like Takemoto, we found chelation of the enolate with a metal cation, specifically lithium, to be crucial to the diastereoselectivity as bases lacking a chelating metal cation (i.e., DABCO) provide significantly lower selectivity. By deprotonating ketoesters **10** with LiOt-Bu prior to introduction of the electrophile, products **12** bearing vicinal tertiary and all-carbon quaternary stereocenters can be obtained in moderate to excellent selectivities with the use of a catalyst derived from $[\text{Ir}(\text{cod})\text{Cl}]_2$ and Me-THQphos (**L2**). While a majority of the cinnamyl carbonates **11** proceed with a high degree of regioselectivity (>90:10), we found that the use of electron-deficient aryl-substituted electrophiles **11** (e.g., $\text{R} = \text{C}_6\text{H}_5\text{NO}_2$ or $\text{C}_6\text{H}_5\text{CF}_3$) lead to a decrease in selectivity (50:50–86:14).

Scheme 1.2 Allylic alkylation of acyclic β -ketoesters by Stoltz



In 2016, Hartwig found that acyclic α -alkoxy ketones **13** undergo selective allylic alkylation reactions with allyl carbonates **14** in the presence of preformed metallacyclic iridium complex **15**, LiHMDS, and CuBr (Scheme 1.3).^{7a} In these reactions, the geometry of the acyclic enolate, formed by deprotonation with the lithium base, is controlled by chelation to a copper(I) salt. Interestingly, the identity of the cation associated with the base is also found to play an integral role in achieving high diastereoselectivities, with KHMDS providing much lower selectivities than LiHMDS. The exact nature of this cation dependence is unknown. It is also worth noting that the scope of this reaction permits the use of crotyl carbonates, albeit in lower diastereoselectivities (ca. 7:1 dr). This is one of only two reports of alkyl-substituted electrophiles in a diastereoselective iridium-catalyzed allylic alkylation.

Scheme 1.3 Allylic alkylation with acyclic α -alkoxy ketones by Hartwig

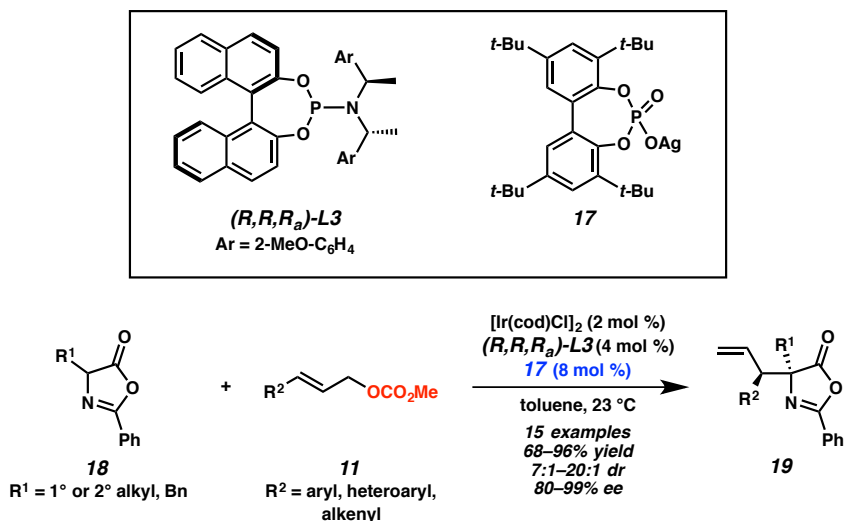


1.2.1.2 Cyclic Nucleophiles

In 2013, Hartwig published the first example of a diastereoselective iridium-catalyzed allylic alkylation of cyclic, prochiral nucleophiles (Scheme 1.4).^{8a} In this report, vicinal tertiary and tetra-substituted stereodyads are created via the allylic alkylation of azlactones **18** with aryl- and alkenyl-substituted allylic carbonates **11** in the

presence of catalytic amounts of achiral silver phosphate **17**, 3 Å molecular sieves, and an iridium catalyst generated in situ from $[\text{Ir}(\text{cod})\text{Cl}]_2$ and ligand **L3**. Through a series of control experiments, the authors were able to determine that both the phosphate and methyl carbonate anions, but not the silver cation, are key to the high reaction diastereoselectivity (up to >20:1 dr). The counteranions are presumed to deprotonate and control the facial attack of the nucleophile while the silver cation is believed to sequester chloride and promote the formation of the active metallacyclic iridium catalyst.

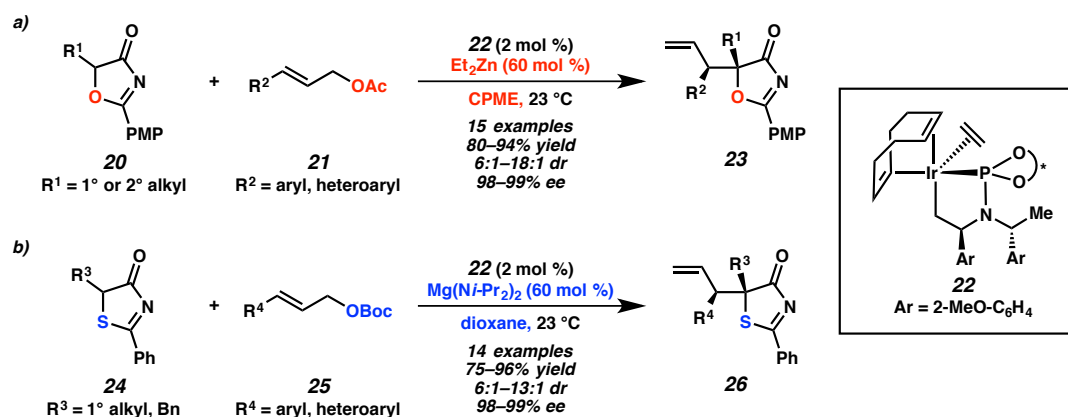
Scheme 1.4 Counterion-assisted iridium-catalyzed allylic alkylation of azlactones by Hartwig



This counterion strategy did not prove fruitful in the iridium-catalyzed allylic alkylation of substituted 5*H*-oxazol-4-ones **20** or 5*H*-thiazol-4-ones **24** (Scheme 1.5).^{8b} Application of the previously developed conditions to the reaction of 5*H*-oxazol-4-ones **20** with cinnamyl carbonates failed to yield desired allylic alkylation products **23** (Scheme 1.5a). The yields were improved by examining a number of organic and inorganic bases in combination with silver phosphate **17**. However, it was not until a substoichiometric amount of diethyl zinc, allylic acetate **21**, and preformed catalyst **22**

were used in place of the silver phosphate that good diastereoselectivities were achieved (up to 18:1 dr). The authors propose that the addition of diethyl zinc leads to the formation of zinc enolate aggregates ranging from dimers to tetramers, which in turn impart facial selectivity to the prochiral nucleophile.

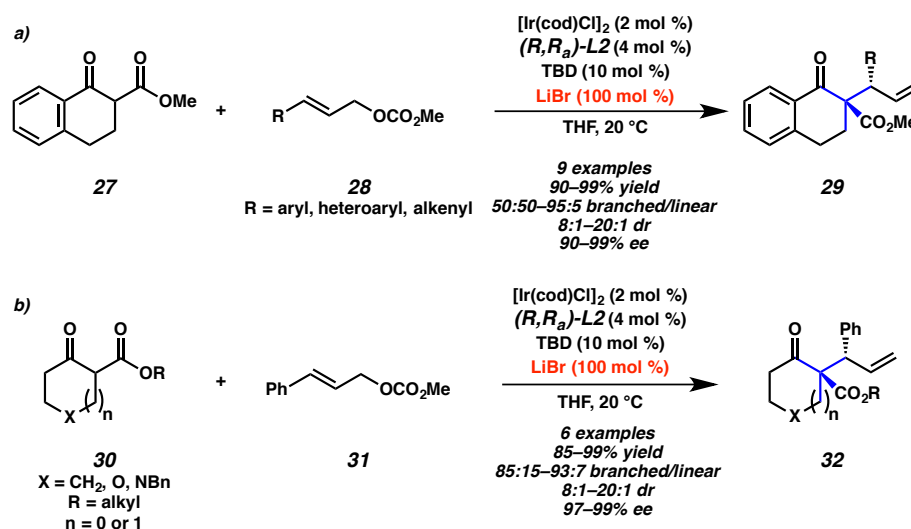
Scheme 1.5 Cation control of diastereoselectivity in iridium-catalyzed allylic alkylation of a) 5*H*-oxazol-4-ones **20** and b) 5*H*-thiazol-4-ones **24** by Hartwig



Application of the optimal conditions developed for 5*H*-oxazol-4-ones **20** using diethyl zinc does not afford a diastereoselective reaction (1.3:1 dr) with substituted 5*H*-thiazol-4-ones **24** (Scheme 1.5b). Instead, the authors achieved diastereoselectivity using a magnesium enolate formed from magnesium bis(diisopropyl)amide. The aggregation states of magnesium enolates, which are generally thought to be higher order aggregates than that of the corresponding zinc enolates, are believed to be responsible for the difference in diastereoselectivity. The authors also found that *tert*-butyl carbonate electrophiles **25** further improve the diastereoselectivities (up to 13:1 dr) for this nucleophile class.

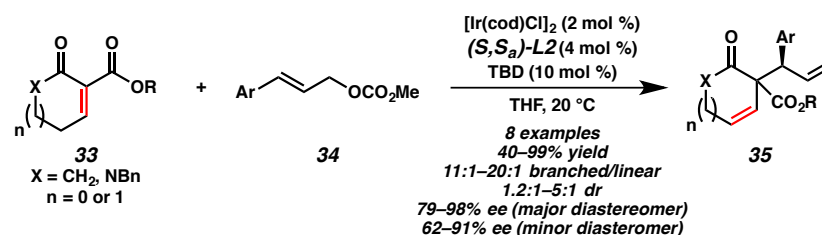
In 2013, our group pioneered the discovery of diastereo- and enantioselective iridium-catalyzed allylic alkylation chemistry of cyclic enolates for the formation of vicinal tertiary and all-carbon quaternary stereocenters (Scheme 1.6).^{6b} Initial investigations involving tetralone **27** revealed that a wide variety of aryl- and heteroaryl-substituted allylic carbonates **28** react to provide products **29** with high yields and stereoselectivities (Scheme 1.6a). The use of Me-THQphos (**L2**) as the chiral ligand and LiBr as a stoichiometric additive were found to be critical in attaining high selectivity. We postulate that LiBr results in lithium enolate aggregates, similar to those proposed by Hartwig.^{8b} In further investigations, we found that reactions involving various monocyclic substrates **30** afford the corresponding products **31** with similarly high yields and selectivities to those of the tetralone-based nucleophiles (Scheme 1.6b). Of note, the use of electron-deficient aryl-substituted electrophiles leads to an erosion in regioselectivity (50:50 to 71:29 branched/linear) in reactions of bicyclic nucleophiles.

Scheme 1.6 Allylic alkylation of a) bicyclic β -ketoesters **27** and b) monocyclic β -ketoesters **30** by Stoltz

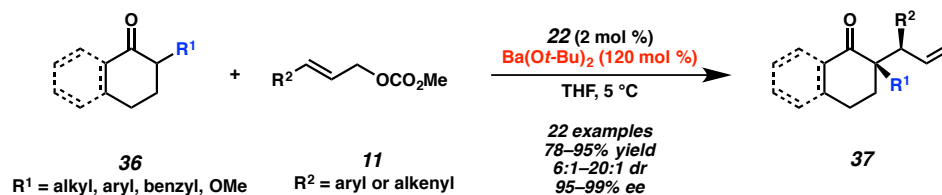


Studies toward substrate scope expansion of this reaction led to the successful allylic alkylation of extended enolates derived from unsaturated β -ketoester **33** (Scheme 1.7).^{6e} Though the yields and selectivities were generally found to be lower than the corresponding saturated analogs (*vide supra*), allylic alkylation at the α -carbon atom of the extended enolate was achieved to provide products **35** bearing an additional olefin for further functionalization of the molecule.

Scheme 1.7 Allylic alkylation of extended enolates by Stoltz

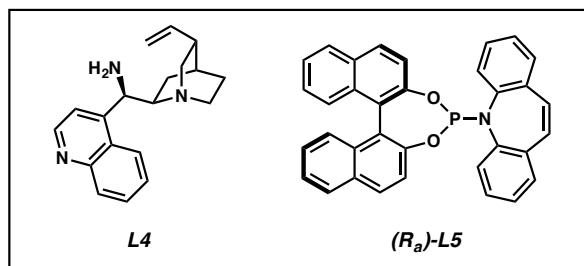
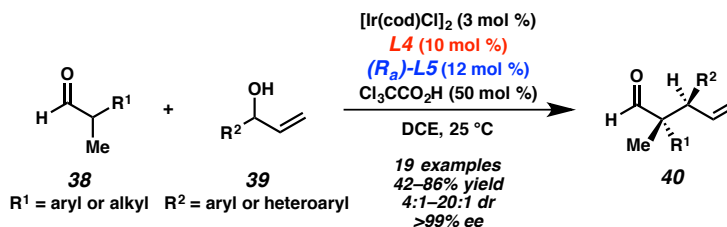


In 2013, Hartwig found that non-stabilized enolates **36** undergo selective iridium-catalyzed allylic alkylation reactions to form vicinal tertiary and all-carbon quaternary stereocenters using preformed iridium complex **22** and BaOt-Bu (Scheme 1.8).^{6d} In all cases, products **37** are afforded with excellent enantioenrichment (>98% ee), and even simple cyclohexanone derivatives provide good selectivity for allylic alkylation of the corresponding thermodynamic enolate. This protocol is currently the only reported set of conditions for cyclic nucleophiles that is not limited to softer enolate equivalents (e.g., malonates and β -ketoesters).

Scheme 1.8 Allylic alkylation of non-stabilized enolates by Hartwig

1.2.2 DUAL CATALYST-CONTROLLED PROCESSES

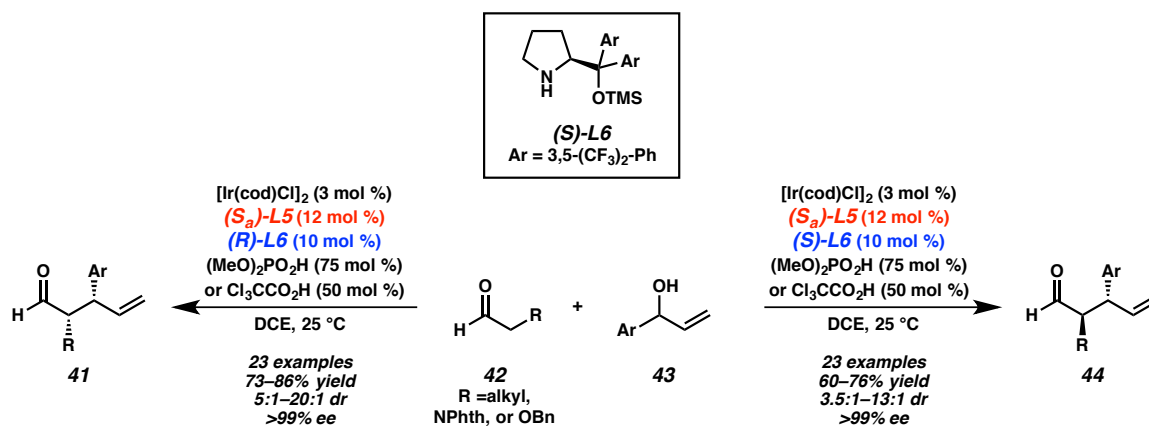
Methodology that allows for the selective synthesis of all four branched stereoisomers from one set of starting materials is highly sought after in the field of allylic alkylation. However, controlling the facial selectivity of both the nucleophile and the electrophile is a daunting task for a single catalyst.⁹ Thus, the use of two catalysts has been required to achieve stereodivergence.

Scheme 1.9 Dual catalyst-promoted allylic alkylation of aldehydes by Carreira

In 2013, Carreira disclosed the first dual catalytic allylic alkylation to construct vicinal tertiary and all-carbon quaternary stereocenters via the use of cinchona alkaloid-derived primary amine **L4** and phosphoramidite ligand **L5** (Scheme 1.9).^{6c} With the

appropriate combination of enantiomers of ligand **L5** and pseudo-enantiomers of **L4**, functionalized aldehyde **40**, or any of the three other corresponding stereoisomers, can be obtained with little erosion of selectivity due to mismatched catalysts from aldehyde **38** and branched alcohol **39**. The authors propose that the lack of an apparent mismatched pair of catalysts likely arises from a high degree of planarity between the two chiral intermediates in the carbon–carbon bond-forming event. During the course of reaction optimization, the authors discovered that an acid co-catalyst is extremely important for high stereoselectivity, with trichloroacetic acid being optimal. This pioneering study set the foundation for future work using the powerful combination of enamine and iridium catalysis.

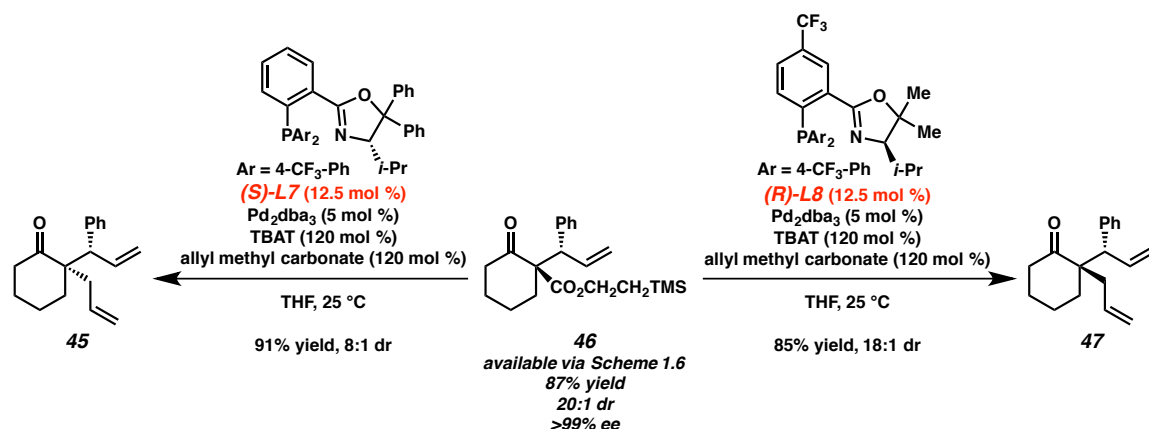
Scheme 1.10 Proline-derived dual catalysis by Carreira



In a second-generation protocol, Carreira utilized proline-derived amine **L6** for the formation of vicinal tertiary stereocenters (Scheme 1.10).^{8c} While seemingly simpler from a steric perspective, this transformation in fact produces a number of additional challenges; specifically, both the starting material and allylic alkylation products are potential electrophiles for aldol processes, and the products are susceptible to

epimerization. Nevertheless, the authors found that the appropriate selection of the enantiomers of **L5** and **L6** allows for the full complement of stereoisomers to be accessed with good to excellent selectivity. Unlike with the cinchona alkaloid-derived catalyst **L4** (Scheme 1.9), a significant mismatched pair of catalysts is observed (7:1 dr mismatched versus 20:1 dr matched). In this work, the authors found dimethyl hydrogen phosphate to be the optimal acid co-catalyst (**42**, R = alkyl). In a follow-up study, the authors reported that this method tolerates α -heteroatoms (**42**, R = NPhth or OBn) in similarly high yields and selectivities, though trichloroacetic acid is required as the co-catalyst.^{8d}

Scheme 1.11 Diastereoablative allylic alkylation of **46** by Stoltz

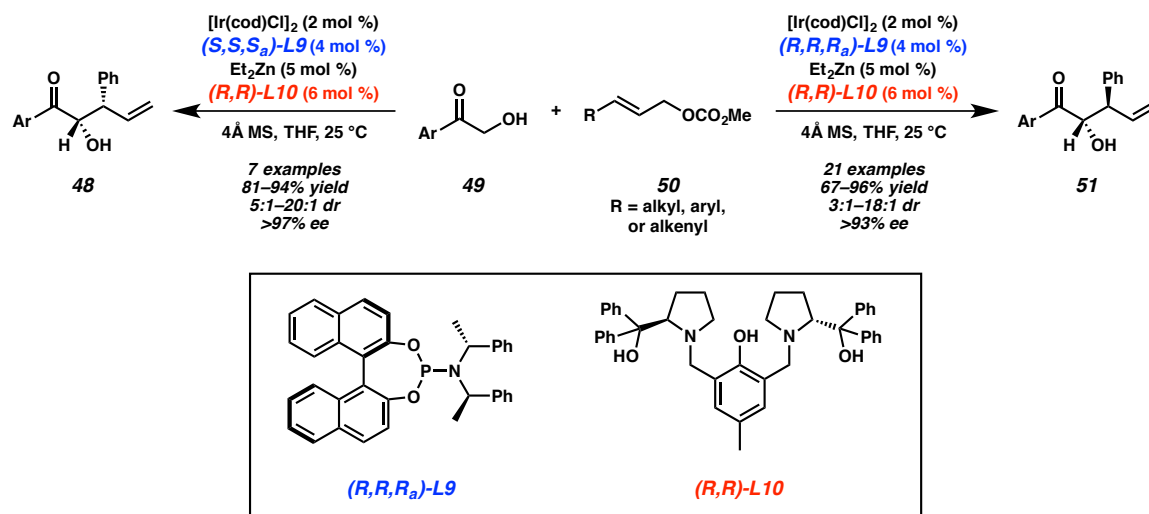


Our group has developed a two-step procedure for the divergent synthesis of various stereoisomers of cyclohexanone derivatives (Scheme 1.11).^{6b} Trimethylsilyl ethyl ester **46** is readily accessible via the aforementioned iridium-catalyzed allylic alkylation (Scheme 1.6). The use of the two pseudo-enantiomeric phosphinooxazoline (PHOX) ligands **L7** and **L8** allows for a fluoride-triggered diastereoablative *palladium-catalyzed* allylic alkylation, delivering either **45** or **47** selectively. While there is a significant difference in selectivities between the two pathways (8:1 dr mismatched versus 18:1 dr

matched), both palladium-catalyzed allylic alkylation products are obtained in good yields with no loss in enantioselectivity.

Finally, in 2016, Zhang developed a bimetallic dual catalysis strategy for the stereodivergent allylic alkylation of α -hydroxyketones **49** using a chiral iridium complex derived from phosphoramidite **L9** and a chiral zinc–ProPhenol (**L10**) species.^{7b} This method does not require the use of an exogenous base and a range of α -hydroxyl- γ,δ -unsaturated ketones **48/51** containing vicinal stereocenters can be accessed in good yields and stereoselectivities utilizing this protocol. Moreover, with the appropriate combination of **L9** and **L10** enantiomers, any stereoisomer of product can be constructed with the dual catalytic strategy; however, a significant mismatched pair of catalysts is observed (15:1 dr matched versus 6:1 dr mismatched).

Scheme 1.12 Bimetallic dual catalytic allylic alkylation by Zhang



1.3 REACTION OPTIMIZATION

Based on the precedent from the aforementioned reports of diastereo-, enantio-, and regioselective iridium-catalyzed allylic alkylation, our studies commenced with an exploration of the efficacy of additives, leaving groups, bases, and ligands on the selectivity of the reaction between α -carboxymethyl tetralone (**52**) and crotyl electrophile **53**. Using our previously reported conditions for iridium-catalyzed allylic alkylations with cinnamyl-derived electrophiles as a starting point,^{6a,b} the reactivity of tetralone **52** was first investigated with crotyl carbonate in the presence of catalytic phosphoramidite **L2**·½[Ir(cod)Cl]₂ and either LiBr (Table 1.1, entry 1),^{6a} LiOt-Bu (entry 2),^{6b} or a combination of LiBr and LiOt-Bu (entry 3). Unfortunately, while these conditions result in excellent conversion and good diastereoselectivity, low levels of regioselectivity were observed. As our earlier work on cinnamyl-derived electrophiles revealed that the regioselectivity improved as carbocation stability increased (i.e., increasingly electron-rich aromatic cinnamyl derivatives),^{6b} we reasoned that the poor regioselectivity in this case was likely due to the minimal stabilization of the carbocation afforded by the methyl substituent of **53**. Specifically, we hypothesized that the attenuated carbocation stability could be effecting slow equilibration between diastereomers of the iridium π -allyl complex, translating into diminished regioselectivity. Previous reports have proposed that LiCl may facilitate the equilibration leading to increased regio- and enantioselectivity,¹⁰ but we noted little improvement in selectivity with the use of LiCl as compared to LiBr (entry 4).

We subsequently turned our attention to the nature of the leaving group on the electrophile. We envisioned that switching from crotyl methyl carbonate to crotyl

chloride would render the anions in solution congruent and perhaps make the effect of the chloride anions more pronounced. To our delight, regioselectivity is dramatically improved with the use of crotyl chloride, albeit with diminished diastereoselectivity (entry 5).

Table 1.1 Optimization of reaction parameters^a

Entry	L	Base (200 mol %)	Additive (mol %)	LG	52:53	Yield 54+55 (%) ^b	54:55 ^c	dr of 54 ^c	ee of 54 (%) ^d
1	L2	–	LiBr (100)	OCO ₂ Me	2:1	100	55:45	6.4:1	–
2	L2	LiOt-Bu	–	OCO ₂ Me	2:1	85	34:66	5.3:1	–
3	L2	LiOt-Bu	LiBr (100)	OCO ₂ Me	2:1	100	45:55	6.8:1	–
4	L2	LiOt-Bu	LiCl (100)	OCO ₂ Me	2:1	69	50:50	7.2:1	–
5	L2	LiOt-Bu	LiCl (100)	Cl	2:1	94	86:14	4.8:1	–
6	L2	proton sponge	LiCl (100)	Cl	2:1	100	93:7	7.9:1	66
7	L9	proton sponge	LiCl (100)	Cl	2:1	79	69:31	2.4:1	–
8	L5	proton sponge	LiCl (100)	Cl	2:1	91	52:48	1.5:1	–
9	L11	proton sponge	LiCl (100)	Cl	2:1	46	95:5	6.0:1	96
10	L11	proton sponge	–	Cl	2:1	trace	–	–	–
11	L11	proton sponge	LiCl (400)	Cl	2:1	78	94:6	6.7:1	97
12	L11	proton sponge	LiCl (400)	Cl	1:1	55	95:5	5.3:1	98
13	L11	proton sponge	LiCl (400)	Cl	1:2	76	>95:5	5.3:1	85

R = H: (S,S_a)-L2
R = Ph: (S,S_a)-L11

(S,S,S_a)-L9

(S_a)-L5

TBD
proton sponge

[a] Reactions performed on 0.1 mmol scale. [b] ¹H NMR yield based on internal standard of the mixture of diastereomers. [c] Determined by ¹H NMR analysis of the crude reaction mixture. [d] Determined by chiral SFC analysis. [e] TBD = 1,3,5-triazabicyclo[4.4.0]dec-5-ene, proton sponge = 1,8-bis(dimethylamino)naphthalene.

Previous work demonstrating the marked effect of bases on regio- and diastereoselectivity in iridium-catalyzed allylic alkylations prompted an extensive

exploration of bases (see Section 1.7.2.2, Table 1.4).⁵⁻⁸ We found that the use of proton sponge in place of LiOt-Bu afforded the desired branched product **54** with high regioselectivity (93:7, **54:55**) and diastereoselectivity (7.9:1 dr), though in a modest 66% enantiomeric excess (entry 6). A brief study of ligand frameworks (entries 7–9)¹¹ revealed 3,3'-diphenyl-phosphoramidite **L11** to be optimal. Using **L11**, allylic alkylation product **54** is obtained in excellent enantioselectivity (96% ee) with comparable regio- and diastereoselectivities to **L2**, though in considerably lower yield (46%, entry 9). Efforts to increase the yield revealed super-stoichiometric levels of LiCl to be both essential and correlative to the conversion (entries 10 and 11). Ultimately, we found that the combination of catalytic phosphoramidite **L11**·½ [Ir(cod)Cl]₂, 200 mol % proton sponge, and 400 mol % LiCl deliver product **54** in 78% yield (entry 11) with an exceptional branched to linear ratio (94:6, **54:55**), diastereoselectivity (6.7:1 dr), and enantioselectivity (97% ee). Finally, it should be noted that we observed optimal conversion and selectivity using a 2:1 nucleophile to electrophile ratio; however, the nucleophile and electrophile stoichiometry can be varied (1:1 or 1:2) without dramatically affecting reaction conversion or selectivity, rendering the reaction synthetically practical (entries 12 and 13). Moreover, the excess equivalent of nucleophile can be re-isolated during purification.

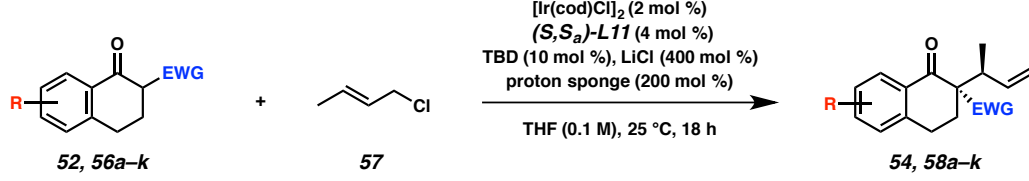
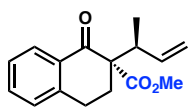
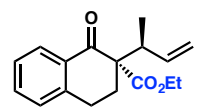
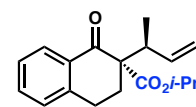
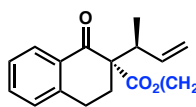
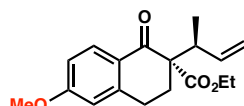
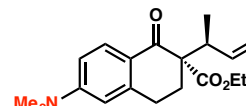
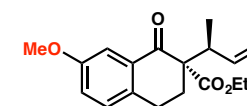
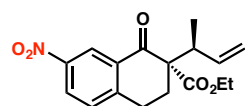
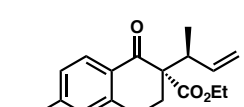
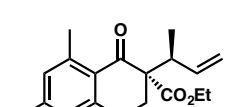
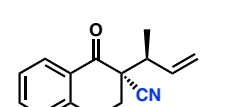
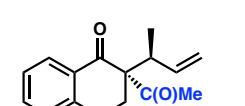
1.4 SUBSTRATE SCOPE EXPLORATION

With the optimized conditions identified, we explored the substrate scope of this diastereo-, enantio-, and regioselective allylic alkylation reaction (Table 1.2). Generally, the process is tolerant of a wide range of substituents and functionality on both the arene

and ester groups. We found that increasing the size of the ester moiety ($-\text{CO}_2\text{Me}$, $-\text{CO}_2\text{Et}$, $-\text{CO}_2i\text{-Pr}$) results in formation of the corresponding products **54**, **58a**, and **58b** in increasingly improved regio- and diastereoselectivity but moderately diminished yields. As a balance between yield and selectivity, we moved forward in our investigation using α -carboxyethyl tetralone derivatives. Moreover, we were pleased to find that a (2-trimethylsilyl)ethyl substrate undergoes allylic alkylation to provide **58c** with good selectivity, albeit in modest yield. Alkylation product **58c** may undergo subsequent fluoride-triggered allylic alkylation mediated by palladium to provide either diastereomer of the bis-alkylation product with catalyst control.¹²

We sought to further examine the scope of the reaction by exploring the diversity of substitution permitted on the tetralone aromatic ring. Gratifyingly, a wide variety of both electron-donating and withdrawing groups are tolerated at varying positions, though an electronic effect was noted on enantioselectivity. We observed that substrates bearing electron-donating groups ($\text{MeO}-$, $\text{Me}_2\text{N}-$) at the 6-position give products **58d** and **58e** with slightly diminished enantioselectivity (84–86% ee). Conversely, substrates with electron-withdrawing groups ($7\text{-MeO}-$, 7-NO_2- , $6\text{-Br}-$) afford the corresponding products **58f**, **58g**, and **58h** in excellent enantioselectivity (94–98% ee). Additionally, 5,7-dimethyl-substituted tetralone **58i** is furnished in comparable selectivity to unsubstituted α -carboxyethyl tetralone **58a**. In all examples, good regio- and diastereoselectivity is observed. Furthermore, during the course of our investigations we found that the β -ketoester moiety is crucial to the reaction. Substrates with this functionality replaced with either a nitrile or ketone provide the corresponding products **58j** and **58k** in decreased selectivities.

Table 1.2 Substrate scope exploration^a

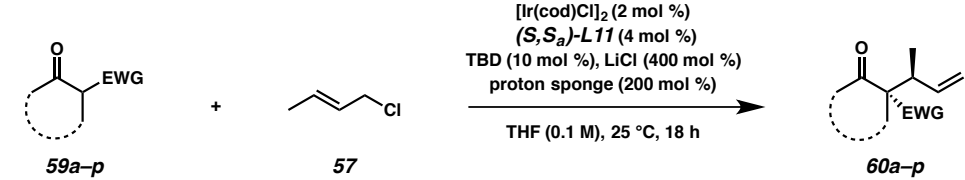
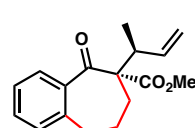
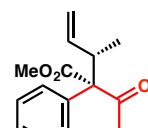
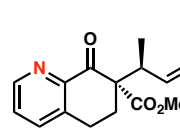
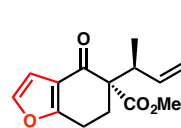
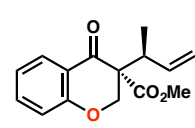
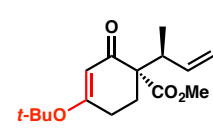
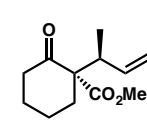
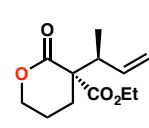
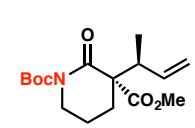
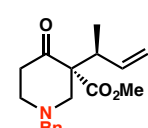
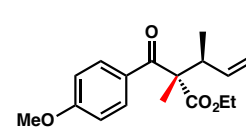
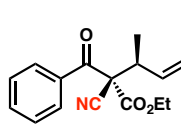
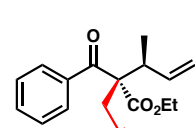
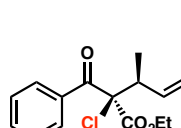
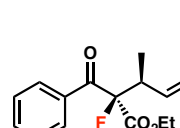
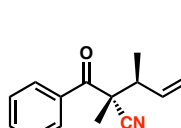
					
 <p>54 74% (74%) yield^b 93:7 b:l^c 6:1 dr^c 96% ee^d</p>		 <p>58a 71% (56%) yield 93:7 b:l 8.9:1 dr 96% ee</p>		 <p>58b 58% (55%) yield 95:5 b:l 17.5:1 dr 96% ee</p>	
 <p>58c 37% (27%) yield 95:5 b:l 12.1:1 dr 89% ee</p>		 <p>58d 65% (55%) yield 92:8 b:l 5.8:1 dr 84% ee</p>		 <p>58e 46% (46%) yield 93:7 b:l 5.4:1 dr 86% ee</p>	
 <p>58f 68% (68%) yield 90:10 b:l 7.6:1 dr 94% ee</p>		 <p>58g 94% (82%) yield 90:10 b:l 15.5:1 dr 93% ee</p>		 <p>58h 78% (63%) yield 92:8 b:l 10.4:1 dr 98% ee</p>	
 <p>58i 66% (52%) yield 94:6 b:l 10.9:1 dr 96% ee</p>		 <p>58j >99% (95%) yield 90:10 b:l 5.1:1 dr 52% ee</p>		 <p>58k 32% (23%) yield 85:15 b:l 1.7:1 dr 65% ee</p>	

[a] Reactions performed on 0.2 mmol scale with 2:1 nucleophile/electrophile. [b] ¹H NMR yield based on internal standard of the mixture of diastereomers; combined isolated yield of branched and linear products given in parentheses. [c] Determined by ¹H NMR analysis of the crude reaction mixture. [d] Determined by chiral SFC or HPLC analysis. [e] Absolute stereochemistry determined via single-crystal X-ray analysis.

A broader investigation of the substrate scope reveals additional limitations of the catalytic system (Table 1.3). Foremost, no allylic alkylation is observed with alkyl-substituted allylic chloride derivatives other than crotyl chloride (**57**). With respect to limitations on the nucleophile substrate scope, altering the saturated ring size (e.g., a benzosuberone-derived nucleophile) or employing a 2-tetralone-derived nucleophile

leads to products **60a** and **60b** in significantly diminished diastereo- and regioselectivities. Additionally, bicyclic nucleophiles containing fused heterocycles give products **60c** and **60d** in decreased yields. Use of a chromanone-based nucleophile affords allylic alkylation product **60e** with no diastereocontrol. Furthermore, we observed that monocyclic nucleophiles, including lactones, lactams, and piperidones, afford the corresponding products **60f**, **60g**, **60h**, **60i**, and **60j** in only modest yields. Moreover, with respect to linear nucleophiles, we noted minimal or no conversion to product when a quaternary stereocenter is formed in the allylic alkylation reaction (e.g., **60k**, **60l**, and **60m**), and in the case of propargyl **60m**, we hypothesize that the alkyne functionality leads to catalyst poisoning. However, we did observe excellent reactivity for α -halogenated linear nucleophiles, which reacted to give products **60n** and **60o** in high yield and regioselectivity, though inconsistent diastereo- and enantioselectivities. Finally, we were interested to find that in contrast to the case with a tetralone-derived nucleophile, exchanging the β -ketoester moiety for a nitrile on a linear nucleophile gave product **60p** in excellent yields and selectivities.

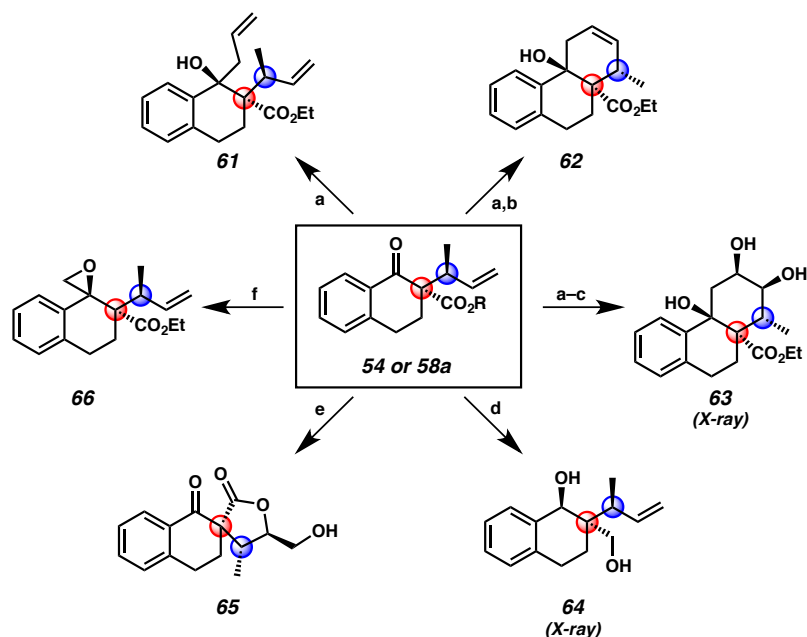
Table 1.3 Substrate scope limitations^a

<p>  </p>				
 <p>60a^b 79% yield^c 78:22 b:l^d 1.2:1 dr^d</p>	 <p>60b^b 90% yield 67:33 b:l 2:1 dr</p>	 <p>60c^b trace yield</p>	 <p>60d 50% yield >95:5 b:l 1.4:1 dr</p>	
 <p>60e^b trace yield 86:14 b:l 1.1:1 dr</p>	 <p>60f^b 56% yield 81:19 b:l 3.3:1 dr</p>	 <p>60g^b 47% yield 86:14 b:l 5.1:1 dr</p>	 <p>60h 51% yield 90:10 b:l 5.2:1 dr</p>	
 <p>60i^b 7% yield – b:l 3.9:1 dr</p>	 <p>60j^b 49% yield 83:17 b:l 3.6:1 dr</p>	 <p>60k^e no reaction</p>	 <p>60l 53% (46%) yield 91:9 b:l 4.5:1 dr 4% ee^f</p>	
 <p>60m^b 19% yield 90:10 b:l 2:1 dr</p>	 <p>60n 96% (93%) yield >95:5 b:l 29:1 dr 85% ee</p>	 <p>60o 95% (47%) yield >95:5 b:l 3.5:1 dr 38% ee</p>	 <p>60p^b 91% yield 90:10 b:l >20:1 dr</p>	

[a] Reactions performed on 0.2 mmol scale with 2:1 nucleophile/electrophile. [b] Reaction performed with (*S,S*_a)-L2. [c] ¹H NMR yield based on internal standard of the mixture of diastereomers; combined isolated yield of branched and linear products given in parentheses. [d] Determined by ¹H NMR analysis of the crude reaction mixture. [e] Reaction performed with 1:1.1 nucleophile/electrophile, 400 mol % proton sponge, and 0.5 M THF. [f] Determined by chiral SFC or HPLC analysis.

1.5 PRODUCT TRANSFORMATIONS

To demonstrate the synthetic utility of this method, we carried out a number of transformations on allylic alkylation products **54** and **58a** (Figure 1.3). We found that the addition of allylmagnesium chloride proceeds smoothly to furnish alcohol **61** in 71% yield as a single diastereomer. In a two-step protocol, addition of allyl Grignard with subsequent ring-closing metathesis allows rapid access to tricycle **62** bearing three contiguous stereocenters in 58% yield over two steps. The resultant cyclohexene moiety undergoes diastereoselective dihydroxylation to provide triol **63** bearing five contiguous stereocenters in 59% yield. Both the ester and the ketone functionalities of **58a** can be reduced to provide 1,3-diol **64** in 43% yield. Dihydroxylation of the pendant olefin of **58a** proceeds with concomitant lactonization to provide highly functionalized γ -butyrolactone **65** in 65% yield. Functionalized γ -butyrolactone moieties are highly prevalent and estimated to be present in about 10% of all natural products.¹³ Additionally, Corey–Chaykovsky epoxidation proceeds smoothly, furnishing **66** in 82% yield. Notably, all six of these derivatizations proceed with excellent diastereoselectivity to facilitate the synthesis of at least three contiguous stereocenters, demonstrating the ease with which complexity can be added to these high-value products.

Figure 1.3 Product transformations of allylic alkylation products **54** and **58a**^a

[a] allylmagnesium chloride, THF, -78°C , 71% yield. [b] HG-II, CH_2Cl_2 , 81% yield. [c] K_2OsO_4 , NMO, THF/ H_2O , 59% yield. [d] DIBAL, THF, -78°C , 43% yield. [e] K_2OsO_4 , NMO, THF/ H_2O , 65% yield. [f] $\text{Me}_3\text{S(O)I}$, NaH, DMSO, 82% yield.

1.6 CONCLUSIONS

In summary, we have developed the first enantioselective transition-metal-catalyzed allylic alkylation reaction forming vicinal tertiary and all-carbon quaternary stereocenters between prochiral enolates and an alkyl-substituted electrophile. Critical to the success of this new reaction is the identity and ubiquity of the chloride counterion in addition to the use of proton sponge, the combination of which affords excellent regio- and enantioselectivities along with good yields and diastereoselectivities. Additionally, a number of transformations were carried out on the alkylation products to demonstrate the value of this method in rapidly accessing highly functionalized, stereochemically rich polycyclic scaffolds.

1.7 EXPERIMENTAL SECTION

1.7.1 MATERIALS AND METHODS

Unless otherwise stated, reactions were performed in flame-dried glassware under an argon or nitrogen atmosphere using dry, deoxygenated solvents. Solvents were dried by passage through an activated alumina column under argon. Commercially obtained reagents were used as received. Chemicals were purchased from Sigma Aldrich/Strem/Alfa Aesar/Oakwood Chemicals and used as received. Reaction temperatures were controlled by an IKA Mag temperature modulator. Glove box manipulations were performed under a nitrogen atmosphere. Thin-layer chromatography (TLC) and preparatory TLC was performed using E. Merck silica gel 60 F254 precoated plates (0.25 mm) and visualized by UV fluorescence quenching, KMnO_4 , or *p*-anisaldehyde staining. SiliaFlash P60 Academic Silica gel (particle size 0.040–0.063 mm) was used for flash chromatography. Preparatory HPLC was performed with an Agilent 1200 Series HPLC equipped with two Agilent Zorbax RX-sil silica columns (9.4 x 250 mm) in series. Analytical chiral HPLC was performed with an Agilent 1100 Series HPLC utilizing a Chiralpak AD-H column (4.6 mm x 25 cm) in series with a Chiralpak AD column (4.6 mm x 25 cm) or a Chiralpak IC column (4.6 mm x 25 cm), all obtained from Daicel Chemical Industries, Ltd. with visualization at 254 nm. Analytical SFC was performed with a Mettler SFC supercritical CO_2 analytical chromatography system utilizing a Chiralpak IC column (4.6 mm x 25 cm) obtained from Daicel Chemical Industries, Ltd. with visualization at 254 nm. ^1H NMR spectra were recorded on a Bruker Avance HD 400 MHz spectrometer and are reported relative to residual CHCl_3 (δ 7.26 ppm). ^{13}C NMR spectra were recorded on a Bruker Avance HD 400 MHz spectrometer

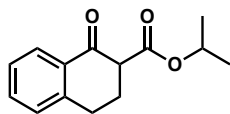
and are reported relative to residual CDCl_3 (δ 77.16 ppm). Data for ^1H NMR are reported as follows: s = singlet, d = doublet, t = triplet, q = quartet, p = pentet, sept = septuplet, m = multiplet, br s = broad singlet. Data for ^{13}C NMR are reported in terms of chemical shifts (δ ppm). Some reported spectra include minor solvent impurities of benzene (δ 7.36 ppm), water (δ 1.56 ppm), ethyl acetate (δ 4.12, 2.05, 1.26 ppm), methylene chloride (δ 5.30 ppm), grease (δ 1.26, 0.86 ppm), and/or silicon grease (δ 0.07 ppm), which do not impact product assignments. IR spectra were obtained using a Perkin Elmer Paragon 1000 spectrometer using thin films deposited on NaCl plates and reported in frequency of absorption (cm^{-1}). High resolution mass spectra (HRMS) were obtained from the Caltech Mass Spectral Facility using a JEOL JMS-600H High Resolution Mass Spectrometer in fast atom bombardment (FAB+) or electron ionization (EI+) mode, or an Agilent 6200 Series TOF with an Agilent G1978A Multimode source in electrospray ionization (ESI+), atmospheric pressure chemical ionization (APCI+), or mixed ionization mode (MM: ESI-APCI+). Optical rotations were measured with a Jasco P-2000 polarimeter operating on the sodium D-line (589 nm), using a 100 mm pathlength cell, and are reported as: $[\alpha]_{\text{D}}^{\text{T}}$ (concentration in g/100 mL, solvent).

1.7.1.1 Preparation of Known Compounds

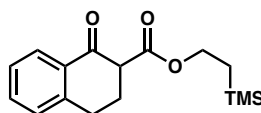
Previously reported methods were used to prepare ligands $(S,S_a)\text{-L2}$,^{11a,14} $(S,S_a)\text{-L11}$,^{11a,14} and $(S_a)\text{-L9}$ ¹⁵ as well as starting materials **52**,¹⁶ **56a**,¹⁶ **56f**,¹⁷ **56d**,¹⁸ **56i**,¹⁹ and **56j**.²⁰

1.7.2 EXPERIMENTAL PROCEDURES AND SPECTROSCOPIC DATA

1.7.2.1 Experimental Procedures and Spectroscopic Data for the Synthesis of Tetralone Substrates

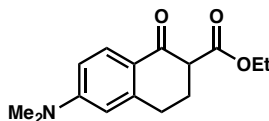


Isopropyl 1-oxo-1,2,3,4-tetrahydronaphthalene-2-carboxylate (56b). A solution of methyl ester **52**¹⁶ (0.75 g, 3.7 mmol, 1 equiv), Bu₂SnO (0.091 g, 0.37 mmol, 0.1 equiv), and IPA (15 mL) was heated under reflux for 72 h then concentrated onto silica and purified by silica gel flash column chromatography (3% Et₂O/hexanes) to give isopropyl ester **56b** (1:1 mixture of enol/keto isomers) as a colorless oil (0.62 g, 72% yield): ¹H NMR (400 MHz, CDCl₃) δ 12.56 (s, 0.5H), 8.05 (ddd, *J* = 7.8, 1.5, 0.6 Hz, 0.5H), 7.81 – 7.77 (m, 0.5H), 7.49 (td, *J* = 7.8, 1.5 Hz, 0.5H), 7.35 – 7.23 (m, 2H), 7.20 – 7.14 (m, 0.5H), 5.14 (dp, *J* = 17.1, 6.2 Hz, 1H), 3.56 (dd, *J* = 10.5, 4.7 Hz, 0.5H), 3.13 – 2.93 (m, 1H), 2.81 (dd, *J* = 8.6, 6.9 Hz, 1H), 2.60 – 2.52 (m, 1H), 2.53 – 2.43 (m, 0.5H), 2.35 (ddt, *J* = 13.5, 5.7, 4.7 Hz, 0.5H), 1.32 (d, *J* = 6.3 Hz, 3H), 1.28 (dd, *J* = 6.3, 2.8 Hz, 3H); ¹³C NMR (101 MHz, CDCl₃) δ 193.6, 172.5, 170.0, 165.0, 143.8, 139.5, 133.9, 132.0, 130.5, 130.3, 128.9, 127.8, 127.5, 127.0, 126.7, 124.4, 97.5, 69.0, 68.2, 54.9, 27.9, 27.8, 26.5, 22.2 (2C), 21.9, 21.9, 20.7; IR (Neat Film, NaCl) 3070, 3027, 2980, 2937, 2847, 1736, 1687, 1644, 1618, 1571, 1454, 1384, 1322, 121, 1214, 1106, 1084, 949, 831, 770, 744 cm⁻¹; HRMS (MM: ESI-APCI+) *m/z* calc'd for C₁₄H₁₇O₃ [M+H]⁺: 233.1172, found 233.1174.



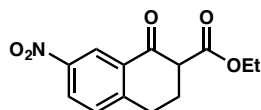
2-(Trimethylsilyl)ethyl 1-oxo-1,2,3,4-tetrahydronaphthalene-2-carboxylate (56c). A solution of LiHMDS (1.83 g, 10.9 mmol, 2 equiv) in THF (20 mL) was added dropwise to a solution of 1-tetralone (0.804 g, 5.50 mmol, 1 equiv) in THF (20 mL) via cannula at $-78\text{ }^{\circ}\text{C}$. After 1.5 h at $-78\text{ }^{\circ}\text{C}$, a solution of 2-(trimethylsilyl)ethyl 1*H*-imidazole-1-carboxylate (1.39 g, 6.55 mmol, 1.2 equiv) in THF (5 mL) was then added. The resulting reaction mixture was allowed to warm to ambient temperature and stirred for 18 h. The reaction was quenched with the addition of saturated NH_4Cl aqueous solution (40 mL) and the aqueous layer was then extracted with Et_2O (3 x 50 mL). The combined organic layers were washed with brine (20 mL), dried over Na_2SO_4 , and concentrated under reduced pressure. The crude residue was purified by CombiFlash EZ Prep (12 g silica, 1 \rightarrow 5% Et_2O /hexanes, 30 min) to provide ester **56c** (3:1 mixture of enol/keto isomers) as a colorless oil (0.40 g, 25%): ^1H NMR (400 MHz, CDCl_3) δ 12.57 (s, 0.75H), 8.08 (dd, $J = 7.8, 1.4\text{ Hz}$, 0.25H), 7.83 (dd, $J = 7.8, 1.4\text{ Hz}$, 0.75H), 7.52 (td, $J = 7.8, 1.4\text{ Hz}$, 0.25H), 7.39 – 7.24 (m, 2H), 7.23 – 7.16 (m, 0.75H), 4.41 – 4.14 (m, 2H), 3.61 (dd, $J = 10.3, 4.7\text{ Hz}$, 0.25H), 3.14 – 2.97 (m, 0.5H), 2.83 (dd, $J = 8.9, 6.6\text{ Hz}$, 1.5H), 2.64 – 2.57 (m, 1.5H), 2.56 – 2.47 (m, 0.25H), 2.38 (m, 0.25H), 1.24 – 0.99 (m, 2H), 0.10 (s, 9H); ^{13}C NMR (101 MHz, CDCl_3) δ 193.4, 173.1, 170.5, 165.1, 155.5, 143.8, 139.5, 134.0, 131.9, 131.0, 130.2, 128.9, 127.9, 127.5, 127.0, 126.7, 124.4, 97.2, 66.2, 63.8, 62.9, 54.8, 27.9, 27.8, 26.5, 20.7, 17.7, 17.5, 17.5, -1.3 , -1.39 , -1.41 ; IR (Neat Film, NaCl) 3071, 3028, 2954, 2898, 2846, 1739, 1689, 1644, 1620, 1571, 1454, 1394, 1355, 1325, 1270, 1212,

1175, 1133, 1084, 859, 837, 769 cm^{-1} ; HRMS (FAB+) m/z calc'd for $\text{C}_{16}\text{H}_{23}\text{O}_3\text{Si}$ $[\text{M}+\text{H}]^+$: 291.1417, found 291.1421.

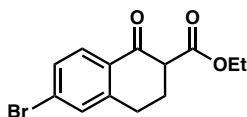


Ethyl 6-(dimethylamino)-1-oxo-1,2,3,4-tetrahydronaphthalene-2-carboxylate (56e).

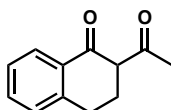
To a suspension of NaH (0.98 g, 29 mmol, 3.7 equiv, 60 wt %) in THF (10 mL) was added diethyl carbonate (1.9 mL, 16 mmol, 2 equiv). The reaction mixture was brought to reflux at which point a solution of 6-(dimethylamino)-3,4-dihydronaphthalene-1(2*H*)-one (1.5 g, 7.9 mmol, 1 equiv) in THF (10 mL) was added dropwise via addition funnel over 15 min. The reaction mixture was heated to reflux for an additional 18 h then allowed to cool to ambient temperature, whereupon it was quenched with conc. AcOH (10 mL) and diluted with Et₂O (30 mL). The organic layer was washed with brine (5 x 10 mL), dried over Na₂SO₄, and concentrated under reduced pressure. The crude residue was purified by CombiFlash EZ Prep (12 g silica, 10→20% EtOAc/hexanes, 30 min) to provide dimethylamine **56e** (keto isomer) as a tan solid (1.36 g, 66%): ¹H NMR (400 MHz, CDCl₃) δ 7.95 (d, J = 9.0 Hz, 1H), 6.60 (dd, J = 9.0, 2.6 Hz, 1H), 6.36 (d, J = 2.6 Hz, 1H), 4.32 – 4.12 (m, 2H), 3.52 (dd, J = 10.2, 4.7 Hz, 1H), 3.06 (s, 6H), 2.99 – 2.83 (m, 2H), 2.44 (m, 1H), 2.29 (m, 1H), 1.29 (t, J = 7.1 Hz, 3H); ¹³C NMR (101 MHz, CDCl₃) δ 191.4, 171.2, 153.8, 145.9, 130.1, 128.5, 120.8, 110.6, 109.3, 61.2, 54.5, 40.2, 28.6, 26.8, 14.4; IR (Neat Film, NaCl) 2935, 1735, 1660, 1593, 1521, 1449, 1372, 1308, 1197, 1121, 1084, 923 cm^{-1} ; HRMS (FAB+) m/z calc'd for $\text{C}_{15}\text{H}_{20}\text{NO}_3$ $[\text{M}+\text{H}]^+$: 262.1443, found 262.1473.



Ethyl 7-nitro-1-oxo-1,2,3,4-tetrahydronaphthalene-2-carboxylate (56g). A solution of LiHMDS (1.8 g, 11 mmol, 2.1 equiv) in THF (20 mL) was added dropwise to a solution of 7-nitro-3,4-dihydronaphthalene-1(2*H*)-one (1.0 g, 5.2 mmol, 1 equiv) in THF (20 mL) via cannula at $-78\text{ }^{\circ}\text{C}$. The reaction was stirred for 1.5 h at $-78\text{ }^{\circ}\text{C}$, whereupon ethyl cyanoformate (0.61 g, 6.2 mmol, 1.2 equiv) was added. The resulting reaction mixture was allowed to warm to ambient temperature and was stirred for 18 h. The reaction was quenched with the addition of saturated NH_4Cl aqueous solution (40 mL) and the aqueous layer was then extracted with Et_2O (3 x 50 mL). The combined organic layers were washed with brine (20 mL), dried over Na_2SO_4 , and concentrated under reduced pressure. The crude residue was purified by silica gel flash column chromatography (8% EtOAc /hexanes) to provide nitroarene **56g** (enol isomer) as a colorless solid (114 mg, 8%): ^1H NMR (400 MHz, CDCl_3) δ 12.45 (s, 1H), 8.65 (d, $J = 2.4\text{ Hz}$, 1H), 8.20 (dd, $J = 8.3, 2.4\text{ Hz}$, 1H), 7.37 (dt, $J = 8.3, 1.0\text{ Hz}$, 1H), 4.34 (q, $J = 7.1\text{ Hz}$, 2H), 2.95 (t, $J = 7.8\text{ Hz}$, 2H), 2.66 (dd, $J = 8.8, 6.9\text{ Hz}$, 2H), 1.39 (t, $J = 7.1\text{ Hz}$, 3H); ^{13}C NMR (101 MHz, CDCl_3) δ 172.4, 162.5, 147.3, 146.3, 131.6, 128.5, 125.0, 119.6, 98.9, 61.2, 28.0, 20.2, 14.4; IR (Neat Film, NaCl) 2996, 2962, 2907, 2858, 1755, 1648, 1514, 1401, 1344, 1270, 1252, 1216, 1068, 1027, 907, 806, 745 cm^{-1} ; HRMS (FAB+) m/z calc'd for $\text{C}_{13}\text{H}_{14}\text{NO}_5$ $[\text{M}+\text{H}]^+$: 264.0872, found 264.0871. *Please note* that a minor amount of keto isomer is present in the spectra, which does not impact the characterization.

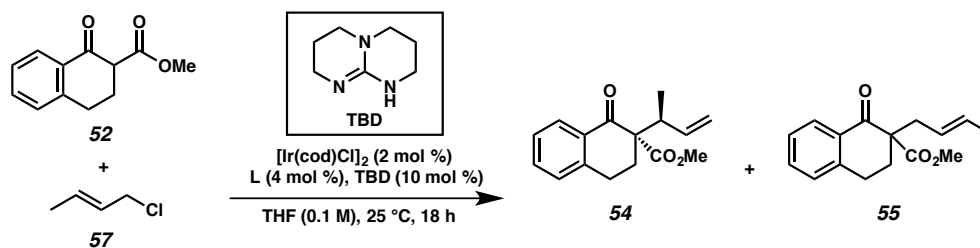


Ethyl 6-bromo-1-oxo-1,2,3,4-tetrahydronaphthalene-2-carboxylate (56h). A solution of LiHMDS (1.8 g, 11 mmol, 2.1 equiv) in THF (20 mL) was added dropwise to a solution of 6-bromo-3,4-dihydronaphthalene-1(2*H*)-one¹⁶ (1.2 g, 5.2 mmol, 1 equiv) in THF (20 mL) via cannula at $-78\text{ }^{\circ}\text{C}$. The reaction was stirred for 1.5 h at $-78\text{ }^{\circ}\text{C}$, whereupon ethyl cyanoformate (0.61 g, 6.2 mmol, 1.2 equiv) was added. The resulting reaction mixture was allowed to warm to ambient temperature and was stirred for 18 h. The reaction was quenched with the addition of saturated NH_4Cl aqueous solution (40 mL) and the aqueous layer was then extracted with Et_2O (3 x 50 mL). The combined organic layers were washed with brine (20 mL), dried over Na_2SO_4 , and concentrated under reduced pressure. The crude residue was purified by CombiFlash EZ Prep (12 g silica, 5 \rightarrow 20% EtOAc/hexanes, 30 min) to provide bromide **56h** (4:1 mixture of enol/keto isomers) as a tan solid (0.63 g, 41%): ^1H NMR (400 MHz, CDCl_3) δ 12.44 (s, 0.8H), 7.90 (d, $J = 8.3$ Hz, 0.2H), 7.64 (d, $J = 8.3$ Hz, 0.8H), 7.46 – 7.38 (m, 1.2H), 7.33 (dd, $J = 2.0, 1.0$ Hz, 0.8H), 4.27 (p, $J = 7.0$ Hz, 2H), 3.58 (dd, $J = 10.0, 4.7$ Hz, 0.2H), 3.09 – 2.90 (m, 0.4H), 2.78 (dd, $J = 8.9, 6.7$ Hz, 1.6H), 2.62 – 2.52 (m, 1.6H), 2.53 – 2.27 (m, 0.4H), 1.34 (t, $J = 7.1$ Hz, 2.4H), 1.29 (t, $J = 7.1$ Hz, 0.6H); ^{13}C NMR (101 MHz, CDCl_3) δ 192.5, 172.7, 170.0, 164.2, 145.4, 141.4, 131.8, 130.7, 130.6, 130.0, 129.9, 129.6, 129.3, 129.1, 126.0, 124.9, 97.4, 61.6, 60.8, 54.4, 27.7, 27.5, 26.3, 20.5, 14.4, 14.3; IR (Neat Film, NaCl) 2979, 2958, 2902, 2848, 1740, 1689, 1645, 1616, 1588, 1558, 1479, 1406, 1377, 1267, 1214, 1195, 1096, 1025, 845, 829, 758 cm^{-1} ; HRMS (FAB+) m/z calc'd for $\text{C}_{13}\text{H}_{14}\text{BrO}_3$ $[\text{M}+\text{H}]^+$: 297.0126, found 297.0134.



2-Acetyl-3,4-dihydronaphthalen-1(2H)-one (56k). To a suspension of NaH (0.49 g, 21 mmol, 2 equiv, 60 wt %) in EtOAc (2 mL) cooled to 0 °C, a solution of 1-tetralone (1.5 g, 10 mmol, 1 equiv) in toluene (0.5 mL) was added dropwise. After H₂ evolution ceased, the resulting solution was heated to 40 °C for 3 h. The reaction mixture was then allowed to cool to ambient temperature, whereupon it was quenched with MeOH (5 mL), poured onto H₂O (20 mL), neutralized with conc. HCl, and extracted with CH₂Cl₂ (3 x 30 mL). The combined organic extracts were washed with brine (30 mL), dried over Na₂SO₄, and concentrated under reduced pressure. The crude residue was purified by silica gel flash column chromatography (10% EtOAc/hexanes) to give ketone **56k** (enol isomer) as a pale yellow solid (0.51 g, 26%): ¹H NMR (400 MHz, CDCl₃) δ 7.94 (dd, *J* = 7.7, 1.4 Hz, 1H), 7.40 (td, *J* = 7.7, 1.4 Hz, 1H), 7.36 – 7.29 (m, 1H), 7.20 (dq, *J* = 7.7, 0.7 Hz, 1H), 2.87 (dd, *J* = 8.5, 6.3 Hz, 2H), 2.68 – 2.59 (m, 2H), 2.24 (s, 3H); ¹³C NMR (101 MHz, CDCl₃) δ 194.0, 177.0, 140.9, 132.0, 131.2, 127.7, 127.0, 126.0, 106.1, 28.4, 24.1, 22.9; IR (Neat Film, NaCl) 3061, 2940, 2893, 2838, 1598, 1567, 1414, 1354, 1294, 1213, 1156, 1079, 1033, 974, 902, 788, 737, 548 cm⁻¹; HRMS (MM: ESI-APCI+) *m/z* calc'd for C₁₂H₁₃O₂ [M+H]⁺: 189.0910, found 189.0908. Please note that the exchangeable enol proton was not observed in the ¹H NMR spectrum.

1.7.2.2 Additional Optimization of Reaction Parameters

Table 1.4 Additional optimization of reaction parameters^a

Entry	L	Base	Additive	Solvent	54:55 ^b	dr of 54 ^b
1	L2	quinoline	LiCl	THF	94:6	4.6:1
2	L2	pyridine	LiCl	THF	89:11	7.2:1
3	L2	triethylamine	LiCl	THF	86:14	4.5:1
4	L2	isoquinoline	LiCl	THF	89:11	11.3:1
5	L2	<i>N</i> -methylimidazole	LiCl	THF	80:20	3.0:1
6	L2	<i>N</i> -methylmorpholine	LiCl	THF	89:11	6.0:1
7	L2	<i>N</i> -methylpiperidine	LiCl	THF	89:11	5.1:1
8	L2	2,4,6-tri- <i>tert</i> -butylpyridine	LiCl	THF	89:11	4.0:1
9	L2	<i>sym</i> -collidine	LiCl	THF	93:7	5.0:1
10	L2	proton sponge	LiCl	THF	92:8	8.3:1
11	L11	proton sponge	LiCl	THF	94:6	6.7:1
12	L11	proton sponge	CsCl	THF	nr	nr
13	L11	proton sponge	TBAC	THF	nr	nr
14	L11	proton sponge	CuCl	THF	88:12	6.8:1
15	L11	proton sponge	LiCl	TBME	80:20	7.7:1
16 ^c	L11	proton sponge	LiCl	toluene	95:5	6.7:1
17	L11	proton sponge	LiCl	dioxane	83:17	4.5:1
18	L11	proton sponge	LiCl	cyclohexane	nr	nr
19	L11	proton sponge	LiCl	CH ₂ Cl ₂	78:22	1.8:1

(S,S,S_a)-L2

(S,S,S_a)-L11

[a] Reactions performed with 0.1 mmol of **53**, 0.2 mmol of **52**, 0.2 mmol of base, and 0.4 mmol of additive. [b] Determined by ¹H NMR analysis of the crude reaction mixture. [c] Trace conversion.

1.7.2.3 General Procedure for Optimization Reactions (Table 1.1 & 1.4)

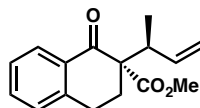
In a nitrogen-filled glove box, to a 1 dram vial (vial A) equipped with a stir bar was added [Ir(cod)Cl]₂ (1.3 mg, 0.0020 mmol, 2 mol %), ligand **L** (0.0040 mmol, 4 mol %), TBD (1.4 mg, 0.010 mmol, 10 mol%), and THF (0.5 mL). Vial A was stirred at 25 °C (ca. 10 min) while another 1 dram vial (vial B) was charged with base, additive, tetralone **52** (0.20 mmol), and THF (0.25 mL). The pre-formed catalyst solution (vial A) was then transferred to vial B followed by 0.25 mL of a solution of crotyl electrophile **53** (0.2 M in THF). The vial was sealed and stirred at 25 °C. After 18 h, the vial was removed from the glove box and filtered through a pad of silica, rinsing with EtOAc. The crude mixture was concentrated and dimethyl maleate (0.050 mmol in 0.5 mL CDCl₃) was added. The NMR yield (measured in reference to dimethyl maleate δ 6.28 ppm (s, 2H)), regioselectivity (branched product to linear product: **54:55**), and diastereoselectivity were determined by ¹H NMR analysis of the crude mixture. The residue was purified by preparatory TLC (10% Et₂O/hexanes) to afford the combined branched (**54/epi-54**) and linear (**55**) products as an inseparable mixture. The major diastereomer (**54**) was isolated by preparatory HPLC (2% EtOAc/hexanes, two Agilent Zorbax RX-sil silica columns in series; flow rate = 15 mL/min; λ = 254 nm) and analyzed by chiral SFC (3% MeOH, 3.5 mL/min, Chiralpak AD-H column, λ = 254 nm).

1.7.2.4 General Procedure for the Iridium-Catalyzed Allylic Alkylation

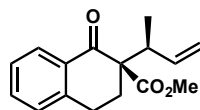
Please note that the absolute configuration was determined only for compound **58f** via x-ray crystallographic analysis. The absolute configuration for all other products

has been inferred by analogy. For respective HPLC and SFC conditions, please refer to Table 1.5.

Methyl (S)-2-((S)-but-3-en-2-yl)-1-oxo-1,2,3,4-tetrahydronaphthalene-2-carboxylate (54). In a nitrogen-filled glove box, to a 1 dram vial (vial A) equipped with a stir bar was added [Ir(cod)Cl]₂ (2.7 mg, 0.0040 mmol, 2 mol %), ligand (*S,S_a*)-**L11** (4.9 mg, 0.0080 mmol, 4 mol %), TBD (2.8 mg, 0.020 mmol, 10 mol %), and THF (1 mL). Vial A was stirred at 25 °C (ca. 10 min) while another 1 dram vial (vial B) was charged with proton sponge (86 mg, 0.40 mmol, 200 mol %), tetralone **52** (82 mg, 0.40 mmol, 200 mol %), LiCl (34 mg, 0.80 mmol, 400 mol %), and THF (0.5 mL). The pre-formed catalyst solution (vial A) was then transferred to vial B followed by a solution of crotyl chloride **57** (18 mg, 0.20 mmol, 100 mol %) in THF (0.5 mL). The vial was sealed and stirred at 25 °C. After 18 h, the vial was removed from the glove box and filtered through a pad of silica, rinsing with EtOAc. The crude mixture was concentrated and dimethyl maleate (0.10 mmol in 0.5 mL CDCl₃) was added. The NMR yield (74%, measured in reference to dimethyl maleate δ 6.28 ppm (s, 2H)), regioselectivity (branched product to linear product, b:l = 93:7), and diastereoselectivity (dr = 6:1) were determined by ¹H NMR analysis of the crude mixture. The residue was purified by preparatory TLC (10% Et₂O/hexanes) to give the isolated yield of the branched and linear products (38.0 mg, 74% combined yield). The diastereomers were separated by preparatory HPLC (2% EtOAc/hexanes, two Agilent Zorbax RX-sil silica columns in series; flow rate = 15 mL/min; λ = 254 nm).

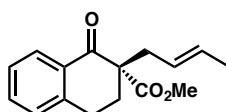


Major diastereomer **54** was isolated as a colorless oil: 96% ee; $[\alpha]_D^{25} -48.5$ (c 0.8, CHCl_3); ^1H NMR (400 MHz, CDCl_3) δ 8.05 (ddd, $J = 7.9, 1.5, 0.5$ Hz, 1H), 7.45 (td, $J = 7.4, 1.5$ Hz, 1H), 7.30 (ddt, $J = 7.3, 6.9, 1.1$ Hz, 1H), 7.20 (dtt, $J = 7.6, 1.3, 0.7$ Hz, 1H), 5.82 (ddd, $J = 17.0, 10.2, 8.9$ Hz, 1H), 5.12 – 4.97 (m, 2H), 3.64 (s, 3H), 3.28 – 3.09 (m, 2H), 2.90 (ddd, $J = 17.4, 4.9, 3.0$ Hz, 1H), 2.43 (ddd, $J = 13.7, 4.7, 3.0$ Hz, 1H), 2.22 (ddd, $J = 13.7, 12.3, 4.9$ Hz, 1H), 1.15 (d, $J = 6.9$ Hz, 3H); ^{13}C NMR (101 MHz, CDCl_3) δ 194.3, 171.2, 143.4, 139.1, 133.6, 132.7, 128.9, 128.2, 126.8, 116.6, 61.2, 52.5, 43.5, 27.8, 26.3, 16.6; IR (Neat Film, NaCl) 3073, 2951, 2850, 1732, 1688, 1600, 1454, 1434, 1290, 1241, 1220, 993, 917, 746 cm^{-1} ; HRMS (MM: ESI-APCI+) m/z calc'd for $\text{C}_{16}\text{H}_{19}\text{O}_3$ $[\text{M}+\text{H}]^+$: 259.1329, found 259.1329; SFC conditions: 3% MeOH, 3.5 mL/min, Chiralpak AD-H column, $\lambda = 254$ nm, t_R (min): major = 5.170, minor = 5.968.



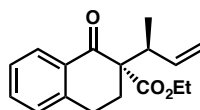
Minor diastereomer **epi-54** (which was inseparable from major diastereomer **54**) was isolated as a colorless oil: ^1H NMR (400 MHz, CDCl_3) δ 8.05 (dd, $J = 7.9, 1.4$ Hz, 1H), 7.46 (td, $J = 7.5, 1.5$ Hz, 1H), 7.34 – 7.27 (m, 1H), 7.23 – 7.16 (m, 1H), 5.98 (ddd, $J = 17.2, 10.3, 7.8$ Hz, 1H), 5.12 – 5.00 (m, 2H), 3.65 (s, 3H), 3.27 – 3.05 (m, 2H), 2.97 – 2.85 (m, 1H), 2.45 (dddd, $J = 19.3, 13.7, 4.7, 3.2$ Hz, 1H), 2.17 – 2.10 (m, 1H), 1.10 (d, $J = 7.0$ Hz, 3H); ^{13}C NMR (101 MHz, CDCl_3) δ 194.5, 171.3, 143.3, 139.9, 133.6, 132.7, 128.8, 128.2, 126.8, 116.2, 61.2, 52.5, 42.5, 28.5, 26.3, 15.0; IR (Neat Film, NaCl) 3072,

2951, 1734, 1686, 1601, 1453, 1438, 1289, 1240, 1219, 1000, 917, 808, 746 cm^{-1} . HRMS (MM: ESI-APCI+) m/z calc'd for $\text{C}_{16}\text{H}_{19}\text{O}_3$ $[\text{M}+\text{H}]^+$: 259.1329, found 259.1332. *Please note* that the provided spectra for **epi-54** reflect the inseparable mixture of **epi-54** and **54**, while the tabulated NMR data is for only **epi-54**.



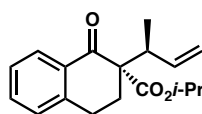
Linear isomer **55** was isolated as a colorless oil: 23% ee; $[\alpha]_{\text{D}}^{25} -5.2$ (c 0.7, CHCl_3); ^1H NMR (400 MHz, CDCl_3) δ 8.14 – 8.06 (m, 1H), 7.60 – 7.47 (m, 1H), 7.36 (tdd, J = 7.8, 1.3, 0.6 Hz, 1H), 7.29 – 7.23 (m, 1H), 5.68 – 5.56 (m, 1H), 5.56 – 5.40 (m, 1H), 3.73 (s, 3H), 3.19 – 3.08 (m, 1H), 2.97 (dt, J = 17.3, 4.9 Hz, 1H), 2.71 (ddt, J = 7.2, 2.5, 1.2 Hz, 2H), 2.57 (dt, J = 13.8, 4.9 Hz, 1H), 2.26 – 2.13 (m, 1H), 1.71 (dq, J = 6.4, 1.2 Hz, 3H); ^{13}C NMR (101 MHz, CDCl_3) δ 195.3, 172.3, 143.5, 133.6, 132.1, 129.8, 128.9, 128.2, 126.9, 125.7, 57.8, 52.6, 37.7, 30.5, 26.0, 18.2; IR (Neat Film, NaCl) 2918, 2850, 1732, 1689, 1601, 1434, 1263, 1236, 1086, 973, 944, 802, 743 cm^{-1} . HRMS (MM: ESI-APCI+) m/z calc'd for $\text{C}_{16}\text{H}_{19}\text{O}_3$ $[\text{M}+\text{H}]^+$: 259.1329, found 259.1324; HPLC conditions: 1% IPA, 1 mL/min, Chiralpak IC column, λ = 254 nm, t_{R} (min): major = 19.785, minor = 24.041.

1.7.2.5 Spectroscopic Data for the Iridium-Catalyzed Allylic Alkylation Products



Ethyl (S)-2-((S)-but-3-en-2-yl)-1-oxo-1,2,3,4-tetrahydronaphthalene-2-carboxylate (58a). Product **58a** was prepared according to the general procedure and isolated by

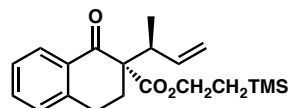
preparatory TLC (10% Et₂O/hexanes) to give the isolated yield of the branched and linear products (30.3 mg, 56% combined yield). The major diastereomer was isolated as a colorless oil by preparatory HPLC (2% EtOAc/hexanes, two Agilent Zorbax RX-sil silica columns in series; flow rate = 15 mL/min; λ = 254 nm): 96% ee; $[\alpha]_D^{25}$ -44.3 (*c* 0.1, CHCl₃); ¹H NMR (400 MHz, CDCl₃) δ 8.04 (dd, *J* = 7.5, 1.5 Hz, 1H), 7.44 (td, *J* = 7.5, 1.5 Hz, 1H), 7.31 – 7.26 (m, 1H), 7.19 (d, *J* = 7.5 Hz, 1H), 5.84 (ddd, *J* = 17.0, 10.2, 8.8 Hz, 1H), 5.20 – 4.96 (m, 2H), 4.24 – 3.95 (m, 2H), 3.26 – 3.08 (m, 2H), 2.89 (ddd, *J* = 17.4, 4.7, 3.0 Hz, 1H), 2.41 (ddd, *J* = 13.7, 4.7, 3.0 Hz, 1H), 2.21 (ddd, *J* = 13.7, 12.3, 4.7 Hz, 1H), 1.19 – 1.09 (m, 6H); ¹³C NMR (101 MHz, CDCl₃) δ 194.4, 170.7, 143.2, 139.1, 133.5, 132.9, 128.8, 128.1, 126.7, 116.5, 61.4, 60.8, 43.4, 28.1, 26.3, 16.6, 14.2; IR (Neat Film, NaCl) 3073, 2978, 2938, 1729, 1693, 1639, 1600, 1454, 1290, 1237, 1220, 1019, 909, 746, 652 cm⁻¹; HRMS (MM: ESI-APCI+) *m/z* calc'd for C₁₇H₂₁O₃ [M+H]⁺: 273.1485, found 273.1493; SFC conditions: 3% MeOH, 3.5 mL/min, Chiralpak AD-H column, λ = 254 nm, *t_R* (min): major = 4.539, minor = 5.113.



Isopropyl (*S*)-2-((*S*)-but-3-en-2-yl)-1-oxo-1,2,3,4-tetrahydronaphthalene-2-

carboxylate (58b). Product **58b** was prepared according to the general procedure and isolated by preparatory TLC (8% EtOAc/hexanes) to give the isolated yield of the branched and linear products (31.3 mg, 55% combined yield). The major diastereomer was isolated as a colorless oil by preparatory HPLC (2% EtOAc/hexanes, two Agilent Zorbax RX-sil silica columns in series; flow rate = 15 mL/min; λ = 254 nm): 96% ee;

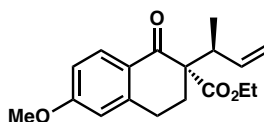
$[\alpha]_D^{25} -61.5$ (*c* 0.6, CHCl_3); ^1H NMR (400 MHz, CDCl_3) δ 8.02 (dd, $J = 7.9, 1.4$ Hz, 1H), 7.43 (td, $J = 7.5, 1.5$ Hz, 1H), 7.37 – 7.22 (m, 1H), 7.18 (d, $J = 7.7$ Hz, 1H), 5.86 (ddd, $J = 17.1, 10.2, 8.8$ Hz, 1H), 5.12 – 4.92 (m, 3H), 3.23 – 3.11 (m, 1H), 3.11 – 2.98 (m, 1H), 2.89 (ddd, $J = 17.5, 5.1, 2.9$ Hz, 1H), 2.39 (ddd, $J = 13.7, 4.8, 2.9$ Hz, 1H), 2.20 (ddd, $J = 13.7, 12.2, 5.0$ Hz, 1H), 1.18 (dd, $J = 6.6, 5.3$ Hz, 6H), 1.02 (d, $J = 6.2$ Hz, 3H); ^{13}C NMR (101 MHz, CDCl_3) δ 194.6, 170.4, 143.0, 139.2, 133.3, 133.2, 128.7, 128.0, 126.7, 116.5, 69.0, 60.6, 43.4, 28.5, 26.3, 21.8, 21.6, 16.7; IR (Neat Film, NaCl) 3073, 2979, 2936, 1724, 1694, 16001, 1456, 1374, 1288, 1244, 1220, 1179, 1144, 1105, 915, 744 cm^{-1} ; HRMS (MM: ESI-APCI+) m/z calc'd for $\text{C}_{18}\text{H}_{23}\text{O}_3$ $[\text{M}+\text{H}]^+$: 287.1642, found 287.1650; HPLC conditions: 1% EtOH/hexanes, 1 mL/min, Chiralpak AD then AD-H column, $\lambda = 254$ nm, t_R (min): major = 10.378, minor = 11.179.



2-(Trimethylsilyl)ethyl (S)-2-((S)-but-3-en-2-yl)-1-oxo-1,2,3,4-

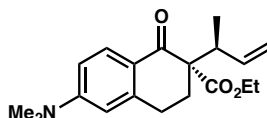
tetrahydronaphthalene-2-carboxylate (58c). Product **58c** was prepared according to the general procedure and isolated by preparatory TLC (5% Et_2O /hexanes) to give the isolated yield of the branched and linear products (18.3 mg, 27% combined yield). The major diastereomer was isolated as a colorless oil by preparatory HPLC (1% EtOAc/hexanes, two Agilent Zorbax RX-sil silica columns in series; flow rate = 15 mL/min; $\lambda = 254$ nm): 89% ee; $[\alpha]_D^{25} -46.0$ (*c* 1.0, CHCl_3); ^1H NMR (400 MHz, CDCl_3) δ 8.04 (dd, $J = 8.0, 1.5$ Hz, 1H), 7.44 (td, $J = 8.0, 1.5$ Hz, 1H), 7.29 (t, $J = 8.0$, 1H), 7.19 (d, $J = 8.0$, 1H), 5.84 (ddd, $J = 17.0, 10.2, 8.8$ Hz, 1H), 5.15 – 5.00 (m, 2H), 4.23 – 4.03

(m, 2H), 3.26 – 3.02 (m, 2H), 2.88 (ddd, $J = 17.4, 4.9, 2.9$ Hz, 1H), 2.40 (ddd, $J = 13.7, 4.7, 2.9$ Hz, 1H), 2.21 (ddd, $J = 13.6, 12.3, 4.9$ Hz, 1H), 1.16 (d, $J = 6.8$ Hz, 3H), 0.89 (dd, $J = 9.3, 8.1$ Hz, 2H), -0.03 (s, 9H); ^{13}C NMR (101 MHz, CDCl_3) δ 194.4, 171.0, 143.3, 139.2, 133.5, 133.0, 128.8, 128.2, 126.7, 116.5, 63.9, 60.8, 43.5, 28.2, 26.3, 17.4, 16.6, -1.5 (3C); IR (Neat Film, NaCl) 3074, 2955, 2899, 1727, 1693, 1601, 1454, 1289, 1251, 1220, 1141, 1041, 918, 860, 837, 746, 695 cm^{-1} ; HRMS (FAB+) m/z calc'd for $\text{C}_{20}\text{H}_{28}\text{O}_3\text{SiNa}$ $[\text{M}+\text{Na}]^+$: 367.1706, found 367.1720; HPLC conditions: 1% EtOH/hexanes, 1 mL/min, Chiralpak AD then AD-H column, $\lambda = 254$ nm, t_R (min): major = 9.018, minor = 9.737.



Ethyl (S)-2-((S)-but-3-en-2-yl)-6-methoxy-1-oxo-1,2,3,4-tetrahydronaphthalene-2-carboxylate (58d). Product **58d** was prepared according to the general procedure and isolated by preparatory TLC (8% Et_2O /hexanes) to give the isolated yield of the branched and linear products (33.0 mg, 55% combined yield). The major diastereomer was isolated as a colorless oil by preparatory HPLC (7% EtOAc/hexanes, two Agilent Zorbax RX-sil silica columns in series; flow rate = 15 mL/min; $\lambda = 254$ nm): 84% ee; $[\alpha]_D^{25} -12.3$ (c 0.5, CHCl_3); ^1H NMR (400 MHz, CDCl_3) δ 8.02 (d, $J = 8.8$ Hz, 1H), 6.81 (ddd, $J = 8.8, 2.6, 0.7$ Hz, 1H), 6.63 (d, $J = 2.6$ Hz, 1H), 5.82 (ddd, $J = 17.1, 10.2, 8.8$ Hz, 1H), 5.12 – 4.97 (m, 2H), 4.20 – 3.99 (m, 2H), 3.84 (s, 3H), 3.26 – 3.08 (m, 2H), 2.84 (ddd, $J = 17.4, 4.9, 3.0$ Hz, 1H), 2.39 (ddd, $J = 13.6, 4.7, 2.9$ Hz, 1H), 2.17 (ddd, $J = 13.7, 12.4, 4.9$ Hz, 1H), 1.16 (t, $J = 7.1$ Hz, 3H), 1.12 (d, $J = 6.9$ Hz, 3H); ^{13}C NMR (101 MHz, CDCl_3) δ 193.0,

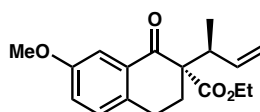
170.8, 163.7, 145.9, 139.2, 130.7, 126.5, 116.4, 113.5, 112.3, 61.4, 60.6, 55.6, 43.3, 27.7, 26.7, 16.5, 14.3; IR (Neat Film, NaCl) 3075, 2964, 2935, 2849, 1727, 1681, 1600, 1494, 1446, 1354, 1253, 1217, 1094, 1022, 917, 854, 824 cm^{-1} ; HRMS (MM: ESI-APCI+) m/z calc'd for $\text{C}_{18}\text{H}_{23}\text{O}_4$ $[\text{M}+\text{H}]^+$: 303.1591, found 303.1583; HPLC conditions: 1% EtOH/hexanes, 1 mL/min, Chiralpak AD then AD-H column, $\lambda = 254$ nm, t_R (min): major = 23.903, minor = 29.498.



Ethyl (S)-2-((S)-but-3-en-2-yl)-6-(dimethylamino)-1-oxo-1,2,3,4-

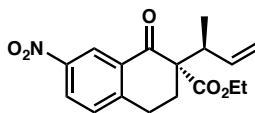
tetrahydronaphthalene-2-carboxylate (58e). Product **58e** was prepared according to the general procedure and isolated by preparatory TLC (10% EtOAc/hexanes) to give the isolated yield of the branched and linear products (29.0 mg, 46% combined yield). The major diastereomer was isolated as a colorless solid by preparatory HPLC (10% EtOAc/hexanes, two Agilent Zorbax RX-sil silica columns in series; flow rate = 15 mL/min; $\lambda = 254$ nm): 86% ee; $[\alpha]_D^{25} +8.5$ (c 0.9, CHCl_3); ^1H NMR (400 MHz, CDCl_3) δ 7.96 (d, $J = 8.9$ Hz, 1H), 6.59 (dd, $J = 9.0, 2.6$ Hz, 1H), 6.31 (d, $J = 2.5$ Hz, 1H), 5.82 (ddd, $J = 17.1, 10.2, 8.7$ Hz, 1H), 5.15 – 4.96 (m, 2H), 4.10 (ddq, $J = 41.7, 10.8, 7.1$ Hz, 2H), 3.31 – 3.12 (m, 2H), 3.04 (s, 6H), 2.78 (ddd, $J = 17.1, 4.8, 3.0$ Hz, 1H), 2.36 (ddd, $J = 13.4, 4.6, 3.0$ Hz, 1H), 2.13 (ddd, $J = 13.4, 12.5, 4.8$ Hz, 1H), 1.18 (t, $J = 7.1$ Hz, 3H), 1.09 (d, $J = 6.8$ Hz, 3H); ^{13}C NMR (101 MHz, CDCl_3) δ 192.1, 171.2, 153.6, 145.5, 139.5, 130.5, 121.9, 116.1, 110.5, 109.2, 61.2, 60.5, 43.2, 40.2 (2C), 27.4, 26.9, 16.4, 14.3; IR (Neat Film, NaCl) 3078, 2935, 1725, 1666, 1595, 1520, 1446, 1370, 1293, 1221,

1196, 1125, 1025, 912, 813 cm^{-1} ; HRMS (MM: ESI-APCI+) m/z calc'd for $\text{C}_{19}\text{H}_{26}\text{NO}_3$ $[\text{M}+\text{H}]^+$: 316.1907, found 316.1912; HPLC conditions: 3% EtOH/hexanes, 1 mL/min, Chiralpak AD then AD-H column, $\lambda = 254$ nm, t_R (min): major = 24.809, minor = 33.026.



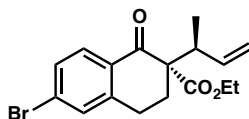
Ethyl (S)-2-((S)-but-3-en-2-yl)-7-methoxy-1-oxo-1,2,3,4-tetrahydronaphthalene-2-carboxylate (58f). Product **58f** was prepared according to the general procedure and isolated by preparatory TLC (8% Et₂O/hexanes) to give the isolated yield of the branched and linear products (41.0 mg, 68% combined yield). The major diastereomer was isolated as a colorless oil by preparatory HPLC (2% EtOAc/hexanes, two Agilent Zorbax RX-sil silica columns in series; flow rate = 15 mL/min; $\lambda = 254$ nm): 94% ee; $[\alpha]_D^{25} -76.8$ (c 0.8, CHCl_3); ^1H NMR (400 MHz, CDCl_3) δ 7.52 (d, $J = 2.8$ Hz, 1H), 7.10 (d, $J = 8.4$ Hz, 1H), 7.03 (dd, $J = 8.4, 2.8$ Hz, 1H), 5.84 (ddd, $J = 17.0, 10.2, 8.9$ Hz, 1H), 5.12 – 4.95 (m, 2H), 4.20 – 4.02 (m, 2H), 3.83 (s, 3H), 3.17 – 3.04 (m, 2H), 2.83 (ddd, $J = 17.2, 5.0, 2.9$ Hz, 1H), 2.39 (ddd, $J = 13.6, 4.6, 2.9$ Hz, 1H), 2.19 (ddd, $J = 13.7, 12.2, 5.0$ Hz, 1H), 1.22 – 1.09 (m, 6H); ^{13}C NMR (101 MHz, CDCl_3) δ 194.4, 170.7, 158.3, 139.0, 135.7, 133.6, 129.9, 122.0, 116.4, 109.6, 61.3, 60.5, 55.5, 43.4, 28.4, 25.4, 16.6, 14.1; IR (Neat Film, NaCl) 3075, 2963, 2936, 2838, 1728, 1688, 1609, 1497, 1463, 1419, 1329, 1279, 1232, 1175, 1143, 1034, 920, 881, 819 cm^{-1} ; HRMS (MM: ESI-APCI+) m/z calc'd for $\text{C}_{18}\text{H}_{23}\text{O}_4$ $[\text{M}+\text{H}]^+$: 303.1591, found 303.1583; HPLC conditions: 1% EtOH/hexanes, 1

mL/min, Chiralpak AD then AD-H column, λ = 254 nm, t_R (min): major = 17.216, minor = 14.519.

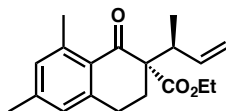


Ethyl (*S*)-2-((*S*)-but-3-en-2-yl)-7-nitro-1-oxo-1,2,3,4-tetrahydronaphthalene-2-

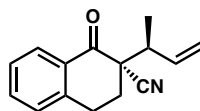
carboxylate (58g). Product **58g** was prepared according to the general procedure and isolated by preparatory TLC (20% EtOAc/hexanes) to give the isolated yield of inseparable branched and linear products (52.0 mg, 82% combined yield): 93% ee; $[\alpha]_D^{25}$ –53.5 (*c* 1.4, CHCl₃); ¹H NMR (400 MHz, CDCl₃, major diastereomer) δ 8.86 (d, *J* = 2.5 Hz, 1H), 8.27 (dd, *J* = 8.4, 2.5 Hz, 1H), 7.39 (dt, *J* = 8.7, 0.9 Hz, 1H), 5.81 (ddd, *J* = 17.1, 10.2, 8.9 Hz, 1H), 5.23 – 4.99 (m, 2H), 4.25 – 3.97 (m, 2H), 3.24 (dddd, *J* = 18.1, 12.3, 4.8, 1.1 Hz, 1H), 3.13 – 2.96 (m, 2H), 2.46 (ddd, *J* = 13.9, 4.8, 2.7 Hz, 1H), 2.24 (ddd, *J* = 13.9, 12.4, 4.9 Hz, 1H), 1.21 – 1.12 (m, 6H); ¹³C NMR (101 MHz, CDCl₃, major diastereomer) δ 192.4, 170.2, 149.7, 147.2, 138.5, 133.8, 130.3, 127.2, 123.4, 117.2, 61.8, 60.8, 43.6, 27.9, 26.7, 16.6, 14.2; IR (Neat Film, NaCl) 3079, 2979, 2938, 1727, 1698, 1612, 1526, 1421, 1347, 1218, 1181, 1018, 931, 740 cm^{–1}; HRMS (FAB+) *m/z* calc'd for C₁₇H₂₀NO₅ [M+H]⁺: 318.1341, found 318.1333; HPLC conditions: 5% EtOH/hexanes, 1 mL/min, Chiralpak AD then AD-H column, λ = 254 nm, t_R (min): major = 14.901, minor = 13.808.



Ethyl (S)-6-bromo-2-((S)-but-3-en-2-yl)-1-oxo-1,2,3,4-tetrahydronaphthalene-2-carboxylate (58h). Product **58h** was prepared according to the general procedure and isolated by silica gel flash column chromatography (5% Et₂O/hexanes) to give the isolated yield of the branched and linear products (44.0 mg, 63% combined yield). The major diastereomer was isolated as a colorless oil by preparatory HPLC (0.8% EtOAc/hexanes, two Agilent Zorbax RX-sil silica columns in series; flow rate = 15 mL/min; λ = 254 nm): 98% ee; $[\alpha]_D^{25}$ -32.7 (*c* 2.3, CHCl₃); ¹H NMR (400 MHz, CDCl₃) δ 7.89 (d, *J* = 8.4 Hz, 1H), 7.42 (ddd, *J* = 8.4, 2.0, 0.8 Hz, 1H), 7.40 – 7.35 (m, 1H), 5.81 (ddd, *J* = 17.1, 10.2, 8.9 Hz, 1H), 5.11 – 4.98 (m, 2H), 4.20 – 3.99 (m, 2H), 3.25 – 3.02 (m, 2H), 2.85 (ddd, *J* = 17.6, 4.9, 2.8 Hz, 1H), 2.40 (ddd, *J* = 13.7, 4.8, 2.9 Hz, 1H), 2.19 (ddd, *J* = 13.8, 12.3, 4.9 Hz, 1H), 1.20 – 1.12 (m, 6H); ¹³C NMR (101 MHz, CDCl₃) δ 193.6, 170.5, 144.9, 138.9, 131.8, 131.7, 130.2, 129.8, 128.7, 116.8, 61.6, 60.7, 43.5, 28.0, 26.1, 16.6, 14.3; IR (Neat Film, NaCl) 3074, 2977, 2936, 1728, 1690, 1587, 1444, 1353, 1279, 1235, 1218, 1182, 1144, 1018, 910, 838, 670 cm⁻¹; HRMS (EI+) *m/z* calc'd for C₁₇H₁₉O₃Br [M]⁺: 350.0518, found 350.0491; SFC conditions: 3% MeOH/hexanes, 3.5 mL/min, Chiralpak AD-H column, λ = 254 nm, *t_R* (min): major = 9.330, minor = 8.616.

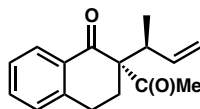


Ethyl (*S*)-2-((*S*)-but-3-en-2-yl)-6,8-dimethyl-1-oxo-1,2,3,4-tetrahydronaphthalene-2-carboxylate (58i**).** Product **58i** was prepared according to the general procedure and isolated by preparatory TLC (9% EtOAc/hexanes) to give the isolated yield of the branched and linear products (31.0 mg, 52% combined yield). The major diastereomer was isolated as a colorless oil by preparatory HPLC (1.5% EtOAc/hexanes, two Agilent Zorbax RX-sil silica columns in series; flow rate = 15 mL/min; λ = 254 nm): 96% ee; $[\alpha]_D^{25}$ –35.1 (*c* 0.3, CHCl₃); ¹H NMR (400 MHz, CDCl₃) δ 7.72 (d, *J* = 2.0 Hz, 1H), 7.22 – 7.08 (m, 1H), 5.85 (ddd, *J* = 17.0, 10.2, 8.9 Hz, 1H), 5.18 – 4.94 (m, 2H), 4.20 – 3.86 (m, 2H), 3.18 – 3.08 (m, 1H), 2.92 (ddd, *J* = 16.9, 11.6, 5.0 Hz, 1H), 2.81 (ddd, *J* = 17.7, 5.6, 3.0 Hz, 1H), 2.45 (ddd, *J* = 13.8, 4.9, 3.0 Hz, 1H), 2.32 (s, 3H), 2.23 (s, 3H), 2.15 (ddd, *J* = 13.8, 11.5, 5.5 Hz, 1H), 1.17 – 1.10 (m, 6H); ¹³C NMR (101 MHz, CDCl₃) δ 194.9, 170.7, 139.2, 138.7, 136.4, 136.0, 135.8, 132.9, 126.0, 116.4, 61.3, 60.2, 42.9, 27.1, 23.3, 21.0, 19.3, 16.5, 14.2; IR (Neat Film, NaCl) 3075, 2976, 2935, 1730, 1688, 1611, 1477, 1445, 1375, 1286, 1236, 1222, 1163, 1139, 1020, 919, 884 cm^{–1}; HRMS (MM: ESI-APCI+) *m/z* calc'd for C₁₉H₂₅O₃ [M+H]⁺: 301.1798, found 301.1801; HPLC conditions: 1% IPA/hexanes, 1 mL/min, Chiralpak IC column, λ = 254 nm, *t_R* (min): major = 9.599, minor = 10.926.



(*R*)-2-((*S*)-but-3-en-2-yl)-1-oxo-1,2,3,4-tetrahydronaphthalene-2-carbonitrile (58j).

Product **58j** was prepared according to the general procedure and isolated by preparatory TLC (17% EtOAc/hexanes) to give the isolated yield of the branched and linear products (43.0 mg, 95% combined yield). The major diastereomer was isolated as a colorless oil by preparatory HPLC (4% EtOAc/hexanes, two Agilent Zorbax RX-sil silica columns in series; flow rate = 15 mL/min; λ = 254 nm): 52% ee; $[\alpha]_D^{25} +11.4$ (c 0.4, CHCl_3); ^1H NMR (400 MHz, CDCl_3) δ 8.03 (dd, J = 8.0, 1.4 Hz, 1H), 7.54 (td, J = 7.5, 1.5 Hz, 1H), 7.45 – 7.32 (m, 1H), 7.29 – 7.25 (m, 1H), 5.91 (ddd, J = 17.0, 10.3, 8.0 Hz, 1H), 5.17 (dt, J = 10.3, 1.1 Hz, 1H), 5.05 (dt, J = 17.1, 1.2 Hz, 1H), 3.27 – 2.89 (m, 3H), 2.43 (ddd, J = 7.1, 5.3, 3.4 Hz, 2H), 1.22 (d, J = 6.8 Hz, 3H); ^{13}C NMR (101 MHz, CDCl_3) δ 190.3, 142.4, 137.1, 134.6, 130.7, 129.0, 128.9, 127.6, 118.5, 118.1, 53.0, 39.8, 28.5, 25.2, 15.3; IR (Neat Film, NaCl) 2975, 2930, 1693, 1600, 1454, 1292, 1223, 1158, 1096, 992, 927, 904, 788, 741 cm^{-1} ; HRMS (FAB+) m/z calc'd for $\text{C}_{15}\text{H}_{16}\text{ON}$ $[\text{M}+\text{H}]^+$: 226.1232, found 226.1240; HPLC conditions: 2% EtOH/hexanes, 1 mL/min, Chiralpak AD then AD-H column, λ = 254 nm, t_R (min): major = 24.027, minor = 26.658.

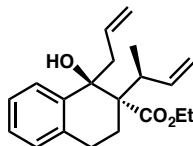


(*R*)-2-acetyl-2-((*S*)-but-3-en-2-yl)-3,4-dihydronaphthalen-1(2*H*)-one (58k).

Product **10k** was prepared according to the general procedure and isolated by preparatory TLC (9% EtOAc/hexanes) to give the isolated yield of the branched and linear products (11.0

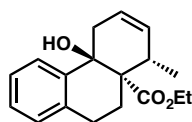
mg, 23% combined yield). The major diastereomer was isolated as a colorless oil by preparatory HPLC (4% EtOAc/hexanes, two Agilent Zorbax RX-sil silica columns in series; flow rate = 15 mL/min; λ = 254 nm): 65% ee; $[\alpha]_D^{25}$ -43.3 (c 0.2, CHCl_3); ^1H NMR (400 MHz, CDCl_3) δ 8.05 (dt, J = 8.0, 0.9 Hz, 1H), 7.47 (td, J = 7.5, 1.5 Hz, 1H), 7.33 – 7.27 (m, 1H), 7.19 (dt, J = 7.7, 1.2, 0.6 Hz, 1H), 5.64 (ddd, J = 17.0, 10.2, 8.8 Hz, 1H), 5.27 – 4.94 (m, 2H), 3.46 – 3.32 (m, 1H), 3.16 (dddt, J = 17.4, 12.6, 4.7, 1.1 Hz, 1H), 2.84 (ddd, J = 17.4, 5.0, 2.7 Hz, 1H), 2.47 (ddd, J = 13.5, 4.7, 2.7 Hz, 1H), 2.12 – 2.06 (m, 1H), 2.09 (s, 3H), 1.06 (d, J = 6.8 Hz, 3H); ^{13}C NMR (101 MHz, CDCl_3) δ 204.7, 196.8, 144.2, 138.3, 134.1, 132.8, 129.0, 128.0, 126.7, 116.5, 68.4, 42.6, 26.9, 25.9, 24.7, 16.3; IR (Neat Film, NaCl) 3076, 2971, 2937, 1708, 1674, 1599, 1446, 1359, 1295, 1231, 1208, 1120, 995, 912, 781, 754, 737 cm^{-1} ; HRMS (FAB+) m/z calc'd for $\text{C}_{16}\text{H}_{19}\text{O}_2$ $[\text{M}+\text{H}]^+$: 243.1385, found 243.1381; HPLC conditions: 1% EtOH/hexanes, 1 mL/min, Chiralpak AD then AD-H column, λ = 254 nm, t_R (min): major = 11.271, minor = 11.944.

1.7.2.6 Experimental Procedures and Spectroscopic Data for the Transformations of Allylic Alkylation Products



Ethyl (1R,2S)-1-allyl-2-((S)-but-3-en-2-yl)-1-hydroxy-1,2,3,4-tetrahydronaphthalene-2-carboxylate (61). Allylmagnesium chloride (0.065 mL, 0.11 mmol, 1.1 equiv, 1.7 M in THF) was added dropwise to a solution of ethyl ester **58a** (27 mg, 1.0 mmol, 1 equiv) in THF (0.5 mL) at -78 °C. The mixture was stirred at -78 °C for

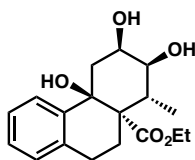
4 h, whereupon the reaction was quenched with a saturated NH_4Cl aqueous solution (1 mL). The aqueous layer was then extracted with EtOAc (3 x 5 mL) and the combined organic layers were washed with brine (5 mL), dried over Na_2SO_4 , and concentrated under reduced pressure. The crude residue was purified by preparatory TLC (9% Et_2O /hexanes) to give alcohol **61** as a colorless oil (31 mg, 71% yield): $[\alpha]_{\text{D}}^{25} +27.3$ (c 0.3, CHCl_3); ^1H NMR (400 MHz, CDCl_3) δ 7.56 – 7.50 (m, 1H), 7.20 – 7.14 (m, 2H), 7.10 – 7.02 (m, 1H), 5.99 (ddd, $J = 17.1, 10.2, 8.5$ Hz, 1H), 5.65 (ddt, $J = 17.2, 10.2, 7.1$ Hz, 1H), 4.98 – 4.85 (m, 2H), 4.85 – 4.76 (m, 1H), 4.68 (ddd, $J = 17.1, 1.9, 1.0$ Hz, 1H), 4.33 – 4.19 (m, 2H), 4.01 (s, 1H), 2.94 – 2.86 (m, 2H), 2.72 (ddt, $J = 8.6, 7.0, 0.8$ Hz, 1H), 2.52 – 2.30 (m, 3H), 2.21 – 2.12 (m, 1H), 1.35 (t, $J = 7.1$ Hz, 3H), 0.80 (d, $J = 7.0$ Hz, 3H); ^{13}C NMR (101 MHz, CDCl_3) δ 175.9, 142.0, 140.7, 134.1, 133.7, 127.9, 126.7, 126.3, 125.5, 117.5, 114.7, 76.6, 61.1, 56.4, 47.2, 41.2, 25.2, 23.3, 16.7, 14.4; IR (Neat Film, NaCl) 3492, 3075, 2978, 2930, 2853, 1732, 1694, 1640, 1455, 1376, 1267, 1213, 1026, 914, 766, 732, 665 cm^{-1} ; HRMS (FAB+) m/z calc'd for $\text{C}_{20}\text{H}_{27}\text{O}_3$ $[\text{M}+\text{H}]^+$: 315.1960, found 315.1954.



Ethyl (4bR,8S,8aS)-4b-hydroxy-8-methyl-5,8,9,10-tetrahydrophenanthrene-

8a(4bH)-carboxylate (62). A solution of bis-olefin **61** (4.0 mg, 0.013 mmol, 1 equiv), Hoveyda-Grubbs Catalyst-II (1.4 mg, 2.6 μmol , 0.2 equiv), and CH_2Cl_2 (0.5 mL) was stirred at ambient temperature for 18 h, whereupon the reaction mixture was concentrated under reduced pressure. The crude residue was purified by preparatory TLC (9%

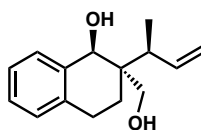
EtOAc/hexanes) to give tricycle **62** as a colorless oil (3.0 mg, 81% yield): $[\alpha]_D^{25} +7.9$ (c 0.2, CHCl₃); ¹H NMR (400 MHz, CDCl₃) δ 7.55 – 7.46 (m, 1H), 7.22 – 7.16 (m, 2H), 7.13 – 7.06 (m, 1H), 5.82 (ddt, J = 10.1, 5.1, 2.6 Hz, 1H), 5.56 (ddt, J = 10.1, 2.6, 1.8 Hz, 1H), 3.96 (qd, J = 7.1, 1.0 Hz, 2H), 3.36 (ddt, J = 18.0, 3.8, 2.6 Hz, 1H), 3.09 – 2.96 (m, 1H), 2.96 – 2.78 (m, 2H), 2.70 – 2.57 (m, 1H), 2.49 – 2.38 (m, 1H), 2.28 – 2.11 (m, 1H), 1.12 (d, J = 7.6 Hz, 3H), 1.07 (t, J = 7.1 Hz, 3H); ¹³C NMR (101 MHz, CDCl₃) δ 172.2, 140.0, 136.0, 130.6, 129.6, 127.9, 126.3, 125.1, 124.1, 70.5, 60.0, 52.2, 36.8, 36.4, 26.4, 25.5, 16.2, 14.2; IR (Neat Film, NaCl) 3488, 3019, 2972, 2934, 1727, 1715, 1451, 1368, 1293, 1251, 1177, 1027, 887, 761, 694 cm⁻¹; HRMS (FAB+) m/z calc'd for C₁₈H₂₃O₃ [M+H]⁺: 287.1647, found 287.1637. Please note that the exchangeable hydroxy proton was not observed in the ¹H NMR spectrum.



Ethyl (4bR,6R,7S,8R,8aS)-4b,6,7-trihydroxy-8-methyl-5,6,7,8,9,10-

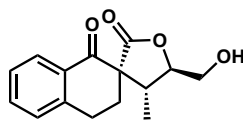
hexahydrophenanthrene-8a(4bH)-carboxylate (63). A solution of olefin **62** (18 mg, 0.058 mmol, 1 equiv), K₂OsO₄ (1.0 mg, 2.8 μ mol, 0.05 equiv), *N*-methylmorpholine *N*-oxide (11 mg, 0.093 mmol, 1.6 equiv), and THF/H₂O (3:1, 0.2 mL) was stirred at ambient temperature for 18 h, whereupon the reaction was quenched with saturated Na₂S₂O₃ aqueous solution (1 mL). The aqueous layer was then extracted with EtOAc (5 x 5 mL) and the combined organic layers were washed with brine (5 mL), dried over Na₂SO₄, and concentrated under reduced pressure. The crude residue was purified by preparatory TLC (17% EtOAc/hexanes) to give triol **63** as a colorless oil (11 mg, 59% yield): $[\alpha]_D^{25} +3.8$ (c

0.2, CHCl₃); ¹H NMR (400 MHz, CDCl₃) δ 7.34 (dd, *J* = 7.8, 1.5 Hz, 1H), 7.19 (td, *J* = 7.4, 1.5 Hz, 1H), 7.16 – 7.05 (m, 2H), 4.26 (q, *J* = 3.3 Hz, 1H), 3.82 (q, *J* = 7.1 Hz, 2H), 3.74 (dd, *J* = 11.0, 3.5 Hz, 1H), 3.70 – 3.56 (m, 1H), 3.06 – 2.92 (m, 3H), 2.78 (dd, *J* = 14.6, 3.0 Hz, 1H), 2.61 – 2.44 (m, 1H), 2.24 – 2.05 (m, 2H), 1.10 (d, *J* = 6.8 Hz, 3H), 0.90 (t, *J* = 7.1 Hz, 3H); ¹³C NMR (101 MHz, CDCl₃) δ 172.9, 139.4, 136.9, 129.6, 128.4, 125.8, 123.8, 73.0, 72.7, 70.5, 60.4, 56.1, 37.3, 35.3, 25.9, 25.1, 13.9, 12.3; IR (Neat Film, NaCl) 3284, 2970, 2928, 1723, 1452, 1382, 1259, 1234, 1189, 1103, 1054, 1020, 867, 834, 763, 722 cm⁻¹; HRMS (MM: ESI-APCI-) *m/z* calc'd for C₁₈H₂₄O₅Cl [M+Cl]⁻: 355.1318, found 355.1326. Please note that two of the exchangeable hydroxy protons were not observed in the ¹H NMR spectrum.



(1*R*,2*R*)-2-((*S*)-But-3-en-2-yl)-2-(hydroxymethyl)-1,2,3,4-tetrahydronaphthalen-1-ol (64). DIBAL (0.071 mL, 0.40 mmol, 4 equiv) was added dropwise to a solution of ethyl ester **58a** (27 mg, 1.0 mmol, 1 equiv) in THF (0.6 mL) at –78 °C. The mixture was stirred at –78 °C for 6 h, whereupon the reaction was quenched with a saturated Rochelle's salt aqueous solution (1 mL) and stirred for 18 h at ambient temperature. The aqueous layer was then extracted with EtOAc (3 x 5 mL) and the combined organic layers were washed with brine (5 mL), dried over Na₂SO₄, and concentrated under reduced pressure. The crude residue was purified by preparatory TLC (20% EtOAc/hexanes) to give diol **64** as a colorless oil (10 mg, 43% yield): [α]_D²⁵ +105.7 (*c* 0.7, CHCl₃); ¹H NMR (400 MHz, CDCl₃) δ 7.49 – 7.44 (m, 1H), 7.24 – 7.18 (m, 2H), 7.11 (ddd, *J* = 5.5, 2.4, 1.2 Hz, 1H),

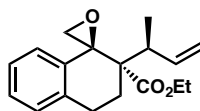
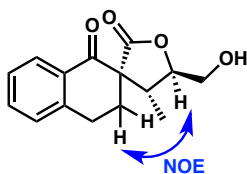
6.30 (ddd, $J = 17.2, 10.1, 9.1$ Hz, 1H), 4.99 (ddd, $J = 10.1, 2.1, 0.6$ Hz, 1H), 4.90 (ddd, $J = 17.3, 2.1, 0.9$ Hz, 1H), 4.80 (d, $J = 7.3$ Hz, 1H), 3.81 (dd, $J = 11.3, 5.5$ Hz, 1H), 3.59 (dd, $J = 11.4, 3.7$ Hz, 1H), 2.91 – 2.66 (m, 2H), 2.65 – 2.57 (m, 2H), 2.19 (bs, 1H), 1.75 (ddd, $J = 13.8, 7.2, 6.5$ Hz, 1H), 1.64 – 1.50 (m, 1H), 1.04 (d, $J = 7.0$ Hz, 3H); ^{13}C NMR (101 MHz, CDCl_3) δ 144.5, 138.9, 135.9, 128.4, 127.3, 127.0, 126.5, 115.1, 75.3, 67.3, 43.7, 39.8, 25.8, 25.7, 15.5; IR (Neat Film, NaCl) 3404, 3069, 3020, 2932, 1634, 1602, 1455, 1417, 1374, 1268, 1217, 1191, 1045, 991, 913, 774, 741, 641 cm^{-1} ; HRMS (FAB+) m/z calc'd for $\text{C}_{15}\text{H}_{19}\text{O}_2$ $[(\text{M}+\text{H})-\text{H}_2]^+$: 231.1385, found 231.1385. Please note that a minor amount of epimeric product is present in the ^1H NMR spectrum.



(3*S*,4*R*)-5-(Hydroxymethyl)-4-methyl-3',4,4',5-tetrahydro-1'*H*,2*H*-spiro[furan-3,2'-naphthalene]-1',2-dione (65). A solution of methyl ester **54** (20.0 mg, 0.077 mmol, 1 equiv), K_2OsO_4 (3.0 mg, 0.0081 mmol, 0.11 equiv), *N*-methylmorpholine *N*-oxide (15 mg, 0.12 mmol, 1.6 equiv), and THF/ H_2O (3:1, 0.4 mL) was stirred at ambient temperature for 12 h, whereupon a second addition of K_2OsO_4 and *N*-methylmorpholine *N*-oxide was added and the reaction was stirred for an additional 24 h. The reaction was quenched with saturated $\text{Na}_2\text{S}_2\text{O}_3$ aqueous solution (1 mL). The aqueous layer was then extracted with EtOAc (5 x 5 mL) and the combined organic layers were washed with brine (5 mL), dried over Na_2SO_4 , and concentrated under reduced pressure. The crude residue was purified by preparatory TLC (33% EtOAc/hexanes) to give lactone **65** as a colorless oil (13 mg, 65% yield): $[\alpha]_{\text{D}}^{25} +7.0$ (c 0.2, CHCl_3); ^1H NMR (400 MHz, CDCl_3)

δ 8.07 (dd, $J = 7.9, 1.4$ Hz, 1H), 7.52 (td, $J = 7.5, 1.5$ Hz, 1H), 7.38 – 7.31 (m, 1H), 4.26 (ddd, $J = 10.5, 5.6, 2.4$ Hz, 1H), 4.01 (ddd, $J = 12.8, 7.0, 2.5$ Hz, 1H), 3.82 (dt, $J = 12.4, 6.0$ Hz, 1H), 3.59 (dq, $J = 10.5, 7.0$ Hz, 1H), 3.47 – 3.34 (m, 1H), 2.98 (dt, $J = 17.0, 3.8$ Hz, 1H), 2.32 – 2.25 (m, 2H), 1.94 (t, $J = 6.7$ Hz, 1H), 1.03 (d, $J = 7.0$ Hz, 3H); ^{13}C NMR (101 MHz, CDCl_3) δ 192.6, 173.5, 144.0, 134.4, 131.8, 129.0, 128.8, 127.2, 84.3, 62.9, 57.7, 36.1, 25.6, 25.3, 10.8; IR (Neat Film, NaCl) 3444, 2928, 2851, 1760, 1682, 1599, 1455, 1308, 1239, 1217, 1166, 1094, 1056, 1021, 914, 759, 733, 656 cm^{-1} ; HRMS (FAB+) m/z calc'd for $\text{C}_{15}\text{H}_{17}\text{O}_4$ $[\text{M}+\text{H}]^+$: 261.1127, found 261.1129.

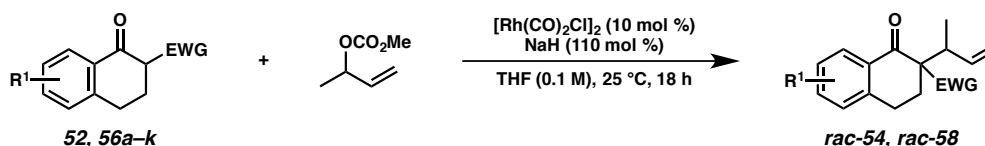
NOE correlation:



Ethyl (1R,2S)-2-((S)-but-3-en-2-yl)-3,4-dihydro-2H-spiro[naphthalene-1,2'-oxirane]-2-carboxylate (66). $(\text{CH}_3)_3\text{SOI}$ (35 mg, 0.17 mmol, 1.7 equiv) and NaH (5.0 mg, 0.15 mmol, 1.5 equiv, 60 wt %) were dissolved in DMSO (1.5 mL). The mixture was stirred for 20 min at ambient temperature, whereupon a solution of ketone **58a** (27 mg, 0.10 mmol, 1 equiv) in DMSO (1.0 mL) was added. The resulting solution was stirred for an additional 18 h. H_2O (2.0 mL) was then added to the reaction mixture and the aqueous layer was extracted with EtOAc (3 x 5 mL). The organic layer was washed with H_2O (5.0 mL) and brine (5.0 mL), dried over Na_2SO_4 , and concentrated under reduced pressure.

The crude residue was purified by preparatory TLC (3% Et₂O/hexanes) to give epoxide **66** as a colorless oil (23 mg, 82% yield): $[\alpha]_D^{25} +10.4$ (c 0.1, CHCl₃); ¹H NMR (400 MHz, CDCl₃) δ 7.23 – 7.15 (m, 3H), 7.15 – 7.07 (m, 1H), 6.07 (ddd, J = 17.1, 10.3, 8.1 Hz, 1H), 4.93 (ddd, J = 10.2, 1.9, 0.8 Hz, 1H), 4.74 (ddd, J = 17.1, 2.0, 1.1 Hz, 1H), 4.29 – 4.06 (m, 2H), 3.01 – 2.94 (m, 1H), 2.98 (d, J = 5.1 Hz, 1H), 2.93 – 2.82 (m, 1H), 2.82 – 2.71 (m, 1H), 2.62 (d, J = 5.1 Hz, 1H), 2.35 (ddd, J = 14.0, 8.2, 5.7 Hz, 1H), 2.09 (ddd, J = 14.2, 6.9, 5.5 Hz, 1H), 1.29 (t, J = 7.1 Hz, 3H), 0.99 (d, J = 6.9 Hz, 3H); ¹³C NMR (101 MHz, CDCl₃) δ : 173.4, 140.9, 138.2, 136.4, 127.8, 127.4, 126.8, 123.4, 115.1, 61.0, 59.1, 56.5, 51.9, 40.2, 28.0, 26.2, 15.8, 14.4; IR (Neat Film, NaCl) 3073, 2977, 2938, 1723, 1489, 1456, 1368, 1296, 1255, 1233, 1213, 1134, 1096, 1025, 915, 760 cm⁻¹; HRMS (FAB+) m/z calc'd for C₁₈H₂₁O₃ [(M+H)–H₂]⁺: 285.1491, found 285.1487. Please note that the relative stereochemistry of **16** has been assigned via analogy to **11** and **14**.

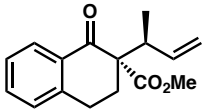
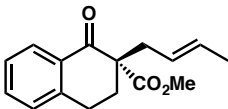
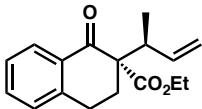
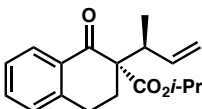
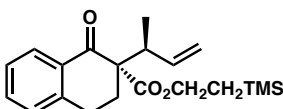
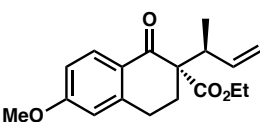
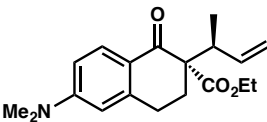
1.7.2.7 Determination of Enantiomeric Excess

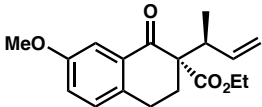
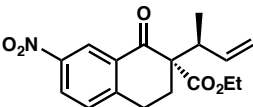
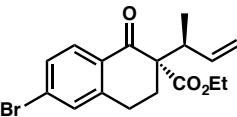
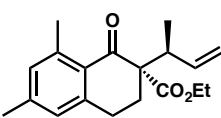
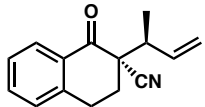
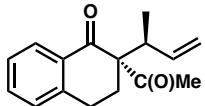


Please note racemic products (**rac-54**, **rac-58**) were synthesized as follows: in a nitrogen-filled glove box, to a 1 dram vial (vial A) equipped with a stir bar was added $[\text{Rh}(\text{CO})_2\text{Cl}]_2$ (10 mol %) and but-3-en-2-yl methyl carbonate (140 mol %) in THF. Vial A was stirred at 25 °C (ca. 10 min) while another 1 dram vial (vial B) was charged with tetralone **52, 56a-k** (100 mol %), NaH (110 mol %), and THF. The pre-formed catalyst solution (vial A) was then transferred to vial B and the vial was sealed and stirred at 25 °C. After 18 h, the vial was removed from the glove box and filtered through celite,

rinsing with EtOAc to give the crude racemic product. The residue was purified as in the general procedure for the Ir-catalyzed allylic alkylation.

Table 1.5 Determination of enantiomeric excess

Entry	Product	Assay Conditions	Retention time of major isomer (min)	Retention time of minor isomer (min)	%ee
1		SFC Chiralpak AD-H 3% MeOH isocratic, 3.5 mL/min	5.170	5.968	96%
2		HPLC Chiralpak IC 1% IPA isocratic, 1 mL/min	19.785	24.041	23%
3		SFC Chiralpak AD-H 3% MeOH isocratic, 3.5 mL/min	4.539	5.113	96%
4		HPLC Chiralpak AD then AD-H 1% EtOH/hexanes isocratic, 1 mL/min	10.378	11.179	96%
5		HPLC Chiralpak AD then AD-H 1% EtOH/hexanes isocratic, 1 mL/min	9.018	9.737	89%
6		HPLC Chiralpak AD then AD-H 1% EtOH/hexanes isocratic, 1 mL/min	23.903	29.498	84%
7		HPLC Chiralpak AD then AD-H 3% EtOH/hexanes isocratic, 1 mL/min	24.809	33.026	86%

Entry	Product	Assay Conditions	Retention time of major isomer (min)	Retention time of minor isomer (min)	%ee
8		HPLC Chiralpak AD then AD-H 1% EtOH/hexanes isocratic, 1 mL/min	17.216	14.519	94%
9		HPLC Chiralpak AD then AD-H 5% EtOH/hexanes isocratic, 1 mL/min	14.901	13.808	93%
10		SFC Chiralpak AD-H 3% MeOH isocratic, 3.5 mL/min	9.330	8.616	98%
11		HPLC Chiralpak IC 1% IPA/hexanes isocratic, 1 mL/min	9.599	10.926	96%
12		HPLC Chiralpak AD then AD-H 2% EtOH/hexanes isocratic, 1 mL/min	24.027	26.658	52%
13		HPLC Chiralpak AD then AD-H 1% EtOH/hexanes isocratic, 1 mL/min	11.271	11.944	65%

1.8 REFERENCES AND NOTES

- (1) (a) Douglas, C. J.; Overman, L. E. *Proc. Natl. Acad. Sci. U.S.A.* **2004**, *101*, 5363–5367; (b) Das, J. P.; Marek, I. *Chem. Commun.* **2011**, *47*, 4593–4623; (c) Quasdorf, K. W.; Overman, L. E. *Nature* **2014**, *516*, 181–191; d) Corey, E. J.; Guzman-Perez, A. *Angew. Chem. Int. Ed.* **1998**, *37*, 388–401; e) Christoffers, J.; Mann, A. *Angew. Chem. Int. Ed.* **2001**, *40*, 4591–4597; (f) Trost, B. M.; Jiang, C. *Synthesis* **2006**,

- 369–396; (g) Denissova, I.; Barriault, L. *Tetrahedron*, **2003**, *59*, 10105–10146; (h) Ling, T.; Rivas, F. *Tetrahedron* **2016**, *72*, 6729–6777; (i) Liu, Y.; Han, S.-J.; Liu, W.-B.; Stoltz, B. M. *Acc. Chem. Res.* **2015**, *48*, 740–751.
- (2) For select reviews, see: (a) Krause, N.; Hoffman-Röder, A. *Synthesis* **2001**, 171–196; (b) Christoffers, J.; Koripelly, G.; Rosiak, A.; Rössle M. *Synthesis* **2007**, 1279–1300; (c) Ito, H.; Taguchi, T. *Chem. Soc. Rev.* **1999**, *28*, 43–50; (d) Castro, A. M. M. *Chem. Rev.* **2004**, *104*, 2939–3002; (e) Ilardi, E. A.; Stivala, C. E.; Zakarian, A. *Chem. Soc. Rev.* **2009**, *38*, 3133–3148.
- (3) For select examples and references therein, see: (a) Streuff, J.; White, D. E.; Virgil, S. C.; Stoltz, B. M. *Nat. Chem.* **2010**, *2*, 192–196; (b) Wong, K. C.; Ng, E.; Wong, W.-T.; Chiu, P. *Chem. Eur. J.* **2016**, *22*, 3709–3712; (c) Jolit, A.; Walleser, P. M.; Yap, G. P. A.; Tius, M. A. *Angew. Chem. Int. Ed.* **2014**, *53*, 6180–6183; (d) Trost, B. M.; Ryan, M. C. *J. Am. Chem. Soc.* **2016**, *138*, 2981–2984; (e) Trost, B. M.; Silverman, S. M.; Stambuli, J. P. *J. Am. Chem. Soc.* **2011**, *133*, 19483–19497; (f) Zhao, J.; Fang, B.; Luo, W.; Hao, X.; Liu, X.; Lin, L.; Feng, X. *Angew. Chem. Int. Ed.* **2015**, *54*, 241–244; (g) Gunes, Y.; Arcelik, N.; Sahin, E.; Fleming, F. F.; Altundas, R. *Eur. J. Org. Chem.* **2015**, 6679–6686; (h) Enders, D.; Knopp, M.; Runsink, J.; Raabe, G. *Angew. Chem. Int. Ed.* **1995**, *34*, 2278–2280.
- (4) For select reviews, see: (a) Helmchen, G.; Dahnz, A.; Dübon, P.; Schelwies, M.; Weihofen, R. *Chem. Commun.* **2007**, 675–691; (b) Hartwig, J. F.; Pouy, M. J. *Top. Organomet. Chem.* **2011**, *34*, 169–208; (c) Liu, W.-B.; Xia, J.-B.; You, S.-L. *Top.*

- Organomet. Chem.* **2012**, *38*, 155–208; (d) Hethcox, J. C.; Shockley, S. E.; Stoltz, B. M. *ACS Catal.* **2016**, *6*, 6207–6213.
- (5) Kanayama, T.; Yoshida, K.; Miyabe, H.; Takemoto, K. *Angew. Chem. Int. Ed.* **2003**, *42*, 2054–2056.
- (6) (a) Liu, W.-B.; Reeves, C. M.; Stoltz, B. M. *J. Am. Chem. Soc.* **2013**, *135*, 17298–17301; (b) Liu, W.-B.; Reeves, C. M.; Virgil, S. C.; Stoltz, B. M. *J. Am. Chem. Soc.* **2013**, *135*, 10626–10629; (c) Krautwald, S.; Sarlah, D.; Schafroth, M. A.; Carreira, E. M. *Science* **2013**, *340*, 1065–1068; (d) Chen, W.; Chen, M.; Hartwig, J. F. *J. Am. Chem. Soc.* **2014**, *136*, 15825–15828; (e) Liu, W.-B.; Okamoto, N.; Alexy, E. J.; Hong, A. Y.; Tran, K.; Stoltz, B. M. *J. Am. Chem. Soc.* **2016**, *138*, 5234–5237.
- (7) (a) Jiang, X.; Chen, W.; Hartwig, J. F. *Angew. Chem. Int. Ed.* **2016**, *55*, 5819–5823; (b) Huo, X.; He, R.; Zhang, W. *J. Am. Chem. Soc.* **2016**, *138*, 11093–11096.
- (8) (a) Chen, W.; Hartwig, J. F. *J. Am. Chem. Soc.* **2013**, *135*, 2068–2071; (b) Chen, W.; Hartwig, J. F. *J. Am. Chem. Soc.* **2014**, *136*, 377–382; (c) Krautwald, S.; Schafroth, M. A.; Sarlah, D.; Carreira, E. M. *J. Am. Chem. Soc.* **2014**, *136*, 3020–3023; (d) Sandmeier, T.; Krautwald, S.; Zipfel, H. F.; Carreira, E. M. *Angew. Chem. Int. Ed.* **2015**, *54*, 14363–14367.
- (9) Allen, A. E.; MacMillan, D. W. C. *Chem. Sci.* **2012**, *3*, 633–658.
- (10) Bartels, B.; Helmchen, G. *Chem. Commun.* **1999**, 741–742; (b) Alexakis, A.; Polet, D. *Org. Lett.* **2004**, *6*, 3529–3532; (c) Polet, D.; Alexakis, A.; Tissot-Croset, K.; Corminboeuf, C.; Ditrach, K.; *Chem. Eur. J.* **2006**, *12*, 3596–3609.

- (11) (a) Liu, W.-B.; Zheng, C.; Zhuo, C.-X.; Dai, L.-X.; You, S.-L. *J. Am. Chem. Soc.* **2012**, *134*, 4812–4821; (b) Zhang, X.; Liu, W.-B.; Cheng, Q.; You, S.-L. *Organometallics* **2016**, *35*, 2467–2472 (c) Cheng, Q.; Wang, Y.; You, S.-L. *Angew. Chem. Int. Ed.* **2016**, *55*, 3496–3499.
- (12) Reeves, C. M.; Behenna, D. C.; Stoltz, B. M. *Org. Lett.* **2014**, *16*, 2314–2317.
- (13) Seitz, M.; Reiser, O. *Curr. Opin. Chem. Biol.* **2005**, *9*, 285–292.
- (14) Liu, W.-B.; He, H.; Dai, L.-X.; You, S.-L. *Synthesis* **2009**, 2076–2082.
- (15) Defieber, C.; Ariger, M. A.; Moriel, P.; Carreira, E. M. *Angew. Chem. Int. Ed.* **2007**, *46*, 3139–3143.
- (16) Cui, L.-Q.; Dong, Z.-L.; Liu, K.; Zhang, C. *Org. Lett.* **2011**, *13*, 6488–6491.
- (17) Manitto, P.; Monti, D.; Zanzola, S.; Speranza, G. *J. Org. Chem.* **1997**, *62*, 6658–6665.
- (18) Breitenlechner, S.; Bach, T. *Angew. Chem. Int. Ed.* **2008**, *47*, 7957–7959.
- (19) Paolo, B.; Diego, V.; Giampietro, B.; Roberto, S. U.S. Patent, 166800 A1, Sept. 4, 2003.
- (20) Ankner, T.; Fridén-Saxin, M.; Pemberton, N.; Seifert, T.; Grøtli, M.; Luthman, K.; Hilmersson, G. *Org. Lett.* **2010**, *12*, 2210–2213.

APPENDIX 1

Spectra Relevant to Chapter 1:

Stereoselective Iridium-Catalyzed Allylic Alkylation

Reactions with Crotyl Chloride

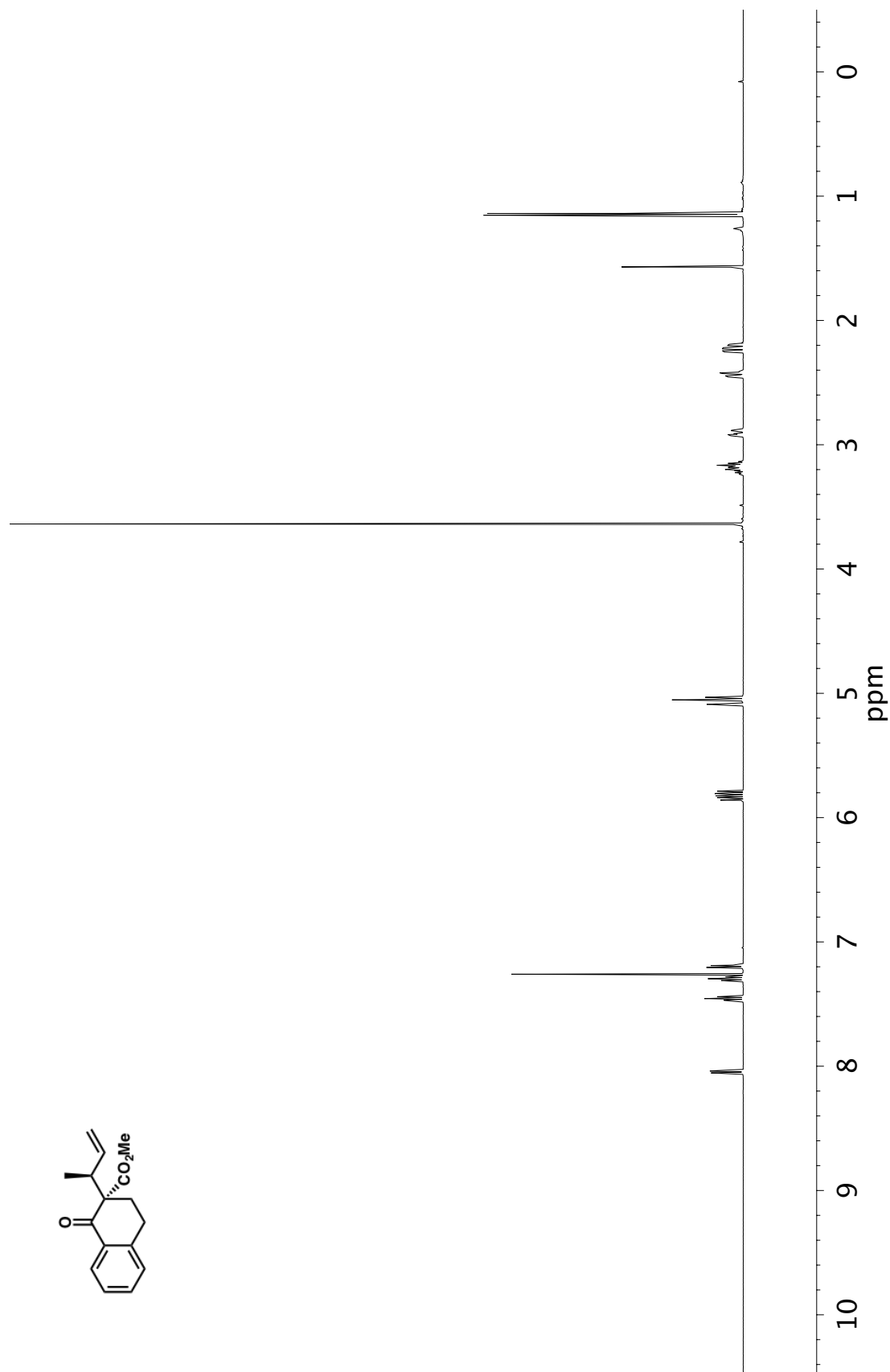


Figure A1.1 ¹H NMR (400 MHz, CDCl₃) of compound 54

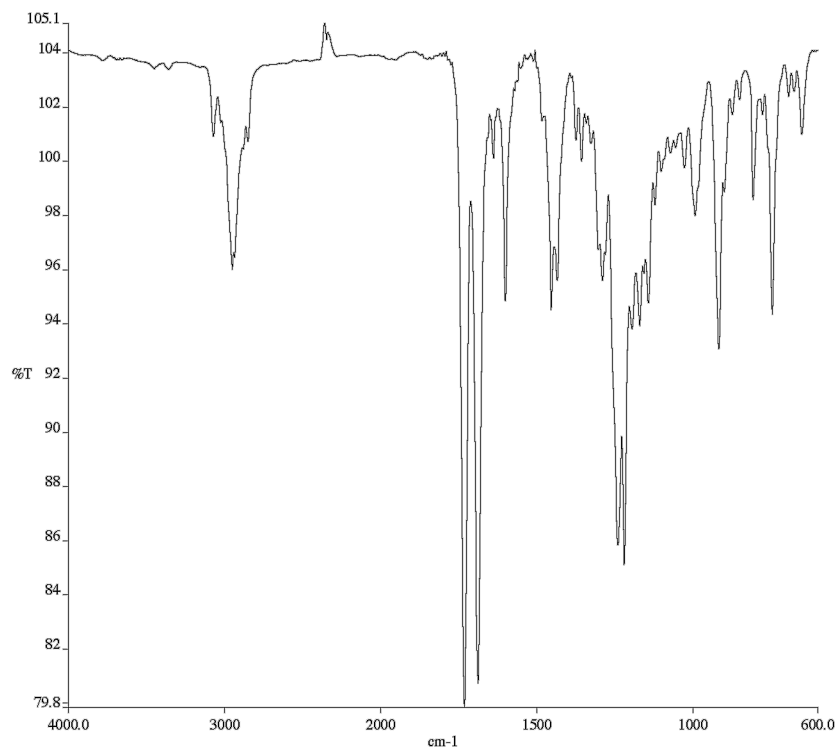


Figure A1.2 Infrared spectrum (Thin Film, NaCl) of compound **54**

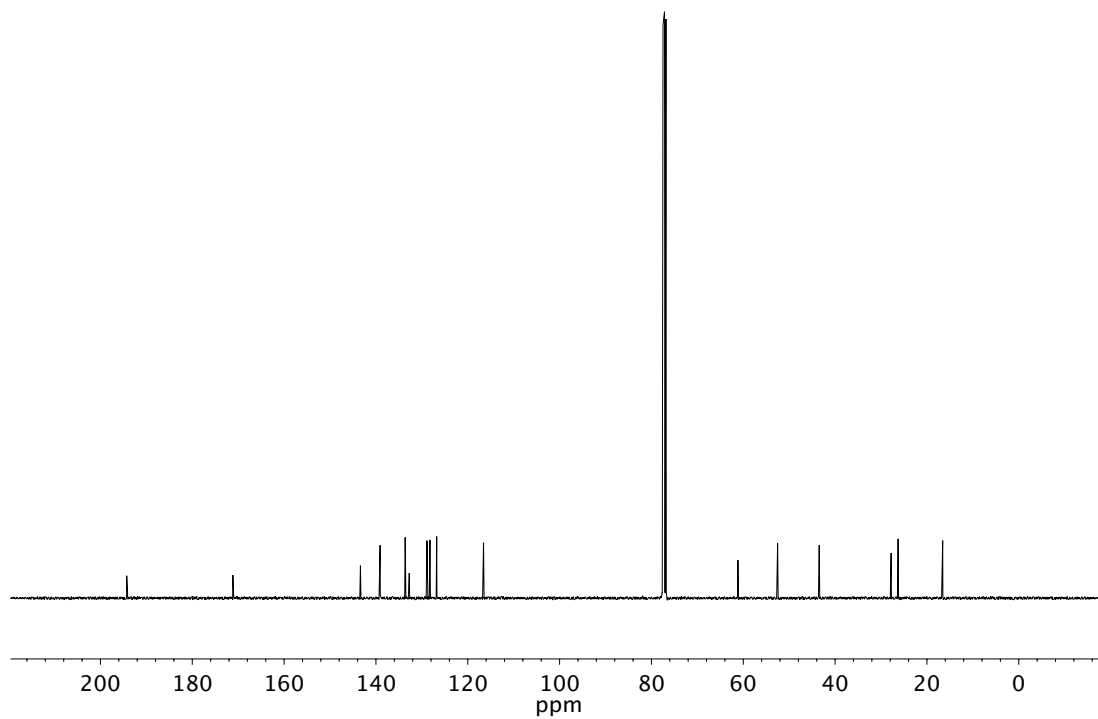


Figure A1.3 ¹³C NMR (101 MHz, CDCl₃) of compound **54**

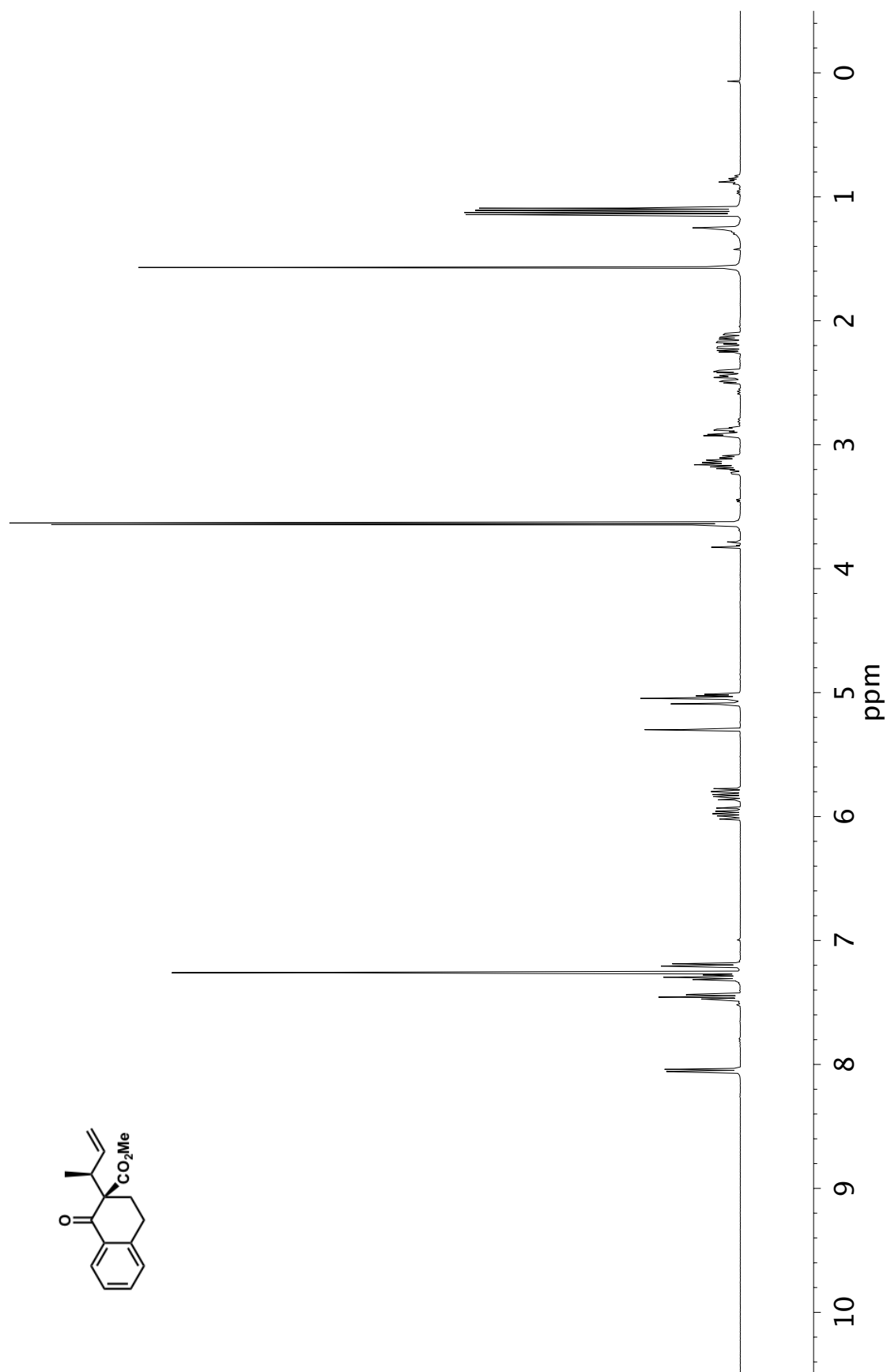


Figure A1.4 ^1H NMR (400 MHz, CDCl_3) of compound **epi-54**

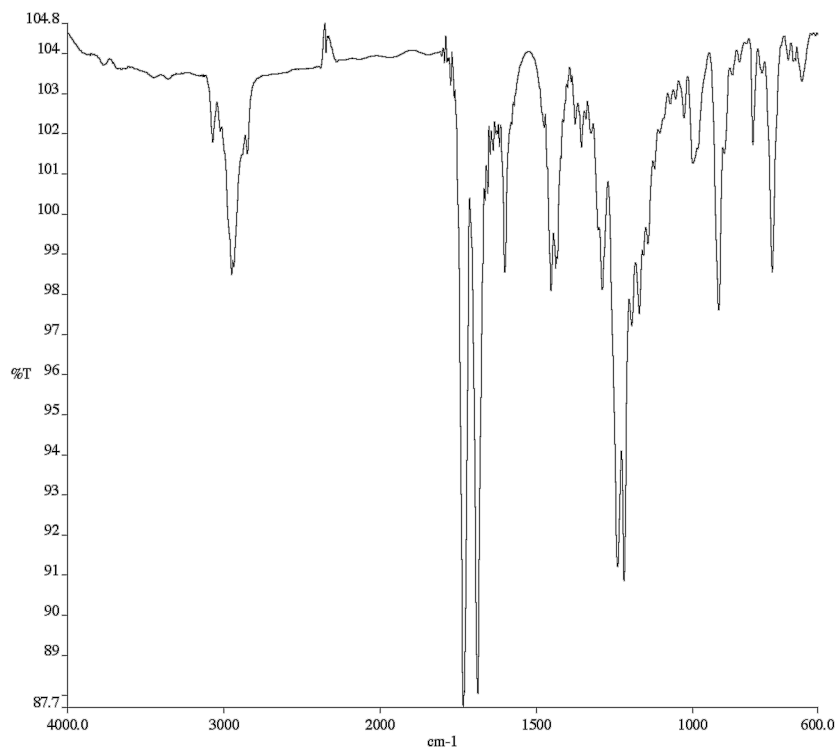


Figure A1.5 Infrared spectrum (Thin Film, NaCl) of compound **epi-54**

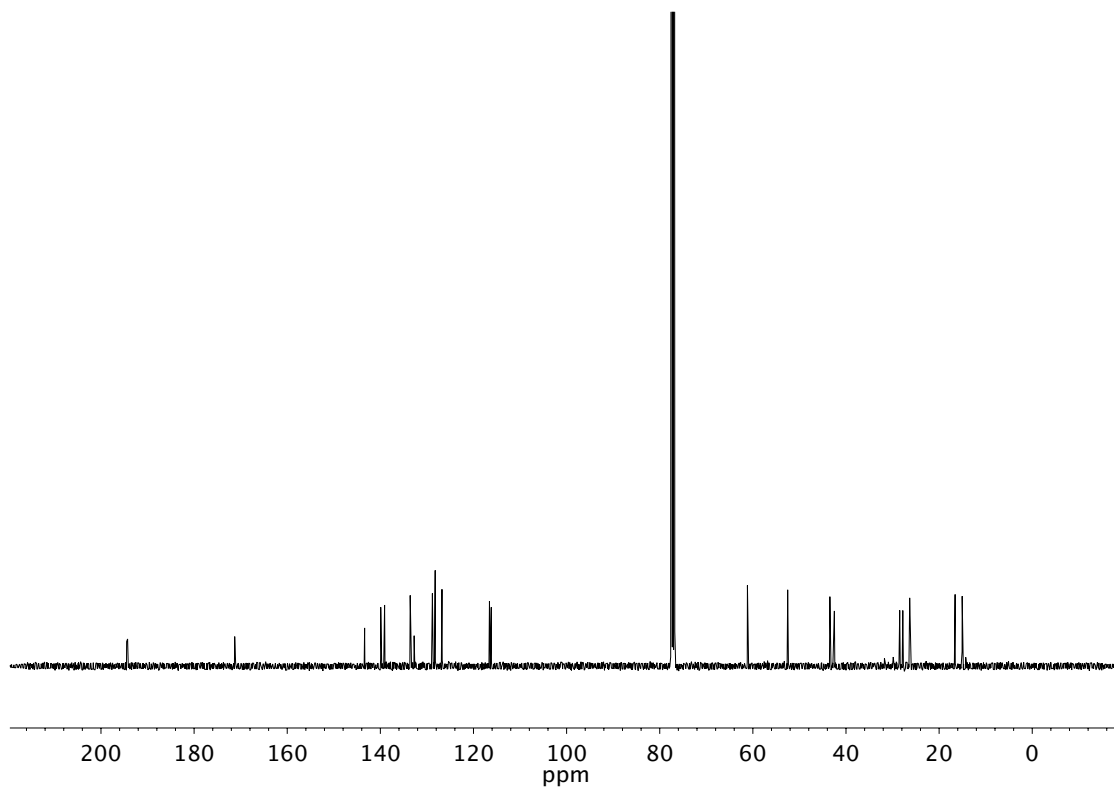
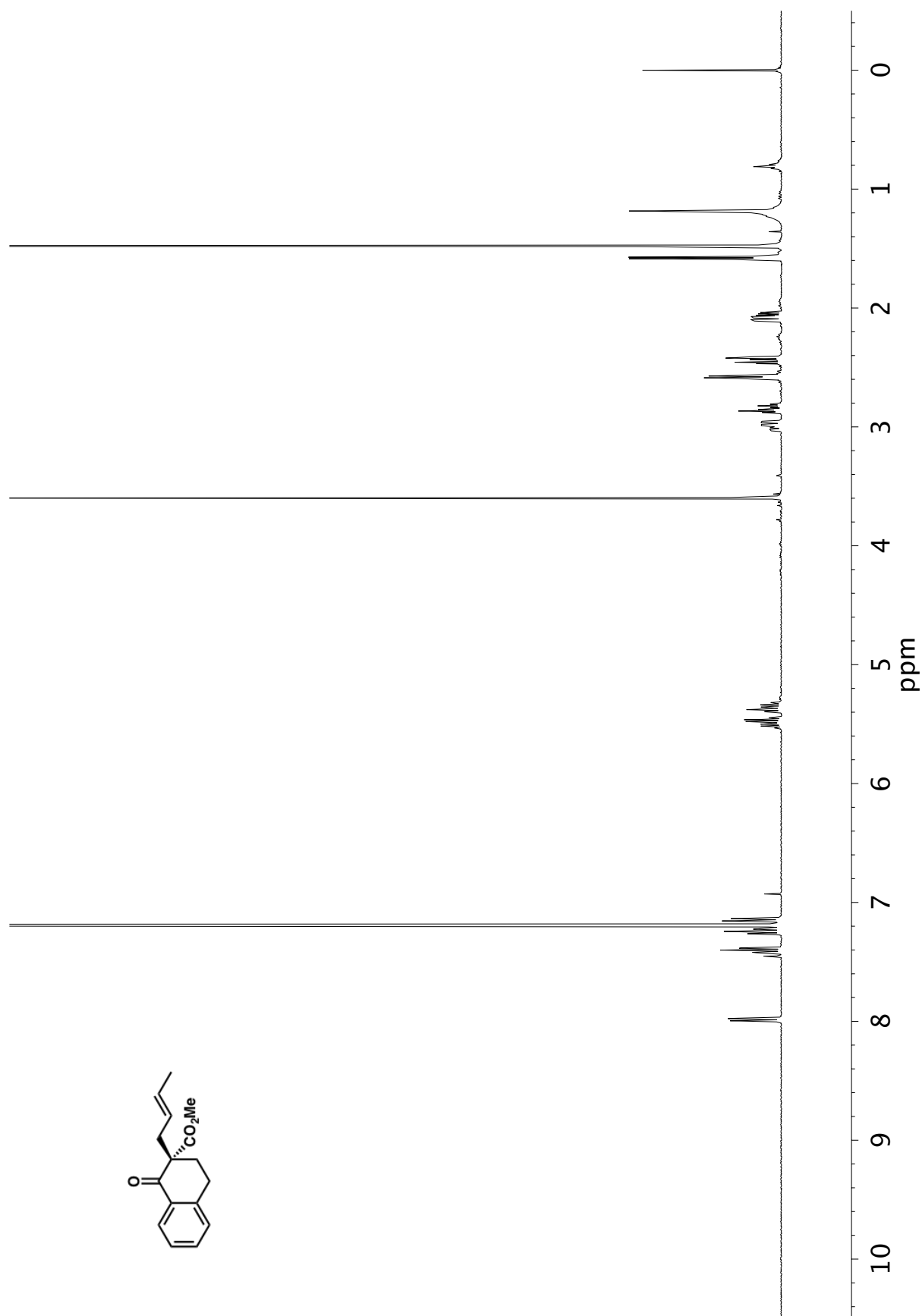


Figure A1.6 ¹³C NMR (101 MHz, CDCl₃) of compound **epi-54**

Figure A1.7 ¹H NMR (400 MHz, CDCl₃) of compound 55

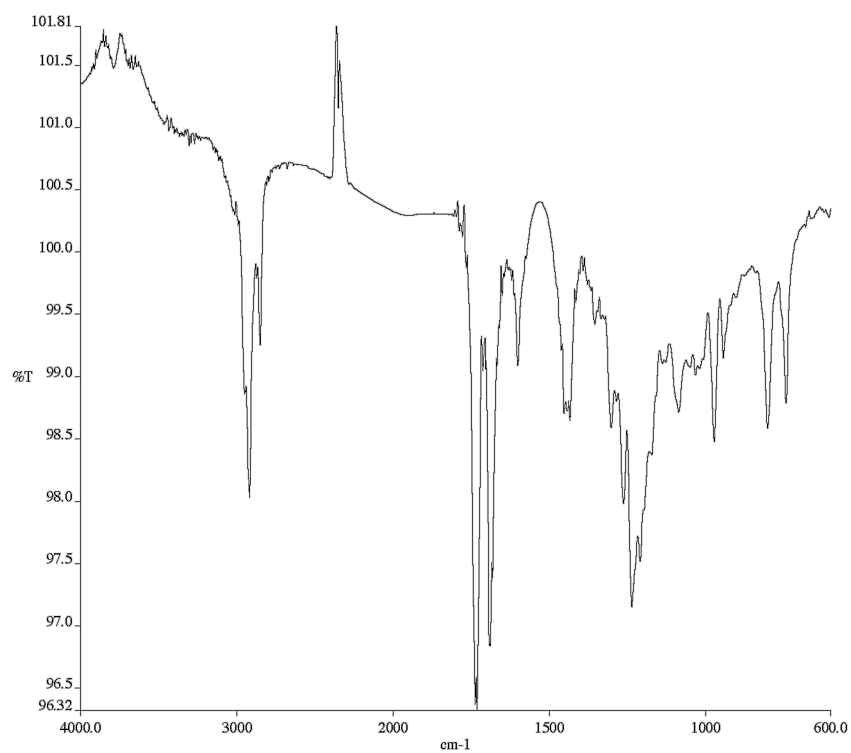


Figure A1.8 Infrared spectrum (Thin Film, NaCl) of compound **55**

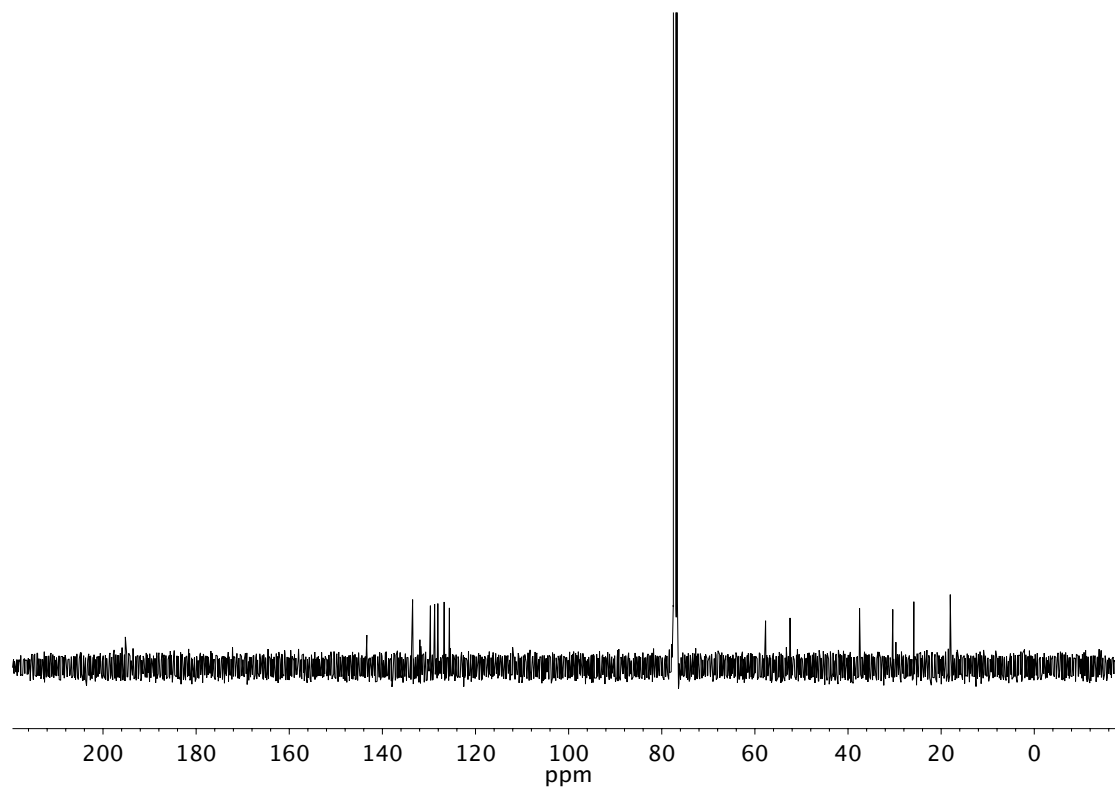


Figure A1.9 ¹³C NMR (101 MHz, CDCl₃) of compound **55**

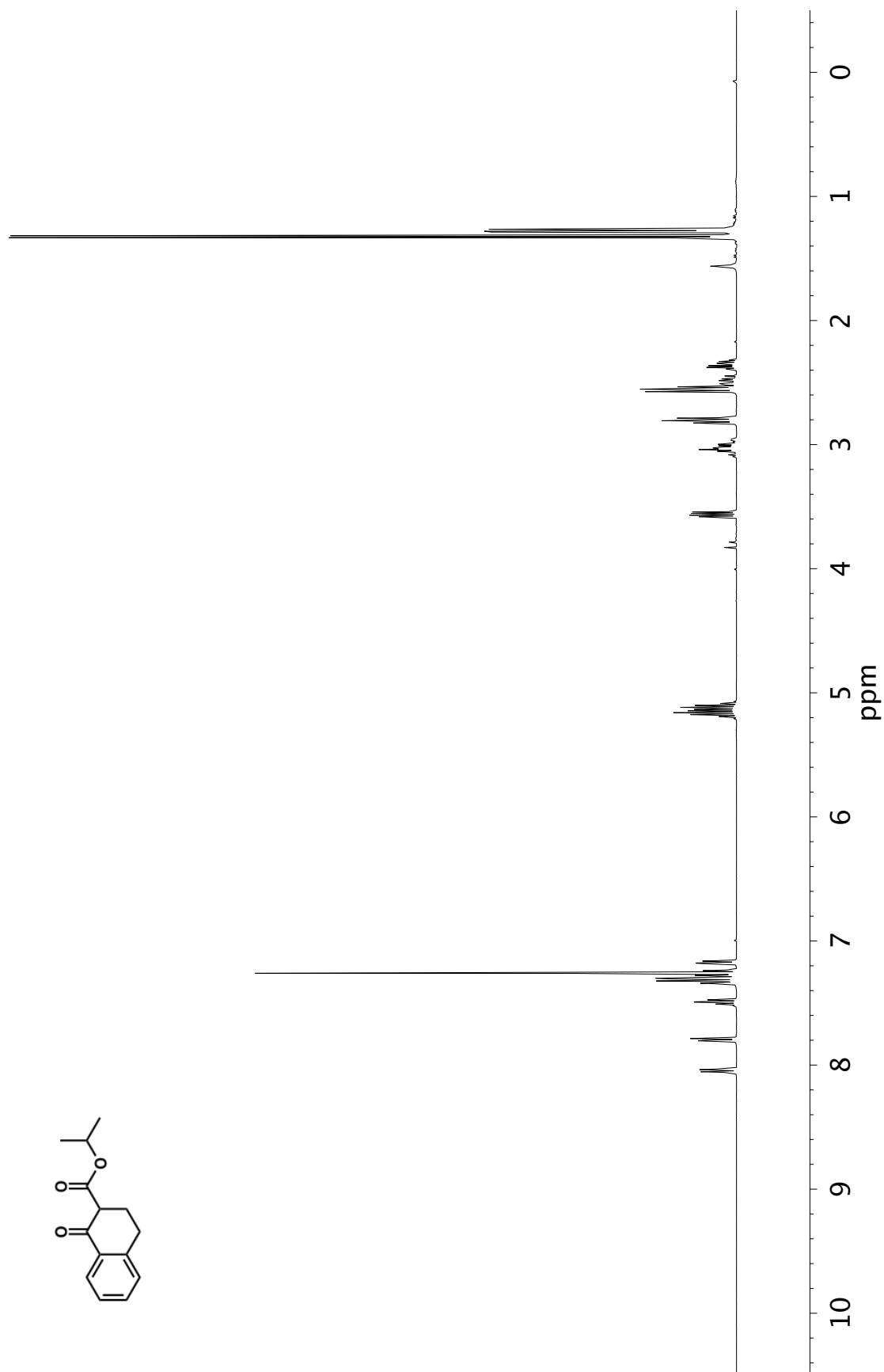
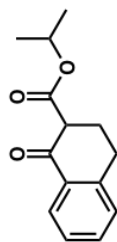


Figure A1.10 ^1H NMR (400 MHz, CDCl_3) of compound **56b**



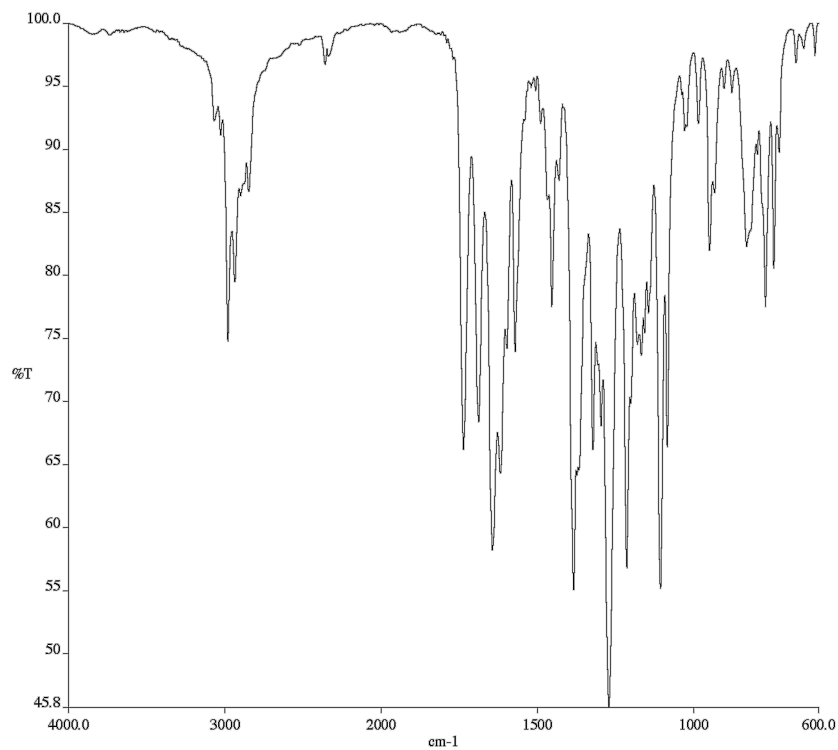


Figure A1.11 Infrared spectrum (Thin Film, NaCl) of compound **56b**

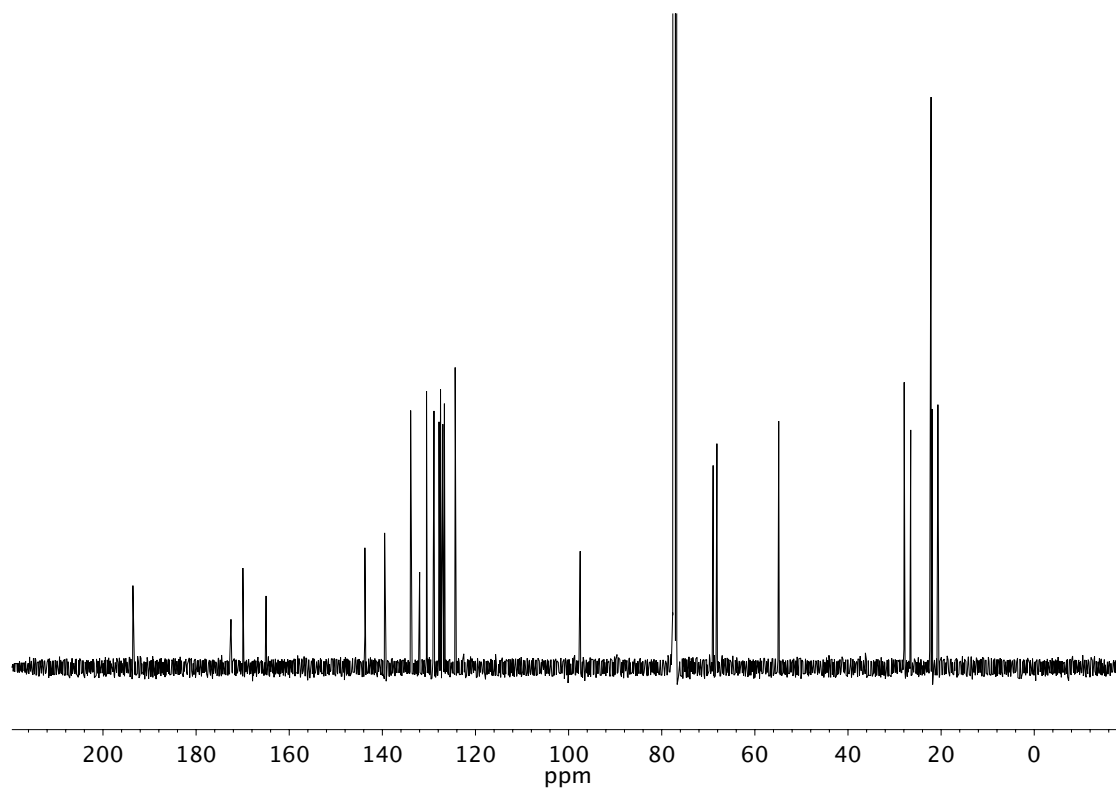


Figure A1.12 ¹³C NMR (101 MHz, CDCl₃) of compound **56b**

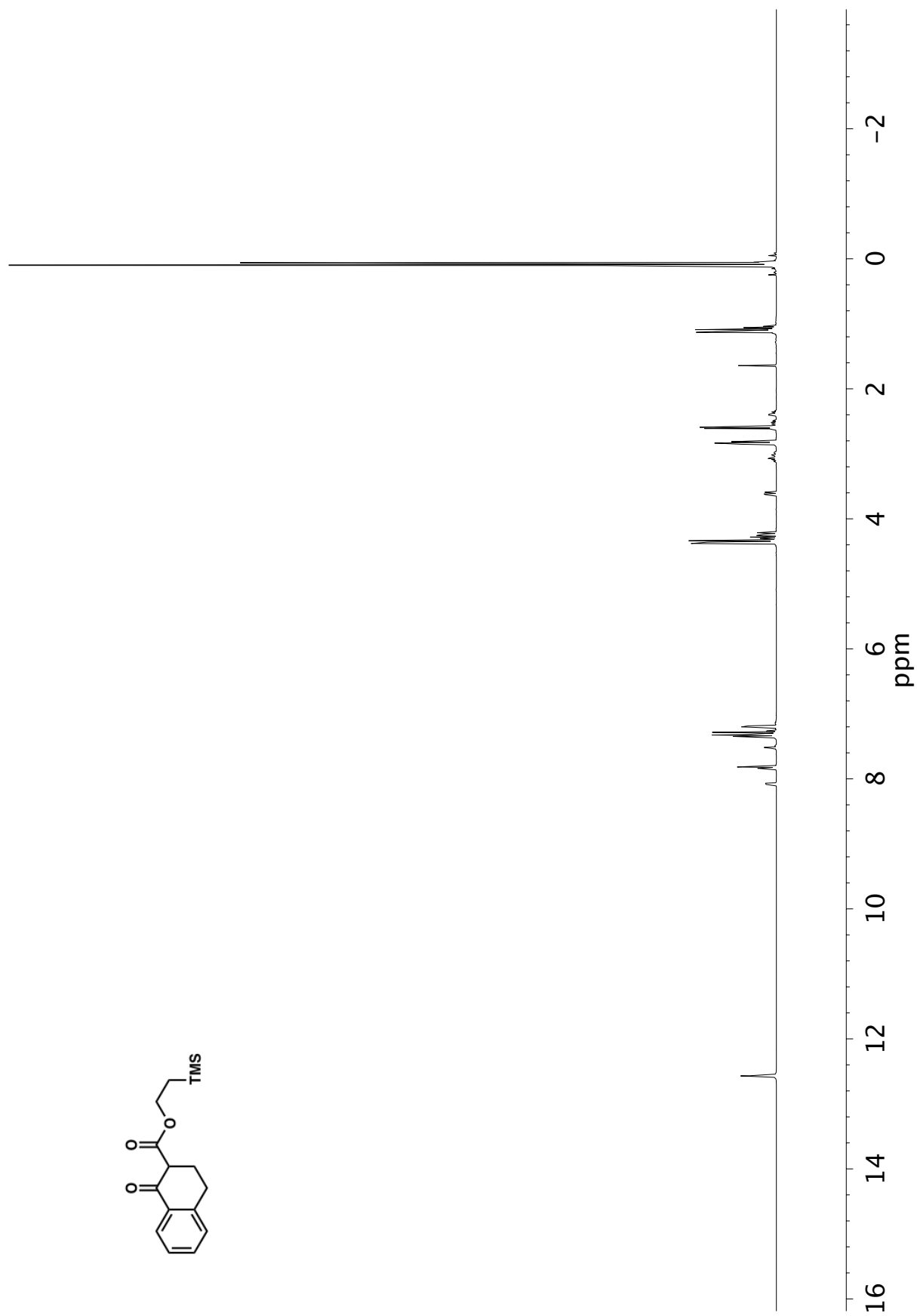


Figure A1.13 ¹H NMR (400 MHz, CDCl₃) of compound 56c

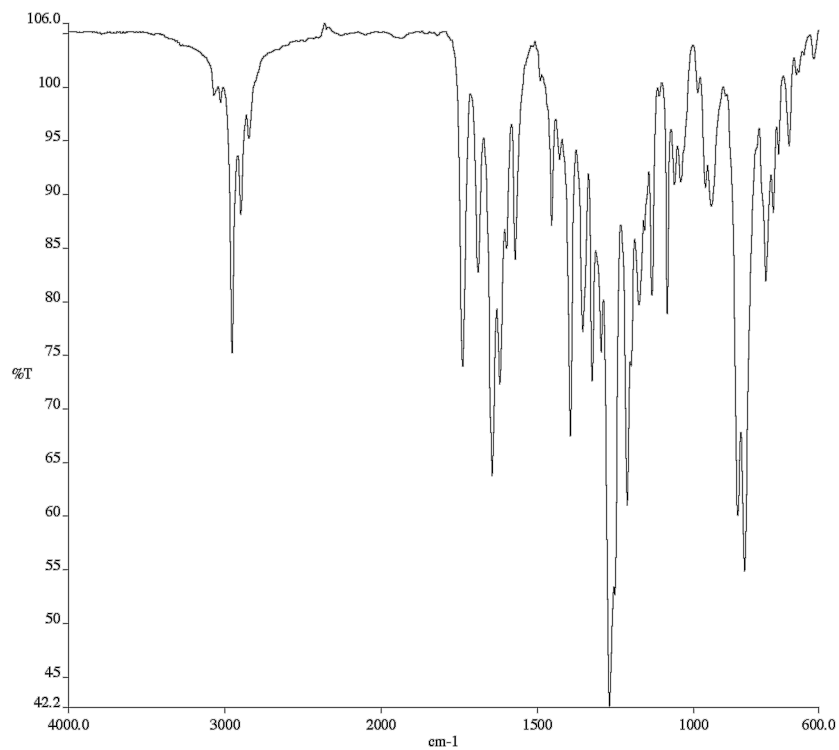


Figure A1.14 Infrared spectrum (Thin Film, NaCl) of compound **56c**

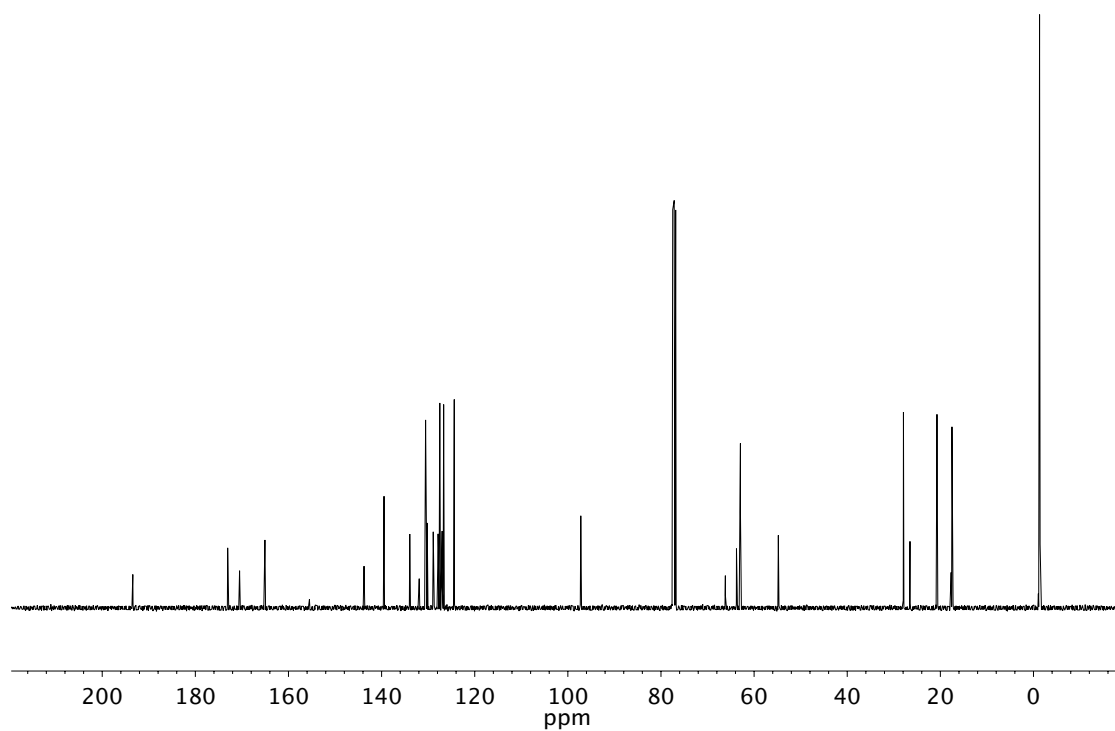


Figure A1.15 ¹³C NMR (101 MHz, CDCl₃) of compound **56c**

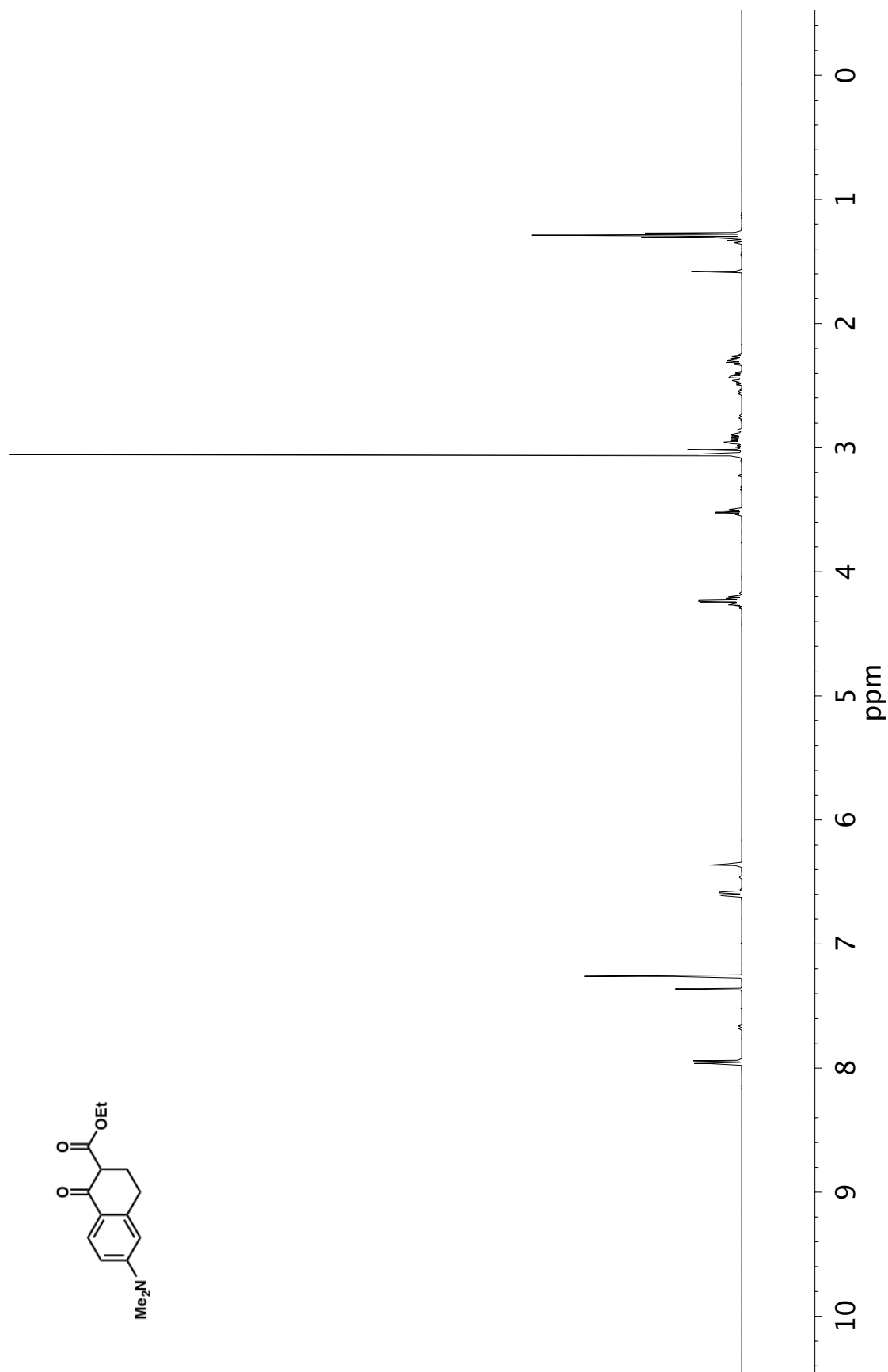


Figure A1.16 ¹H NMR (400 MHz, CDCl₃) of compound **56e**

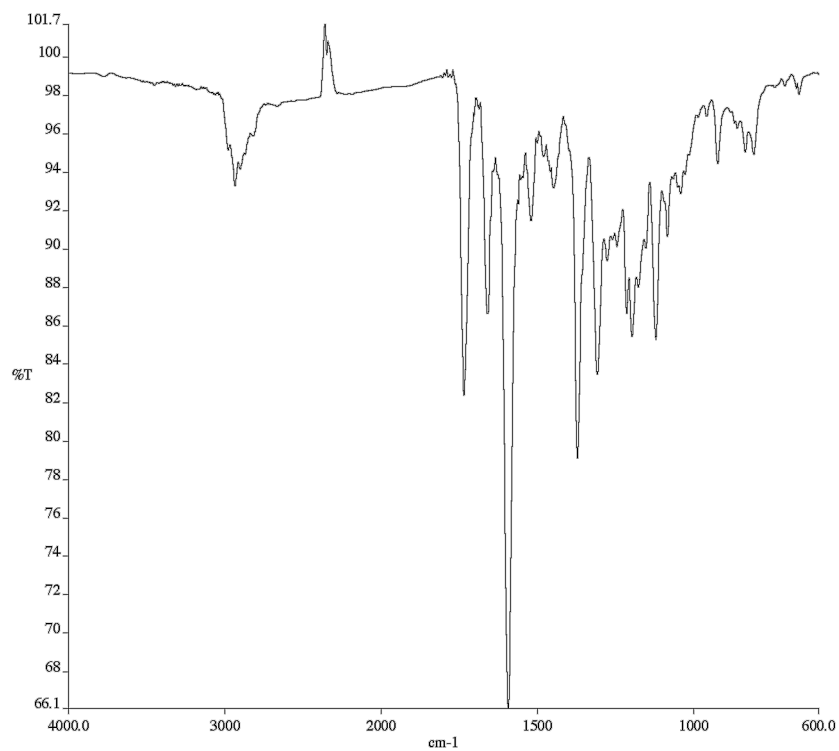


Figure A1.17 Infrared spectrum (Thin Film, NaCl) of compound **56e**

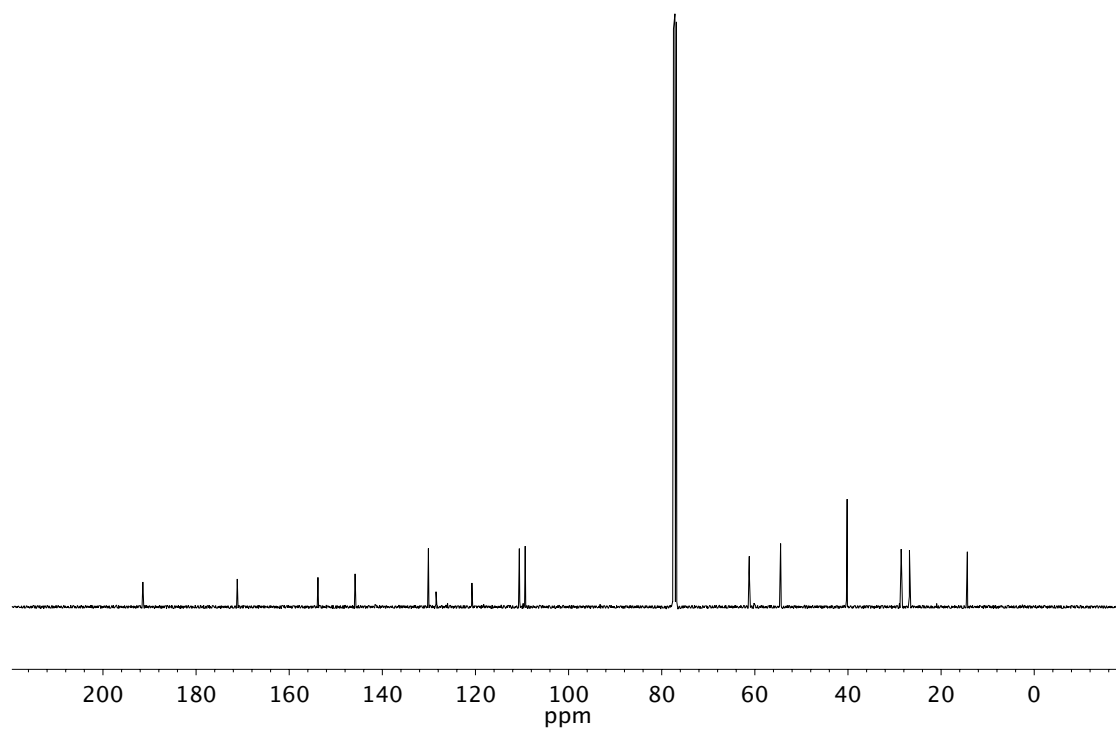


Figure A1.18 ¹³C NMR (101 MHz, CDCl₃) of compound **56e**

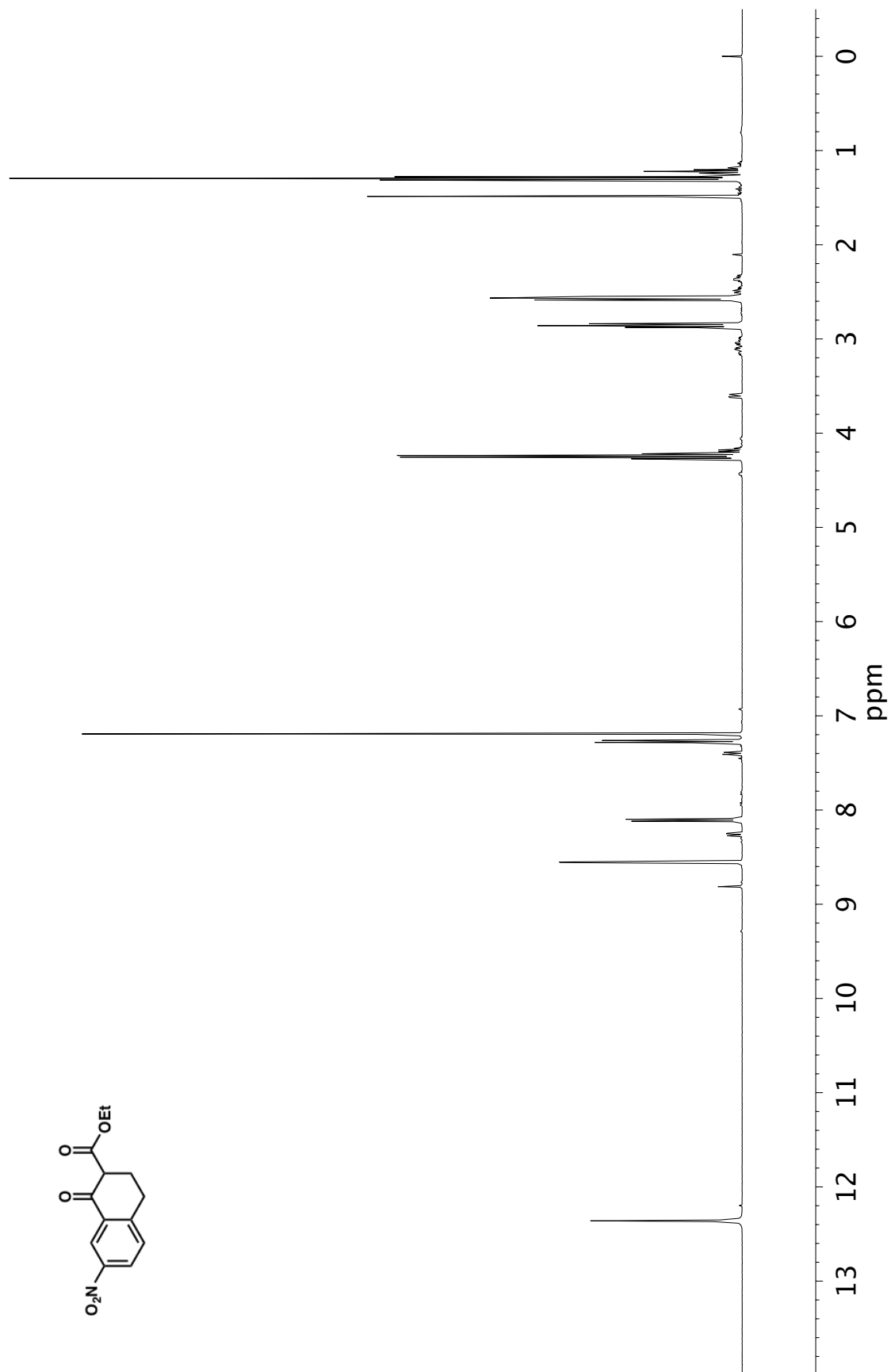


Figure A1.19 ¹H NMR (400 MHz, CDCl₃) of compound 56g

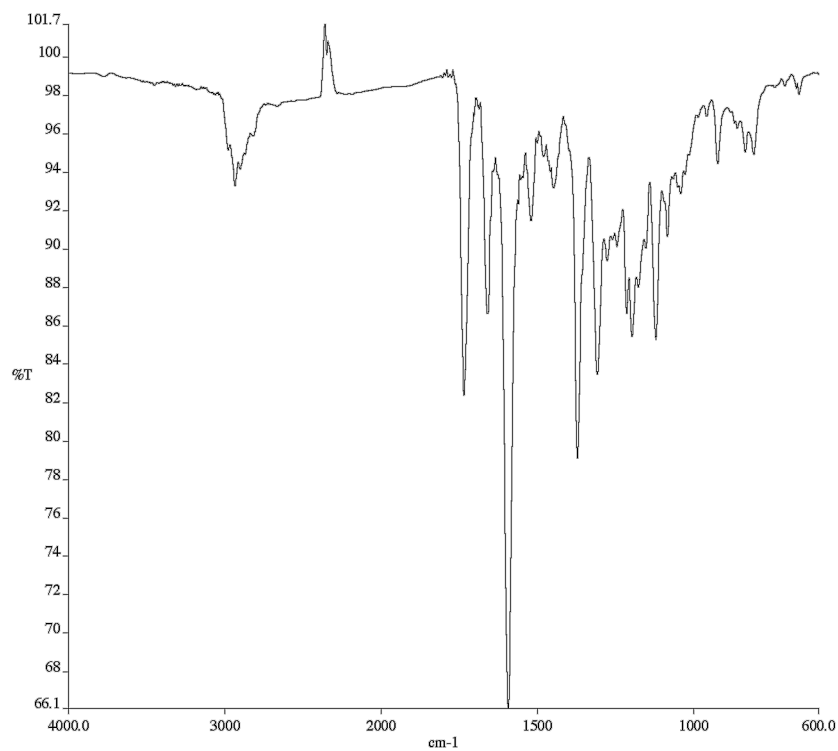


Figure A1.20 Infrared spectrum (Thin Film, NaCl) of compound **56g**

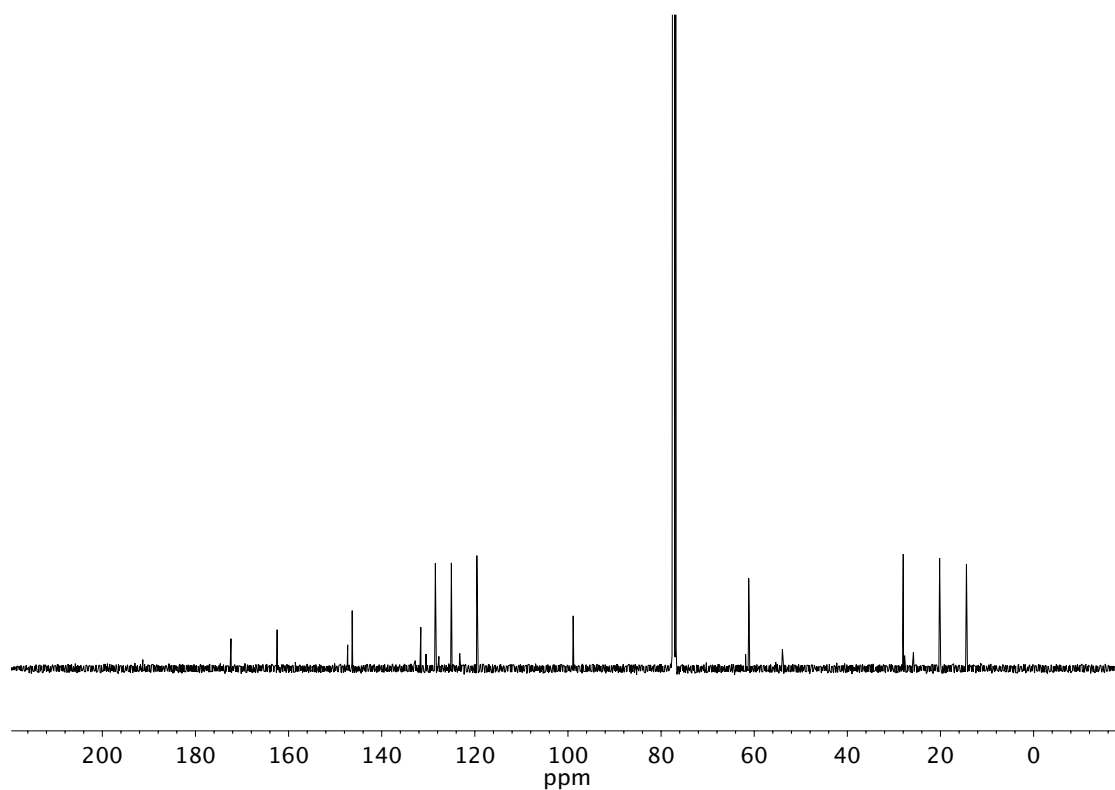


Figure A1.21 ¹³C NMR (101 MHz, CDCl₃) of compound **56g**

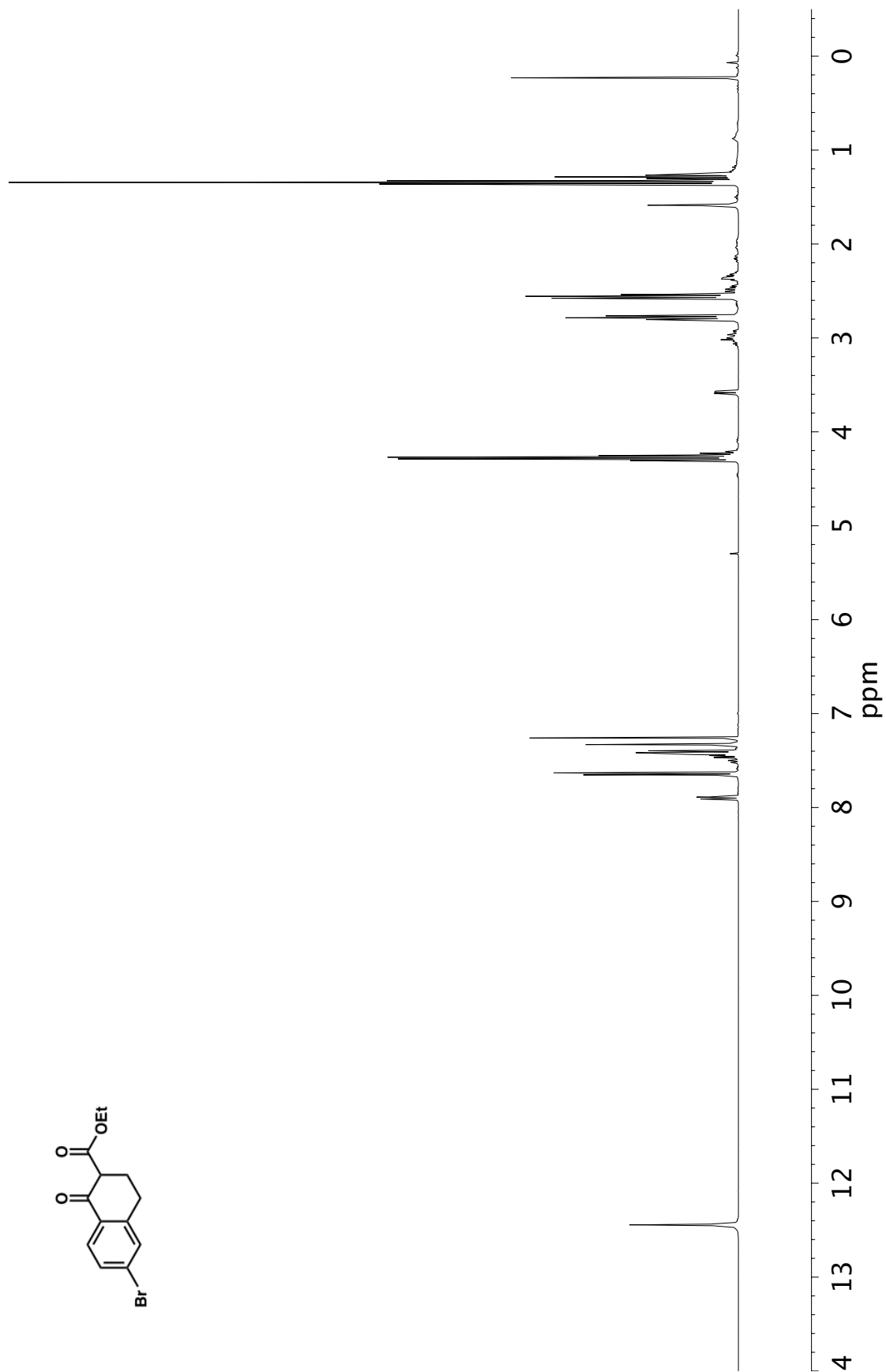


Figure A1.22 ^1H NMR (400 MHz, CDCl_3) of compound **56h**

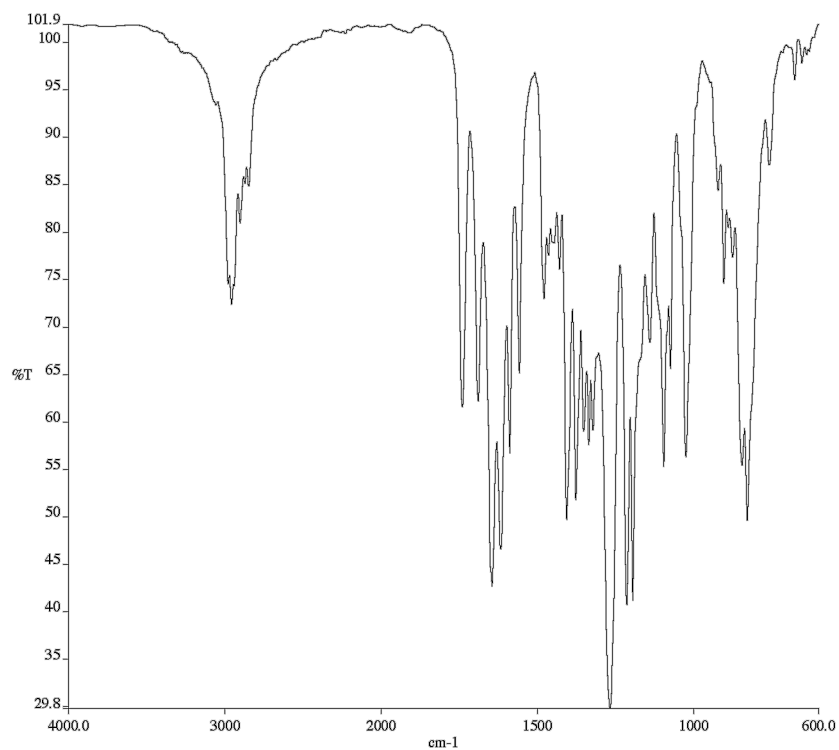


Figure A1.23 Infrared spectrum (Thin Film, NaCl) of compound **56h**

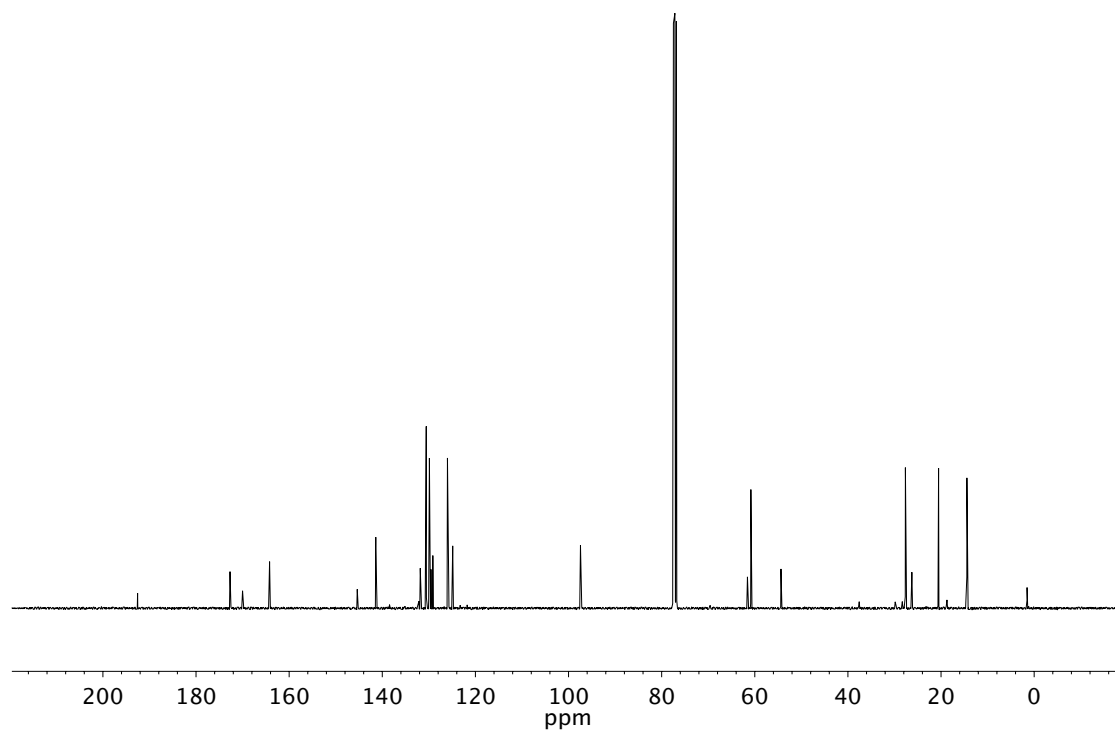


Figure A1.24 ¹³C NMR (101 MHz, CDCl₃) of compound **56h**

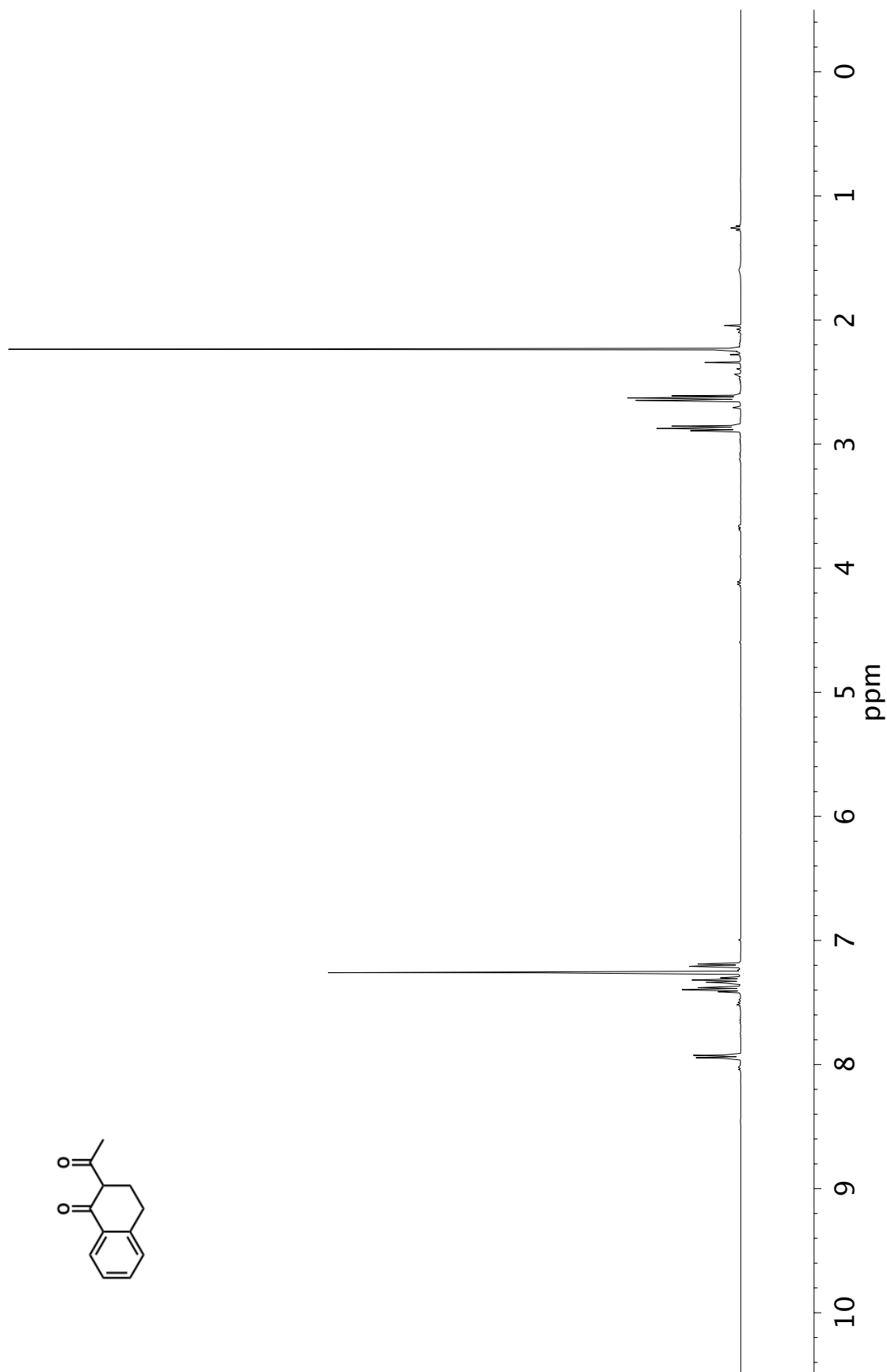


Figure A1.25 ¹H NMR (400 MHz, CDCl₃) of compound 56k

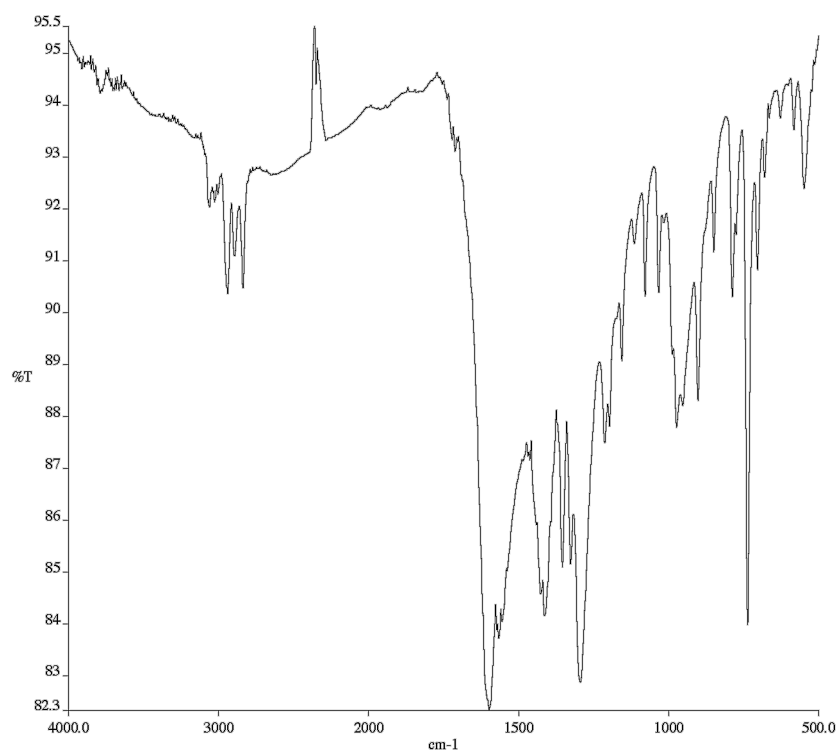


Figure A1.26 Infrared spectrum (Thin Film, NaCl) of compound **56k**

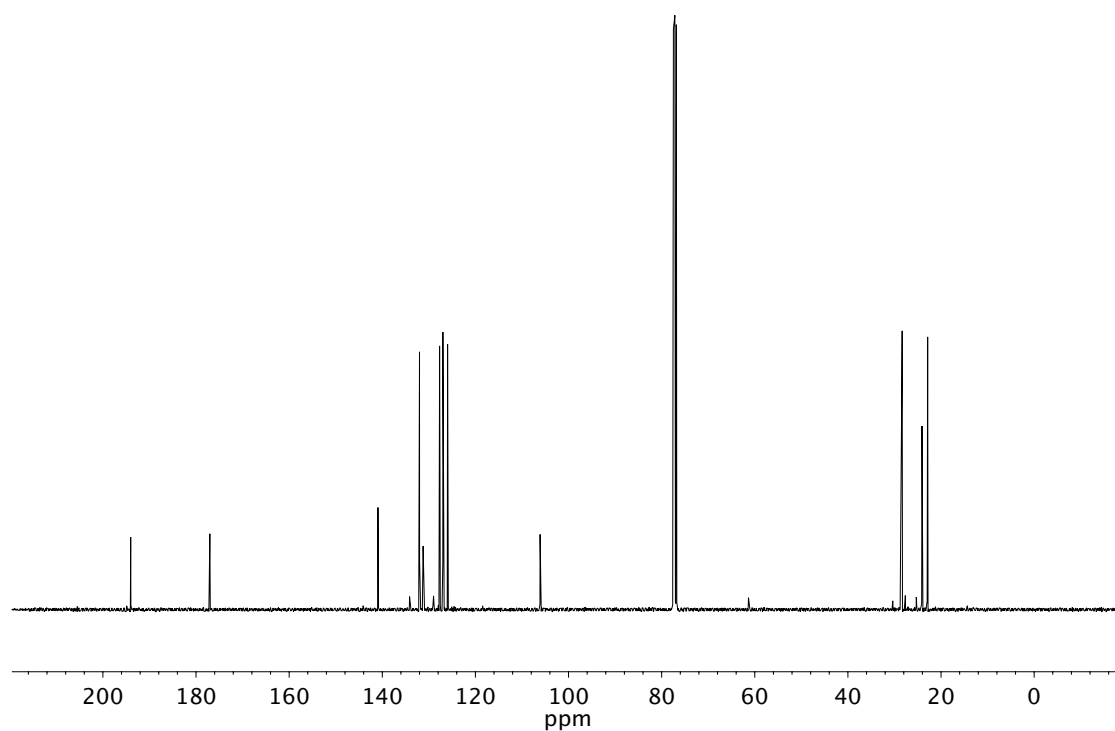


Figure A1.27 ¹³C NMR (101 MHz, CDCl₃) of compound **56k**

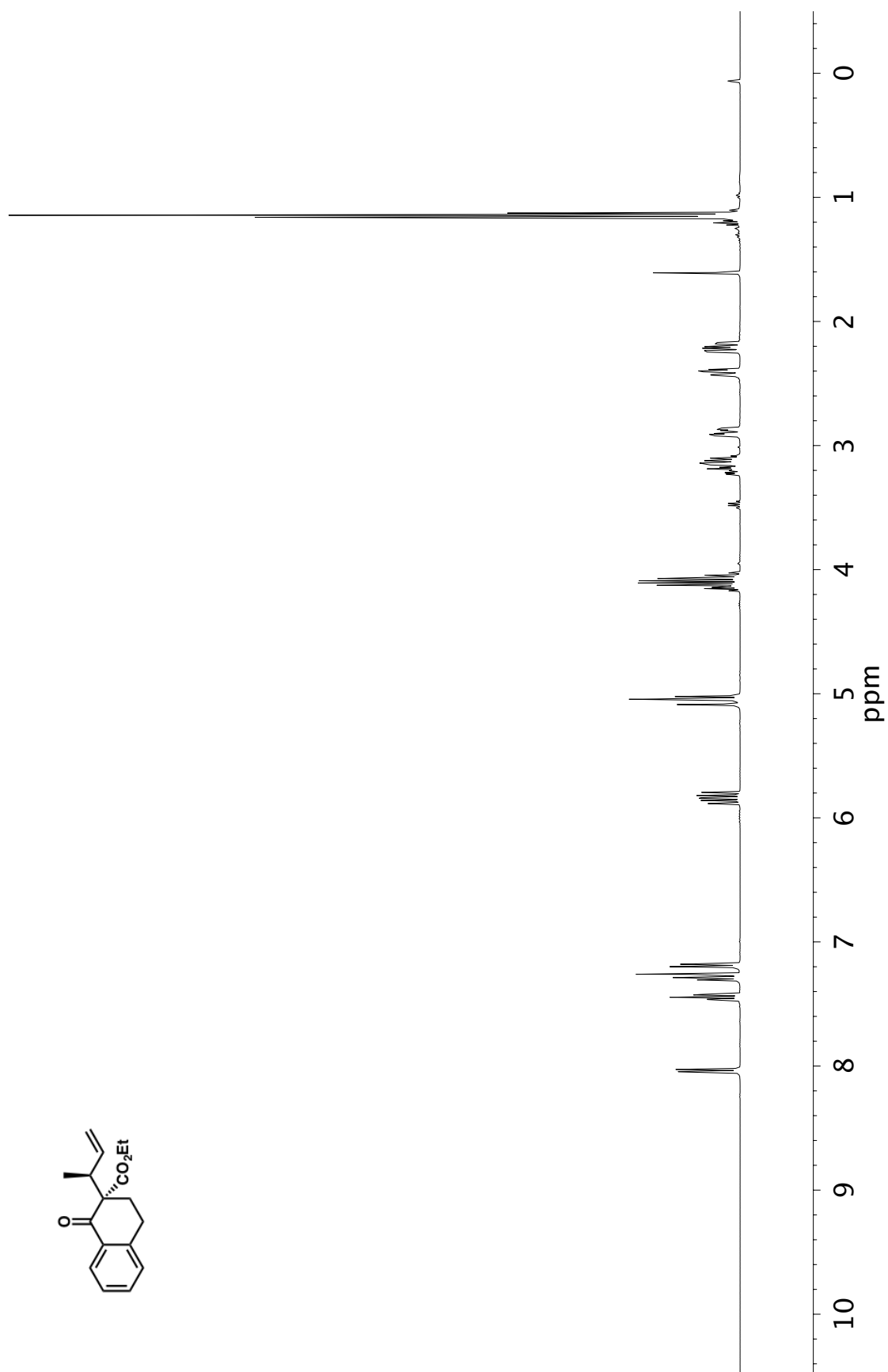


Figure A1.28 ¹H NMR (400 MHz, CDCl₃) of compound 58a

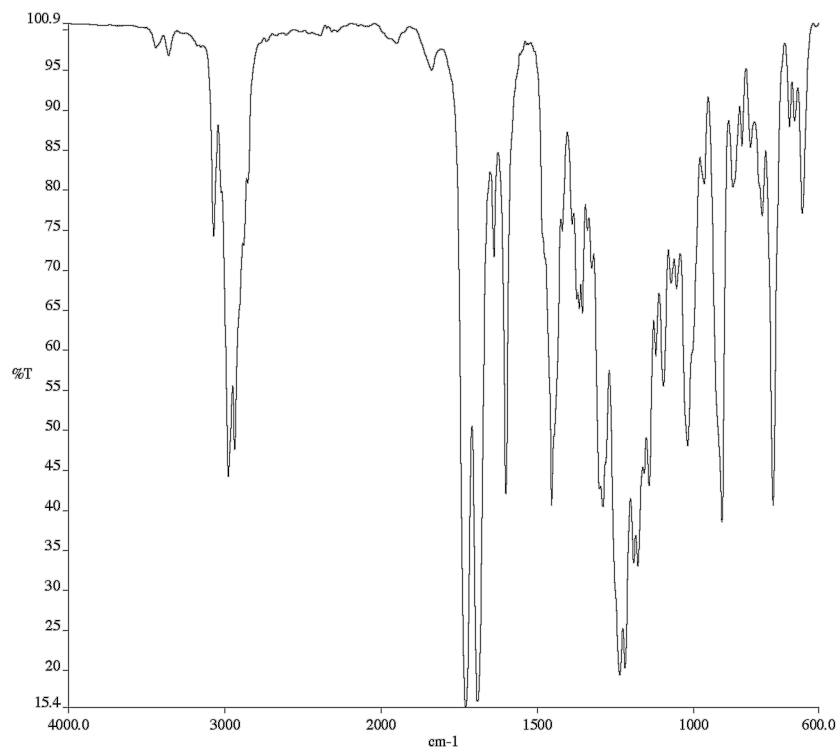


Figure A1.29 Infrared spectrum (Thin Film, NaCl) of compound **58a**

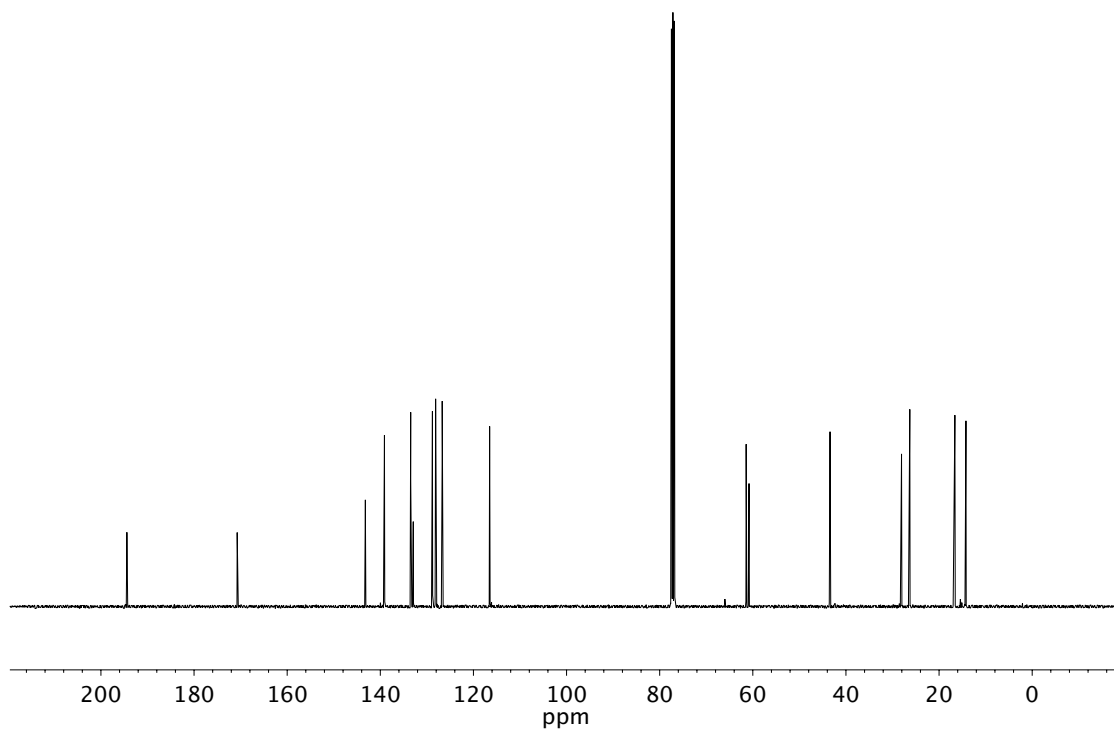


Figure A1.30 ¹³C NMR (101 MHz, CDCl₃) of compound **58a**

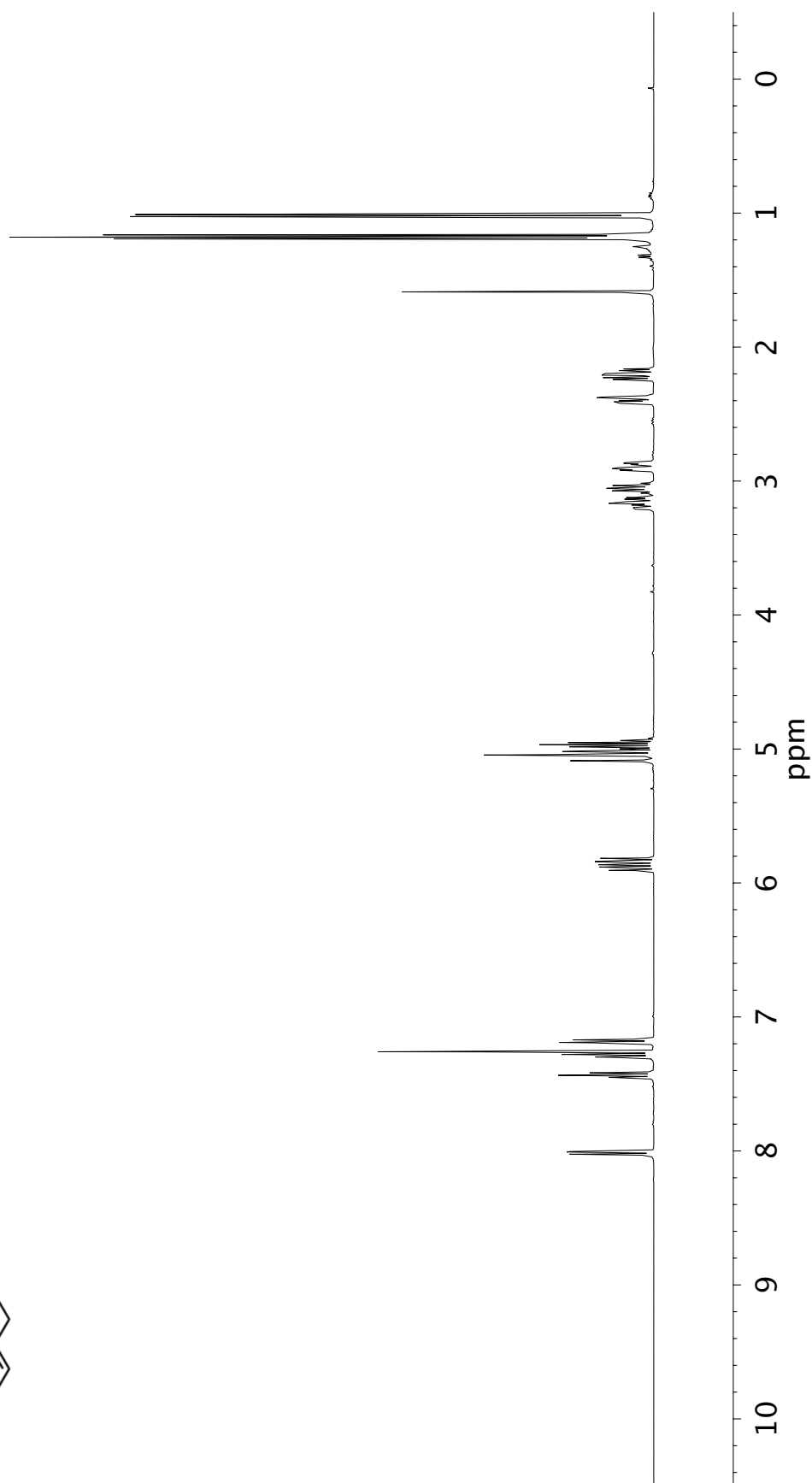
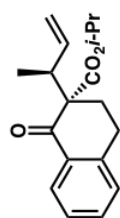


Figure A1.31 ¹H NMR (400 MHz, CDCl₃) of compound 58b

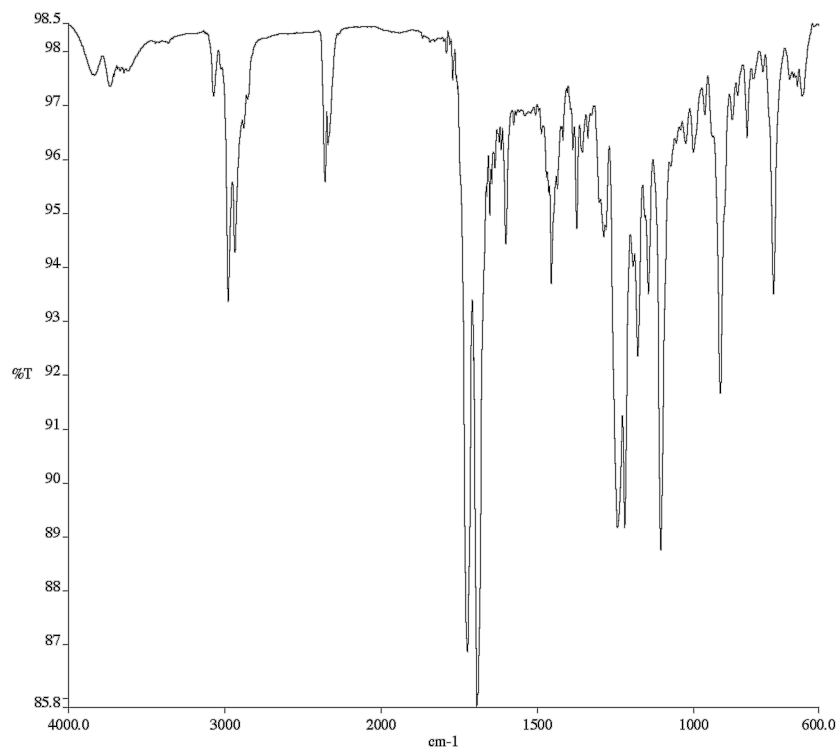


Figure A1.32 Infrared spectrum (Thin Film, NaCl) of compound **58b**

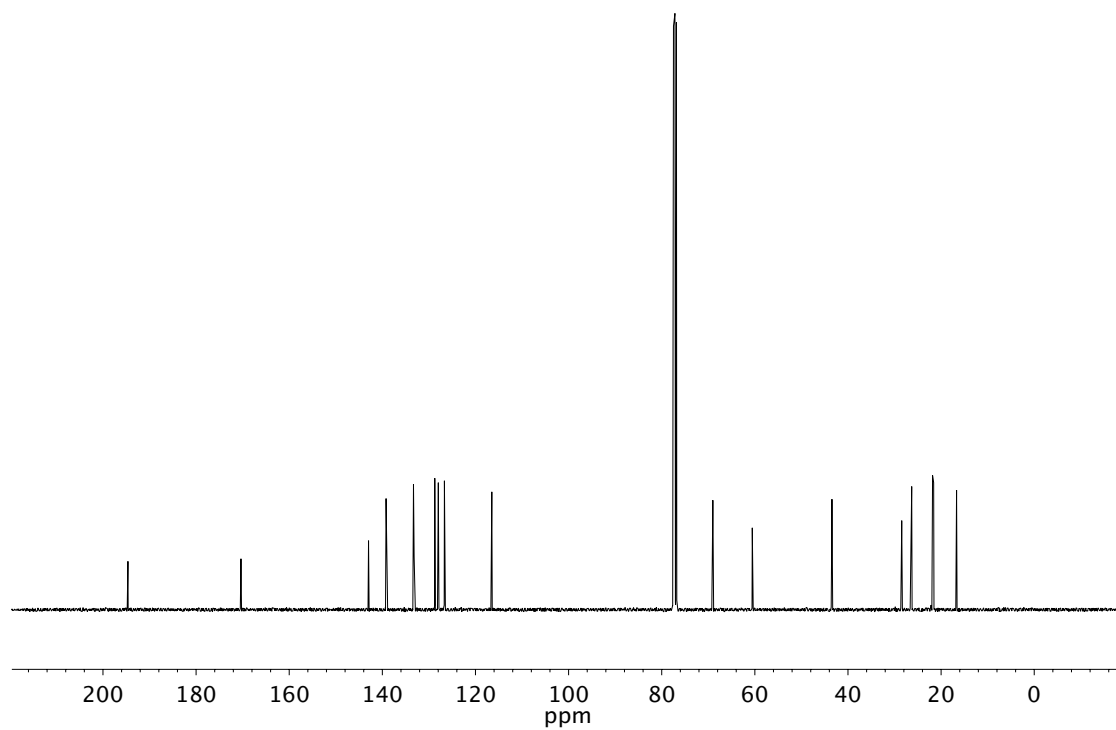


Figure A1.33 ¹³C NMR (101 MHz, CDCl₃) of compound **58b**

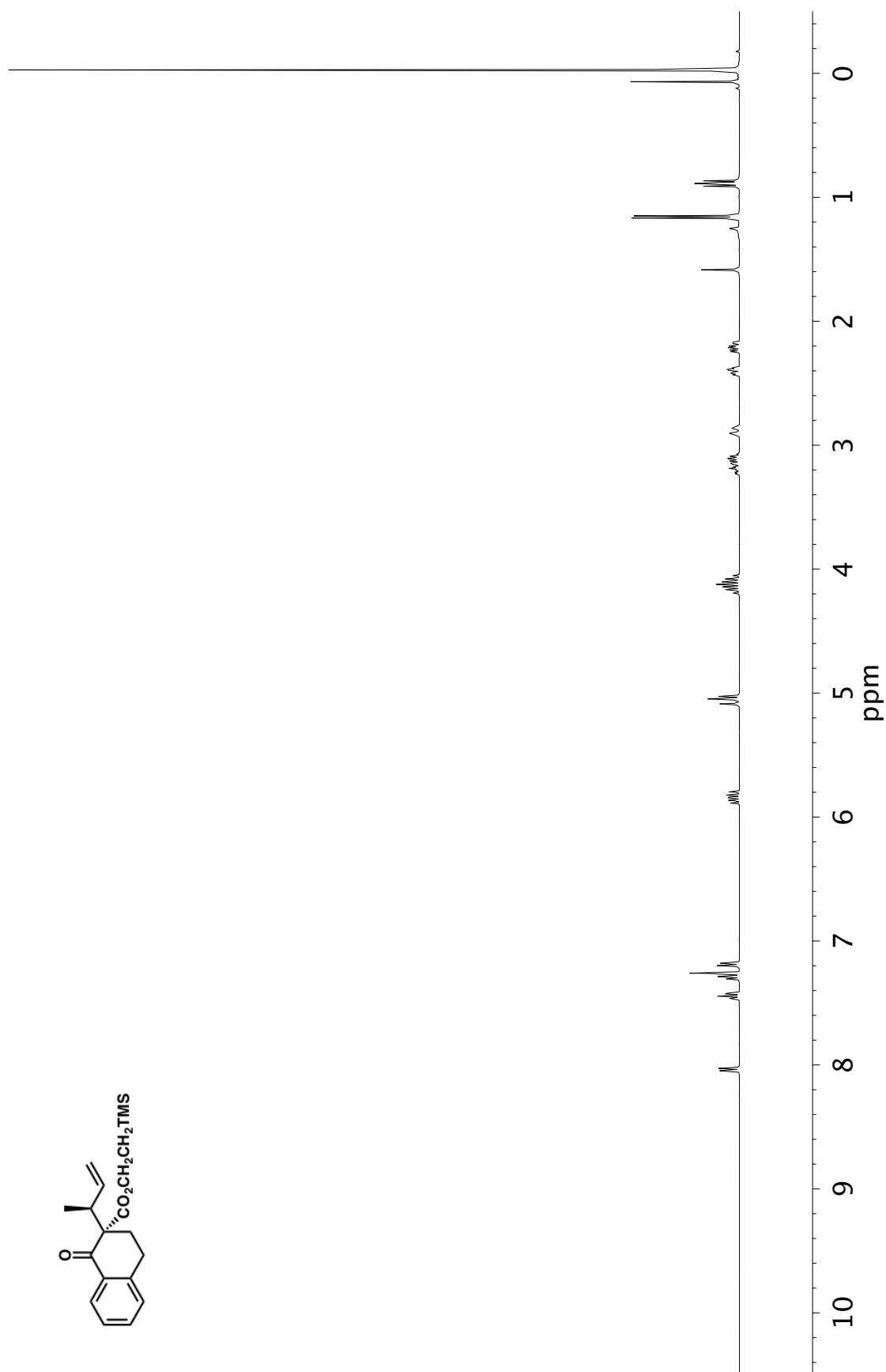


Figure A1.34 ¹H NMR (400 MHz, CDCl₃) of compound 58c

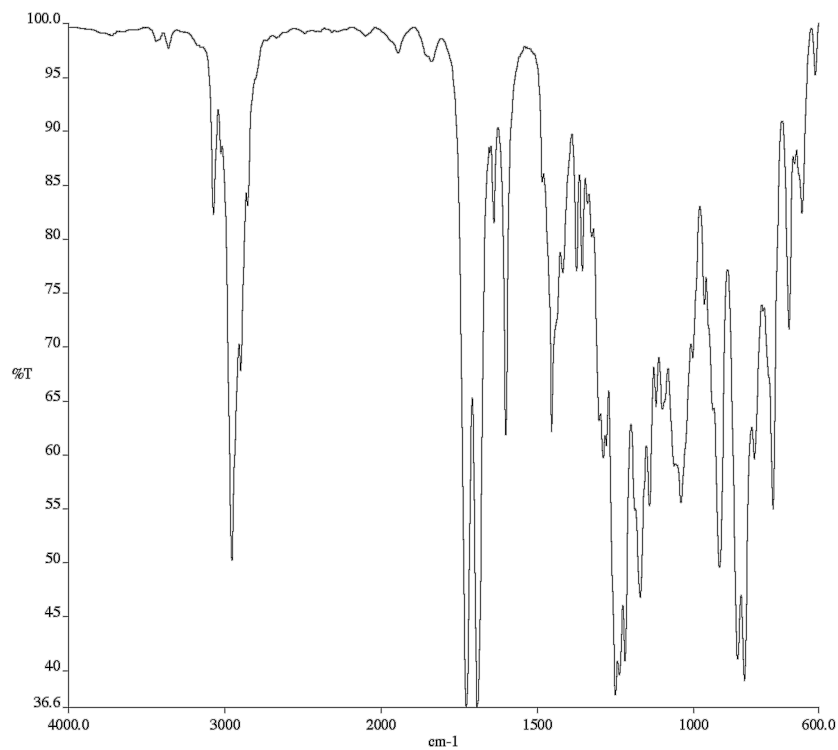


Figure A1.35 Infrared spectrum (Thin Film, NaCl) of compound **58c**

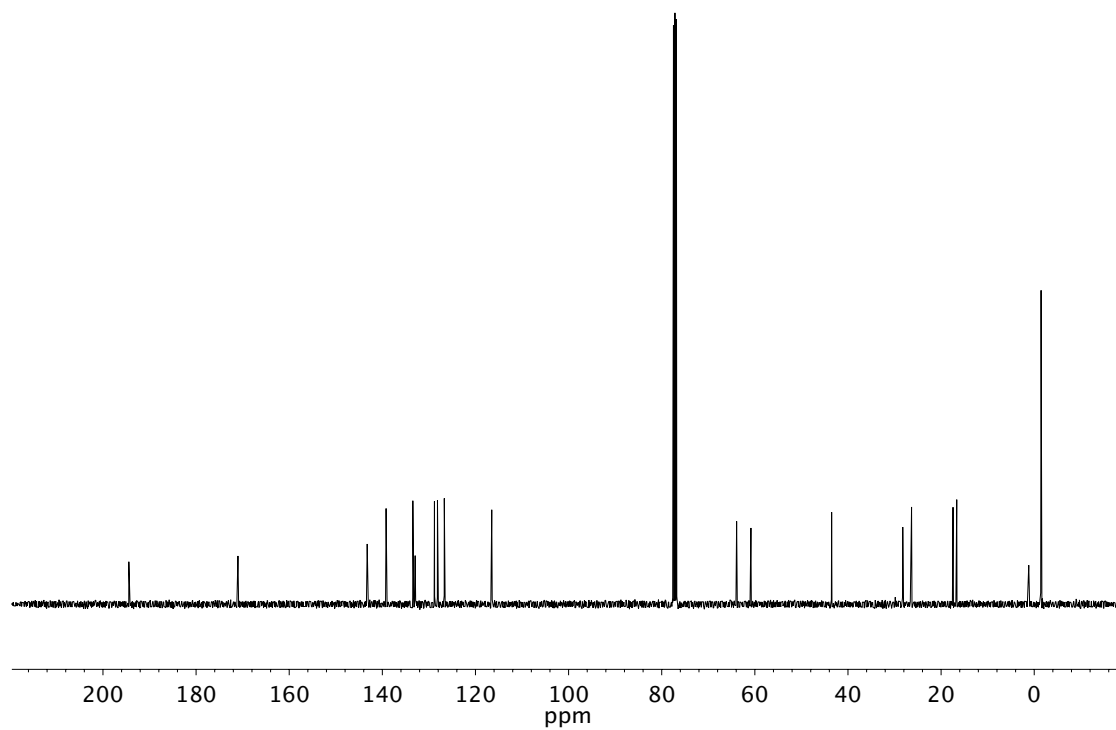


Figure A1.36 ¹³C NMR (101 MHz, CDCl₃) of compound **58c**

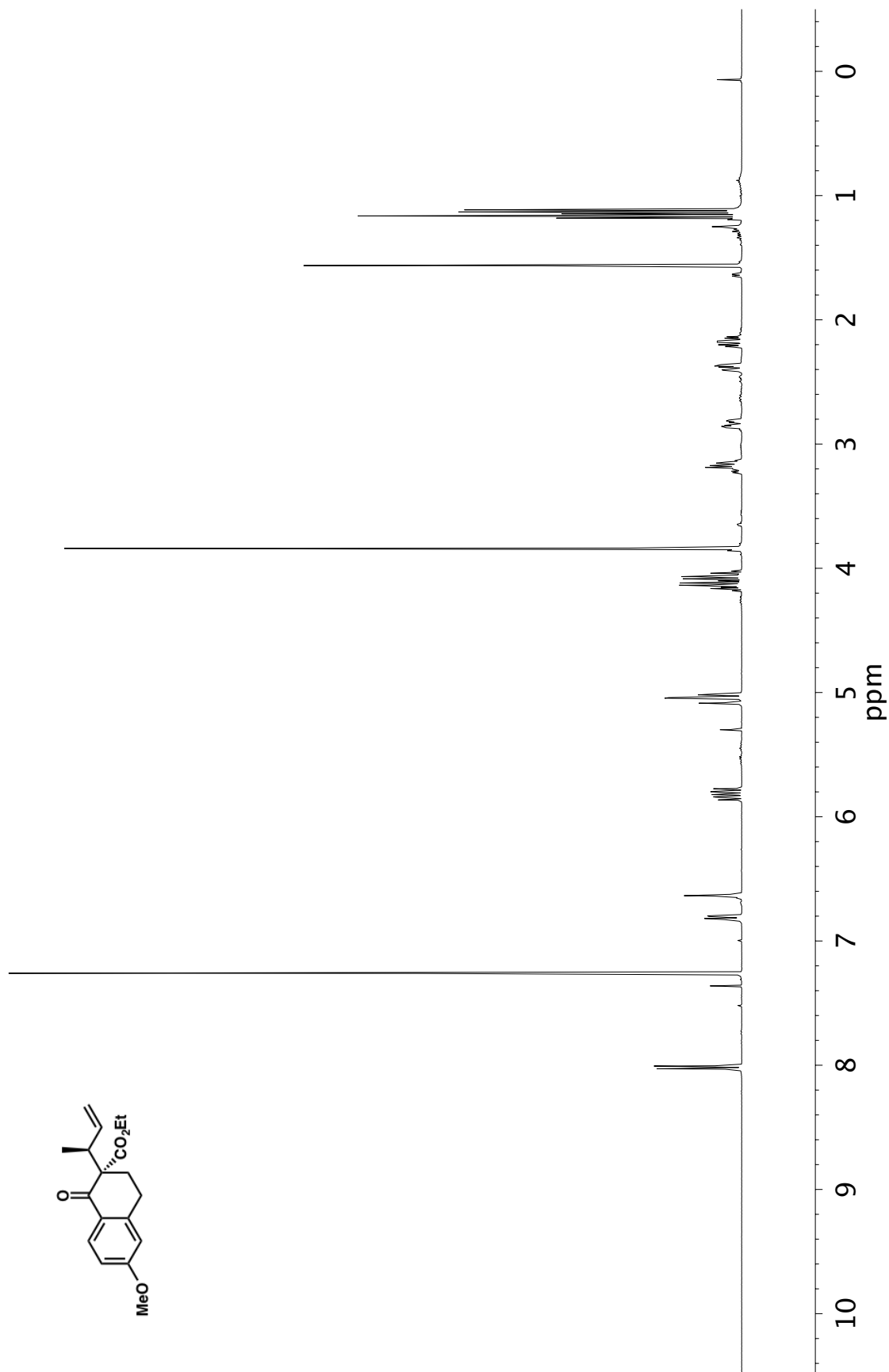


Figure A1.37 ¹H NMR (400 MHz, CDCl₃) of compound 58d

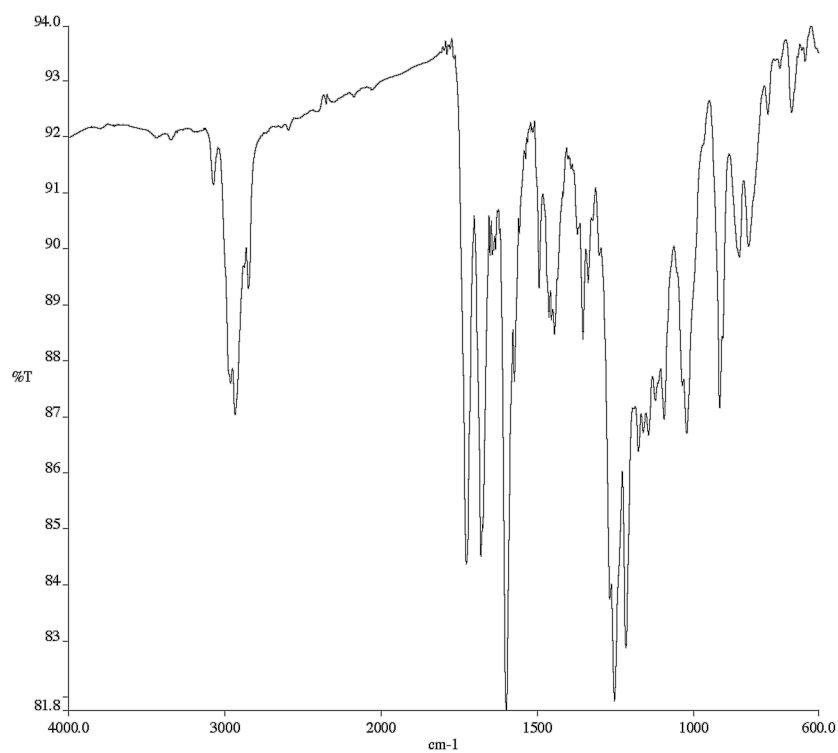


Figure A1.38 Infrared spectrum (Thin Film, NaCl) of compound **58d**

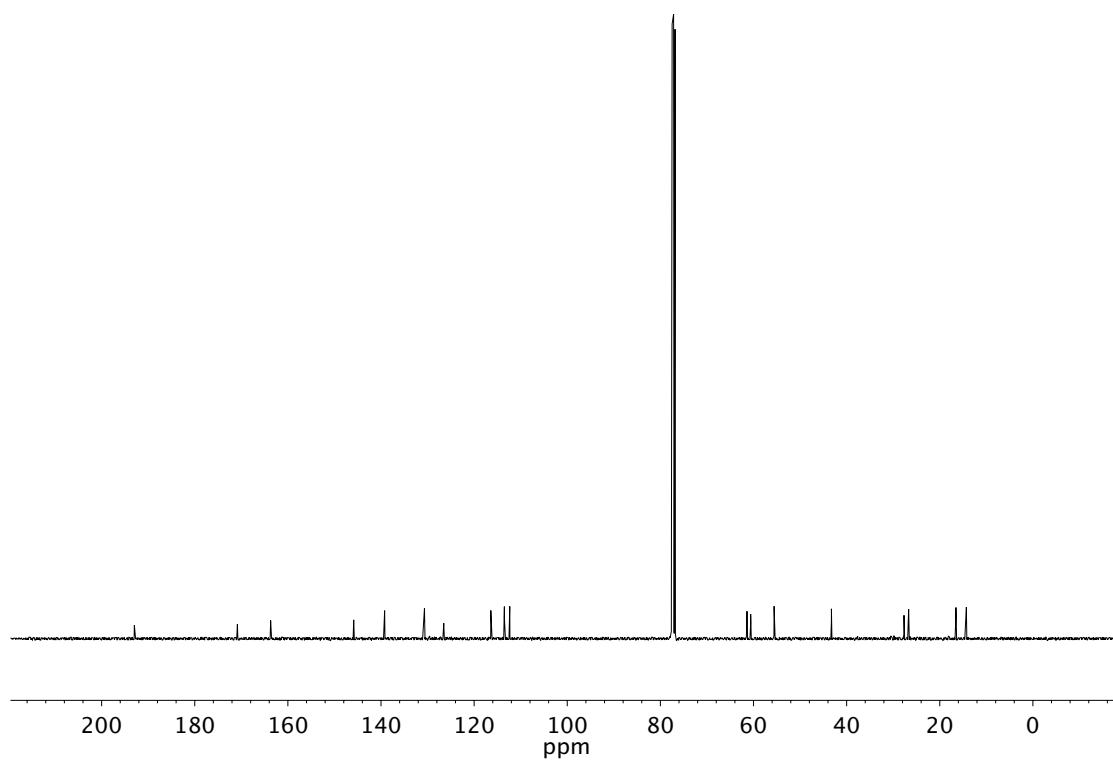


Figure A1.39 ¹³C NMR (101 MHz, CDCl₃) of compound **58d**

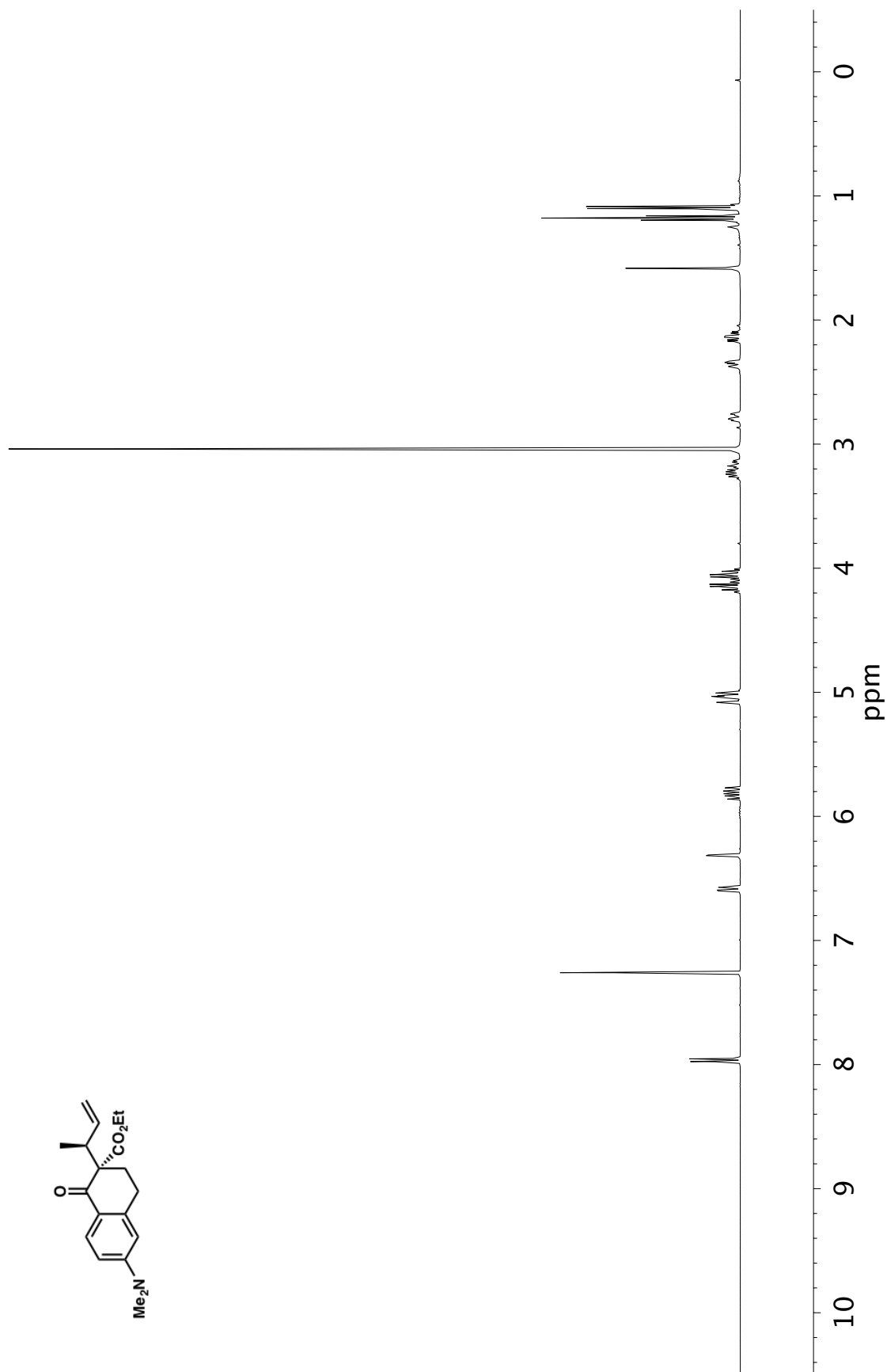


Figure A1.40 ¹H NMR (400 MHz, CDCl₃) of compound 58e

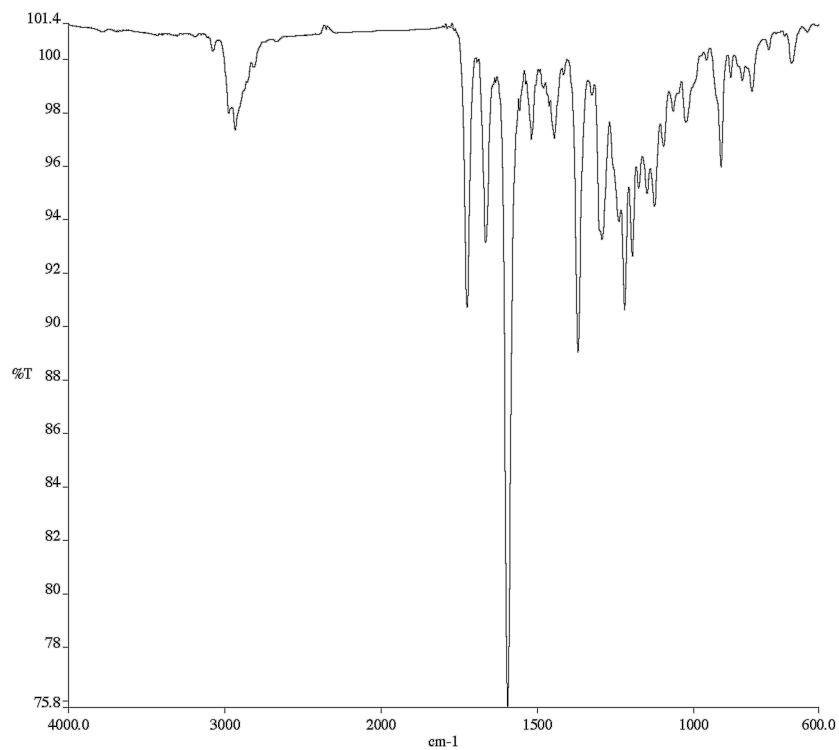


Figure A1.41 Infrared spectrum (Thin Film, NaCl) of compound **58e**

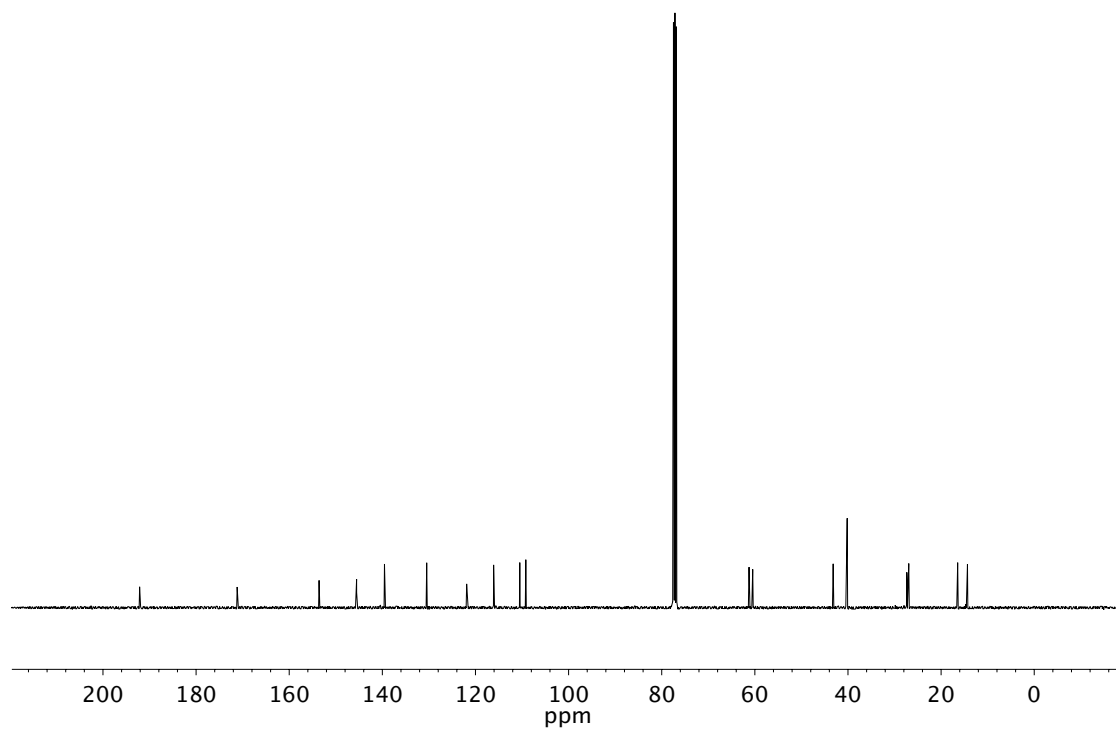


Figure A1.42 ¹³C NMR (101 MHz, CDCl₃) of compound **58e**

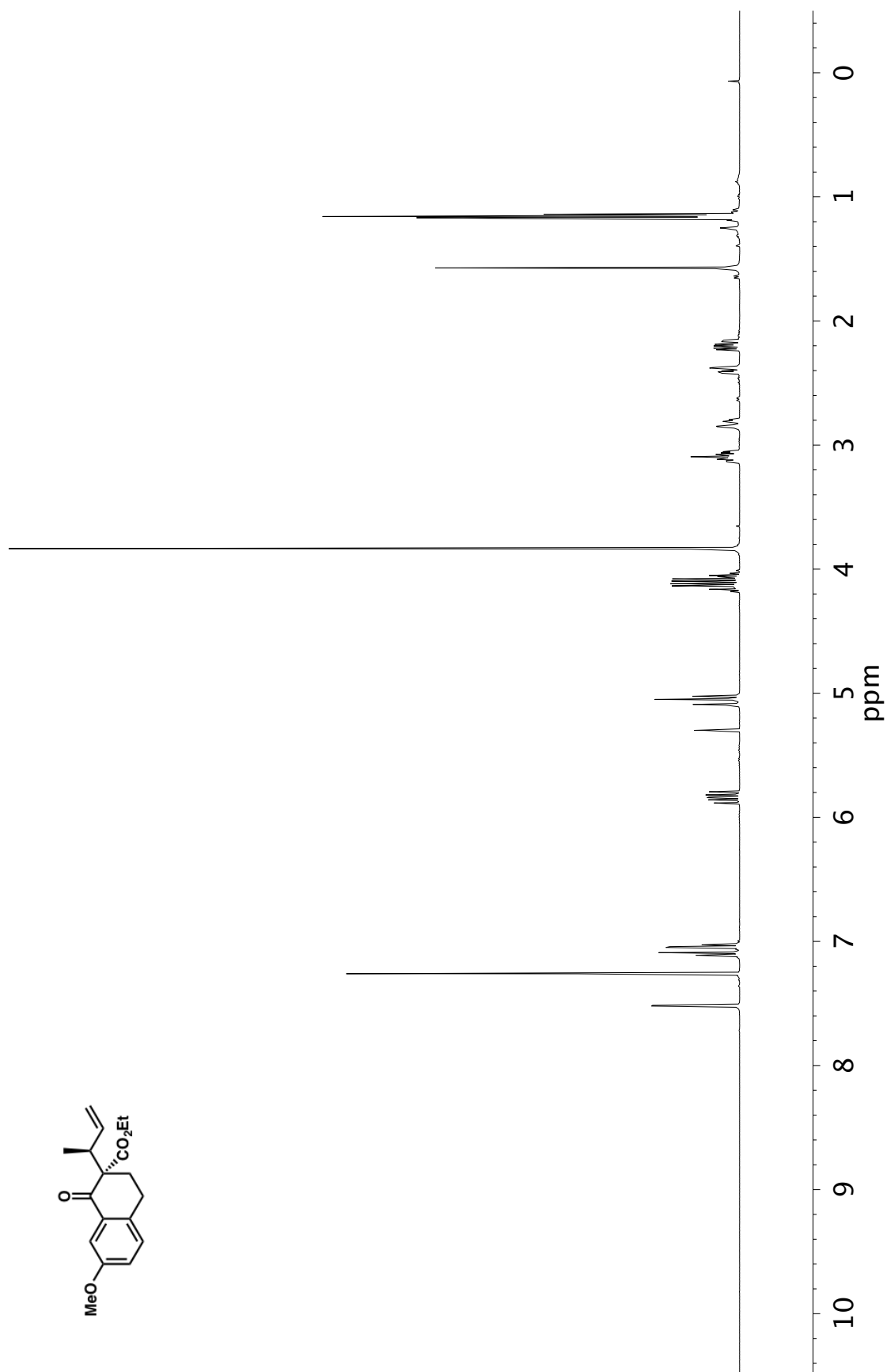


Figure A1.43 ¹H NMR (400 MHz, CDCl₃) of compound **58f**

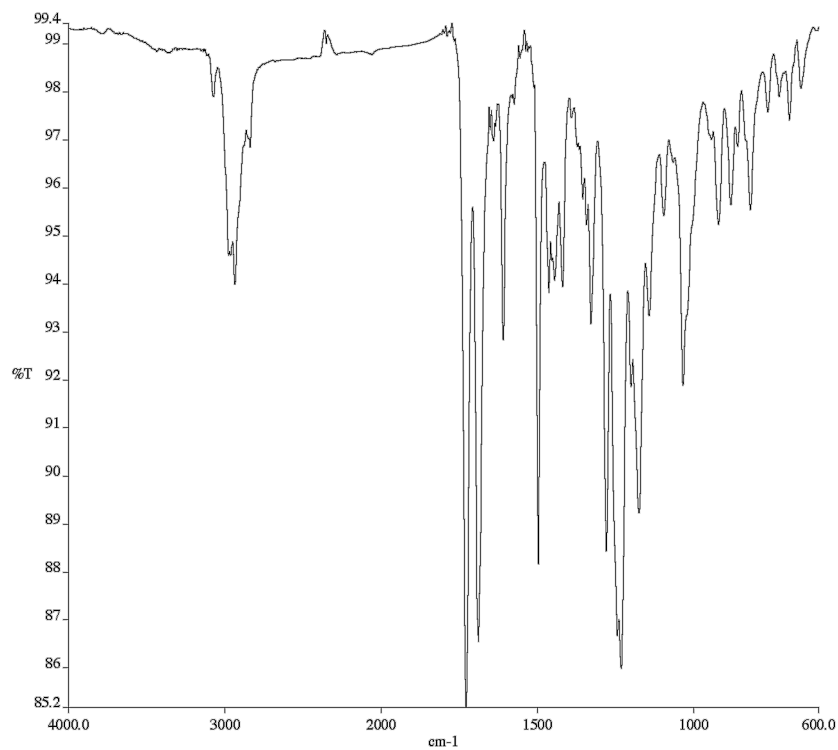


Figure A1.44 Infrared spectrum (Thin Film, NaCl) of compound **58f**

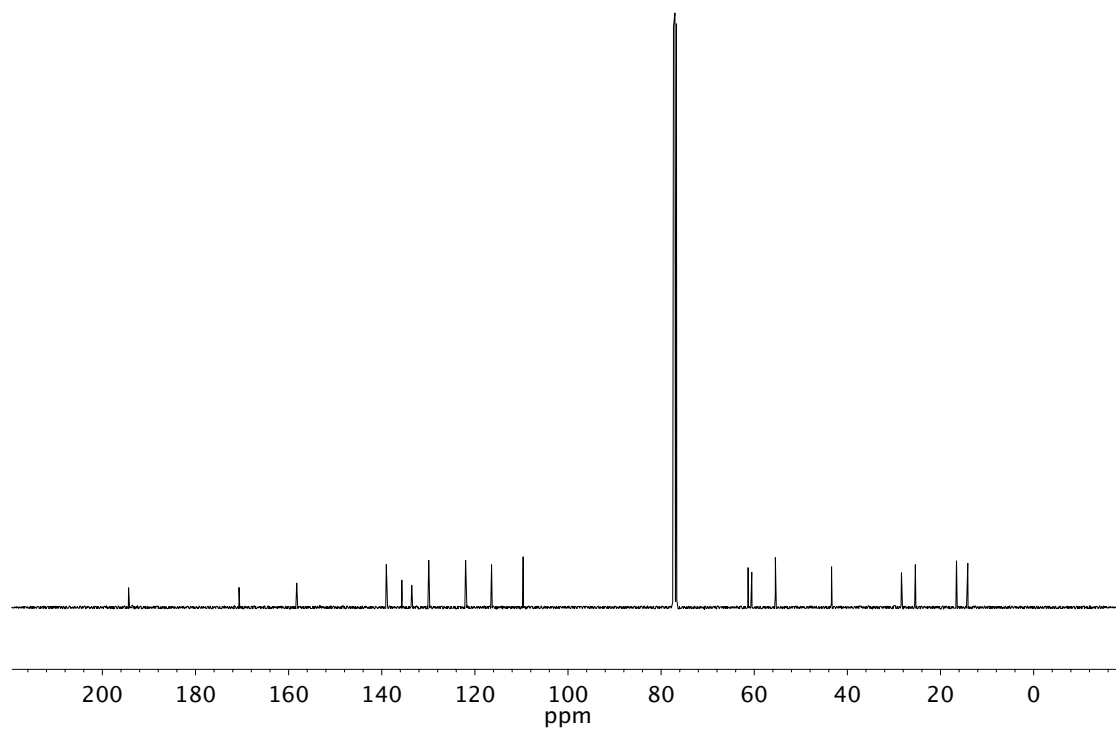


Figure A1.45 ¹³C NMR (101 MHz, CDCl₃) of compound **58f**

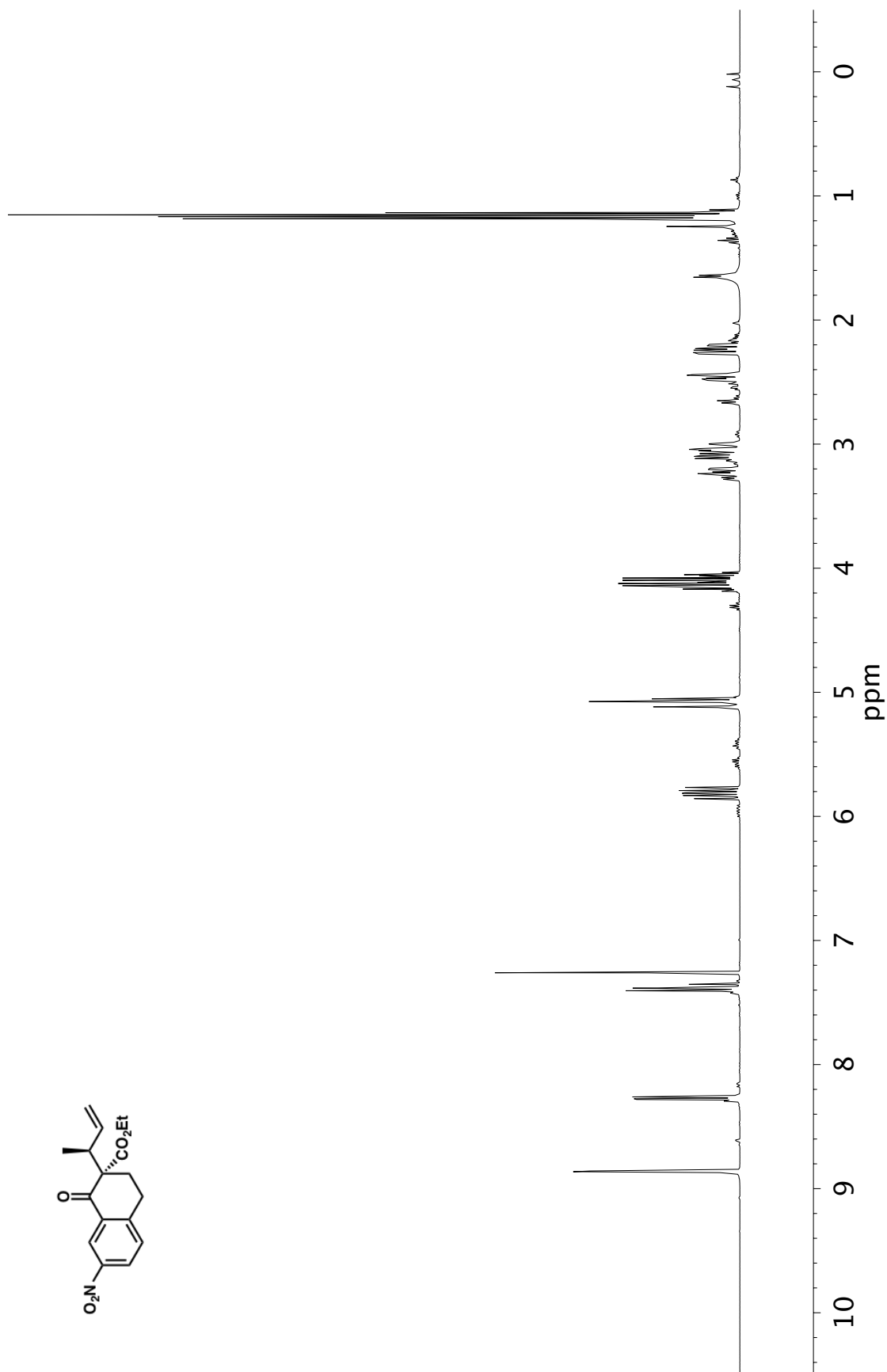


Figure A1.46 ¹H NMR (400 MHz, CDCl₃) of compound 58g

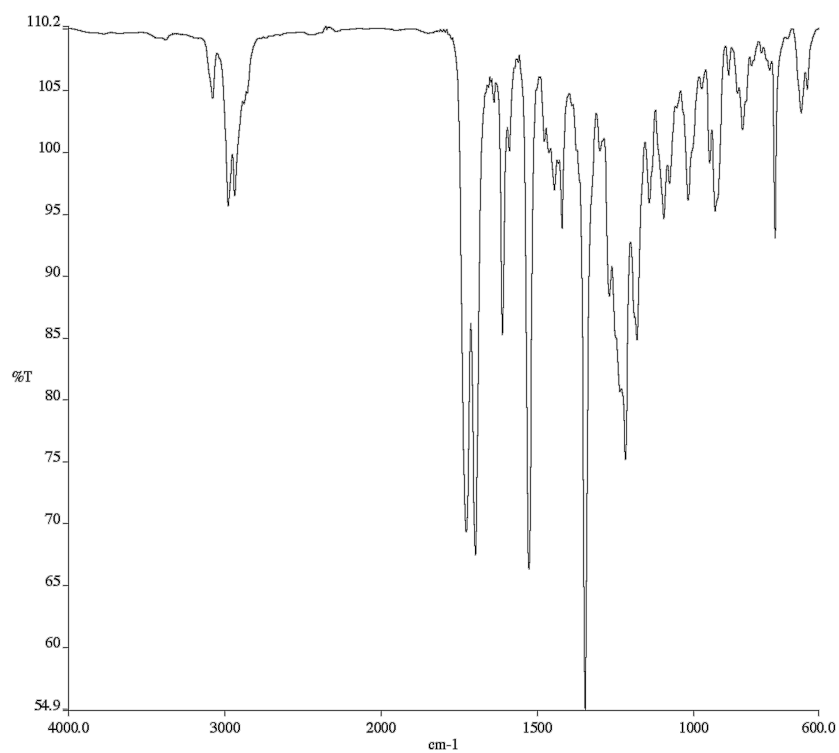


Figure A1.47 Infrared spectrum (Thin Film, NaCl) of compound **58g**

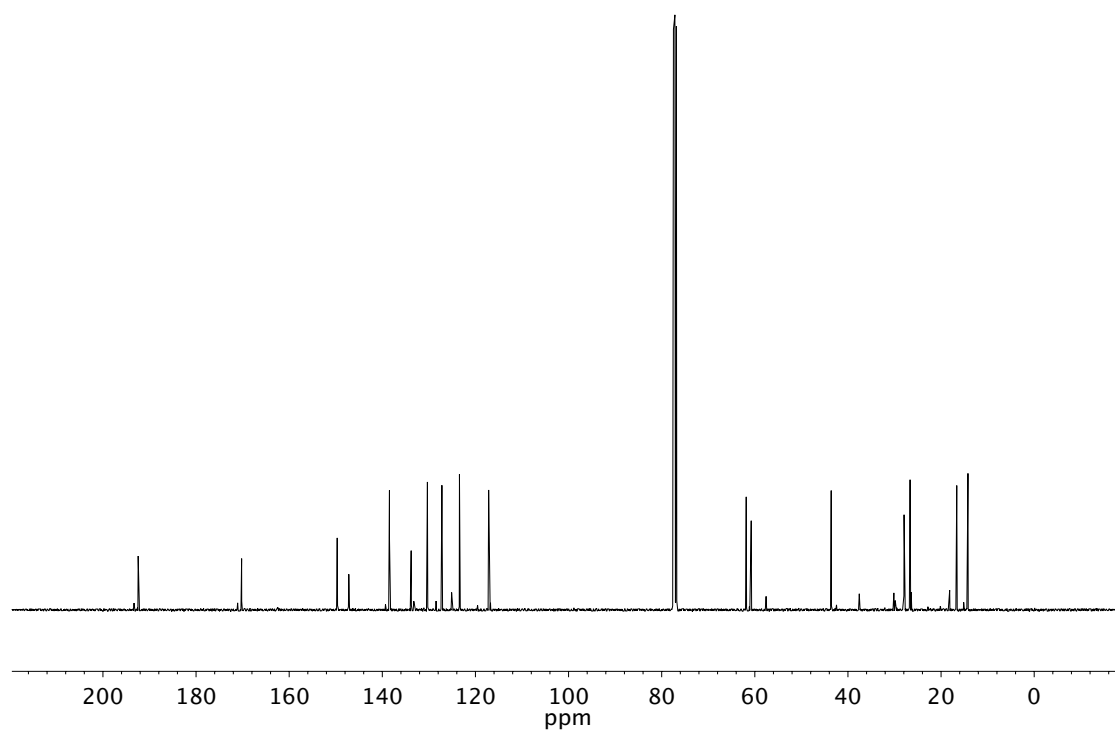


Figure A1.48 ¹³C NMR (101 MHz, CDCl₃) of compound **58g**

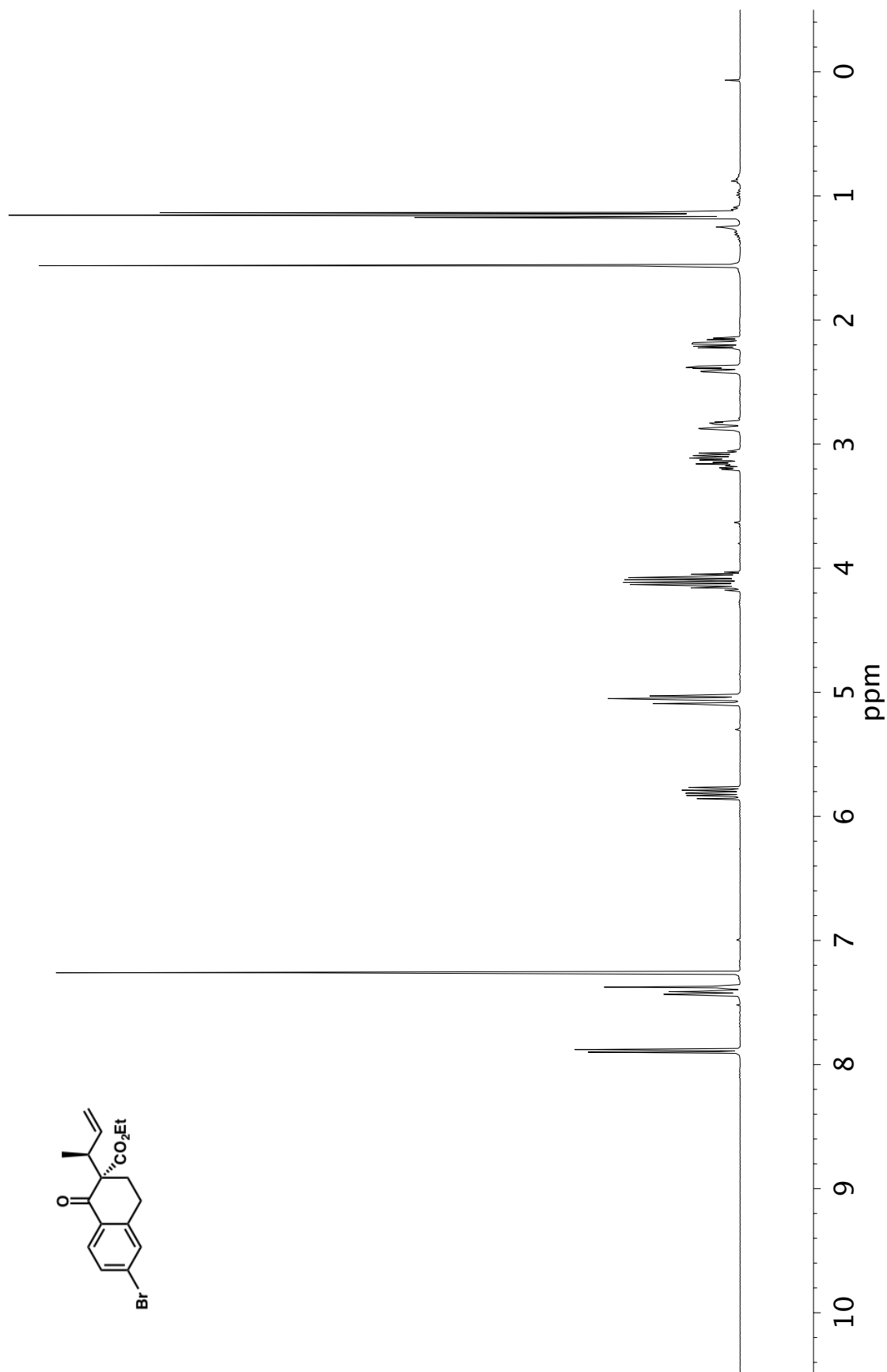


Figure A1.49 ^1H NMR (400 MHz, CDCl_3) of compound **58h**

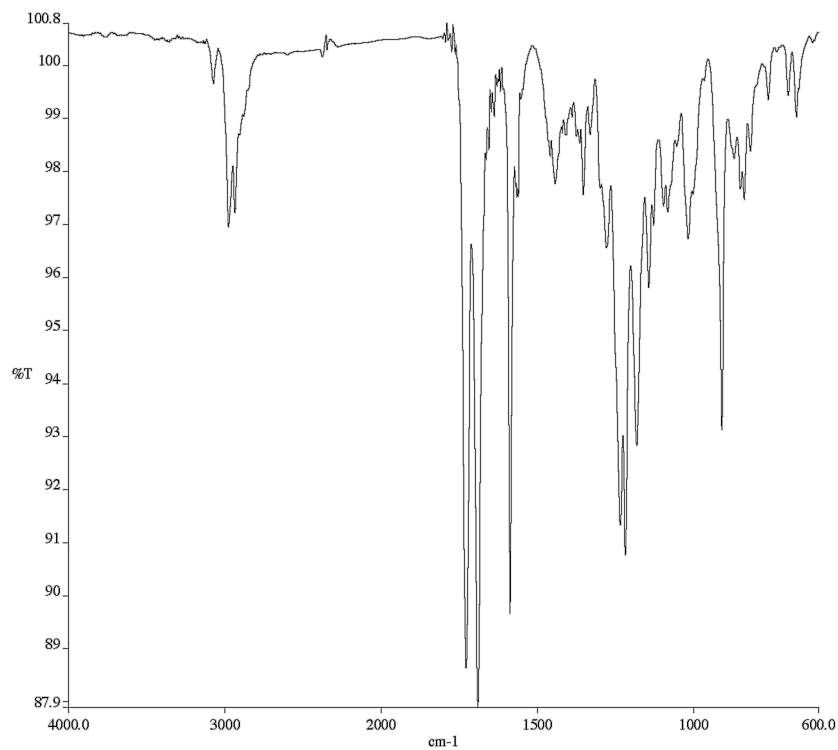


Figure A1.50 Infrared spectrum (Thin Film, NaCl) of compound **58h**

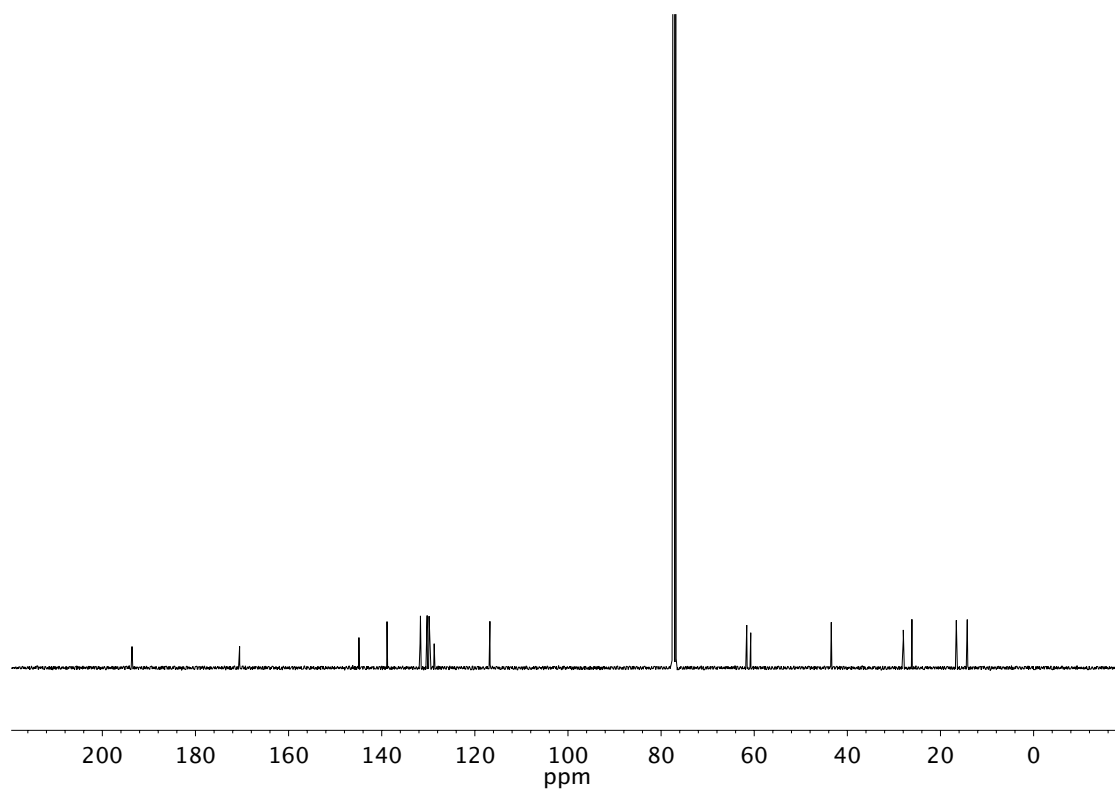


Figure A1.51 ¹³C NMR (101 MHz, CDCl₃) of compound **58h**

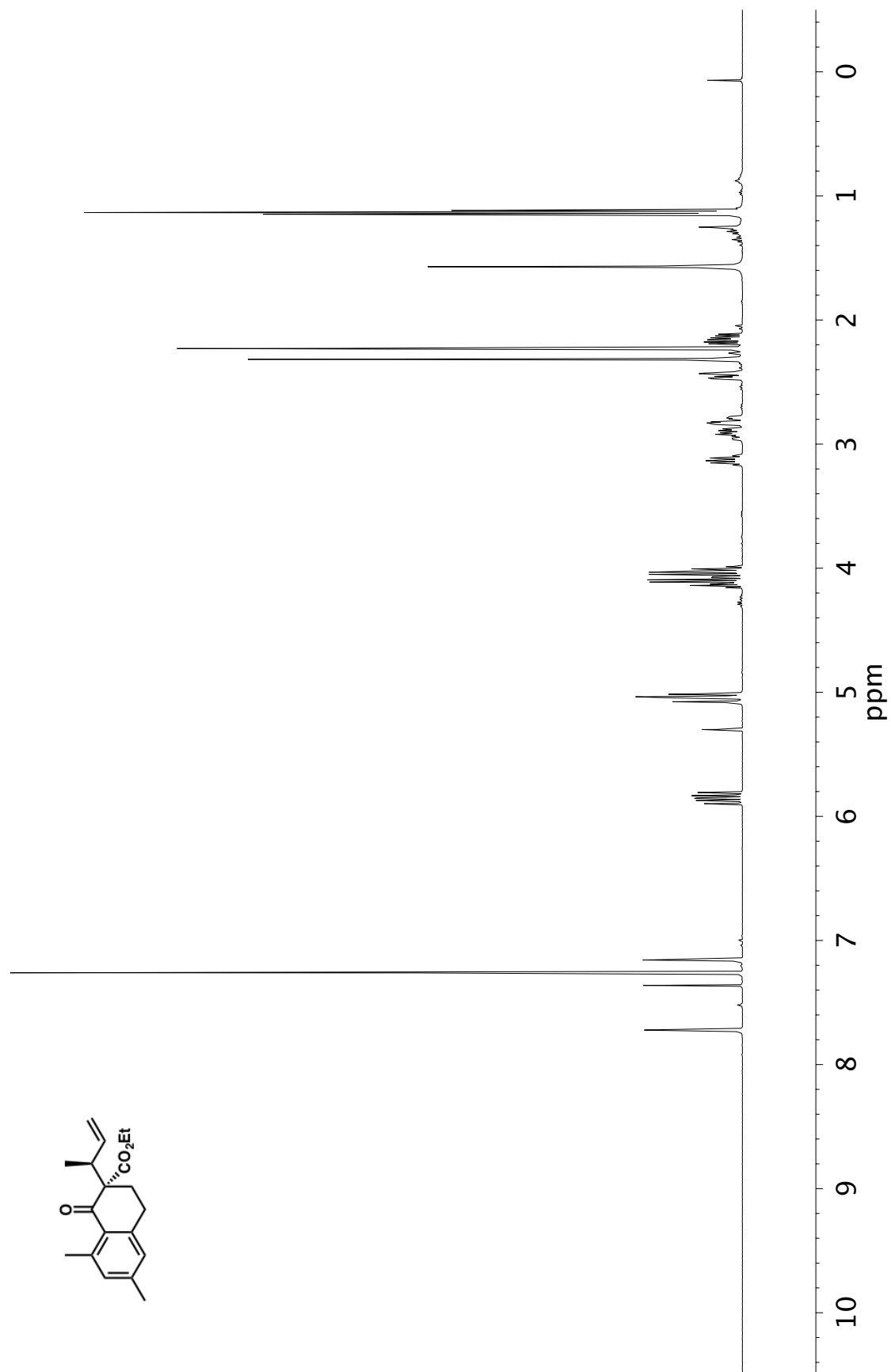


Figure A1.52 ^1H NMR (400 MHz, CDCl_3) of compound **58i**

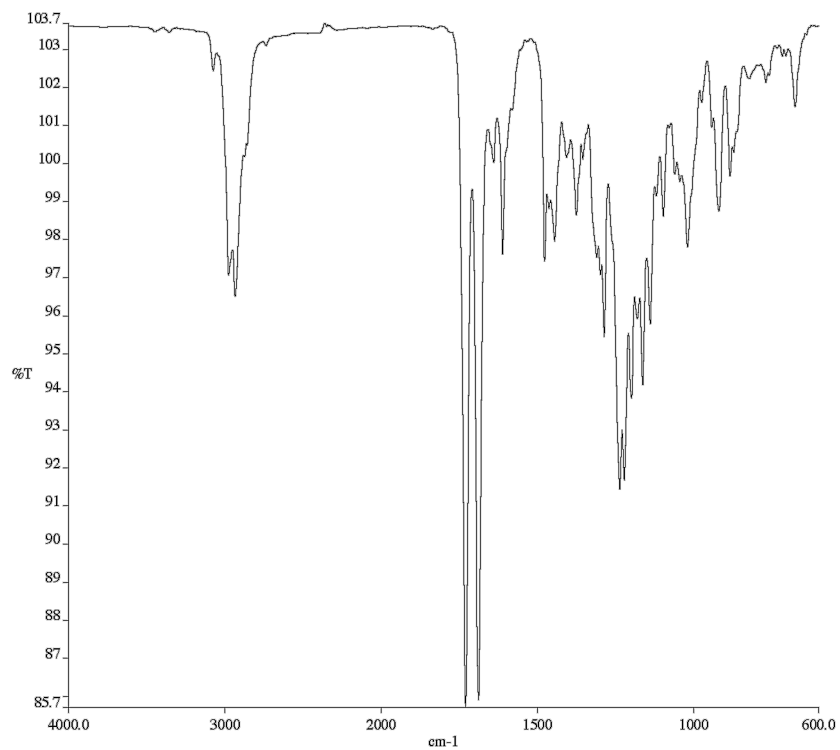


Figure A1.53 Infrared spectrum (Thin Film, NaCl) of compound **58i**

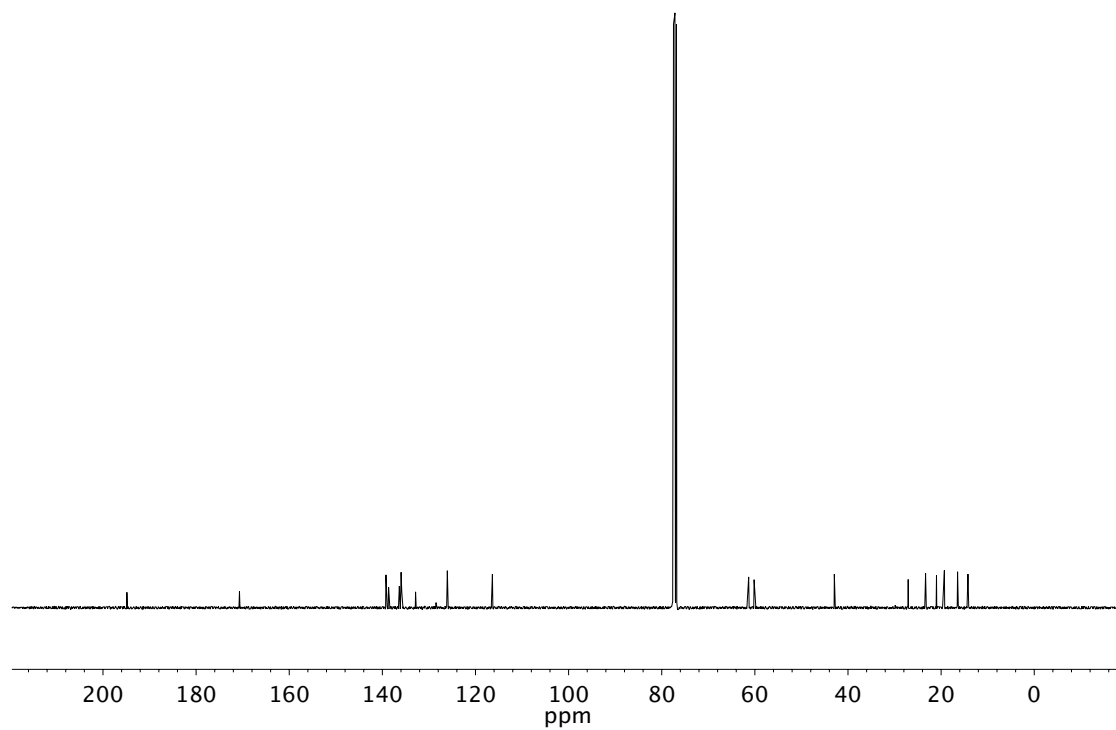


Figure A1.54 ¹³C NMR (101 MHz, CDCl₃) of compound **58i**

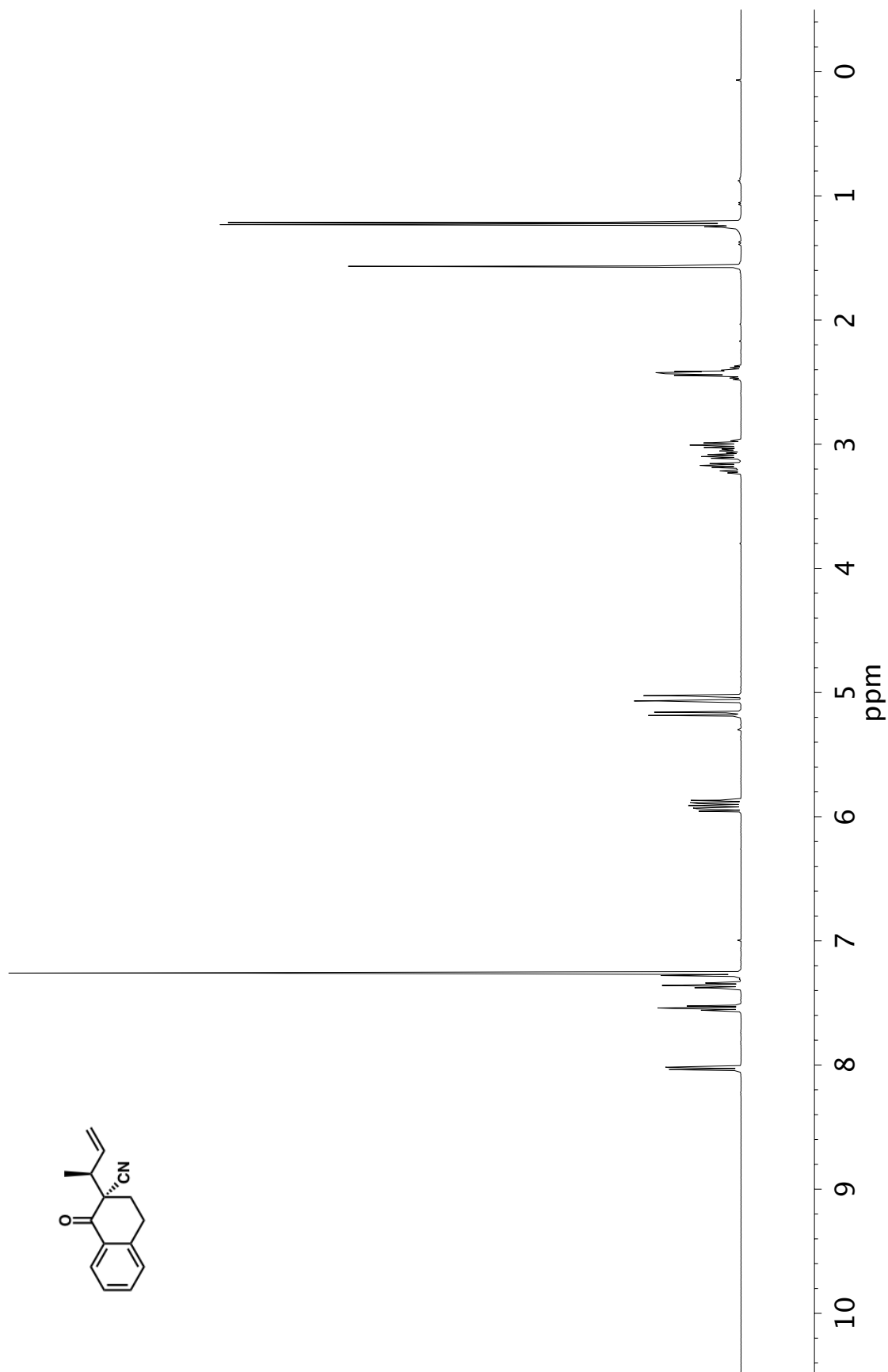


Figure A1.55 ¹H NMR (400 MHz, CDCl₃) of compound **58j**

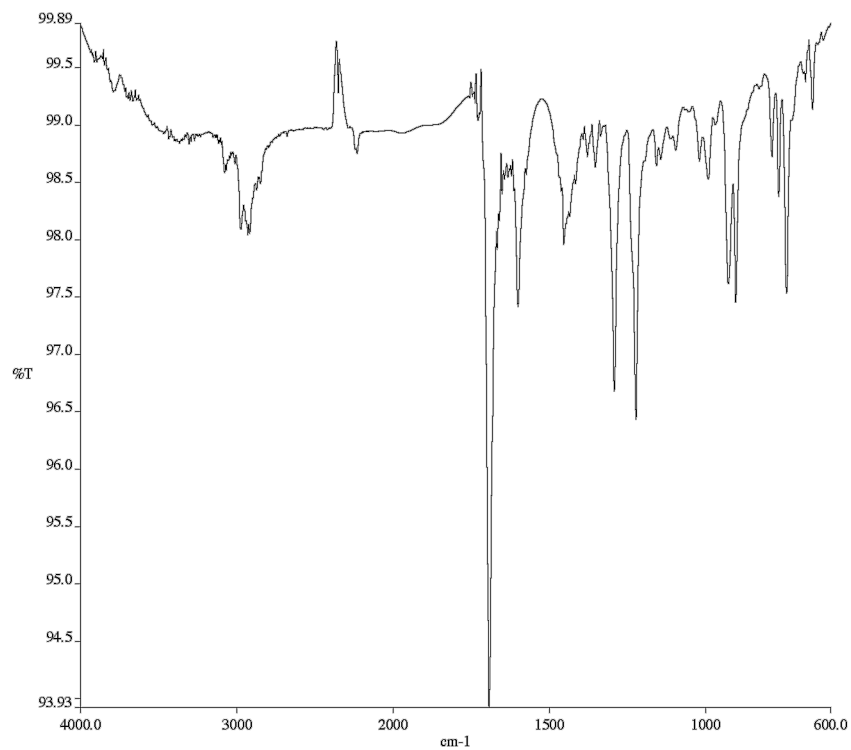


Figure A1.56 Infrared spectrum (Thin Film, NaCl) of compound **58j**

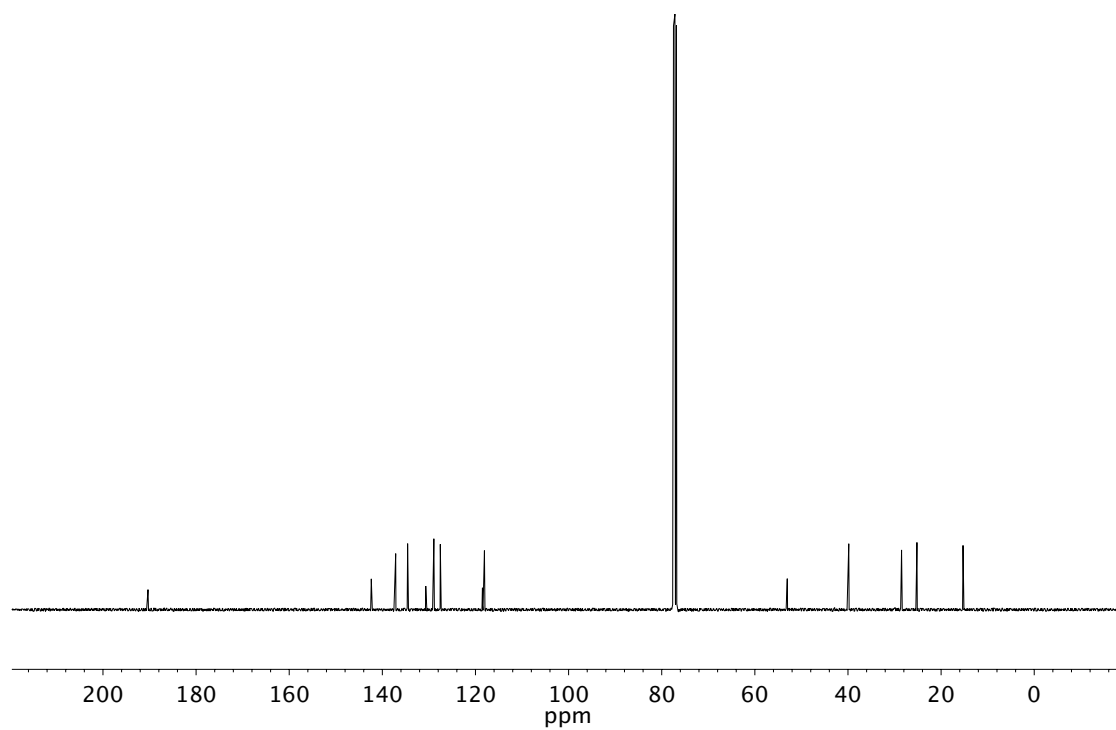


Figure A1.57 ¹³C NMR (101 MHz, CDCl₃) of compound **58j**

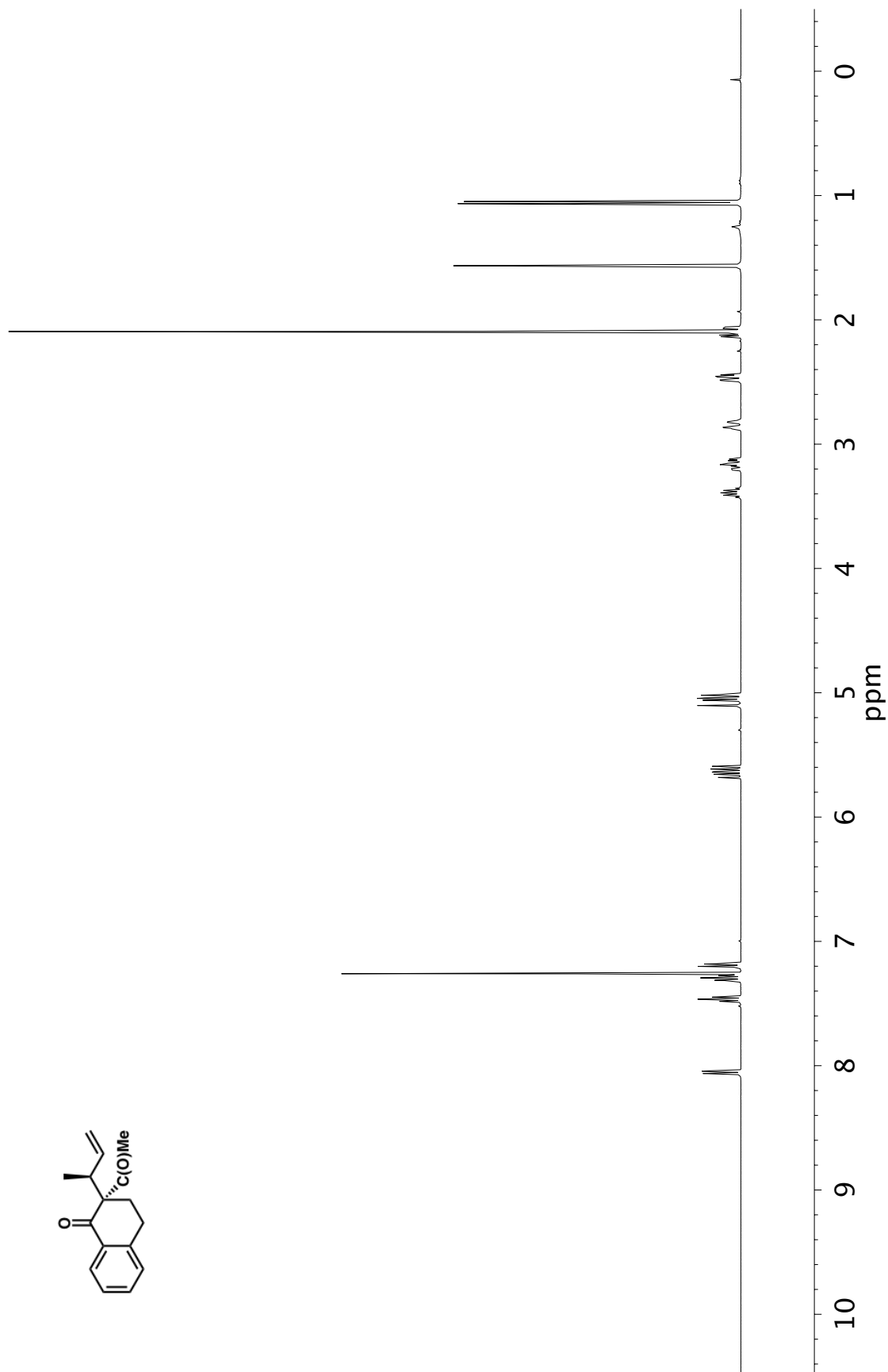


Figure A1.58 ^1H NMR (400 MHz, CDCl_3) of compound **58k**

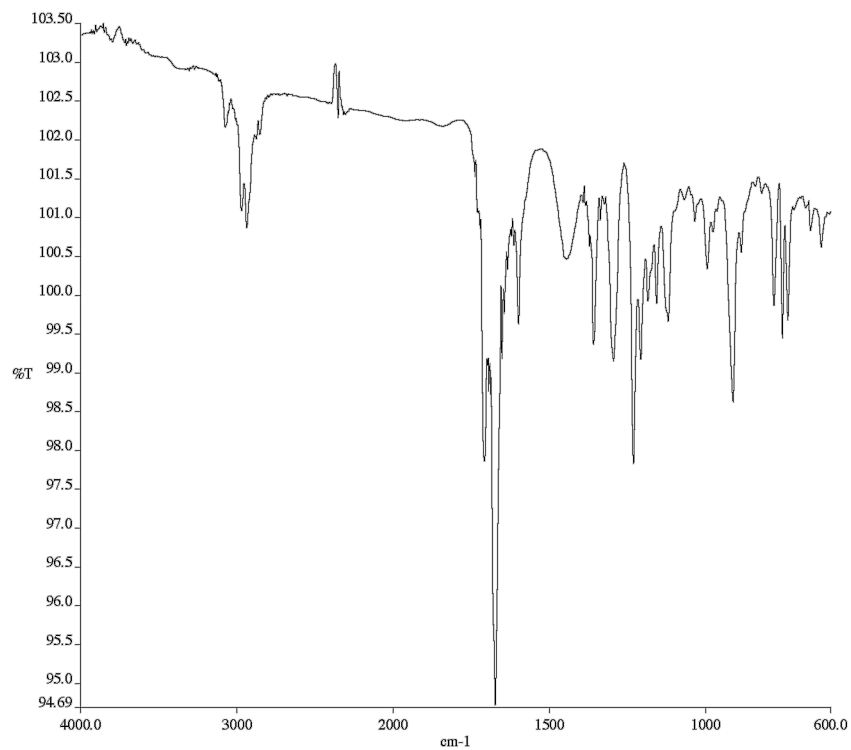


Figure A1.59 Infrared spectrum (Thin Film, NaCl) of compound **58k**

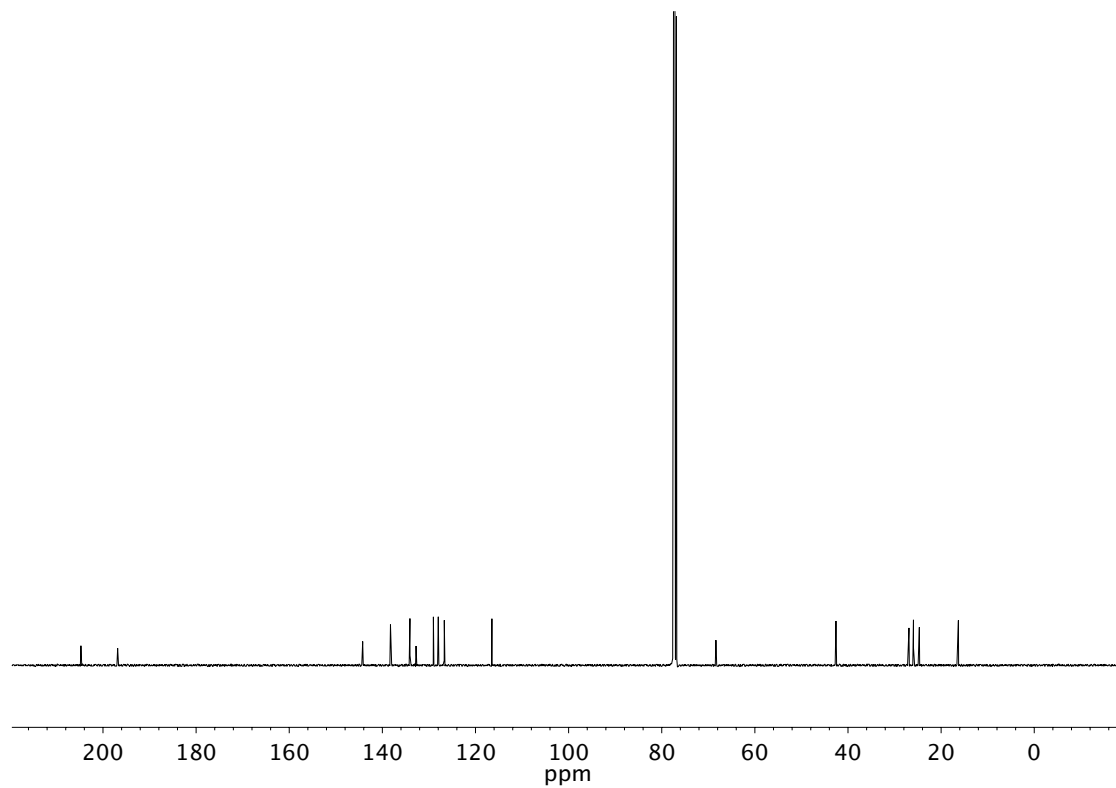


Figure A1.60 ¹³C NMR (101 MHz, CDCl₃) of compound **58k**

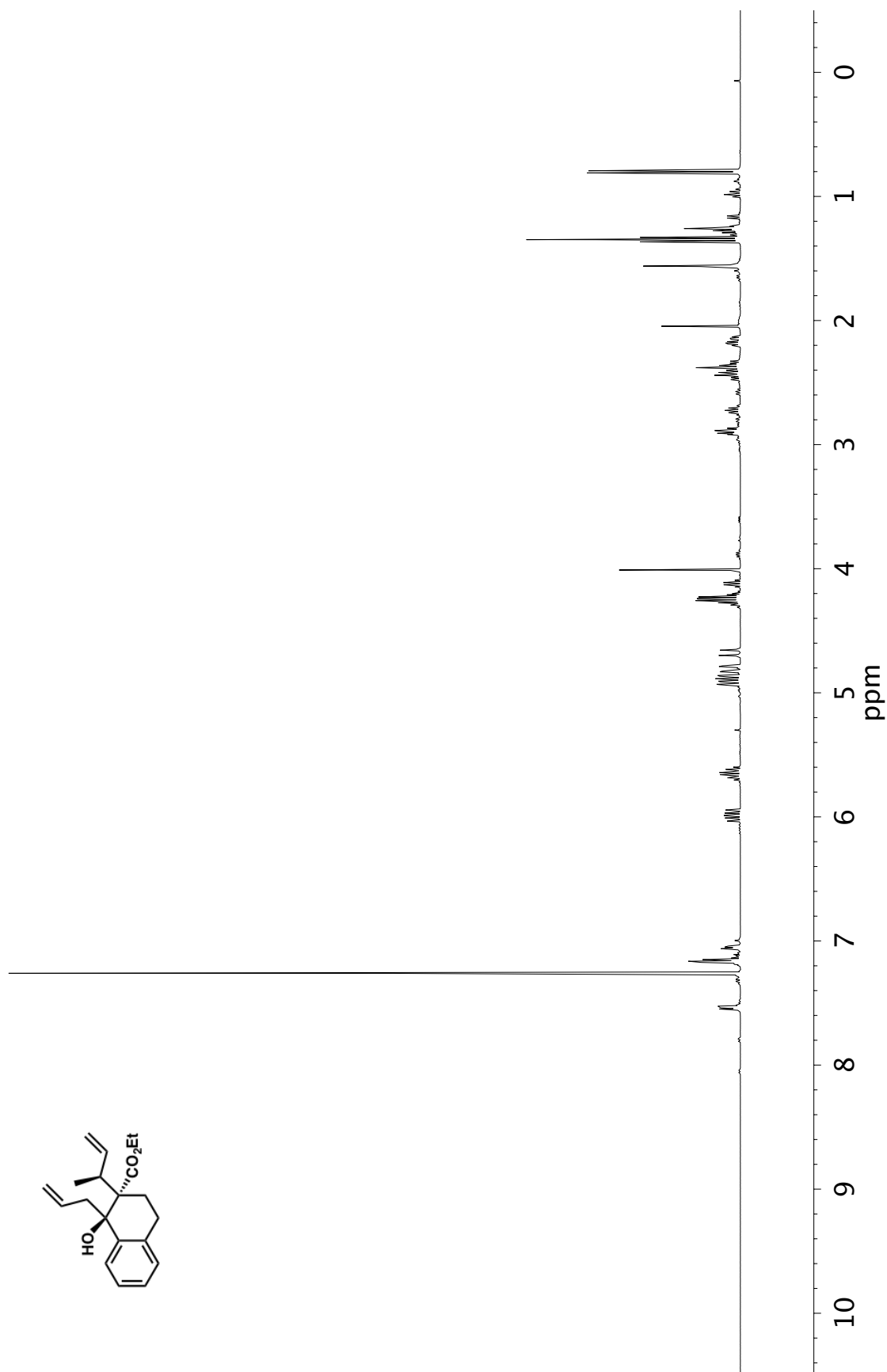


Figure A1.61 ¹H NMR (400 MHz, CDCl₃) of compound **61**

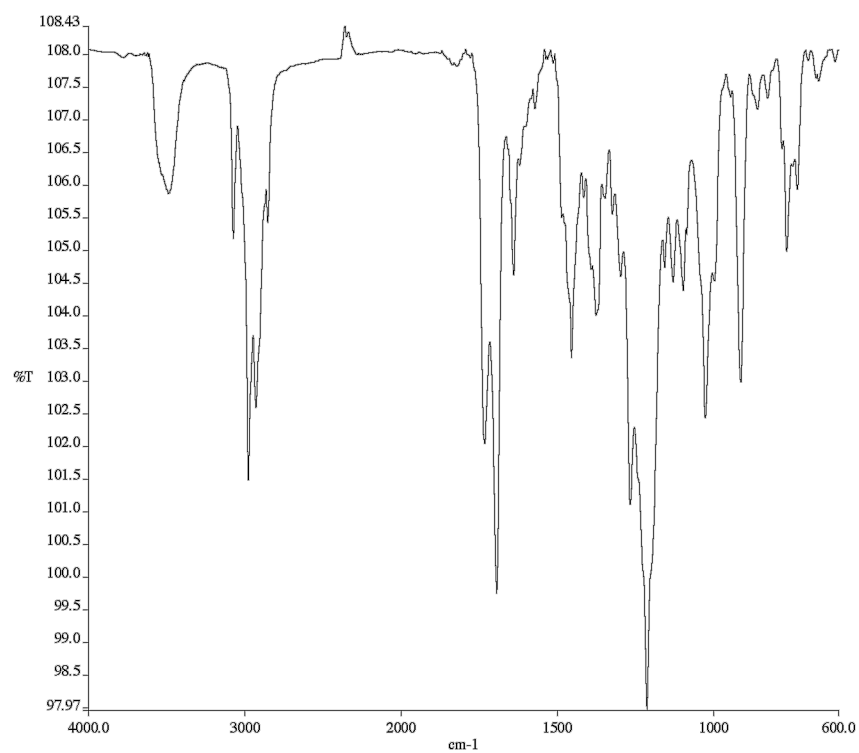


Figure A1.62 Infrared spectrum (Thin Film, NaCl) of compound **61**

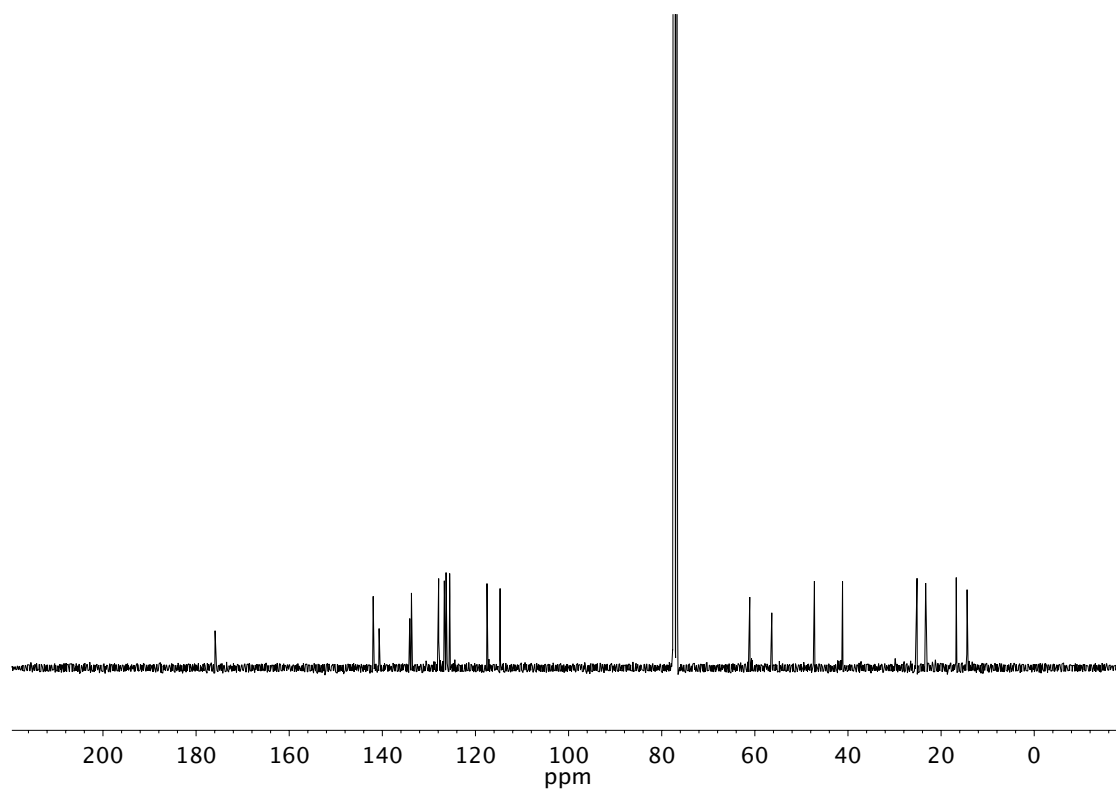


Figure A1.63 ^{13}C NMR (101 MHz, CDCl_3) of compound **61**

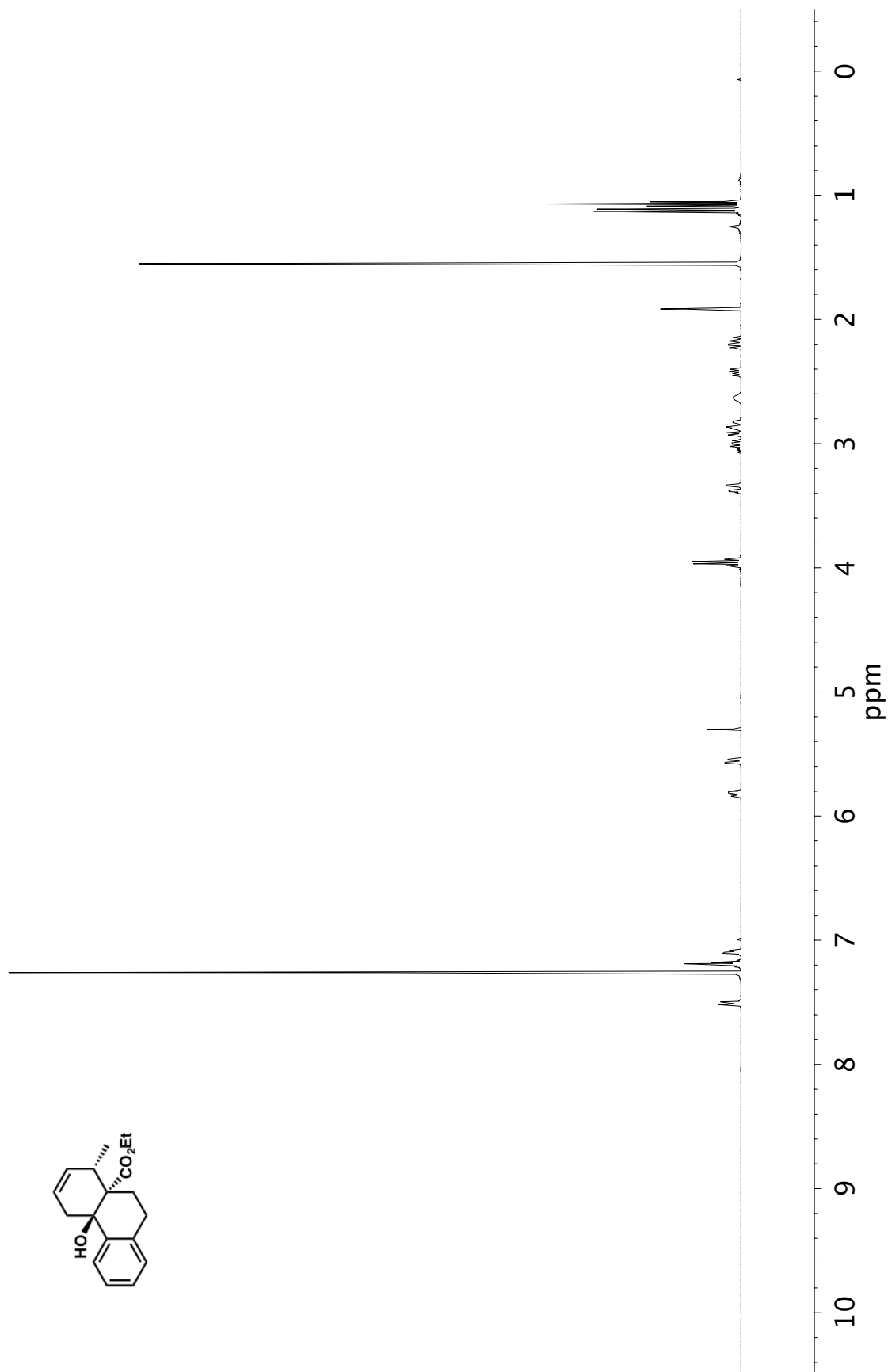


Figure A1.64 ¹H NMR (400 MHz, CDCl₃) of compound **62**

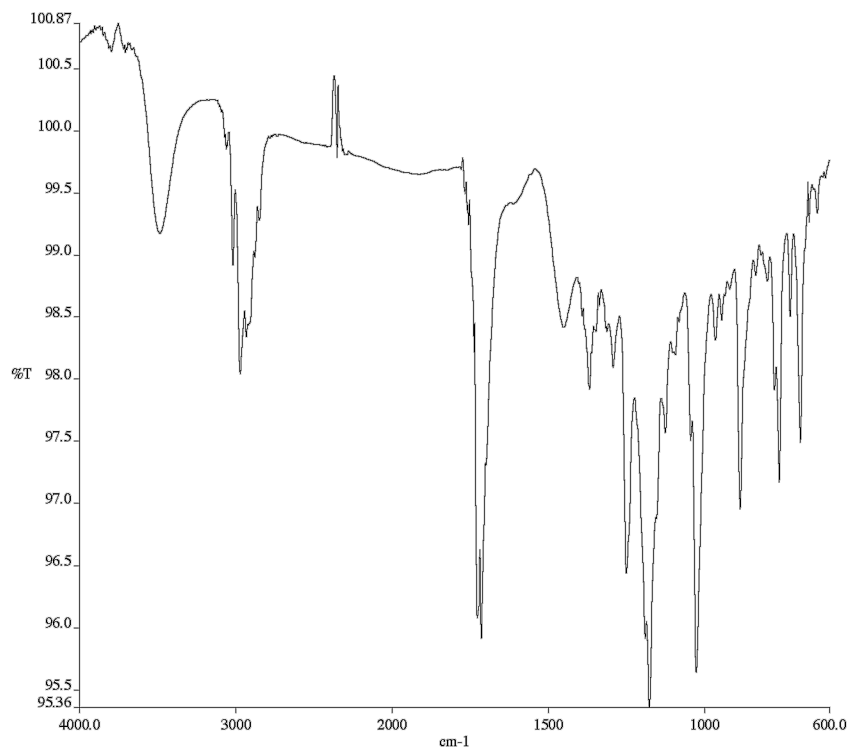


Figure A1.65 Infrared spectrum (Thin Film, NaCl) of compound **62**

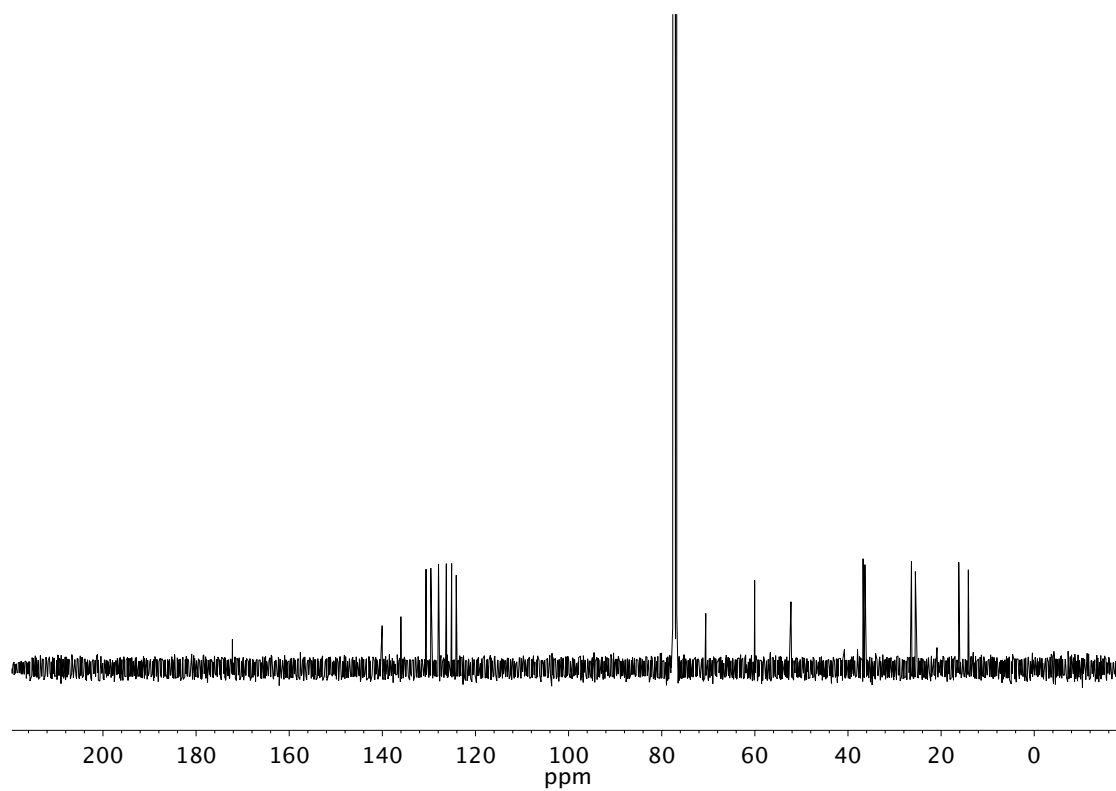


Figure A1.66 ¹³C NMR (101 MHz, CDCl₃) of compound **62**

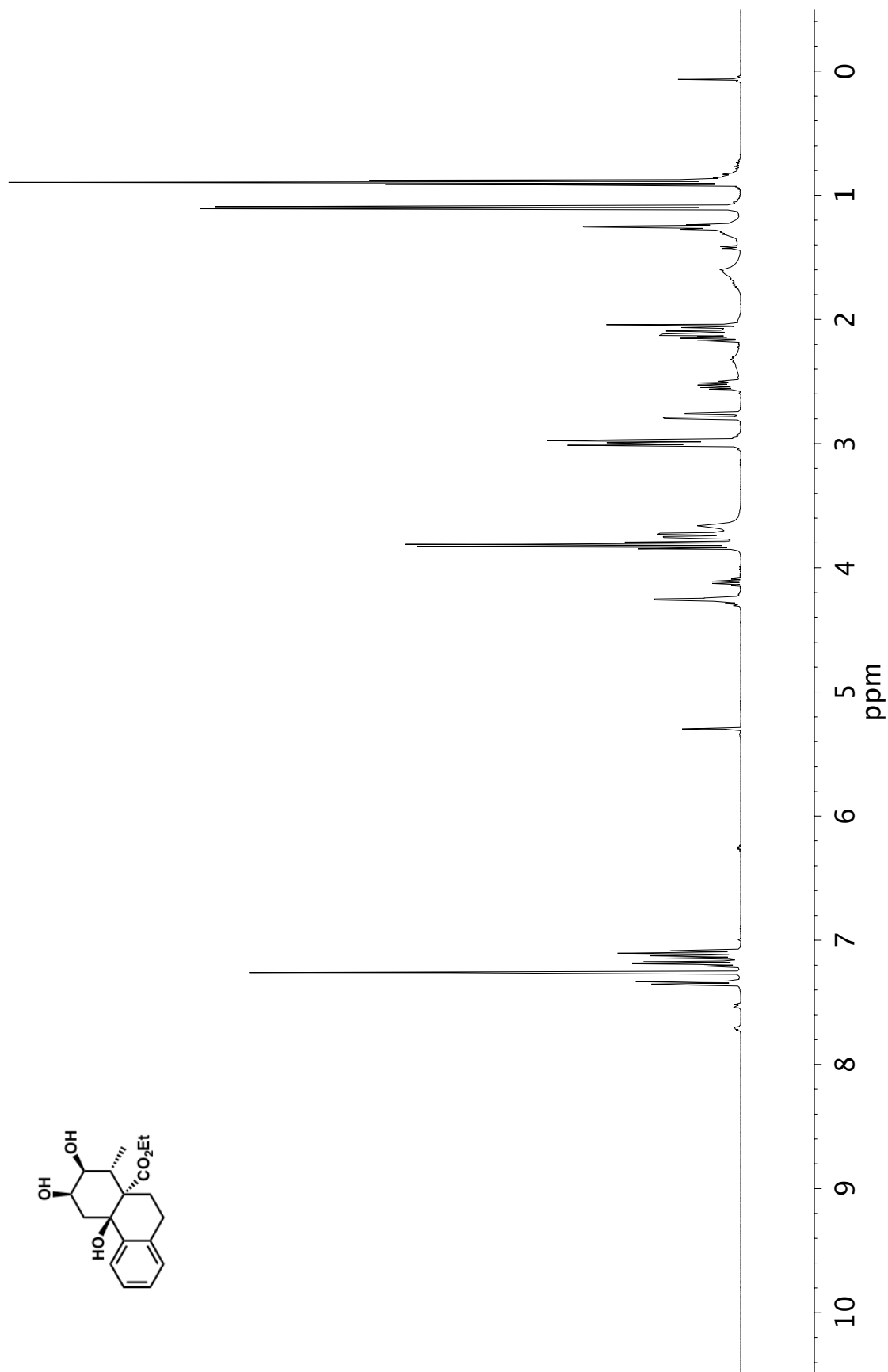


Figure A1.67 ^1H NMR (400 MHz, CDCl_3) of compound **63**

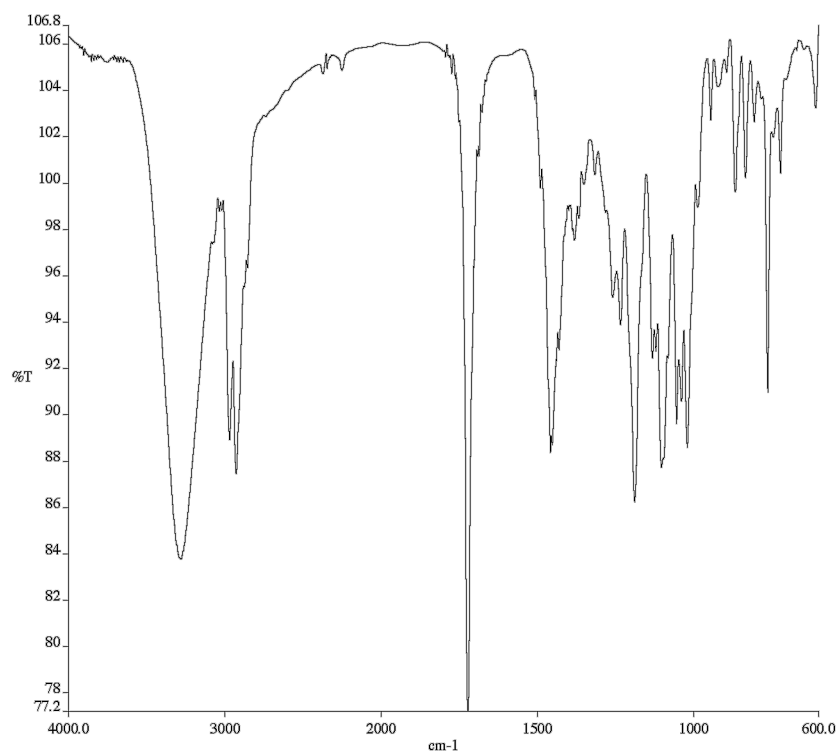


Figure A1.68 Infrared spectrum (Thin Film, NaCl) of compound **63**

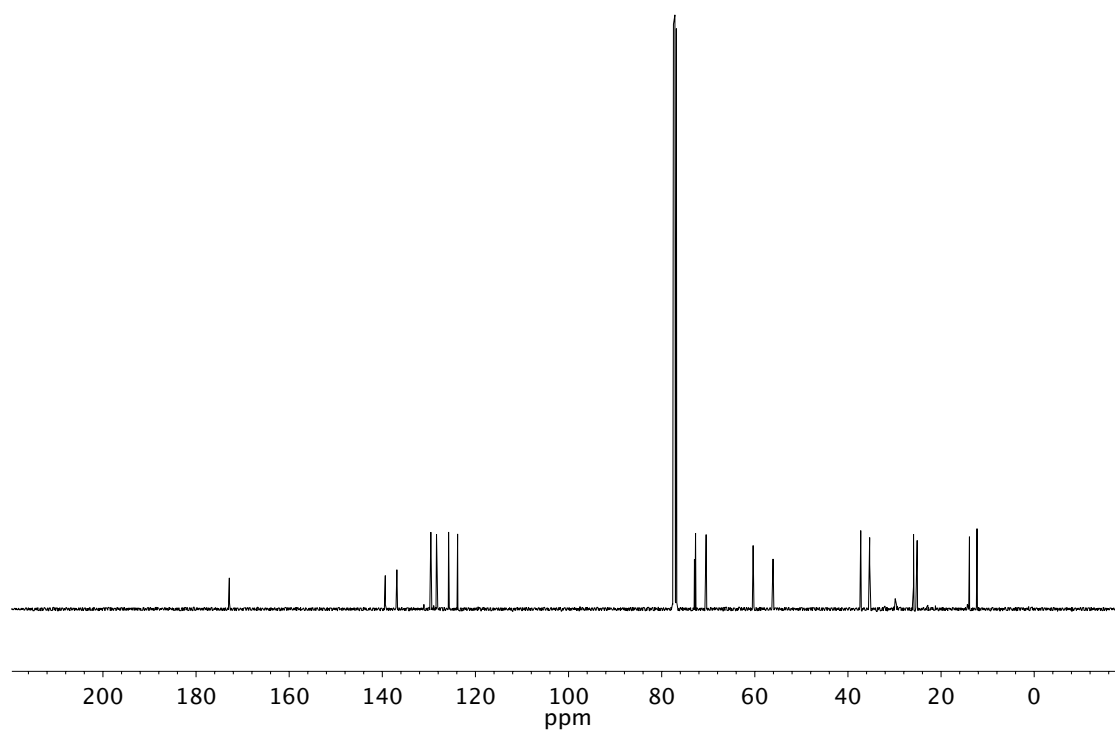


Figure A1.69 ¹³C NMR (101 MHz, CDCl₃) of compound **63**

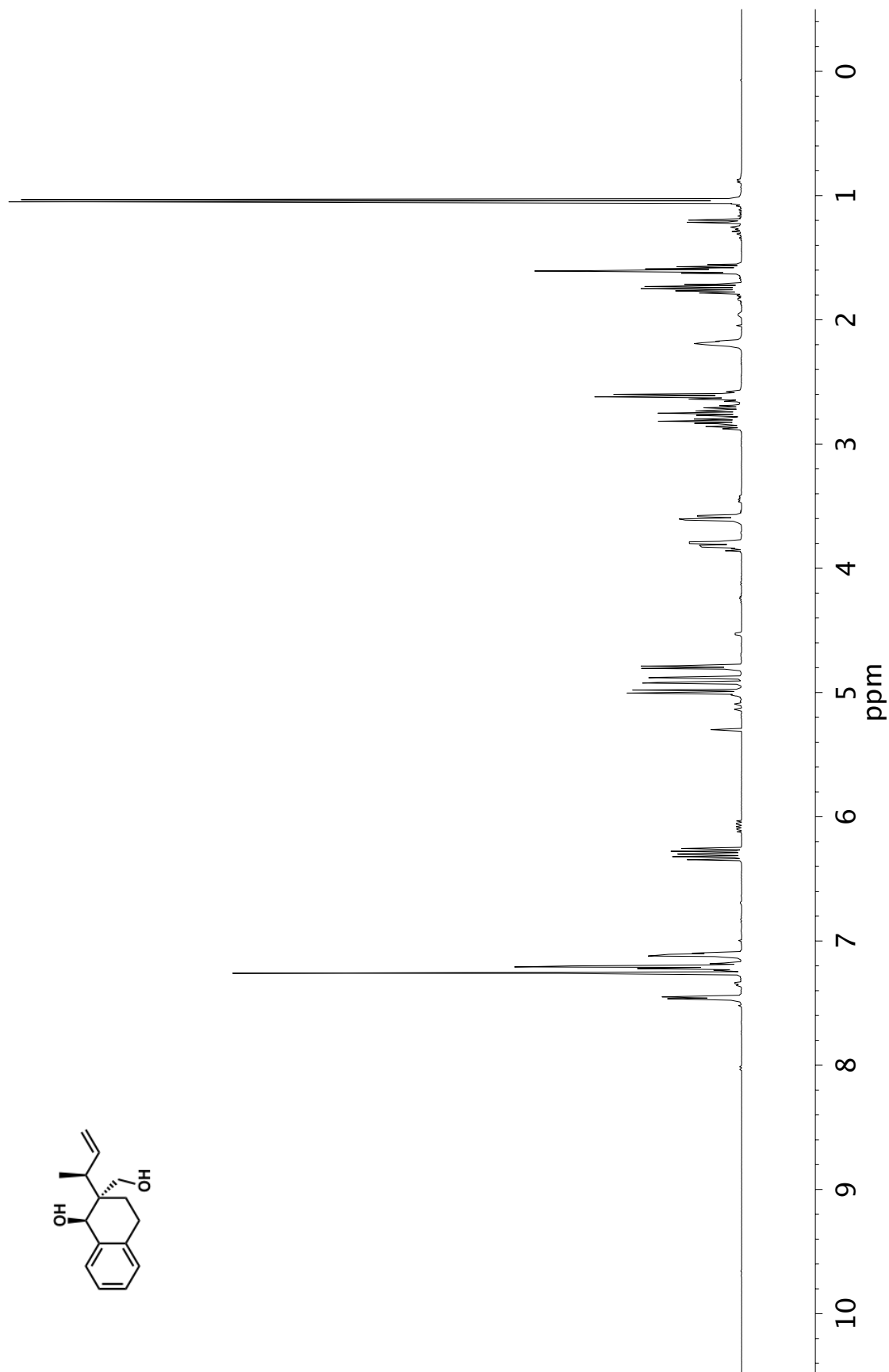


Figure A1.70 ^1H NMR (400 MHz, CDCl_3) of compound **64**

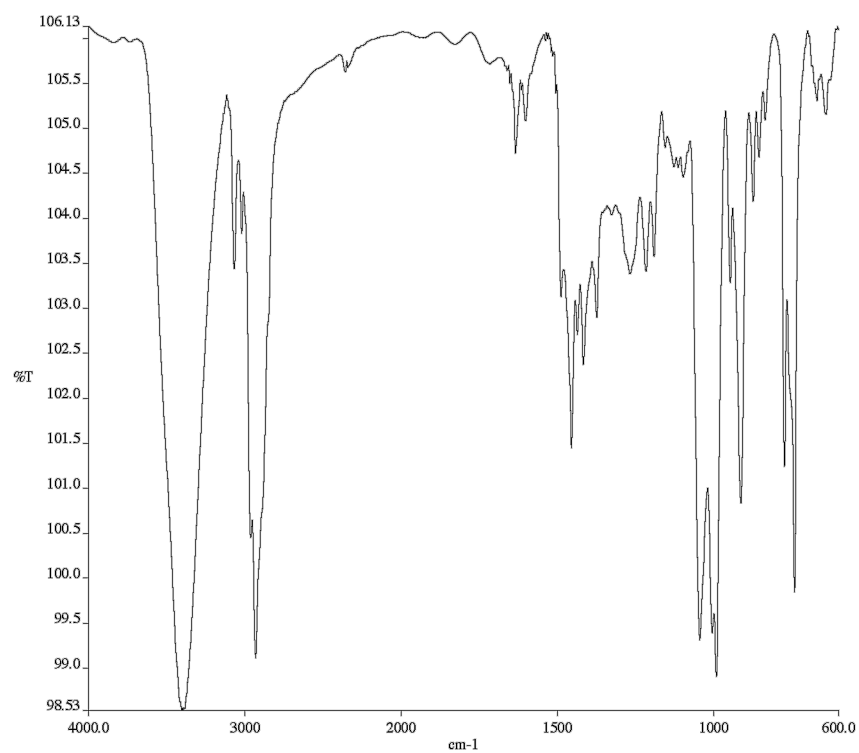


Figure A1.71 Infrared spectrum (Thin Film, NaCl) of compound **64**

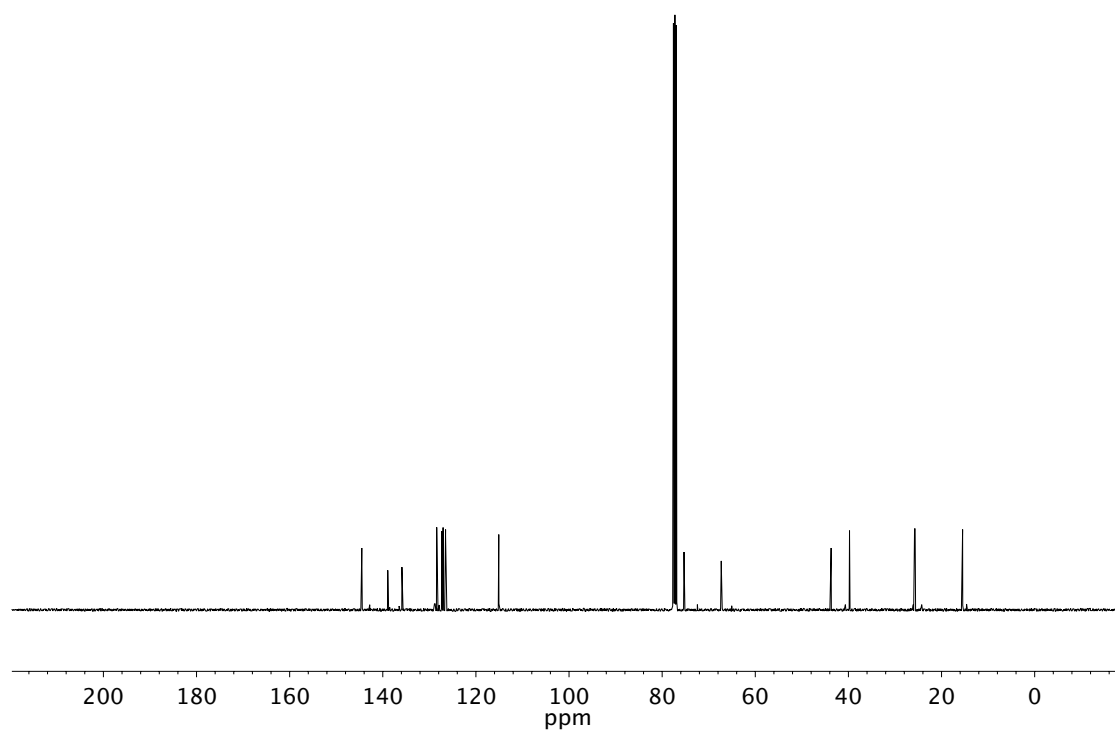


Figure A1.72 ¹³C NMR (101 MHz, CDCl₃) of compound **64**

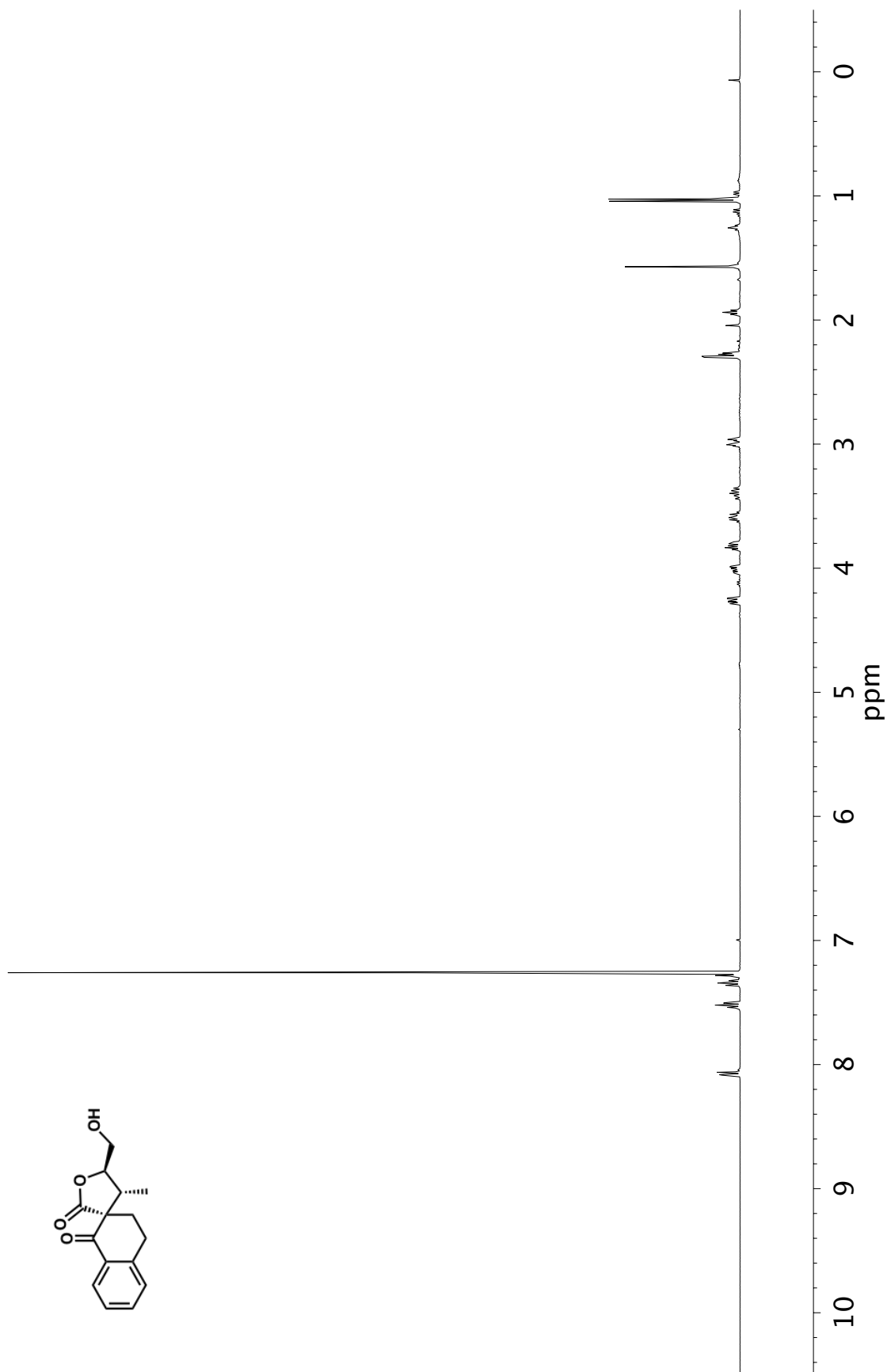


Figure A1.73 ¹H NMR (400 MHz, CDCl₃) of compound **65**

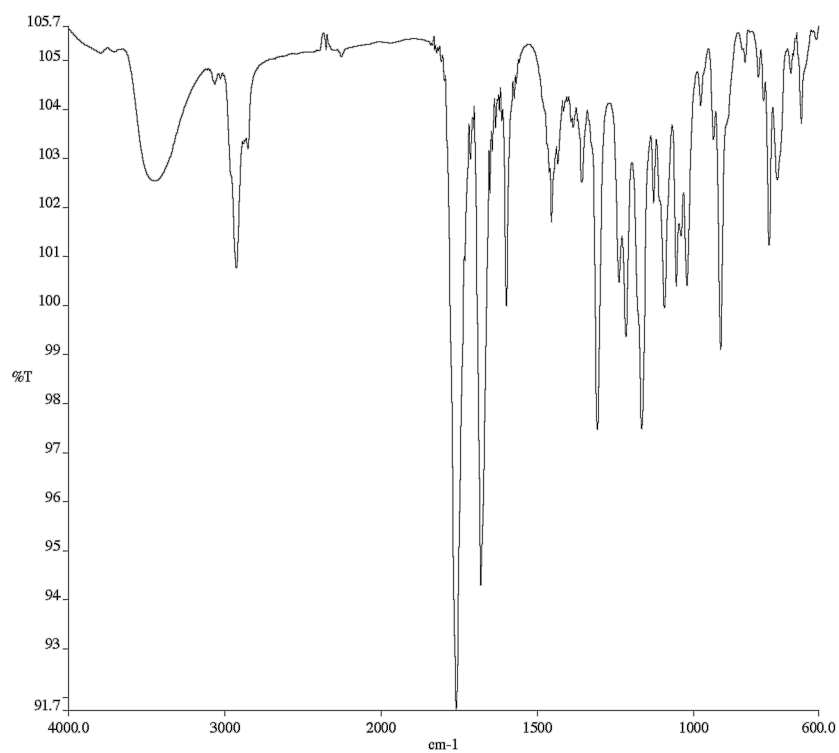


Figure A1.74 Infrared spectrum (Thin Film, NaCl) of compound **65**

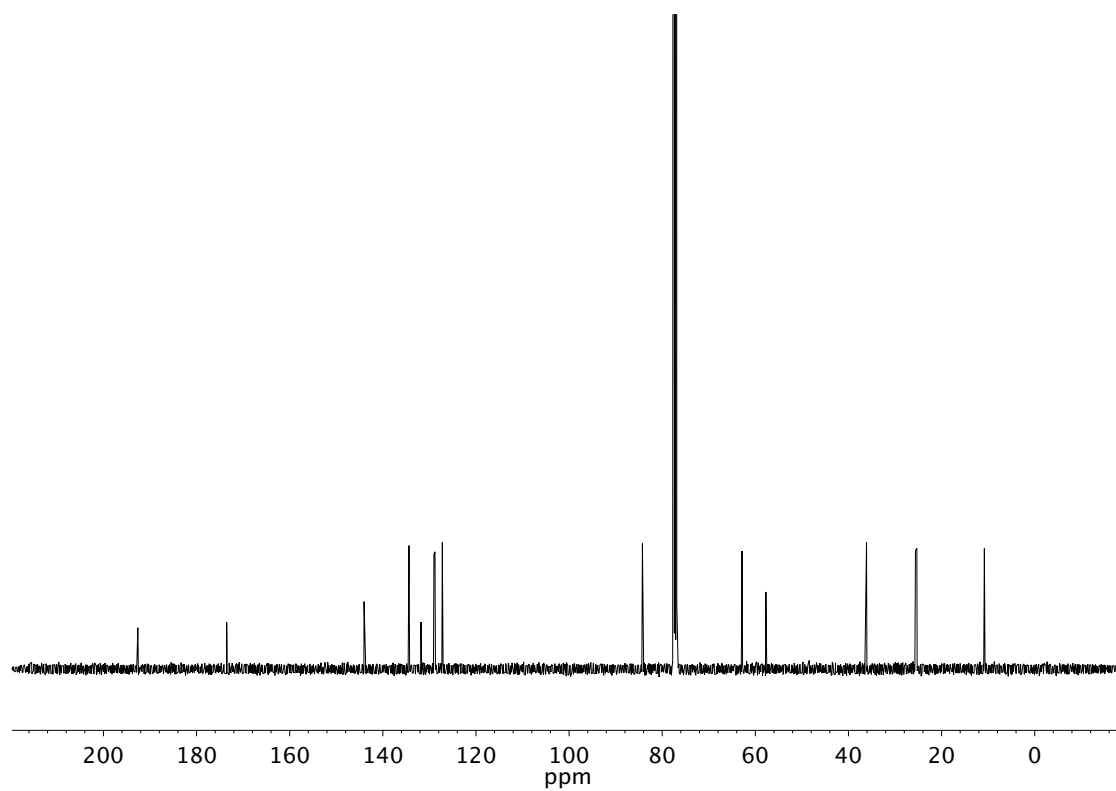


Figure A1.75 ¹³C NMR (101 MHz, CDCl₃) of compound **65**

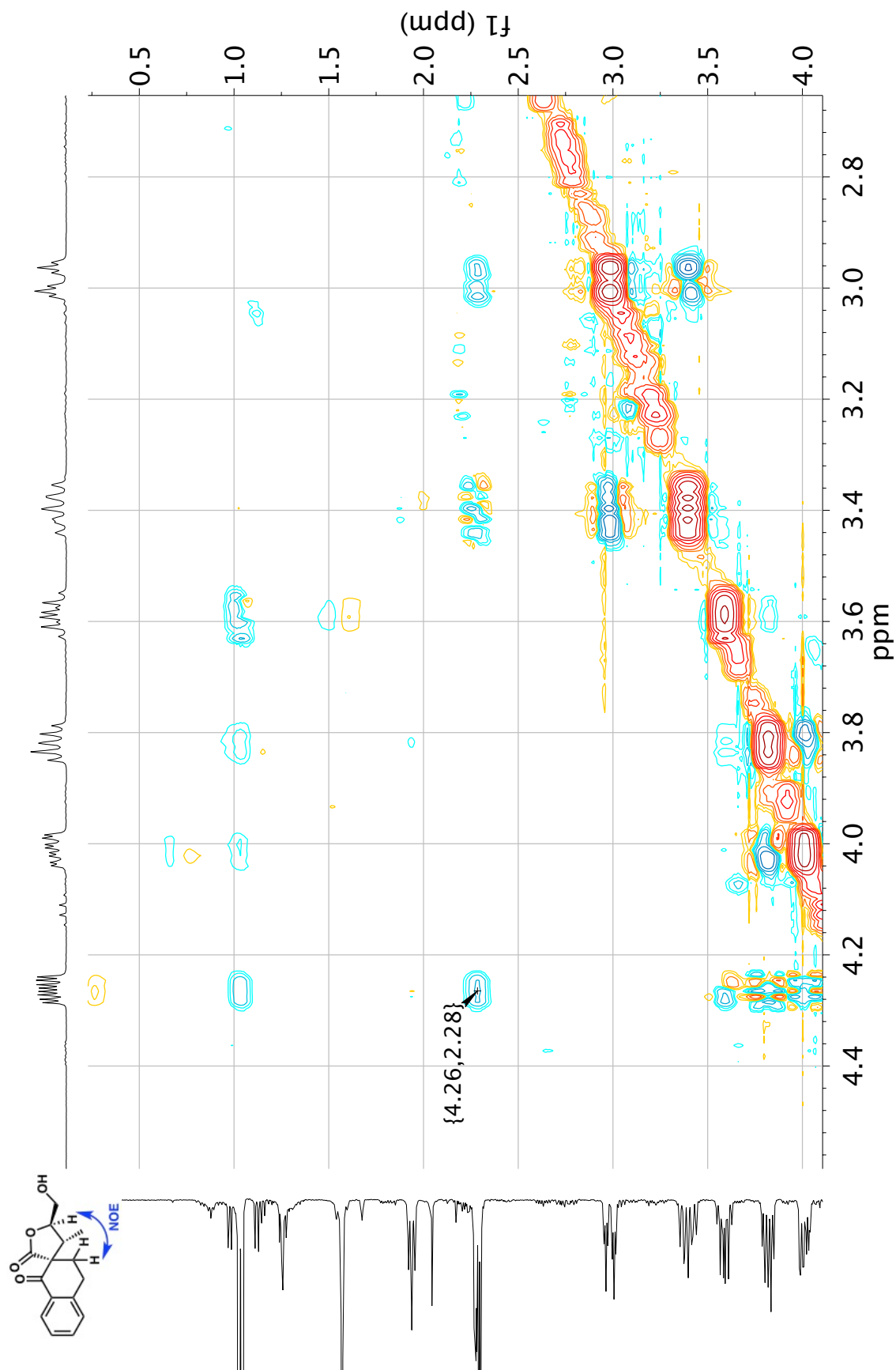


Figure A1.76 NEOSY (400 MHz, CDCl₃) of compound 65

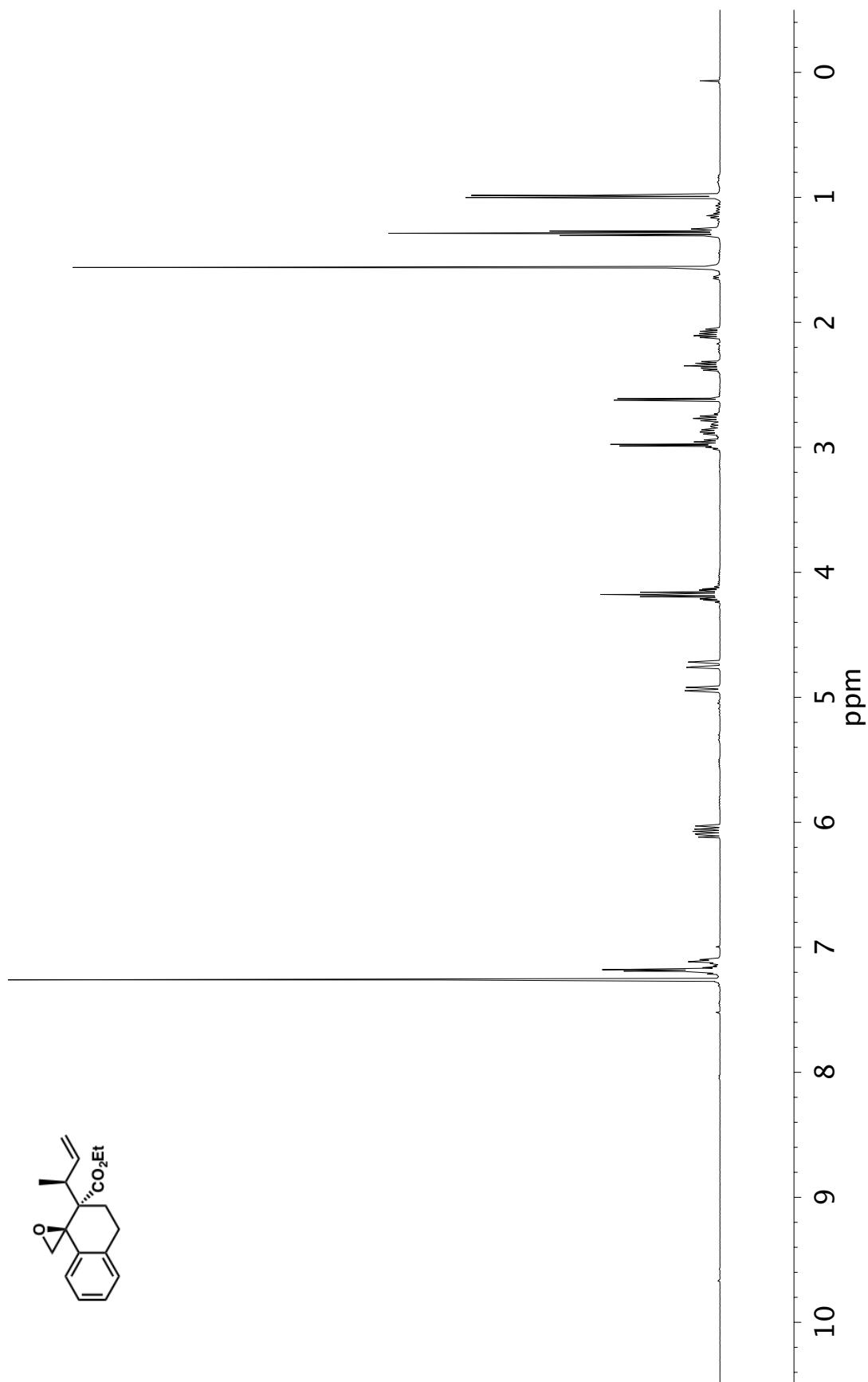


Figure A1.77 ^1H NMR (400 MHz, CDCl_3) of compound **66**

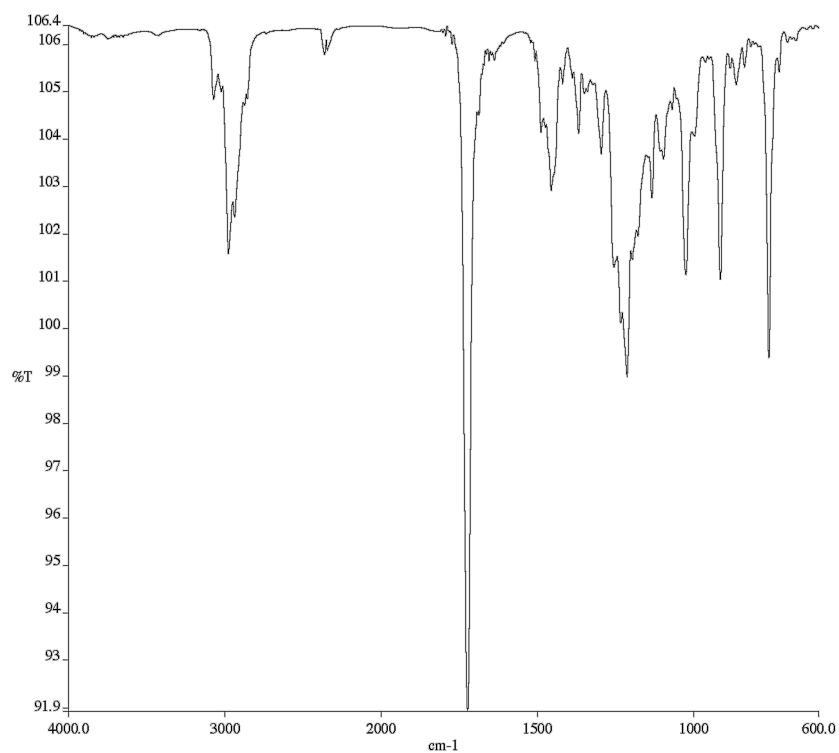


Figure A1.78 Infrared spectrum (Thin Film, NaCl) of compound **66**

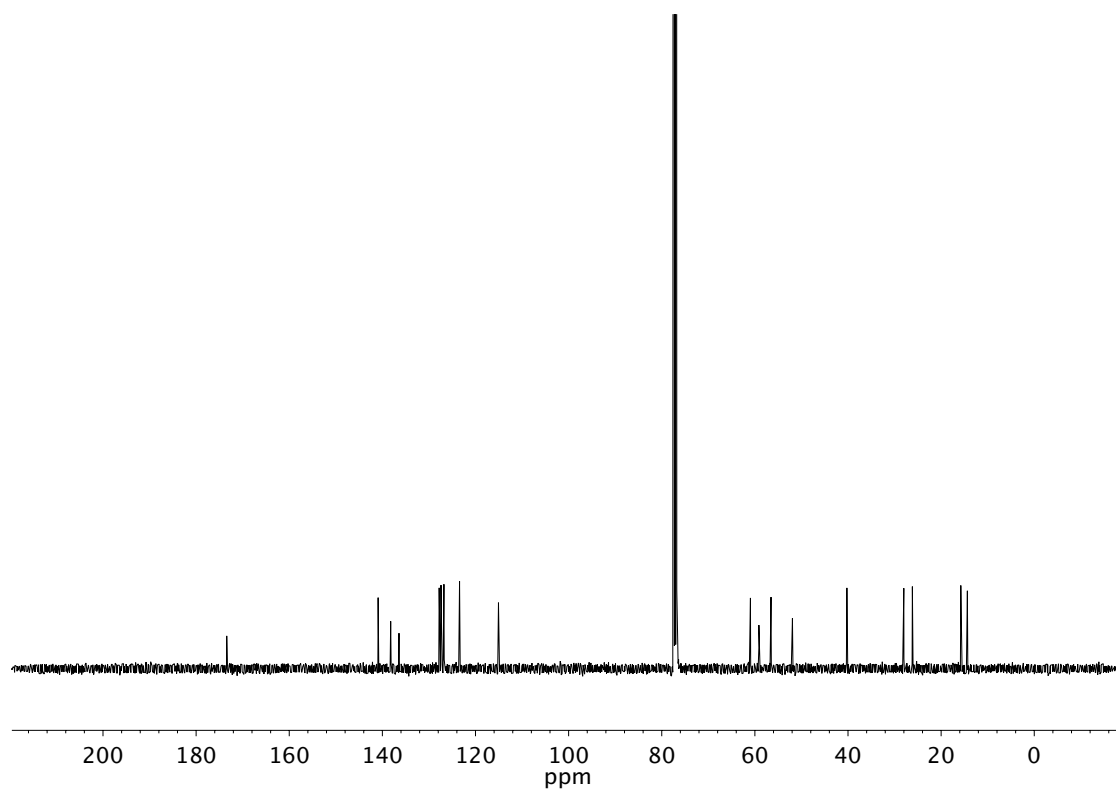


Figure A1.79 ¹³C NMR (101 MHz, CDCl₃) of compound **66**

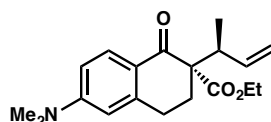
APPENDIX 2

*X-Ray Crystallography Reports Relevant to Chapter 1:
Stereoselective Iridium-Catalyzed Allylic Alkylation Reactions
with Crotyl Chloride*

A2.1 GENERAL EXPERIMENTAL

X-ray crystallographic analysis was obtained from the Caltech X-Ray Crystallography Facility using a Bruker D8 Venture Kappa Duo Photon 100 CMOS diffractometer.

A2.1.1 X-RAY CRYSTAL STRUCTURE ANALYSIS OF ALLYLIC ALKYLATION PRODUCT **58e**



The alkylation product **58e** (86% ee) was recrystallized by slow evaporation of hexanes to provide crystals suitable for X-ray analysis, m.p. = 67 – 69 °C.

Figure A2.1 X-ray crystal structure of allylic alkylation product **58e**

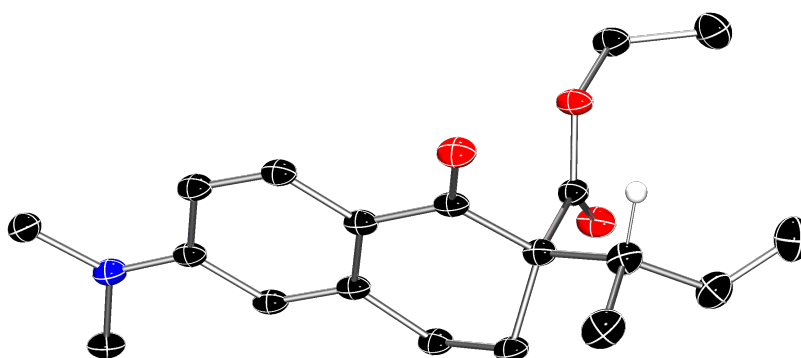


Table A2.1 Crystal data and structure refinement for allylic alkylation product **58e**

Empirical formula	C ₁₉ H ₂₅ N O ₃
Formula weight	315.40
Temperature	100(2) K
Wavelength	1.54178 Å

Crystal system	Monoclinic
Space group	P2 ₁
Unit cell dimensions	a = 7.5983(10) Å a = 90°. b = 6.1333(8) Å b = 99.411(4)°. c = 18.493(3) Å g = 90°.
Volume	850.2(2) Å ³
Z	2
Density (calculated)	1.232 Mg/m ³
Absorption coefficient	0.661 mm ⁻¹
F(000)	340
Crystal size	0.240 x 0.230 x 0.080 mm ³
Theta range for data collection	2.422 to 79.330°.
Index ranges	-9<=h<=8, -7<=k<=7, -23<=l<=23
Reflections collected	26025
Independent reflections	3636 [R(int) = 0.0411]
Completeness to theta = 67.679°	99.6 %
Absorption correction	Semi-empirical from equivalents
Refinement method	Full-matrix least-squares on F ²
Data / restraints / parameters	3636 / 1 / 212
Goodness-of-fit on F ²	1.094
Final R indices [I>2sigma(I)]	R1 = 0.0271, wR2 = 0.0727
R indices (all data)	R1 = 0.0274, wR2 = 0.0730
Absolute structure parameter	0.07(3)
Extinction coefficient	n/a
Largest diff. peak and hole	0.132 and -0.164 e.Å ⁻³

Table A2.2 Atomic coordinates ($\times 10^4$) and equivalent isotropic displacement parameters ($\text{\AA}^2 \times 10^3$) for **58e**. $U(\text{eq})$ is defined as one third of the trace of the orthogonalized U^{ij} tensor.

	x	y	z	U(eq)
O(1)	7683(1)	7250(2)	2322(1)	22(1)
O(2)	3598(1)	7112(2)	1929(1)	22(1)
O(3)	2465(1)	3836(2)	2155(1)	26(1)

N(1)	7877(2)	5287(2)	5723(1)	22(1)
C(1)	6891(2)	5855(2)	2615(1)	18(1)
C(2)	5657(2)	4176(2)	2162(1)	19(1)
C(3)	5859(2)	1974(2)	2564(1)	21(1)
C(4)	5385(2)	2122(2)	3330(1)	21(1)
C(5)	6371(2)	3931(2)	3774(1)	19(1)
C(6)	6627(2)	3825(2)	4533(1)	20(1)
C(7)	7579(2)	5444(2)	4976(1)	19(1)
C(8)	8254(2)	7234(2)	4615(1)	21(1)
C(9)	8014(2)	7309(2)	3861(1)	20(1)
C(10)	7074(2)	5687(2)	3423(1)	19(1)
C(11)	7366(2)	3305(2)	6073(1)	25(1)
C(12)	8987(2)	6890(2)	6164(1)	23(1)
C(13)	3720(2)	4979(2)	2090(1)	19(1)
C(14)	1805(2)	8046(3)	1784(1)	26(1)
C(15)	1022(2)	7841(3)	986(1)	34(1)
C(16)	6100(2)	3994(3)	1368(1)	23(1)
C(17)	4726(2)	2647(3)	886(1)	27(1)
C(18)	3647(2)	3362(3)	300(1)	34(1)
C(19)	7958(2)	3021(3)	1358(1)	30(1)

Table A2.3 Bond lengths [\AA] and angles [$^\circ$] for **58e**

O(1)-C(1)	1.2222(17)
O(2)-C(13)	1.3416(18)
O(2)-C(14)	1.4618(16)
O(3)-C(13)	1.2044(18)
N(1)-C(7)	1.3659(18)
N(1)-C(12)	1.4557(18)
N(1)-C(11)	1.4589(18)
C(1)-C(10)	1.480(2)
C(1)-C(2)	1.5442(18)
C(2)-C(3)	1.537(2)
C(2)-C(13)	1.5374(18)
C(2)-C(16)	1.5650(19)
C(3)-C(4)	1.521(2)
C(3)-H(3A)	0.9900

C(3)-H(3B)	0.9900
C(4)-C(5)	1.5042(19)
C(4)-H(4A)	0.9900
C(4)-H(4B)	0.9900
C(5)-C(6)	1.388(2)
C(5)-C(10)	1.4074(19)
C(6)-C(7)	1.4096(19)
C(6)-H(6)	0.9500
C(7)-C(8)	1.4236(19)
C(8)-C(9)	1.376(2)
C(8)-H(8)	0.9500
C(9)-C(10)	1.4032(19)
C(9)-H(9)	0.9500
C(11)-H(11A)	0.9800
C(11)-H(11B)	0.9800
C(11)-H(11C)	0.9800
C(12)-H(12A)	0.9800
C(12)-H(12B)	0.9800
C(12)-H(12C)	0.9800
C(14)-C(15)	1.505(2)
C(14)-H(14A)	0.9900
C(14)-H(14B)	0.9900
C(15)-H(15A)	0.9800
C(15)-H(15B)	0.9800
C(15)-H(15C)	0.9800
C(16)-C(17)	1.505(2)
C(16)-C(19)	1.535(2)
C(16)-H(16)	1.0000
C(17)-C(18)	1.322(2)
C(17)-H(17)	0.9500
C(18)-H(18A)	0.9500
C(18)-H(18B)	0.9500
C(19)-H(19A)	0.9800
C(19)-H(19B)	0.9800
C(19)-H(19C)	0.9800
C(13)-O(2)-C(14)	116.82(11)
C(7)-N(1)-C(12)	120.26(11)
C(7)-N(1)-C(11)	119.66(12)

C(12)-N(1)-C(11)	119.10(12)
O(1)-C(1)-C(10)	121.63(12)
O(1)-C(1)-C(2)	121.71(12)
C(10)-C(1)-C(2)	116.66(11)
C(3)-C(2)-C(13)	109.99(11)
C(3)-C(2)-C(1)	108.68(11)
C(13)-C(2)-C(1)	108.76(11)
C(3)-C(2)-C(16)	111.84(12)
C(13)-C(2)-C(16)	106.93(11)
C(1)-C(2)-C(16)	110.60(11)
C(4)-C(3)-C(2)	112.21(12)
C(4)-C(3)-H(3A)	109.2
C(2)-C(3)-H(3A)	109.2
C(4)-C(3)-H(3B)	109.2
C(2)-C(3)-H(3B)	109.2
H(3A)-C(3)-H(3B)	107.9
C(5)-C(4)-C(3)	112.26(11)
C(5)-C(4)-H(4A)	109.2
C(3)-C(4)-H(4A)	109.2
C(5)-C(4)-H(4B)	109.2
C(3)-C(4)-H(4B)	109.2
H(4A)-C(4)-H(4B)	107.9
C(6)-C(5)-C(10)	120.11(13)
C(6)-C(5)-C(4)	119.48(12)
C(10)-C(5)-C(4)	120.38(12)
C(5)-C(6)-C(7)	121.95(12)
C(5)-C(6)-H(6)	119.0
C(7)-C(6)-H(6)	119.0
N(1)-C(7)-C(6)	121.49(12)
N(1)-C(7)-C(8)	121.09(12)
C(6)-C(7)-C(8)	117.41(13)
C(9)-C(8)-C(7)	120.20(13)
C(9)-C(8)-H(8)	119.9
C(7)-C(8)-H(8)	119.9
C(8)-C(9)-C(10)	122.17(13)
C(8)-C(9)-H(9)	118.9
C(10)-C(9)-H(9)	118.9
C(9)-C(10)-C(5)	118.13(13)

C(9)-C(10)-C(1)	119.25(12)
C(5)-C(10)-C(1)	122.60(12)
N(1)-C(11)-H(11A)	109.5
N(1)-C(11)-H(11B)	109.5
H(11A)-C(11)-H(11B)	109.5
N(1)-C(11)-H(11C)	109.5
H(11A)-C(11)-H(11C)	109.5
H(11B)-C(11)-H(11C)	109.5
N(1)-C(12)-H(12A)	109.5
N(1)-C(12)-H(12B)	109.5
H(12A)-C(12)-H(12B)	109.5
N(1)-C(12)-H(12C)	109.5
H(12A)-C(12)-H(12C)	109.5
H(12B)-C(12)-H(12C)	109.5
O(3)-C(13)-O(2)	124.23(13)
O(3)-C(13)-C(2)	124.53(13)
O(2)-C(13)-C(2)	111.23(11)
O(2)-C(14)-C(15)	110.68(13)
O(2)-C(14)-H(14A)	109.5
C(15)-C(14)-H(14A)	109.5
O(2)-C(14)-H(14B)	109.5
C(15)-C(14)-H(14B)	109.5
H(14A)-C(14)-H(14B)	108.1
C(14)-C(15)-H(15A)	109.5
C(14)-C(15)-H(15B)	109.5
H(15A)-C(15)-H(15B)	109.5
C(14)-C(15)-H(15C)	109.5
H(15A)-C(15)-H(15C)	109.5
H(15B)-C(15)-H(15C)	109.5
C(17)-C(16)-C(19)	109.29(13)
C(17)-C(16)-C(2)	111.13(11)
C(19)-C(16)-C(2)	112.17(12)
C(17)-C(16)-H(16)	108.0
C(19)-C(16)-H(16)	108.0
C(2)-C(16)-H(16)	108.0
C(18)-C(17)-C(16)	125.47(16)
C(18)-C(17)-H(17)	117.3
C(16)-C(17)-H(17)	117.3

C(17)-C(18)-H(18A)	120.0
C(17)-C(18)-H(18B)	120.0
H(18A)-C(18)-H(18B)	120.0
C(16)-C(19)-H(19A)	109.5
C(16)-C(19)-H(19B)	109.5
H(19A)-C(19)-H(19B)	109.5
C(16)-C(19)-H(19C)	109.5
H(19A)-C(19)-H(19C)	109.5
H(19B)-C(19)-H(19C)	109.5

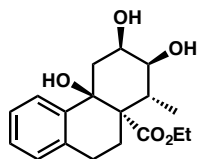
Table A2.4 Anisotropic displacement parameters ($\text{\AA}^2 \times 10^3$) for **58e**. The anisotropic displacement factor exponent takes the form: $-2\pi^2 [h^2 a^{*2} U^{11} + \dots + 2 h k a^* b^* U^{12}]$

	U ¹¹	U ²²	U ³³	U ²³	U ¹³	U ¹²
O(1)	19(1)	17(1)	32(1)	2(1)	6(1)	-3(1)
O(2)	14(1)	16(1)	35(1)	1(1)	1(1)	1(1)
O(3)	16(1)	21(1)	41(1)	4(1)	3(1)	-3(1)
N(1)	22(1)	16(1)	28(1)	1(1)	6(1)	-1(1)
C(1)	11(1)	13(1)	30(1)	2(1)	4(1)	1(1)
C(2)	14(1)	15(1)	28(1)	0(1)	2(1)	-1(1)
C(3)	17(1)	13(1)	32(1)	-1(1)	2(1)	-1(1)
C(4)	18(1)	14(1)	32(1)	2(1)	3(1)	-4(1)
C(5)	12(1)	14(1)	31(1)	1(1)	4(1)	1(1)
C(6)	15(1)	14(1)	31(1)	2(1)	6(1)	-1(1)
C(7)	14(1)	15(1)	28(1)	0(1)	5(1)	3(1)
C(8)	17(1)	14(1)	32(1)	1(1)	3(1)	-2(1)
C(9)	14(1)	14(1)	32(1)	3(1)	3(1)	-1(1)
C(10)	12(1)	15(1)	29(1)	2(1)	3(1)	0(1)
C(11)	28(1)	17(1)	31(1)	3(1)	9(1)	2(1)
C(12)	21(1)	19(1)	29(1)	-2(1)	3(1)	0(1)
C(13)	16(1)	16(1)	24(1)	-1(1)	2(1)	-1(1)
C(14)	16(1)	20(1)	39(1)	-1(1)	0(1)	3(1)
C(15)	27(1)	33(1)	40(1)	1(1)	-7(1)	5(1)
C(16)	19(1)	21(1)	28(1)	-1(1)	6(1)	-2(1)
C(17)	25(1)	27(1)	30(1)	-4(1)	6(1)	-3(1)
C(18)	30(1)	41(1)	31(1)	-3(1)	3(1)	-3(1)

C(19) 22(1) 32(1) 38(1) -5(1) 10(1) 1(1)

Table A2.5 Hydrogen coordinates ($\times 10^4$) and isotropic displacement parameters ($\text{\AA}^2 \times 10^3$) for **58e**

	x	y	z	U(eq)
H(3A)	5075	886	2276	25
H(3B)	7106	1463	2599	25
H(4A)	4085	2369	3292	26
H(4B)	5673	719	3588	26
H(6)	6146	2627	4762	24
H(8)	8872	8379	4895	26
H(9)	8500	8499	3631	24
H(11A)	6078	3077	5938	37
H(11B)	7674	3450	6606	37
H(11C)	8003	2057	5909	37
H(12A)	10166	6934	6015	35
H(12B)	9116	6485	6683	35
H(12C)	8427	8330	6092	35
H(14A)	1857	9604	1927	31
H(14B)	1030	7281	2084	31
H(15A)	1819	8539	688	52
H(15B)	-147	8555	894	52
H(15C)	886	6296	854	52
H(16)	6079	5497	1156	27
H(17)	4624	1157	1013	33
H(18A)	3705	4841	153	41
H(18B)	2815	2397	25	41
H(19A)	7954	1474	1490	45
H(19B)	8840	3797	1712	45
H(19C)	8266	3172	866	45

A2.1.2 X-RAY CRYSTAL STRUCTURE ANALYSIS OF TRIOL 63

Triol **63** was recrystallized by slow evaporation of benzene to provide crystals suitable for X-ray analysis, m.p. = 111 – 115 °C.

Figure A2.2 X-ray crystal structure of triol **63**

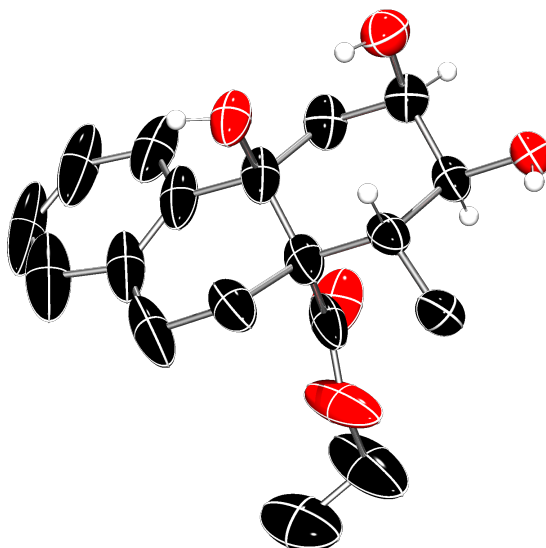


Table A2.6 Crystal data and structure refinement for triol **63**

Empirical formula	C _{28.63} H _{34.63} O ₅	
Formula weight	458.70	
Temperature	100(2) K	
Wavelength	1.54178 Å	
Crystal system	Hexagonal	
Space group	P6 ₅ 22	
Unit cell dimensions	a = 21.3194(5) Å	a = 90°.
	b = 21.3194(5) Å	b = 90°.
	c = 18.6055(6) Å	g = 120°.

Volume	7323.6(4) Å ³
Z	12
Density (calculated)	1.305 Mg/m ³
Absorption coefficient	0.695 mm ⁻¹
F(000)	3108
Crystal size	.2 x .1 x .1 mm ³
Theta range for data collection	2.393 to 58.098°.
Index ranges	-22<=h<=20, -22<=k<=22, -20<=l<=20
Reflections collected	60463
Independent reflections	3412 [R(int) = 0.0731]
Completeness to theta = 67.679°	78.2 %
Absorption correction	Semi-empirical from equivalents
Max. and min. transmission	0.7514 and 0.6563
Refinement method	Full-matrix least-squares on F ²
Data / restraints / parameters	3412 / 1 / 283
Goodness-of-fit on F ²	1.110
Final R indices [I>2sigma(I)]	R1 = 0.0803, wR2 = 0.1889
R indices (all data)	R1 = 0.1100, wR2 = 0.2084
Absolute structure parameter	0.03(8)
Extinction coefficient	n/a
Largest diff. peak and hole	0.290 and -0.263 e.Å ⁻³

Table A2.7 Atomic coordinates ($\times 10^4$) and equivalent isotropic displacement parameters ($\text{\AA}^2 \times 10^3$) for **63**. $U(\text{eq})$ is defined as one third of the trace of the orthogonalized U^{ij} tensor.

	x	y	z	U(eq)
O(1A)	7920(2)	7040(3)	6808(2)	56(1)
O(2A)	9307(3)	7800(3)	6495(3)	58(1)
O(3A)	9815(2)	6894(2)	5959(2)	43(1)
O(4A)	7565(3)	6012(4)	4758(3)	83(2)
O(5A)	7359(4)	5007(4)	5298(3)	109(3)
C(1A)	7758(4)	6774(4)	6067(3)	55(2)

C(2A)	7774(4)	6048(4)	6049(3)	52(2)
C(3A)	7206(4)	5535(4)	6597(4)	63(2)
C(4A)	6454(4)	5377(7)	6424(5)	91(4)
C(5A)	6399(5)	6008(7)	6139(4)	83(3)
C(6A)	5726(6)	5959(9)	6069(5)	125(6)
C(7A)	5634(7)	6481(12)	5755(7)	136(7)
C(8A)	6225(7)	7100(9)	5525(5)	109(5)
C(9A)	6913(5)	7191(6)	5601(4)	81(3)
C(10A)	7009(4)	6657(6)	5911(4)	70(3)
C(11A)	8356(4)	7356(4)	5609(4)	57(2)
C(12A)	9097(4)	7469(4)	5797(3)	48(2)
C(13A)	9114(3)	6767(4)	5770(3)	42(2)
C(14A)	8537(3)	6184(4)	6252(3)	44(2)
C(15A)	8628(4)	5516(4)	6272(4)	63(2)
C(16A)	7550(4)	5710(5)	5293(4)	63(2)
C(17A)	7152(6)	4621(7)	4606(5)	137(6)
C(18A)	6414(7)	4137(6)	4612(5)	113(4)
C(1)	5200(6)	5125(5)	3686(4)	76(3)
C(2)	5804(6)	5643(6)	4044(4)	80(3)
C(3)	6326(6)	6241(6)	3681(5)	91(3)
C(4)	4612(8)	6693(6)	3992(5)	95(3)
C(5)	3968(7)	6673(5)	4078(5)	88(3)
C(6)	5251(7)	7315(7)	4077(5)	100(4)
C(1DA)	7650(90)	9370(50)	5020(80)	520(40)
C(2DA)	8300(80)	9420(50)	5190(40)	520(40)
C(3DA)	8570(40)	9070(70)	4760(80)	520(40)
C(4DA)	8180(80)	8680(50)	4160(70)	520(40)
C(5DA)	7520(80)	8630(60)	4000(60)	520(40)
C(6DA)	7260(40)	8980(70)	4420(100)	520(40)
C(1DB)	9660(90)	9170(100)	4740(60)	410(30)
C(2DB)	10280(80)	9850(100)	4720(70)	410(30)
C(3DB)	10570(30)	10170(40)	4060(110)	410(30)
C(4DB)	10240(80)	9820(80)	3430(60)	410(30)
C(5DB)	9620(80)	9140(70)	3450(60)	410(30)
C(6DB)	9330(50)	8810(40)	4110(100)	410(30)

Table A2.8 Bond lengths [\AA] and angles [$^\circ$] for **63**

O(1A)-C(1A)	1.466(7)
O(2A)-C(12A)	1.438(8)
O(3A)-C(13A)	1.425(7)
O(4A)-C(16A)	1.176(10)
O(5A)-C(16A)	1.344(11)
O(5A)-C(17A)	1.472(10)
C(1A)-C(10A)	1.514(10)
C(1A)-C(11A)	1.519(10)
C(1A)-C(2A)	1.566(11)
C(2A)-C(3A)	1.541(10)
C(2A)-C(16A)	1.543(10)
C(2A)-C(14A)	1.549(9)
C(3A)-C(4A)	1.499(12)
C(4A)-C(5A)	1.504(14)
C(5A)-C(6A)	1.392(14)
C(5A)-C(10A)	1.410(14)
C(6A)-C(7A)	1.35(2)
C(7A)-C(8A)	1.36(2)
C(8A)-C(9A)	1.386(13)
C(9A)-C(10A)	1.382(12)
C(11A)-C(12A)	1.516(9)
C(12A)-C(13A)	1.514(9)
C(13A)-C(14A)	1.527(9)
C(14A)-C(15A)	1.531(10)
C(17A)-C(18A)	1.384(14)
C(1)-C(1)#1	1.341(15)
C(1)-C(2)	1.378(13)
C(2)-C(3)	1.379(13)
C(3)-C(3)#1	1.331(18)
C(4)-C(6)	1.353(15)
C(4)-C(5)	1.363(15)
C(5)-C(5)#2	1.365(19)
C(6)-C(6)#2	1.36(2)
C(1DA)-C(2DA)	1.3900
C(1DA)-C(6DA)	1.3900
C(2DA)-C(3DA)	1.3900

C(3DA)-C(4DA)	1.3900
C(4DA)-C(5DA)	1.3900
C(5DA)-C(6DA)	1.3900
C(1DB)-C(2DB)	1.390(3)
C(1DB)-C(6DB)	1.3900
C(2DB)-C(3DB)	1.3900
C(3DB)-C(4DB)	1.3900
C(4DB)-C(5DB)	1.3900(12)
C(5DB)-C(6DB)	1.3900
C(16A)-O(5A)-C(17A)	117.2(8)
O(1A)-C(1A)-C(10A)	105.6(5)
O(1A)-C(1A)-C(11A)	105.8(6)
C(10A)-C(1A)-C(11A)	114.3(7)
O(1A)-C(1A)-C(2A)	106.6(6)
C(10A)-C(1A)-C(2A)	112.1(7)
C(11A)-C(1A)-C(2A)	111.8(6)
C(3A)-C(2A)-C(16A)	108.7(6)
C(3A)-C(2A)-C(14A)	110.6(6)
C(16A)-C(2A)-C(14A)	111.2(5)
C(3A)-C(2A)-C(1A)	106.8(6)
C(16A)-C(2A)-C(1A)	109.0(7)
C(14A)-C(2A)-C(1A)	110.5(6)
C(4A)-C(3A)-C(2A)	113.0(7)
C(3A)-C(4A)-C(5A)	115.3(8)
C(6A)-C(5A)-C(10A)	117.2(13)
C(6A)-C(5A)-C(4A)	120.3(12)
C(10A)-C(5A)-C(4A)	122.5(8)
C(7A)-C(6A)-C(5A)	123.1(14)
C(6A)-C(7A)-C(8A)	119.2(11)
C(7A)-C(8A)-C(9A)	120.4(14)
C(10A)-C(9A)-C(8A)	120.7(12)
C(9A)-C(10A)-C(5A)	119.3(8)
C(9A)-C(10A)-C(1A)	121.6(9)
C(5A)-C(10A)-C(1A)	119.0(9)
C(12A)-C(11A)-C(1A)	112.5(6)
O(2A)-C(12A)-C(13A)	111.1(5)
O(2A)-C(12A)-C(11A)	109.2(6)
C(13A)-C(12A)-C(11A)	111.9(6)

O(3A)-C(13A)-C(12A)	110.2(5)
O(3A)-C(13A)-C(14A)	110.5(5)
C(12A)-C(13A)-C(14A)	112.2(5)
C(13A)-C(14A)-C(15A)	110.3(5)
C(13A)-C(14A)-C(2A)	110.6(6)
C(15A)-C(14A)-C(2A)	116.1(6)
O(4A)-C(16A)-O(5A)	121.7(7)
O(4A)-C(16A)-C(2A)	126.8(9)
O(5A)-C(16A)-C(2A)	111.4(8)
C(18A)-C(17A)-O(5A)	108.7(8)
C(1)#1-C(1)-C(2)	119.8(5)
C(1)-C(2)-C(3)	120.2(7)
C(3)#1-C(3)-C(2)	120.0(5)
C(6)-C(4)-C(5)	121.4(10)
C(4)-C(5)-C(5)#2	119.2(6)
C(4)-C(6)-C(6)#2	119.5(7)
C(2DA)-C(1DA)-C(6DA)	120.0
C(3DA)-C(2DA)-C(1DA)	120.0
C(2DA)-C(3DA)-C(4DA)	120.00(6)
C(3DA)-C(4DA)-C(5DA)	120.0
C(4DA)-C(5DA)-C(6DA)	120.0
C(5DA)-C(6DA)-C(1DA)	120.00(6)
C(2DB)-C(1DB)-C(6DB)	120.00(11)
C(3DB)-C(2DB)-C(1DB)	120.00(5)
C(4DB)-C(3DB)-C(2DB)	120.00(6)
C(5DB)-C(4DB)-C(3DB)	120.00(12)
C(4DB)-C(5DB)-C(6DB)	120.00(8)
C(5DB)-C(6DB)-C(1DB)	120.00(9)

Symmetry transformations used to generate equivalent atoms:

#1 y,x,-z+2/3 #2 x,x-y+1,-z+5/6

Table A2.9 Anisotropic displacement parameters ($\text{\AA}^2 \times 10^3$) for **63**. The anisotropic displacement factor exponent takes the form: $-2\pi^2 [h^2 a^{*2} U^{11} + \dots + 2 h k a^* b^* U^{12}]$

U ¹¹	U ²²	U ³³	U ²³	U ¹³	U ¹²
-----------------	-----------------	-----------------	-----------------	-----------------	-----------------

O(1A)	51(3)	88(4)	40(2)	-17(3)	-8(2)	43(3)
O(2A)	60(3)	59(3)	61(3)	-10(3)	-5(2)	32(3)
O(3A)	35(3)	45(3)	45(2)	2(2)	1(2)	17(2)
O(4A)	97(5)	137(5)	36(3)	-23(3)	-14(3)	74(4)
O(5A)	115(5)	73(4)	49(3)	-30(3)	24(3)	-21(4)
C(1A)	40(4)	94(6)	34(3)	-17(4)	-9(3)	36(4)
C(2A)	40(4)	73(5)	31(3)	-14(3)	3(3)	19(4)
C(3A)	46(5)	77(5)	37(4)	-16(4)	5(3)	9(4)
C(4A)	34(5)	139(10)	54(5)	-20(6)	8(4)	8(5)
C(5A)	41(6)	157(10)	46(5)	-45(6)	-13(4)	46(6)
C(6A)	56(7)	253(17)	59(6)	-80(9)	-29(5)	71(9)
C(7A)	72(8)	300(20)	75(8)	-109(11)	-54(7)	127(12)
C(8A)	86(8)	231(15)	64(6)	-71(8)	-44(6)	119(10)
C(9A)	85(7)	147(9)	48(5)	-40(5)	-28(4)	86(7)
C(10A)	51(5)	128(8)	38(4)	-34(5)	-11(4)	51(6)
C(11A)	54(5)	79(5)	46(4)	2(4)	-1(4)	39(4)
C(12A)	49(4)	58(5)	40(4)	2(3)	-1(3)	29(4)
C(13A)	33(4)	56(4)	31(3)	-4(3)	0(3)	16(3)
C(14A)	37(4)	46(4)	36(3)	-6(3)	0(3)	12(3)
C(15A)	51(5)	47(5)	77(5)	-3(4)	12(4)	13(4)
C(16A)	33(4)	93(7)	40(5)	-22(5)	4(3)	15(4)
C(17A)	105(9)	133(10)	59(6)	-52(6)	13(6)	-26(8)
C(18A)	129(10)	92(8)	64(6)	-17(5)	-16(6)	16(8)
C(1)	121(8)	92(7)	49(4)	11(5)	0(5)	79(7)
C(2)	136(9)	110(8)	38(4)	-5(5)	-8(5)	95(7)
C(3)	115(8)	106(8)	58(5)	-16(5)	-17(5)	59(7)
C(4)	177(12)	91(8)	57(6)	-8(5)	-21(7)	99(9)
C(5)	132(9)	81(6)	60(5)	-9(5)	-8(6)	60(6)
C(6)	131(9)	146(11)	46(5)	-9(7)	-15(6)	87(9)

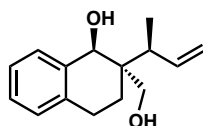
Table A2.10 Hydrogen coordinates ($\times 10^4$) and isotropic displacement parameters ($\text{\AA}^2 \times 10^3$) for

	x	y	z	U(eq)
H(1A)	7550	6986	7001	84

H(2A)	8992	7554	6789	88
H(3A)	9776	6578	6237	65
H(3AA)	7212	5083	6610	76
H(3AB)	7338	5752	7071	76
H(4AA)	6162	5201	6856	109
H(4AB)	6247	4990	6072	109
H(6A)	5320	5549	6245	150
H(7A)	5172	6417	5698	163
H(8A)	6168	7465	5316	131
H(9A)	7313	7616	5440	97
H(11A)	8255	7221	5107	69
H(11B)	8358	7808	5675	69
H(12A)	9445	7802	5444	57
H(13A)	9015	6589	5274	51
H(14A)	8634	6383	6740	52
H(15A)	8599	5337	5793	94
H(15B)	8251	5147	6561	94
H(15C)	9091	5645	6476	94
H(17A)	7272	4964	4216	164
H(17B)	7414	4363	4534	164
H(18A)	6293	3825	5022	169
H(18B)	6279	3852	4180	169
H(18C)	6157	4400	4636	169
H(1)	4846	4724	3933	91
H(2)	5860	5589	4532	96
H(3)	6738	6584	3921	110
H(4)	4613	6270	3873	113
H(5)	3533	6242	4016	106
H(6)	5686	7320	4014	120
H(1DA)	7468	9607	5309	622
H(2DA)	8562	9679	5591	622
H(3DA)	9005	9096	4874	622
H(4DA)	8353	8442	3877	622
H(5DA)	7259	8370	3595	622
H(6DA)	6817	8953	4311	622
H(1DB)	9471	8948	5182	495
H(2DB)	10503	10084	5145	495
H(3DB)	10983	10630	4047	495

H(4DB)	10431	10040	2986	495
H(5DB)	9399	8904	3023	495
H(6DB)	8919	8358	4121	495

A2.1.3 X-RAY CRYSTAL STRUCTURE ANALYSIS OF DIOL 64



Diol **64** was recrystallized in boiling heptane to provide crystals suitable for X-ray analysis, m.p. = 97 – 99 °C.

Figure A2.3 X-ray crystal structure of diol **64**

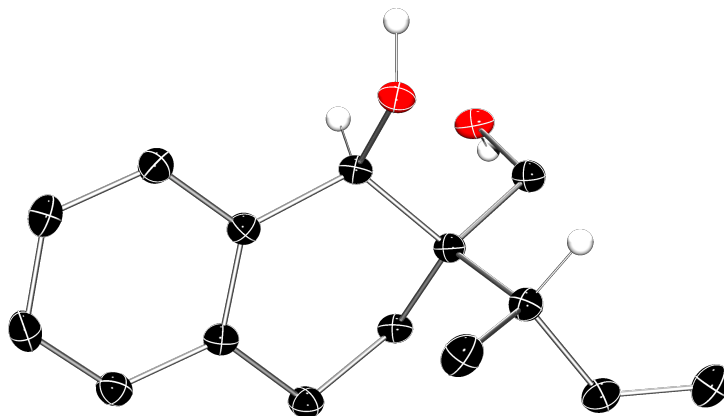


Table A2.11 Crystal data and structure refinement for diol **64**

Empirical formula	C ₁₅ H ₂₀ O ₂
Formula weight	232.31
Temperature	100(2) K
Wavelength	1.54178 Å
Crystal system	Monoclinic
Space group	P2 ₁
Unit cell dimensions	a = 8.0972(3) Å a = 90°.

	$b = 6.3583(2) \text{ \AA}$	$b = 105.4260(10)^\circ$.
	$c = 12.5999(4) \text{ \AA}$	$g = 90^\circ$.
Volume	$625.33(4) \text{ \AA}^3$	
Z	2	
Density (calculated)	1.234 Mg/m^3	
Absorption coefficient	0.630 mm^{-1}	
F(000)	252	
Crystal size	$.1 \times .1 \times .1 \text{ mm}^3$	
Theta range for data collection	$3.639 \text{ to } 79.259^\circ$.	
Index ranges	$-10 \leq h \leq 10, -8 \leq k \leq 8, -15 \leq l \leq 16$	
Reflections collected	20029	
Independent reflections	2647 [$R(\text{int}) = 0.0449$]	
Completeness to $\theta = 67.679^\circ$	100.0 %	
Absorption correction	Semi-empirical from equivalents	
Refinement method	Full-matrix least-squares on F^2	
Data / restraints / parameters	2647 / 3 / 163	
Goodness-of-fit on F^2	1.085	
Final R indices [$I > 2\sigma(I)$]	$R1 = 0.0296, wR2 = 0.0677$	
R indices (all data)	$R1 = 0.0312, wR2 = 0.0687$	
Absolute structure parameter	0.04(8)	
Extinction coefficient	n/a	
Largest diff. peak and hole	$0.144 \text{ and } -0.158 \text{ e.\AA}^{-3}$	

Table A2.12 Atomic coordinates ($\times 10^4$) and equivalent isotropic displacement parameters ($\approx \text{\AA}^2 \times 10^3$) for **64**. $U(\text{eq})$ is defined as one third of the trace of the orthogonalized U^{ij} tensor.

	x	y	z	U(eq)
C(1)	8395(2)	5246(3)	8290(1)	13(1)
C(2)	6809(2)	3826(3)	8166(1)	14(1)
C(3)	6586(2)	2540(3)	7101(1)	15(1)
C(4)	6321(2)	3872(3)	6062(1)	18(1)
C(5)	7576(2)	5670(3)	6196(1)	15(1)
C(6)	7795(2)	6715(3)	5269(1)	18(1)
C(7)	8956(2)	8347(3)	5356(2)	20(1)
C(8)	9945(2)	8942(3)	6391(2)	21(1)
C(9)	9737(2)	7927(3)	7319(2)	18(1)
C(10)	8540(2)	6317(3)	7239(1)	14(1)
O(1)	8491(2)	6779(2)	9145(1)	15(1)
O(2)	8701(2)	1051(2)	9217(1)	18(1)
C(11)	7204(2)	2296(3)	9154(2)	16(1)
C(12)	5173(2)	5063(3)	8245(2)	16(1)
C(13)	4829(2)	7173(3)	7629(2)	21(1)
C(14)	3580(2)	3725(3)	7913(2)	19(1)
C(15)	2772(2)	2878(3)	8592(2)	23(1)

Table A2.13 Bond lengths [\AA] and angles [$^\circ$] for **64**

C(1)-O(1)	1.440(2)
C(1)-C(10)	1.521(2)
C(1)-C(2)	1.543(2)
C(1)-H(1)	1.0000
C(2)-C(3)	1.541(2)
C(2)-C(11)	1.545(2)
C(2)-C(12)	1.566(2)
C(3)-C(4)	1.525(2)
C(3)-H(3A)	0.9900
C(3)-H(3B)	0.9900
C(4)-C(5)	1.509(3)

C(4)-H(4A)	0.9900
C(4)-H(4B)	0.9900
C(5)-C(6)	1.396(2)
C(5)-C(10)	1.400(2)
C(6)-C(7)	1.385(3)
C(6)-H(6)	0.9500
C(7)-C(8)	1.389(3)
C(7)-H(7)	0.9500
C(8)-C(9)	1.384(3)
C(8)-H(8)	0.9500
C(9)-C(10)	1.395(2)
C(9)-H(9)	0.9500
O(1)-H(1O)	0.93(2)
O(2)-C(11)	1.432(2)
O(2)-H(2O)	0.91(2)
C(11)-H(11A)	0.9900
C(11)-H(11B)	0.9900
C(12)-C(14)	1.508(2)
C(12)-C(13)	1.537(3)
C(12)-H(12)	1.0000
C(13)-H(13A)	0.9800
C(13)-H(13B)	0.9800
C(13)-H(13C)	0.9800
C(14)-C(15)	1.322(3)
C(14)-H(14)	0.9500
C(15)-H(15A)	0.9500
C(15)-H(15B)	0.9500
O(1)-C(1)-C(10)	110.31(13)
O(1)-C(1)-C(2)	110.47(13)
C(10)-C(1)-C(2)	115.37(14)
O(1)-C(1)-H(1)	106.7
C(10)-C(1)-H(1)	106.7
C(2)-C(1)-H(1)	106.7
C(3)-C(2)-C(1)	107.46(13)
C(3)-C(2)-C(11)	108.58(14)
C(1)-C(2)-C(11)	107.34(13)
C(3)-C(2)-C(12)	114.66(14)
C(1)-C(2)-C(12)	113.27(15)

C(11)-C(2)-C(12)	105.21(13)
C(4)-C(3)-C(2)	114.18(14)
C(4)-C(3)-H(3A)	108.7
C(2)-C(3)-H(3A)	108.7
C(4)-C(3)-H(3B)	108.7
C(2)-C(3)-H(3B)	108.7
H(3A)-C(3)-H(3B)	107.6
C(5)-C(4)-C(3)	112.78(14)
C(5)-C(4)-H(4A)	109.0
C(3)-C(4)-H(4A)	109.0
C(5)-C(4)-H(4B)	109.0
C(3)-C(4)-H(4B)	109.0
H(4A)-C(4)-H(4B)	107.8
C(6)-C(5)-C(10)	118.84(16)
C(6)-C(5)-C(4)	119.89(15)
C(10)-C(5)-C(4)	121.27(15)
C(7)-C(6)-C(5)	121.68(17)
C(7)-C(6)-H(6)	119.2
C(5)-C(6)-H(6)	119.2
C(6)-C(7)-C(8)	119.20(17)
C(6)-C(7)-H(7)	120.4
C(8)-C(7)-H(7)	120.4
C(9)-C(8)-C(7)	119.79(18)
C(9)-C(8)-H(8)	120.1
C(7)-C(8)-H(8)	120.1
C(8)-C(9)-C(10)	121.30(17)
C(8)-C(9)-H(9)	119.3
C(10)-C(9)-H(9)	119.3
C(9)-C(10)-C(5)	119.13(16)
C(9)-C(10)-C(1)	118.63(15)
C(5)-C(10)-C(1)	122.16(15)
C(1)-O(1)-H(1O)	107.5(19)
C(11)-O(2)-H(2O)	115.1(17)
O(2)-C(11)-C(2)	112.54(14)
O(2)-C(11)-H(11A)	109.1
C(2)-C(11)-H(11A)	109.1
O(2)-C(11)-H(11B)	109.1
C(2)-C(11)-H(11B)	109.1

H(11A)-C(11)-H(11B)	107.8
C(14)-C(12)-C(13)	108.99(15)
C(14)-C(12)-C(2)	111.98(15)
C(13)-C(12)-C(2)	116.67(15)
C(14)-C(12)-H(12)	106.2
C(13)-C(12)-H(12)	106.2
C(2)-C(12)-H(12)	106.2
C(12)-C(13)-H(13A)	109.5
C(12)-C(13)-H(13B)	109.5
H(13A)-C(13)-H(13B)	109.5
C(12)-C(13)-H(13C)	109.5
H(13A)-C(13)-H(13C)	109.5
H(13B)-C(13)-H(13C)	109.5
C(15)-C(14)-C(12)	125.79(17)
C(15)-C(14)-H(14)	117.1
C(12)-C(14)-H(14)	117.1
C(14)-C(15)-H(15A)	120.0
C(14)-C(15)-H(15B)	120.0
H(15A)-C(15)-H(15B)	120.0

Table A2.14 Anisotropic displacement parameters ($\text{\AA}^2 \times 10^3$) for **14**. The anisotropic displacement factor exponent takes the form: $-2\pi^2 [h^2 a^{*2} U^{11} + \dots + 2 h k a^* b^* U^{12}]$

	U ¹¹	U ²²	U ³³	U ²³	U ¹³	U ¹²
C(1)	15(1)	11(1)	13(1)	-1(1)	2(1)	1(1)
C(2)	14(1)	11(1)	14(1)	1(1)	2(1)	-1(1)
C(3)	16(1)	12(1)	16(1)	-1(1)	1(1)	0(1)
C(4)	19(1)	18(1)	16(1)	-1(1)	2(1)	-3(1)
C(5)	15(1)	13(1)	16(1)	0(1)	3(1)	3(1)
C(6)	18(1)	20(1)	16(1)	1(1)	4(1)	2(1)
C(7)	23(1)	21(1)	18(1)	4(1)	9(1)	1(1)
C(8)	20(1)	20(1)	24(1)	1(1)	8(1)	-3(1)
C(9)	17(1)	18(1)	18(1)	-1(1)	5(1)	-1(1)
C(10)	14(1)	14(1)	15(1)	1(1)	4(1)	2(1)
O(1)	17(1)	13(1)	14(1)	-3(1)	2(1)	0(1)

O(2)	18(1)	11(1)	21(1)	1(1)	0(1)	2(1)
C(11)	18(1)	12(1)	16(1)	2(1)	3(1)	1(1)
C(12)	17(1)	14(1)	16(1)	0(1)	4(1)	-1(1)
C(13)	18(1)	16(1)	29(1)	4(1)	6(1)	3(1)
C(14)	17(1)	17(1)	21(1)	-2(1)	3(1)	-1(1)
C(15)	20(1)	19(1)	31(1)	0(1)	9(1)	-1(1)

Table A2.15 Hydrogen coordinates ($\times 10^4$) and isotropic displacement parameters ($\text{\AA}^2 \times 10^3$) for **64**

	x	y	z	U(eq)
H(1)	9423	4319	8540	16
H(3A)	7615	1651	7174	18
H(3B)	5590	1591	7016	18
H(4A)	6441	2964	5448	22
H(4B)	5141	4443	5864	22
H(6)	7130	6296	4560	21
H(7)	9075	9051	4715	24
H(8)	10761	10042	6462	25
H(9)	10423	8336	8024	21
H(10)	9470(30)	6480(50)	9710(20)	52(8)
H(20)	8500(30)	-340(30)	9040(20)	42(8)
H(11A)	7369	3113	9843	19
H(11B)	6210	1351	9090	19
H(12)	5343	5400	9042	19
H(13A)	4478	6913	6834	32
H(13B)	5875	8025	7814	32
H(13C)	3914	7925	7847	32
H(14)	3117	3469	7149	22
H(15A)	3189	3093	9363	28
H(15B)	1773	2054	8308	28

CHAPTER 2

Enantioselective Iridium-Catalyzed Allylic Alkylation Reactions of Masked Acyl Cyanide Equivalents[†]

2.1 INTRODUCTION AND BACKGROUND

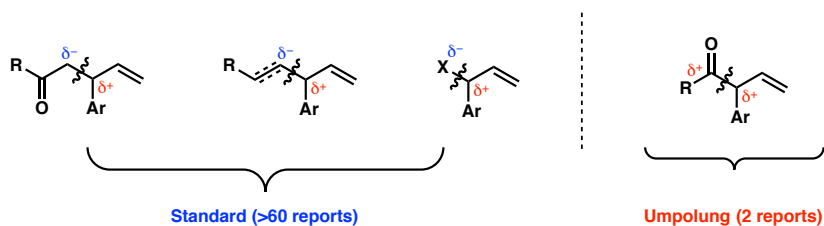
Since the first report of an asymmetric iridium-catalyzed allylic alkylation in 1997,¹ the technology has been widely developed for normal reactivity patterns between electrophilic π -allyl species and nucleophilic enolate equivalents, organometallic reagents, or heteroatoms (Figure 2.1a, left).² However, the application of an umpolung strategy to stitch together a formally electrophilic group and a π -allyl cation via enantioselective iridium-catalyzed allylic alkylation remains underexplored (Figure 2.1a, right).³ To date, only two examples of reverse-polarity nucleophiles in iridium-catalyzed allylic alkylation have been reported (Figure 2.1b). In 2008, Helmchen showed that the extensively explored malononitrile nucleophile can operate as a methoxy carbonyl synthon with the

[†] This work was performed in collaboration with Dr. J. Caleb Hethcox. Portions of this chapter have been reproduced with permission from Hethcox, J. C.;[‡] Shockley, S. E.;[§] Stoltz, B. M. *Org. Lett.* **2017**, *19*, 1527–1529 © 2017 American Chemical Society.

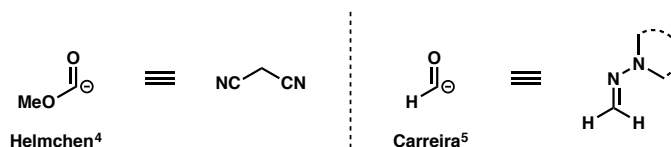
subsequent application of an oxidative degradation process (Figure 2.1b, left).⁴ More recently, Carreira disclosed the use of formaldehyde *N,N*-dialkylhydrazone as a formyl anion equivalent in iridium-catalyzed allylic alkylation reactions (Figure 2.1b, right).⁵ Herein, we describe the first use of an acyl cyanide equivalent in asymmetric iridium-catalyzed allylic alkylation, which formally serves as the addition of carbon monoxide (Figure 2.1c, left).

Figure 2.1 Iridium-catalyzed allylic alkylation strategies

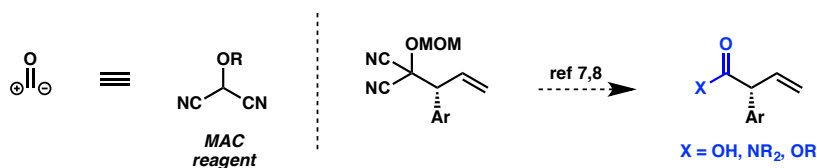
a) Iridium-Catalyzed Allylic Alkylation Strategies



b) Prior Art: Umpolung Strategy Iridium-Catalyzed Allylic Alkylation



c) This Research: Use of an Umpoled Masked Acyl Cyanide (MAC) Reagent



As part of our ongoing research program to develop iridium-catalyzed allylic alkylation methods,⁶ we became interested in exploring the reactivity of masked acyl cyanide (MAC) reagents as reverse-polarity nucleophiles with π -allyl electrophiles. Following reaction with an electrophile, these umpoled synthons, developed by

Yamamoto and Nemoto,⁷ can be unmasked to reveal a transient acyl cyanide intermediate, which can be further transformed into a carboxylic acid, amide, or ester.^{7,8} We envisioned that the novel application of MAC reagents to iridium-catalyzed allylic alkylation chemistry could provide access to highly desirable, enantioenriched vinylated α -aryl carbonyl derivatives, which are otherwise difficult to prepare (Figure 1c, right).⁹

2.2 REACTION OPTIMIZATION

Preliminary studies focused on the identification of a suitable protecting group for MAC nucleophile **67** in order to achieve the allylic alkylation reaction. Using our previously reported conditions for iridium-catalyzed allylic alkylations with cinnamyl-derived electrophiles as a starting point,^{6a} we found that the reaction of either silyl ether **67a** or acetate **67b** with cinnamyl carbonate (**68**) furnishes desired products **69a** and **69b**, respectively, albeit in low yields (Table 2.1, entries 1 and 2). However, the use of methoxymethyl ether **67c** provides allylic alkylation product **69c** in 64% yield (entry 3). Moreover, we were pleased to find that product **69c** can be obtained with excellent enantioselectivity (95% ee), obviating the need for further optimization beyond that of conversion. Of note, as in our prior investigations on iridium-catalyzed allylic alkylation,^{6a} LiBr was found to improve the regioselectivity of the allylic alkylation reaction – the use of 200 mol % (in comparison to 100 mol % as utilized in our previous report^{6a}) provides consistently higher yields of desired branched product **69**.

Efforts to increase the reaction conversion revealed that altering the nucleophile to electrophile ratio from 1:2 to 2:1 improves the yield to 77% with no erosion of enantioselectivity (entries 4 and 5). We observed that extending the reaction time from 18

to 48 hours provides product **69c** in a now synthetically useful 85% yield and 97% ee (entry 6). Ultimately, we found that treatment of a mixture (2:1) of nucleophile **67c** to electrophile **68** with a combination of catalytic Ir(cod)Cl·**L2** (4 mol %) and LiBr (200 mol %) at 60 °C delivers allylic alkylation product **69c** in a high 86% yield with an exceptional 96% enantioselectivity in only 18 hours (entry 7).

Table 2.1 Optimization of reaction parameters^a

Entry	R	67:68	Temp (°C)	Yield (%) ^b	ee (%) ^c
1	TBS (67a)	1:2	23	24	–
2	Ac (67b)	1:2	23	19	–
3	MOM (67c)	1:2	23	64	95
4	MOM (67c)	1:1	23	50	96
5	MOM (67c)	2:1	23	77	96
6 ^d	MOM (67c)	2:1	23	85	97
7	MOM (67c)	2:1	60	86	96

(S,S_a)-L2

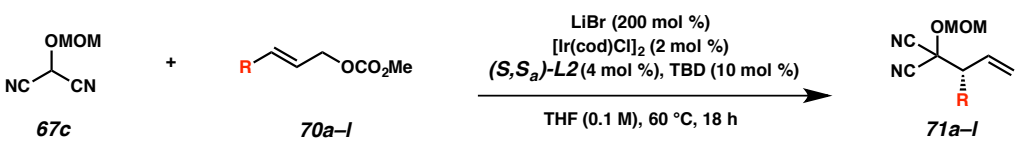
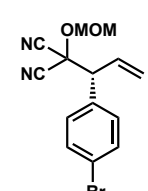
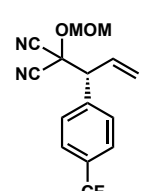
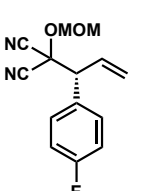
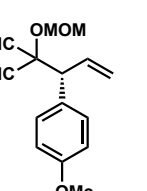
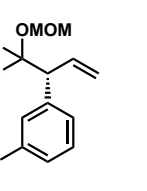
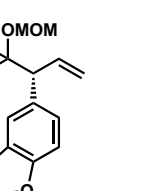
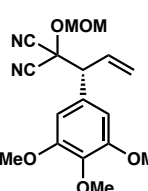
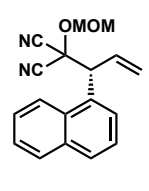
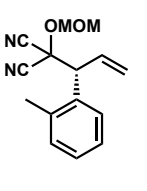
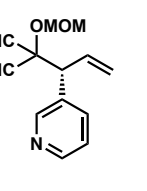
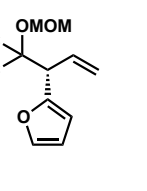
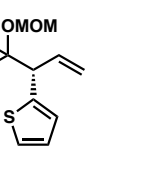
[a] Reactions performed on 0.1 mmol scale. [b] ¹H NMR yield based on internal standard. [c] Determined by chiral HPLC analysis. [d] Reaction run for 48 h. [e] TBD = 1,3,5-triazabicyclo[4.4.0]dec-5-ene.

2.3 SUBSTRATE SCOPE EXPLORATION

With the optimized conditions identified, the substrate scope of the enantioselective umpolung reaction was explored (Table 2.2). Our investigation began by probing the effects of electronics on reaction yield and selectivity. Gratifyingly, we observed that *para*-substituted aryl electrophiles bearing both electron-withdrawing (–Br, –CF₃, –F) and electron-donating (–OMe) groups furnish products **71a–d** with consistently excellent enantioselectivities (>95% ee). While products **71a** (–Br) and **71d** (–OMe) are obtained in high yield (>94% yield), diminished yields (58% and 69% yield,

respectively) are observed for the more electron-poor products **71b** (–CF₃) and **71c** (–F). Further examination of electrophile electronics revealed that *meta*-Cl-substituted **71e**, as well as poly-alkoxylated **71f** and **71g**, are each furnished in good yields (>81%) and high enantioselectivities (92–98% ee), despite varying electronics. Studies involving sterically demanding substrates showed that products **71h** (–2-Np) and **71i** (–*ortho*-Me) can be provided with good selectivities (92% and 89% ee, respectively), albeit in moderate yields (41% and 65%, respectively). Additionally, we were pleased to discover that pyridine **71j**, furan **71k**, and thiophene **71l** are each afforded with excellent enantioselectivities (90–96% ee) and in moderate to high yields (73–94%).

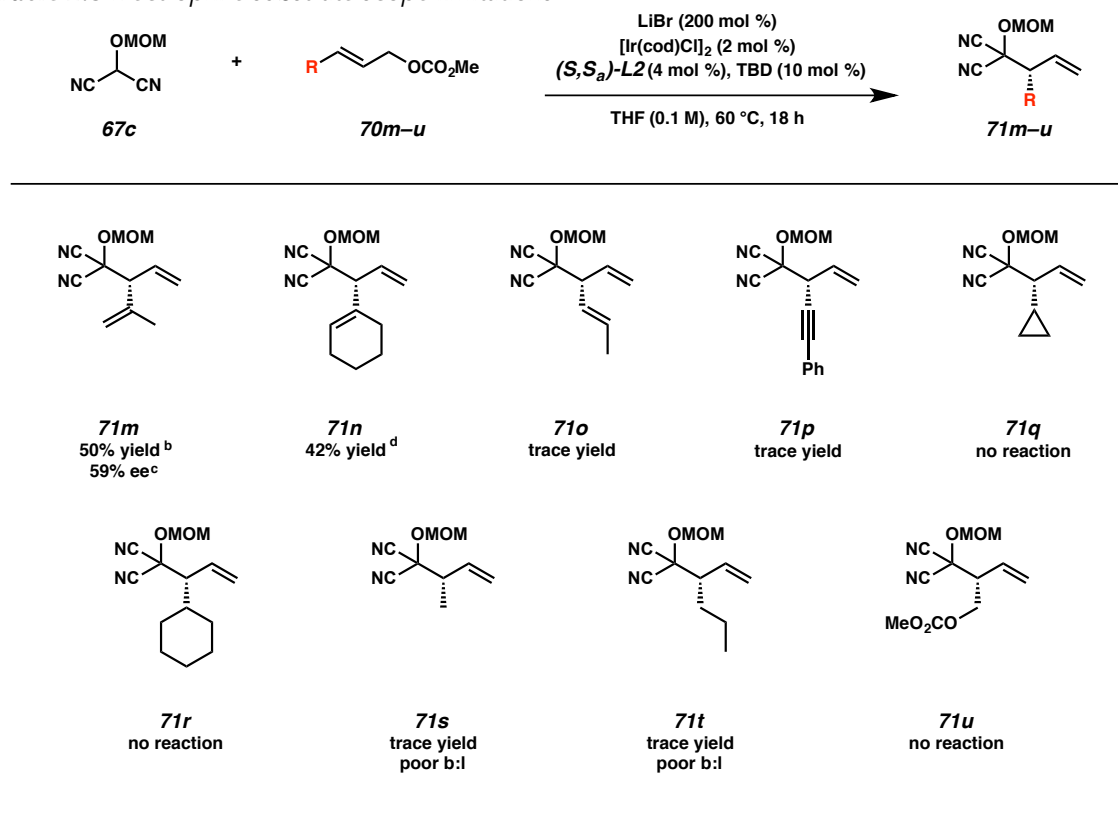
Table 2.2 Electrophile substrate scope^a

					
 71a 94% yield ^b 96% ee ^c	 71b ^d 58% yield 96% ee	 71c 69% yield 96% ee	 71d 95% yield 95% ee	 71e 85% yield 92% ee	 71f 90% yield 96% ee
 71g 81% yield 98% ee	 71h 41% yield 92% ee	 71i 65% yield 89% ee	 71j 74% yield 90% ee	 71k 73% yield 96% ee	 71l 94% yield 93% ee

[a] Reactions performed on 0.2 mmol scale. [b] Isolated yield. [c] Determined by chiral HPLC or SFC analysis. [d] Reaction run for 36 h at 50 °C.

A broader investigation of the substrate scope revealed limitations of the developed catalytic system (Table 2.3). Foremost, alkenyl substitution is not tolerated on allylic electrophile **70** and leads to significantly diminished yields and enantioselectivities, as is observed in the formation of iso-propenyl **71m**, cyclohexyl **71n**, and propenyl **71o**. Additionally, a propargyl-substituted electrophile does not give desired product **71q** in the allylic alkylation reaction, likely due to catalyst poisoning by binding of the alkyne to the metal source. Finally, the optimized reaction conditions fail to provide synthetically useful yields or high regioselectivities when alkyl-substituted allylic electrophiles are employed (e.g., **71q–u**).

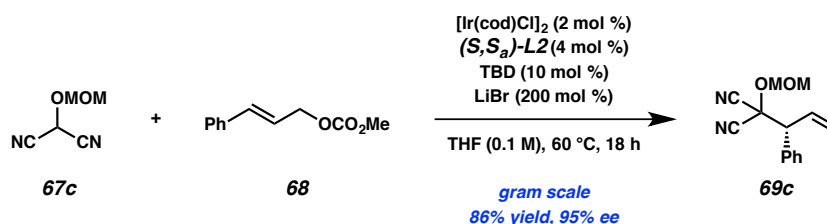
Table 2.3 Electrophile substrate scope limitations^a



[a] Reactions performed on 0.2 mmol scale. [b] Isolated yield. [c] Determined by chiral HPLC or SFC analysis. [d] ¹H NMR yield based on internal standard.

To demonstrate the synthetic utility of this method, a preparatory scale (4 mmol) reaction was performed (Scheme 2.1). Using cinnamyl carbonate (**68**), both the yield and enantioselectivity of the reaction are unchanged from those obtained at 0.1 mmol scale.

Scheme 2.1 Preparatory scale reaction



2.4 CONCLUSIONS

In summary, we have developed the first enantioselective iridium-catalyzed allylic alkylation reaction of masked acyl cyanide (MAC) reagents. The umpolung strategy showcased in this reaction diverges from the normal reactivity patterns employed in all but two of the previously reported iridium-catalyzed allylic alkylations and is the first report of a carbon monoxide synthon in iridium-catalyzed allylic alkylation. Critical to the success of this new reaction is the identity of the methoxymethyl protecting group on the MAC reagent. The developed methodology proceeds with moderate to excellent yields (up to 95%) and high levels of enantioselectivity (up to 98% ee) on up to gram scale for a wide range of aryl- and heteroaryl-substituted allylic electrophiles. Furthermore, MAC adducts bearing resemblance to compound **4c** have been transformed into acids, amides, and esters by unmasking the alkoxy malononitrile moiety.^{7,8} Thus, this methodology serves as an entry to enantioenriched vinylated α -aryl carbonyl derivatives.

2.5 EXPERIMENTAL SECTION

2.5.1 MATERIALS AND METHODS

Unless otherwise stated, reactions were performed in flame-dried glassware under an argon or nitrogen atmosphere using dry, deoxygenated solvents. Solvents were dried by passage through an activated alumina column under argon. Commercially obtained reagents were used as received. Chemicals were purchased from Sigma Aldrich/Strem/Alfa Aesar/Oakwood Chemicals and used as received. Reaction temperatures were controlled by an IKA Mag temperature modulator. Glove box manipulations were performed under a nitrogen atmosphere. Thin-layer chromatography (TLC) and preparatory TLC was performed using E. Merck silica gel 60 F254 precoated plates (0.25 mm) and visualized by UV fluorescence quenching, KMnO_4 or *p*-anisaldehyde staining. SiliaFlash P60 Academic Silica gel (particle size 0.040–0.063 mm) was used for flash chromatography. Analytical chiral HPLC was performed with an Agilent 1100 Series HPLC utilizing a Chiralpak IC column (4.6 mm x 25 cm) or a Chiralpak AD column (4.6 mm x 25 cm), both obtained from Daicel Chemical Industries, Ltd. with visualization at 210 nm. Analytical SFC was performed with a Mettler SFC supercritical CO_2 analytical chromatography system utilizing a Chiralpak IC-3 column (4.6 mm x 25 cm) obtained from Daicel Chemical Industries, Ltd. with visualization at 210 nm. ^1H NMR spectra were recorded on a Bruker Avance HD 400 MHz spectrometer and are reported relative to residual CHCl_3 (δ 7.26 ppm). ^{13}C NMR spectra were recorded on a Bruker Avance HD 400 MHz spectrometer and are reported relative to residual CDCl_3 (δ 77.16 ppm). Data for ^1H NMR are reported as follows: s = singlet, d = doublet, t = triplet, q = quartet, p = pentet, sept = septuplet, m = multiplet, br s = broad singlet.

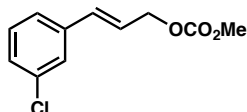
Data for ^{13}C NMR are reported in terms of chemical shifts (δ ppm). Some reported spectra include minor solvent impurities of benzene (δ 7.36 ppm), water (δ 1.56 ppm), ethyl acetate (δ 4.12, 2.05, 1.26 ppm), methylene chloride (δ 5.30 ppm), grease (δ 1.26, 0.86 ppm), and/or silicon grease (δ 0.07 ppm), which do not impact product assignments. IR spectra were obtained using a Perkin Elmer Paragon 1000 spectrometer using thin films deposited on NaCl plates and reported in frequency of absorption (cm^{-1}). High resolution mass spectra (HRMS) were obtained from the Caltech Mass Spectral Facility using a JEOL JMS-600H High Resolution Mass Spectrometer in fast atom bombardment (FAB+) or electron ionization (EI+) mode, or an Agilent 6200 Series TOF with an Agilent G1978A Multimode source in electrospray ionization (ESI+), atmospheric pressure chemical ionization (APCI+), or mixed ionization mode (MM: ESI-APCI+). Optical rotations were measured with a Jasco P-2000 polarimeter operating on the sodium D-line (589 nm), using a 100 mm pathlength cell, and are reported as: $[\alpha]_{\text{D}}^{\text{T}}$ (concentration in g/100 mL, solvent).

2.5.1.1 Preparation of Known Compounds

Previously reported methods were used to prepare ligand (*S,S*)-**L2**¹⁰ as well as starting materials **67a–c**,¹¹ **68**,¹² **70a**,¹¹ **70b**,¹¹ **70c**,¹³ **70d**,¹⁴ **70h**,^{10b} **70i**,¹⁴ **70j**,¹⁵ **70k**,¹⁶ **70l**.¹²

2.5.2 EXPERIMENTAL PROCEDURES AND SPECTROSCOPIC DATA

2.5.2.1 General Procedure for the Synthesis of Electrophiles

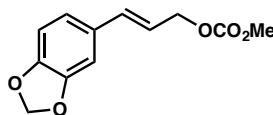


(*E*)-3-(3-Chlorophenyl)allyl methyl carbonate (70e). To a solution of methyl (*E*)-3-(3-chlorophenyl)prop-2-enoate¹⁷ (1.4 g, 7.0 mmol, 1 equiv) in Et₂O (28 mL) at –78 °C was added DIBAL (3.0 g, 21 mmol, 3 equiv) dropwise. The resulting reaction mixture was stirred at –78 °C for 2.5 h, whereupon the reaction was quenched with a saturated aqueous Rochelle’s salt solution (10 mL). The cooling bath was then removed and the reaction was stirred for 18 h at ambient temperature. The aqueous layer was extracted with CH₂Cl₂ (3 x 50 mL) and the combined organic layers were washed with brine (50 mL), dried over Na₂SO₄, and concentrated under reduced pressure.

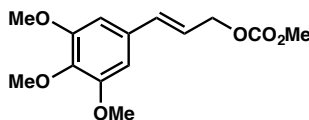
The crude material was then dissolved in CH₂Cl₂ (10 mL) and cooled to 0 °C. Pyridine (1.7 mL, 21 mmol, 3 equiv) was added followed by methyl chloroformate (0.81 mL, 11 mmol, 1.5 equiv) dropwise. The resulting solution was allowed to warm to ambient temperature and stirred for 18 h. The reaction was quenched with the addition of 1 M HCl (10 mL) and the aqueous layer was extracted with CH₂Cl₂ (3 x 50 mL). The combined organic layers were washed with brine (50 mL), dried over Na₂SO₄, and concentrated under reduced pressure. The crude product was purified by silica gel flash column chromatography (5% EtOAc/hexanes) to give carbonate **70e** as a colorless oil (1.0 g, 63% yield): ¹H NMR (400 MHz, CDCl₃) δ 7.43 – 7.37 (m, 1H), 7.30 – 7.23 (m, 3H), 6.69 – 6.60 (m, 1H), 6.32 (dt, *J* = 15.9, 6.3 Hz, 1H), 4.81 (dd, *J* = 6.3, 1.4 Hz, 2H), 3.84 (s, 3H); ¹³C NMR (101 MHz, CDCl₃) δ 155.7, 138.0, 134.7, 133.2, 130.0, 128.3,

126.7, 125.0, 124.2, 68.1, 55.1; IR (Neat Film, NaCl) 3010, 2956, 2856, 1748, 1594, 1567, 1442, 1377, 1261, 1091, 1078, 962, 791, 777, 682 cm^{-1} ; HRMS (MM: FAB+) m/z calc'd for $\text{C}_{11}\text{H}_{11}\text{ClO}_3$ $[\text{M}]^+$: 226.0397, found 226.0398.

2.5.2.2 Spectroscopic Data for the Synthesis of Electrophiles



(E)-3-(Benzo[d][1,3]dioxol-5-yl)allyl methyl carbonate (70f). Carbonate **70f** was prepared from methyl (2*E*)-3-(1,3-benzodioxol-5-yl)acrylate¹⁸ according to the general procedure and isolated by silica gel flash column chromatography (5% EtOAc/hexanes) as a colorless solid (0.79 g, 48% yield): ^1H NMR (400 MHz, CDCl_3) δ 6.93 (d, J = 1.6 Hz, 1H), 6.83 (ddd, J = 7.9, 1.6, 0.5 Hz, 1H), 6.79 – 6.73 (m, 1H), 6.60 (dt, J = 15.7, 1.3 Hz, 1H), 6.12 (dt, J = 15.7, 6.6 Hz, 1H), 5.96 (s, 2H), 4.76 (dd, J = 6.6, 1.3 Hz, 2H), 3.80 (s, 3H); ^{13}C NMR (101 MHz, CDCl_3) δ 155.8, 148.2, 147.9, 134.9, 130.6, 121.8, 120.7, 108.4, 106.0, 101.3, 68.7, 55.0; IR (Neat Film, NaCl) 3003, 2956, 2895, 2781, 1747, 1504, 1491, 1446, 1384, 1355, 1252, 1194, 1126, 1103, 1039, 933, 863, 791 cm^{-1} ; HRMS (FAB+) m/z calc'd for $\text{C}_{12}\text{H}_{12}\text{O}_5$ $[\text{M}]^+$: 236.0685, found 236.0674.



(E)-Methyl (3-(3,4,5-trimethoxyphenyl)allyl) carbonate (70g). Carbonate **70g** was prepared from methyl 3,4,5-trimethoxycinnamate¹⁹ according to the general procedure and isolated by silica gel flash column chromatography (5% EtOAc/hexanes) as a

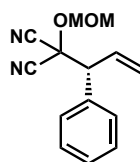
colorless oil (1.2 g, 65% yield): ^1H NMR (400 MHz, CDCl_3) δ 6.65 – 6.56 (m, 3H), 6.21 (dt, J = 15.8, 6.5 Hz, 1H), 4.78 (dd, J = 6.5, 1.3 Hz, 2H), 3.87 (s, 6H), 3.84 (s, 3H), 3.81 (s, 3H); ^{13}C NMR (101 MHz, CDCl_3) δ 155.8, 153.4, 138.4, 135.0, 131.8, 122.0, 103.9, 68.5, 61.1, 56.2, 55.0; IR (Neat Film, NaCl) 2999, 2956, 2840, 1748, 1583, 1508, 1452, 1420, 1339, 1265, 1128, 1010, 941, 850, 792 cm^{-1} ; HRMS (FAB+) m/z calc'd for $\text{C}_{14}\text{H}_{18}\text{O}_6$ $[\text{M}]^+$: 282.1103, found 282.1114.

2.5.2.3 General Procedure for Optimization Reactions (Table 2.1)

In a nitrogen-filled glove box, to a 1 dram vial (vial A) equipped with a stir bar was added $[\text{Ir}(\text{cod})\text{Cl}]_2$ (1.3 mg, 0.0020 mmol, 2 mol %), ligand (*S,S*)-**L2** (1.8 mg, 0.0040 mmol, 4 mol %), TBD (1.4 mg, 0.010 mmol, 10 mol%), and THF (0.5 mL). Vial A was stirred at 25 °C (ca. 10 min) while another 1 dram vial (vial B) was charged with LiBr (17 mg, 0.20 mmol, 200 mol %), MAC nucleophile **67** (0.20 mmol), and THF (0.25 mL). The pre-formed catalyst solution (vial A) was then transferred to vial B followed by 0.25 mL of a solution of cinnamyl carbonate **68** (0.4 M in THF). The vial was sealed and stirred at the specified temperature. After 18 or 48 h, the vial was removed from the glove box and filtered through a pad of silica, rinsing with EtOAc. The crude mixture was concentrated and 1,2,4,5-tetrachloro-3-nitrobenzene (0.10 mmol in 0.5 mL CDCl_3) was added. The NMR yield (measured in reference to 1,2,4,5-tetrachloro-3-nitrobenzene δ 7.74 ppm (s, 1H)) was determined by ^1H NMR analysis of the crude mixture. The residue was purified by preparatory TLC (15% EtOAc/hexanes) to afford product **69**, which was analyzed by chiral HPLC (1% IPA, 1.0 mL/min, Chiralpak IC column, λ = 210 nm).

2.5.2.4 General Procedure for the Iridium-Catalyzed Allylic Alkylation

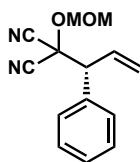
Please note that the absolute configuration of product **69c** was assigned by conversion to (*R*)-2-phenylbutanoic acid.²⁰ All other products (**71a–l**) were assigned by analogy. For respective HPLC and SFC conditions, please refer to Table 2.4.



(*R*)-2-(Methoxymethoxy)-2-(1-phenylallyl)malononitrile (69c). In a nitrogen-filled glove box, to a 1 dram vial (vial A) equipped with a stir bar was added [Ir(cod)Cl]₂ (2.7 mg, 0.0040 mmol, 2 mol %), ligand (*S,S*_a)-**L2** (3.7 mg, 0.0080 mmol, 4 mol %), TBD (2.8 mg, 0.020 mmol, 10 mol %), and THF (1 mL). Vial A was stirred at 25 °C (ca. 10 min) while another 1 dram vial (vial B) was charged with LiBr (35 mg, 0.40 mmol, 200 mol %), MAC nucleophile **67c** (50 mg, 0.40 mmol, 200 mol %), and THF (0.5 mL). The pre-formed catalyst solution (vial A) was then transferred to vial B followed by a solution of cinnamyl carbonate **68** (38 mg, 0.20 mmol, 100 mol %) in THF (0.5 mL). The vial was sealed and stirred at 60 °C. After 18 h, the vial was removed from the glove box and filtered through a pad of silica, rinsing with EtOAc. The crude mixture was concentrated and the resulting residue was purified by silica gel flash column chromatography (10% EtOAc/hexanes) to give the product **69c** as a colorless oil (41 mg, 85% yield): 95% ee; [α]_D²⁵ –41.3 (*c* 2.5, CHCl₃); ¹H NMR (400 MHz, CDCl₃) δ 7.47 – 7.32 (m, 5H), 6.29 (ddd, *J* = 16.9, 10.3, 8.6 Hz, 1H), 5.53 – 5.38 (m, 2H), 5.06 – 4.94 (m, 2H), 3.97 – 3.91 (m, 1H), 3.44 (s, 3H); ¹³C NMR (101 MHz, CDCl₃) δ 134.4, 131.5, 129.6, 129.1, 128.9,

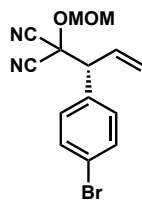
122.7, 112.7, 112.7, 96.5, 69.9, 58.4, 57.4; IR (Neat Film, NaCl) 3065, 3033, 2961, 2904, 2851, 2244, 1750, 1496, 1455, 1420, 1267, 1217, 1164, 1109, 1053, 1033, 967, 940, 791, 732, 700 cm^{-1} ; HRMS (FAB+) m/z calc'd for $\text{C}_{14}\text{H}_{15}\text{N}_2\text{O}_2$ $[\text{M}+\text{H}]^+$: 243.1131, found 243.1134; HPLC conditions: 1% IPA, 1.0 mL/min, Chiralpak IC column, λ = 210 nm, t_R (min): major = 12.831, minor = 17.466.

2.5.2.5 Procedure for the Preparatory Scale Reaction

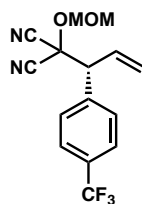


(*R*)-2-(Methoxymethoxy)-2-(1-phenylallyl)malononitrile (69c). In a nitrogen-filled glove box, a solution of $[\text{Ir}(\text{cod})\text{Cl}]_2$ (106 mg, 0.16 mmol, 2 mol %), ligand (*S,S*)-**L2** (145 mg, 0.32 mmol, 4 mol %), TBD (110 mg, 0.79 mmol, 10 mol %) in THF (20 mL) was stirred at 25 °C. After 10 minutes, the catalyst mixture was added to a mixture of LiBr (0.69 g, 7.9 mmol, 200 mol %), MAC nucleophile **67c** (1 g, 7.9 mmol, 200 mol %), and THF (20 mL) followed by cinnamyl carbonate **68** (0.76 g, 4.0 mmol, 100 mol %). The flask was removed from the glove box and stirred at 60 °C. After 18 h, the crude reaction mixture was concentrated and the resulting residue was purified by silica gel flash column chromatography (10% EtOAc/hexanes) to give the product **69c** as a colorless oil (0.82 g, 86% yield): 95% ee, spectroscopic data vide supra.

2.5.2.6 Spectroscopic Data for the Iridium-Catalyzed Allylic Alkylation Products

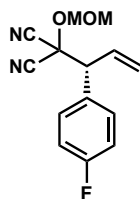


(*R*)-2-(1-(4-Bromophenyl)allyl)-2-(methoxymethoxy)malononitrile (71a). Product **71a** was prepared according to the general procedure and isolated by silica gel flash column chromatography (10% EtOAc/hexanes) to give a colorless oil (60 mg, 94% yield): 96% ee; $[\alpha]_D^{25} -44.3$ (*c* 3.2, CHCl₃); ¹H NMR (400 MHz, CDCl₃) δ 7.56 – 7.50 (m, 2H), 7.32 – 7.28 (m, 2H), 6.23 (ddd, *J* = 16.9, 10.3, 8.6 Hz, 1H), 5.55 – 5.38 (m, 2H), 5.05 – 4.96 (m, 2H), 3.92 (d, *J* = 8.6 Hz, 1H), 3.44 (s, 3H); ¹³C NMR (101 MHz, CDCl₃) δ 133.4, 132.1, 131.3, 130.9, 123.4, 123.2, 112.6, 112.5, 96.6, 69.5, 57.8, 57.5; IR (Neat Film, NaCl) 3013, 2934, 2242, 1488, 1404, 1274, 1216, 1163, 1108, 1034, 1010, 967, 939, 826, 762 cm⁻¹; HRMS (FAB+) *m/z* calc'd for C₁₄H₁₃BrO₂N₂ [M]⁺: 320.0160, found 320.0155; HPLC conditions: 1% IPA, 1.0 mL/min, Chiralpak IC column, λ = 210 nm, *t*_R (min): major = 15.852, minor = 11.623.



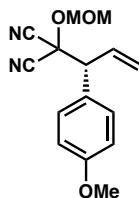
(*R*)-2-(Methoxymethoxy)-2-(1-(4-(trifluoromethyl)phenyl)allyl)malononitrile (71b). Product **71b** was prepared according to the general procedure and isolated by preparatory TLC (5% EtOAc/hexanes, plate eluted three times) to give a pale yellow oil (36 mg, 58%

yield): 96% ee; $[\alpha]_D^{25} -25.2$ (c 1.5, CHCl_3); ^1H NMR (400 MHz, CDCl_3) δ 7.66 (d, J = 8.6 Hz, 2H), 7.55 (d, J = 8.2 Hz, 2H), 6.27 (ddd, J = 16.9, 10.3, 8.7 Hz, 1H), 5.57 – 5.41 (m, 2H), 5.09 – 4.96 (m, 2H), 4.02 (d, J = 8.7 Hz, 1H), 3.44 (s, 3H); ^{13}C NMR (101 MHz, CDCl_3) δ 138.4, 131.5, 131.1, 130.6, 130.2, 125.9 (q, J = 3.9 Hz), 125.3, 123.6, 122.6, 112.5, 112.4, 96.7, 69.4, 58.0, 57.6; IR (Neat Film, NaCl) 2962, 2906, 2835, 2245, 1751, 1618, 1445, 1417, 1445, 1417, 1327, 1269, 1218, 1166, 1127, 1069, 943, 840, 792 cm^{-1} ; HRMS (MM: FAB+) m/z calc'd for $\text{C}_{15}\text{H}_{12}\text{F}_3\text{N}_2\text{O}_2$ $[(\text{M}+\text{H})-\text{H}_2]^+$: 309.0851, found 309.0849; HPLC conditions: 1% IPA, 1.0 mL/min, Chiralpak IC column, λ = 210 nm, t_R (min): major = 10.681, minor = 8.223.

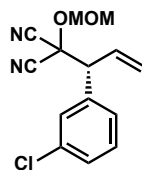


(*R*)-2-(1-(4-Fluorophenyl)allyl)-2-(methoxymethoxy)malononitrile (71c). Product **71c** was prepared according to the general procedure and isolated by preparatory TLC (9% EtOAc/hexanes, plate eluted two times) to give a colorless oil (37 mg, 69% yield): 96% ee; $[\alpha]_D^{25} -35.9$ (c 1.9, CHCl_3); ^1H NMR (400 MHz, CDCl_3) δ 7.47 – 7.32 (m, 2H), 7.15 – 7.02 (m, 2H), 6.25 (ddd, J = 16.9, 10.3, 8.5 Hz, 1H), 5.57 – 5.35 (m, 2H), 5.11 – 4.94 (m, 2H), 3.95 (d, J = 8.5 Hz, 1H), 3.44 (s, 3H); ^{13}C NMR (101 MHz, CDCl_3) δ 164.3, 161.9, 131.5, 131.4, 131.2, 130.2 (d, J = 3.5 Hz), 122.9, 116.1, 115.9, 112.7, 112.6, 96.6, 69.8 (d, J = 1.6 Hz), 57.5 (d, J = 9.2 Hz); IR (Neat Film, NaCl) 3085, 2964, 2847, 2242, 1606, 1511, 1415, 1281, 1230, 1164, 1108, 1053, 968, 940, 798, 766 cm^{-1} ; HRMS (ESI+) m/z calc'd for $\text{C}_{14}\text{H}_{14}\text{N}_2\text{O}_2\text{F}$ $[\text{M}+\text{H}]^+$: 261.1039, found 261.1033; HPLC conditions: 1%

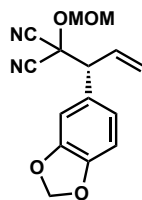
IPA, 1 mL/min, Chiralpak IC column, λ = 210 nm, t_R (min): major = 11.712, minor = 8.971.



(*R*)-2-(Methoxymethoxy)-2-(1-(4-methoxyphenyl)allyl)malononitrile (71d). Product **71d** was prepared according to the general procedure and isolated by silica gel flash column chromatography (5–10% EtOAc/hexanes) to give a colorless oil (52 mg, 95% yield): 95% ee; $[\alpha]_D^{25}$ –51.8 (*c* 2.7, CHCl₃); ¹H NMR (400 MHz, CDCl₃) δ 7.41 – 7.31 (m, 2H), 6.92 (d, *J* = 8.8 Hz, 2H), 6.26 (ddd, *J* = 16.9, 10.3, 8.5 Hz, 1H), 5.61 – 5.34 (m, 2H), 5.08 – 4.94 (m, 2H), 3.91 (d, *J* = 8.5 Hz, 1H), 3.82 (s, 3H), 3.45 (s, 3H); ¹³C NMR (101 MHz, CDCl₃) δ 160.1, 131.7, 130.8, 126.3, 122.3, 114.3, 112.82, 112.78, 96.5, 70.1, 57.6, 57.4, 55.4; IR (Neat Film, NaCl) 3005, 2962, 2939, 2905, 2838, 2244, 2052, 1890, 1610, 1584, 15112, 1459, 1305, 1252, 1216, 1182, 1162, 1107, 1031, 937, 834, 783, 765, 625 cm⁻¹; HRMS (FAB+) *m/z* calc'd for C₁₅H₁₇N₂O₃ [M+H]⁺: 273.1239, found 273.1227; SFC conditions: 3% IPA, 3.5 mL/min, Chiralpak IC-3 column, λ = 210 nm, t_R (min): major = 6.831, minor = 5.267.



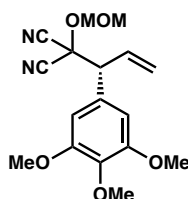
(*R*)-2-(1-(3-Chlorophenyl)allyl)-2-(methoxymethoxy)malononitrile (71e). Product **71e** was prepared according to the general procedure and isolated by silica gel flash column chromatography (10% EtOAc/hexanes) to give a colorless oil (47 mg, 85% yield): 92% ee; $[\alpha]_D^{25} -38.5$ (*c* 2.1, CHCl₃); ¹H NMR (400 MHz, CDCl₃) δ 7.47 – 7.28 (m, 4H), 6.23 (ddd, *J* = 16.9, 10.3, 8.7 Hz, 1H), 5.57 – 5.40 (m, 2H), 5.08 – 4.97 (m, 2H), 3.92 (d, *J* = 8.7 Hz, 1H), 3.45 (s, 3H); ¹³C NMR (101 MHz, CDCl₃) δ 136.4, 134.7, 130.8, 130.2, 129.9, 129.3, 127.8, 123.3, 112.6, 112.4, 96.6, 69.5, 57.9, 57.5; IR (Neat Film, NaCl) 3069, 2962, 2849, 2832, 2244, 1751, 1596, 1576, 1478, 1436, 1418, 1277, 1217, 1164, 1109, 111055, 1032, 967, 940, 884, 797, 760, 730, 713, 690 cm⁻¹; HRMS (ESI+) *m/z* calc'd for C₁₄H₁₄N₂O₂Cl [M+H]⁺: 277.0744, found 277.0715; SFC conditions: 3% IPA, 3.5 mL/min, Chiralpak IC-3 column, λ = 210 nm, *t_R* (min): major = 3.846, minor = 3.428.



(*R*)-2-(1-(Benzo[d][1,3]dioxol-5-yl)allyl)-2-(methoxymethoxy)malononitrile (71f).

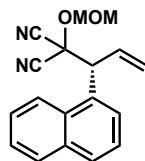
Product **71f** was prepared according to the general procedure and isolated by silica gel flash column chromatography (5–10% EtOAc/hexanes) to give a colorless oil (51 mg, 90% yield): 96% ee; $[\alpha]_D^{25} -40.6$ (*c* 3.4, CHCl₃); ¹H NMR (400 MHz, CDCl₃) δ 6.91 – 6.78 (m, 3H), 6.20 (ddd, *J* = 16.9, 10.3, 8.5 Hz, 1H), 5.99 (s, 2H), 5.51 – 5.37 (m, 2H),

5.03 (d, $J = 1.4$ Hz, 2H), 3.86 (d, $J = 8.5$ Hz, 1H), 3.47 (s, 3H); ^{13}C NMR (101 MHz, CDCl_3) δ 148.2, 148.1, 131.5, 127.9, 123.5, 122.5, 112.7, 109.7, 108.7, 101.5, 96.6, 70.0, 58.1, 57.5; IR (Neat Film, NaCl) 3081, 2972, 2902, 2352, 1505, 1488, 1446, 1368, 1251, 1238, 1164, 1108, 1039, 967, 934, 864, 817, 800, 763 cm^{-1} ; HRMS (ESI+) m/z calc'd for $\text{C}_{15}\text{H}_{15}\text{N}_2\text{O}_4$ $[\text{M}+\text{H}]^+$: 287.1032, found 287.1039; HPLC conditions: 1% IPA, 1.0 mL/min, Chiralpak IC column, $\lambda = 210$ nm, t_R (min): major = 24.142, minor = 19.686.

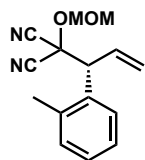


(*R*)-2-(Methoxymethoxy)-2-(1-(3,4,5-trimethoxyphenyl)allyl)malononitrile (71g).

Product **71g** was prepared according to the general procedure and isolated by silica gel flash column chromatography (20% EtOAc/hexanes) to give a colorless oil (54 mg, 81% yield): 98% ee; $[\alpha]_D^{25} -28.2$ (c 3.5, CHCl_3); ^1H NMR (400 MHz, CDCl_3) δ 6.63 (s, 2H), 6.23 (ddd, $J = 16.8, 10.3, 8.5$ Hz, 1H), 5.55 – 5.35 (m, 2H), 5.11 – 4.94 (m, 2H), 3.87 (m, 7H), 3.85 (s, 3H), 3.46 (s, 3H); ^{13}C NMR (101 MHz, CDCl_3) δ 153.4, 138.5, 131.3, 129.7, 122.6, 112.8, 112.7, 106.6, 96.5, 69.9, 61.0, 58.5, 57.5, 56.3; IR (Neat Film, NaCl) 2941, 2840, 244, 1591, 1509, 1463, 1418, 1333, 1245, 1163, 1127, 1034, 1007, 950, 925, 840, 771, 719 cm^{-1} ; HRMS (ESI+) m/z calc'd for $\text{C}_{17}\text{H}_{21}\text{N}_2\text{O}_5$ $[\text{M}+\text{H}]^+$: 333.1450, found 333.1450; HPLC conditions: 7% IPA, 1.0 mL/min, Chiralpak AD column, $\lambda = 210$ nm, t_R (min): major = 17.062, minor = 12.809.

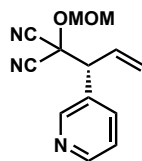


(*R*)-2-(Methoxymethoxy)-2-(1-(naphthalen-1-yl)allyl)malononitrile (71h). Product **71h** was prepared according to the general procedure and isolated by preparatory TLC (9% Et₂O/hexanes, plate eluted two times) to give a colorless oil (24 mg, 41% yield): 92% ee; $[\alpha]_D^{25}$ –30.9 (*c* 1.5, CHCl₃); ¹H NMR (400 MHz, CDCl₃) δ 8.11 (dt, *J* = 8.5, 1.0 Hz, 1H), 7.95 – 7.86 (m, 2H), 7.81 (dd, *J* = 7.4, 1.2 Hz, 1H), 7.60 (ddd, *J* = 8.6, 6.8, 1.5 Hz, 1H), 7.57 – 7.49 (m, 2H), 6.38 (ddd, *J* = 16.7, 10.3, 8.2 Hz, 1H), 5.57 – 5.43 (m, 2H), 5.05 – 4.92 (m, 3H), 3.40 (s, 3H); ¹³C NMR (101 MHz, CDCl₃) δ 134.1, 132.2, 132.1, 130.8, 129.6, 129.3, 126.9, 126.6, 126.1, 125.3, 122.8, 122.7, 113.10, 112.72, 96.5, 70.1, 57.5, 51.6; IR (Neat Film, NaCl) 3051, 2960, 2926, 2851, 2244, 1708, 1398, 1215, 1162, 1106, 1030, 960, 925, 783 cm^{–1}; HRMS (ESI+) *m/z* calc'd for C₁₈H₁₇N₂O₂ [M+H]⁺: 293.1290, found 293.1263; HPLC conditions: 1% IPA, 1.0 mL/min, Chiralpak IC column, λ = 210 nm, *t*_R (min): major = 15.134, minor = 10.197.

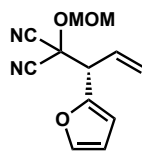


(*R*)-2-(Methoxymethoxy)-2-(1-(*o*-tolyl)allyl)malononitrile (71i). Product **71i** was prepared according to the general procedure and isolated by silica gel flash column chromatography (5% EtOAc/hexanes) to give a colorless oil (33 mg, 65% yield): 89% ee; $[\alpha]_D^{25}$ –68.7 (*c* 1.4, CHCl₃); ¹H NMR (400 MHz, CDCl₃) δ 7.58 – 7.48 (m, 1H), 7.28 –

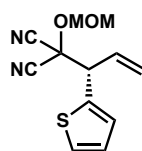
7.19 (m, 3H), 6.22 (ddd, $J = 16.9, 10.2, 8.2$ Hz, 1H), 5.50 – 5.35 (m, 2H), 5.06 – 4.98 (m, 2H), 4.34 (dd, $J = 8.2, 1.0$ Hz, 1H), 3.45 (s, 3H), 2.43 (s, 3H); ^{13}C NMR (101 MHz, CDCl_3) δ 137.4, 133.1, 132.0, 131.2, 128.6, 128.1, 126.6, 122.5, 113.0, 112.8, 96.5, 69.8, 57.5, 53.0, 20.3; IR (Neat Film, NaCl) 3023, 2958, 2360, 2243, 1748, 1640, 1603, 1489, 1445, 1382, 1264, 1164, 1109, 1034, 943, 846, 792, 748, 654 cm^{-1} ; HRMS (FAB+) m/z calc'd for $\text{C}_{15}\text{H}_{17}\text{N}_2\text{O}_2$ $[\text{M}+\text{H}]^+$: 257.1290, found 257.1280; HPLC conditions: 1% IPA, 1.0 mL/min, Chiralpak IC column, $\lambda = 210$ nm, t_R (min): major = 16.719, minor = 9.761.



(R)-2-(Methoxymethoxy)-2-(1-(pyridin-3-yl)allyl)malononitrile (71j). Product **71j** was prepared according to the general procedure and isolated by silica gel flash column chromatography (25% acetone/hexanes) to give a pale yellow oil (36 mg, 74% yield): 90% ee; $[\alpha]_D^{25} -30.8$ (c 2.1, CHCl_3); ^1H NMR (400 MHz, CDCl_3) δ 8.63 (dd, $J = 4.7, 1.7$ Hz, 2H), 7.78 (dddd, $J = 8.0, 2.3, 1.6, 0.5$ Hz, 1H), 7.35 (ddd, $J = 7.9, 4.8, 0.8$ Hz, 1H), 6.27 (ddd, $J = 16.9, 10.3, 8.7$ Hz, 1H), 5.63 – 5.39 (m, 2H), 5.06 – 4.97 (m, 2H), 4.00 (d, $J = 8.7$ Hz, 1H), 3.42 (s, 3H); ^{13}C NMR (101 MHz, CDCl_3) δ 151.1, 150.4, 136.7, 130.4, 130.3, 123.8, 123.7, 112.5, 112.3, 96.7, 69.4, 57.5, 56.0; IR (Neat Film, NaCl) 2963, 2943, 2905, 2833, 2244, 1751, 1718, 1590, 1577, 1480, 1419, 1430, 1271, 1217, 1164, 1109, 2055, 1028, 970, 941, 848, 817, 756, 714 cm^{-1} ; HRMS (FAB+) m/z calc'd for $\text{C}_{13}\text{H}_{14}\text{N}_3\text{O}_2$ $[\text{M}+\text{H}]^+$: 244.1086, found 244.1083; HPLC conditions: 20% IPA, 1.0 mL/min, Chiralpak IC column, $\lambda = 210$ nm, t_R (min): major = 13.161, minor = 23.457.



(R)-2-(1-(Furan-2-yl)allyl)-2-(methoxymethoxy)malononitrile (71k). Product **71k** was prepared according to the general procedure and isolated by silica gel flash column chromatography (10% EtOAc/hexanes) to give a colorless oil (34 mg, 73% yield): 96% ee; $[\alpha]_D^{25} -44.9$ (*c* 1.5, CHCl₃); ¹H NMR (400 MHz, CDCl₃) δ 7.47 (s, 1H), 6.53 – 6.34 (m, 2H), 6.14 (dddd, *J* = 16.9, 10.2, 8.5, 0.8 Hz, 1H), 5.58 – 5.43 (m, 2H), 5.10 – 4.94 (m, 2H), 4.16 (d, *J* = 8.5 Hz, 1H), 3.48 (d, *J* = 0.7 Hz, 3H); ¹³C NMR (101 MHz, CDCl₃) δ 147.4, 143.5, 129.1, 123.5, 112.4, 112.3, 111.0, 110.4, 96.6, 68.9, 57.5, 52.4; IR (Neat Film, NaCl) 3125, 2091, 2964, 2942, 2905, 2833, 2245, 1499, 1444, 14222, 1270, 1217, 1164, 1109, 1030, 922, 797, 743 cm⁻¹; HRMS (ESI+) *m/z* calc'd for C₁₂H₁₃N₂O₃ [M+H]⁺: 233.0926, found 233.0948; HPLC conditions: 1% IPA, 1.0 mL/min, Chiralpak IC column, λ = 210 nm, *t_R* (min): major = 13.297, minor = 10.761.



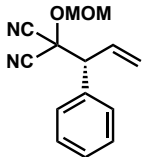
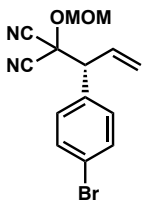
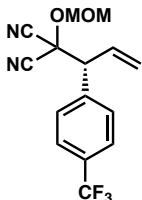
(S)-2-(Methoxymethoxy)-2-(1-(thiophen-2-yl)allyl)malononitrile (71l). Product **71l** was prepared according to the general procedure and isolated by silica gel flash column chromatography (10% EtOAc/hexanes) to give a colorless oil (49 mg, 98% yield): 93% ee; $[\alpha]_D^{25} -40.3$ (*c* 2.5, CHCl₃); ¹H NMR (400 MHz, CDCl₃) δ 7.38 (dd, *J* = 5.1, 1.2 Hz, 1H), 7.20 (ddd, *J* = 3.6, 1.2, 0.7 Hz, 1H), 7.08 (dd, *J* = 5.2, 3.6 Hz, 1H), 6.21 (ddd, *J* = 16.8, 10.2, 8.6 Hz, 1H), 5.59 – 5.48 (m, 2H), 5.09 (d, *J* = 1.7 Hz, 2H), 4.31 (dd, *J* = 8.6,

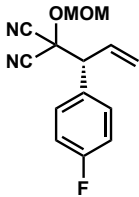
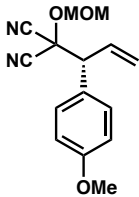
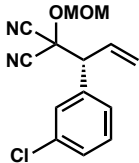
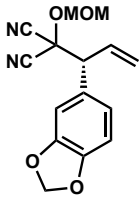
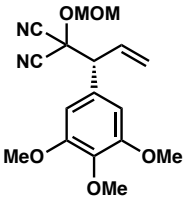
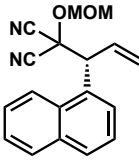
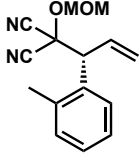
0.8 Hz, 1H), 3.52 (s, 3H); ^{13}C NMR (101 MHz, CDCl_3) δ 135.7, 131.3, 128.3, 127.1, 126.9, 123.0, 112.5, 112.4, 96.7, 69.8, 57.6, 54.0; IR (Neat Film, NaCl) 3090, 2963, 2904, 2833, 2245, 2079, 1639, 1433k 1365, 1270, 1238, 1216, 1162, 1108, 1029, 922, 856, 839, 704 cm^{-1} ; HRMS (ESI+) m/z calc'd for $\text{C}_{12}\text{H}_{13}\text{N}_2\text{O}_2\text{S}$ $[\text{M}+\text{H}]^+$: 249.0698, found 249.0703; SFC conditions: 3% IPA, 3.5 mL/min, Chiralpak IC-3 column, λ = 210 nm, t_R (min): major = 5.289, minor = 4.010.

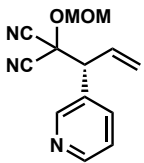
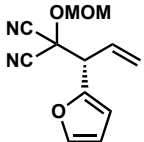
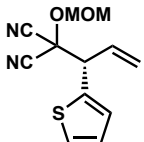
2.5.2.7 Determination of Enantiomeric Excess

Please note racemic products were synthesized using racemic **L2**.

Table 2.4 Determination of enantiomeric excess

Entry	Product	Assay Conditions	Retention time of major isomer (min)	Retention time of minor isomer (min)	%ee
1		HPLC Chiralpak IC 1% IPA isocratic, 1 mL/min	12.831	17.466	95
2		HPLC Chiralpak IC 1% IPA isocratic, 1 mL/min	15.852	11.623	96
3		HPLC Chiralpak IC 1% IPA isocratic, 1 mL/min	10.681	8.223	96

Entry	Product	Assay Conditions	Retention time of major isomer (min)	Retention time of minor isomer (min)	%ee
4		HPLC Chiralpak IC 1% IPA isocratic, 1 mL/min	11.712	8.971	96
5		SFC Chiralpak IC-3 3% IPA isocratic, 3.5 mL/min	6.831	5.267	95
6		SFC Chiralpak IC-3 3% IPA isocratic, 3.5 mL/min	3.846	3.428	92
7		HPLC Chiralpak IC 1% IPA isocratic, 1 mL/min	24.142	19.686	96
8		HPLC Chiralpak AD 7% IPA isocratic, 1 mL/min	17.062	12.809	98
9		HPLC Chiralpak IC 1% IPA isocratic, 1 mL/min	15.134	10.197	92
10		HPLC Chiralpak IC 1% IPA isocratic, 1 mL/min	16.719	9.761	89

Entry	Product	Assay Conditions	Retention time of major isomer (min)	Retention time of minor isomer (min)	%ee
11		HPLC Chiralpak IC 20% IPA isocratic, 1 mL/min	13.161	23.457	90
12		HPLC Chiralpak IC 1% IPA isocratic, 1 mL/min	13.297	10.761	96
13		SFC Chiralpak IC-3 3% IPA isocratic, 3.5 mL/min	5.289	4.010	93

2.6 REFERENCES AND NOTES

- (1) Janssen, J. P.; Helmchen, G. *Tetrahedron Lett.* **1997**, 38, 8025–8026.
- (2) For select reviews of asymmetric iridium-catalyzed allylic alkylation, see: (a) Helmchen, G.; Dahnz, A.; Dübon, P.; Schelwies, M.; Weihofen, R. *Chem. Commun.* **2007**, 675–691; (b) Hartwig, J. F.; Pouy, M. J. *Top. Organomet. Chem.* **2011**, 34, 169–208; (c) Liu, W.-B.; Xia, J. B.; You, S.-L. *Top. Organomet. Chem.* **2012**, 38, 155–208; (d) Hethcox, J. C.; Shockley, S. E.; Stoltz, B. M. *ACS Catal.* **2016**, 6, 6207–6213.
- (3) Nucleophilic additions of methylene imines to iridium π -allyl complexes have been accomplished via an unpoled strategy. However, the reactions deliver products

resembling those of standard iridium-catalyzed allylic alkylation of enolates, see:

Su, Y.-L.; Li, Y.-H.; Chen, Y.-G.; Han, Z.-Y. *Chem. Commun.* **2017**, 53, 1985–1988.

- (4) Förster, S.; Tverskoy, O.; Helmchen, G. *Synlett* **2008**, 18, 2803–2806.
- (5) Breitler, S.; Carreira, E. M. *J. Am. Chem. Soc.* **2015**, 137, 5296–5299.
- (6) (a) Liu, W.-B.; Reeves, C. M.; Virgil, S. C.; Stoltz, B. M. *J. Am. Chem. Soc.* **2013**, 135, 10626–10629; (b) Liu, W.-B.; Reeves, C. M.; Stoltz, B. M. *J. Am. Chem. Soc.* **2013**, 135, 17298–17301; (c) Liu, W.-B.; Okamoto, N.; Alexy, E. J.; Hong, A. J.; Tran, K.; Stoltz, B. M. *J. Am. Chem. Soc.* **2016**, 138, 5234–5237; (d) Hethcox, J. C.; Shockley, S. E.; Stoltz, B. M. *Angew. Chem. Int. Ed.* **2016**, 55, 16092–16095.
- (7) (a) Nemoto, H.; Kubota, Y.; Yamamoto, Y. *J. Org. Chem.* **1990**, 55, 4515–4516; (b) Nemoto, H.; Li, X.; Ma, R.; Suzuki, I.; Shibuya, M. *Tetrahedron Lett.* **2003**, 44, 73–75; (c) Nemoto, H.; Kawamura, T.; Miyoshi, N. *J. Am. Chem. Soc.* **2005**, 127, 14546–14547; (d) Nemoto, H.; Ma, R.; Kawamura, T.; Kamiya, M.; Shibuya, M. *J. Org. Chem.* **2006**, 71, 6038–6043; (e) Nemoto, H.; Kawamura, T.; Kitasaki, K.; Yatsuzuka, K.; Kamiya, M.; Yoshioka, Y. *Synthesis* **2009**, 1694–1702.
- (8) (a) Kociölek, K.; Leplawy, M. T. *Synthesis* **1977**, 778–780; (b) Kubota, Y.; Nemoto, H.; Yamamoto, Y. *J. Org. Chem.* **1991**, 56, 7195–7196; (c) Nemoto, H.; Ma, R.; Ibaragi, T.; Suzuki, I.; Shibuya, M. *Tetrahedron* **2000**, 56, 1463–1468; (d) Yamatsugu, K.; Kanai, M.; Shibasaki, M. *Tetrahedron* **2009**, 65, 6017–6024; (e) Yang, K. S.; Nibbs, A. E.; Türkmen, Y. E.; Rawal, V. H. *J. Am. Chem. Soc.* **2013**, 135, 16050–16053; (f) Yang, K. S.; Rawal, V. H. *J. Am. Chem. Soc.* **2014**, 136,

- 16148–16151; (g) Kagawa, N.; Nibbs, A. E.; Rawal, V. H. *Org. Lett.* **2016**, *18*, 2363–2366.
- (9) (a) Murphy, K. E.; Hoveyda, A. H. *J. Am. Chem. Soc.* **2003**, *125*, 4690–4691; (b) Trost, B. M.; Xu, J. *J. Am. Chem. Soc.* **2005**, *127*, 17180–17181; (c) Yan, S.-S.; Liang, C.-G.; Zhang, Y.; Hong, W.; Cao, B.-X.; Dai, L.-X.; Hou, X.-L. *Angew. Chem. Int. Ed.* **2005**, *44*, 6544–6546; (d) Zheng, W.-H.; Zheng, B.-H.; Zhang, Y.; Hou, X.-L. *J. Am. Chem. Soc.* **2007**, *129*, 7718–7719; (e) Lundin, P. M.; Esquivias, J.; Fu, G. C. *Angew. Chem. Int. Ed.* **2009**, *48*, 154–156; (f) Lou, S.; Fu, G. C. *J. Am. Chem. Soc.* **2010**, *132*, 1264–1266; (g) Cherney, A. H.; Kadunce, N. T.; Reisman, S. E. *J. Am. Chem. Soc.* **2013**, *135*, 7442–7445; (h) Poremba, K. E.; Lee, V. A.; Sculimbrene, B. R. *Tetrahedron* **2014**, *70*, 5463–5467; (i) Liu, Y.; Virgil, S. C.; Grubbs, R. H.; Stoltz, B. M. *Angew. Chem. Int. Ed.* **2015**, *54*, 11800–11803.
- (10) (a) Liu, W.-B.; He, H.; Dai, L.-X.; You, S.-L. *Synthesis* **2009**, 2076–2082; (b) Liu, W.-B.; Zheng, C.; Zhuo, C.-X.; Dai, L.-X.; You, S.-L. *J. Am. Chem. Soc.* **2012**, *134*, 4812–4821.
- (11) (a) Nemoto, H.; Li, X.; Ma, R.; Suzuki, I.; Shibuya, M. *Tetrahedron Lett.* **2003**, *44*, 73–75; (b) Yang, K. S.; Nibbs, A. E.; Türkmen, Y. E.; Rawal, V. H. *J. Am. Chem. Soc.* **2013**, *135*, 16050–16053.
- (12) Pouy, M. J.; Leitner, A.; Weix, D. J.; Ueno, S.; Hartwig, J. F. *Org. Lett.* **2007**, *9*, 3949–3952.
- (13) Trost, B. M.; Miller, J. R.; Hoffman, C. M. Jr. *J. Am. Chem. Soc.* **2011**, *133*, 8165–8167.

- (14) Ohmura, T.; Hartwig, J. F. *J. Am. Chem. Soc.* **2002**, *124*, 15164–15165.
- (15) Welter, C.; Moreno, R. M.; Streiff, S.; Helmchen, G. *Org. Biomol. Chem.* **2005**, *3*, 3266–3268.
- (16) Leitner, A.; Shu, C.; Hartwig, J. F. *Org. Lett.* **2005**, *7*, 1093–1096.
- (17) Cao, W.; Liu, X.; Peng, R.; He, P.; Lin, L.; Feng, X. *Chem. Commun.* **2013**, *49*, 3470–3472.
- (18) Lantaño, B.; Aguirre, J. M.; Ugliarolo, E. A.; Torviso, R.; Pomilio, N.; Moltrasio, G. Y. *Tetrahedron*, **2012**, *68*, 913–921.
- (19) Nguyen, B. H.; Perkins, R. J.; Smith, J. A.; Moeller, K. D. *J. Org. Chem.* **2015**, *80*, 11953–11962.
- (20) Li, W.; Wang, J.; Hu, X.; Shen, K.; Wang, W.; Chu, Y.; Lin, L.; Liu, X.; Feng, X. *J. Am. Chem. Soc.* **2010**, *132*, 8532–8533.

APPENDIX 3

Spectra Relevant to Chapter 2:

*Enantioselective Iridium-Catalyzed Allylic Alkylation Reactions of
Masked Acyl Cyanide Equivalents*

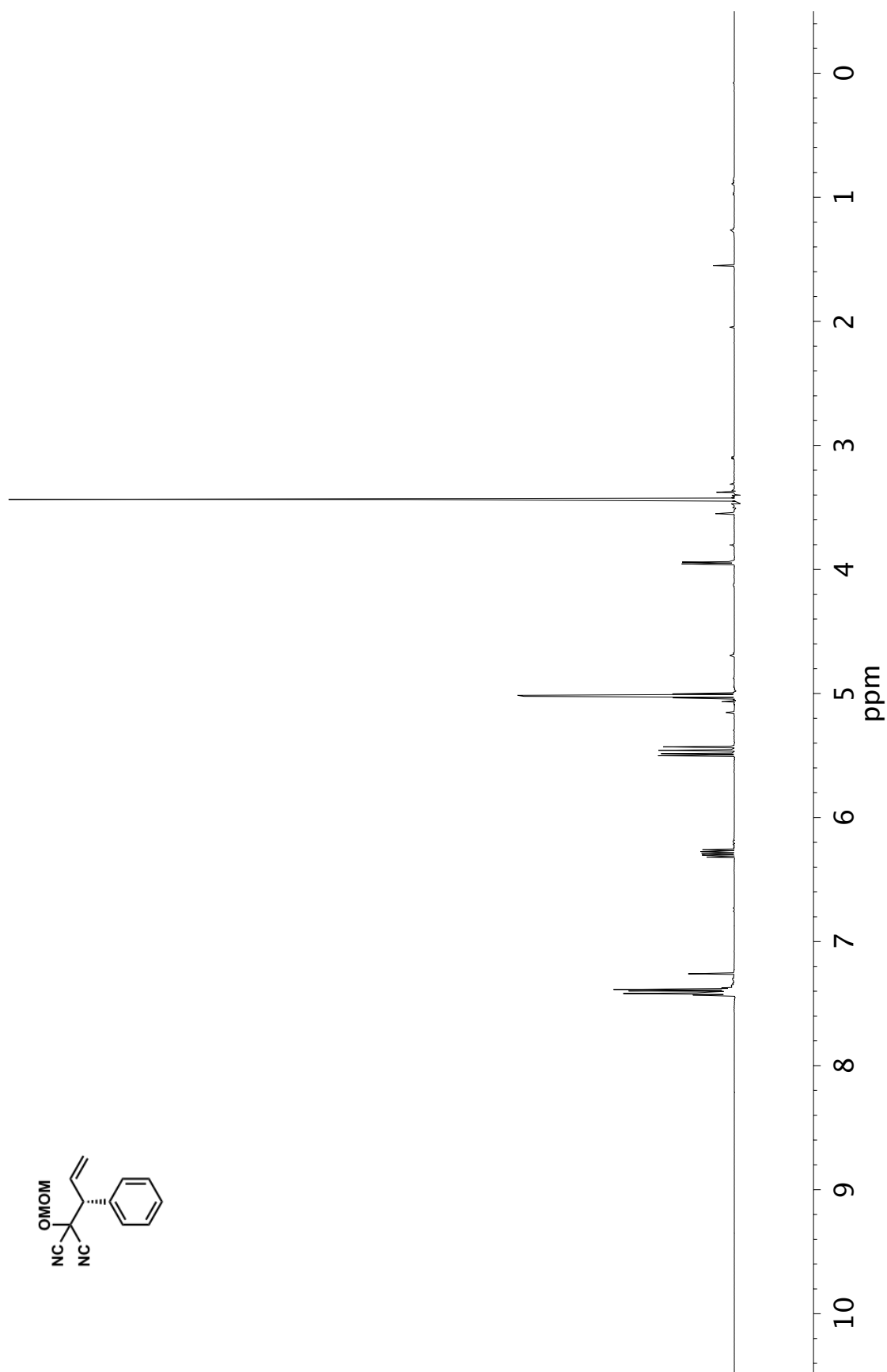


Figure A3.1 ¹H NMR (400 MHz, CDCl₃) of compound **69c**

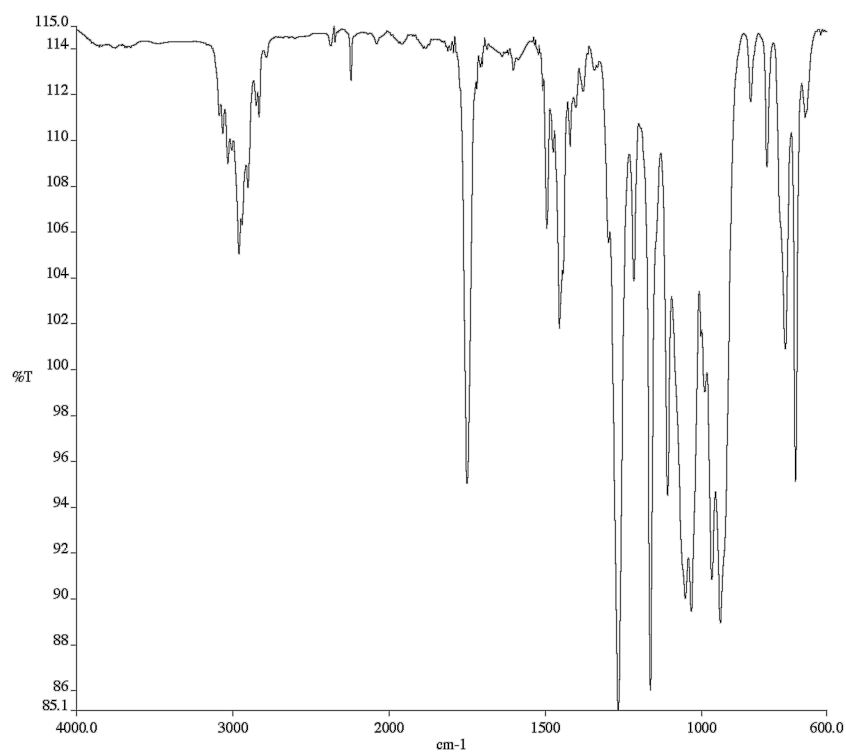


Figure A3.2 Infrared spectrum (Thin Film, NaCl) of compound **69c**

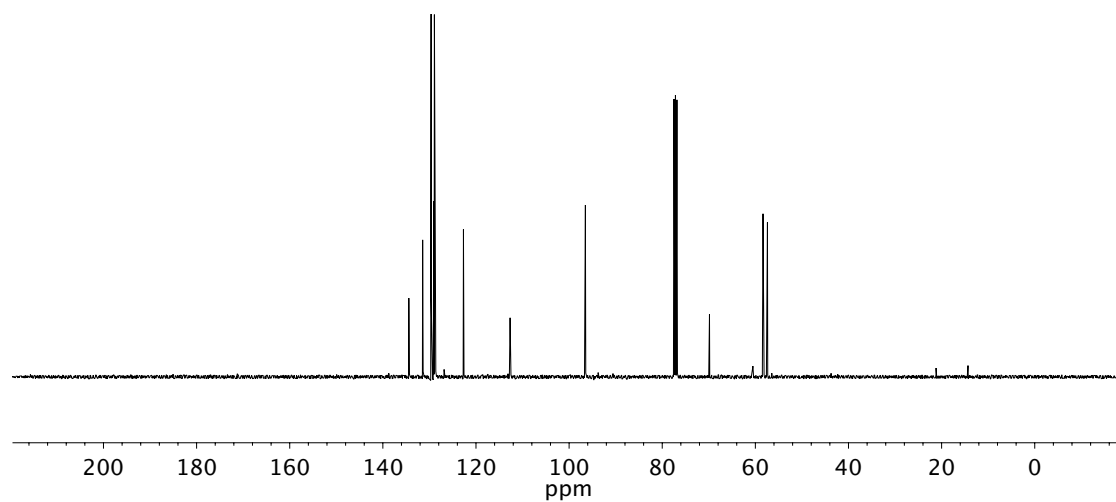


Figure A3.3 ¹³C NMR (101 MHz, CDCl₃) of compound **69c**

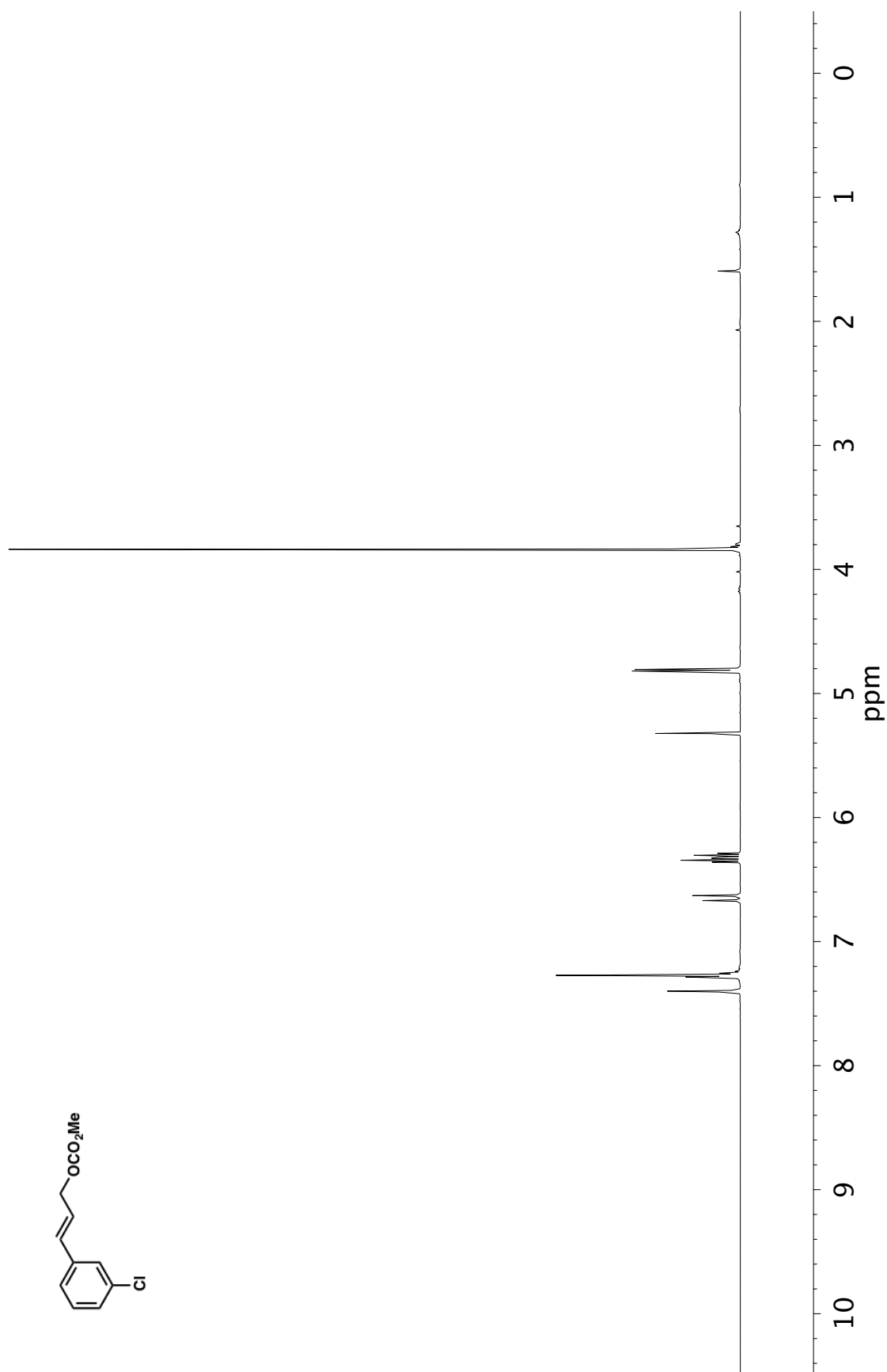


Figure A3.4 ¹H NMR (400 MHz, CDCl₃) of compound **70e**

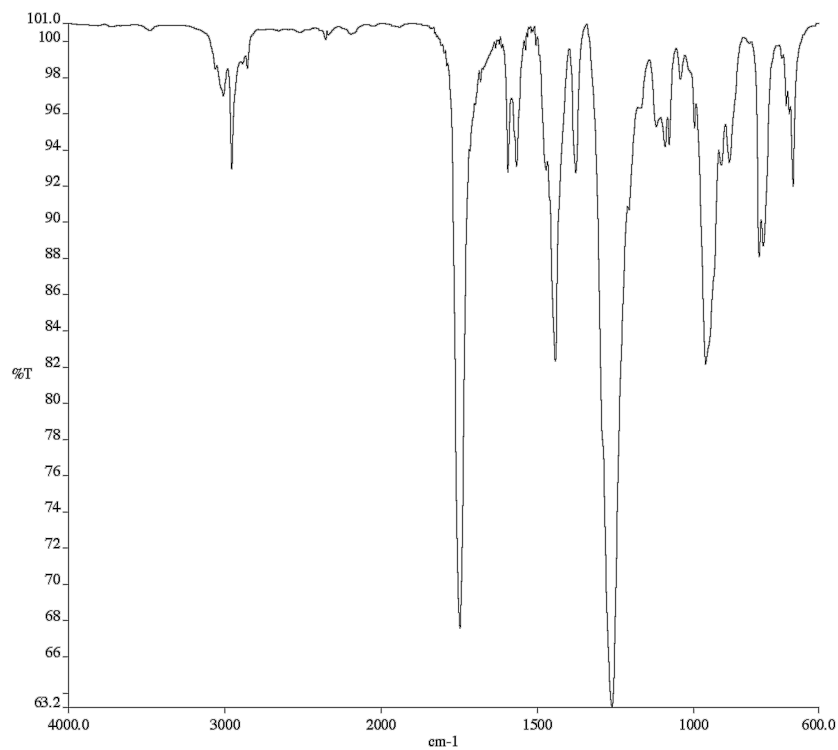


Figure A3.5 Infrared spectrum (Thin Film, NaCl) of compound **70e**

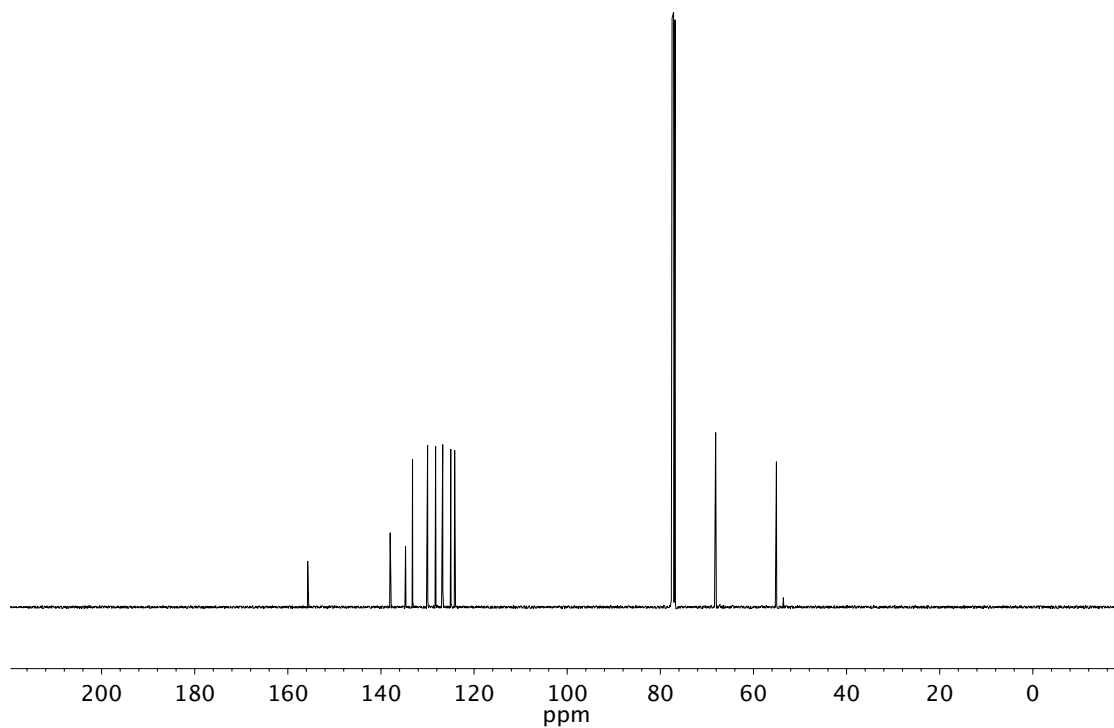


Figure A3.6 ¹³C NMR (101 MHz, CDCl₃) of compound **70e**

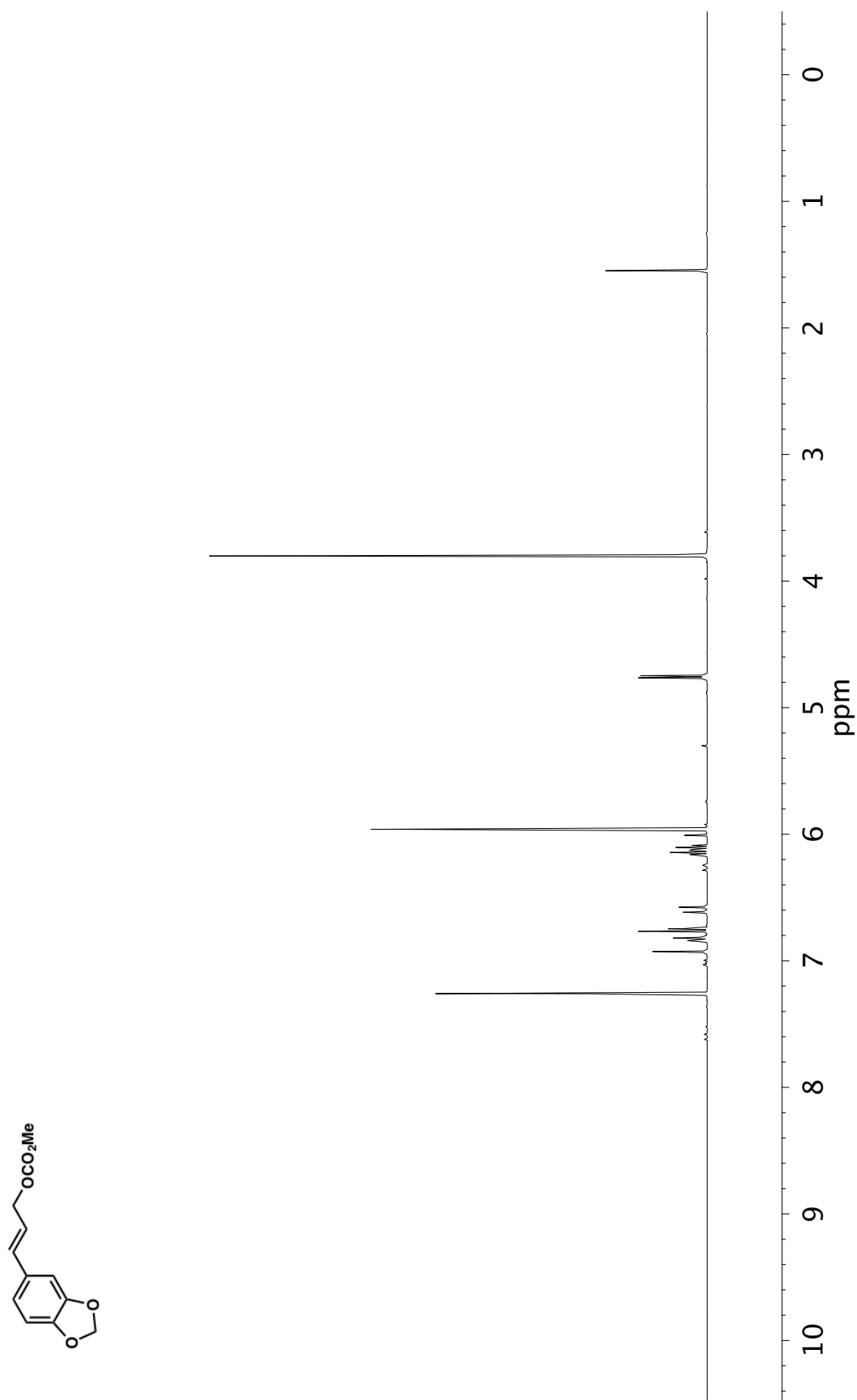


Figure A3.7 ¹H NMR (400 MHz, CDCl₃) of compound 70f

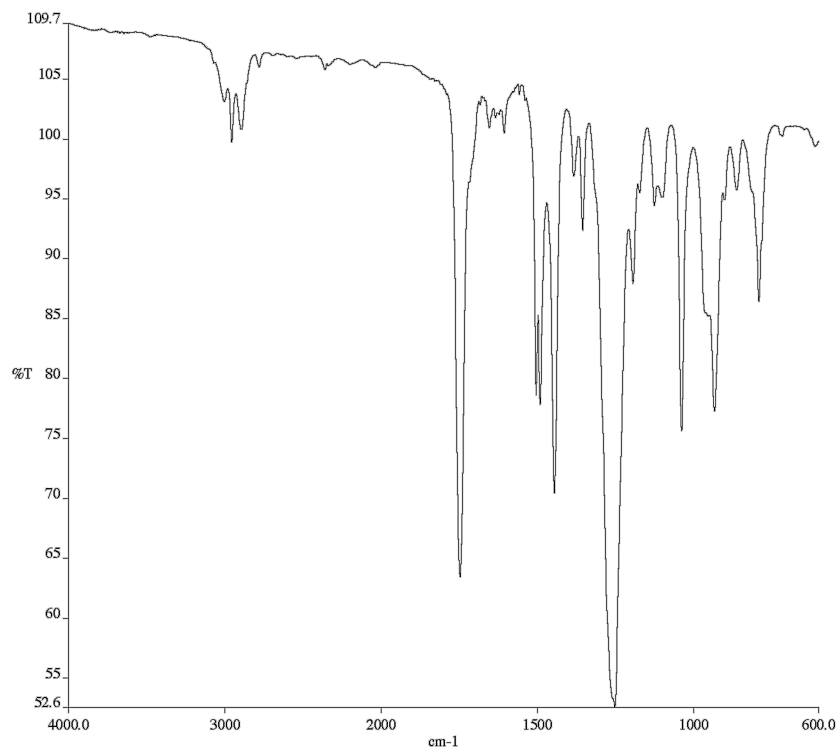


Figure A3.8 Infrared spectrum (Thin Film, NaCl) of compound **70f**

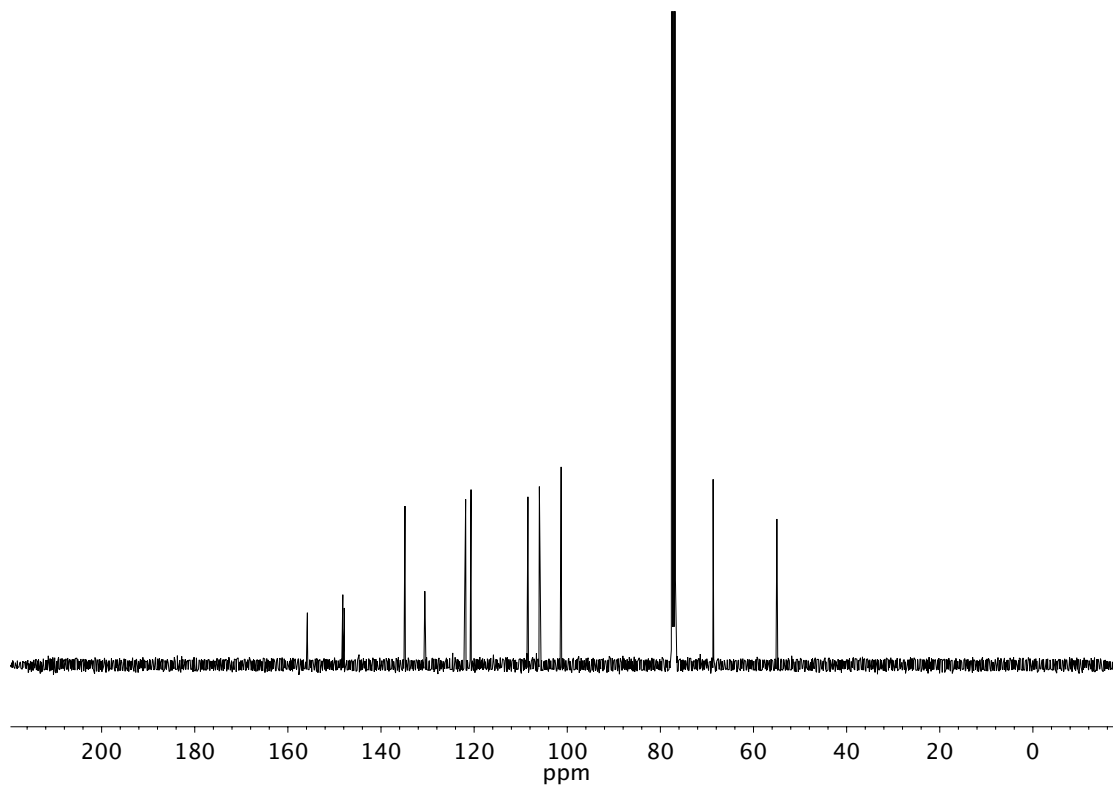


Figure A3.9 ¹³C NMR (101 MHz, CDCl₃) of compound **70f**

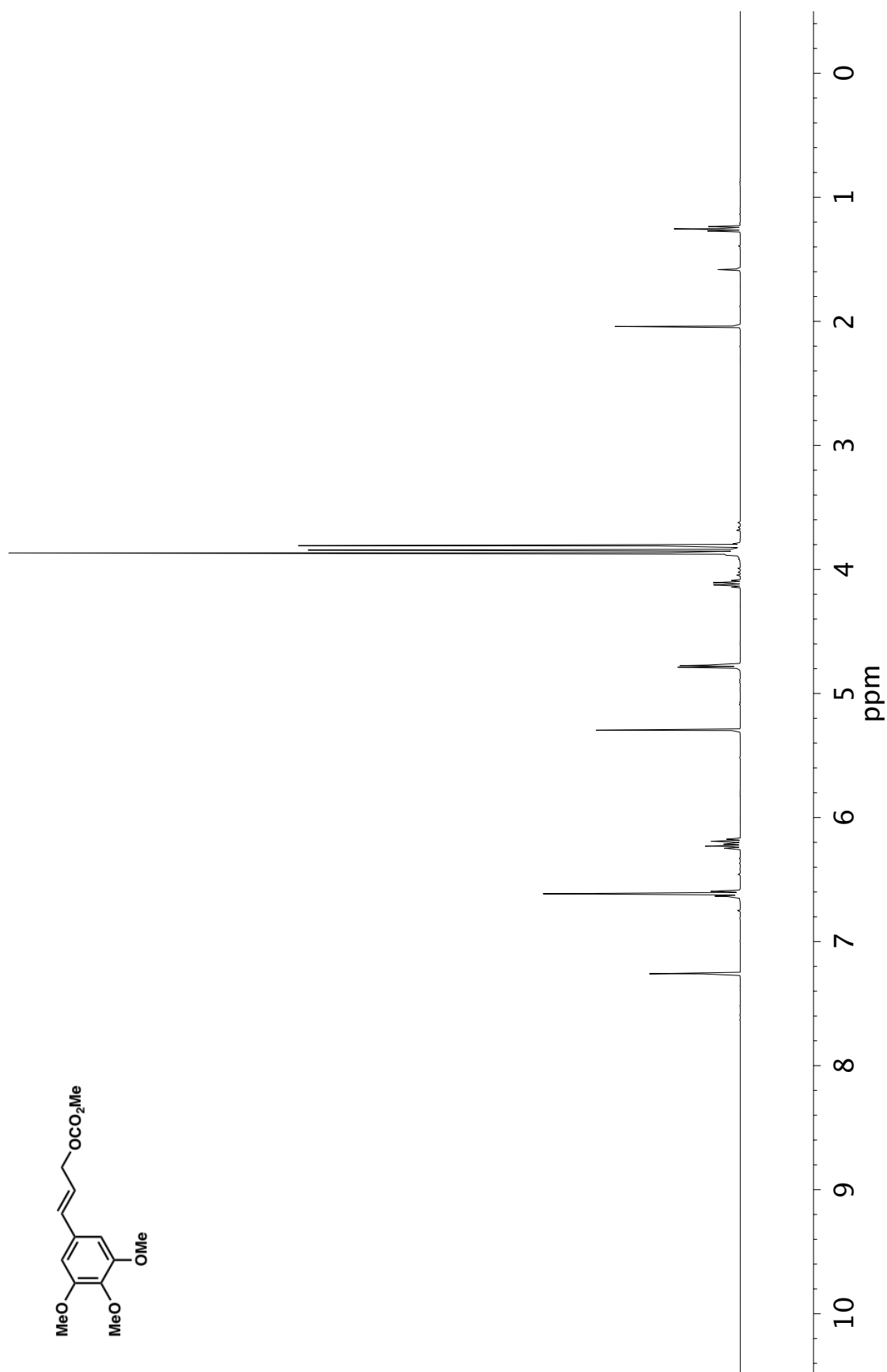


Figure A3.10 ¹H NMR (400 MHz, CDCl₃) of compound 70g

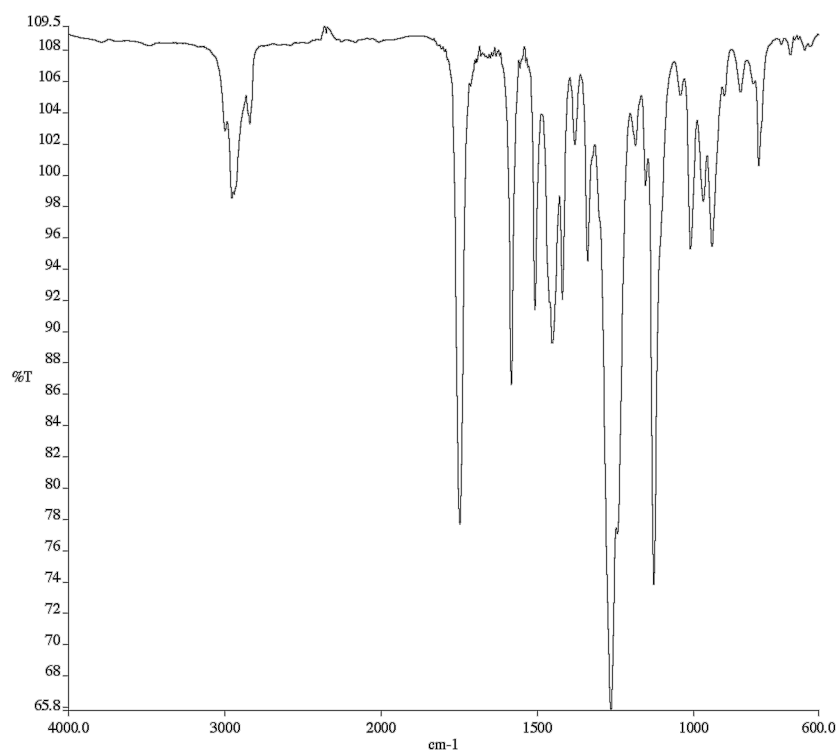


Figure A3.11 Infrared spectrum (Thin Film, NaCl) of compound **70g**

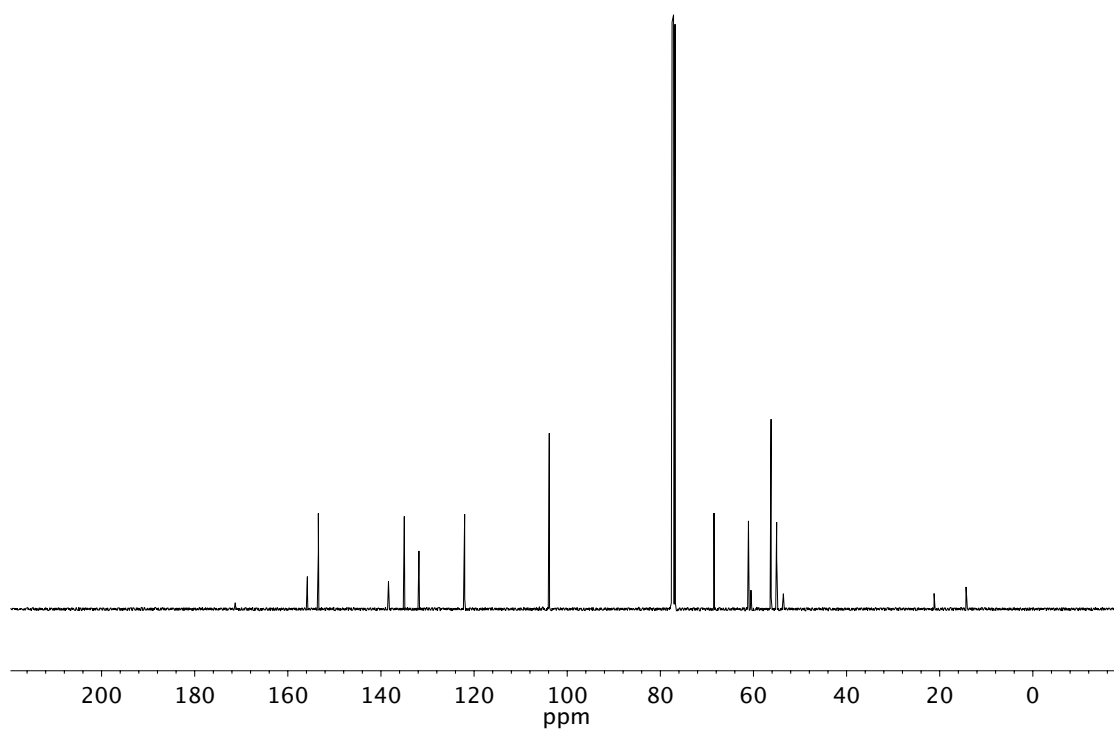


Figure A3.12 ¹³C NMR (101 MHz, CDCl₃) of compound **70g**

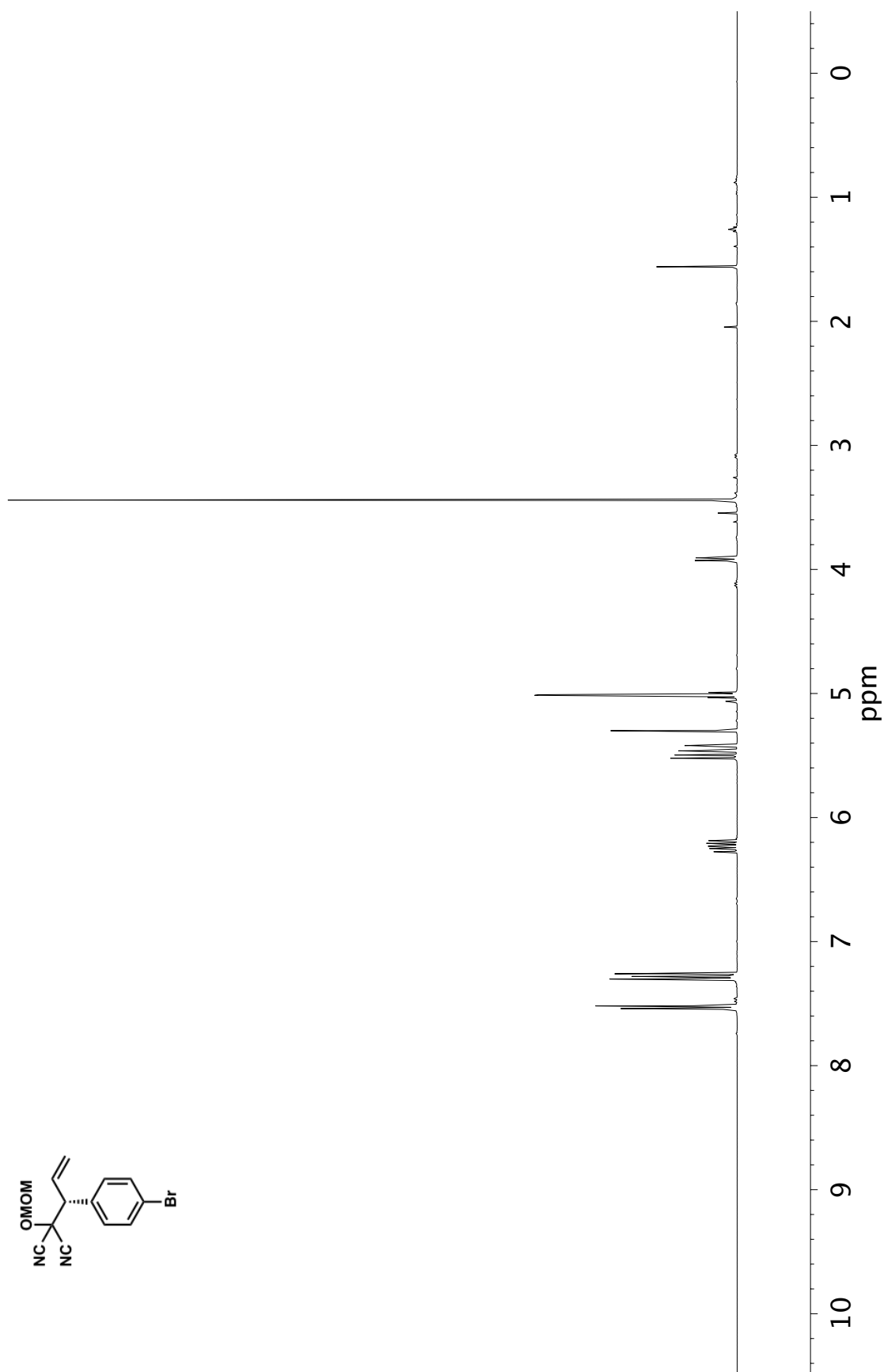


Figure A3.13 ^1H NMR (400 MHz, CDCl_3) of compound **71a**

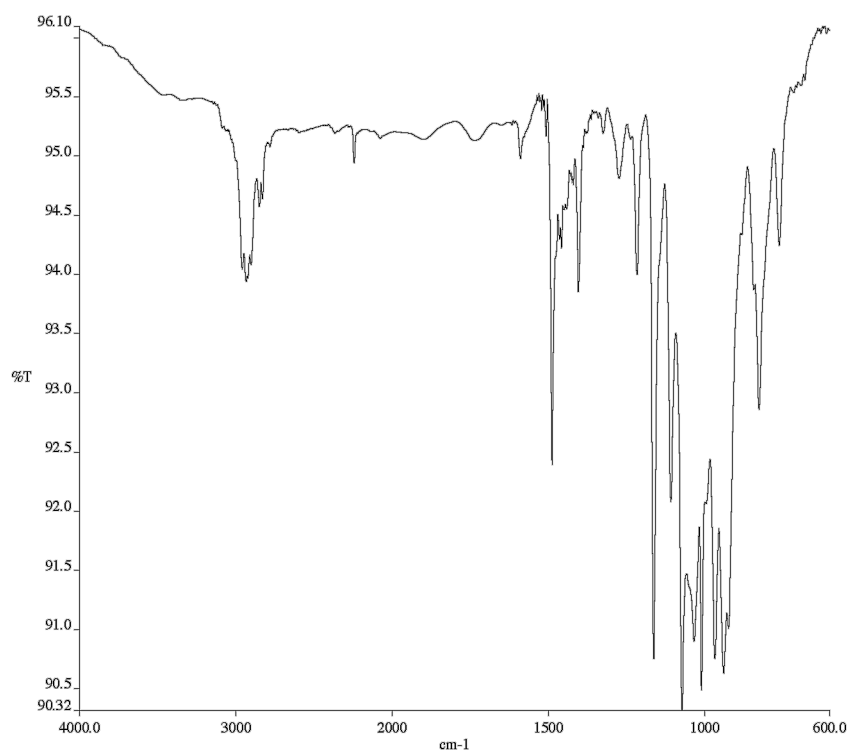


Figure A3.14 Infrared spectrum (Thin Film, NaCl) of compound **71a**

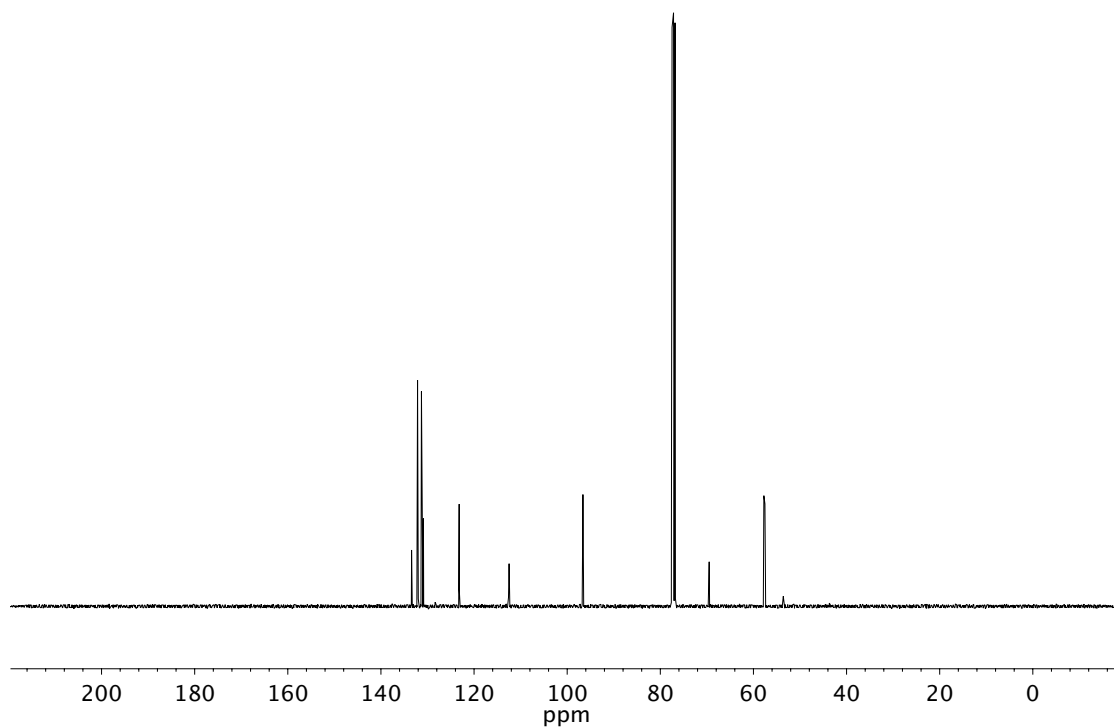


Figure A3.15 ¹³C NMR (101 MHz, CDCl₃) of compound **71a**

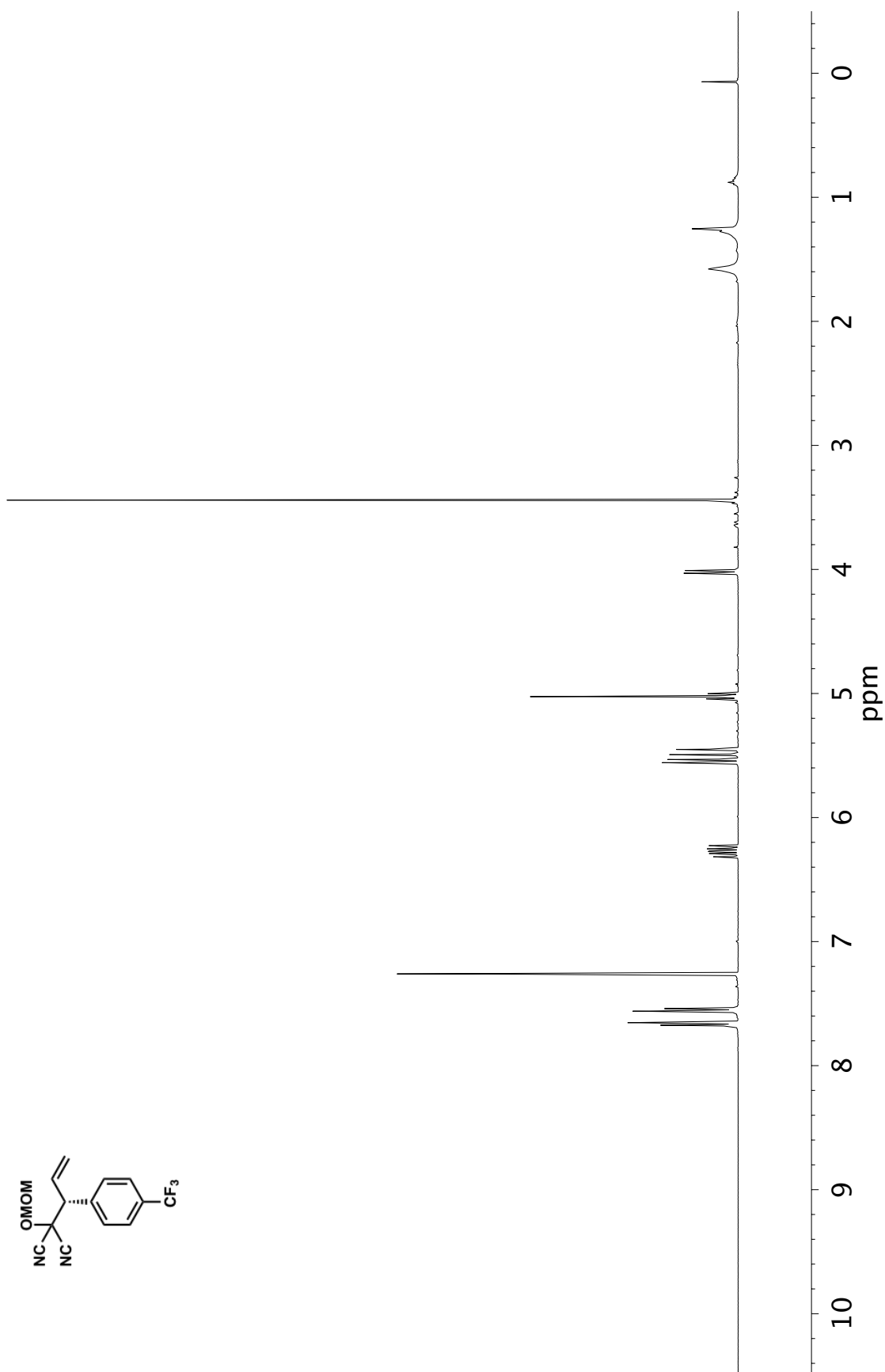


Figure A3.16 ^1H NMR (400 MHz, CDCl_3) of compound **71b**

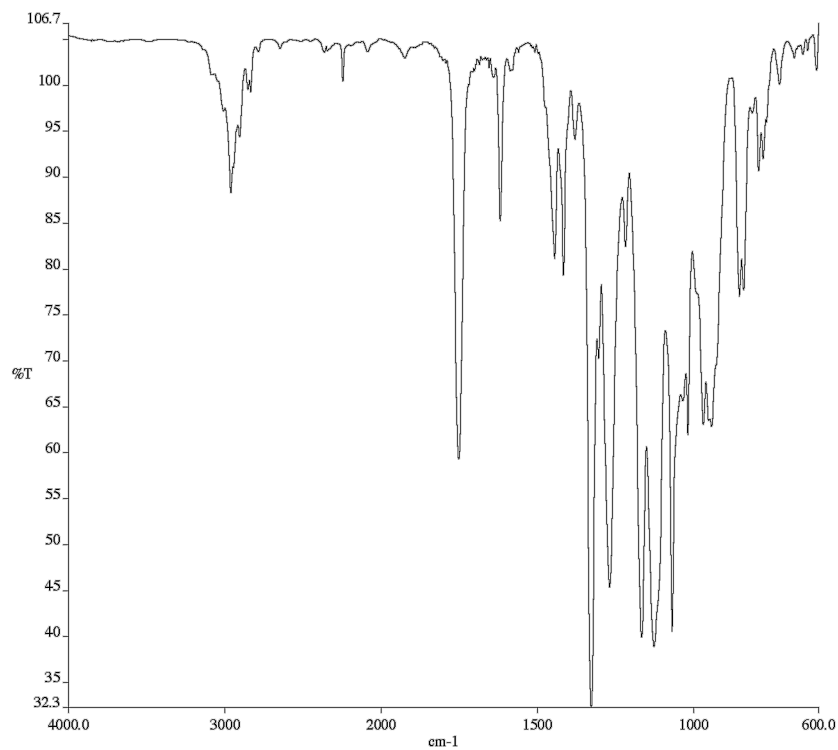


Figure A3.17 Infrared spectrum (Thin Film, NaCl) of compound **71b**

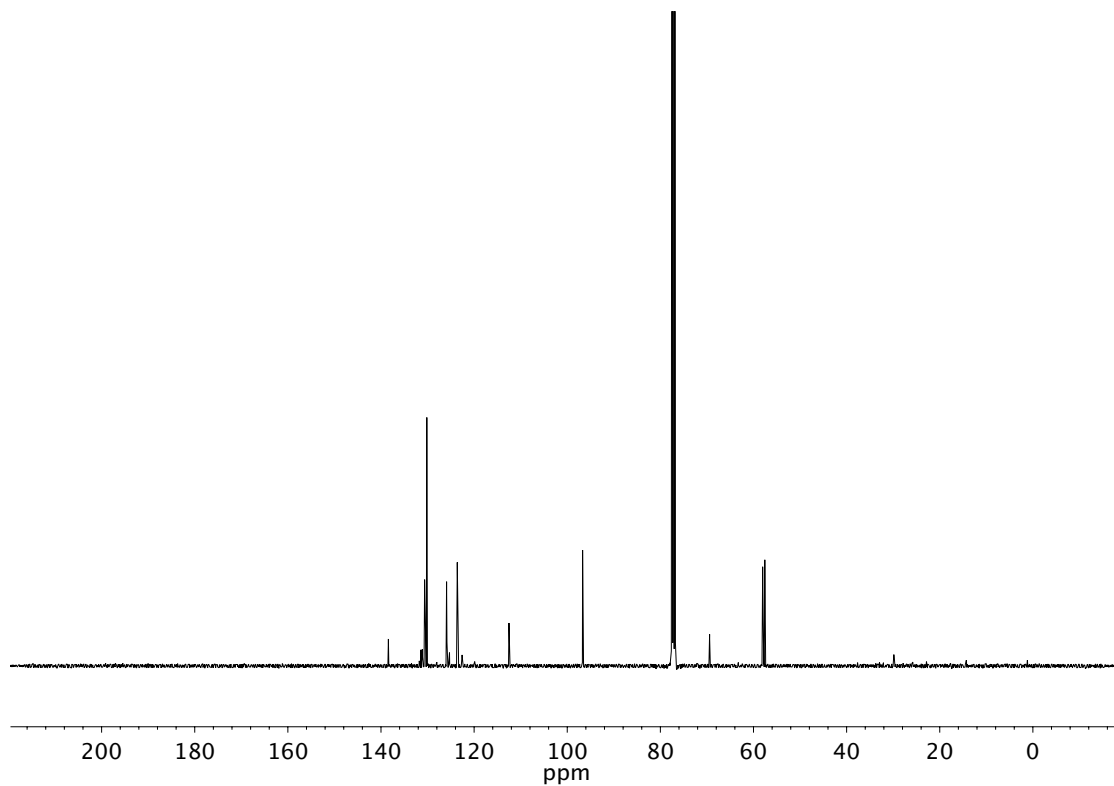


Figure A3.18 ¹³C NMR (101 MHz, CDCl₃) of compound **71b**

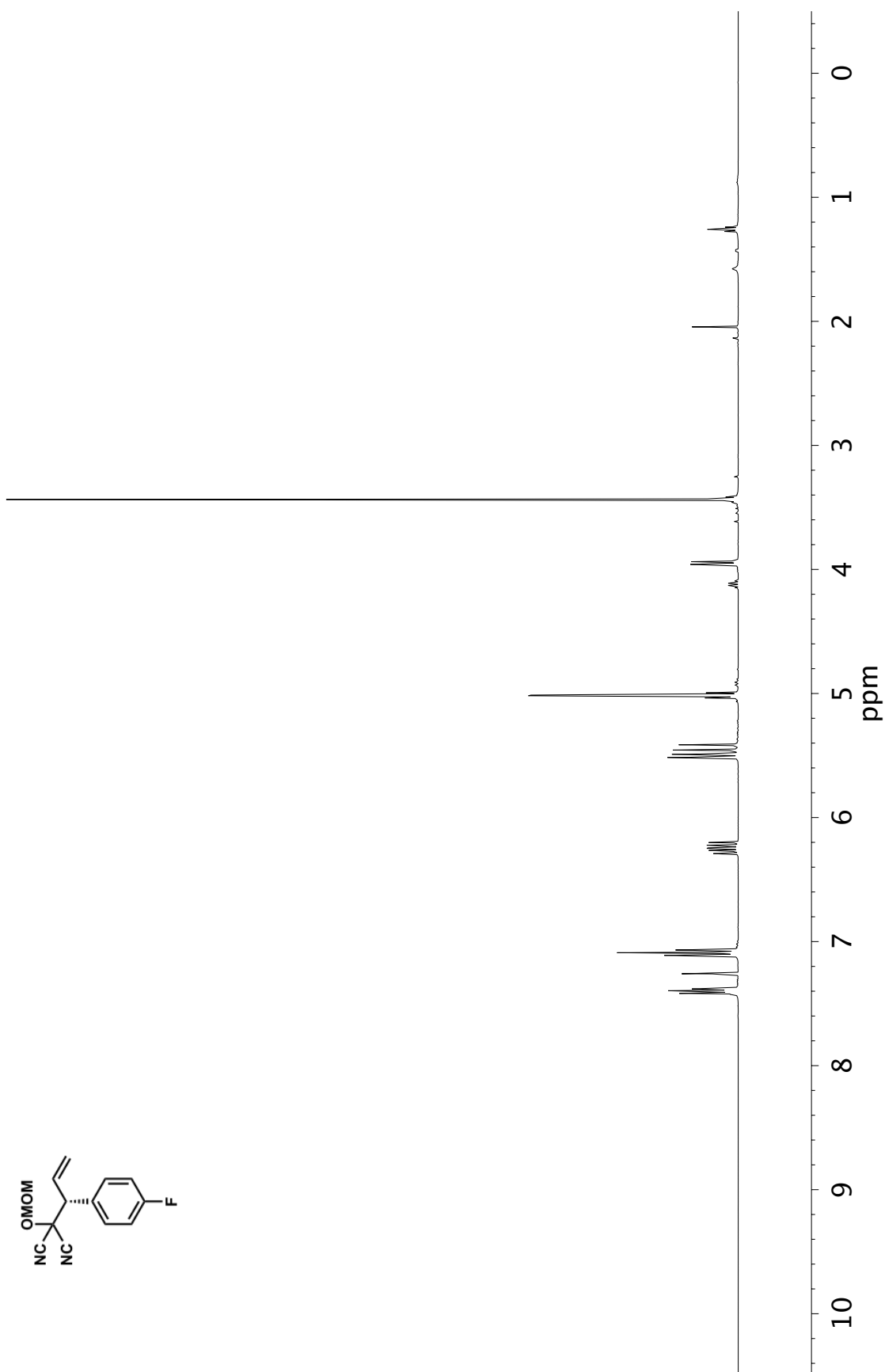


Figure A3.19 ^1H NMR (400 MHz, CDCl_3) of compound **71c**

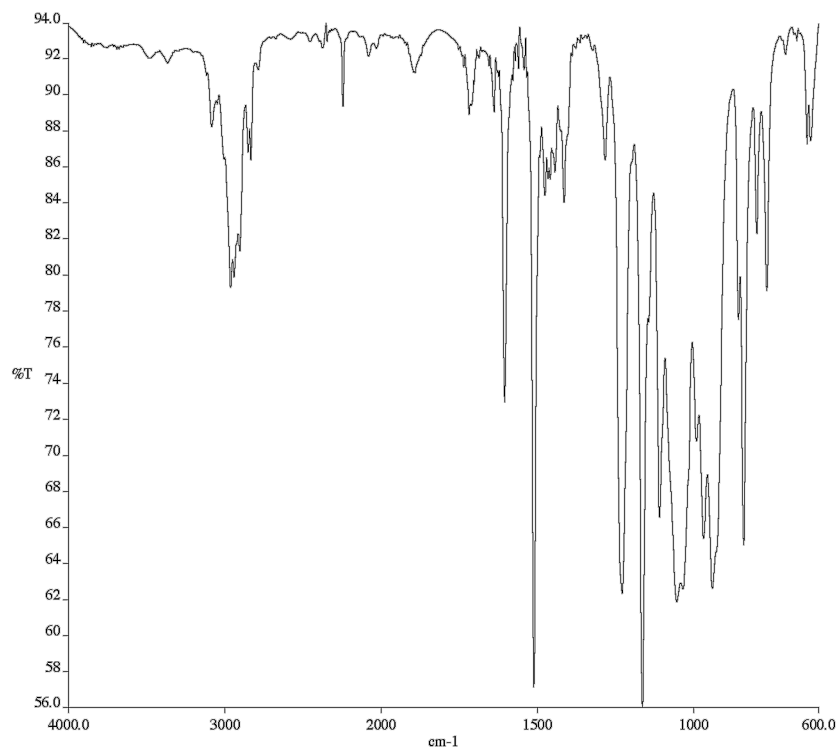


Figure A3.20 Infrared spectrum (Thin Film, NaCl) of compound **71c**

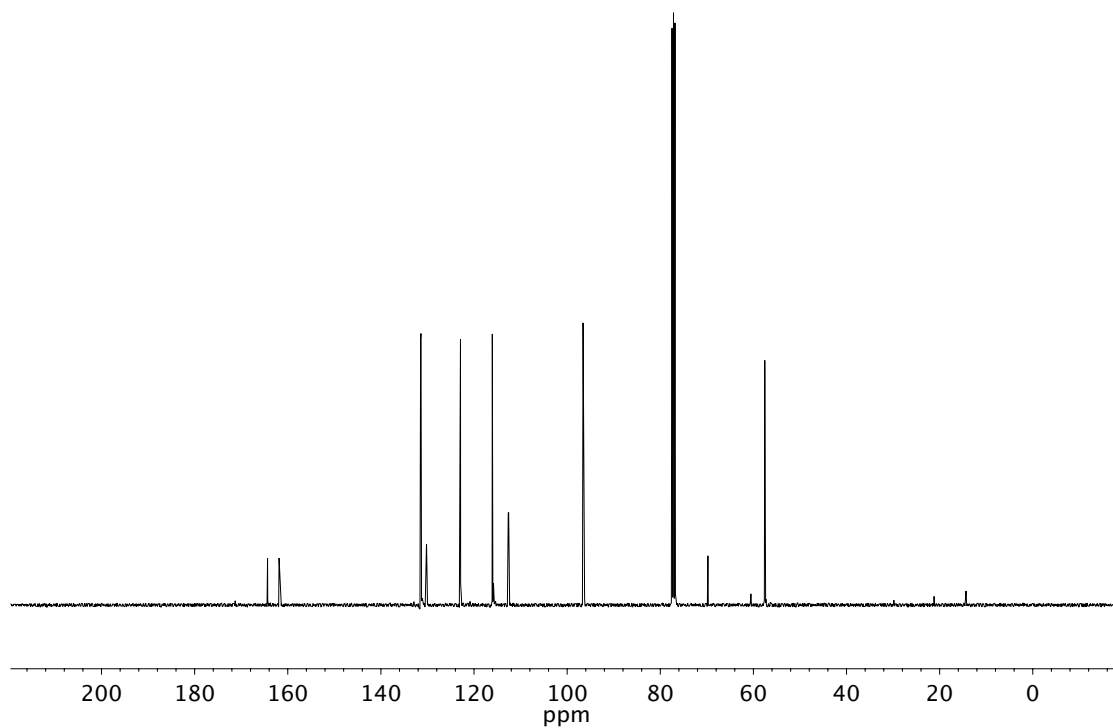


Figure A3.21 ^{13}C NMR (101 MHz, CDCl_3) of compound **71c**

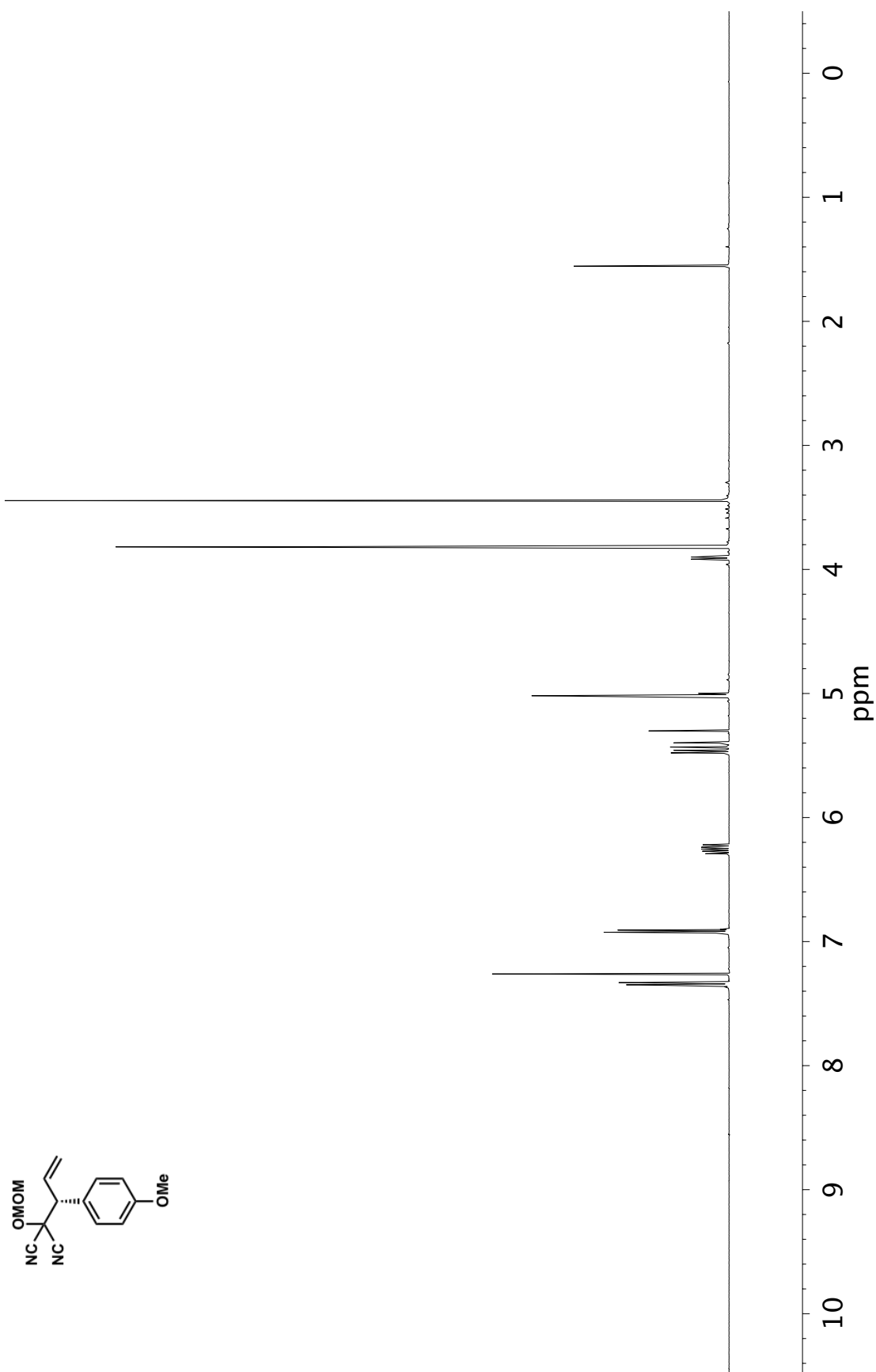


Figure A3.22 ¹H NMR (400 MHz, CDCl₃) of compound **71d**

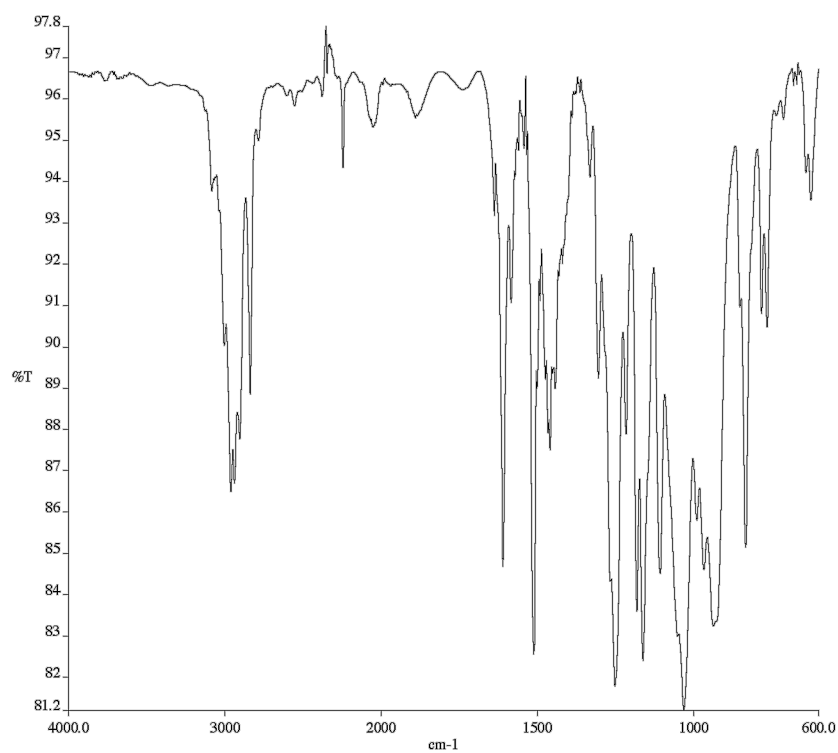


Figure A3.23 Infrared spectrum (Thin Film, NaCl) of compound **71d**

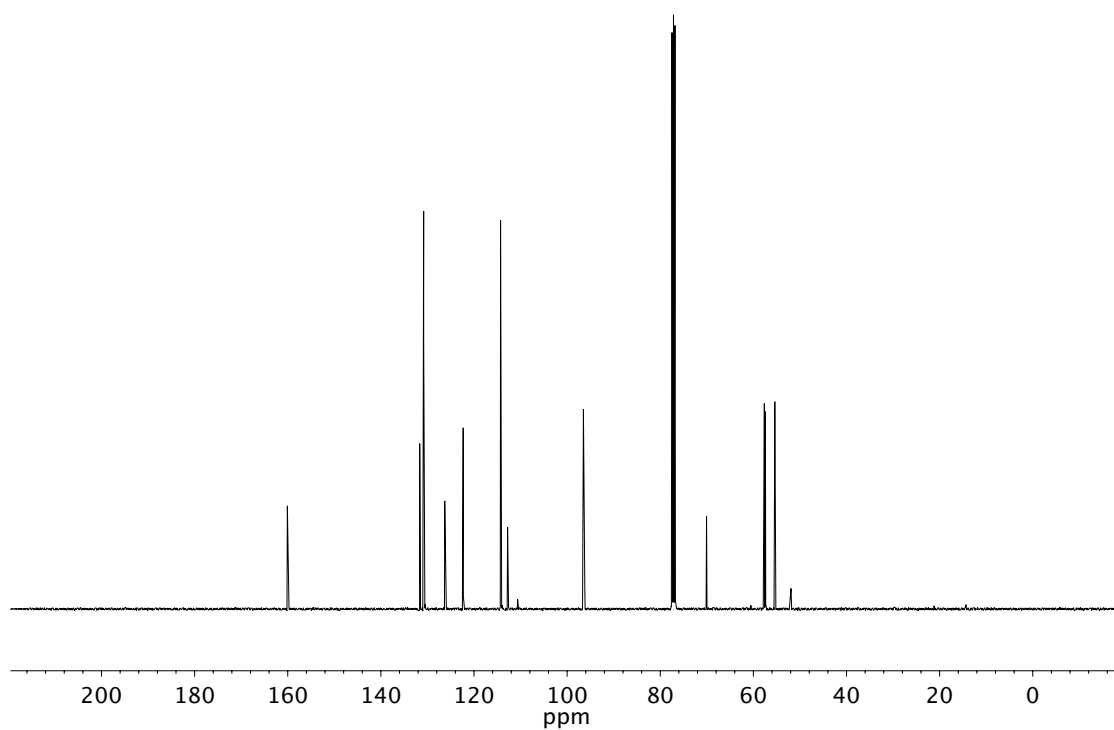


Figure A3.24 ¹³C NMR (101 MHz, CDCl₃) of compound **71d**

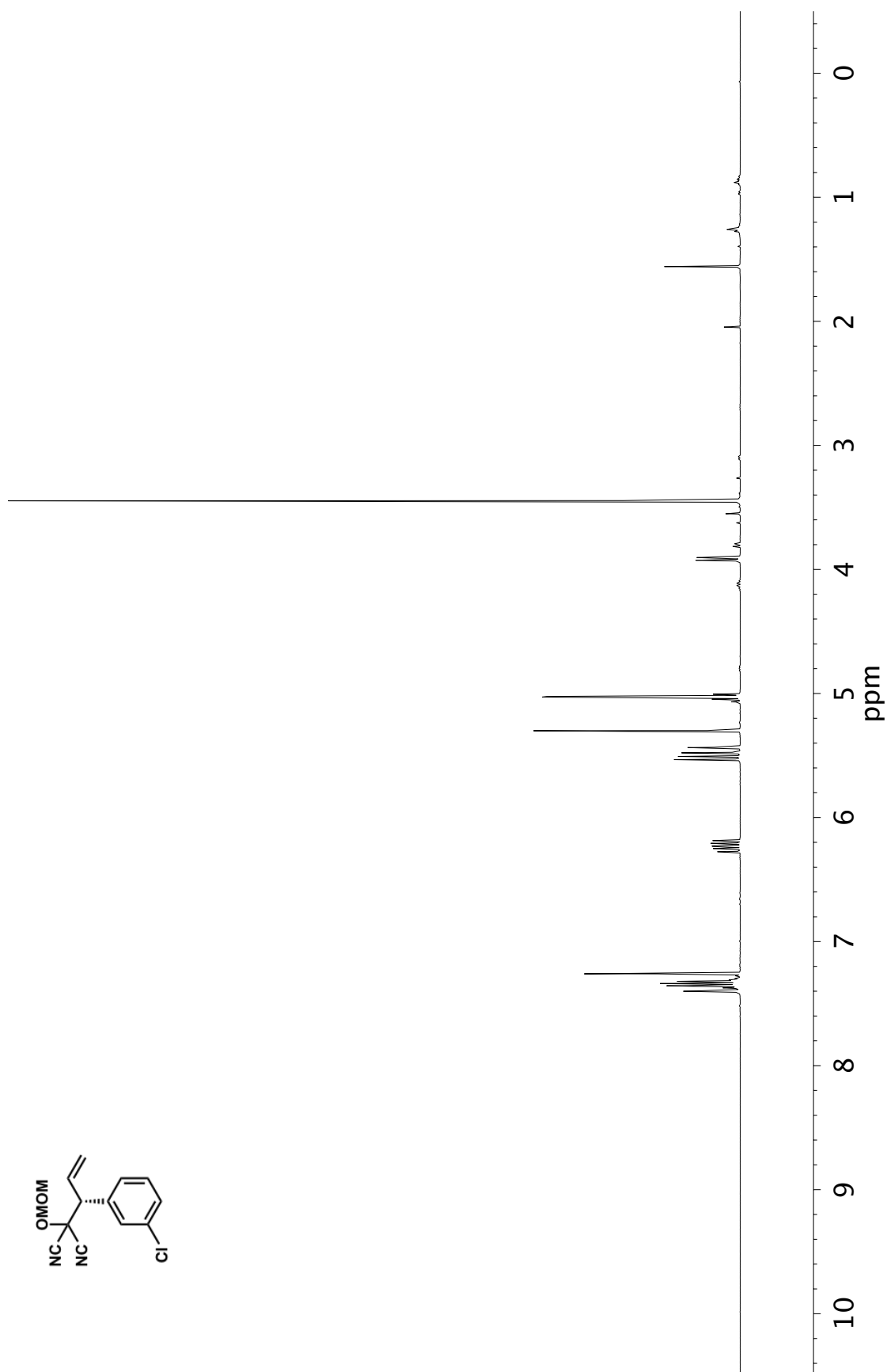


Figure A3.25 ¹H NMR (400 MHz, CDCl₃) of compound **71e**

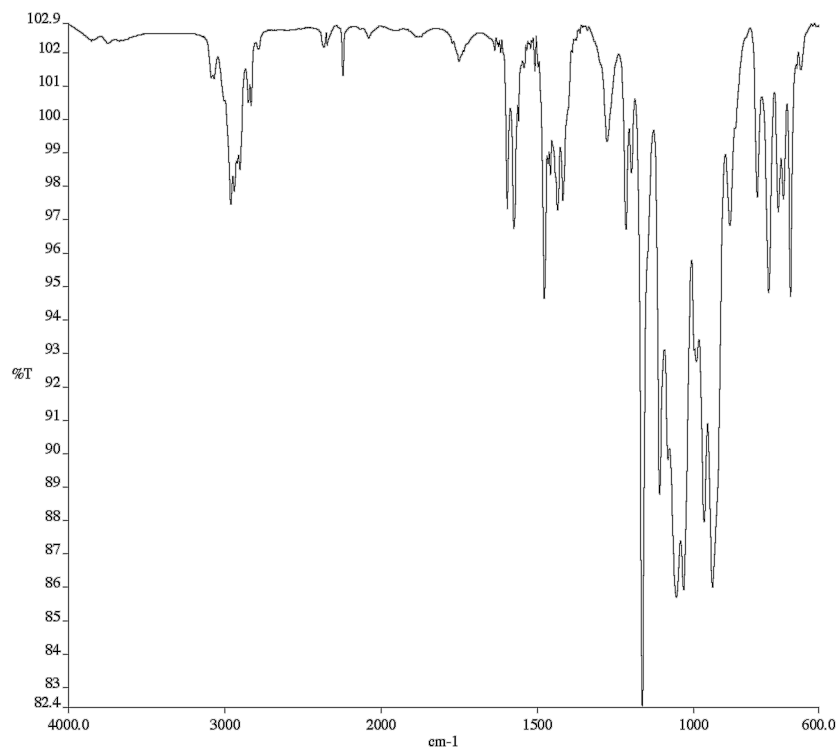


Figure A3.26 Infrared spectrum (Thin Film, NaCl) of compound **71e**

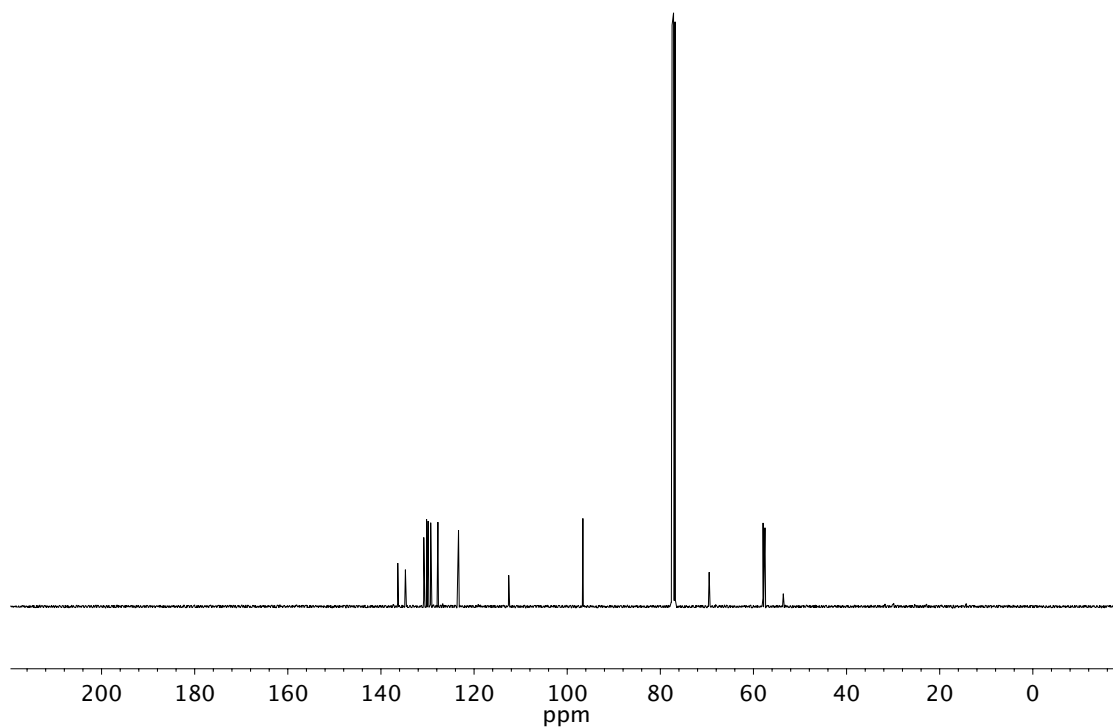


Figure A3.27 ¹³C NMR (101 MHz, CDCl₃) of compound **71e**

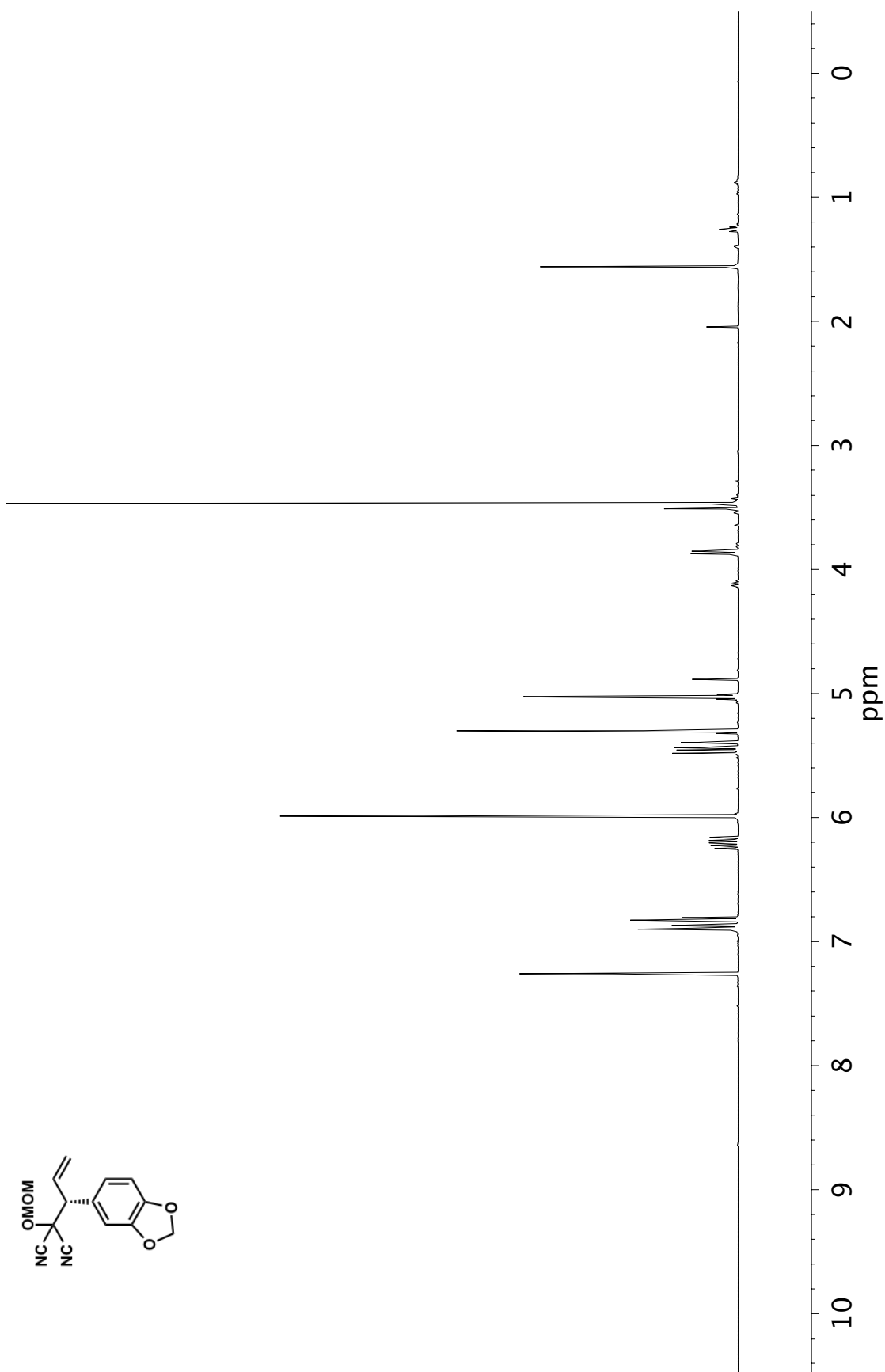


Figure A3.28 ¹H NMR (400 MHz, CDCl₃) of compound **71f**

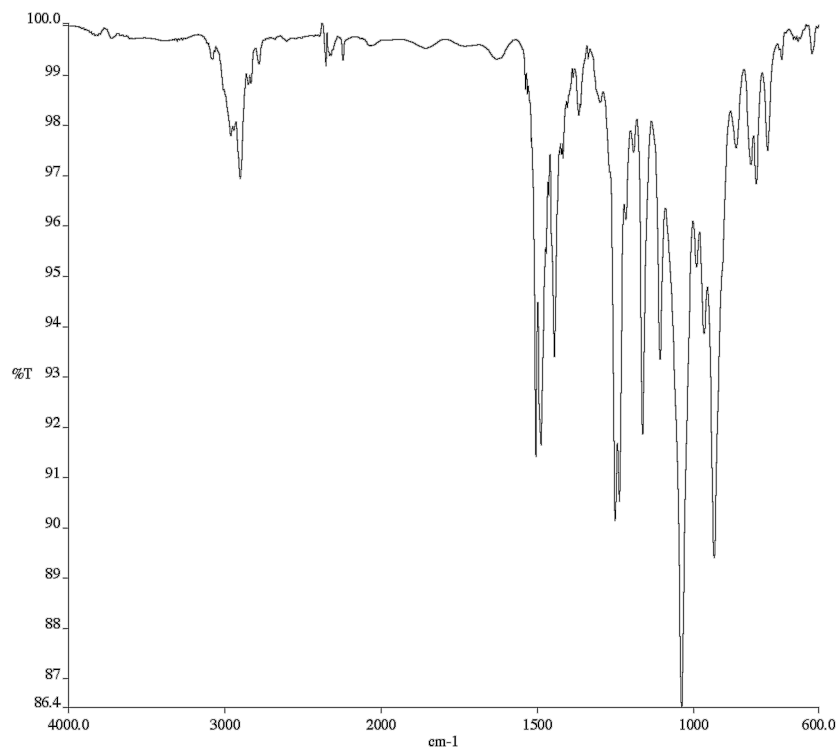


Figure A3.29 Infrared spectrum (Thin Film, NaCl) of compound **71f**

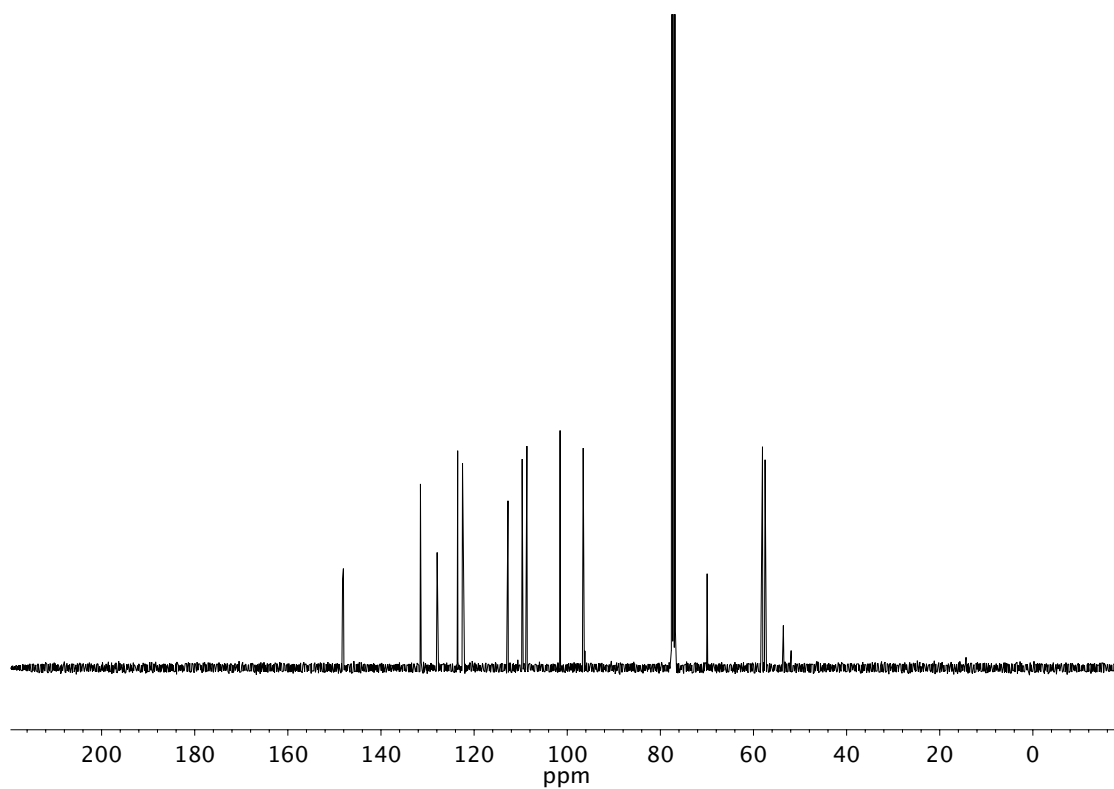


Figure A3.30 ¹³C NMR (101 MHz, CDCl₃) of compound **71f**

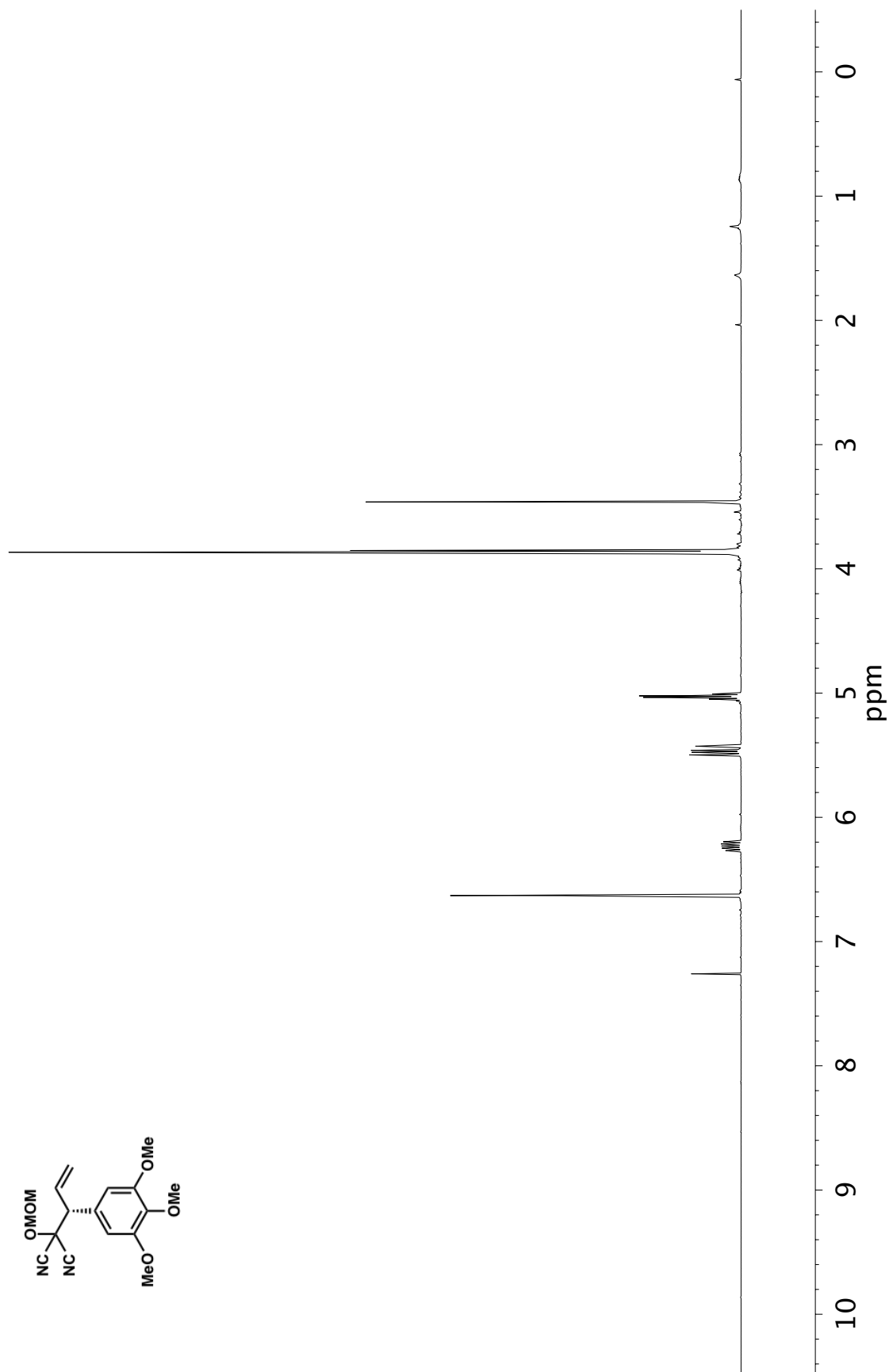


Figure A3.31 ¹H NMR (400 MHz, CDCl₃) of compound **71g**

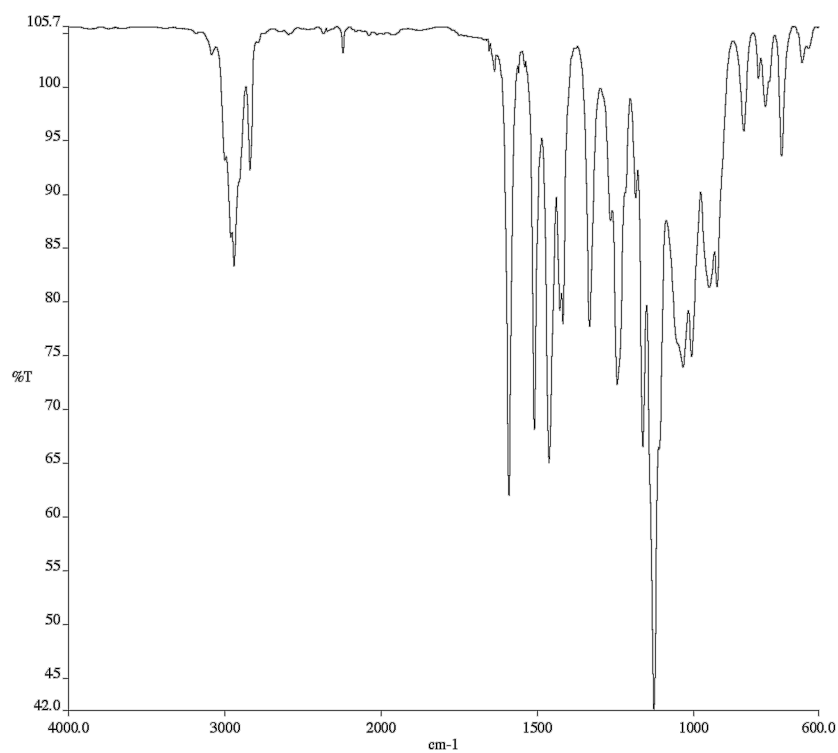


Figure A3.32 Infrared spectrum (Thin Film, NaCl) of compound **71g**

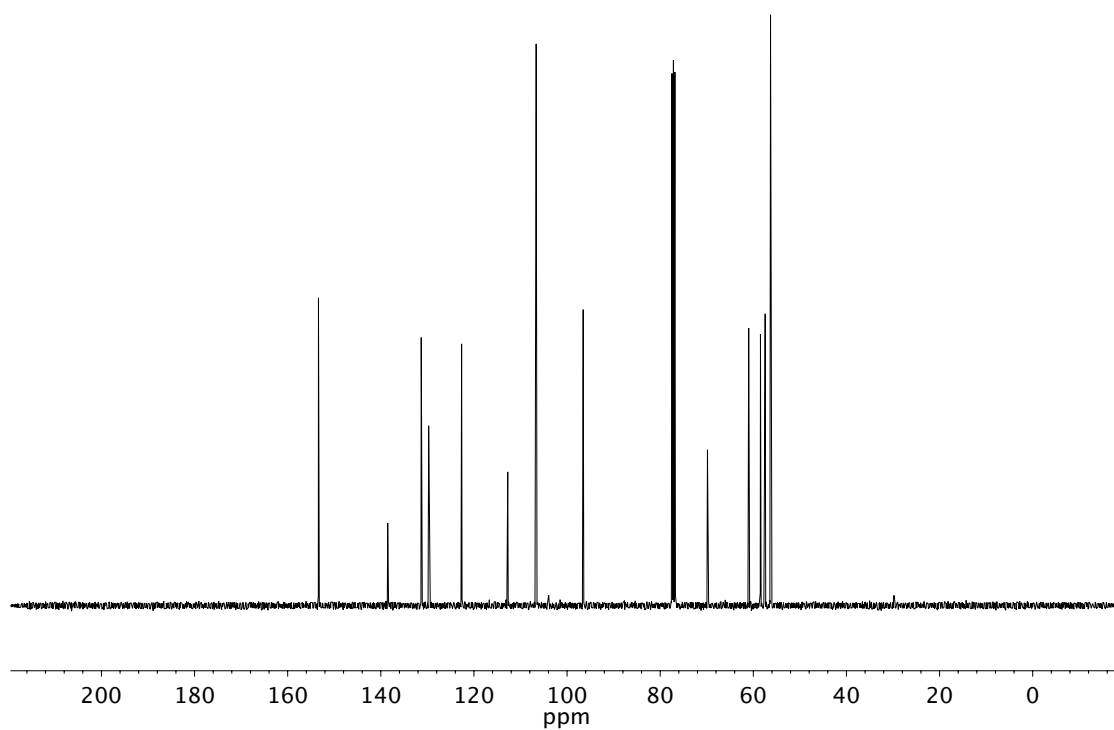


Figure A3.33 ¹³C NMR (101 MHz, CDCl₃) of compound **71g**

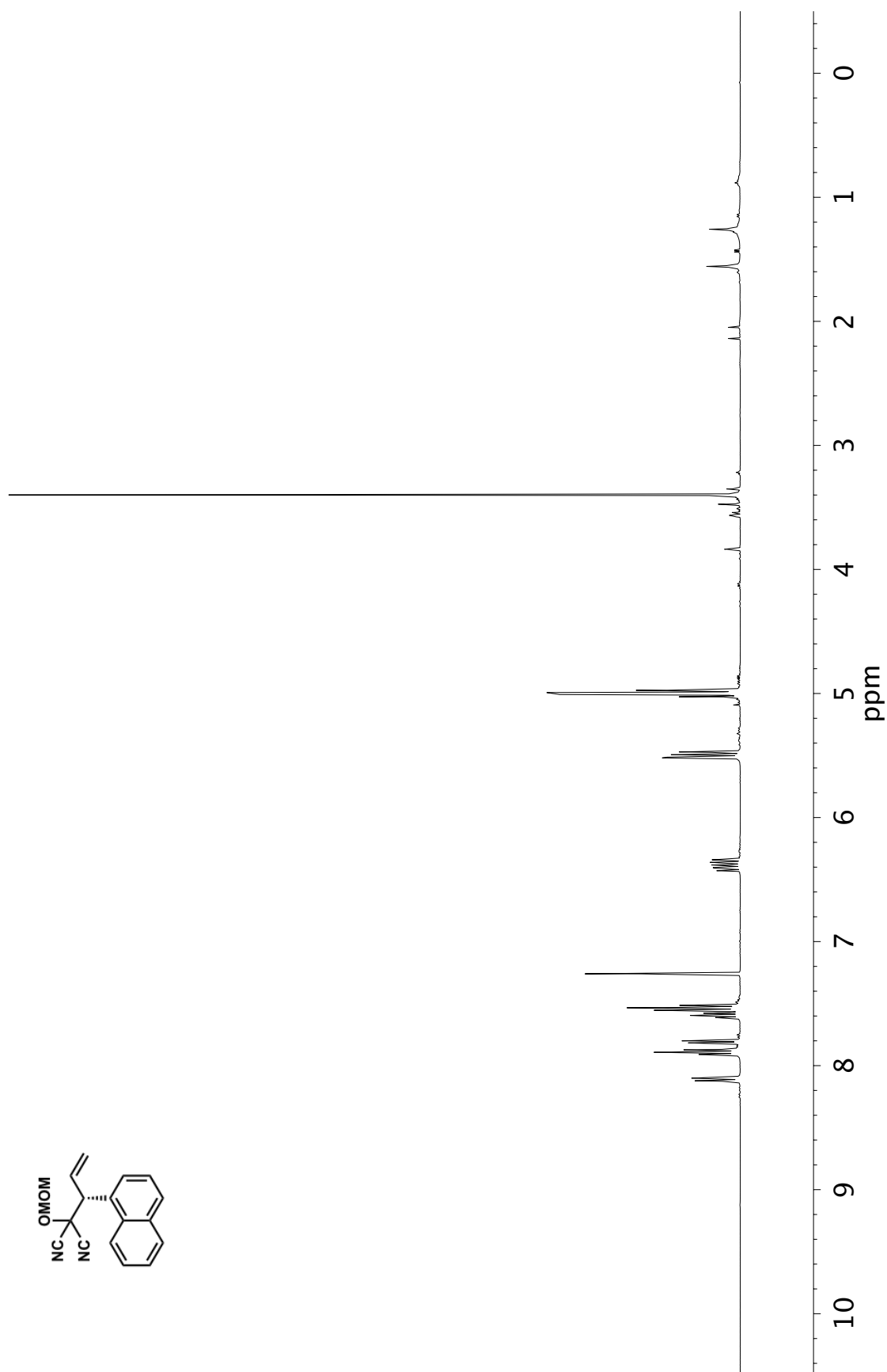


Figure A3.34 ^1H NMR (400 MHz, CDCl_3) of compound **71h**

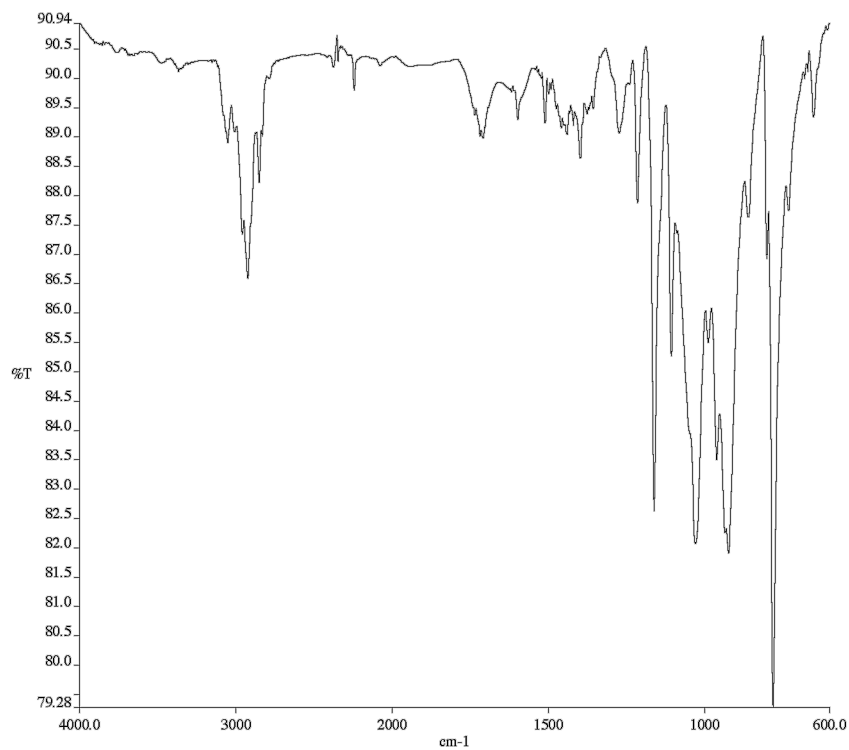


Figure A3.35 Infrared spectrum (Thin Film, NaCl) of compound **71h**

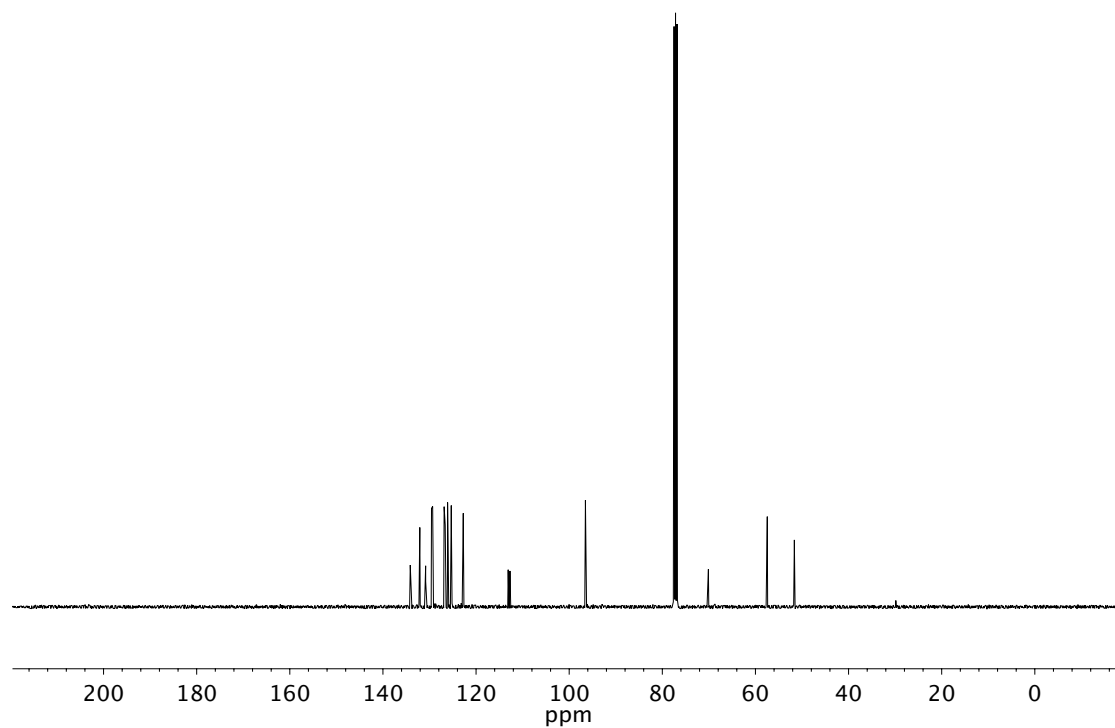


Figure A3.36 ¹³C NMR (101 MHz, CDCl₃) of compound **71h**

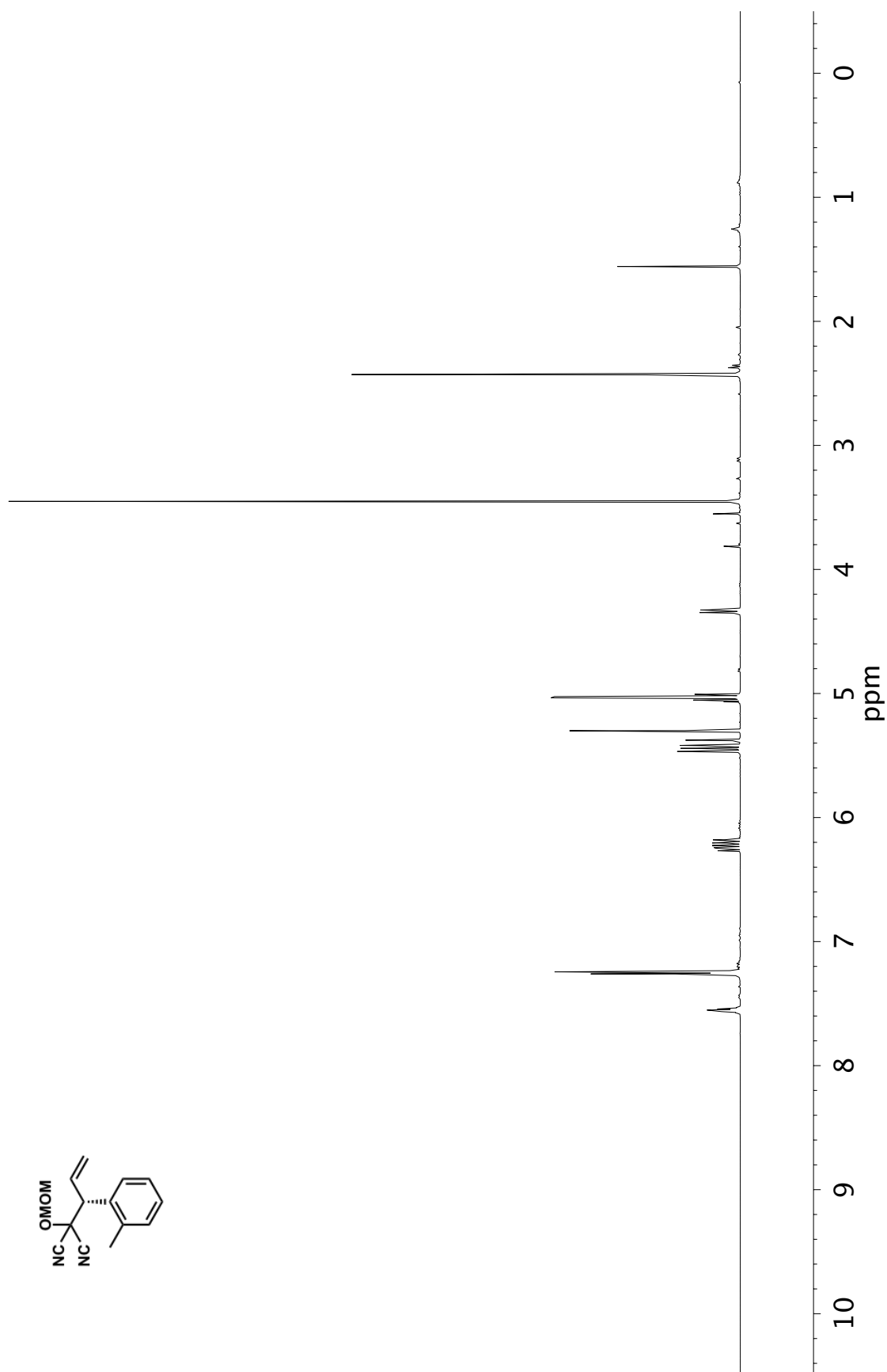


Figure A3.37 ¹H NMR (400 MHz, CDCl₃) of compound **71i**

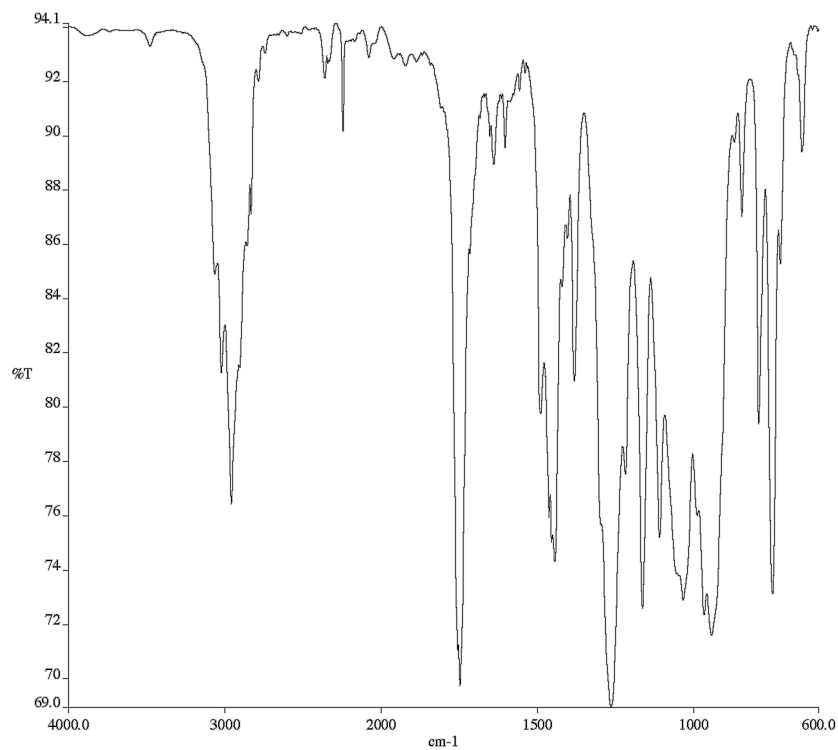


Figure A3.38 Infrared spectrum (Thin Film, NaCl) of compound **71i**

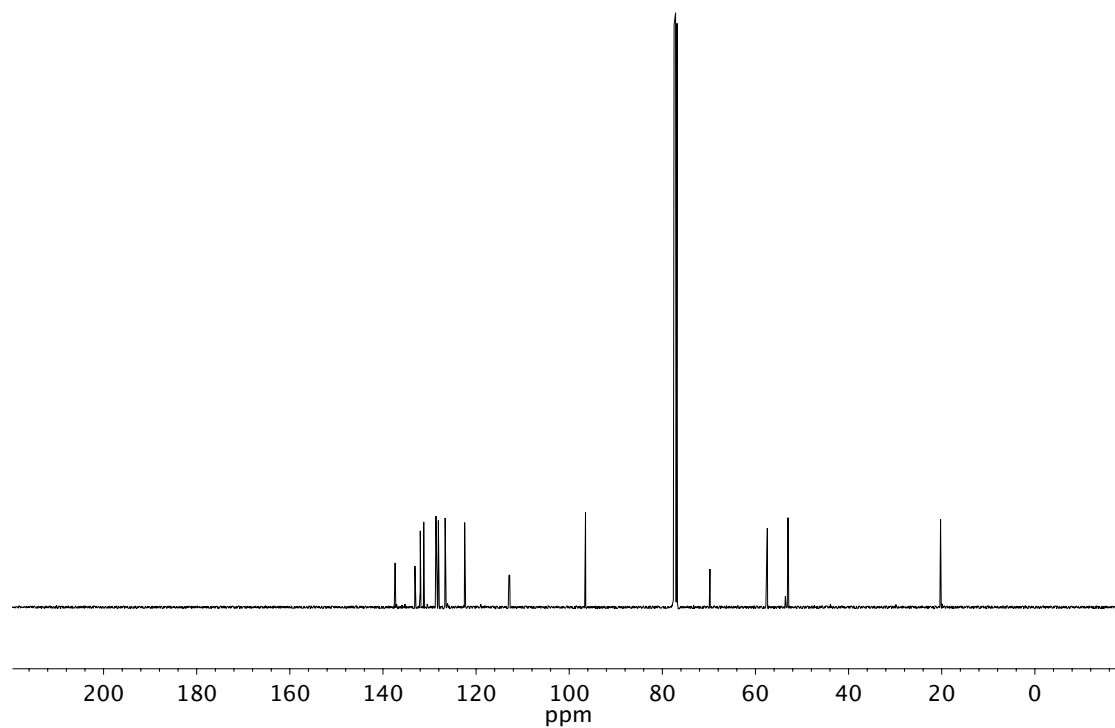


Figure A3.39 ¹³C NMR (101 MHz, CDCl₃) of compound **71i**

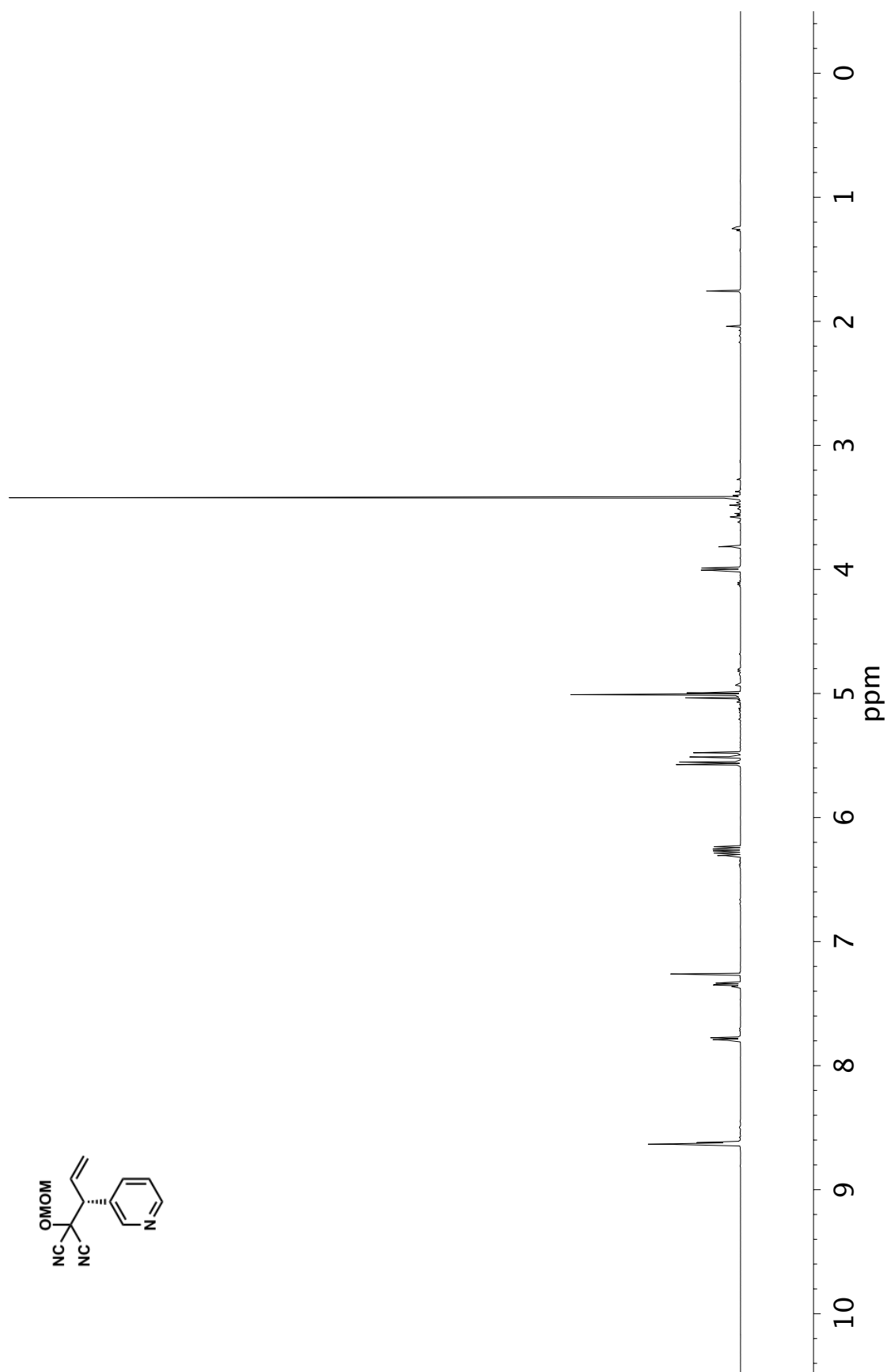


Figure A3.40 ¹H NMR (400 MHz, CDCl₃) of compound **71j**

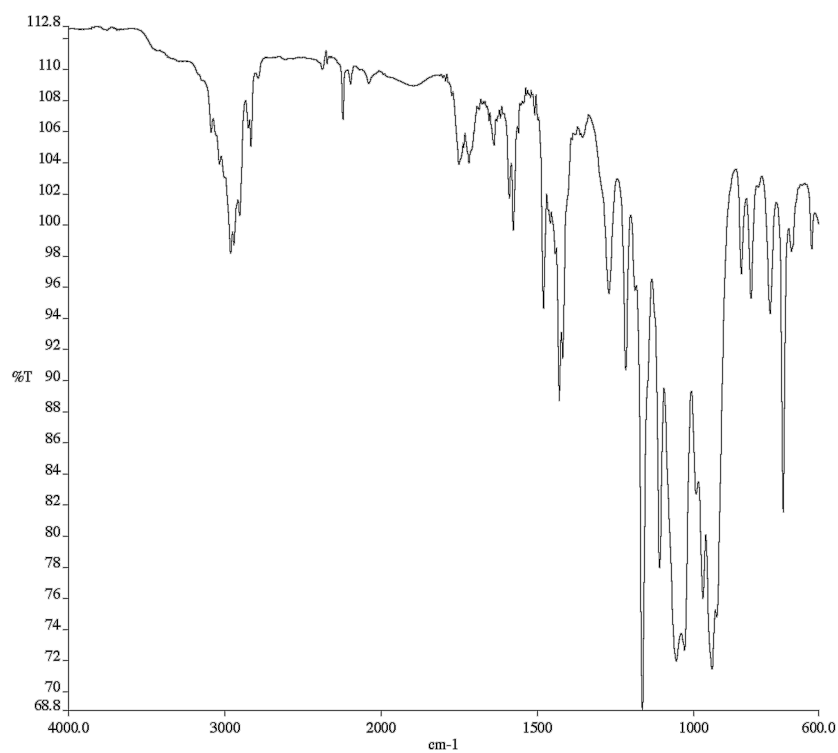


Figure A3.41 Infrared spectrum (Thin Film, NaCl) of compound **71j**

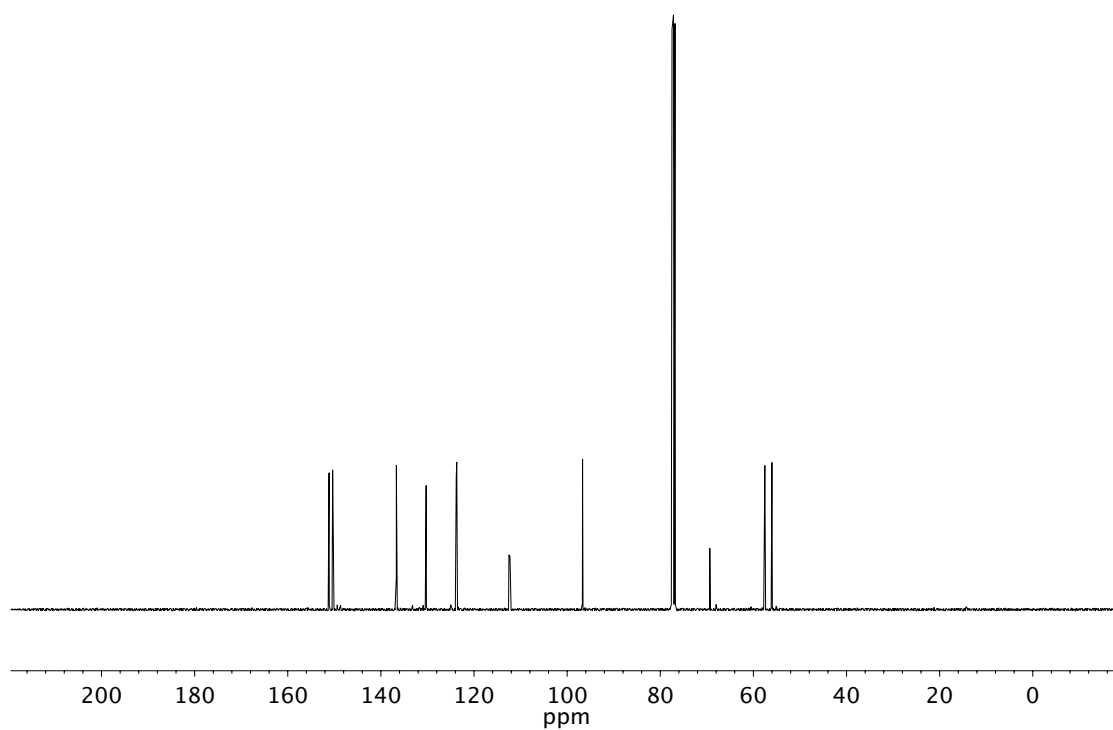


Figure A3.42 ¹³C NMR (101 MHz, CDCl₃) of compound **71j**

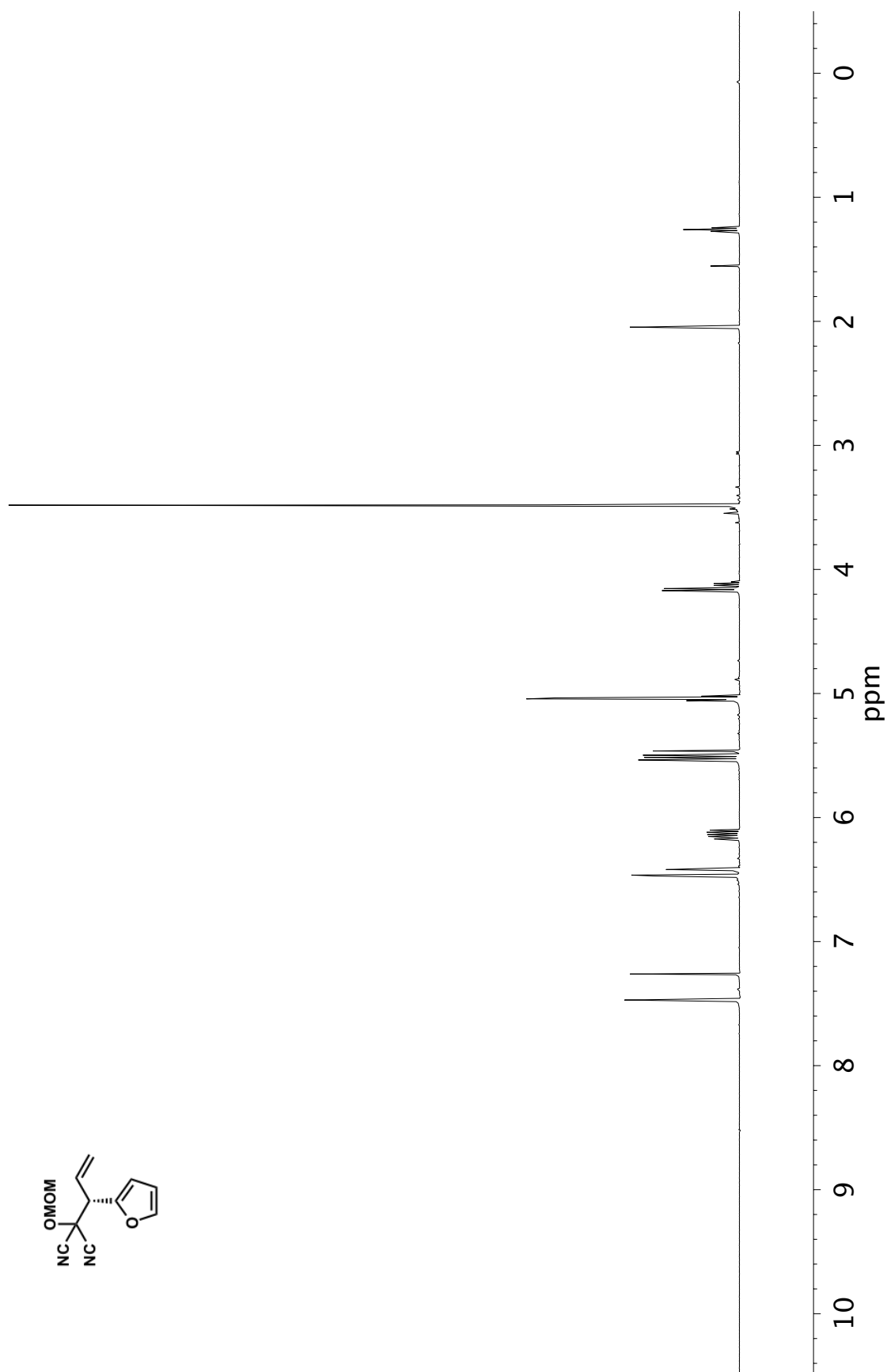


Figure A3.43 ^1H NMR (400 MHz, CDCl_3) of compound **71k**

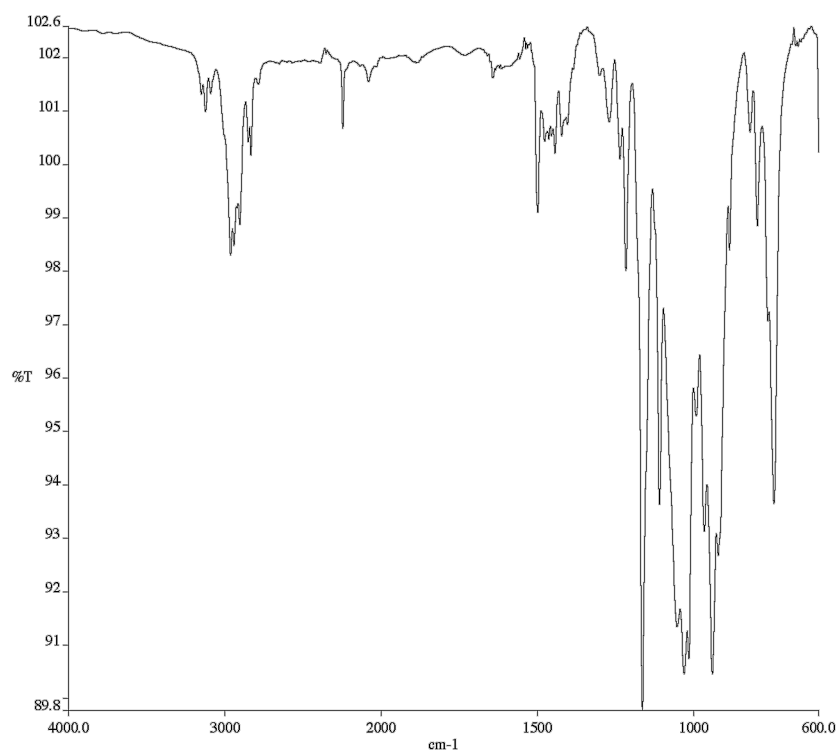


Figure A3.44 Infrared spectrum (Thin Film, NaCl) of compound **71k**

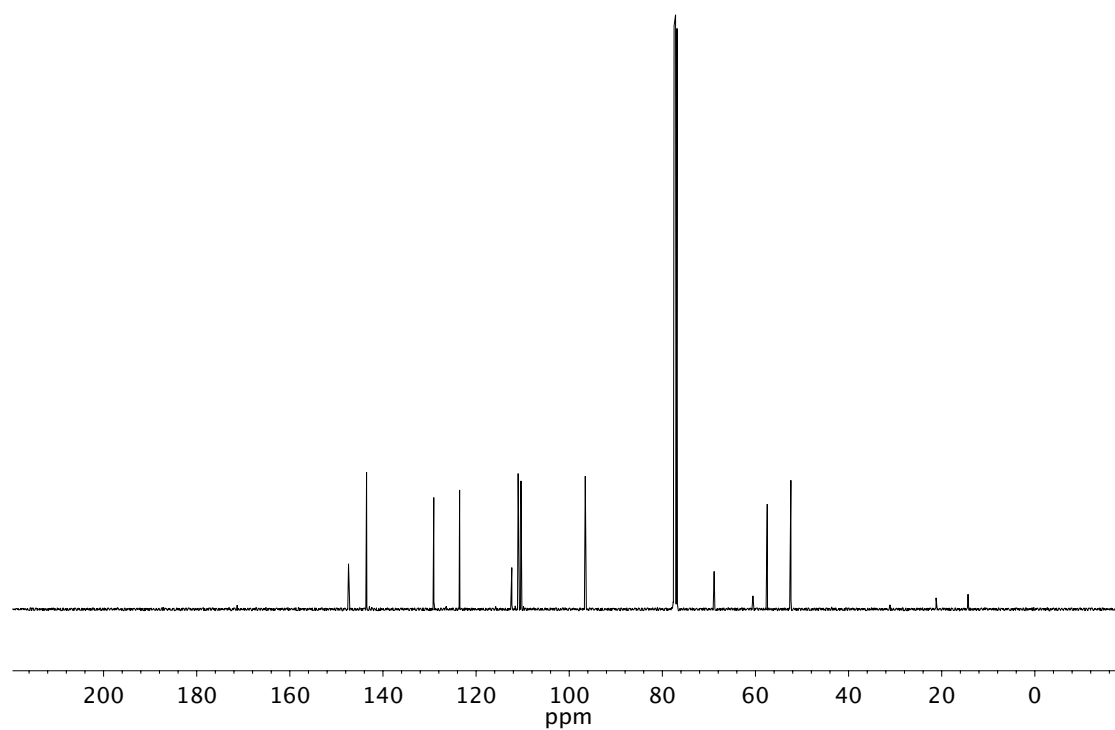


Figure A3.45 ¹³C NMR (101 MHz, CDCl₃) of compound **71k**

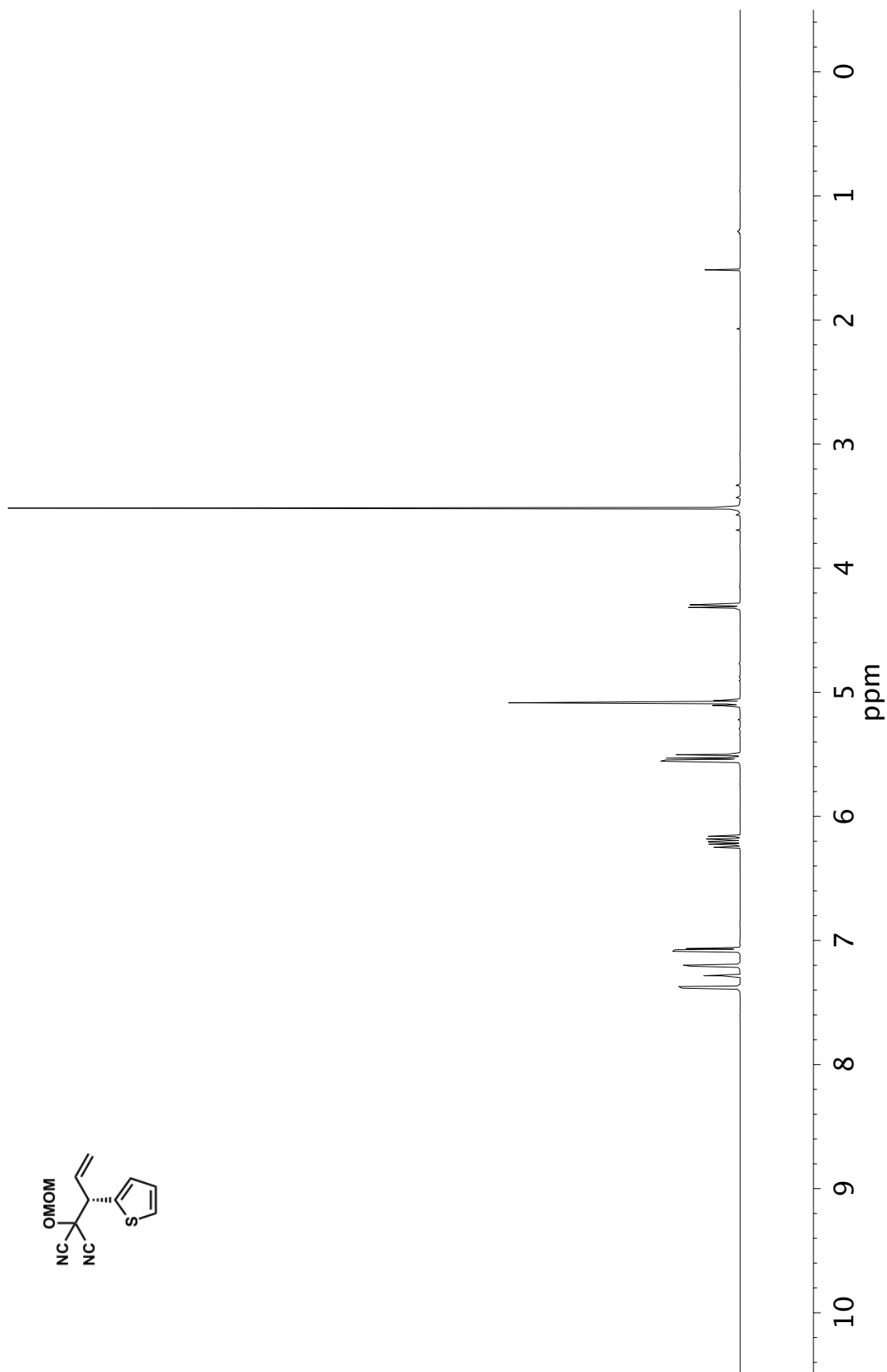


Figure A3.46 ¹H NMR (400 MHz, CDCl₃) of compound **71I**

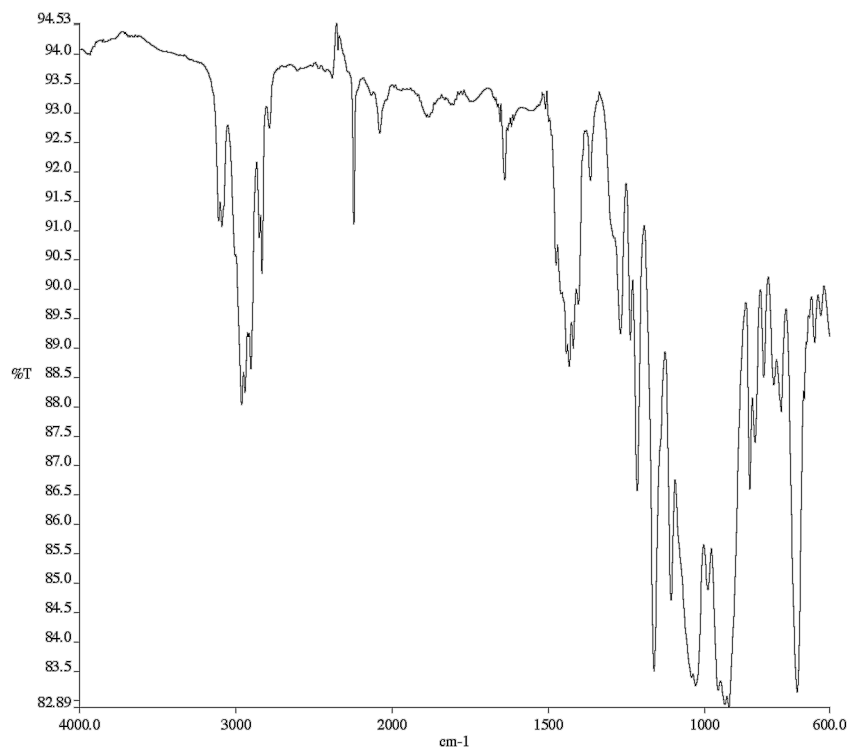


Figure A3.47 Infrared spectrum (Thin Film, NaCl) of compound **71I**

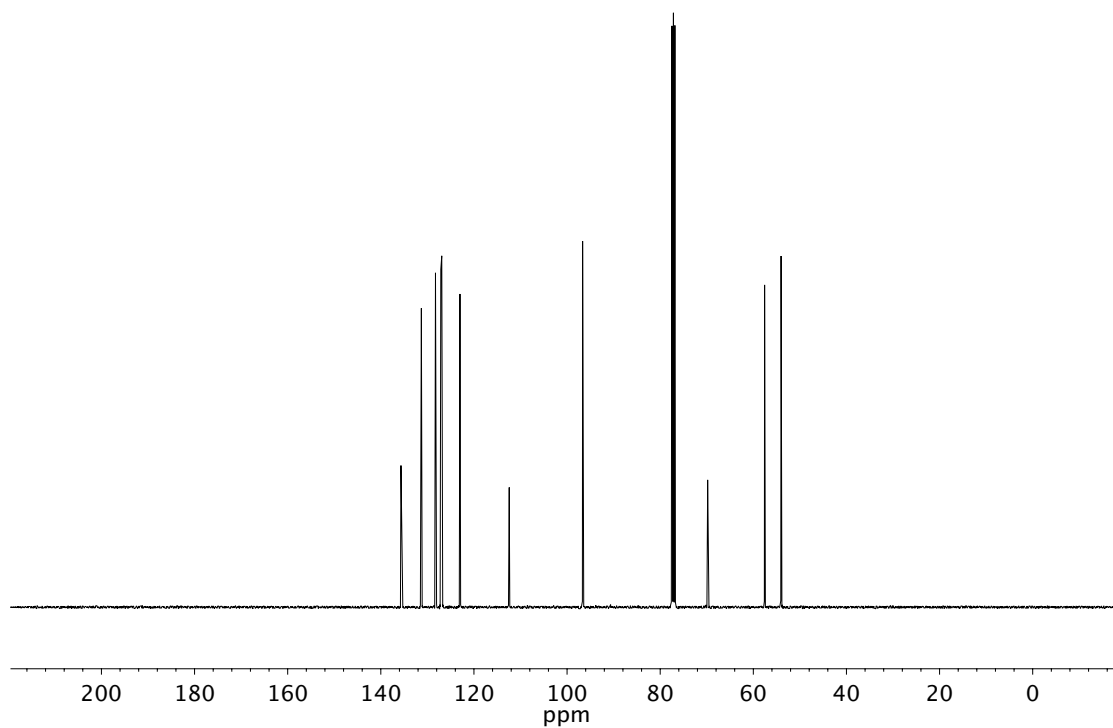


Figure A3.48 ¹³C NMR (101 MHz, CDCl₃) of compound **71I**

CHAPTER 3

Enantioselective Synthesis of Acyclic α -Quaternary Carboxylic Acid Derivatives via Iridium-Catalyzed Allylic Alkylation[†]

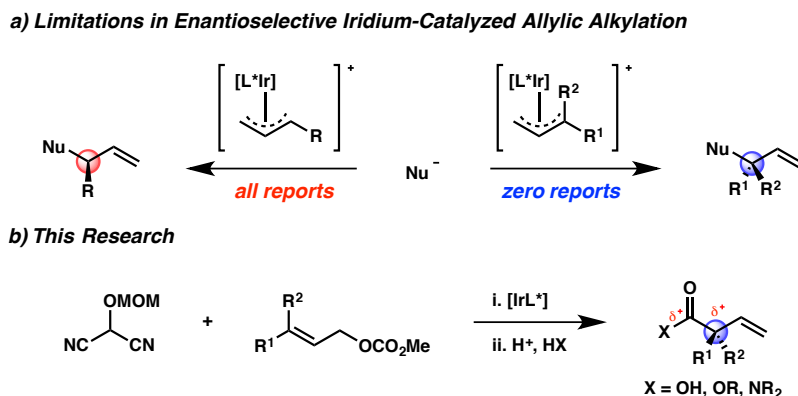
3.1 INTRODUCTION AND BACKGROUND

The field of enantioselective iridium-catalyzed allylic alkylation has flourished in the twenty years since the seminal report by Helmchen.¹ Over these two decades, the substrate scope with respect to the nucleophile has expanded significantly to encompass a vast array of both carbon² and heteroatom³ nucleophiles.⁴ Conversely, the scope of the electrophiles has remained largely unchanged, being limited to those that produce products bearing a tertiary allylic stereocenter (Figure 3.1a, left).⁵ Despite the synthetic community's longstanding interest in the synthesis of enantioenriched quaternary stereocenters as well as the development of other transition metal-catalyzed processes to access all-carbon quaternary allylic stereocenters,^{6,7,8} iridium-catalyzed allylic alkylation

[†] This work was performed in collaboration with Dr. J. Caleb Hethcox. Portions of this chapter have been reproduced with permission from Shockley, S. E.;[‡] Hethcox, J. C.;[‡] Stoltz, B. M. *Angew. Chem. Int. Ed.* **2017**, 56, 11545–11548 © 2017 Wiley-VCH.

reactions that furnish products possessing such a stereocenter remain conspicuously absent from the literature (Figure 3.1a, right).

Figure 3.1 Synthesis of allylic all-carbon quaternary stereocenters via enantioselective iridium-catalyzed allylic alkylation



As part of our ongoing program in developing iridium-catalyzed allylic alkylation technology and our continued interest in the catalytic, asymmetric synthesis of quaternary stereocenters,⁹ we were attracted to this unmet challenge. Moreover, we imagined that an umpolung strategy iridium-catalyzed allylic alkylation reaction of a trisubstituted allylic electrophile with a masked acyl cyanide (MAC) nucleophile would not only give rise to products containing an enantioenriched allylic all-carbon quaternary stereocenter, but also provide access to highly valuable acyclic α -quaternary carboxylic acid derivatives (i.e., acids, esters, amides) upon unmasking of the MAC functionality (Figure 3.1b).^{9e,10} However, success of this strategy hinged upon the implementation of a trisubstituted allylic electrophile, which was predicted to be unreactive in an enantioselective iridium-catalyzed allylic alkylation reaction. It is known that the reaction rates of these processes decrease with increasing substitution on the olefin of the electrophile.^{5,11,12} Herein, we

discuss the unlocking of this heretofore unreactive class of electrophiles to achieve the first example of an enantioselective iridium-catalyzed allylic alkylation reaction forming a quaternary stereocenter at the allylic position.

3.2 REACTION OPTIMIZATION

Preliminary studies focused on identifying a combination of ligand and additive to promote the reaction of MAC **67c** and trisubstituted allylic electrophile **72** (Table 3.1). Application of our standard conditions for iridium-catalyzed allylic alkylation reactions of $[\text{Ir}(\text{cod})\text{Cl}]_2$, **L2**, and LiBr return only starting material (Table 3.1, entry 1).^{9a,c} A brief ligand screen revealed that while ligand **L9** also results in no reaction (entry 2), the phosphoramidite **L5** developed by Carreira provides desired product **73** in 13% yield with a moderate 79% ee (entry 3).^{3b} Attempts to further increase yield and selectivity via an extensive evaluation of additives known to promote iridium-catalyzed allylic alkylations proved ineffective.^{2-4,9} As we hypothesized that the oxidative addition process is slow for trisubstituted allylic electrophiles, we reasoned that the inclusion of a strong Lewis acid would facilitate the ionization of the carbonate during the insertion event, leading to improved reactivity of these recalcitrant electrophiles. Toward this end, we substituted LiBr for triethylborane and were pleased to find that the yield nearly triples and the enantioselectivity rises to 93% ee (entry 4).¹³ Upon varying the stoichiometry of nucleophile **67c** to electrophile **72**, we observed a dramatic increase in yield to 74% with no erosion of enantioselectivity (entry 5). Ultimately, we discovered that exposure of a mixture (1:2) of MAC **67c** and trisubstituted allylic electrophile **72** affords MAC adduct **73** in nearly quantitative yield and in 94% ee (entry 6). Of note, excess electrophile **72** is

not consumed and can be recovered following the iridium-catalyzed allylic alkylation reaction.

Table 3.1 Optimization of reaction parameters^a

Entry	L	1:2	Additive (200 mol %)	Yield (%) ^b	ee (%) ^c
1	L2	2:1	LiBr	0	–
2	L9	2:1	LiBr	0	–
3	L5	2:1	LiBr	13	79
4	L5	2:1	BET ₃	34	93
5	L5	1:1.2	BET ₃	74	92
6	L5	1:2	BET ₃	99	94

(S,S_a)-L2

(S,S,S_a)-L9

(S_a)-L5

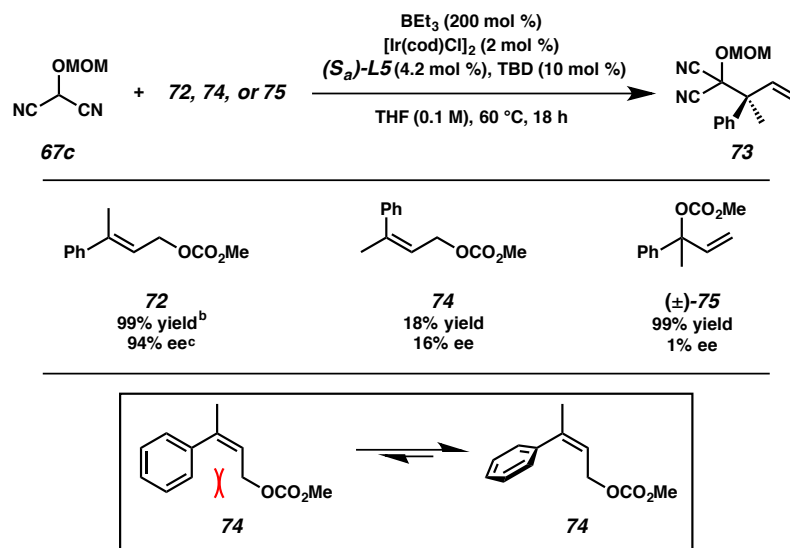
[a] Reactions performed on 0.1 mmol scale. [b] ¹H NMR yield based on internal standard. [c] Determined by chiral HPLC analysis. [d] TBD = 1,3,5-triazabicyclo[4.4.0]dec-5-ene.

3.3 MECHANISTIC INSIGHTS

During the course of our optimization studies, we discovered both the surprising necessity of the guanidine base TBD as well as the importance of electrophile stereochemistry in our newly developed reaction. Though previously reported conditions for the use of **L5** in iridium-catalyzed allylic alkylations do not require a base additive,¹⁴ we found the inclusion of TBD during the catalyst prestir to be critical to the success of the reaction. TBD is included with ligands **L2** and **L9** to form an active iridacycle catalyst; however, Carreira has demonstrated that ligand **L5** does not form an iridacycle.¹⁴

Thus, we hypothesize that TBD may be serving as either a placeholder ligand to prevent the formation of an inactive catalyst or as a base to promote the formation of an active, novel iridicycle.^{2a,c} Additionally, we noted that use of the *E*-trisubstituted allylic electrophile was required, as *Z*-olefin isomer **74** led to markedly decreased yield and selectivity (Table 3.2). We rationalize this difference in reactivity via the preferred conformation of the reactants. Whereas **72** may exist in a planar conformation, the phenyl group of **74** likely prefers to rotate out of plane to alleviate $A^{1,3}$ strain (Table 3.2, bottom). In adopting this perpendicular conformation, the phenyl ring has now increased the sterics above and below the olefin as well as become σ -withdrawing rather than π -donating. Finally, neither a kinetic nor a dynamic kinetic resolution occurs under the reaction conditions with the use of terminal olefin *rac*-**75** (Table 3.2).

Table 3.2 Electrophile isomers^a



[a] Reactions performed with **67c** (0.1 mmol) and **72**, **74**, or **75** (0.2 mmol). [b] ^1H NMR yield based on internal standard. [c] Determined by chiral HPLC analysis.

3.4 SUBSTRATE SCOPE EXPLORATION

Before substrate scope exploration commenced, we identified an additional opportunity for innovation. We imagined that hydrolysis of the MAC functionality of product **73** could be performed in the same reaction vessel as the iridium-catalyzed allylic alkylation reaction to provide direct access to the corresponding carboxylic acid in a one-pot, two-step procedure.¹⁰ Moreover, we envisioned that these carboxylic acid products would be amenable to purification by a simple acid/base extraction. To this end, we subjected the crude allylic alkylation mixture to hydrolysis with 6M HCl at 80 °C and were pleased to find that pure carboxylic acid **77a** is obtained after an aqueous work-up with no need for column chromatography (Table 3.3).

With the optimized protocol in hand, we first explored the effect of substitution on the aryl moiety of electrophile **76** (Table 3.3). We were pleased to find that *para*-substitution was well tolerated to provide acids **77b–f** in consistently high enantioselectivities, though electron-rich substrates provide decreased yields. *Meta*-substituted products **77g** and **77h** are obtained in similarly high enantioselectivities (92% and 87% ee, respectively), and bulky naphthyl-substituted acid **77i** is furnished in 92% ee, albeit in a moderate 66% yield. Further exploration of steric effects using methyl-substituted derivatives demonstrates that while a single *meta*-substituent is tolerated to access **77j** in 68% yield with 93% ee, the bis-*meta*-substituted derivative **77k** is afforded in a drastically lower 32% yield but with good enantioselectivity (85% ee). Finally, we discovered that *ortho*-substitution is not tolerated and only starting material is recovered from the reaction.

Reaction scheme showing the synthesis of **67c** and **72, 76** to form **77**.

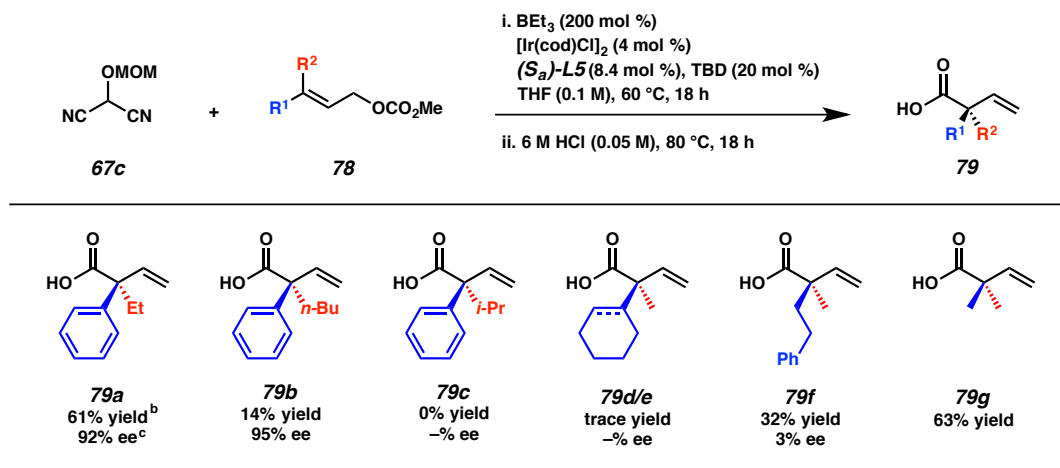
Reagents and conditions:

- i. BEt_3 (200 mol %), $[\text{Ir}(\text{cod})\text{Cl}]_2$ (2 mol %), $(S_a)\text{-L5}$ (4.2 mol %), TBD (10 mol %), THF (0.1 M), 60 °C, 18 h
- ii. 6 M HCl (0.05 M), 80 °C, 18 h

Products **77a** through **77l** are shown with their respective yields and enantiomeric excesses (ee):

Product	Yield	ee
77a	77% yield ^b	95% ee ^c
77b	80% yield	93% ee
77c	90% yield	90% ee
77d	83% yield	92% ee
77e	65% yield	94% ee
77f ^d	51% yield	95% ee
77g ^e	69% yield	92% ee
77h ^f	93% yield	87% ee
77i ^g	66% yield	92% ee
77j ^g	68% yield	93% ee
77k ^g	32% yield	85% ee
77l	0% yield	~9% ee

With the general trends in reactivity corresponding to aryl substitution elucidated, we next turned our attention to the scope of the reaction with respect to the alkyl moiety of the electrophile (Table 3.4). We found that extension of the alkyl chain leads to decreased yields with ethyl-substituted **79a** and *n*-butyl-substituted **79b** able to be isolated in 61% and 14% yield, respectively, though both are obtained in similarly excellent enantioselectivities. Furthermore, branched-substituted electrophiles are unreactive and only starting material is recovered in attempts to prepare isopropyl-substituted **79c**.

Table 3.4 Non-aryl substituent substrate scope^a

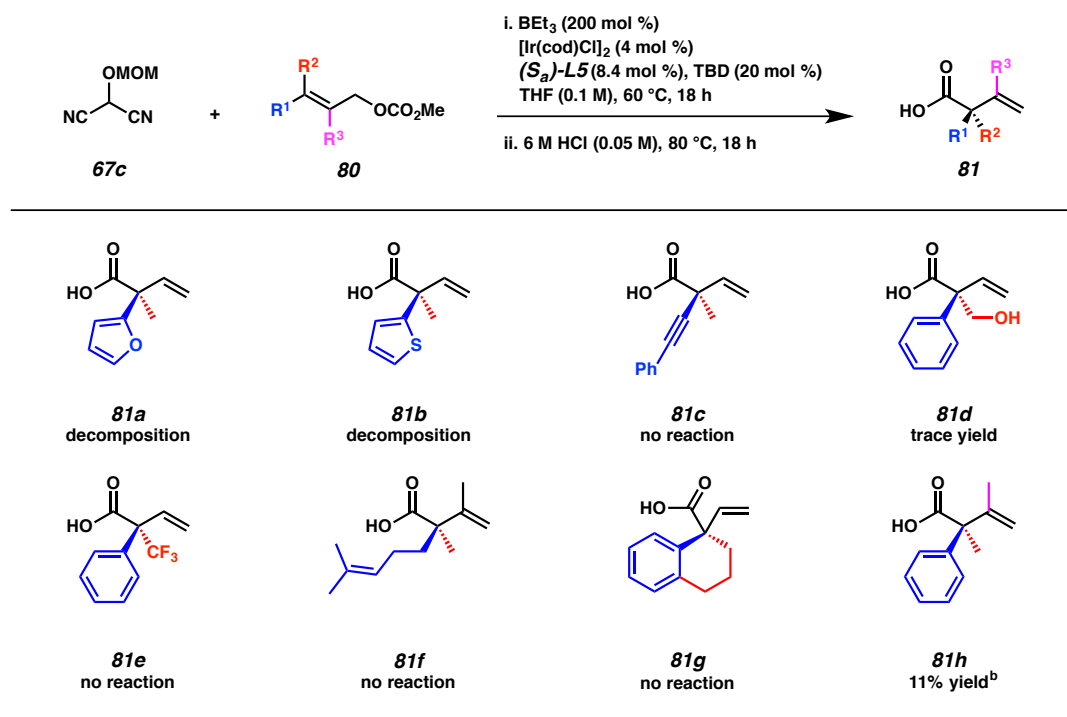
[a] Reactions performed on 0.2 mmol scale. [b] Isolated yield. [c] Determined by chiral HPLC or SFC analysis.

We then moved to explore the necessity of the aryl functionality. We hypothesized that cyclohexyl- and cyclohexenyl-substituted electrophiles **78d** and **78e** would mimic the steric bulk of the phenyl moiety of **76a** when interacting with the chiral catalyst, but we found that only trace products **79d** and **79e** are observed under our reaction conditions (Table 3.4). Use of bis-*n*-alkyl-substituted electrophile **78f** provides the corresponding acid **79f** in moderate yield, though no enantioselectivity is observed. Finally, we were pleased to find that prenyl methyl carbonate (**78g**) is a competent electrophile furnishing acid **79g** in 63% yield.

A wider exploration into the scope of this novel transformation revealed additional limitations of the catalytic system (Table 3.5). Foremost, while furan- and thiophene-substituted allylic electrophiles are well tolerated in the iridium-catalyzed allylic alkylation reaction, the heteroaromatic functionality on the allylic alkylation product is not amenable to the hydrolysis conditions and thus trace **81a** and **81b** are recovered. Moreover, alkenyl substitution is not permitted on allylic electrophile **80**,

likely due to its ability to bind to the iridium catalyst, and no conversion to propargyl-derived **81c** is observed. Additionally, only trace conversion to hydroxymethyl **81d** is noted when corresponding TBS-protected allylic electrophile **80d** is employed. A trifluoromethyl group in place of the methyl substituent on the electrophile shuts down the allylic alkylation reaction entirely, as does the use of a bulky branched geranyl-derived electrophile, resulting in no isolation of **81e** and **81f**, respectively. Also, use of a tethered allylic electrophile (e.g., tetralone **80g**) does not afford corresponding bicyclic product **81g**. Finally, we found that a tetrasubstituted allylic electrophile was able to yield allylic alkylation product **81h**, albeit in a modest 11% yield.

Table 3.5 Substrate scope limitations^a

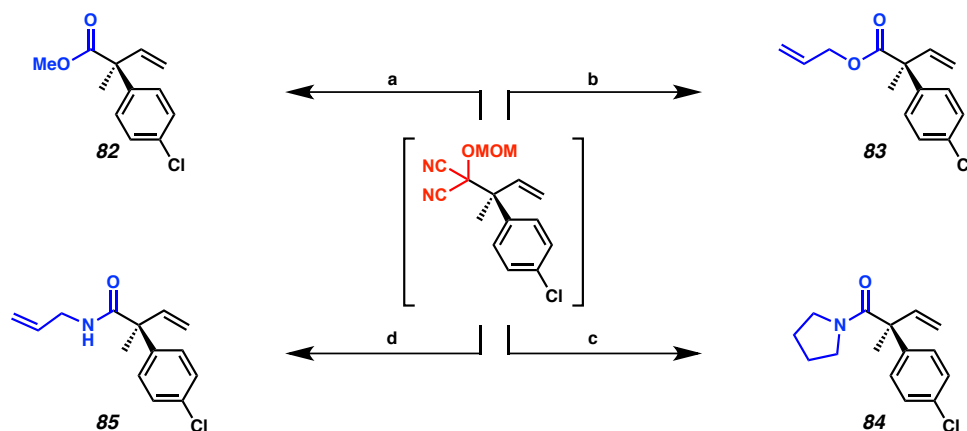


[a] Reactions performed on 0.2 mmol scale. [b] ¹H NMR yield based on internal standard.

3.5 PRODUCT TRANSFORMATIONS

As MAC adducts can be transformed to essentially any carboxylic acid derivative,¹⁰ we endeavored to develop additional one-pot transformations to access both α -quaternary esters and amides. Gratifyingly, we found that alkanolysis of the crude MAC alkylation product with either methanol or allyl alcohol provides methyl ester **82** and allyl ester **83** in 88% and 74% yield, respectively (Figure 3.2). Similarly, aminolysis provides access to both tertiary amide **84** in 61% yield and secondary amide **85** in 63% yield.

Figure 3.2 One-pot transformations to α -quaternary carboxylic acid derivatives^a

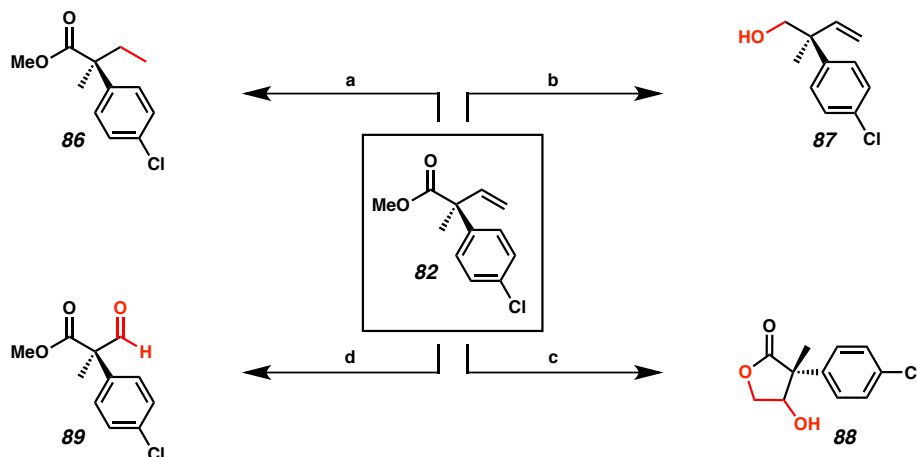


[a] i. CSA, AcOH/DME, 60 °C, 6 h, ii. MeOH, Et₃N, -40 °C → 23 °C, 18 h, 88% yield; [b] i. CSA, AcOH/DME, 60 °C, 6 h, ii. allyl alcohol, Et₃N, 0 °C → 23 °C, 18 h, 74% yield; [c] CSA, AcOH/DME, 60 °C, 6 h, ii. pyrrolidine, Et₃N, -40 °C → 23 °C, 18 h, 61% yield; [d] i. CSA, AcOH/DME, 60 °C, 6 h, ii. allyl amine, Et₃N, 0 °C → 23 °C, 18 h, 63% yield.

In order to demonstrate the synthetic utility of the enantioenriched α -quaternary carboxylic acid derivatives, a series of transformations were performed to access a diverse array of chiral building blocks starting from ester derivative **82** (Figure 3.3). Hydrogenation of olefin **82** delivers ethyl-substituted **86** in 97% yield. Alcohol **87** is accessed via reduction of the ester moiety in 73% yield. Dihydroxylation of the pendant

olefin proceeds with concomitant lactonization to furnish γ -butyrolactone **88** in 82% yield as a mixture (1:1) of diastereomers. Finally, ozonolysis furnishes aldehyde **89** in moderate yield.

Figure 3.3 Product transformations of α -quaternary ester **82**^a



[a] Pd/C, H₂ (balloon), EtOAc, 23 °C, 18 h, 97% yield; [b] DIBAL, Et₂O, 0 °C, 2 h, 73% yield; [c] K₂OsO₄, NMO, THF/H₂O (4:1), 23 °C, 18 h, 82% yield (1:1 dr); [d] i. O₃, NaHCO₃, MeOH/CH₂Cl₂ (1:5), -78 °C, 0.5 h, ii. DMS, -78 °C \rightarrow 23 °C, 18 h, 50% yield.

3.6 CONCLUSIONS

In conclusion, we have developed the first synthesis of all-carbon quaternary allylic stereocenters via enantioselective iridium-catalyzed allylic alkylation. The unprecedented combination of triethylborane and a catalyst prepared from [Ir(cod)Cl]₂, **L5**, and TBD was used to coerce reactivity from a once poorly reactive class of trisubstituted allylic electrophiles. Furthermore, the use of a single masked acyl cyanide nucleophile facilitates the one-pot syntheses of enantioenriched α -quaternary acids, esters, and amides. The protocol is tolerant of a wide range of substitution on the aryl moiety to provide the corresponding products in good yields and excellent enantioselectivities. This methodology is critical in laying the groundwork for the future development of

technology to access vicinal quaternary centers via iridium-catalyzed allylic alkylation of prochiral nucleophiles.

3.7 EXPERIMENTAL SECTION

3.7.1 MATERIALS AND METHODS

Unless otherwise stated, reactions were performed in flame-dried glassware under an argon or nitrogen atmosphere using dry, deoxygenated solvents. Solvents were dried by passage through an activated alumina column under argon. Commercially obtained reagents were used as received. Chemicals were purchased from Sigma Aldrich/Strem/Alfa Aesar/Oakwood Chemicals and used as received. Reaction temperatures were controlled by an IKA Mag temperature modulator. Glove box manipulations were performed under a nitrogen atmosphere. Thin-layer chromatography (TLC) and preparatory TLC was performed using E. Merck silica gel 60 F254 precoated plates (0.25 mm) and visualized by UV fluorescence quenching, KMnO_4 , or *p*-anisaldehyde staining. SiliaFlash P60 Academic Silica gel (particle size 0.040–0.063 mm) was used for flash chromatography. Analytical chiral HPLC was performed with an Agilent 1100 Series HPLC utilizing a Chiralpak IC column (4.6 mm x 25 cm) or a Chiralpak AD-H column (4.6 mm x 25 cm), both obtained from Daicel Chemical Industries, Ltd. with visualization at 210 nm. Analytical SFC was performed with a Mettler SFC supercritical CO_2 analytical chromatography system utilizing a Chiralpak AD-H column (4.6 mm x 25 cm) obtained from Daicel Chemical Industries, Ltd. with visualization at 210 nm. Preparatory HPLC was performed with an Agilent 1200 Series HPLC equipped with a Viridis SFC 2-Ethylpyridine 5 μm column (4.6 x 250 mm). ^1H

NMR spectra were recorded on a Bruker Avance HD 400 MHz spectrometer and are reported relative to residual CHCl_3 (δ 7.26 ppm). ^{13}C NMR spectra were recorded on a Bruker Avance HD 400 MHz spectrometer and are reported relative to residual CDCl_3 (δ 77.16 ppm). Data for ^1H NMR are reported as follows: s = singlet, d = doublet, t = triplet, q = quartet, p = pentet, sept = septuplet, m = multiplet, br s = broad singlet. Data for ^{13}C NMR are reported in terms of chemical shifts (δ ppm). Some reported spectra include minor solvent impurities of benzene (δ 7.36 ppm), water (δ 1.56 ppm), ethyl acetate (δ 4.12, 2.05, 1.26 ppm), methylene chloride (δ 5.30 ppm), grease (δ 1.26, 0.86 ppm), and/or silicon grease (δ 0.07 ppm), which do not impact product assignments. IR spectra were obtained using a Perkin Elmer Paragon 1000 spectrometer using thin films deposited on NaCl plates and reported in frequency of absorption (cm^{-1}). High resolution mass spectra (HRMS) were obtained from the Caltech Mass Spectral Facility using a JEOL JMS-600H High Resolution Mass Spectrometer in fast atom bombardment (FAB+) or electron ionization (EI+) mode, or an Agilent 6200 Series TOF with an Agilent G1978A Multimode source in electrospray ionization (ESI+), atmospheric pressure chemical ionization (APCI+), or mixed ionization mode (MM: ESI-APCI+). Optical rotations were measured with a Jasco P-2000 polarimeter operating on the sodium D-line (589 nm), using a 100 mm pathlength cell, and are reported as $[\alpha]_{\text{D}}^{\text{T}}$ (concentration in g/100 mL, solvent).

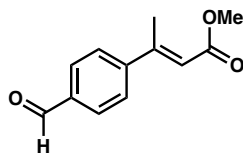
3.7.1.1 Preparation of Known Compounds

Previously reported methods were used to prepare ligands (*S,S*)-**L2**^{2c,15} and (*S*)-**L5**¹⁶ as well as starting materials **67c**,^{10b,17} **72**,¹⁸ **75**,¹⁸ **76a**,¹⁹ **76b**,²⁰ **76d**,¹⁸ **76e**,¹⁸ **76j**,¹⁸ **76l**,¹⁸ **78a**,¹⁸ **78d**,¹⁸ and **78f**¹⁸.

3.7.2 EXPERIMENTAL PROCEDURES AND SPECTROSCOPIC DATA

3.7.2.1 Representative Procedures for the Synthesis of Electrophiles

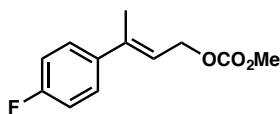
3.7.2.1.1 Representative Procedure #1: Oxidative Heck Reaction²¹



Methyl (E)-3-(4-formylphenyl)but-2-enoate (90). To a solution of (4-formylphenyl)boronic acid (0.75 g, 5.0 mmol, 1 equiv), Pd(OAc)₂ (23 mg, 0.10 mmol, 0.02 equiv), dppp (62 mg, 0.15 mmol, 0.03 equiv) in acetone (8 mL) was added methyl crotonate (1.1 mL, 10.0 mmol, 2 equiv) followed by trifluoroacetic acid (0.12 mL, 1.5 mmol, 0.3 equiv). The resulting slurry was heated under reflux for 48 h, whereupon the reaction was cooled to ambient temperature and concentrated under reduced pressure. The crude product was purified by silica gel flash column chromatography (5% EtOAc/hexanes) to give carbonate **90** as a colorless oil (0.17 g, 17% yield): ¹H NMR (400 MHz, CDCl₃) δ 10.06 (s, 1H), 7.97 – 7.78 (m, 2H), 7.74 – 7.58 (m, 2H), 6.22 (q, *J* = 1.3 Hz, 1H), 3.80 (s, 3H), 2.62 (d, *J* = 1.4 Hz, 3H); ¹³C NMR (101 MHz, CDCl₃) δ 191.8, 167.0, 154.4, 148.2, 136.5, 130.1, 127.1, 119.0, 51.5, 18.1; IR (Neat Film, NaCl) 2950,

2839, 1704, 1631, 1605, 1434, 1349, 1273, 1214, 1171, 1036, 828 cm^{-1} ; HRMS (FAB+) m/z calc'd for $\text{C}_{12}\text{H}_{13}\text{O}_3$ $[\text{M}+\text{H}]^+$: 205.0865, found 205.0860.

3.7.2.1.2 Representative Procedure #2: Reduction & Acylation

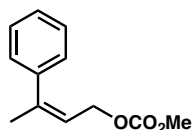


(E)-3-(4-Fluorophenyl)but-2-en-1-yl methyl carbonate (76c). To a solution of methyl (E)-3-(4-fluorophenyl)but-2-enoate²² (0.30 g, 1.6 mmol, 1 equiv) in THF (3.1 mL) at -78 °C was added DIBAL (0.85 mL, 4.8 mmol, 3 equiv) dropwise. The resulting reaction mixture was stirred at -78 °C for 2.5 h, whereupon the reaction was quenched with a saturated aqueous Rochelle's salt solution (5 mL). The cooling bath was then removed and the reaction was stirred for 18 h at ambient temperature. The aqueous layer was extracted with CH_2Cl_2 (3 x 20 mL) and the combined organic layers were washed with brine (20 mL), dried over Na_2SO_4 , and concentrated under reduced pressure.

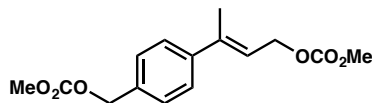
The crude material was then dissolved in CH_2Cl_2 (6.4 mL) and cooled to 0 °C. Pyridine (1.1 mL, 13 mmol, 8.3 equiv) was added followed by methyl chloroformate (0.28 mL, 3.7 mmol, 2.3 equiv) dropwise. The resulting solution was allowed to warm to ambient temperature and stirred for 18 h. The reaction was quenched with the addition of 1 M HCl (5 mL) and the aqueous layer was extracted with CH_2Cl_2 (3 x 20 mL). The combined organic layers were washed with brine (20 mL), dried over Na_2SO_4 , and concentrated under reduced pressure. The crude product was purified by silica gel flash column chromatography (5% EtOAc/hexanes) to give carbonate **76c** as a colorless solid (0.14 g, 38% yield): ^1H NMR (400 MHz, CDCl_3) δ 7.40 – 7.33 (m, 2H), 7.05 – 6.96 (m,

2H), 5.87 (tq, $J = 7.0, 1.4$ Hz, 1H), 4.84 (dd, $J = 7.1, 0.8$ Hz, 2H), 3.80 (s, 3H), 2.11 (dd, $J = 1.4, 0.7$ Hz, 3H); ^{13}C NMR (101 MHz, CDCl_3) δ 163.7, 161.3, 156.0, 140.2, 138.6 (d, $J = 3.3$ Hz), 127.6 (d, $J = 8.0$ Hz), 120.7 (d, $J = 1.3$ Hz), 115.4, 115.1, 65.0, 55.0, 16.5; IR (Neat Film, NaCl) 2961, 1896, 1742, 1649, 1589, 1468, 1442, 1379, 1334, 1252, 1110, 994, 960, 945, 825, 794 cm^{-1} ; HRMS (FAB+) m/z calc'd for $\text{C}_{12}\text{H}_{13}\text{FO}_3$ $[\text{M}]^+$: 224.0849, found 224.0850.

3.7.2.2 Spectroscopic Data for the Synthesis of Electrophiles

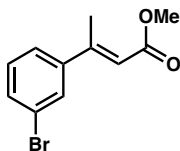


(Z)-methyl (3-phenylbut-2-en-1-yl) carbonate (74). Carbonate **74** was prepared from ethyl (Z)-3-phenylbut-2-enoate²³ according to Representative Procedure #2 and isolated by silica gel flash column chromatography (5% EtOAc/hexanes) as a colorless oil (0.18 g, 49% yield): ^1H NMR (400 MHz, CDCl_3) δ 7.41 – 7.18 (m, 5H), 5.76 – 5.68 (m, 1H), 4.58 (dd, $J = 7.2, 1.1$ Hz, 2H), 3.79 (s, 3H), 2.13 (q, $J = 1.2$ Hz, 3H); ^{13}C NMR (101 MHz, CDCl_3) δ 155.8, 143.8, 140.3, 128.4, 127.8, 127.6, 120.5, 65.8, 54.8, 25.6; IR (Neat Film, NaCl) 3023, 2956, 1748, 1494, 1441, 1382, 1350, 1263, 1024, 944, 792, 765, 702 cm^{-1} ; HRMS (FAB+) m/z calc'd for $\text{C}_{12}\text{H}_{15}\text{O}_3$ $[\text{M}+\text{H}]^+$: 207.1021, found 207.1011.

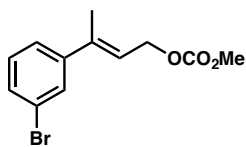


(E)-3-(4-(((Methoxycarbonyl)oxy)methyl)phenyl)but-2-en-1-yl methyl carbonate (76f). Carbonate **76f** was prepared from **90** according to Representative Procedure #2 and

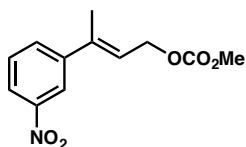
isolated by silica gel flash column chromatography (5% EtOAc/hexanes) as a colorless solid (0.11 g, 46% yield): ^1H NMR (400 MHz, CDCl_3) δ 7.44 – 7.31 (m, 4H), 5.98 – 5.88 (m, 1H), 5.15 (s, 2H), 4.85 (dd, $J = 7.0, 0.9$ Hz, 2H), 3.802 (s, 3H), 3.795 (s, 3H), 2.13 – 2.10 (m, 3H); ^{13}C NMR (101 MHz, CDCl_3) δ 156.0, 155.9, 142.8, 140.6, 134.7, 128.5, 126.3, 121.2, 69.4, 65.0, 55.1, 55.0, 16.4; IR (Neat Film, NaCl) 2959, 1754, 1443, 1385, 1333, 1288, 958, 909, 794, 731 cm^{-1} ; HRMS (FAB+) m/z calc'd for $\text{C}_{15}\text{H}_{18}\text{O}_6$ $[\text{M}]^+$: 294.1103, found 294.1098.



Methyl (*E*)-3-(3-bromophenyl)but-2-enoate (91). Ester **91** was prepared from (3-bromophenyl)boronic acid according to Representative Procedure #1 and isolated by silica gel flash column chromatography (3% EtOAc/hexanes) as a colorless oil (0.54 g, 42% yield): ^1H NMR (400 MHz, CDCl_3) δ 7.65 – 7.59 (m, 1H), 7.51 (ddd, $J = 7.9, 2.0, 1.0$ Hz, 1H), 7.45 – 7.37 (m, 1H), 7.31 – 7.26 (m, 1H), 6.14 (q, $J = 1.3$ Hz, 1H), 3.78 (d, $J = 1.2$ Hz, 3H), 2.57 (d, $J = 1.4$ Hz, 3H); ^{13}C NMR (101 MHz, CDCl_3) δ 167.1, 154.3, 144.4, 132.1, 130.2, 129.6, 125.1, 122.8, 117.9, 51.4, 18.1; IR (Neat Film, NaCl) 3062, 2948, 1719, 1631, 1558, 1435, 1346, 1274, 1191, 1168, 1037, 869, 785, 688 cm^{-1} ; HRMS (FAB+) m/z calc'd for $\text{C}_{11}\text{H}_{12}\text{O}_2\text{Br}$ $[\text{M}+\text{H}]^+$: 255.0021, found 255.0020.

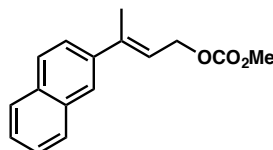


(E)-3-(3-Bromophenyl)but-2-en-1-yl methyl carbonate (76g). Carbonate **76g** was prepared from **91** according to Representative Procedure #2 and isolated by silica gel flash column chromatography (5% EtOAc/hexanes) as a colorless oil (0.47 g, 78% yield): ^1H NMR (400 MHz, CDCl_3) δ 7.54 (t, $J = 1.8$ Hz, 1H), 7.40 (ddd, $J = 7.9, 1.9, 1.0$ Hz, 1H), 7.32 (ddd, $J = 7.8, 1.8, 1.0$ Hz, 1H), 7.22 – 7.14 (m, 1H), 5.96 – 5.88 (m, 1H), 4.88 – 4.76 (m, 2H), 3.81 (s, 3H), 2.12 – 2.08 (m, 3H); ^{13}C NMR (101 MHz, CDCl_3) δ 155.93, 144.65, 139.74, 130.68, 129.96, 129.18, 124.64, 122.65, 122.08, 64.84, 55.02, 16.38; IR (Neat Film, NaCl) 2955, 1748, 1590, 1558, 1442, 1376, 1332, 1263, 946, 789, 690 cm^{-1} ; HRMS (FAB+) m/z calc'd for $\text{C}_{12}\text{H}_{13}\text{O}_3\text{Br}$ $[\text{M}]^+$: 284.0048, found 284.0073.

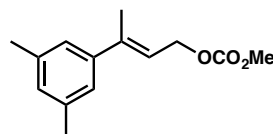


(E)-Methyl (3-(3-nitrophenyl)but-2-en-1-yl) carbonate (76h). Carbonate **76h** was prepared from methyl (E)-3-(3-nitrophenyl)but-2-enoate²⁰ according to Representative Procedure #2 and isolated by silica gel flash column chromatography (10% EtOAc/hexanes) as a colorless oil (0.47 g, 78% yield): ^1H NMR (400 MHz, CDCl_3) δ 8.26 (t, $J = 2.0$ Hz, 1H), 8.14 (ddd, $J = 8.2, 2.3, 1.0$ Hz, 1H), 7.73 (ddd, $J = 7.8, 1.8, 1.1$ Hz, 1H), 7.51 (t, $J = 8.0$ Hz, 1H), 6.10 – 5.91 (m, 1H), 4.88 (dt, $J = 6.9, 0.8$ Hz, 2H), 3.82 (s, 3H), 2.18 (dd, $J = 1.4, 0.7$ Hz, 3H); ^{13}C NMR (101 MHz, CDCl_3) δ 155.9, 148.5, 144.1, 138.7, 131.9, 129.4, 123.6, 122.5, 121.0, 64.7, 55.1, 16.4; IR (Neat Film, NaCl)

3108, 3026, 2969, 2868, 1750, 1530, 1443, 1384, 1353, 1279, 1096, 994, 949, 930, 876, 788, 736, 682 cm^{-1} ; HRMS (FAB+) m/z calc'd for $\text{C}_{12}\text{H}_{14}\text{O}_5\text{N}$ $[\text{M}+\text{H}]^+$: 252.0872, found 252.0884.

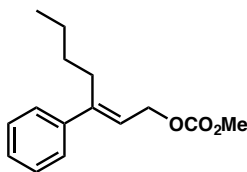


(*E*)-methyl (3-(Naphthalen-2-yl)but-2-en-1-yl) carbonate (76i). Carbonate **76i** was prepared from methyl (*E*)-3-(naphthalen-2-yl)but-2-enoate²⁴ according to Representative Procedure #2 and isolated by silica gel flash column chromatography (5% EtOAc/hexanes) as a colorless oil (0.26 g, 51% yield): ^1H NMR (400 MHz, CDCl_3) δ 7.86 – 7.77 (m, 4H), 7.58 (dd, J = 8.6, 1.9 Hz, 1H), 7.52 – 7.42 (m, 2H), 6.12 – 6.05 (m, 1H), 4.92 (dq, J = 7.0, 0.7 Hz, 2H), 3.82 (s, 3H), 2.29 – 2.22 (m, 3H); ^{13}C NMR (101 MHz, CDCl_3) δ 156.0, 140.9, 139.7, 133.4, 133.0, 128.3, 128.0, 127.7, 126.4, 126.1, 124.9, 124.3, 121.3, 65.2, 55.0, 16.5; IR (Neat Film, NaCl) 3057, 2952, 1752, 1740, 1596, 1467, 1442, 1382, 1248, 997, 941, 818, 794, 740 cm^{-1} ; HRMS (FAB+) m/z calc'd for $\text{C}_{16}\text{H}_{16}\text{O}_3$ $[\text{M}]^+$: 256.1100, found 256.1095.

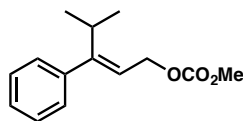


(*E*)-3-(3,5-Dimethylphenyl)but-2-en-1-yl methyl carbonate (76k). Carbonate **76k** was prepared from methyl (*E*)-3-(3,5-dimethylphenyl)but-2-enoate²⁵ according to Representative Procedure #2 and isolated by silica gel flash column chromatography (5%

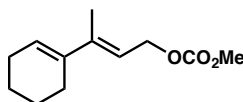
EtOAc/hexanes) as a colorless oil (0.32 g, 86% yield): ^1H NMR (400 MHz, CDCl_3) δ 7.02 (dt, $J = 1.6, 0.8$ Hz, 2H), 6.93 (td, $J = 1.6, 0.8$ Hz, 1H), 5.96 – 5.82 (m, 1H), 4.84 (dd, $J = 7.0, 0.8$ Hz, 2H), 3.80 (s, 3H), 2.31 (d, $J = 0.7$ Hz, 6H), 2.15 – 2.06 (m, 3H); ^{13}C NMR (101 MHz, CDCl_3) δ 156.0, 142.6, 141.5, 137.9, 129.4, 123.9, 120.4, 65.1, 54.9, 21.5, 16.5; IR (Neat Film, NaCl) 2956, 2918, 2862, 1748, 1601, 1443, 1376, 1335, 1262, 944, 905, 849, 792, 699 cm^{-1} ; HRMS (FAB+) m/z calc'd for $\text{C}_{14}\text{H}_{18}\text{O}_3$ $[\text{M}]^+$: 234.1256, found 234.1252.



(*E*)-Methyl (3-phenylhept-2-en-1-yl) carbonate (78b). Carbonate **78b** was prepared from ethyl (*E*)-3-phenylhept-2-enoate²⁶ according to Representative Procedure #2 and isolated by silica gel flash column chromatography (5% EtOAc/hexanes) as a colorless oil (0.31 g, 58% yield): ^1H NMR (400 MHz, CDCl_3) δ 7.48 – 7.27 (m, 5H), 5.89 – 5.71 (m, 1H), 4.84 (d, $J = 7.0$ Hz, 2H), 3.80 (s, 3H), 2.73 – 2.46 (m, 2H), 1.41 – 1.24 (m, 4H), 1.06 – 0.73 (m, 3H); ^{13}C NMR (101 MHz, CDCl_3) δ 156.0, 146.6, 142.0, 128.4, 127.6, 126.6, 121.1, 65.0, 55.0, 31.2, 30.2, 22.7, 14.0; IR (Neat Film, NaCl) 3034, 2957, 2872, 1748, 1644, 1599, 1493, 1444, 1378, 1344, 1262, 1129, 941, 792, 766, 698 cm^{-1} ; HRMS (FAB+) m/z calc'd for $\text{C}_{15}\text{H}_{20}\text{O}_3$ $[\text{M}]^+$: 248.1412, found 248.1424.

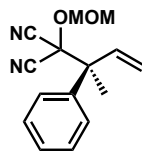


(E)-Methyl (4-methyl-3-phenylpent-2-en-1-yl) carbonate (78c). Carbonate **78c** was prepared from ethyl (*E*)-4-methyl-3-phenylpent-2-enoate²⁷ according to Representative Procedure #2 and isolated by silica gel flash column chromatography (5% EtOAc/hexanes) as a colorless oil (0.17 g, 17% yield): ¹H NMR (400 MHz, CDCl₃) δ 7.37 – 7.27 (m, 3H), 7.11 – 7.02 (m, 2H), 5.61 (td, *J* = 7.0, 1.3 Hz, 1H), 4.46 (dd, *J* = 7.0, 0.8 Hz, 2H), 3.75 (s, 3H), 2.66 – 2.54 (m, 1H), 1.03 (d, *J* = 6.8 Hz, 6H); ¹³C NMR (101 MHz, CDCl₃) δ 155.8, 154.0, 139.7, 128.5, 128.2, 127.3, 117.8, 66.1, 54.8, 36.0, 21.5; IR (Neat Film, NaCl) 2961, 2872, 1749, 1492, 1442, 1263, 942, 792, 771, 703 cm⁻¹; HRMS (FAB+) *m/z* calc'd for C₁₄H₁₉O₃ [M+H]⁺: 235.1334, found 235.1344.



(E)-3-(Cyclohex-1-en-1-yl)but-2-en-1-yl methyl carbonate (78e). Carbonate **78e** was prepared from ethyl (*E*)-3-(cyclohex-1-en-1-yl)but-2-enoate²⁸ according to Representative Procedure #2 and isolated by silica gel flash column chromatography (5% EtOAc/hexanes) as a colorless oil (0.25 g, 73% yield): ¹H NMR (400 MHz, CDCl₃) δ 6.00 – 5.92 (m, 1H), 5.68 – 5.55 (m, 1H), 4.79 (d, *J* = 7.0 Hz, 2H), 3.78 (s, 3H), 2.16 (ddd, *J* = 12.0, 5.9, 3.7 Hz, 4H), 1.85 (d, *J* = 1.1 Hz, 3H), 1.73 – 1.49 (m, 4H); ¹³C NMR (101 MHz, CDCl₃) δ 156.0, 141.2, 137.0, 126.0, 116.8, 65.5, 54.9, 26.1, 25.8, 23.0, 22.3, 14.1; IR (Neat Film, NaCl) 2929, 2859, 1749, 1638, 1443, 1263, 1119, 940, 792 cm⁻¹; HRMS (FAB+) *m/z* calc'd for C₁₂H₁₈O₃ [M]⁺: 210.1256, found 210.1252.

3.7.2.3 General Procedure for Optimization Reactions (Table 3.1)

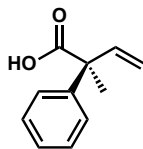


(S)-2-(Methoxymethoxy)-2-(2-phenylbut-3-en-2-yl)malononitrile (73). In a nitrogen-filled glove box, to a 1 dram vial (vial A) equipped with a stir bar was added $[\text{Ir}(\text{cod})\text{Cl}]_2$ (1.3 mg, 0.0020 mmol, 2 mol %), ligand (*S_a*)-**L5** (2.5 mg, 0.0042 mmol, 4.2 mol %), TBD (1.4 mg, 0.010 mmol, 10 mol %), and THF (0.5 mL). Vial A was stirred at 25 °C (ca. 10 min) while another 1 dram vial (vial B) was charged with MAC nucleophile **67c** (0.10 mmol or 0.20 mmol, as specified), THF (0.5 mL), and the Lewis acid additive (200 mol %). The pre-formed catalyst solution (vial A) was then transferred to vial B followed immediately by carbonate **72** (0.20 mmol, 0.10 mmol, or 0.12 mmol, as specified). The vial was sealed and stirred at 60 °C. After 18 h, the vial was removed from the glove box and filtered through a pad of silica, rinsing with EtOAc. The crude mixture was concentrated and 1,2,4,5-tetrachloro-3-nitrobenzene (0.10 mmol in 0.5 mL CDCl_3) was added. The NMR yield (measured in reference to 1,2,4,5-tetrachloro-3-nitrobenzene δ 7.74 ppm (s, 1H)) was determined by ^1H NMR analysis of the crude mixture. The residue was purified by preparatory TLC (15% EtOAc/hexanes) to afford MAC adduct product **73** as a colorless oil. For the purposes of characterization, product **73** was further purified by preparatory HPLC (20% EtOAc/hexanes, Viridis SFC 2-Ethylpyridine 5 μm column, flow rate = 1.5 mL/min; λ = 230 nm): 94% ee (entry 9); $[\alpha]_{\text{D}}^{25} +11.7$ (*c* 0.07, CHCl_3) (entry 9); ^1H NMR (400 MHz, CDCl_3) δ 7.61 – 7.54 (m, 2H), 7.42 – 7.32 (m, 3H), 6.51 (dd, *J* = 17.4, 11.0 Hz, 1H), 5.59 – 5.34 (m, 2H), 5.02 (s, 2H), 3.42 (s, 3H), 1.84 (s, 3H);

^{13}C NMR (101 MHz, CDCl_3) δ 138.3, 137.6, 129.0, 128.57, 238.55, 128.3, 125.2, 119.2, 112.8, 112.7, 96.7, 73.9, 57.5, 52.8, 20.9; IR (Neat Film, NaCl) 3062, 2957, 2896, 2242, 2189, 1750, 1492, 1445, 1358, 1268, 1161, 1108, 1030, 930, 751, 698 cm^{-1} ; HRMS (ESI+) m/z calc'd for $\text{C}_{15}\text{H}_{17}\text{N}_2\text{O}_2$ $[\text{M}+\text{H}]^+$: 257.1290, found 257.1313; HPLC conditions: 1% IPA, 1.0 mL/min, Chiralpak IC column, λ = 210 nm, t_R (min): major = 13.303, minor = 17.243.

3.7.2.4 General Procedure for the Enantioenriched Carboxylic Acid Synthesis

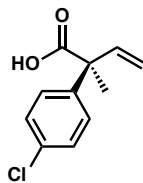
Please note that the absolute configuration was determined only for compound **77h** via x-ray crystallographic analysis. The absolute configuration for all other products has been inferred by analogy. For respective HPLC and SFC conditions, please refer to Table 3.6.



(S)-2-Methyl-2-phenylbut-3-enoic acid (77a). In a nitrogen-filled glove box, to a 1 dram vial (vial A) equipped with a stir bar was added $[\text{Ir}(\text{cod})\text{Cl}]_2$ (2.7 mg, 0.0040 mmol, 2 mol %), ligand (S_a)-**L5** (4.9 mg, 0.0084 mmol, 4.2 mol %), TBD (2.8 mg, 0.020 mmol, 10 mol %), and THF (1 mL). Vial A was stirred at 25 °C (ca. 10 min) while another 1 dram vial (vial B) was charged with MAC nucleophile **67c** (25 mg, 0.20 mmol, 100 mol %), THF (1 mL), and BEt_3 (400 μL , 1M in hexanes). The pre-formed catalyst solution (vial A) was then transferred to vial B followed immediately by carbonate **72** (83 mg, 0.40 mmol, 200 mol %). The vial was sealed and stirred at 60 °C. After 18 h or 48 h,

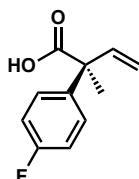
the vial was removed from the glove box, transferred to a 20 mL vial with CH_2Cl_2 , and concentrated. The crude material was heated at 80 °C in 6M HCl (4 mL) for 18 h. Whereupon, the reaction mixture was cooled to 0 °C and basified with 6M NaOH (4.5 mL). The aqueous layer was extracted with CH_2Cl_2 (4 x 8 mL). The combined organic layers were washed with 2M NaOH (8 mL). The combined aqueous layers were acidified with concentrated HCl, extracted with CH_2Cl_2 (4 x 8 mL), dried over Na_2SO_4 , and concentrated under reduced pressure at 0 °C to give the product **77a** as a colorless solid (27 mg, 77% yield): 95% ee; $[\alpha]_{\text{D}}^{25} +13.5$ (c 1.3, CHCl_3); HPLC conditions: 2% IPA, 1.0 mL/min, Chiralpak AD-H column, λ = 210 nm, t_{R} (min): major = 12.198, minor = 11.426. Characterization data match those reported in the literature.²⁹ *Please note* Compounds **77i**, **77j**, **77k**, and **79a–g** were prepared at the same concentration with double catalyst loadings.

3.7.2.5 Spectroscopic Data for the Enantioenriched Carboxylic Acids

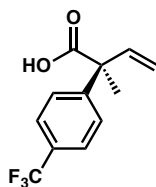


(S)-2-(4-Chlorophenyl)-2-methylbut-3-enoic acid (77b). Product **77b** was prepared according to the general procedure to give a pale yellow oil (33 mg, 80% yield): 93% ee; $[\alpha]_{\text{D}}^{25} +8.1$ (c 1.8, CHCl_3); ^1H NMR (400 MHz, CDCl_3) δ 7.38 – 7.24 (m, 4H), 6.38 (dd, J = 17.5, 10.7 Hz, 1H), 5.44 – 5.16 (m, 2H), 1.66 (s, 3H); ^{13}C NMR (101 MHz, CDCl_3) δ 180.4, 141.1, 140.1, 133.3, 128.7, 128.3, 116.1, 53.3, 23.3; IR (Neat Film, NaCl) 3089, 2987, 2645, 2539, 1705, 1493, 1400, 1282, 1097, 1014, 928, 826, 755 cm^{-1} ; HRMS

(FAB+) m/z calc'd for $C_{11}H_{12}O_2Cl$ $[M+H]^+$: 211.0526, found 211.0528; HPLC conditions: 2% IPA, 1.0 mL/min, Chiralpak AD-H column, λ = 210 nm, t_R (min): major = 15.642, minor = 14.104.

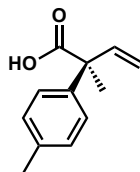


(S)-2-(4-Fluorophenyl)-2-methylbut-3-enoic acid (77c). Product **77c** was prepared according to the general procedure to give a pale yellow oil (35 mg, 90% yield): 90% ee; $[\alpha]_D^{25} +3.4$ (c 1.5, $CHCl_3$); 1H NMR (400 MHz, $CDCl_3$) δ 7.46 – 7.19 (m, 2H), 7.05 (t, J = 8.7 Hz, 2H), 6.39 (dd, J = 17.5, 10.7 Hz, 1H), 5.42 – 5.14 (m, 2H), 1.67 (s, 3H); ^{13}C NMR (101 MHz, $CDCl_3$) δ 180.6, 163.2, 160.7, 140.4, 138.3 (d, J = 3.4 Hz), 128.5 (d, J = 8.1 Hz), 115.9, 115.5, 115.3, 53.2, 23.5; IR (Neat Film, NaCl) 3088, 2987, 2924, 2642, 1704, 1603, 1510, 1462, 1412, 1277, 1234, 1165, 928, 833, 816, 735 cm^{-1} ; HRMS (FAB+) m/z calc'd for $C_{11}H_{12}FO_2$ $[M+H]^+$: 195.0833, found 195.0841; HPLC conditions: 2% IPA, 1.0 mL/min, Chiralpak AD-H column, λ = 210 nm, t_R (min): major = 15.499, minor = 13.811.

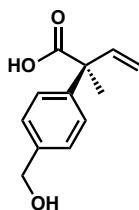


(S)-2-Methyl-2-(4-(trifluoromethyl)phenyl)but-3-enoic acid (77d). Product **77d** was prepared according to the general procedure to give a pale yellow oil (41 mg, 83% yield):

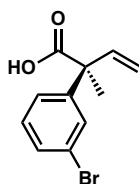
92% ee; $[\alpha]_D^{25} -2.2$ (*c* 2.3, CHCl₃); ¹H NMR (400 MHz, CDCl₃) δ 7.60 (dt, *J* = 8.1, 0.8 Hz, 2H), 7.45 (dt, *J* = 8.3, 0.8 Hz, 2H), 6.38 (dd, *J* = 17.5, 10.7 Hz, 1H), 5.48 – 5.09 (m, 2H), 1.68 (s, 3H); ¹³C NMR (101 MHz, CDCl₃) δ 179.0, 146.6, 139.7, 129.6, 130.0, 129.5, 127.2, 125.6 (q, *J* = 3.7 Hz), 122.8, 116.6, 53.7, 29.9, 23.4; IR (Neat Film, NaCl) 2926, 2649, 1707, 1618, 1413, 1328, 1277, 1167, 1126, 1081, 1016, 930, 940 cm⁻¹; HRMS (FAB+) *m/z* calc'd for C₁₂H₁₂O₂F₃ [M+H]⁺: 245.0789, found 245.0794; SFC conditions: 2% IPA, 2.5 mL/min, Chiralpak AD-H column, λ = 210 nm, *t_R* (min): major = 13.592, minor = 15.745.



(*S*)-2-Methyl-2-(*p*-tolyl)but-3-enoic acid (77e). Product **77e** was prepared according to the general procedure to give a pale yellow oil (24 mg, 63% yield): 94% ee; $[\alpha]_D^{25} +4.6$ (*c* 0.8, CHCl₃); ¹H NMR (400 MHz, CDCl₃) δ 7.42 – 7.01 (m, 4H), 6.40 (dd, *J* = 17.5, 10.7 Hz, 1H), 5.59 – 5.08 (m, 2H), 2.34 (s, 3H), 1.64 (s, 3H); ¹³C NMR (101 MHz, CDCl₃) δ 181.0, 140.7, 139.8, 137.0, 129.3, 126.6, 115.4, 53.3, 23.3, 21.1; IR (Neat Film, NaCl) 2986, 1702, 1636, 1512, 1457, 1412, 1276, 1191, 1132, 1077, 1020, 925, 815, 730 cm⁻¹; HRMS (ESI-) *m/z* calc'd for C₁₂H₁₃O₂ [M-H]⁻: 189.0916, found 189.0903; HPLC conditions: 2% IPA, 1.0 mL/min, Chiralpak AD-H column, λ = 210 nm, *t_R* (min): major = 15.393, minor = 14.288.

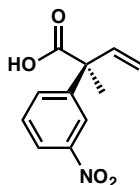


(S)-2-(4-(Hydroxymethyl)phenyl)-2-methylbut-3-enoic acid (77f). Product **77f** was prepared according to the general procedure and isolated by preparatory TLC (30% acetone/hexanes) to give a colorless solid (21 mg, 51% yield): 95% ee; $[\alpha]_D^{25} +3.4$ (c 0.5, CHCl_3); ^1H NMR (400 MHz, CDCl_3) δ 7.33 (q, $J = 8.2$ Hz, 4H), 6.37 (dd, $J = 17.5, 10.7$ Hz, 1H), 5.39 – 5.10 (m, 2H), 4.57 (s, 2H), 1.63 (s, 3H); ^{13}C NMR (101 MHz, CDCl_3) δ 180.1, 143.2, 140.4, 136.4, 128.8, 127.2, 115.8, 53.6, 45.9, 23.4; IR (Neat Film, NaCl) 2985, 2927, 2642, 1703, 1636, 1512, 1460, 1268, 1182, 1076, 926, 836, 731, 683 cm^{-1} ; HRMS (FAB+) m/z calc'd for $\text{C}_{12}\text{H}_{15}\text{O}_3$ $[\text{M}+\text{H}]^+$: 207.1021, found 207.1025; HPLC conditions: 2% IPA, 1.0 mL/min, Chiralpak AD-H column, $\lambda = 210$ nm, t_R (min): major = 15.258, minor = 14.667.

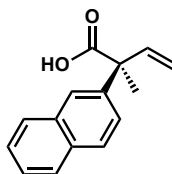


(S)-2-(3-Bromophenyl)-2-methylbut-3-enoic acid (77g). Product **77g** was prepared according to the general procedure to give a pale yellow oil (35 mg, 69% yield): 92% ee; $[\alpha]_D^{25} -2.6$ (c 1.8, CHCl_3); ^1H NMR (400 MHz, CDCl_3) δ 7.47 (t, $J = 1.9$ Hz, 1H), 7.41 (ddd, $J = 7.6, 1.9, 1.2$ Hz, 1H), 7.29 – 7.18 (m, 2H), 6.35 (dd, $J = 17.5, 10.7$ Hz, 1H), 5.42 – 5.09 (m, 2H), 1.65 (s, 3H); ^{13}C NMR (101 MHz, CDCl_3) δ 179.7, 145.0, 139.8,

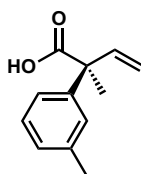
130.5, 130.2, 129.9, 125.5, 122.8, 116.4, 53.5, 23.3; IR (Neat Film, NaCl) 2987, 2644, 1705, 1593, 1566, 1475, 1413, 1280, 1129, 1070, 997, 928, 785, 760, 700 cm^{-1} ; HRMS (ESI-) m/z calc'd for $\text{C}_{11}\text{H}_{10}\text{O}_2\text{Br}$ $[\text{M}-\text{H}]^-$: 252.9864, found 252.9864; HPLC conditions: 2% IPA, 1.0 mL/min, Chiralpak AD-H column, λ = 210 nm, t_R (min): major = 15.217, minor = 14.439.



(S)-2-Methyl-2-(3-nitrophenyl)but-3-enoic acid (77h). Product **77h** was prepared according to the general procedure to give a colorless solid (41 mg, 93% yield): 87% ee; $[\alpha]_D^{25} +94.5$ (c 3.4, CHCl_3); ^1H NMR (400 MHz, CDCl_3) δ 8.22 (t, J = 2.0 Hz, 1H), 8.15 (ddd, J = 8.2, 2.2, 1.0 Hz, 1H), 7.69 (ddd, J = 7.9, 1.9, 1.1 Hz, 1H), 7.53 (t, J = 8.0 Hz, 1H), 6.38 (dd, J = 17.5, 10.7 Hz, 1H), 5.59 – 5.11 (m, 2H), 1.72 (s, 3H); ^{13}C NMR (101 MHz, CDCl_3) δ 179.6, 148.5, 144.7, 139.2, 133.3, 129.6, 122.5, 122.1, 117.2, 53.7, 23.4; IR (Neat Film, NaCl) 3089, 2988, 2924, 2641, 1707, 1530, 1351, 1276, 1106, 929, 808, 738, 688 cm^{-1} ; HRMS (FAB+) m/z calc'd for $\text{C}_{11}\text{H}_{12}\text{O}_4\text{N}$ $[\text{M}+\text{H}]^+$: 222.0766, found 222.0769; HPLC conditions: 3% IPA, 1.0 mL/min, Chiralpak AD-H column, λ = 210 nm, t_R (min): major = 24.060, minor = 20.907.

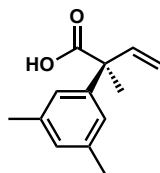


(S)-2-Methyl-2-(naphthalen-2-yl)but-3-enoic acid (77i). Product **77i** was prepared according to the general procedure to give a pale yellow oil (30 mg, 66% yield): 92% ee; $[\alpha]_D^{25} +7.8$ (c 0.6, CHCl_3); ^1H NMR (400 MHz, CDCl_3) δ 7.91 – 7.72 (m, 4H), 7.55 – 7.39 (m, 3H), 6.52 (dd, $J = 17.5, 10.7$ Hz, 1H), 5.57 – 5.11 (m, 2H), 1.77 (s, 3H); ^{13}C NMR (101 MHz, CDCl_3) δ 180.9, 140.5, 140.0, 133.3, 132.5, 128.3, 128.2, 127.6, 126.3, 126.2, 125.3, 125.2, 116.0, 53.9, 23.4; IR (Neat Film, NaCl) 3057, 2984, 1701, 1506, 1458, 1411, 1274, 1182, 1128, 1102, 925, 856, 816, 747 cm^{-1} ; HRMS (FAB+) m/z calc'd for $\text{C}_{15}\text{H}_{14}\text{O}_2$ $[\text{M}]^+$: 226.0994, found 226.0992; HPLC conditions: 2% IPA, 1.0 mL/min, Chiralpak AD-H column, $\lambda = 210$ nm, t_R (min): major = 28.272, minor = 24.870.

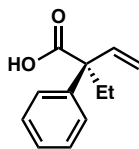


(S)-2-Methyl-2-(*m*-tolyl)but-3-enoic acid (77j). Product **77j** was prepared according to the general procedure to give a pale yellow oil (26 mg, 68% yield): 93% ee; $[\alpha]_D^{25} +5.2$ (c 1.6, CHCl_3); ^1H NMR (400 MHz, CDCl_3) δ 7.25 – 7.04 (m, 4H), 6.40 (dd, $J = 17.5, 10.7$ Hz, 1H), 5.45 – 5.08 (m, 2H), 2.44 – 2.20 (m, 3H), 1.65 (s, 3H); ^{13}C NMR (101 MHz, CDCl_3) δ 180.2, 142.7, 140.6, 138.3, 128.5, 128.1, 127.3, 123.7, 115.6, 53.6, 23.3, 21.7; IR (Neat Film, NaCl) 2984, 2923, 2648, 1703, 1606, 1459, 1411, 1275, 1178, 1127, 1002, 926, 785, 703 cm^{-1} ; HRMS (FAB+) m/z calc'd for $\text{C}_{12}\text{H}_{15}\text{O}_2$ $[\text{M}+\text{H}]^+$: 191.1072,

found 191.1074; HPLC conditions: 2% IPA, 1.0 mL/min, Chiralpak AD-H column, λ = 210 nm, t_R (min): major = 13.800, minor = 12.388.

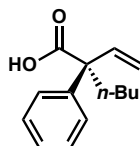


(S)-2-(3,5-Dimethylphenyl)-2-methylbut-3-enoic acid (77k). Product **77k** was prepared according to the general procedure and isolated by preparatory TLC (30% acetone/hexanes) to give a colorless oil (13 mg, 32% yield): 85% ee; $[\alpha]_D^{25}$ -40.6 (c 0.1, CHCl_3); ^1H NMR (400 MHz, CDCl_3) δ 6.94 (d, J = 8.5 Hz, 3H), 6.42 (dd, J = 17.4, 10.6 Hz, 1H), 5.45 – 5.08 (m, 2H), 2.33 (s, 6H), 1.65 (s, 3H); ^{13}C NMR (101 MHz, CDCl_3) δ 180.5, 142.8, 140.8, 138.1, 129.0, 124.4, 115.3, 53.6, 23.3, 21.6; IR (Neat Film, NaCl) 2983, 2919, 2639, 1700, 1602, 1411, 1279, 1125, 923, 848, 708 cm^{-1} ; HRMS (FAB+) m/z calc'd for $\text{C}_{13}\text{H}_{17}\text{O}_2$ $[\text{M}+\text{H}]^+$: 205.1229, found 205.1233; HPLC conditions: 2% IPA, 1.0 mL/min, Chiralpak AD-H column, λ = 210 nm, t_R (min): major = 11.107, minor = 10.064. *Please note* an HMBC has been included due to the low intensity of the carbonyl ^{13}C shift at δ 180.5.

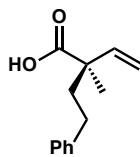


(S)-2-Ethyl-2-phenylbut-3-enoic acid (79a). Product **79a** was prepared according to the general procedure and isolated by preparatory TLC (30% acetone/hexanes) to give a

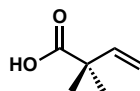
colorless oil (23 mg, 61% yield): 92% ee; $[\alpha]_D^{25} +17.4$ (c 0.4, CHCl_3); ^1H NMR (400 MHz, CDCl_3) δ 7.38 – 7.22 (m, 5H), 6.36 (dd, $J = 17.7, 10.9$ Hz, 1H), 5.35 (d, $J = 10.7$ Hz, 1H), 5.09 (d, $J = 17.6$ Hz, 1H), 2.36 – 2.00 (m, 2H), 0.87 (t, $J = 7.2$ Hz, 3H); ^{13}C NMR (101 MHz, CDCl_3) δ 180.1, 141.3, 139.1, 128.4, 127.6, 127.2, 116.9, 58.0, 29.4, 9.4; IR (Neat Film, NaCl) 3060, 2970, 2928, 2636, 1702, 1495, 1448, 1407, 1381, 1261, 1083, 924, 761, 700 cm^{-1} ; HRMS (FAB+) m/z calc'd for $\text{C}_{12}\text{H}_{15}\text{O}_2$ $[\text{M}+\text{H}]^+$: 191.1072, found 191.1071; HPLC conditions: 1.5% IPA, 1.0 mL/min, two Chiralpak AD-H columns in series, $\lambda = 210$ nm, t_R (min): major = 46.253, minor = 47.271.



(S)-2-Phenyl-2-vinylhexanoic acid (79b). Product **79b** was prepared according to the general procedure and isolated by preparatory TLC (30% acetone/hexanes) to give a colorless oil (6 mg, 14% yield): 95% ee; $[\alpha]_D^{25} -106.0$ (c 0.07, CHCl_3); ^1H NMR (400 MHz, CDCl_3) δ 7.40 – 7.29 (m, 5H), 6.38 (dd, $J = 17.6, 10.9$ Hz, 1H), 5.32 (dd, $J = 10.9, 0.9$ Hz, 1H), 5.06 (dd, $J = 17.6, 0.9$ Hz, 1H), 2.28 – 1.98 (m, 2H), 1.44 – 1.14 (m, 4H), 0.87 (t, $J = 7.2$ Hz, 3H); ^{13}C NMR (101 MHz, CDCl_3) δ 178.4, 141.6, 139.7, 128.4, 127.5, 127.1, 116.6, 57.5, 36.5, 27.0, 23.4, 14.1; IR (Neat Film, NaCl) 2956, 2920, 2851, 1734, 1706, 1466, 1378, 1260, 1098, 925, 800, 722, 700 cm^{-1} ; HRMS (FAB+) m/z calc'd for $\text{C}_{14}\text{H}_{19}\text{O}_2$ $[\text{M}+\text{H}]^+$: 219.1385, found 219.1291; SFC conditions: 5% IPA, 2.5 mL/min, Chiralpak AD-H column, $\lambda = 210$ nm, t_R (min): major = 10.646, minor = 11.952.

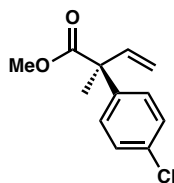


(R)-2-Methyl-2-phenethylbut-3-enoic acid (79f). Product **79f** was prepared according to the general procedure and isolated by preparatory TLC (33% acetone/hexanes) to give a colorless oil (13 mg, 32% yield): 3% ee; $[\alpha]_D^{25} -12.1$ (c 0.7, CHCl_3); ^1H NMR (400 MHz, CDCl_3) δ 7.44 – 7.04 (m, 5H), 6.10 (dd, J = 17.6, 10.7 Hz, 1H), 5.21 (dd, J = 14.0, 3.3 Hz, 2H), 2.60 (dt, J = 11.0, 4.9 Hz, 2H), 2.33 – 1.79 (m, 2H), 1.40 (s, 3H); ^{13}C NMR (101 MHz, CDCl_3) δ 182.0, 142.0, 140.9, 128.54, 128.49, 126.1, 114.7, 48.7, 41.1, 31.2, 20.7; IR (Neat Film, NaCl) 3026, 2927, 1702, 1496, 1454, 1380, 1264, 1097, 925, 748, 700 cm^{-1} ; HRMS (FAB+) m/z calc'd for $\text{C}_{13}\text{H}_{17}\text{O}_2$ $[\text{M}+\text{H}]^+$: 267.1385, found 267.1376; HPLC conditions: 2% IPA, 1.0 mL/min, Chiralpak AD-H column, λ = 210 nm, t_R (min): major = 18.485, minor = 14.652. *Please note* an HMBC has been included due to the low intensity of the carbonyl ^{13}C shift at δ 182.0.



2,2-Dimethylbut-3-enoic acid (79g). Product **79g** was prepared according to the general procedure to give a colorless oil (15 mg, 63% yield). Characterization data match those reported in the literature.³⁰

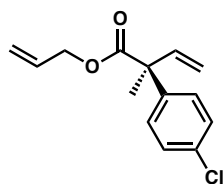
3.7.2.6 Experimental Procedures and Spectroscopic Data for the One-pot Syntheses of Carboxylic Acid Derivatives



Methyl (*S*)-2-(4-chlorophenyl)-2-methylbut-3-enoate (82). In a nitrogen-filled glove box, to a scintillation vial (vial A) equipped with a stir bar was added $[\text{Ir}(\text{cod})\text{Cl}]_2$ (13 mg, 0.02 mmol, 2 mol %), ligand (*S_a*)-**L5** (25 mg, 0.042 mmol, 4.2 mol %), TBD (14 mg, 0.10 mmol, 10 mol %), and THF (5 mL). Vial A was stirred at 25 °C (ca. 10 min) while another scintillation vial (vial B) was charged with MAC nucleophile **67c** (126 mg, 1.0 mmol, 100 mol %), THF (5 mL), and BEt_3 (2.0 mL, 1M in hexanes). The pre-formed catalyst solution (vial A) was then transferred to vial B followed immediately by carbonate **76b** (480 mg, 2.0 mmol, 200 mol %). The vial was sealed and stirred at 60 °C. After 18 h, the vial was removed from the glove box and the reaction mixture was concentrated under reduced pressure.

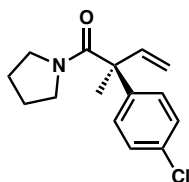
To the vial of crude MAC adduct equipped with a stir bar and septum cap was added 1:1 AcOH/DME (2 mL, 0.5 M) and CSA (0.26 g, 1.1 mmol, 1.1 equiv) under a nitrogen atmosphere. The reaction was heated to 60 °C for 6 h, whereupon the reaction mixture was cooled to ambient temperature, diluted with anhydrous MeOH (2.8 mL), and cooled to –40 °C. A solution of 1:1 MeOH/ Et_3N (5.6 mL, 20.1 equiv of Et_3N) was added dropwise over 10 min. The reaction mixture was allowed to warm to ambient temperature over 18 h, whereupon the reaction was slowly quenched with saturated NH_4Cl aqueous solution (5 mL). The aqueous layer was then extracted with CH_2Cl_2 (3 x 10 mL) and the

combined organic layers were washed with brine (10 mL), dried over Na_2SO_4 , and concentrated under reduced pressure at 0 °C. The crude residue was purified by silica gel flash column chromatography (10% EtOAc/hexanes) to give methyl ester **82** as a colorless oil (0.20 g, 88% yield): $[\alpha]_{\text{D}}^{25} +1.5$ (c 0.8, CHCl_3); ^1H NMR (400 MHz, CDCl_3) δ 7.41 – 6.99 (m, 4H), 6.35 (dd, J = 17.5, 10.7 Hz, 1H), 5.48 – 5.00 (m, 2H), 3.70 (s, 3H), 1.62 (s, 3H); ^{13}C NMR (101 MHz, CDCl_3) δ 175.0, 142.0, 140.6, 132.9, 128.7, 128.1, 115.6, 53.5, 52.7, 23.7; IR (Neat Film, NaCl) 2986, 2952, 1734, 1637, 1493, 1459, 1246, 1181, 1123, 1098, 1014, 926, 828, 757 cm^{-1} ; HRMS (FAB+) m/z calc'd for $\text{C}_{12}\text{H}_{13}\text{ClO}_2$ $[\text{M}]^+$: 224.0604, found 224.0621.



Allyl (*S*)-2-(4-chlorophenyl)-2-methylbut-3-enoate (83). In a nitrogen-filled glove box, to a 1 dram vial (vial A) equipped with a stir bar was added $[\text{Ir}(\text{cod})\text{Cl}]_2$ (2.7 mg, 0.0040 mmol, 2 mol %), ligand (*S_a*)-**L5** (4.9 mg, 0.0084 mmol, 4.2 mol %), TBD (2.8 mg, 0.020 mmol, 10 mol %), and THF (1 mL). Vial A was stirred at 25 °C (ca. 10 min) while another 1 dram vial (vial B) was charged with MAC nucleophile **67c** (25 mg, 0.20 mmol, 100 mol %), THF (1 mL), and BEt_3 (400 μL , 1M in hexanes). The pre-formed catalyst solution (vial A) was then transferred to vial B followed immediately by carbonate **76b** (96 mg, 0.40 mmol, 200 mol %). The vial was sealed and stirred at 60 °C. After 18 h, the vial was removed from the glove box, transferred to a 20 mL vial with CH_2Cl_2 , and concentrated.

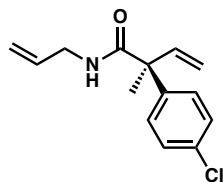
To the vial of crude MAC adduct equipped with a stir bar and septum cap was added 1:1 AcOH/DME (0.4 mL, 0.5 M) and CSA (51 mg, 0.22 mmol, 1.1 equiv) under a nitrogen atmosphere. The reaction was heated to 60 °C for 6 h, whereupon the reaction mixture was cooled to ambient temperature, diluted with allyl alcohol (0.4 mL), and cooled to 0 °C. A solution of 1:1 Et₃N/allyl alcohol (1.1 mL, 20.4 equiv of Et₃N) was added dropwise over 10 min. The reaction mixture was allowed to warm to ambient temperature over 18 h, whereupon the reaction was slowly quenched with saturated NH₄Cl aqueous solution (5 mL). The aqueous layer was then extracted with CH₂Cl₂ (3 x 10 mL) and the combined organic layers were washed with brine (10 mL), dried over Na₂SO₄, and concentrated under reduced pressure at 0 °C. The crude residue was purified by preparatory TLC (8% EtOAc/hexanes) to give allyl ester **83** as a colorless oil (37 mg, 74% yield): [α]_D²⁵ +0.4 (*c* 2.3, CHCl₃); ¹H NMR (400 MHz, CDCl₃) δ 7.35 – 7.12 (m, 4H), 6.36 (dd, *J* = 17.5, 10.7 Hz, 1H), 5.85 (ddt, *J* = 17.2, 10.5, 5.6 Hz, 1H), 5.38 – 5.02 (m, 4H), 4.61 (dt, *J* = 5.6, 1.4 Hz, 2H), 1.63 (s, 3H); ¹³C NMR (101 MHz, CDCl₃) δ 174.1, 142.0, 140.6, 132.9, 131.9, 128.6, 128.1, 118.5, 115.6, 65.9, 53.5, 23.6; IR (Neat Film, NaCl) 3089, 2985, 2930, 2857, 1900, 1734, 1638, 1493, 1236, 1177, 1122, 1097, 1014, 926, 828, 756 cm⁻¹; HRMS (FAB+) *m/z* calc'd for C₁₄H₁₆O₂Cl [M+H]⁺: 251.0839, found 251.0842.



(S)-2-(4-Chlorophenyl)-2-methyl-1-(pyrrolidin-1-yl)but-3-en-1-one (84). In a nitrogen-filled glove box, to a 1 dram vial (vial A) equipped with a stir bar was added $[\text{Ir}(\text{cod})\text{Cl}]_2$ (2.7 mg, 0.0040 mmol, 2 mol %), ligand (*S_a*)-**L5** (4.9 mg, 0.0084 mmol, 4.2 mol %), TBD (2.8 mg, 0.020 mmol, 10 mol %), and THF (1 mL). Vial A was stirred at 25 °C (ca. 10 min) while another 1 dram vial (vial B) was charged with MAC nucleophile **67c** (25 mg, 0.20 mmol, 100 mol %), THF (1 mL), and BEt_3 (400 μL , 1M in hexanes). The pre-formed catalyst solution (vial A) was then transferred to vial B followed immediately by carbonate **76b** (96 mg, 0.40 mmol, 200 mol %). The vial was sealed and stirred at 60 °C. After 18 h, the vial was removed from the glove box, transferred to a 20 mL vial with CH_2Cl_2 , and concentrated.

To the vial of crude MAC adduct equipped with a stir bar and septum cap was added 1:1 AcOH/DME (0.4 mL, 0.5 M) and CSA (51 mg, 0.22 mmol, 1.1 equiv) under a nitrogen atmosphere. The reaction was heated to 60 °C for 6 h, whereupon the reaction mixture was cooled to ambient temperature, diluted with CH_2Cl_2 (0.4 mL), and cooled to –40 °C. A solution of 1:1 pyrrolidine/ CH_2Cl_2 (0.67 mL, 20.4 equiv of pyrrolidine) was added dropwise over 10 min then Et_3N (0.57 mL, 4.1 mmol, 20.4 equiv). The reaction mixture was allowed to warm to ambient temperature over 18 h, whereupon the reaction was slowly quenched with saturated NH_4Cl aqueous solution (5 mL). The aqueous layer was then extracted with CH_2Cl_2 (3 x 10 mL) and the combined organic layers were washed with brine (10 mL), dried over Na_2SO_4 , and concentrated under reduced pressure.

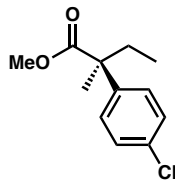
at 0 °C. The crude residue was purified by preparatory TLC (30% acetone/hexanes) to give amide **84** as a colorless oil (32 mg, 61% yield): $[\alpha]_D^{25} -49.5$ (c 1.7, CHCl_3); ^1H NMR (400 MHz, CDCl_3) δ 7.34 – 7.28 (m, 2H), 7.21 – 7.14 (m, 2H), 6.45 (dd, $J = 17.4, 10.7$ Hz, 1H), 5.27 (dd, $J = 10.7, 0.8$ Hz, 1H), 5.10 (dd, $J = 17.4, 0.8$ Hz, 1H), 3.63 – 3.47 (m, 2H), 2.98 (dt, $J = 10.6, 6.3$ Hz, 1H), 2.52 (dt, $J = 10.6, 6.7$ Hz, 1H), 1.78 – 1.62 (m, 2H), 1.64 – 1.55 (m, 5H); ^{13}C NMR (101 MHz, CDCl_3) δ 172.1, 143.2, 139.7, 132.5, 129.0, 127.6, 115.5, 54.3, 47.52, 47.44, 28.4, 26.5, 23.5; IR (Neat Film, NaCl) 2928, 2873, 1742, 1627, 1491, 1396, 1228, 1185, 1096, 1012, 921, 829, 723 cm^{-1} ; HRMS (FAB+) m/z calc'd for $\text{C}_{15}\text{H}_{19}\text{ClNO}$ $[\text{M}+\text{H}]^+$: 264.1155, found 264.1154.



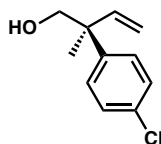
(S)-N-allyl-2-(4-chlorophenyl)-2-methylbut-3-enamide (85). In a nitrogen-filled glove box, to a 1 dram vial (vial A) equipped with a stir bar was added $[\text{Ir}(\text{cod})\text{Cl}]_2$ (2.7 mg, 0.0040 mmol, 2 mol %), ligand (S_d)-**L5** (4.9 mg, 0.0084 mmol, 4.2 mol %), TBD (2.8 mg, 0.020 mmol, 10 mol %), and THF (1 mL). Vial A was stirred at 25 °C (ca. 10 min) while another 1 dram vial (vial B) was charged with MAC nucleophile **67c** (25 mg, 0.20 mmol, 100 mol %), THF (1 mL), and BEt_3 (400 μL , 1M in hexanes). The pre-formed catalyst solution (vial A) was then transferred to vial B followed immediately by carbonate **76b** (96 mg, 0.40 mmol, 200 mol %). The vial was sealed and stirred at 60 °C. After 18 h, the vial was removed from the glove box, transferred to a 20 mL vial with CH_2Cl_2 , and concentrated.

To the vial of crude MAC adduct equipped with a stir bar and septum cap was added 1:1 AcOH/DME (0.4 mL, 0.5 M) and CSA (51 mg, 0.22 mmol, 1.1 equiv) under a nitrogen atmosphere. The reaction was heated to 60 °C for 6 h, whereupon the reaction mixture was cooled to ambient temperature, diluted with allyl amine (0.4 mL), and cooled to 0 °C. A solution of 1:1 Et₃N/allyl amine (1.1 mL, 20.4 equiv of Et₃N) was added dropwise over 10 min. The reaction mixture was allowed to warm to ambient temperature over 18 h, whereupon the reaction was slowly quenched with saturated NH₄Cl aqueous solution (5 mL). The aqueous layer was then extracted with CH₂Cl₂ (3 x 10 mL) and the combined organic layers were washed with brine (10 mL), dried over Na₂SO₄, and concentrated under reduced pressure at 0 °C. The crude residue was purified by preparatory TLC (30% EtOAc/hexanes) to give allyl amide **85** as a colorless oil (31 mg, 63% yield): [α]_D²⁵ +10.2 (*c* 1.6, CHCl₃); ¹H NMR (400 MHz, CDCl₃) δ 7.42 – 7.17 (m, 4H), 6.29 (dd, *J* = 17.4, 10.6 Hz, 1H), 5.90 – 5.75 (m, 1H), 5.64 (s, 1H), 5.33 (dd, *J* = 10.6, 0.8 Hz, 1H), 5.20 – 5.03 (m, 3H), 3.96 – 3.82 (m, 2H), 1.67 (s, 3H); ¹³C NMR (101 MHz, CDCl₃) δ 174.1, 142.0, 141.8, 134.1, 133.1, 128.9, 128.8, 116.6, 116.5, 54.3, 42.3, 24.6; IR (Neat Film, NaCl) 3341, 3085, 2983, 2931, 1739, 1658, 1520, 1493, 1414, 1270, 1096, 1014, 922, 827, 725, 657 cm⁻¹; HRMS (FAB+) *m/z* calc'd for C₁₄H₁₇NOCl [M+H]⁺: 250.0999, found 250.0991.

3.7.2.7 Experimental Procedures and Spectroscopic Data for the Product Transformations of α -Quaternary Ester **82**

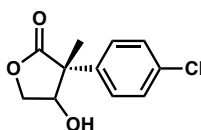


Methyl (S)-2-(4-chlorophenyl)-2-methylbutanoate (86). To a solution of olefin **82** (13 mg, 0.056 mmol, 1 equiv) in EtOAc (1 mL) was added Pd/C (2.5 mg, 20% w/w). The reaction mixture was sparged with a hydrogen gas (balloon) for 5 minutes and then stirred under a hydrogen atmosphere for 18 h, whereupon the reaction was filtered through celite with EtOAc (5 mL) and concentrated under reduced pressure at 0 °C to give alkyl **86** as a colorless oil (12 mg, 97% yield): $[\alpha]_D^{25} +3.6$ (*c* 1.2, CHCl₃); ¹H NMR (400 MHz, CDCl₃) δ 7.41 – 7.15 (m, 4H), 3.67 (s, 3H), 2.31 – 1.80 (m, 2H), 1.53 (s, 3H), 0.83 (t, *J* = 7.4 Hz, 3H); ¹³C NMR (101 MHz, CDCl₃) δ 176.5, 142.4, 132.6, 128.6, 127.7, 52.3, 50.4, 32.0, 22.2, 9.2; IR (Neat Film, NaCl) 2970, 2880, 1731, 1493, 1457, 1383, 1307, 1238, 1147, 1096, 1012, 824, 756, 720 cm⁻¹; HRMS (FAB+) *m/z* calc'd for C₁₂H₁₆O₂Cl [M+H]⁺: 227.0839, found 227.0840.



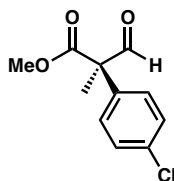
(S)-2-(4-Chlorophenyl)-2-methylbut-3-en-1-ol (87). DIBAL (0.029 mL, 0.16 mmol, 3 equiv) was added dropwise to a solution of methyl ester **82** (13 mg, 0.056 mmol, 1 equiv) in Et₂O (1.0 mL) at 0 °C. The mixture was stirred at 0 °C for 2 h, whereupon the reaction was quenched with a saturated Rochelle's salt aqueous solution (1 mL) and stirred for 18

h at ambient temperature. The aqueous layer was then extracted with CH_2Cl_2 (3 x 5 mL) and the combined organic layers were washed with brine (5 mL), dried over Na_2SO_4 , and concentrated under reduced pressure at 0 °C. The crude residue was purified by preparatory TLC (25% acetone/hexanes) to give alcohol **87** as a colorless oil (8 mg, 73% yield): $[\alpha]_{\text{D}}^{25} +11.0$ (c 0.4, CHCl_3). Characterization data match those reported in the literature.³¹



(3S)-3-(4-Chlorophenyl)-4-hydroxy-3-methyldihydrofuran-2(3H)-one (88). To a solution of olefin **82** (24 mg, 0.10 mmol, 1 equiv) in THF/ H_2O (4:1, 1 mL) was added K_2OsO_4 (4.0 mg, 0.010 mmol, 0.1 equiv) and *N*-methylmorpholine *N*-oxide (19 mg, 0.16 mmol, 1.6 equiv). The reaction mixture was stirred for 18 h, whereupon the reaction was quenched with sodium sulfite (10 mg, 0.079 mmol, 0.79 equiv) and diluted with water (0.5 mL). The aqueous layer was then extracted with EtOAc (3 x 5 mL) and the combined organic layers were washed with brine (5 mL), dried over Na_2SO_4 , and concentrated under reduced pressure at 0 °C. The crude residue was purified by preparatory TLC (30% acetone/hexanes) to give lactone **88** as a colorless oil (19 mg, 82% yield, 1:1 dr): $[\alpha]_{\text{D}}^{25} -115.6$ (c 0.5, CHCl_3); ^1H NMR (400 MHz, CDCl_3) δ 7.43 – 7.26 (m, 4H), 4.58 (dd, J = 4.4, 2.8 Hz, 0.5H), 4.54 (dd, J = 10.2, 4.5 Hz, 0.5H), 4.35 – 4.31 (m, 0.5H), 4.28 – 4.20 (m, 1H), 4.16 (dd, J = 10.1, 2.8 Hz, 0.5H), 1.66 (s, 1.5H), 1.57 (s, 1.5H); ^{13}C NMR (101 MHz, CDCl_3) δ 178.4, 178.1, 138.4, 134.4, 134.0, 133.9, 129.6, 129.4, 129.3, 127.8, 76.5, 76.2, 71.8, 71.6, 53.2, 52.8, 22.3, 18.5; IR (Neat Film,

NaCl) 3448, 2976, 2929, 1761, 1496, 1384, 1218, 1178, 1096, 1072, 1014, 982, 927, 737, 688 cm^{-1} ; HRMS (FAB+) m/z calc'd for $\text{C}_{11}\text{H}_{12}\text{O}_3\text{Cl}$ $[\text{M}+\text{H}]^+$: 227.0475, found 227.0481.

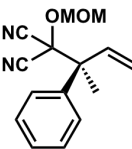
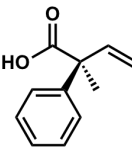
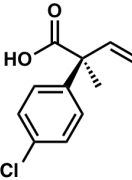
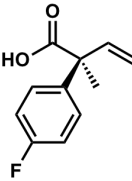
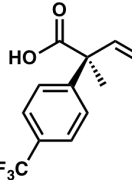
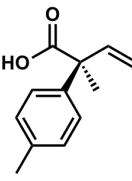


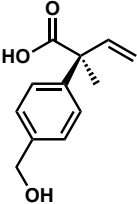
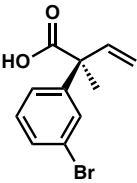
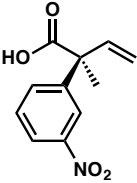
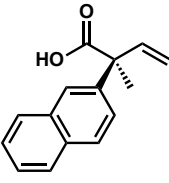
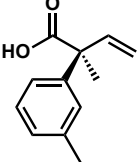
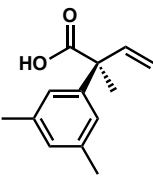
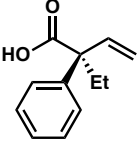
Methyl (*R*)-2-(4-chlorophenyl)-2-methyl-3-oxopropanoate (89). A solution of olefin **82** (10 mg, 0.045 mmol, 1 equiv) and NaHCO_3 (1.0 mg, 0.011 mmol, 0.25 equiv) in $\text{MeOH}/\text{CH}_2\text{Cl}_2$ (1:5, 2.6 mL) was cooled to $-78\text{ }^\circ\text{C}$. Ozone was bubbled through the reaction mixture for 0.5 h, whereupon the reaction mixture was sparged with N_2 and dimethyl sulfide (0.10 mL, 0.14 mmol, 3 equiv) was added. The cooling bath was then removed and the reaction was stirred for 18 h at ambient temperature. The reaction mixture was concentrated under reduced pressure at $0\text{ }^\circ\text{C}$ and the crude residue was purified by preparatory TLC (17% Et_2O /hexanes) to afford aldehyde **89** as a colorless oil (5.0 mg, 50% yield): $[\alpha]_{\text{D}}^{25} +9.1$ (c 0.07, CHCl_3); ^1H NMR (400 MHz, CDCl_3) δ 9.83 (s, 1H), 7.41 – 7.33 (m, 2H), 7.22 – 7.13 (m, 2H), 3.81 (s, 3H), 1.69 (s, 3H); ^{13}C NMR (101 MHz, CDCl_3) δ 196.2, 171.8, 134.8, 134.5, 129.5, 128.5, 61.7, 53.1, 18.0; IR (Neat Film, NaCl) 2992, 2954, 2845, 2726, 1721, 1596, 1494, 1455, 1252, 1122, 1096, 1013, 911, 823, 758, 718 cm^{-1} ; HRMS (FAB+) m/z calc'd for $\text{C}_{11}\text{H}_{12}\text{ClO}_3$ $[\text{M}+\text{H}]^+$: 227.0475, found 227.0479.

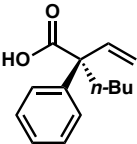
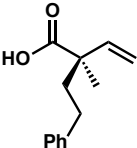
3.7.2.8 Determination of Enantiomeric Excess

Please note racemic products were synthesized using racemic **L5**.

Table 3.6 Determination of enantiomeric excess

Entry	Product	Assay Conditions	Retention time of major isomer (min)	Retention time of minor isomer (min)	%ee
1		HPLC Chiralpak IC 1% IPA isocratic, 1 mL/min	13.303	17.243	94%
2		HPLC Chiralpak AD-H 2% IPA isocratic, 1 mL/min	12.198	11.426	95%
3		HPLC Chiralpak AD-H 2% IPA isocratic, 1 mL/min	15.642	14.104	93%
4		HPLC Chiralpak AD-H 2% IPA isocratic, 1 mL/min	15.499	13.811	90%
5		SFC Chiralpak AD-H 2% IPA isocratic, 2.5 mL/min	13.592	15.745	92%
6		HPLC Chiralpak AD-H 2% IPA isocratic, 1 mL/min	15.393	14.288	94%

Entry	Product	Assay Conditions	Retention time of major isomer (min)	Retention time of minor isomer (min)	%ee
7		HPLC Chiralpak AD-H 2% IPA isocratic, 1 mL/min	15.258	14.667	95%
8		HPLC Chiralpak AD-H 2% IPA isocratic, 1 mL/min	15.217	14.439	92%
9		HPLC Chiralpak AD-H 3% IPA isocratic, 1 mL/min	24.060	20.907	87%
10		HPLC Chiralpak AD-H 2% IPA isocratic, 1 mL/min	28.272	24.870	92%
11		HPLC Chiralpak AD-H 2% IPA isocratic, 1 mL/min	13.800	12.388	93%
12		HPLC Chiralpak AD-H 2% IPA isocratic, 1 mL/min	11.107	10.064	85%
13		HPLC two Chiralpak AD-H in series 1.5% IPA isocratic, 1 mL/min	46.253	47.271	92%

Entry	Product	Assay Conditions	Retention time of major isomer (min)	Retention time of minor isomer (min)	%ee
14		SFC Chiralpak AD-H 5% IPA isocratic, 2.5 mL/min	10.646	11.952	95%
15		HPLC Chiralpak AD-H 2% IPA isocratic, 1 mL/min	18.485	14.652	3%

3.8 REFERENCES AND NOTES

- (1) Janssen, J. P.; Helmchen, G. *Tetrahedron Lett.* **1997**, 38, 8025–8026.
- (2) For select recent examples, see: (a) Jiang, X.; Beiger, J. J.; Hartwig, J. F. *J. Am. Chem. Soc.* **2017**, 139, 87–90; (b) Sandmeier, T.; Krautwald, S.; Zipfel, H. F.; Carreira, E. M. *Angew. Chem. Int. Ed.* **2015**, 54, 14363–14367; (c) Liu, W.-B.; Zheng, C.; Zhuo, C.-X.; Dai, L.-X.; You, S.-L. *J. Am. Chem. Soc.* **2012**, 134, 4812–4821.
- (3) For select recent examples, see: (a) Seehafer, K.; Malakar, C. C.; Bender, M.; Qu, J.; Liang, C.; Helmchen, G. *Eur. J. Org. Chem.* **2016**, 493–501; (b) Defieber, C.; Ariger, M. A.; Moriel, P.; Carreira, E. M. *Angew. Chem. Int. Ed.* **2007**, 46, 3139–3143; (c) Ueda, M.; Hartwig, J. F. *Org. Lett.* **2010**, 12, 92–94.

- (4) For select reviews, see: (a) Helmchen, G.; Dahnz, A.; Dübon, P.; Schelwies, M.; Weihofen, R. *Chem. Commun.* **2007**, 675–691; (b) Hartwig, J. F.; Pouy, M. J. *Top. Organomet. Chem.* **2011**, *34*, 169–208; (c) Liu, W.-B.; Xia, J.-B.; You, S.-L. *Top. Organomet. Chem.* **2012**, *38*, 155–208; (d) Hethcox, J. C.; Shockley, S. E.; Stoltz, B. M. *ACS Catal.* **2016**, *6*, 6207–6213.

- (5) A singular example of an iridium-catalyzed allylic alkylation reaction producing a product bearing an allylic all-carbon stereocenter has been reported with 11% yield and 21% ee: Onodera, G.; Watabe, K.; Matsubara, M.; Oda, K.; Kezuka, S.; Takeuchi, R. *Adv. Synth. Catal.* **2008**, *350*, 2725–2732.

- (6) (a) Douglas, C. J.; Overman, L. E. *Proc. Natl. Acad. Sci. USA* **2004**, *101*, 5363–5367; (b) Das, J. P.; Marek, I. *Chem. Commun.* **2011**, *47*, 4593–4623; (c) Quasdorf, K. W.; Overman, L. E. *Nature* **2014**, *516*, 181–191; (d) Corey, E. J.; Guzman-Perez, A. *Angew. Chem. Int. Ed.* **1998**, *37*, 388–401; (e) Christoffers, J.; Mann, A. *Angew. Chem. Int. Ed.* **2001**, *40*, 4591–4597; (f) Trost, B. M.; Jiang, C. *Synthesis* **2006**, 369–396; (g) Liu, Y.; Han, S.-J.; Liu, W.-B.; Stoltz, B. M. *Acc. Chem. Res.* **2015**, *48*, 740–751.

- (7) For select recent examples of the enantioselective transition metal-catalyzed synthesis of allylic all-carbon quaternary stereocenters, see: (a) Zhang, A.; RajanBabu, T. V. *J. Am. Chem. Soc.* **2006**, *128*, 5620–5621; (b) Falciola, C. A.; Alexakis, A. *Chem. Eur. J.* **2008**, *14*, 10615–10627; (c) Xiong, Y.; Zhang, G. *Org. Lett.* **2016**, *18*, 5094–5097; (d) Guduguntla, S.; Gualtierotti, J.-B.; Goh, S. S.; Feringa, B. L. *ACS Catal.* **2016**, *6*, 6591–6595; (e) Trost, B. M.; Jiang, C. *J. Am.*

- Chem. Soc.* **2001**, *123*, 12907–12908; (f) Hou, X.-L.; Sun, N. *Org. Lett.* **2004**, *6*, 4399–4401; (g) Zhang, P.; Le, H.; Kyne, R. E.; Morken, J. P. *J. Am. Chem. Soc.* **2011**, *133*, 9716–9719.
- (8) For the only enantioselective reports to access acyclic quaternary α -vinyl, α -aryl carbonyl derivatives disclosed at the time, see: (a) Murphy, K. E.; Hoveyda, A. H. *Org. Lett.* **2005**, *7*, 1255–1258; (b) Lee, Y.; Hoveyda, A. H. *J. Am. Chem. Soc.* **2006**, *128*, 15604–15605; (c) Gao, F.; Lee, Y.; Mandai, K.; Hoveyda, A. H. *Angew. Chem. Int. Ed.* **2010**, *49*, 8370–8374; (d) Hojoh, K.; Ohmiya, H.; Sawamura, M. *J. Am. Chem. Soc.* **2017**, *139*, 2184–2187.
- (9) (a) Liu, W.-B.; Reeves, C. M.; Stoltz, B. M. *J. Am. Chem. Soc.* **2013**, *135*, 17298–17301; (b) Liu, W.-B.; Reeves, C. M.; Virgil, S. C.; Stoltz, B. M. *J. Am. Chem. Soc.* **2013**, *135*, 10626–10629; (c) Liu, W.-B.; Okamoto, N.; Alexy, E. J.; Hong, A. Y.; Tran, K.; Stoltz, B. M. *J. Am. Chem. Soc.* **2016**, *138*, 5234–5237; (d) Hethcox, J. C.; Shockley, S. E.; Stoltz, B. M. *Angew. Chem. Int. Ed.* **2016**, *55*, 16092–16095; (e) Hethcox, J. C.; Shockley, S. E.; Stoltz, B. M. *Org. Lett.* **2017**, *19*, 1527–1529.
- (10) (a) Nemoto, H.; Kubota, Y.; Yamamoto, Y. *J. Org. Chem.* **1990**, *55*, 4515–4516; (b) Yang, K. S.; Nibbs, A. E.; Türkmen, Y. E.; Rawal, V. H. *J. Am. Chem. Soc.* **2013**, *135*, 16050–16053.
- (11) (a) Madrahimov, S. T.; Hartwig, J. F. *J. Am. Chem. Soc.* **2012**, *134*, 8136–8147; (b) Madrahimov, S. T.; Li, Q.; Sharma, A.; Hartwig, J. F. *J. Am. Chem. Soc.* **2015**, *137*, 14968–14981.

- (12) One report of a trisubstituted allylic electrophile in an enantioselective iridium-catalyzed allylic alkylation had been disclosed, but the products bear a tertiary allylic stereocenter: Chen, M.; Hartwig, J. F. *Angew. Chem. Int. Ed.* **2016**, *55*, 11651–11655.
- (13) To the best of our knowledge, only one report of a borane additive (Ph_3B) in iridium-catalyzed allylic alkylation reactions had been disclosed: Yamashita, Y.; Gopalarathnam, A.; Hartwig, J. F. *J. Am. Chem. Soc.* **2007**, *129*, 7508–7509.
- (14) Rössler, S. L.; Krautwald, S.; Carreira, E. M. *J. Am. Chem. Soc.* **2017**, *139*, 3603–3606.
- (15) Liu, W.-B.; He, H.; Dai, L.-X.; You, S.-L. *Synthesis* **2009**, 2076–2082.
- (16) Hamilton, J. Y.; Sarlah, D.; Carreira, E. M. *Org. Synth.* **2015**, *92*, 1–12.
- (17) Nemoto, H.; Li, X.; Ma, R.; Suzuki, I.; Shibuya, M. *Tetrahedron Lett.* **2003**, *44*, 73–75.
- (18) (a) Ardolino, M. J.; Morken, J. P. *J. Am. Chem. Soc.* **2014**, *136*, 7092–7100; (b) Evans, P. A.; Oliver, S.; Chae, J. *J. Am. Chem. Soc.* **2012**, *134*, 19314–19317.
- (19) Matsubara, R.; Jamison, T. F. *J. Am. Chem. Soc.* **2010**, *132*, 6880–6881.
- (20) Guzman-Martinez, A.; Hoveyda, A. H. *J. Am. Chem. Soc.* **2010**, *132*, 10634–10637.
- (21) Ruan, J.; Li, X.; Saidi, O.; Xiao, J. *J. Am. Chem. Soc.* **2008**, *130*, 2424–2425.
- (22) Duan, Z.-C.; Hu, X.-P.; Zhang, C.; Zheng, Z. *J. Org. Chem.* **2010**, *75*, 8319–8321.
- (23) Nakatsuji, H.; Ueno, K.; Misaki, T.; Tanabe, Y. *Org. Lett.* **2008**, *10*, 2131–2134.
- (24) Gürtler, C.; Buchwald, S. L. *Chem. Eur. J.* **1999**, *5*, 3107–3112.

- (25) Sano, S.; Yokoyama, K.; Shiro, M.; Nagao, Y. *Chem. Pharm. Bull.* **2002**, *50*, 706–709.
- (26) Ho Oh, C.; Jung, H. H.; Kim, K. S.; Kim, N. *Angew. Chem. Int. Ed.* **2003**, *42*, 805–808.
- (27) Bernasconi, M.; Ramella, V.; Tosatti, P.; Pfaltz, A. *Chem. Eur. J.* **2014**, *20*, 2440–2444.
- (28) Bensch, N.; Höhn, J.; Marschall, H.; Weyerstahl, P. *Eur. J. Inorg. Chem.* **1979**, *112*, 2256–2277.
- (29) Takaya, J.; Iwasawa, N. *J. Am. Chem. Soc.* **2008**, *130*, 15254–15255.
- (30) Duong, H. A.; Huleatt, P. B.; Tan, Q.-W.; Shuying, E. L. *Org. Lett.* **2013**, *15*, 4034–4037.
- (31) Ngai, M.-Y.; Skucas, E.; Krische, M. J. *Org. Lett.* **2008**, *10*, 2705–2708.

APPENDIX 4

Spectra Relevant to Chapter 3:

Enantioselective Synthesis of Acyclic α -Quaternary Carboxylic Acid

Derivatives via Iridium-Catalyzed Allylic Alkylation

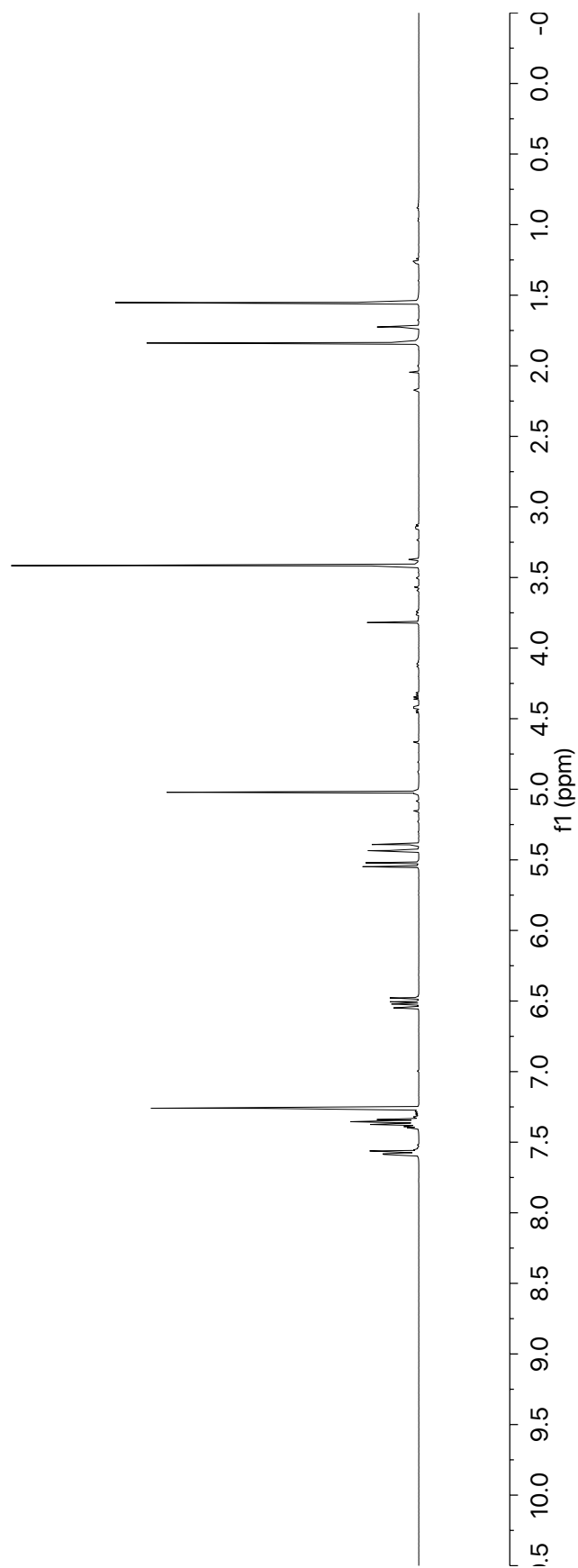
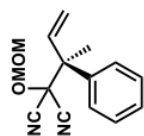


Figure A4.1 ¹H NMR (400 MHz, CDCl₃) of compound 73

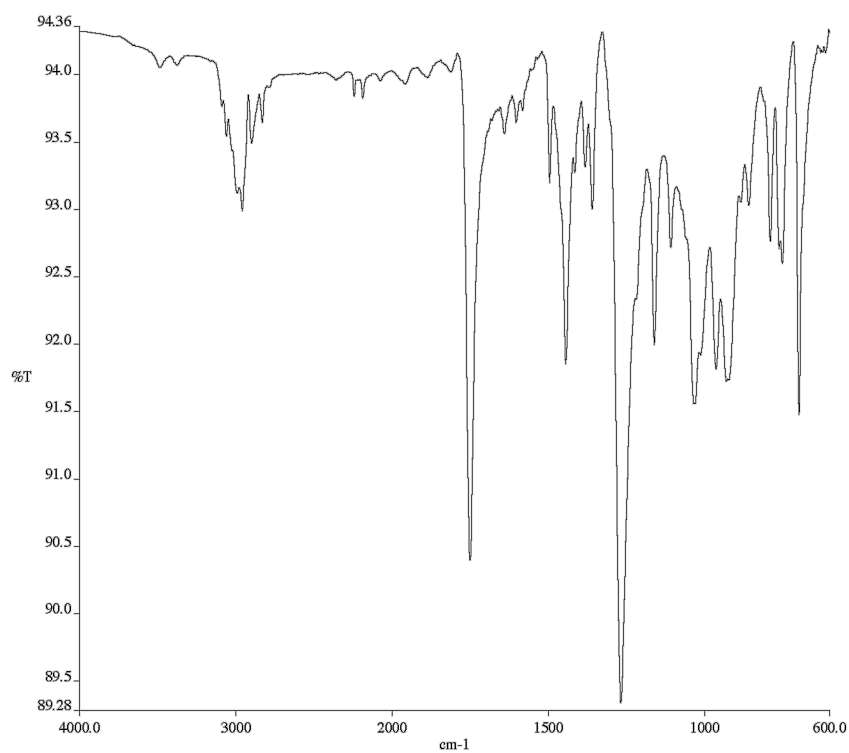


Figure A4.2 Infrared spectrum (Thin Film, NaCl) of compound **73**

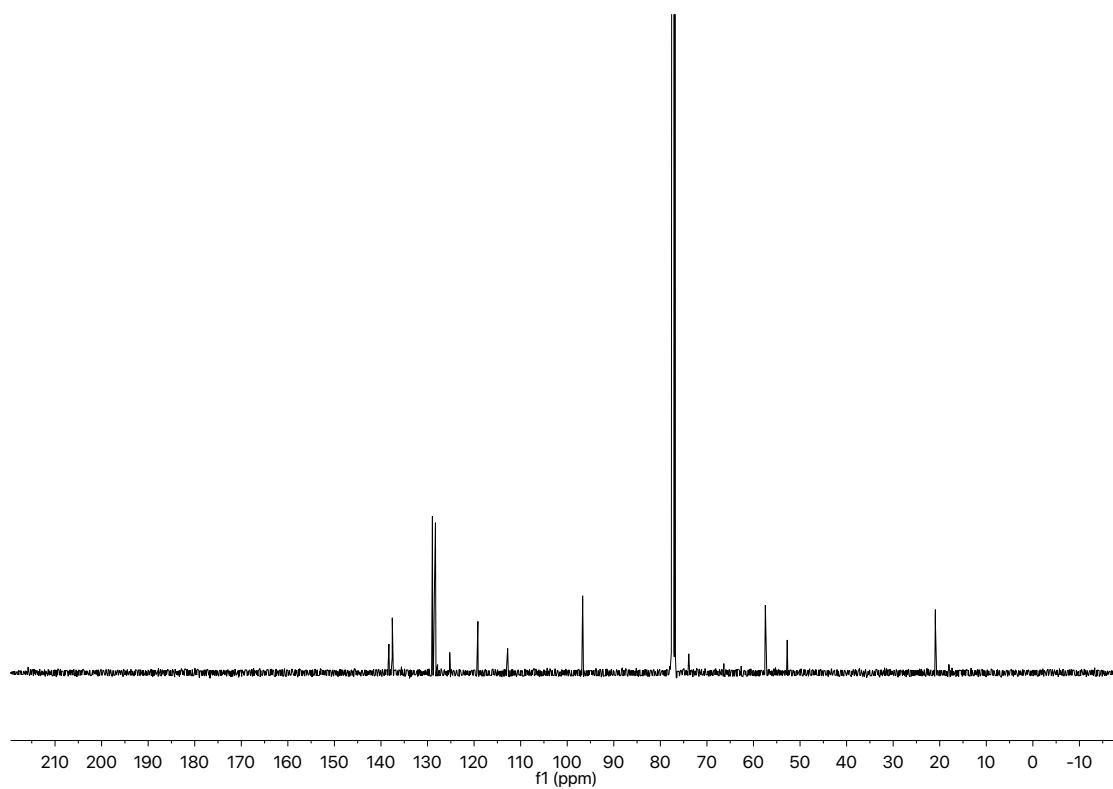


Figure A4.3 ¹³C NMR (101 MHz, CDCl₃) of compound **73**

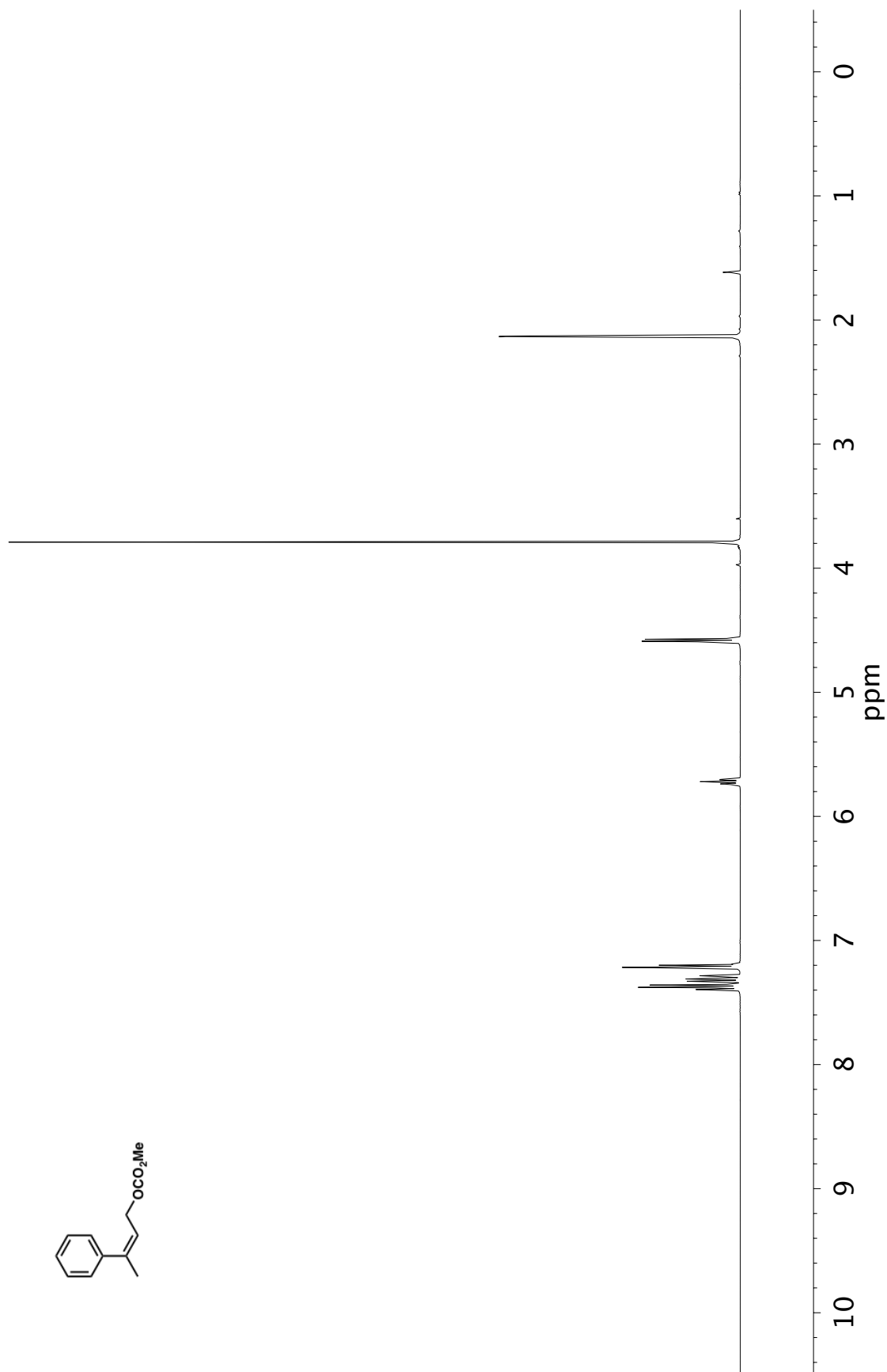


Figure A4.4 ¹H NMR (400 MHz, CDCl₃) of compound 74

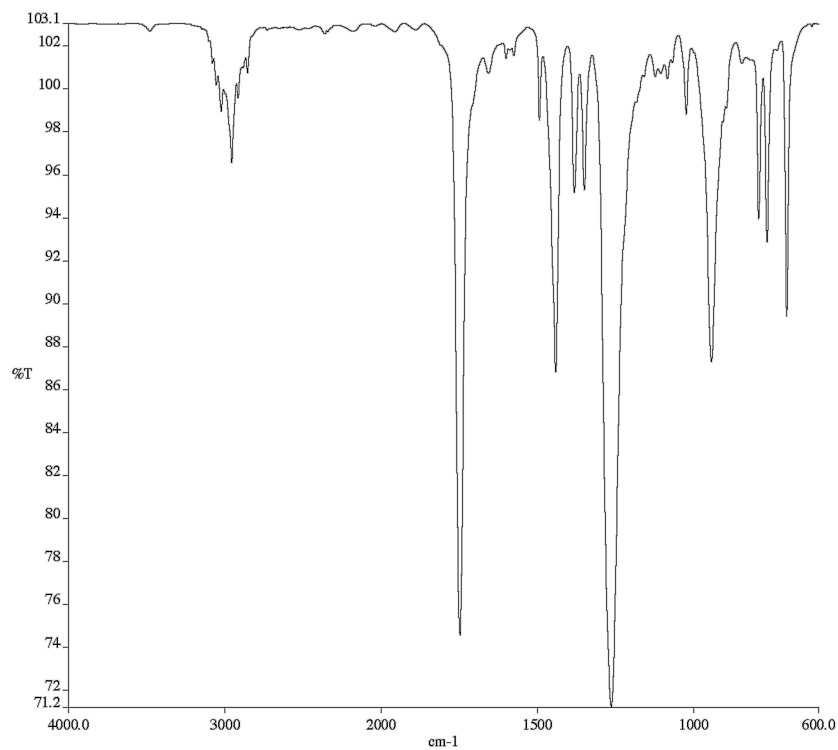


Figure A4.5 Infrared spectrum (Thin Film, NaCl) of compound **74**

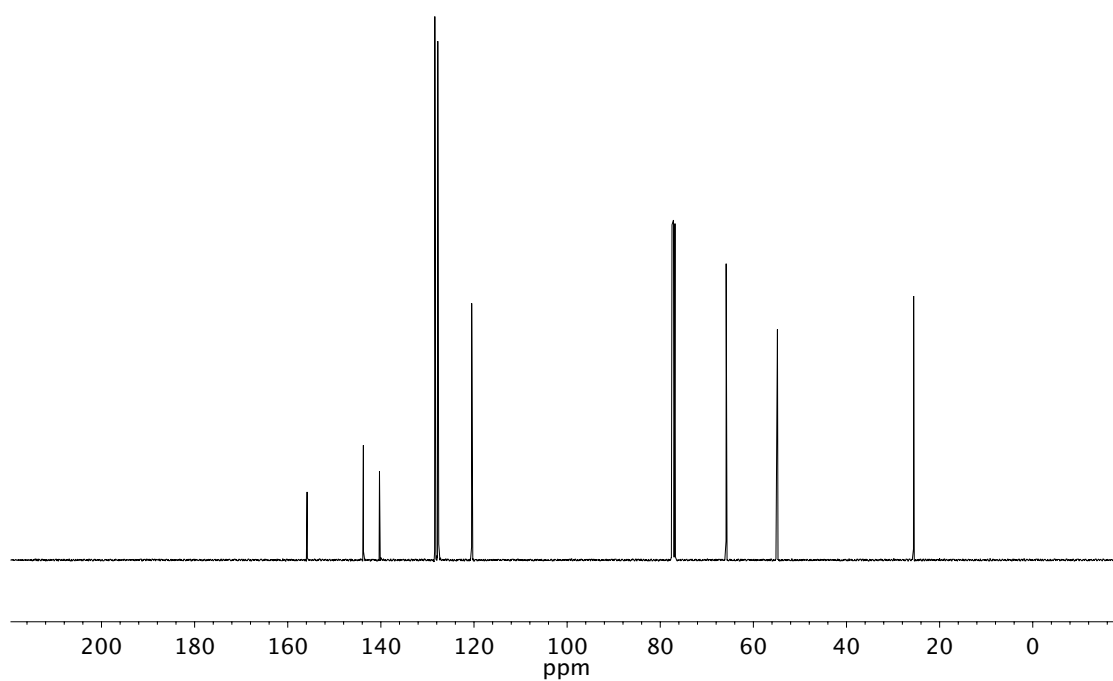


Figure A4.6 ^{13}C NMR (101 MHz, CDCl_3) of compound **74**

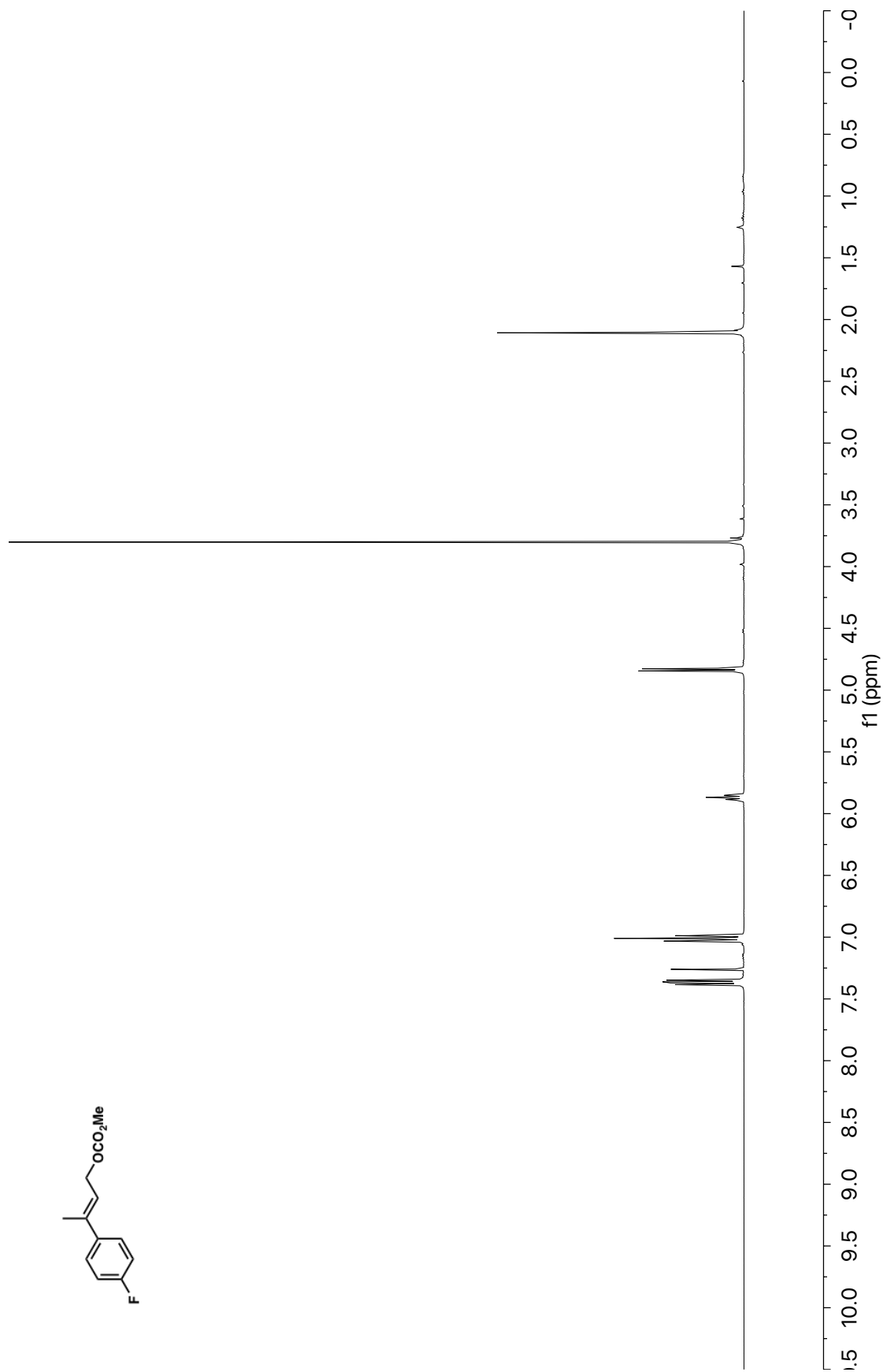


Figure A4.7 ¹H NMR (400 MHz, CDCl₃) of compound **76c**

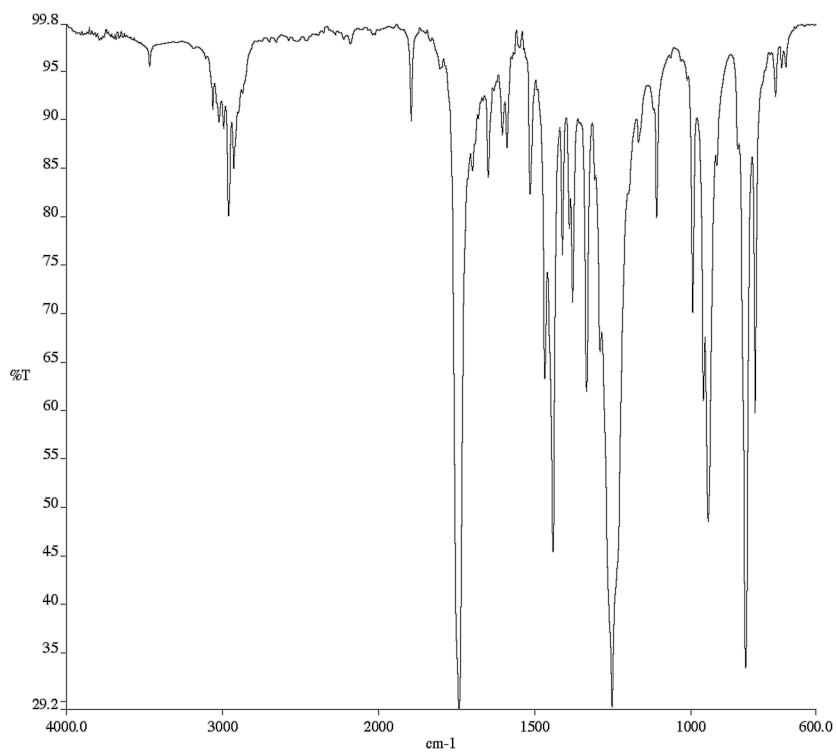


Figure A4.8 Infrared spectrum (Thin Film, NaCl) of compound **76c**

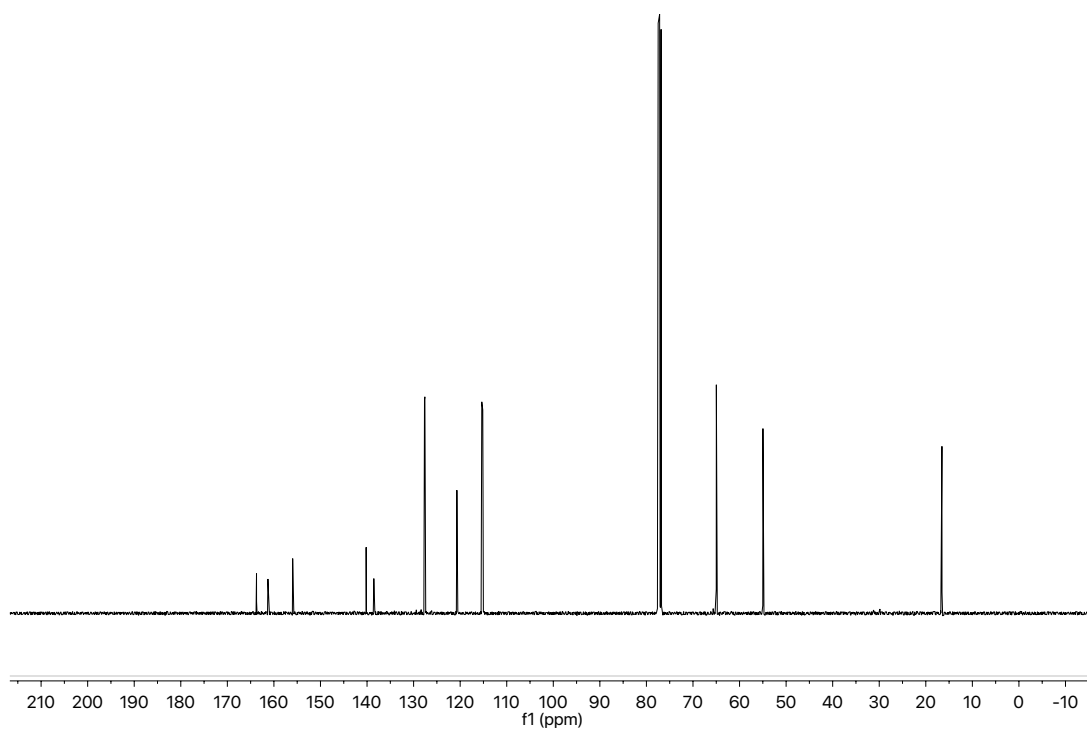


Figure A4.9 ¹³C NMR (101 MHz, CDCl₃) of compound **76c**

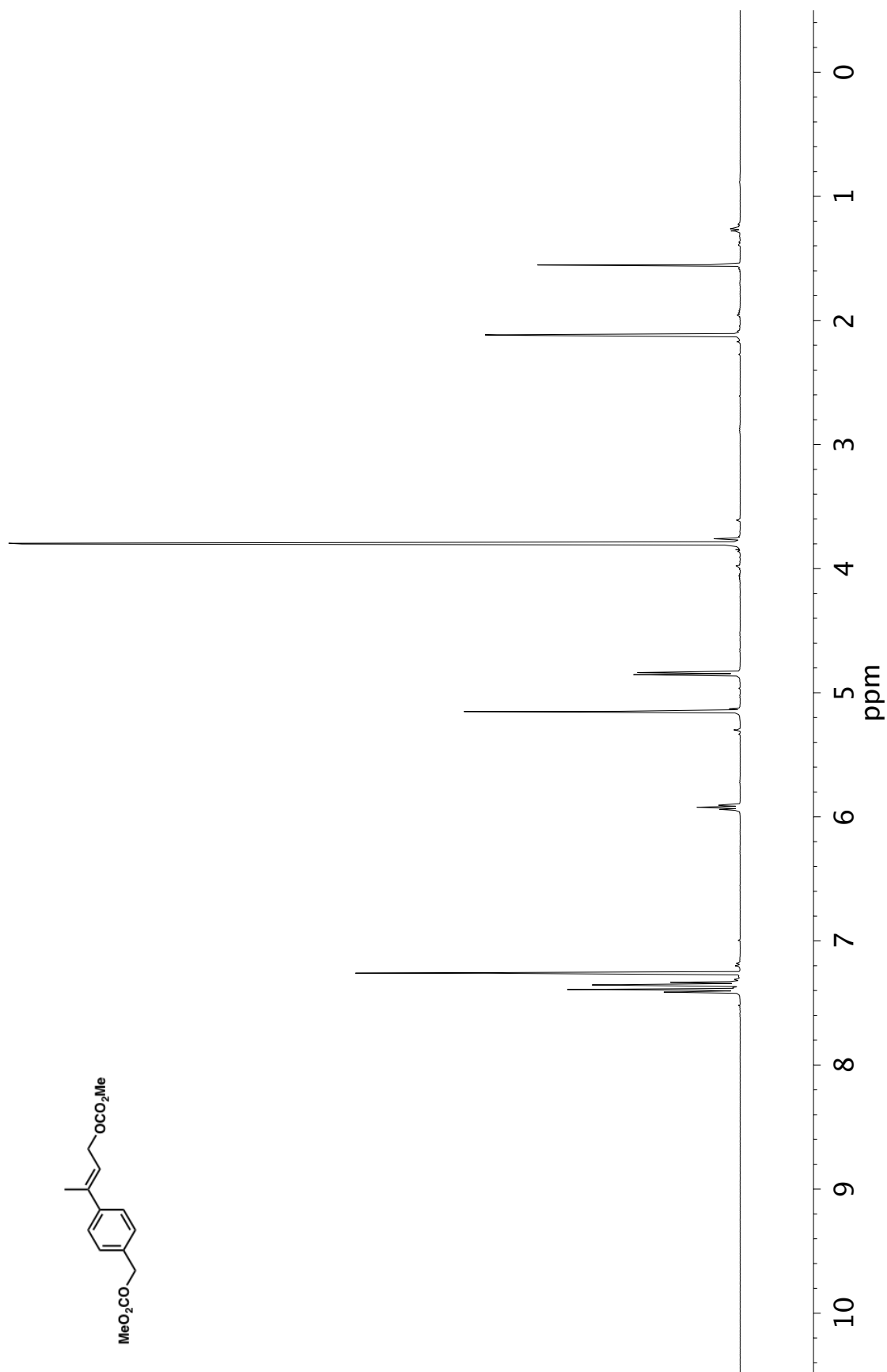


Figure A4.10 ^1H NMR (400 MHz, CDCl_3) of compound **76f**

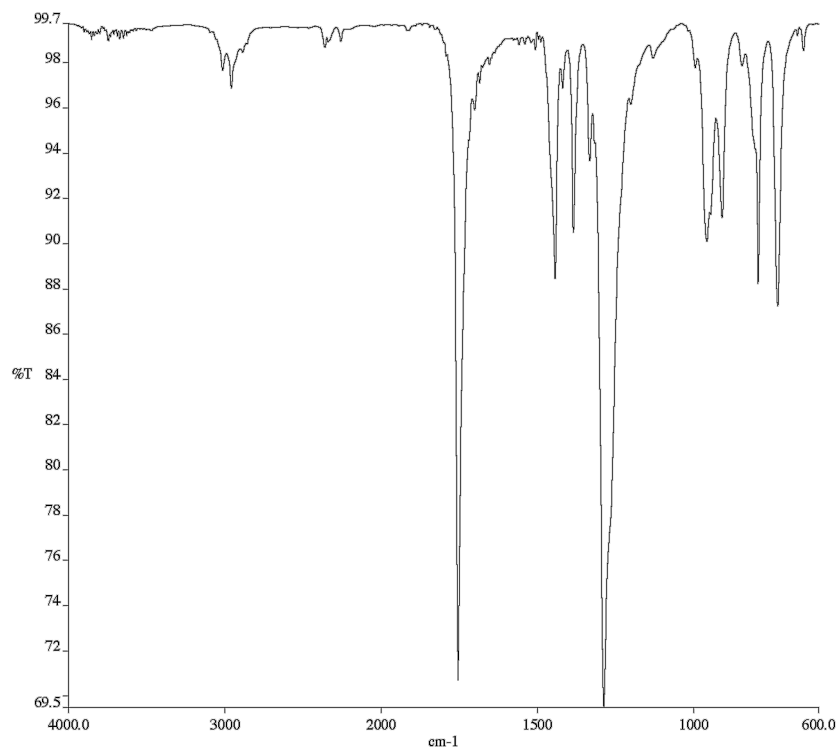


Figure A4.11 Infrared spectrum (Thin Film, NaCl) of compound **76f**

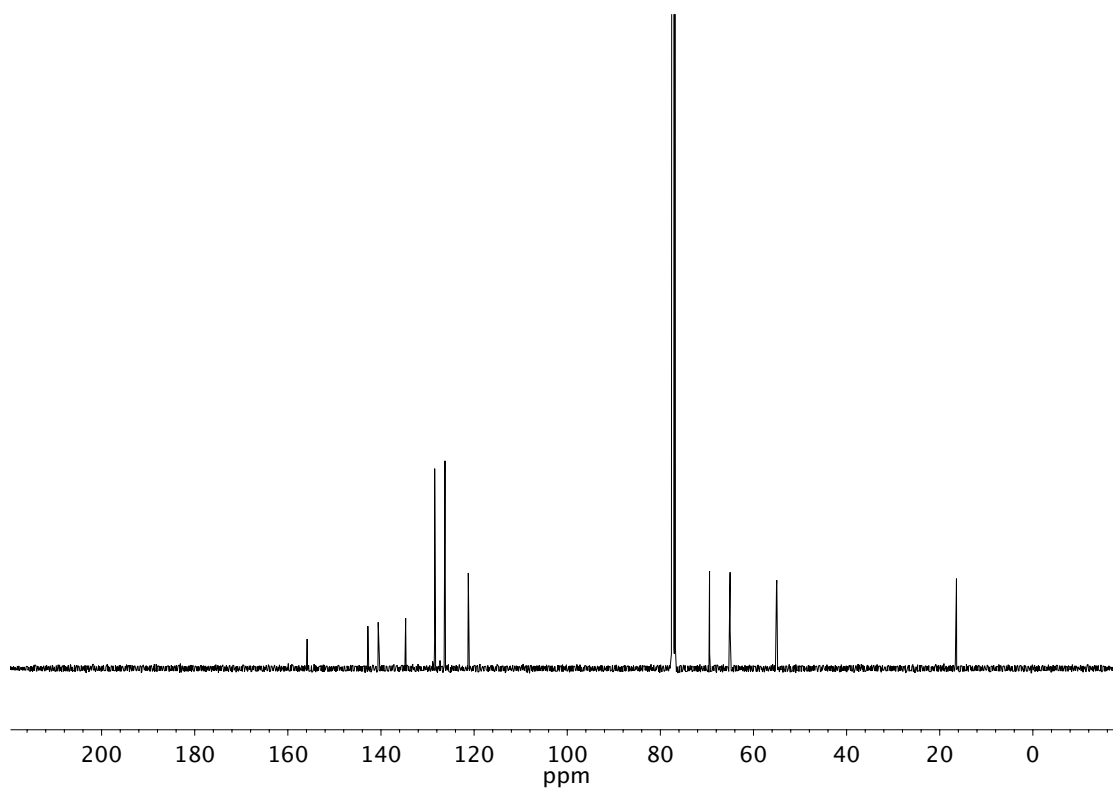


Figure A4.12 ¹³C NMR (101 MHz, CDCl₃) of compound **76f**

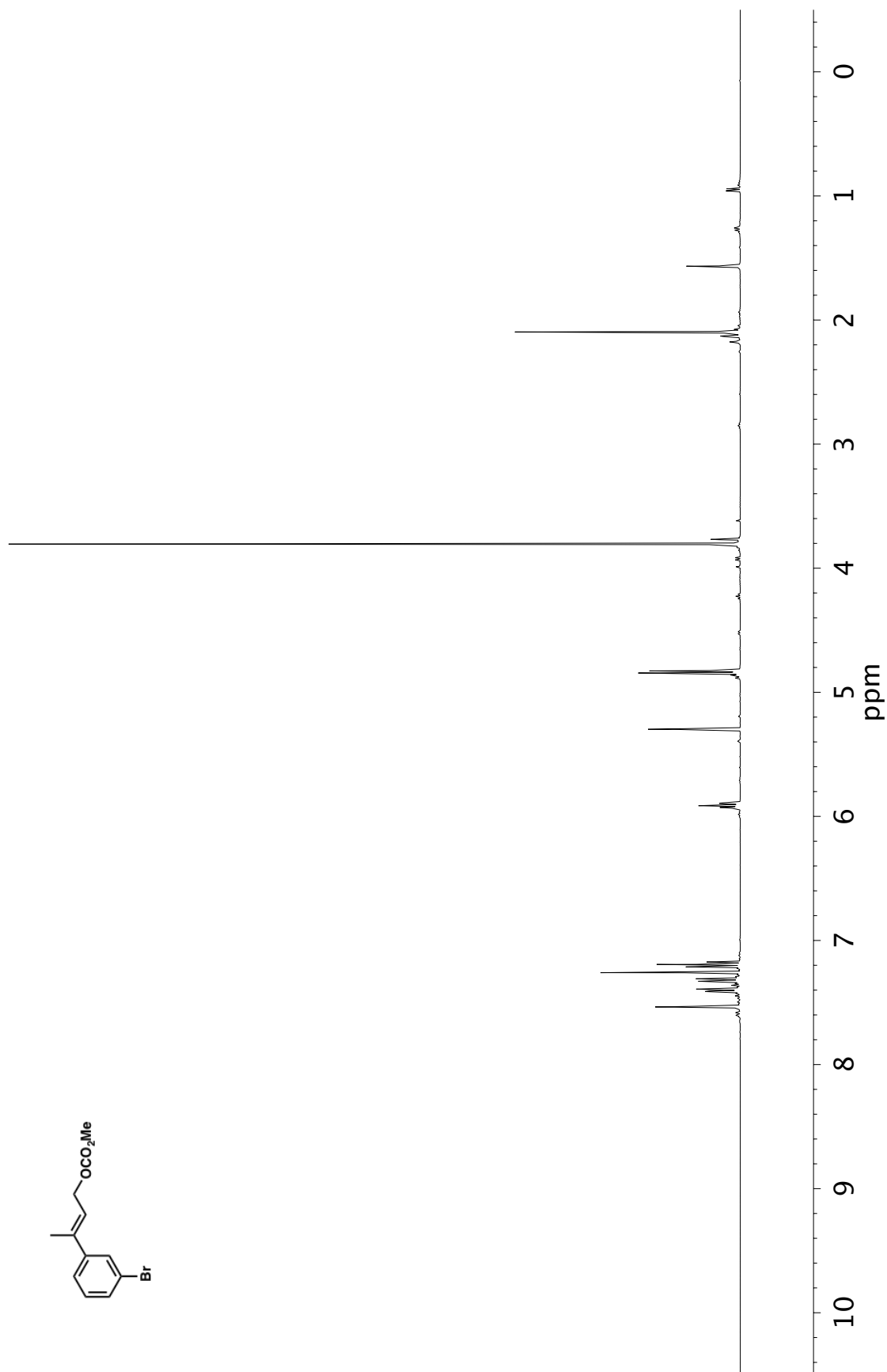


Figure A4.13 ¹H NMR (400 MHz, CDCl₃) of compound 76g

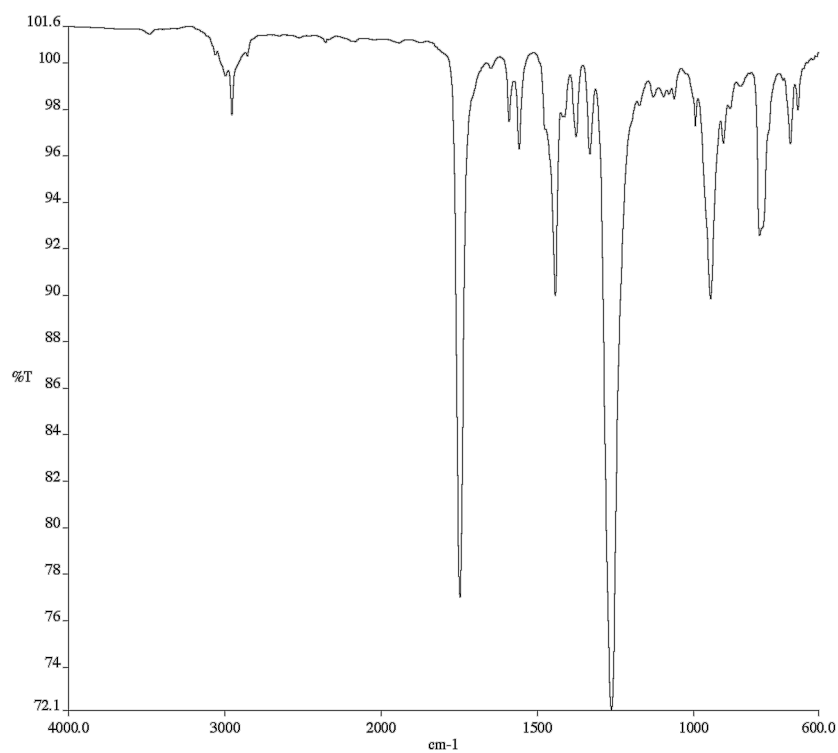


Figure A4.14 Infrared spectrum (Thin Film, NaCl) of compound **76g**

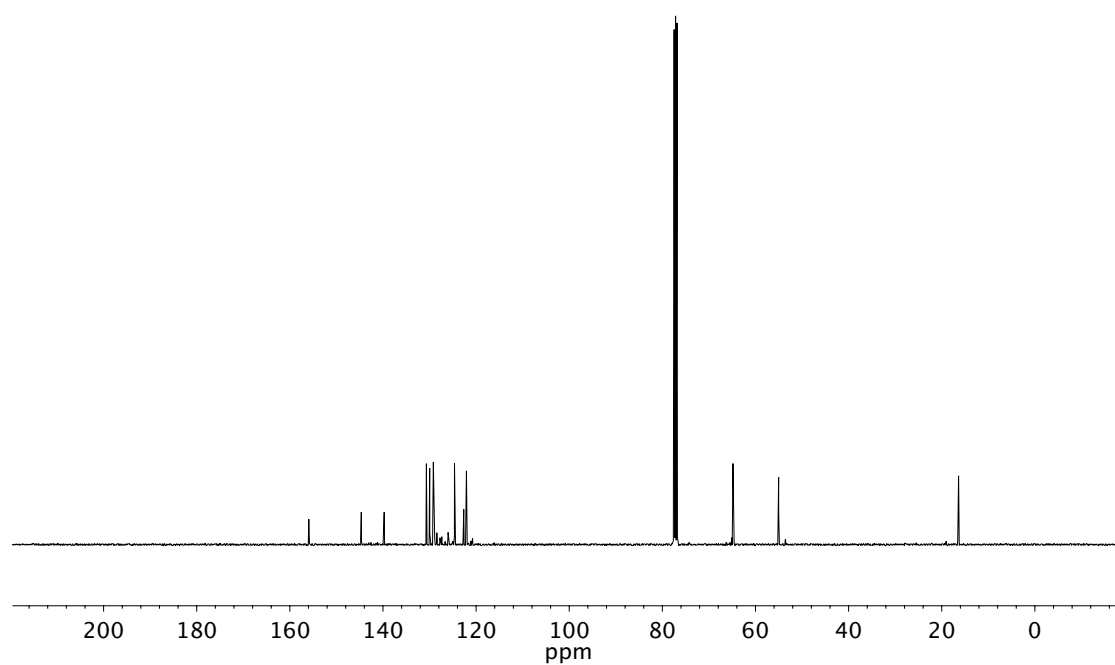


Figure A4.15 ¹³C NMR (101 MHz, CDCl₃) of compound **76g**

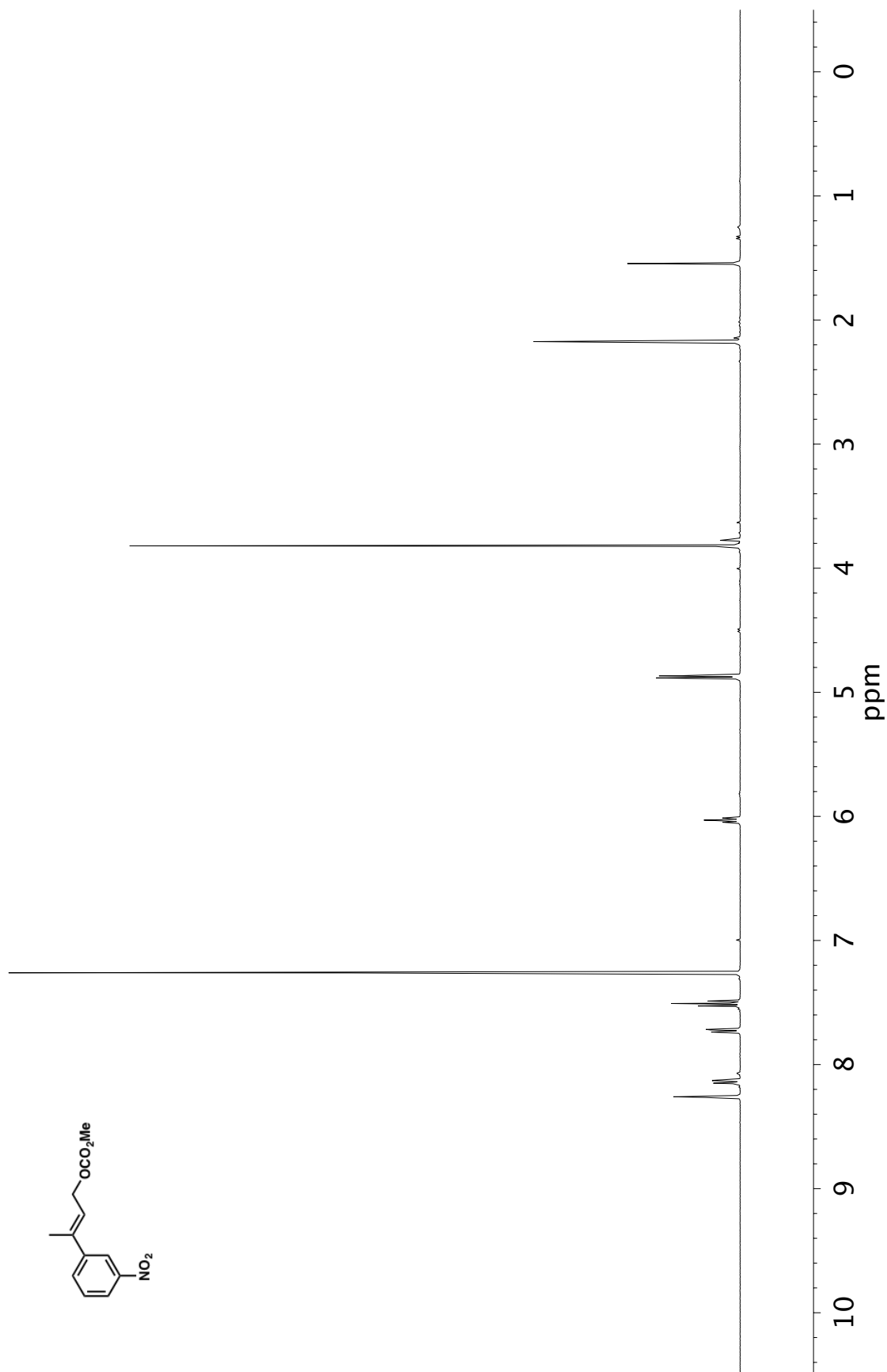


Figure A4.16 ^1H NMR (400 MHz, CDCl_3) of compound **76h**

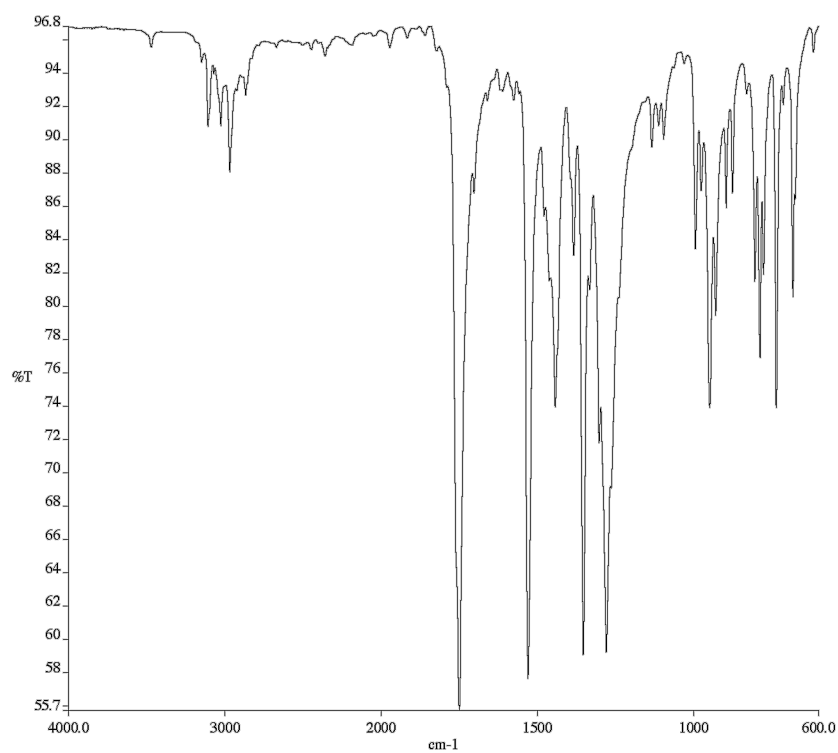


Figure A4.17 Infrared spectrum (Thin Film, NaCl) of compound **76h**

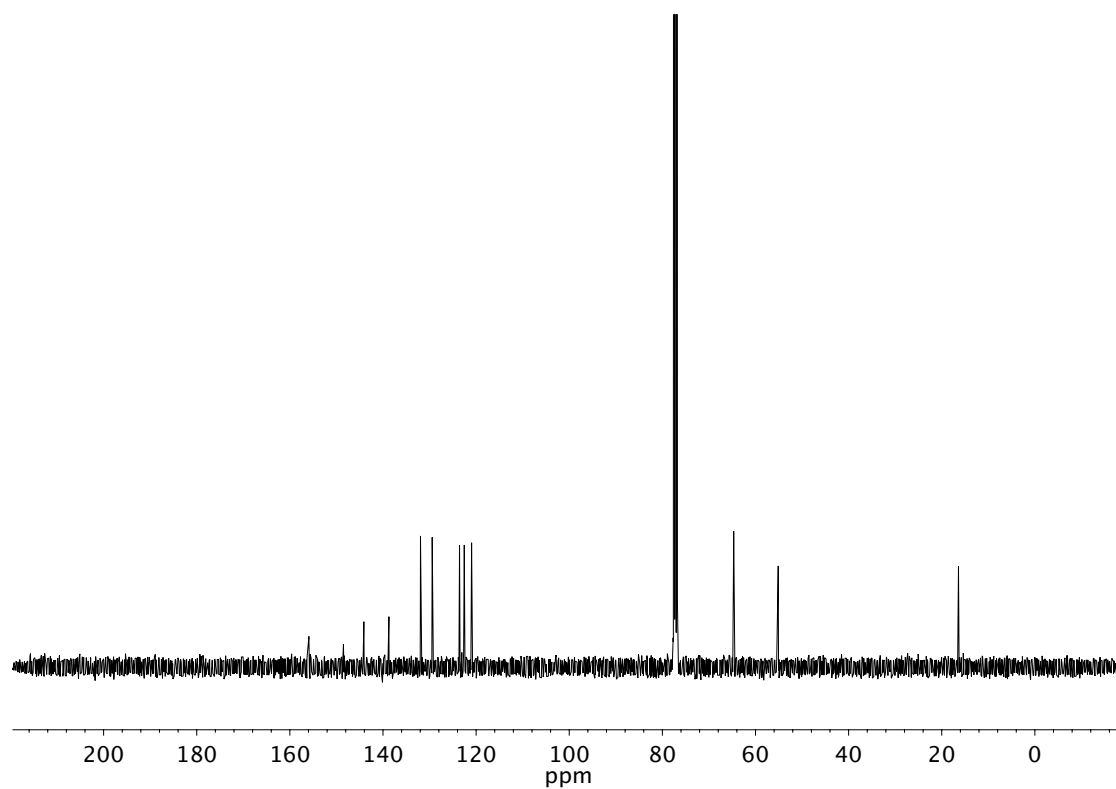


Figure A4.18 ¹³C NMR (101 MHz, CDCl₃) of compound **76h**

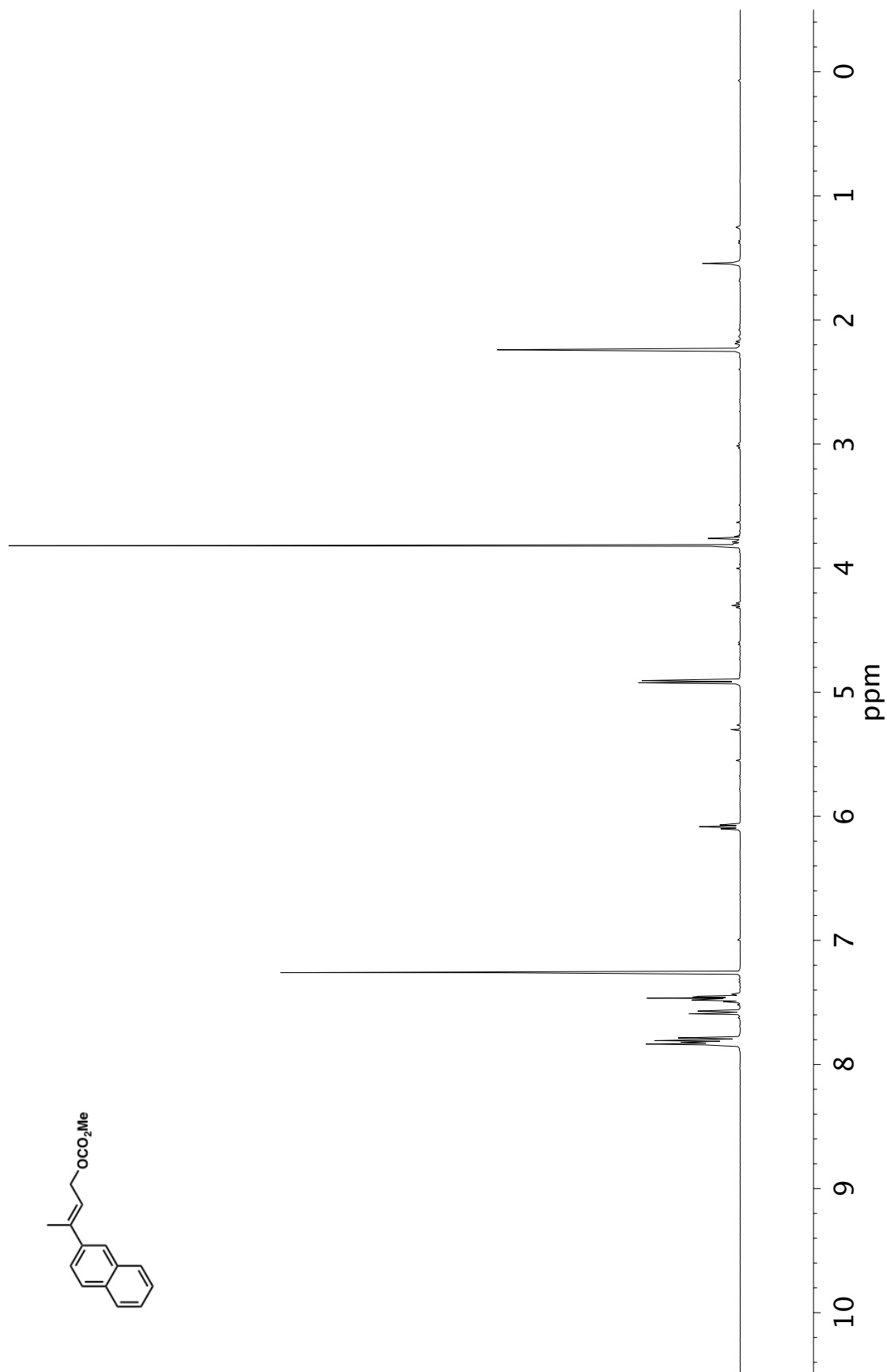


Figure A4.19 ^1H NMR (400 MHz, CDCl_3) of compound **76i**

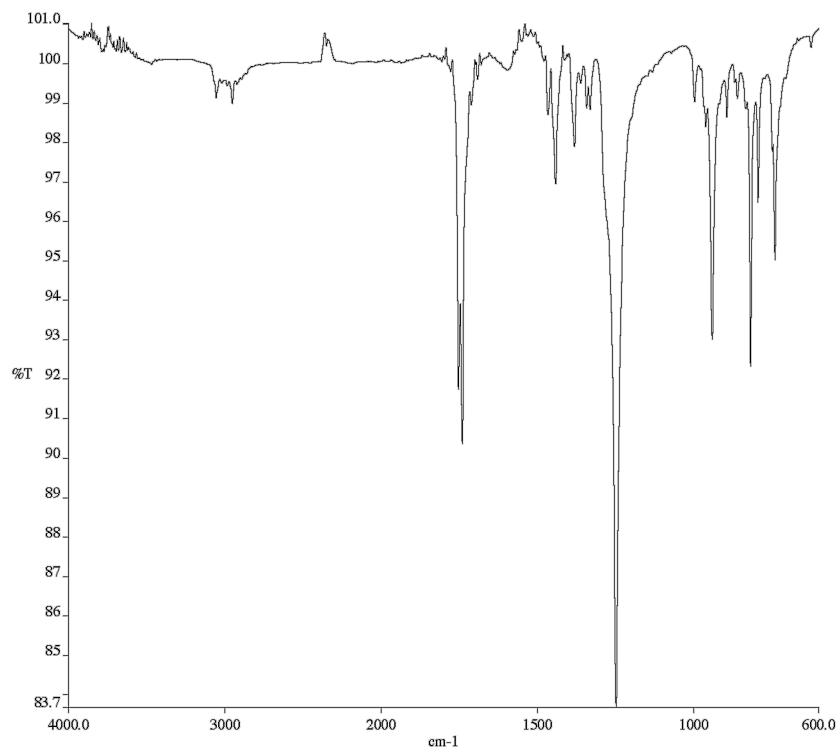


Figure A4.20 Infrared spectrum (Thin Film, NaCl) of compound **76i**

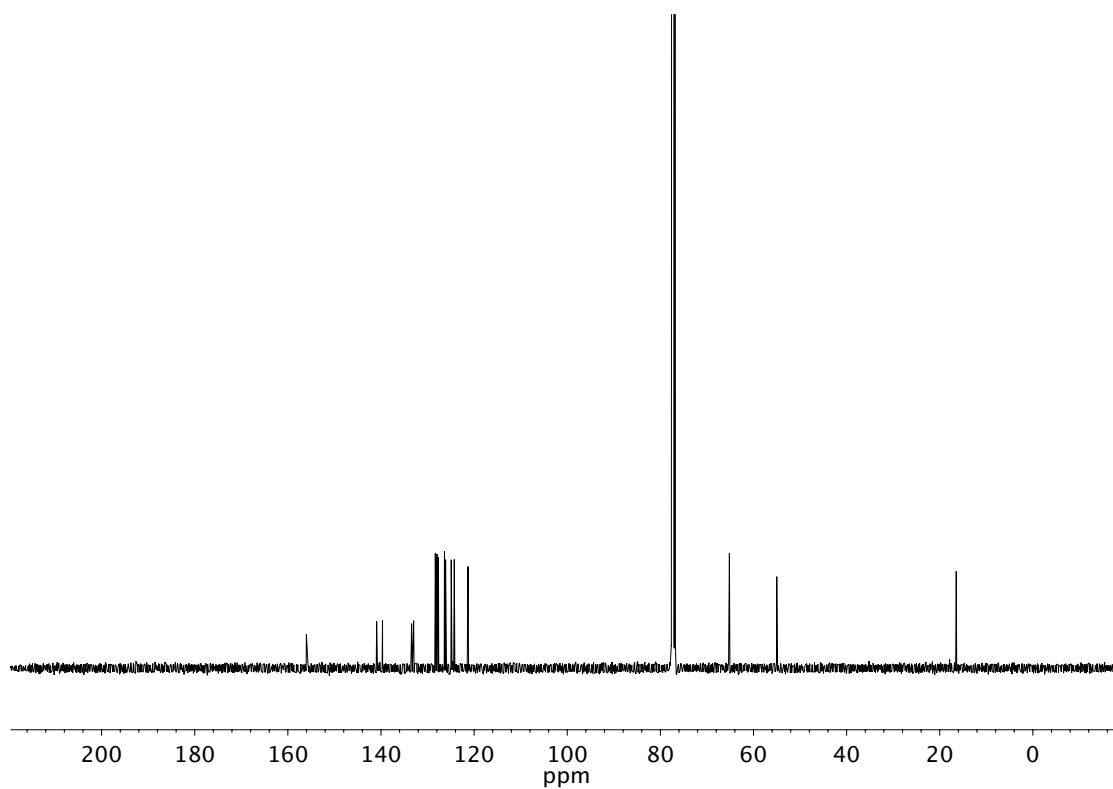


Figure A4.21 ¹³C NMR (101 MHz, CDCl₃) of compound **76i**

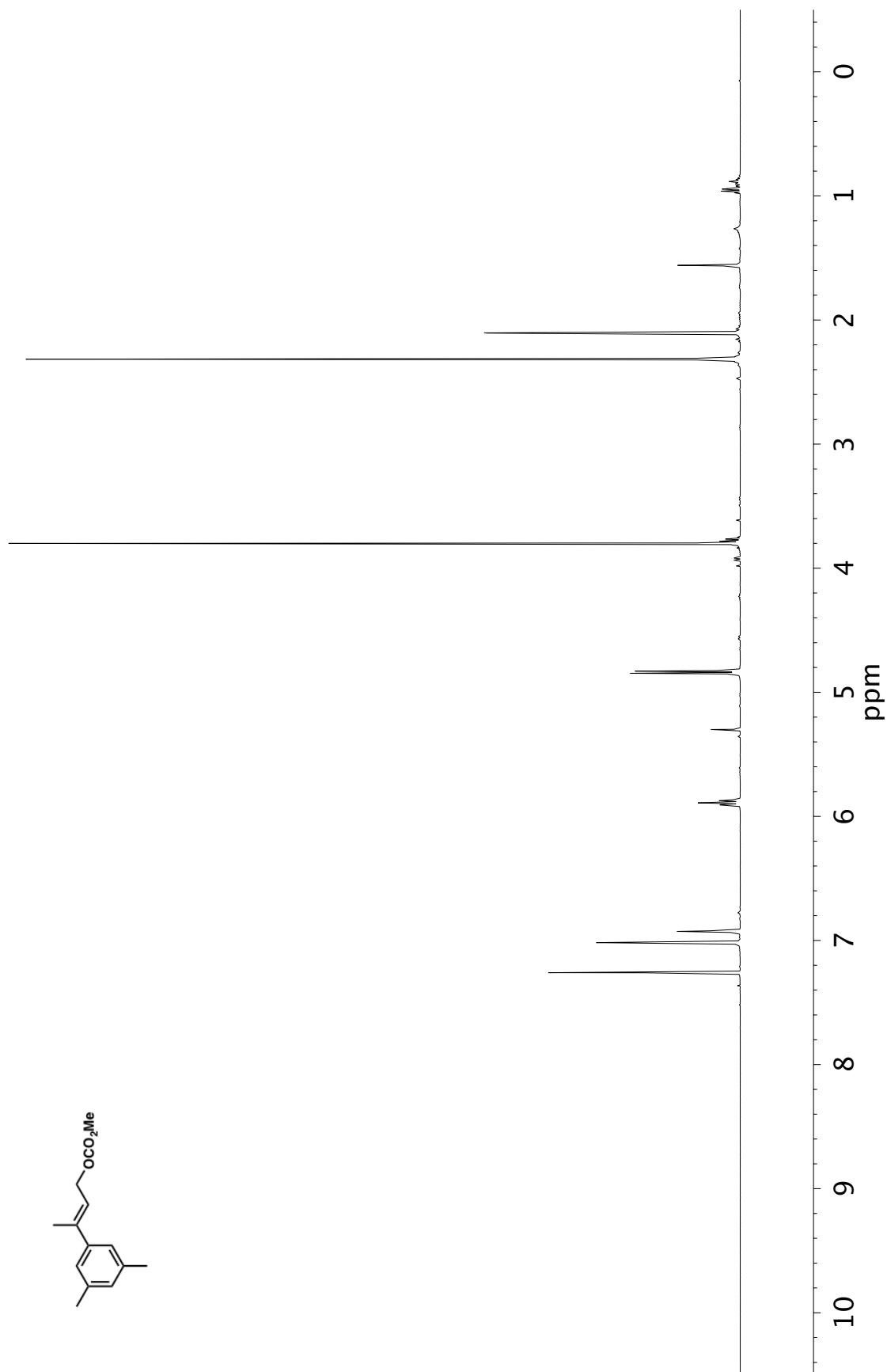


Figure A4.22 ¹H NMR (400 MHz, CDCl₃) of compound 76k

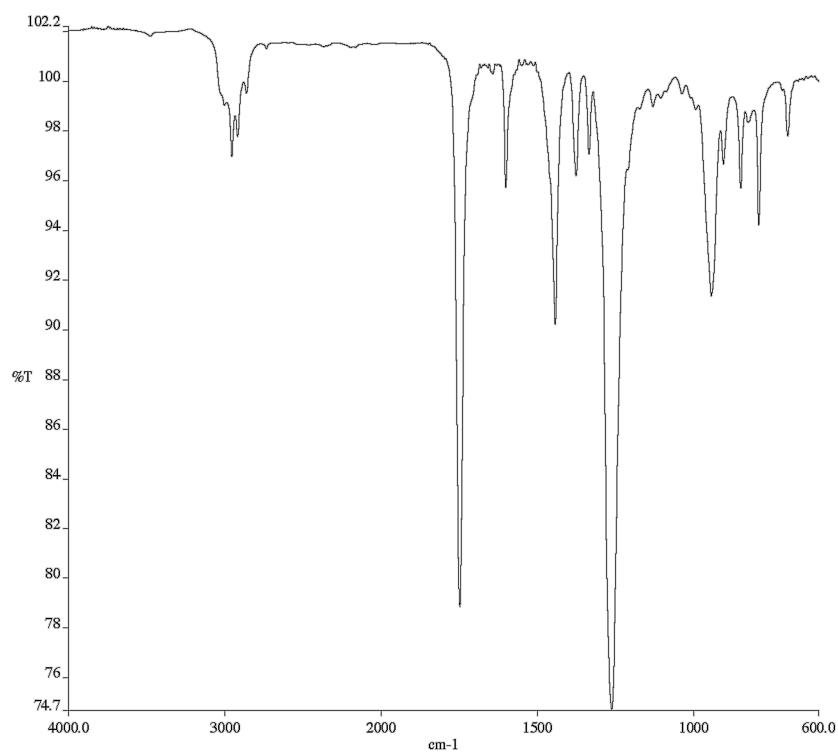


Figure A4.23 Infrared spectrum (Thin Film, NaCl) of compound **76k**

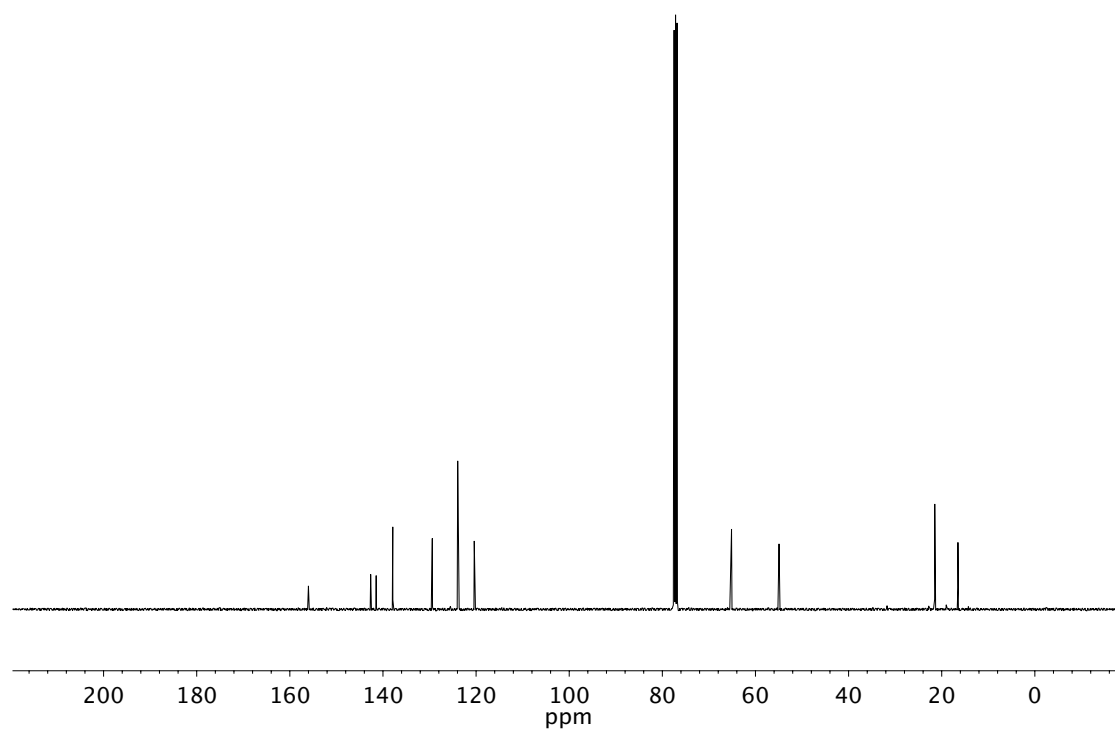


Figure A4.24 ¹³C NMR (101 MHz, CDCl₃) of compound **76k**

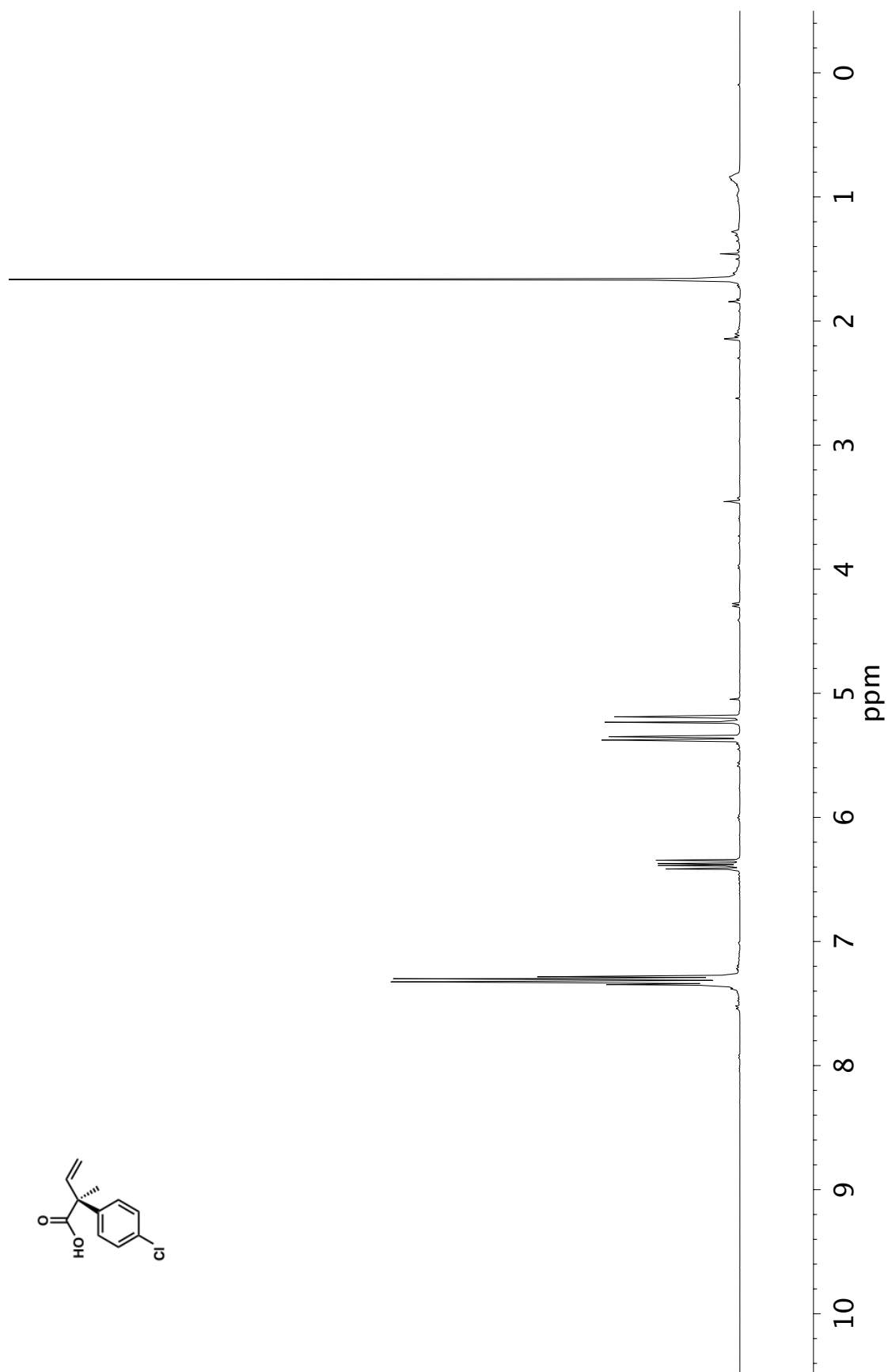


Figure A4.25 ^1H NMR (400 MHz, CDCl_3) of compound 77b

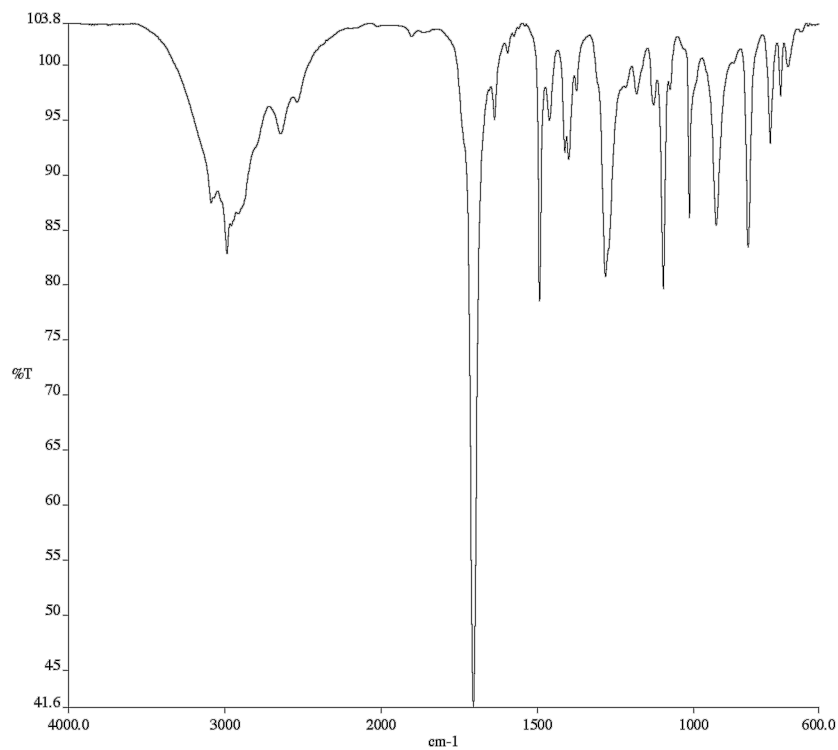


Figure A4.26 Infrared spectrum (Thin Film, NaCl) of compound **77b**

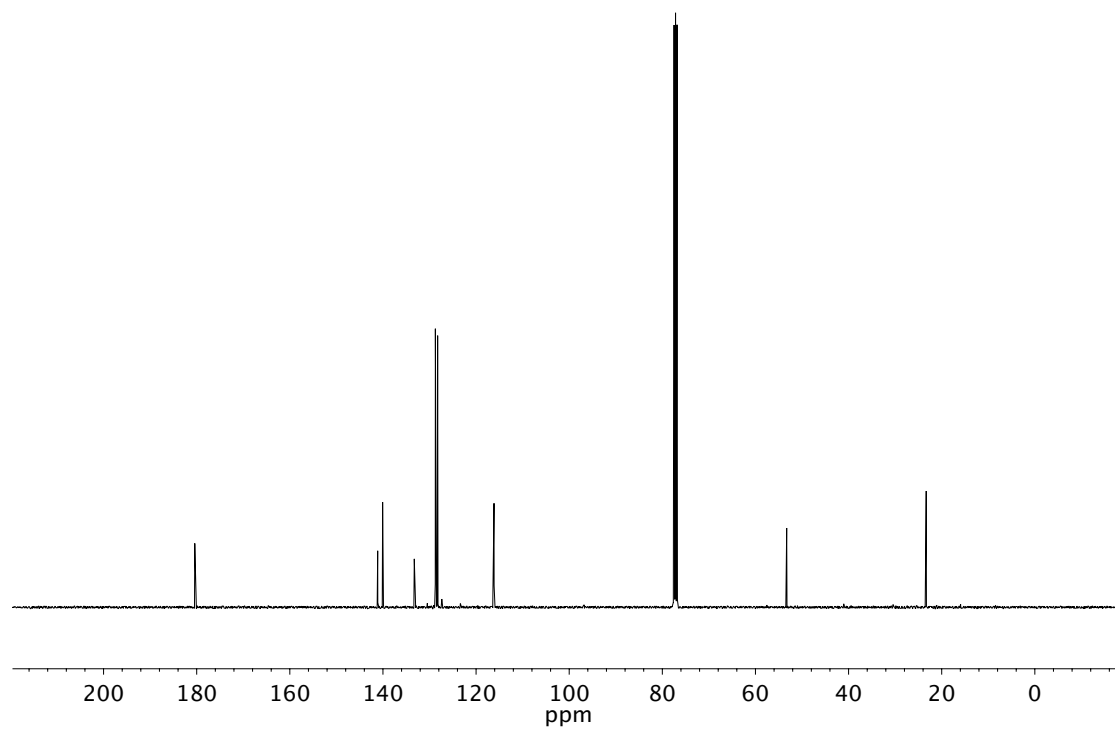


Figure A4.27 ¹³C NMR (101 MHz, CDCl₃) of compound **77b**

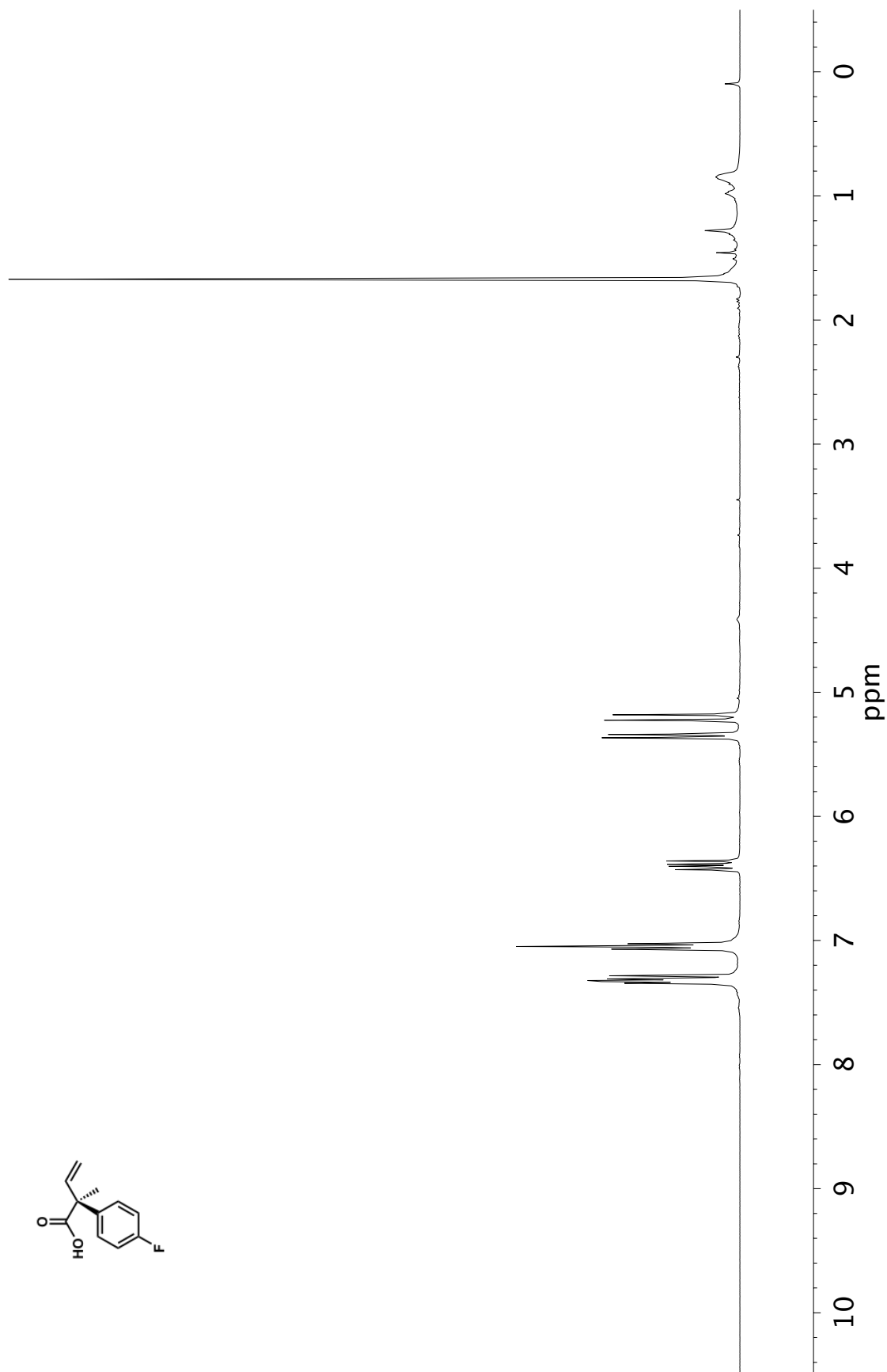


Figure A4.28 ^1H NMR (400 MHz, CDCl_3) of compound 77c

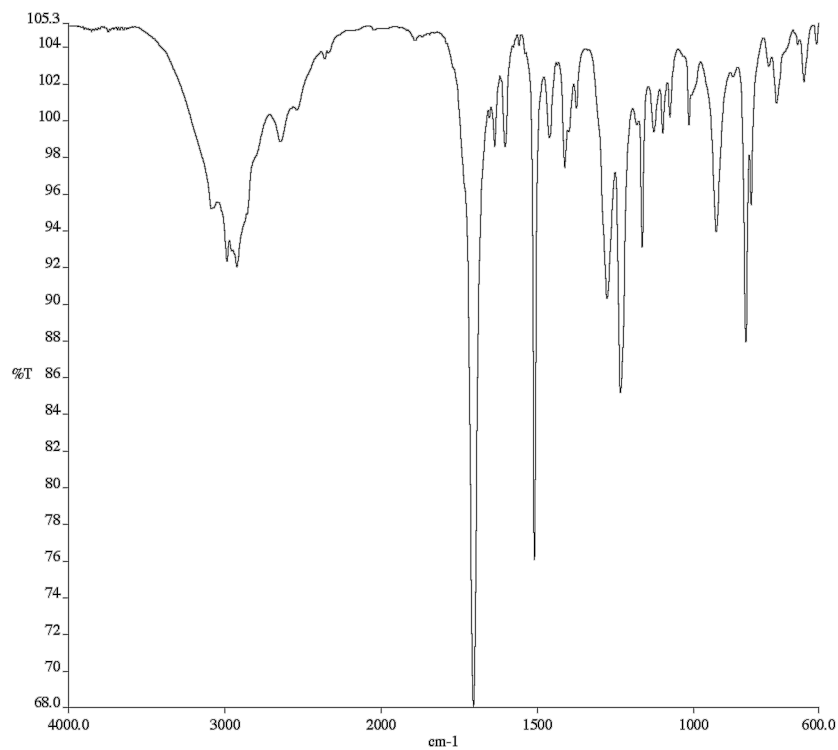


Figure A4.29 Infrared spectrum (Thin Film, NaCl) of compound **77c**

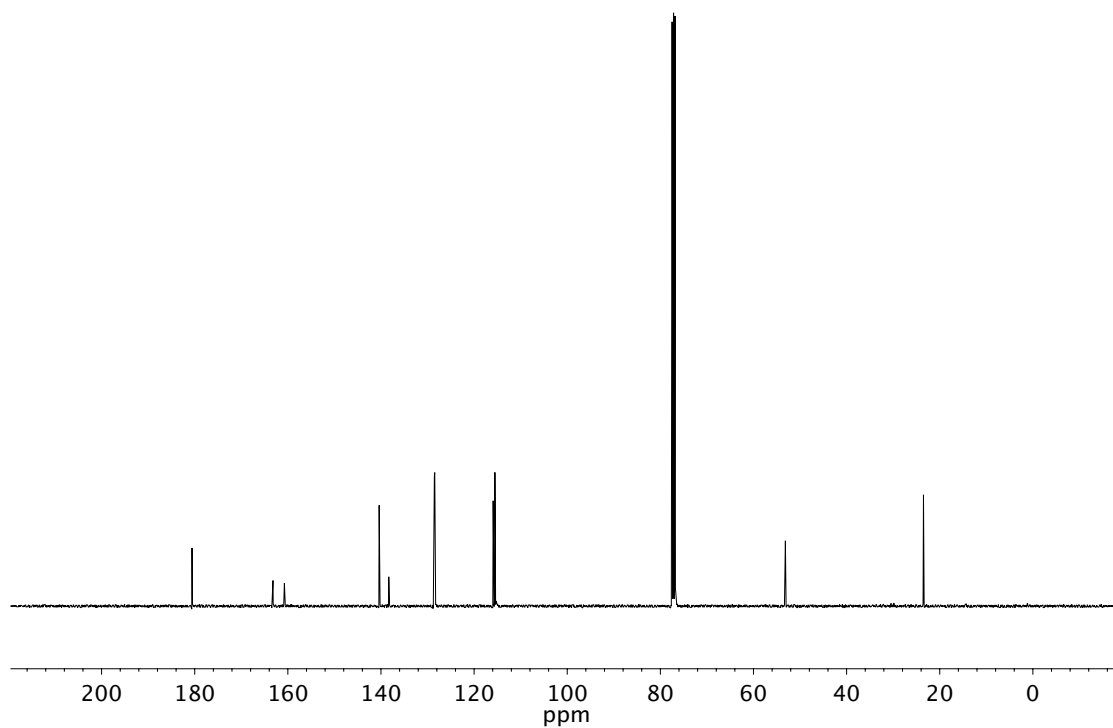


Figure A4.30 ¹³C NMR (101 MHz, CDCl₃) of compound **77c**

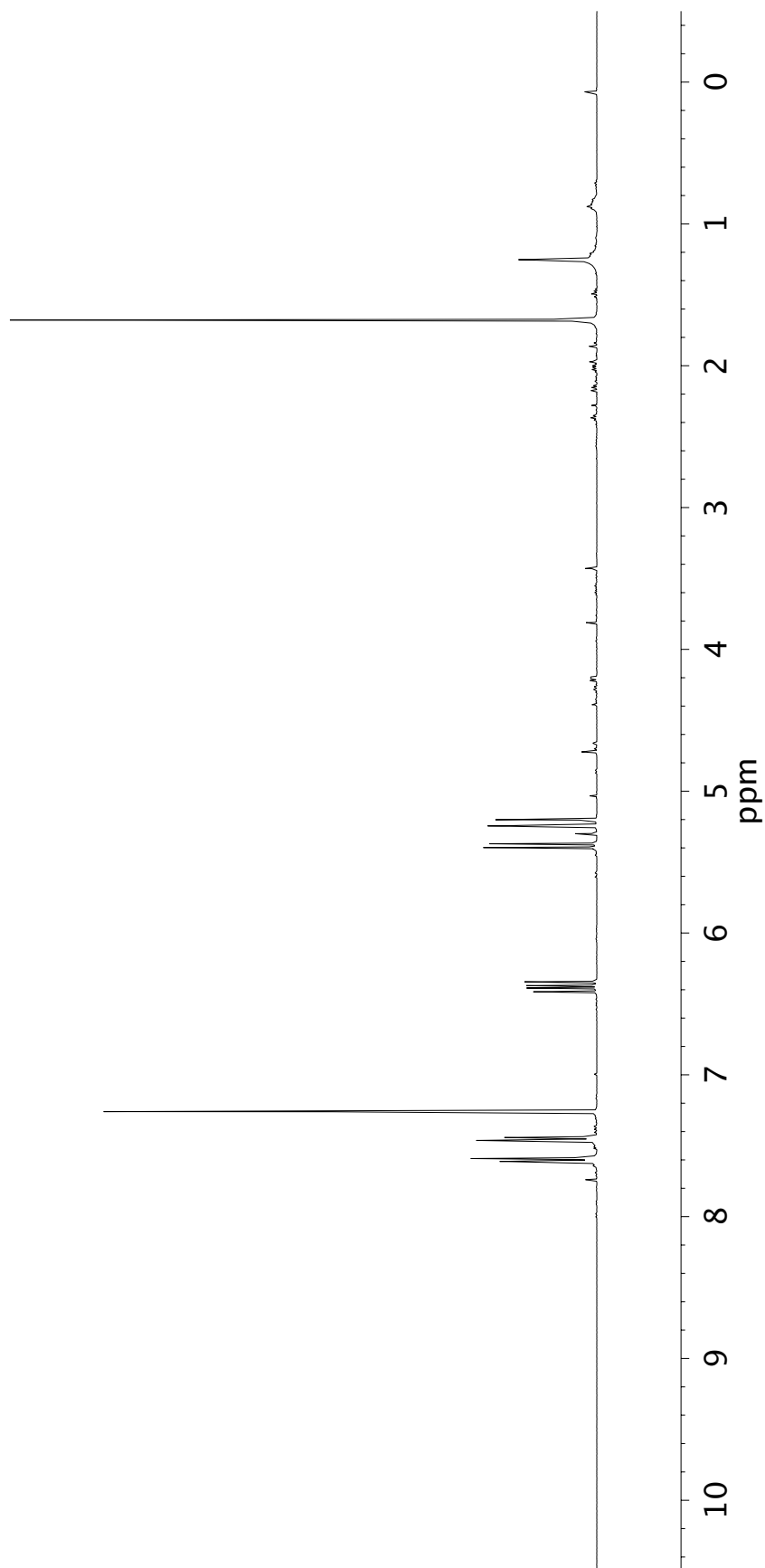
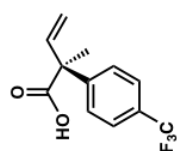


Figure A4.31 ¹H NMR (400 MHz, CDCl₃) of compound 77d

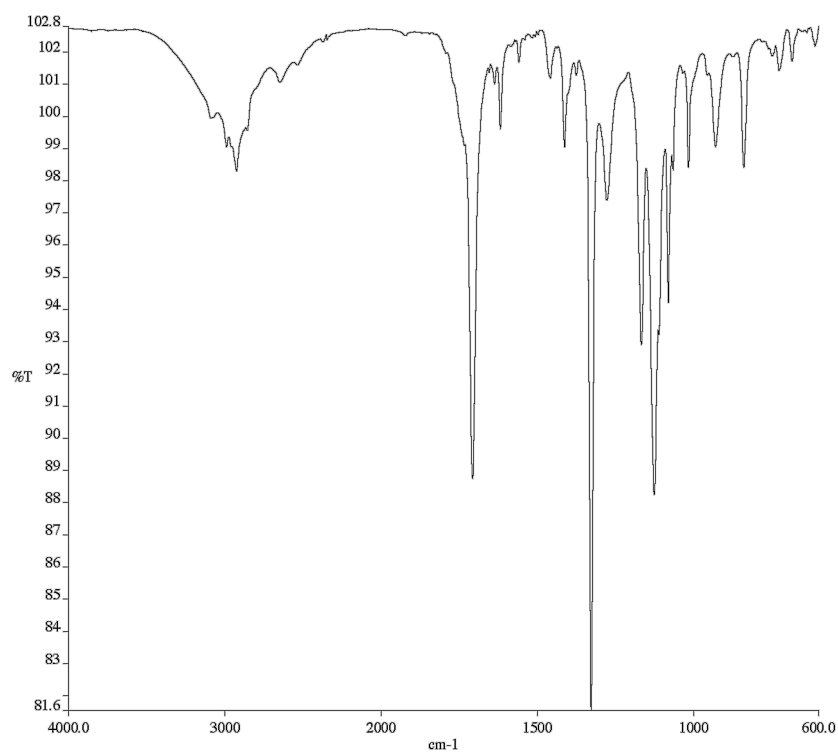


Figure A4.32 Infrared spectrum (Thin Film, NaCl) of compound **77d**

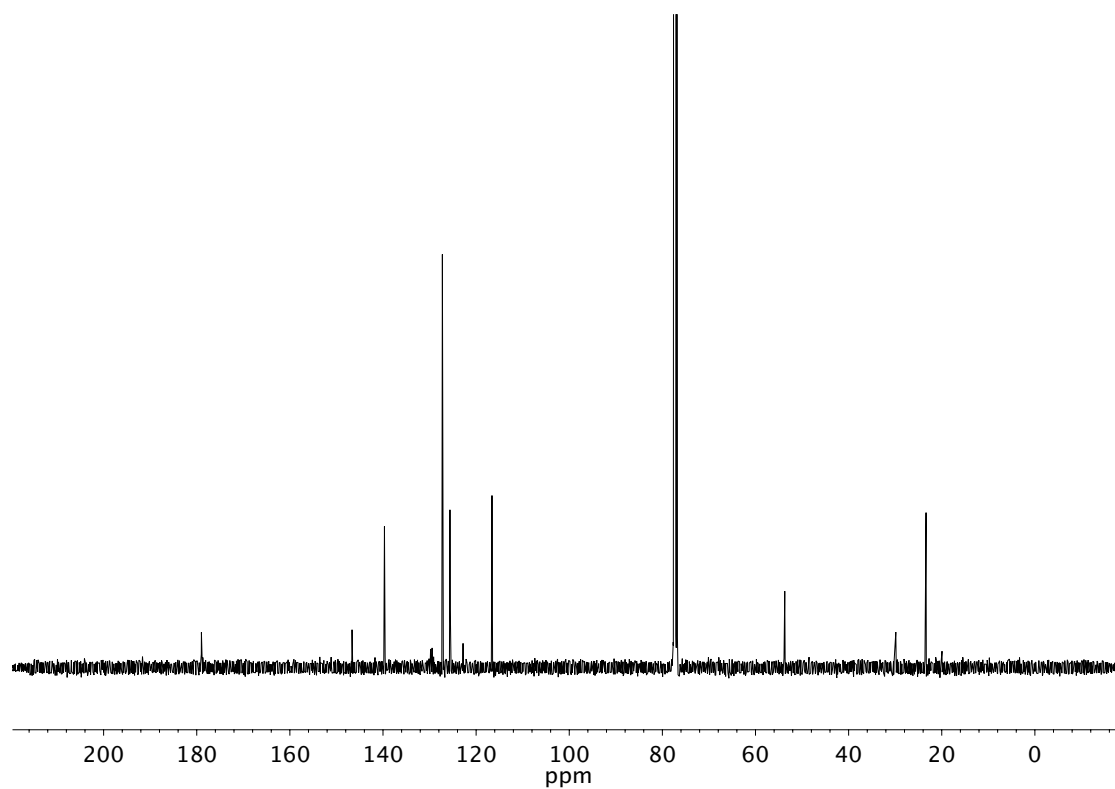


Figure A4.33 ¹³C NMR (101 MHz, CDCl₃) of compound **77d**

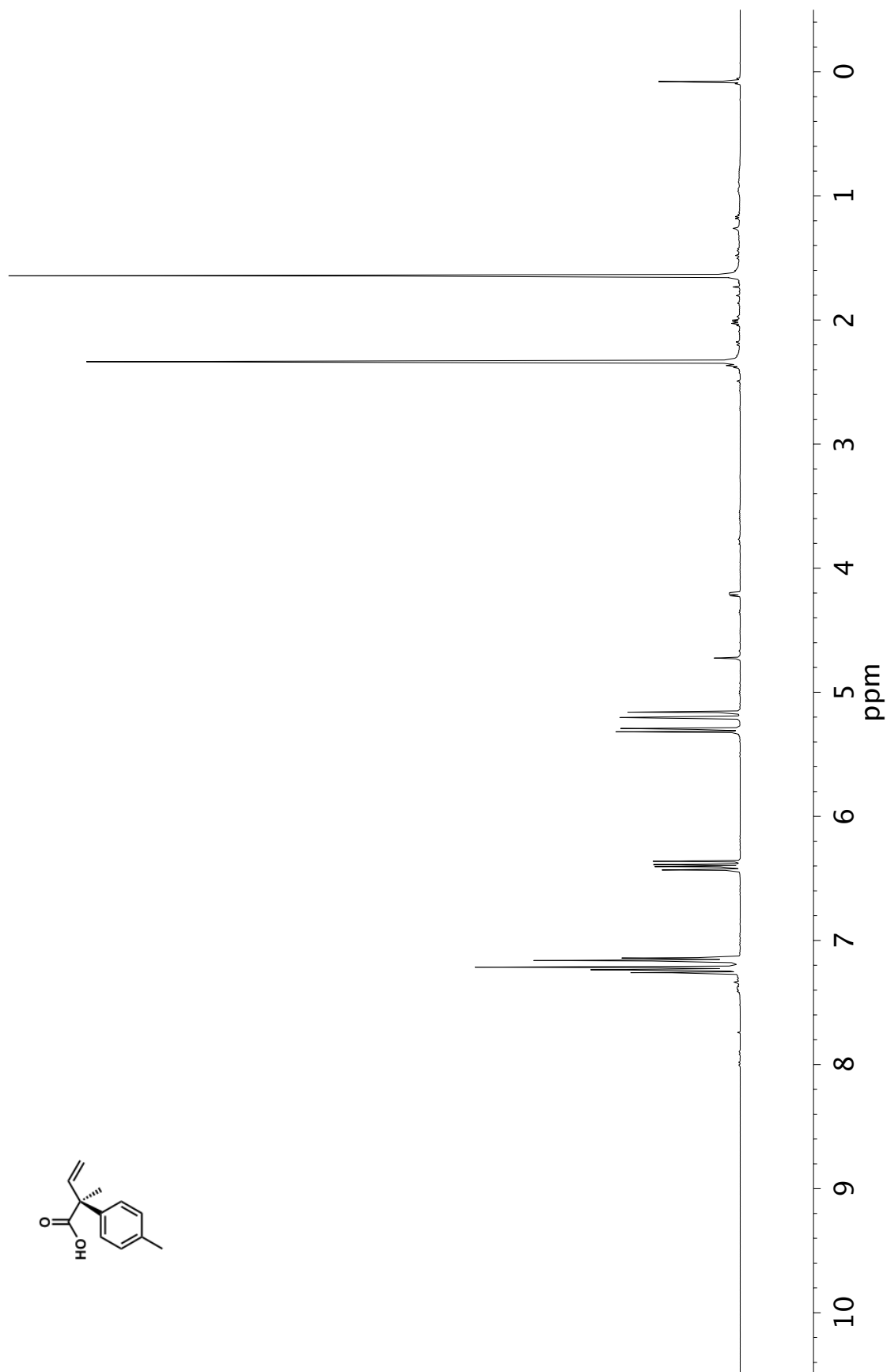


Figure A4.34 ^1H NMR (400 MHz, CDCl_3) of compound 77e

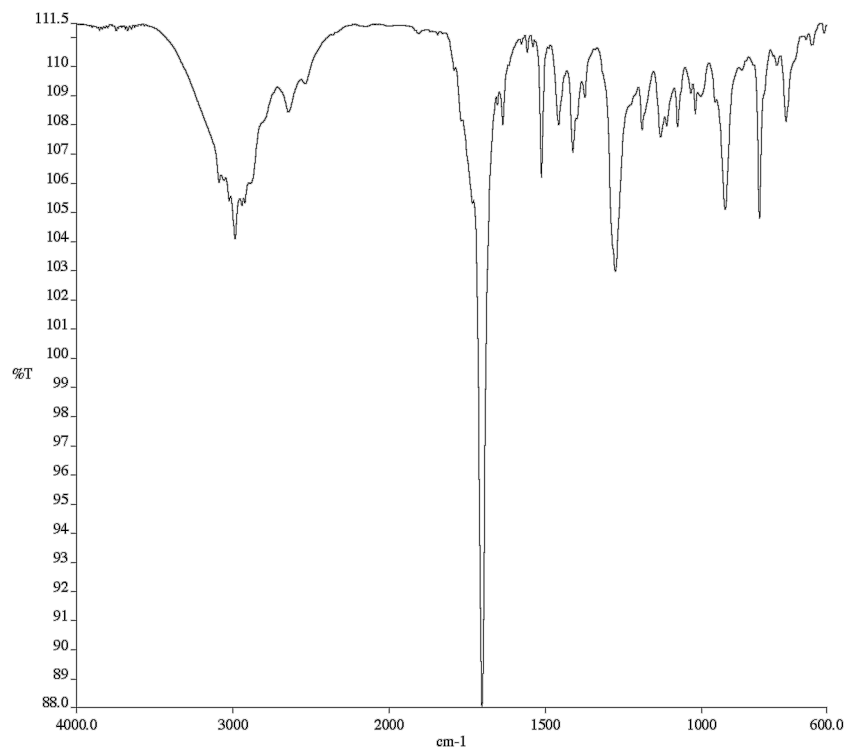


Figure A4.35 Infrared spectrum (Thin Film, NaCl) of compound **77e**

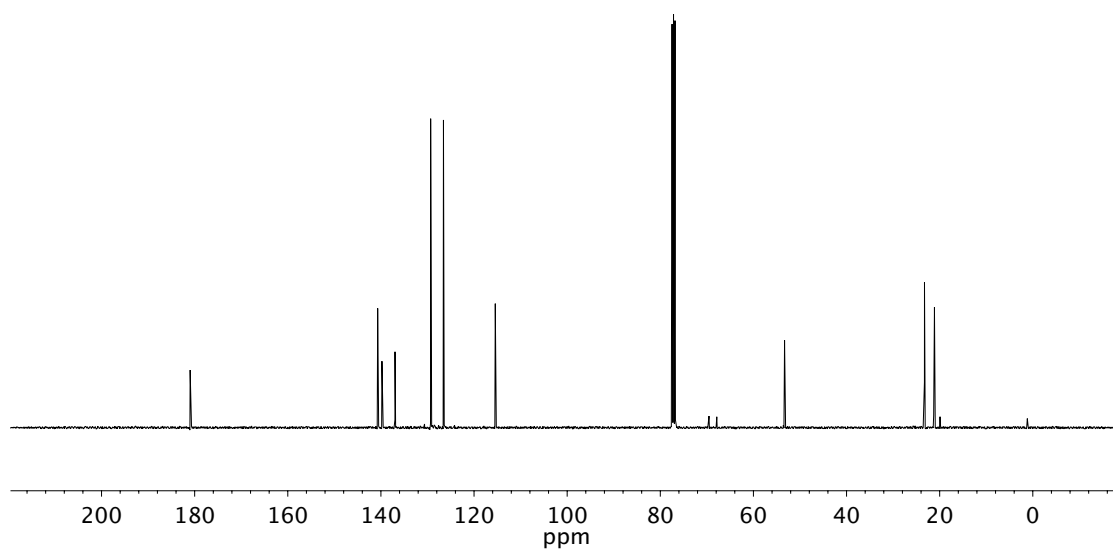


Figure A4.36 ¹³C NMR (101 MHz, CDCl₃) of compound **77e**

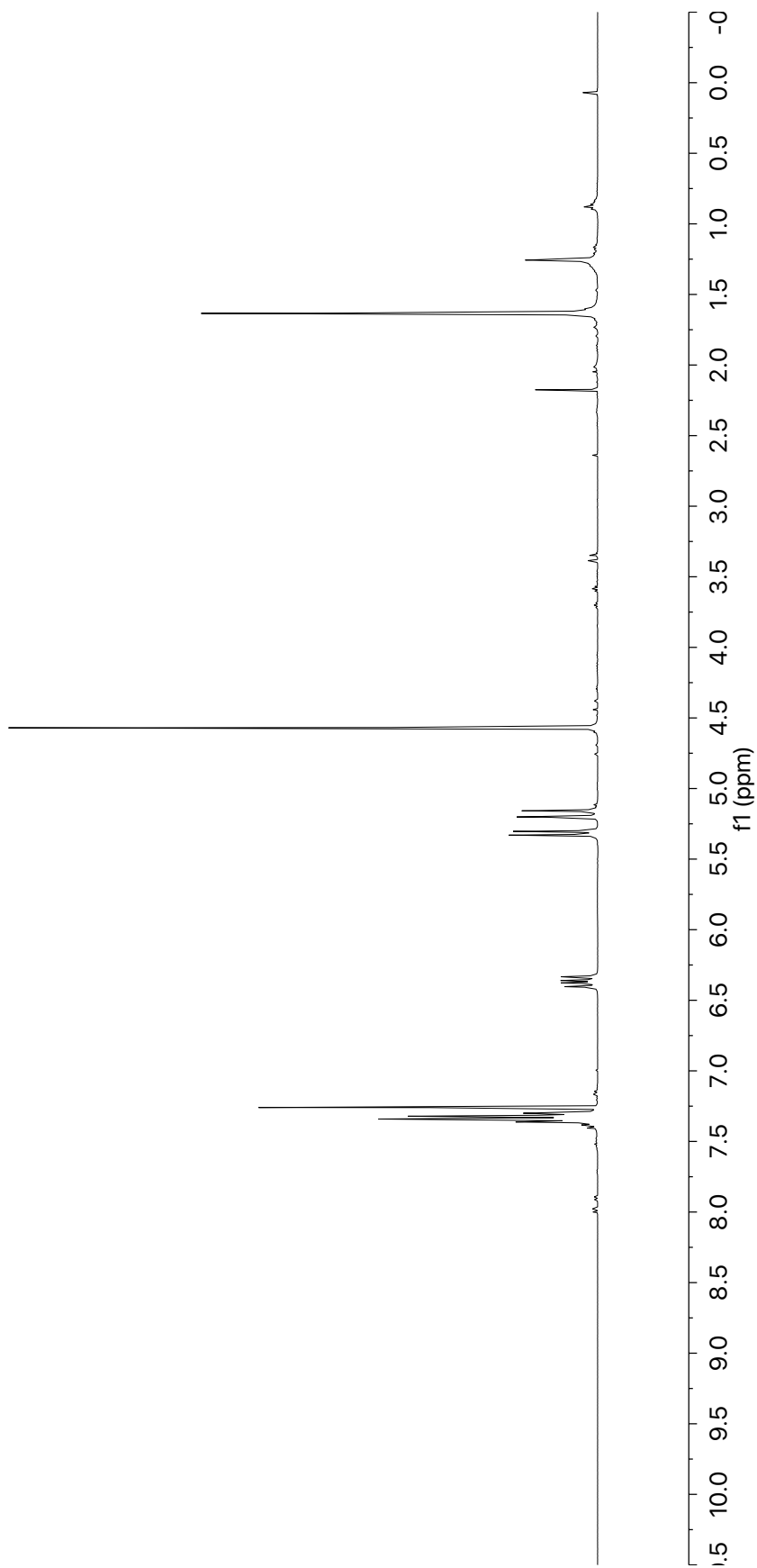
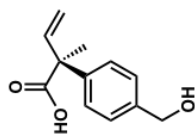


Figure A4.37 ^1H NMR (400 MHz, CDCl_3) of compound **77f**

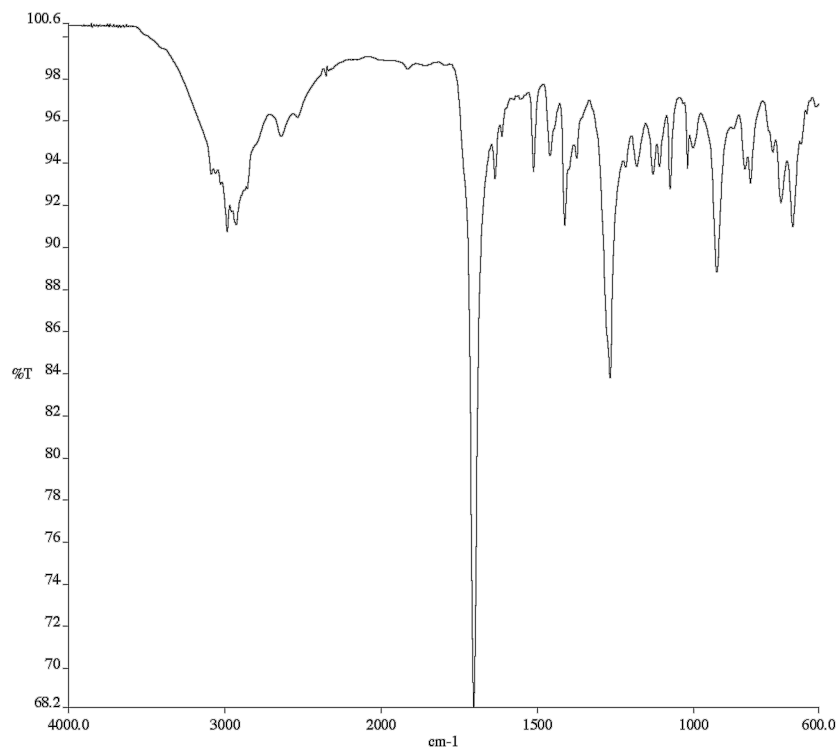


Figure A4.38 Infrared spectrum (Thin Film, NaCl) of compound **77f**

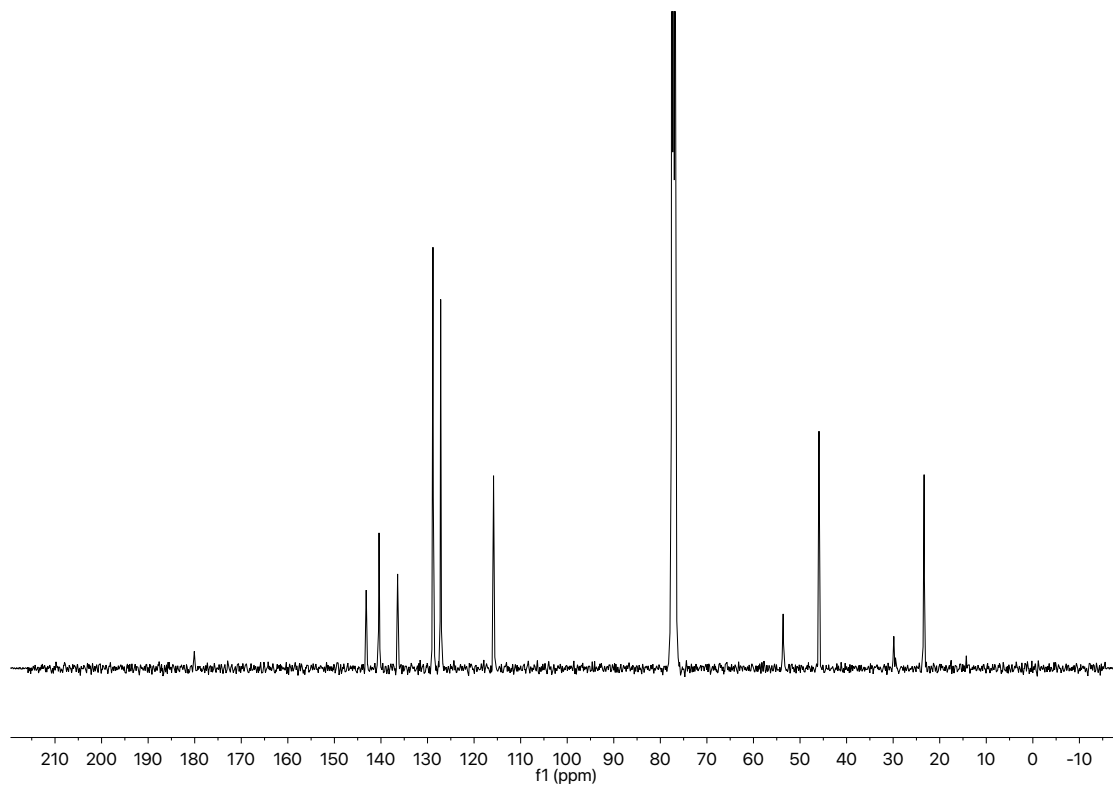


Figure A4.39 ¹³C NMR (101 MHz, CDCl₃) of compound **77f**

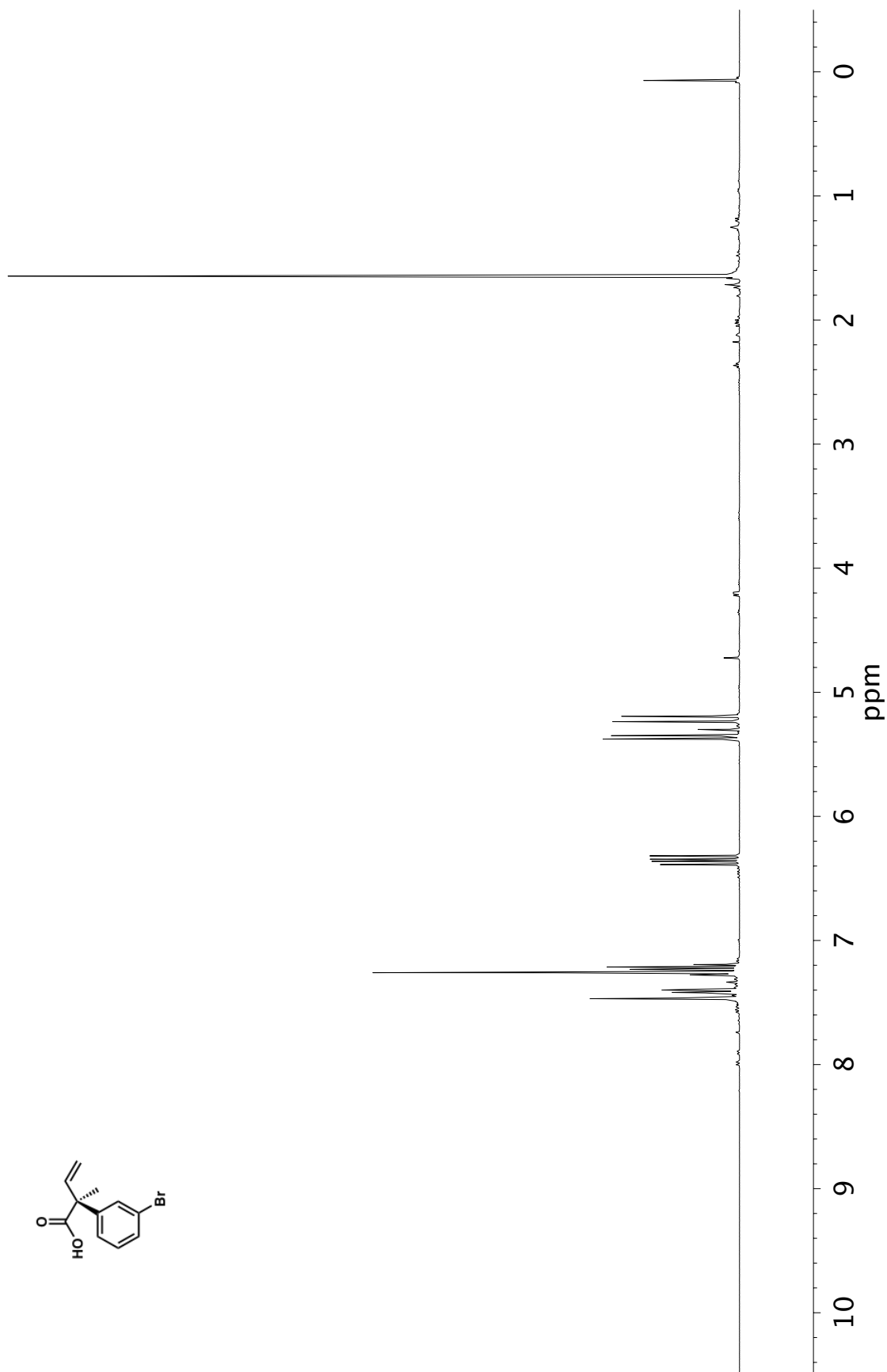


Figure A4.40 ¹H NMR (400 MHz, CDCl₃) of compound 77g

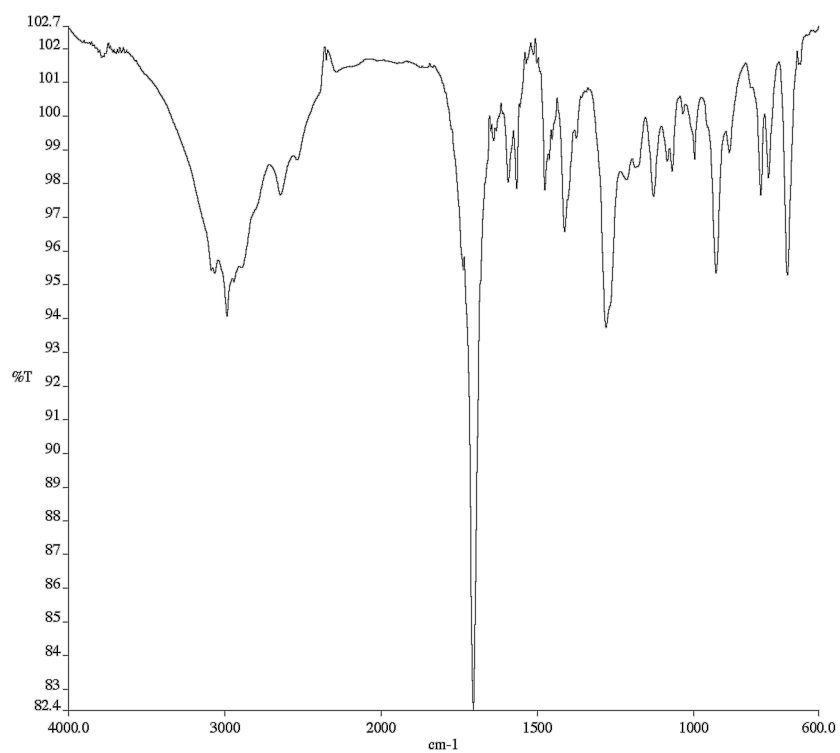


Figure A4.41 Infrared spectrum (Thin Film, NaCl) of compound **77g**

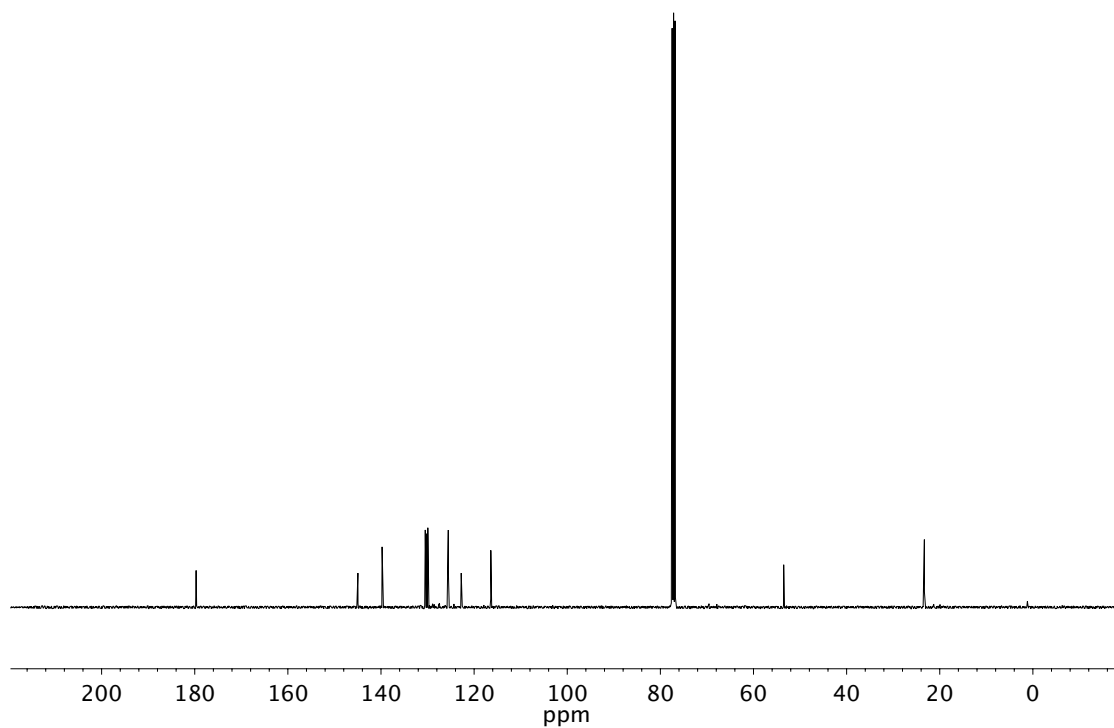


Figure A4.42 ¹³C NMR (101 MHz, CDCl₃) of compound **77g**

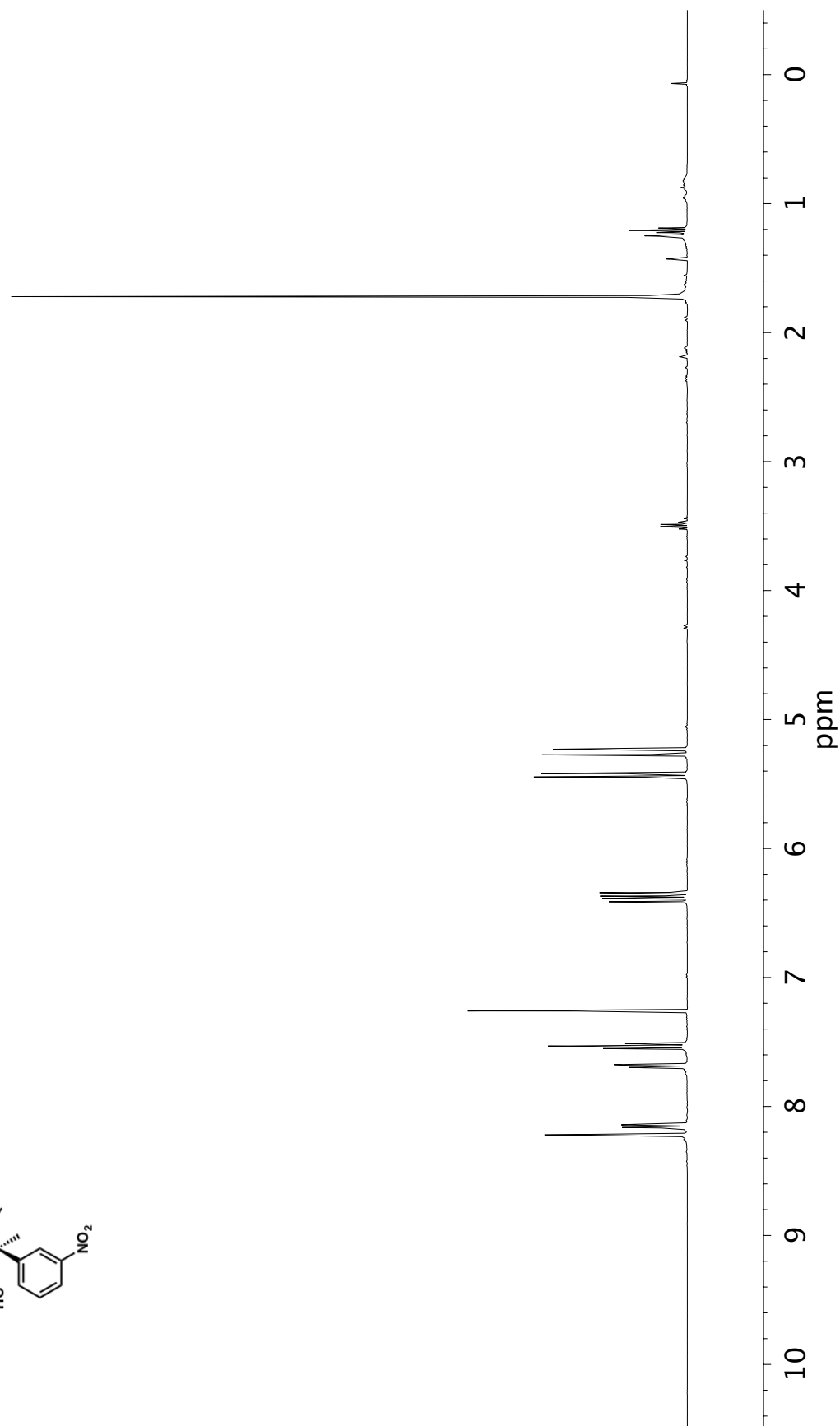
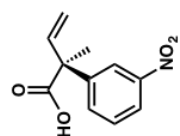


Figure A4.43 ¹H NMR (400 MHz, CDCl₃) of compound 77h

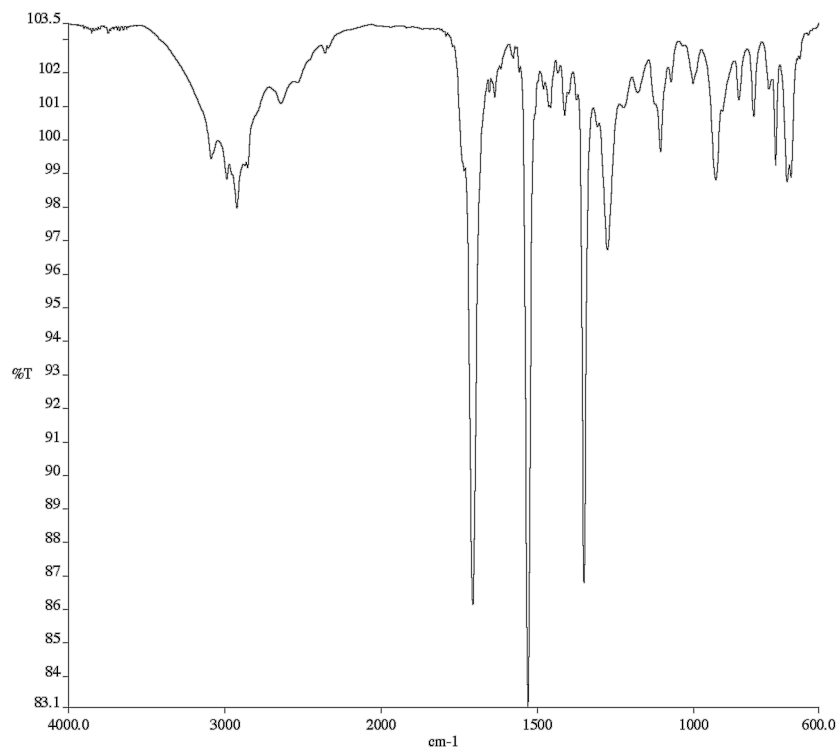


Figure A4.44 Infrared spectrum (Thin Film, NaCl) of compound **77h**

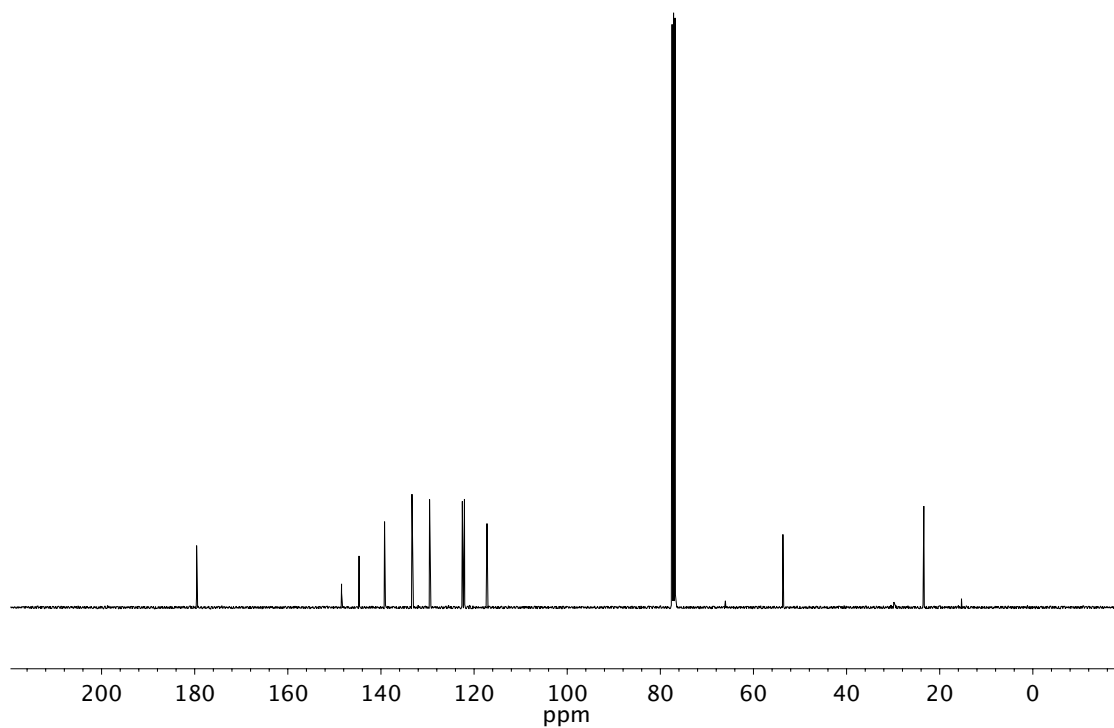


Figure A4.45 ¹³C NMR (101 MHz, CDCl₃) of compound **77h**

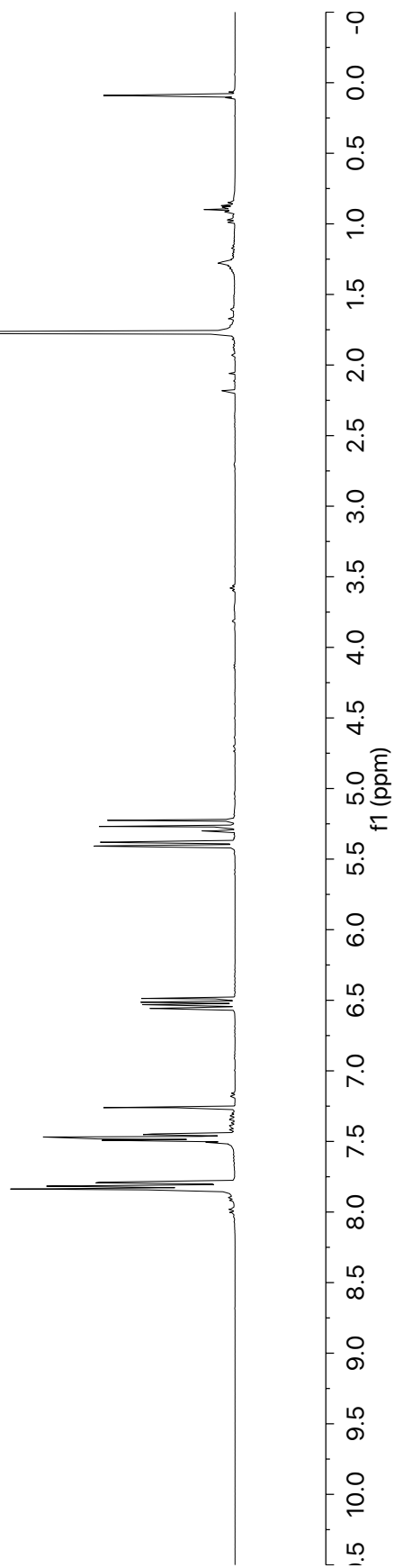
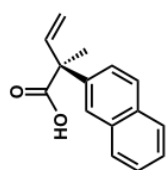


Figure A4.46 ^1H NMR (400 MHz, CDCl_3) of compound **77i**

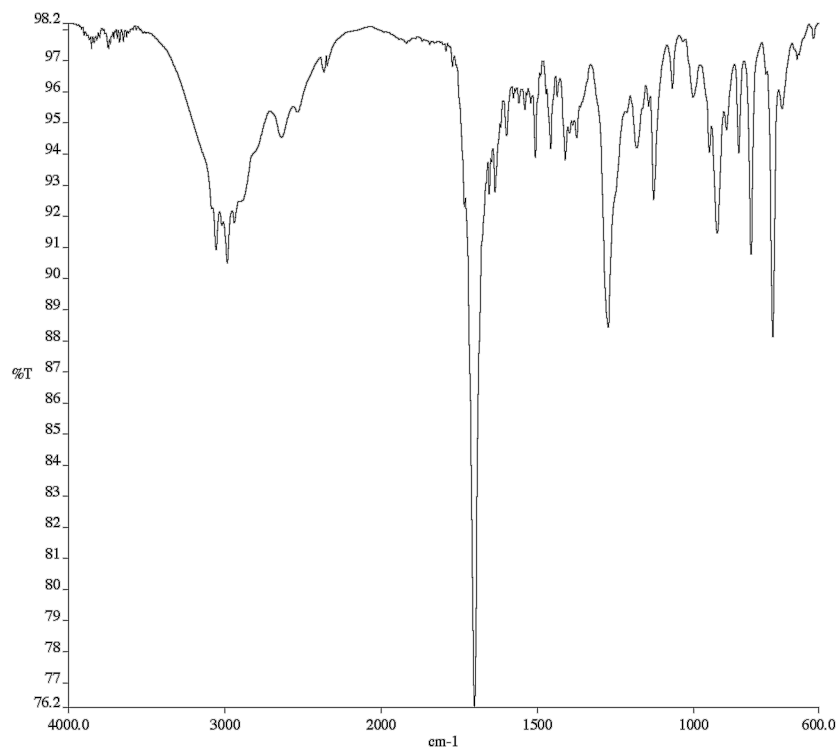


Figure A4.47 Infrared spectrum (Thin Film, NaCl) of compound **77i**

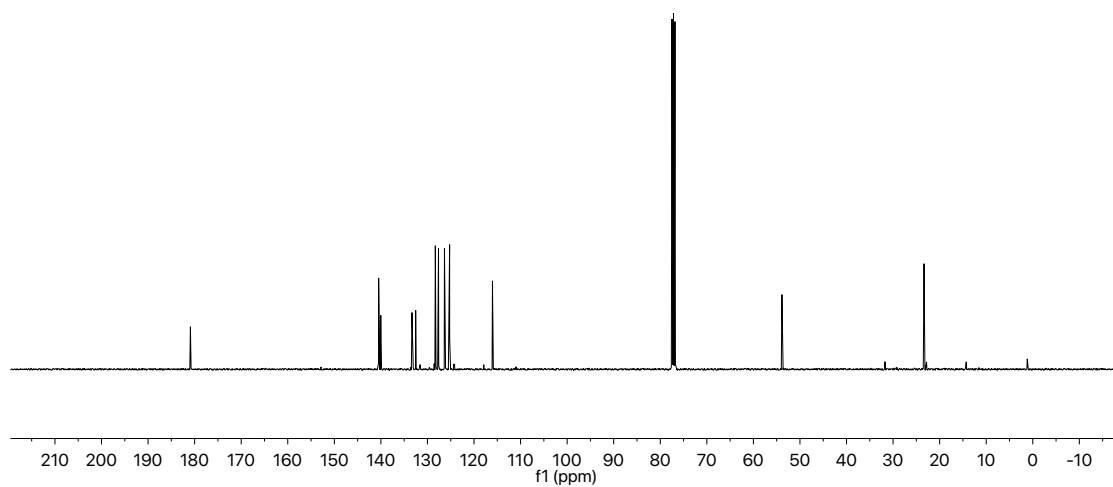


Figure A4.48 ¹³C NMR (101 MHz, CDCl₃) of compound **77i**

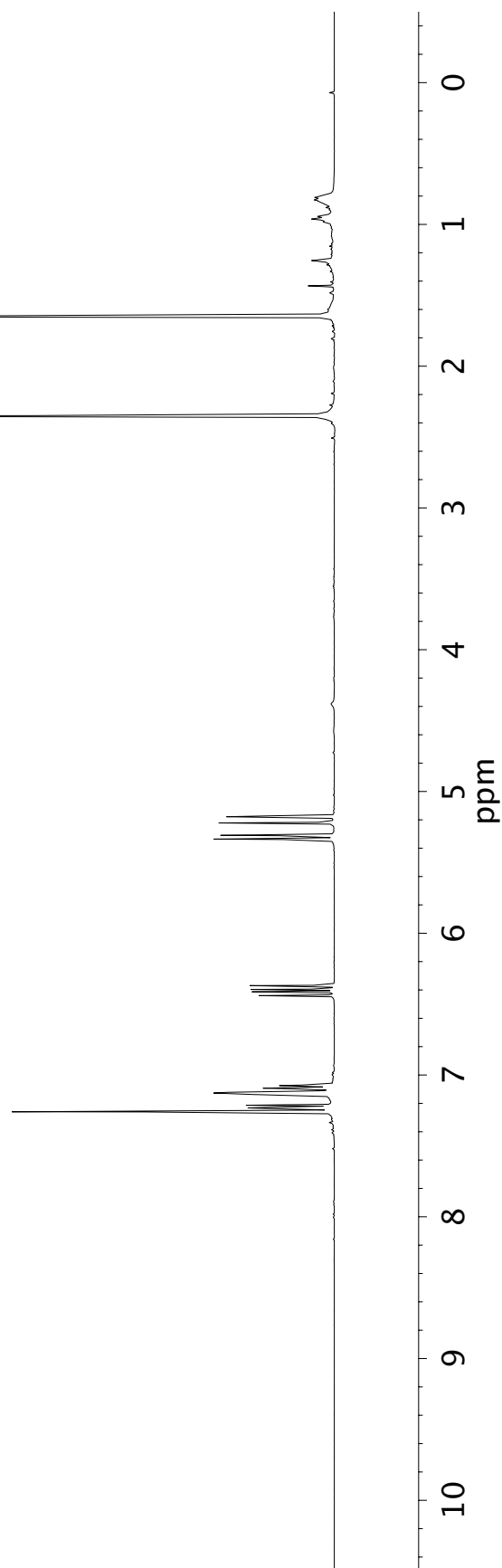
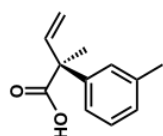


Figure A4.49 ^1H NMR (400 MHz, CDCl_3) of compound **77j**

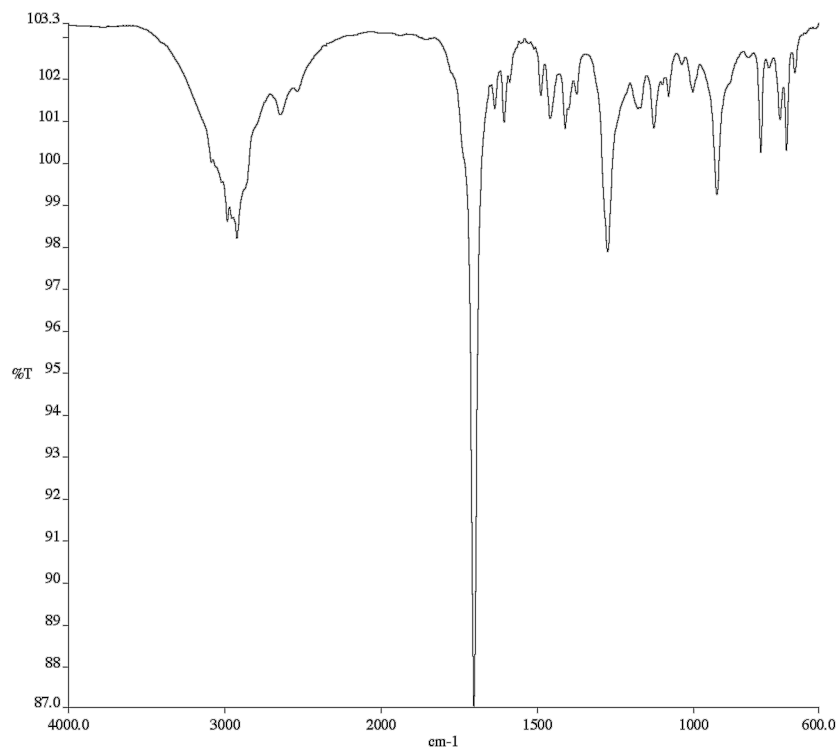


Figure A4.50 Infrared spectrum (Thin Film, NaCl) of compound **77j**

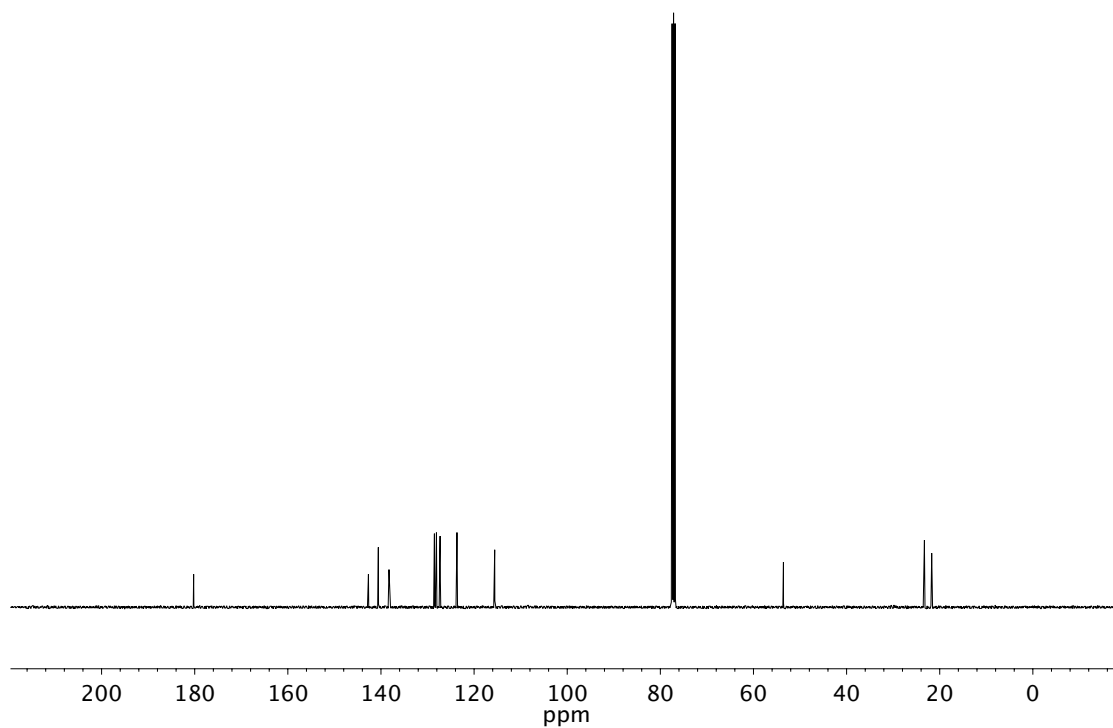
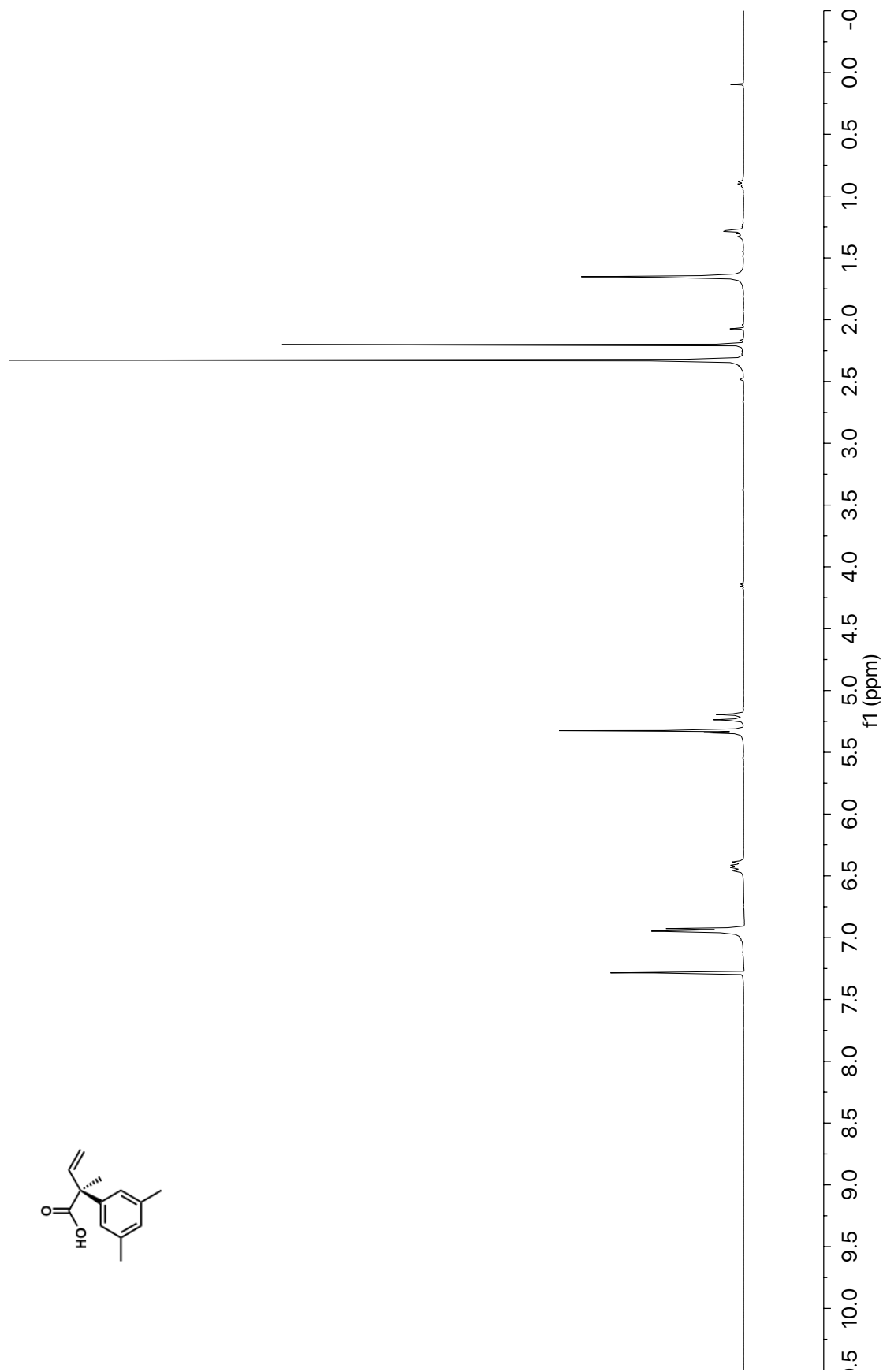


Figure A4.51 ¹³C NMR (101 MHz, CDCl₃) of compound **77j**

**Figure A4.52** ¹H NMR (400 MHz, CDCl₃) of compound 77k

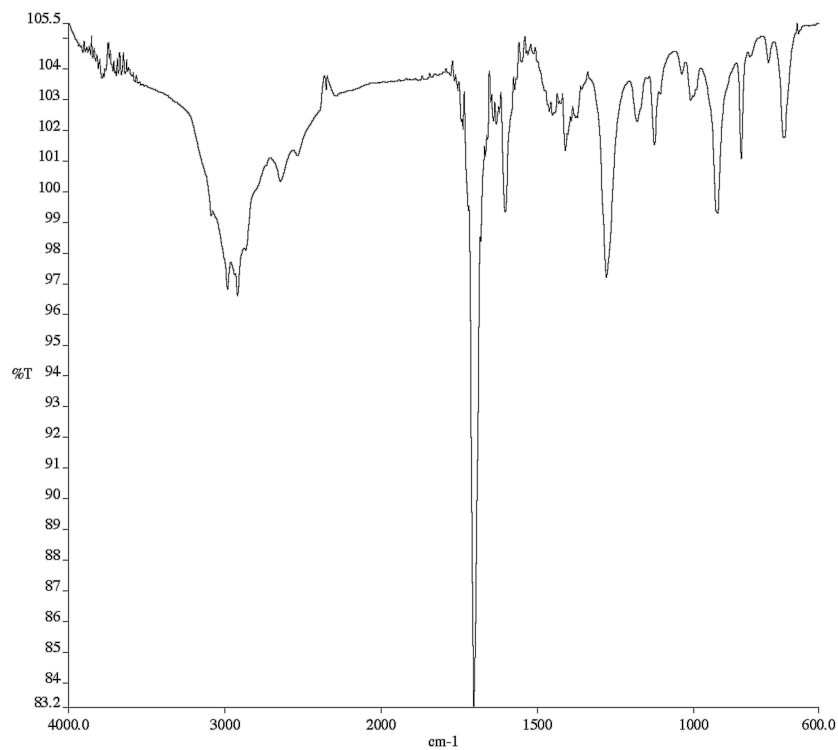


Figure A4.53 Infrared spectrum (Thin Film, NaCl) of compound **77k**

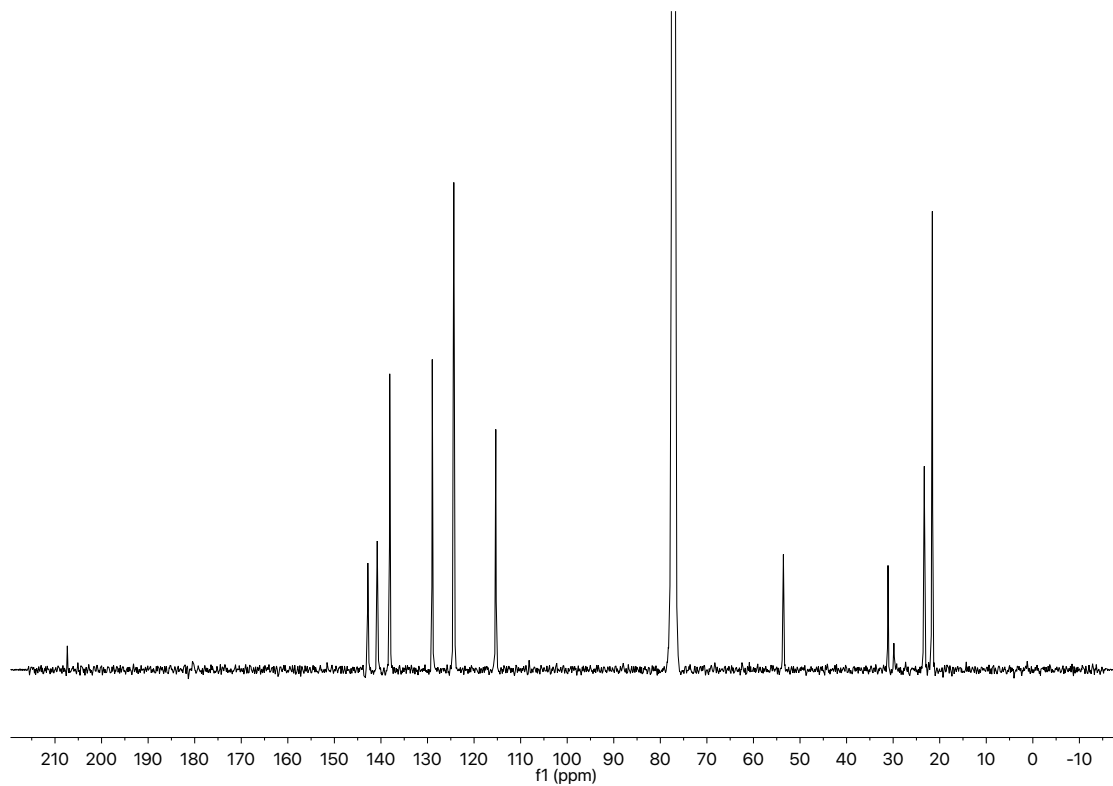


Figure A4.54 ¹³C NMR (101 MHz, CDCl₃) of compound **77k**

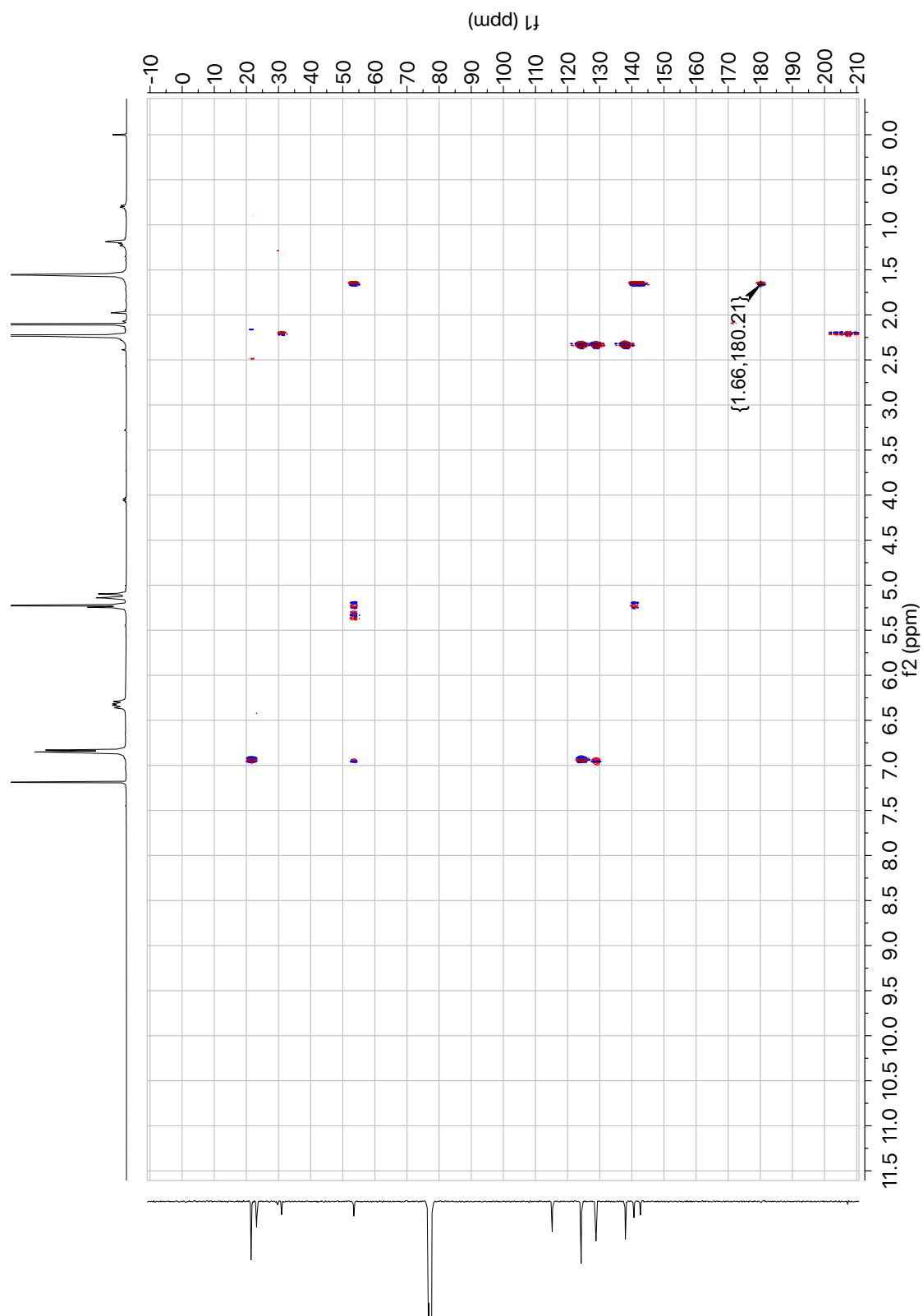


Figure A4.55 HMBC (400 MHz, CDCl_3) of compound **77k**

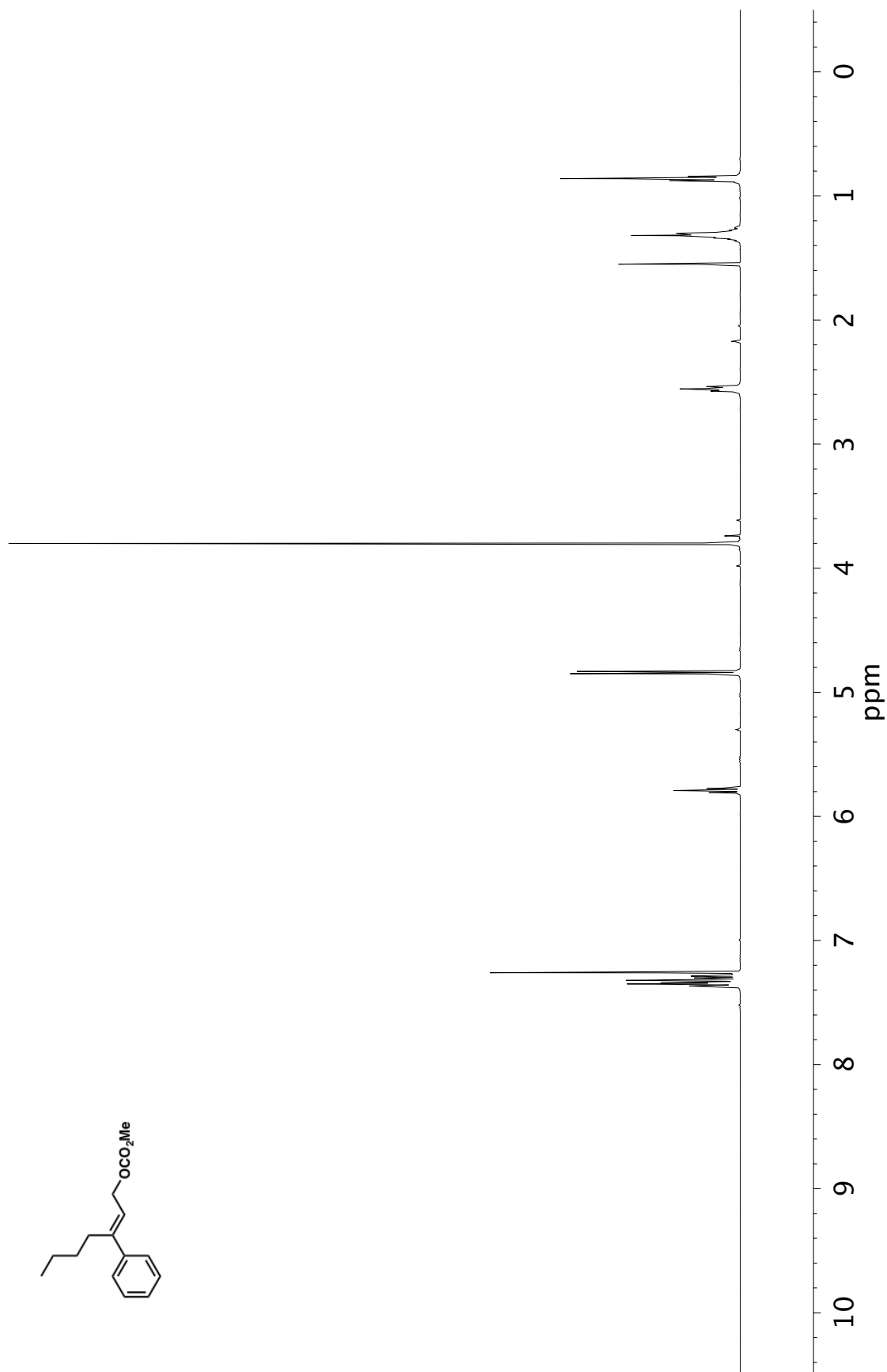


Figure A4.56 ¹H NMR (400 MHz, CDCl₃) of compound 78b

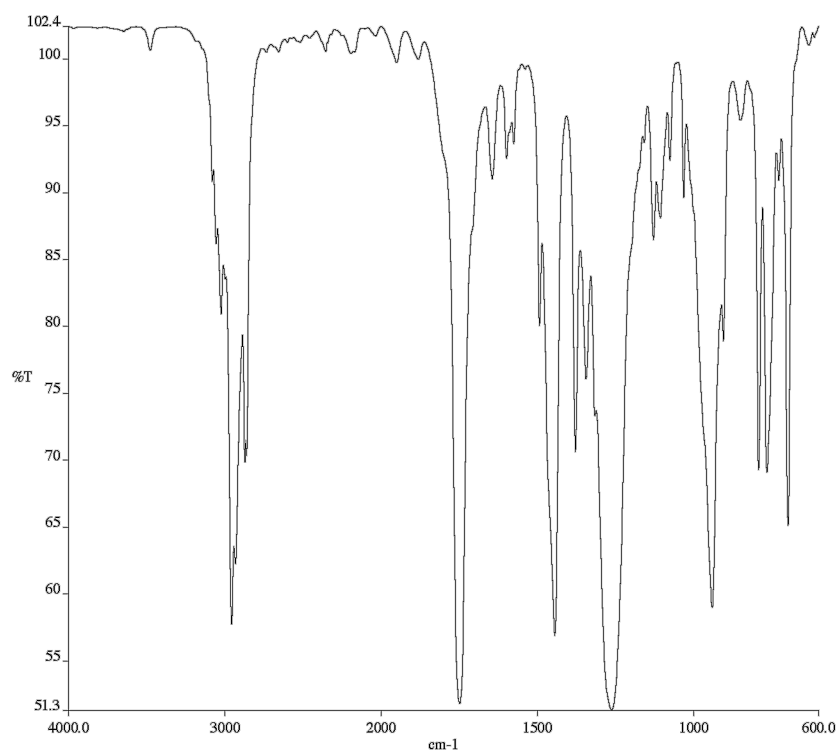


Figure A4.57 Infrared spectrum (Thin Film, NaCl) of compound **78b**

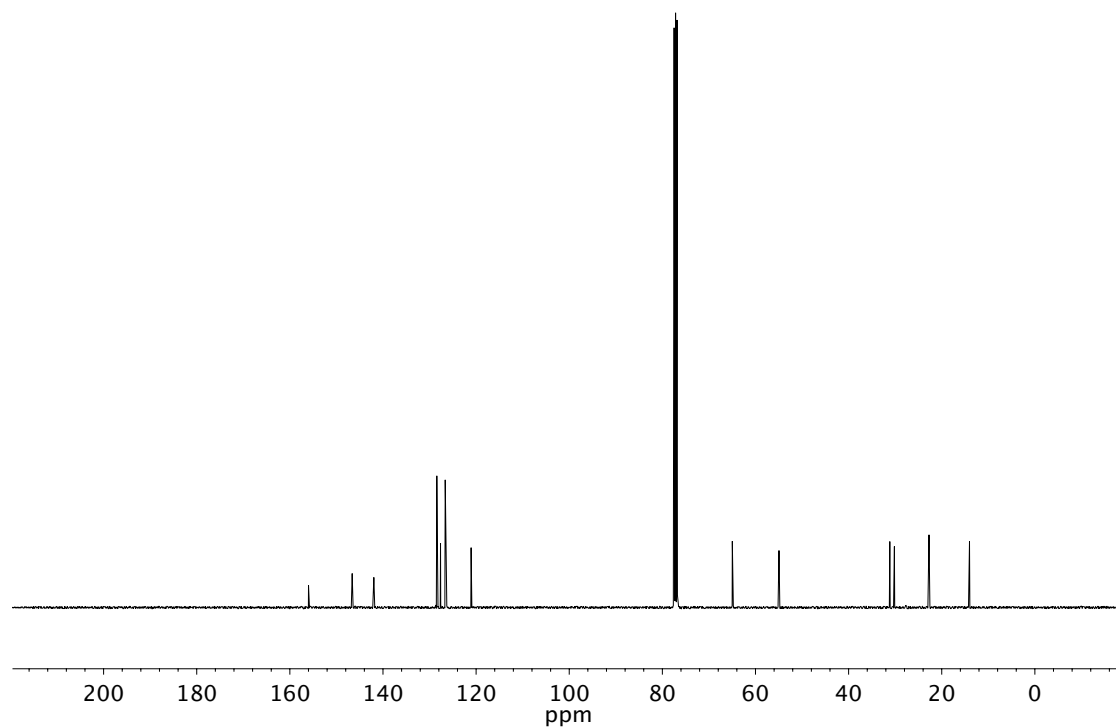


Figure A4.58 ¹³C NMR (101 MHz, CDCl₃) of compound **78b**

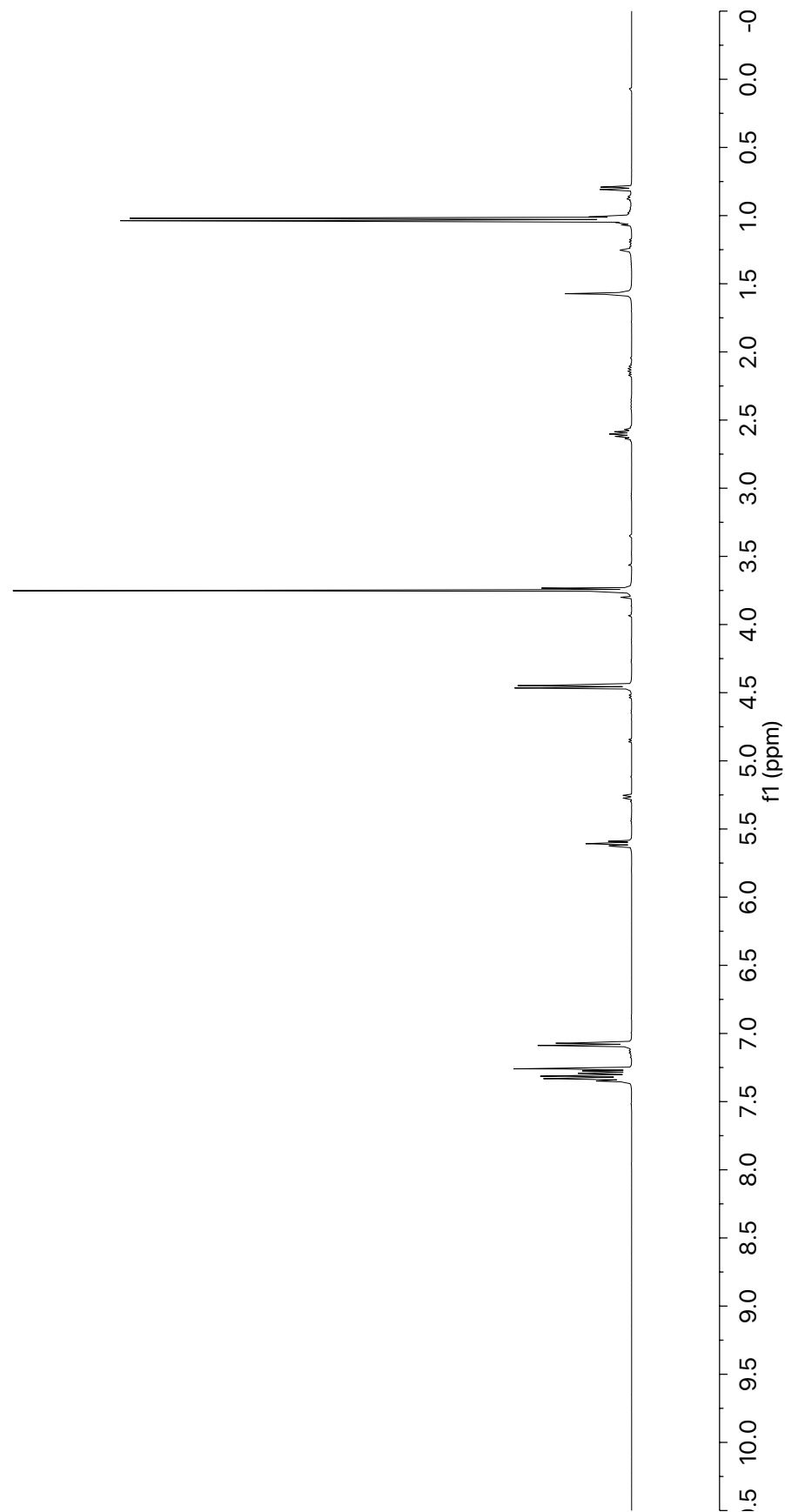
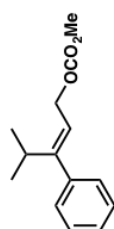


Figure A4.59 ^1H NMR (400 MHz, CDCl_3) of compound 78c

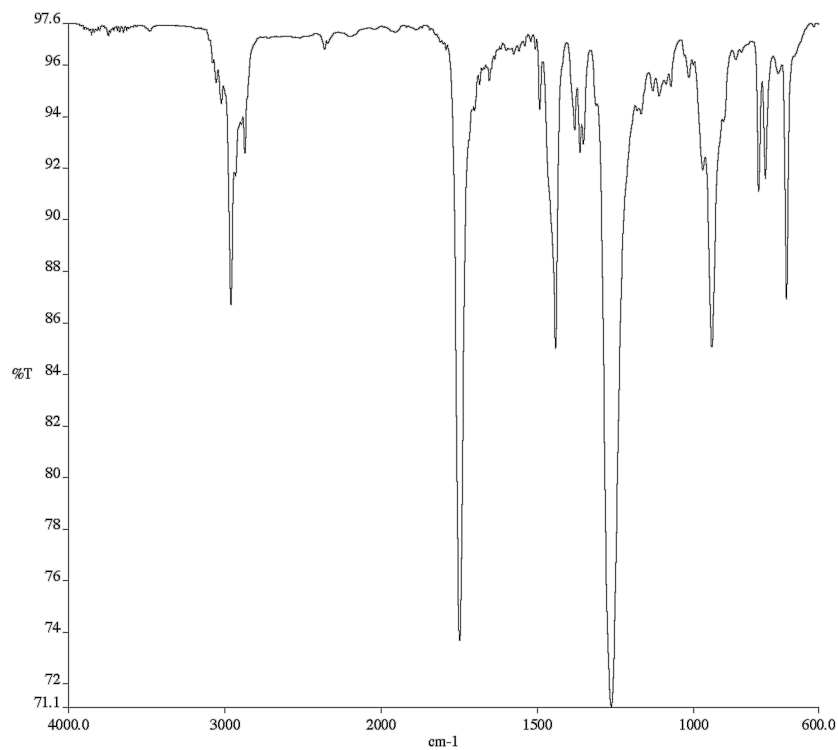


Figure A4.60 Infrared spectrum (Thin Film, NaCl) of compound **78c**

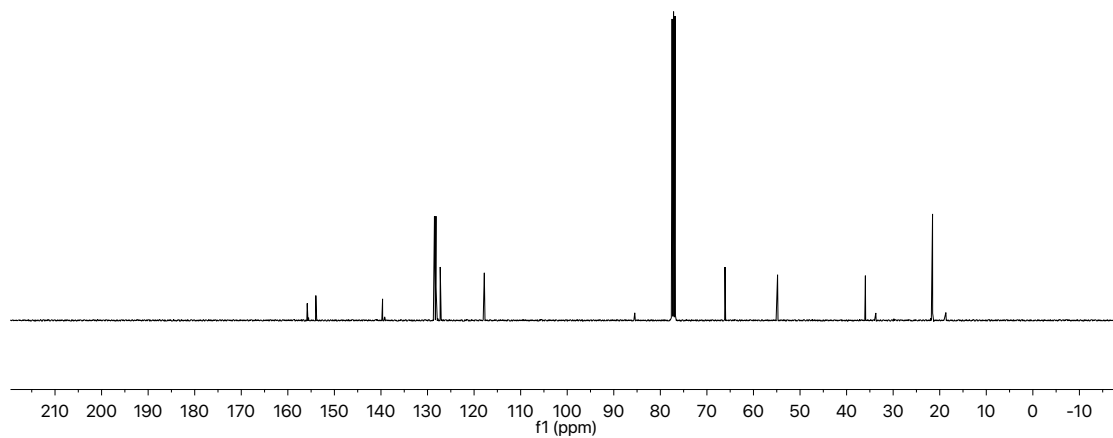


Figure A4.61 ¹³C NMR (101 MHz, CDCl₃) of compound **78c**

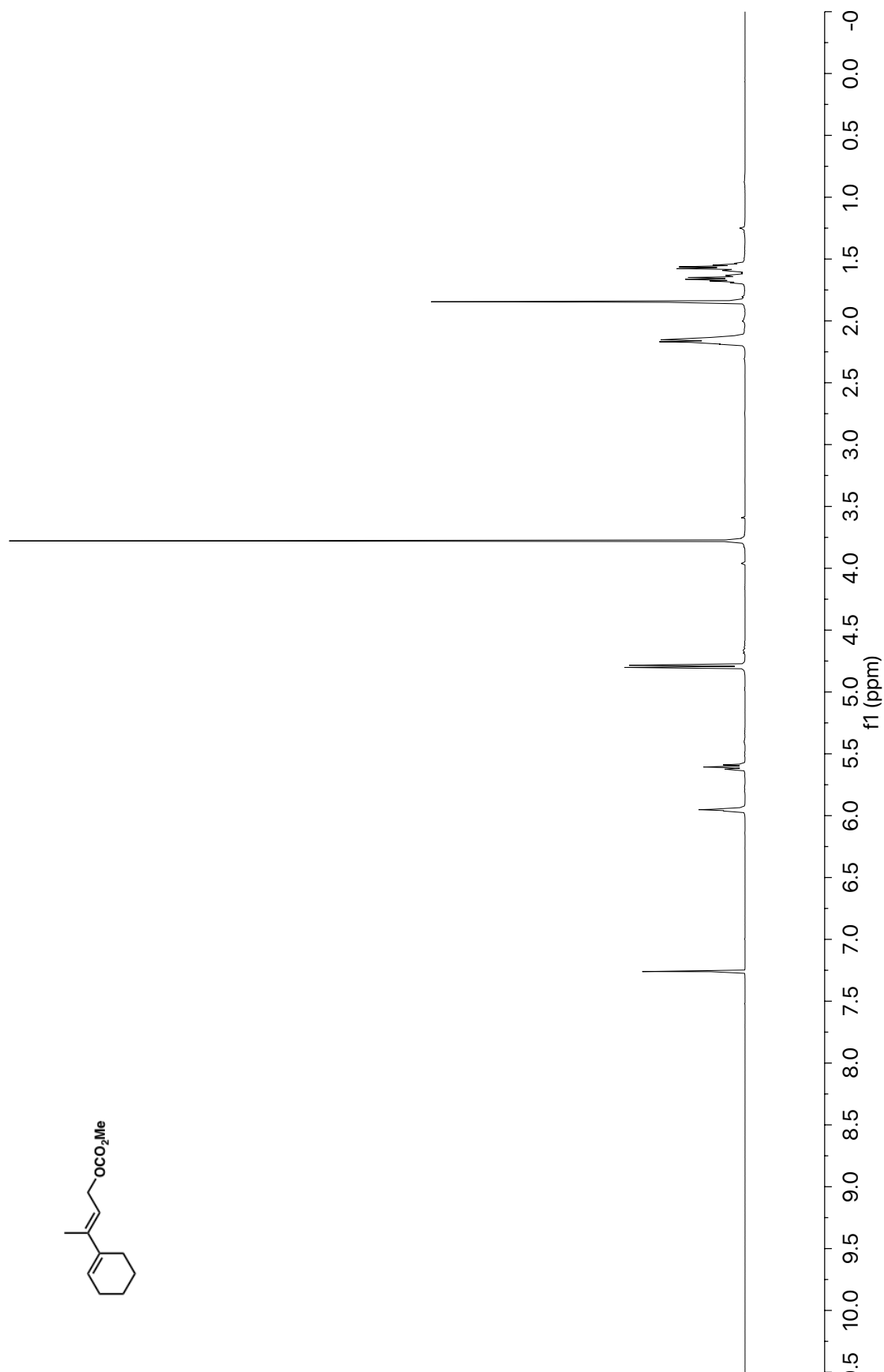


Figure A4.62 ¹H NMR (400 MHz, CDCl₃) of compound 78e

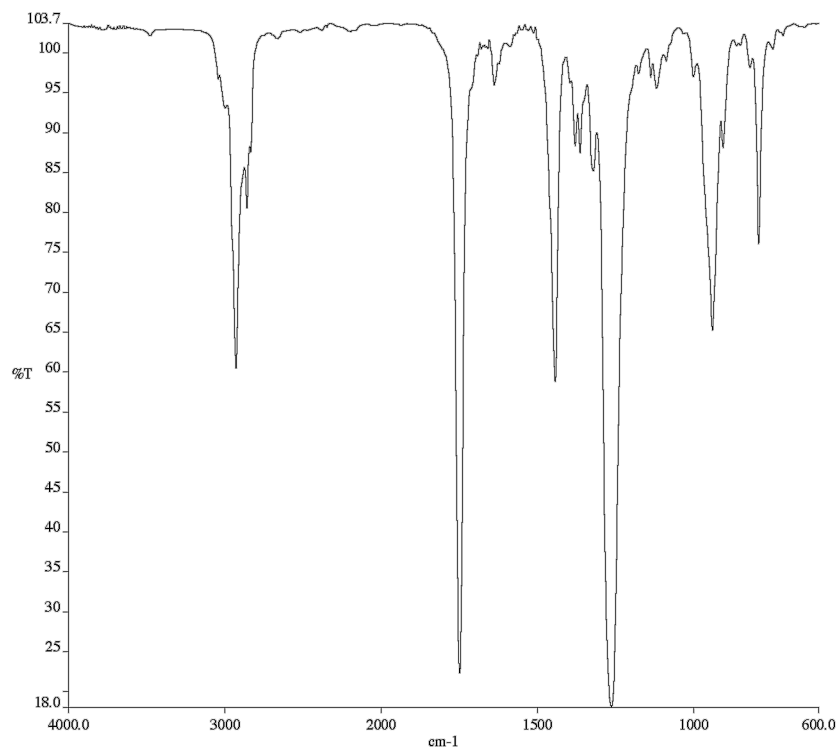


Figure A4.63 Infrared spectrum (Thin Film, NaCl) of compound **78e**

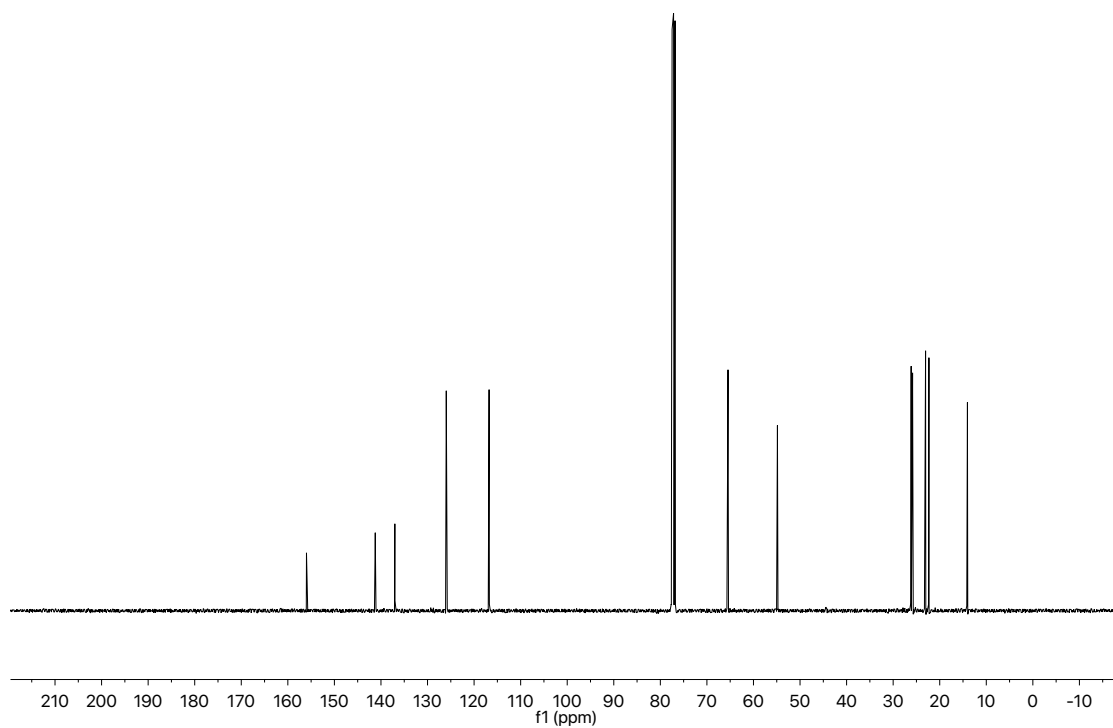


Figure A4.64 ¹³C NMR (101 MHz, CDCl₃) of compound **78e**



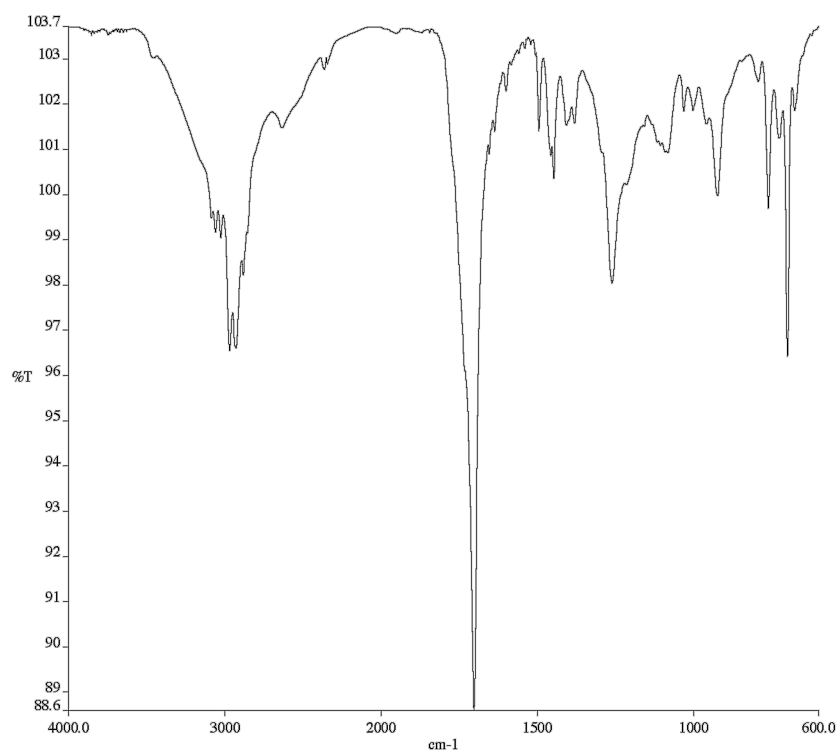


Figure A4.66 Infrared spectrum (Thin Film, NaCl) of compound **79a**

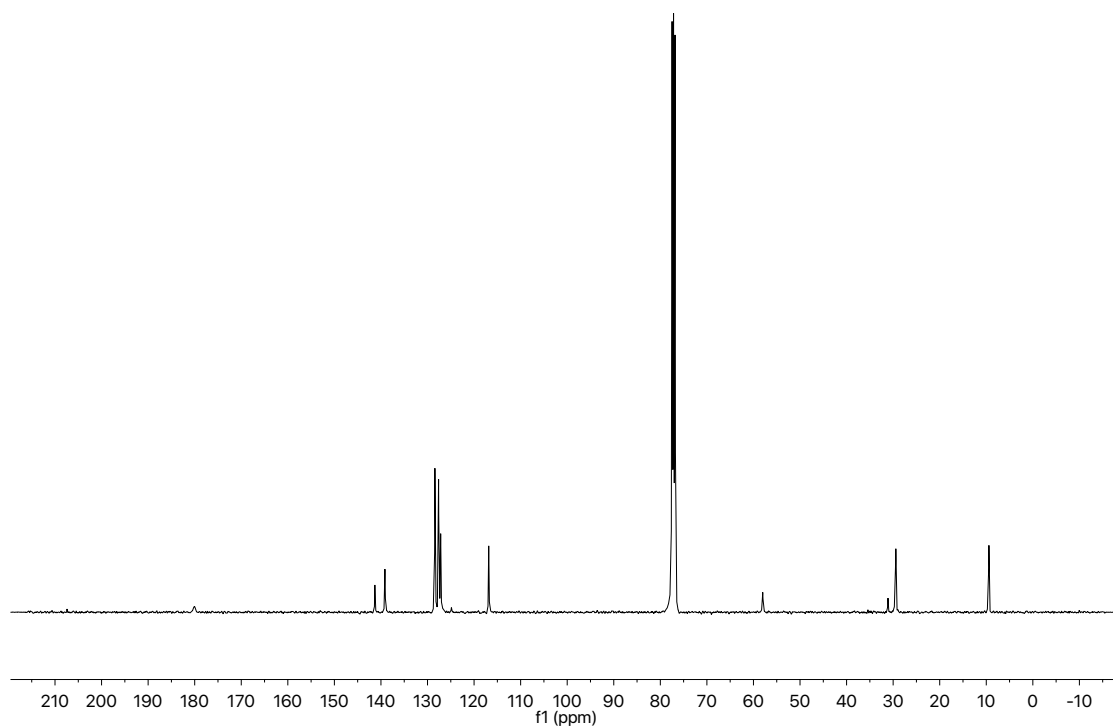


Figure A4.67 ¹³C NMR (101 MHz, CDCl₃) of compound **79a**

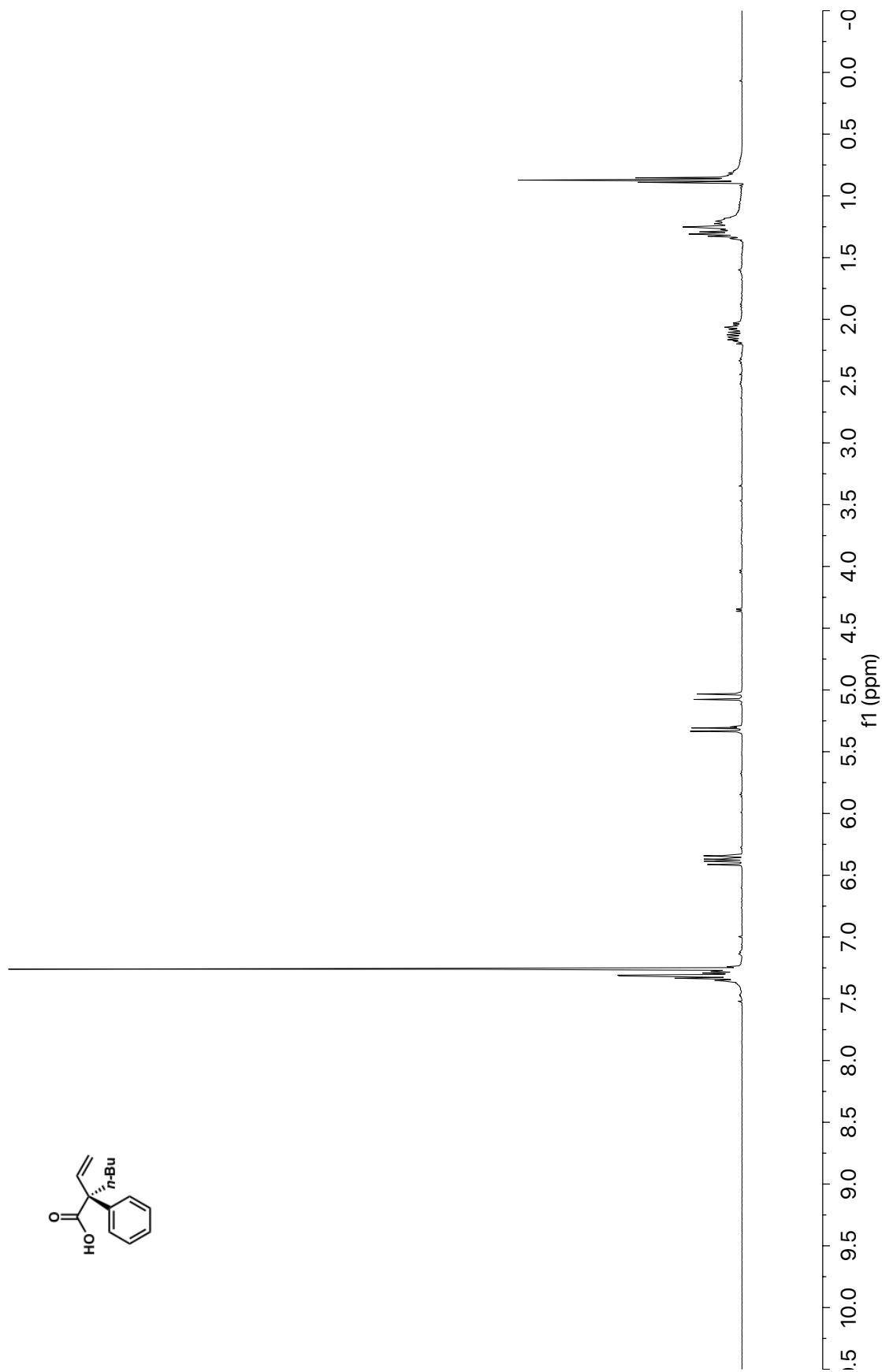


Figure A4.68 ^1H NMR (400 MHz, CDCl_3) of compound **79b**

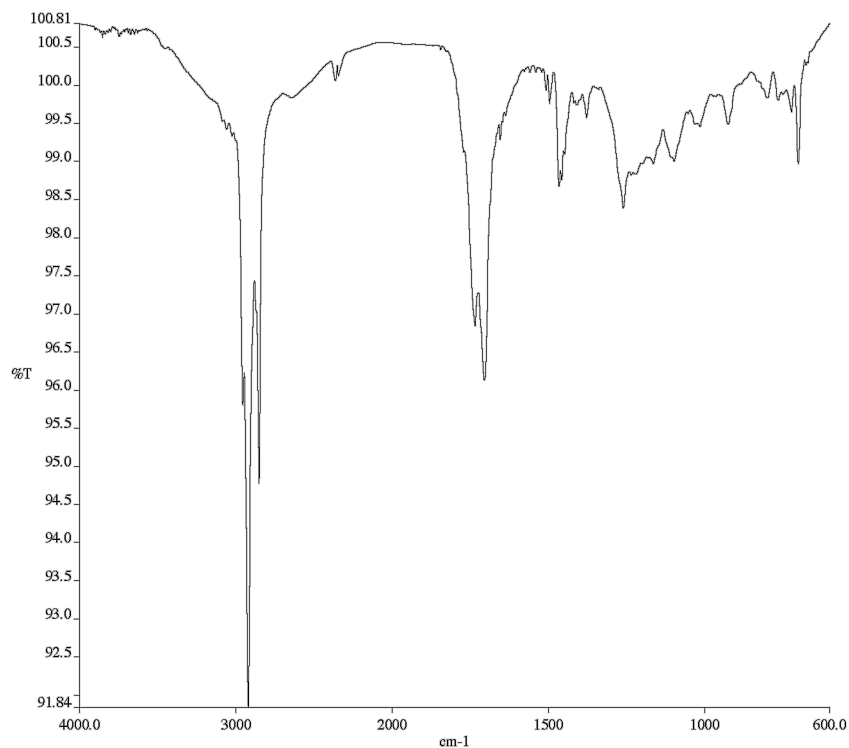


Figure A4.69 Infrared spectrum (Thin Film, NaCl) of compound **79b**

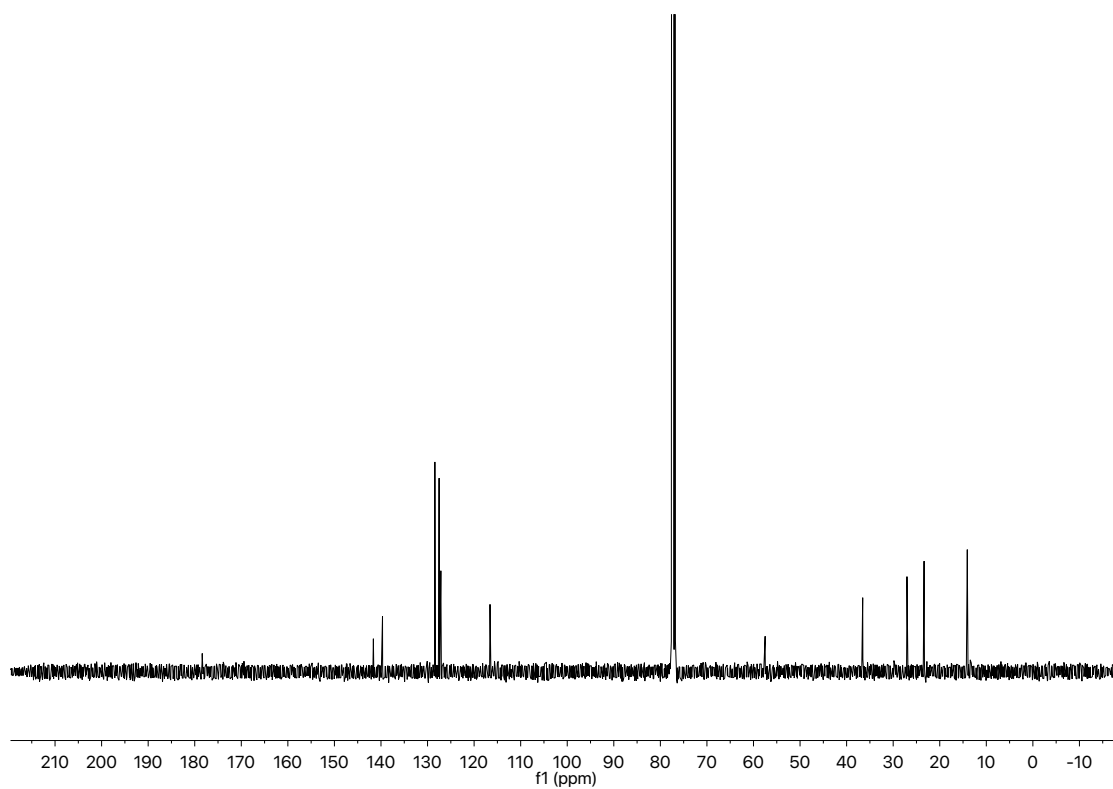


Figure A4.70 ¹³C NMR (101 MHz, CDCl₃) of compound **79b**

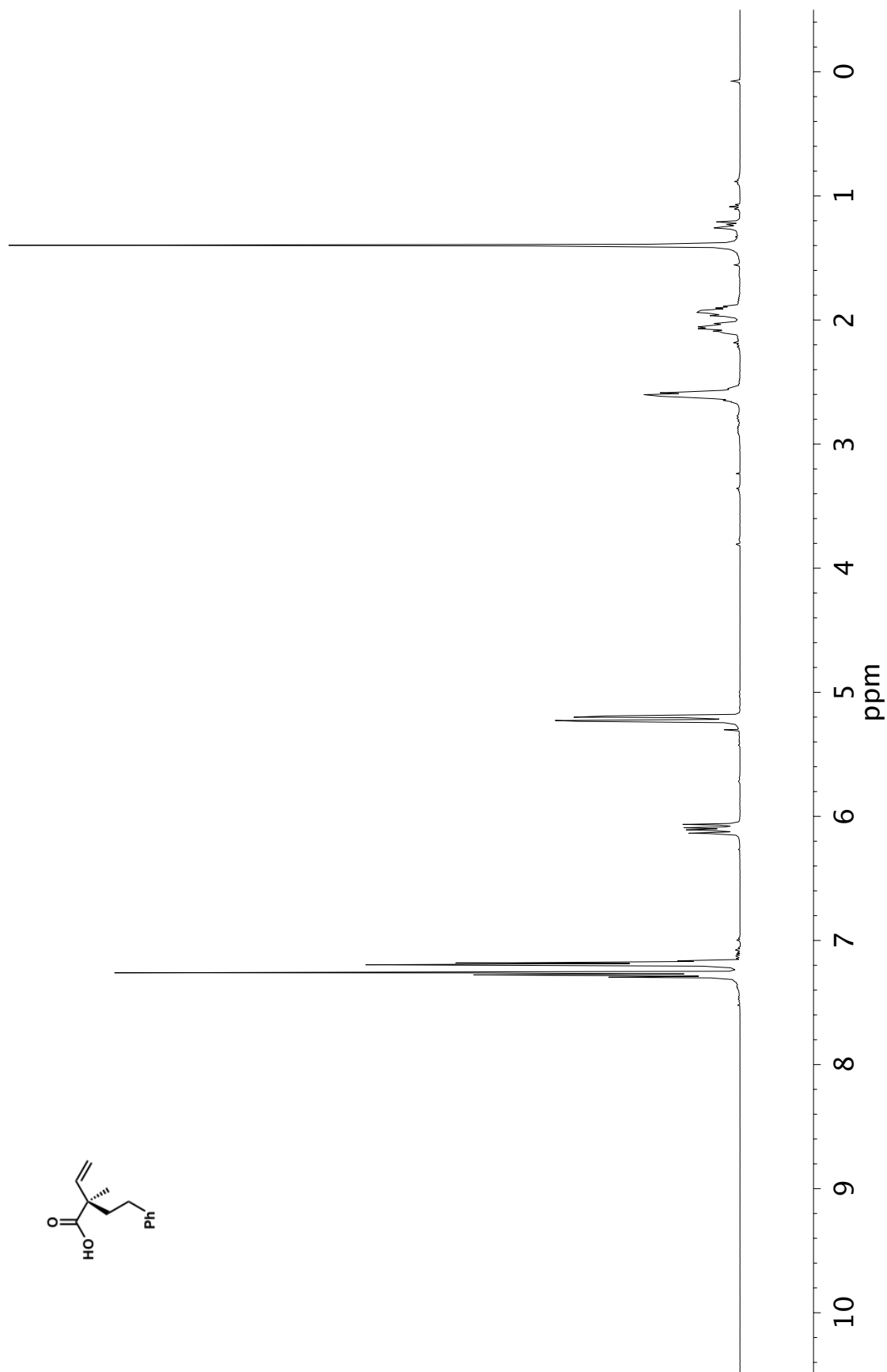
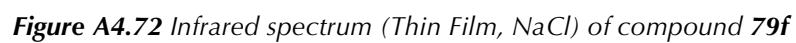


Figure A4.71 ¹H NMR (400 MHz, CDCl₃) of compound **79f**



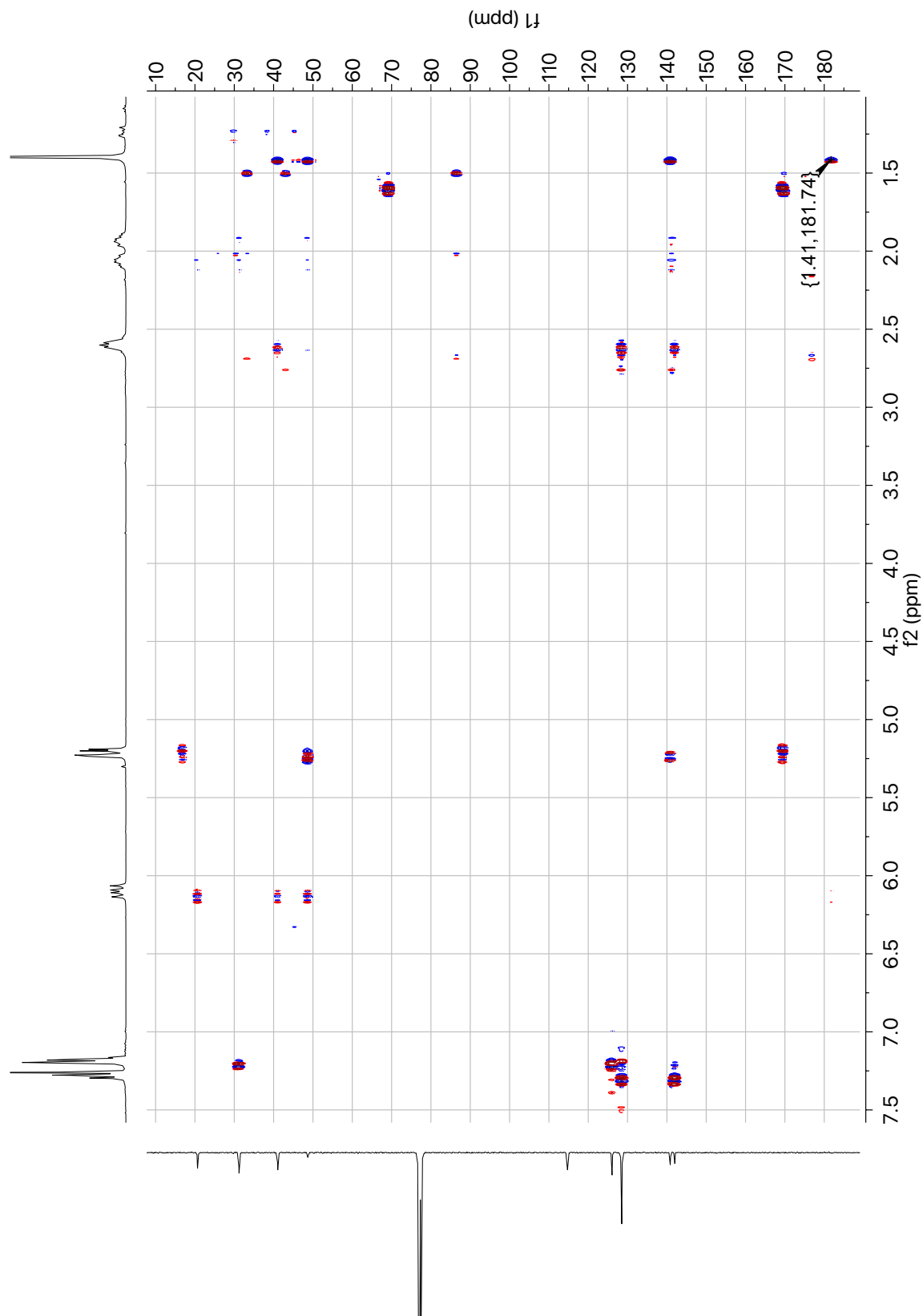


Figure A4.74 HMBC (400 MHz, CDCl_3) of compound **79f**



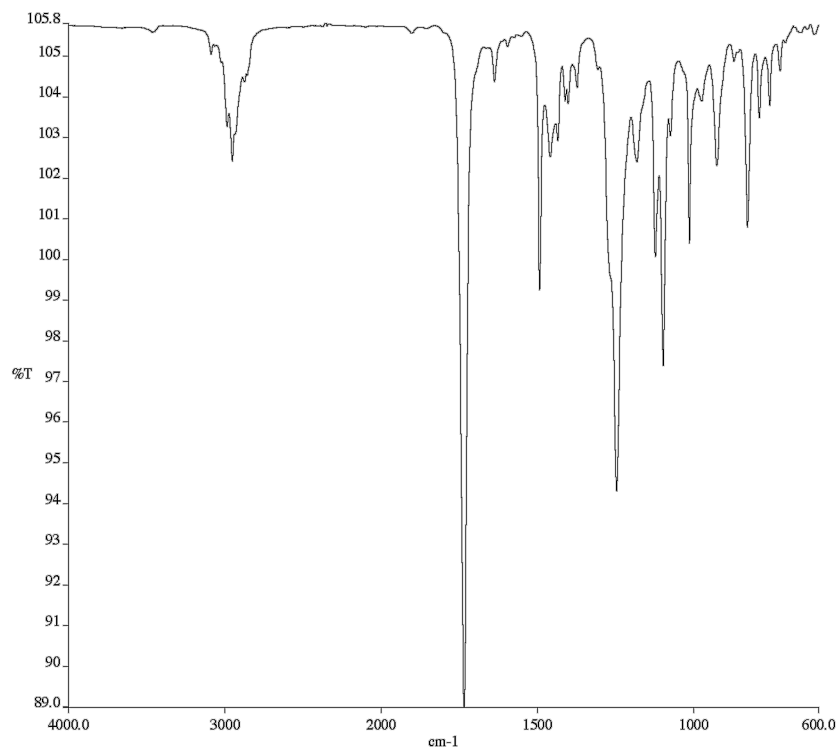


Figure A4.76 Infrared spectrum (Thin Film, NaCl) of compound **82**

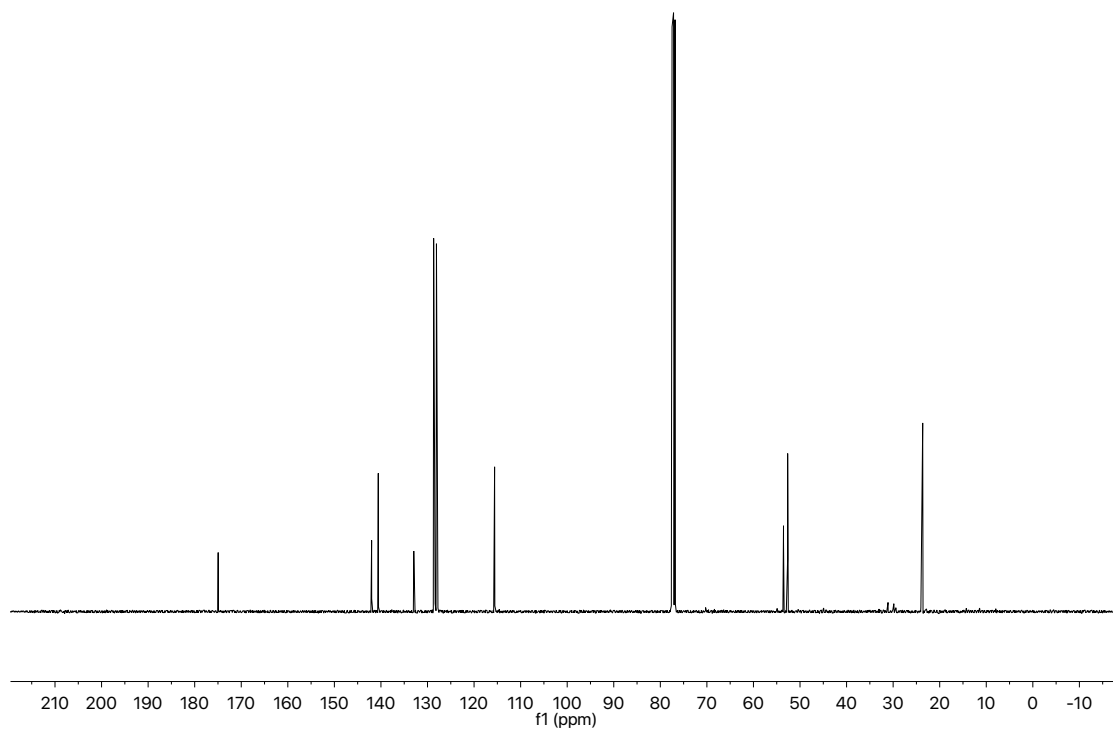


Figure A4.77 ¹³C NMR (101 MHz, CDCl₃) of compound **82**

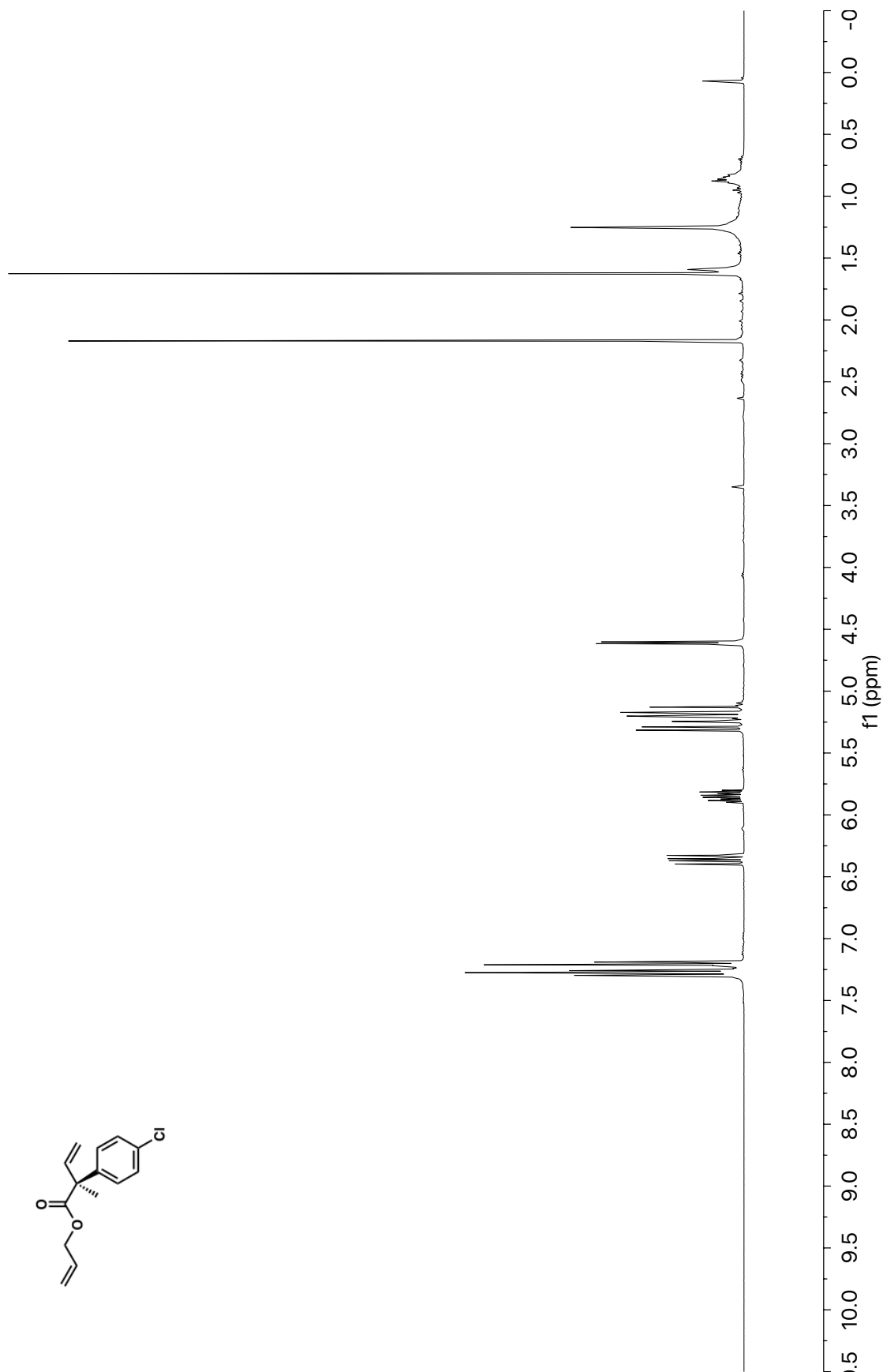


Figure A4.78 ¹H NMR (400 MHz, CDCl₃) of compound **83**

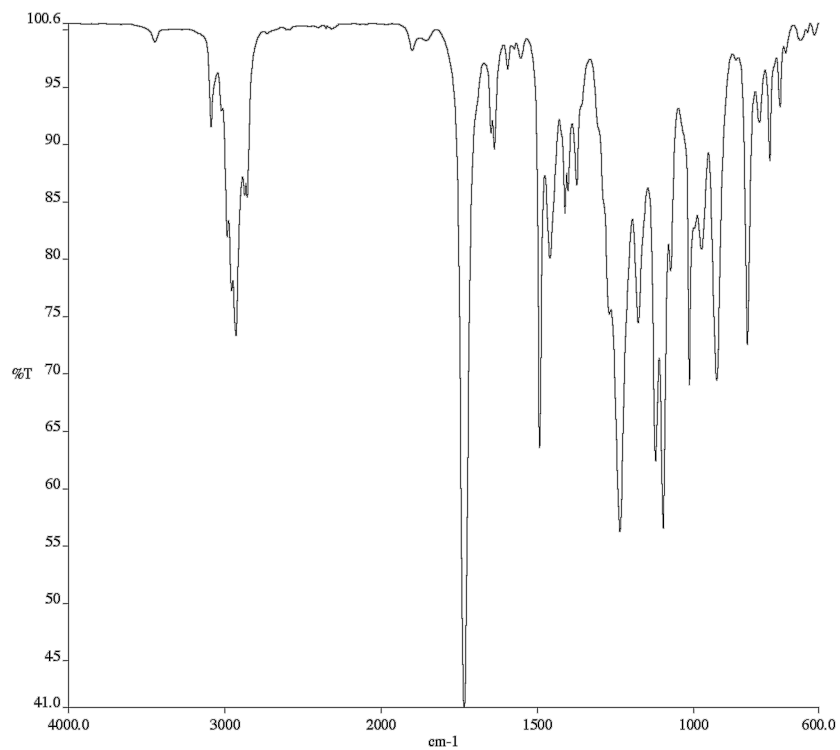


Figure A4.79 Infrared spectrum (Thin Film, NaCl) of compound **83**

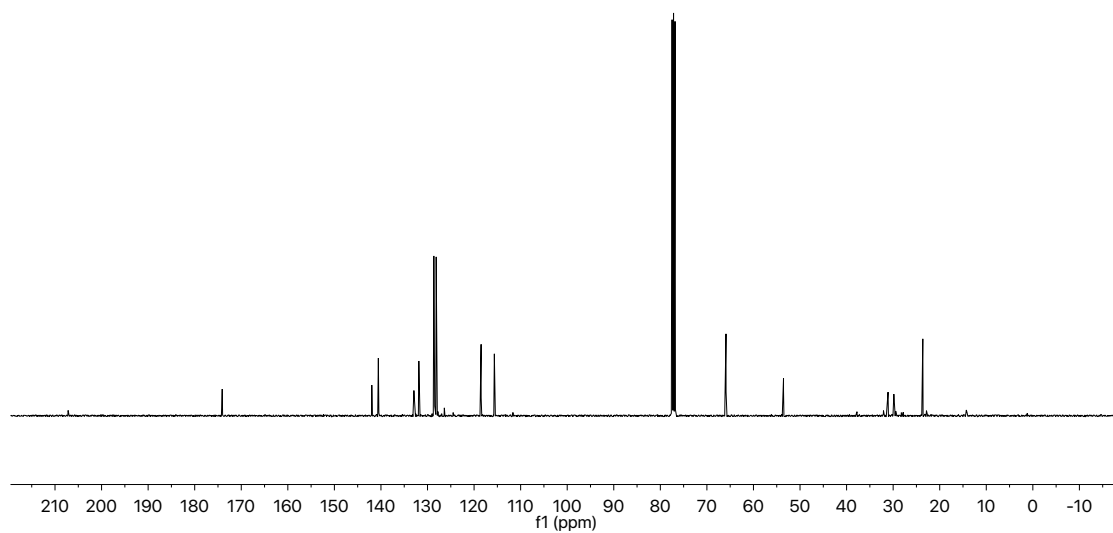


Figure A4.80 ^{13}C NMR (101 MHz, CDCl_3) of compound **83**

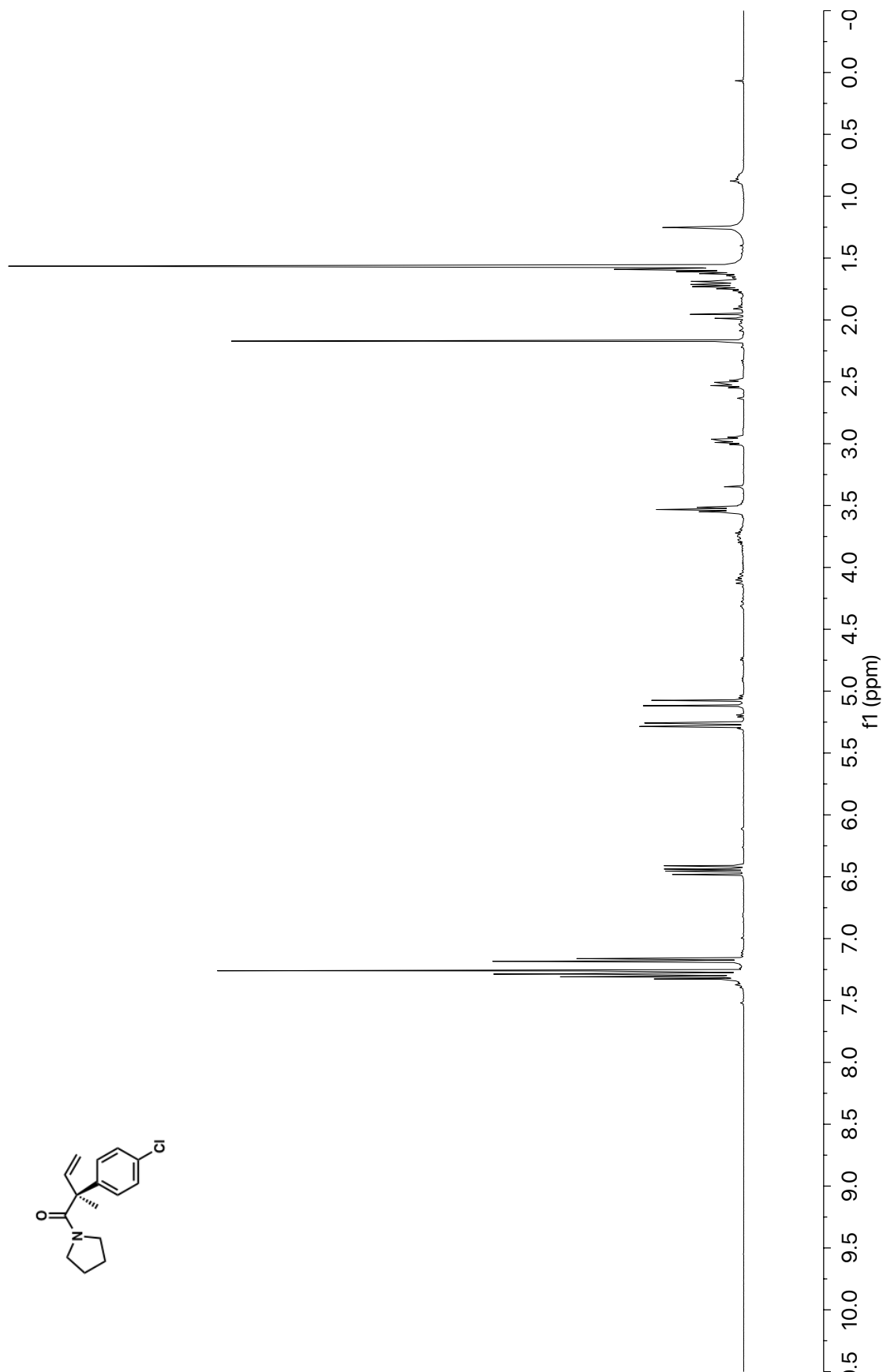


Figure A4.81 ¹H NMR (400 MHz, CDCl₃) of compound **84**

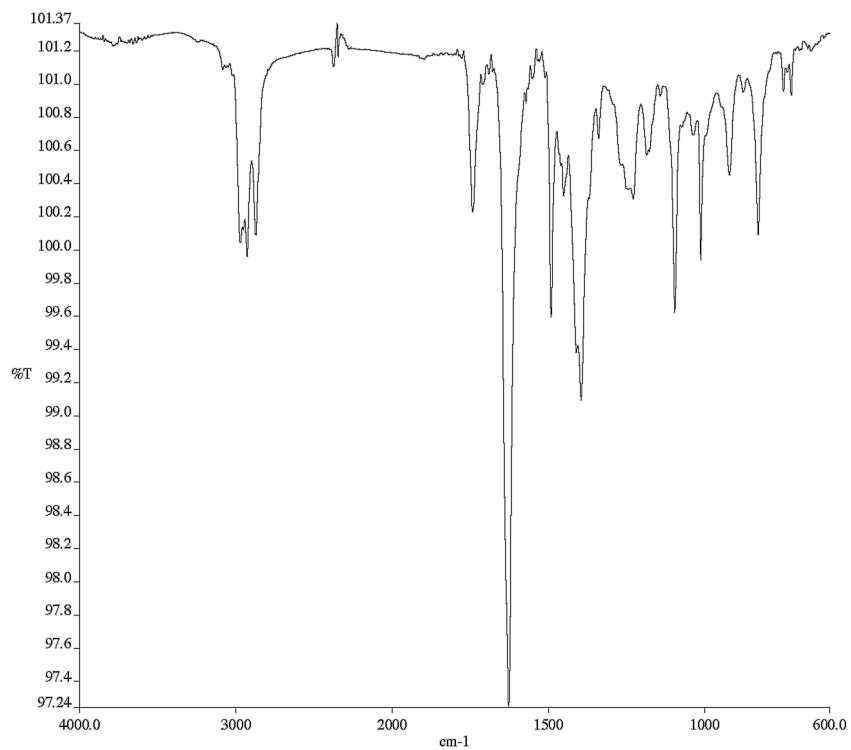


Figure A4.82 Infrared spectrum (Thin Film, NaCl) of compound **84**

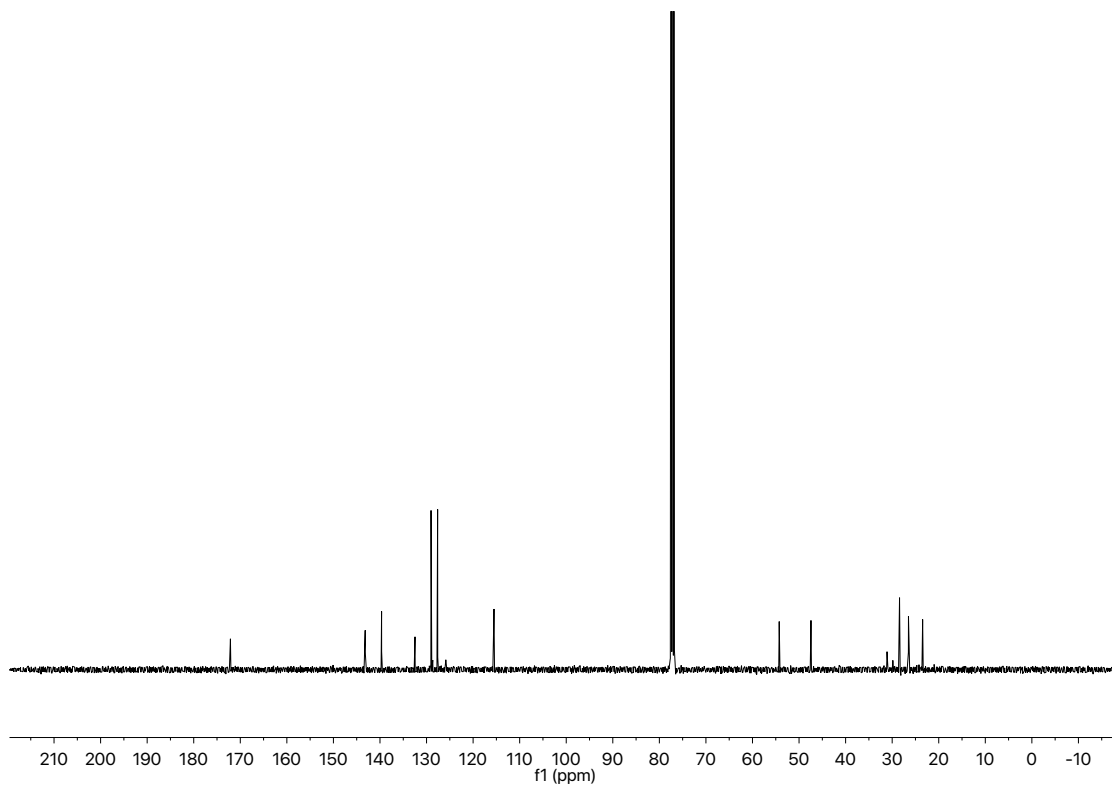


Figure A4.83 ¹³C NMR (101 MHz, CDCl₃) of compound **84**

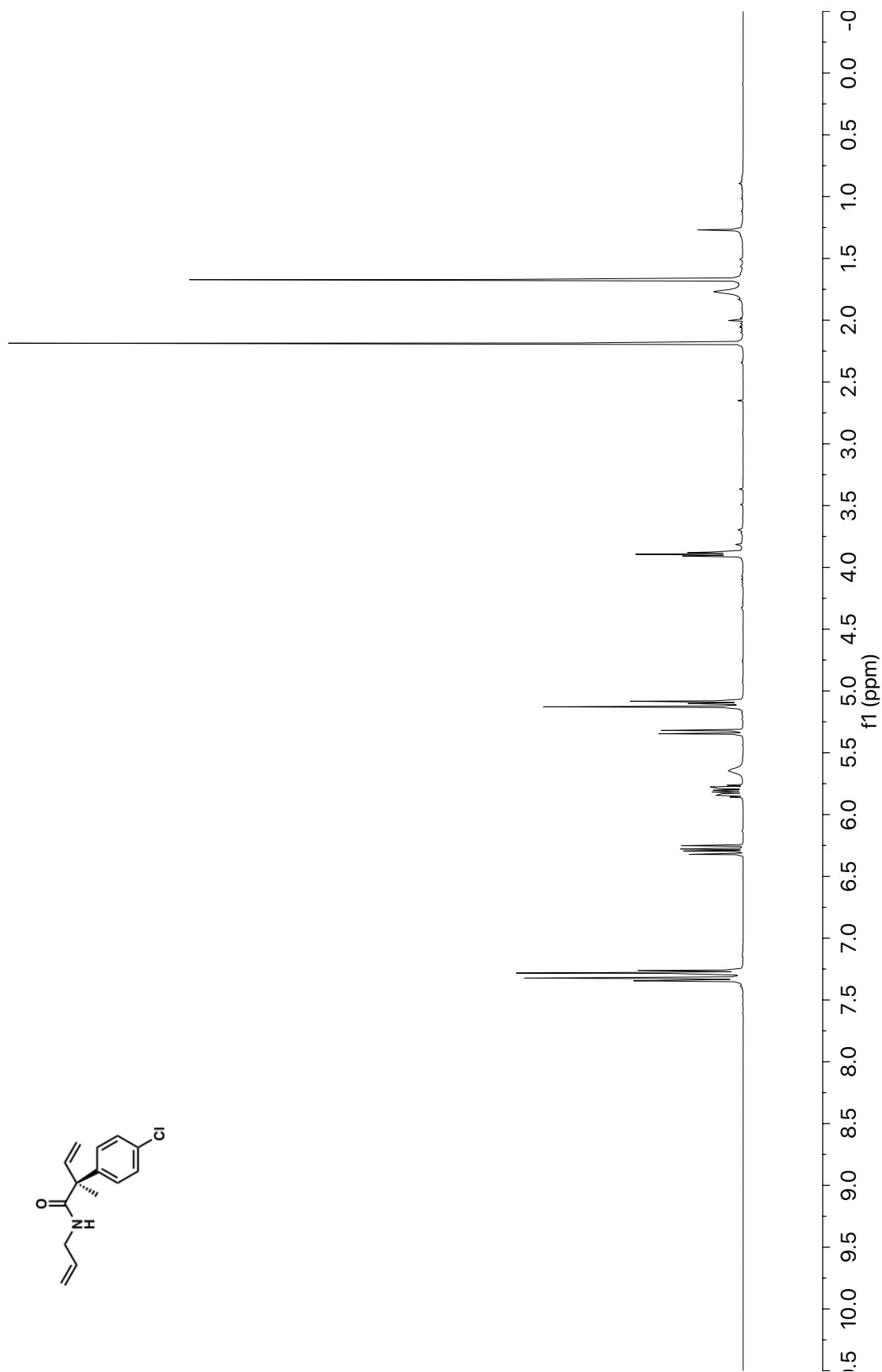


Figure A4.84 ¹H NMR (400 MHz, CDCl₃) of compound **85**

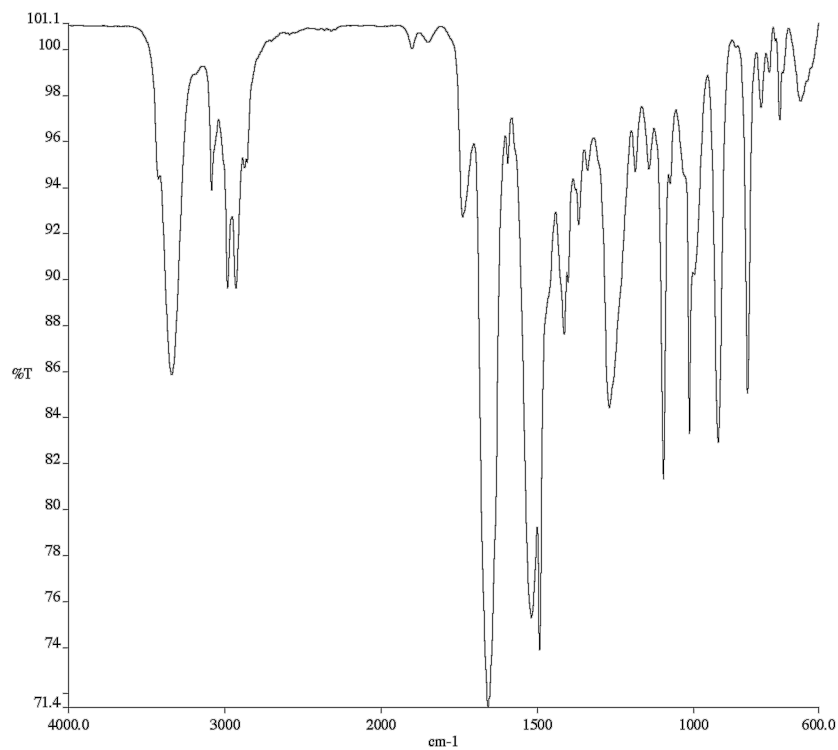


Figure A4.85 Infrared spectrum (Thin Film, NaCl) of compound **85**

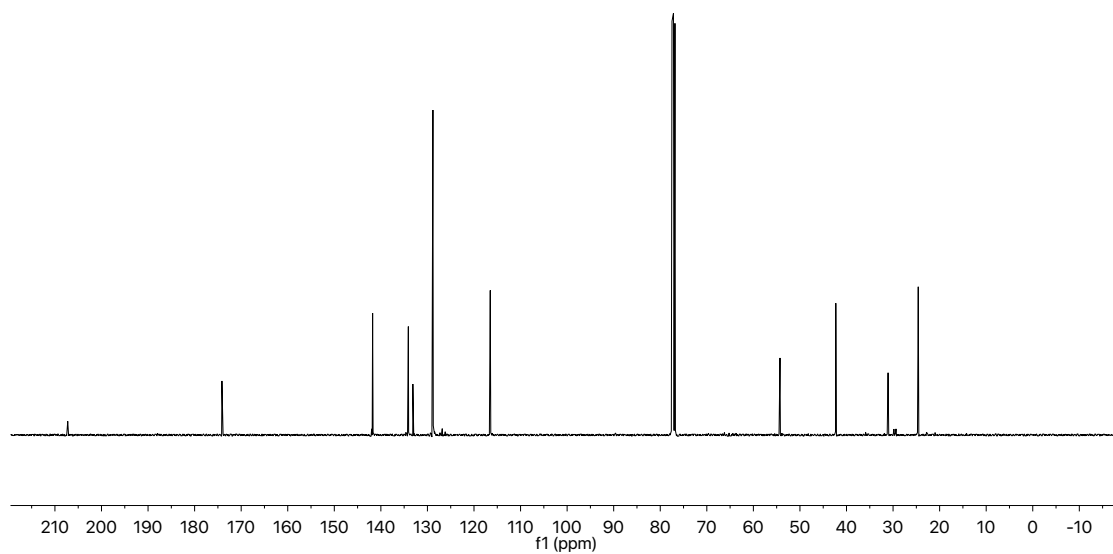


Figure A4.86 ¹³C NMR (101 MHz, CDCl₃) of compound **85**

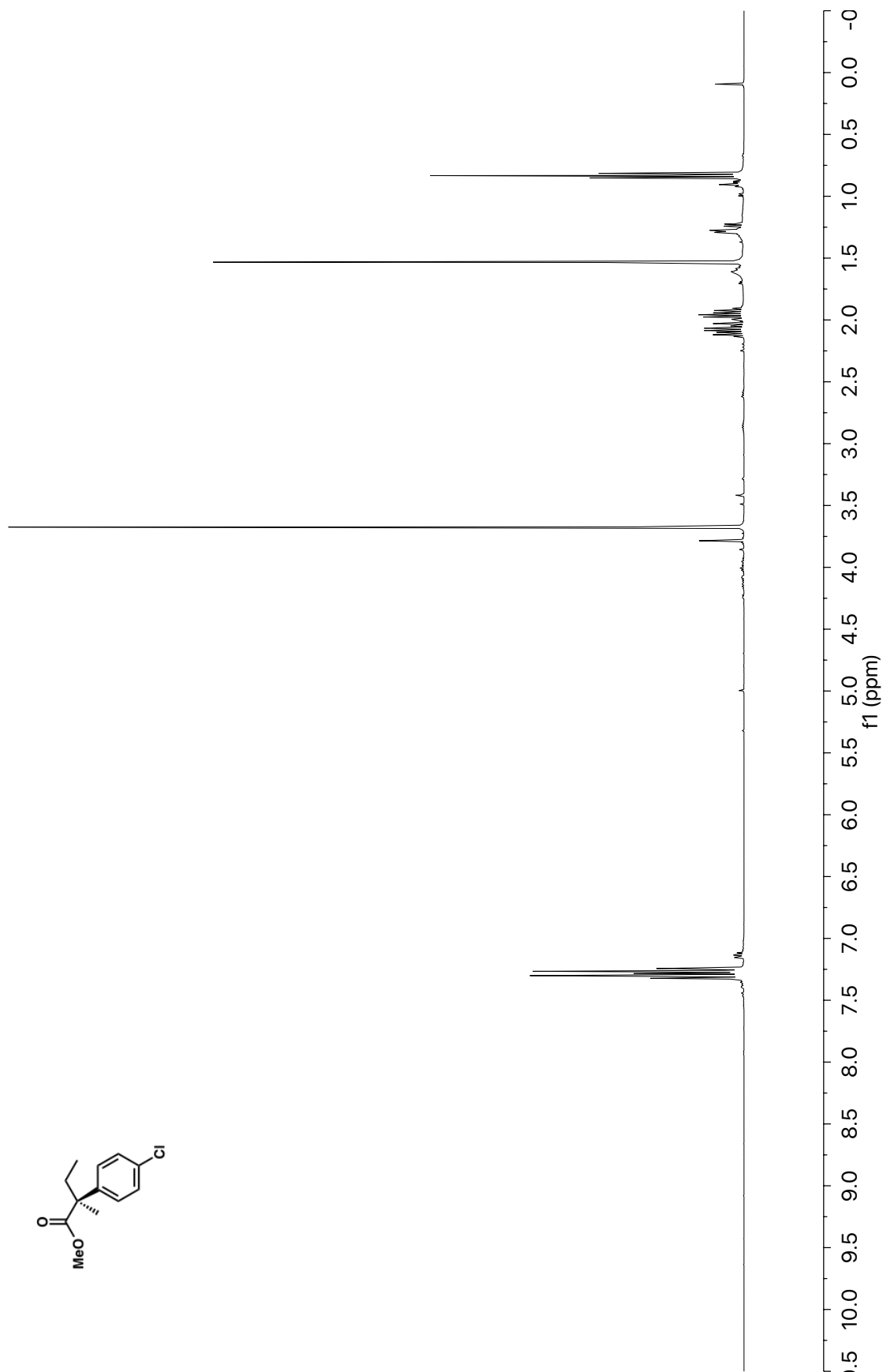


Figure A4.87 ¹H NMR (400 MHz, CDCl₃) of compound **86**

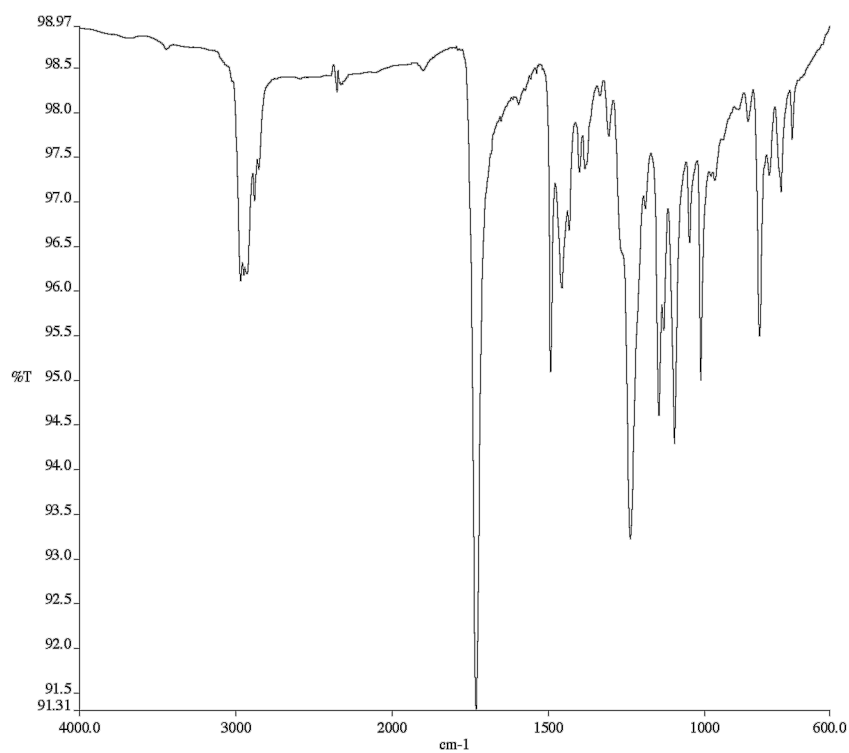


Figure A4.88 Infrared spectrum (Thin Film, NaCl) of compound **86**

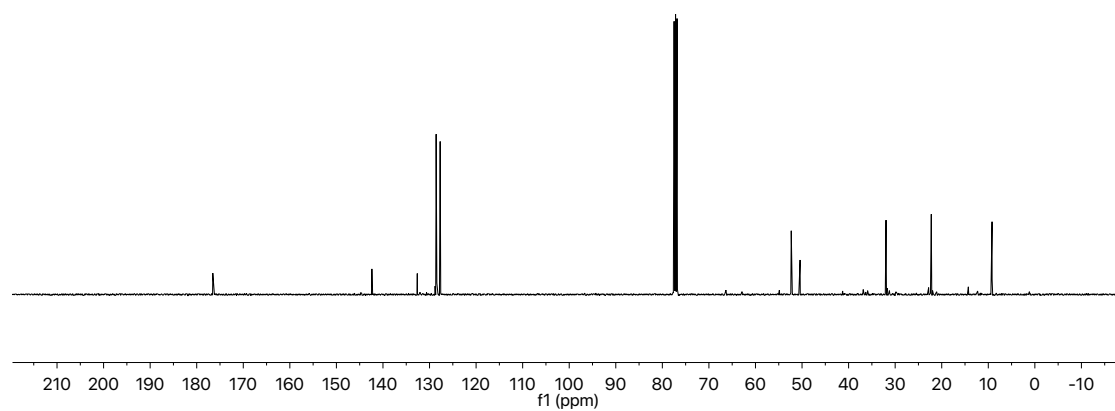


Figure A4.89 ¹³C NMR (101 MHz, CDCl₃) of compound **86**

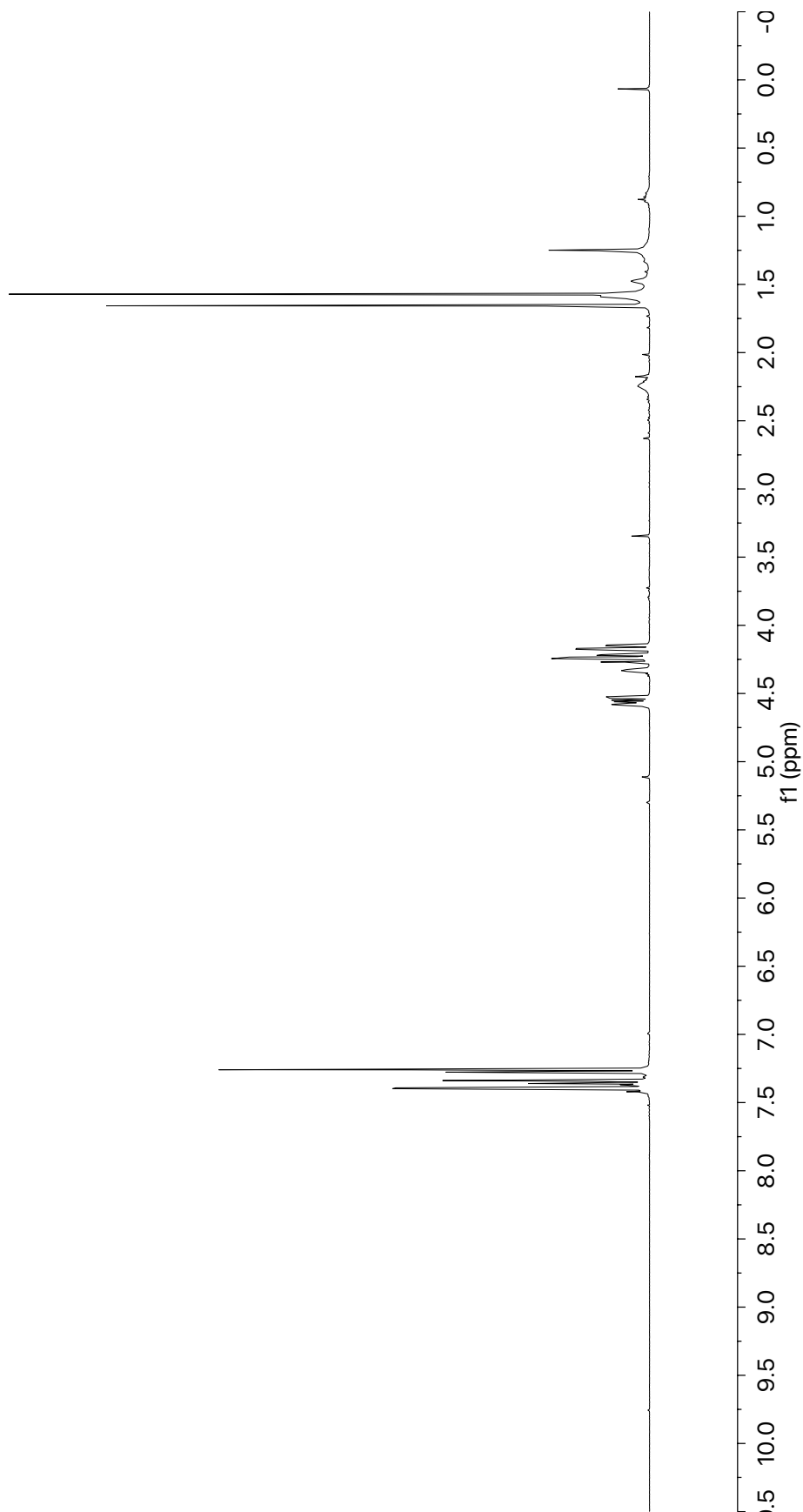
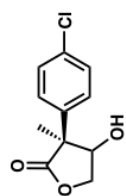


Figure A4.90 ¹H NMR (400 MHz, CDCl₃) of compound **88**

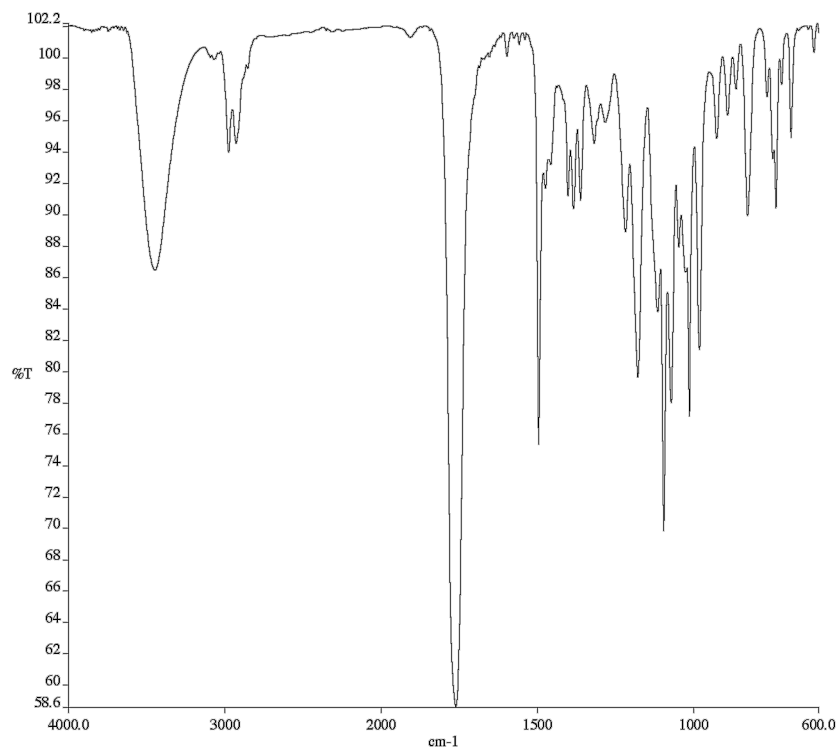


Figure A4.91 Infrared spectrum (Thin Film, NaCl) of compound **88**

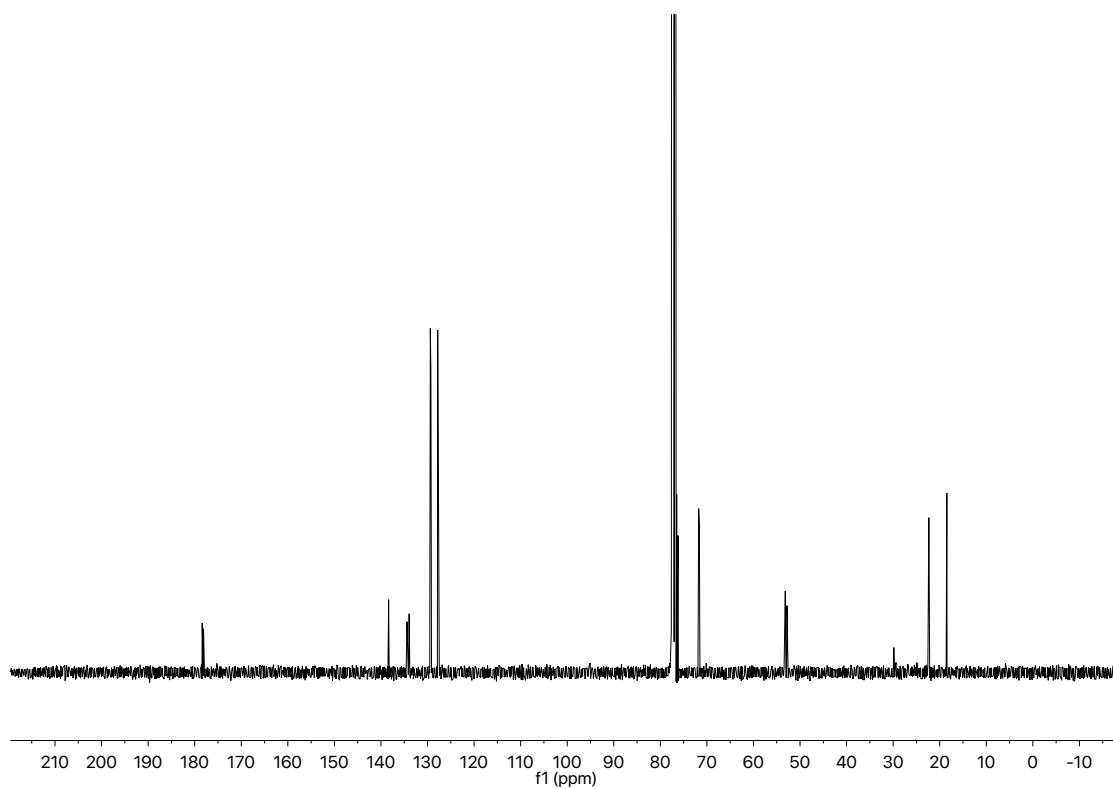


Figure A4.92 ¹³C NMR (101 MHz, CDCl₃) of compound **88**

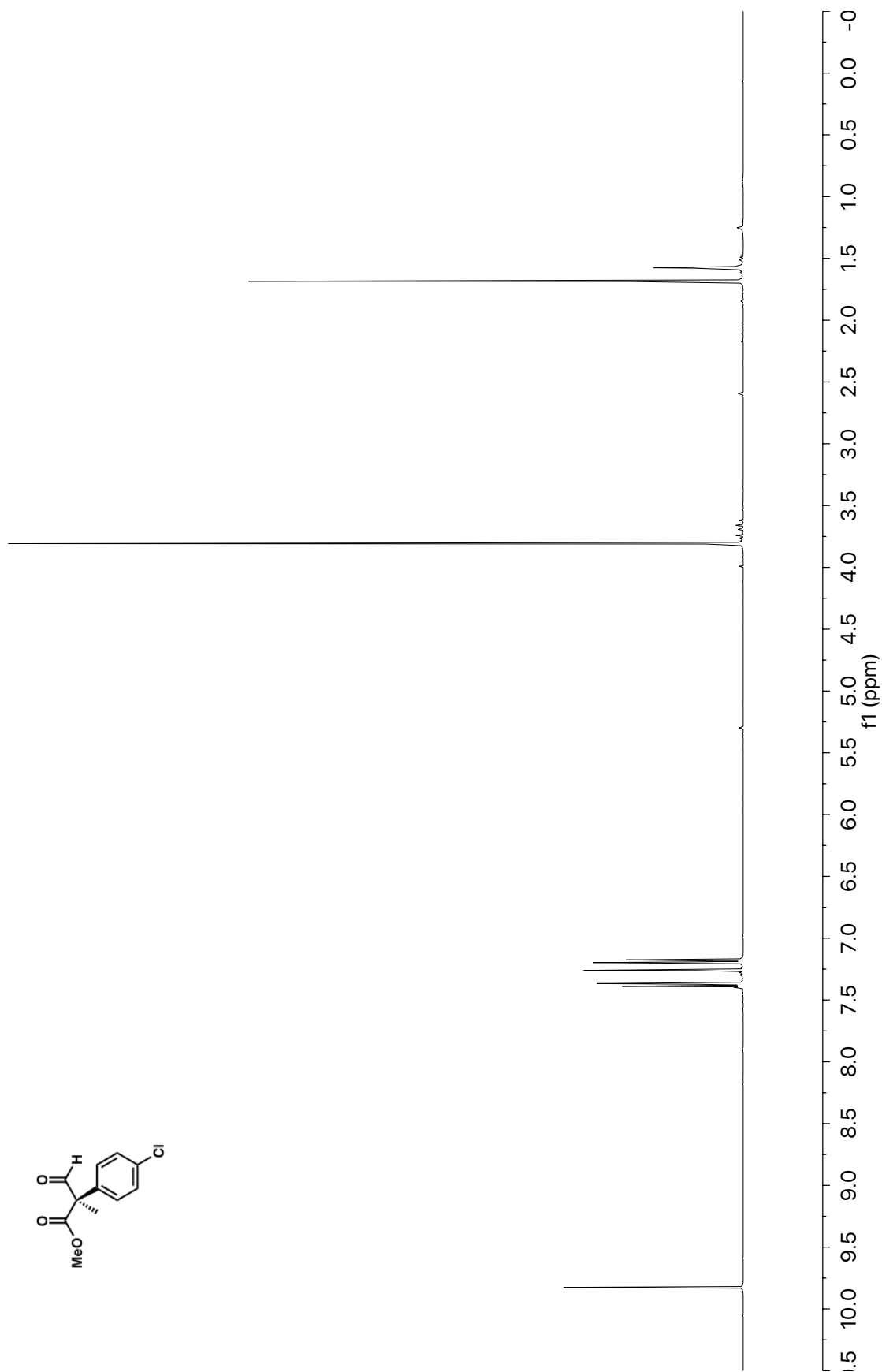


Figure A4.93 ¹H NMR (400 MHz, CDCl₃) of compound **89**

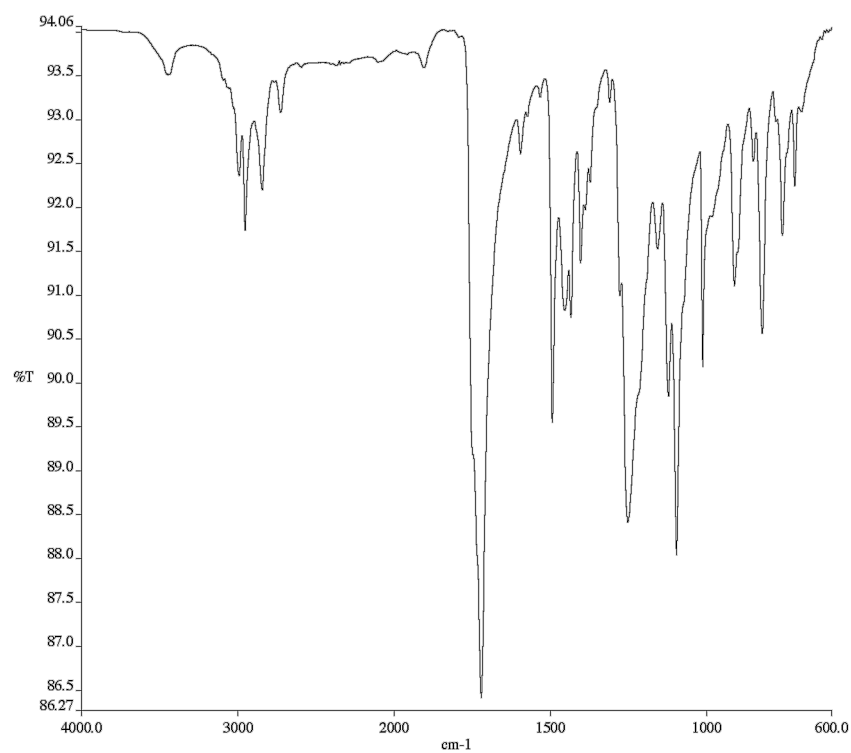


Figure A4.94 Infrared spectrum (Thin Film, NaCl) of compound **89**

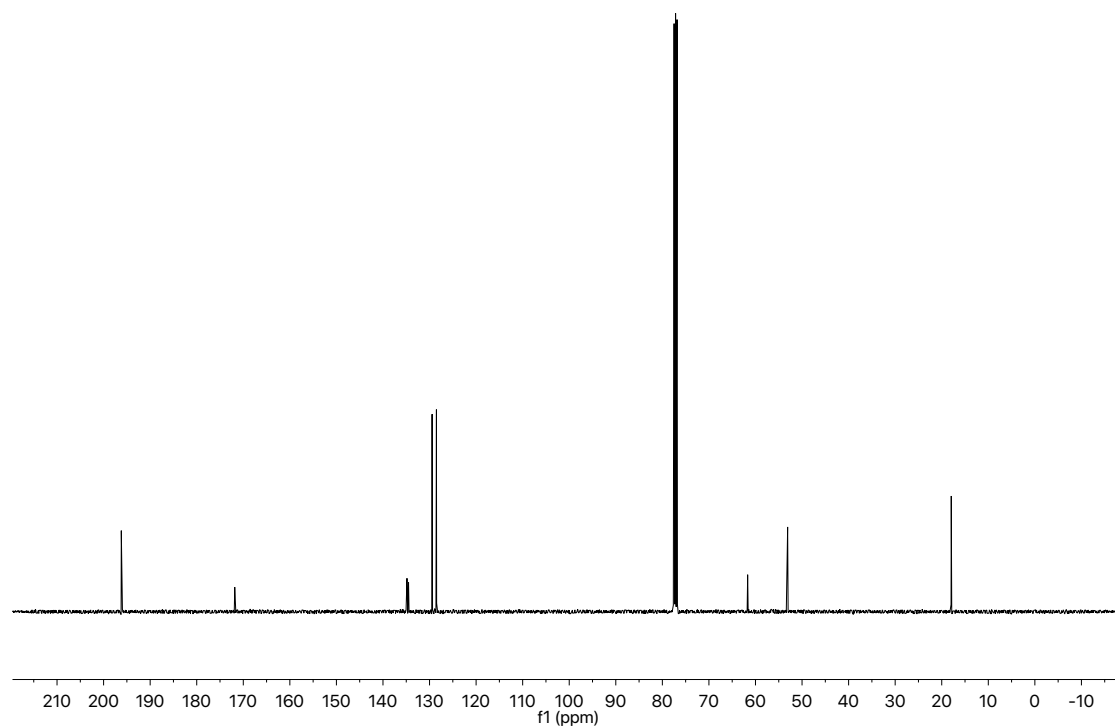


Figure A4.95 ¹³C NMR (101 MHz, CDCl₃) of compound **89**

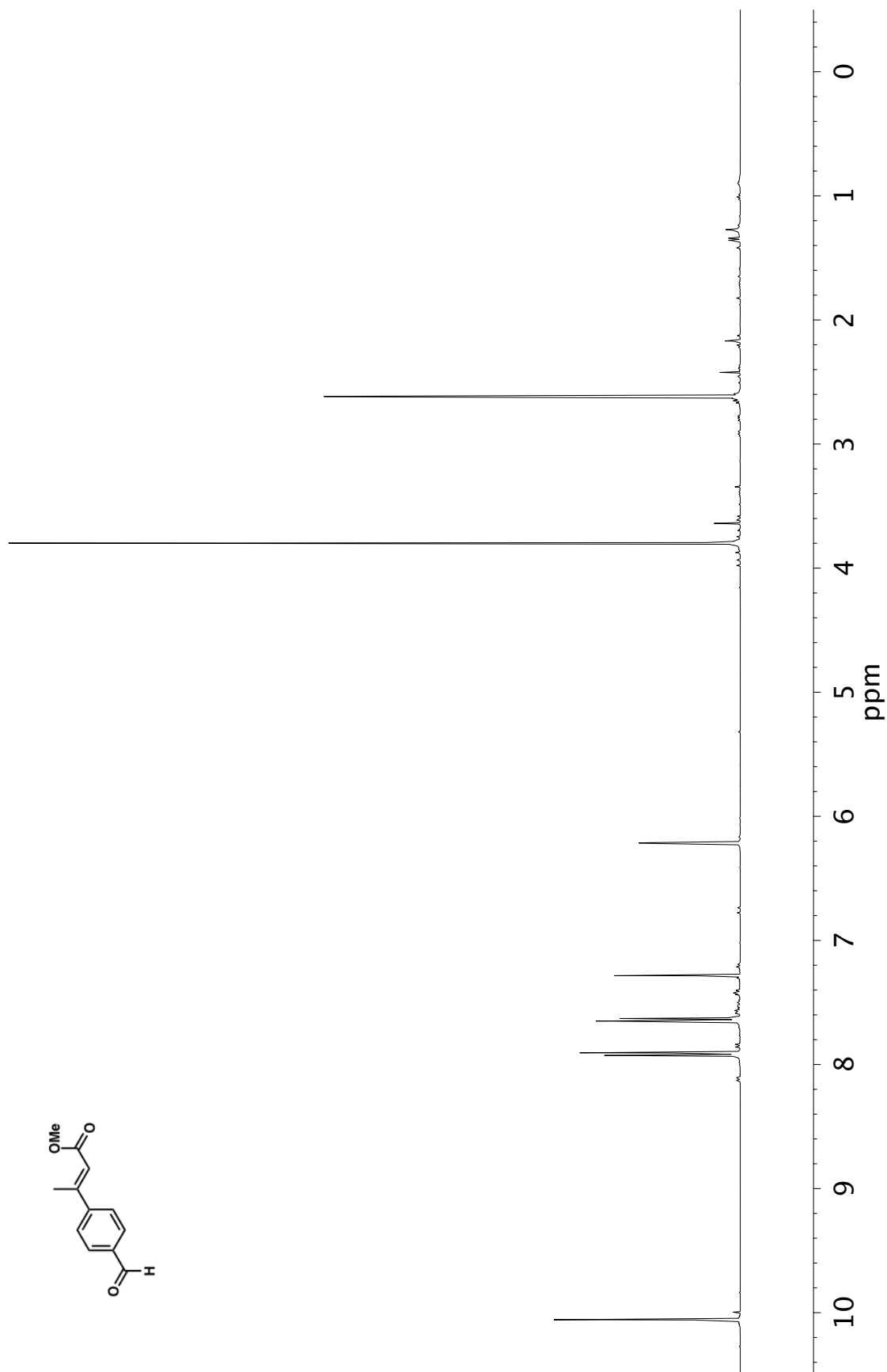


Figure A4.96 ¹H NMR (400 MHz, CDCl₃) of compound **90**

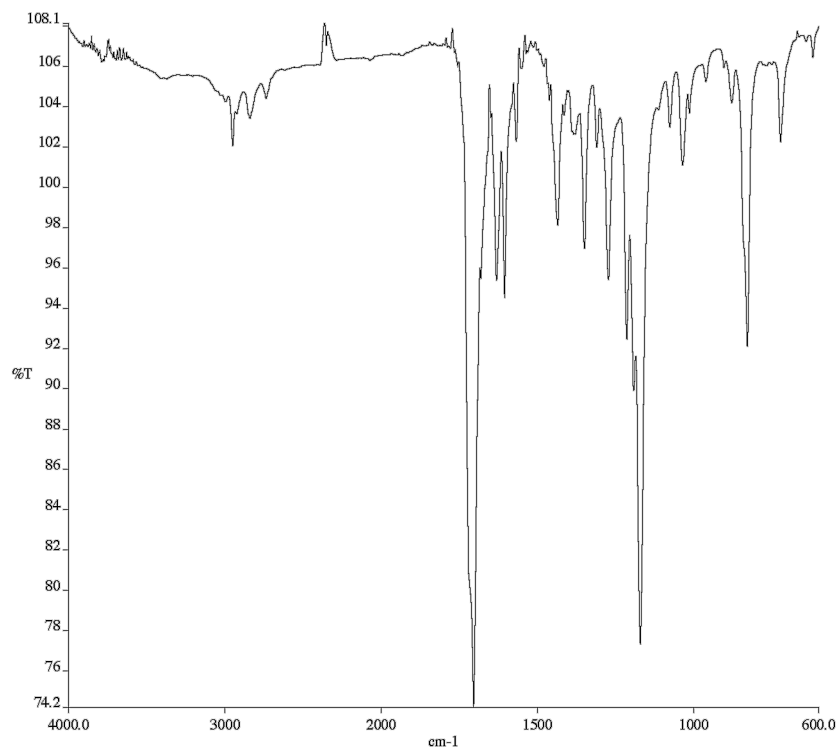


Figure A4.97 Infrared spectrum (Thin Film, NaCl) of compound **90**

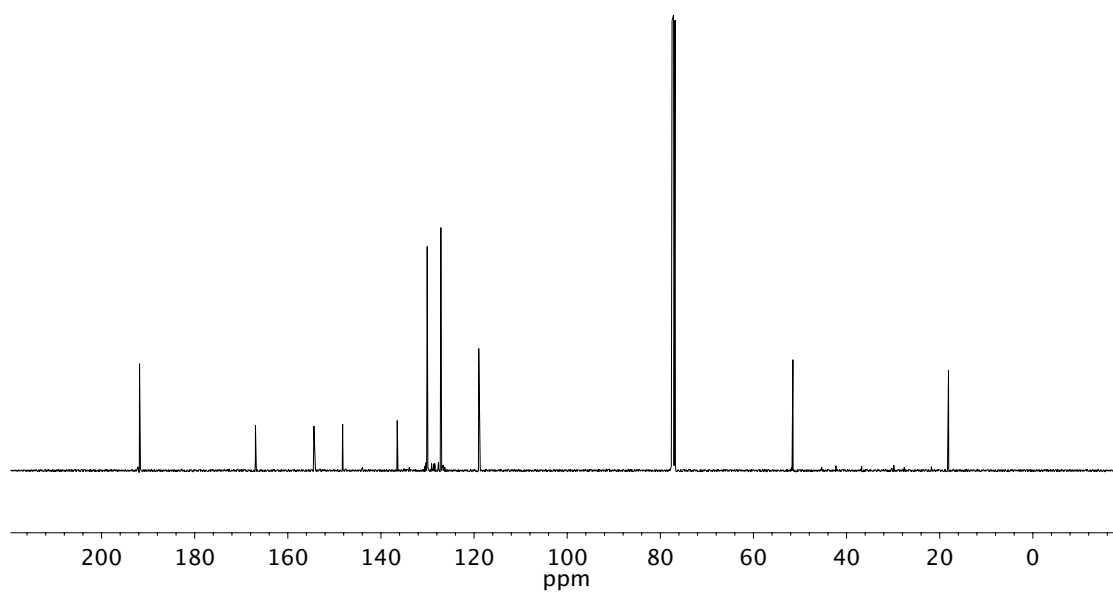


Figure A4.98 ¹³C NMR (101 MHz, CDCl₃) of compound **90**

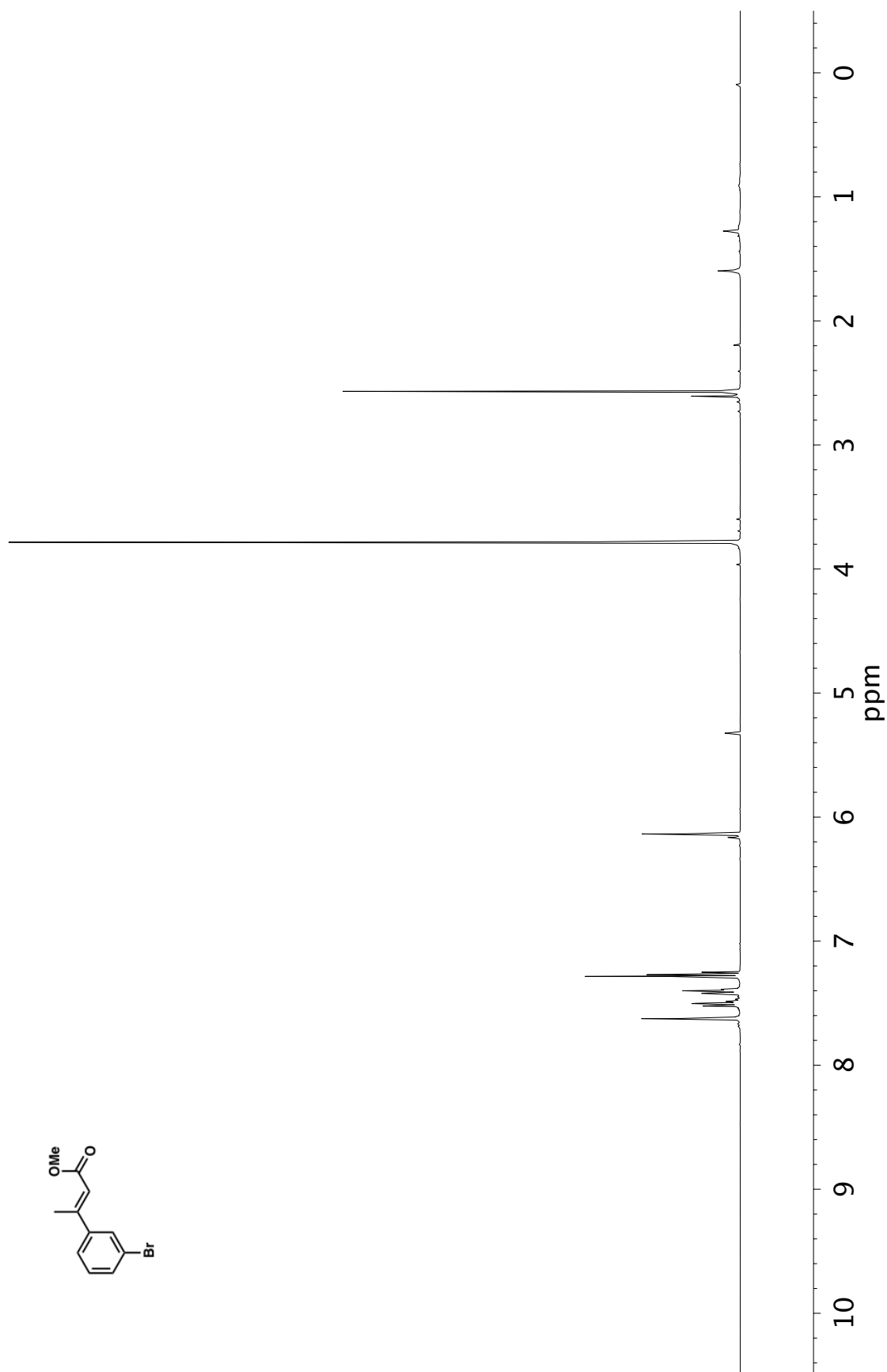


Figure A4.99 ¹H NMR (400 MHz, CDCl₃) of compound **91**

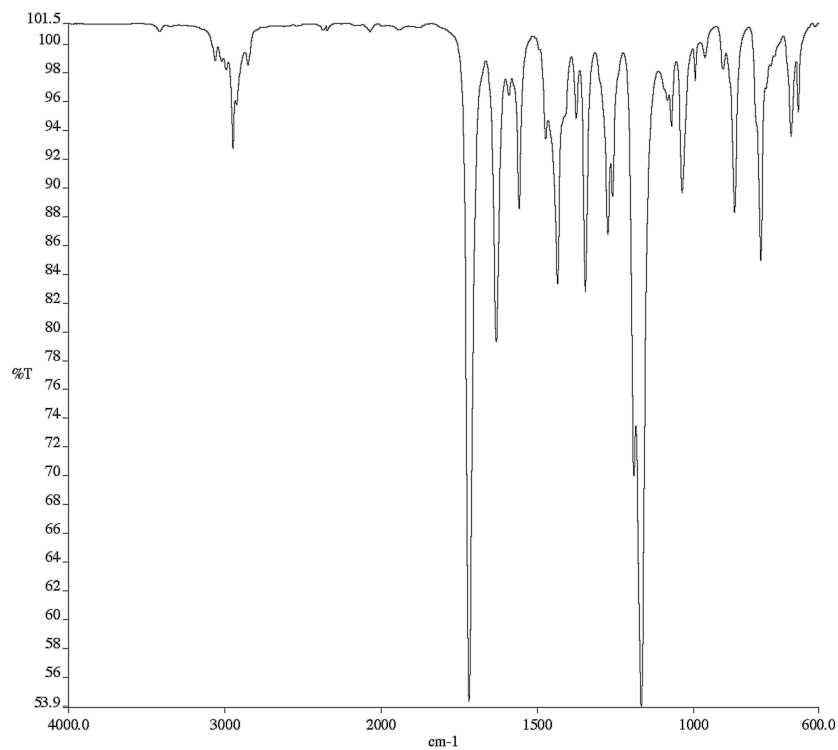


Figure A4.100 Infrared spectrum (Thin Film, NaCl) of compound **91**

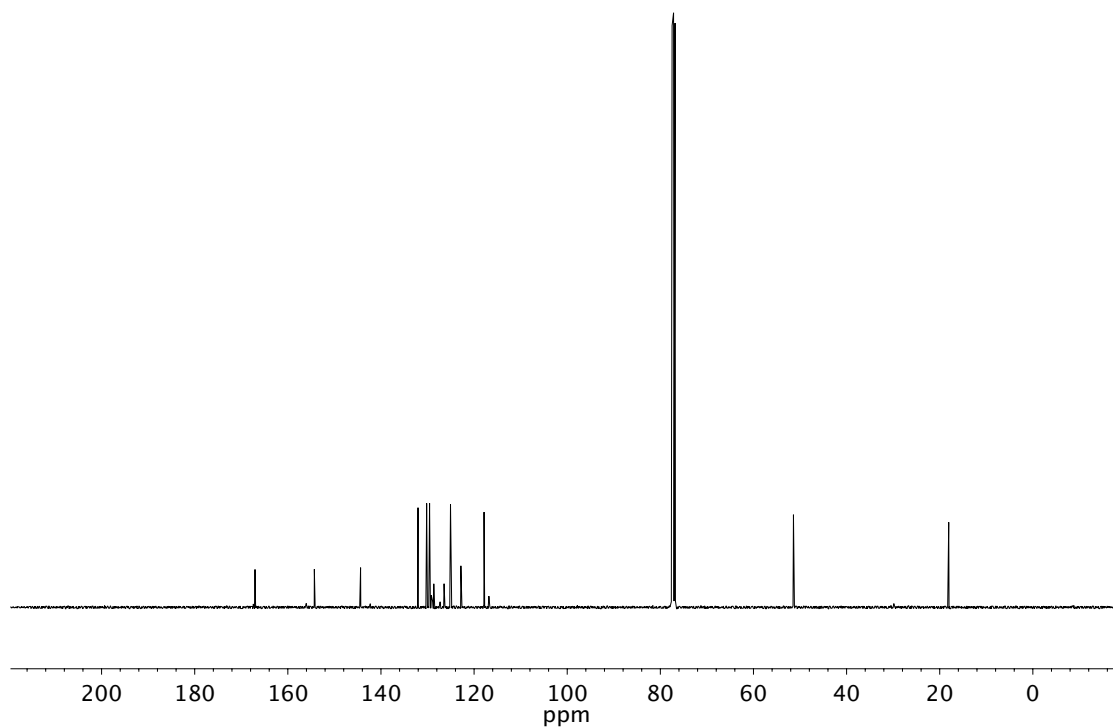


Figure A4.101 ¹³C NMR (101 MHz, CDCl₃) of compound **91**

APPENDIX 5

X-Ray Crystallography Reports Relevant to Chapter 3:

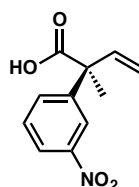
Enantioselective Synthesis of Acyclic α -Quaternary Carboxylic Acid

Derivatives via Iridium-Catalyzed Allylic Alkylation

A5.1 GENERAL EXPERIMENTAL

X-ray crystallographic analysis was obtained from the Caltech X-Ray Crystallography Facility using a Bruker D8 Venture Kappa Duo Photon 100 CMOS diffractometer.

A5.1.1 X-RAY CRYSTAL STRUCTURE ANALYSIS OF CARBOXYLIC ACID **77h**



Carboxylic acid **77h** (87% ee) was recrystallized by slow evaporation of CH₂Cl₂ to provide crystals suitable for X-ray analysis.

Figure A5.1 X-ray crystal structure of carboxylic acid **77h**

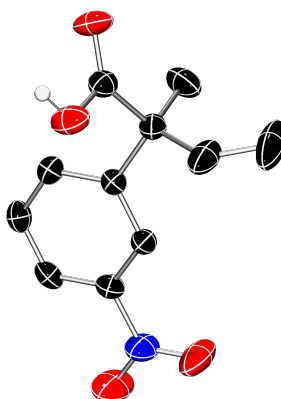


Table A5.1 Crystal data and structure refinement for carboxylic acid **77h**

Empirical formula	C ₁₁ H ₁₁ N O ₄
Formula weight	221.21
Temperature	200(2) K
Wavelength	1.54178 Å

Crystal system	Monoclinic
Space group	P2 ₁
Unit cell dimensions	a = 7.3561(3) Å a = 90° b = 6.7600(3) Å b = 94.5940(10)° c = 10.9461(5) Å g = 90°
Volume	542.57(4) Å ³
Z	2
Density (calculated)	1.354 Mg/m ³
Absorption coefficient	0.879 mm ⁻¹
F(000)	232
Theta range for data collection	4.051 to 72.406°.
Index ranges	-9<=h<=9, -8<=k<=8, -13<=l<=13
Reflections collected	24109
Independent reflections	2132 [R(int) = 0.0427]
Completeness to theta = 67.679°	100.0 %
Absorption correction	Semi-empirical from equivalents
Refinement method	Full-matrix least-squares on F ²
Data / restraints / parameters	2132 / 1 / 146
Goodness-of-fit on F ²	1.315
Final R indices [I>2sigma(I)]	R1 = 0.0495, wR2 = 0.1336
R indices (all data)	R1 = 0.0497, wR2 = 0.1346
Absolute structure parameter	0.08(5)
Extinction coefficient	n/a
Largest diff. peak and hole	0.312 and -0.539 e.Å ⁻³

Table A5.2 Atomic coordinates ($\times 10^4$) and equivalent isotropic displacement parameters ($\text{\AA}^2 \times 10^3$) for **77h**. $U(\text{eq})$ is defined as one third of the trace of the orthogonalized U^{ij} tensor.

	x	y	z	U(eq)
C(1)	6927(3)	5263(3)	4602(2)	32(1)
C(2)	7734(2)	5232(3)	5795(2)	30(1)
C(3)	6640(2)	5267(3)	6762(2)	27(1)
C(4)	4752(2)	5328(3)	6510(2)	33(1)
C(5)	3969(2)	5364(3)	5309(2)	35(1)
C(6)	5062(3)	5332(3)	4329(2)	34(1)
C(7)	7495(2)	5394(3)	8089(2)	33(1)
C(8)	7573(4)	7595(4)	8448(2)	52(1)
C(9)	9331(3)	4360(5)	8210(2)	51(1)
C(10)	10884(3)	5180(9)	8624(2)	86(2)
C(11)	6291(2)	4290(3)	8935(2)	33(1)
O(1)	6125(2)	2390(3)	8666(1)	46(1)
O(2)	5572(2)	5042(3)	9776(1)	49(1)
N(1)	8117(3)	5216(4)	3590(2)	47(1)
O(3)	9753(2)	5210(6)	3825(2)	84(1)
O(4)	7426(3)	5157(6)	2546(2)	81(1)

Table A5.3 Bond lengths [\AA] and angles [$^\circ$] for **77h**

C(1)-C(6)	1.381(3)
C(1)-C(2)	1.390(2)
C(1)-N(1)	1.466(3)
C(2)-C(3)	1.380(2)
C(3)-C(4)	1.395(2)
C(3)-C(7)	1.538(2)
C(4)-C(5)	1.392(3)

C(5)-C(6)	1.391(3)
C(7)-C(9)	1.517(3)
C(7)-C(11)	1.527(2)
C(7)-C(8)	1.539(3)
C(9)-C(10)	1.318(4)
C(11)-O(2)	1.210(2)
C(11)-O(1)	1.321(3)
N(1)-O(3)	1.210(3)
N(1)-O(4)	1.214(3)
C(6)-C(1)-C(2)	123.08(18)
C(6)-C(1)-N(1)	118.68(17)
C(2)-C(1)-N(1)	118.25(17)
C(3)-C(2)-C(1)	119.26(16)
C(2)-C(3)-C(4)	118.74(16)
C(2)-C(3)-C(7)	120.38(14)
C(4)-C(3)-C(7)	120.72(15)
C(5)-C(4)-C(3)	121.17(17)
C(6)-C(5)-C(4)	120.45(17)
C(1)-C(6)-C(5)	117.31(17)
C(9)-C(7)-C(11)	106.08(18)
C(9)-C(7)-C(3)	110.51(16)
C(11)-C(7)-C(3)	109.42(14)
C(9)-C(7)-C(8)	114.1(2)
C(11)-C(7)-C(8)	109.22(15)
C(3)-C(7)-C(8)	107.45(17)
C(10)-C(9)-C(7)	125.3(4)
O(2)-C(11)-O(1)	122.7(2)
O(2)-C(11)-C(7)	124.49(19)
O(1)-C(11)-C(7)	112.85(17)
O(3)-N(1)-O(4)	122.26(19)
O(3)-N(1)-C(1)	118.91(17)
O(4)-N(1)-C(1)	118.82(19)

Table A5.4 Anisotropic displacement parameters ($\text{\AA}^2 \times 10^3$) for **77h**. The anisotropic displacement factor exponent takes the form: $-2p^2 [h^2 a^{*2} U^{11} + \dots + 2 h k a^* b^* U^{12}]$

	U ¹¹	U ²²	U ³³	U ²³	U ¹³	U ¹²
C(1)	38(1)	32(1)	26(1)	-1(1)	2(1)	1(1)
C(2)	29(1)	34(1)	28(1)	0(1)	1(1)	0(1)
C(3)	30(1)	25(1)	27(1)	1(1)	1(1)	-1(1)
C(4)	30(1)	34(1)	35(1)	1(1)	4(1)	1(1)
C(5)	29(1)	34(1)	41(1)	3(1)	-5(1)	-1(1)
C(6)	40(1)	28(1)	32(1)	-2(1)	-8(1)	1(1)
C(7)	31(1)	42(1)	26(1)	0(1)	3(1)	-4(1)
C(8)	72(2)	48(1)	36(1)	-7(1)	6(1)	-24(1)
C(9)	33(1)	91(2)	30(1)	16(1)	4(1)	5(1)
C(10)	32(1)	176(5)	49(1)	35(2)	-6(1)	-14(2)
C(11)	33(1)	39(1)	26(1)	2(1)	1(1)	2(1)
O(1)	62(1)	37(1)	42(1)	0(1)	22(1)	-4(1)
O(2)	60(1)	51(1)	38(1)	-7(1)	22(1)	5(1)
N(1)	50(1)	67(1)	26(1)	2(1)	4(1)	5(1)
O(3)	40(1)	176(3)	36(1)	0(1)	9(1)	5(1)
O(4)	66(1)	151(3)	25(1)	-7(1)	-1(1)	12(1)

Table A5.5 Hydrogen coordinates ($\times 10^4$) and isotropic displacement parameters ($\text{\AA}^2 \times 10^3$) for **77h**

	x	y	z	U(eq)
H(2)	9023	5188	5942	36
H(4)	3987	5347	7168	40
H(5)	2680	5410	5158	42
H(6)	4546	5355	3505	40

H(8A)	8291	8322	7880	78
H(8B)	8145	7730	9284	78
H(8C)	6333	8135	8410	78
H(9)	9363	3012	7967	62
H(10A)	10911	6525	8877	103
H(10B)	11978	4427	8671	103
H(1)	5466	1842	9160	69

CHAPTER 4

Enantioselective Synthesis Vicinal All-Carbon Quaternary Centers via Iridium-Catalyzed Allylic Alkylation[†]

4.1 INTRODUCTION AND BACKGROUND

The enantioselective preparation of singular all-carbon quaternary stereocenters has been a persistent challenge in the synthetic community and a topic of great interest to our research group.¹ However, due to significant progress in this area over recent decades,² the more formidable challenge of constructing vicinal all-carbon quaternary centers has become the forefront of investigation. A limited number of organic³ and transition metal-catalyzed^{4,5} methods for the enantioselective preparation of vicinal all-carbon quaternary stereocenters have been reported,⁶ with enantioselective transition metal-catalyzed allylic alkylation strategies remaining underexplored.

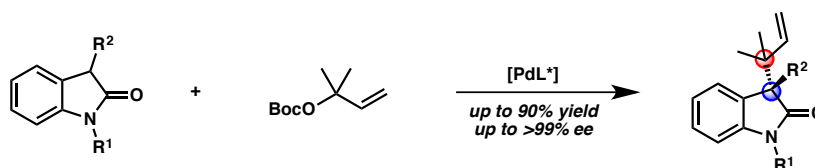
[†] This work was performed in collaboration with Dr. J. Caleb Hethcox. Portions of this chapter have been reproduced with permission from Hethcox, J. C.;[‡] Shockley, S. E.;[‡] Stoltz, B. M. *Angew. Chem. Int. Ed.* **2018**, doi: 10.1002/anie.201804820 © 2018 Wiley-VCH.

In 2011, Trost reported an enantioselective palladium-catalyzed allylic alkylation of oxindoles to provide reverse prenylated products containing a homoallylic quaternary stereocenter vicinal to an all-carbon quaternary center (Figure 4.1a).^{5a,b} In 2014, Ooi^{5c} and Zhang^{5d} each disclosed examples of enantio- and diastereoselective palladium-catalyzed allylic alkylation reactions to form cyclic products bearing vicinal all-carbon quaternary stereocenters (Figure 4.1b). To date, these three methods represent the only enantioselective transition metal-catalyzed allylic alkylation protocols for the synthesis of vicinal all-carbon quaternary centers^{7,8} – none of these reports provide access to acyclic products.

Figure 4.1 State-of-the-art in the enantioselective synthesis of vicinal all-carbon quaternary centers via transition metal-catalyzed allylic alkylation

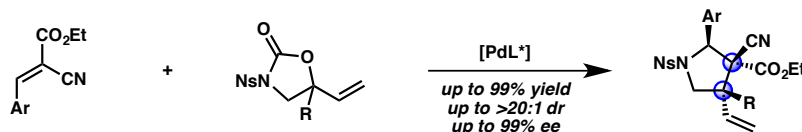
a) Previous Report: Enantioselective Synthesis of Vicinal Quaternary Centers

Trost (2011)

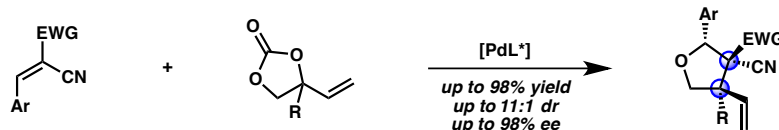


b) Previous Reports: Enantio- and Diastereoselective Synthesis of Vicinal Quaternary Stereocenters

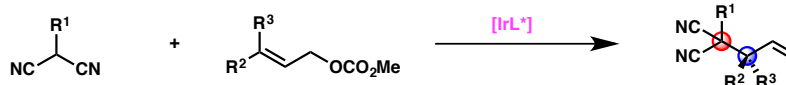
Ooi (2014)



Zhang (2014)



c) This Research: Enantioselective Synthesis of Vicinal Quaternary Centers with Prochiral Electrophile



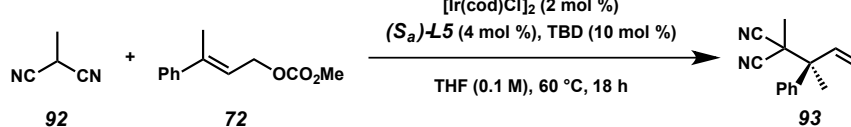
Recently, our group reported the first iridium-catalyzed allylic alkylation method to allow for the synthesis of highly enantioenriched allylic quaternary stereocenters.⁹ Given that iridium-catalyzed allylic alkylation is well known to facilitate the synthesis of vicinal stereocenters ($3^\circ/3^\circ$ and $3^\circ/4^\circ$),¹⁰ we hypothesized that we could utilize our newly developed technology to prepare vicinal all-carbon quaternary centers, with the use of appropriately designed nucleophiles.¹¹ Herein, we discuss the first enantioselective transition metal-catalyzed allylic alkylation to form acyclic products bearing vicinal all-carbon quaternary centers (Figure 4.1c).

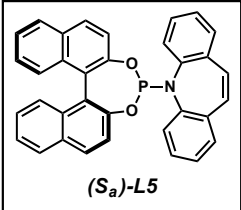
4.2 REACTION OPTIMIZATION

Preliminary studies focused on identifying a suitable catalyst system to promote the reaction of nucleophile **92** and trisubstituted allylic electrophile **72** (Table 4.1). In designing our optimal nucleophile for the allylic alkylation reaction, we imagined that methylmalononitrile (**92**) would mimic both the acidity and steric bulk of the previously utilized masked acyl cyanide (MAC) nucleophile⁹ (Figure 1C, $R^1 = \text{OMOM}$) as well as provide versatile functional handles for derivatizations of product **93**. We were pleased to find that our hypothesis was valid, and when utilizing our optimized conditions for the iridium-catalyzed allylic alkylation of MAC reagents⁹ with nucleophile **92**, product **93** is obtained in nearly quantitative yield, though in only a moderate 73% ee (Table 4.1, entry 1). In an effort to improve the enantioselectivity of the transformation we investigated a range of basic additives, as bases have been reported to have a pronounced effect on selectivity in allylic alkylation reactions.¹² While addition of LiOt-Bu provided only a slight enhancement in enantioselectivity to 81% ee (entry 2), we were delighted to find

that the amine base DABCO affords product **93** in 92% yield and an excellent 95% ee (entry 3). At this time, the specific role of DABCO remains unknown; however, due to the additive's drastic effect on enantioselectivity, we hypothesize that DABCO allows for increased equilibration between diastereomers of an iridium π -allyl complex by slowing the rate of nucleophilic attack.^{13,14} Moreover, while we observed the highest yield for the allylic alkylation reaction using a 1:2 nucleophile to electrophile ratio, the nucleophile and electrophile stoichiometry can be varied (1:1 or 2:1) without affecting reaction selectivity, though yields are diminished (entries 4 and 5). Of note, excess electrophile **72** is unable to be quantitatively recovered as a competing elimination reaction takes place to form a diene byproduct.

Table 4.1 Optimization of reaction parameters^a

		Base (200 mol %) BEt ₃ (200 mol %) [Ir(cod)Cl] ₂ (2 mol %) (<i>S_a</i>)- L5 (4 mol %), TBD (10 mol %) THF (0.1 M), 60 °C, 18 h		
Entry	Nuc:Elec	Base	Yield (%) ^b	ee (%) ^c
1	1:2	—	>99	73
2	1:2	LiOt-Bu	>99	81
3	1:2	DABCO	92	95
4	1:1	DABCO	67	95
5	2:1	DABCO	41	94

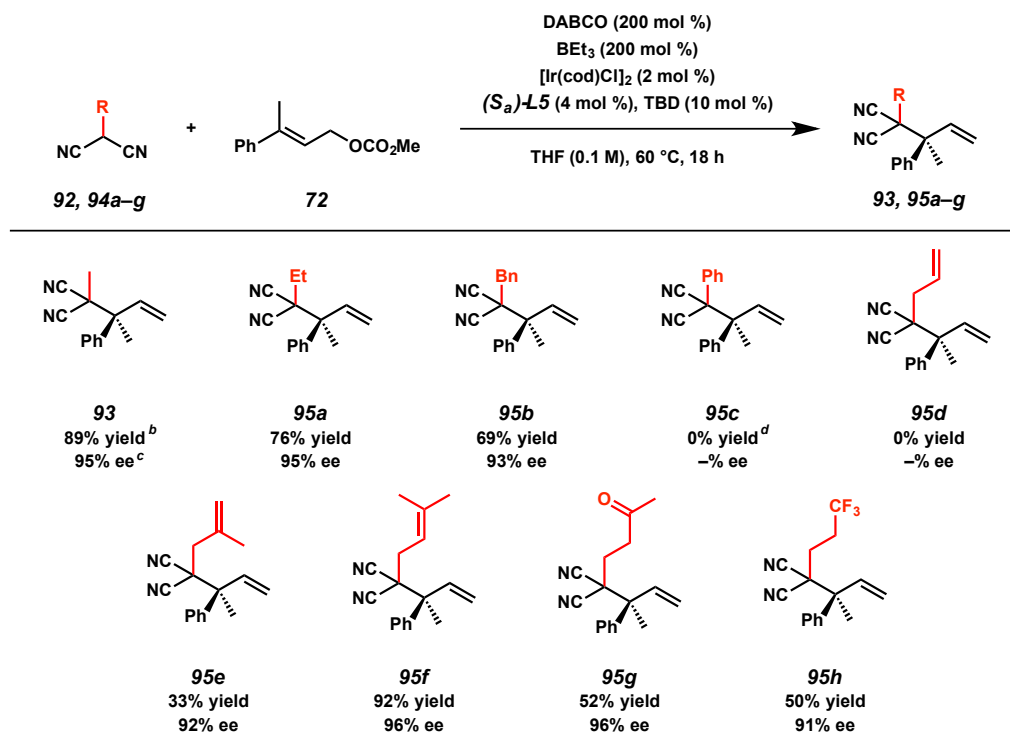


(*S_a*)-**L5**

[a] Reactions performed on 0.1 mmol scale. [b] ¹H NMR yield based on internal standard. [c] Determined by chiral SFC analysis. [d] TBD = 1,3,4-triazabicyclo[4.4.0]dec-5-ene, DABCO = 1,4-diazabicyclo[2.2.2]octane.

4.3 SUBSTRATE SCOPE EXPLORATION

With the optimal conditions identified (Table 4.1, entry 3), we explored the substrate scope for this new transformation. With respect to nucleophile **94**, the process is tolerant of a wide variety of substituted malononitrile derivatives (Table 4.2). Specifically, we were pleased to find that increasing the steric bulk on the nucleophile results in formation of the corresponding ethyl-substituted **95a** and benzyl-substituted **95b** products in only slightly decreased yields (76% and 69%, respectively) and no significant loss in enantioselectivity. Interestingly, phenyl-substituted nucleophile **94c** gives full conversion to the linear product (**105**, Section 4.6.2.5) in the allylic alkylation reaction rather than branched product **95c**. Additionally, olefinic substituents on the nucleophile are tolerated under the reaction conditions provided the olefin is at least di-substituted; allyl-substituted **94d** returns only starting material in the allylic alkylation reaction while methallyl-substituted product **95e** can be prepared in 33% yield with 92% ee and prenyl-substituted product **95f** can be constructed in an excellent 92% yield with 96% ee. We reason that increased olefin substitution decreases the affinity of the olefin to bind to the catalyst,¹⁵ thus leading to increased yields. Furthermore, we were delighted to discover that carbonyl-containing product **95g** can be obtained in a moderate 52% yield with an excellent 96% ee. Finally, fluorinated product **95h** can be accessed in a moderate 50% yield with 91% ee.

Table 4.2 Nucleophile substrate scope^a

[a] Reactions performed on 0.2 mmol scale. [b] Isolated yield. [c] Determined by chiral SFC. [d] 99% conversion by ¹H NMR to linear product **105**.

Pleased to find the reaction amenable to a range of nucleophilic substrates, we sought to further examine the scope of the transformation by exploring the diversity of substitution permitted on trisubstituted allylic electrophile **96** (Table 4.3). Gratifyingly, we observed that a series of *para*-substituted allylic electrophiles bearing both electron-donating (*-p*-Me, *-p*-OMe) and withdrawing groups (*-p*-Ph, *-p*-F) on the aromatic ring furnish the corresponding products **97a–d** in consistently excellent enantioselectivities (>94% ee) when subjected to the reaction conditions utilizing methylmalononitrile (**92**) as the nucleophile. In evaluating the effect of *meta*-substitution, we found that products **97e–h** (*-m*-Me, *-m*-Cl, *-m*-NO₂, 2-Np) can be obtained with similarly high enantiocontrol (>93% ee). Generally, we noted that electron-rich electrophiles (i.e., **96a**,

96b, **96e**) provide the corresponding allylic alkylation products in slightly diminished yields (67–80% versus 84–99%) as compared to electron-poor electrophiles (i.e., **96c**, **96d**, **96f**, **96g**). At this time, *ortho*-substitution (i.e., *-o*-Me) is not tolerated under the reaction conditions and no conversion to product **97i** is observed. However, we were pleased to discover that the reaction is amenable to bis-alkyl-substitution on the allylic electrophile allowing for access to product **97j** in 65% yield and 84% ee as an inseparable mixture (1:1.5) of branched and linear isomers. Additionally, reverse prenylation can be effected to produce achiral product **97k** in 61% yield. Finally, extension of the alkyl chain on the allylic electrophile to an ethyl group leads to a decreased yield with **97l** isolated in 50% yield but with no loss in selectivity (96% ee).

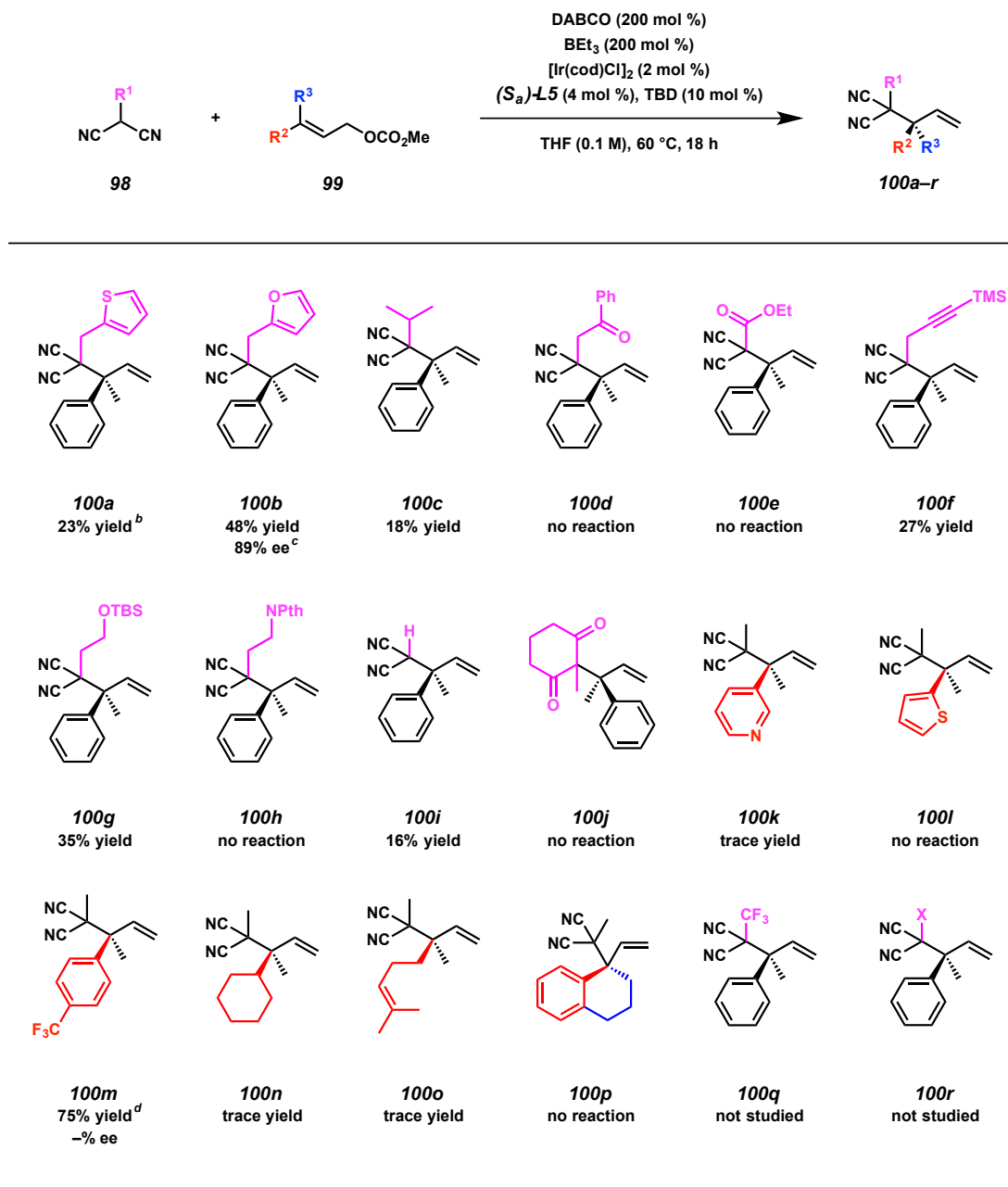
Table 4.3 Electrophile substrate scope^a

97a 80% yield ^b 96% ee ^c	97b 70% yield 96% ee	97c ^d >99% yield 95% ee	97d 99% yield 94% ee	97e 67% yield 95% ee	97f 99% yield 99% ee
97g 84% yield 93% ee	97h 93% yield 95% ee	97i 0% yield –% ee	97j 65% yield ^e 84% ee	97k 61% yield –% ee	97l 50% yield 96% ee

[a] Reactions performed on 0.2 mmol scale. [b] Isolated yield. [c] Determined by chiral HPLC or SFC. [d] Absolute stereochemistry determined by single-crystal X-ray analysis; the absolute stereochemistry of all other compounds was assigned by analogy. [e] Isolated as an inseparable mixture (1:1.5) of linear to branched product.

A deeper investigation into the scope of this novel transformation revealed the limits of the catalytic system (Table 4.4). Foremost, Lewis basic functionalities are not tolerated on nucleophile **98** or electrophile **99**, thus low yields or no reactivity was observed in the formation of thiophene **100a**, furan **100b**, ketone **100d**, alkyne **100f**, pyridine **100k**, and thiophene **100l**. Moreover, branched substitution on the nucleophile is not permitted in the allylic alkylation reaction as isopropyl-substituted **98** ($R^1 = i\text{-Pr}$) returns only starting material. Additionally, drastically altering the pKa of nucleophile **98** shuts down the reaction, as seen with ester-functionalized **100e** ($R^1 = \text{CO}_2\text{Et}$). Also, adding significant steric bulk to nucleophile **98** leads to low to no conversion to product (e.g., **100g**, **100h**). Furthermore, to date, only functionalized-malononitrile nucleophiles have been successful utilized in the reported allylic alkylation reaction, despite studies into other bis-electron-withdrawing group-functionalized nucleophiles (e.g., 1,3-diketone **100j**) and unfunctionalized malononitrile (**100i**). Of note, *para*-trifluoromethyl-substituted allylic alkylation product **100m** can be isolated in a good 75% yield, however the enantiomeric excess could not be determined due to inseparable enantiomers by HPLC and SFC; though we hypothesize that the value would be consistently high as with other electrophile substrates (Table 4.3). With respect to substitution on the electrophile, replacement of the aryl moiety with an alkyl group leads to minimal to no yield of allylic alkylation products **100n**, and **100o**. Use of a cyclic allylic electrophile does not afford corresponding bicyclic product **100p**. Finally, despite the interest and value in the corresponding products (**100q** and **100r**), due to difficulty of substrate preparation, a trifluoromethyl-substitute malononitrile nucleophile and halogen-substituted malononitriles were not explored in the newly developed allylic alkylation reaction.

Table 4.4 Substrate scope limitations^a

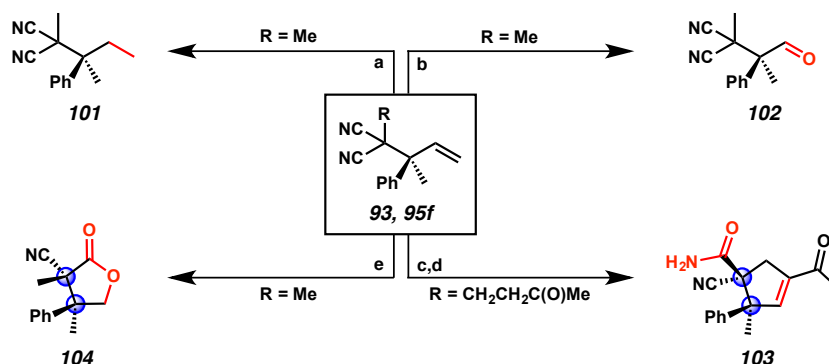


[a] Reactions performed on 0.2 mmol scale. [b] ¹H NMR yield based on internal standard. [c] Determined by chiral HPLC or SFC. [d] Isolated yield.

4.4 PRODUCT TRANSFORMATIONS

With the general reactivity trends for the allylic alkylation reaction explored, we sought to demonstrate the utility of these sterically congested products (Figure 4.2). Though hydrogenation of the olefin in allylic alkylation product **93** using palladium catalysis proved problematic due to competing reduction of the nitrile groups, we found that treatment of **93** with Wilkinson's catalyst under a hydrogen atmosphere chemoselectively reduces the olefin to furnish **101** in 92% yield. Additionally, ozonolysis of olefin **93** proceeds smoothly to give enantioenriched aldehyde **102** in 93% yield,¹⁶ wherein the aldehyde moiety can serve as a valuable functional handle for further manipulation (e.g., reductive aminations, allylations, and olefinations). Allylic alkylation product **95f** was subjected to a two-step ozonolysis/aldol condensation process to deliver a densely functionalized, enantioenriched cyclopentene (**106**, Section 4.6.2.6) in 43% yield, which can then undergo diastereoselective hydration of the bis-nitrile functionality to provide amide **103** in 1:11 dr. Chiral cyclopentenones have been demonstrated to be key building blocks in a number of complex molecule total syntheses.¹⁷ Finally, enantioenriched lactone **104** bearing vicinal all-carbon quaternary stereocenters can be accessed in 65% yield and 1:2.5 dr from allylic alkylation product **93** via ozonolysis followed by reductive quenching. The transformations forming products **103** and **104** showcase that the diastereotopic nitrile functionalities of the allylic alkylation products are amenable to diastereoselective differentiation to afford vicinal all-carbon quaternary stereocenters, which are otherwise difficult to prepare.

Figure 4.2 Product transformations of allylic alkylation products



[a] RhCl(PPh₃)₃, H₂ (balloon), benzene, 23 °C, 18 h, 92% yield; [b] O₃, pyridine, CH₂Cl₂, -78 °C, 4 min, 93% yield; [c] i. O₃, pyridine, CH₂Cl₂, -78 °C, 4 min, ii. *p*-TsOH, benzene, reflux, 18 h, 47% yield; [d] NaOH, EtOH/H₂O (1:1), 60 °C, 18 h, 38% yield, 1:11 dr; [e] i. O₃, MeOH, -78 °C, 0.5 h, ii. NaBH₄, 0 °C, 3 h, 65% yield, 1:2.5 dr.

4.5 CONCLUSIONS

In conclusion, we have developed the first enantioselective transition metal-catalyzed allylic alkylation reaction for the preparation of acyclic products bearing vicinal all-carbon quaternary centers. Key to the success of this new reaction is the use of DABCO in combination with triethylborane and our unique catalyst prepared from [Ir(cod)Cl]₂, (*S_a*)-**L5**, and TBD. The developed method proceeds with moderate to excellent yields and high levels of enantioselectivity for a wide range of substitution on both the malononitrile-derived nucleophile and the trisubstituted allylic electrophile. Furthermore, the allylic alkylation products can be transformed by chemo- and diastereoselective methods to a number of highly valuable, densely functionalized building blocks, including those containing vicinal all-carbon quaternary stereocenters.

4.6 EXPERIMENTAL SECTION

4.6.1 MATERIALS AND METHODS

Unless otherwise stated, reactions were performed in flame-dried glassware under an argon or nitrogen atmosphere using dry, deoxygenated solvents. Solvents were dried by passage through an activated alumina column under argon. Chemicals were purchased from Sigma Aldrich/Strem/Alfa Aesar/Oakwood Chemicals and used as received. Reaction temperatures were controlled by an IKA Mag temperature modulator. Glove box manipulations were performed under a nitrogen atmosphere. Thin-layer chromatography (TLC) and preparatory TLC was performed using E. Merck silica gel 60 F254 precoated plates (0.25 mm) and visualized by UV fluorescence quenching, KMnO_4 , or *p*-anisaldehyde staining. SiliaFlash P60 Academic Silica gel (particle size 0.040–0.063 mm) was used for flash chromatography. Analytical chiral HPLC was performed with an Agilent 1100 Series HPLC utilizing a Chiralpak OJ column (4.6 mm x 25 cm) or a Chiralpak AD-H column (4.6 mm x 25 cm), both obtained from Daicel Chemical Industries, Ltd. with visualization at 210 nm. Analytical SFC was performed with a Mettler SFC supercritical CO_2 analytical chromatography system utilizing a Chiralpak OJ-H column (4.6 mm x 25 cm) obtained from Daicel Chemical Industries, Ltd. with visualization at 210 nm. ^1H NMR spectra were recorded on a Bruker Avance HD 400 MHz spectrometer and are reported relative to residual CHCl_3 (δ 7.26 ppm). ^{13}C NMR spectra were recorded on a Bruker Avance HD 400 MHz spectrometer and are reported relative to residual CDCl_3 (δ 77.16 ppm). Data for ^1H NMR are reported as follows: s = singlet, d = doublet, t = triplet, q = quartet, p = pentet, sept = septuplet, m = multiplet, br s = broad singlet. Data for ^{13}C NMR are reported in terms of chemical shifts (δ ppm).

Some reported spectra include minor solvent impurities of water (δ 1.56 ppm), ethyl acetate (δ 4.12, 2.05, 1.26 ppm), methylene chloride (δ 5.30 ppm), acetone (δ 2.17 ppm), grease (δ 1.26, 0.86 ppm), and/or silicon grease (δ 0.07 ppm), which do not impact product assignments. IR spectra were obtained using a Perkin Elmer Paragon 1000 spectrometer using thin films deposited on NaCl plates and reported in frequency of absorption (cm^{-1}). High resolution mass spectra (HRMS) were obtained from the Caltech Mass Spectral Facility using a JEOL JMS-600H High Resolution Mass Spectrometer in fast atom bombardment (FAB+) or electron ionization (EI+) mode, or an Agilent 6200 Series TOF with an Agilent G1978A Multimode source in electrospray ionization (ESI+), atmospheric pressure chemical ionization (APCI+), or mixed ionization mode (MM: ESI-APCI+). Optical rotations were measured with a Jasco P-2000 polarimeter operating on the sodium D-line (589 nm), using a 100 mm pathlength cell, and are reported as: $[\alpha]_{\text{D}}^{\text{T}}$ (concentration in g/100 mL, solvent).

4.6.1.1 Key Considerations

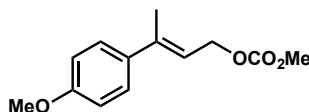
All synthesized reagents (i.e., (S_{a})-**L5**, **92**, **72**, **94**, and **96**) were dried over P_2O_5 and drierite in a vacuum desiccator under vacuum overnight before use in the iridium-catalyzed allylic alkylation reaction. THF was taken directly from an activated alumina column under argon and used immediately to eliminate the possibility of peroxides. Mesitylene or 1,2,4,5-tetrachloro-3-nitrobenzene were used as the internal standard for determining ^1H NMR yields. Prolonged storage of electrophiles **72** and **96** at room temperature under an air atmosphere results in the formation of an unidentified impurity; storage in a $-30\text{ }^{\circ}\text{C}$ freezer allows for prolonged storage.

4.6.1.2 Preparation of Known Compounds

Previously reported methods were used to prepare ligand (*S_a*)-**L5**¹⁸ as well as starting materials **92**,¹⁹ **72**,²⁰ **94a**,²¹ **94b**,¹⁹ **94c**,²² **94d**,²³ **94e**,²⁴ **94f**,²⁴ **94g**,²⁵ **94h**,²⁶ **96a**,²⁷ **96d**,⁹ **96e**,²⁷ **96g**,⁹ **96h**,⁹ **96i**,²⁷ **96j**,²⁷ **96k**,²⁸ and **96l**.²⁷

4.6.2 EXPERIMENTAL PROCEDURES AND SPECTROSCOPIC DATA

4.6.2.1 Representative Procedures for the Synthesis of Electrophiles

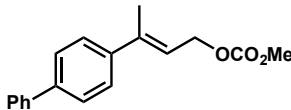


(*E*)-3-(4-Methoxyphenyl)but-2-en-1-yl methyl carbonate (96b). To a solution of methyl (*E*)-3-(4-methoxyphenyl)but-2-enoate²⁹ (0.21 g, 1.0 mmol, 1 equiv) in THF (6.0 mL) at $-78\text{ }^{\circ}\text{C}$ was added DIBAL (0.62 mL, 3.0 mmol, 3.5 equiv) dropwise. The resulting reaction mixture was stirred at $-78\text{ }^{\circ}\text{C}$ for 2.5 h, whereupon the reaction was quenched with a saturated aqueous Rochelle's salt solution (10 mL). The cooling bath was then removed and the reaction was stirred for 18 h at ambient temperature. The aqueous layer was extracted with CH_2Cl_2 (3 x 20 mL) and the combined organic layers were washed with brine (20 mL), dried over Na_2SO_4 , and concentrated under reduced pressure.

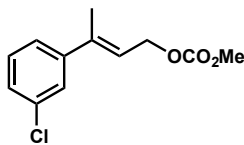
The crude material was dissolved in CH_2Cl_2 (4.0 mL) and cooled to $0\text{ }^{\circ}\text{C}$. Pyridine (0.64 mL, 8.3 mmol, 8.3 equiv) was added followed by methyl chloroformate (0.20 mL, 2.3 mmol, 2.3 equiv) dropwise. The resulting solution was allowed to warm to ambient temperature and was stirred for 18 h. The reaction was quenched with the addition of 1 M HCl (5 mL) and the aqueous layer was extracted with CH_2Cl_2 (3 x 20

mL). The combined organic layers were washed with brine (20 mL), dried over Na₂SO₄, and concentrated under reduced pressure. The crude product was purified by silica gel flash column chromatography (5% EtOAc/hexanes) to give carbonate **96b** as a colorless solid (0.13 g, 53% yield): ¹H NMR (400 MHz, CDCl₃) δ 7.35 (d, *J* = 8.8 Hz, 2H), 6.86 (d, *J* = 8.8 Hz, 2H), 5.92 – 5.82 (m, 1H), 4.84 (dd, *J* = 7.2, 0.8 Hz, 2H), 3.81 (s, 3H), 3.80 (s, 3H), 2.16 – 2.05 (m, 3H); ¹³C NMR (101 MHz, CDCl₃) δ 159.4, 156.0, 140.7, 134.9, 127.1, 119.1, 113.8, 65.2, 55.4, 54.9, 16.4; IR (Neat Film, NaCl) 2958, 2832, 1753, 1740, 1440, 1381, 1336, 1249, 1028, 942, 819, 798 cm⁻¹; HRMS (FAB+) *m/z* calc'd for C₁₃H₁₆O₃ [M]⁺: 236.1049, found 236.1053.

4.6.2.2 Spectroscopic Data for the Synthesis of Electrophiles

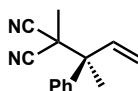


(*E*)-3-([1,1'-Biphenyl]-4-yl)but-2-en-1-yl methyl carbonate (96c). Carbonate **96c** was prepared from methyl (*E*)-3-([1,1'-biphenyl]-4-yl)but-2-enoate³⁰ according to the representative procedure and isolated by silica gel flash column chromatography (5% EtOAc/hexanes) as a colorless oil (0.17 g, 52% yield): ¹H NMR (400 MHz, CDCl₃) δ 7.58 (d, *J* = 19.6 Hz, 4H), 7.51 – 7.41 (m, 4H), 7.35 (t, *J* = 7.3 Hz, 1H), 6.00 (td, *J* = 7.0, 1.4 Hz, 1H), 4.88 (dq, *J* = 7.0, 0.8 Hz, 2H), 3.81 (s, 3H), 2.17 (dt, *J* = 1.3, 0.7 Hz, 3H); ¹³C NMR (101 MHz, CDCl₃) δ 156.0, 141.4, 140.7, 140.7, 140.6, 128.9, 127.5, 127.1, 126.4, 120.8, 65.1, 55.0, 16.4; IR (Neat Film, NaCl) 3032, 2968, 1750, 1740, 1441, 1408, 1340, 1245, 992, 943, 827, 794, 759, 689 cm⁻¹; HRMS (FAB+) *m/z* calc'd for C₁₈H₁₈O₃ [M]⁺: 282.1256, found 282.1253.



(*E*)-3-(3-Chlorophenyl)but-2-en-1-yl methyl carbonate (96f). Carbonate **96f** was prepared from methyl (*E*)-3-(3-chlorophenyl)but-2-enoate ³¹ according to the representative procedure and isolated by silica gel flash column chromatography (10% EtOAc/hexanes) as a colorless oil (0.43 g, 88% yield): ¹H NMR (400 MHz, CDCl₃) δ 7.38 (q, *J* = 1.5 Hz, 1H), 7.30 – 7.22 (m, 3H), 5.92 (ddt, *J* = 6.9, 5.6, 1.4 Hz, 1H), 4.84 (dq, *J* = 7.0, 0.8 Hz, 2H), 3.81 (s, 3H), 2.10 (dt, *J* = 1.4, 0.7 Hz, 3H); ¹³C NMR (101 MHz, CDCl₃) δ 155.9, 144.4, 139.8, 134.4, 129.7, 127.8, 126.3, 124.2, 122.0, 64.9, 55.0, 16.4; IR (Neat Film, NaCl) 2957, 1748, 1594, 1564, 1443, 1377, 1333, 1268, 1172, 1102, 997, 948, 906, 884, 782, 691 cm⁻¹; HRMS (FAB+) *m/z* calc'd for C₁₂H₁₃ClO₃ [M]⁺: 240.0553, found 240.0564.

4.6.2.3 General Procedure for Optimization Reactions (Table 4.1)

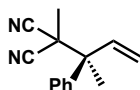


(*S*)-2-Methyl-2-(2-phenylbut-3-en-2-yl)malononitrile (93). In a nitrogen-filled glove box, to a 1 dram vial (vial A) equipped with a stir bar was added [Ir(cod)Cl]₂ (1.3 mg, 0.0020 mmol, 2 mol %), ligand (*S_a*)-**L5** (2.0 mg, 0.004 mmol, 4 mol %), TBD (1.4 mg, 0.010 mmol, 10 mol %), and THF (0.5 mL). Vial A was stirred at 25 °C (ca. 10 min) while another 1 dram vial (vial B) was charged with nucleophile **92** (0.10 mmol or 0.20 mmol, as specified), THF (0.5 mL), and the base additive (0 or 200 mol %). The pre-formed catalyst solution (vial A) was then transferred to vial B followed immediately by

carbonate **72** (0.20 mmol, 0.10 mmol, or 0.20 mmol, as specified). The vial was sealed and stirred at 60 °C. After 18 h, the vial was removed from the glove box concentrated under reduced pressure. To the crude reaction mixture was added 1,2,4,5-tetrachloro-3-nitrobenzene (0.10 mmol in 0.5 mL CDCl₃). The NMR yield (measured in reference to 1,2,4,5-tetrachloro-3-nitrobenzene δ 7.74 ppm (s, 1H)) was determined by ¹H NMR analysis of the crude mixture. The residue was purified by preparatory TLC (15% Et₂O/hexanes, eluted twice) to afford allylic alkylation product **3** as a pale yellow oil.

4.6.2.4 General Procedure for the Iridium-Catalyzed Allylic Alkylation

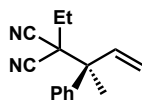
Please note that the absolute configuration was determined only for compound **97c** via X-ray crystallographic analysis. The absolute configuration for all other products has been inferred by analogy. For respective HPLC and SFC conditions, please refer to Table S1.



(S)-2-Methyl-2-(2-phenylbut-3-en-2-yl)malononitrile (93). In a nitrogen-filled glove box, to a 1 dram vial (vial A) equipped with a stir bar was added [Ir(cod)Cl]₂ (2.7 mg, 0.0040 mmol, 2 mol %), ligand (*S_a*)-**L5** (4.0 mg, 0.008 mmol, 4 mol %), TBD (2.8 mg, 0.020 mmol, 10 mol %), and THF (1 mL). Vial A was stirred at 25 °C (ca. 10 min) while another 1 dram vial (vial B) was charged with nucleophile **92** (18 mg, 0.20 mmol, 100 mol %), THF (1 mL), DABCO (45 mg, 0.40 mmol, 200 mol %), and BEt₃ (400 μ L, 1M in hexanes). The pre-formed catalyst solution (vial A) was then transferred to vial B followed immediately by carbonate **72** (83 mg, 0.40 mmol, 200 mol %). The vial was

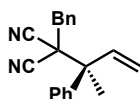
sealed and stirred at 60 °C. After 18 h, the vial was removed from the glove box, transferred to a 20 mL vial with CH₂Cl₂, and concentrated under reduced pressure. The crude residue was purified by preparatory TLC (15% Et₂O/hexanes, eluted twice) to afford allylic alkylation product **93** as a pale yellow oil (37 mg, 89% yield): 95% ee; $[\alpha]_D^{25} +32.9$ (*c* 1.9, CHCl₃); ¹H NMR (400 MHz, CDCl₃) δ 7.61 – 7.52 (m, 2H), 7.44 – 7.33 (m, 3H), 6.49 (dd, *J* = 17.3, 11.0 Hz, 1H), 5.63 – 5.31 (m, 2H), 1.80 (s, 3H), 1.66 (s, 3H); ¹³C NMR (101 MHz, CDCl₃) δ 139.2, 138.3, 128.7, 128.6, 128.1, 119.0, 116.1, 116.0, 49.4, 41.9, 21.8, 21.5; IR (Neat Film, NaCl) 3095, 3062, 2992, 2951, 2247, 1749, 1639, 1600, 1496, 1447, 1417, 1386, 1270, 1217, 1165, 1102, 1074, 1031, 1003, 937, 802, 751, cm⁻¹; HRMS (ESI+) *m/z* calc'd for C₁₄H₁₄N₂ [M]⁺: 210.1157, found 210.1156; SFC conditions: 3% IPA, 2.5 mL/min, Chiralpak OJ–H column, λ = 210 nm, t_R (min): major = 3.832, minor = 4.594.

4.6.2.5 Spectroscopic Data for the Iridium-Catalyzed Allylic Alkylation Products

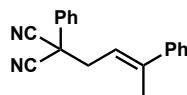


(S)-2-Ethyl-2-(2-phenylbut-3-en-2-yl)malononitrile (95a). Allylic alkylation product **95a** was prepared according to the general procedure and isolated by preparatory TLC (100% toluene, eluted twice) to give a pale yellow oil (34 mg, 76% yield): 95% ee; $[\alpha]_D^{25} +19.0$ (*c* 0.87, CHCl₃); ¹H NMR (400 MHz, CDCl₃) δ 7.63 – 7.51 (m, 2H), 7.45 – 7.31 (m, 3H), 6.51 (dd, *J* = 17.3, 11.0 Hz, 1H), 5.52 (d, *J* = 11.0 Hz, 1H), 5.40 (d, *J* = 17.3 Hz, 1H), 1.90 – 1.72 (m, 5H), 1.27 (t, *J* = 7.3 Hz, 3H); ¹³C NMR (101 MHz, CDCl₃) δ 139.6,

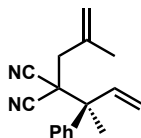
138.7, 128.6, 128.5, 128.2, 118.7, 115.2, 115.1, 49.9, 49.7, 27.7, 22.0, 10.7; IR (Neat Film, NaCl) 3094, 3061, 2959, 2931, 2874, 2244, 1730, 1640, 1600, 1496, 1461, 1446, 1416, 1382, 1271, 1175, 1074, 1031, 1002, 937, 793, 750, 701 cm^{-1} ; HRMS (ESI+) m/z calc'd for $\text{C}_{15}\text{H}_{17}\text{N}_2$ $[\text{M}+\text{H}]^+$: 225.1392, found 225.1395; SFC conditions: 3% IPA, 2.5 mL/min, Chiralpak OJ–H column, $\lambda = 210$ nm, t_R (min): major = 3.378, minor = 4.088.



(S)-2-Benzyl-2-(2-phenylbut-3-en-2-yl)malononitrile (95b). Allylic alkylation product **95b** was prepared according to the general procedure and isolated by preparatory TLC (15% Et_2O /hexanes, eluted twice) to give a pale yellow oil (39 mg, 69% yield): 93% ee; $[\alpha]_D^{25} +11.0$ (c 1.0, CHCl_3); ^1H NMR (400 MHz, CDCl_3) δ 7.68 – 7.62 (m, 2H), 7.51 – 7.29 (m, 8H), 6.64 (dd, $J = 17.3, 11.0$ Hz, 1H), 5.60 (d, $J = 11.0$ Hz, 1H), 5.47 (d, $J = 17.2$ Hz, 1H), 3.07 – 2.90 (m, 2H), 1.93 (s, 3H); ^{13}C NMR (101 MHz, CDCl_3) δ 139.4, 138.5, 132.6, 130.5, 128.9, 128.7, 128.7, 128.6, 128.3, 119.1, 114.9, 114.7, 50.6, 50.3, 39.6, 22.1; IR (Neat Film, NaCl) 3092, 3063, 3034, 2990, 2927, 2245, 1957, 1884, 1810, 1748, 1602, 1498, 1456, 1446, 1416, 1383, 1270, 1212, 1159, 1110, 1080, 1032, 1004, 938, 766, 749 cm^{-1} ; HRMS (FAB+) m/z calc'd for $\text{C}_{20}\text{H}_{19}\text{N}_2$ $[\text{M}+\text{H}]^+$: 287.1548, found 287.1553; SFC conditions: 3% IPA, 2.5 mL/min, Chiralpak OJ–H column, $\lambda = 210$ nm, t_R (min): major = 10.960, minor = 11.727.

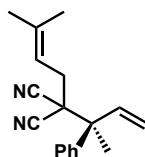


(*E*)-2-Phenyl-2-(3-phenylbut-2-en-1-yl)malononitrile (105). Linear allylic alkylation product **SI-1** was prepared according to the general procedure in 99% conversion by ^1H NMR yield but was inseparable from unreacted electrophile **72**. **105** was prepared via an alternate route for verification and characterization. In a nitrogen-filled glove box, to a 1 dram vial equipped with a stir bar was added $\text{Pd}(\text{PPh}_3)_4$ (11 mg, 0.01 mmol, 0.1 mol %), nucleophile **94c** (21 mg, 0.15 mmol, 1.5 equiv), electrophile **72** (21 mg, 0.10 mmol, 1.0 equiv), and THF (1 mL). The reaction was stirred for 18 h whereupon the vial was removed from the glove box, transferred to a 20 mL vial with CH_2Cl_2 , and concentrated under reduced pressure. The crude residue was purified by preparatory TLC (20% Et_2O /hexanes, eluted twice) to afford **105** as a colorless crystalline solid (23 mg, 43% yield): ^1H NMR (400 MHz, CDCl_3) δ 7.67 – 7.28 (m, 10H), 5.75 (td, $J = 7.8, 1.5$ Hz, 1H), 3.23 – 3.01 (m, 2H), 1.95 (d, $J = 1.4$ Hz, 3H); ^{13}C NMR (101 MHz, CDCl_3) δ 143.8, 142.6, 131.7, 130.1, 129.8, 128.5, 128.0, 126.1, 126.1, 117.2, 115.0, 42.5, 42.0, 16.6; IR (Neat Film, NaCl) 3062, 3032, 2983, 2930, 2246, 1599, 1494, 1451, 1383, 1277, 1027, 861, 756, 692 cm^{-1} ; HRMS (FAB+) m/z calc'd for $\text{C}_{19}\text{H}_{17}\text{N}_2$ $[\text{M}+\text{H}]^+$: 273.1292, found 273.1387.



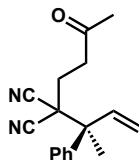
(*S*)-2-(2-methylallyl)-2-(2-phenylbut-3-en-2-yl)malononitrile (95d). Allylic alkylation product **95d** was prepared according to the general procedure and isolated by preparatory

TLC (100% toluene, eluted twice) to give a pale yellow oil (17 mg, 33% yield): 92% ee; $[\alpha]_{\text{D}}^{25} +26.0$ (c 0.94, CHCl_3); ^1H NMR (400 MHz, CDCl_3) δ 7.61 – 7.56 (m, 2H), 7.45 – 7.32 (m, 3H), 6.54 (dd, J = 17.3, 11.0 Hz, 1H), 5.55 (d, J = 11.0 Hz, 1H), 5.41 (d, J = 17.3 Hz, 1H), 5.11 (t, J = 1.4 Hz, 1H), 5.01 (p, J = 1.0 Hz, 1H), 2.50 – 2.35 (m, 2H), 1.91 (dd, J = 1.6, 0.8 Hz, 3H), 1.84 (s, 3H); ^{13}C NMR (101 MHz, CDCl_3) δ 139.4, 138.5, 137.9, 128.7, 128.6, 128.3, 119.1, 118.7, 115.4, 115.2, 50.4, 47.6, 41.5, 23.2, 22.0; IR (Neat Film, NaCl) 3085, 2988, 2242, 1747, 1650, 1496, 1445, 1416, 1381, 1264, 1072, 1004, 910, 792, 750, 698 cm^{-1} ; HRMS (FAB+) m/z calc'd for $\text{C}_{17}\text{H}_{19}\text{N}_2$ $[\text{M}+\text{H}]^+$: 251.1548, found 251.1539; SFC conditions: 3% IPA, 2.5 mL/min, Chiralpak OJ-H column, λ = 210 nm, t_{R} (min): major = 3.138, minor = 3.923.

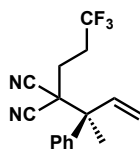


(S)-2-(3-Methylbut-2-en-1-yl)-2-(2-phenylbut-3-en-2-yl)malononitrile (95e). Allylic alkylation product **95e** was prepared according to the general procedure and isolated by preparatory TLC (5% Et_2O /hexanes, eluted twice) to give a colorless oil (49 mg, 92% yield): 96% ee; $[\alpha]_{\text{D}}^{25} +7.87$ (c 6.3, CHCl_3); ^1H NMR (400 MHz, CDCl_3) δ 7.61 – 7.56 (m, 2H), 7.47 – 7.31 (m, 3H), 6.54 (dd, J = 17.3, 11.0 Hz, 1H), 5.54 (d, J = 11.0 Hz, 1H), 5.41 (d, J = 17.3 Hz, 1H), 5.34 – 5.24 (m, 1H), 2.46 (qd, J = 14.1, 7.6 Hz, 2H), 1.84 (s, 3H), 1.78 (d, J = 1.4 Hz, 3H), 1.60 (d, J = 1.4 Hz, 3H); ^{13}C NMR (101 MHz, CDCl_3) δ 140.4, 139.6, 138.7, 128.6, 128.5, 128.1, 118.7, 115.3, 115.3, 115.2, 49.6, 48.9, 32.7, 26.1, 21.9, 18.4; IR (Neat Film, NaCl) 3089, 2987, 2926, 2242, 1497, 1446, 1416, 1383,

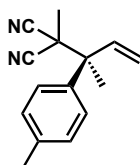
1004, 935, 838, 750, 700 cm^{-1} ; HRMS (FAB+) m/z calc'd for $\text{C}_{18}\text{H}_{21}\text{N}_2$ $[\text{M}+\text{H}]^+$: 265.1705, found 265.1709; SFC conditions: 3% IPA, 2.5 mL/min, Chiralpak OJ–H column, $\lambda = 210$ nm, t_{R} (min): major = 3.095, minor = 4.061.



(S)-2-(3-oxobutyl)-2-(2-phenylbut-3-en-2-yl)malononitrile (95f). Allylic alkylation product **95f** was prepared according to the general procedure and isolated by preparatory TLC (20% Et_2O /hexanes, eluted twice) to give a colorless oil (28 mg, 52% yield): 96% ee; $[\alpha]_{\text{D}}^{25} +16.8$ (c 1.6, CHCl_3); ^1H NMR (400 MHz, CDCl_3) δ 7.62 – 7.53 (m, 2H), 7.46 – 7.30 (m, 3H), 6.50 (dd, $J = 17.2, 10.9$ Hz, 1H), 5.54 (d, $J = 11.0$ Hz, 1H), 5.41 (d, $J = 17.2$ Hz, 1H), 2.86 – 2.75 (m, 2H), 2.19 (s, 3H), 2.17 – 1.97 (m, 2H), 1.82 (s, 3H); ^{13}C NMR (101 MHz, CDCl_3) δ 205.1, 139.2, 138.2, 128.7, 128.6, 128.1, 119.1, 115.0, 114.9, 49.8, 47.7, 40.0, 30.2, 27.8, 21.8; IR (Neat Film, NaCl) 3094, 3061, 2991, 2957, 2246, 1721, 1640, 1601, 1582, 1496, 1446, 1418, 1370, 1288, 1215, 1170, 1118, 1080, 1032, 1002, 938, 754, 702 cm^{-1} ; HRMS (FAB+) m/z calc'd for $\text{C}_{17}\text{H}_{19}\text{N}_2\text{O}$ $[\text{M}+\text{H}]^+$: 267.1497, found 267.1499; SFC conditions: 3% IPA, 2.5 mL/min, Chiralpak OJ–H column, $\lambda = 210$ nm, t_{R} (min): major = 5.022, minor = 7.267.

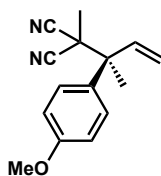


(S)-2-(2-Phenylbut-3-en-2-yl)-2-(3,3,3-trifluoropropyl)malononitrile (95g). Allylic alkylation product **95g** was prepared according to the general procedure and isolated by preparatory TLC (100% toluene, eluted twice) to give a colorless oil (29 mg, 50% yield): 91% ee; $[\alpha]_D^{25} +16.6$ (*c* 1.8, CHCl₃); ¹H NMR (400 MHz, CDCl₃) δ 7.61 – 7.32 (m, 5H), 6.50 (dd, *J* = 17.2, 10.9 Hz, 1H), 5.59 (d, *J* = 11.0 Hz, 1H), 5.44 (d, *J* = 17.2 Hz, 1H), 2.57 – 2.39 (m, 2H), 2.12 – 1.93 (m, 2H), 1.84 (s, 3H); ¹³C NMR (101 MHz, CDCl₃) δ 138.8, 137.7, 128.87, 128.86, 127.9, 125.7 (q, *J* = 276.4 Hz), 119.5, 114.3, 114.1, 49.9, 47.5, 31.7, 31.3 (q, *J* = 30.3 Hz), 27.1 (q, *J* = 3.4 Hz); IR (Neat Film, NaCl) 3096, 3063, 2992, 2928, 2242, 1496, 1447, 1400, 1318, 1257, 1157, 1089, 1046, 940, 845, 752, 701, 624 cm⁻¹; HRMS (ESI+) *m/z* calc'd for C₁₆H₁₅F₃N₂ [M]⁺⁺: 292.1187, found 292.1173; SFC conditions: 1% IPA, 3.0 mL/min, Chiralpak OJ–H column, λ = 210 nm, *t_R* (min): major = 1.651, minor = 1.868.

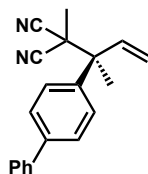


(S)-2-Methyl-2-(2-(*p*-tolyl)but-3-en-2-yl)malononitrile (97a). Allylic alkylation product **97a** was prepared according to the general procedure and isolated by preparatory TLC (15% Et₂O/hexanes, eluted twice) to give a pale yellow oil (36 mg, 80% yield): 96% ee; $[\alpha]_D^{25} +48.7$ (*c* 1.1, CHCl₃); ¹H NMR (400 MHz, CDCl₃) δ 7.47 – 7.39 (m, 2H), 7.23 – 7.16 (m, 2H), 6.48 (dd, *J* = 17.3, 11.0 Hz, 1H), 5.52 (d, *J* = 11.0 Hz, 1H), 5.40 (d, *J* =

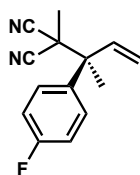
17.3 Hz, 1H), 2.35 (s, 3H), 1.77 (s, 3H), 1.66 (s, 3H); ^{13}C NMR (101 MHz, CDCl_3) δ 138.44, 138.42, 136.2, 129.3, 128.0, 118.8, 116.2, 116.1, 49.2, 42.0, 21.8, 21.5, 21.1; IR (Neat Film, NaCl) 3094, 2992, 2953, 2925, 2247, 1748, 1682, 1639, 1614, 1515, 1454, 1416, 1383, 1268, 1198, 1102, 1074, 1019, 937, 825, 804, 774 cm^{-1} ; HRMS (ESI+) m/z calc'd for $\text{C}_{15}\text{H}_{16}\text{N}_2$ $[\text{M}]^{+}$: 224.1314, found 224.1306; SFC conditions: 1% IPA, 3.0 mL/min, Chiralpak OJ–H column, λ = 210 nm, t_{R} (min): major = 3.658, minor = 4.375.



(S)-2-(2-(4-Methoxyphenyl)but-3-en-2-yl)-2-methylmalononitrile (97b). Allylic alkylation product **97b** was prepared according to the general procedure and isolated by preparatory TLC (20% Et_2O /hexanes, eluted twice) to give a pale yellow oil (34 mg, 70% yield): 96% ee; $[\alpha]_{\text{D}}^{25} +25.4$ (c 2.1, CHCl_3); ^1H NMR (400 MHz, CDCl_3) δ 7.54 – 7.42 (m, 2H), 6.95 – 6.88 (m, 2H), 6.47 (dd, J = 17.3, 11.0 Hz, 1H), 5.52 (d, J = 11.0 Hz, 1H), 5.39 (d, J = 17.3 Hz, 1H), 3.82 (s, 3H), 1.77 (s, 3H), 1.65 (s, 3H); ^{13}C NMR (101 MHz, CDCl_3) δ 159.5, 138.5, 131.0, 129.4, 118.7, 116.2, 116.1, 113.9, 55.4, 49.0, 42.1, 21.7, 21.6; IR (Neat Film, NaCl) 2998, 2934, 2832, 2242, 1609, 1514, 1458, 1298, 1257, 1188, 1029, 932, 832, 808, 774 cm^{-1} ; HRMS (FAB+) m/z calc'd for $\text{C}_{15}\text{H}_{15}\text{ON}_2$ $[(\text{M}+\text{H})-\text{H}_2]^{+}$: 239.1184, found 239.1198; SFC conditions: 3% IPA, 2.5 mL/min, Chiralpak OJ–H column, λ = 210 nm, t_{R} (min): major = 5.019, minor = 5.890.

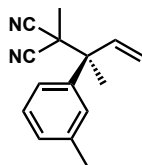


(S)-2-(2-([1,1'-Biphenyl]-4-yl)but-3-en-2-yl)-2-methylmalononitrile (97c). Allylic alkylation product **97c** was prepared according to the general procedure and isolated by preparatory TLC (20% Et₂O/hexanes, eluted twice) to give a colorless crystalline solid (58 mg, 99% yield): 95% ee; $[\alpha]_D^{25} +42.3$ (*c* 1.9, CHCl₃); ¹H NMR (400 MHz, CDCl₃) δ 7.67 – 7.32 (m, 9H), 6.53 (dd, *J* = 17.3, 10.9 Hz, 1H), 5.58 (d, *J* = 10.9 Hz, 1H), 5.46 (d, *J* = 17.3 Hz, 1H), 1.84 (s, 3H), 1.71 (s, 3H); ¹³C NMR (101 MHz, CDCl₃) δ 141.3, 140.1, 138.2, 138.1, 129.0, 128.5, 127.8, 127.24, 127.21, 119.1, 116.1, 116.0, 49.3, 41.9, 21.8, 21.5; IR (Neat Film, NaCl) 3059, 3032, 2992, 2952, 2247, 1749, 1488, 1450, 1416, 1386, 1267, 1214, 1168, 1102, 1076, 1007, 937, 842, 766, 749, 698 cm⁻¹; HRMS (FAB+) *m/z* calc'd for C₂₀H₁₈N₂ [M]⁺: 286.1470, found 286,1466; SFC conditions: 1% IPA, 2.5 mL/min, Chiralpak OJ–H column, λ = 210 nm, *t_R* (min): major = 43.531, minor = 40.798.

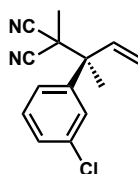


(S)-2-(2-(4-fluorophenyl)but-3-en-2-yl)-2-methylmalononitrile (97d). Allylic alkylation product **97d** was prepared according to the general procedure and isolated by preparatory TLC (15% Et₂O/hexanes, eluted twice) to give a colorless oil (45 mg, 99% yield): 94% ee; $[\alpha]_D^{25} +23.5$ (*c* 3.4, CHCl₃); ¹H NMR (400 MHz, CDCl₃) δ 7.54 (dd, *J* = 9.0, 5.1 Hz, 2H), 7.09 (dd, *J* = 9.1, 8.3 Hz, 2H), 6.46 (dd, *J* = 17.3, 11.0 Hz, 1H), 5.55 (d,

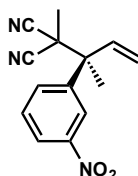
$J = 11.0$ Hz, 1H), 5.41 (d, $J = 17.3$ Hz, 1H), 1.78 (s, 3H), 1.67 (s, 3H); ^{13}C NMR (101 MHz, CDCl_3) δ 162.6 (d, $J = 249.0$ Hz), 138.1, 135.1 (d, $J = 3.3$ Hz), 130.1, 130.0, 119.3, 115.9 (d, $J = 10.2$ Hz), 115.6 (d, $J = 21.4$ Hz), 49.1, 42.0, 21.7, 21.7; IR (Neat Film, NaCl) 3074, 2993, 2247, 1752, 16001, 1509, 1453, 1416, 1386, 1239, 1170, 1097, 1014, 936, 838, 820, 782, 643 cm^{-1} ; HRMS (ESI+) m/z calc'd for $\text{C}_{14}\text{H}_{13}\text{FN}_2$ $[\text{M}]^{+}$: 228.1063, found 228.1036; HPLC conditions: 3% IPA, 1 mL/min, Chiralpak OJ column, $\lambda = 210$ nm, t_{R} (min): major = 22.493, minor = 29.003.



(S)-2-Methyl-2-(2-(*m*-tolyl)but-3-en-2-yl)malononitrile (97e). Allylic alkylation product **97e** was prepared according to the general procedure and isolated by preparatory TLC (15% Et_2O /hexanes, eluted twice) to give a colorless oil (30 mg, 67% yield): 95% ee; $[\alpha]_{\text{D}}^{25} +29.8$ (c 1.8, CHCl_3); ^1H NMR (400 MHz, CDCl_3) δ 7.39 – 7.33 (m, 2H), 7.32 – 7.22 (m, 1H), 7.17 (ddt, $J = 7.4, 1.4, 0.7$ Hz, 1H), 6.48 (dd, $J = 17.3, 11.0$ Hz, 1H), 5.53 (d, $J = 11.0$ Hz, 1H), 5.42 (d, $J = 17.3$ Hz, 1H), 2.38 (d, $J = 0.8$ Hz, 3H), 1.78 (s, 3H), 1.66 (s, 3H); ^{13}C NMR (101 MHz, CDCl_3) δ 139.1, 138.4, 138.3, 129.2, 128.7, 128.5, 125.1, 118.8, 116.1, 116.0, 49.2, 41.8, 21.8, 21.8, 21.4; IR (Neat Film, NaCl) 3092, 2992, 2951, 2924, 2246, 1638, 1606, 1588, 1492, 1454, 1417, 1384, 1250, 1162, 1106, 1042, 1002, 937, 794, 766, 705 cm^{-1} ; HRMS (ESI+) m/z calc'd for $\text{C}_{15}\text{H}_{17}\text{N}_2$ $[\text{M}+\text{H}]^{+}$: 225.1392, found 225.1387; SFC conditions: 3% IPA, 2.5 mL/min, Chiralpak OJ-H column, $\lambda = 210$ nm, t_{R} (min): major = 2.897, minor = 3.290.

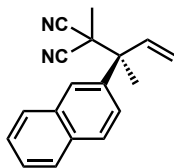


(S)-2-(2-(3-Chlorophenyl)but-3-en-2-yl)-2-methylmalononitrile (97f). Allylic alkylation product **97f** was prepared according to the general procedure and isolated by preparatory TLC (15% Et₂O/hexanes, eluted twice) to give a pale yellow oil (48 mg, 99% yield): 99% ee; $[\alpha]_D^{25} +3.2$ (*c* 3.2, CHCl₃); ¹H NMR (400 MHz, CDCl₃) δ 7.55 – 7.43 (m, 2H), 7.40 – 7.30 (m, 2H), 6.43 (dd, *J* = 17.3, 10.9 Hz, 1H), 5.58 (d, *J* = 11.0 Hz, 1H), 5.43 (d, *J* = 17.3 Hz, 1H), 1.78 (s, 3H), 1.68 (s, 3H); ¹³C NMR (101 MHz, CDCl₃) δ 141.4, 137.6, 134.7, 129.9, 128.8, 128.5, 126.2, 119.6, 115.8, 115.7, 49.3, 41.7, 21.7, 21.4; IR (Neat Film, NaCl) 3071, 2992, 2957, 2247, 1880, 1752, 1637, 1594, 1571, 1478, 1458, 1414, 1261, 1217, 1168, 1094, 999, 938, 885, 811, 739, 695 cm⁻¹; HRMS (ESI+) *m/z* calc'd for C₁₄H₁₃ClN₂ [M]⁺: 244.0767, found 244.0773; SFC conditions: 3% IPA, 2.5 mL/min, Chiralpak OJ–H column, λ = 210 nm, *t*_R (min): major = 3.255, minor = 4.955.



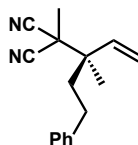
(S)-2-Methyl-2-(2-(3-nitrophenyl)but-3-en-2-yl)malononitrile (97g). Allylic alkylation product **97g** was prepared according to the general procedure and isolated by preparatory TLC (25% Et₂O/hexanes) to give a pale yellow solid (43 mg, 84% yield): 93% ee; $[\alpha]_D^{25} +38.6$ (*c* 2.2, CHCl₃); ¹H NMR (400 MHz, CDCl₃) δ 8.41 (t, *J* = 2.1 Hz, 1H), 8.25 (ddd, *J*

= 8.3, 2.2, 1.0 Hz, 1H), 7.98 (ddd, J = 8.0, 2.1, 1.0 Hz, 1H), 7.63 (t, J = 8.1 Hz, 1H), 6.50 (dd, J = 17.2, 10.9 Hz, 1H), 5.66 (d, J = 11.0 Hz, 1H), 5.46 (d, J = 17.2 Hz, 1H), 1.85 (s, 3H), 1.73 (s, 3H); ^{13}C NMR (101 MHz, CDCl_3) δ 148.3, 141.8, 136.9, 134.1, 129.8, 123.7, 123.3, 120.5, 115.4, 115.3, 49.4, 41.7, 21.7, 21.3; IR (Neat Film, NaCl) 3093, 2994, 2957, 2927, 2248, 1749, 1534, 1455, 1418, 1379, 1351, 1266, 1218, 1107, 1002, 942, 906, 854, 812, 795, 739, 721, 688 cm^{-1} ; HRMS (ESI+) m/z calc'd for $\text{C}_{14}\text{H}_{13}\text{N}_2\text{O}_2$ $[\text{M}]^+$: 255.1008, found 255.0983; HPLC conditions: 6% IPA, 1 mL/min, Chiralpak AD–H column, λ = 210 nm, t_{R} (min): major = 12.542, minor = 11.851.

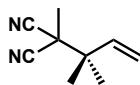


(S)-2-Methyl-2-(2-(naphthalen-2-yl)but-3-en-2-yl)malononitrile (97h). Allylic alkylation product **97h** was prepared according to the general procedure and isolated by preparatory TLC (15% Et_2O /hexanes, eluted twice) to give a colorless oil (48 mg, 93% yield): 95% ee; $[\alpha]_{\text{D}}^{25} +57.9$ (c 3.6, CHCl_3); ^1H NMR (400 MHz, CDCl_3) δ 8.01 (d, J = 2.2 Hz, 1H), 7.93 – 7.80 (m, 3H), 7.70 (dd, J = 8.8, 2.1 Hz, 1H), 7.57 – 7.49 (m, 2H), 6.60 (dd, J = 17.3, 10.9 Hz, 1H), 5.60 (d, J = 11.0 Hz, 1H), 5.46 (d, J = 17.3 Hz, 1H), 1.91 (s, 3H), 1.70 (s, 3H); ^{13}C NMR (101 MHz, CDCl_3) δ 138.4, 136.5, 132.9, 132.8, 128.6, 128.3, 127.8, 127.5, 127.0, 126.7, 125.4, 119.2, 116.1, 116.0, 49.6, 41.8, 21.8 (2C); IR (Neat Film, NaCl) 3060, 2992, 2950, 2246, 1748, 1637, 1598, 1507, 1453, 1416, 1386, 1277, 1194, 1164, 1130, 1103, 999, 937, 902, 859, 819, 779, 747, 666 cm^{-1} ; HRMS (ESI+) m/z calc'd for $\text{C}_{18}\text{H}_{17}\text{N}_2$ $[\text{M}+\text{H}]^+$: 261.1392, found 261.1378; SFC conditions: 4%

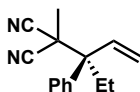
IPA, 2.5 mL/min, Chiralpak OJ–H column, λ = 210 nm, t_R (min): major = 11.637, minor = 13.691.



(*R*)-2-Methyl-2-(3-methyl-5-phenylpent-1-en-3-yl)malononitrile (97j). Allylic alkylation product **97j** was prepared according to the general procedure and isolated by preparatory TLC (20% Et₂O/hexanes, eluted twice) to give a pale yellow oil (31 mg, 65% yield as a 1:1.5 mixture of linear to branched products): 84% ee; $[\alpha]_D^{25} +17.0$ (c 1.9, CHCl₃); ¹H NMR (400 MHz, CDCl₃) δ 7.28 – 7.06 (m, 13.5H), 5.80 (dd, J = 17.3, 10.8 Hz, 1.5H), 5.48 (dd, J = 10.8, 0.5 Hz, 1.5H), 5.30 (dd, J = 17.4, 0.6 Hz, 1.5H), 5.19 – 5.11 (m, 1H), 2.70 (dd, J = 8.9, 6.7 Hz, 2.5H), 2.57 (dq, J = 7.7, 0.7 Hz, 2H), 2.54 – 2.40 (m, 3H), 2.34 (ddd, J = 8.6, 6.4, 1.1 Hz, 2H), 1.94 (ddd, J = 10.3, 6.8, 5.6 Hz, 3H), 1.71 – 1.67 (m, 3H), 1.64 (s, 4.5H), 1.55 (s, 3H), 1.30 (s, 4.5H); ¹³C NMR (101 MHz, CDCl₃) δ 143.7, 141.4, 141.1, 137.0, 128.7, 128.5, 128.4, 126.4, 126.1, 120.5, 116.3, 115.8, 115.7, 115.3, 46.2, 41.8, 41.5, 38.7, 37.4, 34.2, 31.8, 30.9, 23.8, 20.5, 17.1, 16.9; IR (Neat Film, NaCl) 3087, 3064, 3028, 2989, 2930, 2864, 2247, 1949, 1871, 1812, 1638, 1604, 1497, 1453, 1418, 1385, 1277, 1179, 1104, 1074, 1030, 1002, 936, 751, 714, 699, 624 cm⁻¹; HRMS (ESI+) m/z calc'd for C₁₆H₁₉N₂ [M+H]⁺: 239.1548, found 239.1530; SFC conditions: 0.1% IPA, 2.5 mL/min, Chiralpak OJ–H column, λ = 210 nm, t_R (min): major = 7.621, minor = 7.163.



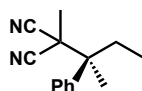
2-Methyl-2-(2-methylbut-3-en-2-yl)malononitrile (97k). Allylic alkylation product **97k** was prepared according to the general procedure and isolated by preparatory TLC (20% Et₂O/hexanes, eluted twice) to give a colorless oil (18 mg, 61% yield): ¹H NMR (400 MHz, CDCl₃) δ 5.92 (dd, *J* = 17.2, 10.8 Hz, 1H), 5.45 – 5.04 (m, 2H), 1.68 (s, 3H), 1.35 (s, 6H); ¹³C NMR (101 MHz, CDCl₃) δ 138.8, 118.2, 115.8, 42.9, 41.2, 22.9, 20.6; IR (Neat Film, NaCl) 3095, 2981, 2941, 2885, 2248, 1643, 1459, 1419, 1383, 1176, 1155, 1112, 998, 934, 735, 688 cm⁻¹; HRMS (ESI+) *m/z* calc'd for C₉H₁₁N₂ [(M+H)–H₂]⁺: 147.0922, found 147.0945.



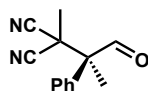
(S)-2-Methyl-2-(3-phenylpent-1-en-3-yl)malononitrile (97l). Allylic alkylation product **97l** was prepared according to the general procedure and isolated by preparatory TLC (15% Et₂O/hexanes, eluted twice) to give a colorless oil (23 mg, 50% yield): 96% ee; [α]_D²⁵ +30.4 (*c* 1.6, CHCl₃); ¹H NMR (400 MHz, CDCl₃) δ 7.55 – 7.46 (m, 2H), 7.46 – 7.29 (m, 3H), 6.19 (ddd, *J* = 17.6, 11.3, 0.7 Hz, 1H), 5.69 (d, *J* = 11.3 Hz, 1H), 5.42 (d, *J* = 17.6 Hz, 1H), 2.50 (dq, *J* = 14.3, 7.2, 0.7 Hz, 1H), 2.15 (dq, *J* = 14.4, 7.2 Hz, 1H), 1.60 (s, 3H), 0.87 (t, *J* = 7.2 Hz, 3H); ¹³C NMR (101 MHz, CDCl₃) δ 134.8, 134.7, 129.8, 128.58, 128.57, 121.2, 116.3, 116.1, 54.4, 42.6, 26.4, 21.9, 9.1; IR (Neat Film, NaCl) 3094, 3061, 2981, 2944, 2884, 2246, 1638, 1601, 1496, 1448, 1414, 1382, 1180, 1161, 1083, 1002, 940, 751, 704 cm⁻¹; HRMS (FAB+) *m/z* calc'd for C₁₅H₁₇N₂ [M+H]⁺:

225.1392, found 225.1377; SFC conditions: 3% IPA, 2.5 mL/min, Chiralpak OJ–H column, $\lambda = 210$ nm, t_R (min): major = 3.270, minor = 4.727.

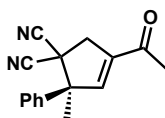
4.6.2.6 Experimental Procedures and Spectroscopic Data for the Product Transformations of Allylic Alkylation Products



(S)-2-Methyl-2-(2-phenylbutan-2-yl)malononitrile (101). In a nitrogen-filled glove box, to a 1 dram vial equipped with a stir bar was added olefin **93** (25 mg, 0.12 mmol, 1 equiv), $\text{RhCl}(\text{PPh}_3)_3$ (11 mg, 0.012 mmol, 10 mol %) and benzene (1.2 mL). The reaction mixture was removed from the glove box, sparged with hydrogen (balloon) for 5 minutes, and stirred under a hydrogen atmosphere for 18 h, whereupon the reaction was concentrated under reduced pressure. The crude residue was purified by preparatory TLC (20% EtOAc/hexanes) to give alkyl **101** as a colorless oil (23 mg, 92% yield): $[\alpha]_D^{25} +16.6$ (c 1.2, CHCl_3); ^1H NMR (400 MHz, CDCl_3) δ 7.49 – 7.31 (m, 5H), 2.58 – 2.46 (m, 1H), 1.94 (dq, $J = 13.6, 7.2$ Hz, 1H), 1.65 (d, $J = 0.9$ Hz, 3H), 1.56 (s, 3H), 0.83 (t, $J = 7.3$ Hz, 3H); ^{13}C NMR (101 MHz, CDCl_3) δ 136.9, 128.7, 128.3 (2C), 116.3, 116.3, 47.3, 43.3, 29.5, 21.2, 20.5, 8.8; IR (Neat Film, NaCl) 3059, 2979, 2943, 2885, 2245, 1602, 15001, 1451, 1391, 1192, 1164, 1098, 1030, 806, 774, 741, 702, 662 cm^{-1} ; HRMS (ESI+) m/z calc'd for $\text{C}_{14}\text{H}_{16}\text{N}_2$ $[\text{M}]^{+}$: 212.1314, found 212.1291.



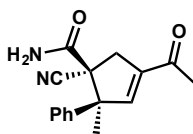
(S)-2-Methyl-2-(1-oxo-2-phenylpropan-2-yl)malononitrile (102). A solution of olefin **93** (40.0 mg, 0.19 mmol, 1 equiv) and pyridine (0.038 mL, 0.48 mmol, 2.5 equiv) in CH_2Cl_2 (2.0 mL) was cooled to $-78\text{ }^\circ\text{C}$. Ozone was bubbled through the resulting solution for 4 min, whereupon the reaction mixture was sparged with O_2 , warmed to ambient temperature, and diluted with CH_2Cl_2 (5.0 mL). The reaction mixture was washed with saturated aqueous NaHCO_3 (5 mL) and the aqueous layer was further extracted with CH_2Cl_2 (2 x 5 mL). The combined organic layers were washed with 1 M HCl (5 mL), brine (5 mL), dried over Na_2SO_4 , and concentrated under reduced pressure to give aldehyde **102** as a colorless solid (37 mg, 93% yield): $[\alpha]_{\text{D}}^{25} -46.9$ (*c* 2.1, CHCl_3); ^1H NMR (400 MHz, CDCl_3) δ 9.45 (s, 1H), 7.55 – 7.45 (m, 3H), 7.41 – 7.30 (m, 2H), 1.88 (s, 3H), 1.70 (s, 3H); ^{13}C NMR (101 MHz, CDCl_3) δ 194.9, 131.1, 130.2, 129.6, 128.9, 115.3, 115.2, 58.3, 37.4, 21.4, 16.3; IR (Neat Film, NaCl) 3033, 3063, 2985, 2954, 2832, 2720, 2249, 1726, 1498, 1448, 1395, 1376, 1262, 1190, 1172, 1080, 923, 869, 764, 703 cm^{-1} ; HRMS (ESI+) *m/z* calc'd for $\text{C}_{13}\text{H}_{12}\text{N}_2\text{O}$ $[\text{M}]^{+}$: 212.0950, found 212.0948.



(S)-4-Acetyl-2-methyl-2-phenylcyclopent-3-ene-1,1-dicarbonitrile (106). A solution of olefin **95f** (42 mg, 0.16 mmol, 1 equiv) and pyridine (0.031 mL, 0.39 mmol, 2.5 equiv) in CH_2Cl_2 (2.0 mL) was cooled to $-78\text{ }^\circ\text{C}$. Ozone was bubbled through the resulting solution for 4 min, whereupon the reaction mixture was sparged with O_2 , warmed to

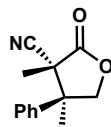
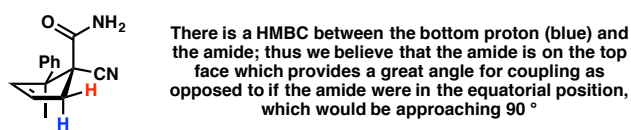
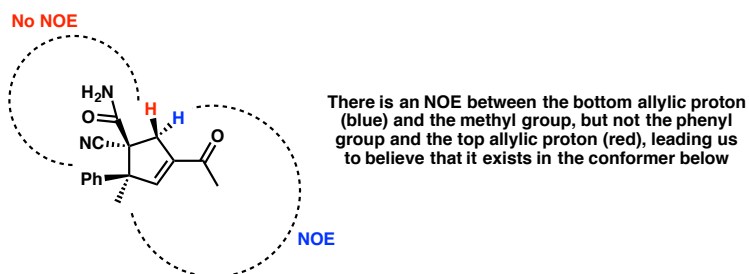
ambient temperature, and diluted with CH₂Cl₂ (5.0 mL). The reaction mixture was washed with saturated aqueous NaHCO₃ (5 mL) and the aqueous layer was further extracted with CH₂Cl₂ (2 x 5 mL). The combined organic layers were washed with 1 M HCl (5 mL), brine (5 mL), dried over Na₂SO₄, and concentrated under reduced pressure.

The crude material was dissolved in benzene (10 mL) and *p*-toluenesulfonic acid (30.0 mg, 0.16 mmol, 1 equiv) was added. The resulting solution was stirred at ambient temperature for 0.5 h and then heated under reflux for 18 h, whereupon the reaction mixture was cooled to ambient temperature and diluted with Et₂O (10 mL). Saturated aqueous NaHCO₃ (10 mL) was added to the resulting solution and allowed to stir for 5 min. The organic layer was then separated and washed further with saturated aqueous NaHCO₃ (10 mL), brine (10 mL), dried over Na₂SO₄, and concentrated under reduced pressure. The crude residue was purified by preparatory TLC (33% acetone/hexanes) to give enone **106** as a colorless oil (19 mg, 47% yield over two steps): [α]_D²⁵ -27.3 (*c* 1.2, CHCl₃); ¹H NMR (400 MHz, CDCl₃) δ 7.52 – 7.36 (m, 5H), 6.91 (dd, *J* = 2.2, 1.2 Hz, 1H), 3.56 (dd, *J* = 16.7, 1.2 Hz, 1H), 3.39 (dd, *J* = 16.7, 2.1 Hz, 1H), 2.48 (s, 3H), 1.82 (s, 3H); ¹³C NMR (101 MHz, CDCl₃) δ 194.6, 145.4, 140.5, 138.8, 129.5 (d, *J* = 2.6 Hz), 126.3, 114.7, 114.4, 61.4, 45.7, 42.2, 26.8, 23.6; IR (Neat Film, NaCl) 3063, 2978, 2934, 2249, 1676, 1629, 1499, 1446, 1371, 1335, 1267, 1098, 1026, 953, 896, 764, 699 cm⁻¹; HRMS (FAB+) *m/z* calc'd for C₁₆H₁₅ON₂ [M+H]⁺: 251.1184, found 251.1197.



(1*S*,2*S*)-4-acetyl-1-cyano-2-methyl-2-phenylcyclopent-3-ene-1-carboxamide (103). A solution of bis-nitrile **106** (19 mg, 0.074 mmol, 1 equiv), NaOH (10 mg, 0.25 mmol, 3.4 equiv) in EtOH/H₂O (1:1, 1.0 mL) was heated to 60 °C for 18 h, whereupon the resulting mixture was cooled to ambient temperature and diluted with EtOAc (5 mL). The solution was washed with brine (5 mL), dried over Na₂SO₄, and concentrated under reduced pressure. The crude product was purified by preparatory TLC (50% acetone/hexanes) to give amide **103** as a colorless oil (7.5 mg, 38% yield, 1:11 dr): $[\alpha]_D^{25} +4.4$ (*c* 1.2, CHCl₃); ¹H NMR (400 MHz, CDCl₃) δ 7.47 – 7.38 (m, 5H), 6.65 (dd, *J* = 2.3, 1.1 Hz, 1H), 5.76 (s, 2H), 3.71 (dd, *J* = 17.0, 2.3 Hz, 1H), 3.22 (dd, *J* = 17.0, 1.1 Hz, 1H), 2.44 (s, 3H), 1.58 (s, 3H); ¹³C NMR (101 MHz, CDCl₃) δ 195.4, 165.9, 146.5, 141.9, 129.8, 129.0, 127.4, 124.9, 120.6, 60.5, 59.0, 39.2, 26.9, 21.4; IR (Neat Film, NaCl) 3338, 3201, 3062, 2980, 2929, 2854, 2242, 1732, 1694, 1673, 1604, 1498, 1446, 1371, 1338, 1259, 1102, 1046, 913, 767. 734, 702 cm⁻¹; HRMS (FAB+) *m/z* calc'd for C₁₆H₁₇O₂N₂ [M+H]⁺: 269.1290, found 269.1282. *Please note* that the NMR data listed is for the major diastereomer, though both diastereomers can be seen in the NMR spectra in a 1:11 ratio.

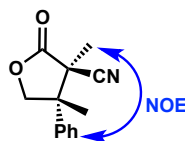
Stereochemical Assignment:



(3R,4S)-3,4-dimethyl-2-oxo-4-phenyltetrahydrofuran-3-carbonitrile (104). A solution of olefin **93** (100.0 mg, 0.48 mmol, 1 equiv) in MeOH (5.0 mL) was cooled to $-78\text{ }^{\circ}\text{C}$. Ozone was bubbled through the reaction mixture for 0.5 h, whereupon the resulting solution was sparged with O_2 and NaBH_4 (0.80 mg, 2.1 mmol, 4.4 equiv) was added. The reaction was then warmed to $0\text{ }^{\circ}\text{C}$ and stirred for 3 h. The reaction mixture was quenched with the addition of 1 M HCl (5 mL) and the aqueous layer was extracted with EtOAc (3 x 20 mL). The combined organic layers were washed with brine (20 mL), dried over Na_2SO_4 , and concentrated under reduced pressure. The crude product was purified by silica gel flash column chromatography (20% acetone/hexanes) to give lactone **104** as a colorless solid (66 mg, 65% yield, 1:2.5 dr): $[\alpha]_{\text{D}}^{25} +21.3$ (c 3.0, CHCl_3); ^1H NMR (400 MHz, CDCl_3) δ 7.47 – 7.33 (m, 3H), 7.26 – 7.23 (m, 2H), 4.78 (dt, $J = 9.1, 0.8$ Hz, 1H), 4.50 (d, $J = 9.1$ Hz, 1H), 1.74 (d, $J = 0.8$ Hz, 3H), 1.33 (s, 3H); ^{13}C NMR (101 MHz,

CDCl_3) δ 171.7, 138.7, 129.6, 128.5, 125.6, 117.7, 74.6, 49.6, 49.0, 27.1, 18.9; IR (Neat Film, NaCl) 2979, 2930, 2355, 2242, 1783, 1498, 1445, 1381, 1279, 1172, 1092, 1012, 764, 699 cm^{-1} ; HRMS (ESI+) m/z calc'd for $\text{C}_{13}\text{H}_{13}\text{NO}_2$ $[\text{M}]^{++}$: 215.0946, found 215.0966. Please note that the NMR data listed is for the major diastereomer.

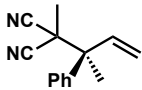
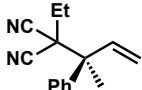
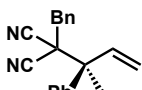
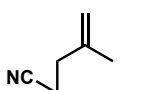
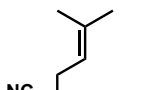
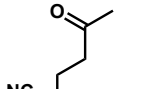
NOE correlation:

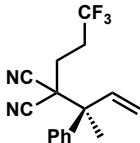
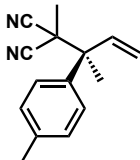
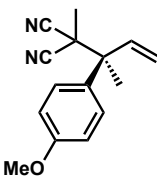
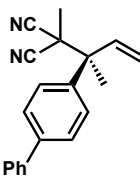
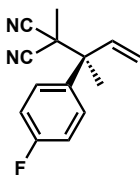
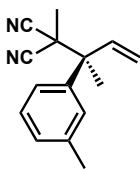
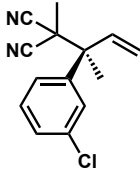


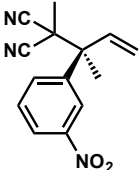
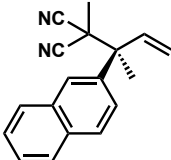
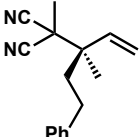
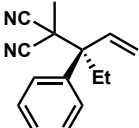
4.6.2.7 Determination of Enantiomeric Excess

Please note racemic products were synthesized using racemic **L5**.

Table 4.5 Determination of enantiomeric excess

Entry	Product	Assay Conditions	Retention time of major isomer (min)	Retention time of minor isomer (min)	%ee
1		SFC Chiralpak OJ–H 3% IPA isocratic, 2.5 mL/min	3.832	4.594	95%
2		SFC Chiralpak OJ–H 3% IPA isocratic, 2.5 mL/min	3.378	4.088	95%
3		SFC Chiralpak OJ–H 3% IPA isocratic, 2.5 mL/min	10.960	11.727	93%
4		SFC Chiralpak OJ–H 3% IPA isocratic, 2.5 mL/min	3.138	3.923	92%
5		SFC Chiralpak OJ–H 3% IPA isocratic, 2.5 mL/min	3.095	4.061	96%
6		SFC Chiralpak OJ–H 3% IPA isocratic, 2.5 mL/min	5.022	7.267	96%

Entry	Product	Assay Conditions	Retention time of major isomer (min)	Retention time of minor isomer (min)	%ee
7		SFC Chiralpak OJ–H 1% IPA isocratic, 3.0 mL/min	1.651	1.868	91%
8		SFC Chiralpak OJ–H 1% IPA isocratic, 3.0 mL/min	3.658	4.375	96%
9		SFC Chiralpak OJ–H 3% IPA isocratic, 2.5 mL/min	5.019	5.890	96%
10		SFC Chiralpak OJ–H 1% IPA isocratic, 2.5 mL/min	43.531	40.798	95%
11		HPLC Chiralpak OJ 3% IPA isocratic, 1 mL/min	22.493	29.003	94%
12		SFC Chiralpak OJ–H 3% IPA isocratic, 2.5 mL/min	2.897	3.290	95%
13		SFC Chiralpak OJ–H 3% IPA isocratic, 2.5 mL/min	3.255	4.955	99%

Entry	Product	Assay Conditions	Retention time of major isomer (min)	Retention time of minor isomer (min)	%ee
14		HPLC Chiralpak AD-H 6% IPA isocratic, 1 mL/min	12.542	11.851	93%
15		SFC Chiralpak OJ-H 4% IPA isocratic, 2.5 mL/min	11.637	13.691	95%
16		SFC Chiralpak OJ-H 0.1% IPA isocratic, 2.5 mL/min	7.621	7.163	84%
17		SFC Chiralpak OJ-H 3% IPA isocratic, 2.5 mL/min	3.270	4.727	96%

4.7 REFERENCES AND NOTES

- (1) For select reviews, see: (a) Douglas, C. J.; Overman, L. E. *Proc. Natl. Acad. Sci. USA* **2004**, *101*, 5363–5367; (b) Das, J. P.; Marek, I. *Chem. Commun.* **2011**, 47, 4593–4623; (c) Quasdorf, K. W.; Overman, L. E. *Nature* **2014**, *516*, 181–191; (d) Corey, E. J.; Guzman-Perez, A. *Angew. Chem. Int. Ed.* **1998**, *37*, 388–401; (e)

- Christoffers, J.; Mann, A. *Angew. Chem. Int. Ed.* **2001**, *40*, 4591–4597; (f) Trost, B. M.; Jiang, C. *Synthesis* **2006**, 369–396; (g) Denissova, I.; Barriault, L. *Tetrahedron* **2003**, *59*, 10105–10146; (h) Ling, T.; Rivas, F. *Tetrahedron* **2016**, *72*, 6729–6777; (i) Liu, Y.; Han, S.-J.; Liu, W.-B.; Stoltz, B. M. *Acc. Chem. Res.* **2015**, *48*, 740–751.
- (2) For select reviews, see: (a) Peterson, E. A.; Overman, L. E. *Proc. Natl. Acad. Sci. USA* **2004**, *101*, 11943–11948; (b) Long, R.; Huang, J.; Gong, J.; Yang, Z. *Nat. Prod. Rep.* **2015**, *32*, 1584–1601.
- (3) For recent examples, see: (a) Uyeda, C.; Rötheli, A. R.; Jacobsen, E. N. *Angew. Chem. Int. Ed.* **2010**, *49*, 9753–9756; (b) Gao, L.; Hwang, G.-S.; Ryu, D. H. *J. Am. Chem. Soc.* **2011**, *133*, 20708–20711; (c) Jolit, A.; Wallester, P. M.; Yap, G. P. A.; Tius, M. A. *Angew. Chem. Int. Ed.* **2014**, *53*, 6180–6183; (d) Ohmatsu, K.; Ando, Y.; Ooi, T. *J. Am. Chem. Soc.* **2013**, *135*, 18706–18709.
- (4) For reports of transition metal-catalyzed methods, excluding allylic alkylation protocols, see: (a) DeAngelis, A.; Dmitrenko, O.; Yap, G. P. A.; Fox, J. M. *J. Am. Chem. Soc.* **2009**, *131*, 7230–7231; (b) Zhang, H.; Hong, L.; Kang, H.; Wang, R. *J. Am. Chem. Soc.* **2013**, *135*, 14098–14101; (c) Cao, Z.-Y.; Wang, X.; Tan, C.; Zhao, X.-L.; Zhou, J.; Ding, K. *J. Am. Chem. Soc.* **2013**, *135*, 8197–8200; (d) Zheng, J.; Lin, L.; Dai, L.; Tang, Q.; Liu, X.; Feng, X. *Angew. Chem. Int. Ed.* **2017**, *56*, 13107–13111.
- (5) For reports of enantioselective transition metal-catalyzed allylic alkylation, see: (a) Trost, B. M.; Malhotra, S.; Chan, W. H. *J. Am. Chem. Soc.* **2011**, *133*, 7328–7331; (b) Trost, B. M.; Chan, W. H.; Malhotra, S. *Chem. Eur. J.* **2017**, *23*, 4405–4414; (c)

- Ohmatsu, K.; Imagawa, N.; Ooi, T. *Nat. Chem.* **2014**, *6*, 47–51; (d) Khan, A.; Yang, L.; Xu, J.; Jin, L. Y.; Zhang, Y. J. *Angew. Chem. Int. Ed.* **2014**, *53*, 11257–11260.
- (6) For select reports of the preparation of vicinal all-carbon quaternary centers but not stereocenters, see: (a) Ramachary, D. B.; Reddy, P. S.; Shruthi, K. S.; Madhavachary, R.; Reddy, P. V. G. *Eur. J. Org. Chem.* **2016**, 5220–5226; (b) Trost, B. M.; Cramer, N.; Silverman, S. M. *J. Am. Chem. Soc.* **2007**, *129*, 12396–12397.
- (7) For reports of *enantiospecific* transition metal-catalyzed allylic alkylation, see: (a) Kawatsura, M.; Sato, M.; Tsuji, H.; Ata, F.; Itoh, T. *J. Org. Chem.* **2011**, *76*, 5485–5488; (b) Huang, X.; Wu, S.; Wu, W.; Li, P.; Fu, C.; Ma, S. *Nat. Commun.* **2016** doi: 10.1038/ncomms12382.
- (8) For reports of enantio- and diastereoselective preparation of vicinal all-carbon quaternary stereocenters via *two sequential allylic alkylations*, see: (a) Ghosh, S.; Bhunia, S.; Kakde, B. N.; De, S.; Bisai, A. *Chem. Commun.* **2014**, *50*, 2434–2437; (b) Trost, B. M.; Osipov, M. *Angew. Chem. Int. Ed.* **2013**, *52*, 9176–9181.
- (9) Shockley, S. E.; Hethcox, J. C.; Stoltz, B. M. *Angew. Chem. Int. Ed.* **2017**, *56*, 11545–11548.
- (10) For a recent review, see: Hethcox, J. C.; Shockley, S. E.; Stoltz, B. M. *ACS Catal.* **2016**, *6*, 6207–6213.
- (11) *Diastereoselective* reverse prenylation of indoles via iridium-catalyzed allylic alkylation has been reported, see: (a) Ruchti, J.; Carreira, E. M. *J. Am. Chem. Soc.* **2014**, *136*, 16756–16759; (b) Müller, J. M.; Stark, C. B. W. *Angew. Chem. Int. Ed.* **2016**, *55*, 4798–4802.

- (12) For select examples, see: (a) Kanayama, T.; Yoshida, K.; Miyabe, H.; Takemoto, Y. *Angew. Chem. Int. Ed.* **2003**, *42*, 2054–2056; (b) Jiang, X.; Chen, W.; Hartwig, J. F. *Angew. Chem. Int. Ed.* **2016**, *55*, 5819–5823; (c) Huo, X.; He, R.; Zhang, X.; Zhang, W. *J. Am. Chem. Soc.* **2016**, *138*, 11093–11096; (d) Chen, W.; Hartwig, J. F. *J. Am. Chem. Soc.* **2013**, *135*, 2068–2071; (e) Chen, W.; Hartwig, J. F. *J. Am. Chem. Soc.* **2014**, *136*, 377–382; (f) Krautwald, S.; Schafroth, M. A.; Sarlah, D.; Carreira, E. M. *J. Am. Chem. Soc.* **2014**, *136*, 3020–3023; (g) Sandmeier, T.; Krautwald, S.; Zipfel, Carreira, E. M. *Angew. Chem. Int. Ed.* **2015**, *54*, 14363–14367; (h) Liu, W.-B.; Reeves, C. M.; Virgil, S. C.; Stoltz, B. M. *J. Am. Chem. Soc.* **2013**, *135*, 10626–10629; (i) Hethcox, J. C.; Shockley, S. E.; Stoltz, B. M. *Angew. Chem. Int. Ed.* **2016**, *55*, 16092–16095.
- (13) DABCO has been previously utilized in iridium-catalyzed allylic alkylation leading to higher yields but slower rates of reaction, see: Bondzic, B. P.; Farwick, A.; Liebich, J.; Eilbracht, P. *Org. Biomol. Chem.* **2008**, *6*, 3723–3731.
- (14) Previous reports have hypothesized that facile equilibration between diastereomers of the iridium π -allyl complex leads to higher selectivities, see: (a) Bartels, B.; Helmchen, G. *Chem. Commun.* **1999**, 741–742; (b) Alexakis, A.; Polet, D. *Org. Lett.* **2004**, *6*, 3529–3532; (c) Polet, D.; Alexakis, A.; Tissot-Croset, K.; Corminboeuf, C.; Ditrich, K. *Chem. Eur. J.* **2006**, *12*, 3596–3609; (d) ref. 12h.
- (15) Schurig, V. *Inorg. Chem.* **1986**, *25*, 945–949.
- (16) Willand-Charnley, R.; Fisher, T. J.; Johnson, B. M.; Dussault, P. H. *Org. Lett.* **2012**, *14*, 2242–2245.

- (17) (a) Hu, X.; Xu, S.; Maimone, T. J. *Angew. Chem. Int. Ed.* **2017**, *56*, 1624–1628; (b) Brown, B.; Hegedus, L. S. *J. Org. Chem.* **2000**, *65*, 1865–1872; (c) Suzuki, M.; Yanagisawa, A.; Noyori, R. *J. Am. Chem. Soc.* **1988**, *110*, 4718–4726; (d) Schnermann, M. J.; Overman, L. E. *Angew. Chem. Int. Ed.* **2012**, *51*, 9576–9580.
- (18) Hamilton, J. Y.; Sarlah, D.; Carreira, E. M. *Org. Synth.* **2015**, *92*, 1–12.
- (19) Ghorai, M. K.; Talukdar, R.; Tiwari, D. P. *Org. Lett.* **2014**, *16*, 2204–2207.
- (20) Matsubara, R.; Jamison, T. F. *J. Am. Chem. Soc.* **2010**, *132*, 6880–6881.
- (21) Díez-Barra, E.; de la Hoz, A.; Moreno, A.; Sánchez-Verdú, P. *J. Chem. Soc., Perkin Trans. 1* **1991**, *0*, 2589–2592.
- (22) Gao, C.; Tao, X.; Qian, Y.; Huang, J. *Synlett* **2003**, *11*, 1716–1718.
- (23) Fernández-Mateos, A.; Teijón, P. H.; Burón, L. M.; Clemente, R. R.; González, R. *J. Org. Chem.* **2007**, *72*, 9973–9982.
- (24) Benati, L.; Bencivenni, G.; Leardini, R.; Minozzi, M.; Nanni, D.; Scialpi, R.; Spagnolo, P.; Zanardi, G.; Rizzoli, C. *Org. Lett.* **2004**, *6*, 417–420.
- (25) Paganelli, S.; Sehionato, A.; Botteghi, C. *Tetrahedron Lett.* **1991**, *32*, 2807–2810.
- (26) Okada, S.; Oohira, D.; Otaka, K. Patent WO2004020399 (A1), March 11, 2004.
- (27) Guzman-Martinez, A.; Hoveyda, A. H. *J. Am. Chem. Soc.* **2010**, *132*, 10634–10637.
- (28) Ghosh, S.; Chaudhuri, S.; Bisai, A. *Org. Lett.* **2015**, *17*, 1373–1376.
- (29) Sharma, S.; Kumar, S.; Shil, A. K.; Guha, N. R.; Bandna; Das, P. *Tetrahedron Lett.* **2012**, *53*, 7044–7051.

- (30) (a) Franke, A.; Mattern, G.; Traber, W. *Helv. Chim. Acta* **1975**, *58*, 268–278; (b) Rossi, D.; Baraglia, A. C.; Serra, M.; Azzolina, O.; Collina, S. *Molecules* **2010**, *15*, 5928–5942.
- (31) Zhang, T.; Jiang, J.; Yao, L.; Geng, H.; Zhang, X. *Chem. Commun.* **2017**, *53*, 9258–9261.

APPENDIX 6

Spectra Relevant to Chapter 4:

Enantioselective Synthesis of Vicinal All-Carbon Quaternary Centers

via Iridium-Catalyzed Allylic Alkylation

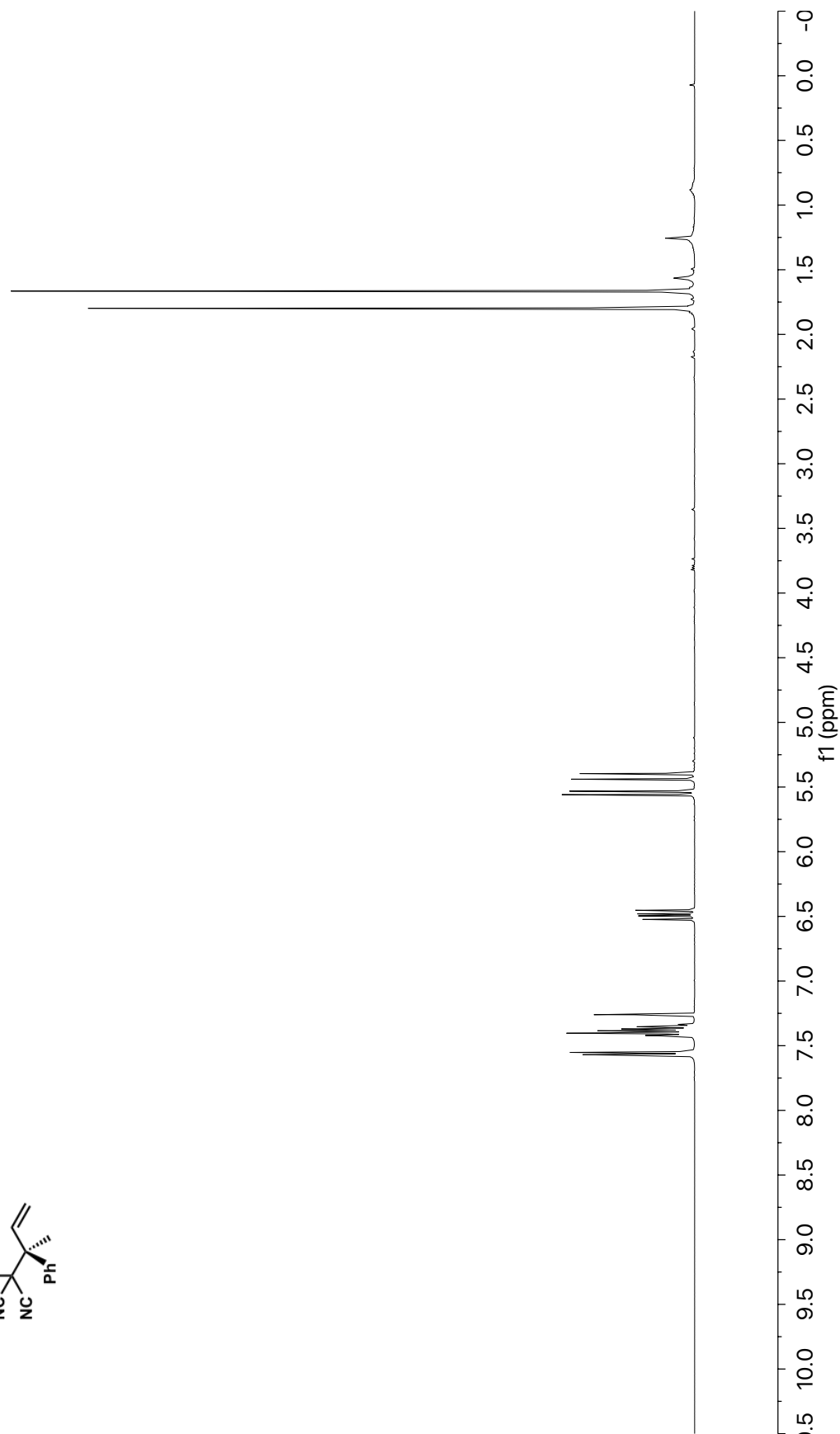
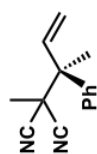


Figure A6.1 ^1H NMR (400 MHz, CDCl_3) of compound **93**

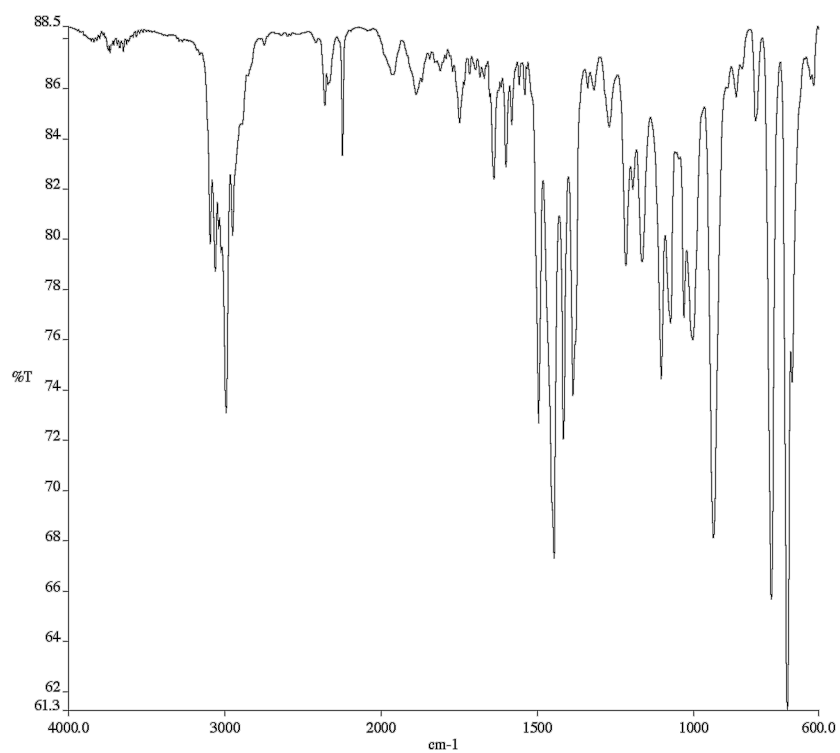


Figure A6.2 Infrared spectrum (Thin Film, NaCl) of compound **93**

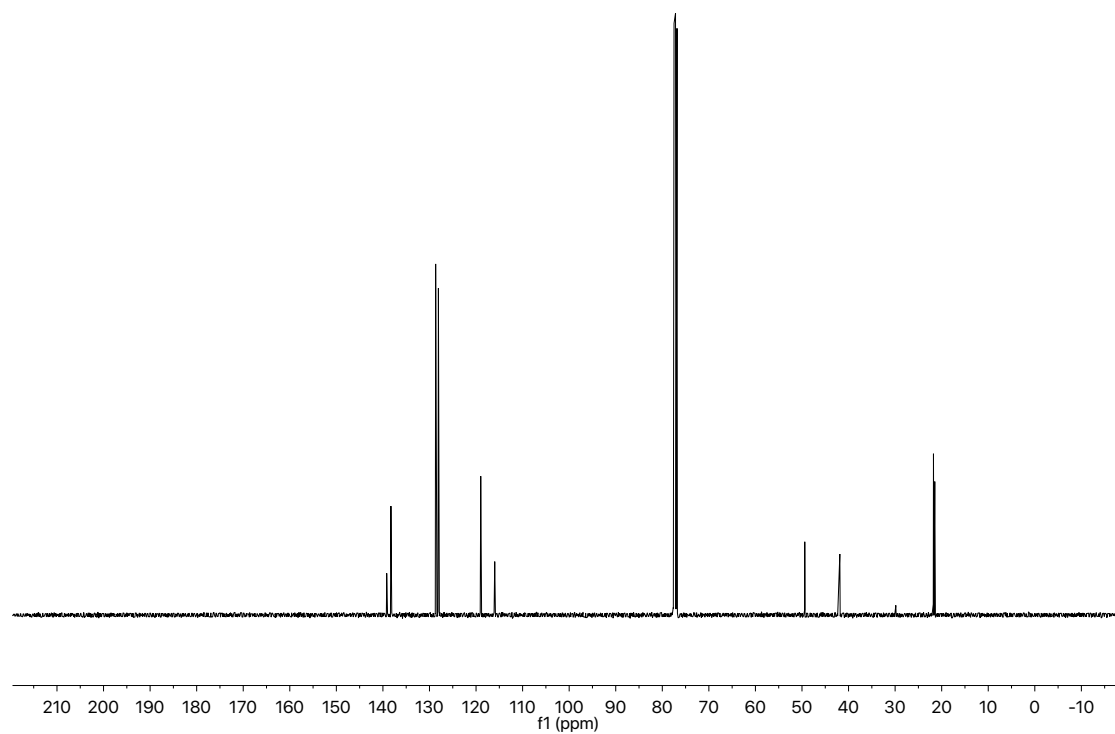


Figure A6.3 ¹³C NMR (101 MHz, CDCl₃) of compound **93**

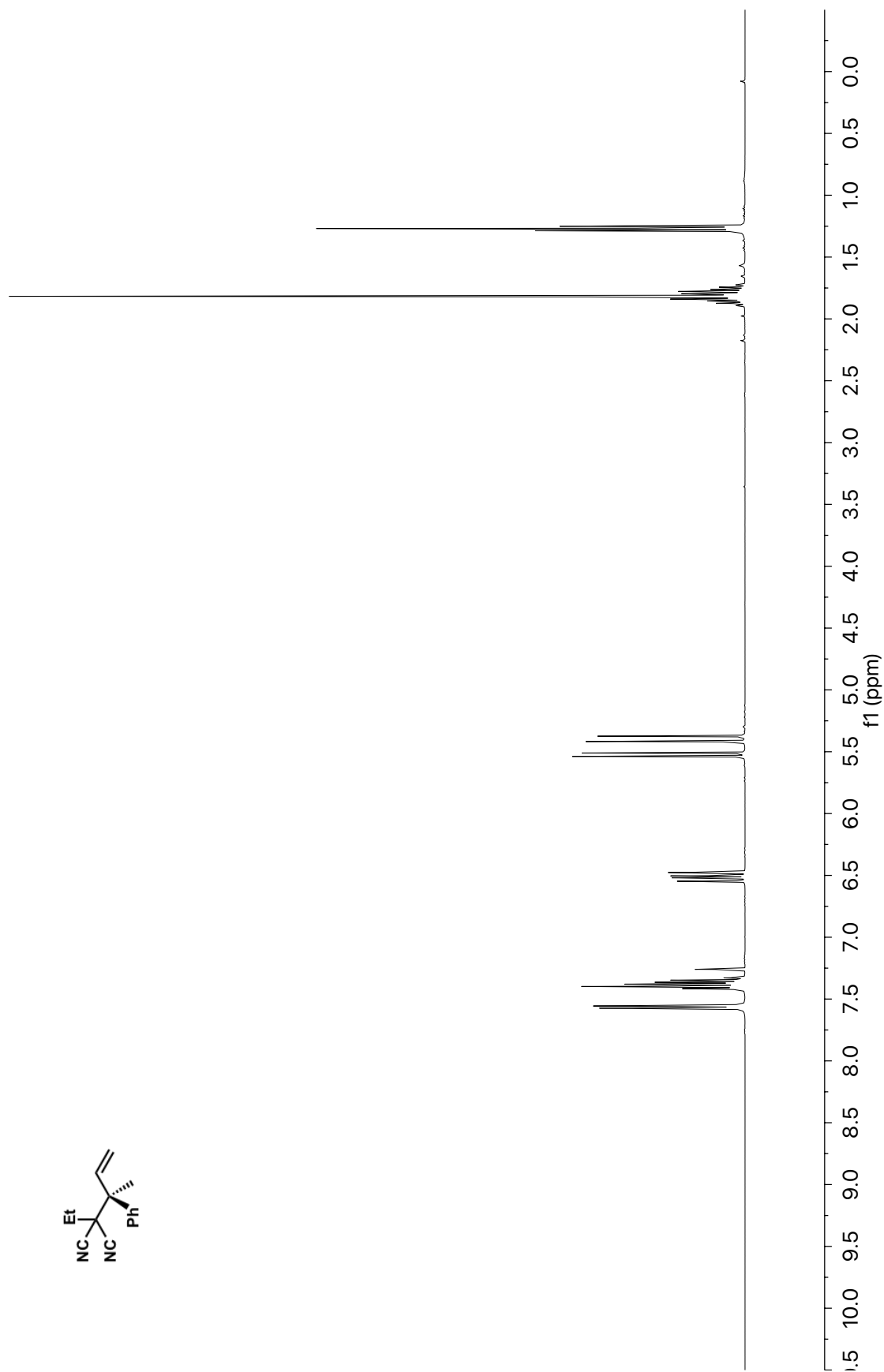


Figure A6.4 ¹H NMR (400 MHz, CDCl₃) of compound 95a

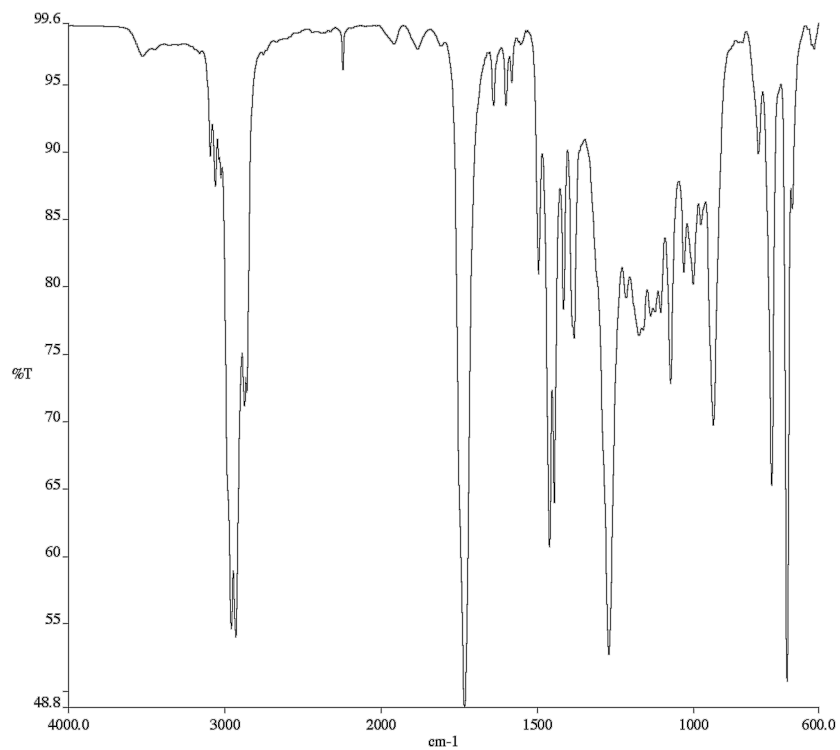


Figure A6.5 Infrared spectrum (Thin Film, NaCl) of compound **95a**

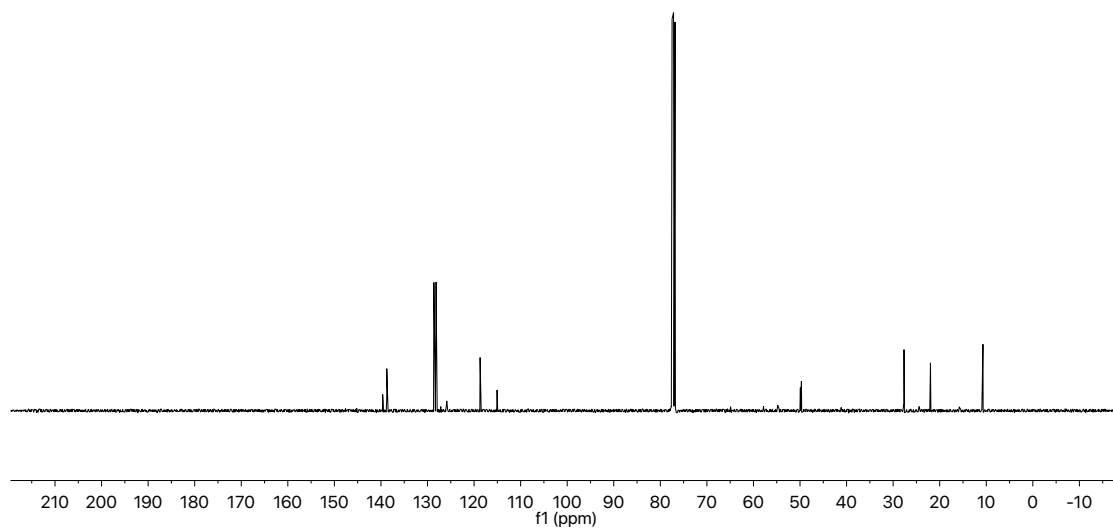


Figure A6.6 ¹³C NMR (101 MHz, CDCl₃) of compound **95a**

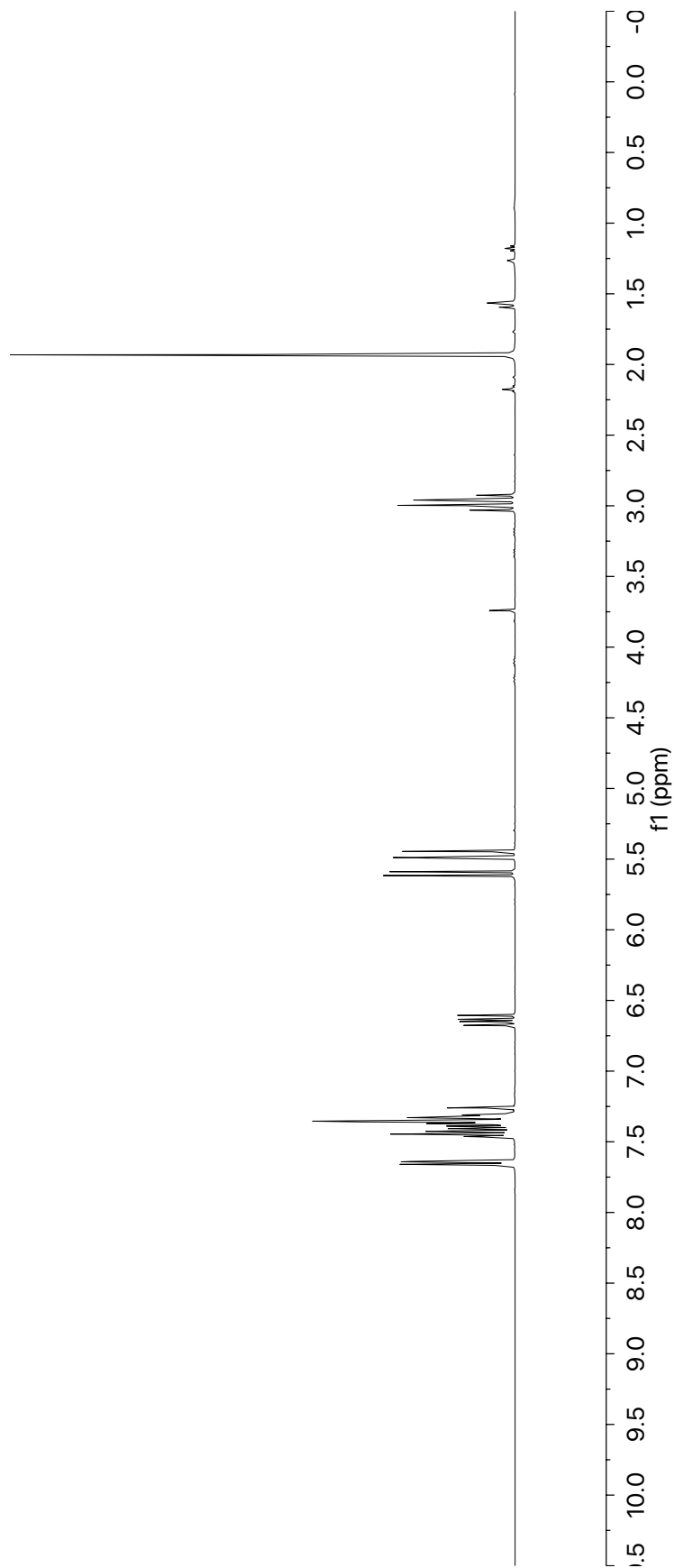
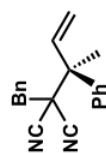


Figure A6.7 ^1H NMR (400 MHz, CDCl_3) of compound **95b**

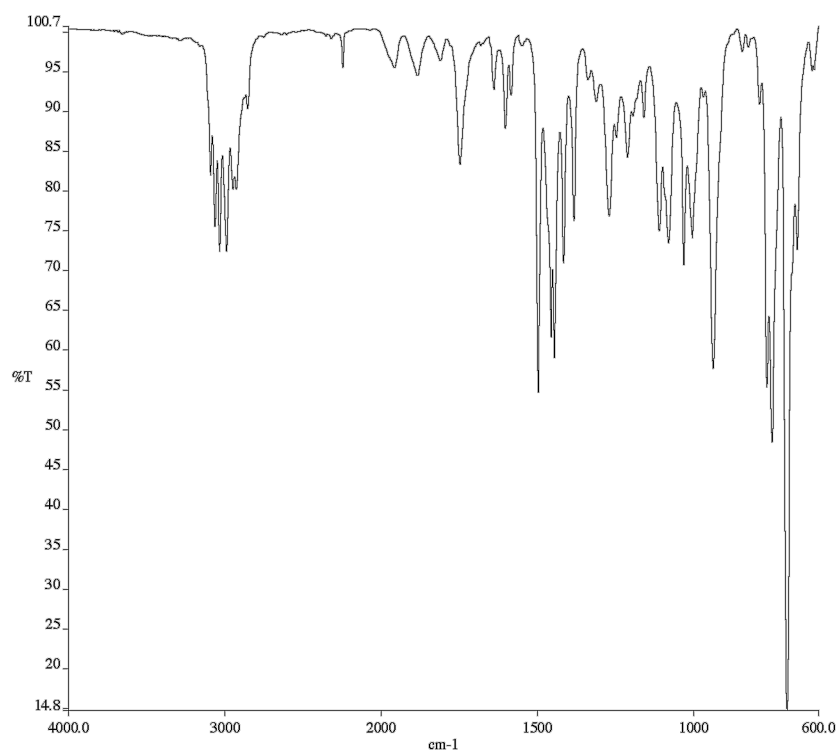


Figure A6.8 Infrared spectrum (Thin Film, NaCl) of compound **95b**

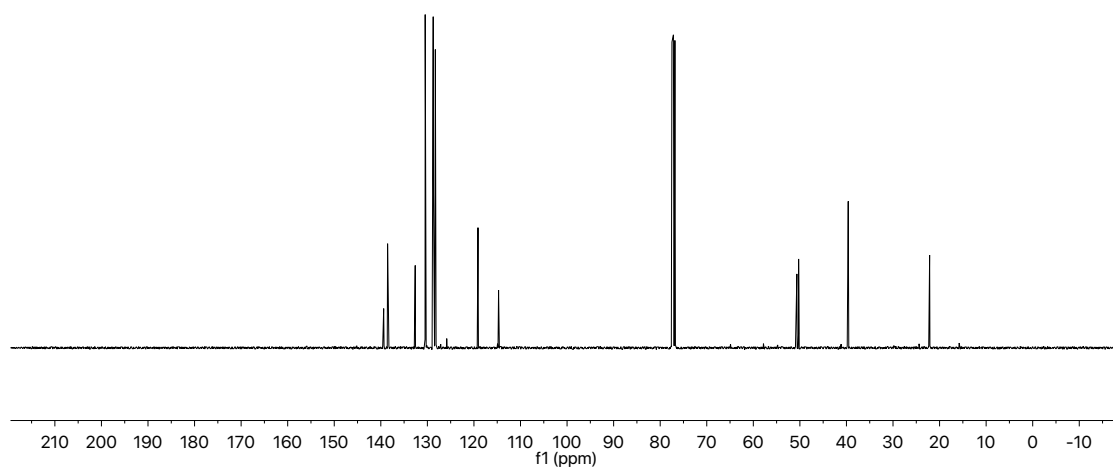


Figure A6.9 ¹³C NMR (101 MHz, CDCl₃) of compound **95b**



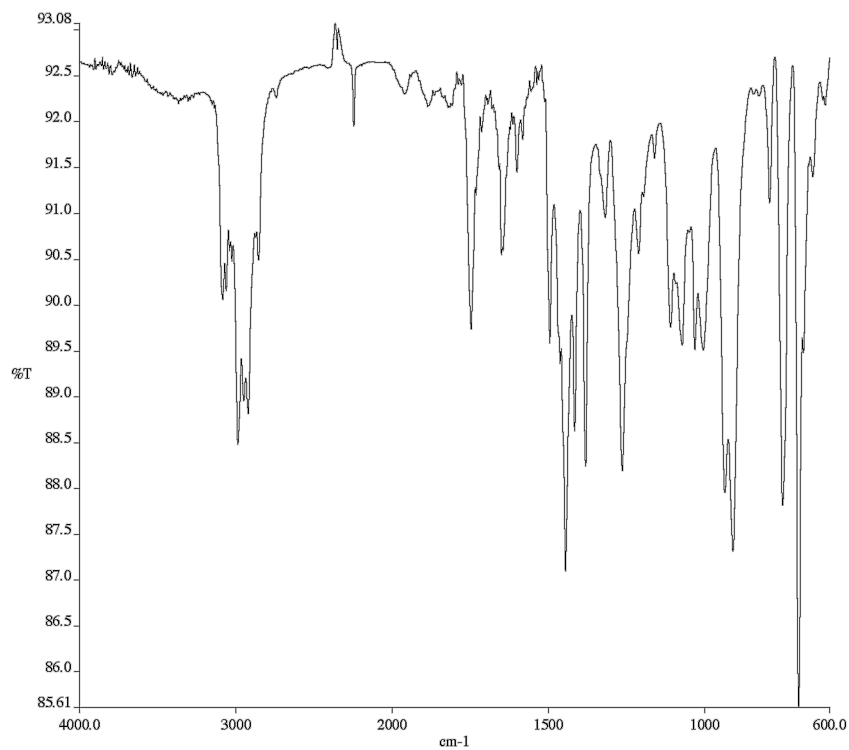


Figure A6.11 Infrared spectrum (Thin Film, NaCl) of compound **95d**

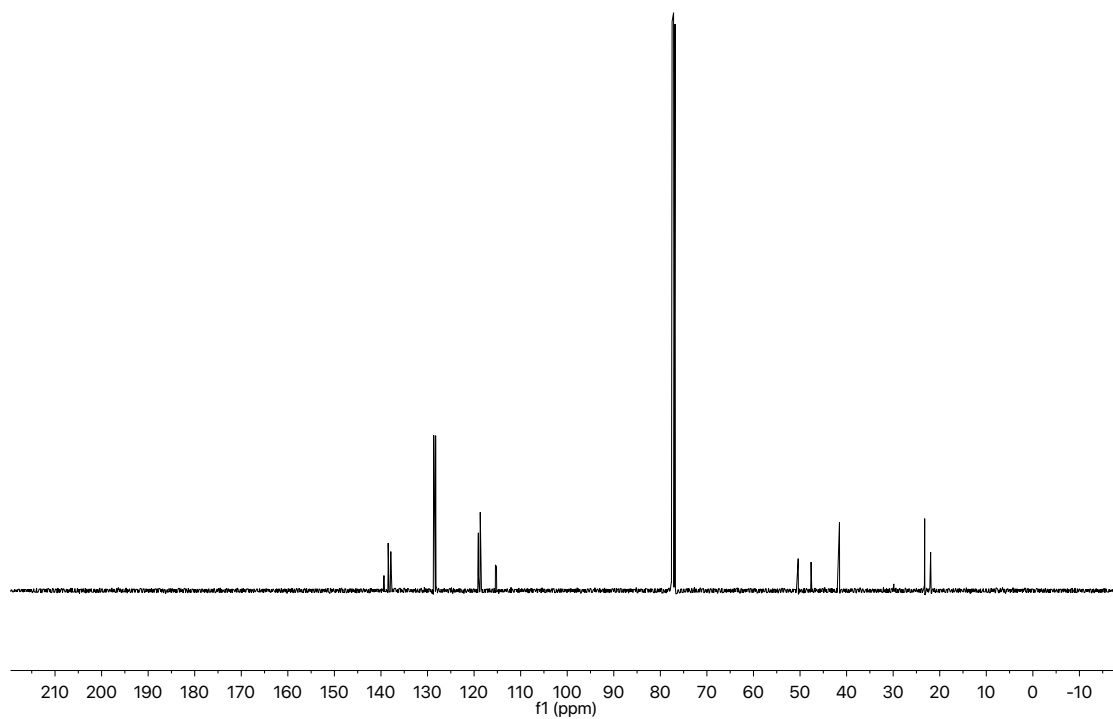


Figure A6.12 ¹³C NMR (101 MHz, CDCl₃) of compound **95d**

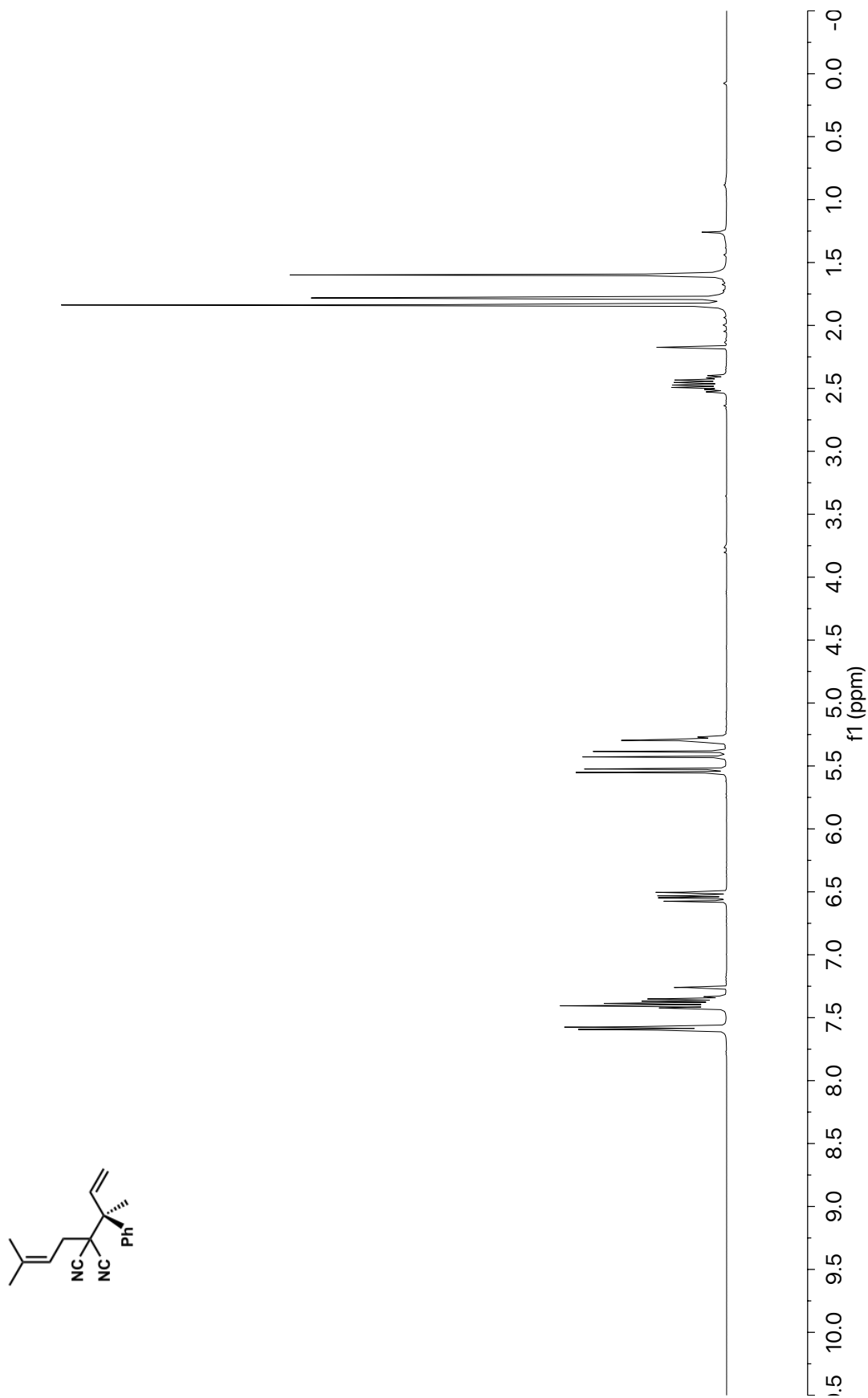


Figure A6.13 ¹H NMR (400 MHz, CDCl₃) of compound **95e**

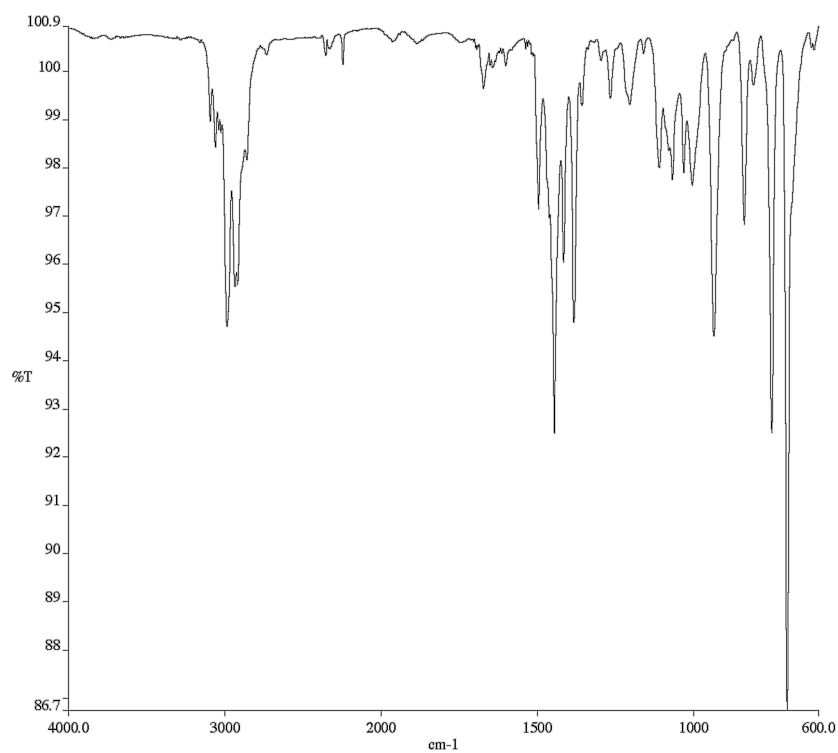


Figure A6.14 Infrared spectrum (Thin Film, NaCl) of compound **95e**

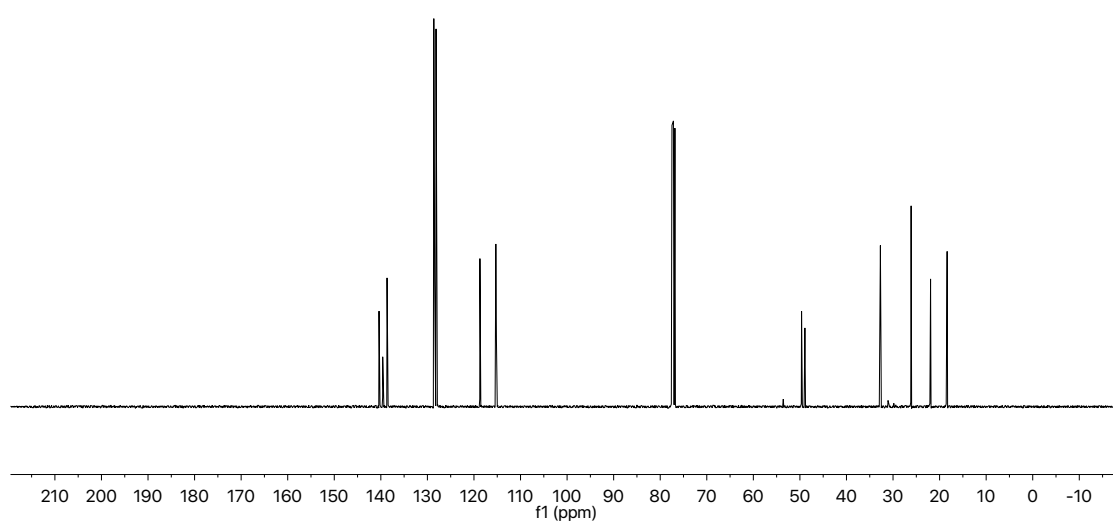


Figure A6.15 ¹³C NMR (101 MHz, CDCl₃) of compound **95e**

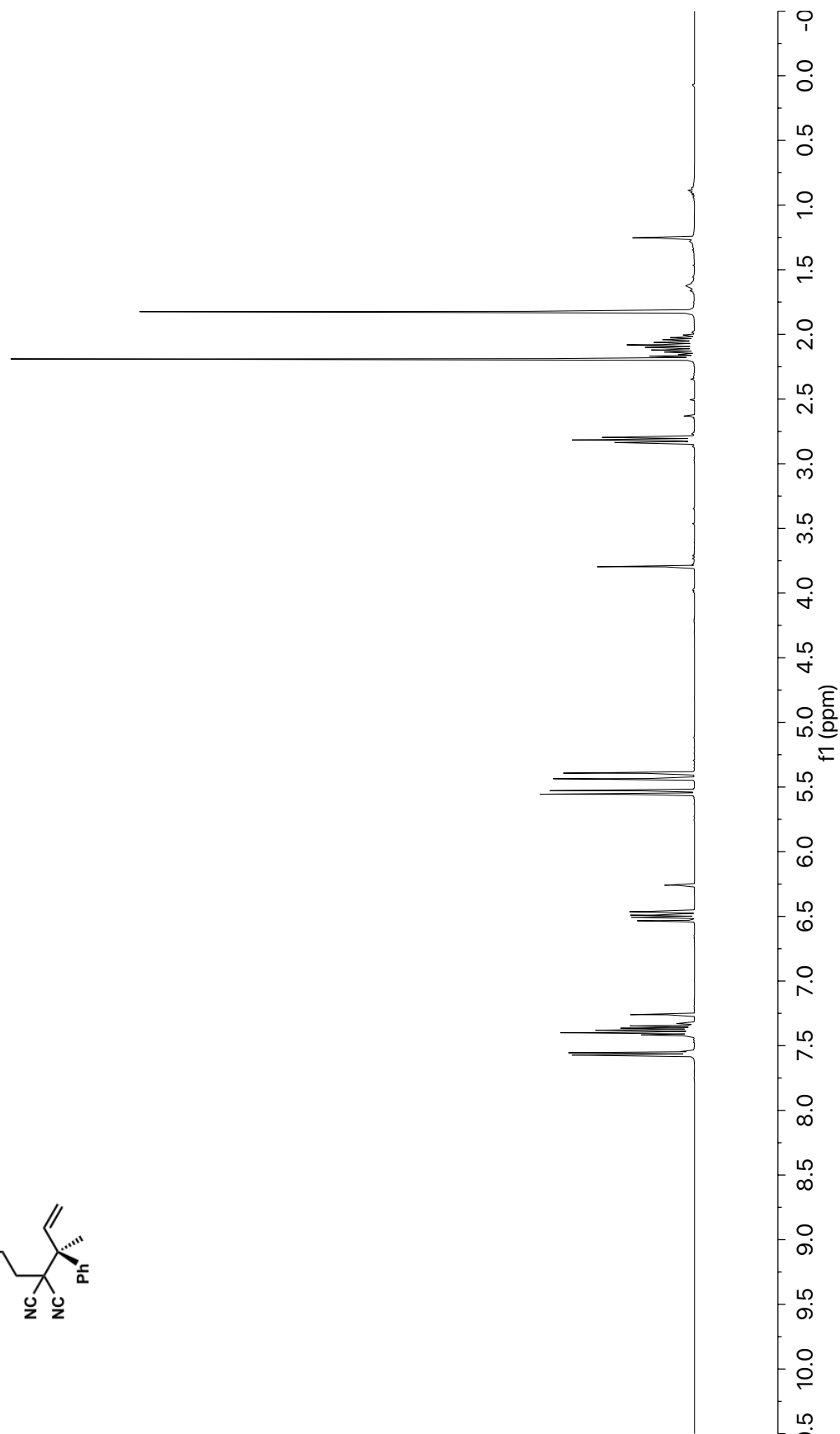
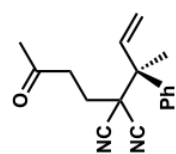


Figure A6.16 ^1H NMR (400 MHz, CDCl_3) of compound **95f**

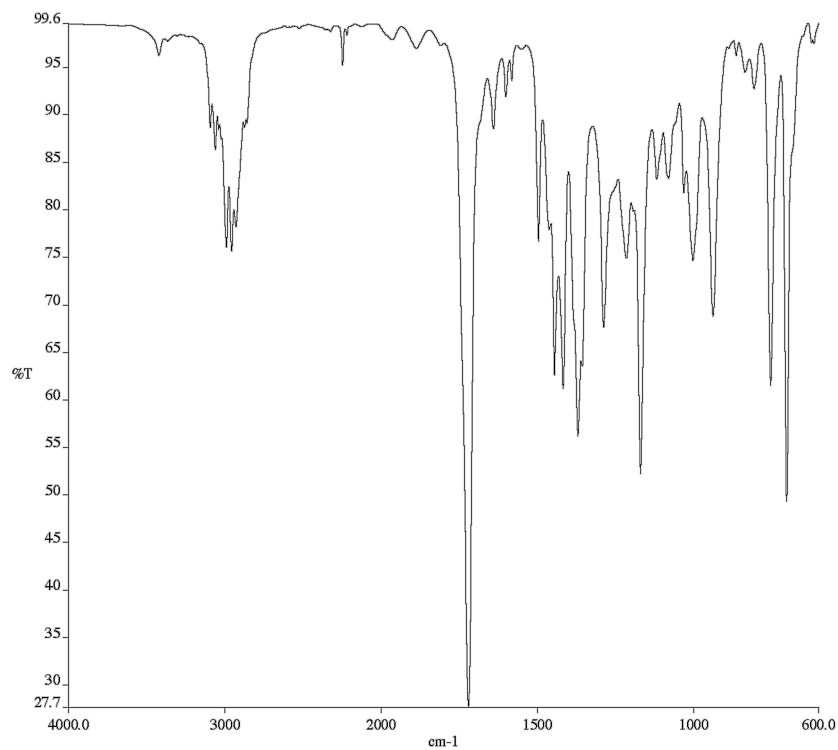


Figure A6.17 Infrared spectrum (Thin Film, NaCl) of compound **95f**

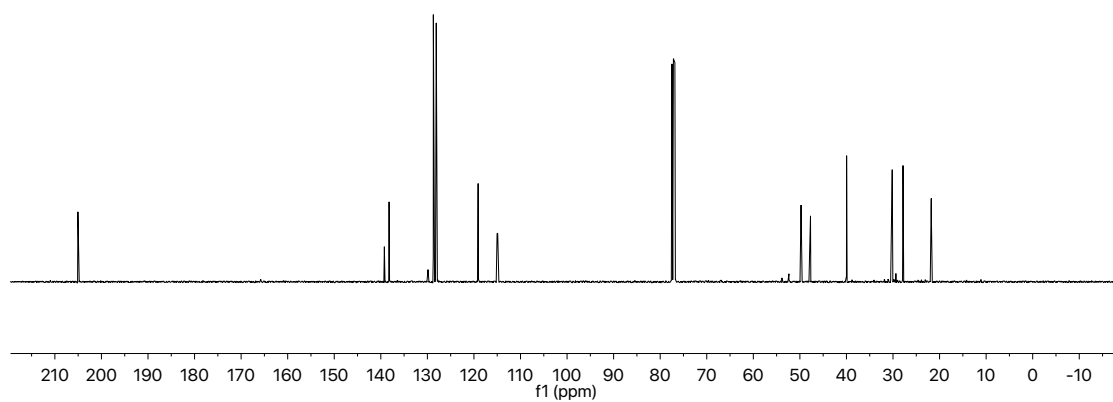


Figure A6.18 ¹³C NMR (101 MHz, CDCl₃) of compound **95f**

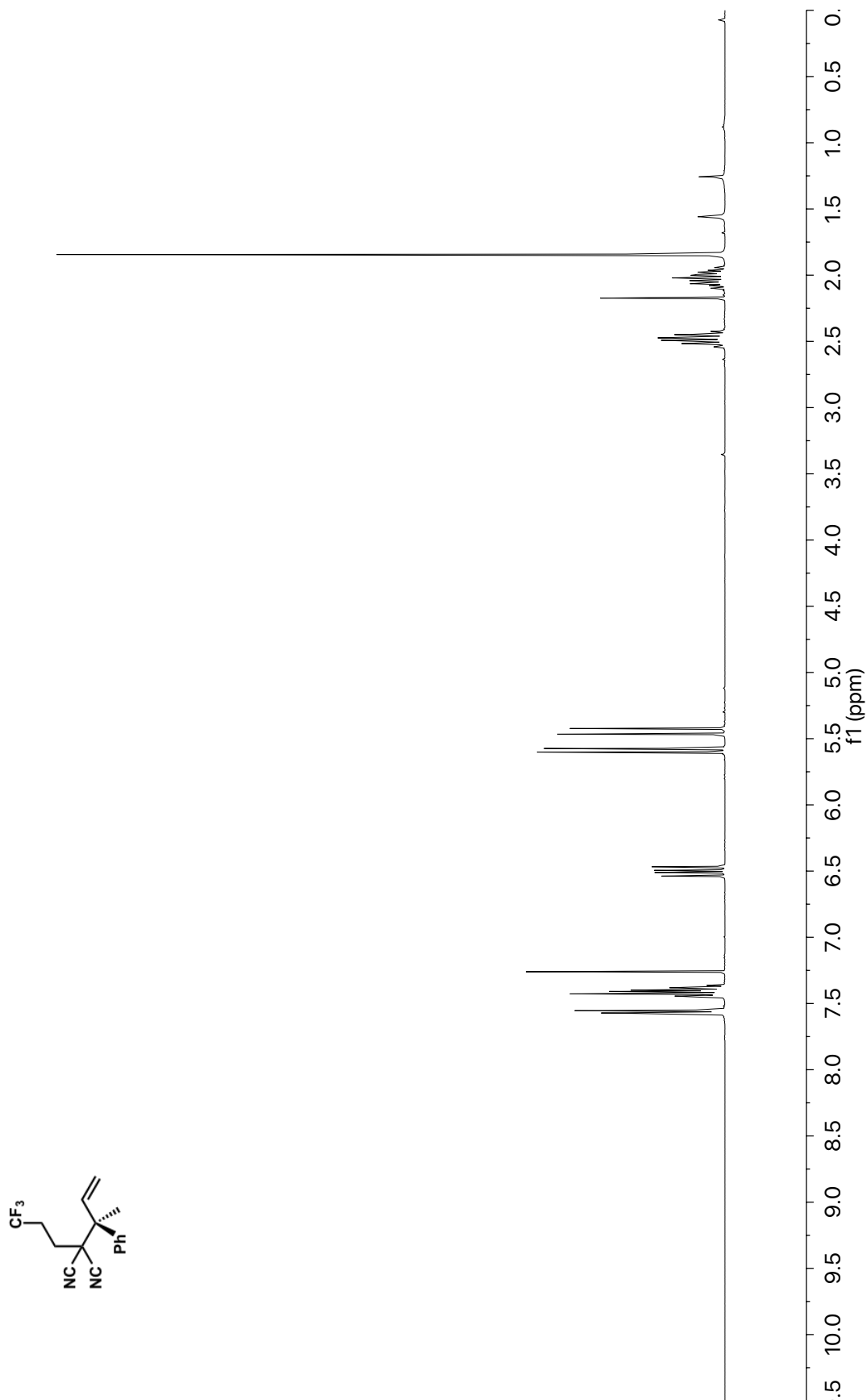


Figure A6.19 ¹H NMR (400 MHz, CDCl₃) of compound **95g**

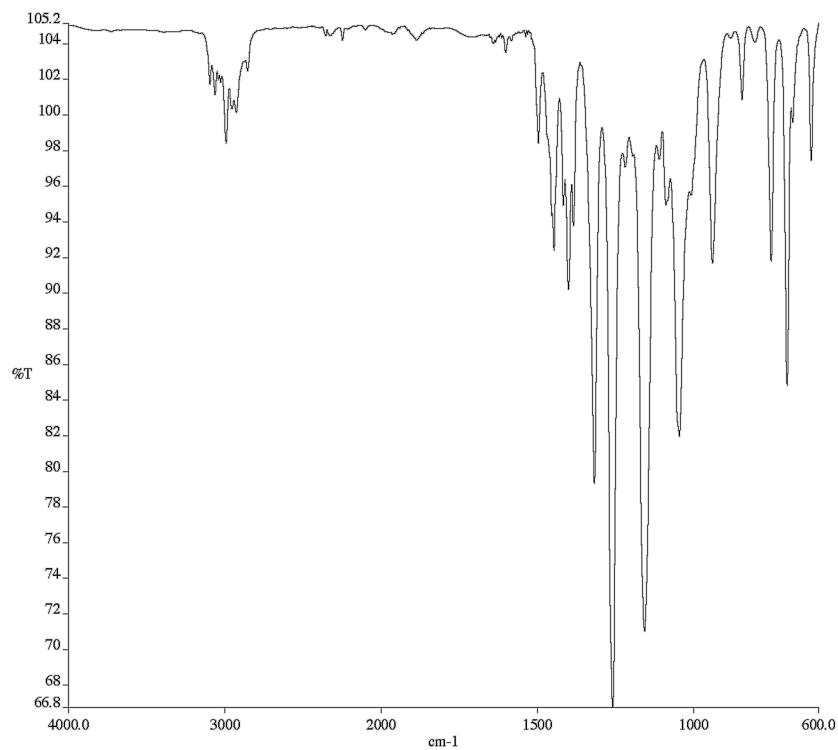


Figure A6.20 Infrared spectrum (Thin Film, NaCl) of compound **95g**

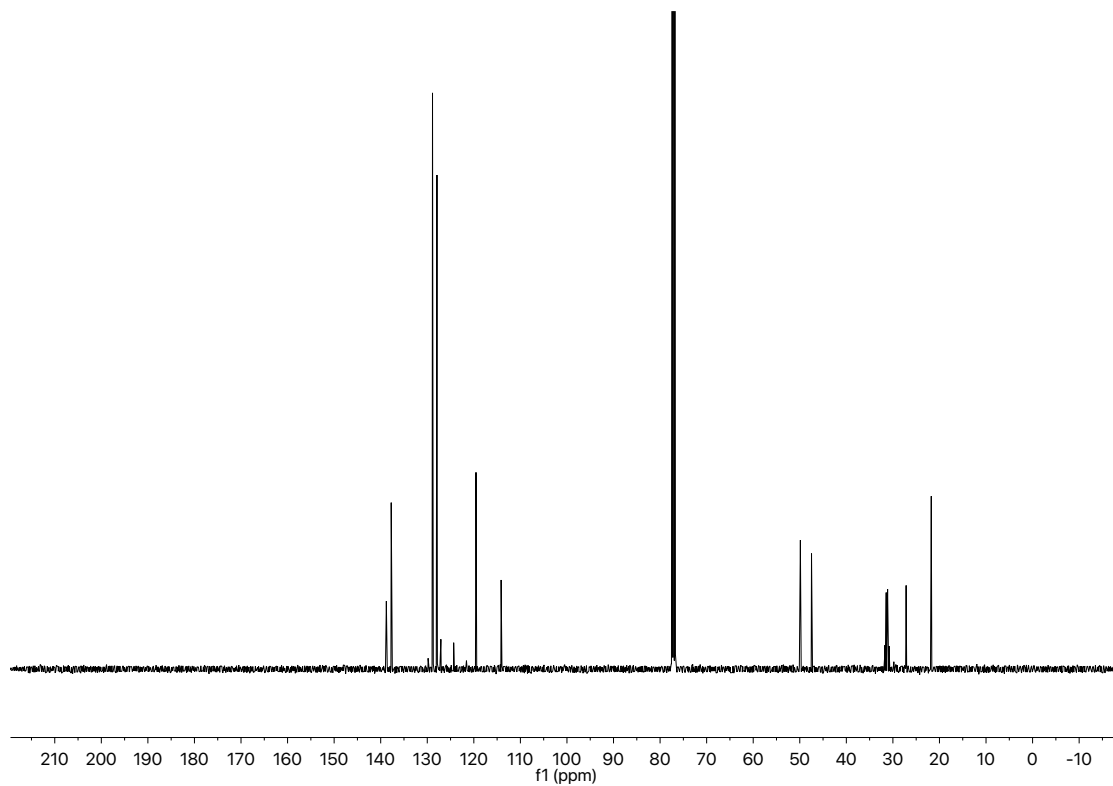


Figure A6.21 ¹³C NMR (101 MHz, CDCl₃) of compound **95g**

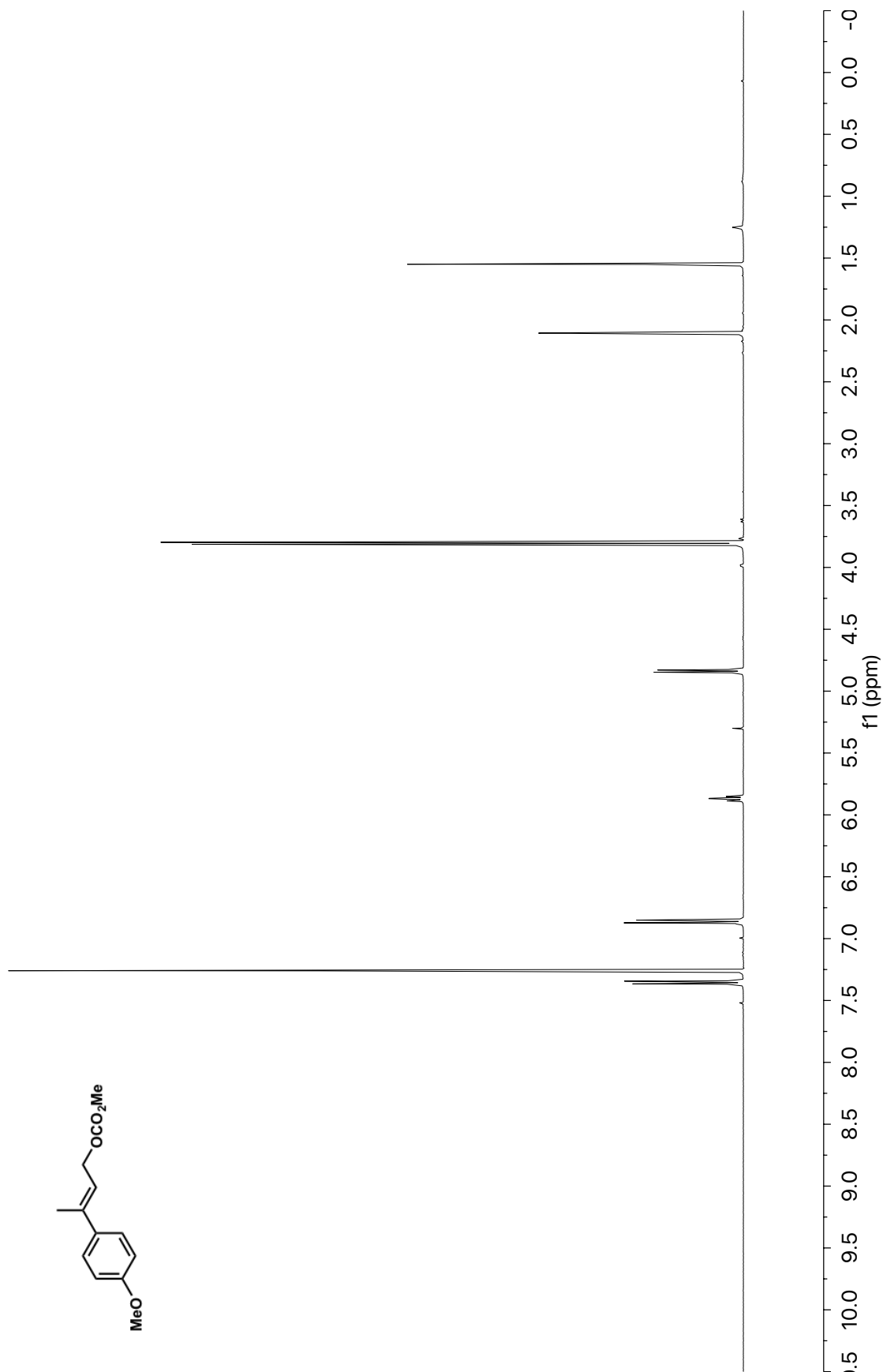


Figure A6.22 ¹H NMR (400 MHz, CDCl₃) of compound **96b**

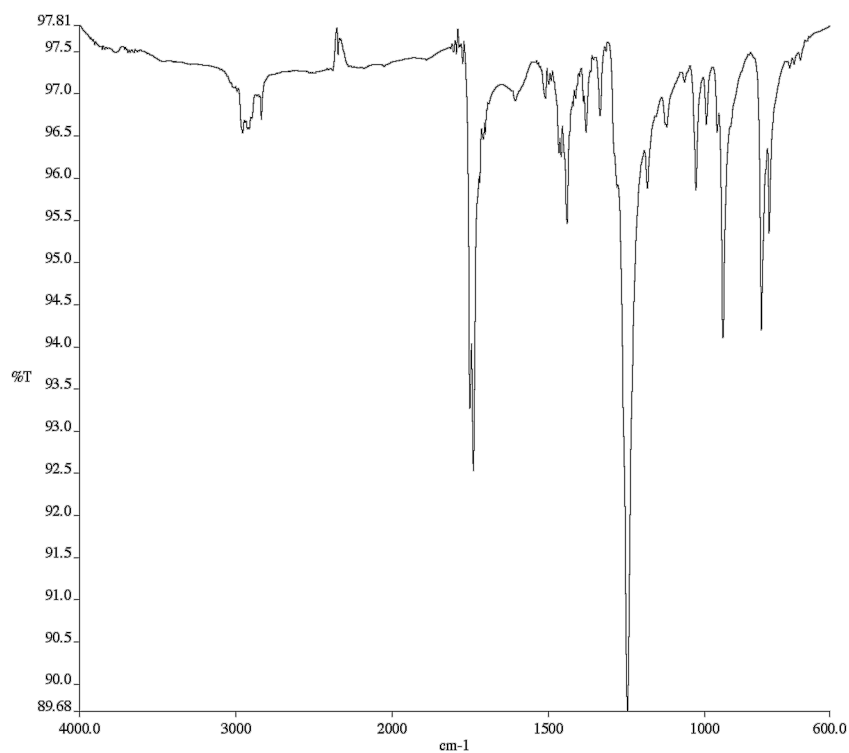


Figure A6.23 Infrared spectrum (Thin Film, NaCl) of compound **96b**

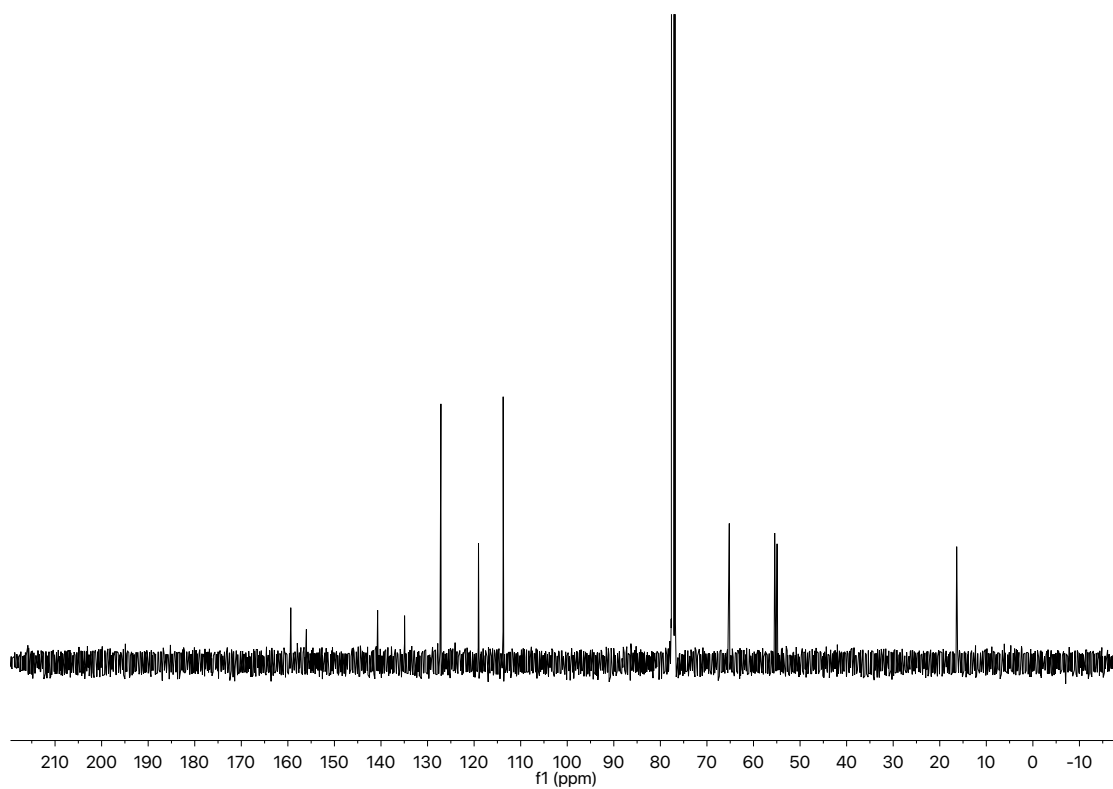


Figure A6.24 ¹³C NMR (101 MHz, CDCl₃) of compound **96b**

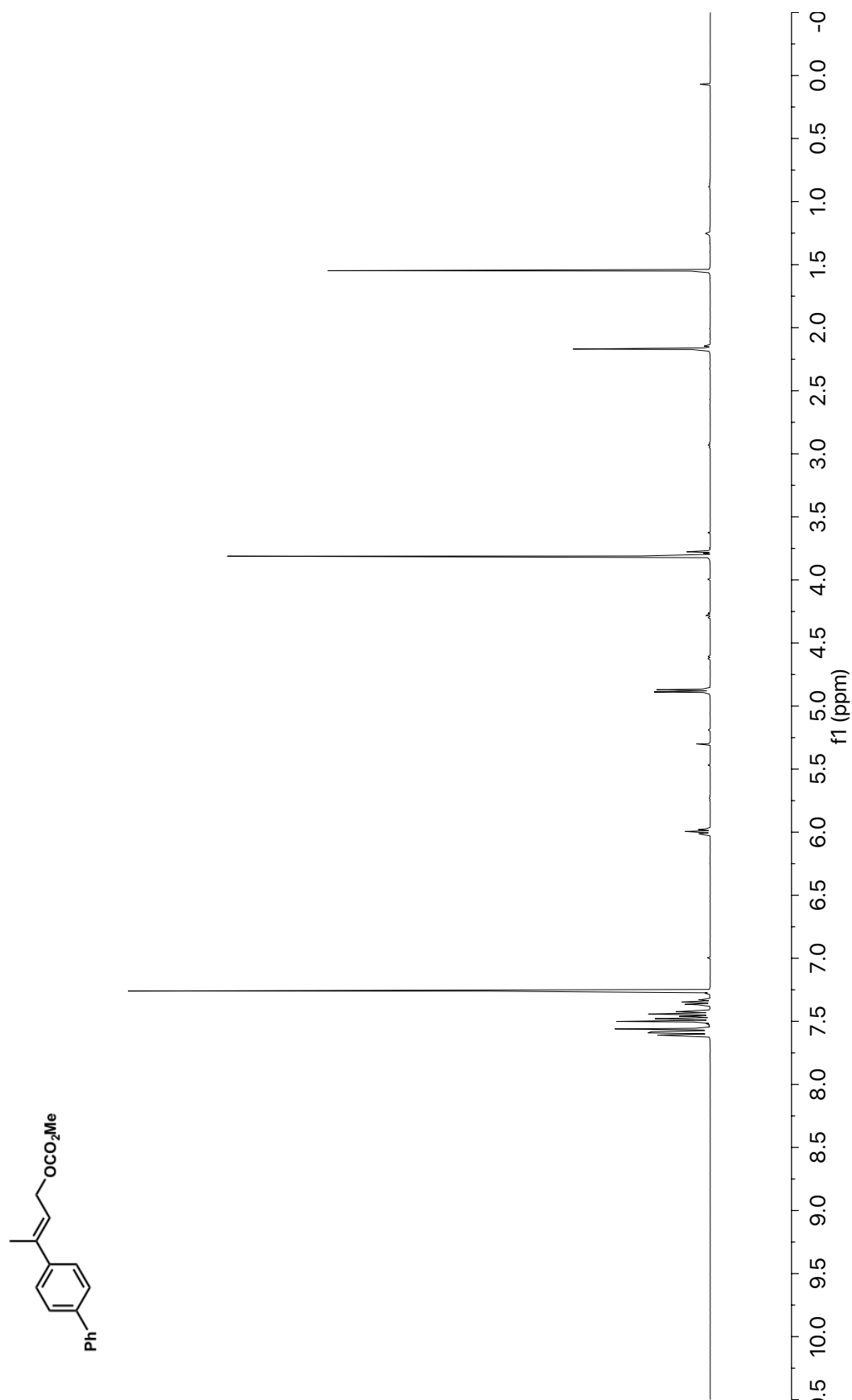


Figure A6.25 ^1H NMR (400 MHz, CDCl_3) of compound **96c**

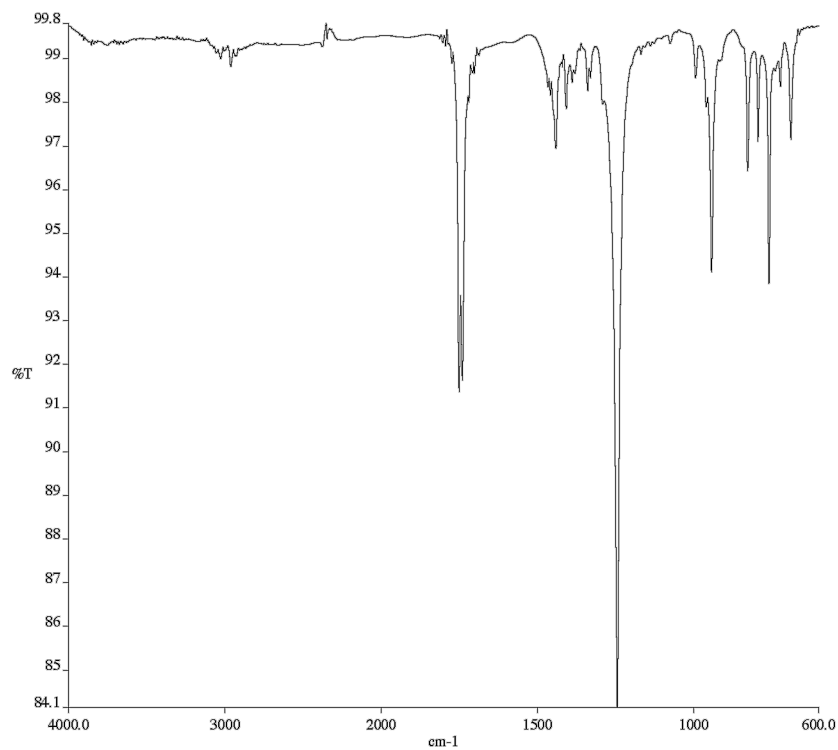


Figure A6.26 Infrared spectrum (Thin Film, NaCl) of compound **96c**

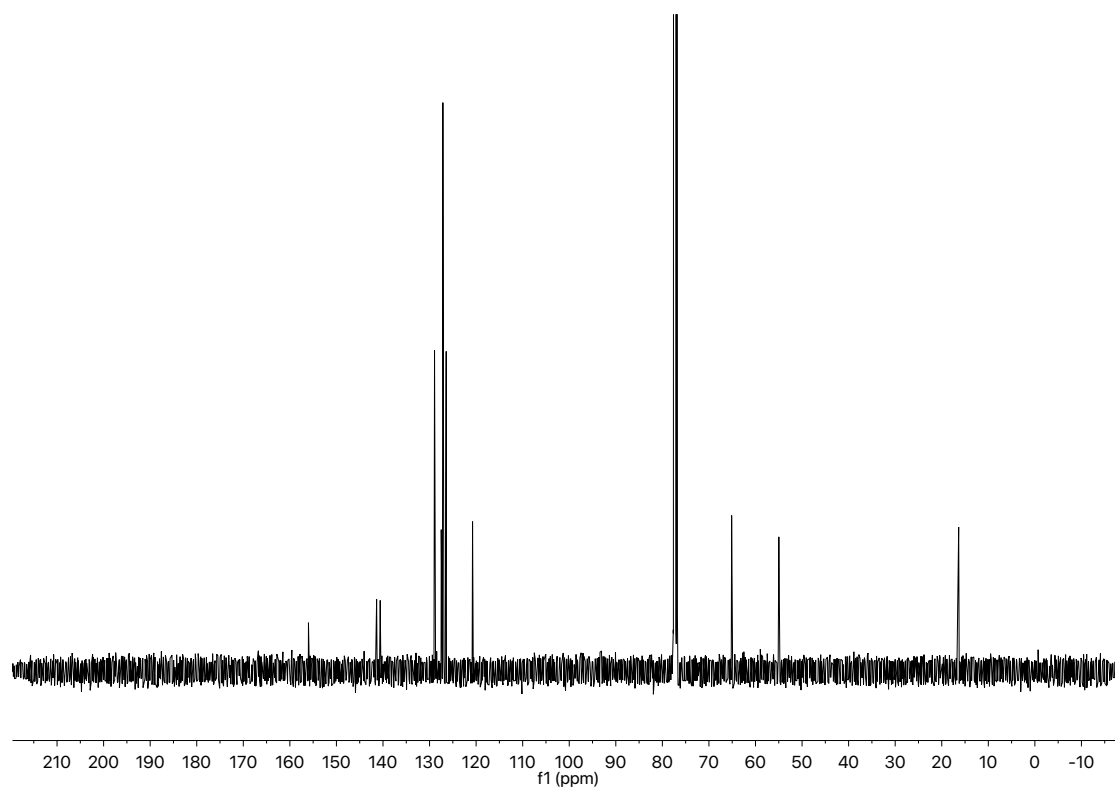


Figure A6.27 ¹³C NMR (101 MHz, CDCl₃) of compound **96c**

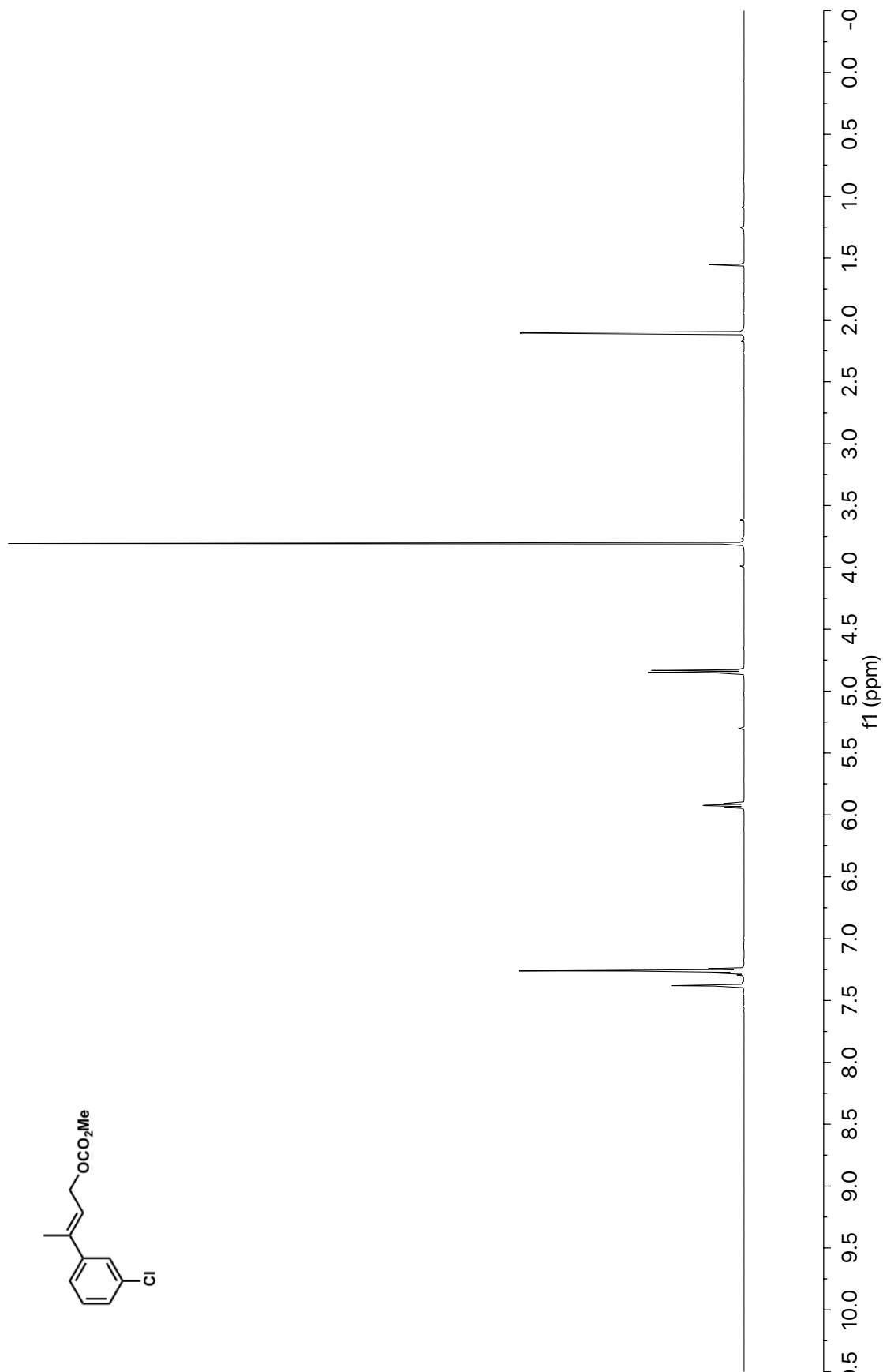


Figure A6.28 ¹H NMR (400 MHz, CDCl₃) of compound **96f**

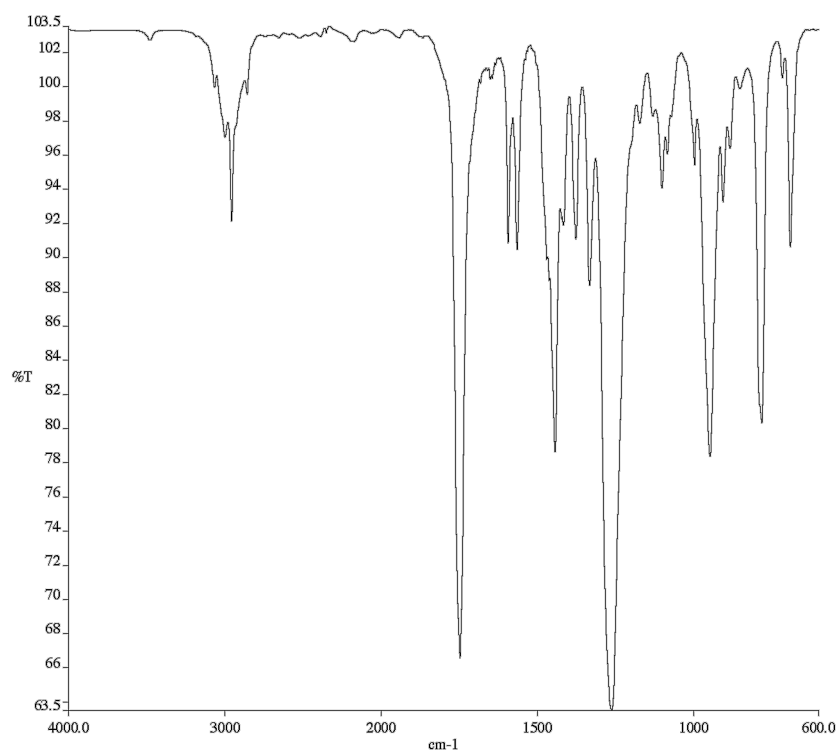


Figure A6.29 Infrared spectrum (Thin Film, NaCl) of compound **96f**

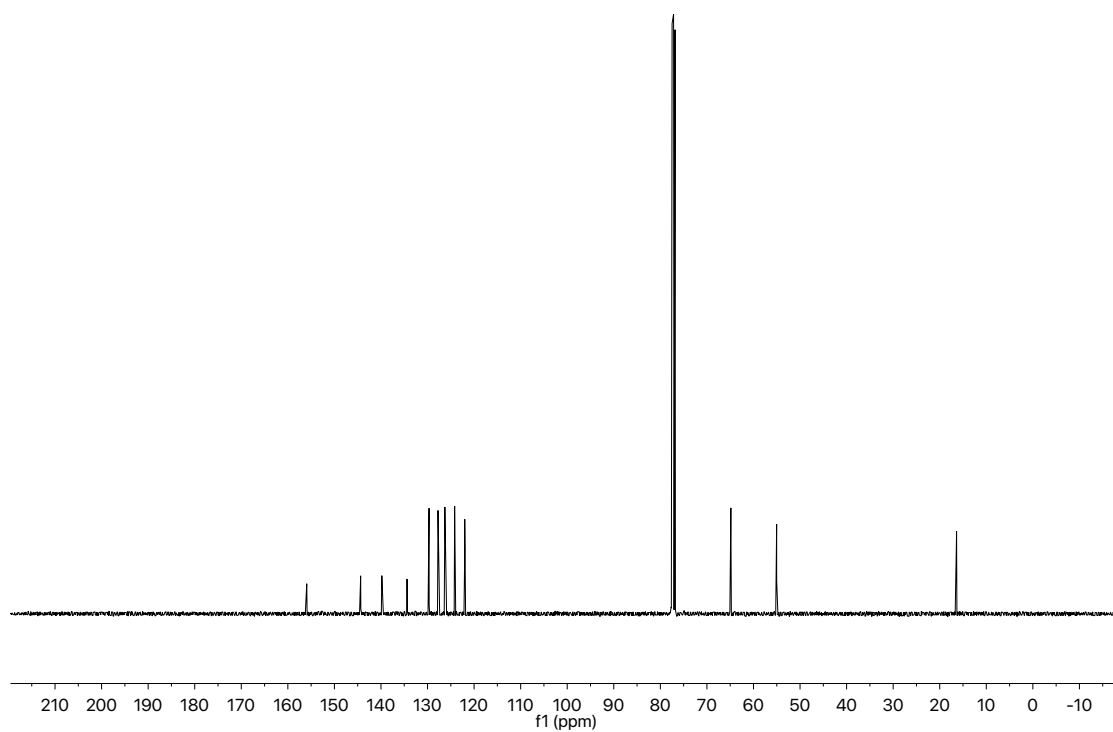


Figure A6.30 ¹³C NMR (101 MHz, CDCl₃) of compound **96f**

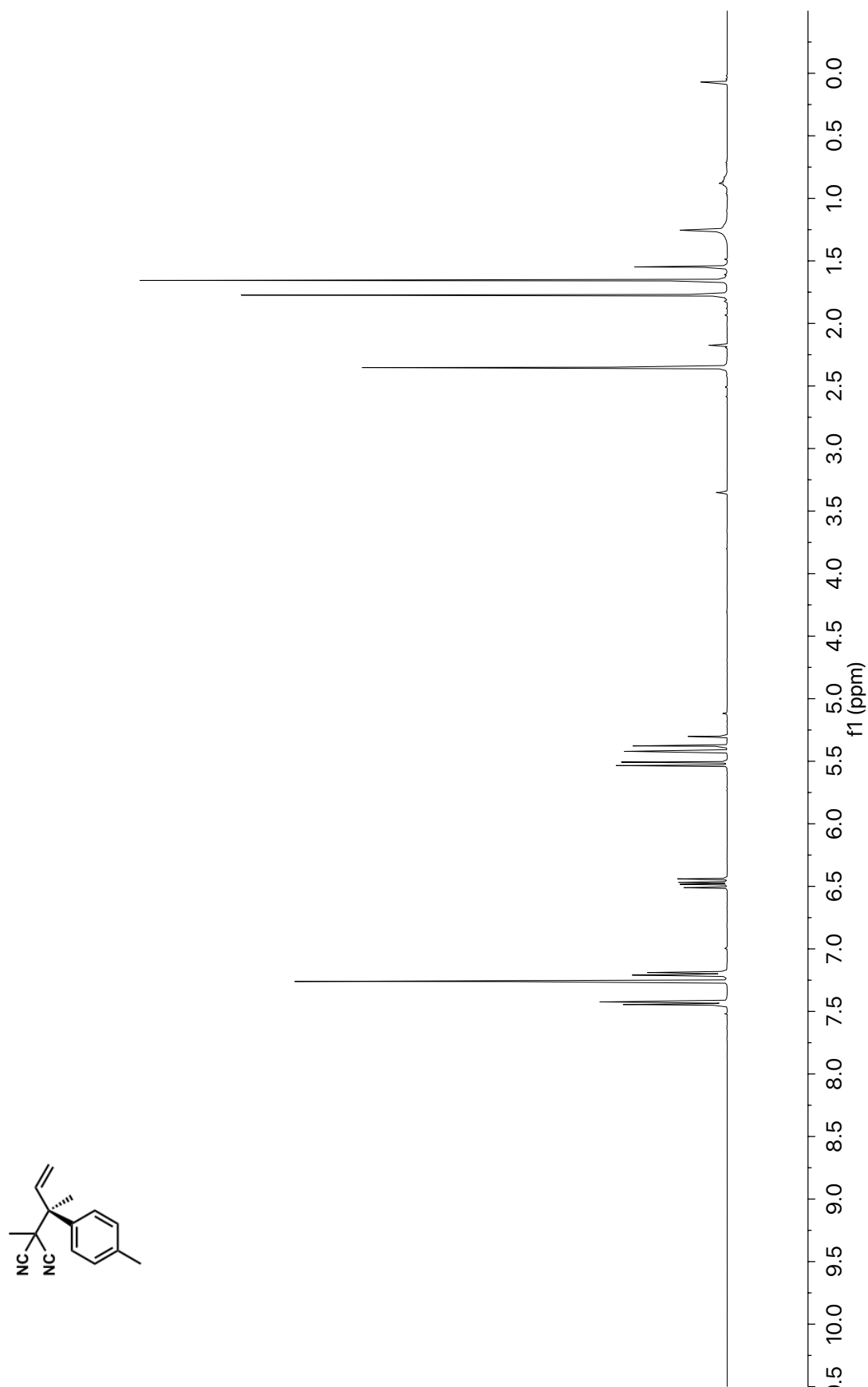


Figure A6.31 ¹H NMR (400 MHz, CDCl₃) of compound **97a**

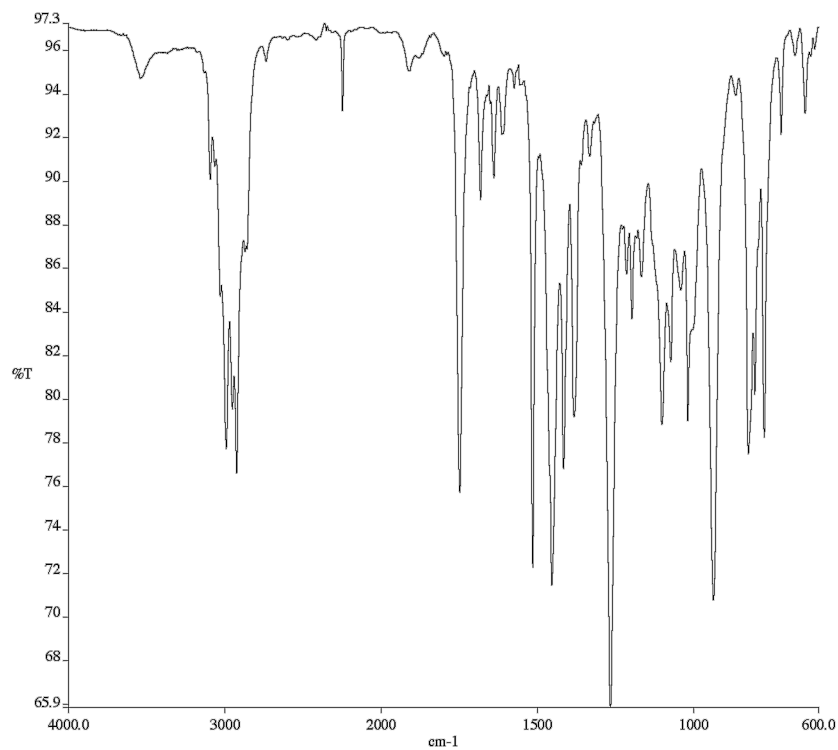


Figure A6.32 Infrared spectrum (Thin Film, NaCl) of compound **97a**

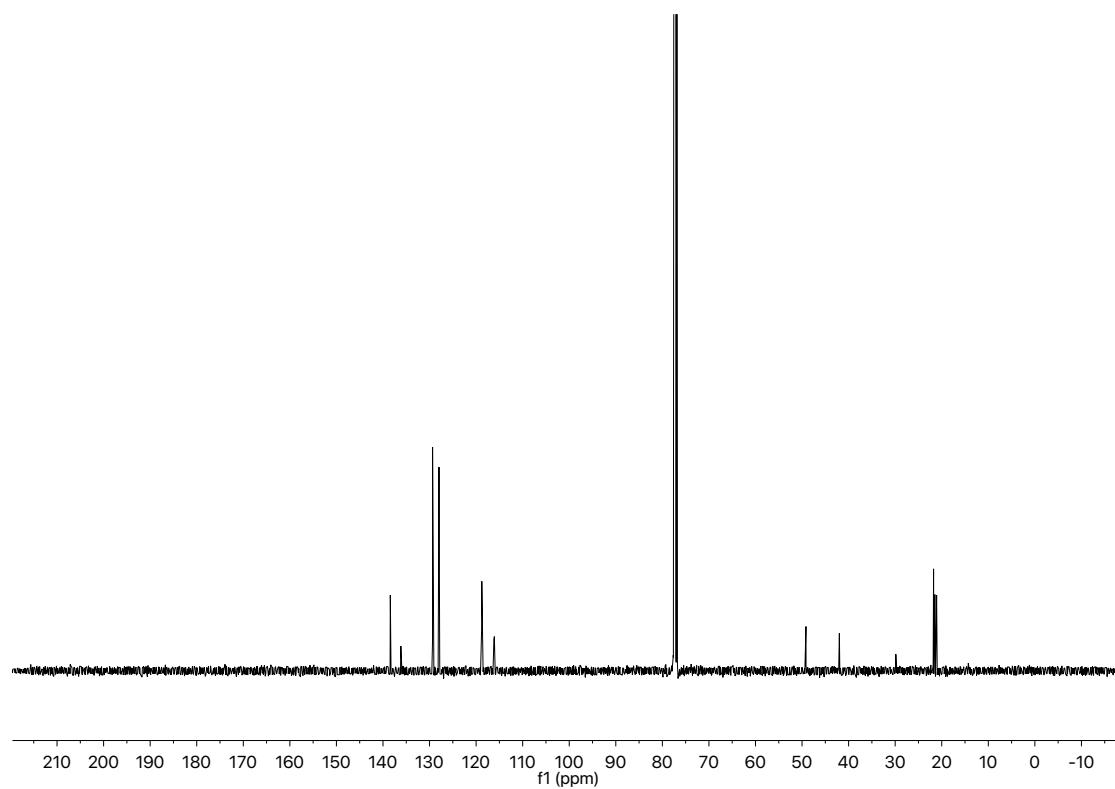


Figure A6.33 ¹³C NMR (101 MHz, CDCl₃) of compound **97a**

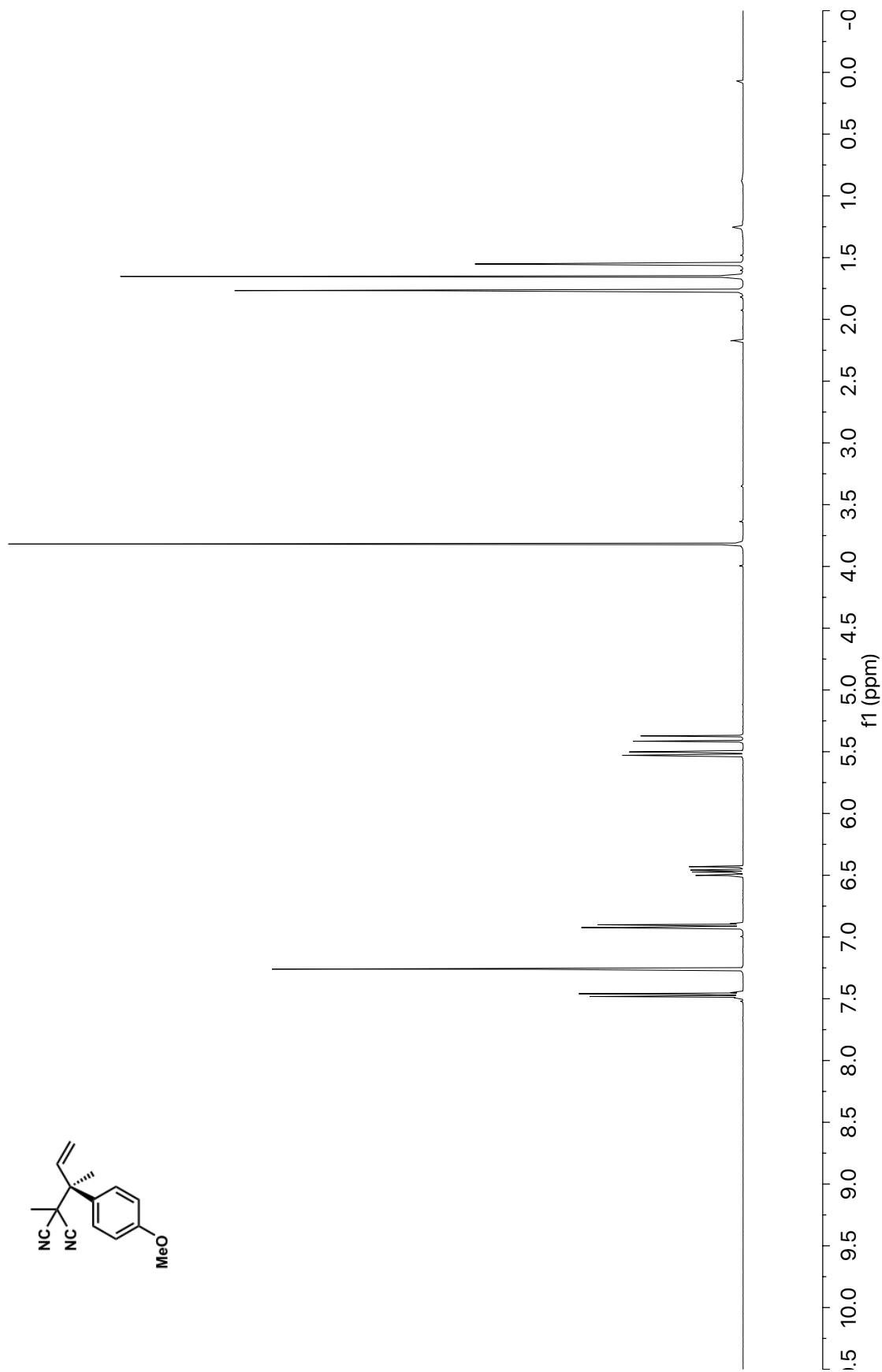


Figure A6.34 ¹H NMR (400 MHz, CDCl₃) of compound **97b**

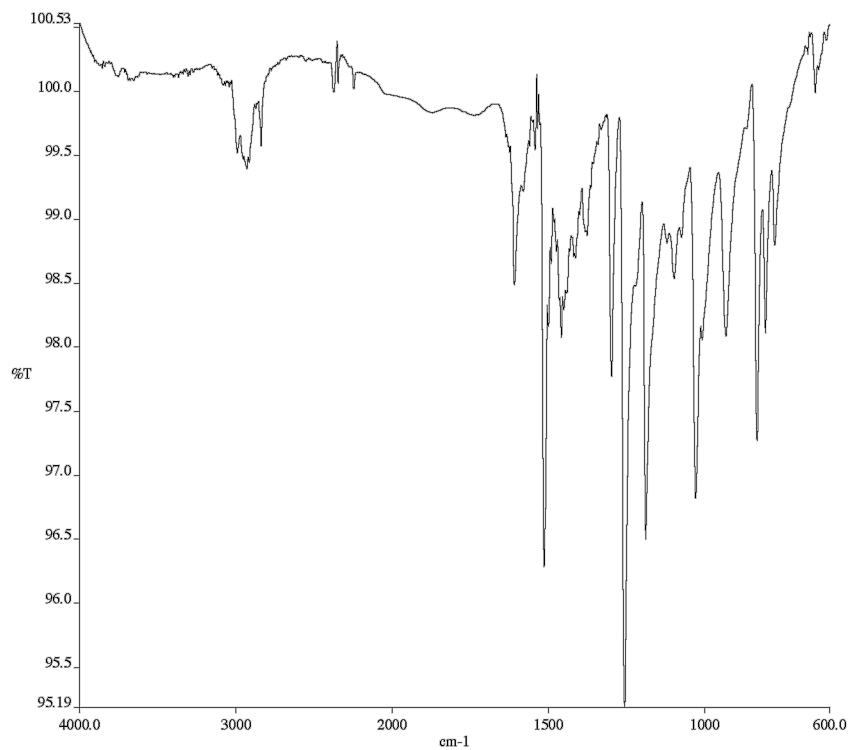


Figure A6.35 Infrared spectrum (Thin Film, NaCl) of compound **97b**

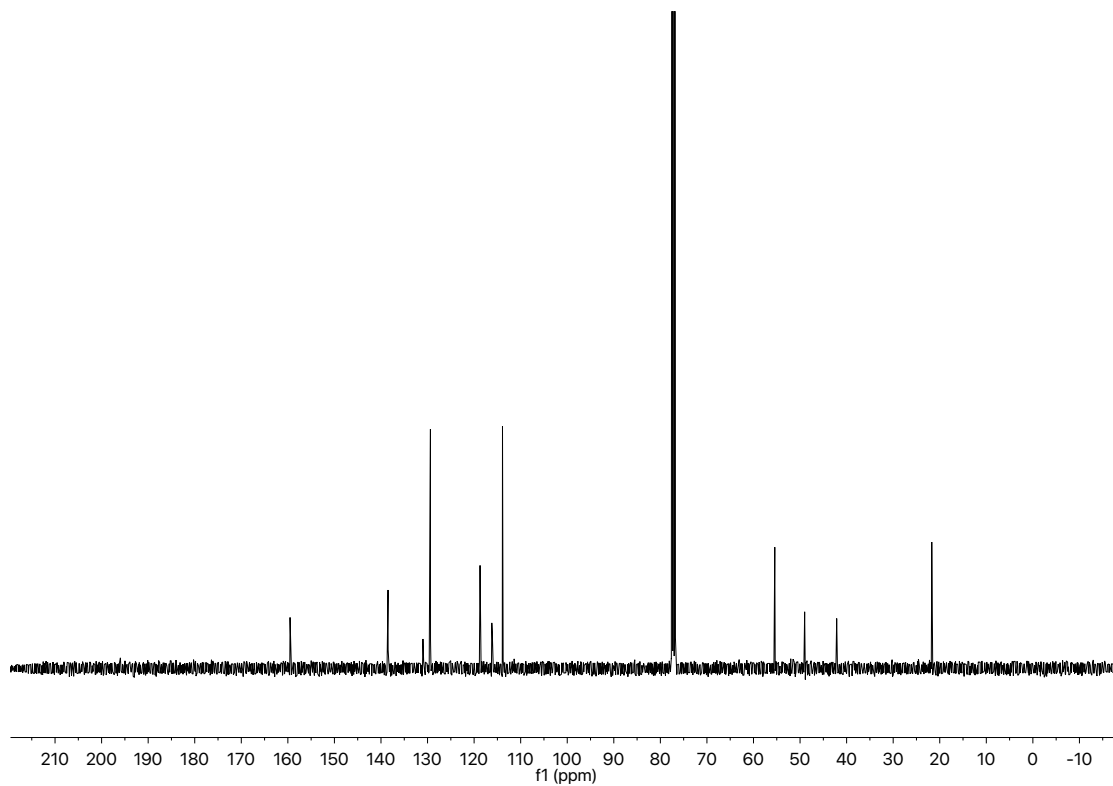


Figure A6.36 ¹³C NMR (101 MHz, CDCl₃) of compound **97b**

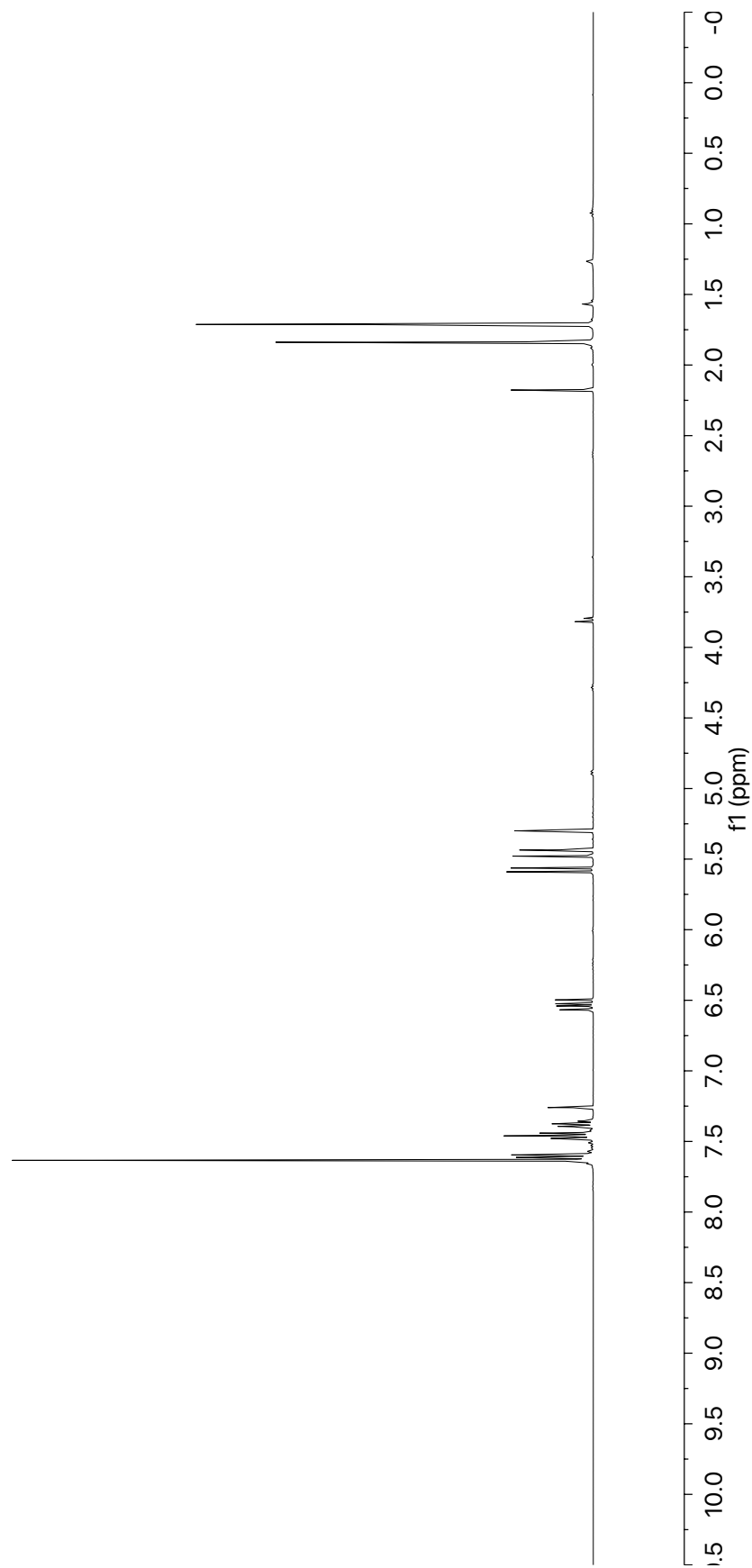
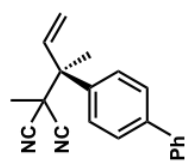


Figure A6.37 ¹H NMR (400 MHz, CDCl₃) of compound **97c**

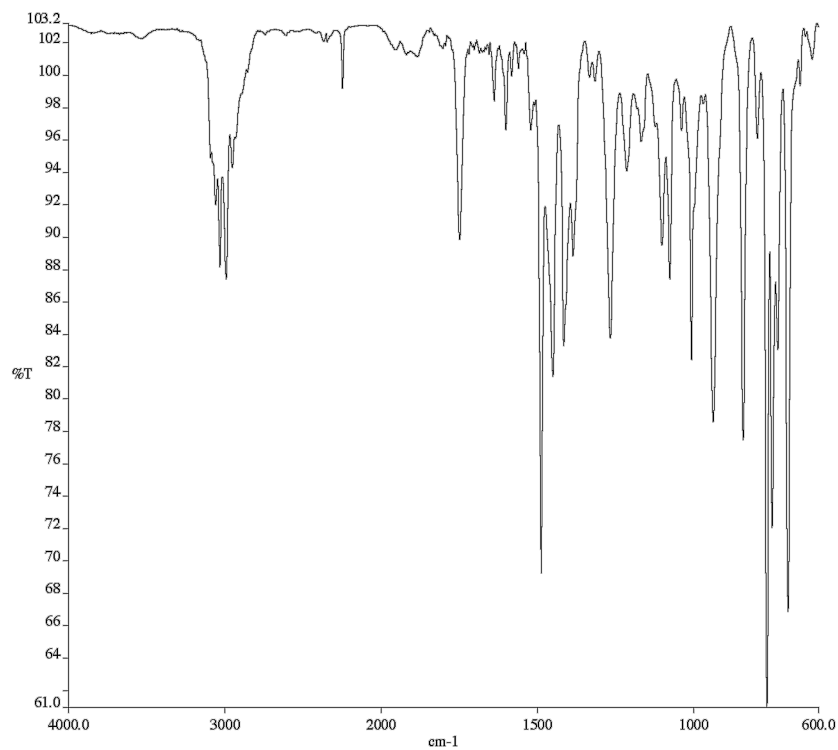


Figure A6.38 Infrared spectrum (Thin Film, NaCl) of compound **97c**

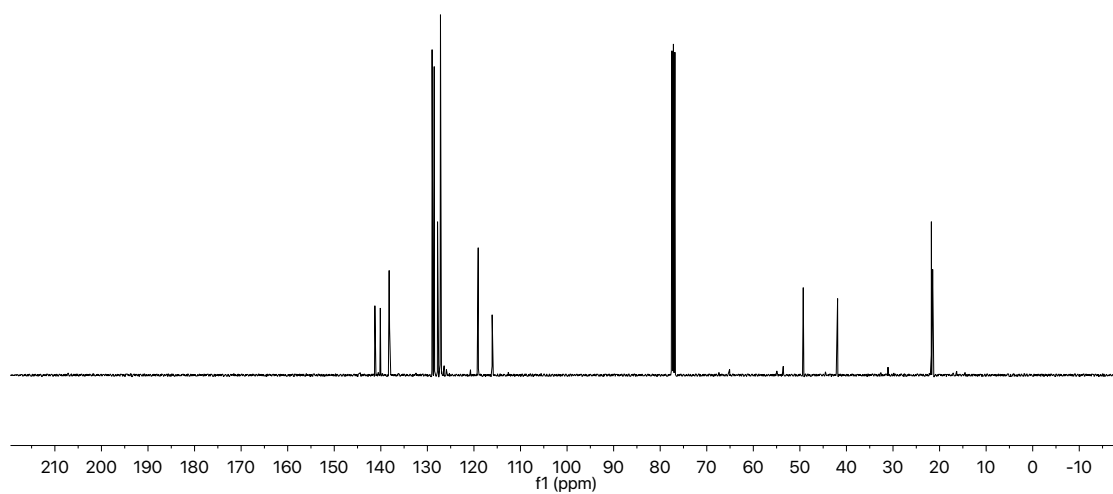


Figure A6.39 ¹³C NMR (101 MHz, CDCl₃) of compound **97c**

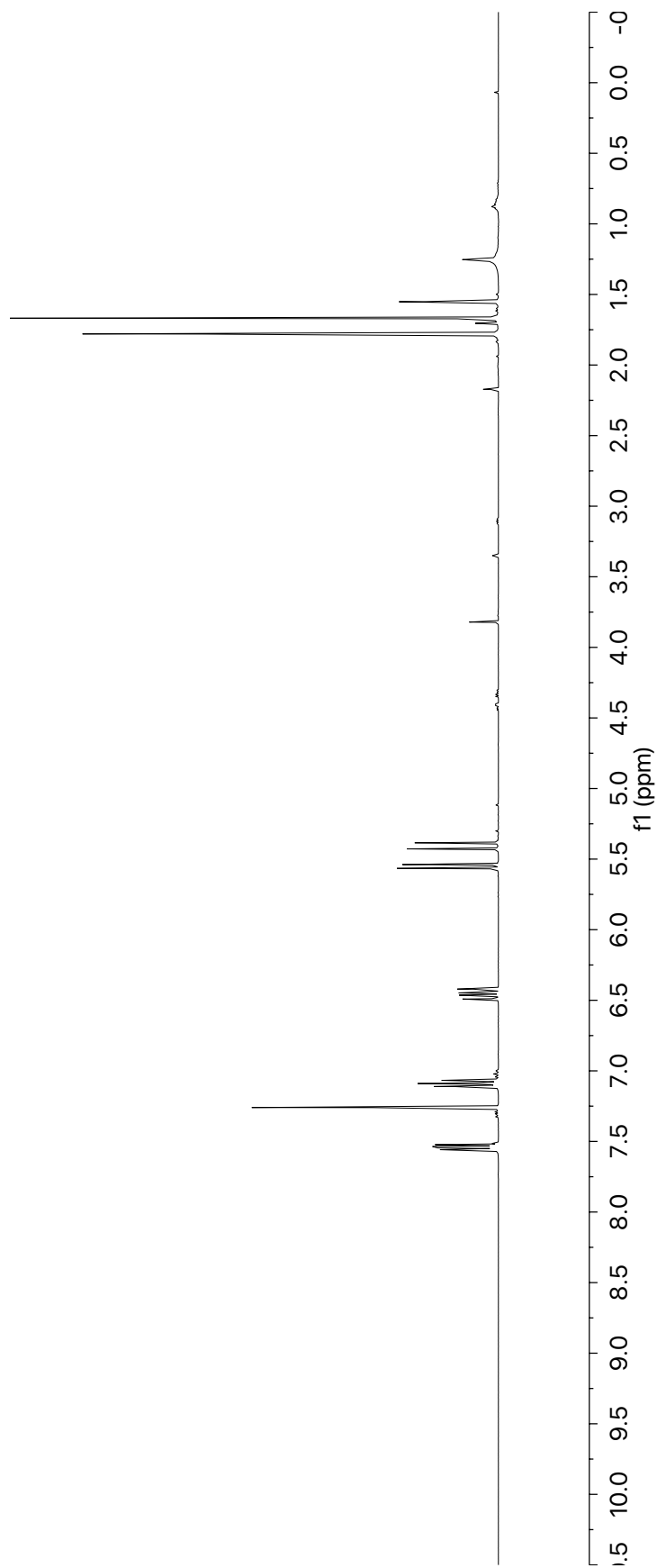
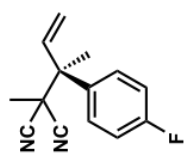


Figure A6.40 ¹H NMR (400 MHz, CDCl₃) of compound **97d**

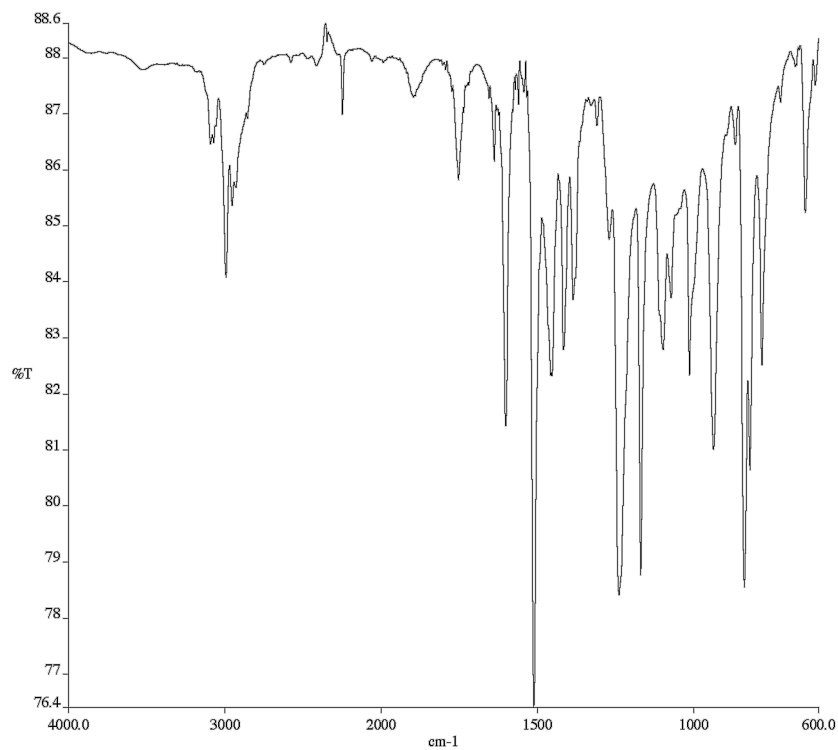


Figure A6.41 Infrared spectrum (Thin Film, NaCl) of compound **97d**

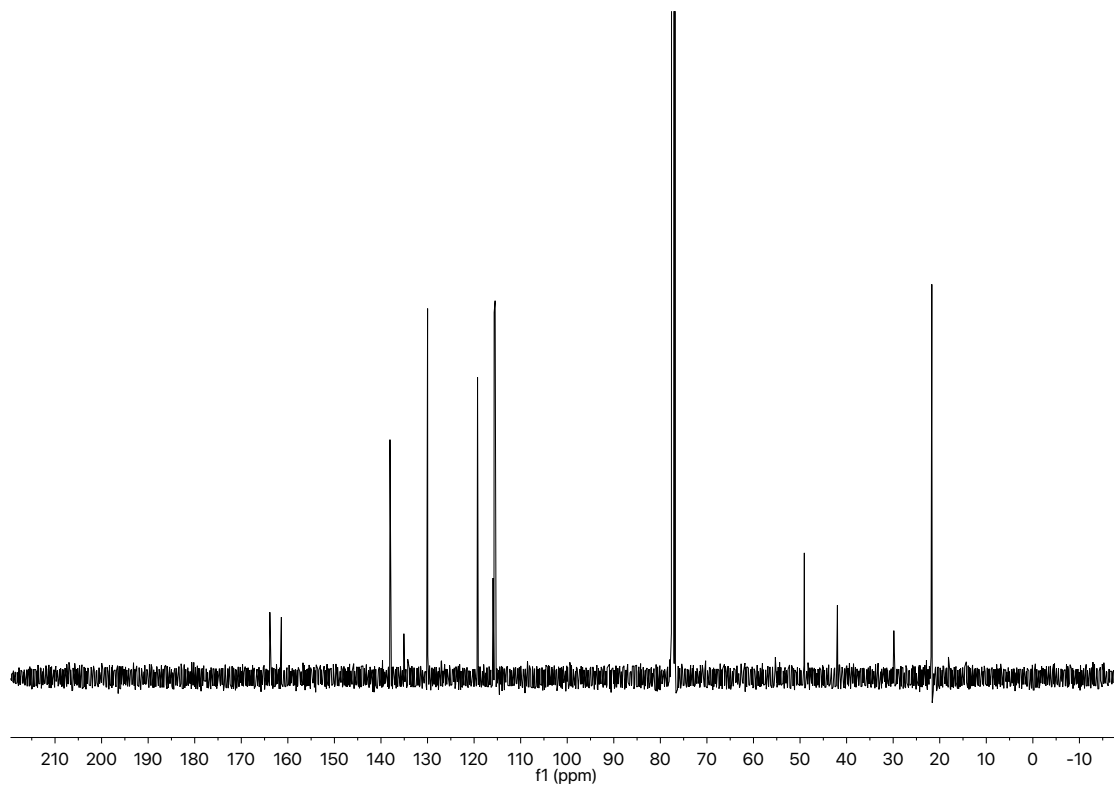


Figure A6.42 ¹³C NMR (101 MHz, CDCl₃) of compound **97d**

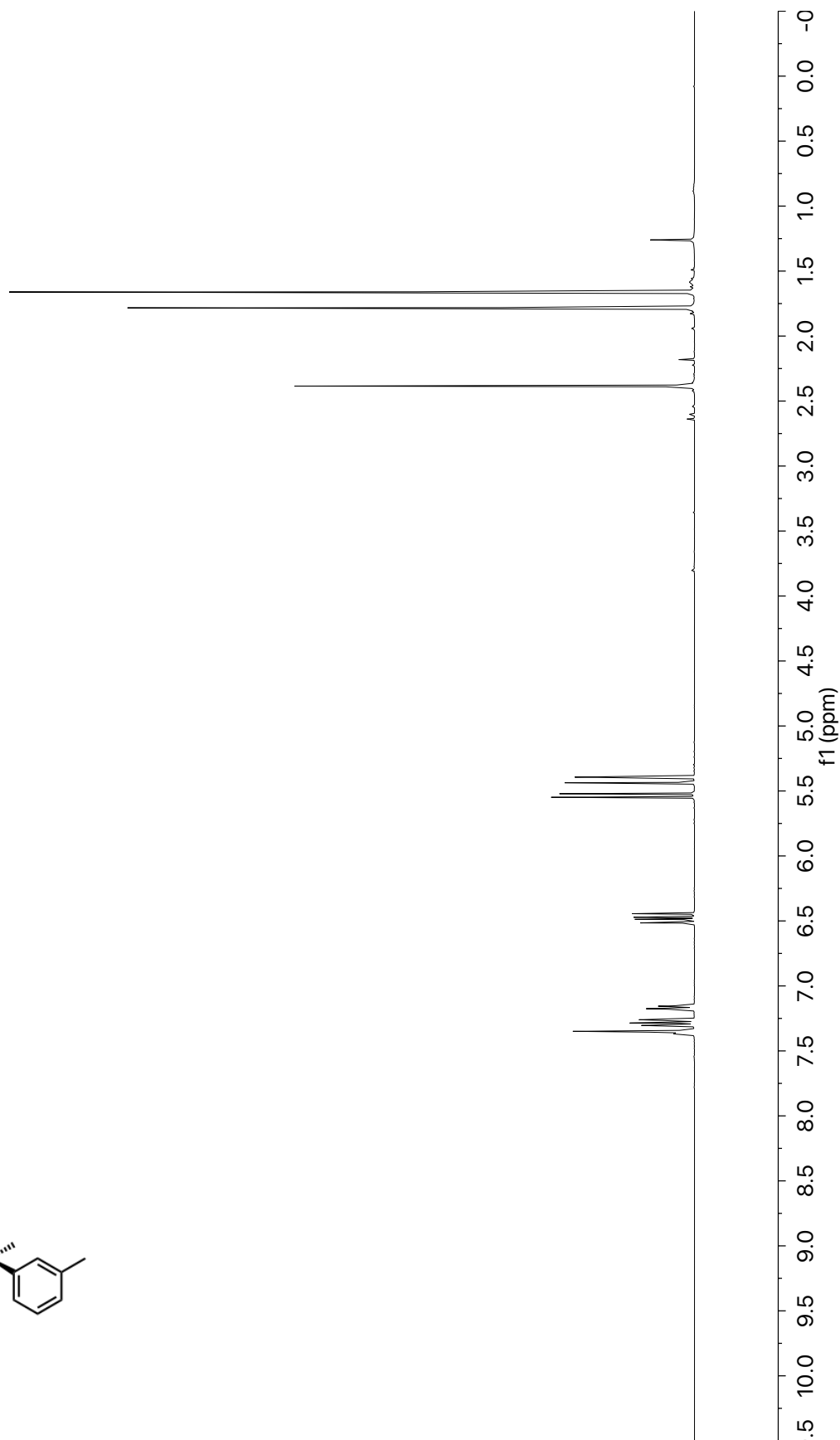
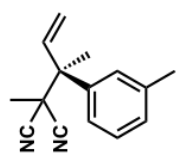


Figure A6.43 ^1H NMR (400 MHz, CDCl_3) of compound **97e**

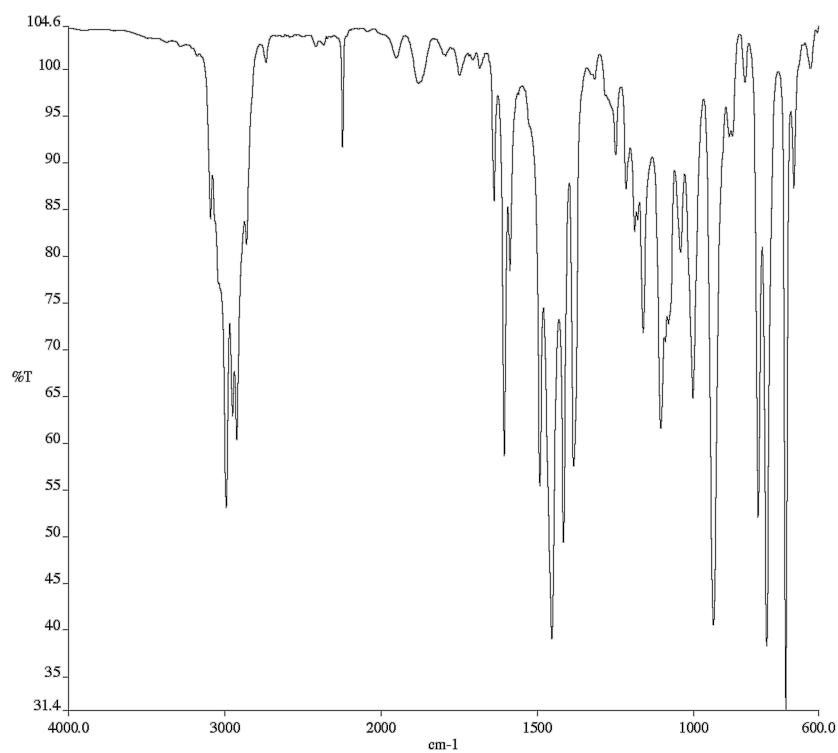


Figure A6.44 Infrared spectrum (Thin Film, NaCl) of compound **97e**

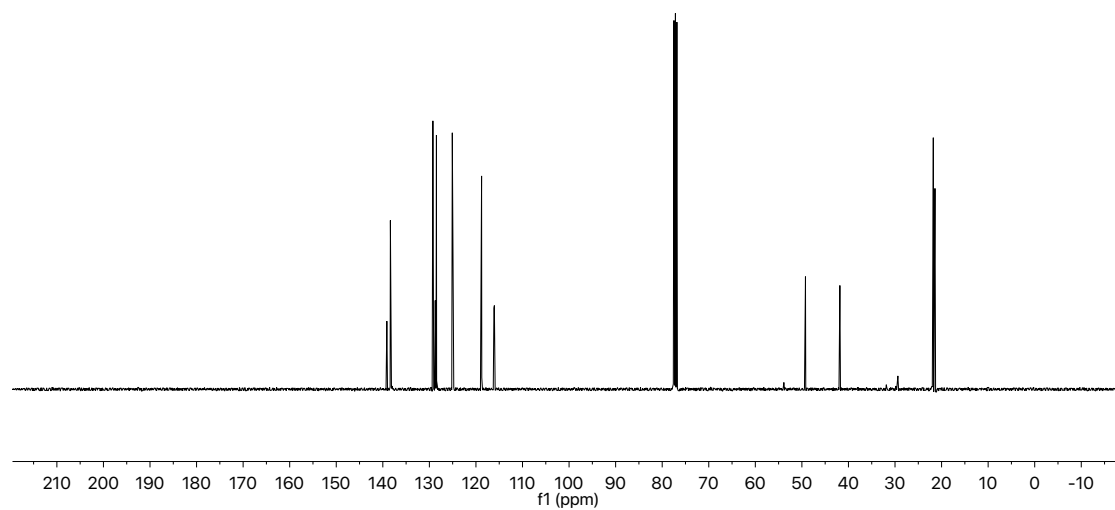


Figure A6.45 ¹³C NMR (101 MHz, CDCl₃) of compound **97e**

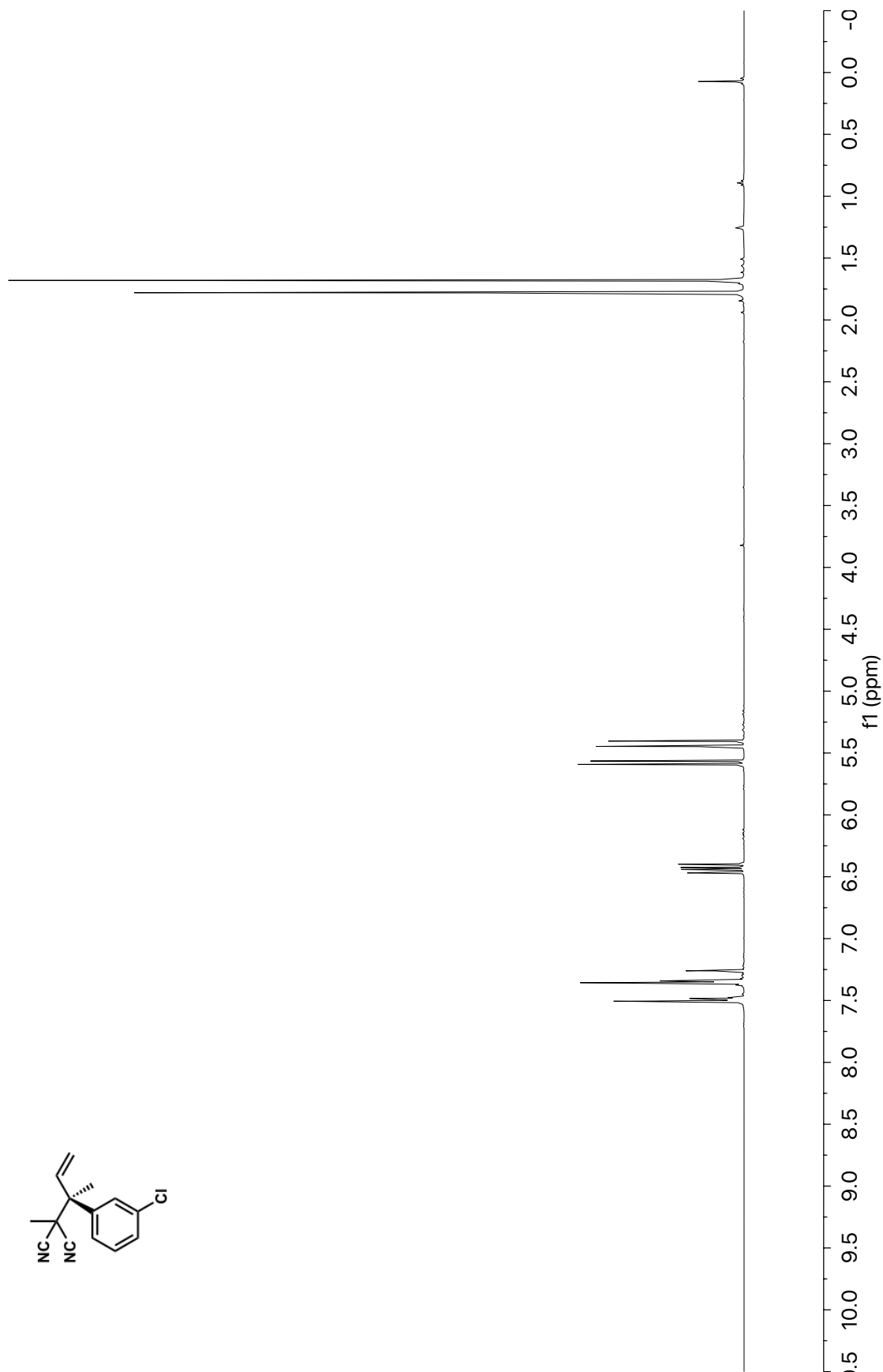


Figure A6.46 ¹H NMR (400 MHz, CDCl₃) of compound **97f**

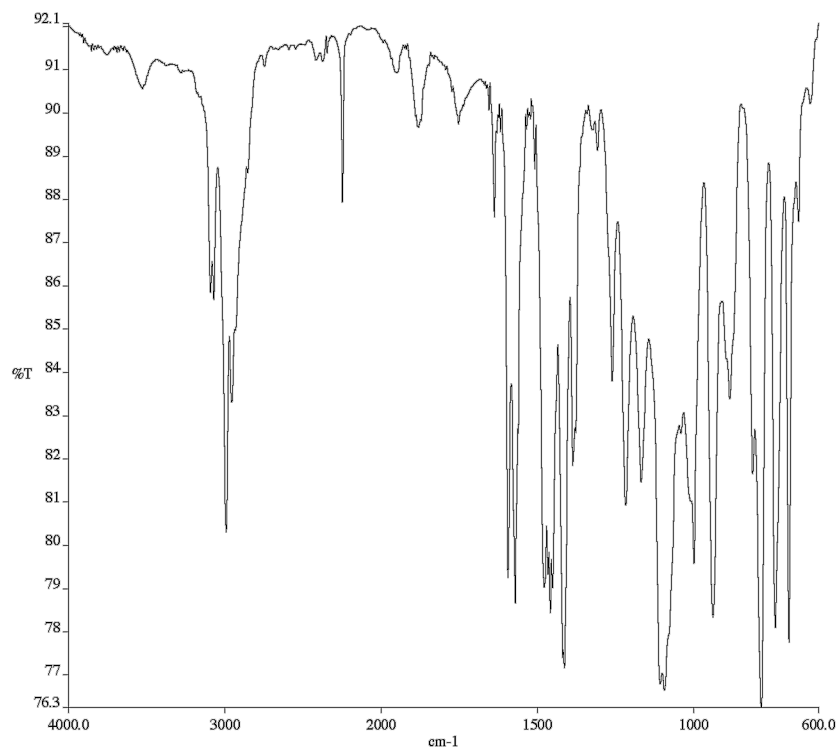


Figure A6.47 Infrared spectrum (Thin Film, NaCl) of compound **97f**

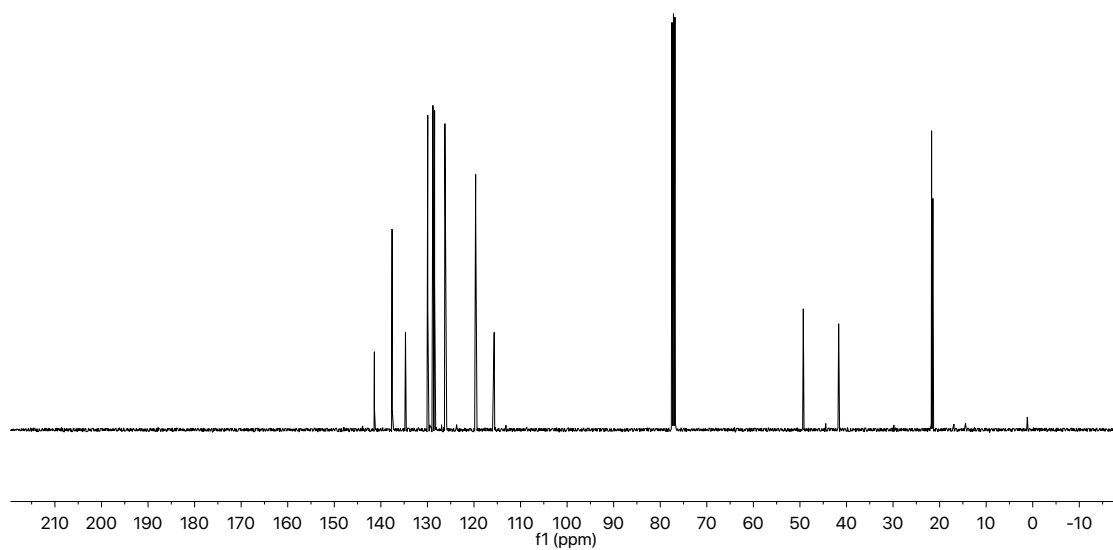


Figure A6.48 ¹³C NMR (101 MHz, CDCl₃) of compound **97f**

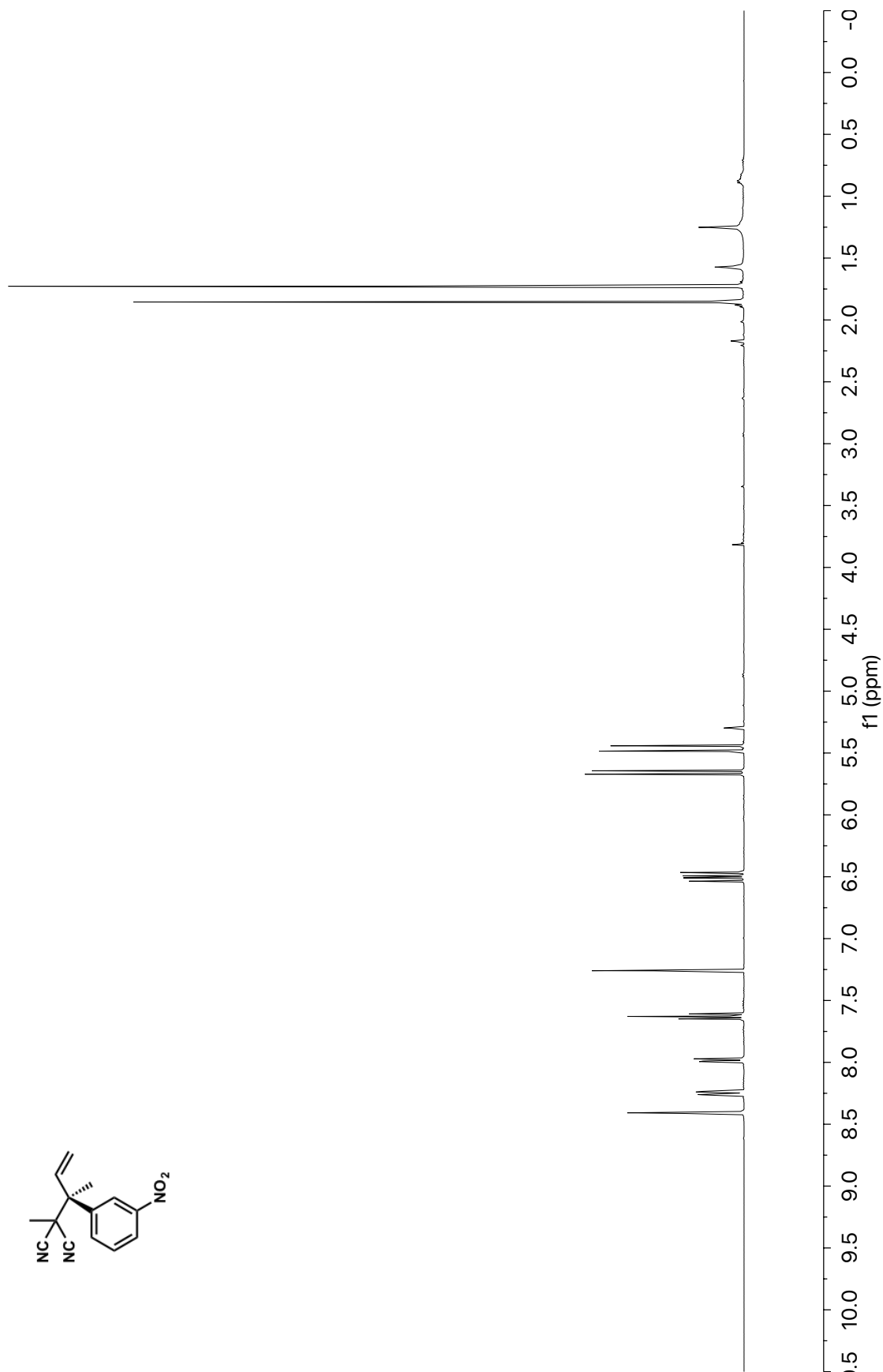


Figure A6.49 ¹H NMR (400 MHz, CDCl₃) of compound **97g**

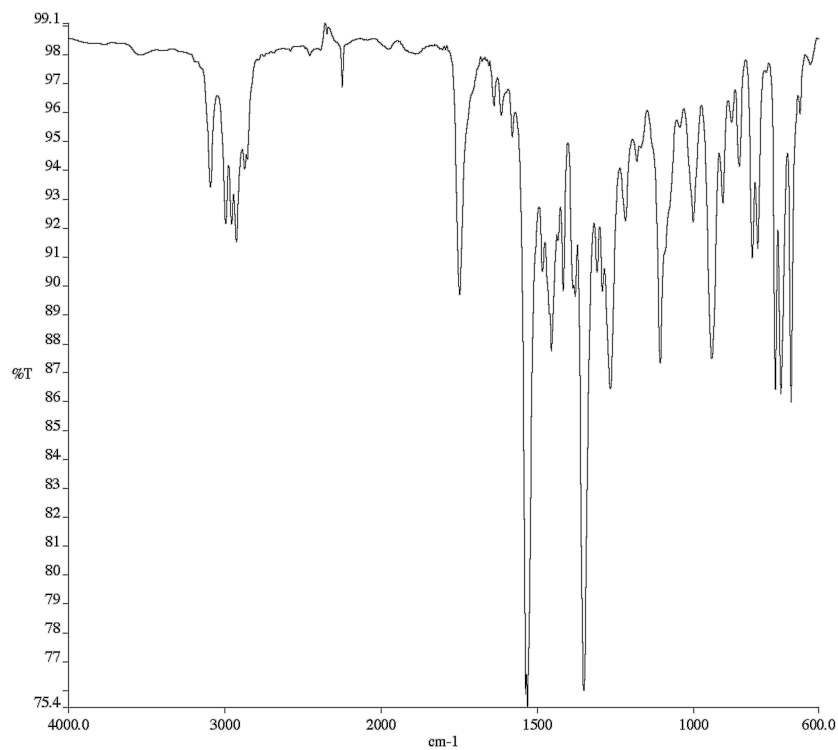


Figure A6.50 Infrared spectrum (Thin Film, NaCl) of compound **97g**

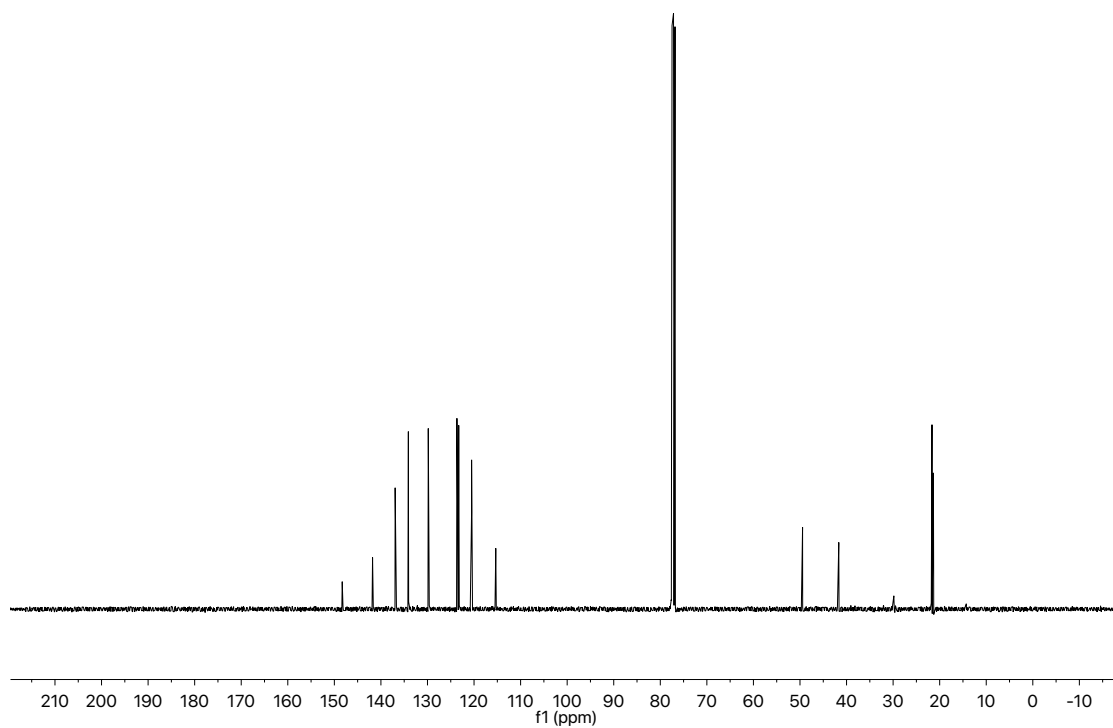


Figure A6.51 ¹³C NMR (101 MHz, CDCl₃) of compound **97g**

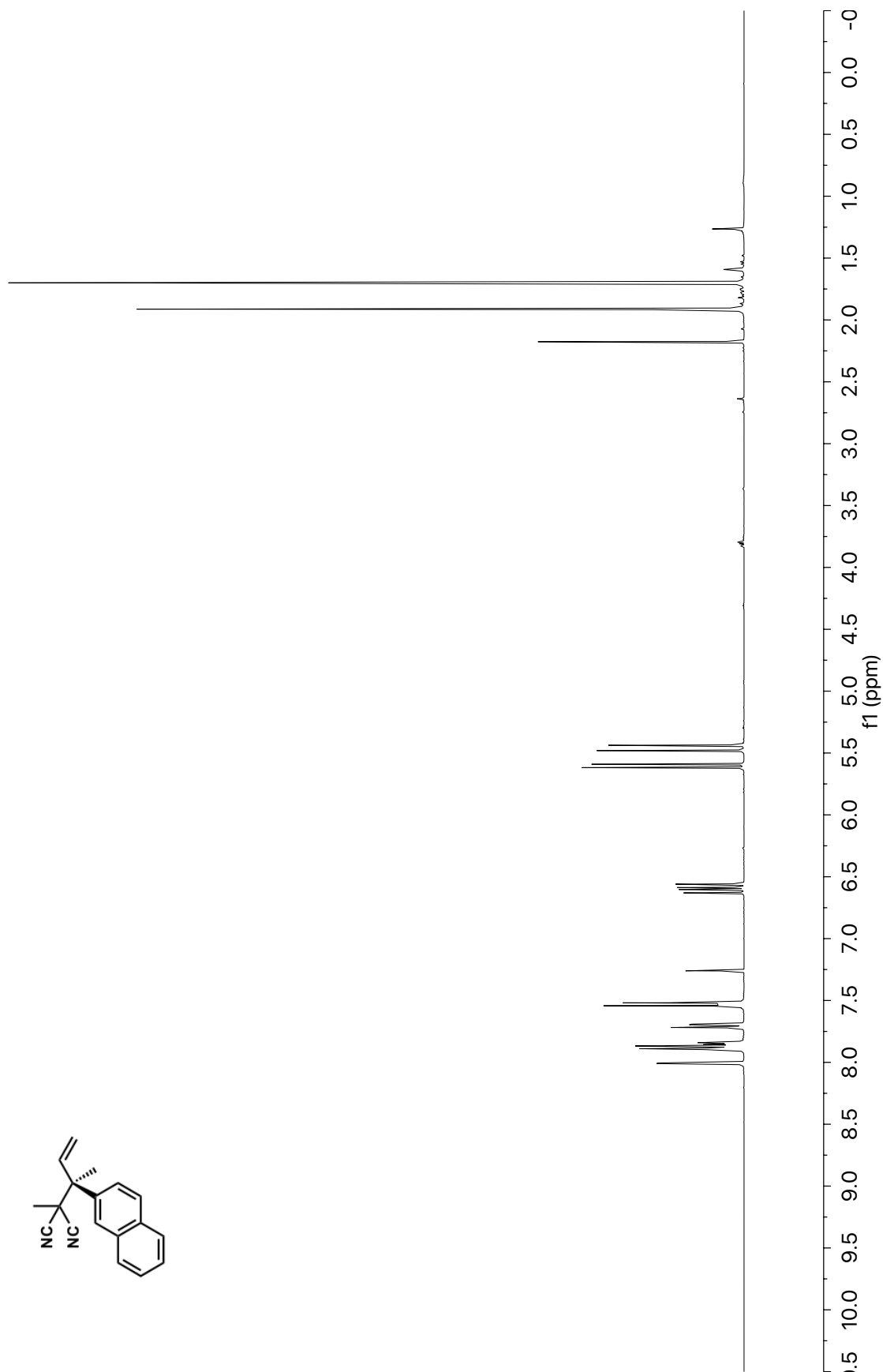


Figure A6.52 ¹H NMR (400 MHz, CDCl₃) of compound **97h**

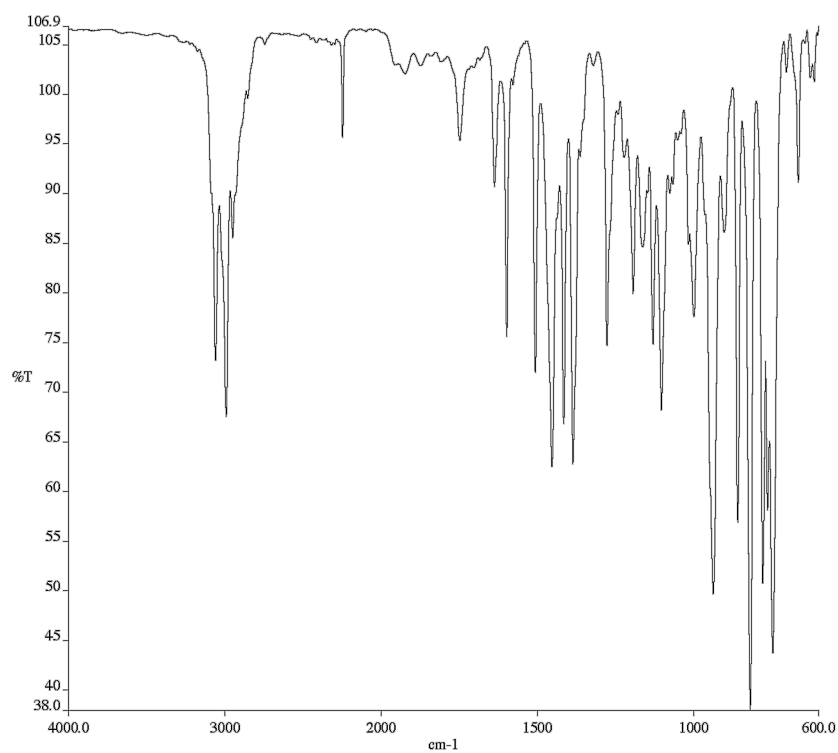


Figure A6.53 Infrared spectrum (Thin Film, NaCl) of compound **97h**

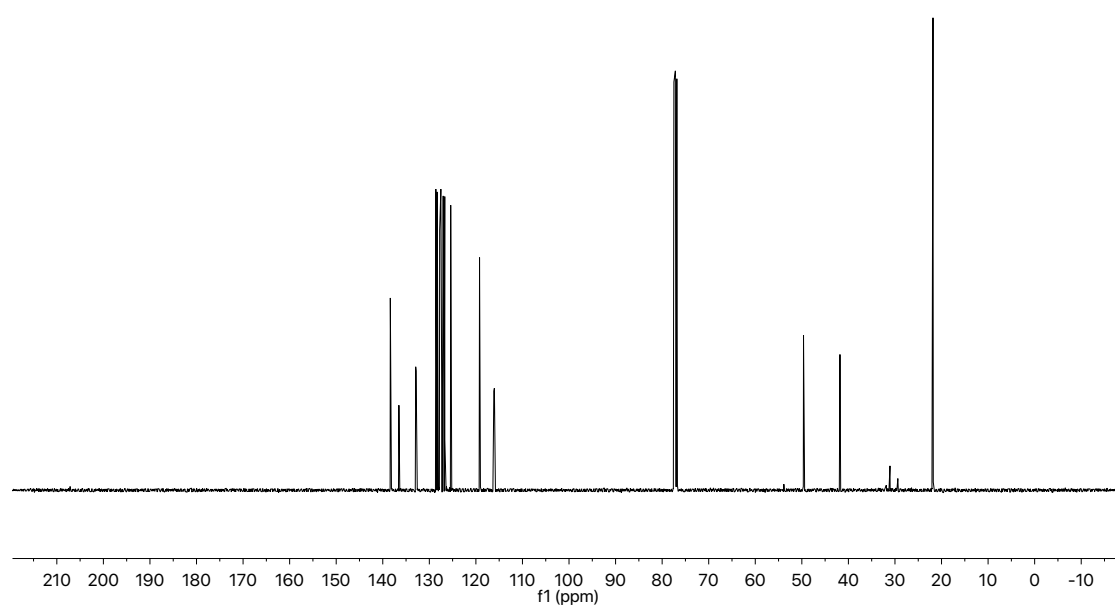


Figure A6.54 ¹³C NMR (101 MHz, CDCl₃) of compound **97h**

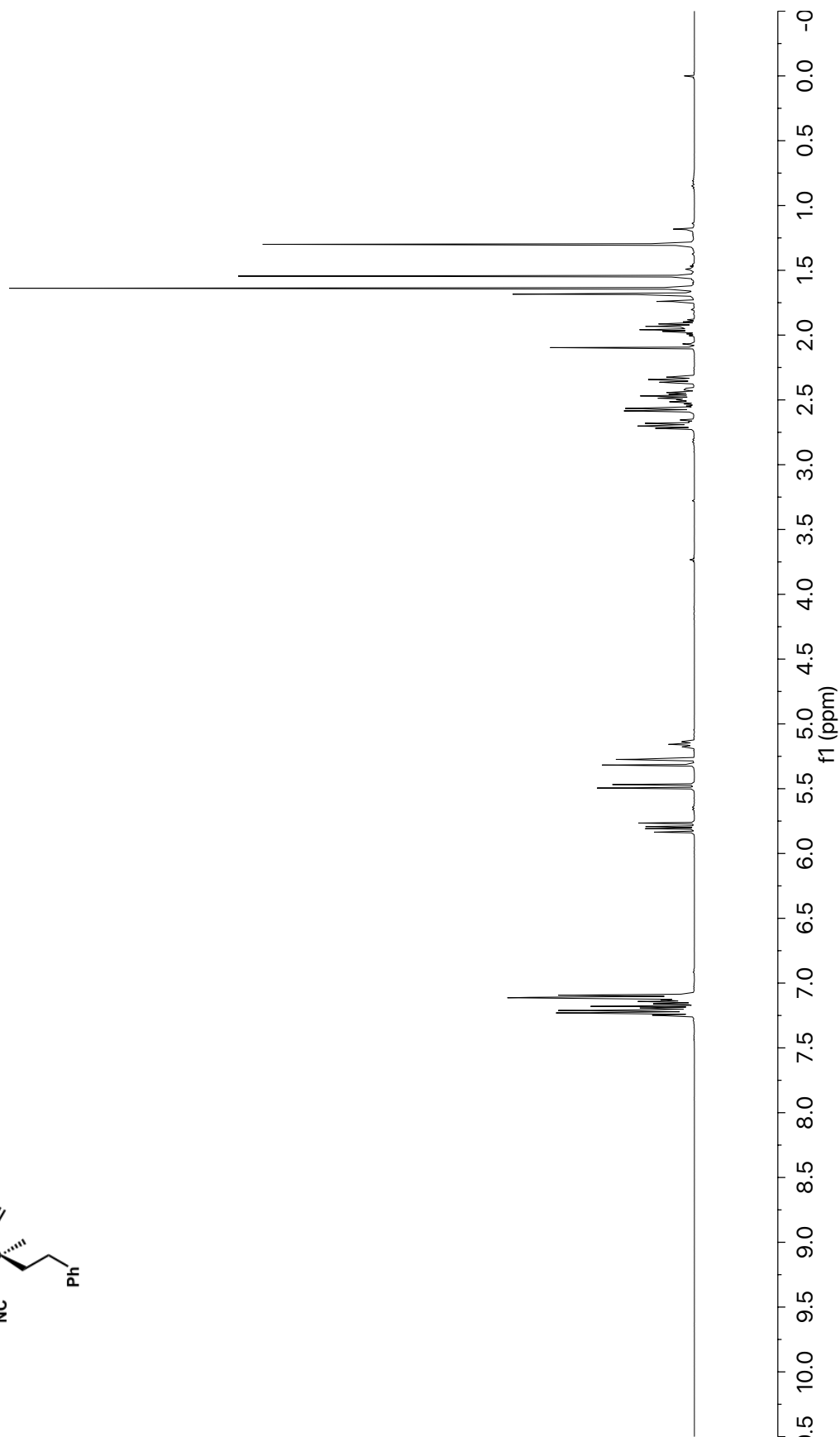
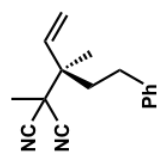


Figure A6.55 ^1H NMR (400 MHz, CDCl_3) of compound **97j**

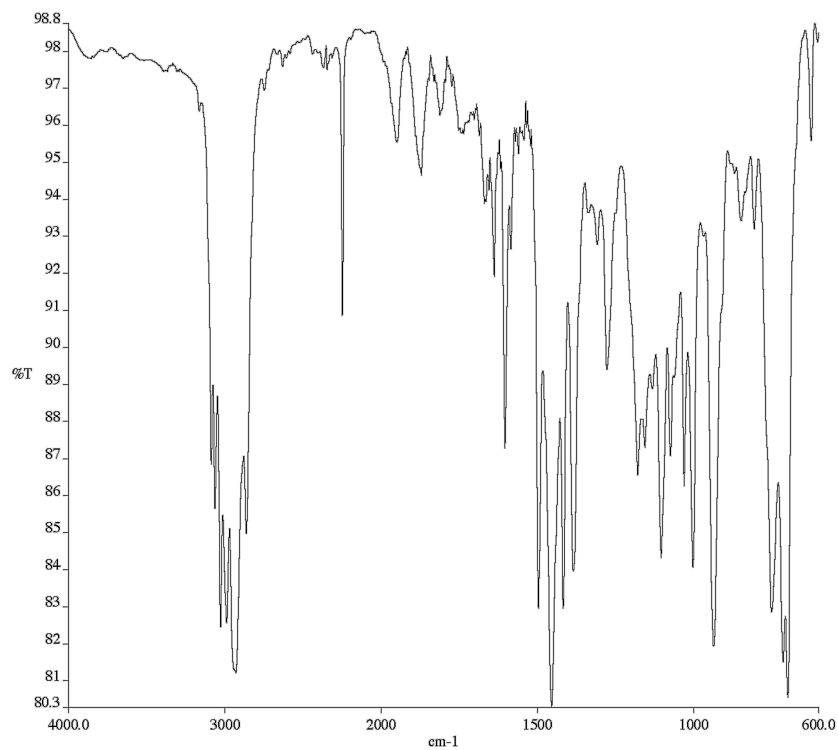


Figure A6.56 Infrared spectrum (Thin Film, NaCl) of compound **97j**

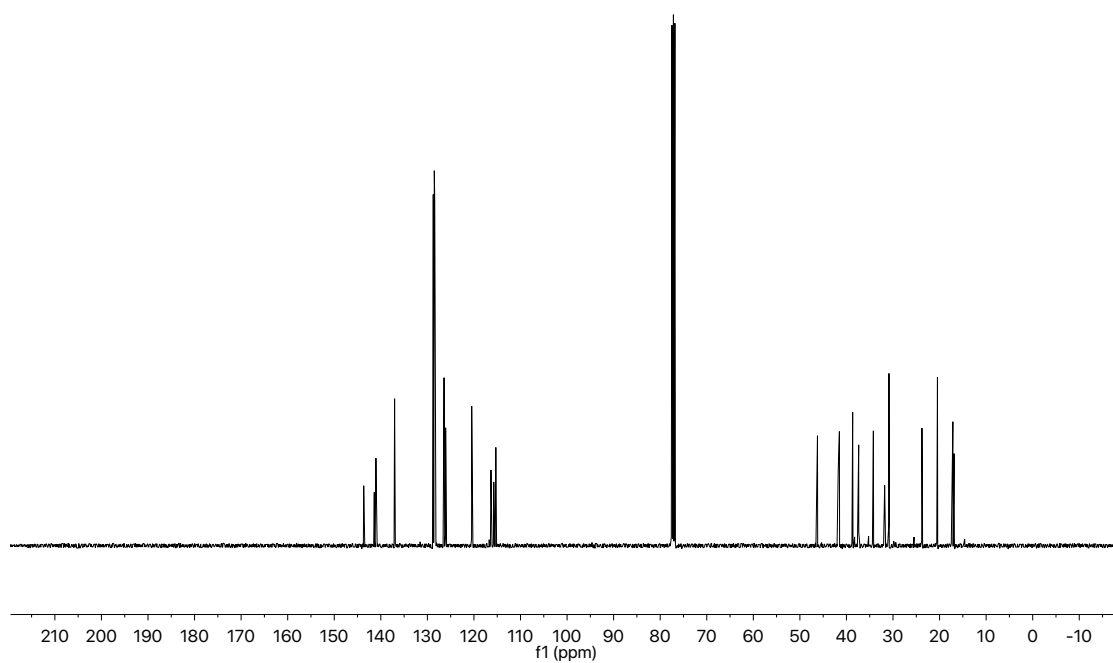


Figure A6.57 ¹³C NMR (101 MHz, CDCl₃) of compound **97j**

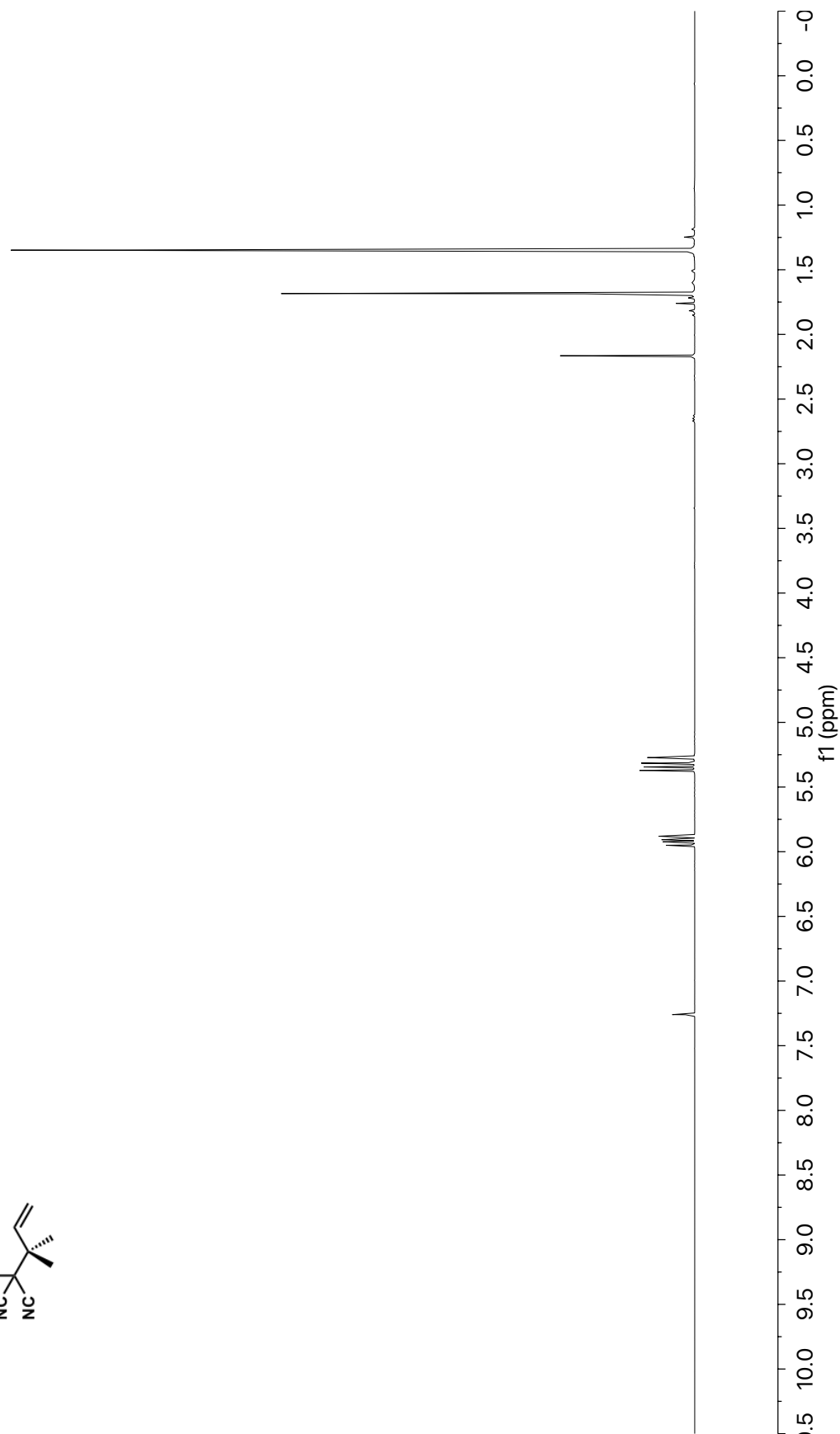


Figure A6.58 ¹H NMR (400 MHz, CDCl₃) of compound **97k**

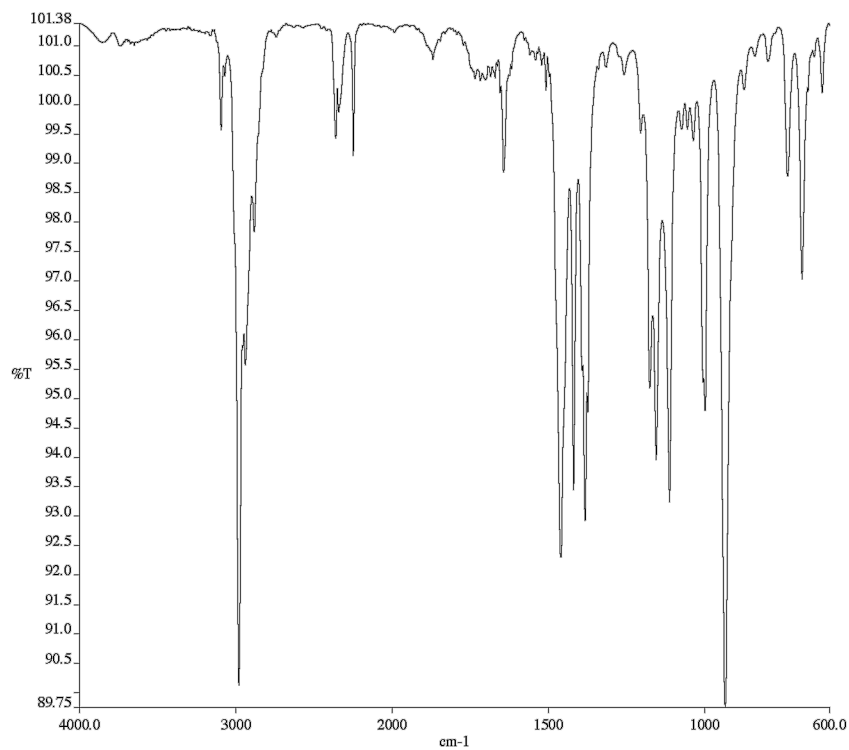


Figure A6.59 Infrared spectrum (Thin Film, NaCl) of compound **97k**

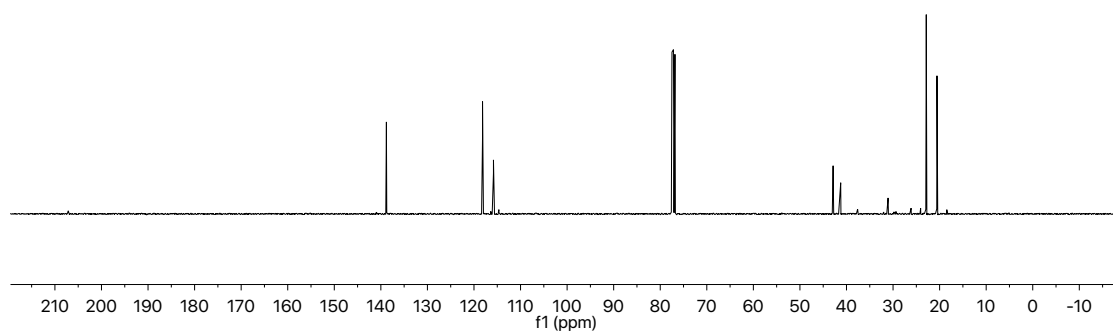


Figure A6.60 ¹³C NMR (101 MHz, CDCl₃) of compound **97k**

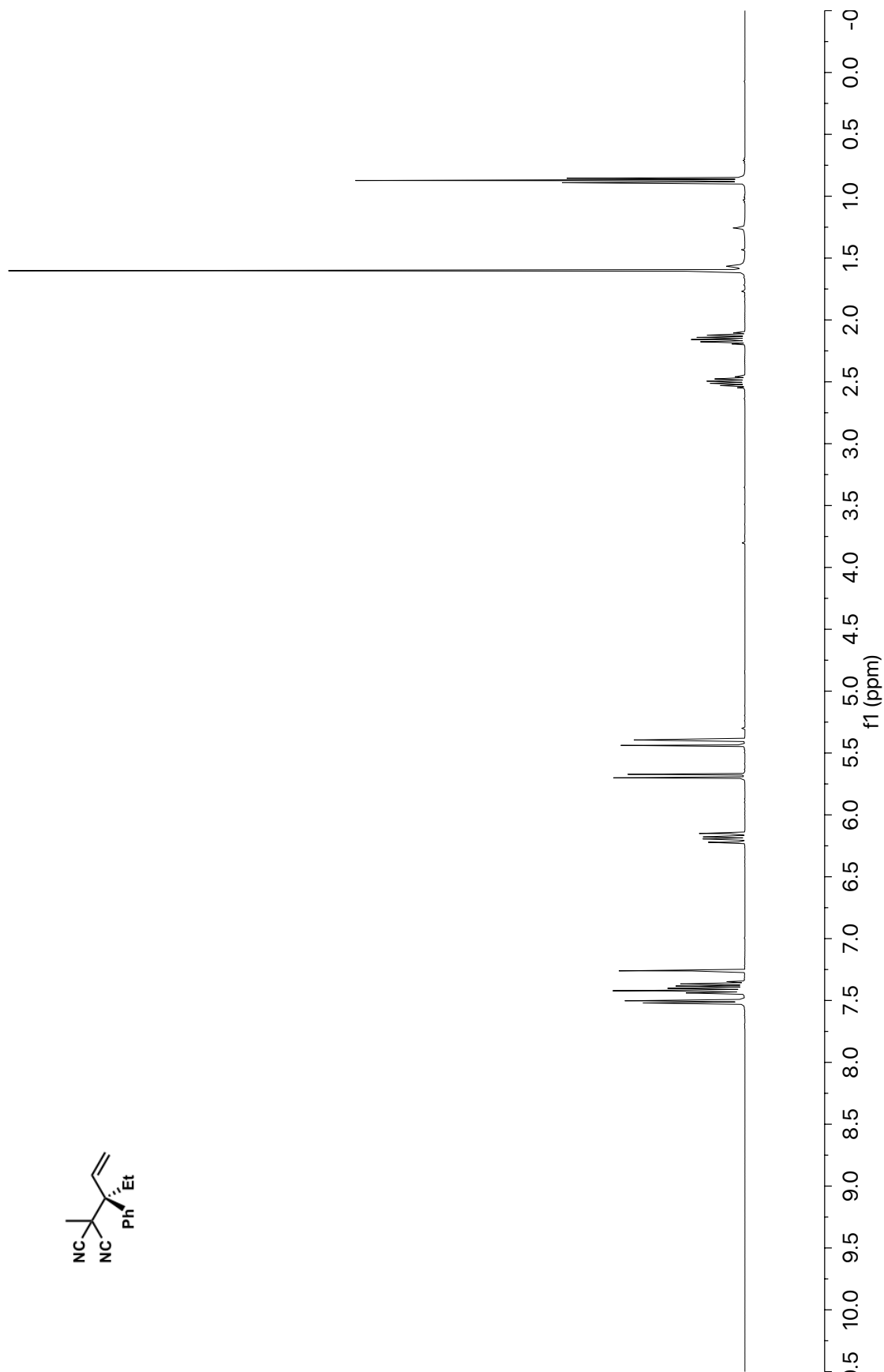


Figure A6.61 ¹H NMR (400 MHz, CDCl₃) of compound **97I**

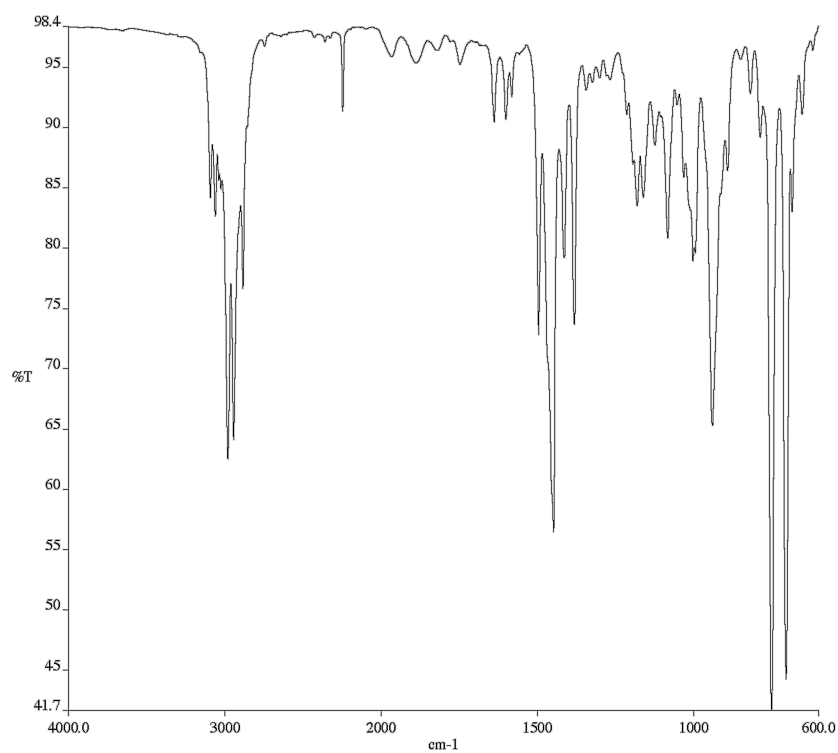


Figure A6.62 Infrared spectrum (Thin Film, NaCl) of compound **97I**

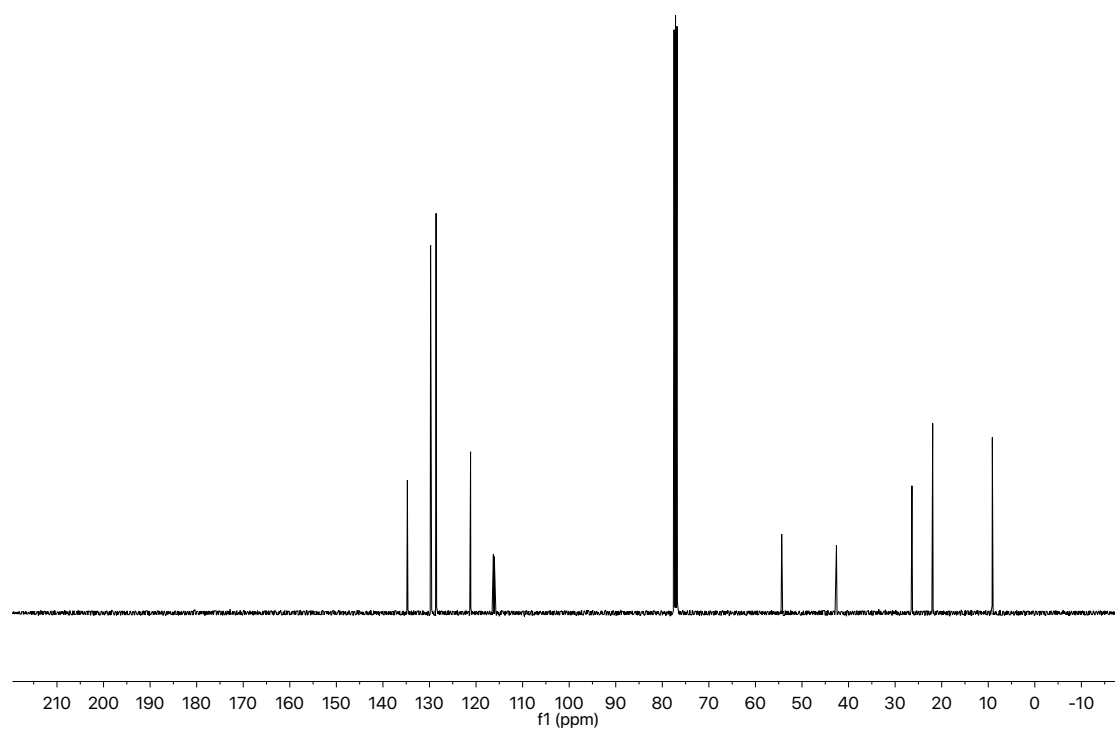


Figure A6.63 ¹³C NMR (101 MHz, CDCl₃) of compound **97I**

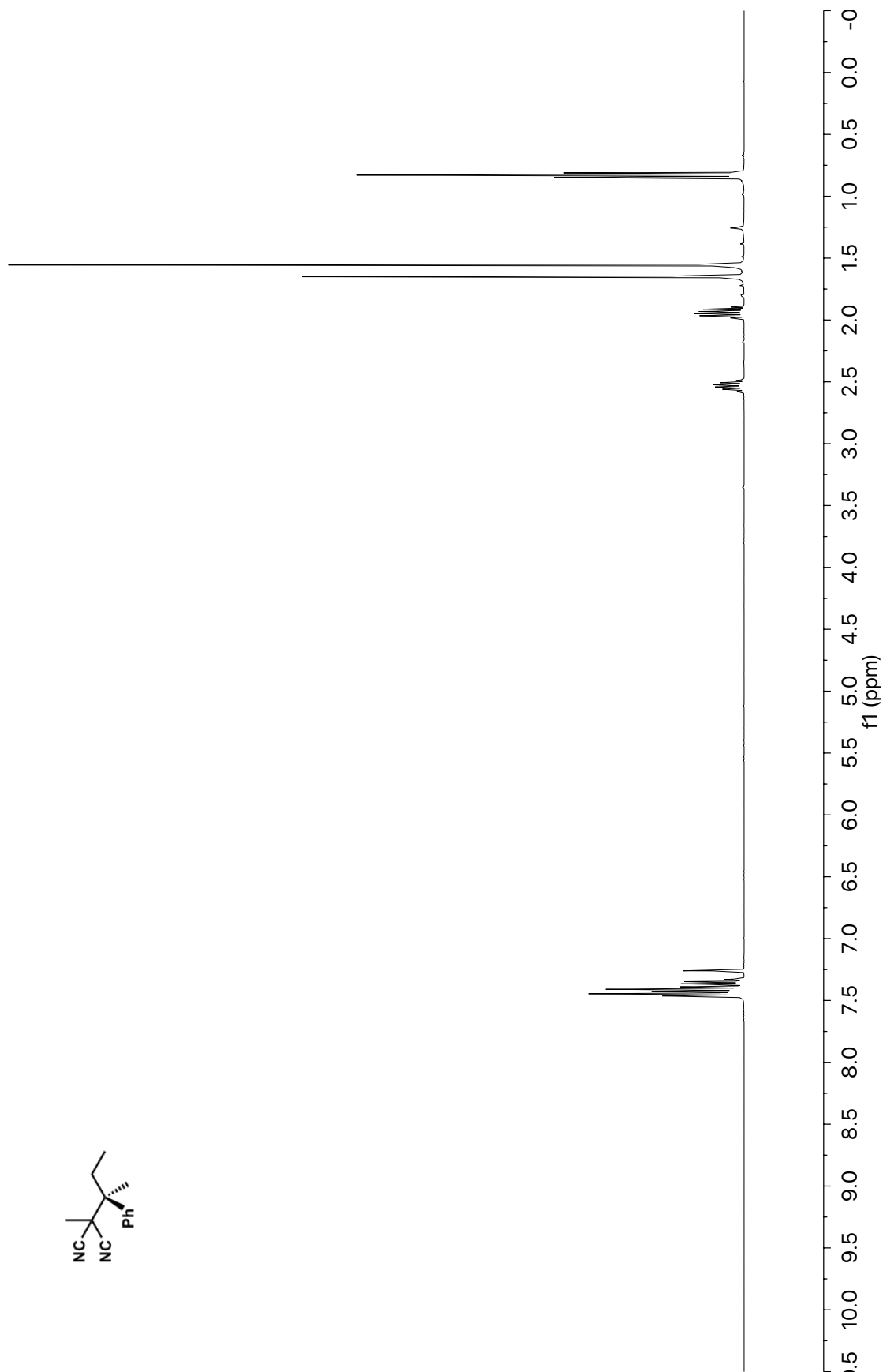


Figure A6.64 ¹H NMR (400 MHz, CDCl₃) of compound **101**

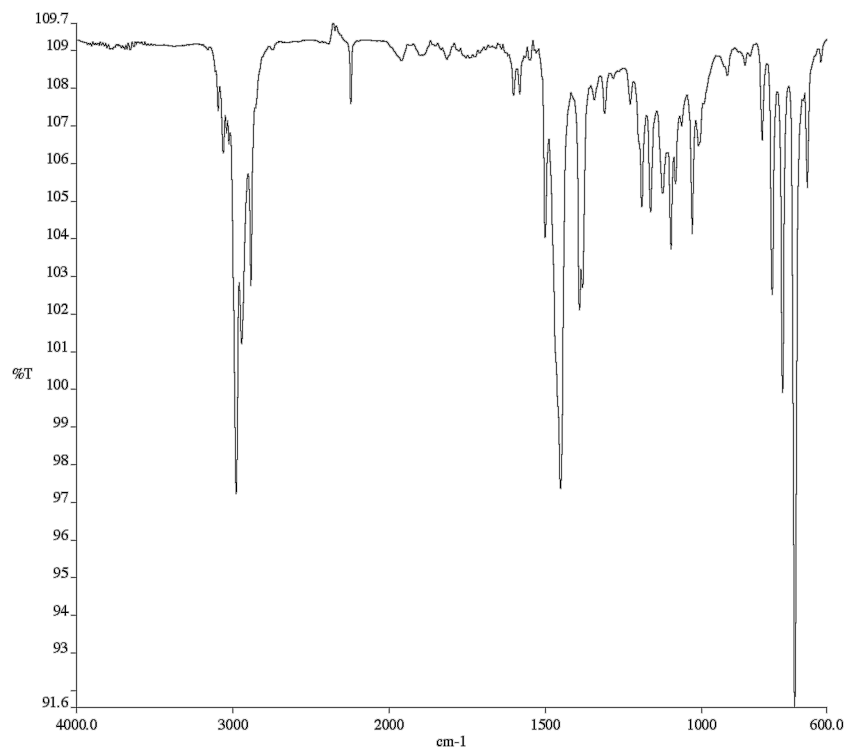


Figure A6.65 Infrared spectrum (Thin Film, NaCl) of compound **101**

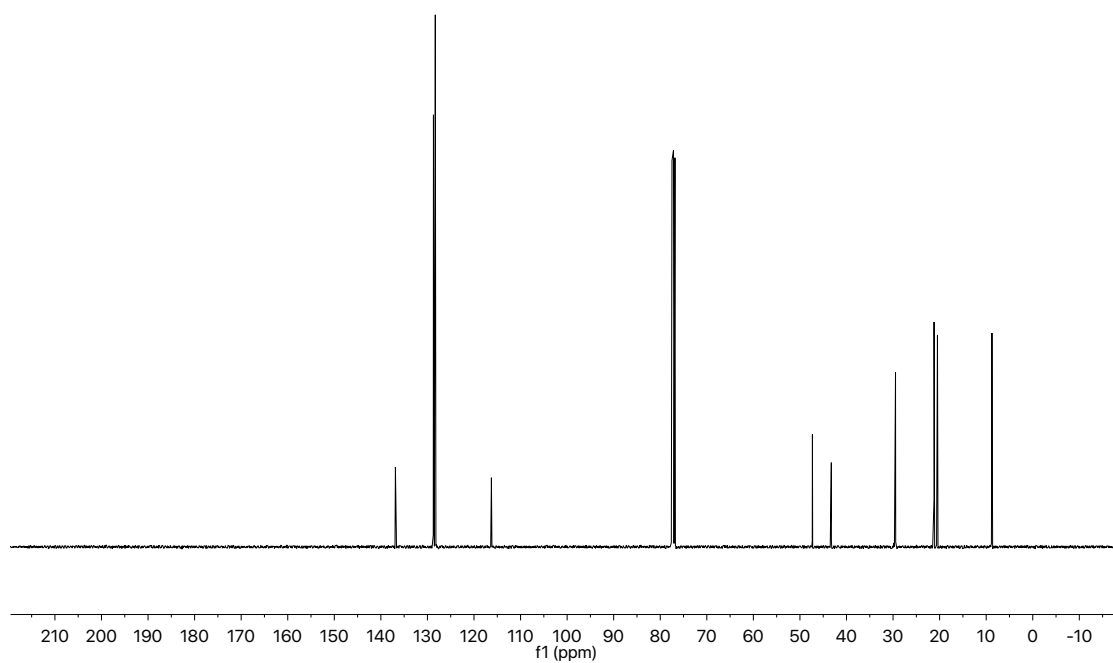


Figure A6.66 ¹³C NMR (101 MHz, CDCl₃) of compound **101**

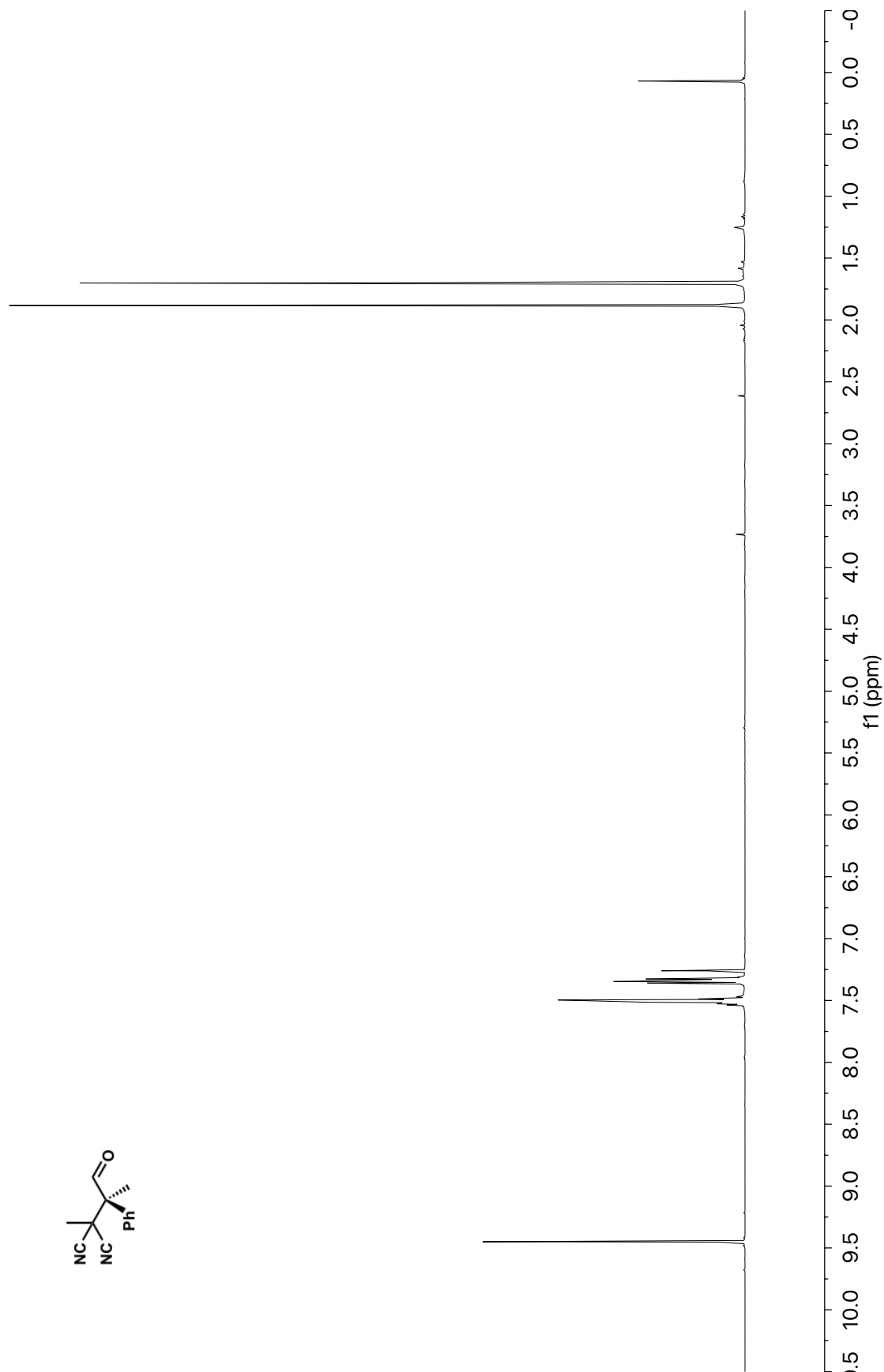


Figure A6.67 ¹H NMR (400 MHz, CDCl₃) of compound **102**

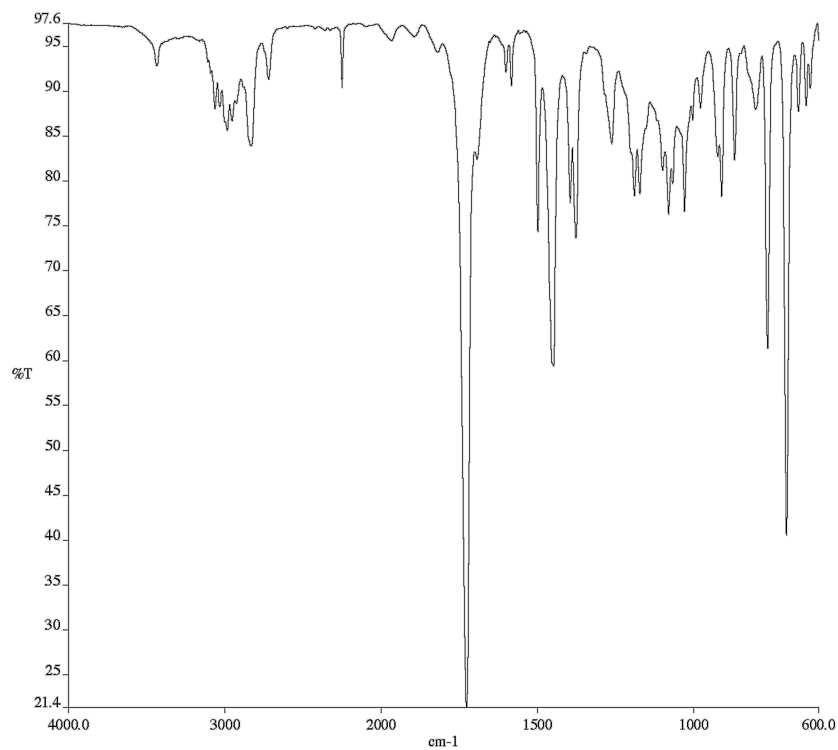


Figure A6.68 Infrared spectrum (Thin Film, NaCl) of compound **102**

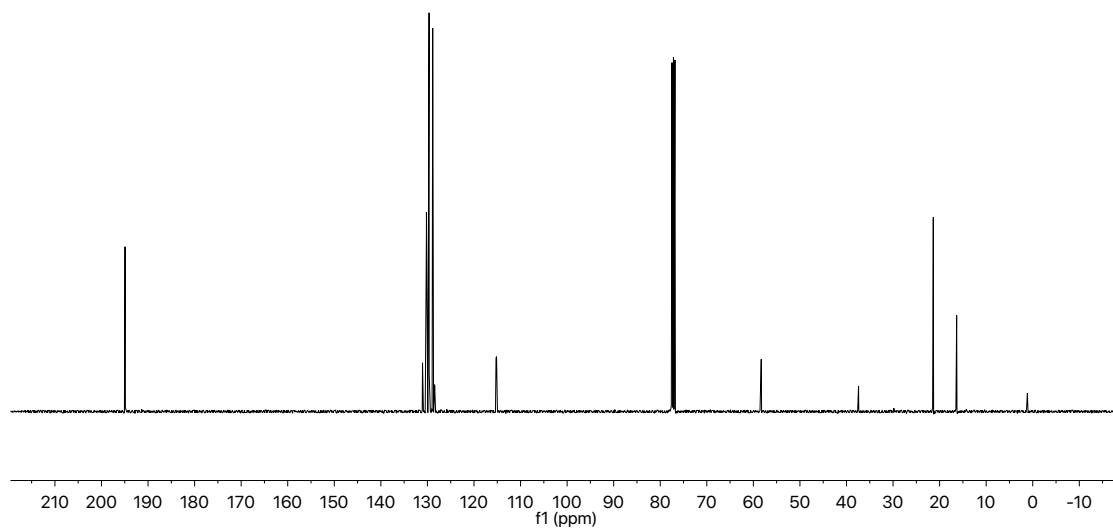


Figure A6.69 ¹³C NMR (101 MHz, CDCl₃) of compound **102**

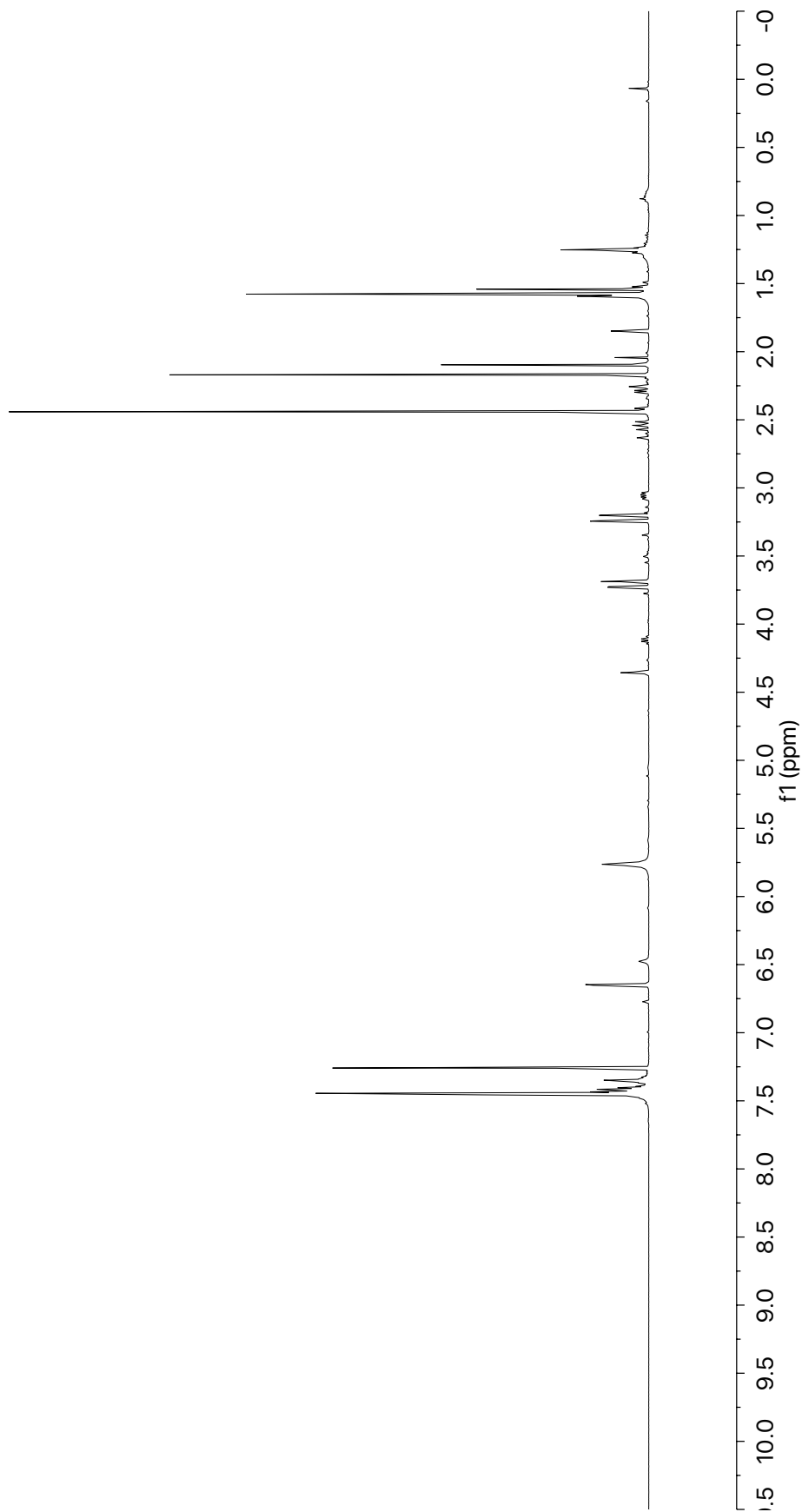
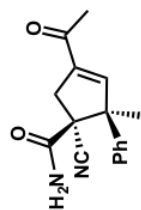


Figure A6.70 ¹H NMR (400 MHz, CDCl₃) of compound **103**

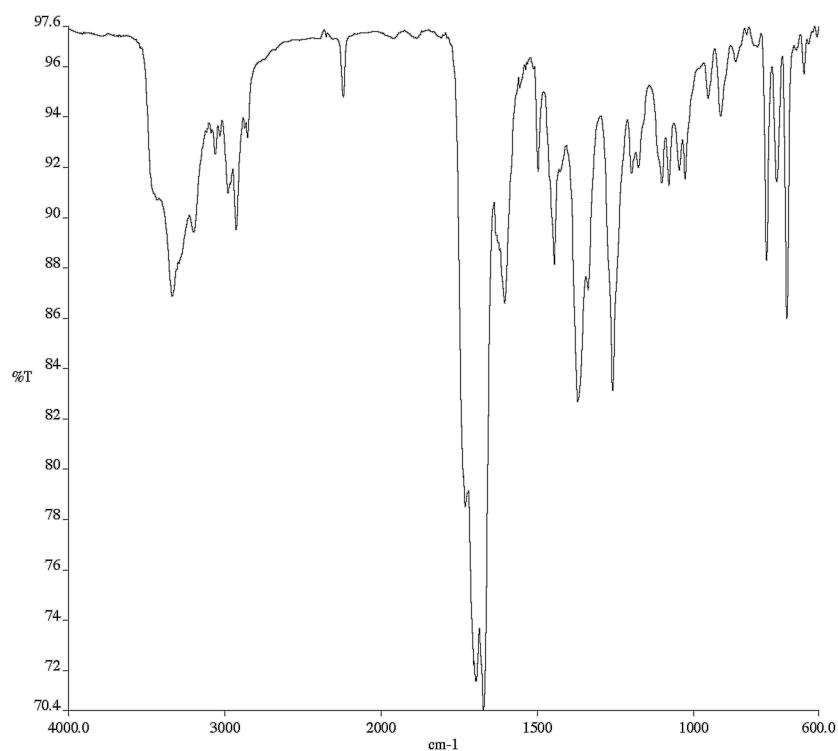


Figure A6.71 Infrared spectrum (Thin Film, NaCl) of compound **103**

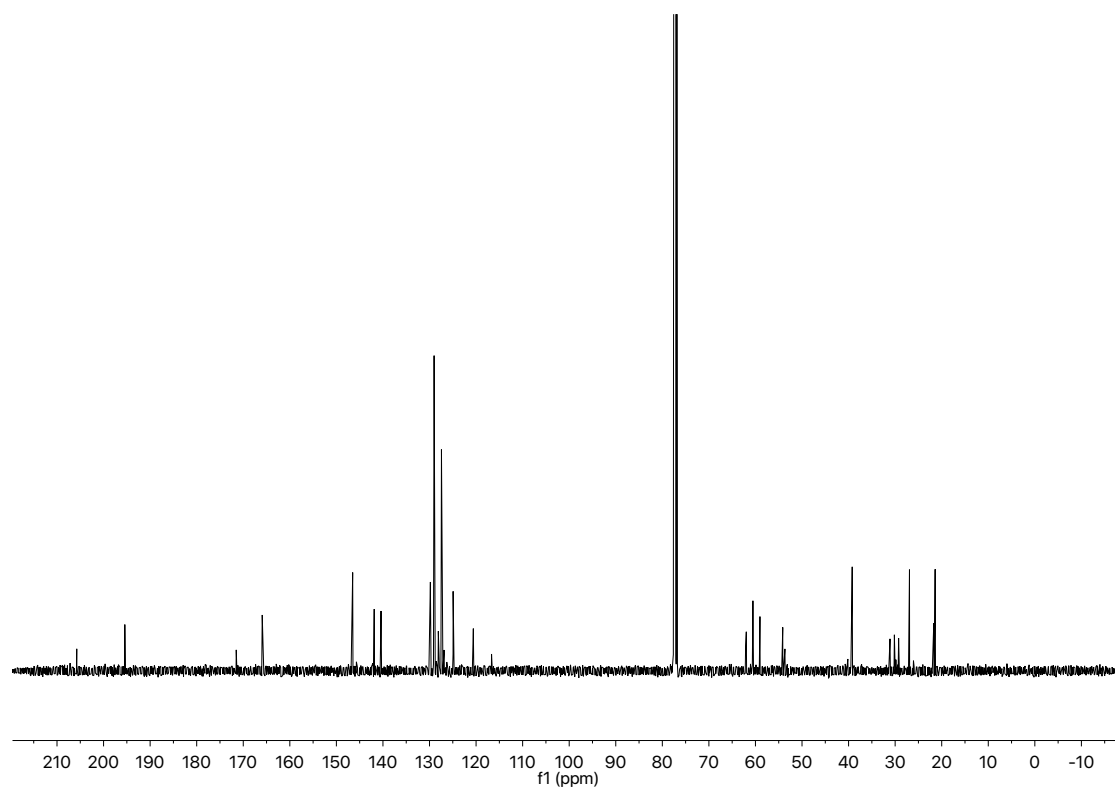


Figure A6.72 ¹³C NMR (101 MHz, CDCl₃) of compound **103**

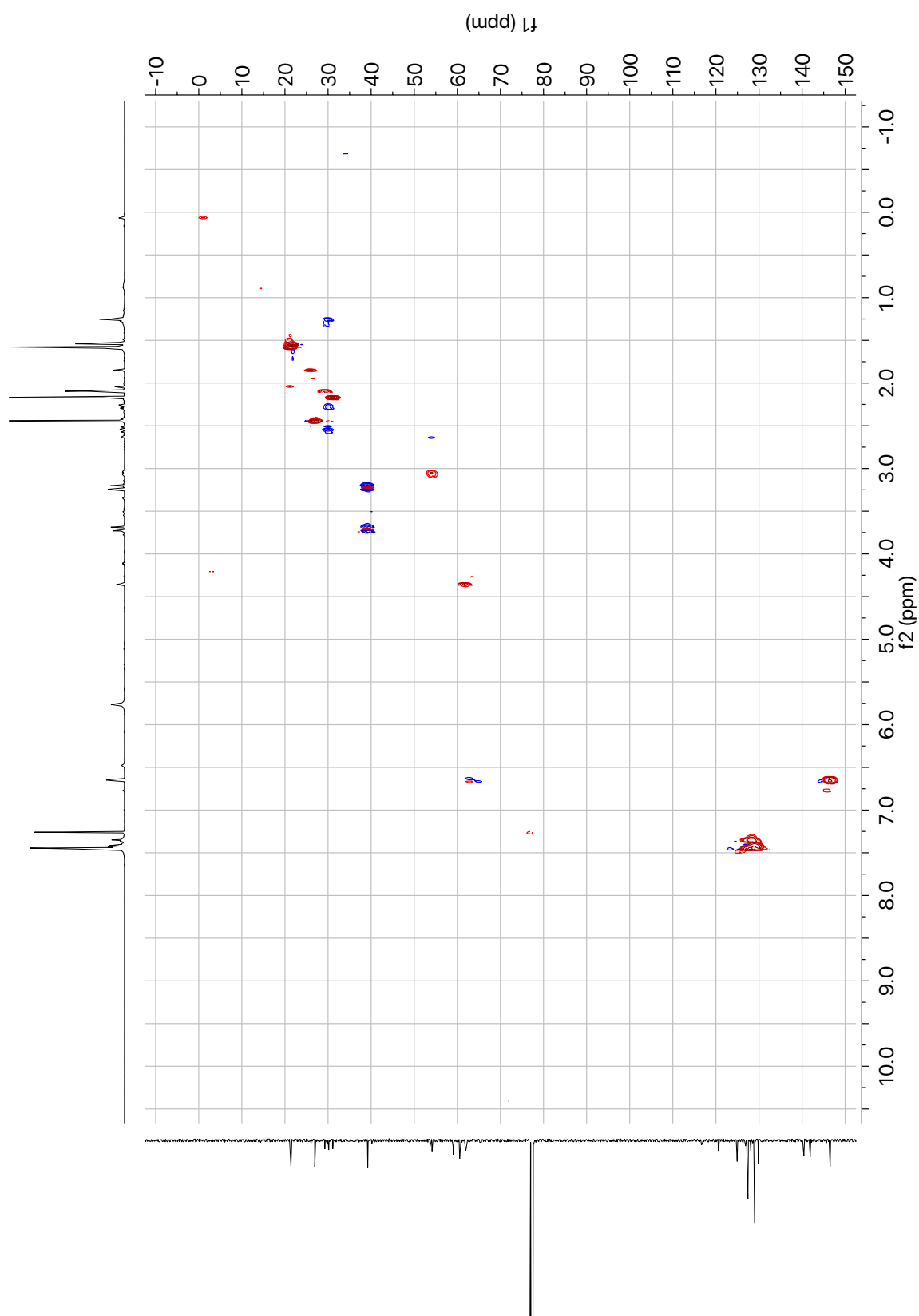


Figure A6.73 HSQC (400 MHz, CDCl_3) of compound **103**

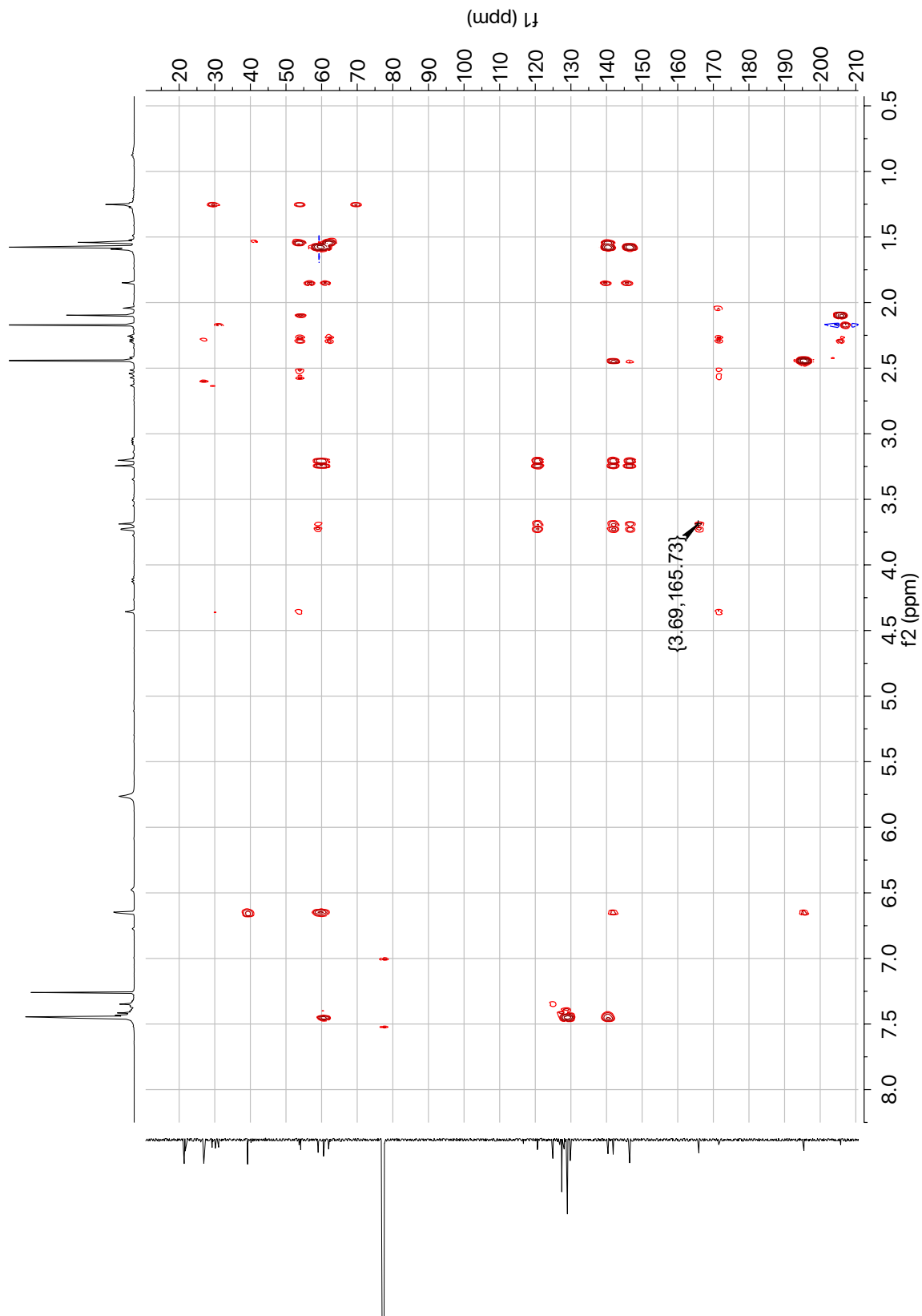


Figure A6.74 HMBC (400 MHz, CDCl_3) of compound **103**

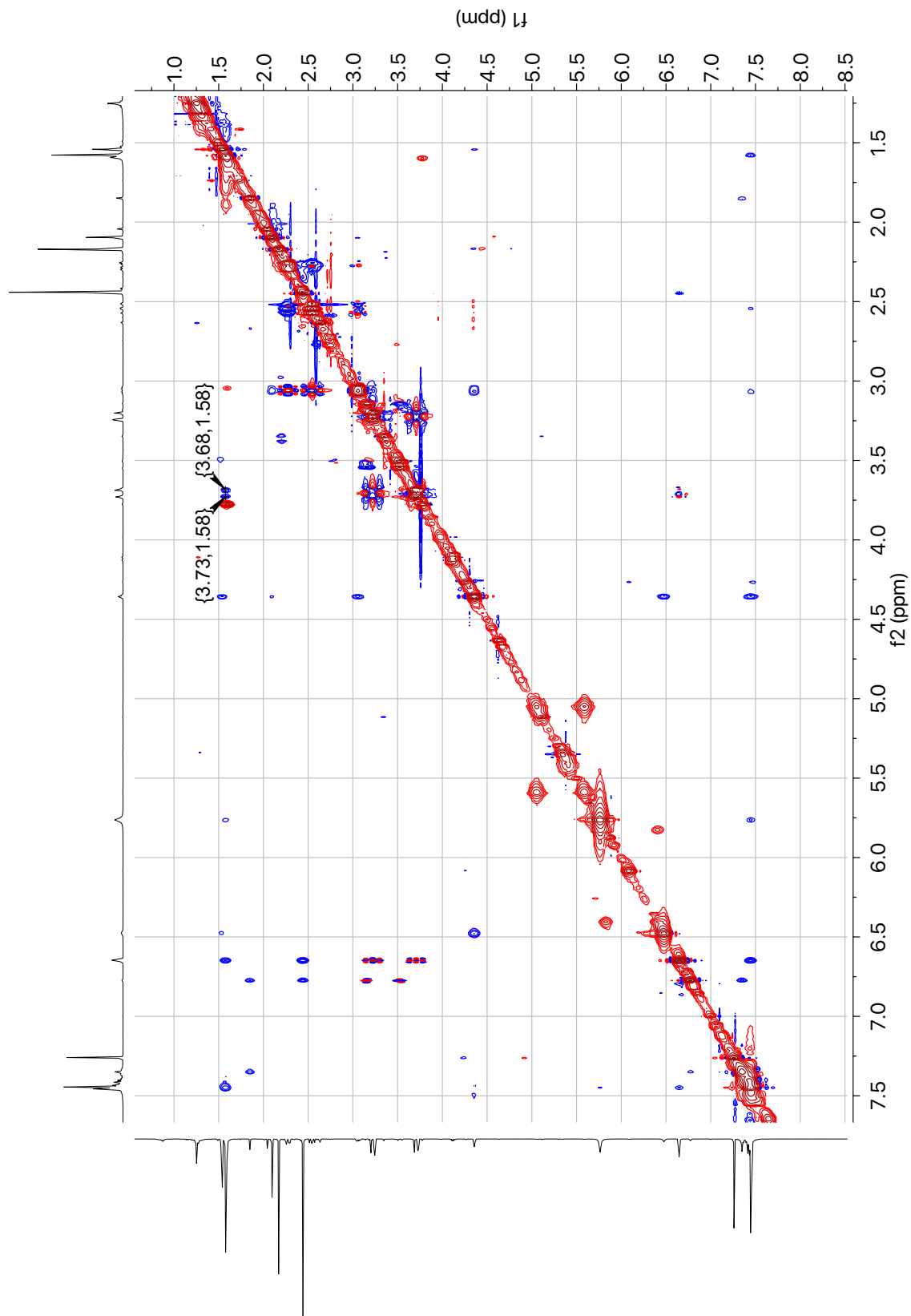


Figure A6.75 NOESY (400 MHz, CDCl_3) of compound **103**

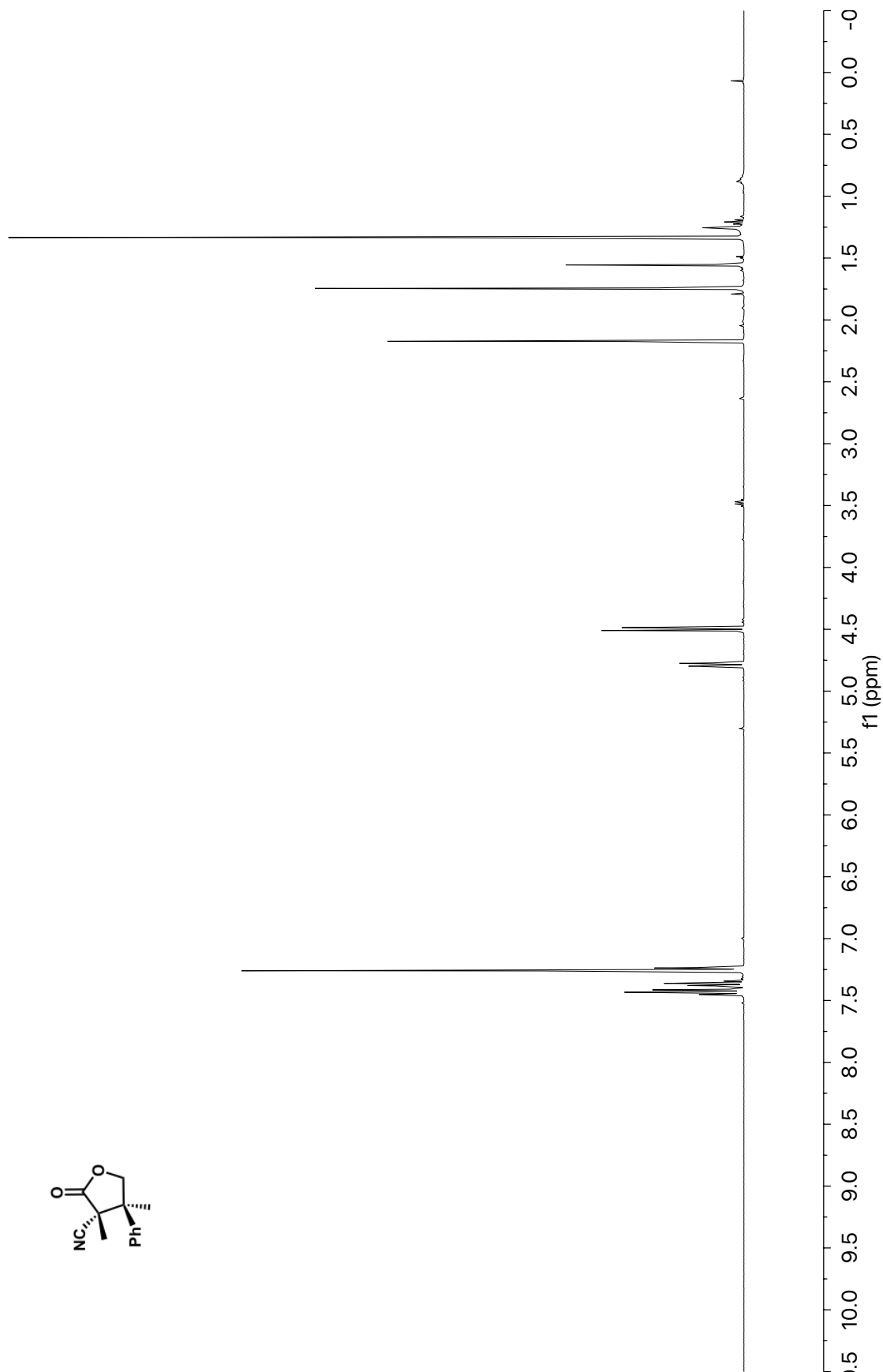


Figure A6.76 ¹H NMR (400 MHz, CDCl₃) of compound **104**

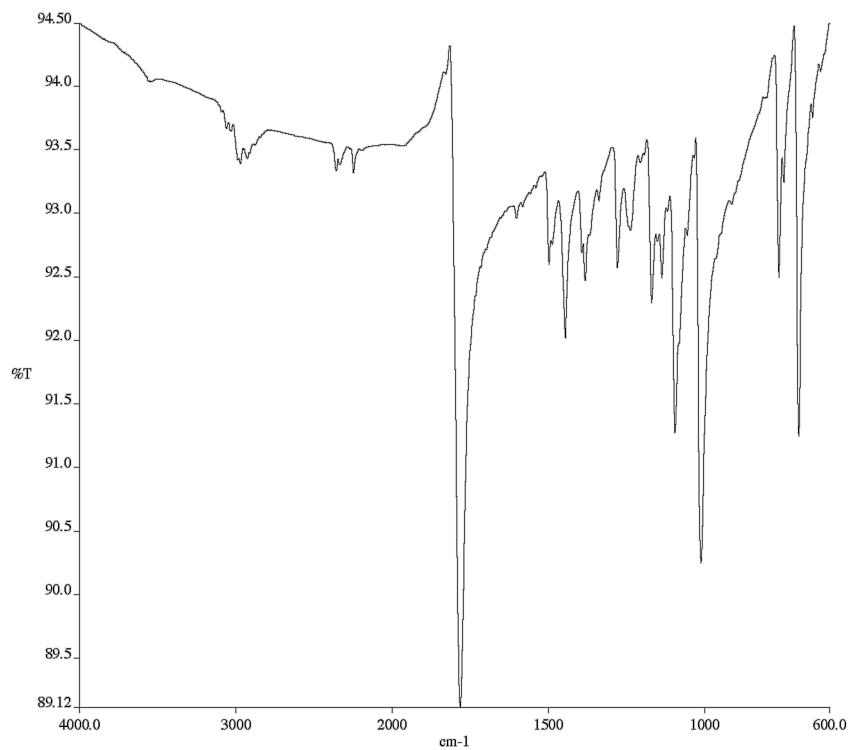


Figure A6.77 Infrared spectrum (Thin Film, NaCl) of compound **104**

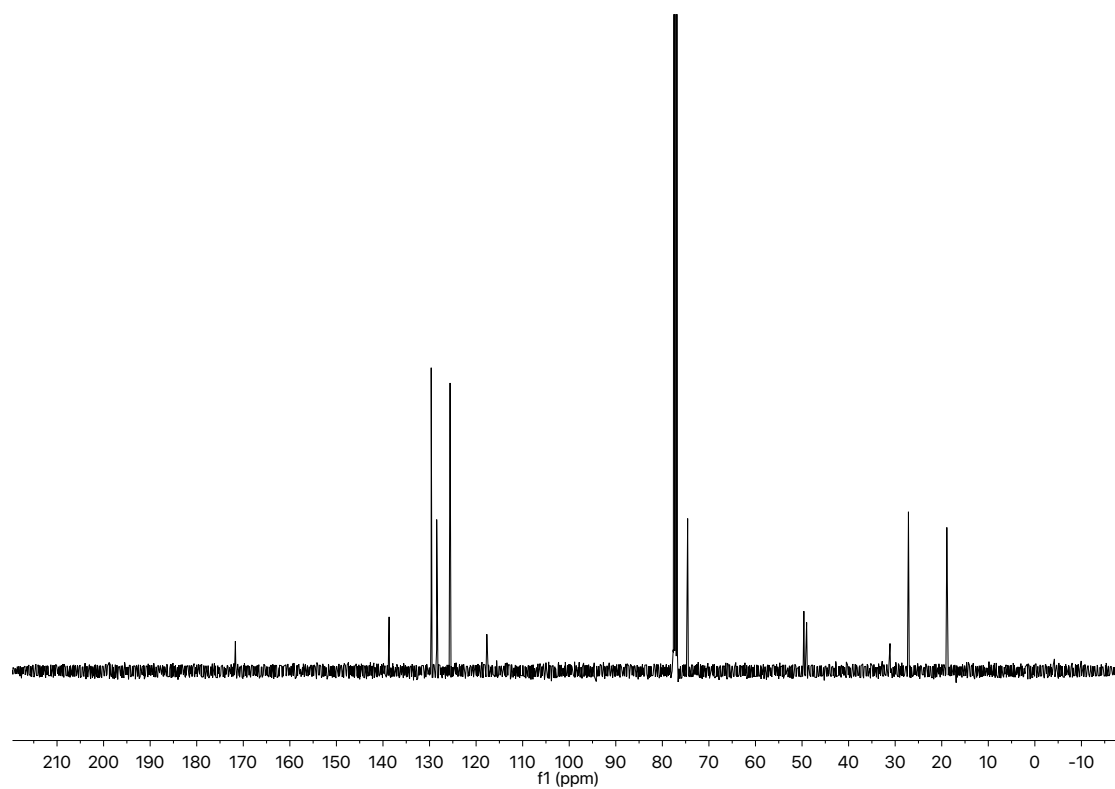


Figure A6.78 ¹³C NMR (101 MHz, CDCl₃) of compound **104**

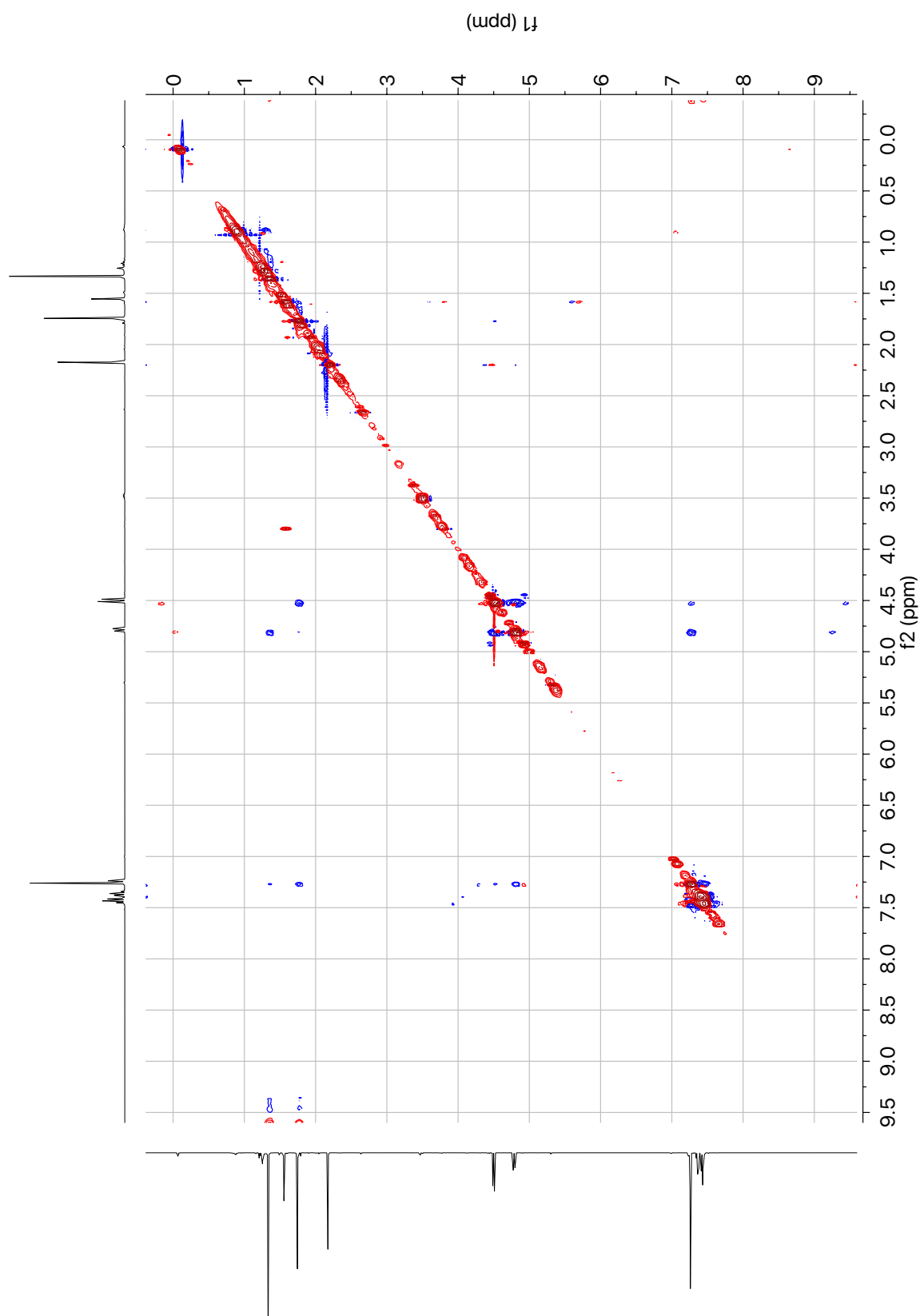


Figure A6.79 NOESY (400 MHz, CDCl_3) of compound **104**

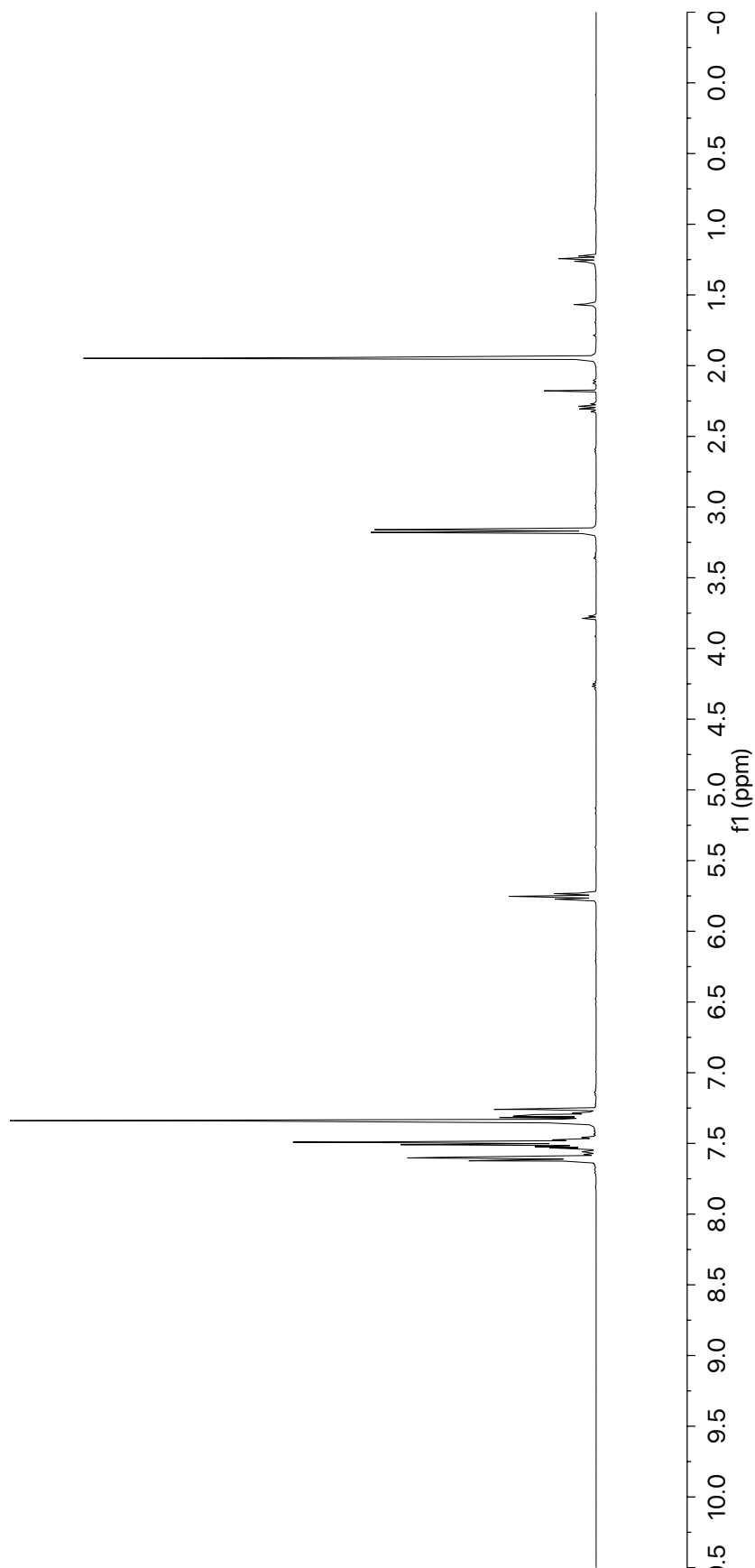
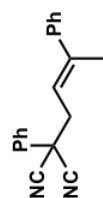


Figure A6.80 ^1H NMR (400 MHz, CDCl_3) of compound **105**

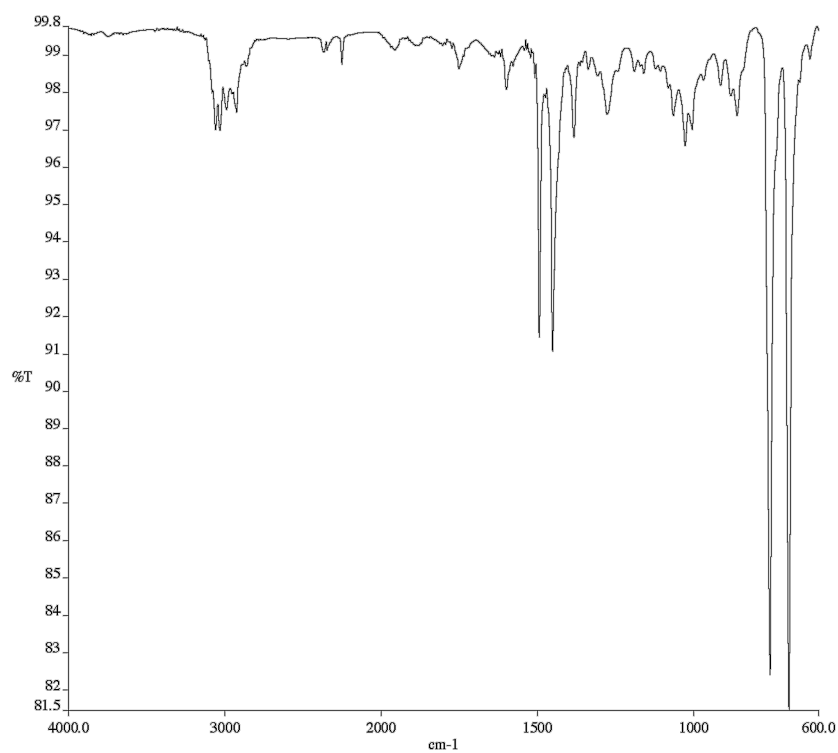


Figure A6.81 Infrared spectrum (Thin Film, NaCl) of compound **105**

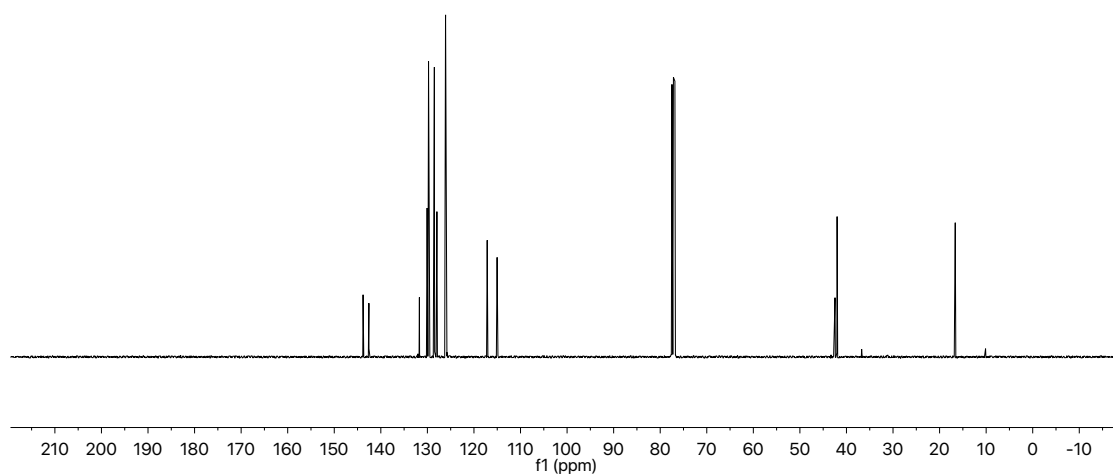


Figure A6.82 ¹³C NMR (101 MHz, CDCl₃) of compound **105**

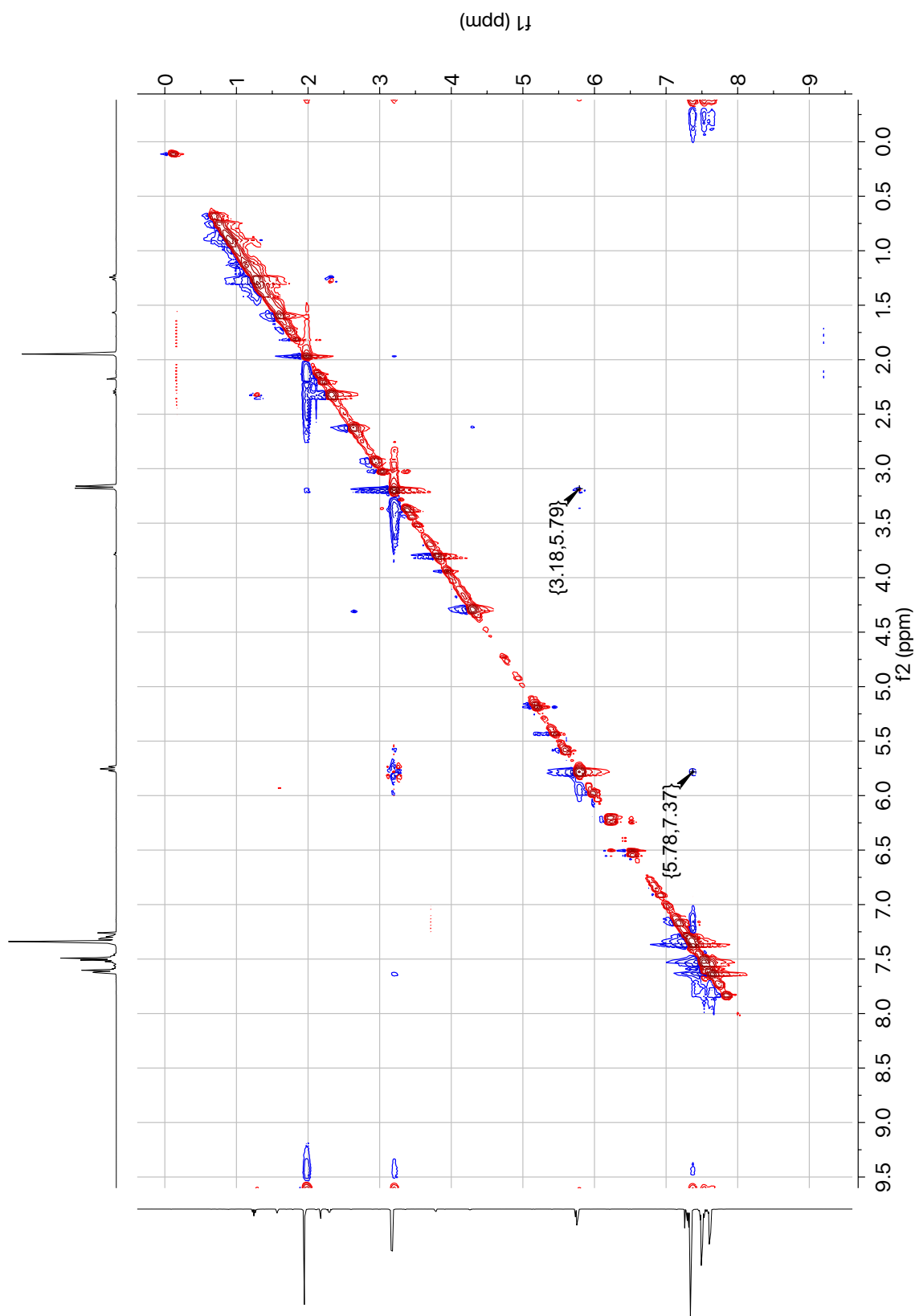


Figure A6.83 NOESY (400 MHz, CDCl_3) of compound **105**

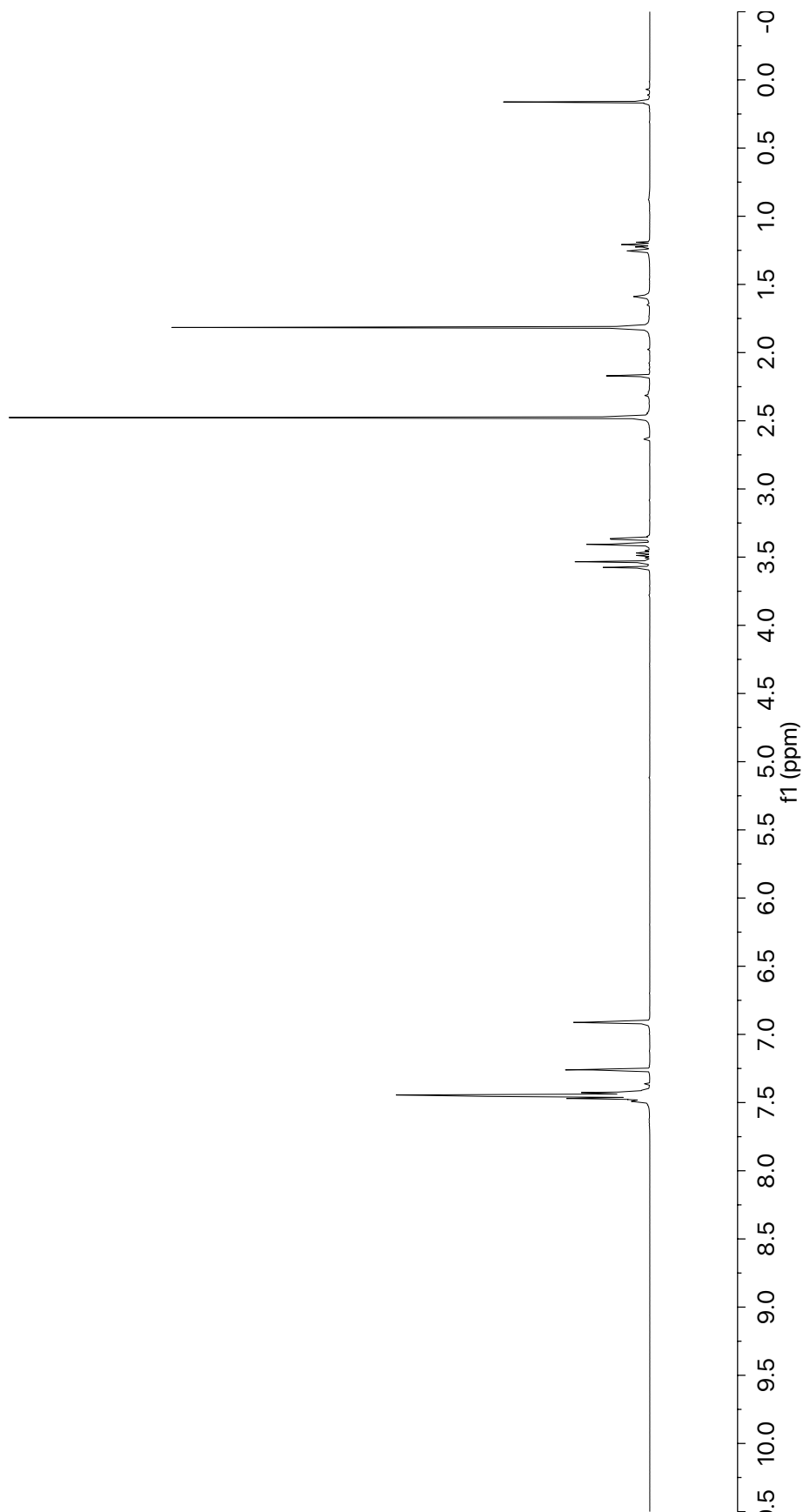
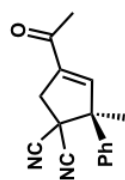


Figure A6.84 ^1H NMR (400 MHz, CDCl_3) of compound **106**

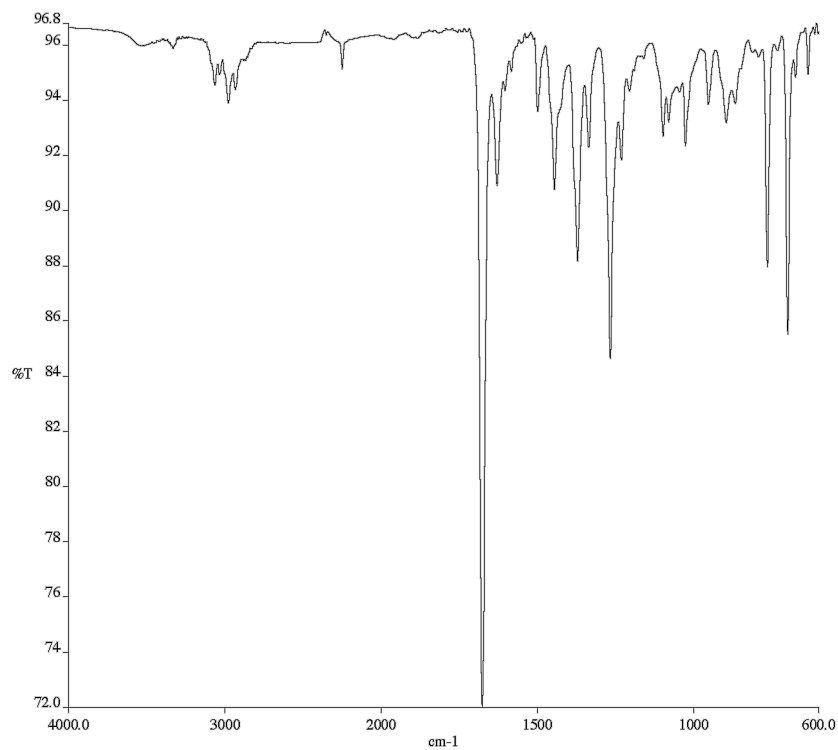


Figure A6.85 Infrared spectrum (Thin Film, NaCl) of compound **106**

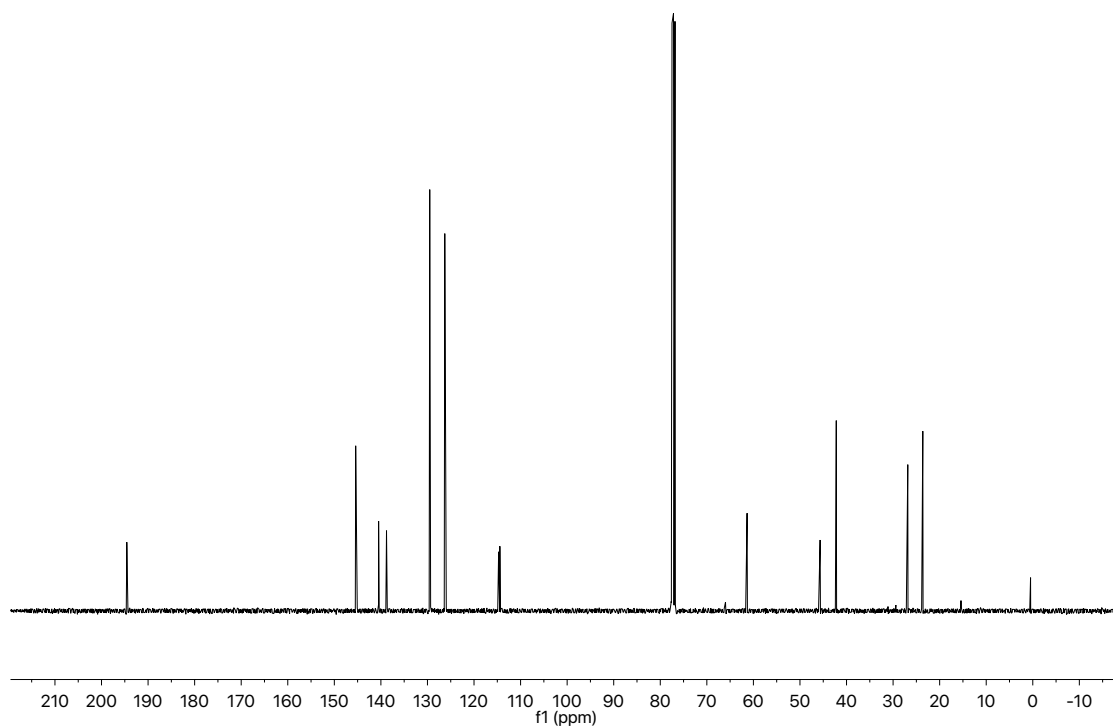


Figure A6.86 ¹³C NMR (101 MHz, CDCl₃) of compound **106**

APPENDIX 7

*X-Ray Crystallography Reports Relevant to Chapter 4:
Enantioselective Synthesis of Vicinal All-Carbon Quaternary Centers
via Iridium-Catalyzed Allylic Alkylation*

A7.1 GENERAL EXPERIMENTAL

Low-temperature diffraction data (ϕ - and ω -scans) were collected on a Bruker AXS D8 VENTURE KAPPA diffractometer coupled to a PHOTON II CPAD detector with Cu K_{α} radiation ($\lambda = 1.54178 \text{ \AA}$) from an I μ S micro-source for the structure of compound **97c**. The structure was solved by direct methods using SHELXS¹ and refined against F^2 on all data by full-matrix least squares with SHELXL-2016² using established refinement techniques.³ All non-hydrogen atoms were refined anisotropically. All hydrogen atoms were included into the model at geometrically calculated positions and refined using a riding model. The isotropic displacement parameters of all hydrogen atoms were fixed to 1.2 times the U value of the atoms they are linked to (1.5 times for methyl groups). All disordered atoms were refined with the help of similarity restraints on the 1,2- and 1,3-distances and displacement parameters as well as enhanced rigid bond restraints for anisotropic displacement parameters.

Compound **97c** crystallizes in the tetragonal space group $I4_1$ with half a molecule in the asymmetric unit. The molecule is located near a crystallographic 2-fold rotation axis and is disordered by the rotation. The phenyl moiety was disordered over four positions, two of which are pairwise related to the other two by the 2-fold rotation. This requires a number of SADI restraints during refinement. We note that a Bayesian analysis of the Friedel pairs (performed using the "Bijvoet-Pair Analysis" routine of PLATON) confirms the absolute stereochemical assignment based on the Flack x . The output of this analysis gives:

Bayesian Statistics

Student_T Nu 99

Select Pairs 752

Theta_Min .. 5.23

Theta_Max ..74.45

P2(true).... 1.000

P3(true).... 0.999

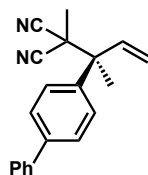
P3(rac-twin) 0.8E-03

P3(false) ..0.8E-08

G 2.0938

G (su) 0.4726

Hooft y -0.5(2)

A7.1.1 X-RAY CRYSTAL STRUCTURE ANALYSIS OF BIS-NITRILE 97c

Bis-nitrile **97c** (95% ee) was recrystallized from boiling hexane to provide crystals suitable for X-ray analysis.

Figure A7.1 X-ray crystal structure of bis-nitrile **97c**

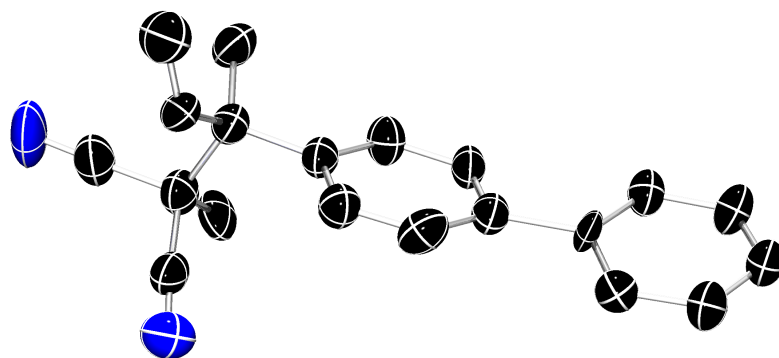


Table A7.1 Crystal data and structure refinement for bis-nitrile **97c**

Empirical formula	C ₂₀ H ₁₈ N ₂	
Formula weight	286.36	
Temperature	100(2) K	
Wavelength	1.54178 Å	
Crystal system	Tetragonal	
Space group	I4 ₁	
Unit cell dimensions	a = 10.0971(4) Å	a = 90°.
	b = 10.0971(4) Å	b = 90°.
	c = 15.5215(7) Å	g = 90°.
Volume	1582.44(14) Å ³	
Z	4	
Density (calculated)	1.202 Mg/m ³	
Absorption coefficient	0.545 mm ⁻¹	
F(000)	608	
Crystal size	0.600 x 0.150 x 0.150 mm ³	
Theta range for data collection	5.226 to 74.482°.	
Index ranges	-12 ≤ h ≤ 12, -12 ≤ k ≤ 12, -17 ≤ l ≤ 19	
Reflections collected	10160	
Independent reflections	1590 [R(int) = 0.0381]	
Completeness to theta = 67.679°	99.6 %	
Absorption correction	Semi-empirical from equivalents	
Max. and min. transmission	0.7538 and 0.5549	
Refinement method	Full-matrix least-squares on F ²	
Data / restraints / parameters	1590 / 823 / 256	
Goodness-of-fit on F ²	1.044	
Final R indices [I > 2σ(I)]	R1 = 0.0422, wR2 = 0.1227	
R indices (all data)	R1 = 0.0433, wR2 = 0.1248	
Absolute structure parameter	-0.6(3)	
Extinction coefficient	n/a	
Largest diff. peak and hole	0.211 and -0.114 e.Å ⁻³	

Table A7.2 Atomic coordinates ($\times 10^4$) and equivalent isotropic displacement parameters ($\text{\AA}^2 \times 10^3$) for **97c**. $U(\text{eq})$ is defined as one third of the trace of the orthogonalized U^j_i tensor.

	x	y	z	U(eq)
C(11)	4978(4)	4611(3)	4288(2)	41(1)
C(12)	3831(6)	4487(6)	4770(4)	50(1)
C(13)	3815(16)	4637(13)	5665(6)	44(2)
C(14)	4960(20)	4930(50)	6109(3)	47(3)
C(15)	6113(19)	5045(15)	5612(9)	58(3)
C(16)	6135(6)	4925(6)	4736(4)	50(1)
C(21)	5150(20)	4990(50)	7046(10)	44(3)
C(22)	4028(19)	5180(30)	7561(12)	58(4)
C(23)	4064(18)	5150(30)	8460(12)	68(4)
C(24)	5262(18)	4980(40)	8853(12)	63(5)
C(25)	6388(16)	4750(30)	8376(10)	69(4)
C(26)	6337(17)	4800(30)	7479(10)	54(3)
C(21A)	4840(30)	4910(40)	7104(13)	43(5)
C(22A)	3718(19)	4470(30)	7512(12)	47(4)
C(23A)	3681(18)	4450(20)	8410(11)	57(4)
C(24A)	4750(30)	4830(40)	8896(17)	56(6)
C(25A)	5830(20)	5330(30)	8484(15)	57(4)
C(26A)	5890(20)	5390(30)	7587(15)	52(4)
C(1)	5012(4)	4373(4)	3312(3)	45(1)
C(2)	6410(11)	3889(10)	3042(7)	52(2)
C(3)	6731(6)	2674(6)	2858(5)	78(2)
C(4)	3908(17)	3438(17)	3046(13)	70(5)
C(5)	4782(5)	5744(4)	2825(3)	51(1)
C(6)	3509(14)	6450(11)	3020(8)	65(3)
C(7)	5866(16)	6713(17)	3030(10)	50(2)
N(1)	6596(5)	7446(5)	3232(4)	78(1)
C(8)	4876(5)	5491(6)	1886(3)	64(1)
N(2)	5010(30)	5250(20)	1173(3)	100(6)

Table A7.3 Bond lengths [\AA] and angles [$^\circ$] for **97c**

C(11)-C(12)	1.385(7)
C(11)-C(16)	1.396(7)
C(11)-C(1)	1.534(6)
C(12)-C(13)	1.398(11)
C(12)-H(12)	0.9500
C(13)-C(14)	1.380(16)
C(13)-H(13)	0.9500
C(14)-C(15)	1.400(16)
C(14)-C(21)	1.467(18)
C(15)-C(16)	1.366(14)
C(15)-H(15)	0.9500
C(16)-H(16)	0.9500
C(21)-C(26)	1.390(17)
C(21)-C(22)	1.397(17)
C(22)-C(23)	1.396(17)
C(22)-H(22)	0.9500
C(23)-C(24)	1.366(18)
C(23)-H(23)	0.9500
C(24)-C(25)	1.376(16)
C(24)-H(24)	0.9500
C(25)-C(26)	1.394(15)
C(25)-H(25)	0.9500
C(26)-H(26)	0.9500
C(21A)-C(22A)	1.374(19)
C(21A)-C(26A)	1.384(19)
C(22A)-C(23A)	1.395(17)
C(22A)-H(22A)	0.9500
C(23A)-C(24A)	1.37(2)
C(23A)-H(23A)	0.9500
C(24A)-C(25A)	1.36(2)
C(24A)-H(24A)	0.9500
C(25A)-C(26A)	1.395(18)
C(25A)-H(25A)	0.9500
C(26A)-H(26A)	0.9500
C(1)-C(4)	1.518(16)
C(1)-C(2)	1.551(11)

C(1)-C(5)	1.594(6)
C(2)-C(3)	1.301(10)
C(2)-H(2)	0.9500
C(3)-H(3A)	0.9500
C(3)-H(3B)	0.9500
C(4)-H(4A)	0.9800
C(4)-H(4B)	0.9800
C(4)-H(4C)	0.9800
C(5)-C(8)	1.482(7)
C(5)-C(6)	1.501(13)
C(5)-C(7)	1.503(15)
C(6)-H(6A)	0.9800
C(6)-H(6B)	0.9800
C(6)-H(6C)	0.9800
C(7)-N(1)	1.091(15)
C(8)-N(2)	1.141(9)
C(12)-C(11)-C(16)	116.9(3)
C(12)-C(11)-C(1)	122.6(4)
C(16)-C(11)-C(1)	120.5(4)
C(11)-C(12)-C(13)	122.5(8)
C(11)-C(12)-H(12)	118.8
C(13)-C(12)-H(12)	118.8
C(14)-C(13)-C(12)	120.7(9)
C(14)-C(13)-H(13)	119.7
C(12)-C(13)-H(13)	119.7
C(13)-C(14)-C(15)	116.0(5)
C(13)-C(14)-C(21)	127.6(17)
C(15)-C(14)-C(21)	115.9(18)
C(16)-C(15)-C(14)	123.8(11)
C(16)-C(15)-H(15)	118.1
C(14)-C(15)-H(15)	118.1
C(15)-C(16)-C(11)	120.1(9)
C(15)-C(16)-H(16)	119.9
C(11)-C(16)-H(16)	119.9
C(26)-C(21)-C(22)	116.1(14)
C(26)-C(21)-C(14)	126(2)
C(22)-C(21)-C(14)	118(2)
C(23)-C(22)-C(21)	123.3(16)

C(23)-C(22)-H(22)	118.3
C(21)-C(22)-H(22)	118.3
C(24)-C(23)-C(22)	118.1(16)
C(24)-C(23)-H(23)	121.0
C(22)-C(23)-H(23)	121.0
C(23)-C(24)-C(25)	120.9(15)
C(23)-C(24)-H(24)	119.5
C(25)-C(24)-H(24)	119.5
C(24)-C(25)-C(26)	120.0(15)
C(24)-C(25)-H(25)	120.0
C(26)-C(25)-H(25)	120.0
C(21)-C(26)-C(25)	121.3(13)
C(21)-C(26)-H(26)	119.3
C(25)-C(26)-H(26)	119.3
C(22A)-C(21A)-C(26A)	119.6(19)
C(21A)-C(22A)-C(23A)	119.1(16)
C(21A)-C(22A)-H(22A)	120.5
C(23A)-C(22A)-H(22A)	120.5
C(24A)-C(23A)-C(22A)	121.7(17)
C(24A)-C(23A)-H(23A)	119.1
C(22A)-C(23A)-H(23A)	119.1
C(25A)-C(24A)-C(23A)	118(2)
C(25A)-C(24A)-H(24A)	120.8
C(23A)-C(24A)-H(24A)	120.8
C(24A)-C(25A)-C(26A)	121(2)
C(24A)-C(25A)-H(25A)	119.5
C(26A)-C(25A)-H(25A)	119.5
C(21A)-C(26A)-C(25A)	119.8(18)
C(21A)-C(26A)-H(26A)	120.1
C(25A)-C(26A)-H(26A)	120.1
C(4)-C(1)-C(11)	110.4(8)
C(4)-C(1)-C(2)	113.5(9)
C(11)-C(1)-C(2)	109.7(6)
C(4)-C(1)-C(5)	107.7(7)
C(11)-C(1)-C(5)	109.2(3)
C(2)-C(1)-C(5)	106.2(5)
C(3)-C(2)-C(1)	125.7(8)
C(3)-C(2)-H(2)	117.1

C(1)-C(2)-H(2)	117.1
C(2)-C(3)-H(3A)	120.0
C(2)-C(3)-H(3B)	120.0
H(3A)-C(3)-H(3B)	120.0
C(1)-C(4)-H(4A)	109.5
C(1)-C(4)-H(4B)	109.5
H(4A)-C(4)-H(4B)	109.5
C(1)-C(4)-H(4C)	109.5
H(4A)-C(4)-H(4C)	109.5
H(4B)-C(4)-H(4C)	109.5
C(8)-C(5)-C(6)	109.6(7)
C(8)-C(5)-C(7)	105.9(7)
C(6)-C(5)-C(7)	105.8(8)
C(8)-C(5)-C(1)	107.9(4)
C(6)-C(5)-C(1)	116.2(5)
C(7)-C(5)-C(1)	111.0(8)
C(5)-C(6)-H(6A)	109.5
C(5)-C(6)-H(6B)	109.5
H(6A)-C(6)-H(6B)	109.5
C(5)-C(6)-H(6C)	109.5
H(6A)-C(6)-H(6C)	109.5
H(6B)-C(6)-H(6C)	109.5
N(1)-C(7)-C(5)	174.5(14)
N(2)-C(8)-C(5)	176(2)

Table A7.4 Anisotropic displacement parameters ($\text{\AA}^2 \times 10^3$) for **97c**. The anisotropic displacement factor exponent takes the form: $-2\pi^2 [h^2 a^{*2} U^{11} + \dots + 2 h k a^* b^* U^{12}]$

	U ¹¹	U ²²	U ³³	U ²³	U ¹³	U ¹²
C(11)	47(2)	43(2)	34(2)	1(1)	1(1)	4(2)
C(12)	42(2)	67(3)	43(2)	2(3)	5(2)	2(3)
C(13)	53(3)	48(5)	32(3)	2(3)	8(2)	3(3)
C(14)	65(3)	39(7)	37(2)	1(4)	6(5)	7(3)
C(15)	55(3)	62(8)	58(4)	-15(4)	-8(3)	-3(4)
C(16)	49(2)	56(3)	46(3)	-3(3)	4(2)	-5(3)

C(21)	56(8)	31(5)	44(5)	-5(6)	10(5)	1(8)
C(22)	63(9)	67(8)	45(6)	1(6)	4(5)	-1(8)
C(23)	80(9)	83(9)	40(6)	-1(6)	9(6)	-2(10)
C(24)	85(10)	69(10)	36(6)	-5(6)	11(6)	-3(10)
C(25)	82(9)	89(9)	36(5)	-11(4)	5(5)	-14(8)
C(26)	64(8)	72(8)	26(4)	-3(4)	3(4)	-7(7)
C(21A)	64(10)	47(10)	18(6)	-10(7)	4(7)	2(9)
C(22A)	51(8)	55(9)	36(6)	0(5)	5(5)	7(7)
C(23A)	64(9)	69(10)	37(6)	-11(6)	5(6)	5(7)
C(24A)	75(11)	58(11)	35(8)	-3(6)	2(7)	-2(8)
C(25A)	71(10)	63(10)	38(7)	1(7)	-4(7)	-4(9)
C(26A)	64(10)	46(8)	46(7)	1(7)	4(6)	-3(9)
C(1)	48(2)	47(2)	39(2)	-5(2)	4(2)	-2(1)
C(2)	66(3)	41(4)	49(3)	-11(3)	19(2)	-3(3)
C(3)	82(3)	66(3)	86(4)	-8(3)	32(3)	0(3)
C(4)	79(7)	73(8)	57(6)	-24(5)	15(5)	-25(6)
C(5)	57(2)	59(2)	37(3)	2(2)	-3(2)	-2(2)
C(6)	91(5)	51(6)	53(3)	21(3)	18(3)	17(3)
C(7)	67(4)	48(3)	36(4)	-1(3)	-2(3)	2(3)
N(1)	86(3)	62(2)	84(3)	-4(2)	7(2)	-12(2)
C(8)	64(3)	84(3)	45(3)	4(2)	0(2)	-21(3)
N(2)	100(3)	164(18)	35(2)	-7(4)	8(4)	-60(11)

Table A7.5 Hydrogen coordinates ($\times 10^4$) and isotropic displacement parameters ($\text{\AA}^2 \times 10^3$) for **97c**

	x	y	z	U(eq)
H(12)	3024	4292	4482	61
H(13)	3007	4534	5971	53
H(15)	6925	5212	5901	70
H(16)	6940	5055	4430	60
H(22)	3202	5331	7286	70
H(23)	3277	5256	8789	81
H(24)	5318	5012	9463	76
H(25)	7201	4562	8658	83
H(26)	7131	4701	7157	65

H(22A)	2977	4171	7187	57
H(23A)	2893	4179	8693	68
H(24A)	4744	4738	9506	67
H(25A)	6561	5645	8813	69
H(26A)	6643	5751	7309	62
H(2)	7091	4536	3009	62
H(3A)	6082	1995	2883	93
H(3B)	7615	2467	2698	93
H(4A)	3973	3256	2428	104
H(4B)	3049	3848	3172	104
H(4C)	3988	2607	3368	104
H(6A)	3559	7361	2805	98
H(6B)	3364	6462	3644	98
H(6C)	2773	5988	2738	98

Table A7.6 Torsion angles [°] for **97c**

C(16)-C(11)-C(12)-C(13)	-1.3(8)
C(1)-C(11)-C(12)-C(13)	176.6(7)
C(11)-C(12)-C(13)-C(14)	1(3)
C(12)-C(13)-C(14)-C(15)	-1(5)
C(12)-C(13)-C(14)-C(21)	-173(4)
C(13)-C(14)-C(15)-C(16)	3(5)
C(21)-C(14)-C(15)-C(16)	175(3)
C(14)-C(15)-C(16)-C(11)	-3(3)
C(12)-C(11)-C(16)-C(15)	2.5(9)
C(1)-C(11)-C(16)-C(15)	-175.4(8)
C(13)-C(14)-C(21)-C(26)	154(3)
C(15)-C(14)-C(21)-C(26)	-18(6)
C(13)-C(14)-C(21)-C(22)	-22(6)
C(15)-C(14)-C(21)-C(22)	166(3)
C(26)-C(21)-C(22)-C(23)	-1(3)
C(14)-C(21)-C(22)-C(23)	175(4)
C(21)-C(22)-C(23)-C(24)	2(3)
C(22)-C(23)-C(24)-C(25)	-4(4)
C(23)-C(24)-C(25)-C(26)	5(4)

C(22)-C(21)-C(26)-C(25)	2(3)
C(14)-C(21)-C(26)-C(25)	-174(4)
C(24)-C(25)-C(26)-C(21)	-4(3)
C(26A)-C(21A)-C(22A)-C(23A)	-3(3)
C(21A)-C(22A)-C(23A)-C(24A)	-2(3)
C(22A)-C(23A)-C(24A)-C(25A)	6(5)
C(23A)-C(24A)-C(25A)-C(26A)	-4(5)
C(22A)-C(21A)-C(26A)-C(25A)	4(3)
C(24A)-C(25A)-C(26A)-C(21A)	-1(4)
C(12)-C(11)-C(1)-C(4)	-25.7(9)
C(16)-C(11)-C(1)-C(4)	152.2(8)
C(12)-C(11)-C(1)-C(2)	-151.5(6)
C(16)-C(11)-C(1)-C(2)	26.4(6)
C(12)-C(11)-C(1)-C(5)	92.6(5)
C(16)-C(11)-C(1)-C(5)	-89.6(5)
C(4)-C(1)-C(2)-C(3)	-20.9(15)
C(11)-C(1)-C(2)-C(3)	103.2(11)
C(5)-C(1)-C(2)-C(3)	-138.9(9)
C(4)-C(1)-C(5)-C(8)	-62.4(9)
C(11)-C(1)-C(5)-C(8)	177.7(4)
C(2)-C(1)-C(5)-C(8)	59.5(6)
C(4)-C(1)-C(5)-C(6)	61.1(11)
C(11)-C(1)-C(5)-C(6)	-58.8(8)
C(2)-C(1)-C(5)-C(6)	-177.0(8)
C(4)-C(1)-C(5)-C(7)	-178.0(10)
C(11)-C(1)-C(5)-C(7)	62.1(7)
C(2)-C(1)-C(5)-C(7)	-56.1(8)

A7.2 REFERENCES AND NOTES

- (1) Sheldrick, G. M. *Acta Cryst.* **1990**, A46, 467–473.
- (2) Sheldrick, G. M. *Acta Cryst.* **2015**, C71, 3–8.
- (3) Müller, P. *Crystallography Reviews* **2009**, 15, 57–83.

CHAPTER 5

Stereoselective Iridium-Catalyzed Allylic Alkylation

in the Stoltz Laboratory: A Summary[†]

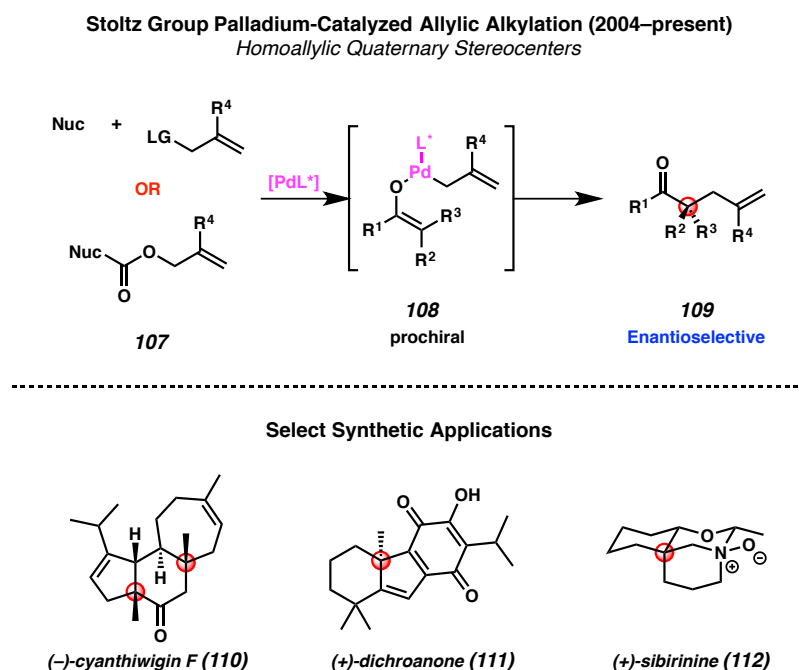
5.1 INTRODUCTION

To enable our ongoing research program focused on the synthesis of complex natural products, we became interested in developing robust methods for the synthesis of stereochemically rich building blocks containing quaternary stereocenters. As a result, our group has developed a range of technologies for the enantioselective preparation of all-carbon quaternary stereocenters.¹ Perhaps most notably, we reported a general asymmetric palladium-catalyzed allylic alkylation method to provide access to a wide variety of products **109** bearing a homoallylic quaternary stereocenter (Figure 5.1, top).² Over the past decade, we have expanded this methodology to a broad array of substrates **107**³ and applied this chemistry to facilitate expedient total syntheses of a variety of

[†] Portions of this chapter have been reproduced from Shockley, S. E.,[‡] Hethcox, J. C.,[‡] Stoltz, B. M. *Manuscript submitted*.

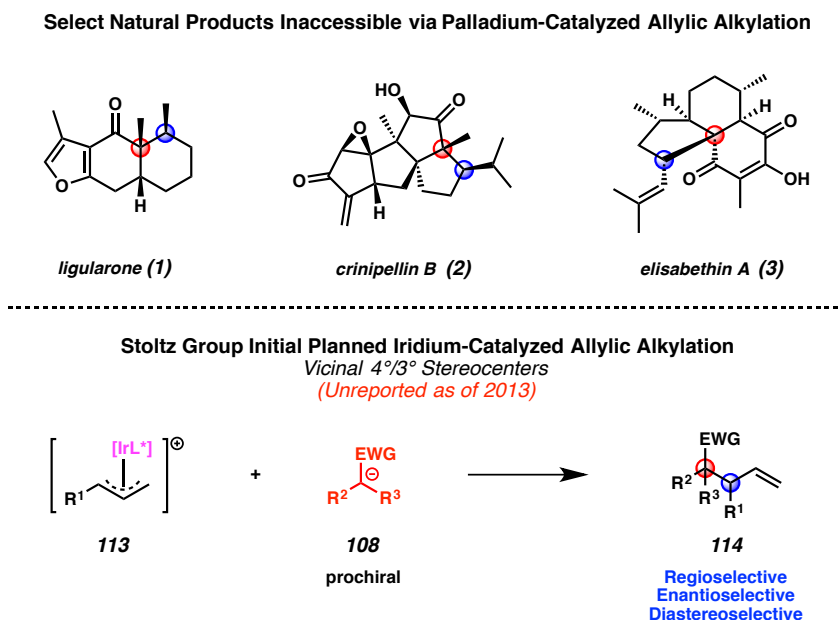
natural products, including (–)-cyanthiwigin F (**110**),⁴ (+)-dichroanone (**111**),⁵ and (+)-sibirinine (**112**, Figure 5.1, bottom).⁶

Figure 5.1 Stoltz group contributions to palladium-catalyzed allylic alkylation methodology and application in natural product total synthesis



Despite its extensive substrate tolerance, our palladium-catalyzed allylic alkylation technology is limited to the synthesis of isolated stereocenters. Thus, to date, this methodology is not amenable to the direct preparation of vicinal stereocenters, which are found in a variety of synthetic targets such as ligularone (**1**), crinipellin B (**2**), and elisabethin A (**3**, Figure 5.2, top). Inspired by these diverse and numerous stereodyad-containing natural products, we sought to expand our stereoselective allylic alkylation research program to include iridium-catalyzed processes that do enable the construction of such vicinal stereocenters **114** (Figure 5.2, bottom).

Figure 5.2 Stereodyad-containing natural products as inspiration for the development of novel iridium-catalyzed allylic alkylation technology

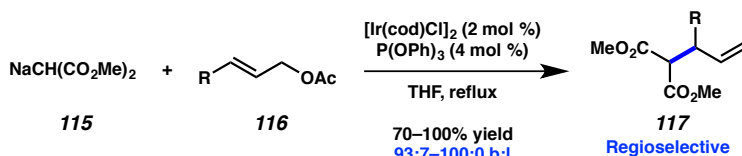


While the aforementioned palladium-catalyzed allylic alkylation has been under exploration since the 1960s,⁷ iridium-catalyzed allylic alkylation is a relatively new area of research. Takeuchi reported the first example of iridium-catalyzed allylic alkylation in 1997 using malonate nucleophiles **115**, demonstrating that iridium catalysts can provide high branched selectivity (branched to linear ratio, b:l) in contrast to palladium catalysts that favor the synthesis of linear products (Figure 5.3a).^{8,9} Shortly thereafter, Helmchen reported that the reaction could be rendered enantioselective with the inclusion of chiral phosphinooxazoline ligand **L12** (Figure 5.3b).¹⁰ In 2003, Takemoto disclosed the first report of a diastereoselective iridium-catalyzed allylic alkylation reaction, wherein prochiral nucleophiles **120** were utilized to form vicinal trisubstituted and tertiary stereocenters **122** (Figure 5.3c, top).¹¹ It was then a decade later before the next report of diastereoselective iridium-catalyzed allylic alkylation was disclosed, which this time

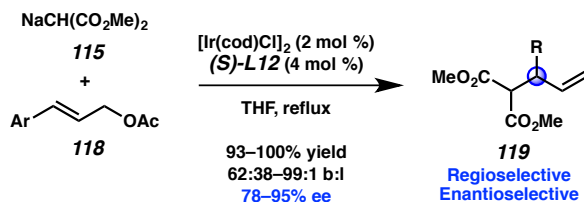
enabled the preparation of vicinal tertiary and tetra-substituted stereocenters **125** (Figure 5.3c, bottom).¹²

Figure 5.3 Timeline for the development of iridium-catalyzed allylic alkylation prior to the Stoltz group's entry into the field

a) First Report of Iridium-Catalyzed Allylic Alkylation Takeuchi (1997)

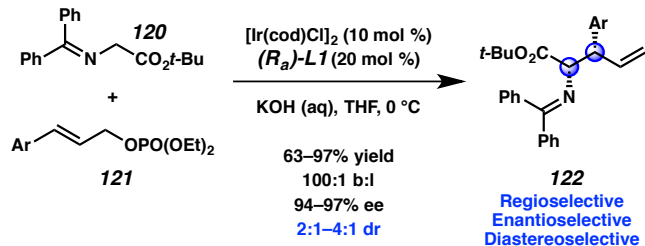


b) First Enantioselective Iridium-Catalyzed Allylic Alkylation Helmchen (1997)

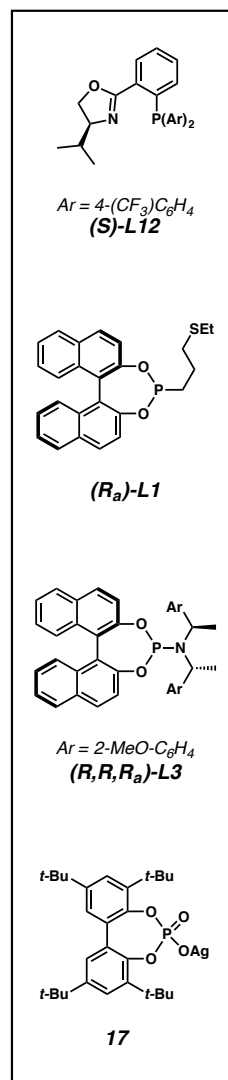
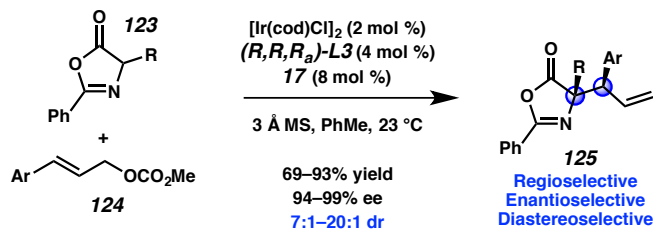


c) First Diastereoselective Iridium-Catalyzed Allylic Alkylations

Takemoto (2003)



Hartwig (2013)



Despite these seminal reports, when our group entered the field in 2013, there were no examples of an iridium-catalyzed allylic alkylation reaction to form a single all-

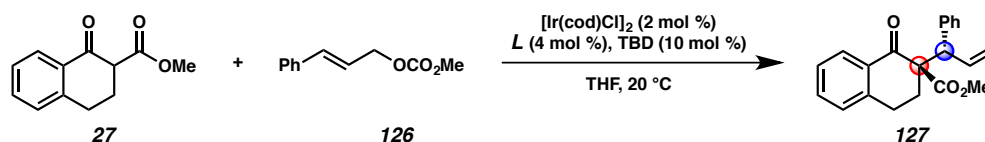
carbon quaternary stereocenter, let alone a stereocenter containing an all-carbon quaternary stereocenter.¹³ Therefore, we were highly intrigued by the possibility of developing new iridium-catalyzed allylic alkylation technology that would allow for the preparation of sterically congested enantioenriched quaternary stereocenters, and thus potentially open the door to the synthesis of a range of new natural product targets (Figure 5.2, top).

5.2 SYNTHESIS OF VICINAL TERTIARY AND ALL-CARBON QUATERNARY STEREOCENTERS VIA ENANTIO- AND DIASTEREOSELECTIVE IRIIDIUM-CATALYZED ALLYLIC ALKYLATION

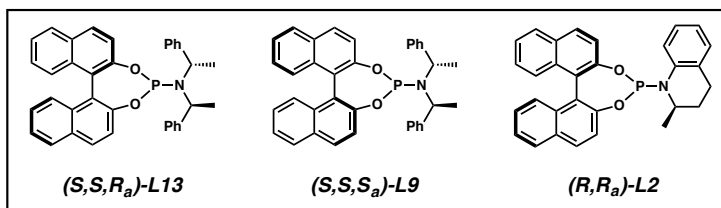
5.2.1 CYCLIC NUCLEOPHILES^{14,15}

In our quest to develop the first iridium-catalyzed allylic alkylation reaction to form vicinal tertiary and all-carbon quaternary stereocenters, we initially selected cyclic prochiral enolates as our nucleophiles in order to obviate the need to control enolate geometry during the allylic alkylation reaction.^{1,16} Thus, our preliminary exploration into this research area commenced with tetralone **27**. We rapidly found that the standard phosphoramidite ligands **L13** and **L9**, which were at the time typically utilized in iridium-catalyzed allylic alkylation with enolate equivalents, were not amenable to the synthesis of a quaternary stereocenter, as neither provided high levels of diastereoselectivity (Table 5.1, entries 1 and 2). Inspired by the work of the You group on the allylic alkylation of heterocycles,¹⁷ we evaluated the effect of MeTHQPhos (**L2**) as the ligand and found that it provided product **127** with a high degree of regio-, diastereo-, and enantioselectivity (entry 3).

Table 5.1 Development of conditions for the iridium-catalyzed allylic alkylation reaction of cyclic nucleophiles forming vicinal tertiary and all-carbon quaternary stereocenters^a



Entry	L	Additive (X mol %)	b:l ^b	dr ^b	ee (%) ^c
1	L13	NaH (200)	>95:5	1:1	99
2	L9	NaH (200)	>95:5	1:2	32
3	L2	NaH (200)	95:5	>20:1	98
4	L2	–	80:20	11:1	96
5	L2	LiCl (100)	88:12	14:1	98
6	L2	LiBr (100)	95:5	>20:1	>99



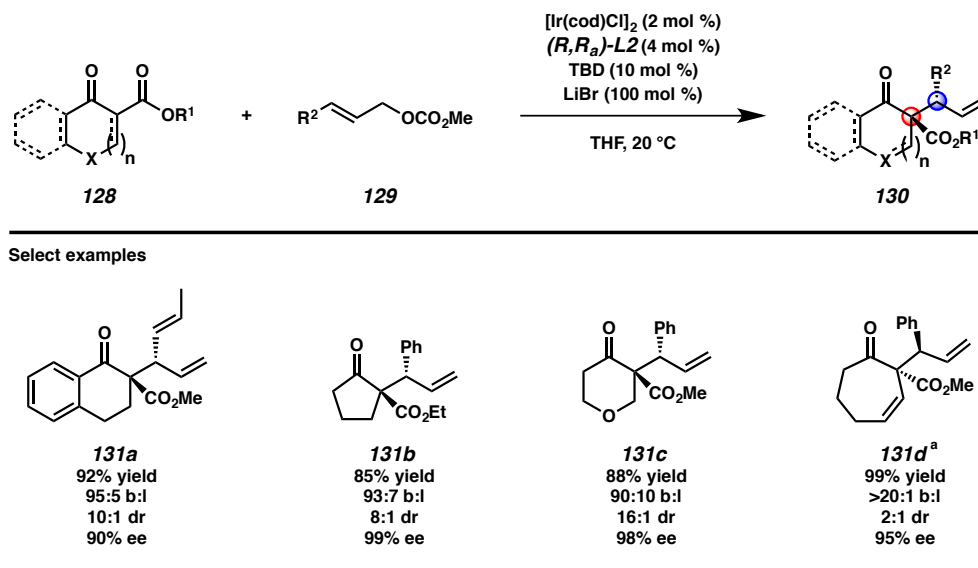
[a] Reactions performed with 0.1 mmol of **126**, 0.2 mmol of **27** in THF (0.1M) and allowed to proceed to complete consumption of **126**. [b] Determined by ¹H NMR and UHPLC-MS analysis of the crude mixture. [c] Determined by chiral HPLC analysis of the major diastereomer. [d] TBD = 1,3,5-triazabicyclo[4.4.0]dec-5-ene.

At this point in our optimization efforts, we realized that the reaction conditions could be simplified if the exogenous base was removed and the carbonate leaving group was instead relied on as the stoichiometric base required for enolate formation. Toward this end, sodium hydride was excluded from the reaction, but we observed diminished selectivity (Table 5.1, entry 4). Previous literature reports documented the beneficial effects of halide salts on selectivity in iridium-catalyzed allylic alkylation reactions.¹⁸ When this strategy was explored in our reaction conditions, LiCl provided only minor enhancement in selectivity (entry 5). However, LiBr led to a pronounced enhancement in

both conversion and selectivity, providing us with our optimized reaction conditions (entry 6).

Upon investigating the substrate scope of the developed transformation, we found the reaction amenable to a wide variety of substitution on both the allylic electrophile and the nucleophile (Scheme 5.1).¹⁴ Though, as a general trend, branched regioselectivity increases with greater carbocation stability on the allylic electrophile, thus electron-rich aromatics **129** ($R^2 = \text{EDG-Ar}$) provide higher branched to linear ratios. Additionally, the reaction is not limited to aryl substitution on the allylic electrophile, as both heteroaryl and alkenyl substitution provide the corresponding products in good yields and selectivities (e.g., **131a**). A key limitation to this initial report is that alkyl-substituted allylic electrophiles are not tolerated and instead proceed with poor conversions and selectivities. With respect to nucleophile **128**, we found that the aryl ring of tetralone **27**, used as the optimization substrate, could be removed without diminishing reactivity or stereoselectivity of the reaction (e.g., as seen in products **131b** and **131c**). Finally, we observed that unsaturated nucleophiles **128** are tolerated, allowing for access to products bearing a 1,5-diene (e.g., **131d**) for subsequent functionalization, though the addition of LiBr was not required in these reactions.¹⁵

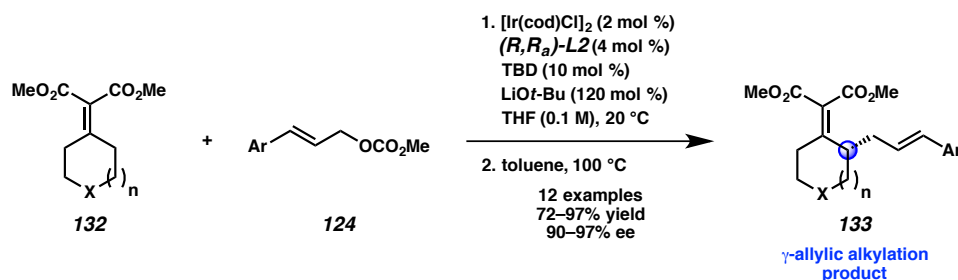
Scheme 5.1 Enantio- and diastereoselective iridium-catalyzed allylic alkylation of cyclic nucleophiles **128**



[a] Reaction performed with (S,S) -**L2** without LiBr.

Upon further optimization, we found that the reactions of unsaturated nucleophiles (e.g., **132**) progressed with a higher degree of selectivity when LiOt-Bu was utilized as a base additive in place of LiBr.¹⁵ These allylic alkylation conditions followed by a subsequent thermal Cope rearrangement, allow unsaturated compounds **132** to formally undergo allylic alkylation at the γ -position to produce compounds such as **35** with a high degree of enantioselectivity (Scheme 5.2).

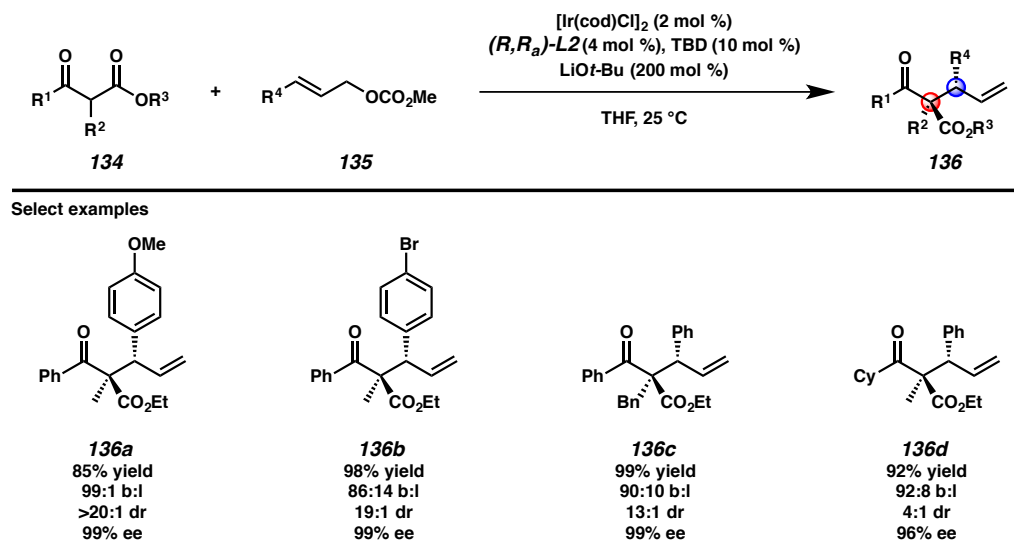
Scheme 5.2 Iridium-catalyzed allylic alkylation/Cope rearrangement sequence



5.2.2 ACYCLIC NUCLEOPHILES¹⁹

In looking to expand our iridium-catalyzed allylic alkylation reaction from cyclic enolate nucleophiles to acyclic variants, we fortuitously discovered that our conditions for cyclic nucleophiles provide satisfactory reactivity and selectivity for acyclic nucleophile **134** (Scheme 5.3). With further optimization though, we ultimately found LiOt-Bu to be the optimal additive as it led to shorter reaction times. With respect to the substrate scope of this transformation, we again observed that reaction regioselectivity is directly affected by the electronics of the aryl functionality on allylic electrophile **135**, however, enantio- and diastereoselectivities remain consistently excellent. Moreover, heteroaryl-substituted allylic electrophiles are tolerated, as are various substituents at the α -position of acyclic β -ketoester nucleophile **134**. However, in contrast to the cyclic variants, we noted pronounced decreases in the diastereomeric ratio of product **136** when ketone **134** was not an aryl ketone (e.g., **136a** versus **136d**).

Scheme 5.3 Enantio- and diastereoselective iridium-catalyzed allylic alkylation of acyclic nucleophiles **134**



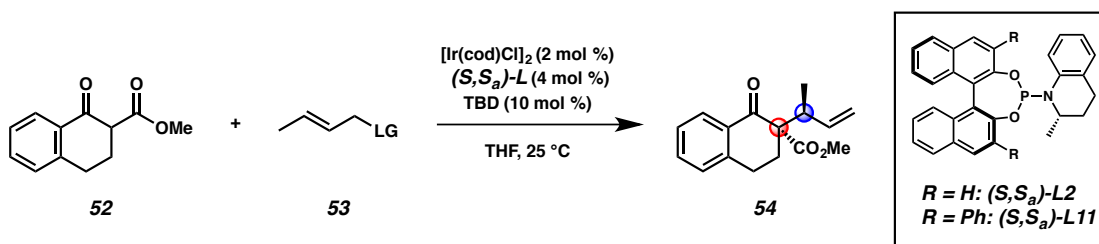
5.2.3 ALKYL-SUBSTITUTED ELECTROPHILES²⁰

After disclosing methods for the synthesis of vicinal tertiary and all-carbon quaternary stereocenters using cyclic,¹⁴ acyclic,¹⁹ and extended enolate¹⁵ nucleophiles in iridium-catalyzed allylic alkylation, we noted that none of these protocols tolerated the use of alkyl-substituted electrophiles. In fact, at the time, no transition metal-catalyzed process enabled the construction of an alkyl-substituted stereodiyad between neighboring tertiary and quaternary carbon atoms. Realizing that many synthetic targets require the installation of this specific stereodiyad, we became intrigued with the possibility of further developing our enantio- and diastereoselective iridium-catalyzed allylic alkylation chemistry to allow for the use of allylic electrophiles bearing an sp^3 -hybridized substituent.

Based on our prior efforts in optimizing iridium-catalyzed allylic alkylation reactions, we anticipated that we would need to explore new combinations of additives and ligands in order to effect selectivity in the reaction between tetralone nucleophile **52**, utilized in our seminal report¹⁴ (Table 5.1), and alkyl-substituted electrophile **53** (Table 5.2). Indeed, when we employed our previously reported conditions for cyclic or acyclic nucleophiles,^{14,19} we observed excellent yields and good diastereoselectivities but poor branched to linear ratios (Table 5.2, entries 1 and 2). Given the trends established in our earlier work where regioselectivity increases with increasing carbocation stability of the iridium π -allyl cation, these findings were not surprising as the methyl group is less stabilizing than an aryl substituent. We hypothesized that decreasing carbocation stability results in slow equilibration between iridium π -allyl diastereomers. Thus, we sought to employ LiCl as an additive, which has been proposed to facilitate iridium π -allyl

equilibration and therefore improve regio- and enantioselectivity in iridium-catalyzed allylic alkylation reactions.¹⁸ While we did not see a marked effect by adding LiCl alone (entry 3), we postulated that by rendering all anions in solution congruent, the effect of the chloride additive would be more pronounced. This hypothesis led us to replace the methyl carbonate leaving group of crotyl electrophile **53** with chloride, and in doing so we noted a significant increase in reaction regioselectivity, though the diastereoselectivity was now only moderate (entry 4).

Table 5.2 Optimization of iridium-catalyzed allylic alkylation reaction of alkyl-substituted electrophile **53**^a



Entry	L	Base (200 mol %)	Additive (mol %)	LG	Yield (%) ^b	b:l ^c	dr ^c	ee (%) ^d
1	L2	—	LiBr (100)	OCO ₂ Me	100	55:45	6.4:1	—
2	L2	LiOt-Bu	—	OCO ₂ Me	85	34:66	5.3:1	—
3	L2	LiOt-Bu	LiCl (100)	OCO ₂ Me	69	50:50	7.2:1	—
4	L2	LiOt-Bu	LiCl (100)	Cl	94	86:14	4.8:1	—
5	L2	proton sponge	LiCl (100)	Cl	100	93:7	7.9:1	66
6	L11	proton sponge	LiCl (100)	Cl	46	95:5	6.0:1	96
7	L11	proton sponge	LiCl (400)	Cl	78	94:6	6.7:1	97

[a] Reactions performed on 0.1 mmol of **53**, 0.2 mmol of **52** in THF (0.1 M) for 18 h. [b] ¹H NMR yield of the mixture of diastereomers based on internal standard. [c] Determined by ¹H NMR analysis of the crude reaction mixture. [d] Determined by chiral SFC analysis. [e] Proton sponge = 1,8-bis(dimethylamino)naphthalene.

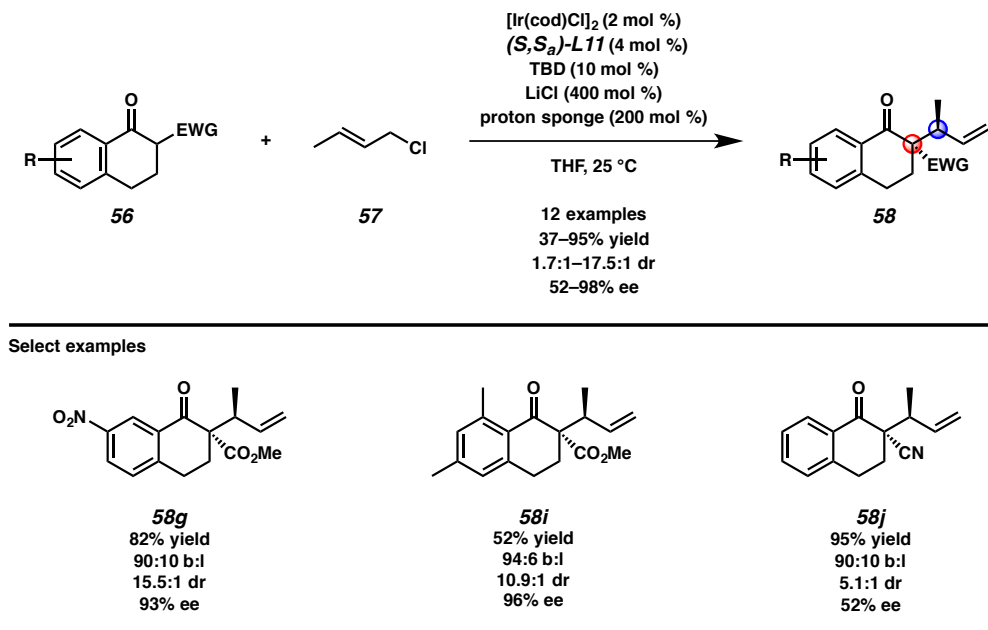
We next sought to improve the diastereoselectivity of the reaction by investigating additional bases other than LiOt-Bu, as we had found in our prior work that bases had a significant effect on selectivity.^{14,15,19} After an extensive screen of bases, we

identified that the bulky amine base, proton sponge, allowed our transformation to proceed in good yield, regio- and diastereoselectivity, but poor enantioselectivity (entry 5). In order to increase the enantioselectivity of our desired reaction, we moved to employ bulkier phosphoramidite ligand **L11**, which led to excellent enantioselectivity, though at the expense of yield (entry 6). Ultimately, we discovered that we could improve the reaction yield, with no effect on selectivity, by increasing the amount of the inexpensive LiCl additive to 400 mol % (entry 7). This extensive fine-tuning of reaction parameters is included here as an illustrative example of how altering one reaction partner (e.g., the substituent on the electrophile) in an iridium-catalyzed allylic alkylation reaction necessitates complete reoptimization of the system.

The optimized conditions allow for a wide range of substituted tetralone nucleophiles **56** to undergo a highly selective iridium-catalyzed allylic alkylation reaction with crotyl chloride (**57**, Scheme 5.4). However, at this time, the nucleophile scope is limited to β -ketoester-based tetralones. We postulate that this limitation is due to both pKa restrictions of the nucleophile that prevent the use of tetralones bearing other α -electron withdrawing groups (e.g., nitrile, ketone; **58j** versus **54**) as well as the necessity of sp^2 -hybridized bulk at the carbonyl α' position to induce selectivity. With respect to the electrophile, longer chain alkyl-substituted electrophiles result in diminished yields and selectivities, likely due to increased sterics. Limitations aside, this transformation represents the first transition metal-catalyzed allylic alkylation reaction forming vicinal tertiary and all-carbon quaternary stereocenters between prochiral enolates and an alkyl-substituted electrophile.²⁰ We envision that with further exploration of new catalytic

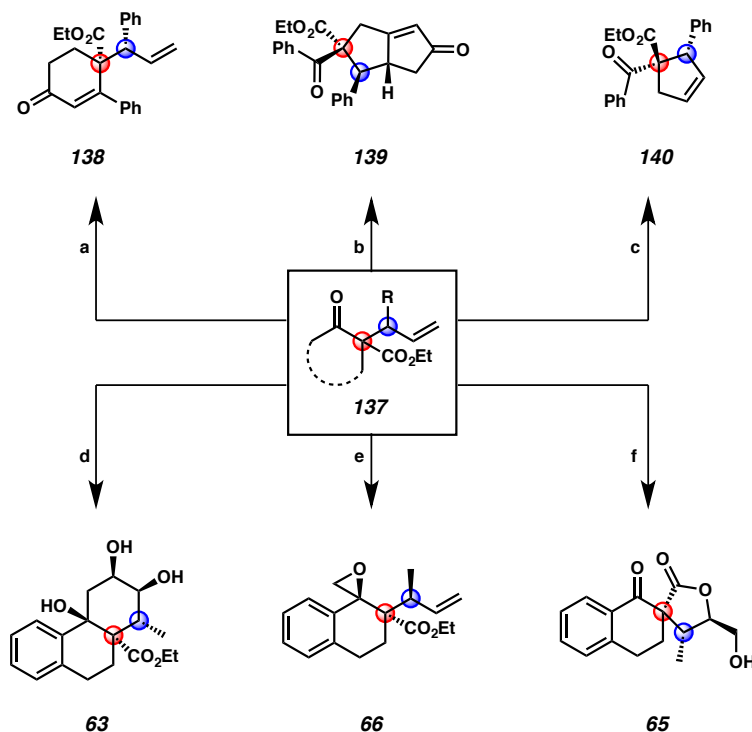
systems that the substrate scope of this transformation can be expanded to additional alkyl-substituted electrophiles in the future.

Scheme 5.4 Enantio- and diastereoselective iridium-catalyzed allylic alkylation reactions with crotyl chloride (**57**)



In order to demonstrate the synthetic utility of our enantio- and diastereoselective iridium-catalyzed allylic alkylation methodology, we carried out series of product transformations on allylic alkylation products **137** (Figure 5.4). Notably, all of these derivatizations proceed with excellent diastereoselectivity to facilitate the synthesis of complex building blocks, demonstrating the ease with which complexity can be added to these high-value products.

Figure 5.4 Select examples of diverse product transformations of enantio- and diastereoselective iridium-catalyzed allylic alkylation products **137**^a



[a] pyrrolidine, AcOH, *t*-BuOMe, reflux, 95% yield; [b] $\text{Co}_2(\text{CO})_8$, CH_2Cl_2 , then $\text{Me}_3\text{NO} \cdot 2\text{H}_2\text{O}$, >20:1 dr, 99% yield; [c] HG-II (10 mol %), CH_2Cl_2 , 40 °C, 96% yield; [d] i) allylmagnesium chloride, THF, -78 °C, 71% yield, ii) HG-II, CH_2Cl_2 , 81% yield, iii) K_2OsO_4 , NMO, THF/ H_2O , 59% yield; [e] $\text{Me}_3\text{S}(\text{O})\text{I}$, NaH, DMSO, 82% yield; [f] K_2OsO_4 , NMO, THF/ H_2O , 65% yield.

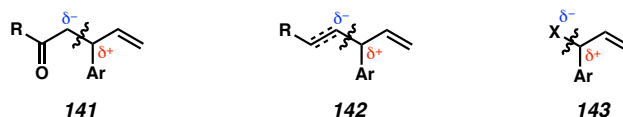
5.3 UMPOLED IRIIDIUM-CATALYZED ALLYLIC ALKYLATION REACTIONS

After four years of expanding the limits of enantio- and diastereoselective iridium-catalyzed allylic alkylation, we became aware of another limitation in the field. Specifically, we noted that over the past two decades of iridium-catalyzed allylic alkylation research since the seminal report,⁸ the technology had been widely developed for standard reactivity patterns between electrophilic π -allyl species and nucleophilic enolate equivalents (**141**), carbanion equivalents (**142**), or heteroatoms (**143**, Figure

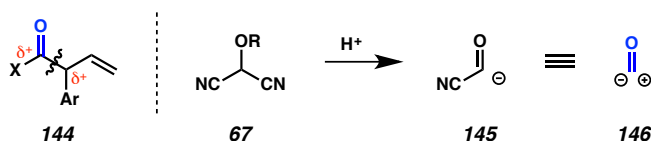
5.5a).^{13,21} However, the application of an umpolung strategy in iridium-catalyzed allylic alkylation to stitch together two formally electrophilic species remained underexplored (**144**, Figure 5.5b, left). At the time, only two examples of reverse-polarity nucleophiles had been reported for this chemistry,²² though neither were in the carboxylic acid oxidation state which would allow for direct access to either enantioenriched amides, esters, or carboxylic acids.

Figure 5.5 Iridium-catalyzed allylic alkylation strategies

a) Standard Iridium-Catalyzed Allylic Alkylation



b) Umpolung Strategy Iridium-Catalyzed Allylic Alkylation via MAC Reagent



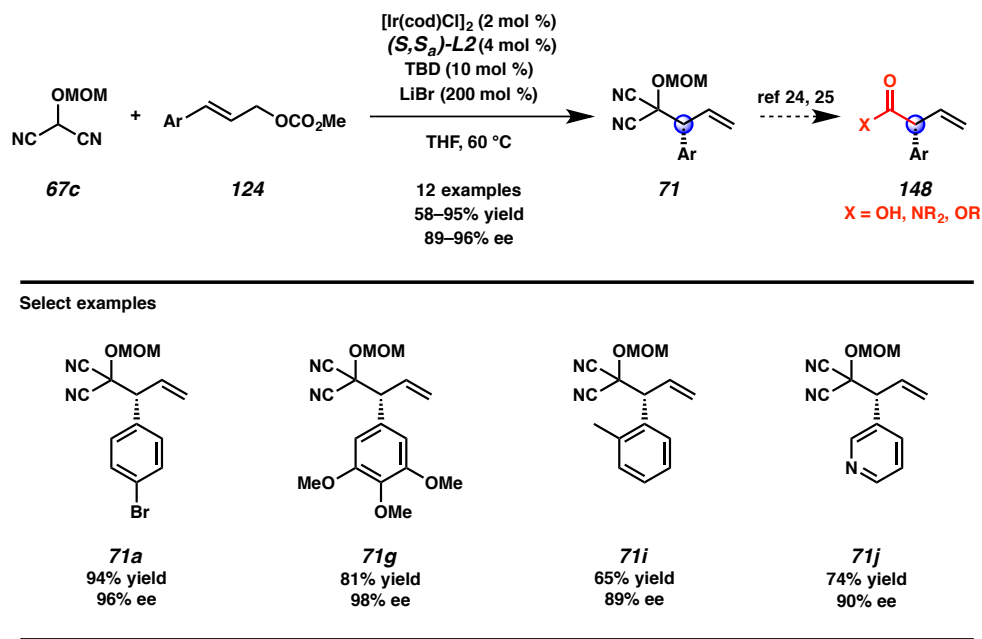
5.3.1 TERTIARY ALLYLIC STEREOCENTERS²³

With this gap in the literature noted we set forth to develop an iridium-catalyzed allylic alkylation method for accessing carboxylic acid derivatives and we identified masked acyl cyanide (MAC) reagents **67** as potential nucleophiles (Figure 5.5b, left). These MAC reagents which were developed by Nemoto and Yamamoto, and popularized by Rawal, can expel an equivalent of cyanide when exposed to acid therefore allowing them to function as acyl cyanide nucleophiles (**145**, Figure 5.5b, right).²⁴ As acyl cyanides are highly electrophilic, the MAC reagent truly functions as a carbon monoxide

synthon (**146**). Thus, we envisioned that if the MAC reagent could react with an iridium- π allyl species to generate an alkylation product, we could use extensive literature precedent to unmask the MAC adduct and further transform the transient acyl cyanide to carboxylic acid derivatives **144** upon treatment with heteroatom nucleophiles (e.g., H_2O , RNH_2 , ROH).^{24,25} As a result, the MAC reagent would function as each an amide, ester, and carboxylic acid synthon.

Employing our previously disclosed conditions for the iridium-catalyzed allylic alkylation of cyclic nucleophiles to form vicinal tertiary and all-carbon quaternary stereocenters,¹⁴ we were able to rapidly establish that the MAC reagent was a competent nucleophile in the iridium-catalyzed reaction given the judicious choice of protecting group on the hydroxyl moiety. Specifically, we found that a methoxymethyl (MOM) group (**67c**) was required in order to access products **71** in high yields (Scheme 5.5). We hypothesize that this protecting group is optimal due to its small steric profile as well as its potential to coordinate and be activated by the LiBr additive. Using these optimized conditions, we discovered that a range of cinnamyl-derived electrophiles, including heteroaryl-substituted allylic electrophiles, react in high yields and excellent enantioselectivities in up to gram scale to provide allylic alkylation products **71**, which are amenable to the synthesis of highly desirable, enantioenriched vinylated α -aryl carboxylic acid derivatives.²³

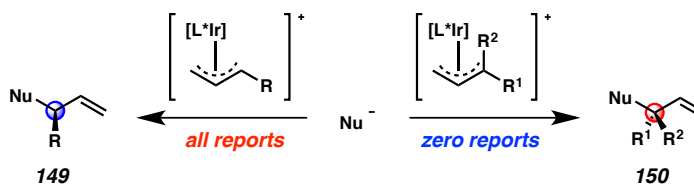
Scheme 5.5 First report of MAC reagent **67c** in an asymmetric transition-metal catalyzed reaction



5.3.2 QUATERNARY ALLYLIC STEREOCENTERS²⁶

After having developed the iridium-catalyzed allylic alkylation chemistry for MAC nucleophile **67c**,²³ we sought to further leverage the utility of the MAC reagents to access an even more challenging class of compounds – acyclic α -quaternary carbonyl derivatives. However, our proposed allylic alkylation strategy had one major caveat, namely, enantioenriched quaternary allylic stereocenters had never been synthesized via iridium-catalyzed allylic alkylation reactions (Figure 5.6).²⁷

Figure 5.6 Limitations in enantioselective iridium-catalyzed allylic alkylation prior to 2017

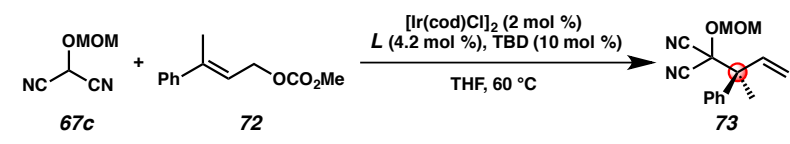


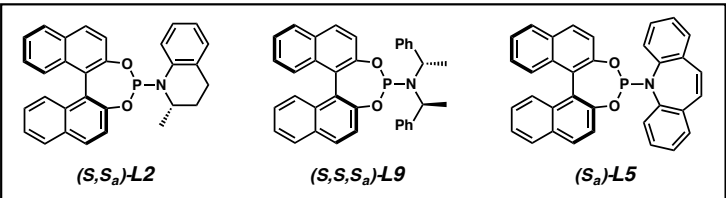
Over the past twenty years, enantioselective iridium-catalyzed allylic alkylation reactions have been exclusively limited to those synthesizing tertiary allylic stereocenters **149** (Figure 5.6, left).^{13,21} In contrast, use of a 1,1-disubstituted π -allyl to forge quaternary allylic stereocenters **150** was unreported (Figure 5.6, right). In order to access such a geminal-disubstituted π -allyl species, a trisubstituted allylic electrophile would need to be utilized; however, this class of electrophile was predicted to be unreactive in iridium-catalyzed allylic alkylation chemistry. Literature reports have demonstrated that the reaction rates of these processes decrease with increasing substitution on the olefin of the electrophile.²⁸ Therefore, we anticipated that our preliminary experiments into this research area would focus on identifying a method in which to unlock reactivity from a heretofore unreactive trisubstituted allylic electrophile **72** (Table 5.3).

As we anticipated, application of our standard conditions for the iridium-catalyzed allylic alkylation of cyclic nucleophiles failed to invoke reactivity from trisubstituted allylic electrophile **72**, instead returning starting material (Table 5.3, entry 1). We rationalized that we would need to explore other phosphoramidite ligand frameworks in order to identify a more reactive catalyst (entries 2 and 3). Ultimately, we identified that phosphoramidite **L5**, developed by Carreira, was uniquely effective in providing desired product **73**, though in only modest yield (entry 3).²⁹ In an effort to increase the yield and selectivity of the transformation, we performed an extensive investigation into alternative additives that have proven successful in promoting iridium-catalyzed allylic alkylation reactions. However, it was not until we identified the necessity of a strong Lewis acid co-catalyst to promote oxidative addition via facilitating the ionization of the carbonate leaving group from allylic electrophile **72** that we saw

improved reactivity. Specifically, we discovered that the addition of Lewis acidic triethylborane to the reaction provided access to desired product **73** in nearly triple the conversion and excellent enantioselectivity (entry 4). Finally, we found that we could further improve reaction yield by altering the nucleophile to electrophile stoichiometry such that an excess of electrophile is present (entry 5). Of note, the *E*-olefin isomer of allylic electrophile **72** is required, as the *Z*-trisubstituted allylic electrophile gave significantly decreased yields and selectivities.

Table 5.3 Optimization of the enantioselective synthesis of products **73** bearing allylic quaternary stereocenters

					
Entry	L	67c:72	Additive (200 mol %)	Yield ^b	ee (%) ^c
1	L2	2:1	LiBr	0	–
2	L9	2:1	LiBr	0	–
3	L5	2:1	LiBr	12	79
4	L5	2:1	BEt ₃	34	93
5	L5	1:2	BEt ₃	99	94



(*S,S_a*)-**L2** (*S,S,S_a*)-**L9** (*S_a*)-**L5**

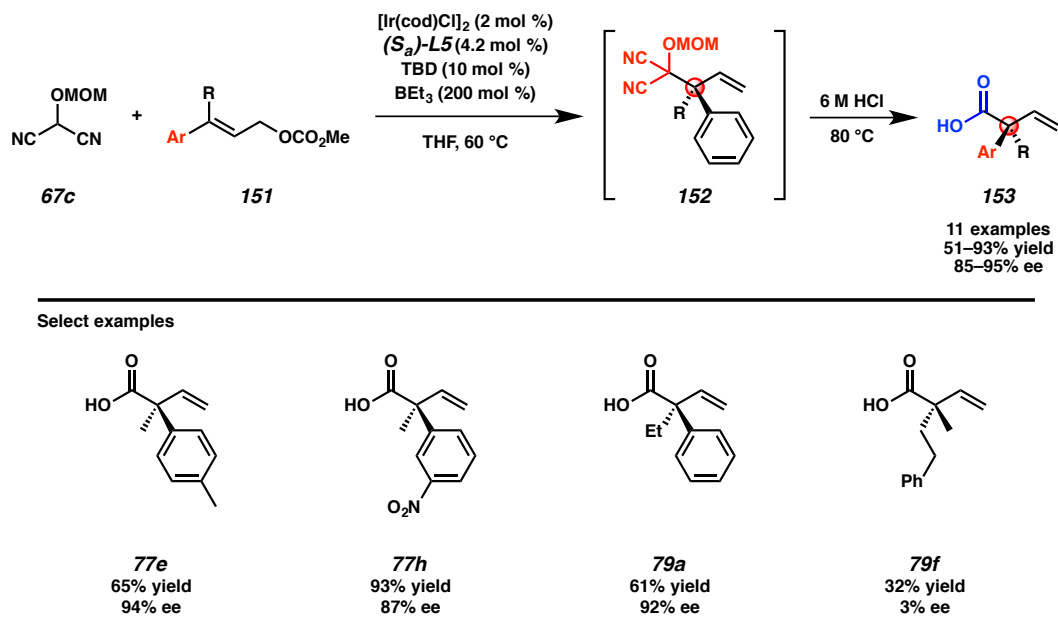
[a] Reactions performed on 0.1 mmol scale. [b] ¹H NMR yield based on internal standard. [c] Determined by chiral HPLC analysis.

While optimizing the reaction parameters for this novel transformation, we noted the importance of the guanidine base, 1,3,5-triazabicyclo[4.4.0]dec-5-ene (TBD), on reactivity. Typically, TBD is utilized as a substoichiometric base additive to promote the

formation of an active iridicycle catalyst.³⁰ However, Carreira has reported that phosphoramidite **L5** does not form an iridicycle and thus a base additive is not required when employing this ligand in iridium-catalyzed allylic alkylation reactions.³¹ We postulate that in the case of our developed reaction, TBD may be serving as a labile placeholder ligand to prevent the formation of an inactive catalyst or as a base to promote the formation of a novel active iridicycle.

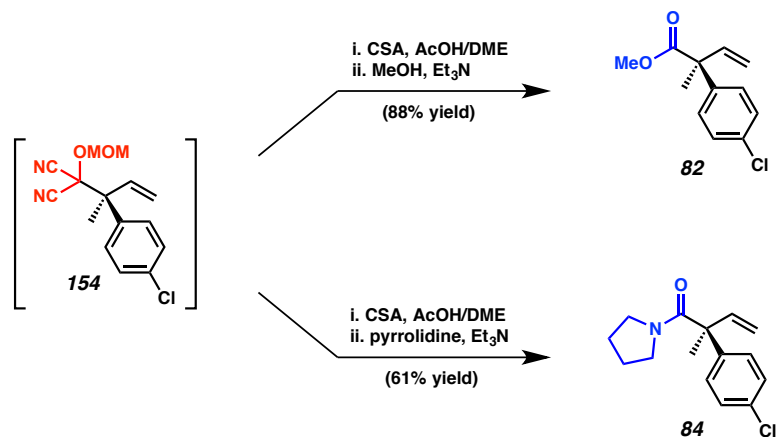
In looking to how this new reaction could be even further improved, we envisioned that hydrolysis of the MAC functionality of allylic alkylation product **152** could be carried out in the same reaction vessel as the iridium-catalyzed reaction to provide direct access to the corresponding carboxylic acid in a one-pot, two-step procedure (Scheme 5.6).^{25e} Moreover, we hypothesized that carboxylic acid products **153** could be isolated in high purity after a simple acid/base work up alone, with no need for column chromatography. We were pleased to find that our hypothesis was valid and with our optimized conditions a range of acyclic α -quaternary carboxylic acids **153** were prepared with varying substitution at the α -position. Specifically, both electron withdrawing and donating groups are well tolerated at the *para* and *meta* positions of the aryl substituent on electrophile **151**, though diminished yields are observed for bis-*meta*-substituted arenes and no reactivity is observed with *ortho*-substituted aryl groups. With respect to the alkyl substituent (R), lengthening the *n*-alkyl group beyond an ethyl moiety results in poor yields, as does the use of branched alkyl substituents. Also of note, bis-alkyl-substituted allylic electrophiles do not currently fare well in this chemistry (cf., **79f**).

Scheme 5.6 Enantioselective synthesis of acyclic α -quaternary carboxylic acids **153**



As MAC adducts can be transformed into essentially any carboxylic acid derivative, we sought to develop additional one-pot methods to access α -quaternary esters and amides.^{25e} Toward this end, we were pleased to find that MAC adduct **154** could be advanced in a one-pot fashion to a variety of esters (e.g., **82**), as well as amides (e.g., **84**) in moderate to high yields following cleavage of the MOM group and interception of the transient acyl cyanide by the appropriate nucleophile (Figure 5.7).

Figure 5.7 Enantioselective synthesis of acyclic α -quaternary esters **82** and amides **84**

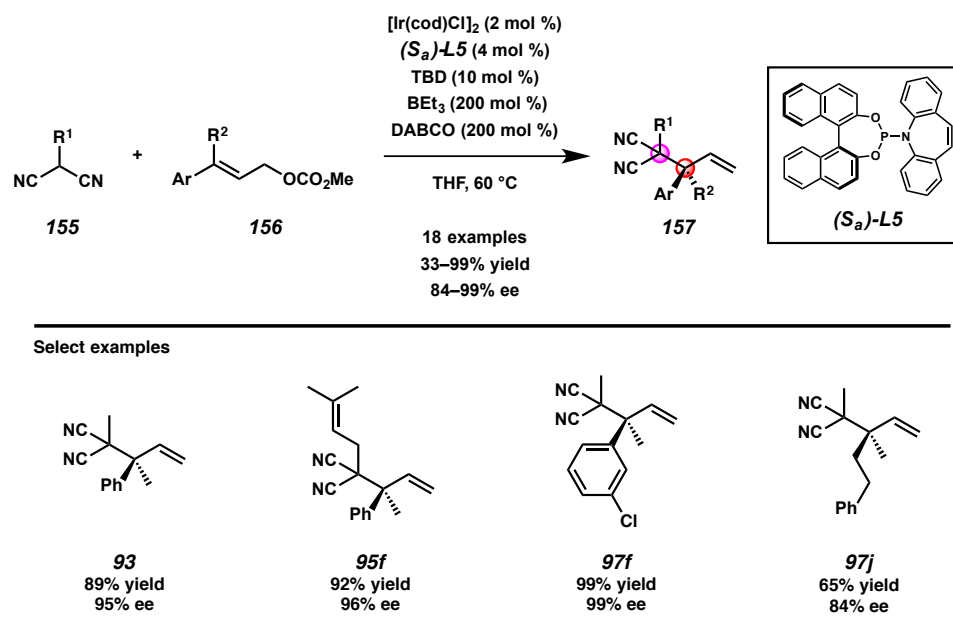


5.4 SYNTHESIS OF VICINAL ALL-CARBON QUATERNARY CENTERS VIA ENANTIOSELECTIVE IRIIDIUM-CATALYZED ALLYLIC ALKYLATION³²

Noting that our preparation of enantioenriched α -quaternary carboxylic acid derivatives progresses through intermediate **152**, bearing vicinal tetra-substituted and quaternary centers, led us to imagine that we could utilize this iridium-catalyzed allylic alkylation methodology to synthesize highly congested vicinal all-carbon quaternary centers. In designing a nucleophile for this desired reaction, we postulated that the most facile reaction development would be achieved if the malononitrile functionality of the previously utilized MAC nucleophile **67c** was kept intact and the α -substitution were not more sterically demanding than the MOM group. Indeed, our previously reported conditions for the synthesis of α -quaternary carboxylic acid derivatives using MAC reagent **67c** translated directly to the reaction of methylmalononitrile (**155**, R¹ = Me) with trisubstituted allylic electrophile **156**, though the enantioselectivity was low (Scheme 5.7). As our early work demonstrated that basic additives have pronounced effects on

selectivity, we explored the effect of base on our current reaction. Ultimately, DABCO was revealed to be uniquely effective for this transformation, providing products **157** bearing vicinal all-carbon quaternary centers in moderate to good yields and excellent enantioselectivities for a variety of substituted malononitrile nucleophiles **155** and trisubstituted allylic electrophiles **156**. At this time, we believe that the DABCO increases the enantioselectivity of the transformation by allowing for increased equilibration between diastereomers of an iridium π -allyl complex by slowing the rate of nucleophilic attack.^{18,33}

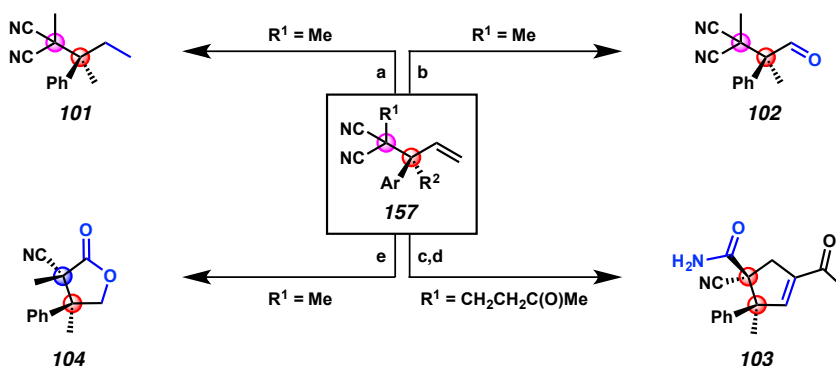
Scheme 5.7 Synthesis of vicinal all-carbon quaternary centers **157** via enantioselective iridium-catalyzed allylic alkylation



As we are inspired and driven by the application of our methods in complex molecule synthesis, we sought to demonstrate the feasibility of chemoselective manipulation of allylic alkylation product **157** (Figure 5.8). The olefin functionality of

157 can either be chemoselectively reduced or oxidized via ozonolysis. Furthermore, multistep procedures can be utilized to prepare densely-functionalized compounds bearing two contiguous all-carbon quaternary stereocenters, such as **103** and **104**.

Figure 5.8 Product derivatizations of iridium-catalyzed allylic alkylation products **157** bearing vicinal all-carbon quaternary centers^a



[a] $\text{RhCl}(\text{PPh}_3)_3$, H_2 (balloon), benzene, 23 °C, 18 h, 92% yield; [b] O_3 , pyridine, CH_2Cl_2 , -78 °C, 4 min, 93% yield; [c] i. O_3 , pyridine, CH_2Cl_2 , -78 °C, 4 min, ii. $p\text{-TsOH}$, benzene, reflux, 18 h, 47% yield; [d] NaOH , $\text{EtOH}/\text{H}_2\text{O}$ (1:1), 60 °C, 18 h, 38% yield, 1:11 dr; [e] i. O_3 , MeOH , -78 °C, 0.5 h, ii. NaBH_4 , 0 °C, 3 h, 65% yield, 1:2.5 dr.

5.5 CONCLUSIONS AND FUTURE OUTLOOK

Building on our group's longstanding interest in the synthesis of enantioenriched quaternary stereocenters, we have sought to expand the limits of iridium-catalyzed allylic alkylation chemistry to encompass the synthesis of sterically congested all-carbon quaternary stereocenters. Initially, we focused on the development of enantio- and diastereoselective iridium-catalyzed allylic alkylation technology for the construction of vicinal tertiary and all-carbon quaternary stereocenters. Our work has enabled the use of both cyclic and acyclic nucleophiles, as well as alkyl-substituted allylic electrophiles in this methodology. We then shifted our attention to umpolung strategy iridium-catalyzed allylic alkylation chemistry and developed MAC reagents as nucleophiles. Continued

study of the umpolung chemistry led to the synthesis of allylic quaternary stereocenters via the use of trisubstituted allylic electrophiles in conjunction with a Lewis acid co-catalyst. Most recently, we have discovered iridium-catalyzed allylic alkylation technology that provides access to vicinal all-carbon quaternary centers.

Despite these advances by our group, as well as beautiful work from other groups in the area,^{13,21} this emerging field is not without limitations. While there have been extensive advances to widen the substrate scope with respect to the nucleophile partner, the allylic electrophile remains largely limited to aryl- and alkenyl-substitution, aside from our reported method for the use of crotyl chloride as an electrophile.²⁰ Most importantly though, no general method for iridium-catalyzed allylic alkylation exists. As demonstrated *vide supra*, even minor changes to either the nucleophile or electrophile partner necessitate complete reoptimization of the reaction parameters. Ideally, a single catalyst system will be developed in the future which enables highly selective iridium-catalyzed allylic alkylation reactions for any combination of nucleophile and electrophile.

In looking forward, we envision that the field will shift its attention to the development of enantio- and diastereoselective iridium-catalyzed allylic alkylation for the synthesis of vicinal all-carbon quaternary stereocenters; a highly challenging motif to access that has also become a holy grail for many other areas of synthetic methodology. We hope that our recent work on the synthesis of vicinal quaternary centers will inspire and enable these studies. Ultimately, we look forward to a time when the broader synthetic community embraces iridium-catalyzed allylic alkylation as an enabling and reliable technology for the synthesis of complex targets.

5.6 REFERENCES AND NOTES

- (1) Liu, Y.; Han, S.-J.; Liu, W.-B.; Stoltz, B. M. *Acc. Chem. Res.* **2015**, *48*, 740–751.
- (2) Behena, D. C.; Mohr, J. T.; Sherden, N. H.; Marinescu, S. C.; Harned, A. M.; Tani, K.; Seto, M.; Ma, S.; Novák, Z.; Krout, M. R.; McFadden, R. M.; Roizen, J. L.; Enquist, J. A., Jr.; White, D. E.; Levine, S. R.; Petrova, K. V.; Iwashita, A.; Virgil, S. C.; Stoltz, B. M. *Chem. Eur. J.* **2011**, *17*, 14199–14223.
- (3) For select examples, see: (a) Reeves, C. M.; Eidamshaus, C.; Kim, J.; Stoltz, B. M. *Angew. Chem. Int. Ed.* **2013**, *52*, 6718–6721; (b) Korch, K. M.; Eidamshaus, C.; Behenna, D. C.; Nam, S.; Horne, D.; Stoltz, B. M. *Angew. Chem. Int. Ed.* **2015**, *54*, 179–183; (c) Numajiri, Y.; Jiménez-Osés, G.; Wang, B.; Houk, K. N.; Stoltz, B. M. *Org. Lett.* **2015**, *17*, 1082–1085; (d) Craig, R. A., II; Loskot, S. A.; Mohr, J. T.; Behenna, D. C.; Harned, A. M.; Stoltz, B. M. *Org. Lett.* **2015**, *17*, 5160–5163.
- (4) Enquist, J. A., Jr.; Stoltz, B. M. *Nature* **2008**, *453*, 1228–1231.
- (5) McFadden, R. M.; Stoltz, B. M. *J. Am. Chem. Soc.* **2006**, *128*, 7738–7739.
- (6) Numajiri, Y.; Pritchett, B. P.; Chiyoda, K.; Stoltz, B. M. *J. Am. Chem. Soc.* **2015**, *137*, 1040–1043.
- (7) Tsuji, J.; Takahashi, H.; Morikawa, M. *Tetrahedron Lett.* **1965**, *6*, 4387–4388.
- (8) Takeuchi, R.; Kashio, M. *Angew. Chem. Int. Ed.* **1997**, *36*, 263–265.
- (9) For examples where palladium-catalyzed allylic alkylation favors branched products, see: (a) Prétôt, R.; Pfaltz, A. *Angew. Chem. Int. Ed.* **1998**, *37*, 323–325; (b) Hayashi, T.; Kawatsura, M.; Uozumi, Y. *J. Am. Chem. Soc.* **1998**, *120*, 1681–1687; (c) You, S.-L.; Zhu, X.-Z.; Luo, Y.-M.; Hou, X.-L.; Dai, L.-X. *J. Am.*

- Chem. Soc.* **2001**, *123*, 7471–7472; (d) Zheng, W.-H.; Sun, N.; Hou, X.-L. *Org. Lett.* **2005**, *7*, 5151–5154; (e) Zheng, W.-H.; Zheng, B.-H.; Zhang, Y.; Hou, X.-L. *J. Am. Chem. Soc.* **2007**, *129*, 7718–7719; (f) Liu, W.; Chen, D.; Zhu, X.-Z.; Wan, X.-L.; Hou, X.-L. *J. Am. Chem. Soc.* **2009**, *131*, 8734–8735; (g) Fang, P.; Ding, C.-H.; Hou, X.-L.; Dai, L.-X. *Tetrahedron: Asymmetry* **2010**, *21*, 1176–1178; (h) Chen, J.-P.; Ding, C.-H.; Liu, W.; Hou, X.-L.; Dai, L.-X. *J. Am. Chem. Soc.* **2010**, *132*, 15493–15495.
- (10) Janssen, J. P.; Helmchen, G. *Tetrahedron Lett.* **1997**, *38*, 8025–8026.
- (11) Kanayama, T.; Yoshida, K.; Miyabe, H.; Takemoto, Y. *Angew. Chem. Int. Ed.* **2003**, *42*, 2054–2056.
- (12) Chen, W.; Hartwig, J. F. *J. Am. Chem. Soc.* **2013**, *135*, 2068–2071.
- (13) For a review on diastereoselective iridium-catalyzed allylic alkylation, see: Hethcox, J. C.; Shockley, S. E.; Stoltz, B. M. *ACS Catal.* **2016**, *6*, 6207–6213.
- (14) Liu, W.-B.; Reeves, C. M.; Virgil, S. C.; Stoltz, B. M. *J. Am. Chem. Soc.* **2013**, *135*, 10626–10629.
- (15) Liu, W.-B.; Okamoto, N.; Alexy, E. J.; Hong, A. Y.; Tran, K.; Stoltz, B. M. *J. Am. Chem. Soc.* **2016**, *138*, 5234–5237.
- (16) (a) Douglas, C. J.; Overman, L. E. *Proc. Natl. Acad. Sci. USA* **2004**, *101*, 5363–5367; (b) Das, J. P.; Marek, I. *Chem. Commun.* **2011**, *47*, 4593–4623; (c) Quasdorf, K. W.; Overman, L. E. *Nature* **2014**, *516*, 181–191; (d) Corey, E. J.; Guzman-Perez, A. *Angew. Chem. Int. Ed.* **1998**, *37*, 388–401; (e) Christoffers, J.; Mann, A. *Angew. Chem. Int. Ed.* **2001**, *40*, 4591–4597; (f) Trost, B. M.; Jiang, C. *Synthesis*

- 2006**, 369–396; (g) Denissova, I.; Barriault, L. *Tetrahedron* **2003**, *59*, 10105–10146; (h) Ling, T.; Rivas, F. *Tetrahedron* **2016**, *72*, 6729–6777.
- (17) (a) Liu, W.-B.; He, H.; Dai, L.-X.; You, S.-L. *Synthesis* **2009**, 2076–2082; (b) Liu, W.-B.; Zheng, C.; Zhuo, C.-X.; Dai, L.-X.; You, S.-L. *J. Am. Chem. Soc.* **2012**, *134*, 4812–4821.
- (18) (a) Bartels, B.; Helmchen, G. *Chem. Commun.* **1999**, 741–742; (b) Alexakis, A.; Polet, D. *Org. Lett.* **2004**, *6*, 3529–3532; (c) Polet, D.; Alexakis, A.; Tissot-Croset, K.; Corminboeuf, C.; Ditrich, K.; *Chem. Eur. J.* **2006**, *12*, 3596–3609.
- (19) Liu, W.-B.; Reeves, C. M.; Stoltz, B. M. *J. Am. Chem. Soc.* **2013**, *135*, 17298–17301.
- (20) Hethcox, J. C.; Shockley, S. E.; Stoltz, B. M. *Angew. Chem. Int. Ed.* **2016**, *55*, 16092–16095.
- (21) For selected reviews of asymmetric iridium-catalyzed allylic alkylation, see: (a) Helmchen, G.; Dahnz, A.; Dübon, P.; Schelwies, M.; Weihofen, R. *Chem. Commun.* **2007**, 675–691; (b) Hartwig, J. F.; Pouy, M. J. *Top. Organomet. Chem.* **2011**, *34*, 169–208; (c) Liu, W.-B.; Xia, J. B.; You, S.-L. *Top. Organomet. Chem.* **2011**, *38*, 155–208.
- (22) (a) Förster, S.; Tverskoy, O.; Helmchen, G. *Synlett* **2008**, 2803–2806; (b) Breitler, S.; Carreira, E. M. *J. Am. Chem. Soc.* **2015**, *137*, 5296–5299.
- (23) Hethcox, J. C.; Shockley, S. E.; Stoltz, B. M. *Org. Lett.* **2017**, *19*, 1527–1529.
- (24) (a) Nemoto, H.; Kubota, Y.; Yamamoto, Y. *J. Org. Chem.* **1990**, *55*, 4515–4516; (b) Nemoto, H.; Li, X.; Ma, R.; Suzuki, I.; Shibuya, M. *Tetrahedron Lett.* **2003**, *44*,

- 73–75; (c) Nemoto, H.; Kawamura, T.; Miyoshi, N. *J. Am. Chem. Soc.* **2005**, *127*, 14546–14547; (d) Nemoto, H.; Ma, R.; Kawamura, T.; Kamiya, M.; Shibuya, M. *J. Org. Chem.* **2006**, *71*, 6038–6043; (e) Nemoto, H.; Kawamura, T.; Kitasaki, K.; Yatsuzuka, K.; Kamiya, M.; Yoshioka, Y. *Synthesis* **2009**, 1694–1702; (f) Yang, K. S.; Nibbs, A. E.; Türkmen, Y. E.; Rawal, V. H. *J. Am. Chem. Soc.* **2013**, *135*, 16050–16053; (g) Yang, K. S.; Rawal, V. H. *J. Am. Chem. Soc.* **2014**, *136*, 16148–16151; (h) Kagawa, N.; Nibbs, A. E.; Rawal, V. H. *Org. Lett.* **2016**, *18*, 2363–2366.
- (25) (a) Kociölek, K.; Leplawy, M. T. *Synthesis* **1977**, 778–780; (b) Kubota, Y.; Nemoto, H.; Yamamoto, Y. *J. Org. Chem.* **1991**, *56*, 7195–7196; (c) Nemoto, H.; Ma, R.; Ibaragi, T.; Suzuki, I.; Shibuya, M. *Tetrahedron* **2000**, *56*, 1463–1468; (d) Yamatsugu, K.; Kanai, M.; Shibasaki, M. *Tetrahedron* **2009**, *65*, 6017–6024; (e) Yang, K. S.; Nibbs, A. E.; Türkmen, Y. E.; Rawal, V. H. *J. Am. Chem. Soc.* **2013**, *135*, 16050–16053; (f) Yang, K. S.; Rawal, V. H. *J. Am. Chem. Soc.* **2014**, *136*, 16148–16151; (g) Kagawa, N.; Nibbs, A. E.; Rawal, V. H. *Org. Lett.* **2016**, *18*, 2363–2366.
- (26) Shockley, S. E.; Hethcox, J. C.; Stoltz, B. M. *Angew. Chem. Int. Ed.* **2017**, *56*, 11545–11548.
- (27) At the time of publication, a singular example of an iridium-catalyzed allylic alkylation reaction producing a product bearing an allylic all-carbon stereocenter has been reported with 11% yield and 21% ee: Onodera, G.; Watabe, K.; Matsubara, M.; Oda, K.; Kezuka, S.; Takeuchi, R. *Adv. Synth. Catal.* **2008**, *350*, 2725–2732.

- (28) (a) Madrahimov, S. T.; Hartwig, J. F. *J. Am. Chem. Soc.* **2012**, *134*, 8136–8147; (b) Madrahimov, S. T.; Li, Q.; Sharma, A.; Hartwig, J. F. *J. Am. Chem. Soc.* **2015**, *137*, 14968–14981.
- (29) Defieber, C.; Ariger, M. A.; Moriel, P.; Carreira, E. M. *Angew. Chem. Int. Ed.* **2007**, *46*, 3139–3143.
- (30) For examples of the formation of active iridicycles, see: (a) Jiang, X.; Beiger, J. J.; Hartwig, J. F. *J. Am. Chem. Soc.* **2017**, *139*, 87–90; (b) Liu, W.-B.; Zheng, C.; Zhuo, C.-X.; Dai, L.-X.; You, S.-L. *J. Am. Chem. Soc.* **2012**, *134*, 4812–4821.
- (31) Rössler, S. L.; Krautwald, S.; Carreira, E. M. *J. Am. Chem. Soc.* **2017**, *139*, 3603–3606.
- (32) Hethcox, J. C.; Shockley, S. E.; Stoltz, B. M. *Angew. Chem. Int. Ed.* **2018**, doi: 10.1002/anie.201804820.
- (33) DABCO has been previously utilized in iridium-catalyzed allylic alkylation leading to higher yields but slower rates of reaction, see: B. P. Bondzic, A. Farwick, J. Liebich, P. Eilbracht, *Org. Biomol. Chem.* **2008**, *6*, 3723–3731.

APPENDIX 8

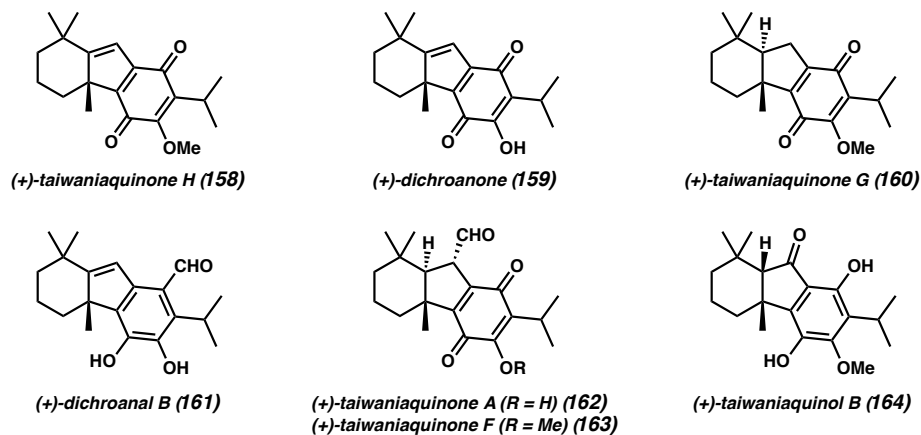
A Catalytic, Enantioselective Formal Synthesis of (+)-Dichroanone and (+)-Taiwaniaquinone H[†]

A8.1 INTRODUCTION

First isolated in 1995, the taiwaniaquinoid natural products are a family of tricyclic diterpenoids with a unique [6,5,6]-*abeo*-abietane skeleton (**158–164**, Figure A8.1).¹ Since their isolation, the taiwaniaquinoids have attracted significant attention from the synthetic community, resulting in a multitude of total and formal syntheses.² Interest in these compounds stems from their reported biological activity,³ in addition to their unique architecture containing a benzylic quaternary stereocenter. Due to the limited number of methodologies capable of installing benzylic quaternary stereocenters, only four catalytic, enantioselective syntheses of taiwaniaquinoids have been published to date.^{2e,m,q,t}

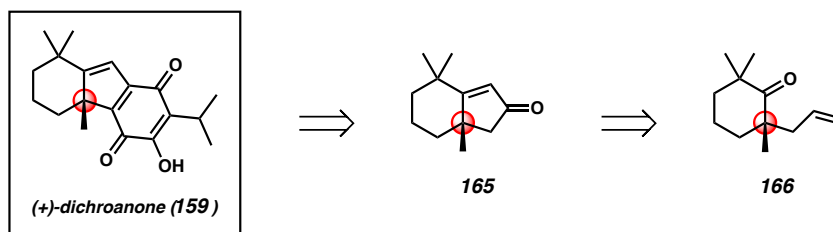
[†] This work was performed in collaboration with Dr. Jeffrey C. Holder. Portions of this chapter have been reproduced with permission from Shockley, S. E.;[‡] Holder, J. C.;[‡] Stoltz, B. M. *Org. Lett.* **2014**, *16*, 6362–6365 © 2014 American Chemical Society and Shockley, S. E.; Holder, J. C.; Stoltz, B. M. *Org. Process Res. Dev.* **2015**, *19*, 974–981 © 2015 American Chemical Society.

Figure A8.1 Taiwaniaquinoid natural products



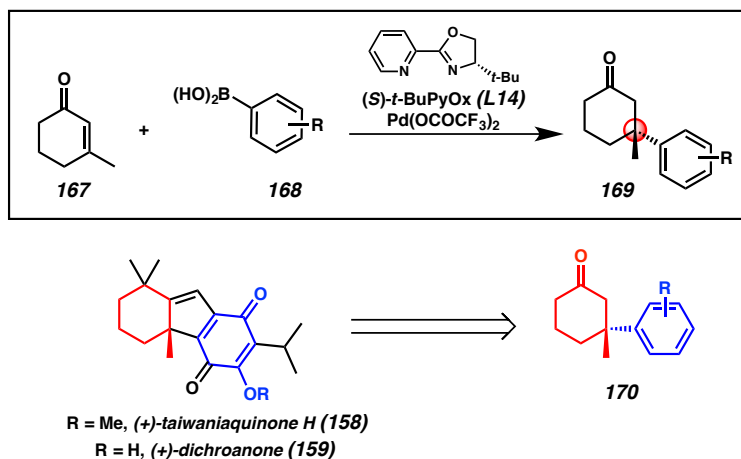
Our laboratory has a longstanding interest in the development of methods for the enantioselective synthesis of quaternary stereocenters and the application of these technologies to the synthesis of natural product targets. In 2006, our group reported the first catalytic, enantioselective total synthesis of (+)-dichroanone (**159**) via enantioselective palladium-catalyzed allylic alkylation (Scheme A8.1).^{2e} This work featured a linear synthetic sequence, elaborating palladium-catalyzed allylic alkylation product **166** to bicyclic enone **165** by Wacker oxidation and subsequent aldol condensation. The final ring was appended by another aldol condensation, and a novel series of oxidations provided the natural product in only 11 steps.

Scheme A8.1 Stoltz group retrosynthesis of (+)-dichroanone (**159**)



In 2011, the Stoltz group disclosed the first enantioselective palladium-catalyzed conjugate addition methodology to form quaternary stereocenters in high yields and enantioselectivities (Figure A8.2, top).⁴ Following this report, we recognized that the β -aryl ketone motif found in these conjugate addition products **169** mapped onto the scaffold of the taiwaniaquinoid terpene natural products, and we envisioned that a more convergent synthesis of these natural products could be achieved by employing β -aryl ketone **170** as the key intermediate (Figure A8.2, bottom). This modified retrosynthetic analysis facilitates a highly convergent, catalytic, enantioselective key step that brings together 13 of the 19 carbon atoms of the taiwaniaquinoid tricyclic core, including the quaternary stereocenter, in a single chemical transformation. Herein, we discuss the rational design of high-yielding and highly enantioselective conjugate addition reactions of arylboronic acids that facilitate the catalytic, enantioselective formal synthesis of (+)-taiwaniaquinone H (**158**) and (+)-dichroanone (**159**) in >99% ee.

Figure A8.2 Stoltz group conjugate addition chemistry as inspiration for revised retrosynthetic analysis of (+)-taiwaniaquinone H (**158**) and (+)-dichroanone (**159**)

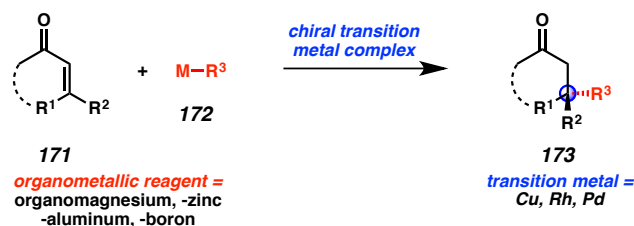


A8.2 BACKGROUND TO THE STOLTZ GROUP'S ENANTIOSELECTIVE PALLADIUM-CATALYZED CONJUGATE ADDITION CHEMISTRY

A8.2.1 INTRODUCTION TO ENANTIOSELECTIVE TRANSITION METAL- CATALYZED CONJUGATE ADDITION CHEMISTRY

Enantioselective conjugate addition has become a powerful synthetic tool for the assembly of structurally complex molecules.⁵ Recently, new developments in this transformation have served as solutions to the persistent challenge of the catalytic, enantioselective synthesis of all-carbon quaternary stereocenters (Scheme A8.2).⁶ To date, copper catalysis has dominated the field of enantioselective conjugate addition, however, these copper-catalyzed methods require the use of highly reactive organometallic reagents (e.g., diorganozinc,⁷ triorganoaluminum,⁸ and organomagnesium⁹ reagents). Thus, these reactions typically necessitate rigorously anhydrous reaction conditions and often operate at cryogenic temperatures. Alternatively, chiral rhodium catalysts in combination with air-stable, easily handled organoboron reagents have been shown to produce a wide array of conjugate addition adducts in very high yield and enantiomeric excess.^{10,11,12} Although extremely effective, these rhodium catalysts are expensive, air-sensitive, and many of the most widely used precatalysts are not commercially available. Additionally, rhodium-catalyzed conjugate additions to form quaternary stereocenters require boroxine or tetraarylborate reagents rather than widely available arylboronic acids. Furthermore, large excesses of the boron reagents are necessary to drive the reactions to completion. These factors diminish the appeal of such rhodium-catalyzed methods in complex molecule synthesis where custom aromatic units are often desired and thus the arene material is of high value.^{8,13}

Scheme A8.2 Enantioselective transition metal-catalyzed conjugate addition



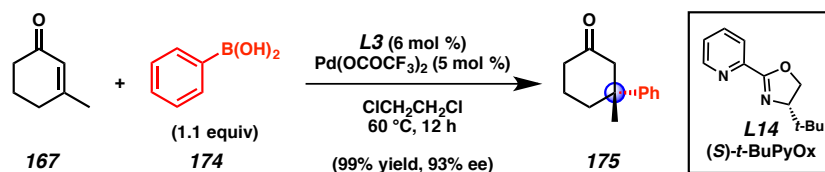
Palladium-catalyzed conjugate addition reactions are less developed than those using copper and rhodium but offer significant advantages. For example, palladium-catalyzed conjugate addition reactions utilize commercially available, air-stable, and functional group-tolerant boron nucleophiles. Furthermore, the reactions are typically not sensitive to water or oxygen. Together, these features comprise an operationally simple and robust transformation.¹⁴ At the time the Stoltz group began our work in this area, there were only examples of the enantioselective synthesis of *tertiary* stereocenters in the palladium literature and a single report of the synthesis of quaternary stereocenters, albeit as a racemate.¹⁵ It was not until our report in 2011 that a palladium-derived catalyst was employed to construct an enantioenriched quaternary stereocenter via conjugate addition methodology.^{4a} Subsequent to our studies, similar palladium-catalyzed conjugate additions to forge quaternary stereocenters were reported by Minnaard and de Vries¹⁶ as well as Stanley.¹⁷

A8.2.2 INITIAL DISCOVERIES

Our initial studies involved the enantioselective conjugate addition of arylboronic acids to β -substituted carbocyclic enones to generate benzylic all-carbon quaternary stereocenters.^{4a} We began these efforts by investigating the reaction of 3-

methylcyclohexen-2-one (**167**) with phenylboronic acid (**174**, Scheme A8.3). Building on the precedent for bidentate, dinitrogen ligands in conjugate addition chemistry,^{15,18} we found that a catalyst formed in situ from the combination of $\text{Pd}(\text{OCOCF}_3)_2$ and the chiral pyridinooxazoline ligand, (*S*)-*t*-BuPyOx (**L14**),¹⁹ proved effective in forming β -quaternary ketone product **175** in high yield and enantioselectivity. Many other ligands were examined in the course of our studies but none provided the high selectivities observed with *t*-BuPyOx (**L14**). Further optimization revealed that polar, coordinating solvents hindered the reaction while non-polar solvents provided higher conversions and superior enantioinduction. Ultimately, we found that 1,2-dichloroethane allowed for the fastest reaction times (12–24 h) with minimization of side product formation. Furthermore, we were pleased to find that the amount of phenylboronic acid could be reduced to 1.1 equivalents with no detrimental effect on the reactivity other than increased reaction times.

Scheme A8.3 Initial Stoltz group enantioselective palladium-catalyzed conjugate addition with (*S*)-*t*-BuPyOx (**L14**)



Based on control studies, we found the reaction to be insensitive to adventitious moisture and air atmosphere as neither the high yield nor enantioselectivity were impacted upon addition of water (up to 10 equivalents) and no improvements were noted under inert gas atmospheres. Therefore, the reactions may be conducted under ambient

air in screw-top vials without the need for purification or distillation of any commercially obtained materials. Moreover, the optimal chiral ligand, (*S*)-*t*-BuPyOx (**L14**), can be expediently prepared on relatively large scale in two steps from readily available starting materials.²⁰

Gratifyingly, a wide range of arylboronic acids and enones undergo highly enantioselective reactions under the developed conditions (Table A8.1). With respect to the nucleophile scope, *para*-substituted arylboronic acids are well tolerated. Alkyl-substituted arylboronic acids react with good yields and enantioselectivities to give products such as 4-methyl- and 4-ethyl-substituted ketones **177a** and **177b**. However, we noted a distinct electronic trend on selectivity, wherein electron-rich nucleophiles tend to furnish more modest yields and enantioselectivities (**177c**, **177d**, and **177h**). Conversely, arylboronic acids bearing electron-withdrawing substituents produce ketone products in excellent enantioselectivities. Specifically, the electron-poor substitution can include carbonyl (**177e**), trifluoromethyl (**177f**) or halide (**177g**) functional groups. Additionally, reactions involving *meta*-substituted nucleophiles fare well with alkyl (**177i**), ester (**177j**), halide (**177k**), or even nitro groups (**177l**) on the arylboronic acid. Notably, substituents at the 2-position of the arylboronic acid result in slower reactions and furnish diminished yields of the ketone products in low enantioselectivity (e.g., 2-methylphenylboronic acid results in 13% of its corresponding product in 22% ee). These *ortho*-arylboronic acid substrates react with higher yields and enantioselectivities in the palladium-catalyzed conjugate addition manifold described by Minnaard and de Vries.^{16b}

Table A8.1 Scope of arylboronic acid and enone conjugate acceptors^a

 176	 168
<p>L14 (6 mol %) Pd(OCOCF₃)₂ (5 mol %) ClCH₂CH₂Cl 40–80 °C, 12–24 h</p>	
 177	
<hr/>	
 177a 99% yield ^b 87% ee ^c	 177b 90% yield 85% ee
 177c 96% yield 74% ee	 177d 58% yield 69% ee
 177e 99% yield 96% ee	
 177f 99% yield 96% ee	 177g 84% yield 92% ee
 177h 52% yield 82% ee	 177i 99% yield 91% ee
 177j 91% yield 95% ee	
 177k 55% yield 96% ee	 177l 40% yield 92% ee
 177m 84% yield 91% ee	 177n 85% yield 93% ee
 177o 96% yield 92% ee	
 177p 95% yield 91% ee	 177q 74% yield 91% ee
 177r 86% yield 79% ee	 177s 68% yield 88% ee
 177t 65% yield 91% ee	

[a] Reactions performed with arylboronic acid (0.50 mmol), cycloalkenone (0.25 mmol), Pd(OCOCF₃)₂ (5 mol %), and **L14** (6 mol %) in ClCH₂CH₂Cl (1 mL) at 60 °C for 12 h. [b] Isolated yield. [c] Determined by chiral HPLC.

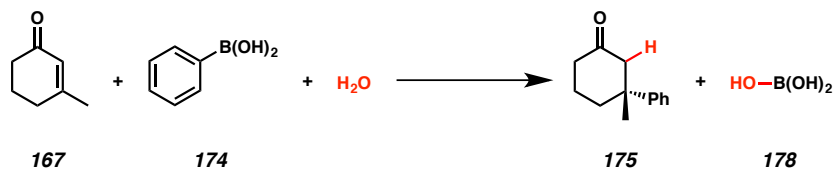
Cyclic enones of different ring sizes, and with a range of β-substitution, react to afford enantioenriched β-quaternary ketone products (Table A8.1). Cyclohexanone products bearing both linear (**177o–q**) and branched β-substituents (**177r** and **177s**) as

well as functionalized side chains (**177t**) are formed in good to excellent yields and selectivity from their corresponding substituted Michael acceptors. Moreover, altering the ring size has no deleterious effect on reactivity and furnishes products with five- (**177m**) or seven-membered (**177n**) cycloalkanones in high yields and enantioselectivity. To the best of our knowledge, this represents the first example of a single catalyst system that successfully constructs quaternary stereocenters via enantioselective conjugate addition to 5-, 6-, and 7-membered enones.

A8.2.3 FURTHER REACTION DEVELOPMENT

Following our initial communication of the construction of quaternary stereocenters by enantioselective palladium-catalyzed conjugate addition,^{4a} we sought to further generalize the substrate scope, reduce the catalyst loading, and lower the reaction temperature.^{4b} While we noted that the addition of water had no deleterious effect in our initial report, we did not consider adventitious water to be a crucial component. Thus, it came as a surprise when attempts to perform the reaction on large scale failed to fully convert enone **167** to product ketone **175**. We rationalized that, on small scale, the moisture in the air and on the glassware provided sufficient water to drive the reaction to completion, however, on larger scale this trace moisture was insufficient. Analysis of the balanced equation for the overall transformation indicated that the addition of water is necessary to achieve catalyst turnover (Scheme A8.4). Thus, we found that the addition of 5 equivalents of water to the reaction mixture restored the reactivity when performing reactions on multi-gram scale. To date, reactions as large as 35 mmol scale have been successfully conducted.

Scheme A8.4 Necessity of water in developed enantioselective palladium-catalyzed conjugate addition

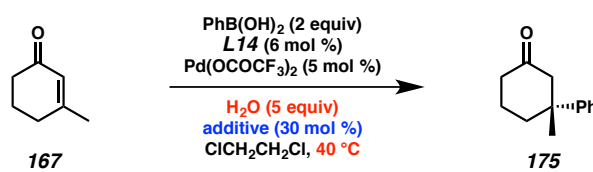


Examination of deuterium incorporation in the product ketone supported our hypothesis of water's role in catalyst turnover. In reactions performed with deuterium oxide in place of water, we found significant deuterium incorporation at the α -methylene position of the carbonyl. This observation was true in reactions run to low conversion as well. These experiments, in combination with the scalability problems encountered without water as an additive, suggested that water is the reagent assisting turnover, rather than the boron nucleophile (Scheme A8.4).

Based on literature reports detailing palladium-catalyzed conjugate addition employing cationic or dicationic precatalysts possessing weakly coordinating anions (PF_6^- , SbF_6^- , BF_4^- , etc.),¹⁴ we sought to evaluate the effect of salt additives on the reaction rate with the hope of achieving milder reaction conditions (Table A8.2). At 40 °C, with no additives, the addition of phenylboronic acid to 3-methylcyclohexenone (**167**) is very slow and rarely goes to full conversion before the catalyst decomposes. At this same temperature, we observed that the addition of strongly coordinating anions (e.g., chloride, entry 1) shutdown the reaction while sodium salts with weakly coordinating anions greatly enhanced the reaction rate, albeit with diminished enantioselectivity (e.g., NaPF_6 , entry 2). Other additives required extended reaction times (e.g., $(n\text{-Bu})_4\text{NPF}_6$, entry 3). A larger examination of salt additives containing weakly

coordinating counterions revealed that NH_4PF_6 gave the optimal combination of short reaction time with minimized loss of enantioselectivity (entry 4). We posit that these additives alter the catalyst resting state and result in a larger percentage of dissolved palladium species in the catalytic cycle.

Table A8.2 Effect of additives on reaction rate, yield, and enantioselectivity^a

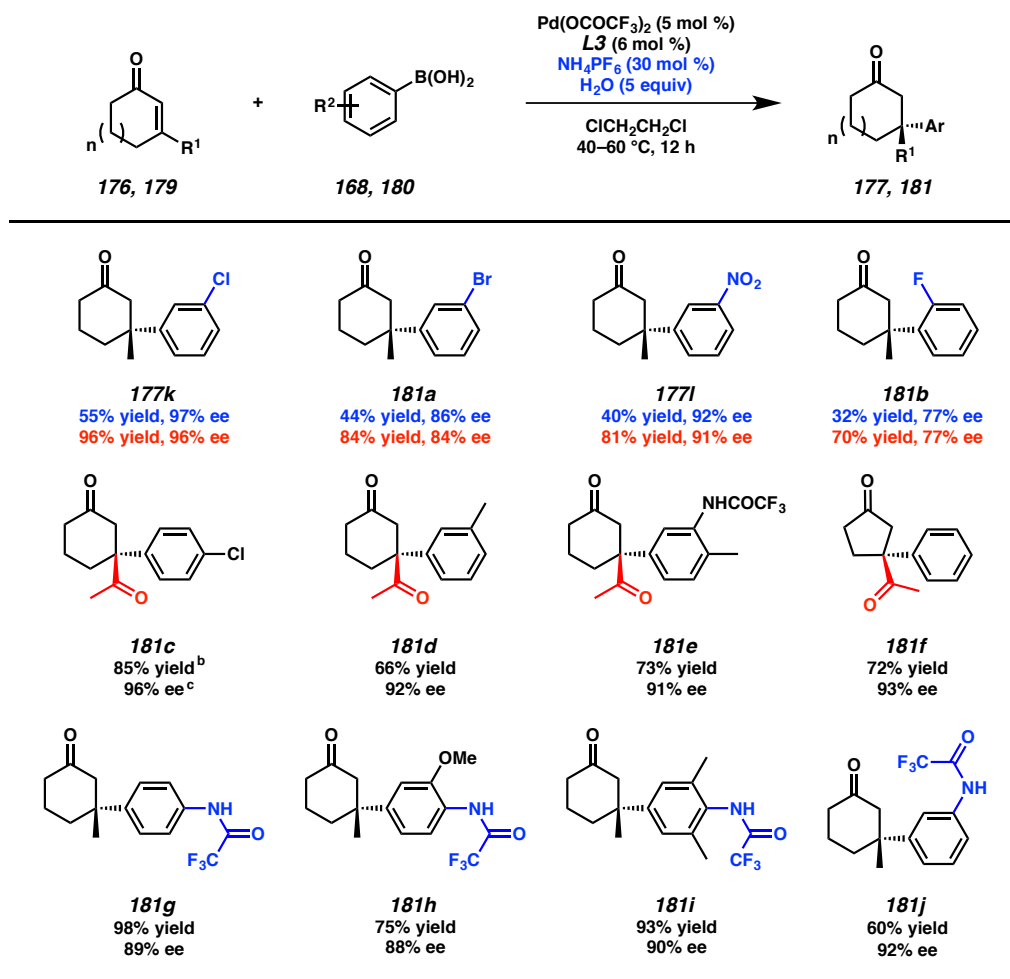
				
Entry	Additive	Time (h)	Yield (%) ^b	ee (%) ^c
1	NaCl	24	trace	—
2	NaPF_6	6	97	87
3	$(n\text{-Bu})_4\text{NPF}_6$	24	98	90
4	NH_4PF_6	12	96	91

[a] Reactions performed with phenylboronic acid (0.5 mmol), **167** (0.25 mmol), NH_4PF_6 (30 mol %), water (5 equiv), $\text{Pd}(\text{OCOCF}_3)_2$ (5 mol %), and **L14** (6 mol %) in $\text{ClCH}_2\text{CH}_2\text{Cl}$ (1 mL) at 40 °C. [b] GC yield utilizing tridecane standard. [c] Determined by chiral HPLC.

Incorporation of the optimized additives (5 equivalents water, 30 mol % NH_4PF_6) into the reaction conditions allowed for reactions to be conducted at decreased temperatures (23–40 °C) and significantly broadened the substrate scope. Many of the previously studied substrates that contained temperature-sensitive functionalities (e.g., silyl ethers) or groups that may react with trace palladium(0) formed by off-cycle pathways (e.g., arylbromides) afforded higher desired product yields under the modified conditions. For example, ketones **177k**, **181a**, **177l**, and **181b** were obtained in nearly double the yield under the new conditions (Table A8.3). Furthermore, at 40 °C the combination of additives allowed catalyst loadings of only 2.5 mol % of palladium and 3 mol % of ligand for most reactions. Moreover, the additives facilitated the reactions of

two new substrate classes: (1) β -acyl cyclic enones and (2) arylboronic acids containing nitrogen substituents. We were pleased to note that β -acyl enone substrates provided access to enantioenriched 1,4-dicarbonyl compounds, with only the olefin insertion process forming the quaternary stereocenter observed (**181c–f**), as opposed to the isomeric insertion products that would afford tertiary stereocenters. We also observed that aniline-derived boronic acid substrates protected with a trifluoroacetyl group did not poison the catalyst and allowed for the synthesis of heteroatom-substituted products (**181e**, **181g–j**).

Table A8.3 Expanded substrate scope with improved reaction conditions^a



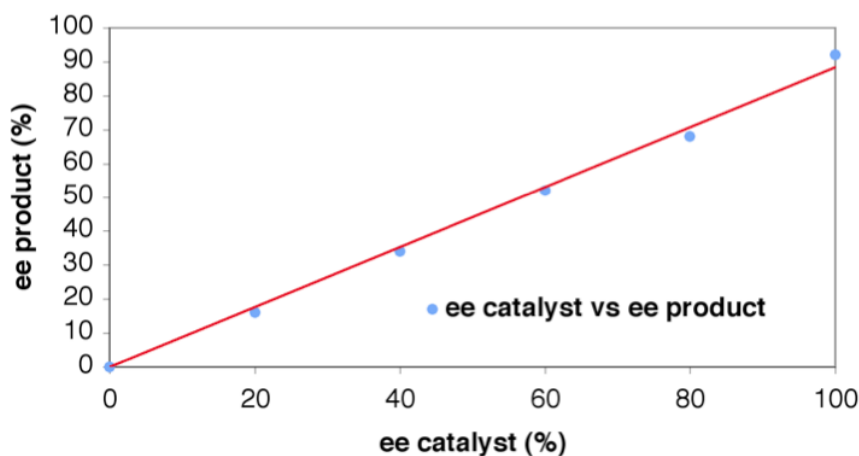
[a] Blue font: reported yield and ee of the product in the absence of NH_4PF_6 and water, with reactions performed at 60 °C. Red font: yield and ee of the product with additives. Conditions: reactions were performed with arylboronic acid (1.0 mmol), cycloalkenone (0.5 mmol), NH_4PF_6 (30 mol %), water (5 equiv), $\text{Pd}(\text{OCOCF}_3)_2$ (5 mol %), and **L14** (6 mol %) in $\text{ClCH}_2\text{CH}_2\text{Cl}$ (2 mL) at 40 °C. [b] Isolated yield. [c] Determined by chiral HPLC.

A8.2.4 MECHANISTIC HYPOTHESIS

Studies have been conducted to elucidate the catalytic cycle active in our enantioselective conjugate addition chemistry.^{4b} A range of Lewis and π -acidic metal salts were substituted for palladium with no product observed, signifying that palladium-catalyzed conjugate addition is not a Lewis acid-catalyzed process. The reaction proceeds

in the presence of mercury drops, which would poison a heterogeneous catalyst, indicating that a soluble complex likely catalyzes the reaction. Furthermore, a nonlinear effect study supported the action of a single, monomeric ML-type catalyst as the kinetically relevant species (Figure A8.3).²¹ The linear relationship between catalyst ee and product ee argues against the kinetic relevance of palladium/ligand dimers in solution, as opposed to some catalysts that are known to aggregate in reservoirs.^{15,22}

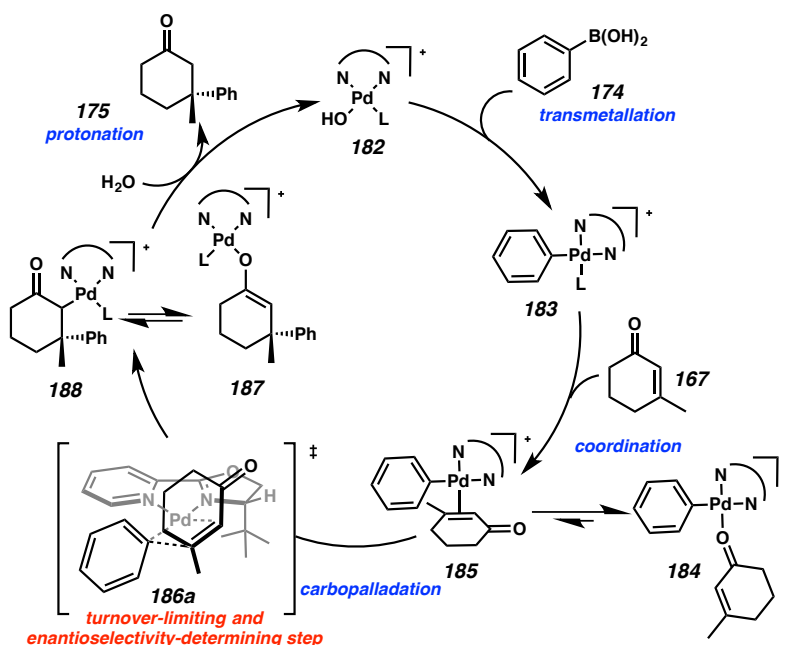
Figure A8.3 Linear relationship of catalyst ee to product ee



Density functional theory (DFT) calculations, performed in collaboration with the Houk laboratory, support the cationic catalytic cycle shown in Figure A8.4.^{4b,23} We postulate that the active catalyst is a cationic palladium(II) hydroxide species, which are known to undergo rapid transmetallation with arylboronic acids without added base.²⁴ We envision that arylpalladium **183** forms by transmetallation of the arylboronic acid with cationic catalyst **182**. Substrate association via the carbonyl yields an equilibrating mixture of carbonyl-bound complex **184** and olefin-bound complex **185**. C-bound enolate **188** is the initial product of alkene insertion into the aryl C–Pd bond. Notably, this

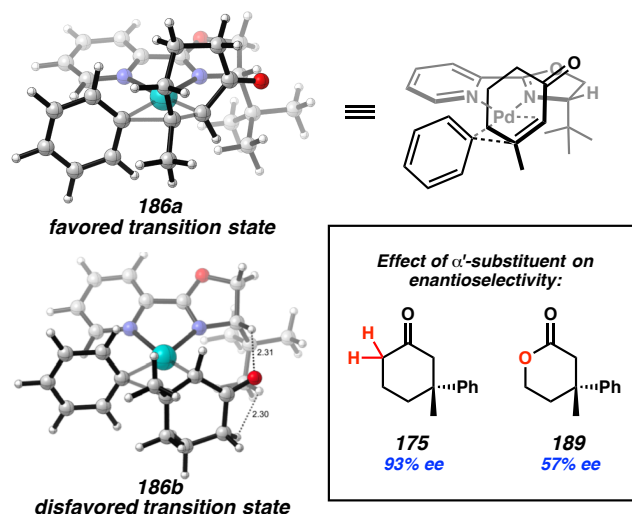
insertion is calculated to be both the enantiodetermining and turnover-limiting step of the catalytic cycle. Subsequent isomerization to *O*-bound tautomer **187** followed by protonation affords the product ketone and regenerates the catalyst (**182**).²⁵ This proposed mechanism was experimentally substantiated by a recent collaboration with the Zare laboratory in which arylpalladium cation **183** and enone complex **184/185** were identified by DESI-MS monitoring of the reaction mixture.²⁶ No intermediates occurring after the predicted turnover-limiting step were observed. The observation of enone-arylpladium complex **184** for a variety of arylboronic acid substrates led us to hypothesize that complex **184** may be the resting state. The enantiodetermining alkene insertion step involves a four-membered cyclic transition state, with the lowest energy diastereomer calculated to be transition state **186a**, which leads to the observed (*R*)-product. Diastereomer **186a** is the most stable as the bulky *t*-Bu group on the ligand points away from the substrate. Analysis of the effects of substituents on the ligand at the 4-position of the oxazoline revealed that replacing the *t*-Bu functionality with smaller groups, such as *i*-Pr, *i*-Bu, or Ph, significantly reduced the selectivity. If instead the oxazoline is substituted at the 5-position practically no enantioselectivity is afforded. Electronic perturbation of the pyridine moiety of the ligand did not erode enantioselectivity, though rates were greatly changed. Therefore, enantioselectivity is primarily attributed to the ligand/substrate steric interactions.

Figure A8.4 Proposed catalytic cycle for the enantioselective conjugate addition of arylboronic acids to cyclic enones catalyzed by the combination of $\text{Pd}(\text{OCOCF}_3)_2$ and (*S*)-*t*-BuPyOx (**L14**)



Transition state calculations suggested that stereocontrol predominantly arises from the repulsion of the α' -methylene hydrogens on the cyclohexenone substrate with the ligand (Figure A8.5). In the disfavored diastereomeric transition state (**186b**), these atoms are only 2.3 Å apart and thus incur a significant energetic penalty. Consequently, replacing the CH₂ group with an oxygen atom (e.g., lactone **189**, Figure A8.5) decreases the energy difference between the two diastereomeric transition states and leads to an observed decrease in enantioselectivity from 93% ee to 57% ee. Of note, α,β -unsaturated lactone substrates afford high enantioselectivity in the enantioselective palladium-catalyzed conjugate addition described by Minnaard and de Vries.^{16a}

Figure A8.5 Calculated transition states and effect of α' -substituents on enantioselectivity



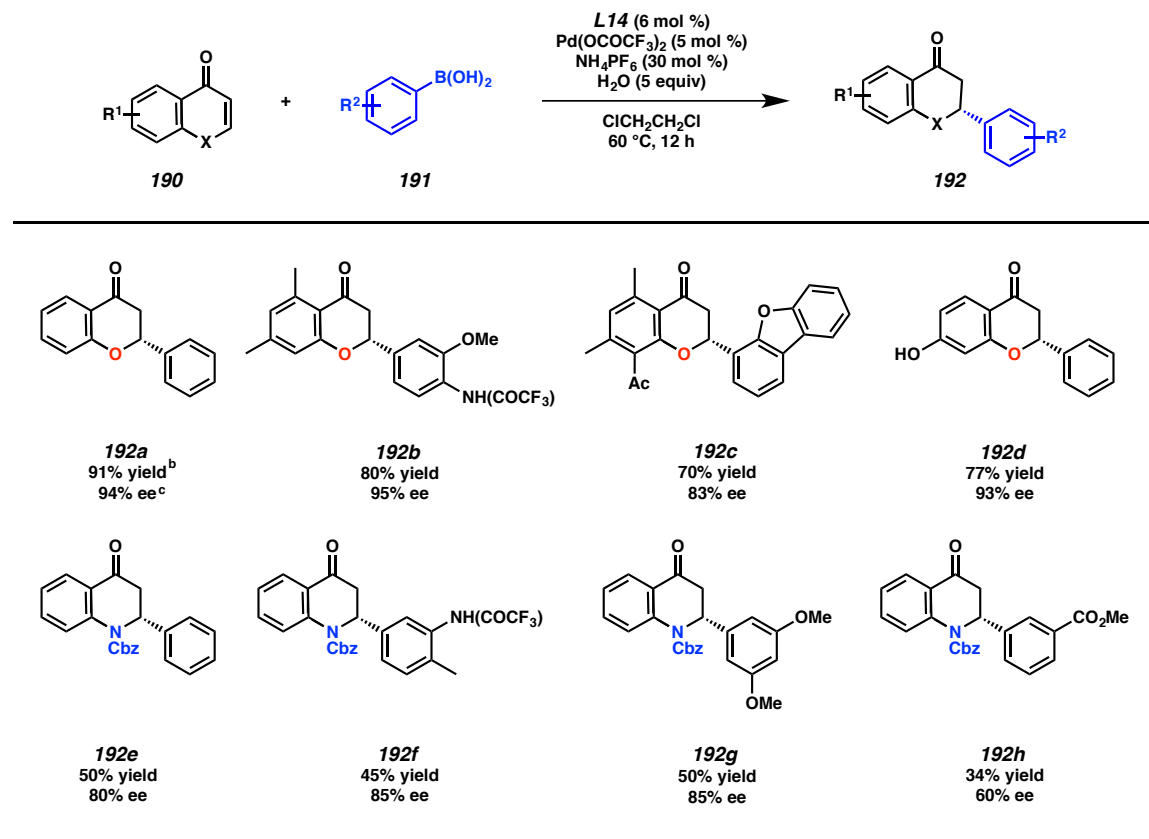
A8.2.5 HETEROCYCLIC ACCEPTORS

We wished to extend our conjugate addition methodology to the synthesis of stereochemically complex heterocyclic molecules. We found that the palladium-catalyzed conjugate addition of arylboronic acids to chromones and 4-quinolones delivered *tertiary* stereocenters in high yield and enantioselectivities across multiple heterocyclic scaffolds with a wide range of arylboronic acids (Table A8.4).^{4c} While chromones^{27,28} and 4-quinolones²⁹ have been successfully employed in rhodium-catalyzed conjugate addition, to our knowledge, these are the first examples of enantioselective transition metal-catalyzed conjugate additions to chromones and 4-quinolones using either palladium catalysis or arylboronic acid nucleophiles.³⁰

Overall, a total of 38 adducts were prepared in moderate to excellent yield and high enantioselectivity. Furthermore, the stability of the reaction components to air and moisture affords unprecedented functional group tolerance. Thus, heterocyclic products

bearing heterocyclic substitution (**192c**), free phenolic groups (**192d**), and *N*-substituted arenes (**192b** and **192f**) could be obtained via the conjugate addition methodology.

Table A8.4 Enantioselective conjugate addition of arylboronic acids to heterocyclic conjugate acceptors^a



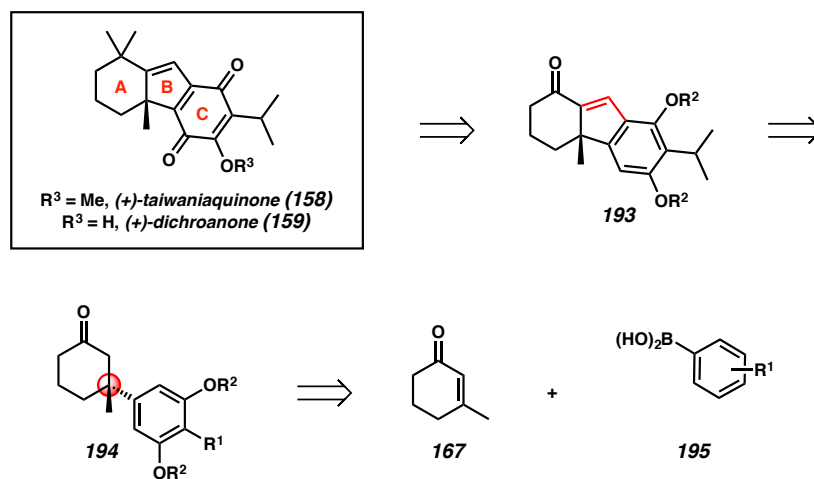
[a] Reactions performed with arylboronic acid (0.50 mmol), heterocyclic acceptor (0.25 mmol), NH_4PF_6 (30 mol %), water (5 equiv), $\text{Pd}(\text{OCOCF}_3)_2$ (5 mol %), and **L14** (6 mol %) in $\text{ClCH}_2\text{CH}_2\text{Cl}$ (1 mL) at 60 °C for 12 h. [b] Isolated yield. [c] Determined by chiral HPLC.

A8.3 RETROSYNTHETIC ANALYSIS

The formal synthesis of (+)-taiwaniaquinone H (**158**) and (+)-dichroanone (**159**) provided an optimal forum for demonstrating the breadth and generality of our aforementioned palladium-catalyzed conjugate addition chemistry. Our preliminary

strategic disconnections of (+)-taiwaniaquinone H (**158**) and (+)-dichroanone (**159**) involved late stage introduction of the gem-dimethyl functionality and oxidation of the C-ring of enone **193** to the quinone (Figure A8.6).^{31,2f} In turn, the B-ring of tricycle **193** was envisioned to be established through *ortho*-formylation of phenol **194** and subsequent aldol condensation. Finally, we anticipated that the all-carbon quaternary stereocenter could be constructed by enantioselective palladium-catalyzed conjugate addition of 3-methyl-2-cyclohexenone (**167**) with an appropriate arylboronic acid **195**.⁴

Figure A8.6 Planned retrosynthesis of (+)-taiwaniaquinone H (**158**) and (+)-dichroanone (**159**)

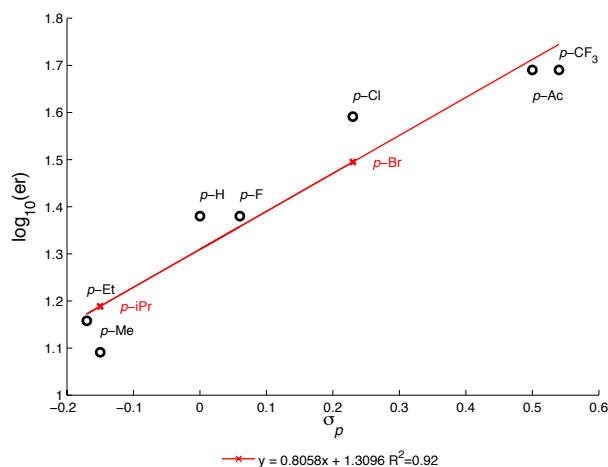


A8.4 FIRST GENERATION ROUTE

We first selected *para*-acetylphenylboronic acid **199** (Scheme A8.5) as our conjugate addition substrate. In our previous work we noted that electron-withdrawing substituents at the *para*-position of the arylboronic acid often afforded highly enantioenriched β -quaternary ketone products.⁴ A plot of the enantiomeric ratio versus the Hammett value (σ_p) for a variety of *para*-substituted phenylboronic acids demonstrates a strong positive linear correlation, $R^2 = 0.92$ (Figure A8.7).³² The positive value of ρ

(0.81) suggests that the difference in energy between the diastereomeric transition states leading to the enantiomeric (*S*) and (*R*) products increases as the boronic acid becomes increasingly electron deficient. Thus, the best selectivity in the conjugate addition reaction is achieved with electron-withdrawing substituents in the *para*-position. Therefore, we chose to mask the isopropyl group as a methyl ketone to achieve a selective conjugate addition reaction.

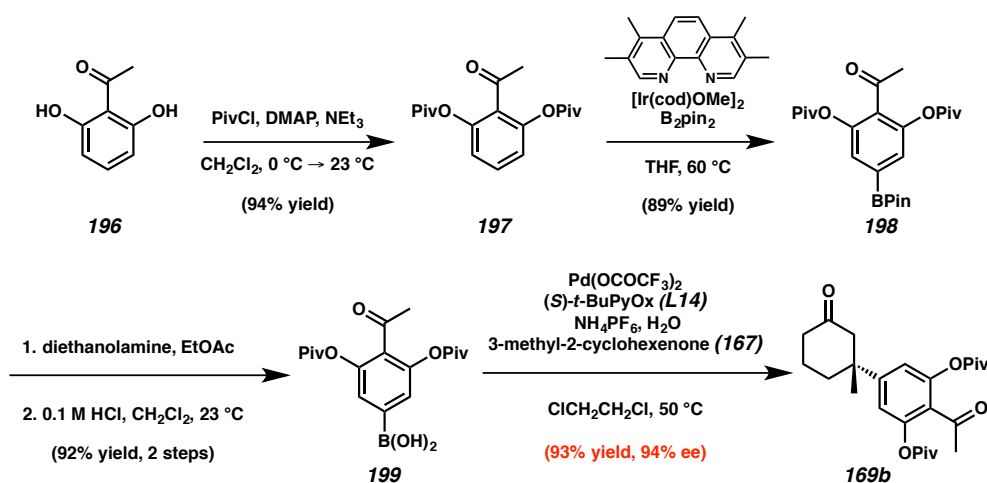
Figure A8.7 Hammett plot of $\log_{10}(er)$ vs σ_p for select boronic acids in the palladium-catalyzed conjugate addition reaction



Access to *para*-acetylphenylboronic acid **199** began with acylation of 2,6-dihydroxyacetophenone (**196**) with pivaloyl chloride to provide arene **197** (Scheme A8.5). Installation of the boryl substituent was accomplished through an iridium-catalyzed C–H borylation.³³ This reaction provided pinacol boronate ester **198** as the exclusive product in 89% yield. Empirically, we identified that protecting the *meta*-hydroxyl substituents with pivalate groups allowed for the highest yields in this borylation chemistry. After exhaustive exploration of deprotection conditions, we found

that treatment with diethanolamine and subsequent acid-catalyzed hydrolysis of the transesterified intermediate afforded arylboronic acid **199** in 92% yield.³⁴ Boronic acid **199** was treated with 3-methyl-2-cyclohexenone (**167**) in the presence of Pd(OCOCF₃)₂, (*S*)-*t*-BuPyOx (**L14**), and NH₄PF₆ at 50° C to afford enantioenriched ketone **169b** in 93% yield and 94% ee.^{4b}

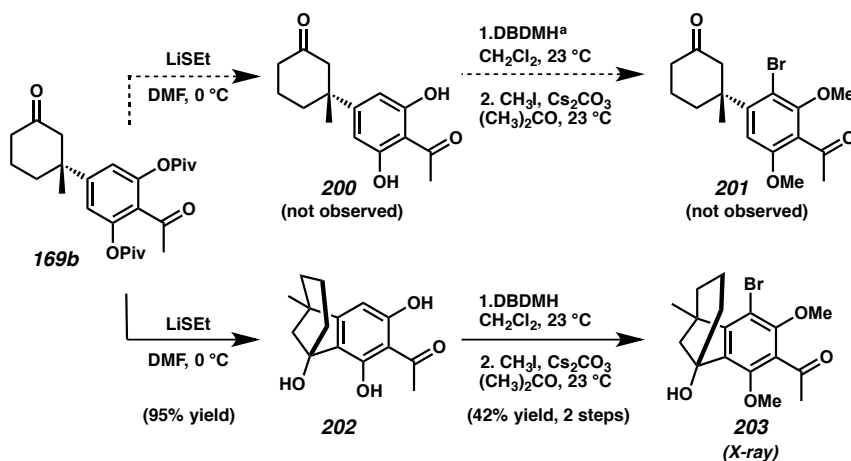
Scheme A8.5 Synthesis of acetyl conjugate addition product **169b**



With ketone **169b** in hand, we turned our attention to the installation of the final carbon of the tricyclic core and completion of the B-ring. Regrettably, attempts to formylate arene **169b** were unsuccessful. We rationalized that the sterically congested environment surrounding the arene C–H bonds prohibited installation of a functional group handle. Moreover, deprotection of the hydroxyl groups of ketone **169b** was not facile, and required treatment with LiSEt to cleanly remove both pivaloyl groups and afford what we predicted to be resorcinol **200** (Scheme A8.6). Though HRMS data matched the molecular formula of desired resorcinol **200**, the ¹H NMR spectra did not

match that of a typical β -quaternary ketone conjugate addition product. We suspected that an unproductive cyclization may have occurred and sought to crystallize derivatives of ketone **202** to confirm the new structure by single crystal X-ray diffraction. Bromination and methylation of compound **202** provided bromoarene **203** as a white crystalline solid. As we suspected, a cyclization had occurred and the structure proved to be [3.2.1]bicycle **203**. Thus, we were able to properly assign the structures of cyclization product **202** and arene bromination adduct **203**. This X-ray structure also confirms the absolute stereochemistry imparted in enantioselective conjugate addition reactions of arylboronic acids to cyclic conjugate acceptors facilitated by the catalyst derived from the combination of (*S*)-*t*-BuPyOx (**L14**) and Pd(OCOCF₃)₂.

Scheme A8.6 Unexpected cyclization of phenolic intermediate^a



[a] DBDMH = 1,3-dibromo-5,5-dimethylhydantoin

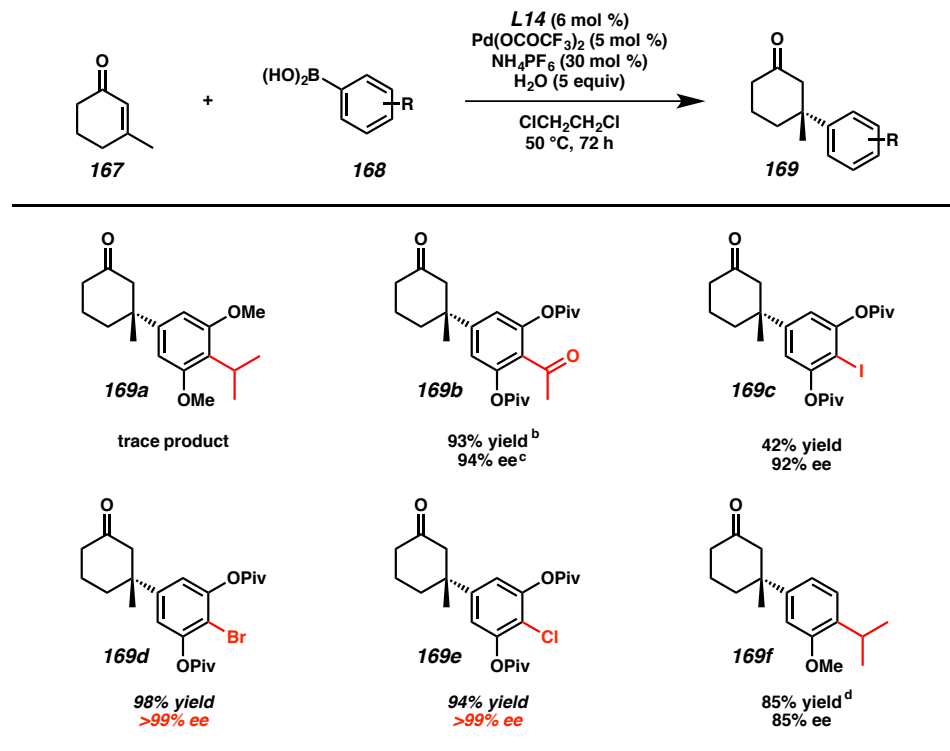
Cyclizations of β -aryl ketones to form [3.2.1] bicycles are rare; the few other reports of this transformation require treatment with strong Lewis³⁵ or Brønsted acids³⁶ at elevated temperatures. These reactions presumably operate via an electrophilic aromatic substitution mechanism. While it is possible that our noted cyclization proceeds through a

similar mechanism, we did not observe cyclization with substrates bearing protected phenols, which suggests that the hydroxyl group or phenoxide may be involved in the cyclization mechanism. This observation led us to propose that this unexpected cyclization may instead occur through a carbonyl ene or lithium phenoxide aldol reaction pathway.

A8.5 SECOND GENERATION ROUTE

As we were unable to functionalize ketone **169b** without causing the undesired cyclization, we decided to redesign the arylboronic acid substrate and began examining alternative conjugate addition reactions. Removing the acetyl group would obviate the need to differentiate the benzylic carbonyl from the cyclic ketone while installing the requisite isopropyl group in the first-generation conjugate addition product **169b**. We envisioned that a *para*-halogenated arylboronic acid derivative would allow for facile installation of the isopropyl group via cross-coupling chemistry. Additionally, based on our Hammett plot analysis, we posited that the *para*-halide would serve as a necessary *para*-electron-withdrawing group to impart high enantioselectivity in the palladium/**L14** conjugate addition chemistry (Figure A8.7).⁴ Gratifyingly, we found that use of these boronic acids furnished products bearing *para*-iodo (**169c**), *para*-bromo (**169d**), and *para*-chloro (**169e**) arenes in high enantioselectivity and moderate to high yields (Table A8.5).

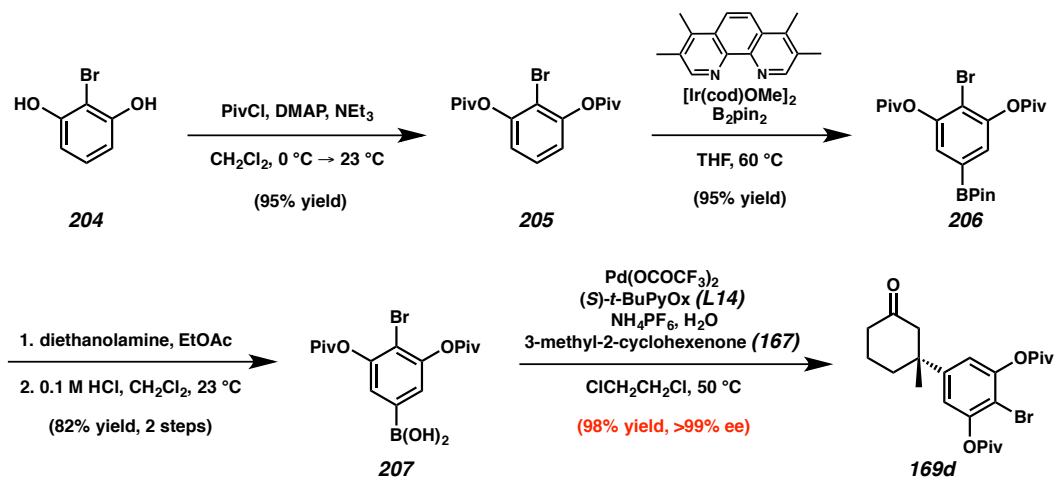
Table A8.5 Identification of a suitable conjugate addition system^a



[a] Reactions performed with boronic acid (1.5 equiv), **167** (1 equiv), NH_4PF_6 (30 mol %), water (5 equiv), $\text{Pd(OCOCF}_3)_2$ (5 mol %), and **L14** (6 mol %) in $\text{ClCH}_2\text{CH}_2\text{Cl}$ at 50°C for 12 h. [b] Isolated yield. [c] Determined by chiral HPLC or SFC.

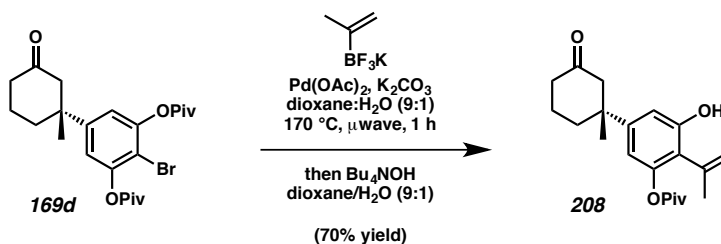
We consequently pursued a revised approach to the natural products via bromoarene **169d**, selected both for its superior reactivity in palladium-catalyzed conjugate addition chemistry and facile cross-coupling ability. To access this intermediate, 2-bromoresorcinol **204** was converted to *para*-bromophenyl boronic acid derivative **207** in 73% yield over four steps (Scheme A8.7). Subsequent catalytic, enantioselective conjugate addition furnished ketone **169d** in 98% yield and >99% ee.

Scheme A8.7 Synthesis of para-bromo conjugate addition product **169d**



Having installed the quaternary stereocenter, we next sought to append the isopropyl group. Attempts to directly cross-couple an isopropyl zinc reagent with bromide **169d** gave an inseparable mixture of iso- and *n*-propyl products.³⁷ The steric hindrance of the nearby pivaloyl groups thwarted our attempts to cross couple **169d** with isopropenyl organometallic reagents, but we ultimately achieved success using Molander's protocol for Suzuki-Miyaura couplings of potassium isopropenyltrifluoroborate salts.³⁸ Our optimized conditions ($170\text{ }^\circ\text{C}$, 1 h, microwave) gave a crude mixture of both cross coupled product and mono-protected cross coupled product that could be stirred with tetrabutylammonium hydroxide to furnish isopropenyl phenol **208** in 70% yield (Scheme A8.8).

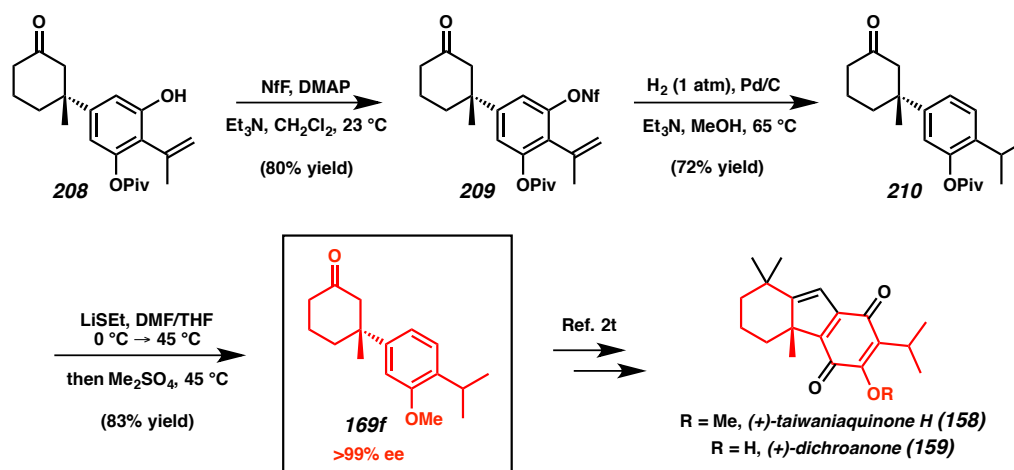
Scheme A8.8 Isopropenyl cross-coupling



With a route to mono-deprotected arene **208** established, we turned our efforts once more toward the formation of the B-ring. However, despite the successful removal of one pivaloyl group, the system proved resistant to a number of metal and non-metal mediated *ortho*-formylations, directed *ortho*-metalations, and halogenations, regardless of protection of the ketone. We speculate that the failure of these efforts may again be attributed to the formidable steric environment of the arene C–H bonds.

Recognizing that significant steric hindrance would prevent the formation of the B-ring, we sought to diminish the steric environment of the arene by reductive removal of the free phenol. Activation of phenol **208** by exposure to excess perfluorobutanesulfonyl fluoride led to the generation of nonaflate **209** in 80% yield (Scheme A8.9). Subsequent hydrogenation with Pd/C simultaneously cleaved the nonaflate and reduced the isopropenyl functionality to afford isopropyl arene **210** in 72% yield.³⁹ Finally, the pivaloyl group was replaced with a methyl group by one pot deprotection and methylation with LiSEt and Me_2SO_4 to provide ketone **169f** in 83% yield. With the less substituted arene **169f** in hand, we believed that the necessary tricycle could now be readily formed by *ortho*-formylation.

Scheme A8.9 Synthesis of key intermediate **169f**



Concurrent with our synthetic efforts, Qin and coworkers reported a formal total synthesis of (+)-taiwaniaquinone H (**158**) and (+)-dichroanone (**159**) via enantioselective conjugate addition of (4-isopropyl-3-methoxyphenyl)boronic acid to 3-methyl-2-cyclohexenone (**167**) in 85% yield and 85% ee (**169f**, Table A8.5) using the catalyst developed in our laboratory.^{2t,4a} However, Qin was unable to optimize the conjugate addition substrates to achieve yields or enantioselectivities over 85%. This result aligns well with our Hammett plot analysis; the determined linear relationship predicts an enantioselectivity of 88% for the electron-donating isopropyl group (Figure A8.7). Moreover, this study demonstrated that our common intermediate **169f** could be further transformed into the taiwaniaquinoid tricyclic skeleton by *ortho*-formylation followed by aldol condensation. Therefore, our synthesis of ketone **169f** in >99% ee constitutes a formal synthesis of (+)-taiwaniaquinone H (**158**) and (+)-dichroanone (**159**) in the highest reported enantioselectivity to date.

A8.6 CONCLUSIONS

In summary, we have completed the formal catalytic, enantioselective total syntheses of (+)-taiwaniaquinone H (**158**) and (+)-dichroanone (**159**) in 35% overall yield, starting from commercially available 2-bromoresorcinol (**204**). Investigation of electronic effects of arylboronic acid substituents on enantioselectivity enabled the rational design of a highly enantioselective reaction that furnished established intermediate **169f** in exceptionally high yield and enantioselectivity. Additionally, an unexpected cyclization to form a [3.2.1] bicycle permitted the unambiguous determination of the absolute stereochemistry of the quaternary stereocenter installed by the palladium/**L14**-catalyzed conjugate addition reaction by X-ray diffraction analysis.

A8.7 EXPERIMENTAL SECTION

A8.7.1 MATERIALS AND METHODS

Unless otherwise stated, reactions were performed in flame-dried glassware under an argon or nitrogen atmosphere using dry, deoxygenated solvents. Solvents were dried by passage through an activated alumina column under argon. Triethylamine was distilled over CaH_2 prior to use. Purified water was obtained using a Barnstead NANOpure Infinity UV/UF system. Chemicals were purchased from Sigma Aldrich/Strem/Alfa Aesar and used as received. Reaction temperatures were controlled by an IKAmag temperature modulator. Microwave-assisted reactions were performed in a Biotage Initiator 2.5 microwave reactor. Glove box manipulations were performed under a nitrogen atmosphere. Thin-layer chromatography (TLC) was performed using E. Merck silica gel 60 F254 precoated plates (0.25 mm) and visualized by UV fluorescence

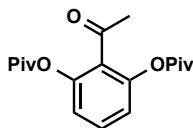
quenching or *p*-anisaldehyde staining. SiliaFlash P60 Academic Silica gel (particle size 0.040–0.063 mm) was used for flash chromatography. ^1H NMR spectra were recorded on a Varian Inova 500 MHz spectrometer or a Bruker Avance HD 400 MHz spectrometer and are reported relative to residual CHCl_3 (δ 7.26 ppm) or $(\text{CH}_3)_2\text{SO}$ (δ 2.50 ppm). ^{13}C NMR spectra were recorded on a Varian Inova 500 MHz spectrometer and are reported relative to residual CDCl_3 (δ 77.16 ppm), $(\text{CD}_3)_2\text{SO}$ (δ 39.52 ppm) or $(\text{CD}_3)_2\text{CO}$ (δ 29.84 ppm). Data for ^1H NMR are reported as follows: s = singlet, d = doublet, t = triplet, q = quartet, p = pentet, sept = septuplet, m = multiplet, br s = broad singlet, app = apparent. Data for ^{13}C NMR are reported in terms of chemical shifts (δ ppm). IR spectra were obtained using a Perkin Elmer Paragon 1000 spectrometer using thin films deposited on NaCl plates and reported in frequency of absorption (cm^{-1}). High resolution mass spectra (HRMS) were obtained from an Agilent 6200 Series TOF with Agilent G1978A Multimode source in mixed ionization mode (MultiMode ESI/APCI) or from a JEOL JMS-600H in fast atom bombardment (FAB+). Optical rotations were measured with a Jasco P-2000 polarimeter operating on the sodium D-line (589 nm), using a 100 mm pathlength cell, and are reported as $[\alpha]_{\text{D}}^{\text{T}}$ (concentration in g/100 mL, solvent).

A8.7.1.1 Preparation of Known Compounds

Previously reported methods were used to prepare ligand (*S*)-*t*-BuPyOx (**L14**).^{20b}

A8.7.2 EXPERIMENTAL PROCEDURES AND SPECTROSCOPIC DATA

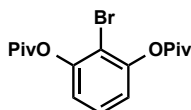
A8.7.2.1 General Procedure and Spectroscopic Data for the Synthesis of Resorcinol Pivaloyl Esters



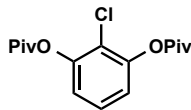
2-Acetyl-1,3-phenylene bis(2,2-dimethylpropanoate) (197). An oven-dried 1 L round-bottom flask was charged with a magnetic stir bar, 2,6-dihydroxyacetophenone (10 g, 65.7 mmol, 1 equiv) and DMAP (800 mg, 6.57 mmol, 10 mol %). The flask was evacuated under vacuum and back-filled three times with argon. The solids were suspended in CH_2Cl_2 (450 mL), and NEt_3 (23 mL, 165 mmol, 2.5 equiv) was added, at which time the solution became homogenous and a transparent, pale yellow color was observed. The reaction solution was cooled to 0 °C in an ice/water bath and pivaloyl chloride (17 mL, 138 mmol, 2.1 equiv) was added via mechanical syringe pump addition over the course of 2 h. Slow addition is essential to maintain an internal temperature of less than 5 °C and minimize formation of side products. Upon complete addition, the ice/water bath was removed and the reaction mixture was allowed to warm to ambient temperature. After 1 h, the starting material was consumed by TLC analysis (30% acetone/hexanes, stain *p*-anisaldehyde), and the reaction mixture was quenched with sat. NH_4Cl (aq, 300 mL). The mixture was diluted with CH_2Cl_2 (400 mL) and transferred to a separatory funnel. The aqueous layer was extracted with CH_2Cl_2 (3 x 100 mL) and the combined organic extracts were washed with 1M HCl (3 x 100 mL) and brine (1 x 100 mL), dried over MgSO_4 and concentrated under reduced pressure. The crude mixture was purified by silica gel flash column chromatography (150 g silica gel, eluent: 20%

acetone/hexanes) to afford pivaloyl **197** as a white, crystalline solid (19.73 g, 94% yield):

^1H NMR (500 MHz, CDCl_3) δ 7.40 (t, $J = 8.3$ Hz, 1H), 6.99 (d, $J = 8.2$ Hz, 2H), 2.45 (s, 3H), 1.32 (s, 18H); ^{13}C NMR (125 MHz, CDCl_3) δ 198.7, 176.4, 147.9, 130.4, 128.6, 120.1, 39.2, 31.7, 27.1; IR (Neat Film, NaCl): 3487, 3395, 2976, 2936, 2874, 1755, 1705, 1611, 1576, 1478, 1457, 1397, 1368, 1274, 1251, 1233, 1117, 1101 cm^{-1} ; HRMS (MultiMode ESI/APCI-) m/z calc'd for $\text{C}_{18}\text{H}_{23}\text{O}_5$ $[\text{M}-\text{H}]^-$: 319.1551, found 319.1542.

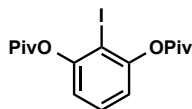


2-Bromo-1,3-phenylene bis(2,2-dimethylpropanoate) (205). White, crystalline solid (3.77 g, 95% yield): ^1H NMR (500 MHz, CDCl_3) δ 7.33 (t, $J = 8.2$ Hz, 1H), 7.00 (d, $J = 8.2$ Hz, 2H), 1.40 (s, 18H); ^{13}C NMR (125 MHz, CDCl_3) δ 175.8, 149.9, 128.0, 120.9, 111.4, 39.6, 27.4; IR (Neat Film, NaCl): 2971, 2934, 2972, 1762, 1586, 1479, 1460, 1396, 1365, 1274, 1254, 1233, 1093, 1031, 884 cm^{-1} ; HRMS (MultiMode ESI/APCI+) m/z calc'd for $\text{C}_{16}\text{H}_{25}\text{BrNO}_4$ $[\text{M}+\text{NH}_4]^+$: 374.0961, found 374.0960.



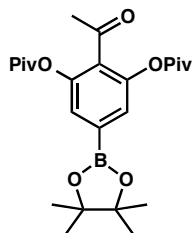
2-Chloro-1,3-phenylene bis(2,2-dimethylpropanoate) (211). White, crystalline solid (7.57 g, 98% yield): ^1H NMR (500 MHz, CDCl_3) δ 7.28 (t, $J = 8.2$ Hz, 1H), 7.03 (d, $J = 8.2$ Hz, 2H), 1.40 (s, 18H); ^{13}C NMR (125 MHz, CDCl_3) δ 175.8, 148.4, 127.0, 121.0, 121.0, 39.3, 27.1; IR (Neat Film, NaCl): 2970, 2935, 2874, 1765, 1749, 1583, 1478,

1463, 14552, 1397, 1368, 1273, 1259, 1235, 1112, 1033 cm^{-1} ; HRMS (MultiMode ESI/APCI+) m/z calc'd for $\text{C}_{16}\text{H}_{25}\text{ClNO}_4$ $[\text{M}+\text{NH}_4]^+$: 330.1467, found 330.1472.



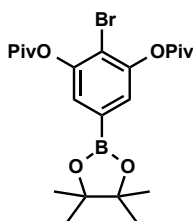
2-Iodo-1,3-phenylene bis(2,2-dimethylpropanoate) (212). White, crystalline solid (14.0 g, 96% yield): ^1H NMR (500 MHz, CDCl_3) δ 7.35 (t, $J = 8.1$ Hz, 1H), 6.95 (d, $J = 8.1$ Hz, 2H), 1.42 (s, 18H); ^{13}C NMR (125 MHz, CDCl_3) δ 175.9, 152.9, 129.5, 120.0, 88.0, 39.5, 27.5; IR (Neat Film, NaCl): 2972, 2873, 1755, 1583, 1479, 1451, 1396, 1367, 1274, 1244, 1218, 1095, 1029, 967, 941, 886 cm^{-1} ; HRMS (MultiMode ESI/APCI-) m/z calc'd for $\text{C}_{16}\text{H}_{20}\text{IO}_4$ $[\text{M}-\text{H}]^-$: 403.0412, found 403.0413.

A8.7.2.2 General Procedure and Spectroscopic Data for the Synthesis of Borylated Arenes



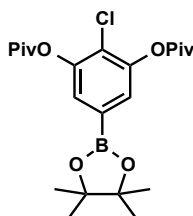
2-Acetyl-5-(4,4,5,5-tetramethyl-1,3,2-dioxaborolan-2-yl)-1,3-phenylene bis(2,2-dimethylpropanoate) (198). In a nitrogen-filled glove box, a 500 mL round-bottom flask with a Kontes valve was charged with a stir bar, arene **197** (16.02 g, 50.0 mmol, 1.0 equiv), B_2Pin_2 (9.5 g, 37.5 mmol, 0.75 equiv), $[\text{Ir}(\text{cod})(\text{OMe})_2]$ (33 mg, 0.05 mmol, 0.1 mol %), and tetramethylphenanthroline (24 mg, 0.10 mmol, 0.2 mol %). The solids were

suspended in THF (50 mL), and the flask was sealed and removed from the glove box. The reaction mixture was stirred in an oil bath heated at 60 °C for 45 h, at which time the reaction was complete by TLC analysis (20% acetone/hexanes, *p*-anisaldehyde stain). The reaction mixture was cooled to ambient temperature and filtered through a silica gel plug (50 g silica gel, eluent: acetone), and concentrated under reduced pressure. The crude reaction mixture was further purified by silica gel flash chromatography (200 g silica gel, eluent: 20% acetone/hexanes) to afford borylated **198** as an amorphous off-white solid (19.85 g, 89% yield): ¹H NMR (500 MHz, CDCl₃) δ 7.38 (s, 2H), 2.43 (s, 3H), 1.33 (s, 12H), 1.32 (s, 18H); ¹³C NMR (125 MHz, CDCl₃) δ 198.8, 176.5, 147.3, 131.0, 126.0, 120.1, 84.6, 39.2, 31.5, 27.2, 25.0; IR (Neat Film, NaCl): 3509, 2981, 2935, 1766, 1707, 1482, 1459, 1405, 1396, 1354, 1331, 1259, 1212, 1147 cm⁻¹; HRMS (MultiMode ESI/APCI+) *m/z* calc'd for C₂₄H₃₉BNO₇ [M+NH₄]⁺: 463.2850, found 463.2852.

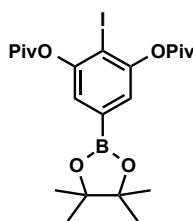


2-Bromo-5-(4,4,5,5-tetramethyl-1,3,2-dioxaborolan-2-yl)-1,3-phenylene bis(2,2-dimethylpropanoate) (206). Amorphous off-white solid (2.04 g, 96% yield): ¹H NMR (500 MHz, CDCl₃) δ 7.38 (s, 2H), 1.39 (s, 18H), 1.32 (s, 12H); ¹³C NMR (125 MHz, CDCl₃) δ 175.8, 149.5, 129.8, 126.6, 114.9, 84.6, 39.5, 27.4, 25.0; IR (Neat Film, NaCl): 2977, 1764, 1600, 1479, 1397, 1389, 1364, 1329, 1274, 1211, 1141, 1094, 1036 cm⁻¹;

HRMS (MultiMode ESI/APCI+) m/z calc'd for $C_{22}H_{36}BBrNO_6$ $[M+NH_4]^+$: 499.1850,
found 499.1834.



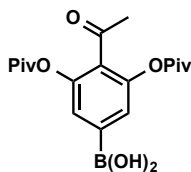
2-Chloro-5-(4,4,5,5-tetramethyl-1,3,2-dioxaborolan-2-yl)-1,3-phenylene bis(2,2-dimethylpropanoate) (213). Amorphous off-white solid (9.01 g, 99% yield): 1H NMR (400 MHz, $CDCl_3$) δ 7.41 (s, 2H), 1.38 (s, 18H), 1.33 (s, 12H); ^{13}C NMR (100 MHz, $CDCl_3$) δ 175.9, 148.1, 128.6, 126.8, 124.1, 84.6, 39.4, 27.3, 23.0; IR (Neat Film, NaCl): 2977, 2935, 2873, 1763, 1605, 1480, 1404, 1365, 1326, 1270, 1213, 1145, 1121, 1094, 1036 cm^{-1} ; HRMS (MultiMode ESI/APCI+) m/z calc'd for $C_{22}H_{36}BClNO_6$ $[M+NH_4]^+$: 455.2355, found 455.2358.



2-Iodo-5-(4,4,5,5-tetramethyl-1,3,2-dioxaborolan-2-yl)-1,3-phenylene bis(2,2-dimethylpropanoate) (214). Amorphous off-white solid (12.5 g, 95% yield): 1H NMR (300 MHz, $CDCl_3$) δ 7.30 (s, 2H), 1.41 (s, 18H), 1.32 (s, 12H); ^{13}C NMR (125 MHz, $CDCl_3$) δ 175.9, 152.6, 131.2, 125.7, 92.3, 84.6, 39.5, 27.5, 25.0; IR (Neat Film, NaCl): 2974, 2935, 2873, 1761, 1598, 1549, 1480, 1463, 1395, 1360, 1330, 1274, 1209, 1142,

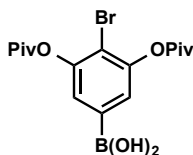
1094, 1034, 965, 900, 848 cm^{-1} ; HRMS (MultiMode ESI/APCI-) m/z calc'd for $\text{C}_{22}\text{H}_{32}\text{BFIO}_6$ $[\text{M}+\text{F}]^-$: 549.1321, found 549.1337.

A8.7.2.3 General Procedure and Spectroscopic Data for the Synthesis of Boronic Acid Analogues

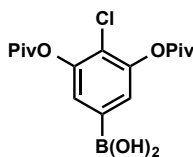


(4-Acetyl-3,5-bis(pivaloyloxy)phenyl)boronic acid (199). A 250 mL round-bottom flask was charged with a stir bar and pinacol boronate ester **198** (8.65 g, 19.27 mmol, 1.0 equiv). The solid was dissolved in EtOAc (250 mL), and diethanolamine (2.35 mL, 24.10 mmol, 1.25 equiv) was added with vigorous stirring. (Note: a glass pipette was cut to have a wide bore, and this wide-bored pipet was used to add the viscous diethanolamine.) Upon addition of diethanolamine, a white precipitate formed. This suspension was stirred vigorously for a further 4 h at ambient temperature, at which time the mixture was concentrated under reduced pressure. The crude white semi-solid reaction residue was suspended in Et₂O (300 mL) and stirred vigorously for 30 min. The suspension was then cooled to -20 °C in a freezer overnight. The white solid was collected by vacuum filtration, and the compound was washed with additional portions of Et₂O (3 x 50 mL). The collected white solid (7.38 g) was suspended in 0.5 M HCl (200 mL) and stirred vigorously. CH₂Cl₂ (ca. 50 mL) was added until the solid fully dissolved. The biphasic mixture was stirred for 12 h with extreme vigor. The mixture was then subjected to continuous extraction with boiling CH₂Cl₂ (300 mL) for 6 h. The combined organic

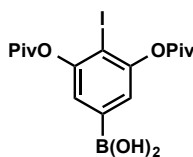
extracts were concentrated *in vacuo* and dried under high vacuum to afford boronic acid **199** as an off-white, flaky solid (6.45 g, 92% yield over two steps): ^1H NMR (300 MHz, CDCl_3) δ 7.35 (s, 2H), 2.19 (s, 3H), 1.08 (s, 18H); ^{13}C NMR (125 MHz, acetone- d_6) δ 198.5, 176.7, 148.1, 138.0, 131.2, 126.2, 39.5, 31.7, 27.2; IR (Neat Film, NaCl): 3446, 2975, 2359, 1751, 1700, 1653, 1635, 1558, 1540, 1480, 1456, 1407, 1340, 1247, 1100, 1038 cm^{-1} ; HRMS (MultiMode ESI/APCI+) m/z calc'd for $\text{C}_{18}\text{H}_{29}\text{BNO}_7$ $[\text{M}+\text{NH}_4]^+$: 381.2068, found 381.2061.



(4-Bromo-3,5-bis(pivaloyloxy)phenyl)boronic acid (207). Please note 2 M H_2SO_4 and THF were used in place of 0.5 M HCl and CH_2Cl_2 , a continuous extraction was not required. Off-white, flaky solid (11.0 g, 82% yield over two steps): ^1H NMR (500 MHz, $\text{DMSO}-\text{d}_6$) δ 7.50 (s, 2H), 1.40 (s, 18H); ^{13}C NMR (125 MHz, $\text{DMSO}-\text{d}_6$) δ 175.3, 148.6, 135.6, 126.3, 112.8, 38.8, 26.8; IR (Neat Film, NaCl): 3454, 3364, 2976, 2937, 2874, 1755, 1733, 1736, 1480, 1454, 1426, 1365, 1342, 1271, 1218, 1137, 1108, 1038 cm^{-1} ; HRMS (MultiMode ESI/APCI-) m/z calc'd for $\text{C}_{16}\text{H}_{22}\text{BBr}_2\text{O}_6$ $[\text{M}+\text{Br}]^-$: 477.9918, found 477.9923.

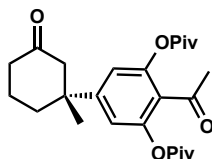


(4-Chloro-3,5-bis(pivaloyloxy)phenyl)boronic acid (215). *Please note* 2 M H₂SO₄ and THF were used in place of 0.5 M HCl and CH₂Cl₂, a continuous extraction was not required. Off-white, flaky solid (3.50 g, 86% yield over two steps): ¹H NMR (400 MHz, DMSO-d₆) δ 7.53 (s, 2H), 1.34 (s, 18H); ¹³C NMR (100 MHz, DMSO-d₆) δ 175.3, 147.2, 134.8, 126.3, 121.5, 38.8, 26.7; IR (Neat Film, NaCl): 3377, 2980, 1753, 1735, 1639, 1480, 1463, 1428, 1366, 1342, 1280, 1139, 1113, 1089 cm⁻¹; HRMS (MultiMode ESI/APCI-) *m/z* calc'd for C₁₆H₂₂BCl₂O₆ [M+Cl]⁻: 390.0928, found 390.0936.



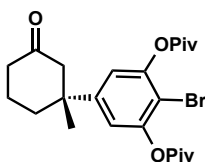
(4-Iodo-3,5-bis(pivaloyloxy)phenyl)boronic acid (216). *Please note* 2 M H₂SO₄ and THF were used in place of 0.5 M HCl and CH₂Cl₂, a continuous extraction was not required. Off-white, flaky solid (4.82 g, 94% yield over two steps): ¹H NMR (500 MHz, DMSO-d₆) δ 7.37 (s, 2H), 1.37 (s, 18H); ¹³C NMR (125 MHz, DMSO-d₆) δ 175.4, 152.0, 136.5, 125.2, 92.0, 38.8, 27.0; IR (Neat Film, NaCl): 3369, 2975, 1759, 1735, 1395, 1360, 1277, 1095, 1034, 904 cm⁻¹; HRMS (MultiMode ESI/APCI-) *m/z* calc'd for C₁₆H₂₂BClIO₆ [M+Cl]⁻: 482.0284, found 482.0296.

A8.7.2.4 General Procedure and Spectroscopic Data for the Enantioselective Palladium-Catalyzed Conjugate Addition of Arylboronic Acids

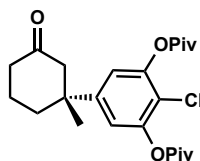


(*R*)-2-Acetyl-5-(1-methyl-3-oxocyclohexyl)-1,3-phenylene bis(2,2-dimethylpropanoate) (169b). A 20 mL screw-top vial was charged with a stir bar, Pd(OCOCF₃)₂ (25 mg, 0.075 mmol, 2.5 mol %), (*S*)-*t*-BuPyOx (18 mg, 0.099 mmol, 3 mol %), NH₄PF₆ (145 mg, 0.99 mmol, 30 mol %), and the solids were dissolved in 1,2-dichloroethane (2 mL) and stirred at ambient temperature for 5 min. Not all solids dissolved at this time. A 100 mL round bottom flask was charged with a stir bar, boronic acid **19** (1.20 g, 3.30 mmol, 1.1 equiv), and 1,2-dichloroethane (10 mL), and stirred at ambient temperature. The catalyst solution was filtered through a pipet plugged with a Kimwipe and added to the suspension of boronic acid in one portion. 3-methylcyclohexen-2-one (340 μ L, 3.00 mmol, 1.0 equiv) and water (270 μ L, 15 mmol, 5 equiv) were added by syringe and the flask was stirred in an oil bath heated to 50 $^{\circ}$ C for 72 h. When the starting material was consumed as determined by TLC analysis (10% acetone/hexanes, *p*-anisaldehyde stain), the mixture was cooled to ambient temperature and filtered through a plug of silica gel (eluent: CH₂Cl₂) and concentrated under reduced pressure. The crude residue was purified by silica gel flash chromatography (200 g silica gel, eluent gradient: 5% acetone/hexanes to 10% acetone/hexanes) to afford conjugate addition product **169b** as a colorless oil (1.19 g, 93% yield): 94% ee; [α]_D²⁵ -36.1° (*c* 1.85, CHCl₃); ¹H NMR (500 MHz, CDCl₃) δ 6.91 (s, 2H), 2.77 (d, *J* = 14.1 Hz, 1H), 2.42 (s, 4H), 2.33 (t, *J* = 6.8 Hz, 2H), 2.12 (s, 1H), 1.99 – 1.84 (m, 2H), 1.82 – 1.71 (m,

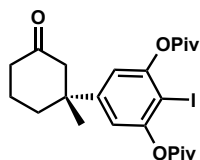
¹H), 1.32 (s, 21H); ¹³C NMR (125 MHz, CDCl₃) δ 210.4, 198.5, 176.4, 151.3, 148.0, 126.5, 117.5, 52.8, 43.0, 40.8, 39.2, 37.6, 31.5, 28.9, 27.2, 27.1, 27.1, 22.0; IR (Neat Film, NaCl): 3404, 2973, 2937, 2874, 1758, 1708, 1620, 1562, 1480, 1408, 1397, 1257, 1095 cm⁻¹; HRMS (MultiMode ESI/APCI+) *m/z* calc'd for C₂₅H₃₄NaO₆ [M+Na]⁺: 453.2248, found 453.2234; HPLC conditions: 5% IPA, 1.0 mL/min, Chiralpak AD-H column, λ = 210 nm, t_R (min): major = 6.454, minor = 6.227.



(R)-2-Bromo-5-(1-methyl-3-oxocyclohexyl)-1,3-phenylene bis(2,2-dimethylpropanoate) (169d). *Please note* 1.5 equiv of boronic acid were employed. Colorless solid (4.57 g, 98% yield): >99% ee; [α]_D²⁵ −34.5° (c 1.41, CHCl₃); ¹H NMR (500 MHz, CDCl₃) δ 6.93 (s, 2H), 2.76 (d, *J* = 14.1 Hz, 1H), 2.44 (d, 14.1 Hz, 1H), 2.33 (t, *J* = 6.7 Hz, 2H), 2.19 – 2.06 (m, 1H), 1.98 – 1.85 (m, 2H), 1.80 – 1.74 (m, 1H), 1.40 (s, 18H), 1.30 (s, 3H); ¹³C NMR (125 MHz, CDCl₃) δ 210.2, 175.8, 149.8, 149.0, 118.4, 108.9, 53.0, 42.8, 40.8, 39.6, 37.7, 28.8, 27.4, 22.1; IR (Neat Film, NaCl): 2973, 2936, 2874, 1763, 1713, 1601, 1571, 1480, 1463, 1408, 1397, 1365, 1272, 1227, 1096, 1037, 894 cm⁻¹; HRMS (MultiMode ESI/APCI+) *m/z* calc'd for C₂₃H₃₅BrNO₅ [M+NH₄]⁺: 484.1693, found 484.1693; HPLC conditions: 20% IPA, 1.0 mL/min, Chiralpak IC column, λ = 210 nm, t_R (min): major = 5.795, minor = 6.232.



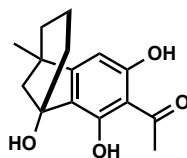
(R)-2-Chloro-5-(1-methyl-3-oxocyclohexyl)-1,3-phenylene bis(2,2-dimethylpropanoate) (169e). *Please note* 1.5 equiv of boronic acid were employed. Colorless solid (0.74 g, 94% yield): >99% ee; $[\alpha]_D^{25} -38.9^\circ$ (*c* 2.59, CHCl₃); ¹H NMR (500 MHz, CDCl₃) δ 6.95 (s, 2H), 2.76 (d, *J* = 14.1 Hz, 1H), 2.43 (d, *J* = 14.1 Hz, 1H), 2.32 (t, *J* = 6.7 Hz, 2H), 2.15 – 2.06 (m, 1H), 1.98 – 1.84 (m, 2H), 1.82 – 1.71 (m, 1H), 1.38 (s, 18H), 1.30 (s, 3H); ¹³C NMR (125 MHz, CDCl₃) δ 210.3, 175.7, 148.2, 147.8, 118.4, 118.3, 52.8, 42.6, 40.6, 39.3, 37.5, 28.7, 27.2, 21.9; IR (Neat Film, NaCl): 2972, 2936, 2874, 2256, 1763, 1713, 1607, 1574, 1479, 1413, 1397, 1352, 1316, 1272, 1227, 1050, 1038, 895, 734 cm⁻¹; HRMS (MultiMode ESI/APCI+) *m/z* calc'd for C₂₃H₃₅ClNO₅ [M+NH₄]⁺: 440.2198, found 440.2197; SFC conditions: 3% IPA, 2.5 mL/min, Chiralpak AS-H column, λ = 210 nm, *t_R* (min): major = 5.393, minor = 6.285.



(R)-2-Iodo-5-(1-methyl-3-oxocyclohexyl)-1,3-phenylene bis(2,2-dimethylpropanoate) (169c). *Please note* 1.5 equiv of boronic acid were employed. Colorless solid (0.40 g, 42% yield): 92% ee; $[\alpha]_D^{25} -29.2^\circ$ (*c* 4.47, CHCl₃); ¹H NMR (500 MHz, CDCl₃) δ 6.87 (s, 2H), 2.75 (d, *J* = 14.1 Hz, 1H), 2.42 (d, 14.1 Hz, 1H), 2.30 (t, *J* = 6.8 Hz, 2H), 2.12 – 2.06 (m, 1H), 1.92 – 1.85 (m, 2H), 1.77 – 1.72 (m, 1H), 1.40 (s, 18H), 1.28 (s, 3H); ¹³C

NMR (125 MHz, CDCl₃) δ 210.4, 175.9, 152.7, 150.4, 117.6, 85.0, 52.8, 42.7, 40.7, 39.4, 37.5, 28.7, 27.4, 22.0; IR (Neat Film, NaCl): 2972, 2936, 2873, 1759, 1711, 1598, 1560, 1480, 1461, 1396, 1368, 1314, 1271, 1226, 1098, 1036, 938, 914, 894, 754, 733 cm⁻¹; HRMS (MultiMode ESI/APCI+) m/z calc'd for C₂₃H₃₅INO₅ [M+NH₄]⁺: 532.1554, found 532.1567; HPLC conditions: 20% IPA, 1.0 mL/min, Chiralpak IC column, λ = 210 nm, t_R (min): major = 6.130, minor = 7.008.

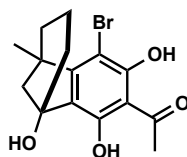
A8.7.2.5 Procedures and Spectroscopic Data for Synthetic Intermediates



(R)-1-(1,3,9-Trihydroxy-5-methyl-6,7,8,9-tetrahydro-5H-5,9-

methanobenzo[7]annulen-2-yl)ethanone (202). A 250 mL round-bottom flask was charged with a stir bar, flame-dried under vacuum, back-filled with argon, and charged with THF (25 mL). The solution was cooled to 0 °C in an ice/water bath and ethanethiol (0.890 mL, 12.5 mmol, 2.7 equiv) was added via syringe. *n*-BuLi (2.5 M solution in hexanes, 5.5 mL, 13.75 mmol, 2.97 equiv) was added dropwise, and a white precipitate was observed at the completion of the addition. DMF (25 mL) was added until the solution became homogenous and clear. The solution was allowed to stir at 0 °C for 30 min. A flame-dried, 25 mL conical flask was charged with ketone **169b** (1.99 g, 4.62 mmol, 1 equiv) and DMF (10 mL). The ketone solution was transferred *via* cannula to the cooled, freshly-prepared solution of LiSEt dropwise over 10 min. The ice/water bath was removed and the reaction was allowed to stir and warm to ambient temperature over 30

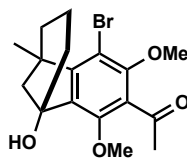
min, at which time the starting material was consumed as determined by TLC analysis (20% EtOAc/hexanes, *p*-anisaldehyde stain). The reaction was quenched by addition of sat. NH₄Cl solution (aq, 50 mL), diluted with CH₂Cl₂ (200 mL) and water (200 mL) and transferred to a separatory funnel. 1M HCl (aq) was added until the aqueous layer was pH 2–4. The aqueous layer was extracted with CH₂Cl₂ (5 x 50 mL) and the combined organic extracts were washed with water (7 x 50 mL), brine (1 x 50 mL), dried with Na₂SO₄ and concentrated under reduced pressure. The crude residue was purified via silica gel flash chromatography (90 g silica gel, eluent gradient: 10% EtOAc/hexanes to 20% EtOAc/hexanes) to afford tricycle **202** as a pale yellow oil (1.15 g, 95% yield): $[\alpha]_D^{25} -19.0^\circ$ (*c* 0.26, CHCl₃); ¹H NMR (500 MHz, CDCl₃) δ 13.30 (s, 1H), 8.30 (s, 1H), 6.23 (d, *J* = 1.9 Hz, 1H), 2.71 (s, 3H), 2.58 (bs, 1H), 2.12 (ddd, *J* = 9.5, 2.9, 2.2 Hz, 1H), 2.01–1.89 (m, 1H), 1.76–1.59 (m, 3H), 1.48–1.32 (m, 2H), 1.31 (s, 3H), 1.03–0.81 (m, 1H); ¹³C NMR (125 MHz, CDCl₃) δ 204.9, 165.8, 156.1, 154.4, 118.8, 109.1, 102.4, 82.3, 59.0, 45.7, 35.4, 34.5, 33.2, 22.9, 21.4; IR (Neat Film, NaCl): 3338, 2934, 2867, 1641, 1588, 1435, 1375, 1324, 1270, 1243, 1124, 1055, 1027, 973, 839 cm⁻¹; HRMS (MultiMode ESI/APCI+) *m/z* calc'd for C₁₅H₁₉O₄ [M+H]⁺: 263.1278, found 263.1272.



(*R*)-1-(4-Bromo-1,3,9-trihydroxy-5-methyl-6,7,8,9-tetrahydro-5H-5,9-

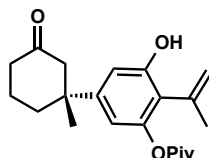
methanobenzo[7]annulen-2-yl)ethanone (217). A 50 mL, flame-dried, round-bottom flask was charged with a stir bar, tricycle **202** (110 mg, 0.419 mmol, 1 equiv) and

dibromodimethylhydantoin (151 mg, 0.461 mmol, 1.1 equiv). The flask was evacuated under vacuum and back-filled with argon, and the solids were dissolved in CH₂Cl₂ (5 mL) and stirred at ambient temperature. After 30 min, an aliquot was partitioned between EtOAc (1 mL) and sat. Na₂S₂O₃ (aq, 1 mL), and the organic layer was subjected to LCMS analysis, where no starting material was observed. The red-colored reaction was quenched by the addition of 20% Na₂S₂O₃ solution (aq, 20 mL) and stirred vigorously for 3 h, until the orange/red color was no longer observed. The mixture was partitioned between CH₂Cl₂ (20 mL) and water (20 mL) and transferred to a separatory funnel. 1M HCl was added until the aqueous layer was pH 3. The aqueous layer was extracted with CH₂Cl₂ (5 x 25 mL) and the combined organic extracts were dried over Na₂SO₄ and concentrated under reduced pressure. The crude residue was purified by silica gel column chromatography (12 g silica gel, eluent gradient: 10% EtOAc/hexanes to 25% EtOAc/hexanes) to afford bromo arene **217** as a yellow, semi-crystalline solid (92 mg, 66% yield): $[\alpha]_D^{25} -20.8^\circ$ (*c* 1.26, CHCl₃); ¹H NMR (500 MHz, CDCl₃) δ 13.37 (s, 1H), 9.10 (s, 1H), 2.74 (s, 3H), 2.55 (s, 1H), 2.22 (ddd, *J* = 9.7, 3.0, 2.2 Hz, 1H), 1.93 (ddd, *J* = 11.2, 6.2, 3.0 Hz, 1H), 1.75 – 1.64 (m, 4H), 1.61 (s, 3H), 1.35 (td, *J* = 13.0, 5.5 Hz, 1H), 0.96 – 0.80 (m, 1H); ¹³C NMR (125 MHz, CDCl₃) δ 204.5, 154.3, 151.9, 120.2, 110.2, 109.9, 97.9, 81.4, 59.1, 48.8, 34.4, 33.1, 33.0, 24.6, 21.6; IR (Neat Film, NaCl): 3381, 2936, 2852, 1631, 1566, 1415, 1373, 1326, 1274, 1233 cm⁻¹; HRMS (MultiMode ESI/APCI-) *m/z* calc'd for C₁₅H₁₆BrO₄ [M-H]⁻: 339.0237, found 339.0230.



(R)-1-(4-Bromo-9-hydroxy-1,3-dimethoxy-5-methyl-6,7,8,9-tetrahydro-5H-5,9-methanobenzo[7]annulen-2-yl)ethanone (203). A flame-dried 20 mL vial was charged with a stir bar, bromo-diphenol **217** (92 mg, 0.270 mmol, 1 equiv), Cs₂CO₃ (194 mg, 0.595 mmol, 2.2 equiv), and acetone (5 mL). The vial was stirred under argon atmosphere at ambient temperature, and methyl iodide (0.037 mL, 0.595 mmol, 2.2 equiv) was added in one portion. The yellow reaction slurry was stirred for 40 h at ambient temperature, at which time the color had faded to a white slurry and the starting material was consumed as determined by TLC analysis (20% EtOAc/hexanes, *p*-anisaldehyde stain). The reaction was quenched with sat. NH₄Cl solution (aq, 5 mL) and stirred for 12 h at ambient temperature. The reaction was diluted with EtOAc (10 mL) and water (10 mL), and the mixture was transferred to a separatory funnel. The aqueous layer was extracted with EtOAc (3 x 10 mL) and the combined organic extracts were washed with water (2 x 10 mL) and brine (1 x 10 mL), dried over MgSO₄ and concentrated under reduced pressure. The crude residue was purified by silica gel flash chromatography (12 g silica gel, eluent gradient 10% EtOAc/hexanes to 20% EtOAc/hexanes) to afford **203** as a clear oil that solidified to an amorphous white solid upon standing (62 mg, 63% yield): $[\alpha]_D^{25} -5.8^\circ$ (*c* 0.73, CHCl₃); ¹H NMR (500 MHz, CDCl₃) δ 3.81 (s, 3H), 3.80 (s, 3H), 2.56 (s, 3H), 2.24 (dt, *J* = 10.1, 2.5 Hz, 1H), 1.84 – 1.71 (m, 2H), 1.71 – 1.61 (m, 4H), 1.60 (s, 3H), 1.35 (td, *J* = 12.9, 5.8 Hz, 1H), 0.81 – 0.67 (m, 1H). ¹³C NMR (125 MHz, CDCl₃) δ 201.8, 153.9, 151.0, 148.1, 135.9, 130.5,

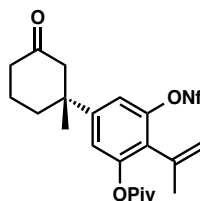
108.9, 79.7, 63.9, 63.1, 58.6, 48.0, 36.7, 33.2, 32.6, 25.1, 21.6; IR (Neat Film, NaCl): 3429, 2938, 2853, 1704, 1642, 1590, 1450, 1382, 1323, 1237, 1120, 1077 cm^{-1} ; HRMS (MultiMode ESI/APCI+) m/z calc'd for $\text{C}_{17}\text{H}_{22}\text{BrO}_4$ $[\text{M}+\text{H}]^+$: 369.0696, found 369.0690.



(R)-3-Hydroxy-5-(1-methyl-3-oxocyclohexyl)-2-(prop-1-en-2-yl)phenyl pivalate (208). Four 20 mL microwave vials were each charged with a stir bar, ketone **169d** (0.594 g, 1.27 mmol, 1 equiv), potassium isopropenyltrifluoroborate (281 mg, 1.91 mmol, 1.25 equiv), K_2CO_3 (263 g, 1.91 mmol, 1.5 equiv), PPh_3 (33 mg, 0.127 mmol, 10 mol %), and $\text{Pd}(\text{OAc})_2$ (14 mg, 0.0635 mmol, 5 mol %), and capped with a microwave septum top. The vials were evacuated with vacuum and back-filled with argon three times. The solids were suspended in degassed dioxane/ H_2O (9:1 ratio, 20 mL) before the reaction was stirred in the microwave reactor for 1 h at 170 $^\circ\text{C}$ on very high absorbance mode. The mixture was cooled to ambient temperature and filtered through a plug of silica gel (eluent: EtOAc) and concentrated under reduced pressure to afford a brown oil.

A 100 mL round-bottom flask was charged with the combined crude reaction residues, a stir bar, Bu_4NOH (4.7 mL, 7.15 mmol, 2.4 equiv), and dioxane/ H_2O (9:1 ratio, 50 mL). The reaction was stirred at ambient temperature for 10 h, at which point the starting material was consumed as determined by TLC analysis (20% EtOAc/hexanes, *p*-anisaldehyde stain). The reaction was quenched with sat. NH_4Cl (aq, 25 mL) and transferred to a separatory funnel. The aqueous layer was extracted with EtOAc (3 x 100

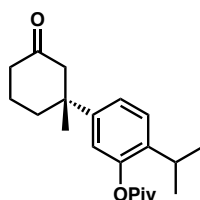
mL), and the combined organic extracts were washed with brine (1 x 100 mL), dried over MgSO_4 and concentrated under reduced pressure. The crude residue was purified by silica gel flash chromatography (50 g silica gel, eluent gradient: 10% EtOAc/hexanes to 20% EtOAc/hexanes) to afford isopropenyl **208** as a yellow oil (1.23 g, 70% yield over 2 steps): $[\alpha]_D^{25} -37.4^\circ$ (*c* 1.26, CHCl_3); ^1H NMR (500 MHz, CDCl_3) δ 6.79 (d, $J = 1.8$ Hz, 1H), 6.53 (d, $J = 1.8$ Hz, 1H), 5.52 (s, 1H), 5.43 (s, 1H), 5.04 (s, 1H), 2.79 (d, $J = 14.1$ Hz, 1H), 2.41 (d, $J = 14.1$ Hz, 1H), 2.32 (t, $J = 6.7$ Hz, 2H), 2.14 – 2.08 (m, 1H), 2.00 (s, 3H), 1.91 – 1.84 (m, 2H), 1.83 – 1.73 (m, 1H), 1.31 (s, 9H), 1.29 (s, 3H); ^{13}C NMR (125 MHz, CDCl_3) δ 211.0, 176.8, 152.9, 149.1, 148.7, 138.1, 121.3, 119.3, 111.9, 110.3, 53.2, 42.8, 40.9, 39.2, 37.8, 29.0, 27.3, 23.6, 22.2; IR (Neat Film, NaCl): 3418, 3083, 2970, 2874, 1712, 1620, 1480, 1414, 1368, 1316, 1278, 1230, 1122, 1073, 1035, 1017, 943, 901, 758 cm^{-1} ; HRMS (MultiMode ESI/APCI-) m/z calc'd for $\text{C}_{21}\text{H}_{27}\text{O}_4$ $[\text{M}-\text{H}]^-$: 343.1915, found 343.1926.



(R)-5-(1-Methyl-3-oxocyclohexyl)-3-(perfluorobutoxy)-2-(prop-1-en-2-yl)phenyl

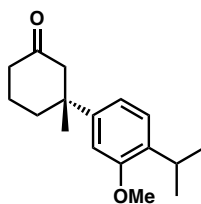
pivalate (209). A 15 mL, flame-dried, round-bottom flask was charged with a stir bar, phenol **208** (165 mg, 0.479 mmol, 1 equiv) and DMAP (3 mg, 0.024 mmol, 5 mol%). The flask was evacuated under vacuum and back-filled with argon three times. The solids were dissolved in CH_2Cl_2 (5 mL), and NEt_3 (1.34 mL, 9.58 mmol, 20 equiv) was added. Perfluorobutanesulfonyl fluoride (1.72 mL, 9.58 mmol, 20 equiv) was then added

dropwise and the resulting solution was stirred at ambient temperature for 18 h, at which time the starting material was consumed as determined by TLC analysis (30% EtOAc/hexanes, *p*-anisaldehyde stain). The mixture was washed with water (10 mL) and brine (10 mL), and the organic extracts were dried over MgSO₄ and concentrated under reduced pressure. The crude residue was purified by silica gel column chromatography (9 g silica gel, gradient: 10% EtOAc/hexanes) to afford nonaflate **209** as a colorless oil (0.2694 g, 80% yield): $[\alpha]_D^{25} -22.1^\circ$ (*c* 1.31, CHCl₃); ¹H NMR (400 MHz, CDCl₃) δ 7.12 (d, *J* = 1.8 Hz, 1H), 7.00 (d, *J* = 1.9 Hz, 1H), 5.39 (t, *J* = 1.2 Hz, 1H), 5.00 (t, *J* = 1.2 Hz, 1H), 2.76 (d, *J* = 14.0 Hz, 1H), 2.47 (d, *J* = 14.0 Hz, 1H), 2.35 (t, *J* = 6.8 Hz, 2H), 2.19 – 2.05 (m, 1H), 2.00 (s, 3H), 1.99 – 1.87 (m, 2H), 1.86 – 1.74 (m, 1H), 1.32 (s, 9H), 1.31 (s, 3H). ¹³C NMR (100 MHz, CDCl₃) δ 210.1, 176.7, 149.5, 149.5, 147.3, 135.1, 129.6, 120.3, 120.3, 117.0, 116.4, 114.3, 109.9, 108.0, 52.9, 42.9, 40.8, 39.2, 37.6, 28.8, 27.2, 23.1, 22.0; ¹⁹F (376 MHz, CDCl₃) δ -80.94 (t, *J* = 9.9 Hz, 3F), -109.86 (t, *J* = 14.0 Hz, 2F), -121.04 – -120.86 (m, 2F), -126.04 (dt, *J* = 13.9, 13.5, 4.9 Hz, 2F). IR (Neat Film, NaCl): 2971, 2877, 1759, 1720, 1649, 1623, 1553, 1482, 1427, 1353, 1240, 1200, 1145, 1107, 1032, 1011, 985, 944, 922 cm⁻¹. HRMS (FAB+) *m/z* calc'd for C₂₅H₂₈F₉O₆S [M+H]⁺: 627.1457, found 627.2216.



(R)-2-Isopropyl-5-(1-methyl-3-oxocyclohexyl)phenyl pivalate (210). A 25 mL Schlenk flask was charged with a stir bar, nonaflate **209** (62.1 mg, 0.110 mmol, 1 equiv), 10%

Pd/C (62.1 mg, equal weight to that of the nonaflate), Et₃N (38 μ L, 0.276 mmol, 2.5 equiv), and MeOH (5 mL). The reaction mixture was degassed then back-filled with H₂ gas (1 atm) using Schlenk technique. The flask was sealed and stirred in an oil bath heated to 65 °C for 11 h. The mixture was cooled to ambient temperature, filtered through a silica gel plug (10 g silica gel, eluent: EtOAc) and concentrated under reduced pressure. The crude residue was purified by silica gel flash chromatography (9 g silica gel, eluent: 5% EtOAc/hexanes) to afford pivaloyl **209** as a colorless oil (26.4 mg, 72% yield): $[\alpha]_D^{25}$ -41.4° (*c* 1.30, CHCl₃); ¹H NMR (400 MHz, CDCl₃) δ 7.28 (d, *J* = 2.4 Hz, 1H), 7.16 (dd, *J* = 8.2, 2.1 Hz, 1H), 6.90 (d, *J* = 2.1 Hz, 1H), 3.13 (p, *J* = 6.9 Hz, 1H), 2.84 (d, *J* = 14.1 Hz, 1H), 2.45 (d, *J* = 14.2 Hz, 1H), 2.33 (t, *J* = 6.7 Hz, 2H), 2.19 – 2.12 (m, 1H), 1.99 – 1.84 (m, 2H), 1.84 – 1.70 (m, 1H), 1.41 (s, 9H), 1.32 (s, 3H), 1.21 (d, *J* = 6.9 Hz, 6H); ¹³C NMR (100 MHz, CDCl₃) δ 211.4, 177.2, 148.6, 146.5, 138.0, 126.5, 123.3, 119.5, 53.2, 42.6, 40.9, 39.3, 37.9, 29.3, 27.4, 27.1, 23.0, 22.9, 22.2; IR (Neat Film, NaCl): 2963, 2872, 1750, 1714, 1619, 1504, 1462, 1410, 1365, 1276, 1229, 1160, 1120, 1055, 1030, 932, 904 cm⁻¹; HRMS (MultiMode ESI/APCI+) *m/z* calc'd for C₂₁H₃₄NO₃ [M+NH₄]⁺: 348.2533, found 348.2518.



(R)-3-(4-Isopropyl-3-methoxyphenyl)-3-methylcyclohexane-1-one (169f). A 25 mL round bottom flask was charged with a stir bar, flame-dried under vacuum, back-filled with argon, and charged with THF (2 mL). The solution was cooled to 0 °C in an

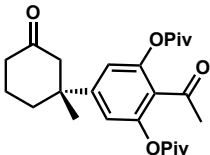
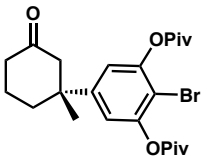
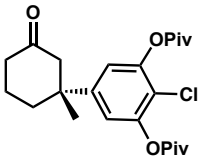
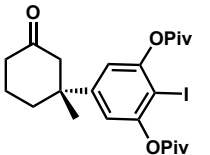
ice/water bath and ethanethiol (57 μ L, 0.787 mmol, 10 equiv) was added *via* syringe. *n*-BuLi (2.5 M solution in hexanes, 322 μ L, 0.802 mmol, 10.2 equiv) was added dropwise, and a white precipitate was observed at the completion of the addition. The solution was allowed to stir at 0 °C for 1 h. A flame-dried 15 mL conical flask was charged with pivaloyl **210** (26.0 mg, 0.079 mmol, 1 equiv) and DMF (1 mL). The ketone solution was transferred *via* cannula to the cooled, freshly-prepared solution of LiSEt dropwise over 5 min. The ice/water bath was removed and the reaction was stirred in an oil bath heated to 45 °C for 6 h, at which time the starting material was consumed as determined by TLC analysis (30% EtOAc/hexanes, *p*-anisaldehyde stain). Me₂SO₄ (112 μ L, 1.185 mmol, 15 equiv) was added to the reaction mixture and stirred at 45 °C for an additional 15 min, at which time the reaction was complete as determined by TLC analysis (30% EtOAc/hexanes, *p*-anisaldehyde stain). The reaction was quenched with NH₄OH (aq, 5 mL) and stirred at 45 °C for another 15 min then diluted with H₂O (10 mL). The aqueous layer was extracted with EtOAc (3 x 10 mL), dried with MgSO₄ and concentrated under reduced pressure. The crude residue was purified *via* silica gel flash chromatography (9 g silica gel, eluent: 2.5% EtOAc/hexanes) to afford key intermediate **169f** as a colorless oil (17.0 mg, 83 % yield): $[\alpha]_D^{25}$ -60.4° (*c* 1.49, CHCl₃); ¹H NMR (400 MHz, CDCl₃) δ 7.14 (d, *J* = 8.0 Hz, 1H), 6.86 (dd, *J* = 8.0, 1.9 Hz, 1H), 6.78 (d, *J* = 1.9 Hz, 1H) 3.82 (s, 3H), 3.26 (p, *J* = 6.9 Hz, 1H), 2.87 (d, *J* = 14.2 Hz, 1H), 2.43 (d, *J* = 14.1 Hz, 1H), 2.31 (t, *J* = 6.8 Hz, 2H), 2.20 – 2.14 (m, 1H), 1.93 – 1.82 (m, 2H), 1.72 – 1.62 (m, 1H), 1.33 (s, 3H), 1.19 (d, *J* = 6.9 Hz, 6H); ¹³C NMR (100 MHz, CDCl₃) δ 211.8, 156.8, 146.1, 134.9, 126.1, 117.8, 108.3, 55.5, 53.4, 43.0, 41.0, 38.3, 30.1, 26.6, 22.8, 22.2; IR (Neat Film, NaCl): 2958, 2869, 1713, 1611, 1573, 1504, 1462, 1409, 1350, 1305, 1254, 1240, 1164,

1092, 1038, 920 cm^{-1} ; HRMS (FAB+) m/z calc'd for $\text{C}_{17}\text{H}_{24}\text{O}_2$ $[\text{M}]^+$: 260.1776, found 260.1782.

A8.7.2.6 Determination of Enantiomeric Excess

Please note racemic products were synthesized using racemic *i*-Pr-PyOx.

Table A8.6 Determination of enantiomeric excess

Entry	Product	Assay Conditions	Retention time of major isomer (min)	Retention time of minor isomer (min)	%ee
1		HPLC Chiralpak AD-H 5% IPA in hexanes isocratic, 1.0 mL/min	6.454	6.227	94
2		HPLC Chiralpak IC 20% IPA in hexanes isocratic, 1.0 mL/min	5.795	6.232	>99
3		SFC Chiralpak AS-H 3% IPA in hexanes isocratic, 2.5 mL/min	5.393	6.285	>99
4		HPLC Chiralpak IC 20% IPA in hexanes isocratic, 1.0 mL/min	6.130	7.008	92

A8.7.2.7 Hammett Plot Data^{4a,b}

Table A8.7 Data for Hammett analysis of enantioselectivity for select boronic acids

phenylboronic acid	σ_p^2	ee ³	er	log ₁₀ (er)
<i>p</i> -Et	-0.15	85	12	1.1
<i>p</i> -Me	-0.17	87	14	1.2
<i>p</i> -H	0	92	24	1.4
<i>p</i> -F	0.06	92	24	1.4
<i>p</i> -Cl	0.23	95	39	1.6
<i>p</i> -Ac	0.50	96	49	1.7
<i>p</i> -CF ₃	0.54	96	49	1.7
<i>p</i> -Br	0.23			
<i>p</i> -iPr	-0.15			

A8.8 REFERENCES AND NOTES

- (1) (a) Majetich, G.; Shimkus, J. M. *J. Nat. Prod.* **2010**, *73*, 284–298; (b) Lin, W.-H.; Fang, J.-M.; Cheng, Y.-S. *Phytochemistry* **1995**, *40*, 871–873; (c) Lin, W.-H.; Fang, J.-M.; Cheng, Y.-S. *Phytochemistry* **1996**, *42*, 1657–1663; (d) Kawazoe, K.; Yamamoto, M.; Takaishi, Y.; Honda, G.; Fujita, T.; Sezik, E.; Yesilada, E. *Phytochemistry* **1999**, *50*, 493–497; (e) Chang, C. -I.; Chien, S.-C.; Lee, S.-M.; Kuo, Y.-H. *Chem. Pharm. Bull.* **2003**, *51*, 1420–1422; (f) Chang, C.-I.; Chang, J.-Y.; Kuo, C.-C.; Pan, W.-Y.; Kuo, Y.-H. *Planta Med.* **2005**, *71*, 72–76.
- (2) (a) Banerjee, M.; Mukhopadhyay, R.; Achari, B.; Banerjee, A. K. *Org. Lett.* **2003**, *5*, 3931–3933; (b) Fillion, E.; Fishlock, D. *J. Am. Chem. Soc.* **2005**, *127*, 13144–13145; (c) Banerjee, M.; Mukhopadhyay, R.; Achari, B.; Banerjee, A. K. *J. Org.*

Chem. **2006**, *71*, 2787–2796; (d) Planas, L.; Mogi, M.; Takita, H.; Kajimoto, T.; Node, M. *J. Org. Chem.* **2006**, *71*, 2896–2898; (e) McFadden, R. M.; Stoltz, B. M. *J. Am. Chem. Soc.* **2006**, *128*, 7738–7739; (f) Liang, G.; Xu, Y.; Seiple, I. B.; Trauner, D. *J. Am. Chem. Soc.* **2006**, *128*, 11022–11023; (g) Li, S.; Chiu, P. *Tetrahedron Lett.* **2008**, *49*, 1741–1744; (h) Tang, S.; Xu, Y.; He, J.; He, Y.; Zheng, J.; Pan, X.; She, X. *Org. Lett.* **2008**, *10*, 1855–1858; (i) Majetich, G.; Shimkus, J. M. *Tetrahedron Lett.* **2009**, *50*, 3311–3313; (j) Alvarez-Manzaneda, E.; Chahboun, R.; Cabrera, E.; Alvarez, E.; Alvarez-Manzaneda, R.; Meneses, R.; Es-Samti, H.; Fernández, A. *J. Org. Chem.* **2009**, *74*, 3384–3388; (k) Alvarez-Manzaneda, E.; Chahboun, R.; Cabrera, E.; Alvarez, E.; Haidour, A.; Ramos, J. M.; Alvarez-Manzaneda, R.; Charrah, Y.; Es-Samti, H. *Org. Biomol. Chem.* **2009**, *7*, 5146–5155; (l) Alvarez-Manzaneda, E.; Chahboun, R.; Cabrera, E.; Alvarez, E.; Haidour, A.; Ramos, J. M.; Alvarez-Manzaneda, R.; Hmamouchi, M.; Es-Samti, H. *Chem. Commun.* **2009**, 592–594; (m) Node, M.; Ozeki, M.; Planas, L.; Nakano, M.; Takita, H.; Mori, D.; Tamatani, S.; Kajimoto, T. *J. Org. Chem.* **2010**, *75*, 190–196; (n) Jana, C. K.; Scopelliti, R.; Gademann, K. *Synthesis* **2010**, 2223–2232; (o) Jana, C. K.; Scopelliti, R.; Gademann, K. *Chem.–Eur. J.* **2010**, *16*, 7692–7695; (p) Alvarez-Manzaneda, E.; Chahboun, R.; Alvarez, E.; Tapia, R.; Alvarez-Manzaneda, R. *Chem. Commun.* **2010**, *46*, 9244–9246; (q) Liao, X.; Stanley, L. M.; Hartwig, J. F. *J. Am. Chem. Soc.* **2011**, *133*, 2088–2091; (r) Tapia, R.; Guardia, J. J.; Alvarez, E.; Haidour, A.; Ramos, J. M.; Alvarez-Manzaneda, R.; Chahboun, R.; Alvarez-Manzaneda, E. *J. Org. Chem.* **2012**, *77*, 573–584; (s) Deng, J.; Li, R.; Luo, Y.; Li,

- J.; Zhou, S.; Li, Y.; Hu, J.; Li, A. *Org. Lett.* **2013**, *15*, 2022–2025; (t) Li, L.-Q.; Li, M.-M.; Chen, D.; Liu, H.-M.; Geng, H.-C.; Lin, J.; Qin, H.-B. *Tetrahedron Lett.* **2014**, *55*, 5960–5962.
- (3) (a) Iwamoto, M.; Ohtsu, H.; Tokuda, H.; Nishino, H.; Matsunaga, S.; Tanaka, R. *Bioorg. Med. Chem.* **2001**, *9*, 1911–1921; (b) Minami, T.; Iwamoto, M.; Ohtsu, H.; Ohishi, H.; Tanaka, R.; Yoshitake, A. *Planta Med.* **2002**, *68*, 742–745; (c) Katoh, T.; Akagi, T.; Noguchi, C.; Kajimoto, T.; Node, M.; Tanaka, R.; Nishizawa, M.; Ohtsu, H.; Suzuki, N.; Saito, K. *Bioorg. Med. Chem.* **2007**, *15*, 2736–2748.
- (4) (a) Kikushima, K.; Holder, J. C.; Gatti, M.; Stoltz, B. M. *J. Am. Chem. Soc.* **2011**, *133*, 6902–6905; (b) Holder, J. C.; Zou, L.; Marziale, A. N.; Liu, P.; Lan, Y.; Gatti, M.; Kikushima, K.; Houk, K. N.; Stoltz, B. M. *J. Am. Chem. Soc.* **2013**, *135*, 14996–15007; (c) Holder, J. C.; Marziale, A. N.; Gatti, M.; Mao, B.; Stoltz, B. M. *Chem.–Eur. J.* **2013**, *19*, 74–77.
- (5) (a) Perlmutter, P. *Conjugate Addition Reactions in Organic Synthesis*, Tetrahedron Organic Chemistry Series 9; Pergamon: Oxford, 1992; (b) Rossiter, B. E.; Swingle, N. M. *Chem. Rev.* **1992**, *92*, 771–806; (c) Tomioka, K.; Nagaoka, Y., In *Comprehensive Asymmetric Catalysis*, Vol. 3; Jacobsen, E. N., Pfaltz, A., Yamamoto, H. Eds.; Springer-Verlag: New York, 1999; Chapter 31; (d) Sibi, M. P.; Manyem, S. *Tetrahedron* **2000**, *56*, 8033–8061; (e) Gini, F.; Hessen, B.; Feringa, B. L.; Minnaard, A. J. *Chem. Commun.* **2007**, 710–712; (f) Cordova, A. *Catalytic Asymmetric Conjugate Reactions*, Wiley & Sons: Weinheim, 2010.

- (6) For a comprehensive review, see: Hawner, C.; Alexakis, A. *Chem. Commun.* **2010**, 7295–7306.
- (7) (a) Feringa, B. L. *Acc. Chem. Res.* **2000**, *33*, 346–353; (b) Wu, J.; Mampreian, D. M.; Hoveyda, A. H. *J. Am. Chem. Soc.* **2005**, *127*, 4584–4585; (c) Hird, A. W.; Hoveyda, A. H. *J. Am. Chem. Soc.* **2005**, *127*, 14988–14989; (d) Fillion, E.; Wilsily, A. *J. Am. Chem. Soc.* **2006**, *128*, 2774–2775; (e) Lee, K.-S.; Brown, M. K.; Hird, A. W.; Hoveyda, A. H. *J. Am. Chem. Soc.* **2006**, *128*, 7182–7184; (f) Brown, M. K.; May, T. L.; Baxter, C. A.; Hoveyda, A. H. *Angew. Chem. Int. Ed.* **2007**, *46*, 1097–1100; (g) Wilsily, A.; Fillion, E. *Org. Lett.* **2008**, *10*, 2801–2804; (h) Wilsily, A.; Fillion, E. *J. Org. Chem.* **2009**, *74*, 8583–8594; (i) Dumas, A. M.; Fillion, E. *Acc. Chem. Res.* **2010**, *43*, 440–454.
- (8) (a) d’Augustin, M.; Palais, L.; Alexakis, A. *Angew. Chem. Int. Ed.* **2005**, *44*, 1376–1378; (b) Fuchs, N.; d’Augustin, M.; Humam, M.; Alexakis, A.; Taras, R.; Gladiali, S. *Tetrahedron: Asymmetry* **2005**, *16*, 3143–3146; (c) Vuagnoux-d’Augustin, M.; Alexakis, A. *Chem.—Eur. J.* **2007**, *13*, 9647–9662; (d) Vuagnoux-d’Augustin, M.; Kehrli, S.; Alexakis, A. *Synlett* **2007**, 2057–2060; (e) Palais, L.; Mikhel, I. S.; Bournaud, C.; Micouin, L.; Falciola, C. A.; Vuagnoux-d’Augustin, M.; Rosset, S.; Bernardinelli, G.; Alexakis, A. *Angew. Chem. Int. Ed.* **2007**, *46*, 7462–7465; (f) May, T. L.; Brown, M. K.; Hoveyda, A. H. *Angew. Chem. Int. Ed.* **2008**, *47*, 7358–7362; (g) Hawner, C.; Li, K.; Cirriez, V.; Alexakis, A. *Angew. Chem. Int. Ed.* **2008**, *47*, 8211–8214; (h) Ladjel, C.; Fuchs, N.; Zhao, J.; Bernardinelli, G.; Alexakis, A. *Eur. J. Org. Chem.* **2009**, 4949–4955; (i) Palais, L.; Alexakis, A. *Chem.—Eur. J.*

- 2009**, *15*, 10473–10485; (j) Müller, D.; Hawner, C.; Tissot, M.; Palais, L.; Alexakis, A. *Synlett* **2010**, 1694–1698; (k) Hawner, C.; Müller, D.; Gremaud, L.; Felouat, A.; Woodward, S.; Alexakis, A. *Angew. Chem. Int. Ed.* **2010**, *49*, 7769–7772.
- (9) (a) Martin, D.; Kehrli, S.; d’Augustin, M.; Clavier, H.; Mauduit, M.; Alexakis, A. *J. Am. Chem. Soc.* **2006**, *128*, 8416–8417; (b) Kehrli, S.; Martin, D.; Rix, D.; Mauduit, M.; Alexakis, A. *Chem.—Eur. J.* **2010**, *16*, 9890–9904; (c) Hénon, H.; Mauduit, M.; Alexakis, A. *Angew. Chem. Int. Ed.* **2008**, *47*, 9122–9124; (d) Matsumoto, Y.; Yamada, K.-i.; Tomioka, K. *J. Org. Chem.* **2008**, *73*, 4578–4581.
- (10) (a) For the seminal report in this area, see: Takaya, Y.; Ogasawara, M.; Hayashi, T.; Sakai, M.; Miyaura, N. *J. Am. Chem. Soc.* **1998**, *120*, 5579–5580; (b) For an excellent review, see: Hayashi, T.; Yamasaki, K. *Chem. Rev.* **2003**, *103*, 2829–2844.
- (11) For select recent examples, see: (a) Hayashi, T.; Ueyama, K.; Tokunaga, N.; Yoshida, K. *J. Am. Chem. Soc.* **2003**, *125*, 11508–11509; (b) Fischer, C.; Defieber, C.; Suzuki, T.; Carreira, E. M. *J. Am. Chem. Soc.* **2004**, *126*, 1628–1629; (c) Shintani, R.; Ueyama, K.; Yamada, I.; Hayashi, T. *Org. Lett.* **2004**, *6*, 3425–3427; (d) Otomaru, Y.; Okamoto, K.; Shintani, R.; Hayashi, T. *J. Org. Chem.* **2005**, *70*, 2503–2508; (e) Paquin, J.-F.; Defieber, C.; Stephenson, C. R. J.; Carreira, E. M. *J. Am. Chem. Soc.* **2005**, *127*, 10850–10851.

- (12) (a) Mauleón, P.; Carretero, J. C. *Chem. Commun.* **2005**, 4961–4963; (b) Shintani, R.; Duan, W.-L.; Hayashi, T. *J. Am. Chem. Soc.* **2006**, *128*, 5628–5629; (c) Shintani, R.; Hayashi, T. *Org. Lett.* **2011**, *13*, 350–352.
- (13) A paper describing the use of Rh·OlefOX (olefin-oxazoline) complex provided a single example of a phenylboronic acid addition to 3-methylcyclohexen-2-one (e.g., **167** + **174** → **175**). However, ketone **175** was isolated in only 36% yield and 85% ee, see: Hahn, B. T.; Tewes, F.; Fröhlich, R.; Glorius, F. *Angew Chem. Int. Ed.* **2010**, *49*, 1143–1146.
- (14) For review articles, see: (a) Gutnov, A. *Eur. J. Org. Chem.* **2008**, 4547–4554; (b) Christoffers, J.; Koripelly, G.; Rosiak, A.; Rössle, M. *Synthesis* **2007**, 1279–1300.
- (15) Lin, S.; Lu, X. *Org. Lett.* **2010**, *12*, 2536–2539.
- (16) (a) Gottumukkala, A. L.; Matcha, K.; Lutz, M.; de Vries, J. G.; Minnaard, A. J. *Chem.–Eur. J.* **2012**, *18*, 6907–6914; (b) Buter, J.; Moezelaar, R.; Minnaard, A. J. *Org. Biomol. Chem.* **2014**, *12*, 5883–5890.
- (17) Kadam, A. A.; Ellern, A.; Stanley, L. M. *Org. Lett.* **2017**, *15*, 4062–4065.
- (18) (a) Lu, X.; Lin, S. *J. Org. Chem.* **2005**, *70*, 9651–9653; (b) Lin, S.; Lu, X. *Tetrahedron Lett.* **2006**, *47*, 7167–7170.
- (19) Brunner, H.; Obermann, U. *Chem. Ber.* **1989**, *122*, 499–507.
- (20) (a) Shimizu, H.; Holder, J. C.; Stoltz, B. M. *Beilstein J. Org. Chem.* **2013**, *9*, 1637–1642; (b) Holder, J. C.; Shockley, S. E.; Wiesenfeldt, M. P.; Shimizu, H.; Stoltz, B. M. *Org. Synth.* **2015**, *92*, 247–266.

- (21) Guillaneux, D.; Zheo, S.-H.; Samuel, O.; Rainford, D.; Kagan, H. B. *J. Am. Chem. Soc.* **1994**, *116*, 9430–9439.
- (22) Duan, W.-L.; Iwamura, H.; Shintani, R.; Hayashi, T. *J. Am. Chem. Soc.* **2007**, *129*, 2130–2138.
- (23) All calculations were performed with Gaussian 03. Frisch, M. J.; et al. *Gaussian 03*, Revision C.02; Gaussian, Inc.: Wallingford, CT, 2004.
- (24) Carrow, B. P.; Hartwig, J. F. *J. Am. Chem. Soc.* **2011**, *133*, 2116–2119.
- (25) Our initial hypothesis concerning the reaction mechanism was well informed by the seminal work of Miyaura, see: Nishitaka, T.; Yamamoto, Y.; Miyaura, N. *Organometallics* **2004**, *23*, 4317–4324.
- (26) Boeser, C. L.; Holder, J. C.; Taylor, B. L. H.; Houk, K. N.; Stoltz, B. M.; Zare, R. N. *Chem. Sci.* **2015**, *6*, 1917–1922.
- (27) (a) Chen, J.; Chen, J.; Lang, F.; Zhang, X.; Cun, L.; Zhu, J.; Deng, J.; Liao, J. *J. Am. Chem. Soc.* **2010**, *132*, 4552–4553; (b) Han, F.; Chen, G.; Zhang, X.; Liao, J. *Eur. J. Org. Chem.* **2011**, 2928–2931; (c) Korenaga, T.; Hayashi, K.; Akaki, Y.; Maenishi, R.; Sakai, T. *Org. Lett.* **2011**, *13*, 2022–2025.
- (28) For a recent example, see: He, Q.; So, C. M.; Bian, Z.; Hayashi, T.; Wang, J. *Chem. Asian J.* **2015**, *10*, 540–543.
- (29) (a) Shintani, R.; Yamagami, T.; Kimura, T.; Hayashi, T. *Org. Lett.* **2005**, *7*, 5317–5319; (b) Zhang, X.; Chen, J.; Han, F.; Cun, L.; Liao, J. *Eur. J. Org. Chem.* **2011**, 1443–1446.

- (30) For an isolated example of a palladium-catalyzed non-enantioselective conjugate addition to a chromone, see: Huang, S.-H.; Wu, T.-M.; Tsai, F.-Y. *Appl. Organomet. Chem.* **2010**, *24*, 619–624.
- (31) Reetz, M. T.; Westermann, J.; Steinbach, R. *J. Chem. Soc. Chem. Commun.* **1981**, 237–239.
- (32) Hansch, C.; Leo, A.; Taft, R. W. *Chem. Rev.* **1991**, *91*, 165–195. Red crosses in Figure A8.7 are interpolated from the linear least square regression using the known Hammett values (σ_p) for *para*-Br and *para*-iPr.
- (33) Ishiyama, T.; Takagi, J.; Ishida, K.; Miyauchi, N.; Anastasi, N. R.; Hartwig, J. F. *J. Am. Chem. Soc.* **2002**, *124*, 390–391.
- (34) Sun, J.; Perfetti, M. T.; Santos, W. L. *J. Org. Chem.* **2011**, *76*, 3571–3575.
- (35) Johnston, M. D.; Shapiro, B. L.; Shapiro, M. J.; Proulx, T. W.; Godwin, A. D.; Pearce, H. L. *J. Am. Chem. Soc.* **1975**, *97*, 542–554.
- (36) Takeda, M.; Inoue, H.; Noguchi, K.; Honma, Y.; Kawamori, M.; Tsukamoto, G.; Yamawaki, Y.; Saito, S. *Chem. Pharm. Bull.* **1976**, *24*, 1514–1526.
- (37) Han, C.; Buchwald, S. L. *J. Am. Chem. Soc.* **2009**, *131*, 7532–7533.
- (38) Molander, G. A.; Rivero, M. R. *Org. Lett.* **2002**, *4*, 107–109.
- (39) Saá, J. M.; Dopico, M.; Martorell, G.; García-Raso, A. *J. Org. Chem.* **1990**, *55*, 991–995.

APPENDIX 9

Spectra Relevant to Appendix 8:

*A Catalytic, Enantioselective Formal Synthesis of (+)-Dichroanone
and (+)-Taiwaniaquinone H*

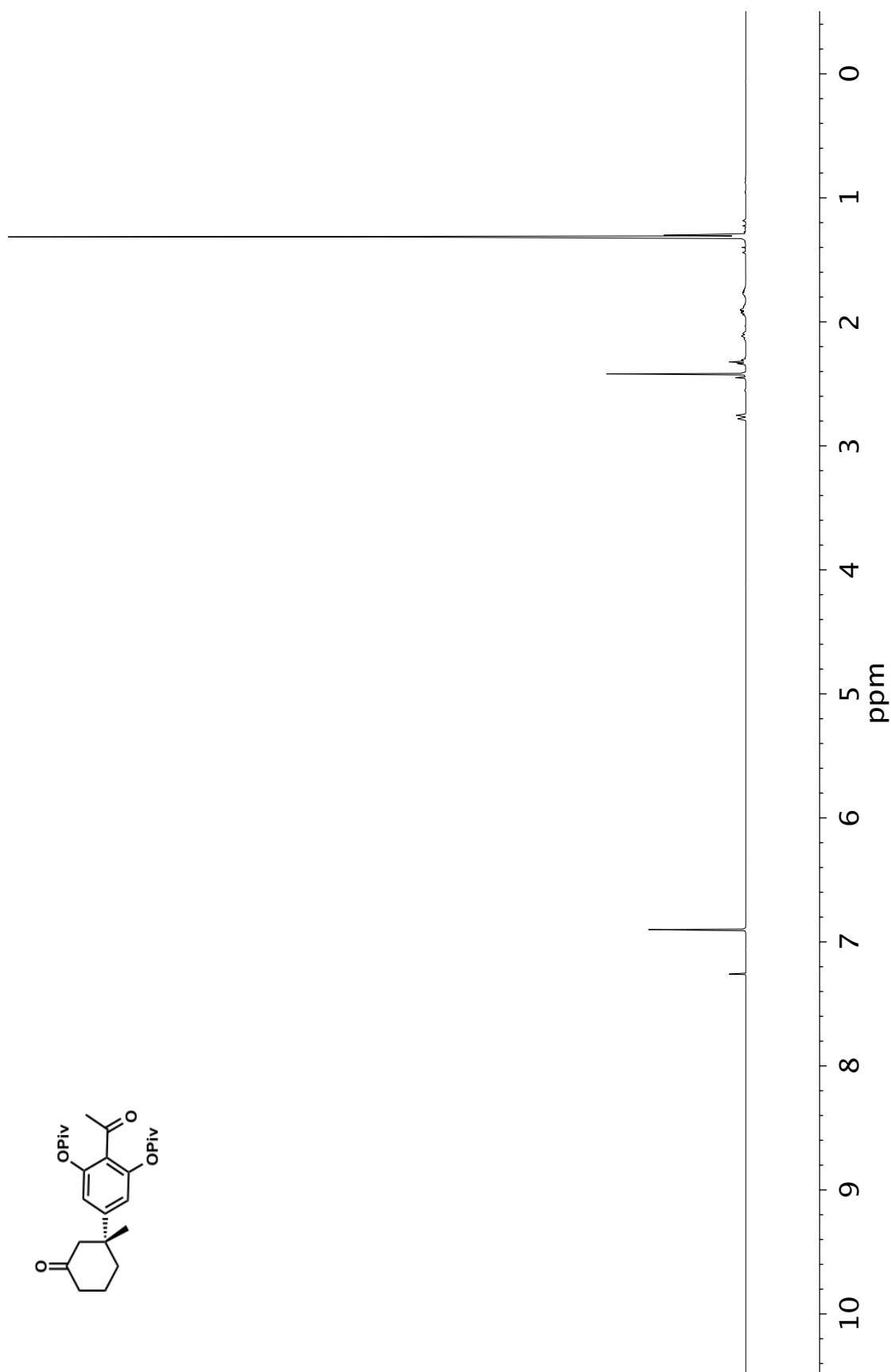


Figure A9.1 ¹H NMR (500 MHz, CDCl₃) of compound **169b**

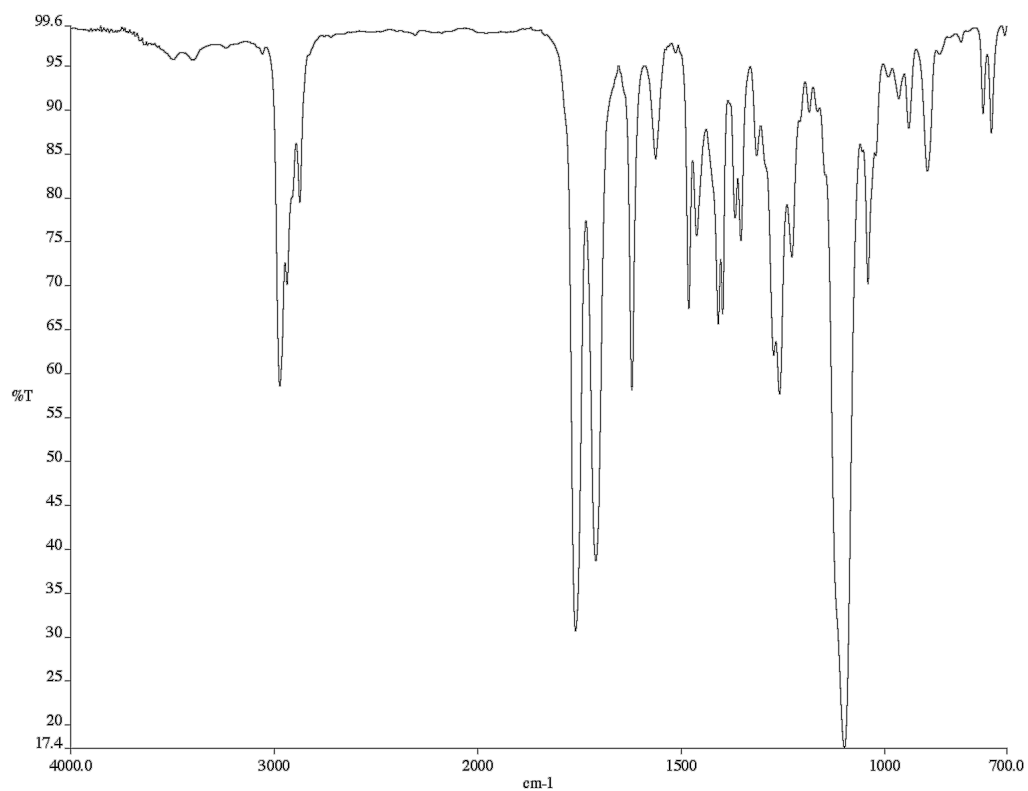


Figure A9.2 Infrared spectrum (Thin Film, NaCl) of compound **169b**

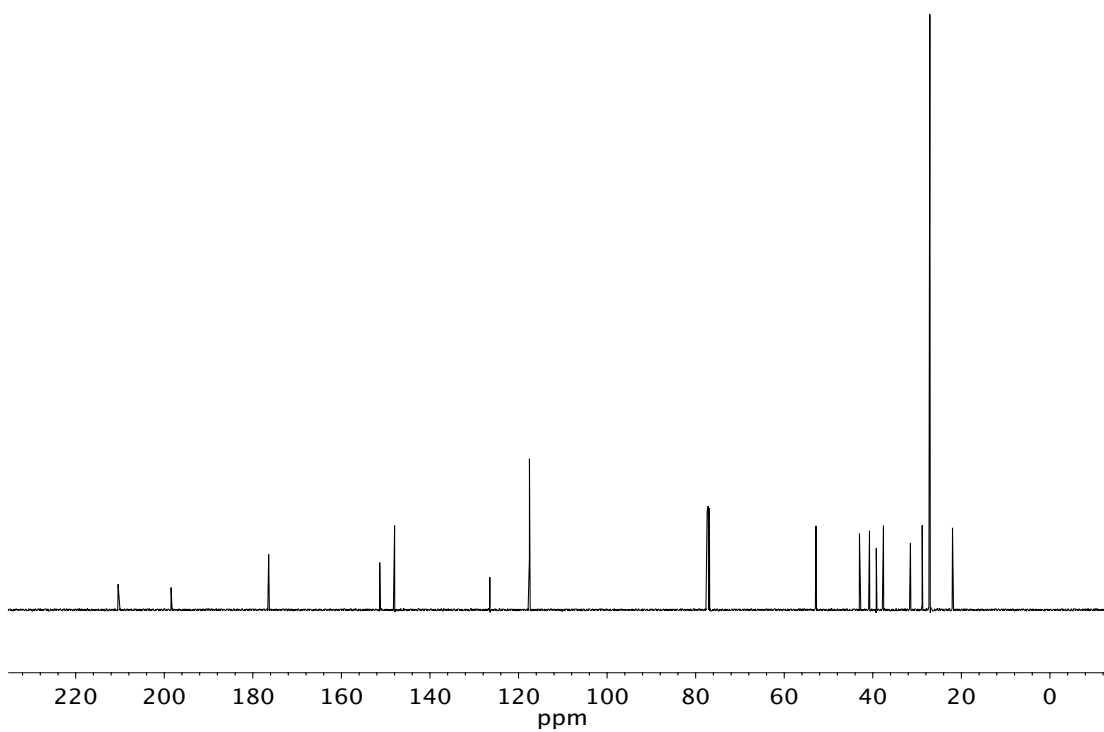


Figure A9.3 ¹³C NMR (125 MHz, CDCl₃) of compound **169b**

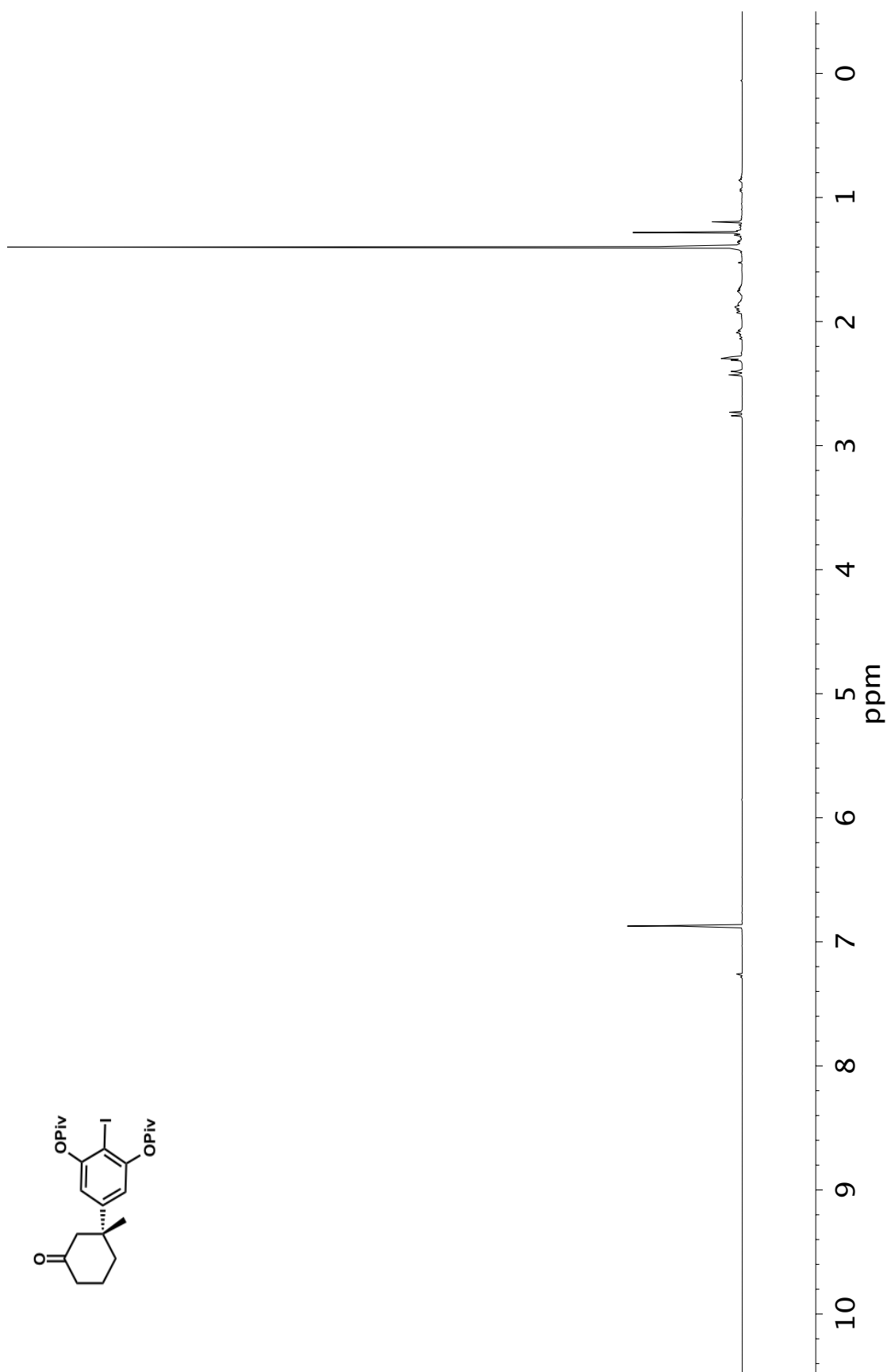


Figure A9.4 ^1H NMR (500 MHz, CDCl_3) of compound **169c**

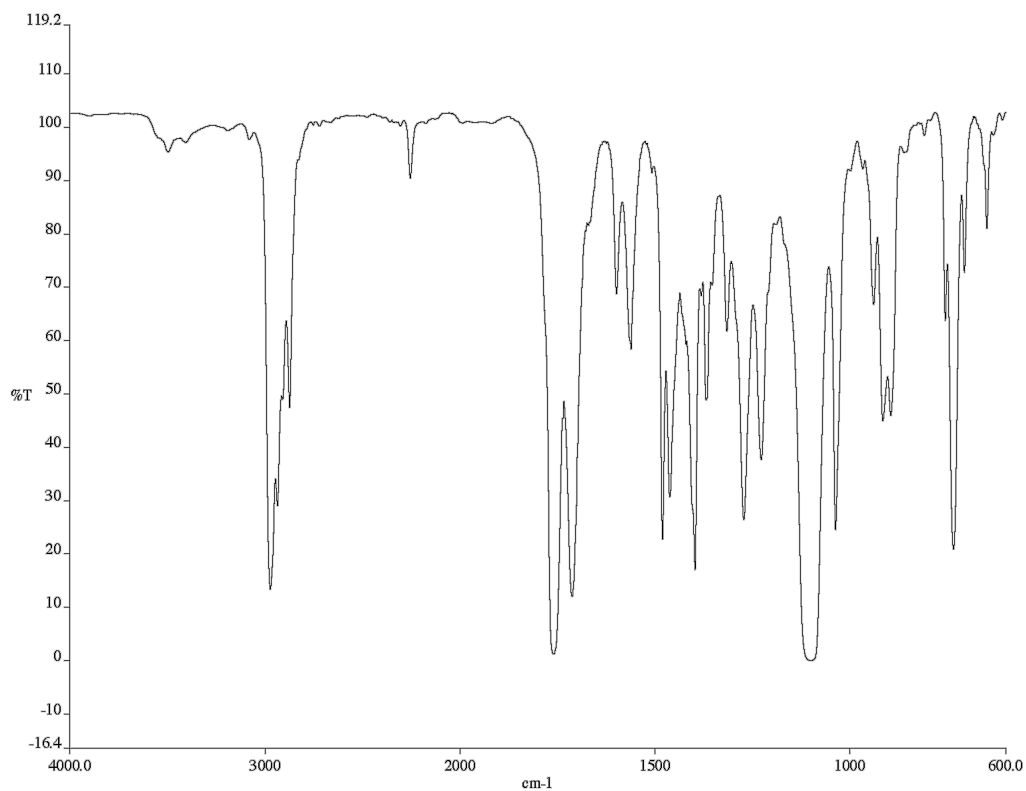


Figure A9.5 Infrared spectrum (Thin Film, NaCl) of compound **169c**

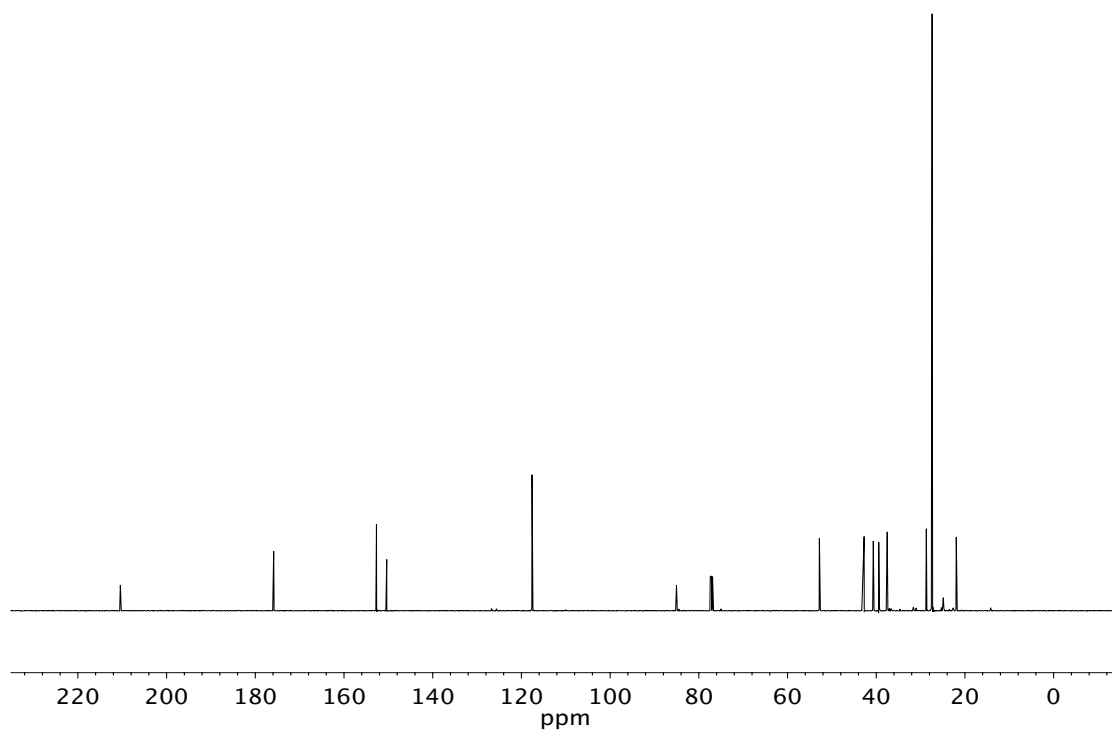


Figure A9.6 ¹³C NMR (125 MHz, CDCl₃) of compound **169c**

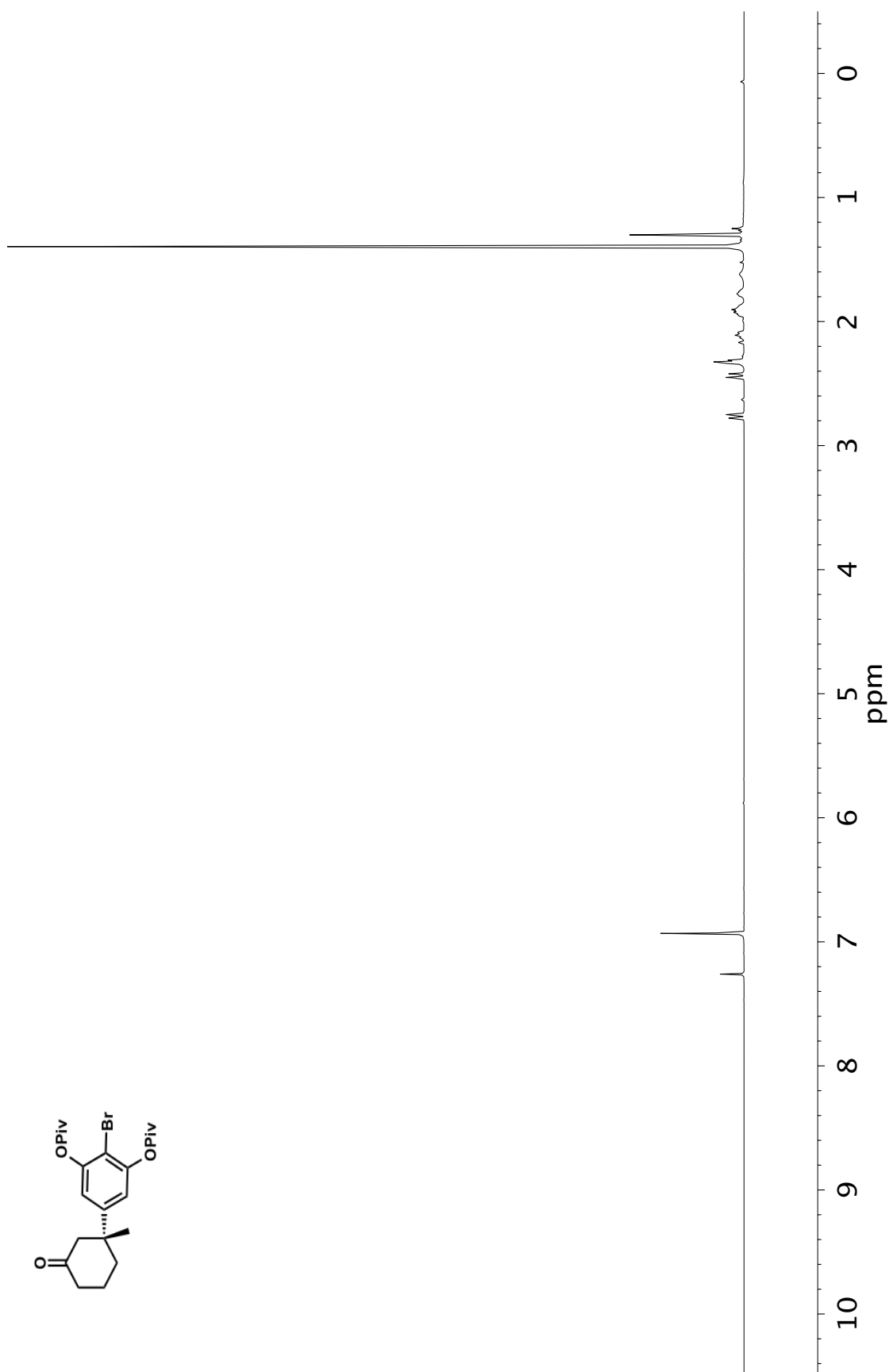


Figure A9.7 ^1H NMR (500 MHz, CDCl_3) of compound **169d**

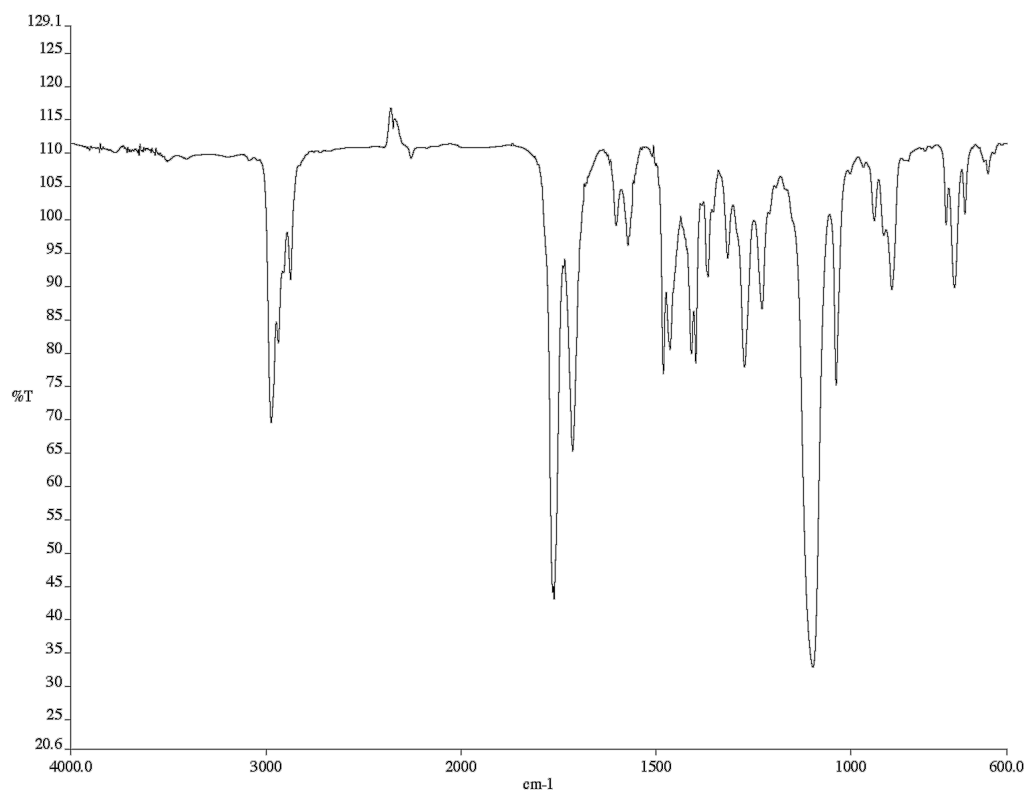


Figure A9.8 Infrared spectrum (Thin Film, NaCl) of compound **169d**

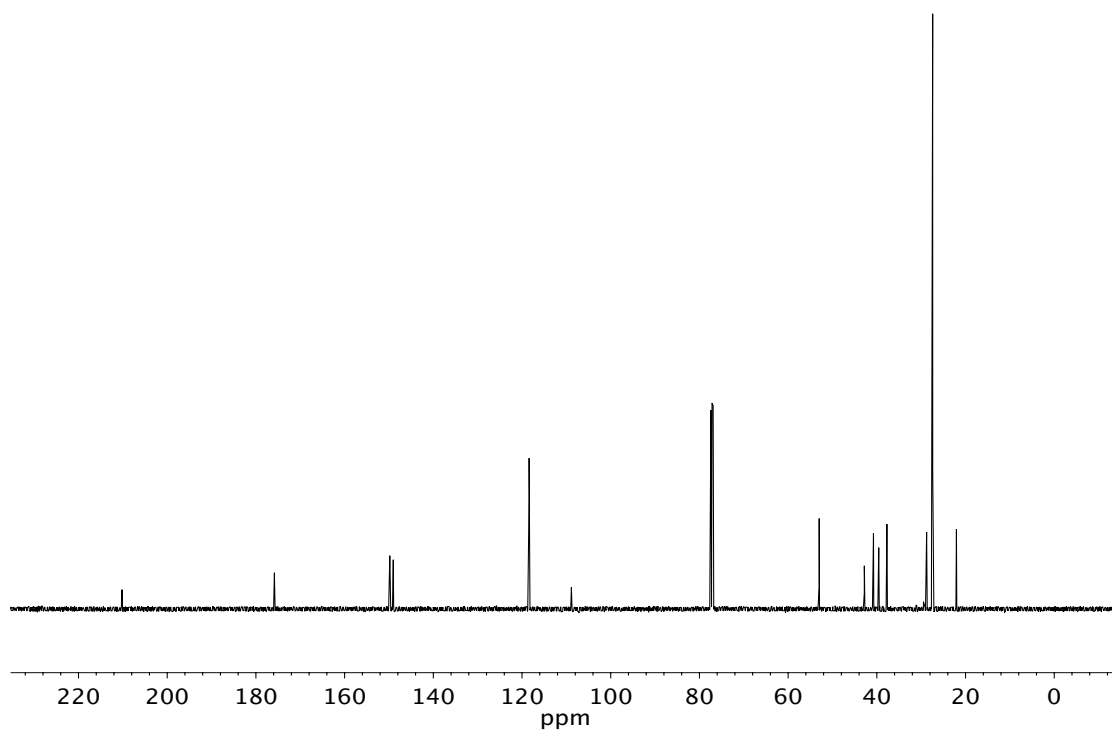


Figure A9.9 ¹³C NMR (125 MHz, CDCl₃) of compound **169d**

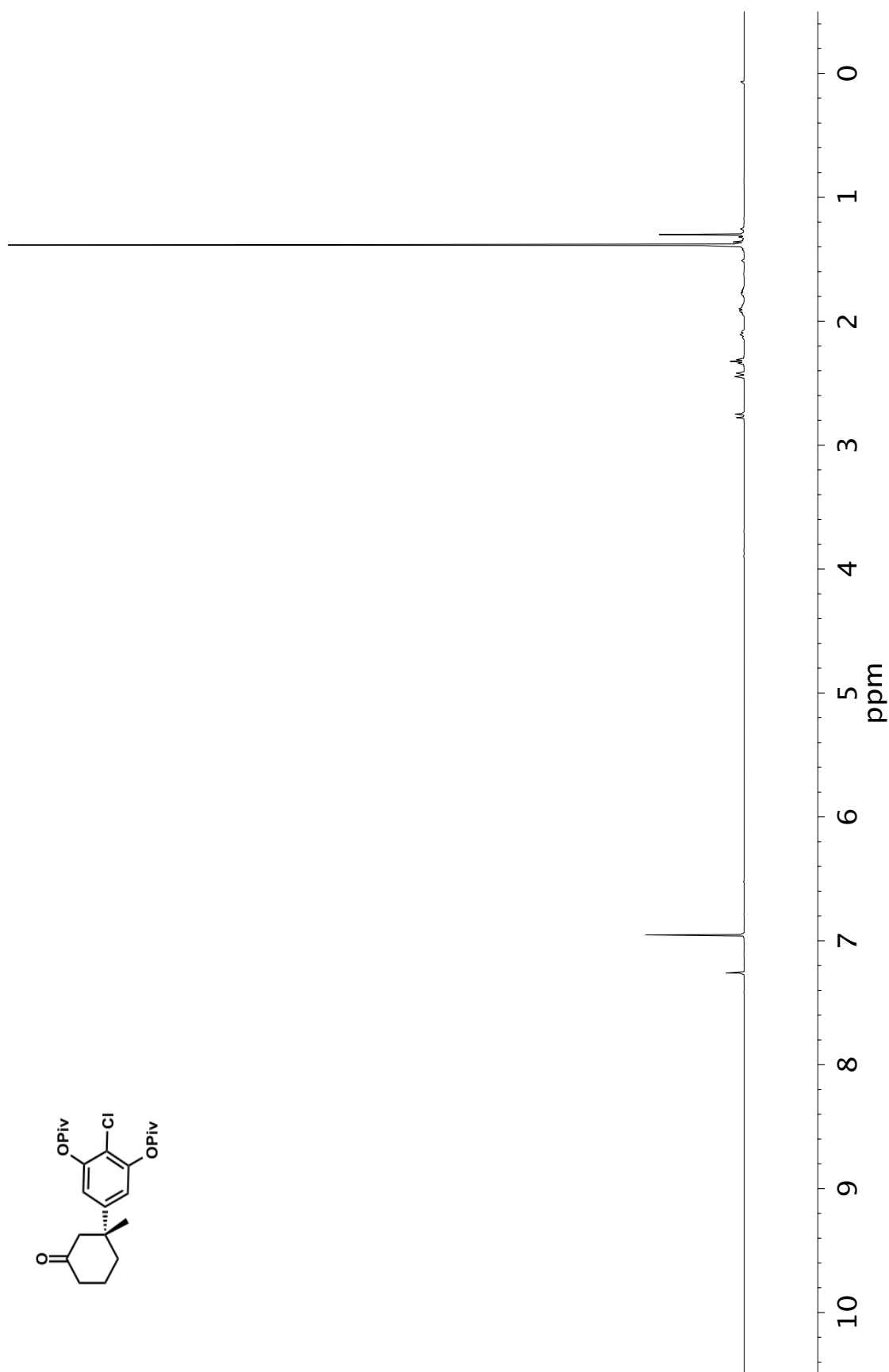


Figure A9.10 ^1H NMR (500 MHz, CDCl_3) of compound **169e**

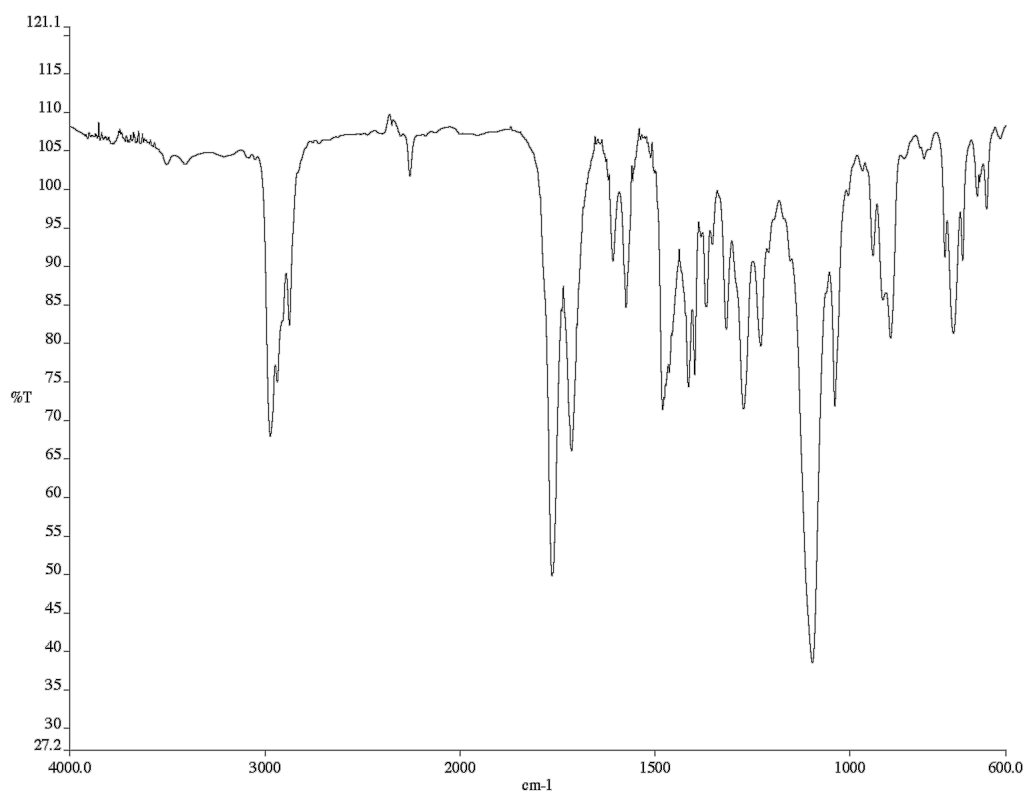


Figure A9.11 Infrared spectrum (Thin Film, NaCl) of compound **169e**

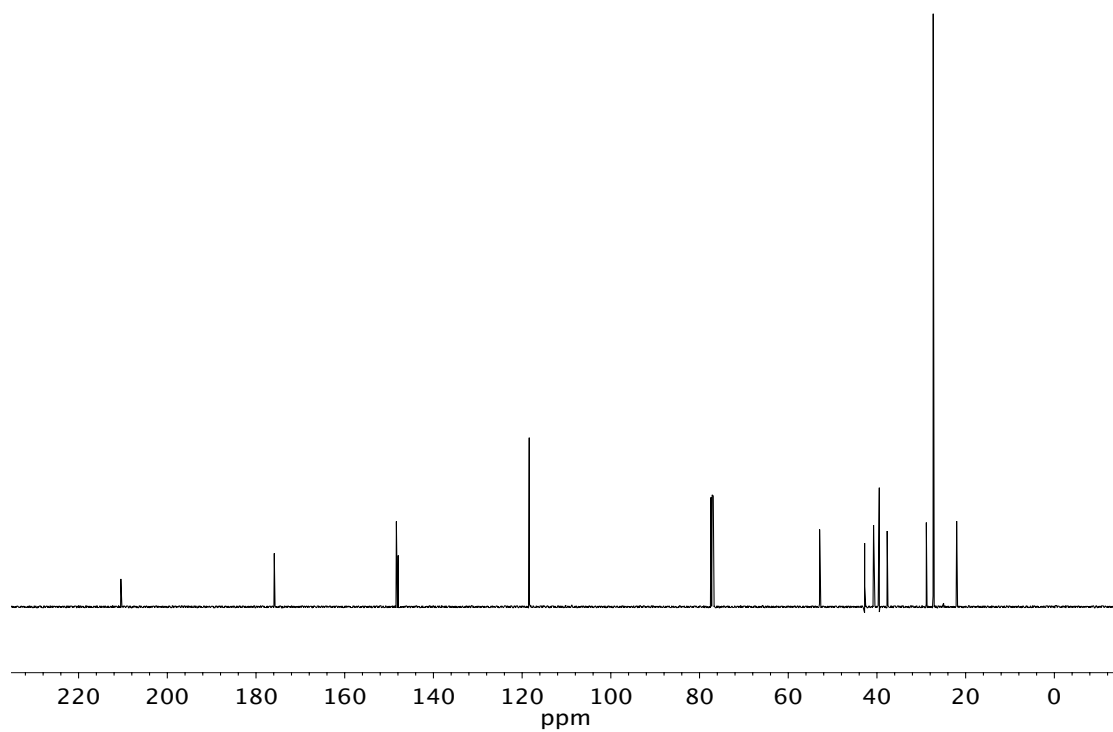


Figure A9.12 ¹³C NMR (125 MHz, CDCl₃) of compound **169e**

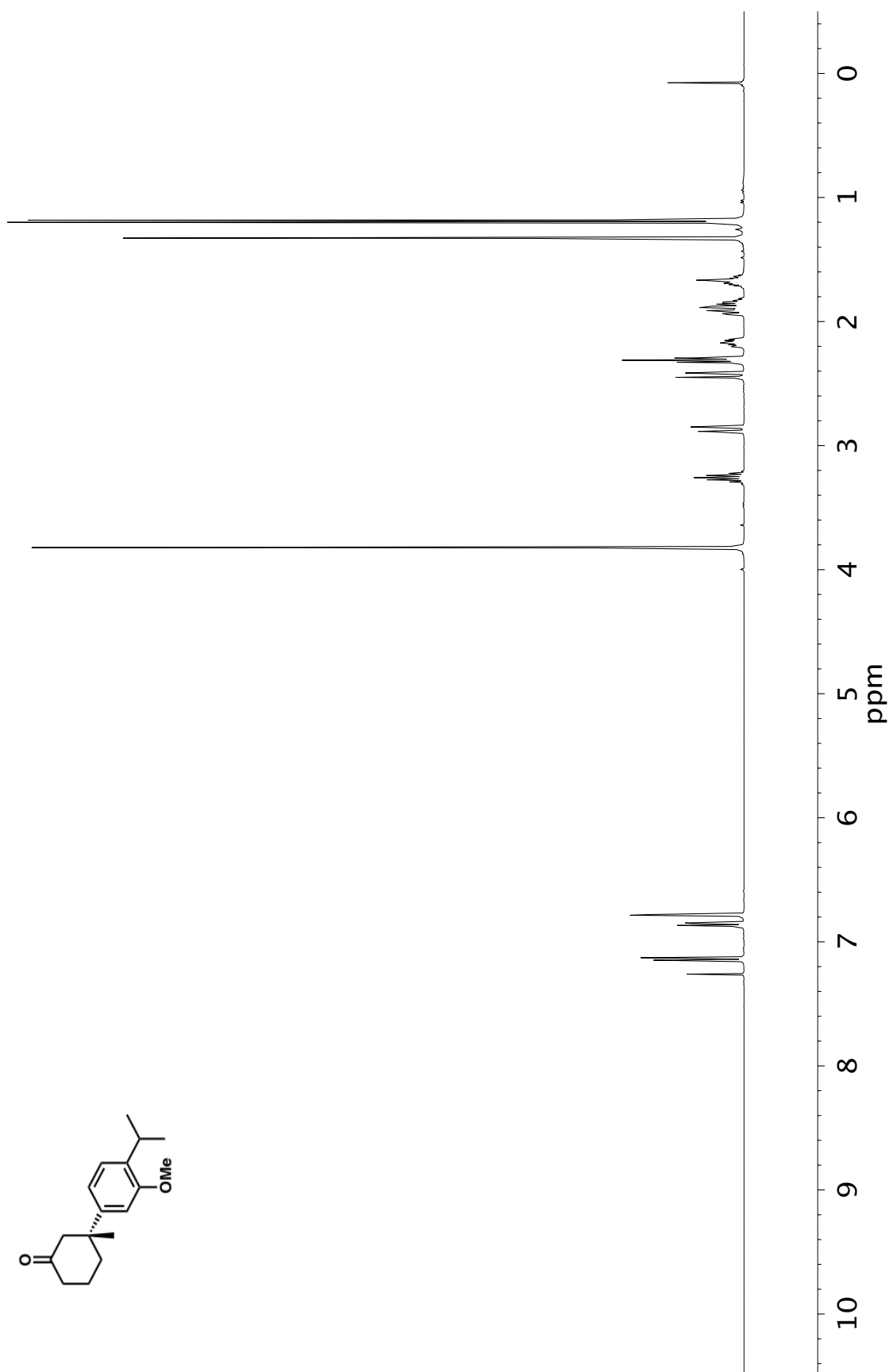


Figure A9.13 ¹H NMR (500 MHz, CDCl₃) of compound **169f**

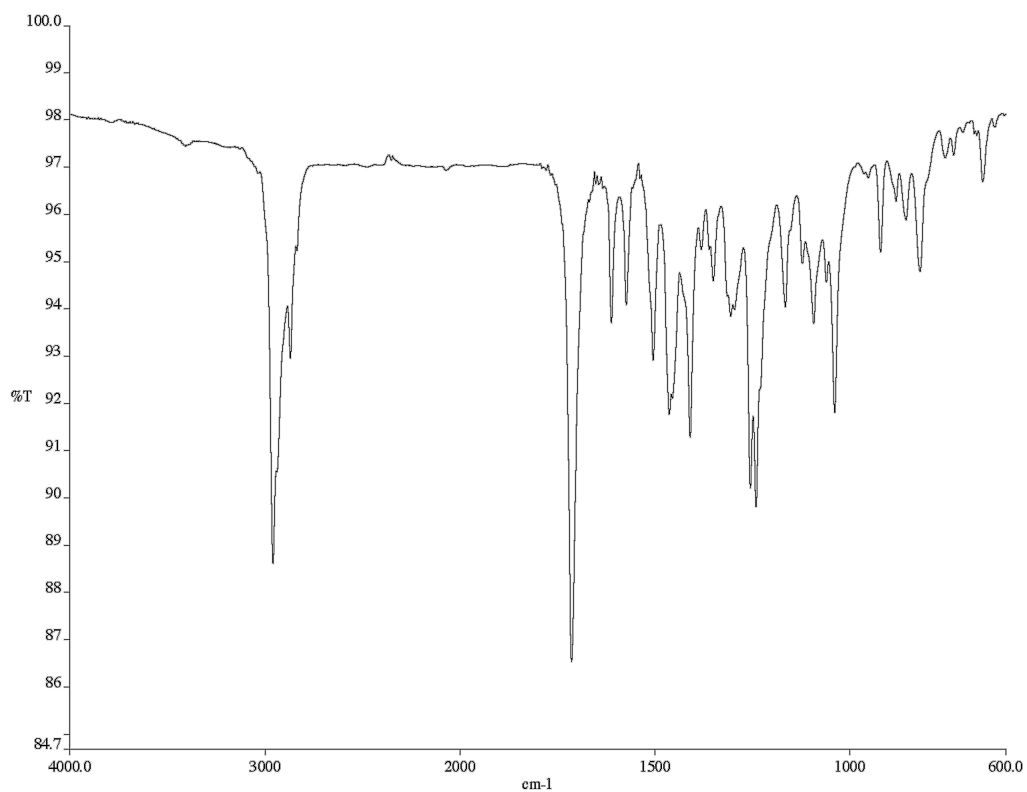


Figure A9.14 Infrared spectrum (Thin Film, NaCl) of compound **169f**

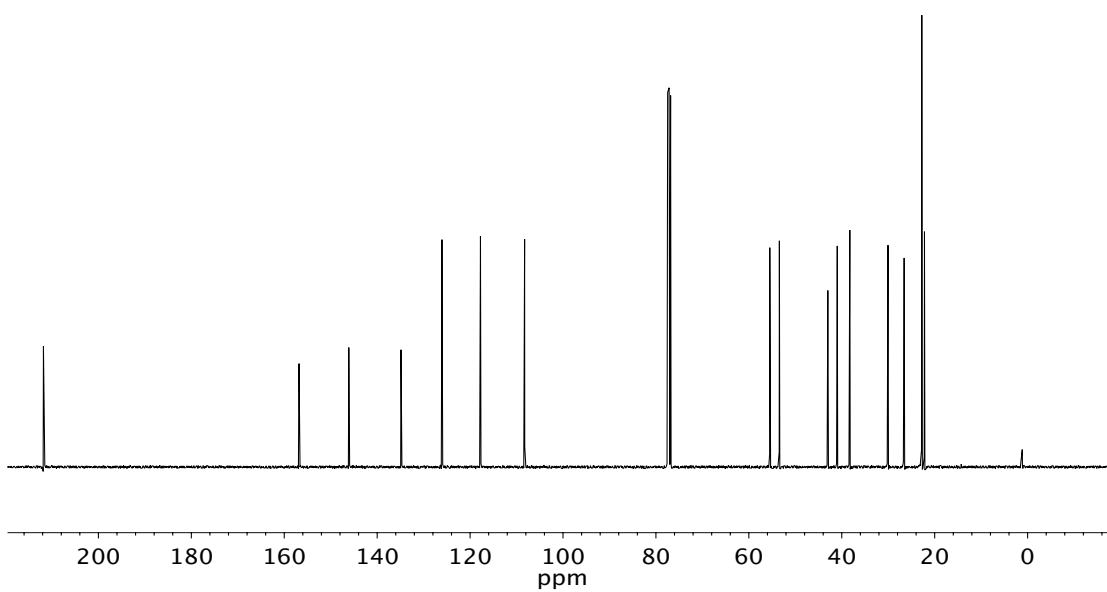


Figure A9.15 ¹³C NMR (125 MHz, CDCl₃) of compound **169f**

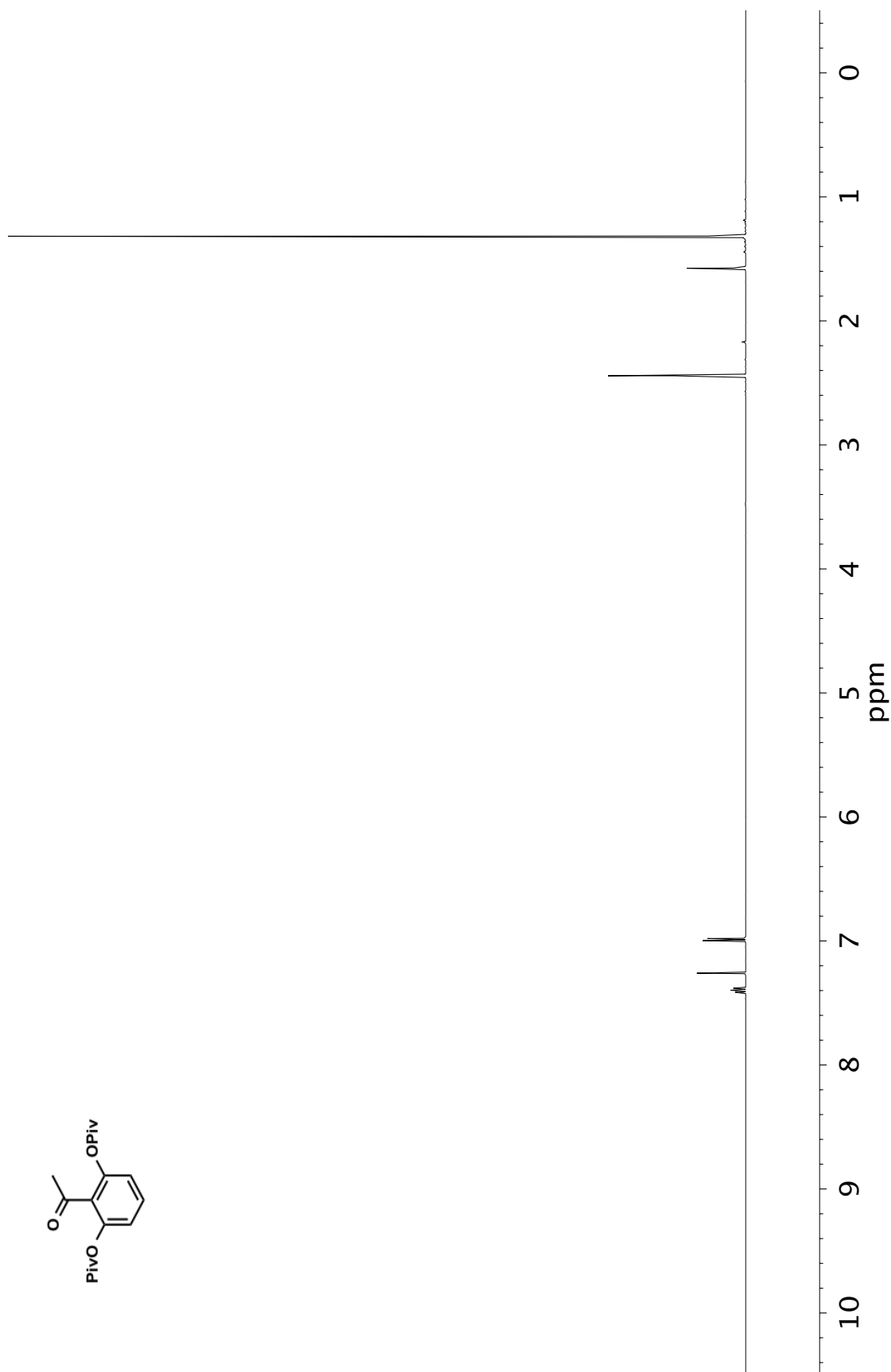


Figure A9.16 ^1H NMR (500 MHz, CDCl_3) of compound **197**

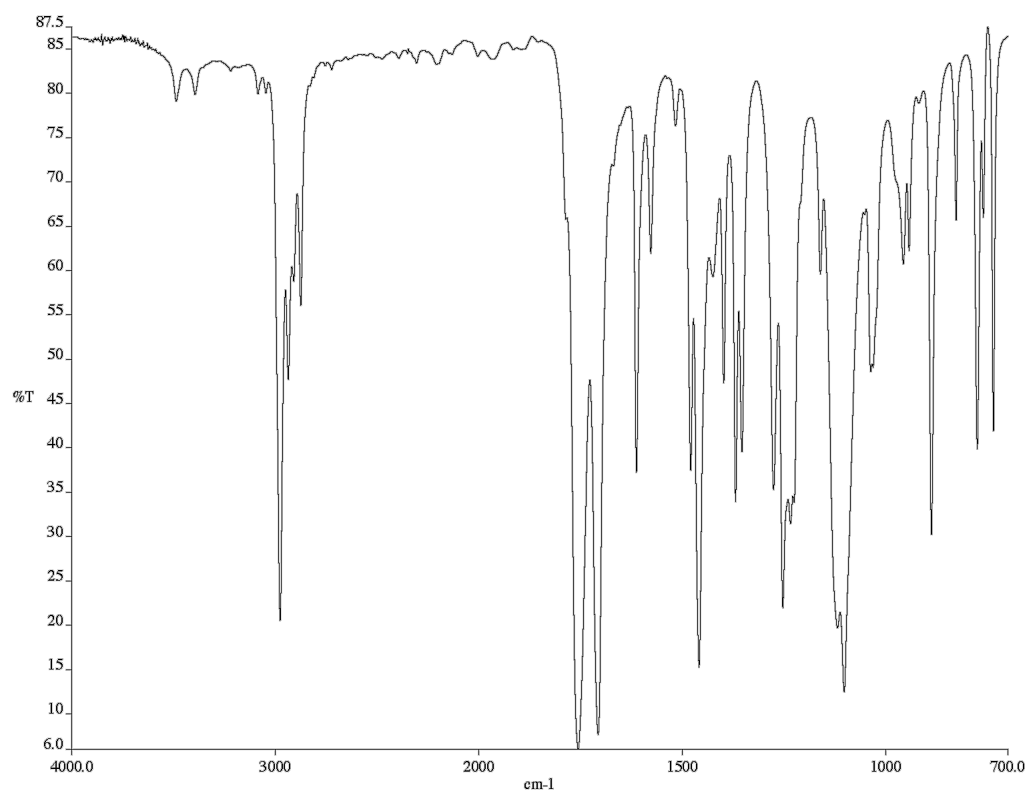


Figure A9.17 Infrared spectrum (Thin Film, NaCl) of compound **197**

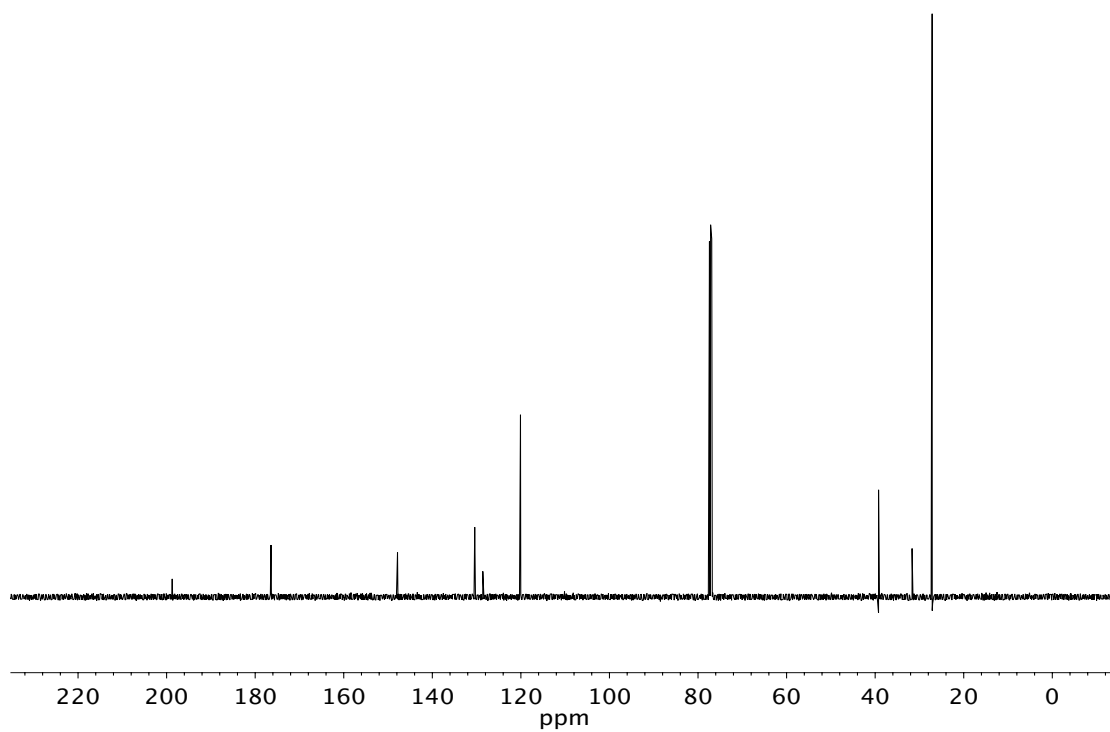


Figure A9.18 ¹³C NMR (125 MHz, CDCl₃) of compound **197**

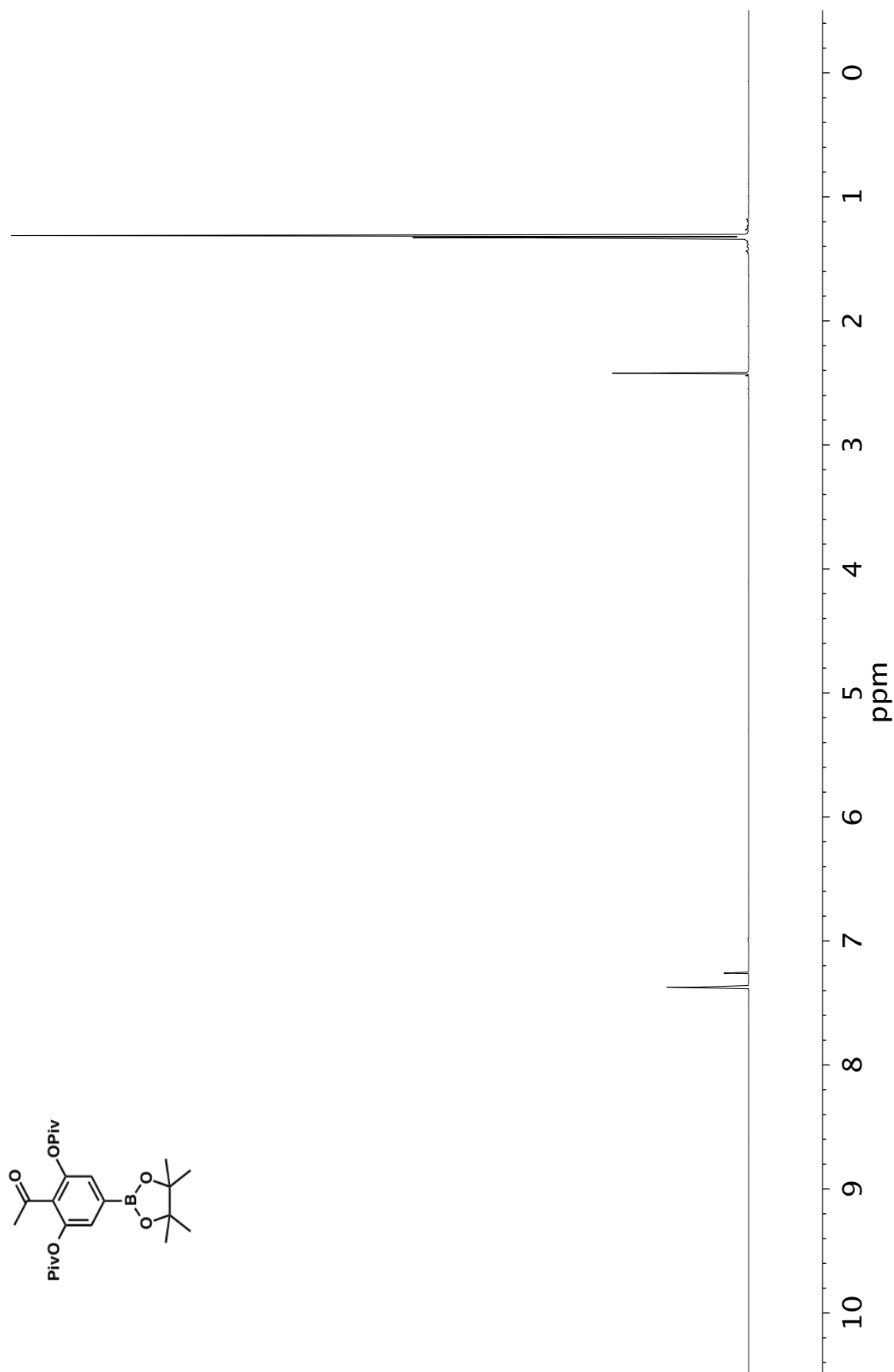


Figure A9.19 ^1H NMR (500 MHz, CDCl_3) of compound **198**

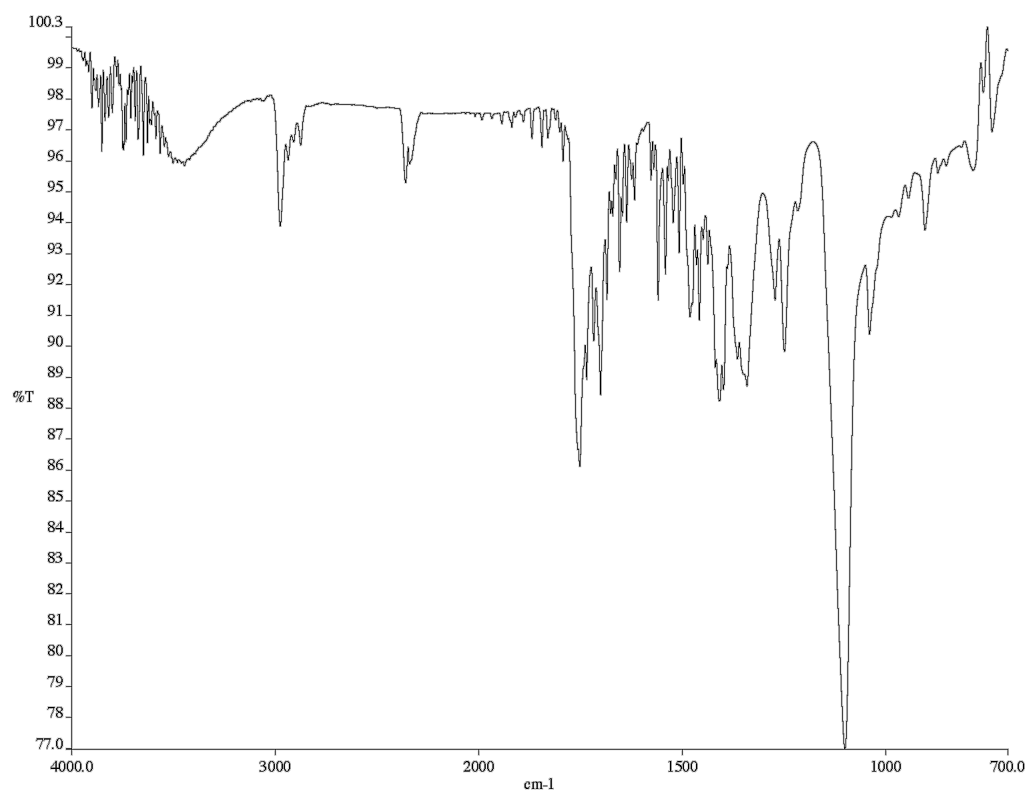


Figure A9.20 Infrared spectrum (Thin Film, NaCl) of compound **198**

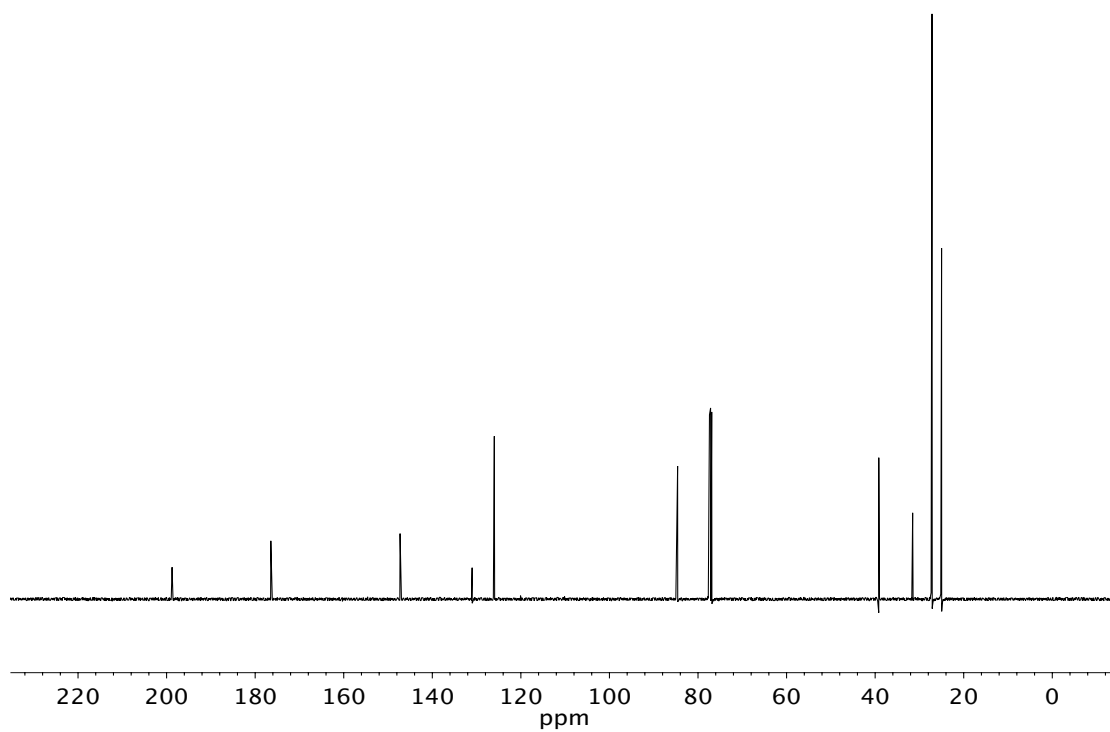


Figure A9.21 ¹³C NMR (125 MHz, CDCl₃) of compound **198**

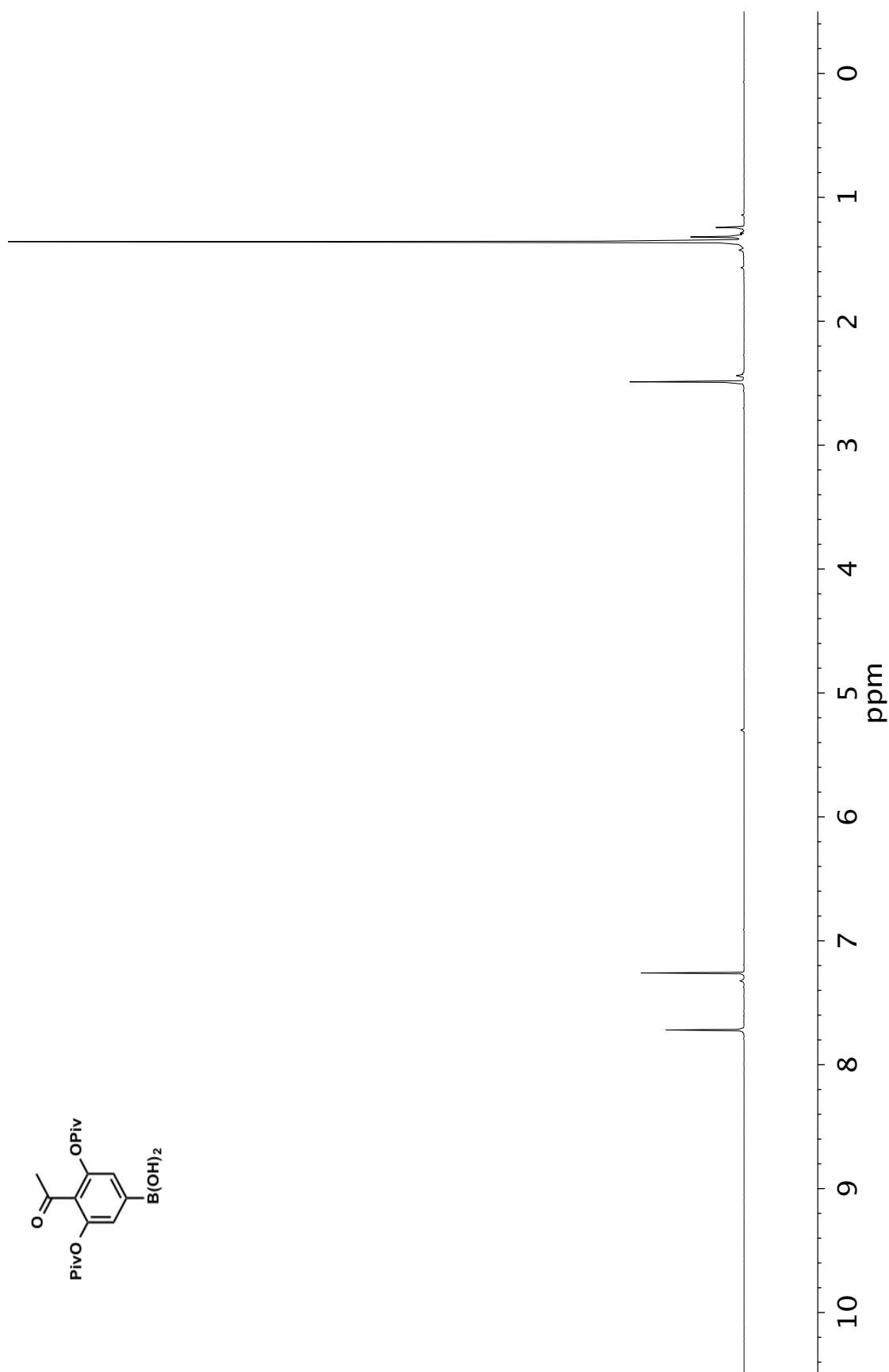


Figure A9.22 ¹H NMR (500 MHz, CDCl₃) of compound **199**

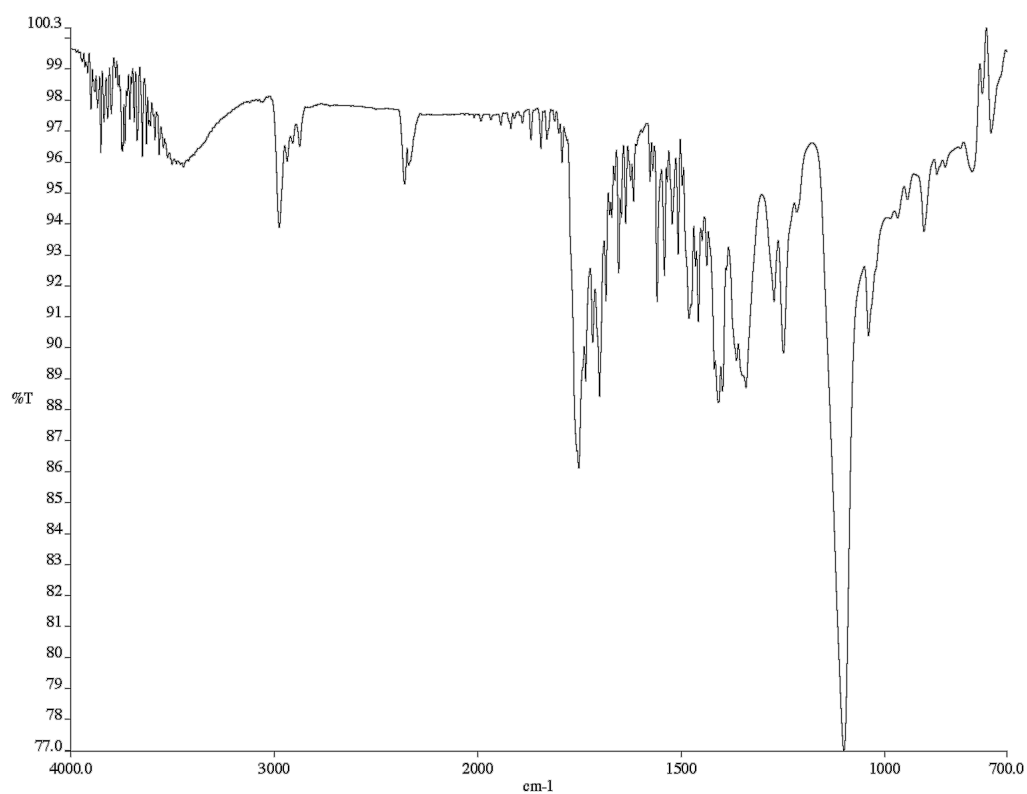


Figure A9.23 Infrared spectrum (Thin Film, NaCl) of compound **199**

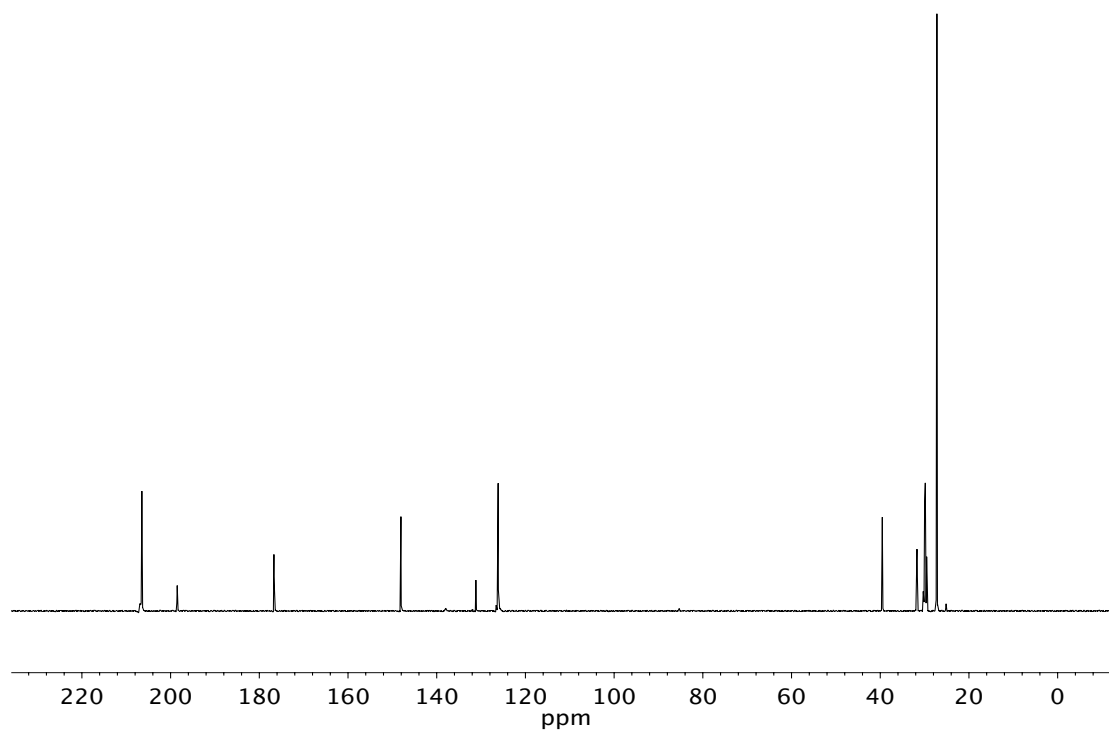


Figure A9.24 ¹³C NMR (125 MHz, CDCl₃) of compound **199**

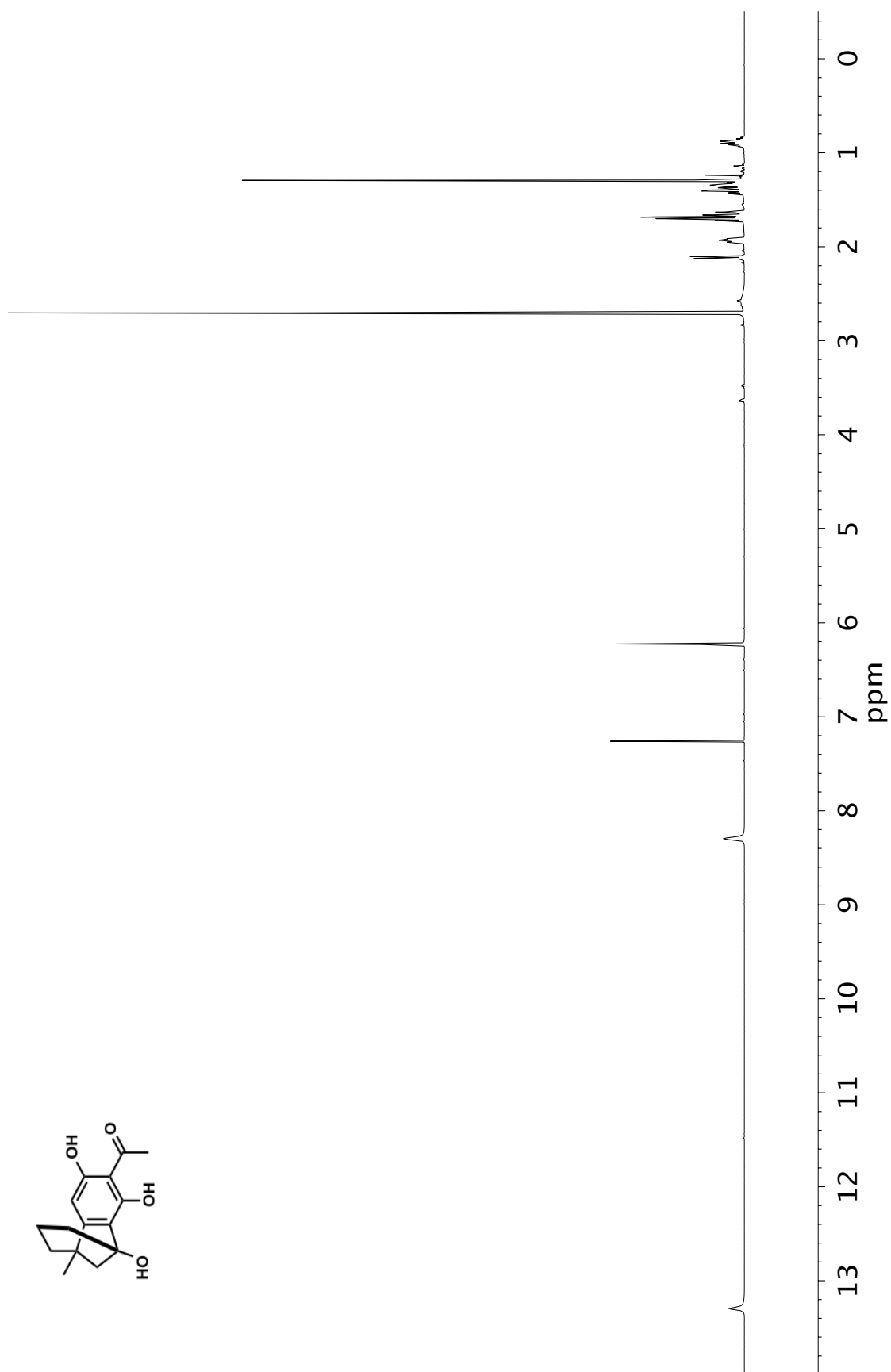


Figure A9.25 ¹H NMR (500 MHz, CDCl₃) of compound 202

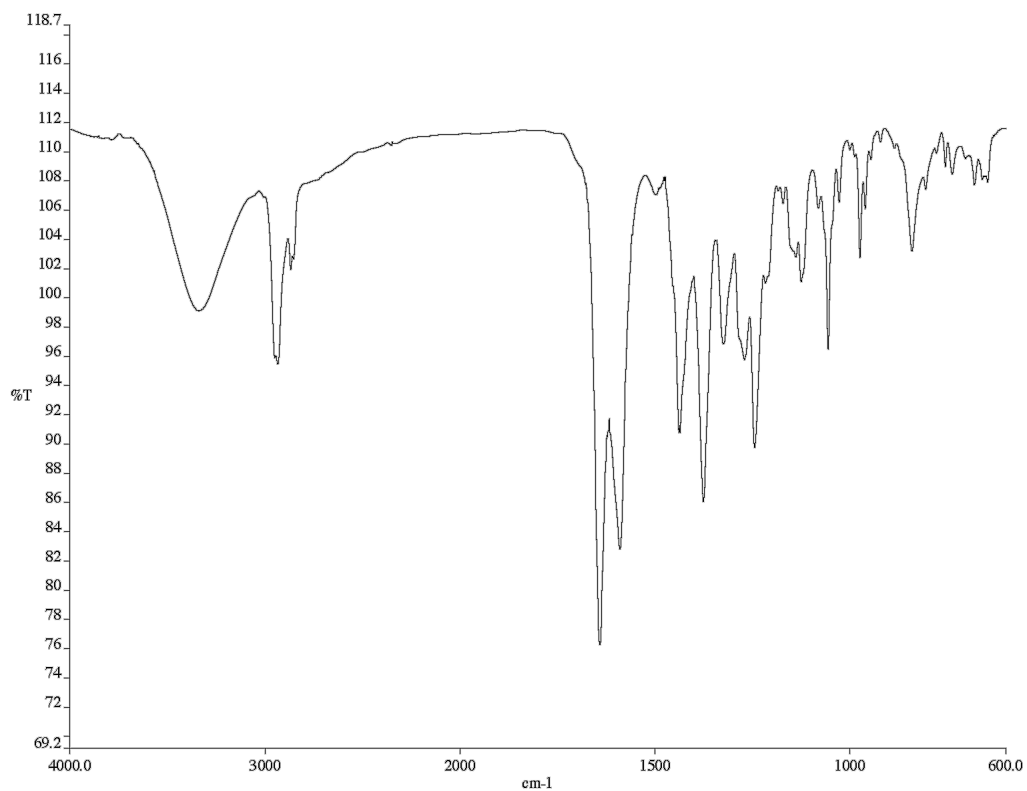


Figure A9.26 Infrared spectrum (Thin Film, NaCl) of compound **202**

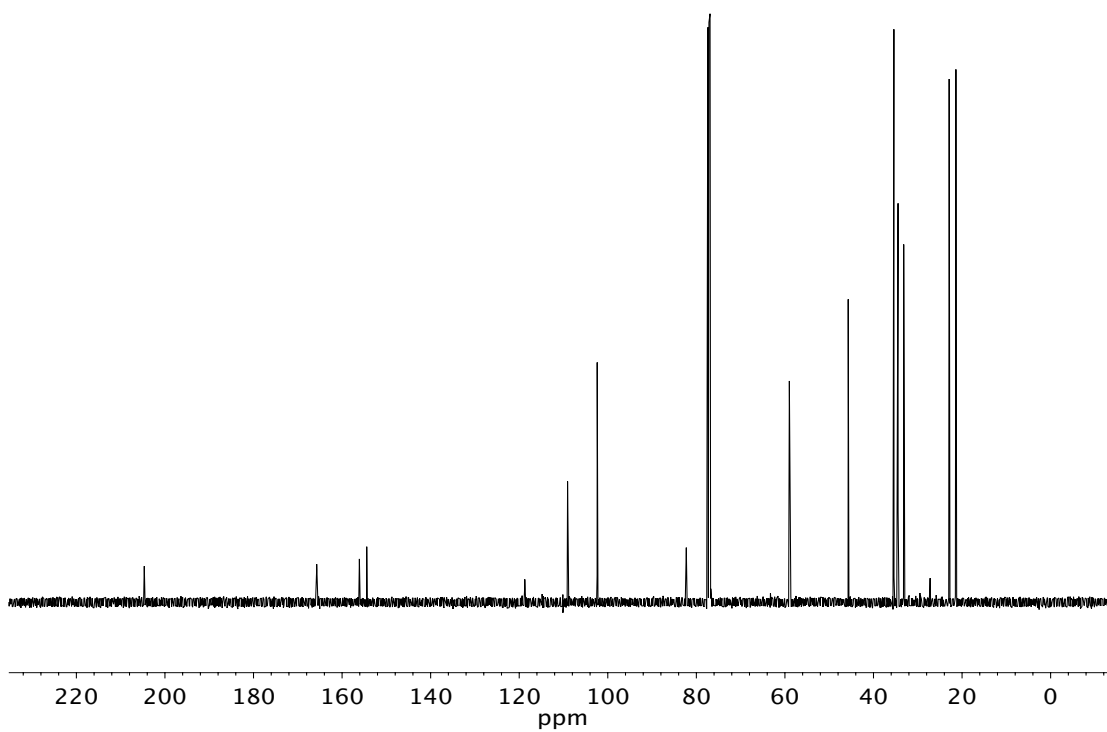


Figure A9.27 ¹³C NMR (125 MHz, CDCl₃) of compound **202**

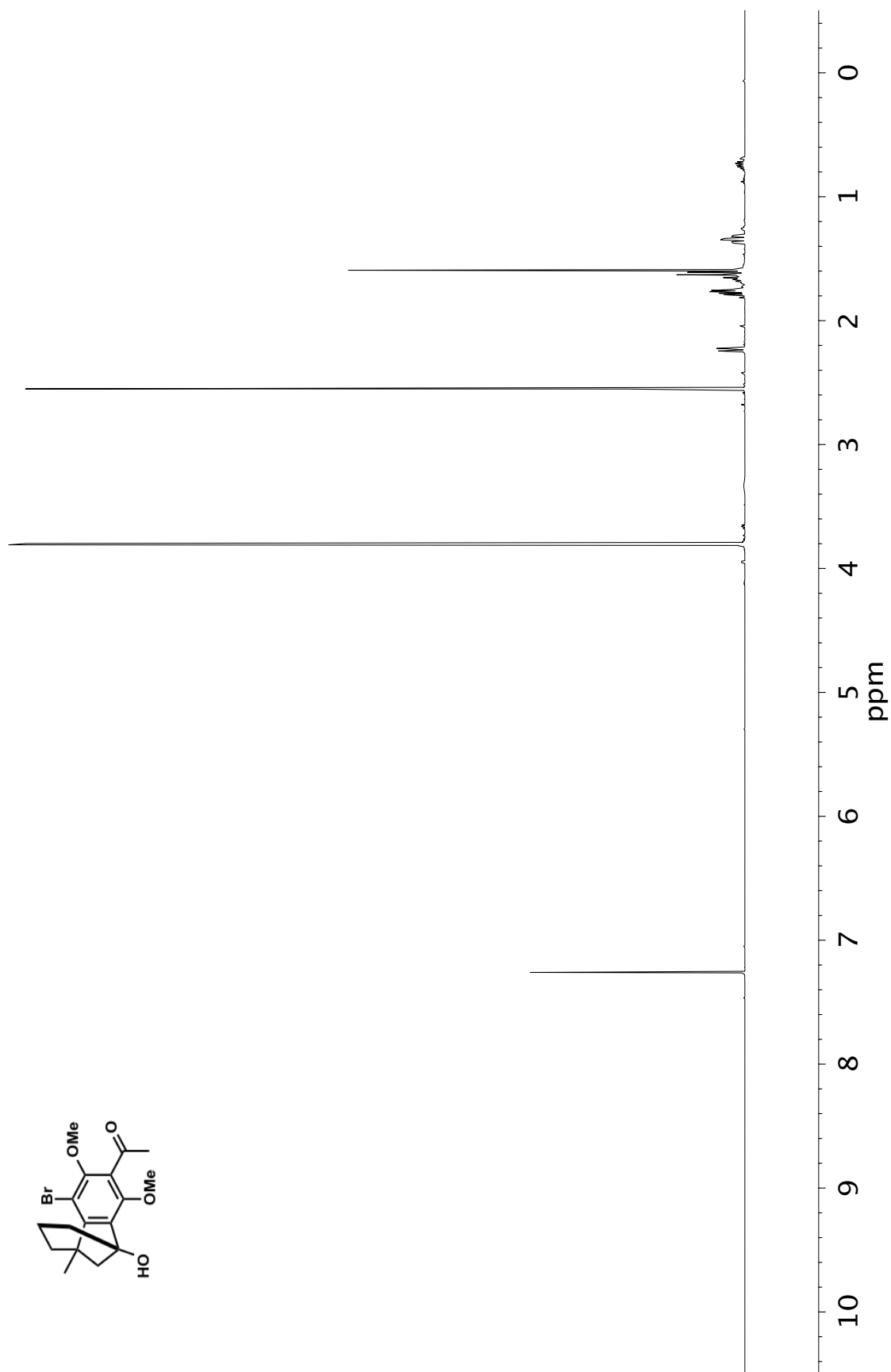


Figure A9.28 ^1H NMR (500 MHz, CDCl_3) of compound 203

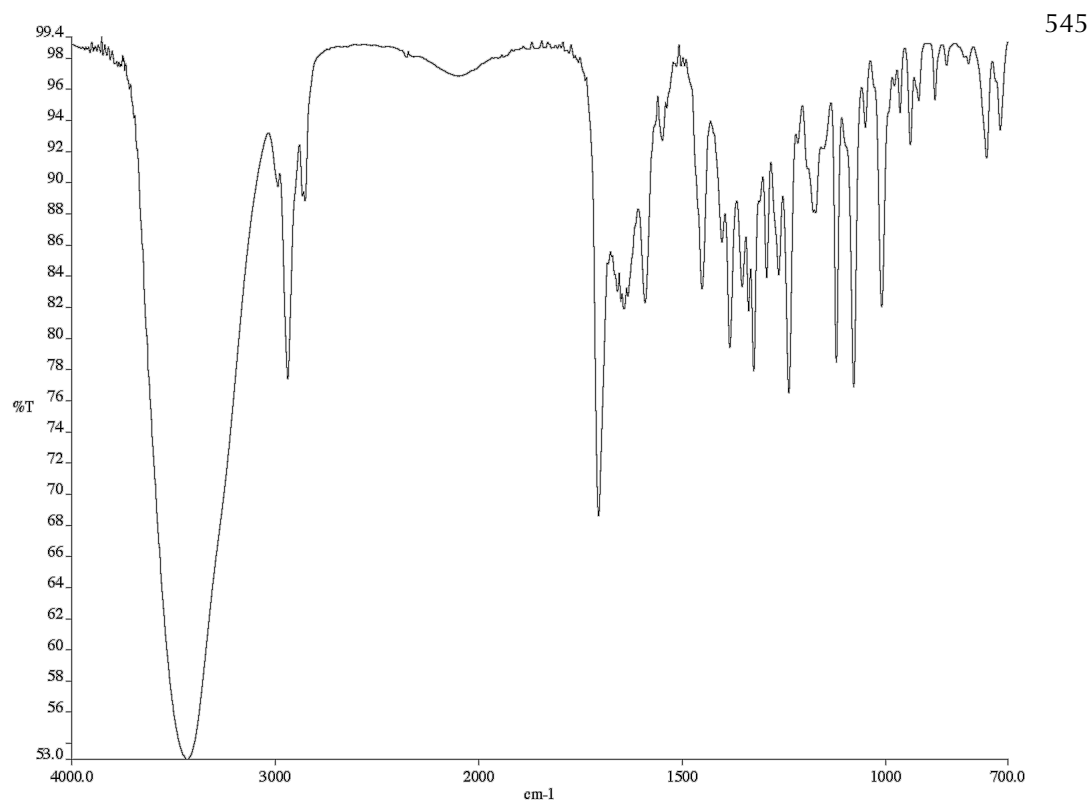


Figure A9.29 Infrared spectrum (Thin Film, NaCl) of compound **203**

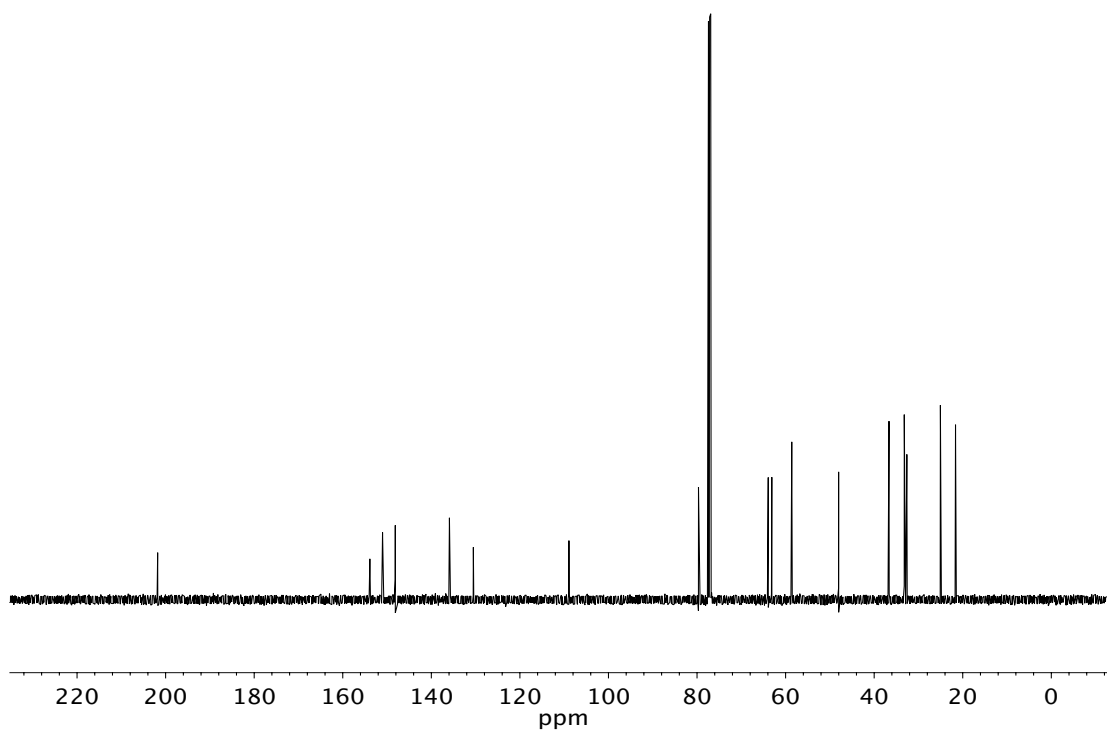


Figure A9.30 ^{13}C NMR (125 MHz, CDCl_3) of compound **203**

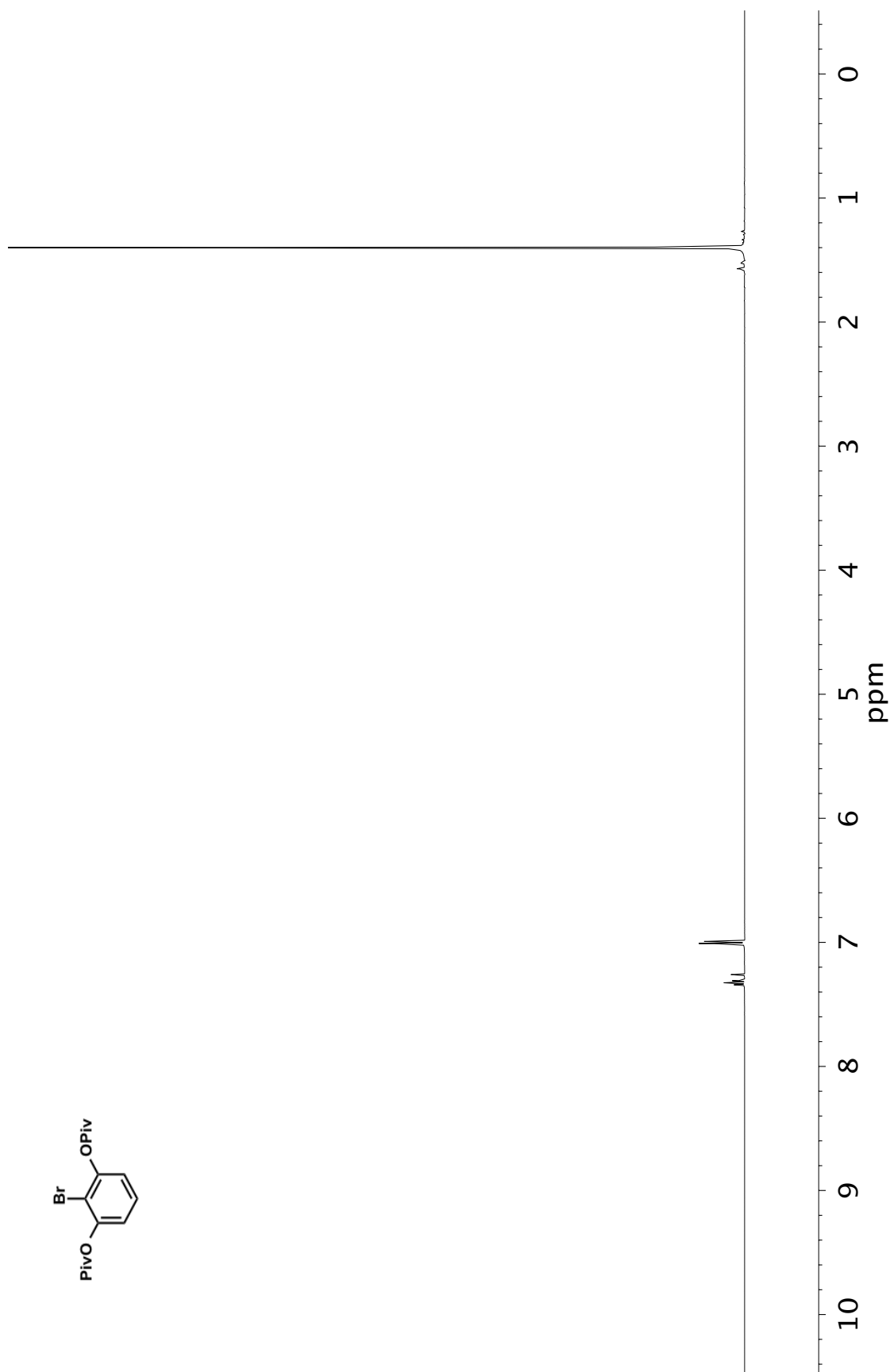


Figure A9.31 ^1H NMR (500 MHz, CDCl_3) of compound 205

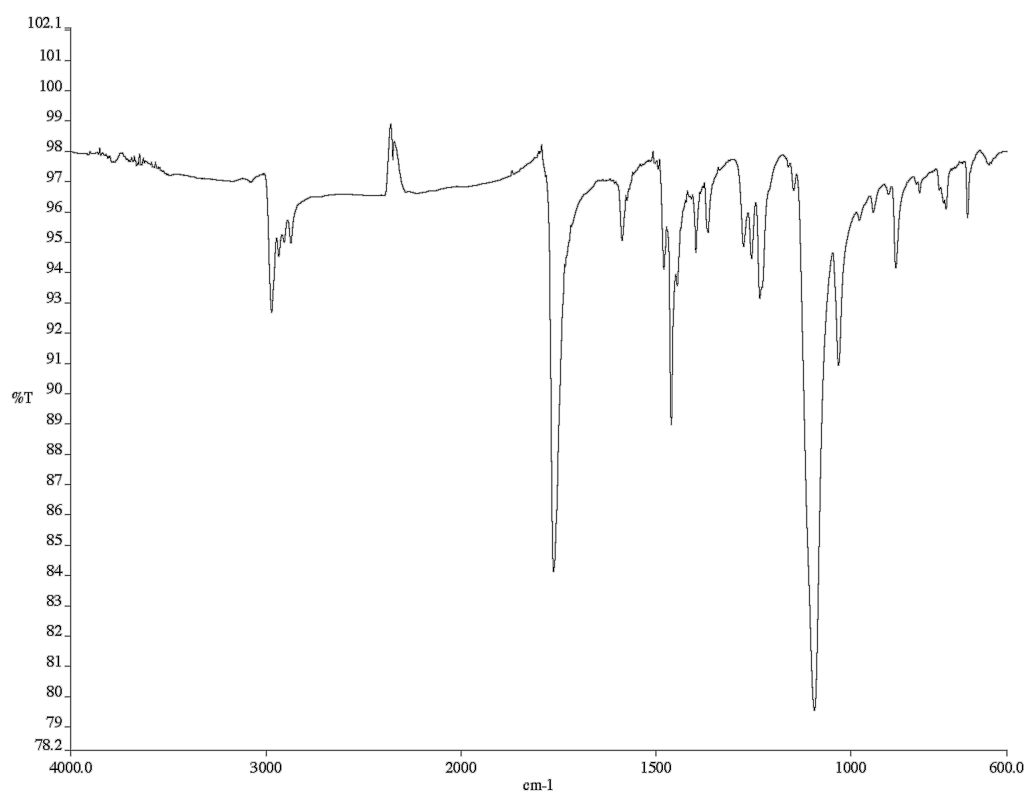


Figure A9.32 Infrared spectrum (Thin Film, NaCl) of compound **205**

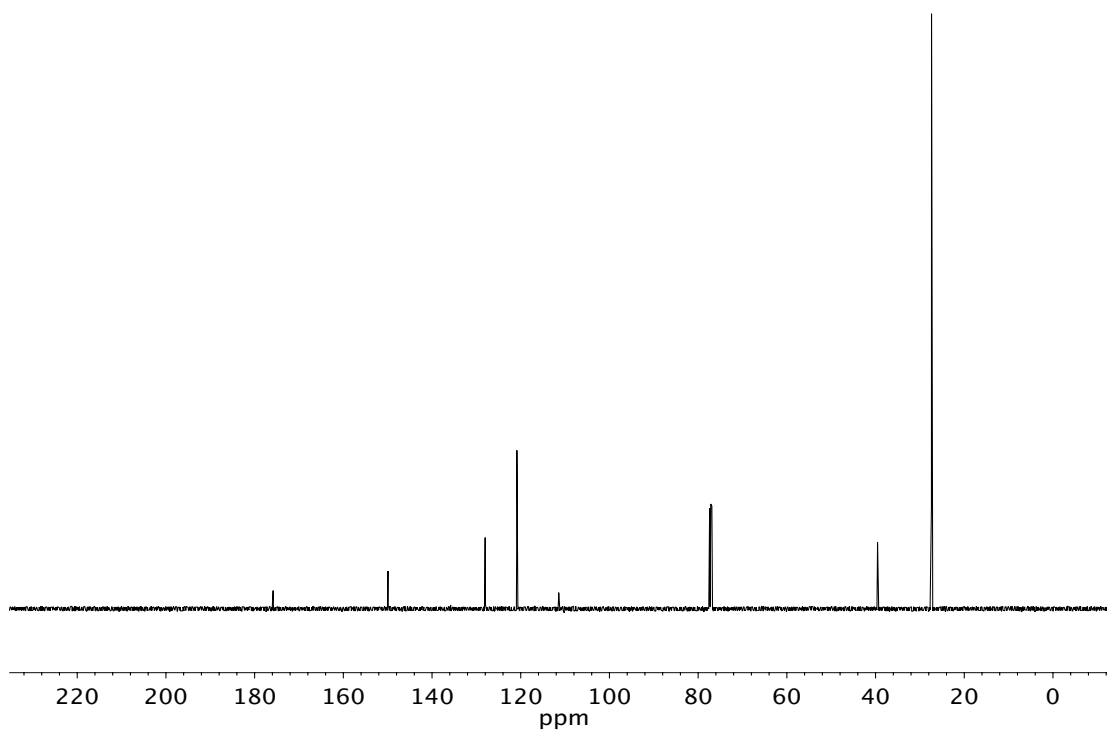
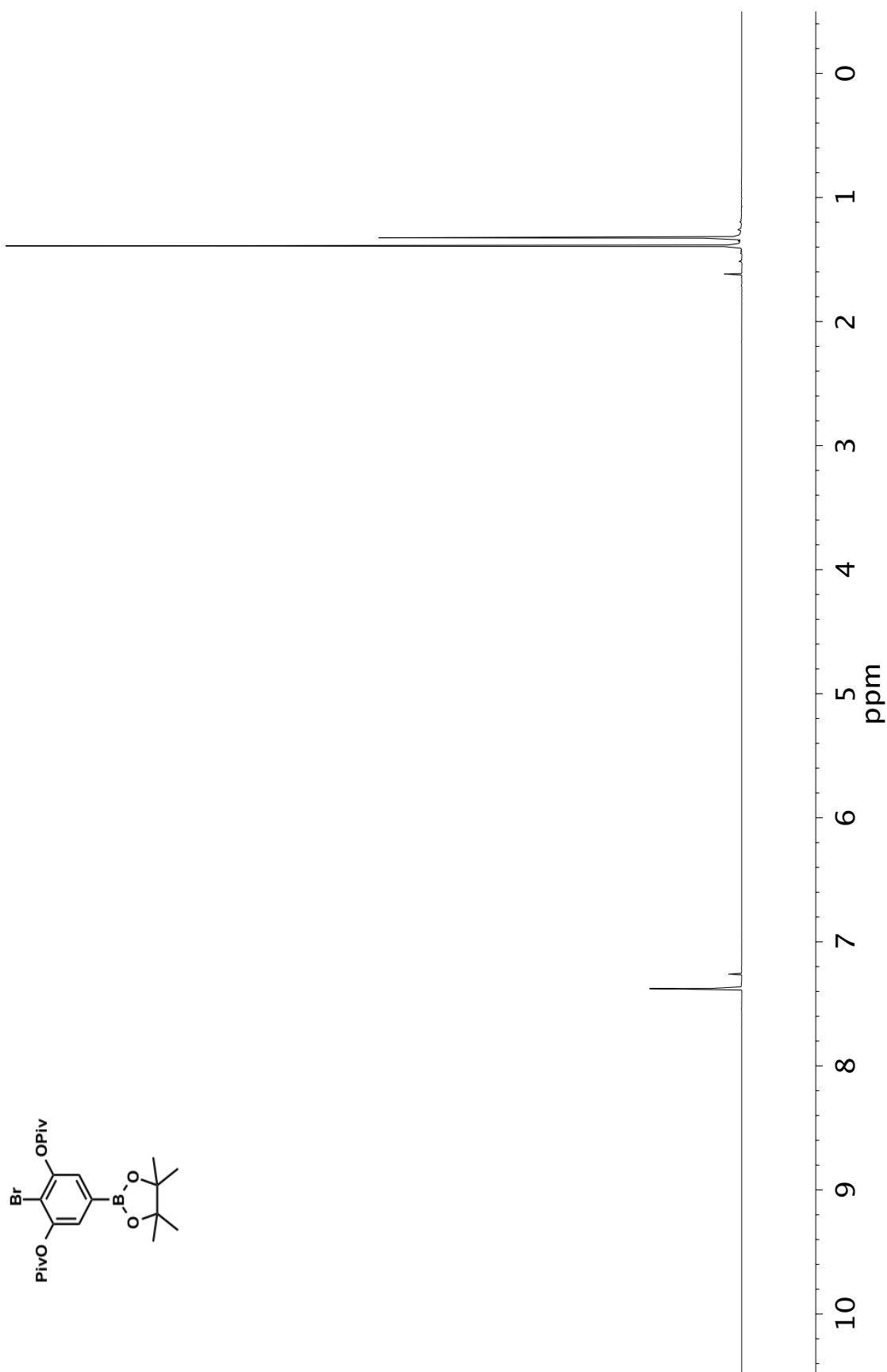


Figure A9.33 ¹³C NMR (125 MHz, CDCl₃) of compound **205**

Figure A9.34 ¹H NMR (500 MHz, CDCl₃) of compound 206

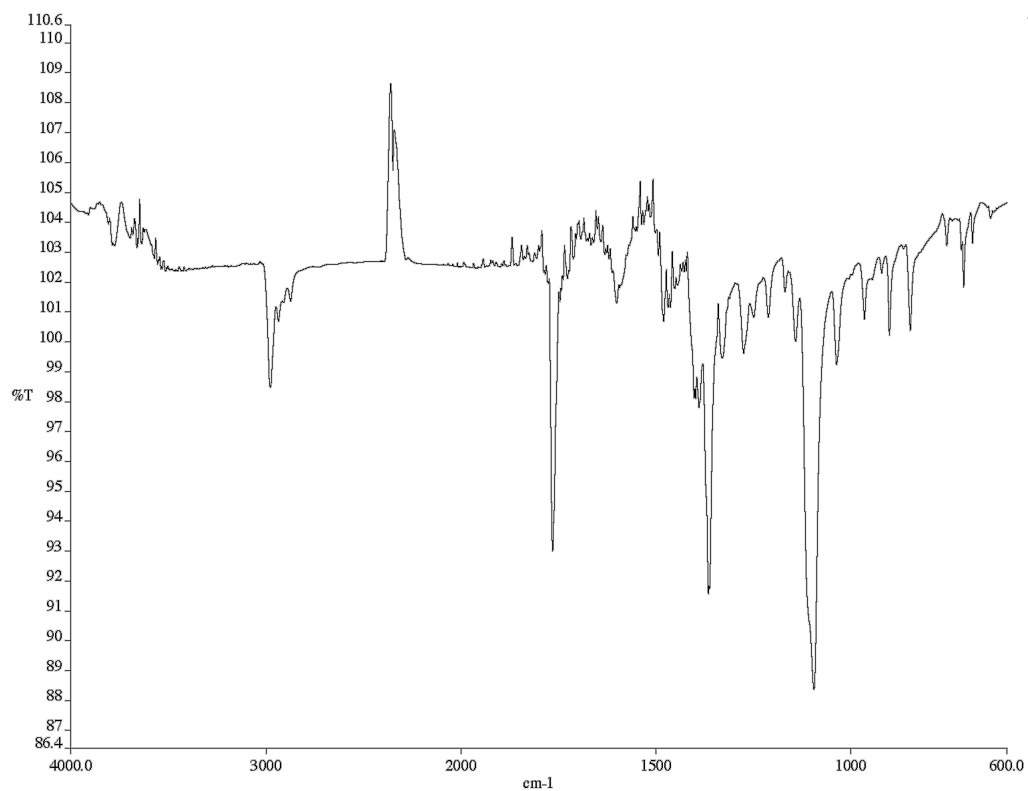


Figure A9.35 Infrared spectrum (Thin Film, NaCl) of compound **206**

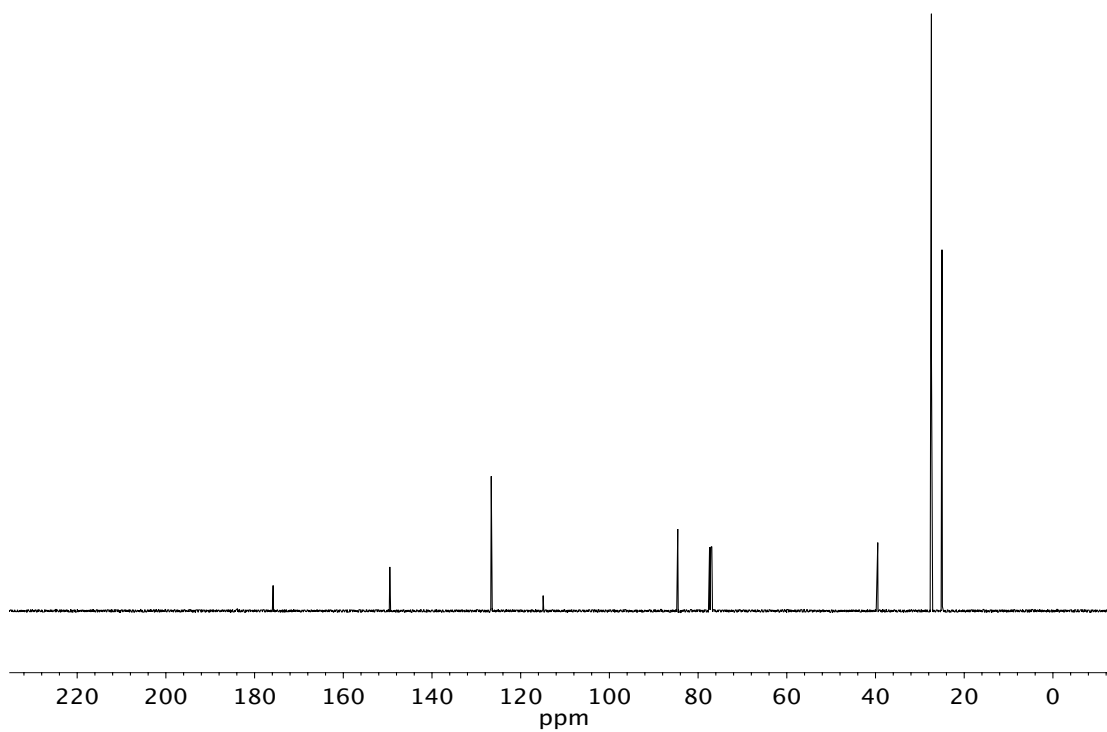


Figure A9.36 ¹³C NMR (125 MHz, CDCl₃) of compound **206**

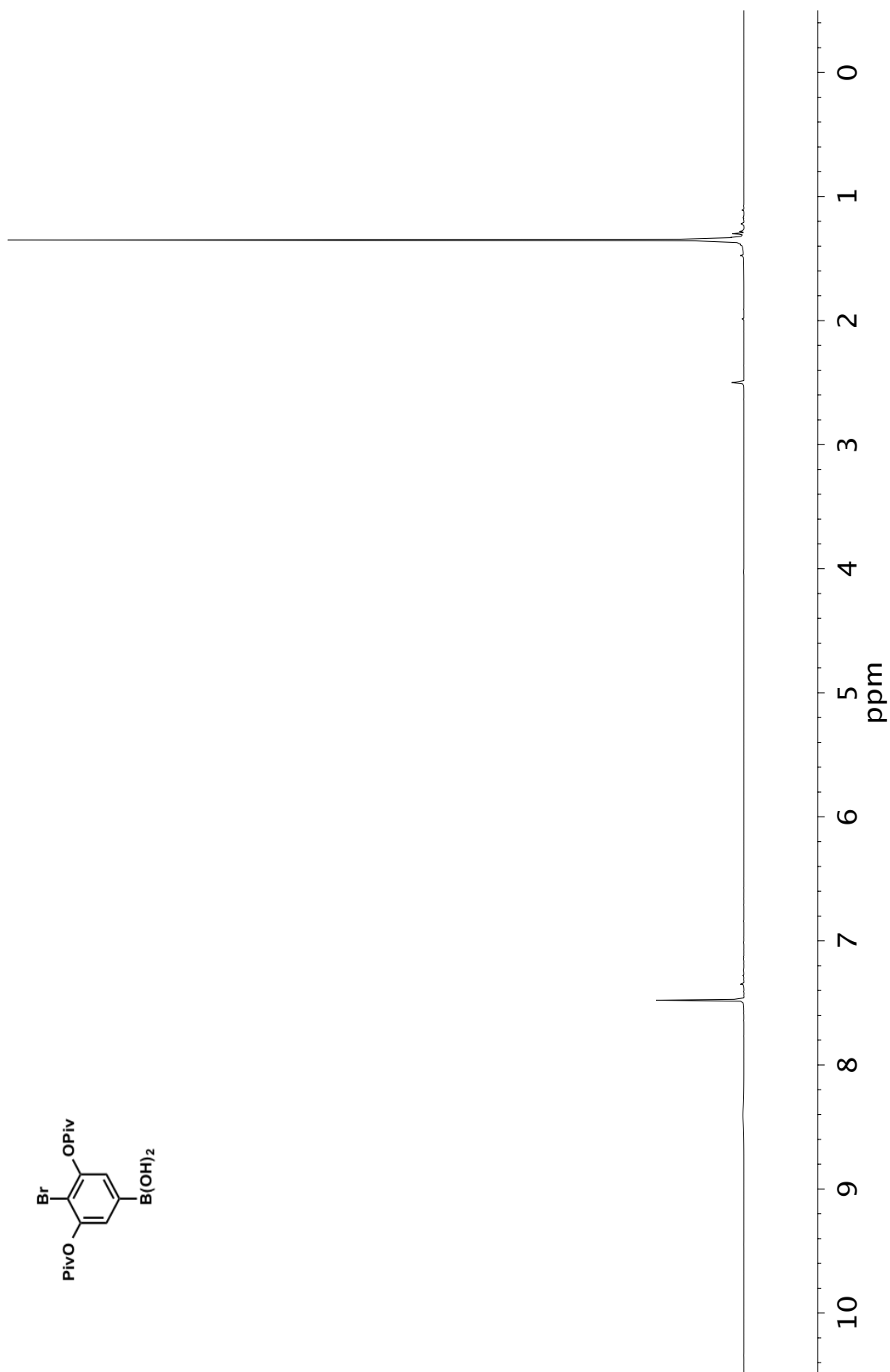


Figure A9.37 ¹H NMR (500 MHz, CDCl₃) of compound **207**

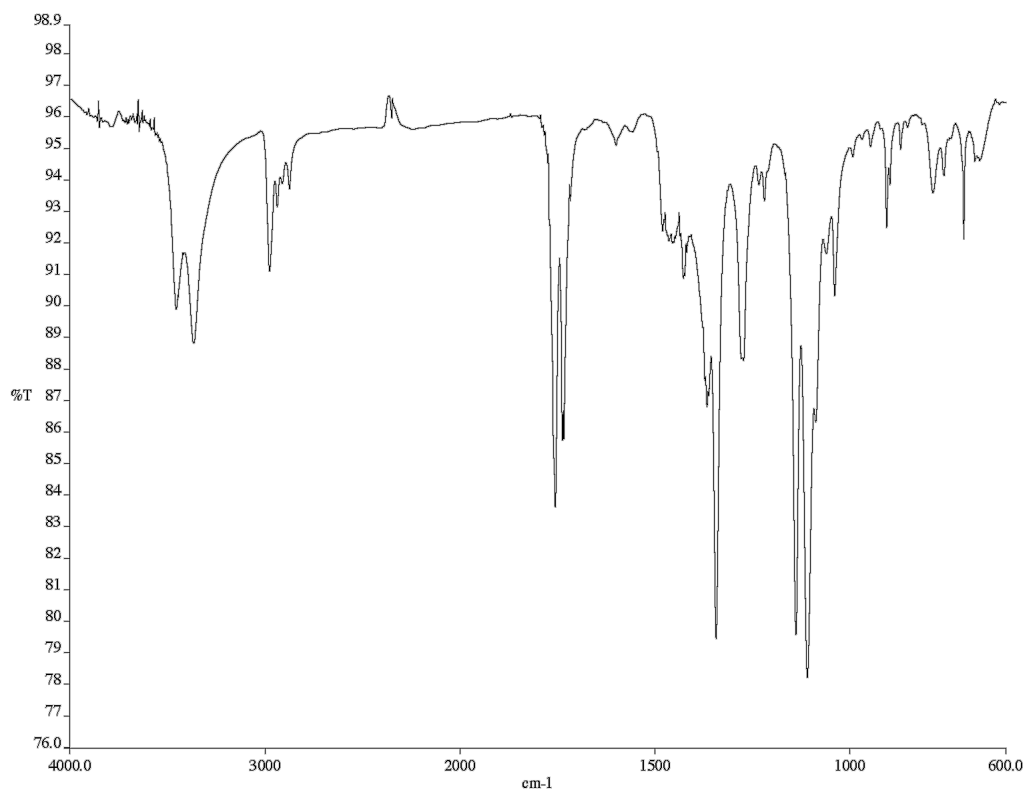


Figure A9.38 Infrared spectrum (Thin Film, NaCl) of compound **207**

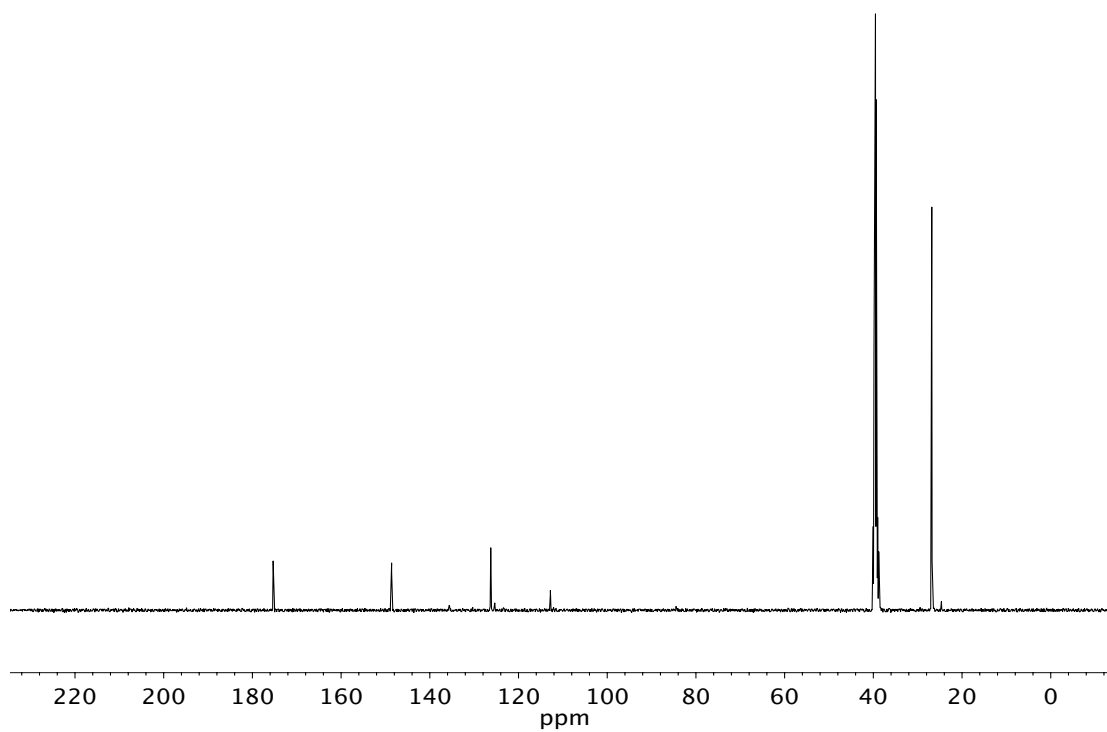


Figure A9.39 ¹³C NMR (125 MHz, CDCl₃) of compound **207**

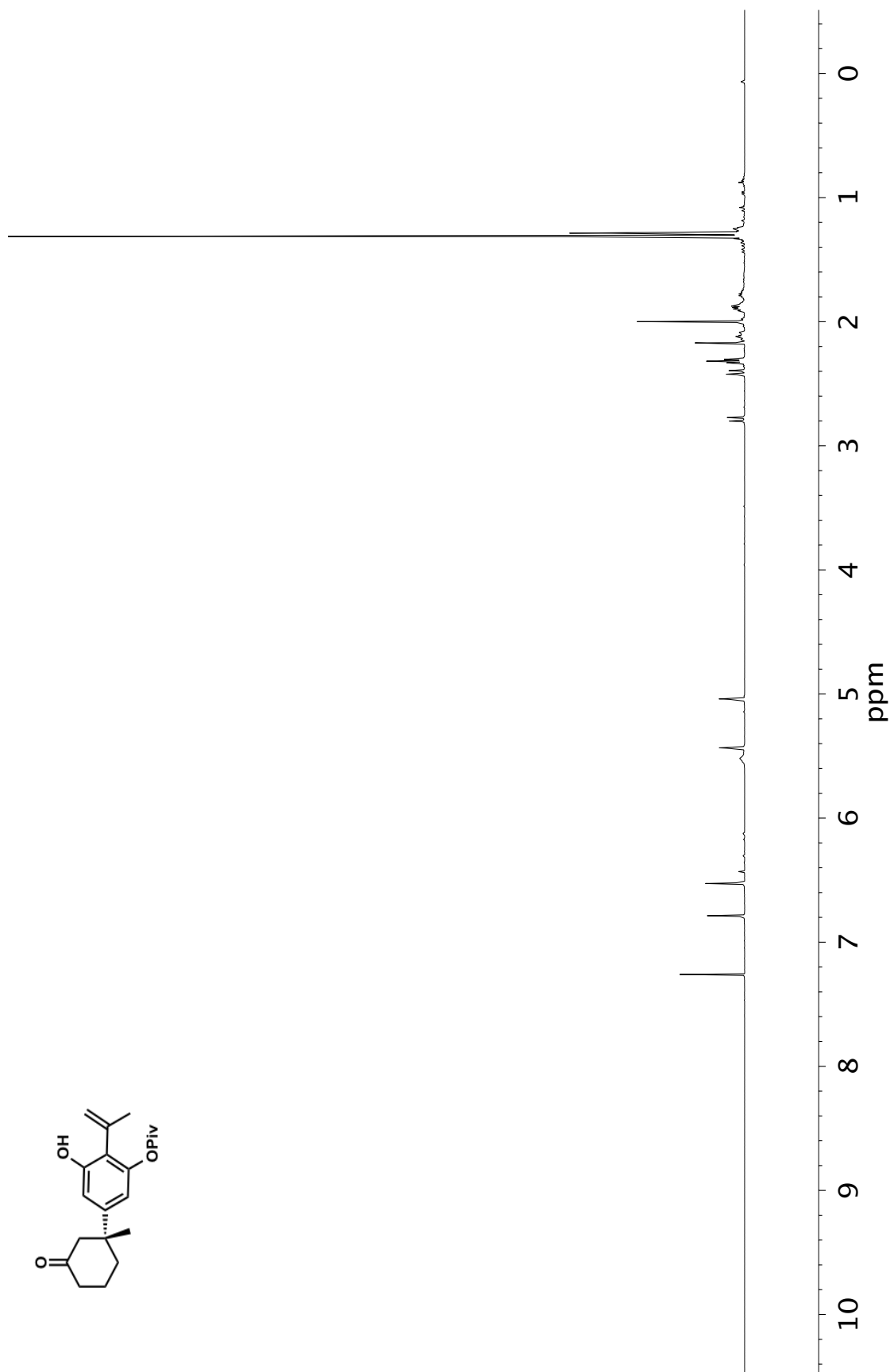


Figure A9.40 ¹H NMR (500 MHz, CDCl₃) of compound 208

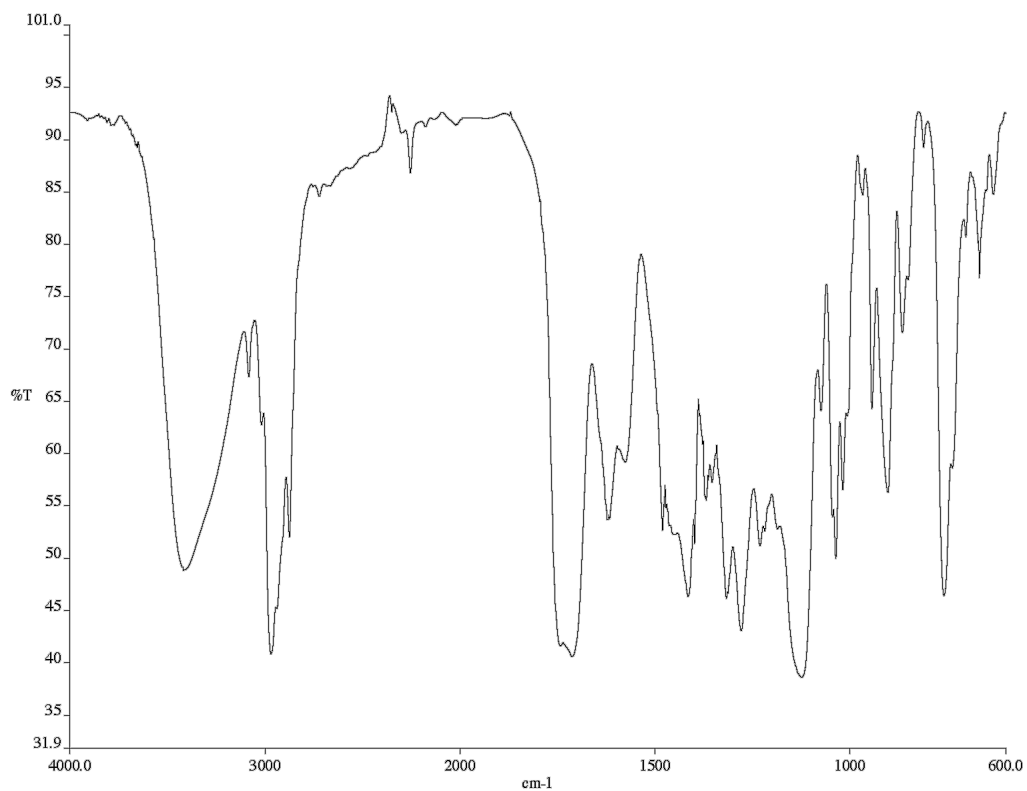


Figure A9.41 Infrared spectrum (Thin Film, NaCl) of compound **208**

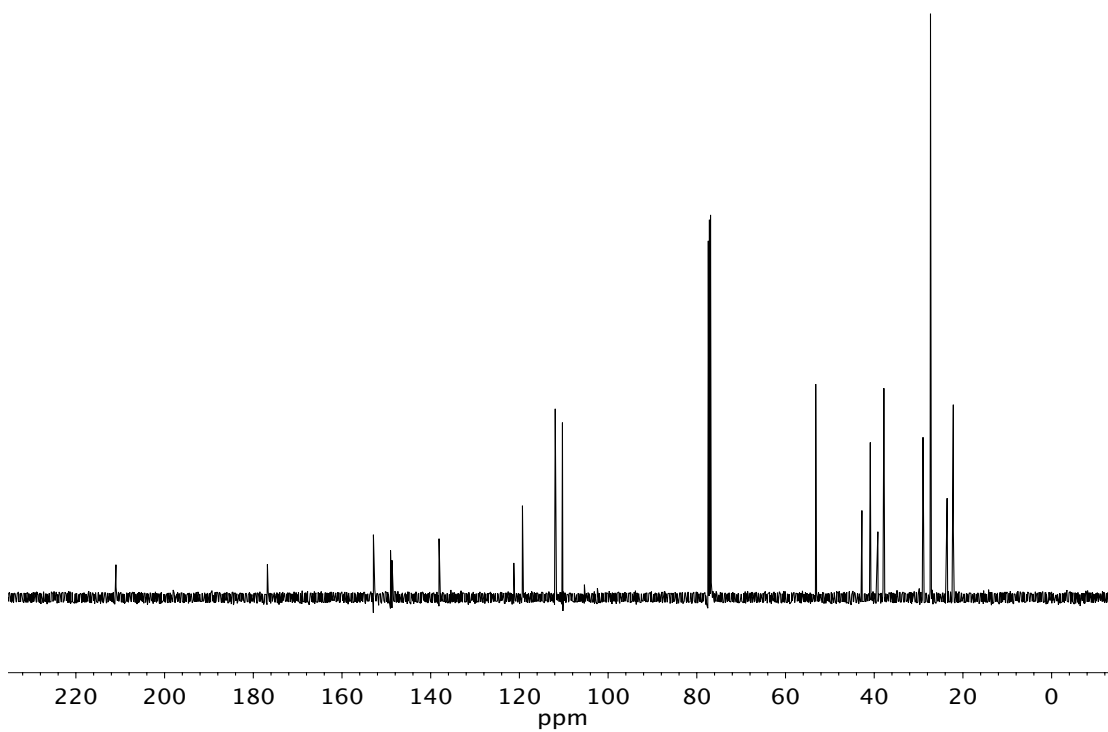


Figure A9.42 ¹³C NMR (125 MHz, CDCl₃) of compound **208**

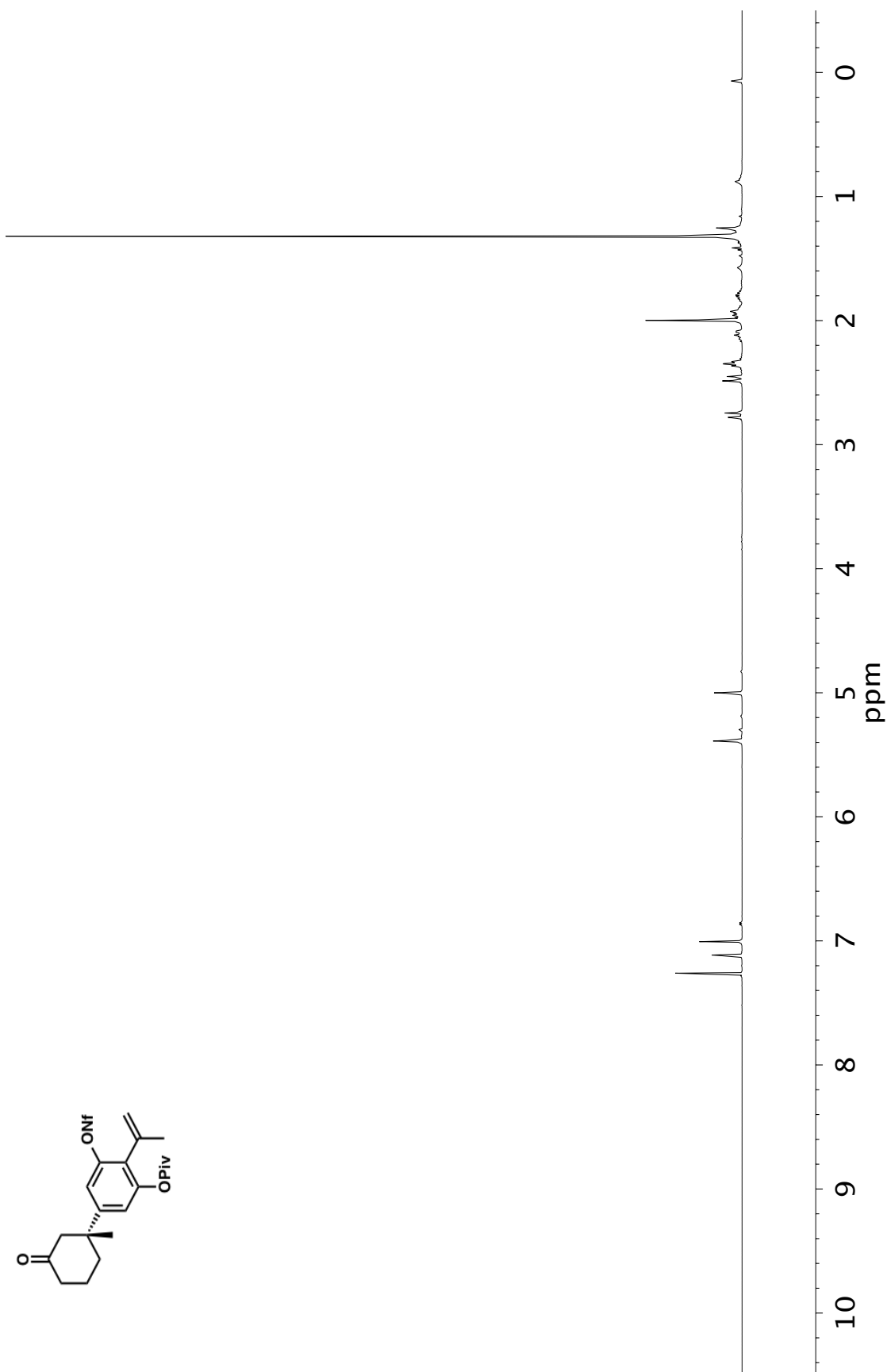


Figure A9.43 ¹H NMR (500 MHz, CDCl₃) of compound 209

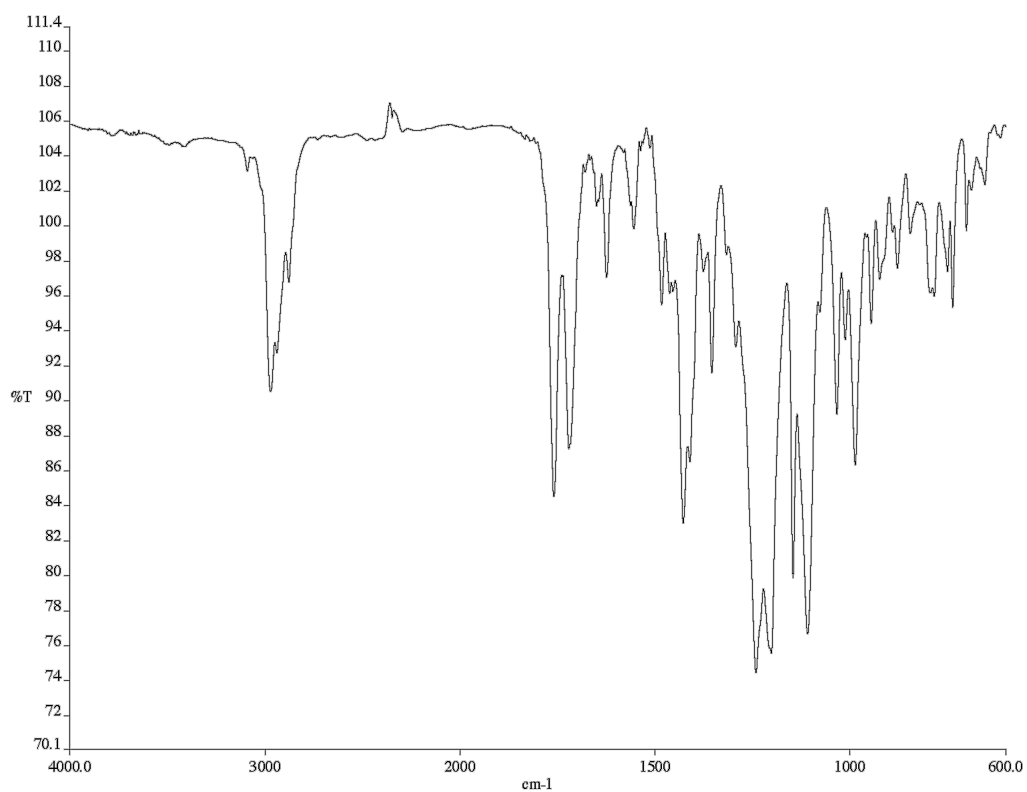


Figure A9.44 Infrared spectrum (Thin Film, NaCl) of compound **209**

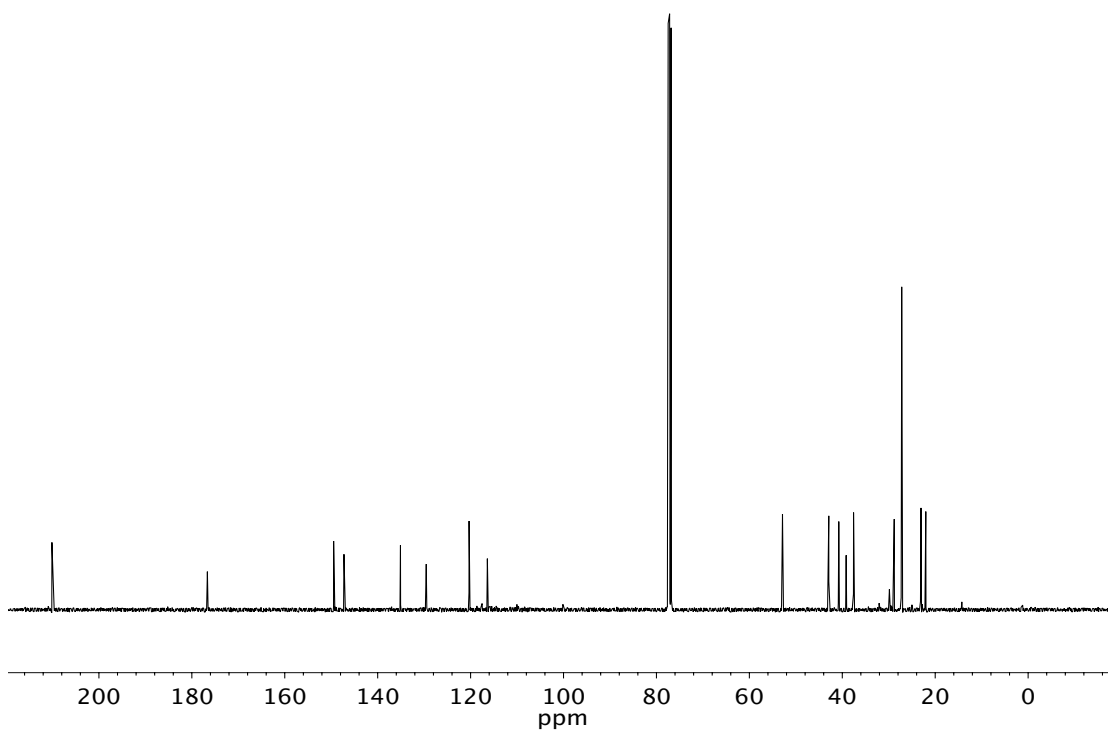


Figure A9.45 ¹³C NMR (125 MHz, CDCl₃) of compound **209**

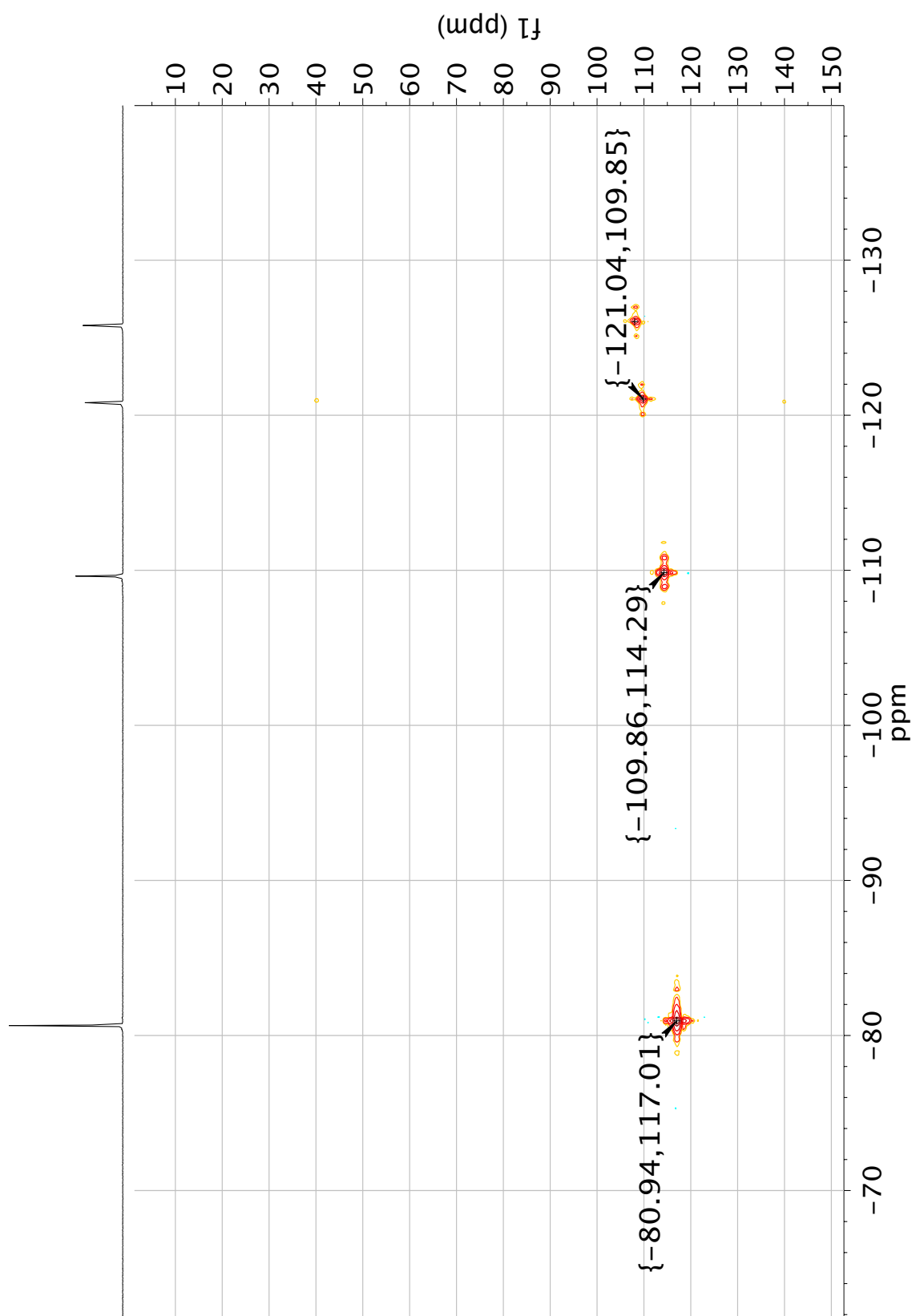
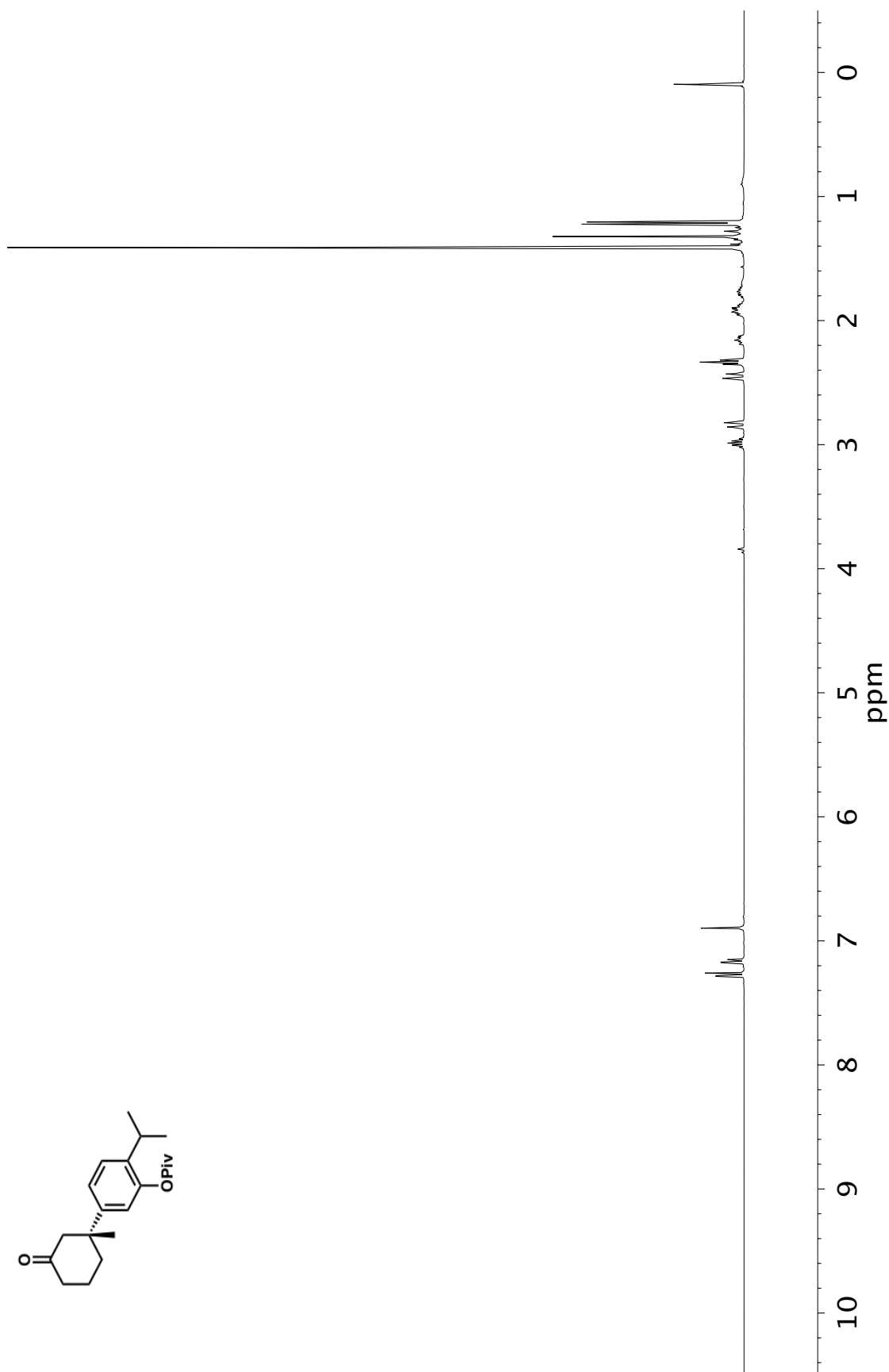


Figure A9.46 ^{19}F vs ^{13}C HSQC NMR (376 MHz, CDCl_3) of compound **209**



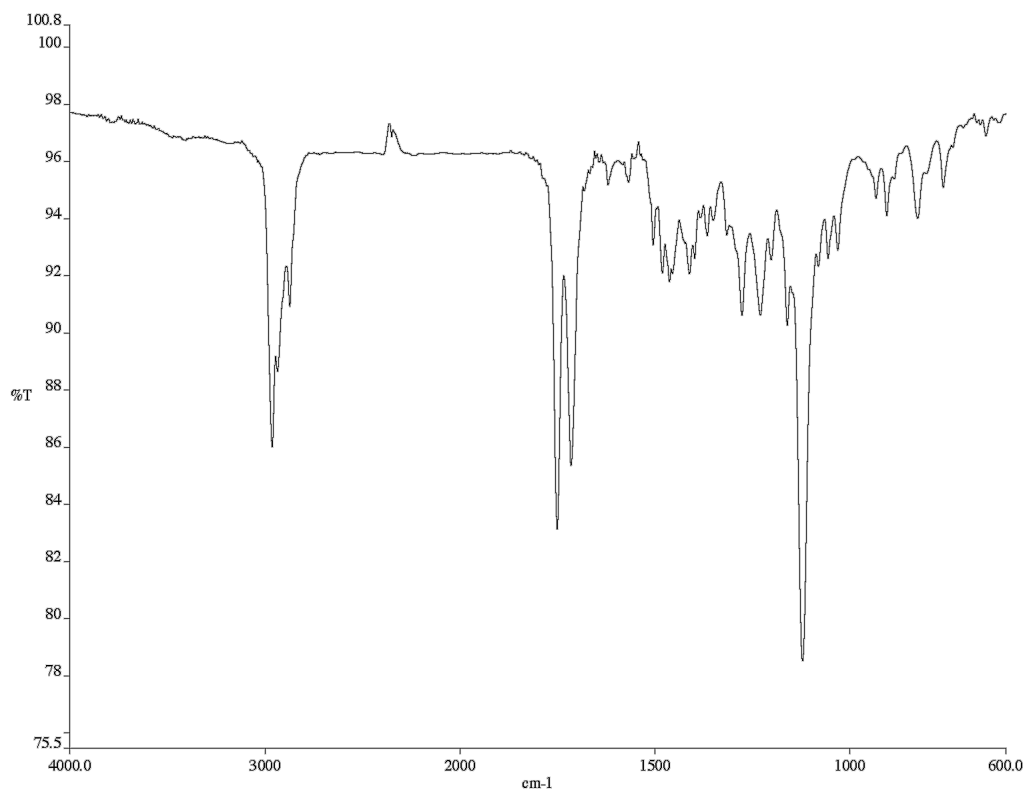


Figure A9.48 Infrared spectrum (Thin Film, NaCl) of compound **210**

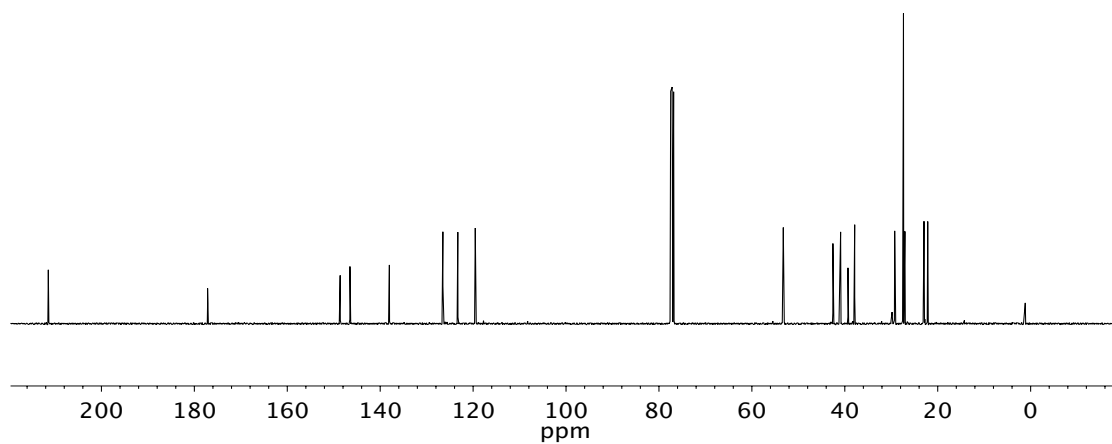


Figure A9.49 ¹³C NMR (125 MHz, CDCl₃) of compound **210**

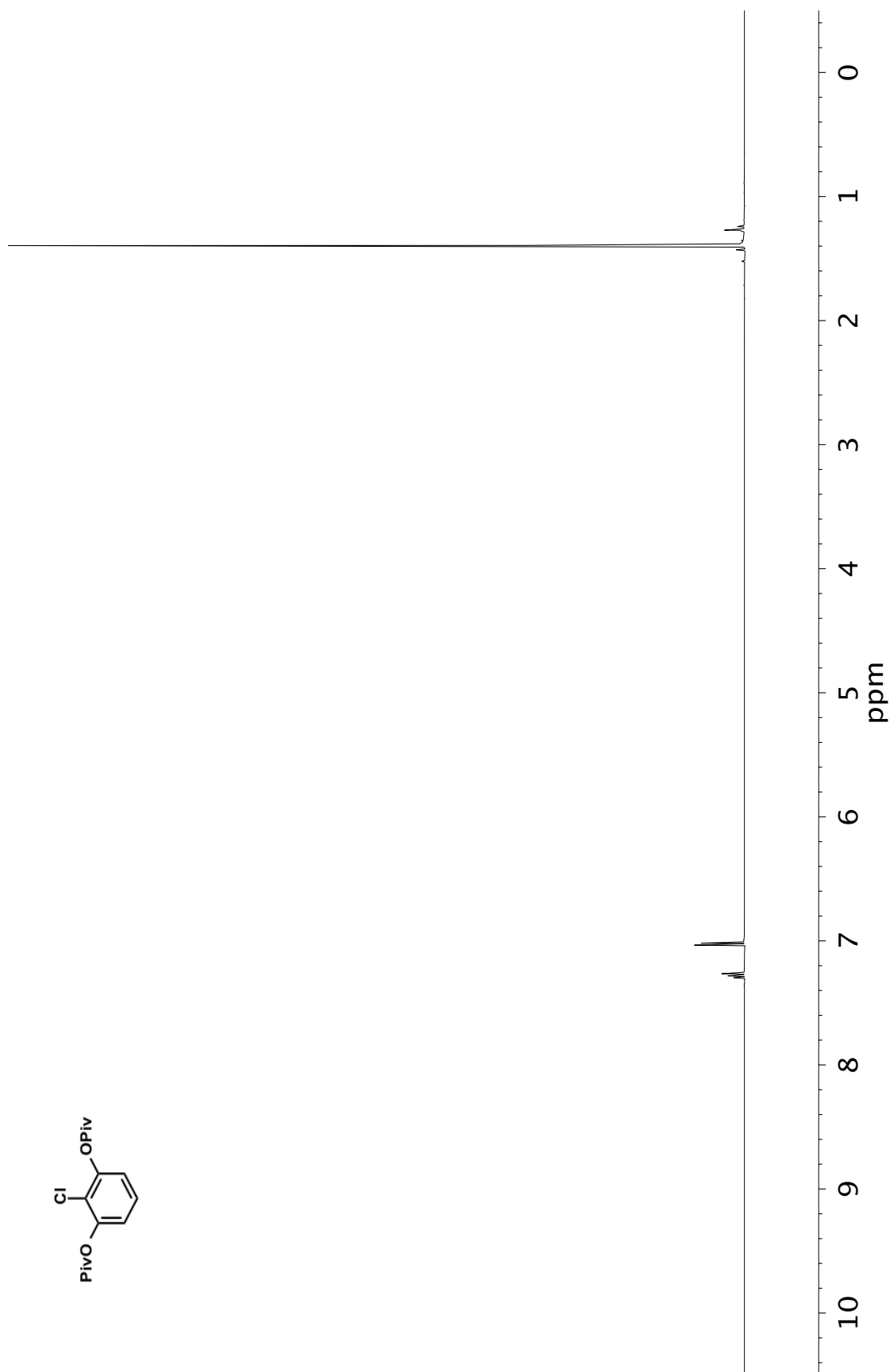


Figure A9.50 ^1H NMR (500 MHz, CDCl_3) of compound **211**

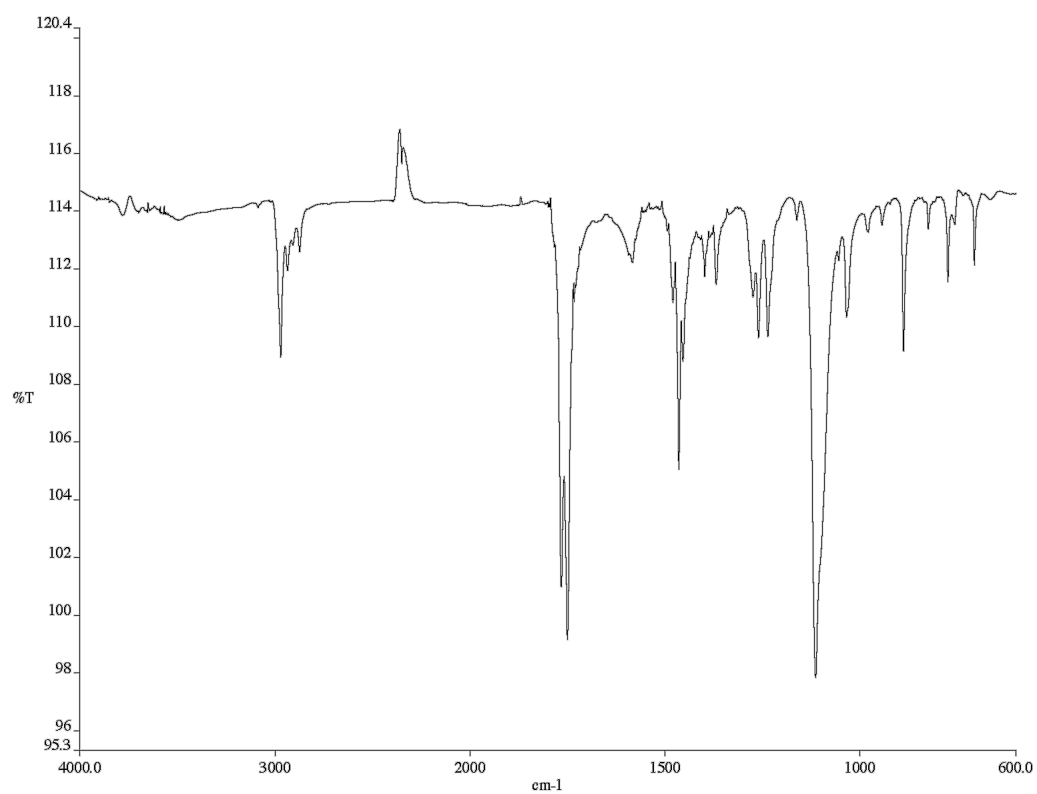


Figure A9.51 Infrared spectrum (Thin Film, NaCl) of compound **211**

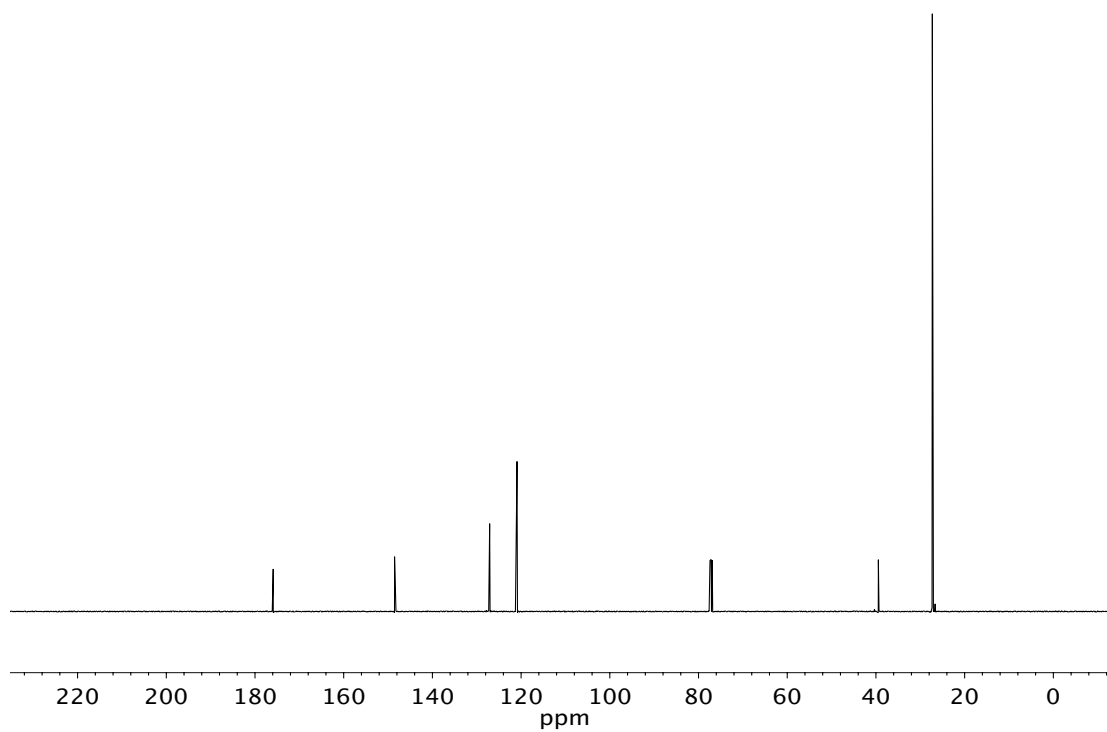


Figure A9.52 ¹³C NMR (125 MHz, CDCl₃) of compound **211**

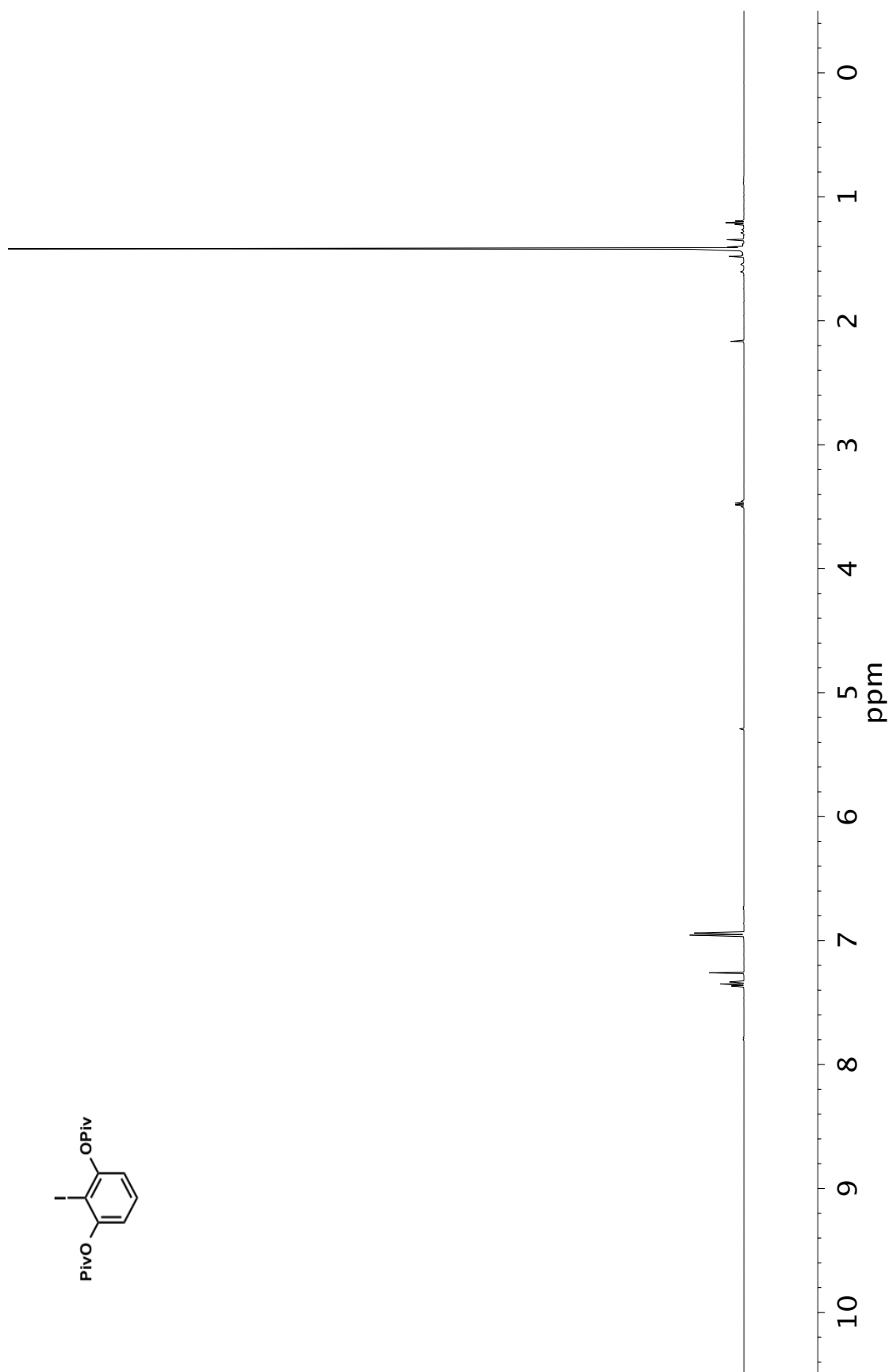


Figure A9.53 ¹H NMR (500 MHz, CDCl₃) of compound **212**

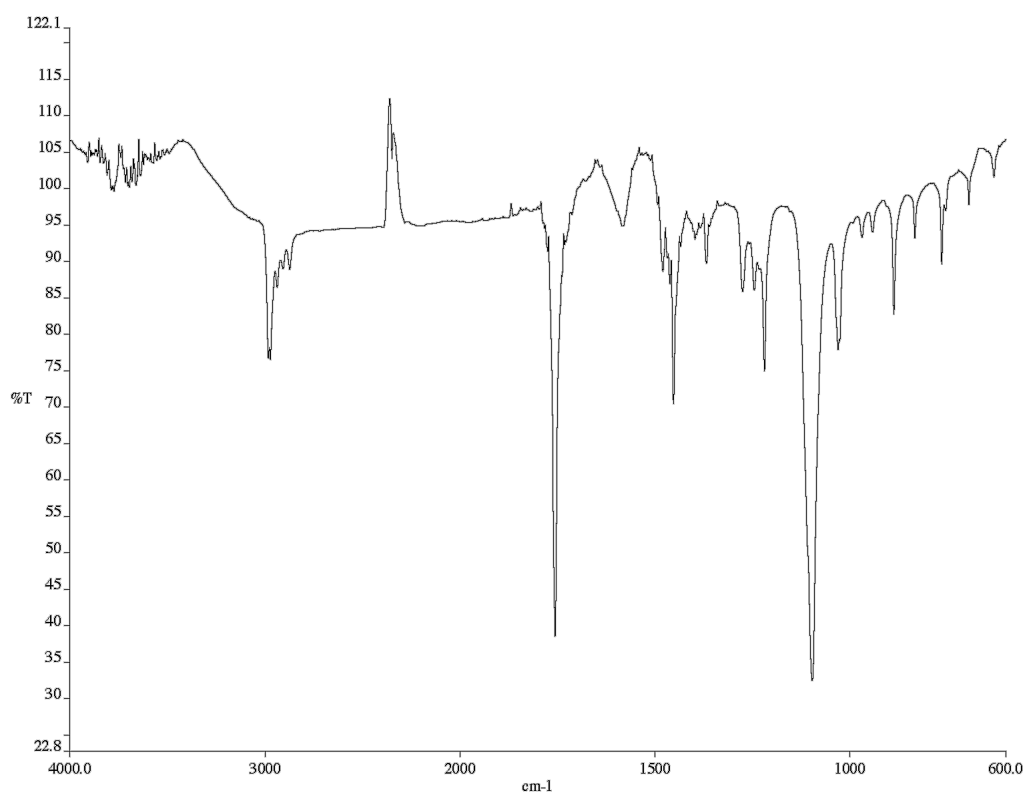


Figure A9.54 Infrared spectrum (Thin Film, NaCl) of compound **212**

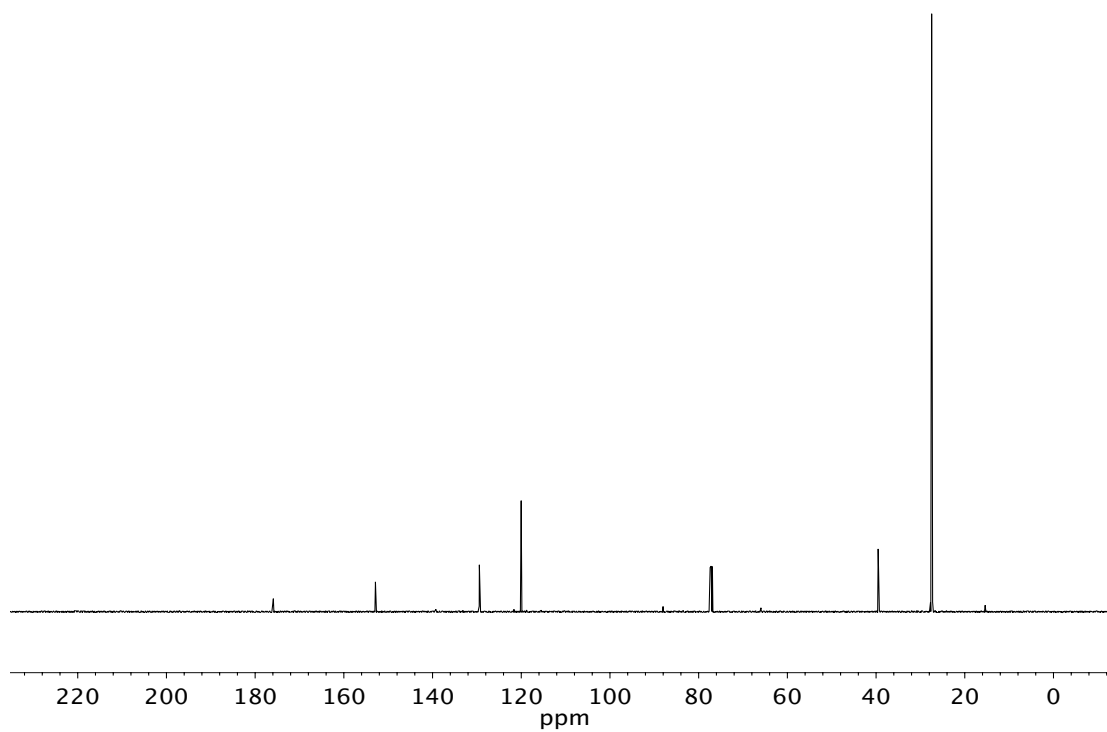


Figure A9.55 ¹³C NMR (125 MHz, CDCl₃) of compound **212**

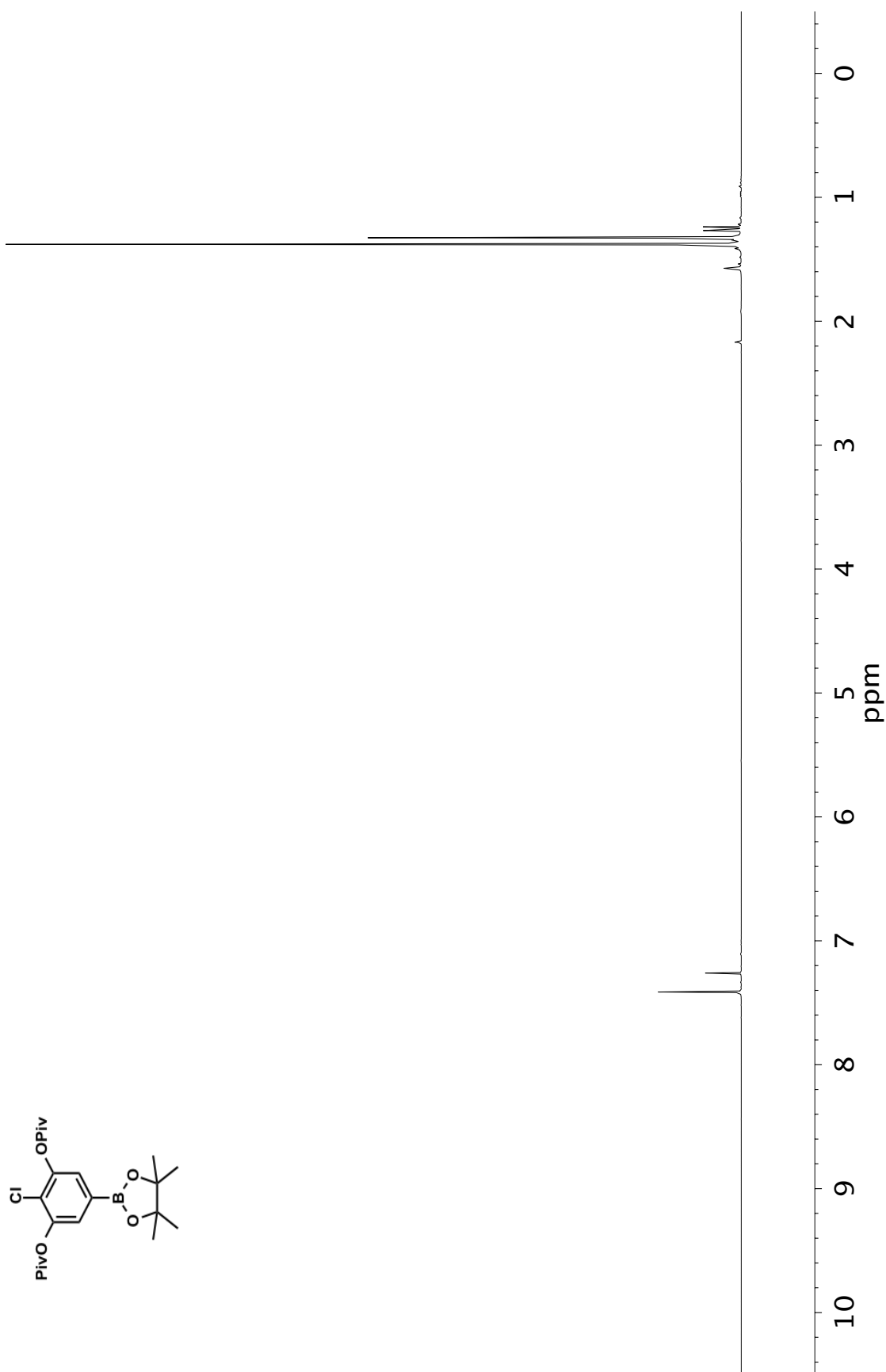


Figure A9.56 ^1H NMR (500 MHz, CDCl_3) of compound **213**

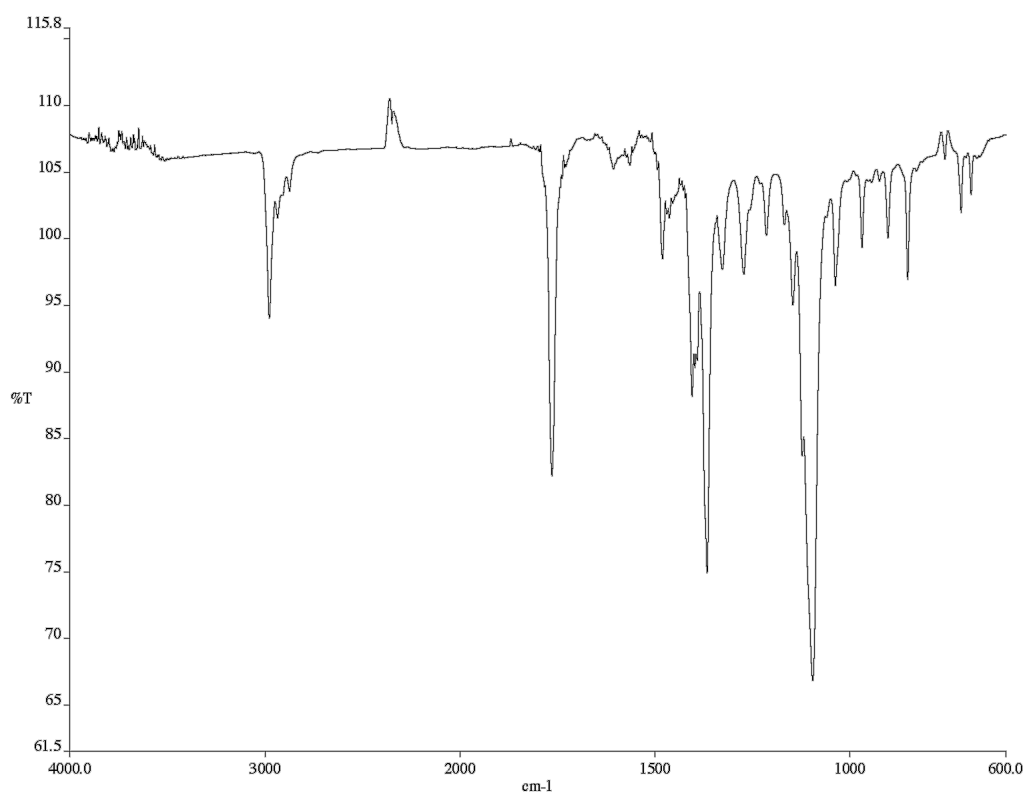


Figure A9.57 Infrared spectrum (Thin Film, NaCl) of compound **213**

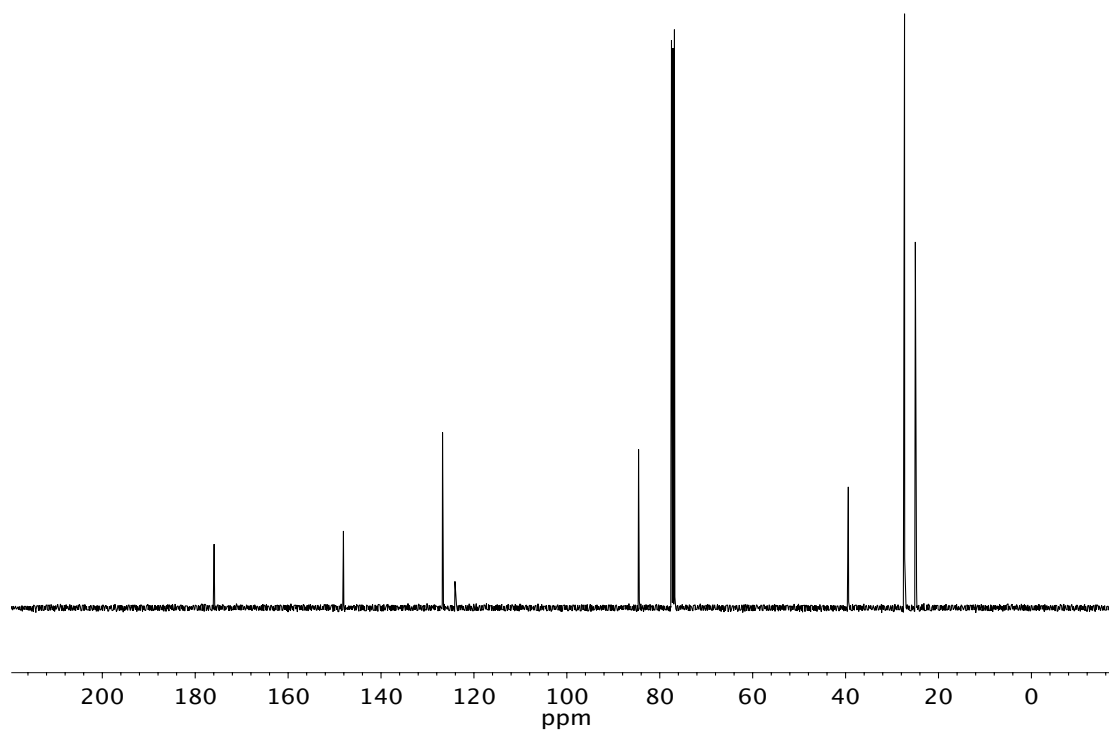


Figure A9.58 ¹³C NMR (125 MHz, CDCl₃) of compound **213**

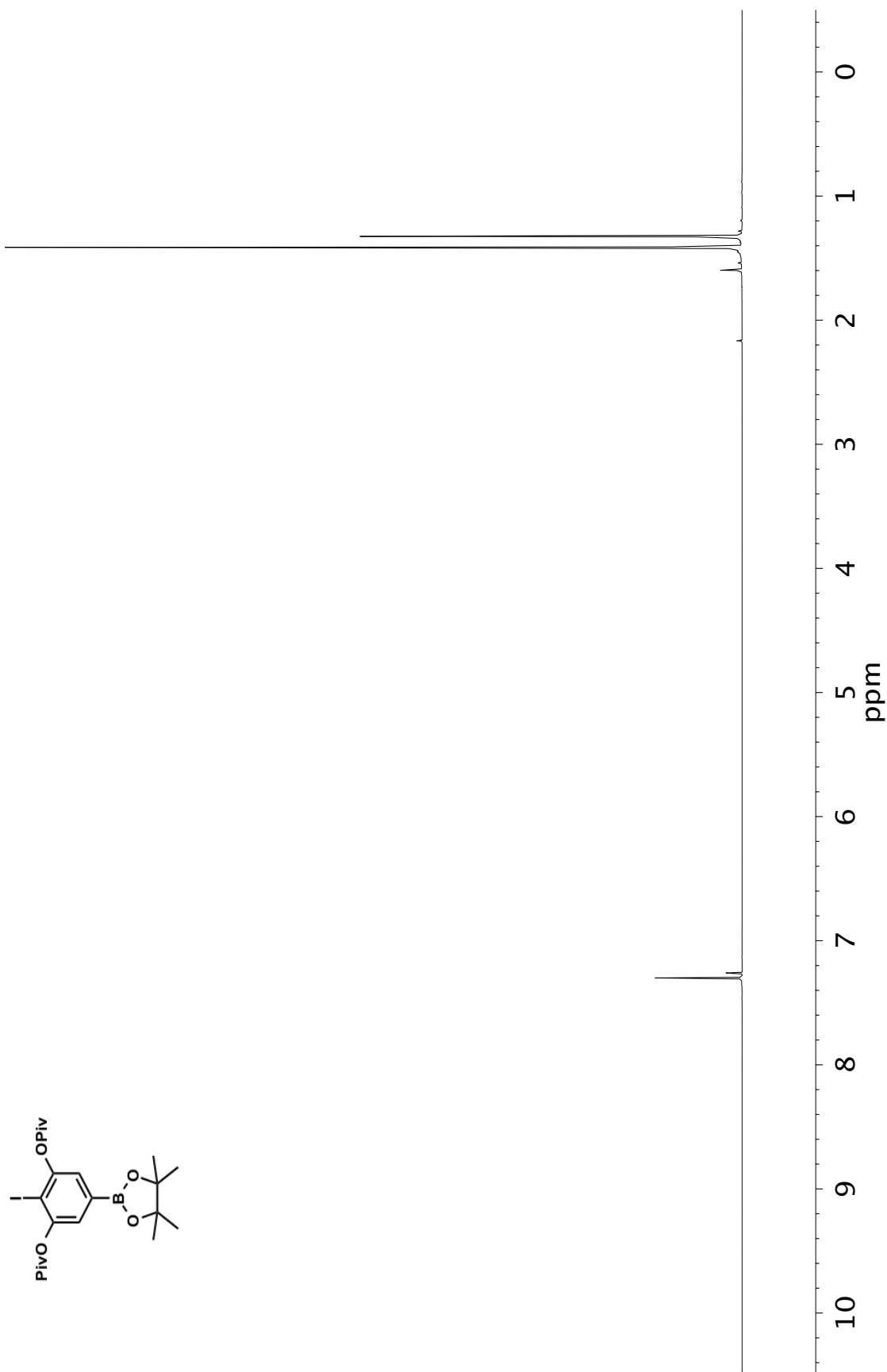


Figure A9.59 ^1H NMR (500 MHz, CDCl_3) of compound **214**

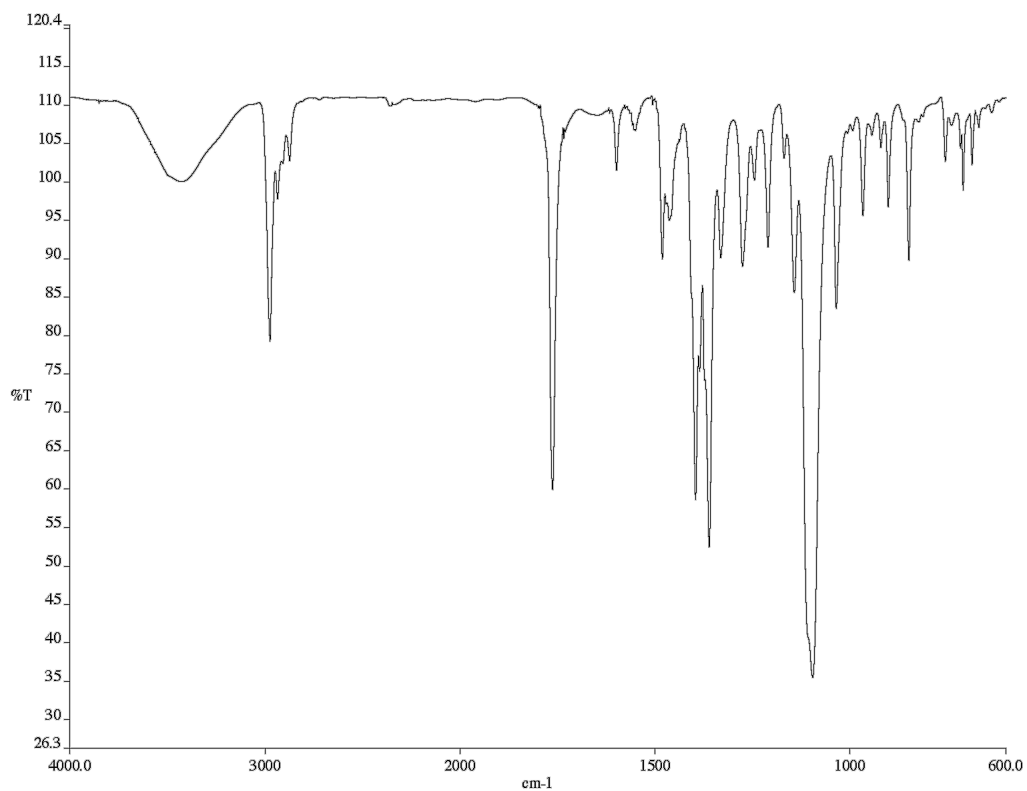


Figure A9.60 Infrared spectrum (Thin Film, NaCl) of compound **214**

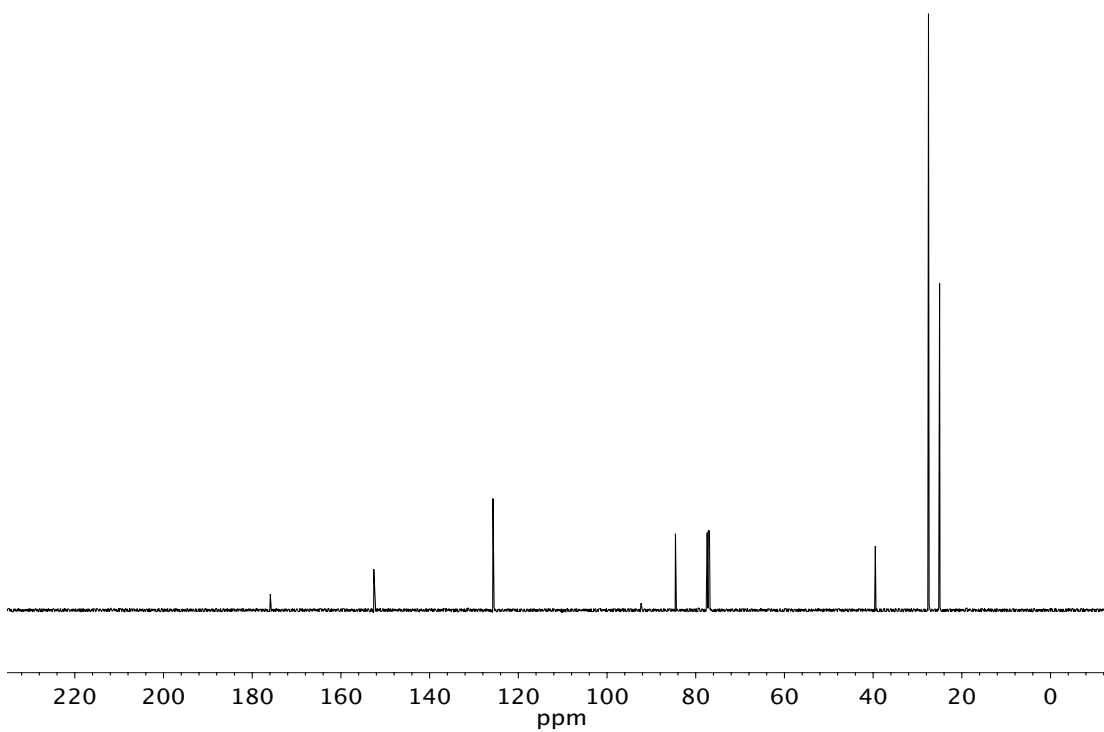
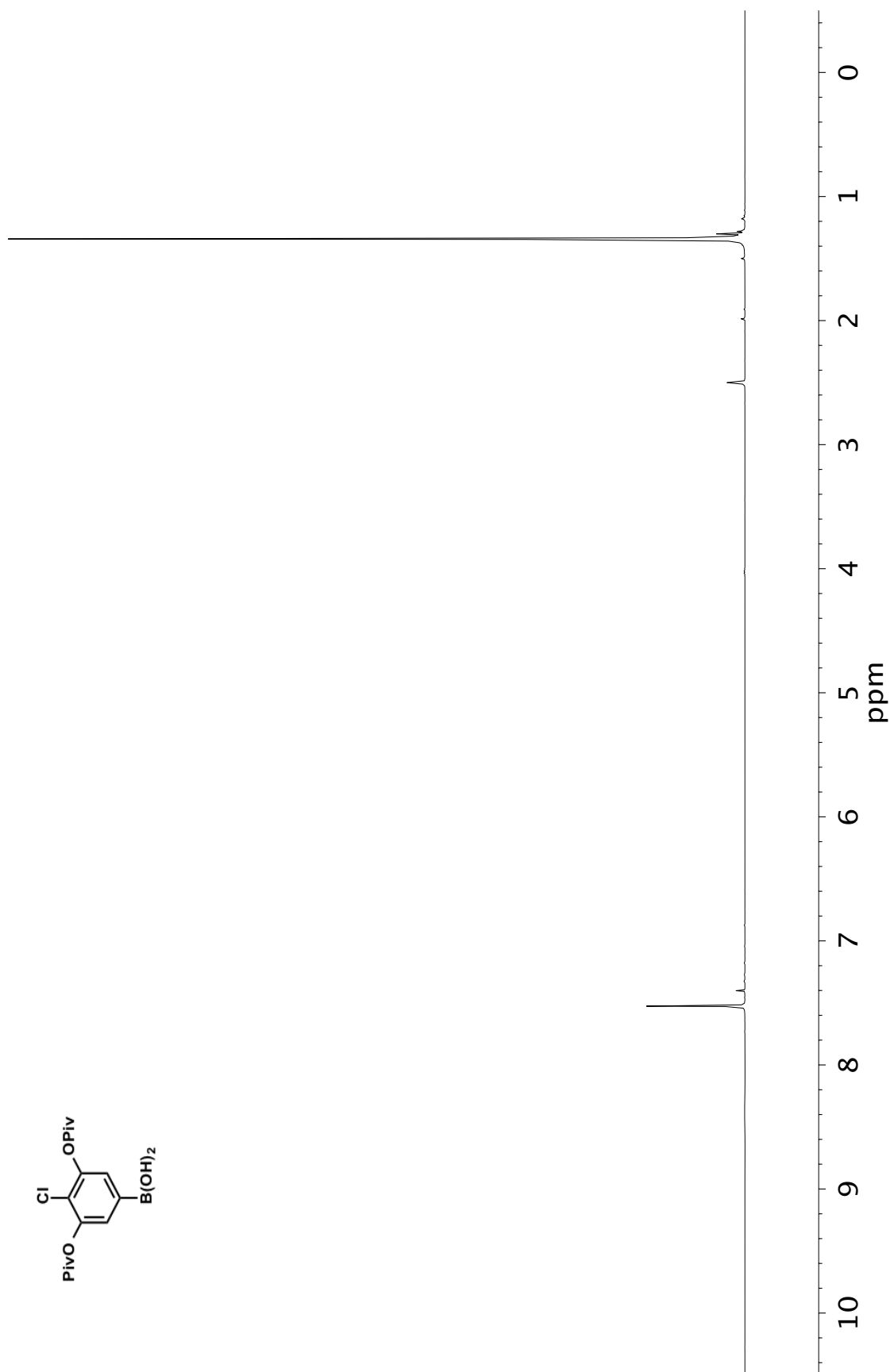


Figure A9.61 ¹³C NMR (125 MHz, CDCl₃) of compound **214**

Figure A9.62 ¹H NMR (500 MHz, CDCl₃) of compound 215

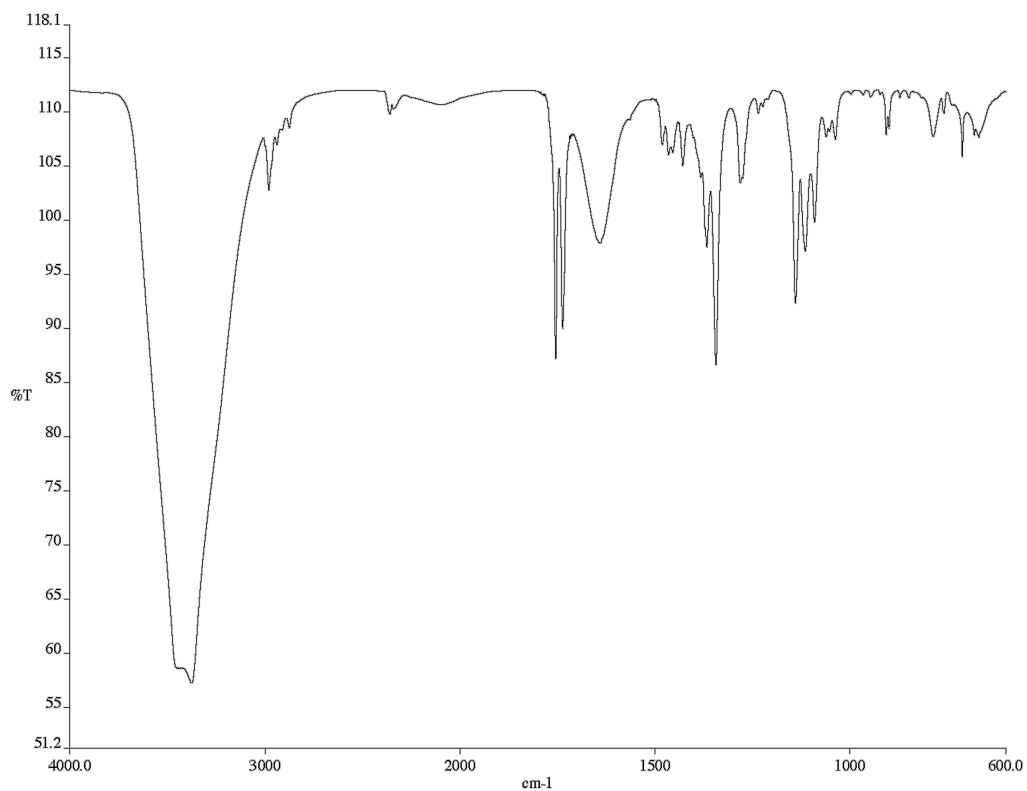


Figure A9.63 Infrared spectrum (Thin Film, NaCl) of compound **215**

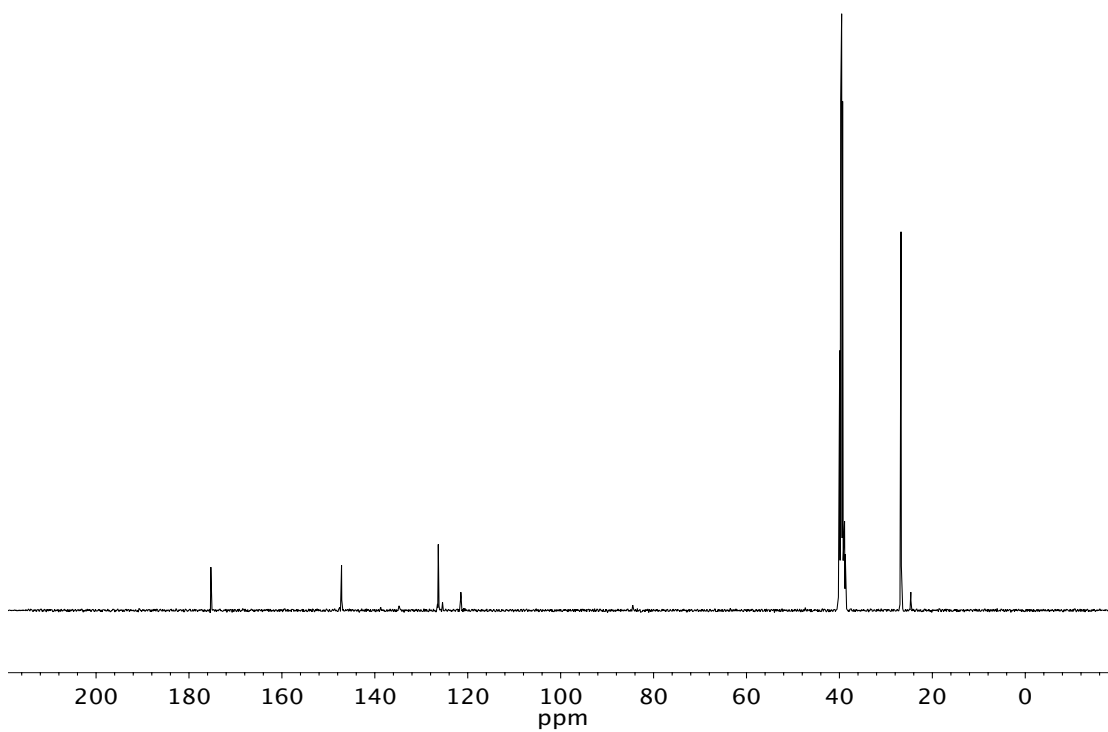
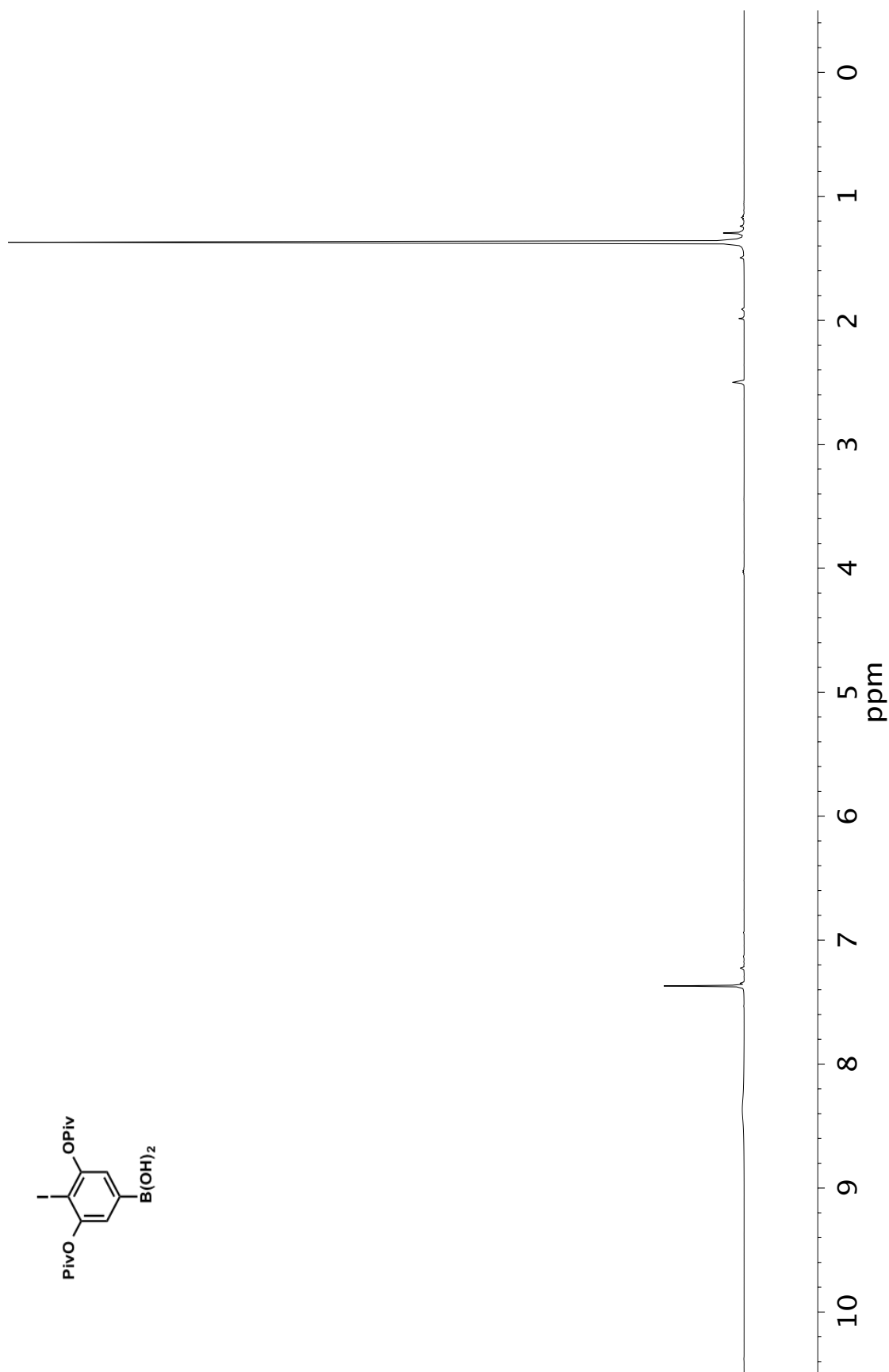


Figure A9.64 ¹³C NMR (125 MHz, CDCl₃) of compound **215**

Figure A9.65 ^1H NMR (500 MHz, CDCl_3) of compound **216**

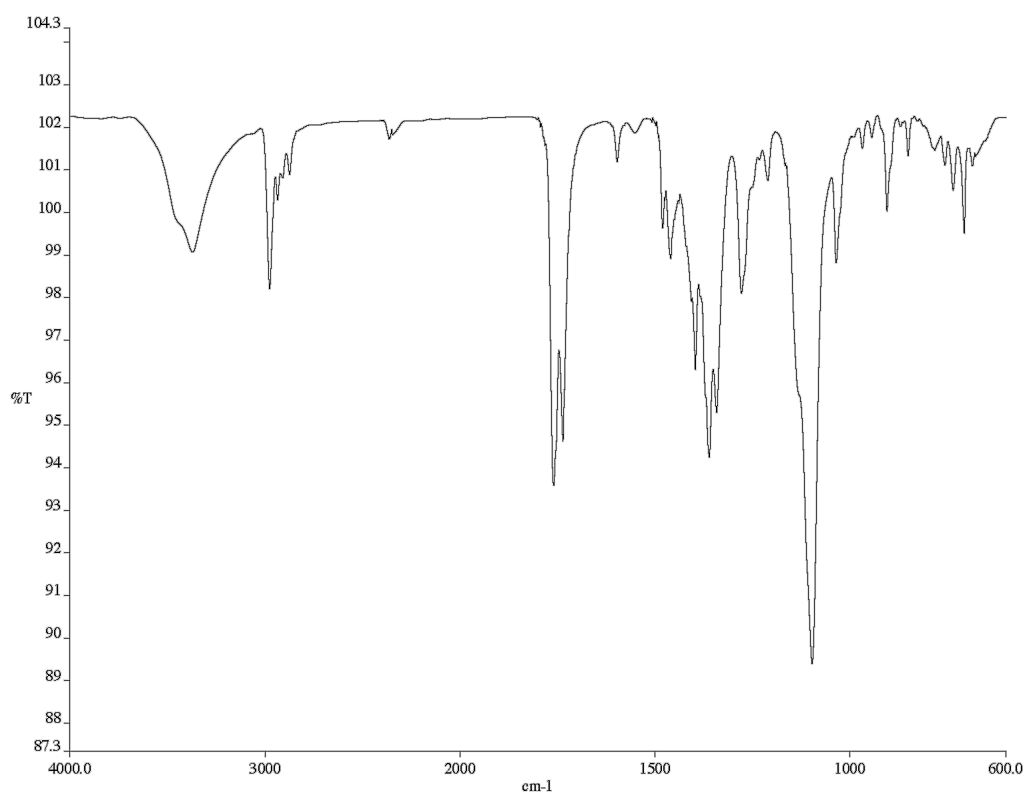


Figure A9.66 Infrared spectrum (Thin Film, NaCl) of compound **216**

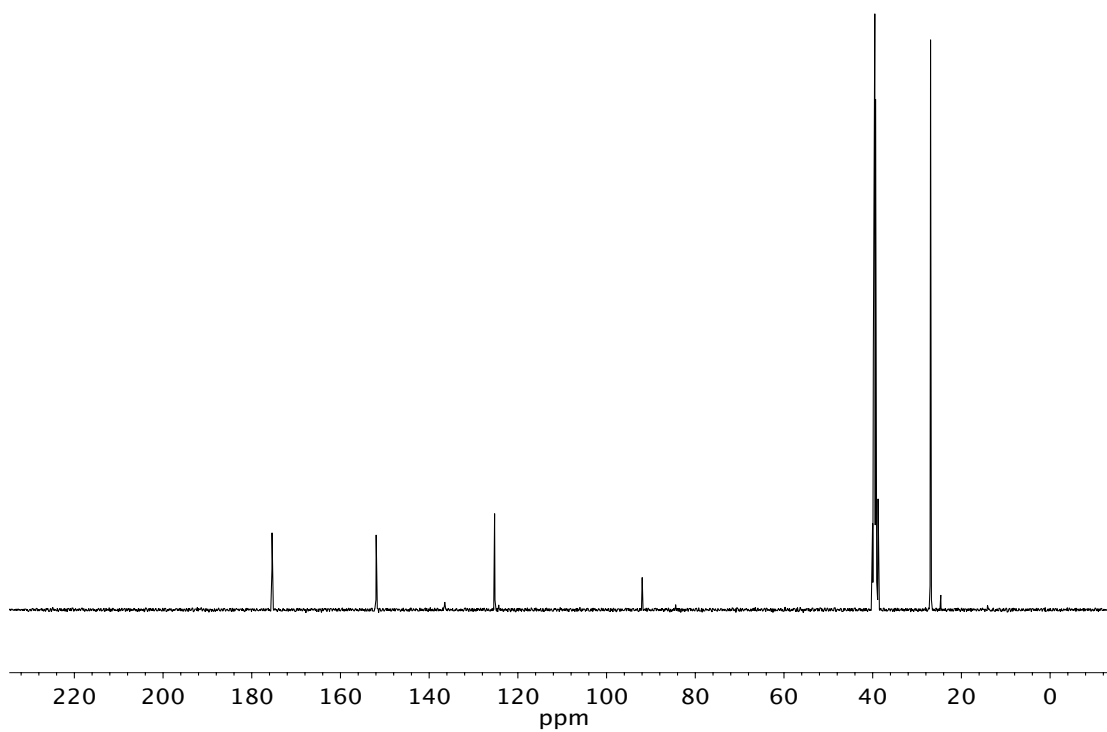


Figure A9.67 ¹³C NMR (125 MHz, CDCl₃) of compound **216**

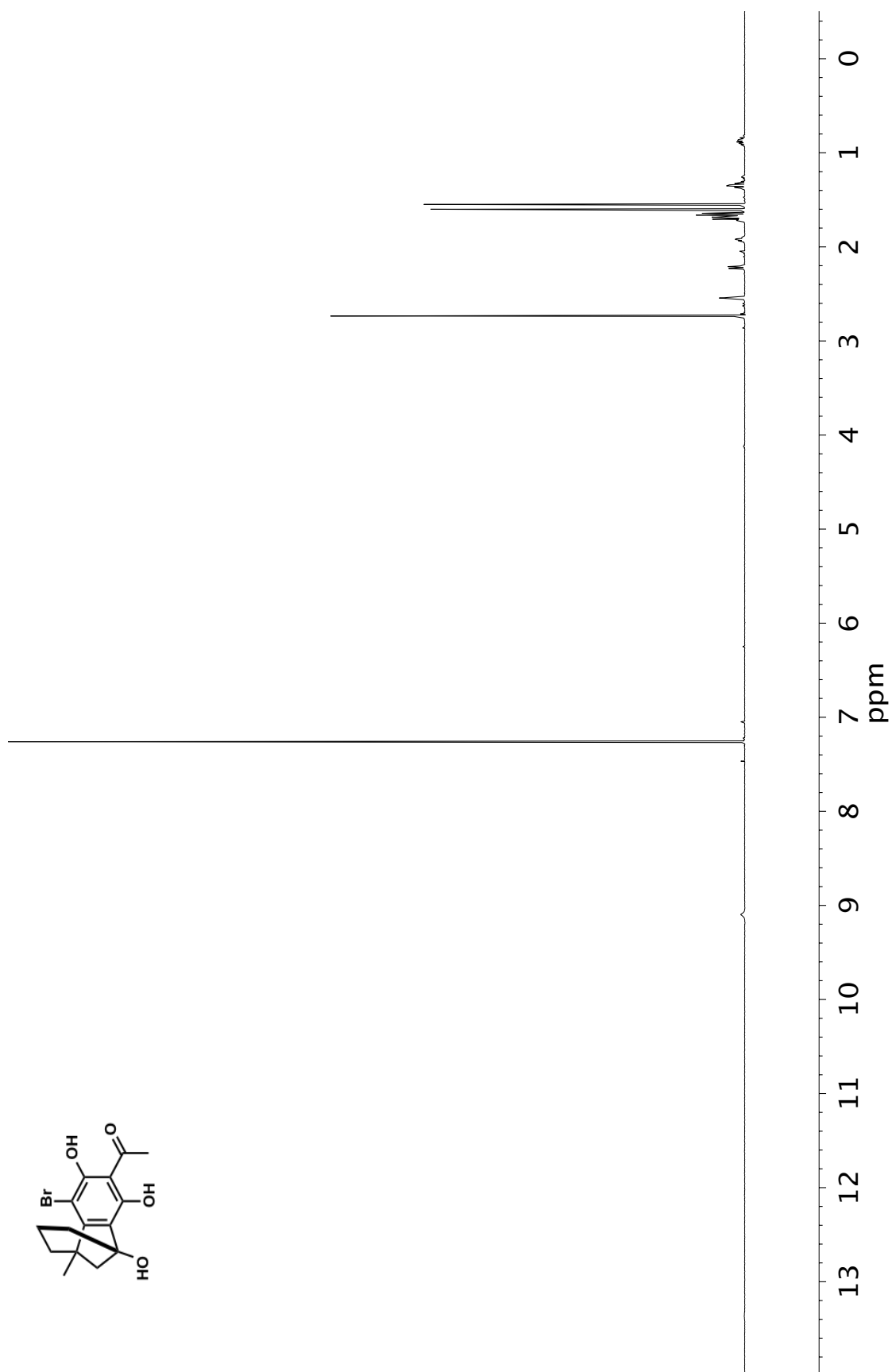


Figure A9.68 ^1H NMR (500 MHz, CDCl_3) of compound **217**

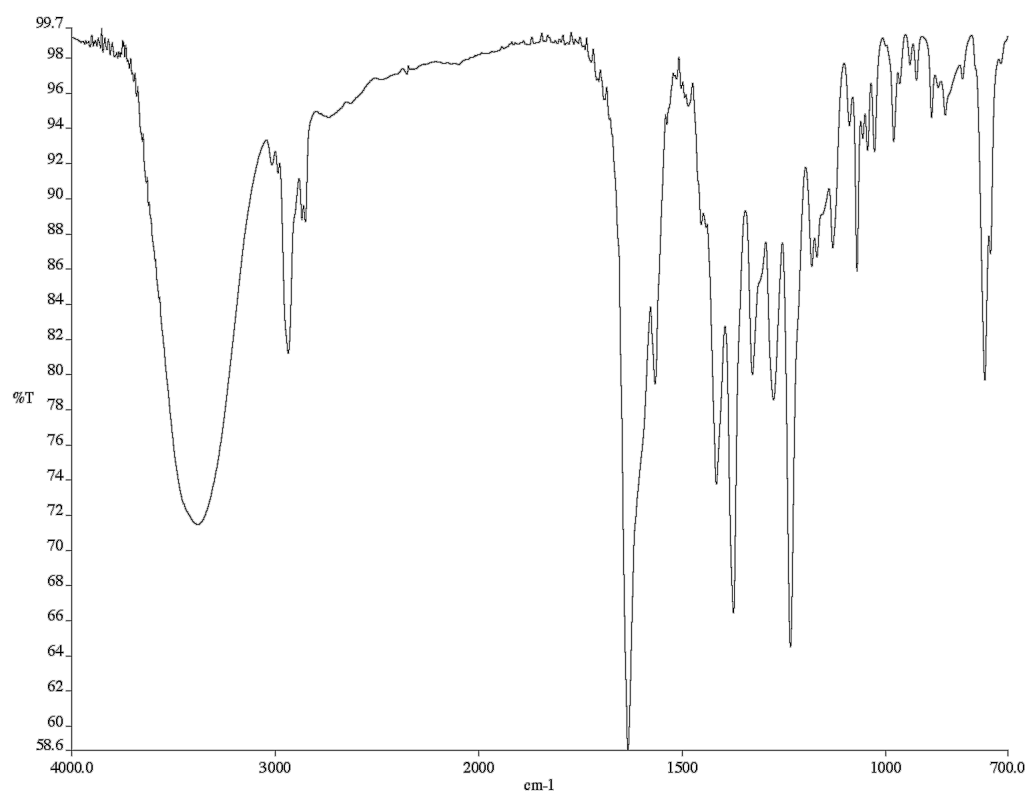


Figure A9.69 Infrared spectrum (Thin Film, NaCl) of compound **217**

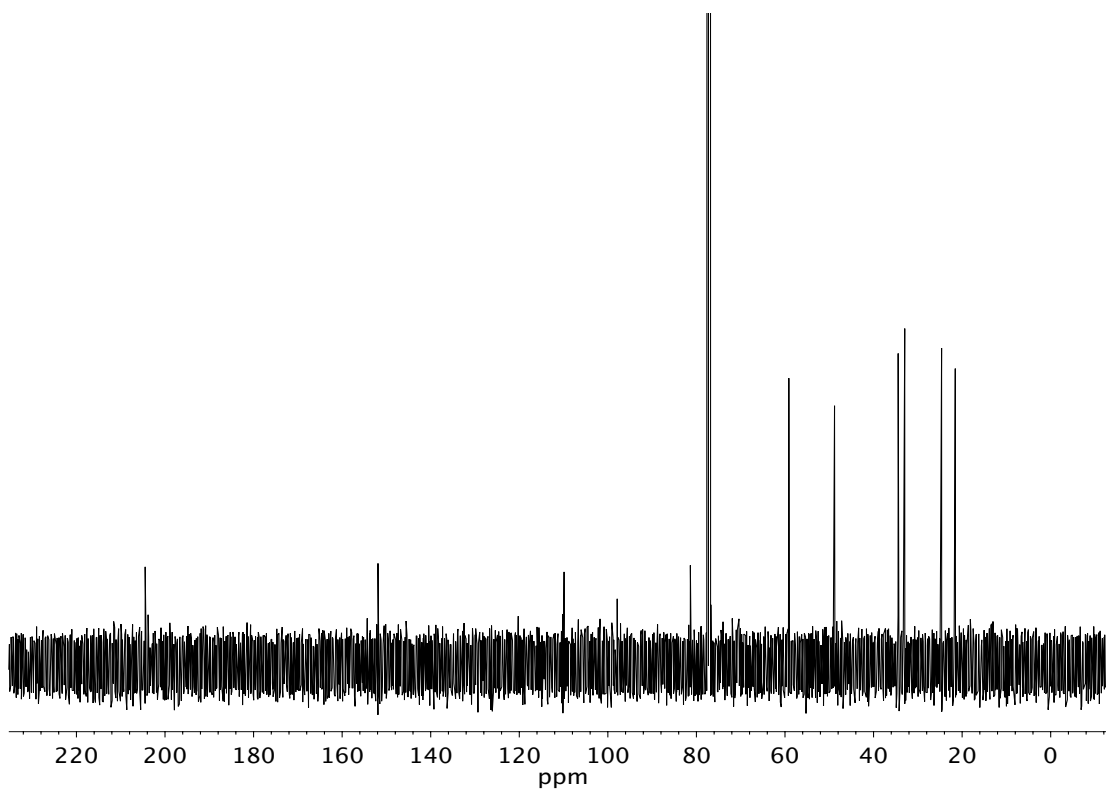


Figure A9.70 ¹³C NMR (125 MHz, CDCl₃) of compound **217**

APPENDIX 10

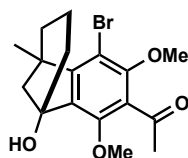
X-Ray Crystallography Reports Relevant to Appendix 8:

*A Catalytic, Enantioselective Formal Synthesis of (+)-Dichroanone
and (+)-Taiwaniaquinone*

A10.1 GENERAL EXPERIMENTAL

X-ray crystallographic analysis was obtained from the Caltech X-Ray Crystallography Facility using a Bruker D8 Venture Kappa Duo Photon 100 CMOS diffractometer.

A10.1.1 X-RAY CRYSTAL STRUCTURE ANALYSIS OF UNDESIRED TRICYCLE 203



Undesired tricycle **203** was recrystallized by slow evaporation of CH₂Cl₂ and hexanes to provide crystals suitable for X-ray analysis.

Figure A10.1 X-ray crystal structure of undesired tricycle **203**

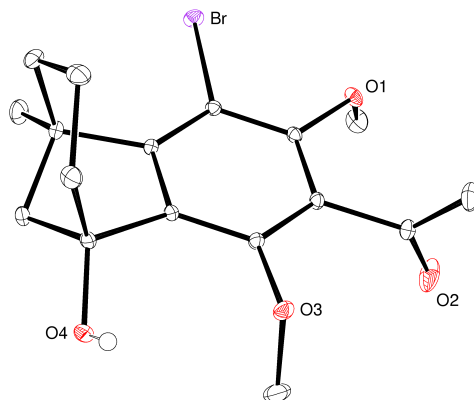


Table A10.1 Crystal data and structure refinement for undesired tricycle **203**

Empirical formula	C ₁₇ H ₂₃ Br O ₅
Formula weight	387.26
Temperature	100 K
Wavelength	0.71073 Å

Crystal system	Monoclinic
Space group	C 1 2 1
Unit cell dimensions	a = 18.8295(9) Å a = 90°. b = 7.8451(4) Å b = 95.208(2)°. c = 11.4443(5) Å g = 90°.
Volume	1683.56(14) Å ³
Z	4
Density (calculated)	1.528 Mg/m ³
Absorption coefficient	2.464 mm ⁻¹
F(000)	800
Crystal size	0.43 x 0.42 x 0.29 mm ³
Theta range for data collection	1.787 to 48.826°.
Index ranges	-39<=h<=39, -16<=k<=16, -22<=l<=24
Reflections collected	78240
Independent reflections	16574 [R(int) = 0.0370]
Completeness to theta = 25.000°	99.8 %
Absorption correction	Semi-empirical from equivalents
Max. and min. transmission	0.5777 and 0.4462
Refinement method	Full-matrix least-squares on F ²
Data / restraints / parameters	16574 / 1 / 299
Goodness-of-fit on F ²	0.966
Final R indices [I>2sigma(I)]	R1 = 0.0256, wR2 = 0.0521
R indices (all data)	R1 = 0.0344, wR2 = 0.0538
Absolute structure parameter	0.0289(17)
Extinction coefficient	n/a
Largest diff. peak and hole	0.653 and -0.707 e.Å ⁻³

Table A10.2 Atomic coordinates ($\times 10^4$) and equivalent isotropic displacement parameters ($\text{\AA}^2 \times 10^3$) for **203**. $U(\text{eq})$ is defined as one third of the trace of the orthogonalized U^{ij} tensor.

	x	y	z	U(eq)
Br(1)	2611(1)	10106(1)	9689(1)	15(1)
O(1)	3623(1)	7401(1)	8867(1)	14(1)
O(2)	3898(1)	5319(1)	6487(1)	32(1)
O(3)	2081(1)	4751(1)	5906(1)	15(1)
O(4)	746(1)	6695(1)	5256(1)	15(1)
C(1)	1792(1)	8548(1)	7722(1)	10(1)
C(2)	2444(1)	8611(1)	8398(1)	10(1)
C(3)	2985(1)	7448(1)	8188(1)	10(1)
C(4)	2858(1)	6206(1)	7328(1)	10(1)
C(5)	2190(1)	6066(1)	6697(1)	10(1)
C(6)	1663(1)	7235(1)	6896(1)	9(1)
C(7)	883(1)	7289(1)	6423(1)	11(1)
C(8)	433(1)	6312(1)	7261(1)	15(1)
C(9)	584(1)	6889(1)	8542(1)	17(1)
C(10)	655(1)	8831(1)	8680(1)	17(1)
C(11)	1110(1)	9610(1)	7757(1)	12(1)
C(12)	734(1)	9187(1)	6539(1)	13(1)
C(13)	4140(1)	8608(2)	8543(1)	21(1)
C(14)	3440(1)	4958(1)	7122(1)	14(1)
C(15)	3422(1)	3280(1)	7728(1)	21(1)
C(16)	2247(1)	5220(2)	4744(1)	23(1)
C(17)	1200(1)	11532(1)	7918(1)	21(1)
O(5)	4353(1)	8297(2)	5398(1)	43(1)

Table A10.3 Bond lengths [\AA] and angles [$^\circ$] for **203**

Br(1)-C(2)	1.8906(8)
O(1)-C(3)	1.3713(9)
O(1)-C(13)	1.4310(12)
O(2)-C(14)	1.2111(12)
O(3)-C(5)	1.3751(10)
O(3)-C(16)	1.4412(14)
O(4)-H(4A)	0.70(4)
O(4)-C(7)	1.4158(11)
C(1)-C(2)	1.3921(11)
C(1)-C(6)	1.4044(11)
C(1)-C(11)	1.5333(11)
C(2)-C(3)	1.4041(11)
C(3)-C(4)	1.3893(12)
C(4)-C(5)	1.3969(11)
C(4)-C(14)	1.5033(12)
C(5)-C(6)	1.3859(11)
C(6)-C(7)	1.5183(10)
C(7)-C(8)	1.5397(13)
C(7)-C(12)	1.5231(12)
C(8)-H(8A)	0.98(2)
C(8)-H(8B)	0.949(19)
C(8)-C(9)	1.5366(14)
C(9)-H(9A)	1.035(18)
C(9)-H(9B)	1.01(2)
C(9)-C(10)	1.5357(16)
C(10)-H(10A)	0.98(2)
C(10)-H(10B)	0.906(18)
C(10)-C(11)	1.5458(13)
C(11)-C(12)	1.5417(13)
C(11)-C(17)	1.5262(13)
C(12)-H(12A)	0.993(18)
C(12)-H(12B)	0.961(15)
C(13)-H(13A)	0.92(2)
C(13)-H(13B)	0.98(2)
C(13)-H(13C)	0.932(18)
C(14)-C(15)	1.4899(15)

C(15)-H(15A)	0.97(3)
C(15)-H(15B)	0.95(2)
C(15)-H(15C)	1.00(2)
C(16)-H(16A)	1.02(2)
C(16)-H(16B)	0.97(2)
C(16)-H(16C)	0.84(3)
C(17)-H(17A)	0.96(2)
C(17)-H(17B)	0.93(2)
C(17)-H(17C)	1.19(2)
O(5)-H(5A)	0.83(4)
O(5)-H(5B)	0.93(8)
C(3)-O(1)-C(13)	114.67(7)
C(5)-O(3)-C(16)	112.54(9)
C(7)-O(4)-H(4A)	108(4)
C(2)-C(1)-C(6)	119.34(7)
C(2)-C(1)-C(11)	131.62(7)
C(6)-C(1)-C(11)	108.83(6)
C(1)-C(2)-Br(1)	122.18(6)
C(1)-C(2)-C(3)	119.90(7)
C(3)-C(2)-Br(1)	117.73(6)
O(1)-C(3)-C(2)	122.13(7)
O(1)-C(3)-C(4)	117.87(7)
C(4)-C(3)-C(2)	119.80(7)
C(3)-C(4)-C(5)	120.65(7)
C(3)-C(4)-C(14)	119.20(7)
C(5)-C(4)-C(14)	120.09(7)
O(3)-C(5)-C(4)	118.31(7)
O(3)-C(5)-C(6)	122.49(7)
C(6)-C(5)-C(4)	119.20(7)
C(1)-C(6)-C(7)	108.75(7)
C(5)-C(6)-C(1)	120.90(7)
C(5)-C(6)-C(7)	130.12(7)
O(4)-C(7)-C(6)	114.47(7)
O(4)-C(7)-C(8)	111.11(7)
O(4)-C(7)-C(12)	112.59(7)
C(6)-C(7)-C(8)	109.45(7)
C(6)-C(7)-C(12)	100.13(6)
C(12)-C(7)-C(8)	108.47(7)

C(7)-C(8)-H(8A)	110.3(9)
C(7)-C(8)-H(8B)	100.8(11)
H(8A)-C(8)-H(8B)	108.1(15)
C(9)-C(8)-C(7)	112.54(7)
C(9)-C(8)-H(8A)	111.3(9)
C(9)-C(8)-H(8B)	113.4(11)
C(8)-C(9)-H(9A)	112.7(10)
C(8)-C(9)-H(9B)	107.0(11)
H(9A)-C(9)-H(9B)	102.1(15)
C(10)-C(9)-C(8)	113.37(8)
C(10)-C(9)-H(9A)	107.8(11)
C(10)-C(9)-H(9B)	113.4(12)
C(9)-C(10)-H(10A)	108.4(13)
C(9)-C(10)-H(10B)	109.6(12)
C(9)-C(10)-C(11)	111.74(8)
H(10A)-C(10)-H(10B)	108.0(17)
C(11)-C(10)-H(10A)	110.9(12)
C(11)-C(10)-H(10B)	108.2(12)
C(1)-C(11)-C(10)	108.71(7)
C(1)-C(11)-C(12)	100.11(7)
C(12)-C(11)-C(10)	107.17(7)
C(17)-C(11)-C(1)	117.14(8)
C(17)-C(11)-C(10)	111.74(8)
C(17)-C(11)-C(12)	111.01(8)
C(7)-C(12)-C(11)	102.47(6)
C(7)-C(12)-H(12A)	110.7(10)
C(7)-C(12)-H(12B)	108.1(9)
C(11)-C(12)-H(12A)	111.6(10)
C(11)-C(12)-H(12B)	112.1(9)
H(12A)-C(12)-H(12B)	111.5(14)
O(1)-C(13)-H(13A)	108.7(14)
O(1)-C(13)-H(13B)	112.7(11)
O(1)-C(13)-H(13C)	109.0(12)
H(13A)-C(13)-H(13B)	105.4(18)
H(13A)-C(13)-H(13C)	106.8(17)
H(13B)-C(13)-H(13C)	113.8(16)
O(2)-C(14)-C(4)	120.71(9)
O(2)-C(14)-C(15)	122.24(9)

C(15)-C(14)-C(4)	117.05(8)
C(14)-C(15)-H(15A)	106.0(16)
C(14)-C(15)-H(15B)	108.4(13)
C(14)-C(15)-H(15C)	110.2(13)
H(15A)-C(15)-H(15B)	102(2)
H(15A)-C(15)-H(15C)	120(2)
H(15B)-C(15)-H(15C)	109.7(18)
O(3)-C(16)-H(16A)	112.2(11)
O(3)-C(16)-H(16B)	110.1(12)
O(3)-C(16)-H(16C)	102.7(17)
H(16A)-C(16)-H(16B)	111.1(18)
H(16A)-C(16)-H(16C)	110(2)
H(16B)-C(16)-H(16C)	110.8(19)
C(11)-C(17)-H(17A)	113.8(12)
C(11)-C(17)-H(17B)	105.1(16)
C(11)-C(17)-H(17C)	114.3(10)
H(17A)-C(17)-H(17B)	103.5(19)
H(17A)-C(17)-H(17C)	102.8(16)
H(17B)-C(17)-H(17C)	117.1(19)
H(5A)-O(5)-H(5B)	108(5)

Table A10.4 Anisotropic displacement parameters ($\text{\AA}^2 \times 10^3$) for **203**. The anisotropic displacement factor exponent takes the form: $-2\pi^2 [h^2 a^{*2} U^{11} + \dots + 2 h k a^* b^* U^{12}]$

	U ¹¹	U ²²	U ³³	U ²³	U ¹³	U ¹²
Br(1)	16(1)	16(1)	13(1)	-6(1)	0(1)	-2(1)
O(1)	9(1)	19(1)	15(1)	2(1)	-3(1)	-1(1)
O(2)	24(1)	30(1)	44(1)	12(1)	22(1)	12(1)
O(3)	15(1)	14(1)	14(1)	-5(1)	1(1)	1(1)
O(4)	12(1)	20(1)	11(1)	-3(1)	-2(1)	1(1)
C(1)	9(1)	10(1)	10(1)	0(1)	1(1)	1(1)
C(2)	10(1)	11(1)	9(1)	-1(1)	1(1)	-1(1)
C(3)	8(1)	12(1)	10(1)	1(1)	0(1)	0(1)
C(4)	8(1)	12(1)	12(1)	1(1)	1(1)	1(1)
C(5)	9(1)	11(1)	10(1)	-1(1)	1(1)	1(1)

C(6)	7(1)	12(1)	9(1)	0(1)	0(1)	1(1)
C(7)	8(1)	16(1)	10(1)	0(1)	0(1)	1(1)
C(8)	10(1)	20(1)	16(1)	2(1)	1(1)	-2(1)
C(9)	14(1)	25(1)	14(1)	4(1)	3(1)	-3(1)
C(10)	12(1)	25(1)	14(1)	-2(1)	4(1)	2(1)
C(11)	10(1)	13(1)	13(1)	0(1)	2(1)	4(1)
C(12)	10(1)	16(1)	13(1)	2(1)	0(1)	4(1)
C(13)	11(1)	26(1)	26(1)	1(1)	-1(1)	-6(1)
C(14)	10(1)	16(1)	16(1)	0(1)	2(1)	3(1)
C(15)	21(1)	15(1)	29(1)	4(1)	4(1)	6(1)
C(16)	22(1)	33(1)	15(1)	-8(1)	4(1)	1(1)
C(17)	22(1)	14(1)	26(1)	-3(1)	0(1)	6(1)
O(5)	34(1)	31(1)	66(1)	17(1)	12(1)	2(1)

Table A10.5 Hydrogen coordinates ($\times 10^4$) and isotropic displacement parameters ($\text{\AA}^2 \times 10^{-3}$) for **203**

	x	y	z	U(eq)
H(4A)	730(20)	5810(50)	5270(40)	110(14)
H(8A)	504(8)	5090(30)	7183(13)	18(3)
H(8B)	-34(10)	6580(30)	6933(16)	24(4)
H(9A)	199(10)	6480(30)	9068(15)	23(4)
H(9B)	1018(11)	6250(30)	8880(17)	27(5)
H(10A)	863(11)	9080(30)	9475(18)	33(5)
H(10B)	216(9)	9320(20)	8589(16)	24(4)
H(12A)	213(9)	9400(20)	6506(16)	21(4)
H(12B)	947(8)	9770(20)	5920(13)	12(3)
H(13A)	4561(12)	8430(30)	9001(19)	37(5)
H(13B)	4005(10)	9790(30)	8697(17)	34(5)
H(13C)	4233(10)	8410(20)	7769(16)	23(4)
H(15A)	3716(14)	2520(40)	7310(20)	53(7)
H(15B)	2962(11)	2800(30)	7559(18)	34(5)
H(15C)	3523(11)	3430(30)	8598(19)	35(5)
H(16A)	2770(12)	5560(30)	4724(17)	36(6)
H(16B)	1930(11)	6120(30)	4436(18)	31(5)

H(16C)	2168(13)	4320(30)	4360(20)	43(6)
H(17A)	1378(10)	11860(30)	8703(18)	29(5)
H(17B)	737(13)	11970(30)	7840(20)	42(6)
H(17C)	1619(10)	12150(30)	7333(18)	32(5)
H(5A)	4075(17)	7470(50)	5340(30)	76(10)
H(5B)	4760(40)	8000(110)	5030(90)	114

Table A10.6 Torsion angles [°] for **203**

Br(1)-C(2)-C(3)-O(1)	-1.53(11)
Br(1)-C(2)-C(3)-C(4)	173.23(6)
O(1)-C(3)-C(4)-C(5)	172.81(7)
O(1)-C(3)-C(4)-C(14)	-4.40(12)
O(3)-C(5)-C(6)-C(1)	179.12(8)
O(3)-C(5)-C(6)-C(7)	5.42(14)
O(4)-C(7)-C(8)-C(9)	178.38(7)
O(4)-C(7)-C(12)-C(11)	-164.95(7)
C(1)-C(2)-C(3)-O(1)	-176.65(8)
C(1)-C(2)-C(3)-C(4)	-1.89(12)
C(1)-C(6)-C(7)-O(4)	150.32(7)
C(1)-C(6)-C(7)-C(8)	-84.20(8)
C(1)-C(6)-C(7)-C(12)	29.65(9)
C(1)-C(11)-C(12)-C(7)	40.37(8)
C(2)-C(1)-C(6)-C(5)	-3.86(12)
C(2)-C(1)-C(6)-C(7)	171.06(7)
C(2)-C(1)-C(11)-C(10)	-84.97(11)
C(2)-C(1)-C(11)-C(12)	162.89(9)
C(2)-C(1)-C(11)-C(17)	42.84(14)
C(2)-C(3)-C(4)-C(5)	-2.18(12)
C(2)-C(3)-C(4)-C(14)	-179.38(8)
C(3)-C(4)-C(5)-O(3)	-176.12(8)
C(3)-C(4)-C(5)-C(6)	3.18(12)
C(3)-C(4)-C(14)-O(2)	-84.34(12)
C(3)-C(4)-C(14)-C(15)	95.72(11)
C(4)-C(5)-C(6)-C(1)	-0.15(12)
C(4)-C(5)-C(6)-C(7)	-173.85(8)

C(5)-C(4)-C(14)-O(2)	98.44(12)
C(5)-C(4)-C(14)-C(15)	-81.50(11)
C(5)-C(6)-C(7)-O(4)	-35.38(12)
C(5)-C(6)-C(7)-C(8)	90.10(11)
C(5)-C(6)-C(7)-C(12)	-156.05(9)
C(6)-C(1)-C(2)-Br(1)	-170.04(6)
C(6)-C(1)-C(2)-C(3)	4.85(12)
C(6)-C(1)-C(11)-C(10)	89.61(8)
C(6)-C(1)-C(11)-C(12)	-22.54(9)
C(6)-C(1)-C(11)-C(17)	-142.58(9)
C(6)-C(7)-C(8)-C(9)	50.99(10)
C(6)-C(7)-C(12)-C(11)	-42.94(8)
C(7)-C(8)-C(9)-C(10)	42.10(11)
C(8)-C(7)-C(12)-C(11)	71.66(8)
C(8)-C(9)-C(10)-C(11)	-43.70(11)
C(9)-C(10)-C(11)-C(1)	-47.37(10)
C(9)-C(10)-C(11)-C(12)	60.01(9)
C(9)-C(10)-C(11)-C(17)	-178.18(8)
C(10)-C(11)-C(12)-C(7)	-72.96(8)
C(11)-C(1)-C(2)-Br(1)	4.07(13)
C(11)-C(1)-C(2)-C(3)	178.96(8)
C(11)-C(1)-C(6)-C(5)	-179.21(8)
C(11)-C(1)-C(6)-C(7)	-4.29(9)
C(12)-C(7)-C(8)-C(9)	-57.35(9)
C(13)-O(1)-C(3)-C(2)	-83.51(11)
C(13)-O(1)-C(3)-C(4)	101.63(10)
C(14)-C(4)-C(5)-O(3)	1.06(12)
C(14)-C(4)-C(5)-C(6)	-179.64(8)
C(16)-O(3)-C(5)-C(4)	-91.05(10)
C(16)-O(3)-C(5)-C(6)	89.68(10)
C(17)-C(11)-C(12)-C(7)	164.77(8)

Table A10.7 Hydrogen bonds for **203** [\AA and $^\circ$]

D-H...A	d(D-H)	d(H...A)	d(D...A)	<(DHA)
O(4)-H(4A)...O(5)#1	0.70(4)	2.11(4)	2.7707(15)	158(5)
C(12)-H(12A)...O(2)#2	0.993(18)	2.577(18)	3.5655(12)	173.5(14)
C(13)-H(13B)...Br(1)	0.98(2)	2.963(19)	3.4746(12)	113.5(13)
C(16)-H(16B)...O(4)	0.97(2)	2.54(2)	3.1572(13)	121.7(15)
O(5)-H(5A)...O(2)	0.83(4)	2.18(4)	2.8176(15)	133(3)
O(5)-H(5B)...O(5)#3	0.93(8)	1.80(7)	2.678(3)	155(8)

Symmetry transformations used to generate equivalent atoms:

#1 $-x+1/2, y-1/2, -z+1$ #2 $x-1/2, y+1/2, z$ #3 $-x+1, y, -z+1$

APPENDIX 11

Asymmetric Synthesis of All-Carbon Quaternary Spirocycles via an Enantioselective Allylic Alkylation Strategy[†]

A11.1 INTRODUCTION AND BACKGROUND

The widespread prevalence of spirocycles in biologically active molecules has inspired the development of many methods for the synthesis¹ and, more recently, the enantioselective synthesis² of this motif. During the course of our ongoing efforts in natural product synthesis, the preparation of an enantioenriched spirocyclic cyclohexenone derivative bearing both an all-carbon quaternary stereogenic spirocenter as well as a 1,4-dicarbonyl moiety spanning the spirocenter was required. This goal was challenging not only due to the difficulties in constructing 1,4-dicarbonyls,³ but also due to the inherent challenges of enantioselectively synthesizing an all-carbon quaternary stereocenter.⁴ As the enantioselective synthesis of all-carbon quaternary stereocenters via

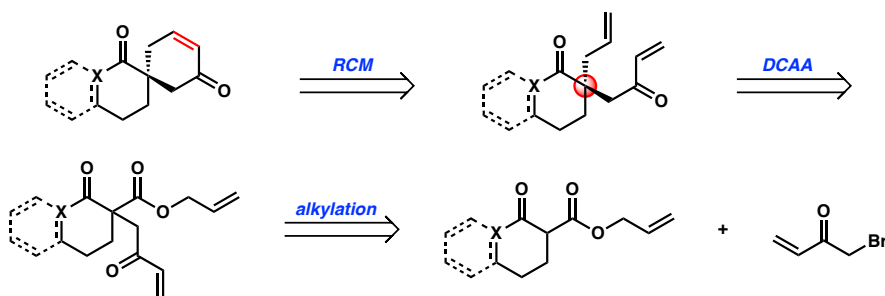
[†] This work was performed in collaboration with Dr. J. Caleb Hethcox. Portions of this chapter have been reproduced with permission from Shockley, S. E.,[‡] Hethcox, J. C.,[‡] Stoltz, B. M. *Tetrahedron Lett.* **2017**, 58, 3341–3343 © 2017 Elsevier Ltd.

palladium-catalyzed allylic alkylation has been developed extensively by our group,⁵ we envisioned that rapid entry to the spirocyclic cyclohexenone framework could be achieved if the olefin was disconnected via a ring-closing metathesis reaction (RCM) and the resultant α -quaternary carbonyl derivative could be synthesized asymmetrically via our allylic alkylation methodology (Figure A11.1a). In addition to the application to our own synthetic endeavor, we imagined that this strategy would be amenable to the synthesis of a wide array of all-carbon quaternary spirocyclic compounds, such as acorenone, laurencenone B, and α -chamigrene (Figure A11.1b).⁶ However, this plan hinged on the challenging use of bromomethyl vinyl ketone as an alkylating reagent.

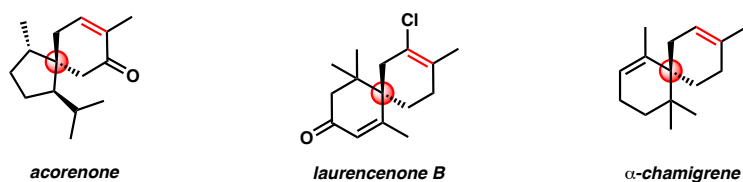
Nucleophilic addition to bromomethyl vinyl ketone can be problematic due to the three electrophilic positions on the molecule, which include positions for Michael addition, 1,2-addition, and S_N2 displacement (Figure A11.1c, left). As a solution to this issue, Funk has developed the use of 6-(bromomethyl)-4*H*-1,3-dioxin as a bromomethyl vinyl ketone surrogate (Figure A11.1c, left).⁷ Following alkylation, the dioxin functionality of this reagent can be unmasked under thermal conditions to release formaldehyde and reveal the latent enone. Therefore, we envisioned that we could obviate the challenges of using bromomethyl vinyl ketone by utilizing Funk's dioxin reagent in our planned strategy (Figure A11.1c, right). However, the use of a substrate bearing such a bulky substituent with Lewis basic oxygens had not yet been explored in our palladium-catalyzed allylic alkylation chemistry.

Figure A11.1. Strategy and inspiration for the catalytic enantioselective synthesis of all-carbon quaternary spirocycles

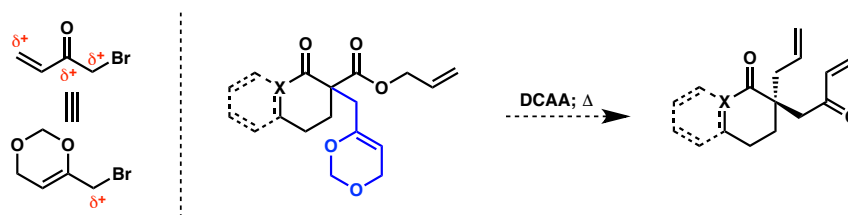
a) Planned strategy for spirocycle synthesis



b) Select spirocyclic natural products



c) Bromomethyl vinyl ketone surrogate

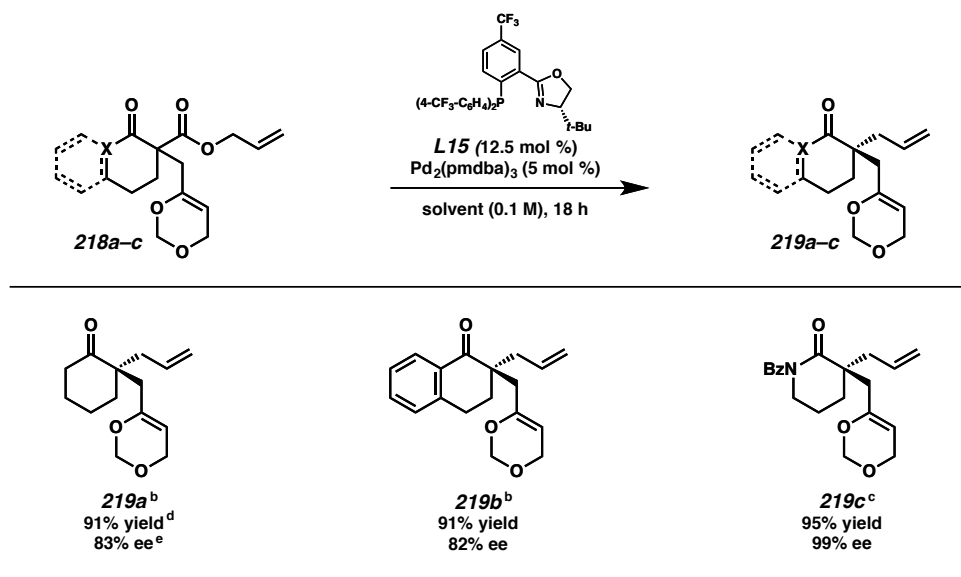


A11.2 REACTION DEVELOPMENT

We fortuitously discovered that the standard conditions developed by our group for palladium-catalyzed allylic alkylation reactions were adaptable to this new substrate class (Table A11.1). The use of a catalyst prepared from $\text{Pd}_2(\text{pmdba})_3$ and (*S*)- $(\text{CF}_3)_3$ -*t*-Bu-PHOX (**L15**) provided access to a variety of dioxin-substituted allylic alkylation products in consistently high yields and enantioselectivities. Cyclohexanone **219a** was obtained in 91% yield and 83% ee. Moreover, tetralone **219b** was afforded in similarly

high yield and selectivity, and we were pleased to find that lactam **219c** could be accessed in an excellent 95% yield and 99% ee. Based on these results in combination with the previously established trends in our palladium-catalyzed allylic alkylation methodology,⁵ we infer that the masked methyl vinyl ketone substituent should be broadly applicable to all of the ring systems tolerated in this chemistry.

Table A11.1 Enantioselective palladium-catalyzed allylic alkylations with substrates bearing a masked methyl vinyl ketone^a

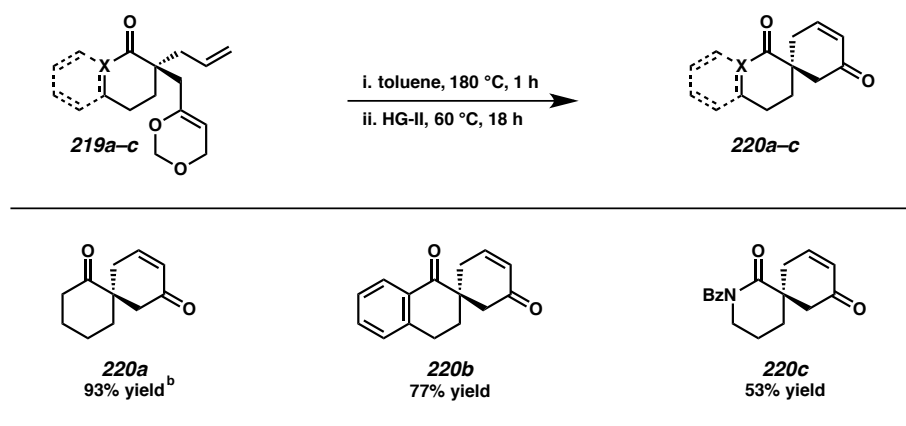


[a] Reactions performed on 0.2 mmol scale. [b] Performed using THF at 23 °C. [c] Performed using toluene at 40 °C. [d] Isolated yield. [e] Determined by chiral HPLC or SFC.

With the feasibility of utilizing substrates bearing a masked methyl vinyl ketone functionality in our allylic alkylation chemistry established, we moved to demonstrate the ease with which this strategy can provide access to the desired spirocyclic compounds. Though the masked methyl vinyl ketone synthon has been shown to provide access to bridged and fused bicyclic systems,⁷ to the best of our knowledge, the utility of this reagent for the synthesis of spirocycles has yet to be demonstrated. We were pleased to

find that the planned thermal unmasking/RCM sequence proceeded smoothly in a single reaction vessel (Table A11.2). In this procedure, dioxin **219** is unmasked via heating in toluene at 180 °C for one hour, whereupon the reaction is cooled to 60 °C and a solution of Hoveyda-Grubbs second-generation catalyst is introduced to complete the annulation. Using this newly developed protocol, spirocyclic cyclohexenones **220a**, **220b**, and **220c** were obtained in good to excellent yields, thus demonstrating the viability of this strategy for the synthesis of enantioenriched spirocycles.

Table A11.2 One-pot synthesis of spirocyclic compounds^a



[a] Reactions performed on 0.1 mmol scale. [b] Isolated yield.

A11.3 CONCLUSIONS

In summary, we have demonstrated that substrates bearing a bulky, highly oxygenated methyl vinyl ketone surrogate can be utilized in an enantioselective palladium-catalyzed allylic alkylation reaction. The resulting allylic alkylation products are obtained in high yields and selectivities with neither the increased sterics nor the added Lewis basic oxygen atoms adversely affecting reactivity. Furthermore, we

developed a one-pot unmasking/RCM procedure showcasing that these allylic alkylation products can be easily advanced to enantioenriched spirocycles bearing both an all-carbon quaternary stereogenic spirocenter as well as a 1,4-dicarbonyl functionality spanning the spirocenter. This simple two-step strategy is amenable to the synthesis of a range of enantioenriched spirocyclic natural products.

A11.4 EXPERIMENTAL SECTION

A11.4.1 MATERIALS AND METHODS

Unless otherwise stated, reactions were performed in flame-dried glassware under an argon or nitrogen atmosphere using dry, deoxygenated solvents. Solvents were dried by passage through an activated alumina column under argon. Commercially obtained reagents were used as received. Chemicals were purchased from Sigma Aldrich/Strem/Alfa Aesar/Oakwood Chemicals and used as received. Reaction temperatures were controlled by an IKA Mag temperature modulator. Glove box manipulations were performed under a nitrogen atmosphere. Thin-layer chromatography (TLC) and preparatory TLC was performed using E. Merck silica gel 60 F254 precoated plates (0.25 mm) and visualized by UV fluorescence quenching, KMnO₄, or *p*-anisaldehyde staining. SiliaFlash P60 Academic Silica gel (particle size 0.040–0.063 mm) was used for flash chromatography. Analytical chiral HPLC was performed with an Agilent 1100 Series HPLC utilizing a Chiralpak IC column (4.6 mm x 25 cm) or Chiralpak AD-H column (4.6 mm x 25 cm), both obtained from Daicel Chemical Industries, Ltd. with visualization at 210 nm. Analytical SFC was performed with a

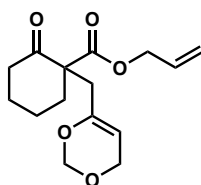
Mettler SFC supercritical CO₂ analytical chromatography system utilizing a Chiralpak OJ-H column (4.6 mm x 25 cm) obtained from Daicel Chemical Industries, Ltd. with visualization at 210 nm. ¹H NMR spectra were recorded on a Bruker Avance HD 400 MHz spectrometer and are reported relative to residual CHCl₃ (δ 7.26 ppm). ¹³C NMR spectra were recorded on a Bruker Avance HD 400 MHz spectrometer and are reported relative to residual CDCl₃ (δ 77.16 ppm). Data for ¹H NMR are reported as follows: s = singlet, d = doublet, t = triplet, q = quartet, p = pentet, sept = septuplet, m = multiplet, br s = broad singlet. Data for ¹³C NMR are reported in terms of chemical shifts (δ ppm). Some reported spectra include minor solvent impurities of benzene (δ 7.36 ppm), water (δ 1.56 ppm), ethyl acetate (δ 4.12, 2.05, 1.26 ppm), methylene chloride (δ 5.30 ppm), grease (δ 1.26, 0.86 ppm), and/or silicon grease (δ 0.07 ppm), which do not impact product assignments. IR spectra were obtained using a Perkin Elmer Paragon 1000 spectrometer using thin films deposited on NaCl plates and reported in frequency of absorption (cm⁻¹). High resolution mass spectra (HRMS) were obtained from the Caltech Mass Spectral Facility using a JEOL JMS-600H High Resolution Mass Spectrometer in fast atom bombardment (FAB+) or electron ionization (EI+) mode, or an Agilent 6200 Series TOF with an Agilent G1978A Multimode source in electrospray ionization (ESI+), atmospheric pressure chemical ionization (APCI+), or mixed ionization mode (MM: ESI-APCI+). Optical rotations were measured with a Jasco P-2000 polarimeter operating on the sodium D-line (589 nm), using a 100 mm pathlength cell, and are reported as: $[\alpha]_D^T$ (concentration in g/100 mL, solvent).

A11.4.1.1 Preparation of Known Compounds

Previously reported methods were used to prepare ligand (*S*)-**L15**⁸ and 6-(bromomethyl)-4*H*-1,3-dioxin⁷.

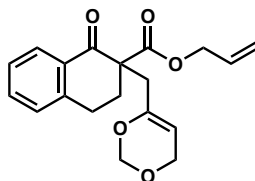
A11.4.2 EXPERIMENTAL PROCEDURES AND SPECTROSCOPIC DATA

A11.4.2.1 Experimental Procedures and Spectroscopic Data for the Synthesis of Allylic Alkylation Substrates



Allyl 1-((4*H*-1,3-dioxin-6-yl)methyl)-2-oxocyclohexane-1-carboxylate (218a). Allyl 2-oxocyclohexane-1-carboxylate⁹ (0.20 g, 1.1 mmol, 1 equiv), K₂CO₃ (0.76 g, 5.5 mmol, 5 equiv), and 6-(bromomethyl)-4*H*-1,3-dioxin⁷ (0.30 g, 1.7 mmol, 1.5 equiv) were dissolved in acetone (5 mL). The resulting reaction mixture was heated under reflux for 18 h, whereupon the reaction was cooled to ambient temperature, filtered through celite with acetone (10 mL), and concentrated under reduced pressure. The crude product was purified by silica gel flash column chromatography (15% EtOAc/hexanes) to give ester **218a** as a colorless oil (0.26 g, 84% yield): ¹H NMR (400 MHz, CDCl₃) δ 5.83 (ddt, *J* = 17.2, 10.4, 5.9 Hz, 1H), 5.31 – 5.12 (m, 2H), 4.89 – 4.80 (m, 2H), 4.66 (t, *J* = 2.6 Hz, 1H), 4.57 – 4.48 (m, 2H), 4.14 – 4.09 (m, 2H), 2.76 (dt, *J* = 15.0, 1.6 Hz, 1H), 2.56 (dt, *J* = 13.9, 3.2 Hz, 1H), 2.43 – 2.25 (m, 2H), 2.24 – 2.16 (m, 1H), 2.01 – 1.89 (m, 1H), 1.82 – 1.63 (m, 2H), 1.56 (dddd, *J* = 17.0, 12.4, 8.4, 4.4 Hz, 1H), 1.36 (ddd, *J* = 13.9, 12.2, 4.7 Hz, 1H); ¹³C NMR (101 MHz, CDCl₃) δ 206.4, 170.4, 150.3, 131.6, 118.8, 100.8, 90.3, 65.9, 63.7, 59.8, 40.9, 38.8, 35.7, 27.5, 22.3; IR (Neat Film, NaCl) 3083, 2944, 2867,

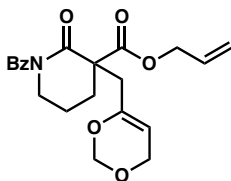
2796, 1715, 1682. 1648, 1451, 1372, 1314, 1175, 1092, 990, 927, 847, 761 cm^{-1} ; HRMS
(FAB+) m/z calc'd for $\text{C}_{15}\text{H}_{19}\text{O}_5$ $[\text{M}+\text{H}]-\text{H}_2$: 279.1232, found 279.1224.



Allyl 2-((4H-1,3-dioxin-6-yl)methyl)-1-oxo-1,2,3,4-tetrahydronaphthalene-2-carboxylate (218b). Allyl 1-oxo-1,2,3,4-tetrahydronaphthalene-2-carboxylate⁹ (0.60 g, 2.8 mmol, 1 equiv), Cs_2CO_3 (1.6 g, 5.0 mmol, 1.8 equiv), and 6-(bromomethyl)-4H-1,3-dioxin⁷ (0.55 g, 3.1 mmol, 1.1 equiv) were dissolved in DMF (19 mL). The resulting reaction mixture was heated to 70 °C for 18 h, whereupon the reaction was cooled to ambient temperature, poured into H_2O (40 mL), and the aqueous layer was extracted with EtOAc (3 x 25 mL). The combined organics were washed with brine (25 mL), dried over Na_2SO_4 , and concentrated under reduced pressure. The crude product was purified by silica gel flash column chromatography (10% EtOAc/hexanes) to give ester **218b** as a pale yellow oil (0.65 g, 71% yield): ^1H NMR (400 MHz, CDCl_3) δ 8.04 (dd, $J = 7.9, 1.4$ Hz, 1H), 7.47 (td, $J = 7.5, 1.5$ Hz, 1H), 7.34 – 7.27 (m, 1H), 7.21 (dd, $J = 7.6, 1.2$ Hz, 1H), 5.80 (ddt, $J = 17.2, 10.5, 5.5$ Hz, 1H), 5.27 – 5.06 (m, 2H), 4.93 (s, 2H), 4.83 (t, $J = 2.6$ Hz, 1H), 4.56 (dq, $J = 5.6, 1.6$ Hz, 2H), 4.20 (dt, $J = 2.6, 1.3$ Hz, 2H), 3.22 – 3.07 (m, 1H), 3.01 – 2.73 (m, 3H), 2.64 (dt, $J = 13.9, 4.6$ Hz, 1H), 2.23 – 2.11 (m, 1H); ^{13}C NMR (101 MHz, CDCl_3) δ 194.2, 170.8, 150.5, 143.3, 133.6, 132.0, 131.6, 128.9, 128.3, 126.8, 118.3, 101.4, 90.5, 66.0, 64.0, 56.8, 38.4, 30.5, 26.1; IR (Neat Film, NaCl) 2929, 2852,

1730, 1688, 1600, 1453, 1371, 1313, 1294, 1232, 1172, 1093, 987, 950, 846, 744 cm^{-1} ;

HRMS (FAB+) m/z calc'd for $\text{C}_{19}\text{H}_{19}\text{O}_5$ $[\text{M}+\text{H}]-\text{H}_2$: 327.1232, found 3267.1223.

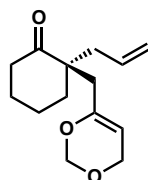


Allyl 3-((4H-1,3-dioxin-6-yl)methyl)-1-benzoyl-2-oxopiperidine-3-carboxylate (218c).

Allyl 1-benzoyl-2-oxopiperidine-3-carboxylate^{5e} (0.20 g, 0.70 mmol, 1 equiv), Cs_2CO_3 (0.41 g, 1.3 mmol, 1.8 equiv), and 6-(bromomethyl)-4H-1,3-dioxin⁷ (0.14 g, 0.77 mmol, 1.1 equiv) were dissolved in DMF (5 mL). The resulting reaction mixture was heated to 70 °C for 18 h, whereupon the reaction was cooled to ambient temperature, poured into H_2O (40 mL), and the aqueous layer was extracted with EtOAc (3 x 10 mL). The combined organics were washed with brine (10 mL), dried over Na_2SO_4 , and concentrated under reduced pressure. The crude product was purified by silica gel flash column chromatography (25% EtOAc/hexanes) to give ester **218c** as a pale yellow oil (0.13 g, 49% yield): ^1H NMR (400 MHz, CDCl_3) δ 7.73 – 7.66 (m, 2H), 7.53 – 7.42 (m, 1H), 7.42 – 7.33 (m, 2H), 5.99 (ddt, $J = 17.2, 10.4, 6.0$ Hz, 1H), 5.49 – 5.28 (m, 2H), 5.05 – 4.93 (m, 2H), 4.78 (dt, $J = 3.0, 1.5$ Hz, 1H), 4.72 (ddt, $J = 6.0, 1.7, 0.8$ Hz, 2H), 4.20 (dq, $J = 2.7, 1.2$ Hz, 2H), 3.94 – 3.66 (m, 2H), 2.98 – 2.87 (m, 1H), 2.74 – 2.62 (m, 1H), 2.50 – 2.33 (m, 1H), 2.14 – 1.92 (m, 3H); ^{13}C NMR (101 MHz, CDCl_3) δ 175.1, 171.4, 171.3, 150.0, 135.9, 131.9, 131.5, 128.3, 128.1, 119.8, 101.7, 90.7, 66.9, 64.0, 55.3, 46.5, 39.3, 30.3, 20.6; IR (Neat Film, NaCl) 2934, 2856, 1732, 1678, 1448, 1371, 1272, 1231,

1170, 1145, 1090, 985, 939, 845, 721, 694, 647 cm^{-1} ; HRMS (FAB+) m/z calc'd for $\text{C}_{21}\text{H}_{24}\text{O}_6\text{N}$ $[\text{M}+\text{H}]^+$: 386.1604, found 386.1619.

A11.4.2.2 General Procedure for the Asymmetric Palladium-Catalyzed Allylic Alkylation

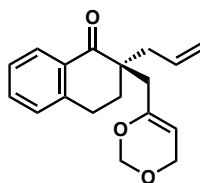


(S)-2-((4H-1,3-Dioxin-6-yl)methyl)-2-allylcyclohexan-1-one (219a). In a nitrogen-filled glove box, to a 1 dram vial equipped with a stir bar was added $\text{Pd}_2(\text{pmdba})_3$ (11 mg, 0.01 mmol, 5 mol %), ligand (*S*)-**L1** (13 mg, 0.025 mmol, 12.5 mol %), and THF (2 mL). The resulting mixture was stirred at 25 °C for 30 min, whereupon substrate **218a** (56 mg, 0.20 mmol, 1 equiv) was added. The vial was sealed, removed from the glove box, and stirred at 25 °C. After 18 h, the reaction mixture was concentrated under reduced pressure and the crude product was purified by preparatory TLC (10% EtOAc/hexanes) to give allyl **219a** as a colorless oil (43 mg, 91% yield): 83% ee; $[\alpha]_{\text{D}}^{25} -13.1$ (c 1.9, CHCl_3); ^1H NMR (400 MHz, CDCl_3) δ 5.66 (ddt, J = 16.5, 10.6, 7.3 Hz, 1H), 5.09 – 4.99 (m, 2H), 4.95 (d, J = 5.4 Hz, 1H), 4.88 (d, J = 5.4 Hz, 1H), 4.68 (t, J = 2.6 Hz, 1H), 4.26 – 4.11 (m, 2H), 2.58 – 2.45 (m, 2H), 2.39 – 2.28 (m, 3H), 2.18 (d, J = 14.5 Hz, 1H), 1.84 (tdd, J = 6.7, 3.4, 1.6 Hz, 1H), 1.79 – 1.69 (m, 5H); ^{13}C NMR (101 MHz, CDCl_3) δ 213.9, 151.5, 134.0, 118.4, 100.7, 90.4, 63.9, 51.0, 39.5, 39.4, 39.0, 36.8, 27.3, 21.0; IR (Neat Film, NaCl) 3391, 3074, 2924, 2854, 2795, 1705, 1681, 1638, 1445, 1372, 1311, 1196, 1172, 1124, 1093, 1021, 990, 911, 847, 755, 640 cm^{-1} ; HRMS (FAB+) m/z calc'd for $\text{C}_{14}\text{H}_{19}\text{O}_3$

[M+H]–H₂: 235.1334, found 235.1341; HPLC conditions: 3% IPA, 1.0 mL/min, Chiralpak AD–H column, λ = 210 nm, t_R (min): major = 7.066, minor = 7.722.

A11.4.2.3 Spectroscopic Data for the Asymmetric Palladium-Catalyzed Allylic Alkylation Products

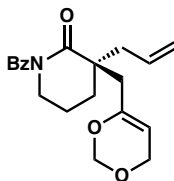
Please note that the absolute configurations of **219a–c** were determined by analogy.^{5e,g} For respective HPLC conditions, please refer to Table A11.3.



(*S*)-2-((4*H*-1,3-Dioxin-6-yl)methyl)-2-allyl-3,4-dihydronaphthalen-1(2*H*)-one (**219b**).

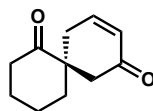
Product **219b** was prepared according to the general procedure to give a colorless oil (52 mg, 91% yield): 82% ee; $[\alpha]_D^{25} +0.254$ (*c* 2.0, CHCl₃); ¹H NMR (400 MHz, CDCl₃) δ 8.05 (dd, *J* = 7.8, 1.4 Hz, 1H), 7.47 (td, *J* = 7.5, 1.5 Hz, 1H), 7.35 – 7.29 (m, 1H), 7.27 – 7.19 (m, 1H), 5.79 (dddd, *J* = 17.0, 10.3, 7.8, 7.0 Hz, 1H), 5.17 – 5.00 (m, 2H), 5.00 – 4.88 (m, 2H), 4.74 (t, *J* = 2.6 Hz, 1H), 4.21 (dt, *J* = 2.5, 1.2 Hz, 2H), 3.02 (dd, *J* = 7.2, 5.5 Hz, 2H), 2.69 (dq, *J* = 14.3, 1.3 Hz, 1H), 2.55 (ddt, *J* = 14.1, 7.0, 1.3 Hz, 1H), 2.34 – 2.27 (m, 1H), 2.27 – 2.21 (m, 1H), 2.11 (ddt, *J* = 6.0, 4.8, 3.2 Hz, 2H); ¹³C NMR (101 MHz, CDCl₃) δ 200.5, 151.5, 143.2, 133.9, 133.2, 132.0, 128.8, 128.2, 126.7, 118.7, 100.8, 90.4, 64.0, 47.8, 39.6, 38.8, 30.4, 25.3; IR (Neat Film, NaCl) 3072, 3004, 2929, 2859, 2794, 1677, 1600, 1454, 1432, 1371, 1289, 1225, 1193, 1172, 1093, 1023, 989, 918, 847, 742 cm⁻¹; HRMS (FAB+) *m/z* calc'd for C₁₈H₁₉O₃ [M+H]–H₂: 283.1334, found

283.1338; HPLC conditions: 4% IPA, 1.0 mL/min, Chiralpak IC column, λ = 210 nm, t_R (min): major = 29.702, minor = 23.387.



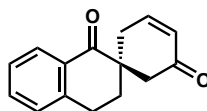
(S)-3-((4H-1,3-Dioxin-6-yl)methyl)-3-allyl-1-benzoylpiperidin-2-one (219c). Product **219c** was prepared according to the general procedure (toluene used in place of THF, reaction mixture heated to 40 °C) to give a pale yellow oil (66 mg, 95% yield): 99% ee; $[\alpha]_D^{25} +11.4$ (c 3.3, CHCl_3); ^1H NMR (400 MHz, CDCl_3) δ 7.61 – 7.31 (m, 5H), 5.76 (dddd, J = 17.1, 10.3, 7.7, 6.9 Hz, 1H), 5.21 – 5.09 (m, 2H), 5.06 – 4.98 (m, 2H), 4.74 (td, J = 2.7, 0.8 Hz, 1H), 4.23 (ddd, J = 2.6, 1.7, 0.8 Hz, 2H), 3.91 – 3.67 (m, 2H), 2.76 (dtd, J = 14.3, 1.7, 0.9 Hz, 1H), 2.59 (ddt, J = 13.8, 6.9, 1.3 Hz, 1H), 2.31 (ddt, J = 13.8, 7.7, 1.1 Hz, 1H), 2.15 – 2.09 (m, 1H), 2.04 – 1.95 (m, 3H), 1.93 – 1.83 (m, 1H); ^{13}C NMR (101 MHz, CDCl_3) δ 177.1, 175.6, 151.2, 136.7, 133.3, 131.5, 128.2, 127.8, 119.6, 101.2, 90.6, 64.1, 47.0 (2C), 43.5, 41.7, 30.0, 20.0; IR (Neat Film, NaCl) 3346, 3072, 2945, 2868, 2795, 1678, 1600, 1477, 1449, 1386, 1372, 1286, 1150, 1172, 1092, 1023, 990, 919, 846, 792, 725, 696 cm^{-1} ; HRMS (FAB+) m/z calc'd for $\text{C}_{20}\text{H}_{24}\text{NO}_4$ $[\text{M}+\text{H}]^+$: 342.1705, found 342.1714; SFC conditions: 5% IPA, 2.5 mL/min, Chiralpak OJ-H column, λ = 210 nm, t_R (min): major = 11.165, minor = 10.427.

A11.4.2.4 General Procedure for Spirocyclic Formation



(S)-Spiro[5.5]undec-9-ene-1,8-dione (220a). To a sealed Biotage microwave vial, allyl **219a** (24 mg, 0.10 mmol, 1 equiv) and toluene (0.7 mL) were added. The reaction mixture was heated to 180 °C for 1 h, whereupon the reaction was cooled to 60 °C and a solution of Hoveyda-Grubbs 2nd generation catalyst (6.3 mg, 0.010 mmol, 0.10 equiv) in toluene (0.3 mL) was added. The reaction mixture was then stirred an additional 18 h at 60 °C, cooled to ambient temperature, and directly purified by preparatory TLC (15% EtOAc/hexanes) to give spirocycle **220a** as a colorless oil (17 mg, 93% yield): $[\alpha]_D^{25} -1.4$ (*c* 1.1, CHCl₃); ¹H NMR (400 MHz, CDCl₃) δ 6.81 (dt, *J* = 10.1, 4.1 Hz, 1H), 5.99 (dt, *J* = 10.0, 2.1 Hz, 1H), 2.84 (ddt, *J* = 18.8, 4.4, 1.4 Hz, 1H), 2.80 – 2.71 (m, 1H), 2.47 – 2.32 (m, 4H), 1.95 – 1.73 (m, 6H); ¹³C NMR (101 MHz, CDCl₃) δ 212.3, 197.4, 146.0, 129.5, 51.5, 45.7, 38.2, 38.1, 33.7, 27.7, 20.8; IR (Neat Film, NaCl) 3037, 2936, 2865, 1705, 1678, 1446, 1424, 1387, 1252, 1135, 736 cm⁻¹; HRMS (FAB+) *m/z* calc'd for C₁₁H₁₅O₂ [M+H]⁺: 179.1072, found 179.1078.

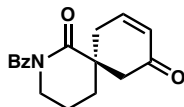
A11.4.2.5 Spectroscopic Data for Spirocyclic Compounds



(S)-3',4'-dihydro-1'H-spiro[cyclohexane-1,2'-naphthalen]-3-ene-1',5-dione (220b).

Product **220b** was prepared according to the general procedure to give a colorless oil (18 mg, 77% yield) after preparatory TLC (15% EtOAc/hexanes): $[\alpha]_D^{25} -1.5$ (*c* 1.2, CHCl₃);

^1H NMR (400 MHz, CDCl_3) δ 8.01 (dd, $J = 7.8, 1.4$ Hz, 1H), 7.50 (td, $J = 7.5, 1.5$ Hz, 1H), 7.40 – 7.30 (m, 1H), 7.26 – 7.20 (m, 1H), 6.91 – 6.77 (m, 1H), 6.10 (dt, $J = 10.3, 2.1$ Hz, 1H), 3.09 – 2.89 (m, 3H), 2.82 (d, $J = 16.2$ Hz, 1H), 2.50 – 2.38 (m, 2H), 2.27 – 2.02 (m, 2H); ^{13}C NMR (101 MHz, CDCl_3) δ 199.2, 197.4, 145.6, 142.7, 133.9, 130.8, 129.5, 128.9, 128.5, 127.2, 47.7, 44.6, 32.5, 32.3, 25.0; IR (Neat Film, NaCl) 3034, 2926, 2858, 1683, 1601, 1455, 1388, 1250, 1224, 1157, 946, 750 cm^{-1} ; HRMS (FAB+) m/z calc'd for $\text{C}_{15}\text{H}_{15}\text{O}_2$ $[\text{M}+\text{H}]^+$: 227.1072, found 227.1074.

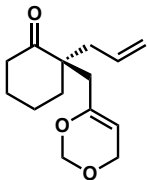
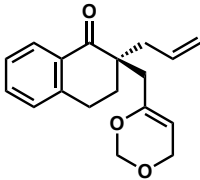
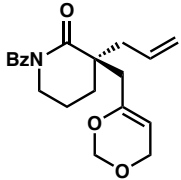


(S)-2-benzoyl-2-azaspiro[5.5]undec-9-ene-1,8-dione (220c). Product **220c** was prepared according to the general procedure to give a colorless oil (15 mg, 53% yield) after preparatory TLC (40% EtOAc/hexanes): $[\alpha]_{\text{D}}^{25} +29.7$ (c 0.9, CHCl_3); ^1H NMR (400 MHz, CDCl_3) δ 7.54 – 7.32 (m, 5H), 6.87 (ddd, $J = 10.2, 5.0, 3.3$ Hz, 1H), 6.06 (dt, $J = 10.1, 2.1$ Hz, 1H), 3.91 – 3.74 (m, 2H), 3.09 (dt, $J = 18.9, 3.0$ Hz, 1H), 2.96 (d, $J = 16.1$ Hz, 1H), 2.59 (dd, $J = 16.2, 1.3$ Hz, 1H), 2.49 (ddt, $J = 18.9, 5.0, 1.6$ Hz, 1H), 2.09 – 1.95 (m, 4H); ^{13}C NMR (101 MHz, CDCl_3) δ 196.4, 177.0, 175.1, 145.8, 135.8, 131.9, 129.2, 128.5, 127.6, 47.1, 47.0, 46.4, 34.8, 32.5, 19.3; IR (Neat Film, NaCl) 2949, 1679, 1449, 1388, 1281, 1151, 919, 729, 694, 665 cm^{-1} ; HRMS (FAB+) m/z calc'd for $\text{C}_{17}\text{H}_{18}\text{O}_3\text{N}$ $[\text{M}+\text{H}]^+$: 284.1287, found 284.1277.

A11.4.2.6 Determination of Enantiomeric Excess

Please note racemic products were synthesized using $\text{Pd}(\text{PPh}_3)_4$ in place of $\text{Pd}_2(\text{pmdba})_3$ and (*S*)-**L15**.

Table A11.3 Determination of enantiomeric excess

Entry	Product	Assay Conditions	Retention time of major isomer (min)	Retention time of minor isomer (min)	%ee
1		HPLC Chiralpak AD-H 3% IPA isocratic, 1 mL/min	7.066	7.722	83
2		HPLC Chiralpak IC 4% IPA isocratic, 1 mL/min	29.702	23.387	82
3		SFC Chiralpak OJ-H 5% IPA isocratic, 2.5 mL/min	11.165	10.427	99

A11.5 REFERENCES AND NOTES

- (1) For reviews on the synthesis of spirocycles, see: (a) Krapcho A. P. *Synthesis* **1974**, 383–419; (b) Sannigrahi, M. *Tetrahedron* **1999**, 55, 9007–9071; (c) Pradhan, R.; Patra, M.; Behera, A. K.; Mishra, B. K.; Behera, R. K.; *Tetrahedron* **2006**, 62, 779–

- 828; (d) Kotha, S.; Deb, A. C.; Lahiri, K.; Manivannan, E. *Synthesis* **2009**, 165–193; (e) Zhuo, C.-X.; Zheng, C.; You, S.-L. *Acc. Chem. Res.* **2014**, *47*, 2558–2573; (f) D'yakonov, V. A.; Trapeznikova, O. A.; de Meijere, A.; Dzhemilev, U. M. *Chem. Rev.* **2014**, *114*, 5775–5814.
- (2) For reviews on the enantioselective synthesis of spirocycles, see: (a) Rios, R. *Chem. Soc. Rev.* **2012**, *41*, 1060–1074; (b) Franz, A. K.; Hanhan, N. V.; Ball-Jones, N. R. *ACS Catal.* **2013**, *3*, 540–553; (c) Ball-Jones, N. R.; Badillo, J. J.; Franz, A. K. *Org. Biomol. Chem.* **2012**, *10*, 5165–5181; (d) Trost, B. M.; Brennan, M. K. *Synthesis* **2009**, 3003–3025; (e) Cheng, D.; Ishihara, Y.; Tan, B.; Barbas, C. F., III. *ACS Catal.* **2014**, *4*, 743–762.
- (3) (a) Arason, K. M.; Bergmeier, S. C. *Org. Prep. Proced. Int.* **2002**, *34*, 337–366; (b) DeMartino, M. P.; Chen, K.; Baran, P. S. *J. Am. Chem. Soc.* **2008**, *130*, 11546–11560.
- (4) For reviews on the synthesis of quaternary stereocenters, see: (a) Douglas, C. J.; Overman, L. E. *Proc. Natl. Acad. Sci. USA* **2004**, *101*, 5363–5367; (b) Das, J. P.; Marek, I. *Chem. Commun.* **2011**, *47*, 4593–4623; (c) Quasdorf, K. W.; Overman, L. E. *Nature* **2014**, *516*, 181–191; (d) Corey, E. J.; Guzman-Perez, A. *Angew. Chem. Int. Ed.* **1998**, *37*, 388–401; (e) Christoffers, J.; Mann, A. *Angew. Chem. Int. Ed.* **2001**, *40*, 4591–4597; (f) Trost, B. M.; Jiang, C. *Synthesis* **2006**, 369–396; (g) Liu, Y.; Han, S.-J.; Liu, W.-B.; Stoltz, B. M. *Acc. Chem. Res.* **2015**, *48*, 740–751.
- (5) (a) Craig, R. A., II.; Loskot, S. A.; Mohr, J. T.; Behenna, D. C.; Harned, A. M.; Stoltz, B. M. *Org. Lett.* **2015**, *17*, 5160–5163; (b) Numajiri, Y.; Jiménez-Osés, G.;

- Wang, B.; Houk, K. N.; Stoltz, B. M. *Org. Lett.* **2015**, *17*, 1082–1085; (c) Reeves, C. M.; Eidamshaus, C.; Kim, J.; Stoltz, B. M. *Angew. Chem. Int. Ed.* **2013**, *52*, 6718–6721; (d) Bennett, N. B.; Duquette, D. C.; Kim, J.; Liu, W.-B.; Marziale, A. N.; Behenna, D. C.; Virgil, S. C.; Stoltz, B. M. *Chem. Eur. J.* **2013**, *19*, 4414–4418; (e) Behenna, D. C.; Liu, Y.; Yurino, T.; Kim, J.; White, D. E.; Virgil, S. C.; Stoltz, B. M. *Nat. Chem.* **2012**, *4*, 130–133; (f) Behenna, D. C.; Mohr, J. T.; Sherden, N. H.; Marinescu, S. C.; Harned, A. M.; Tani, K.; Seto, M.; Ma, S.; Novák, Z.; Krout, M. R.; McFadden, R. M.; Roizen, J. L.; Enquist, J. A.; White, D. E.; Levine, S. R.; Petrova, K. V.; Iwashita, A.; Virgil, S. C.; Stoltz, B. M. *Chem. Eur. J.* **2011**, *17*, 14199–14223; (g) Behenna, D. C.; Stoltz, B. M. *J. Am. Chem. Soc.* **2004**, *126*, 15044–15045.
- (6) Smith, L. K.; Baxendale, I. R. *Org. Biomol. Chem.* **2015**, *13*, 9907–9933.
- (7) Greshock, T. J.; Funk, R. L. *J. Am. Chem. Soc.* **2002**, *124*, 754–755.
- (8) McDougal, N. T.; Streuff, J.; Mukherjee, H.; Virgil, S. C.; Stoltz, B. M. *Tetrahedron Lett.* **2010**, *51*, 5550–5554.
- (9) Mohr, J. T.; Behenna, D. C.; Harned, A. M.; Stoltz, B. M. *Angew. Chem. Int. Ed.* **2005**, *44*, 6924–6927.

APPENDIX 12

Spectra Relevant to Appendix 11:

*Asymmetric Synthesis of All-Carbon Quaternary Spirocycles
via an Enantioselective Allylic Alkylation Strategy*

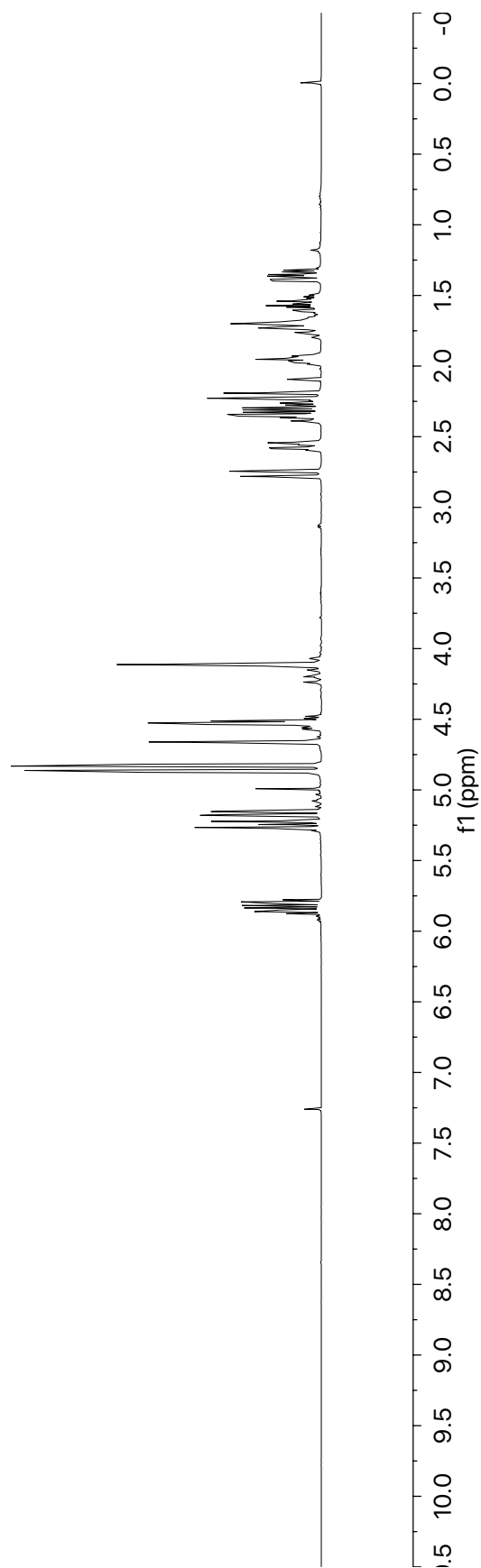
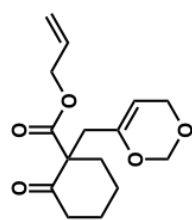


Figure A12.1 ¹H NMR (400 MHz, CDCl₃) of compound **218a**

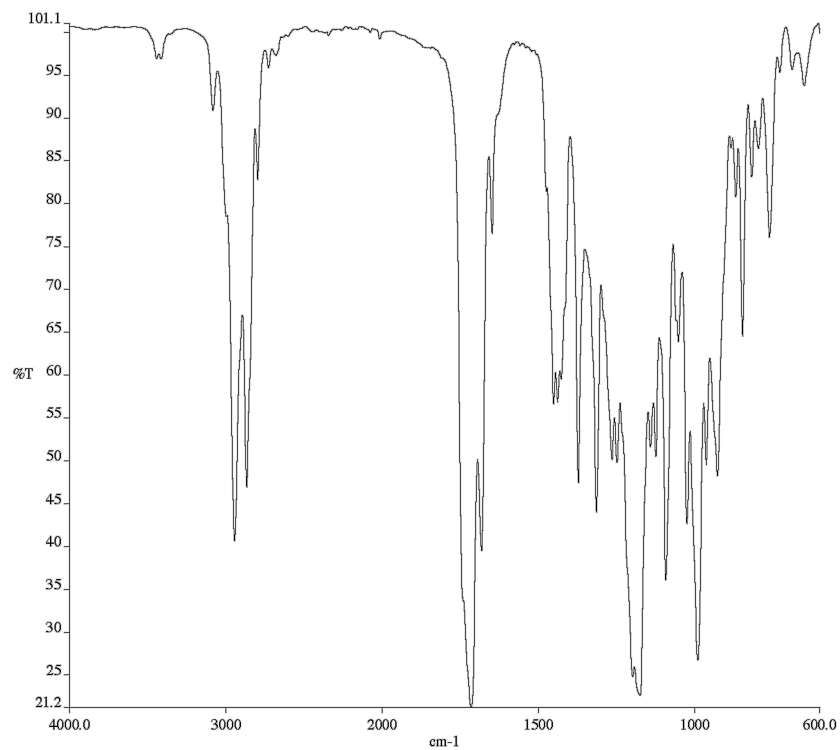


Figure A12.2 Infrared spectrum (Thin Film, NaCl) of compound **218a**

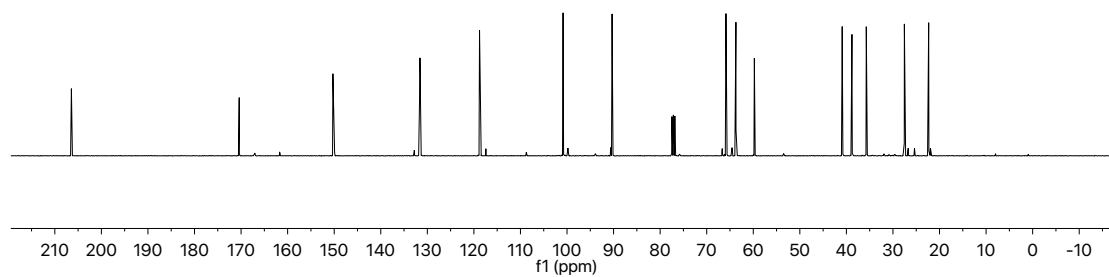


Figure A12.3 ^{13}C NMR (101 MHz, CDCl_3) of compound **218a**

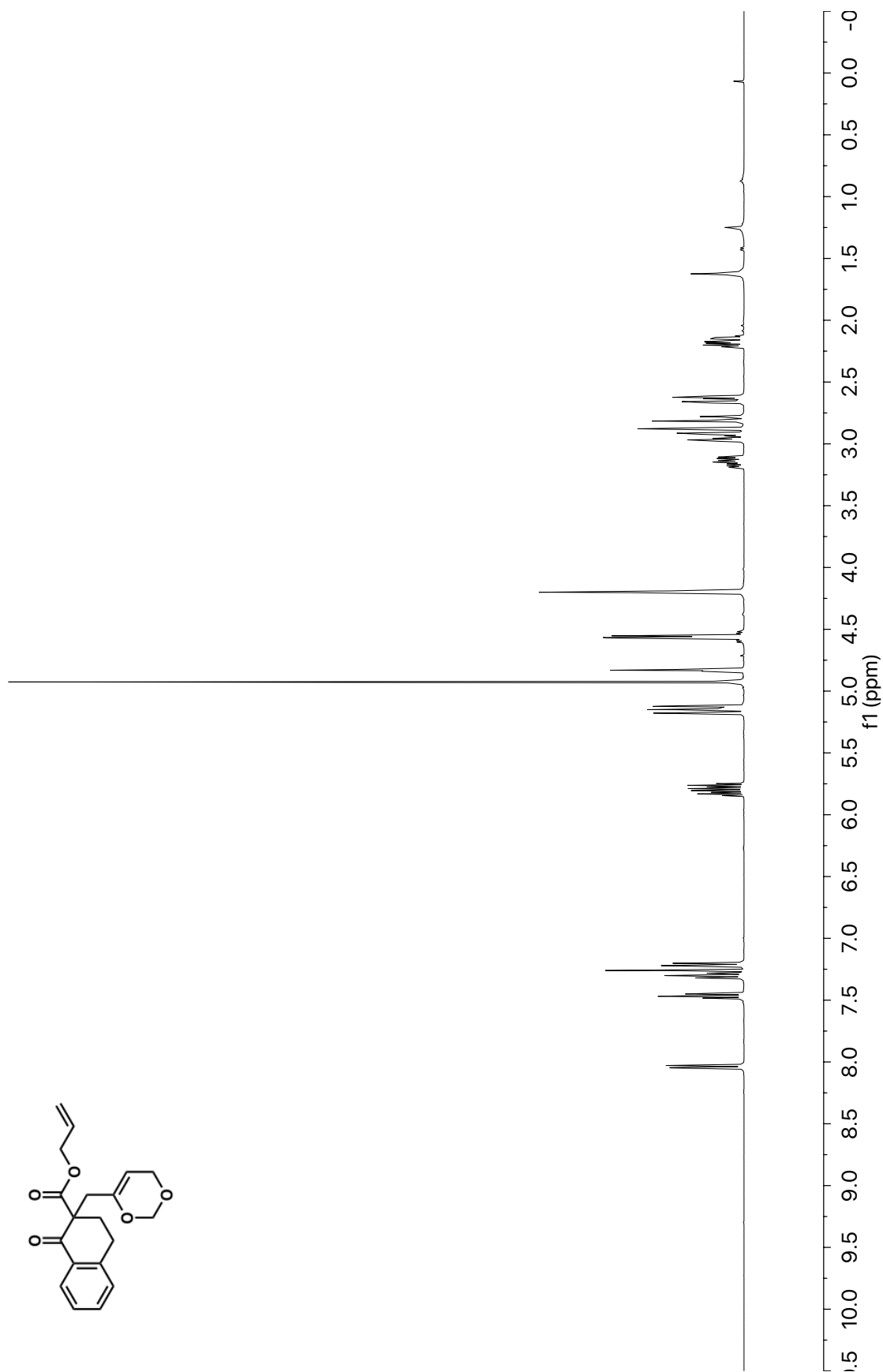


Figure A12.4 ¹H NMR (400 MHz, CDCl₃) of compound **218b**

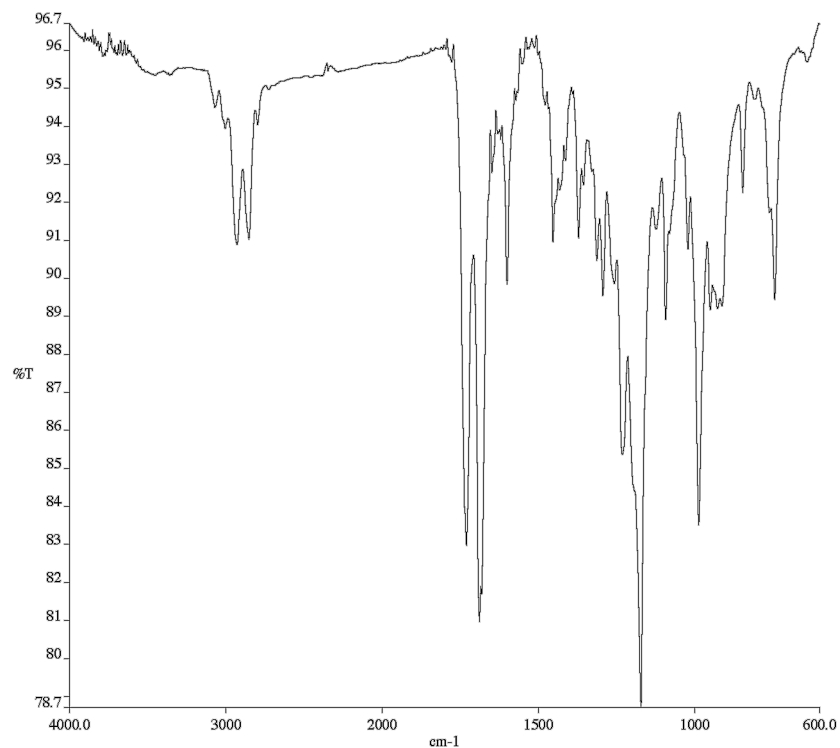


Figure A12.5 Infrared spectrum (Thin Film, NaCl) of compound **218b**

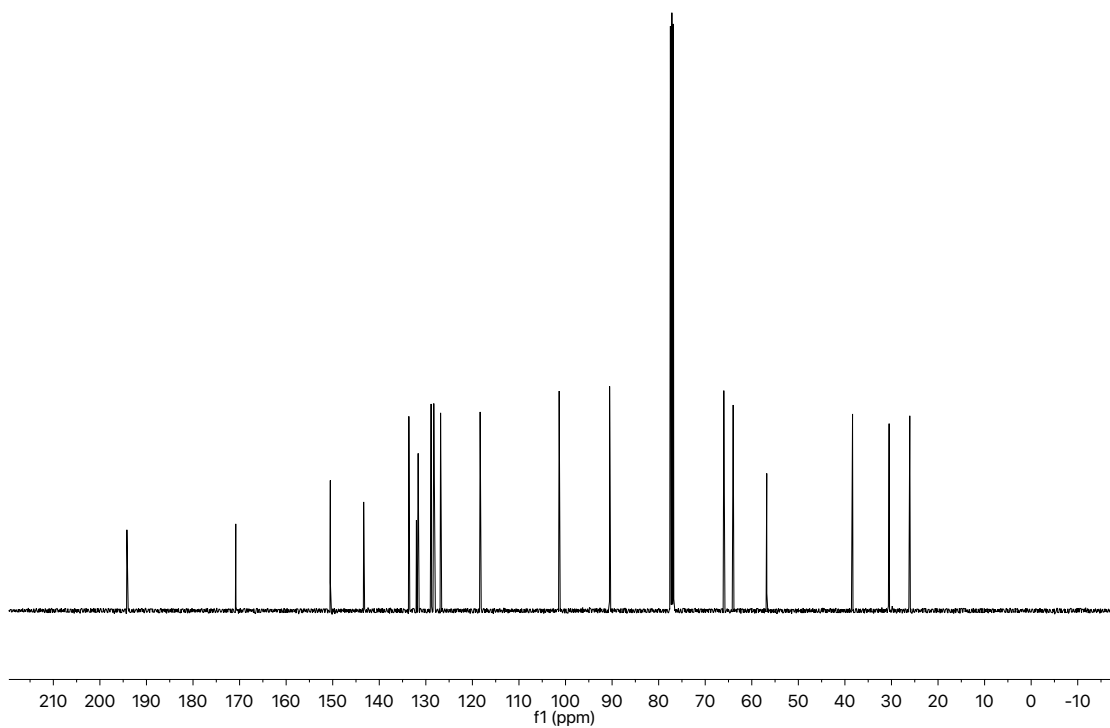


Figure A12.6 ¹³C NMR (101 MHz, CDCl₃) of compound **218b**

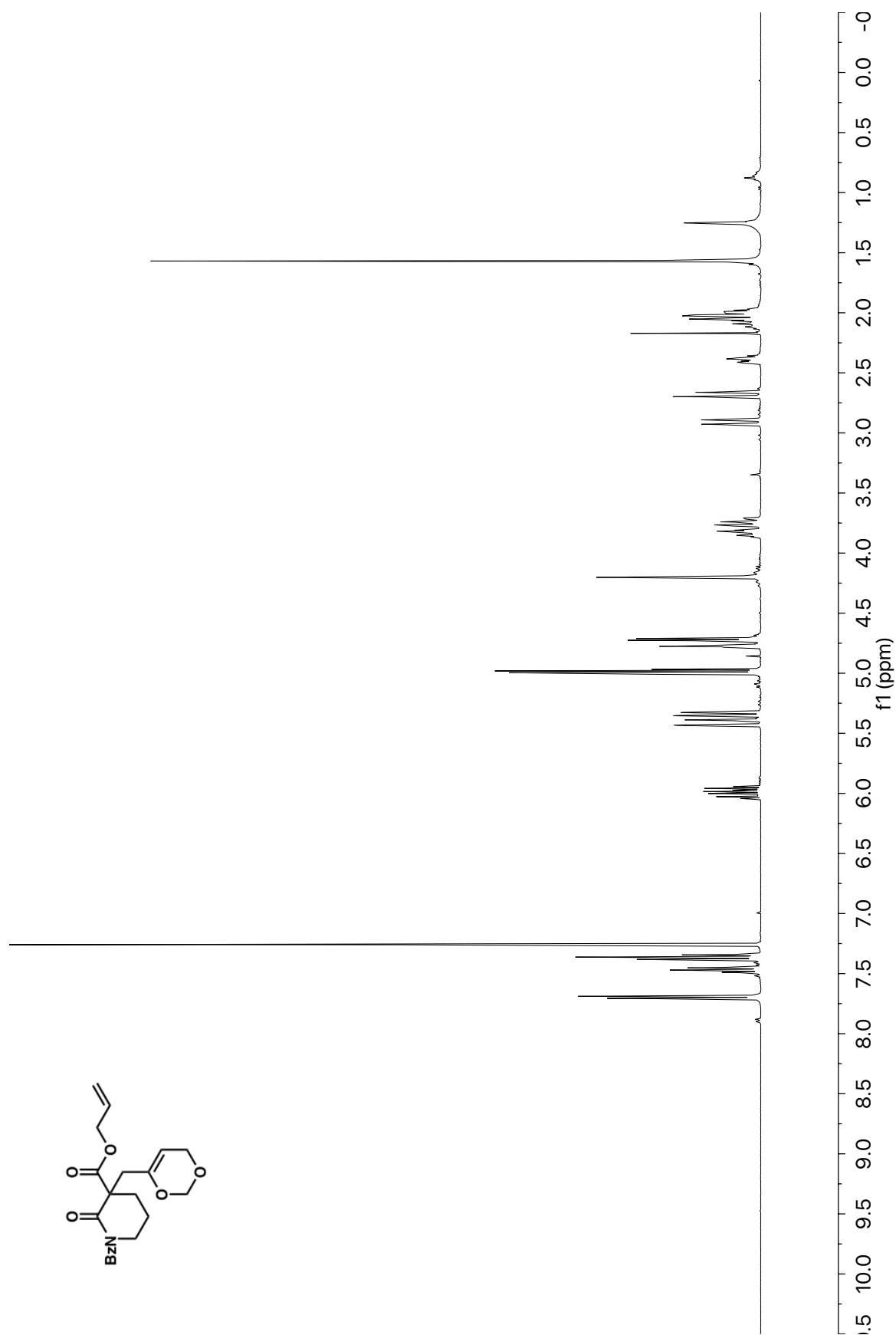


Figure A12.7 ^1H NMR (400 MHz, CDCl_3) of compound **218c**

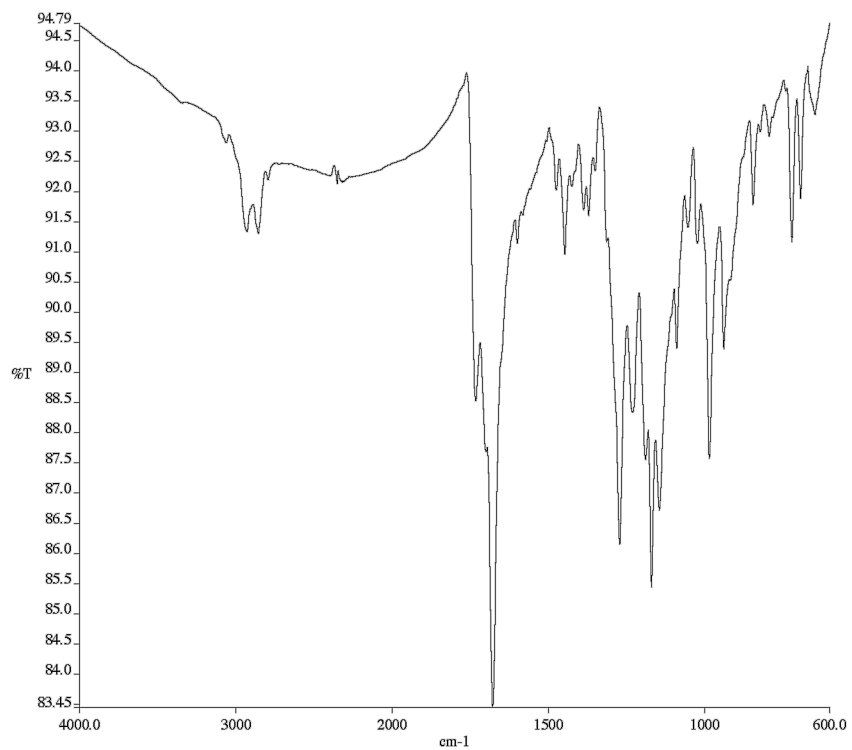


Figure A12.8 Infrared spectrum (Thin Film, NaCl) of compound **218c**

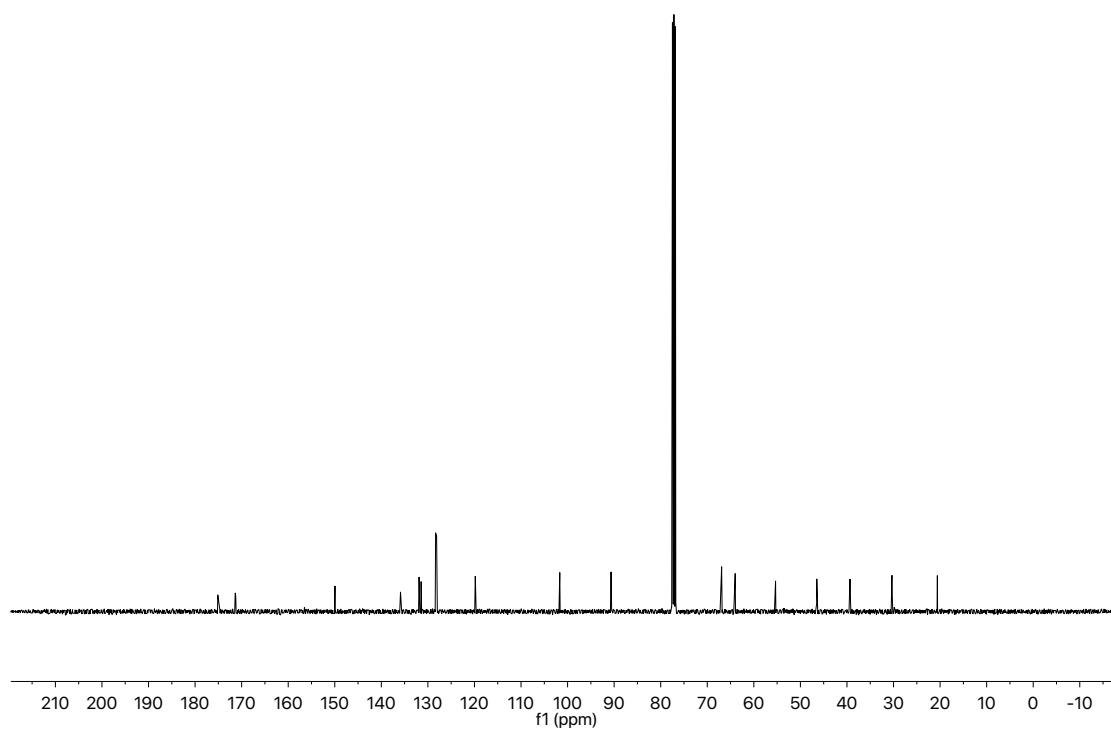


Figure A12.9 ¹³C NMR (101 MHz, CDCl₃) of compound **218c**

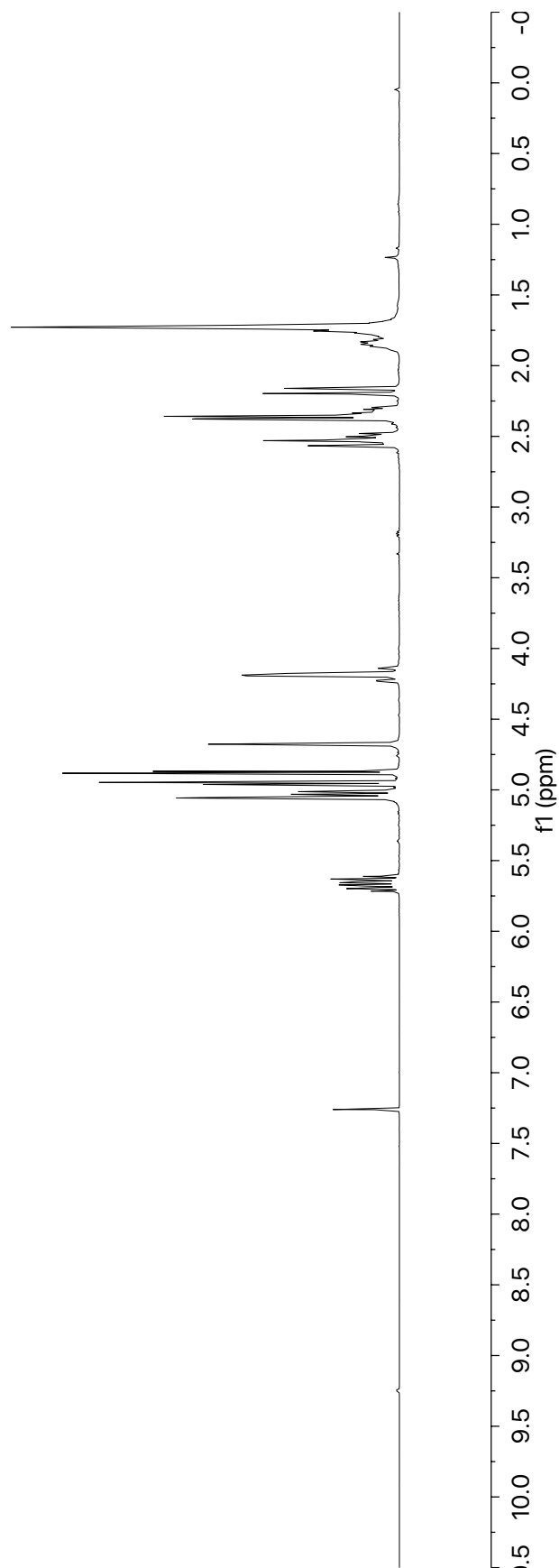
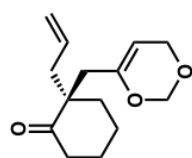


Figure A12.10 ^1H NMR (400 MHz, CDCl_3) of compound **219a**

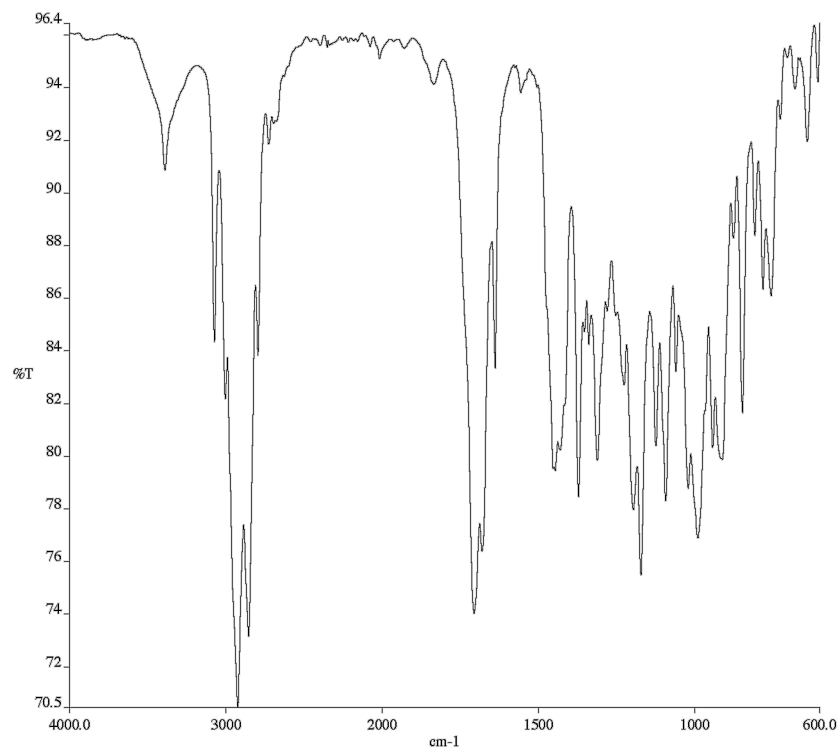


Figure A12.11 Infrared spectrum (Thin Film, NaCl) of compound **219a**

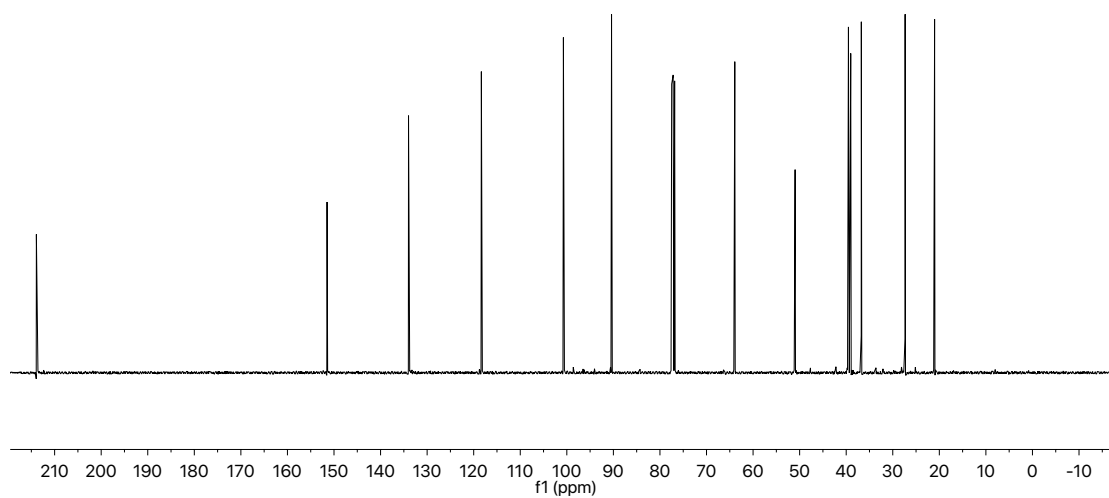


Figure A12.12 ¹³C NMR (101 MHz, CDCl₃) of compound **219a**

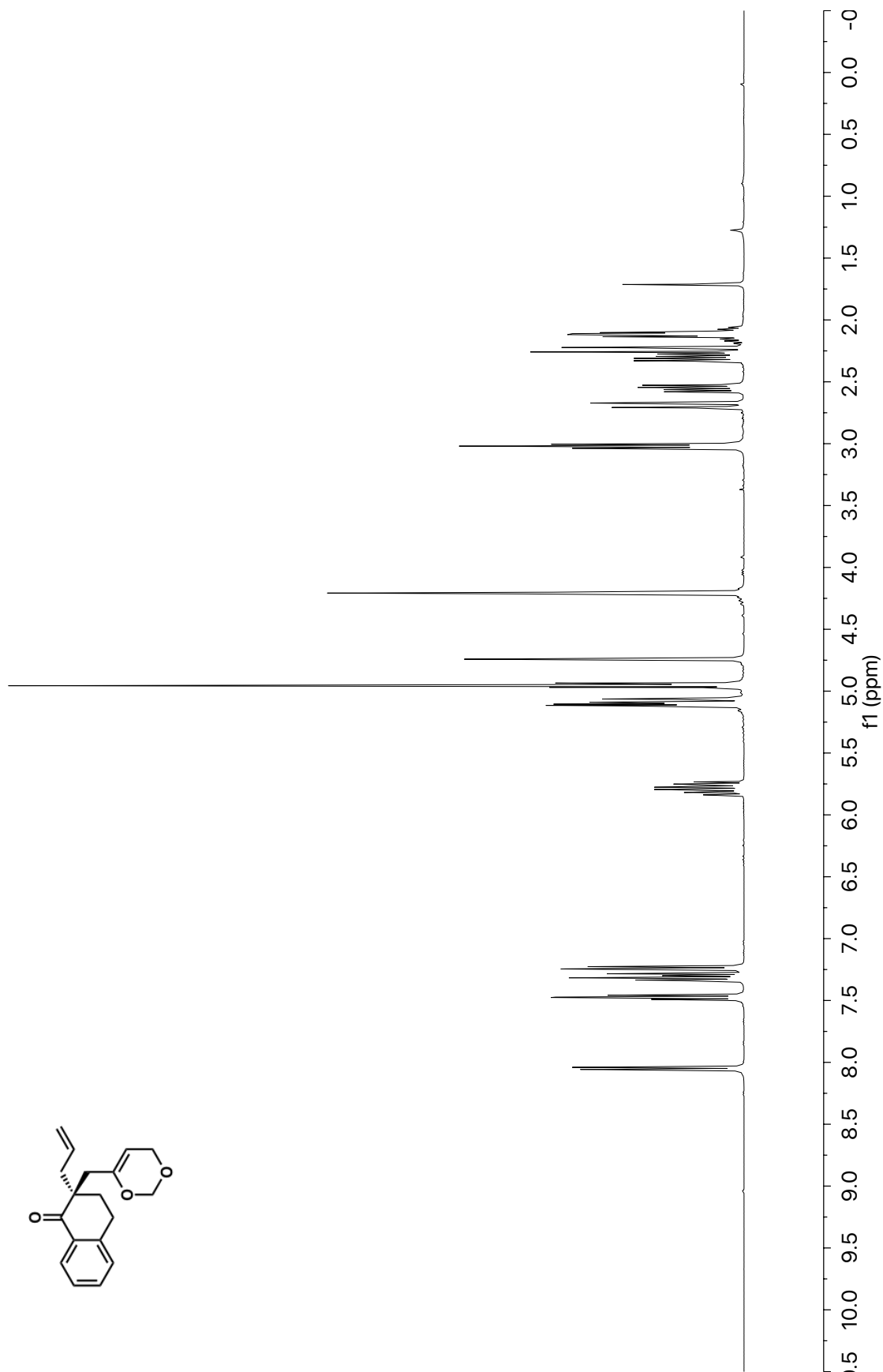


Figure A12.13 ^1H NMR (400 MHz, CDCl_3) of compound **219b**

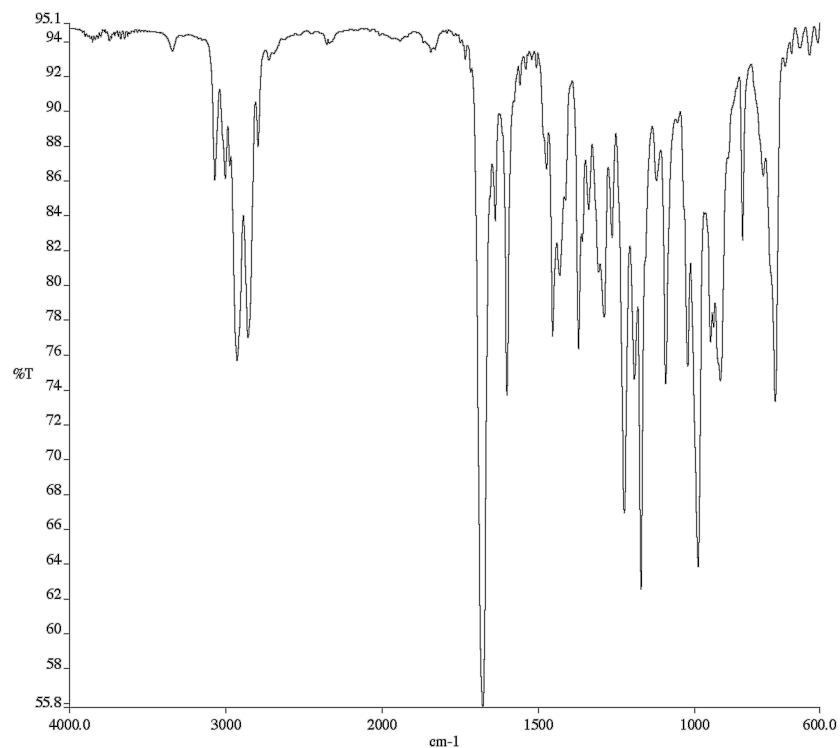


Figure A12.14 Infrared spectrum (Thin Film, NaCl) of compound **219b**

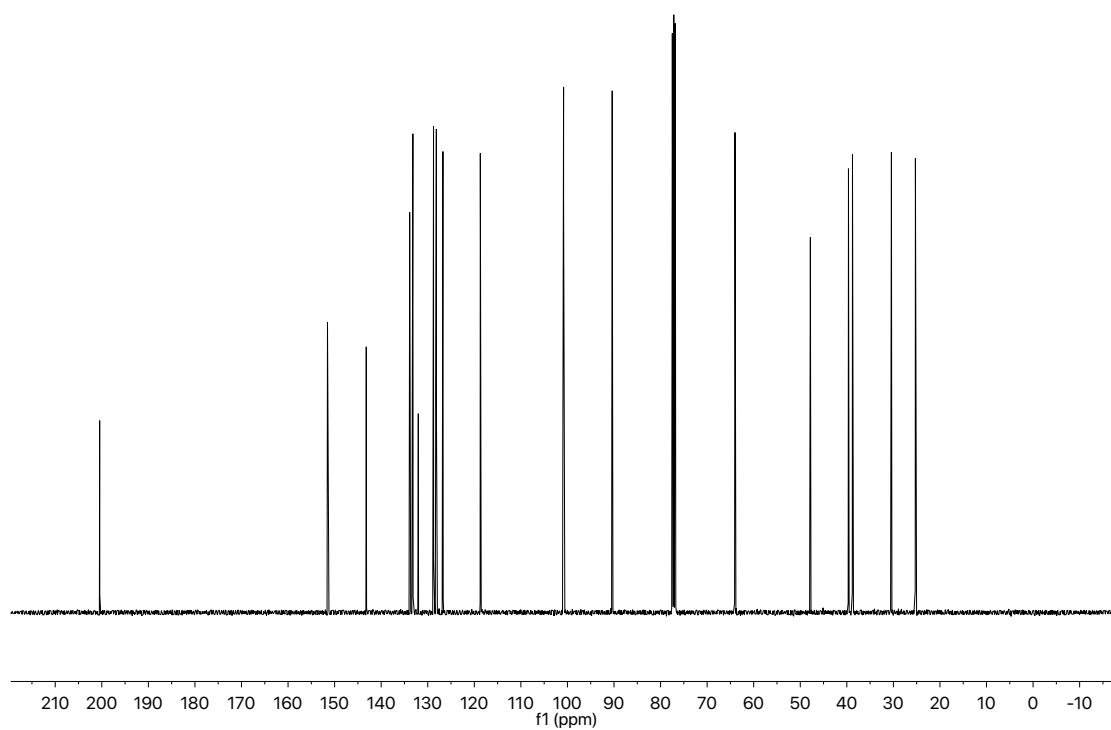


Figure A12.15 ¹³C NMR (101 MHz, CDCl₃) of compound **219b**

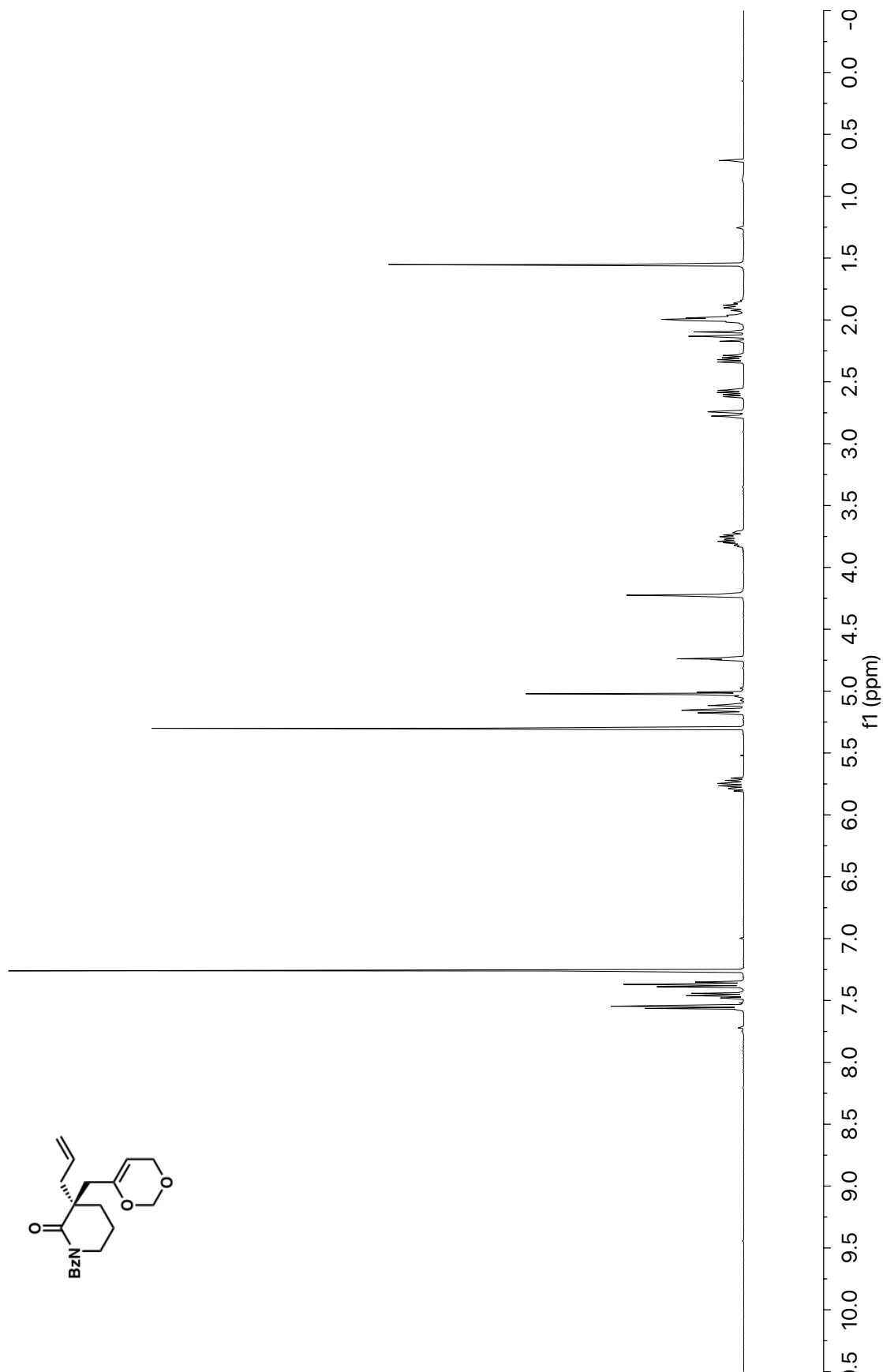


Figure A12.16 ^1H NMR (400 MHz, CDCl_3) of compound **219c**

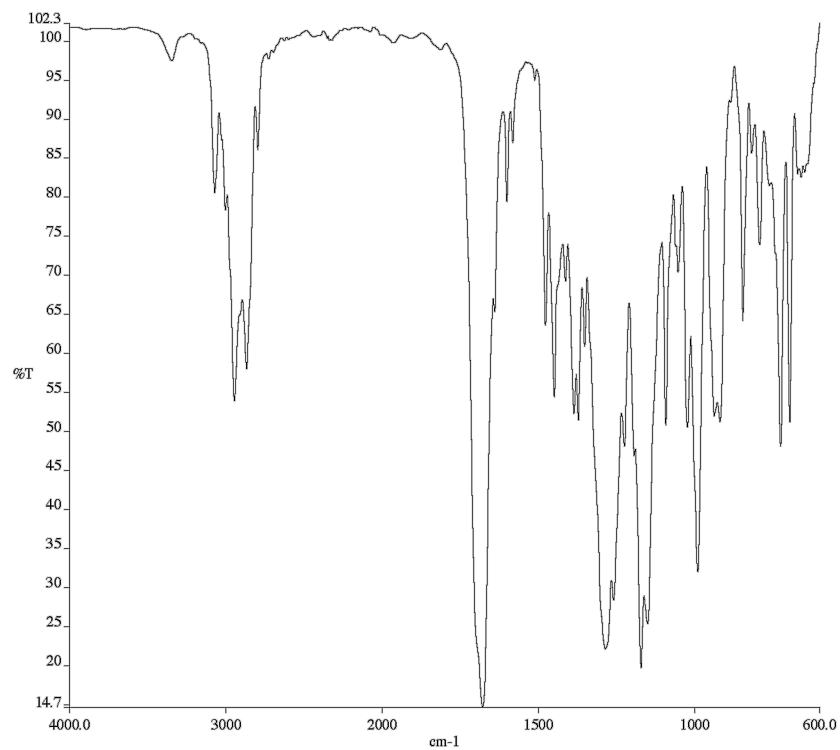


Figure A12.17 Infrared spectrum (Thin Film, NaCl) of compound **219c**

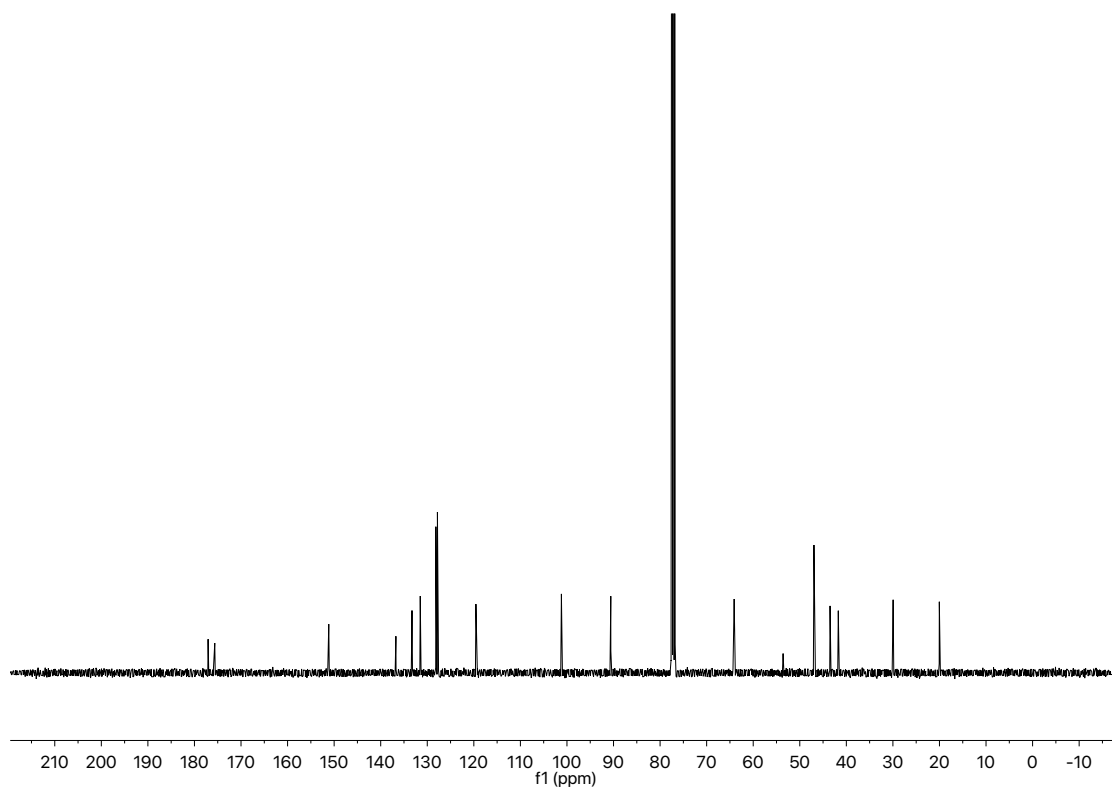
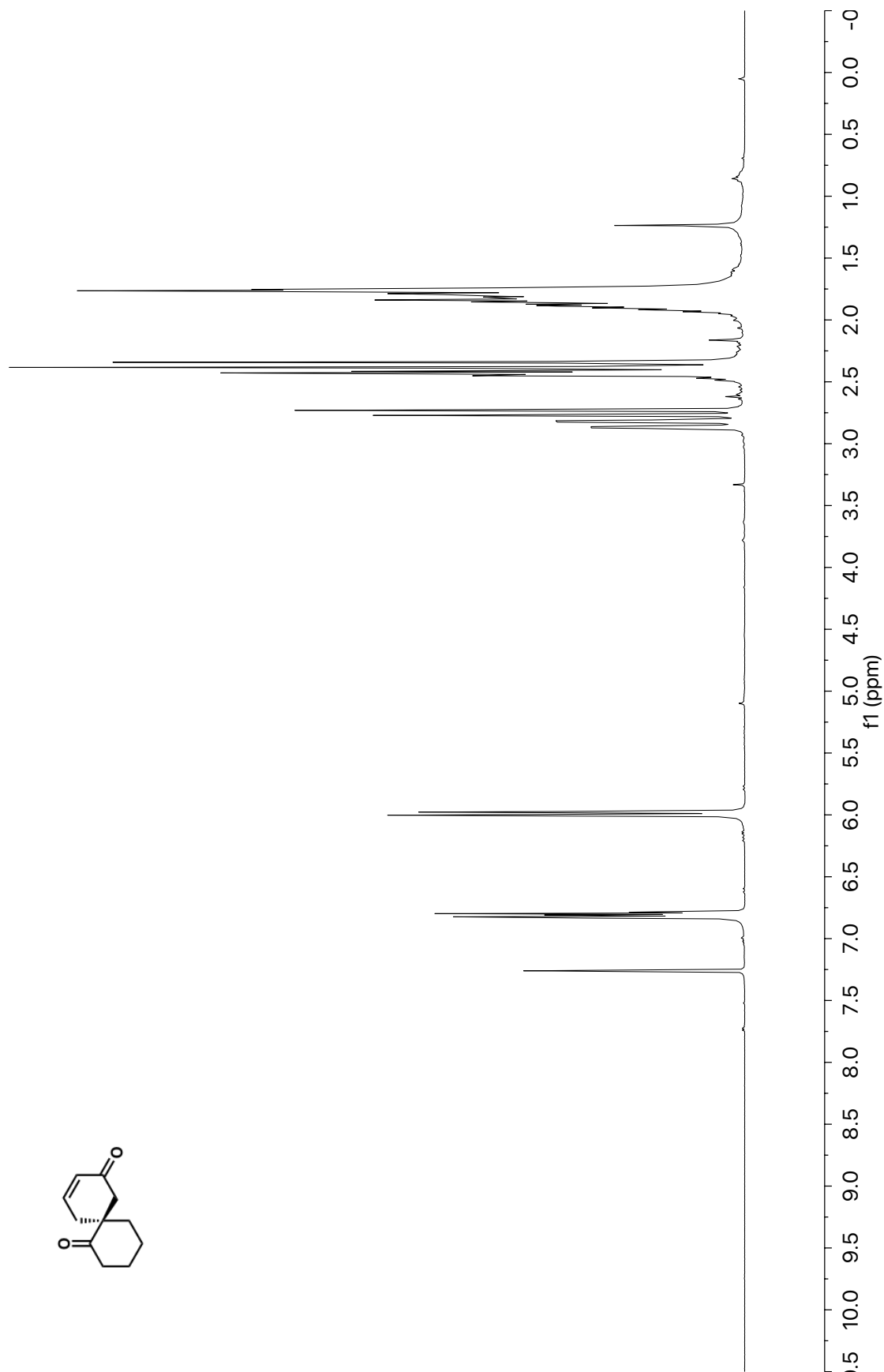


Figure A12.18 ¹³C NMR (101 MHz, CDCl₃) of compound **219c**

**Figure A12.19** ^1H NMR (400 MHz, CDCl_3) of compound **220a**

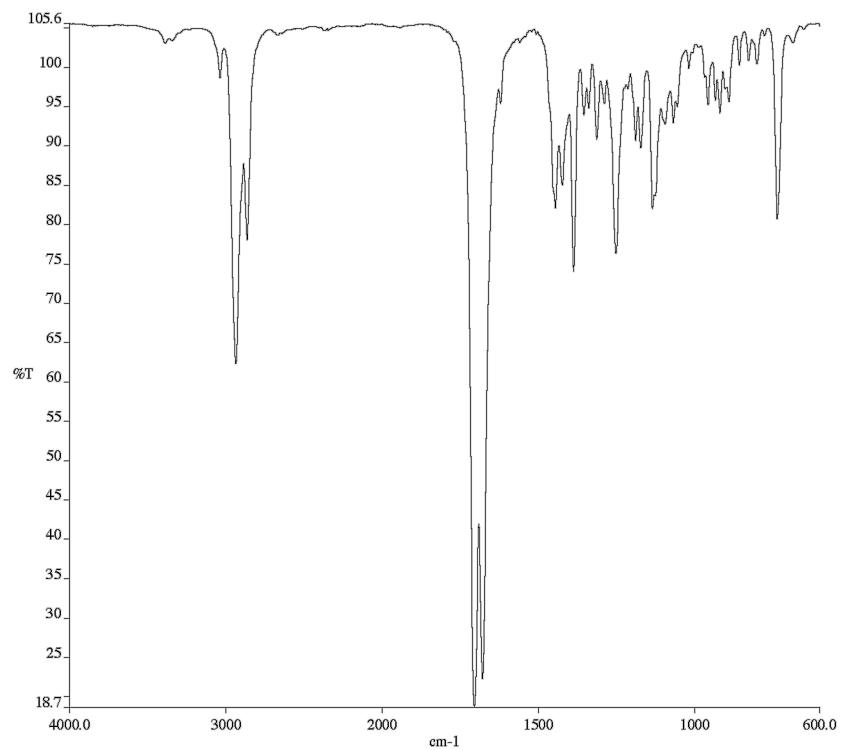


Figure A12.20 Infrared spectrum (Thin Film, NaCl) of compound **220a**

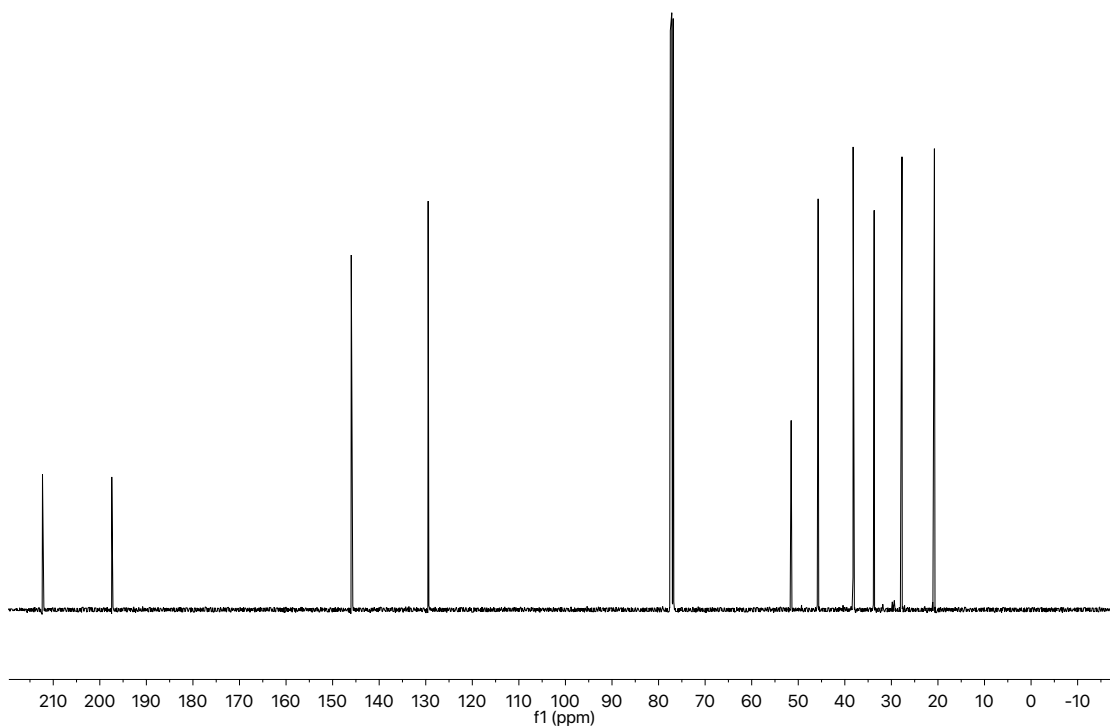


Figure A12.21 ^{13}C NMR (101 MHz, CDCl_3) of compound **220a**

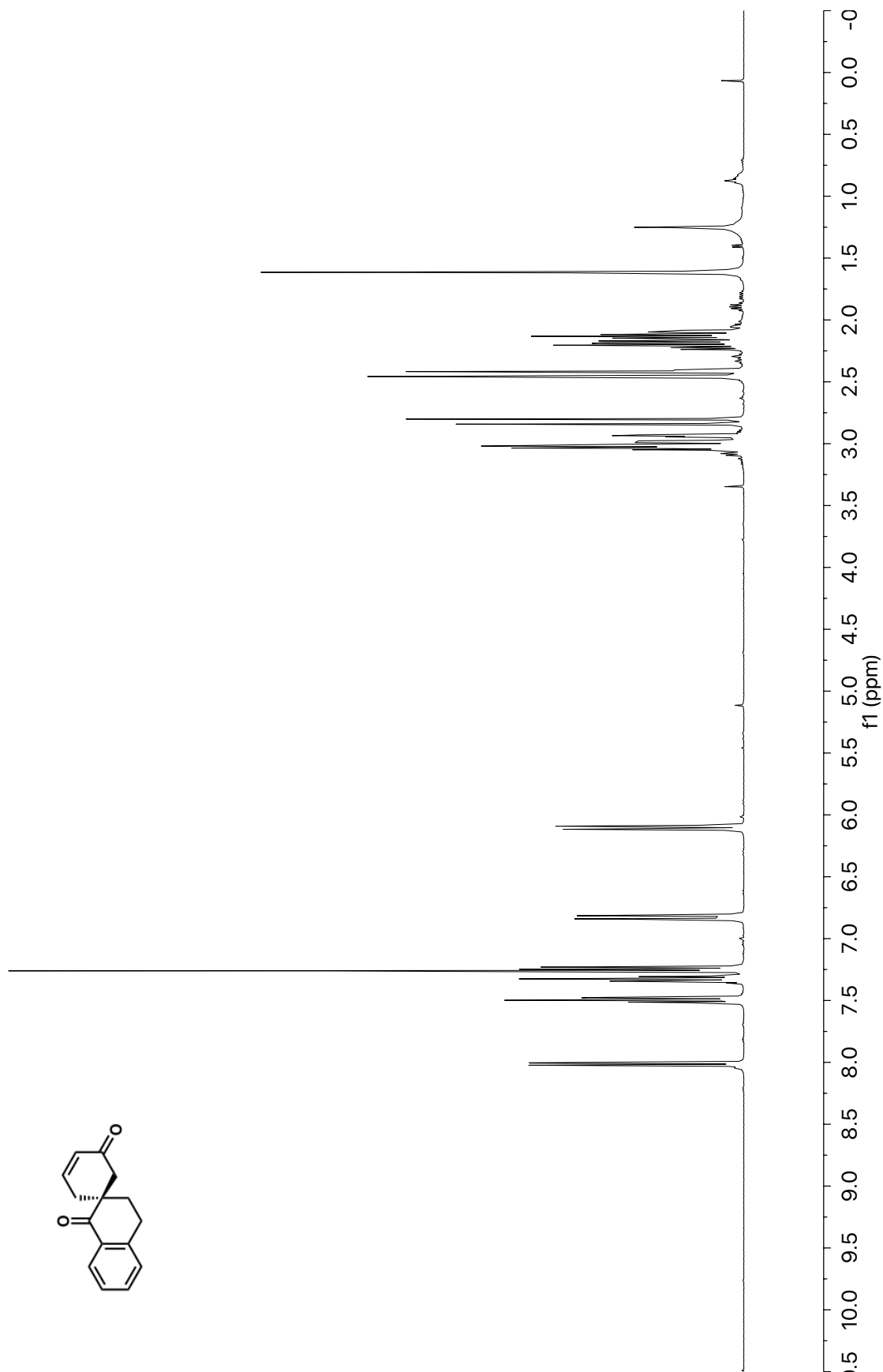


Figure A12.22 ^1H NMR (400 MHz, CDCl_3) of compound **220b**

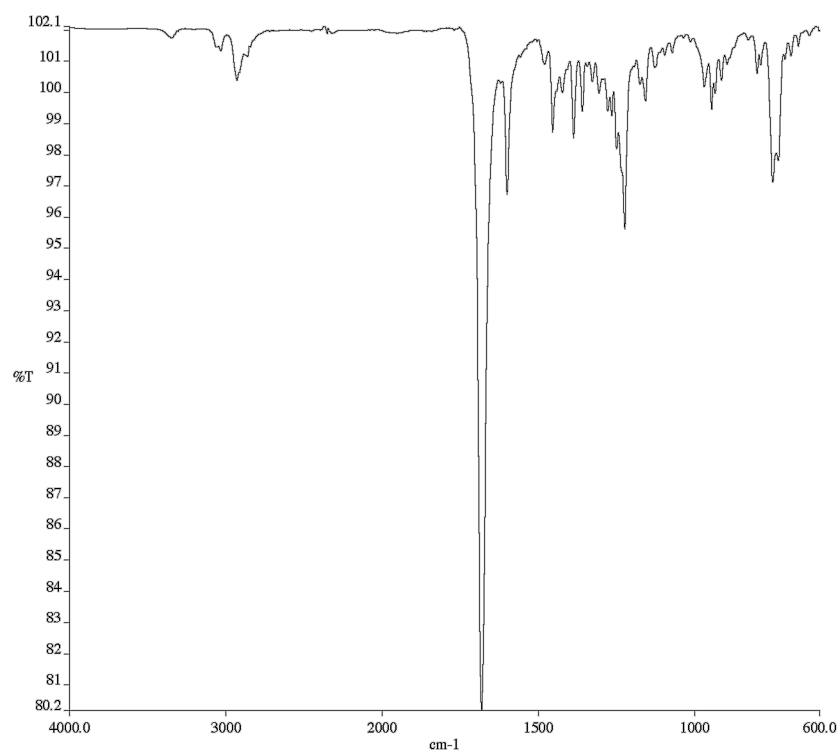


Figure A12.23 Infrared spectrum (Thin Film, NaCl) of compound **220b**

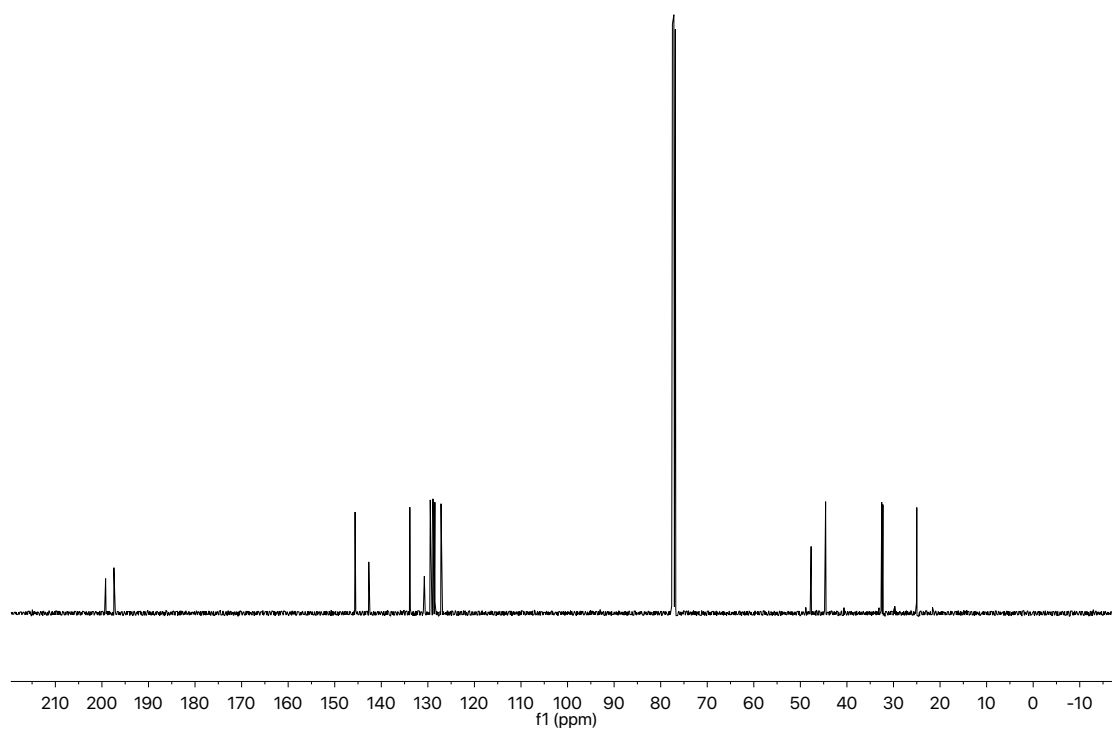


Figure A12.24 ¹³C NMR (101 MHz, CDCl₃) of compound **220b**

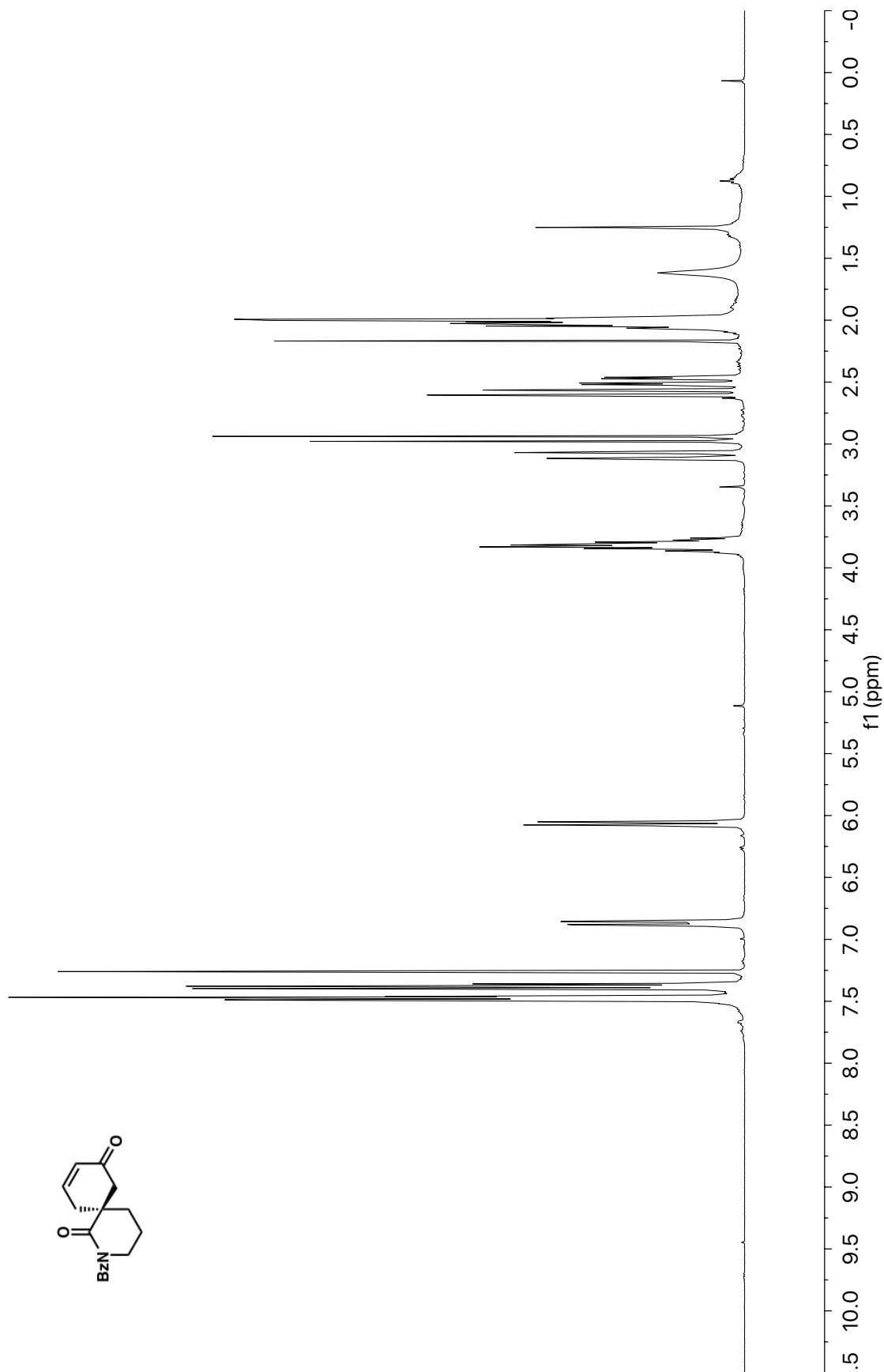


Figure A12.25 ^1H NMR (400 MHz, CDCl_3) of compound **220c**

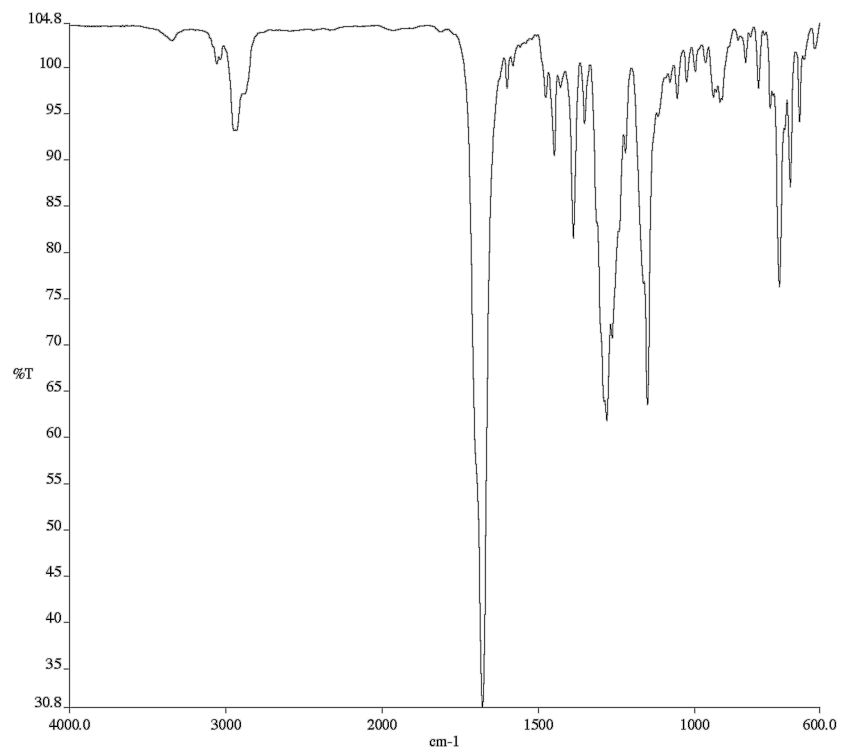


Figure A12.26 Infrared spectrum (Thin Film, NaCl) of compound **220c**

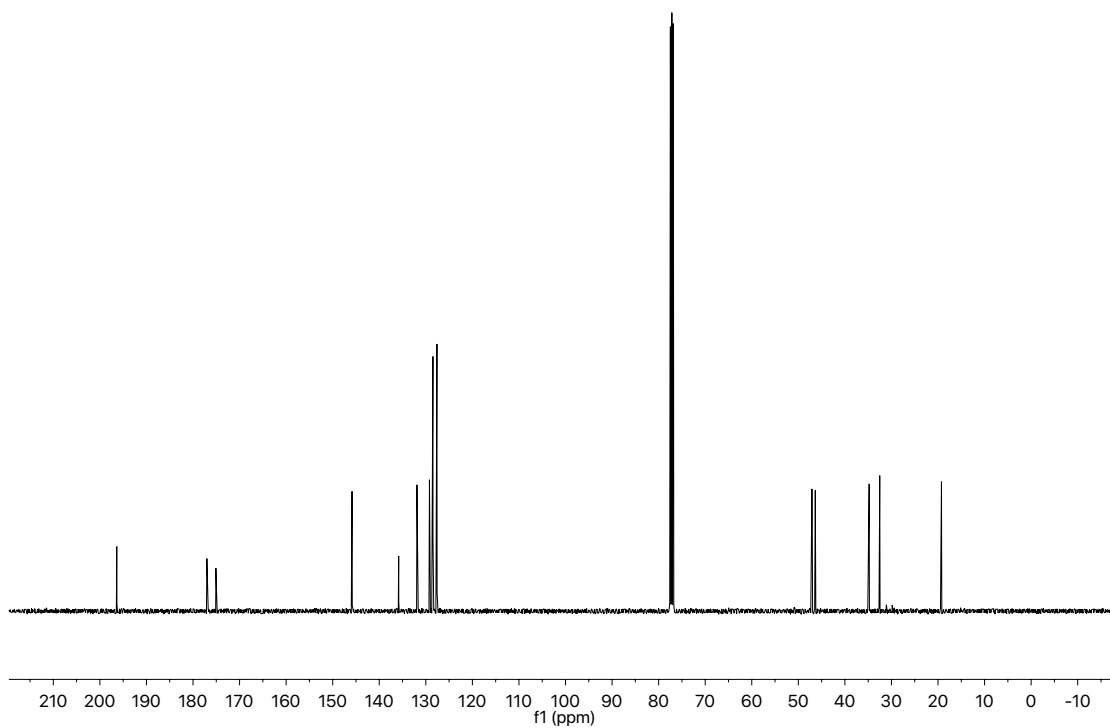


Figure A12.27 ¹³C NMR (101 MHz, CDCl₃) of compound **220c**

APPENDIX 13

Progress Toward the Synthesis of (+)-Isopalhinine A[†]

A13.1 INTRODUCTION AND BACKGROUND

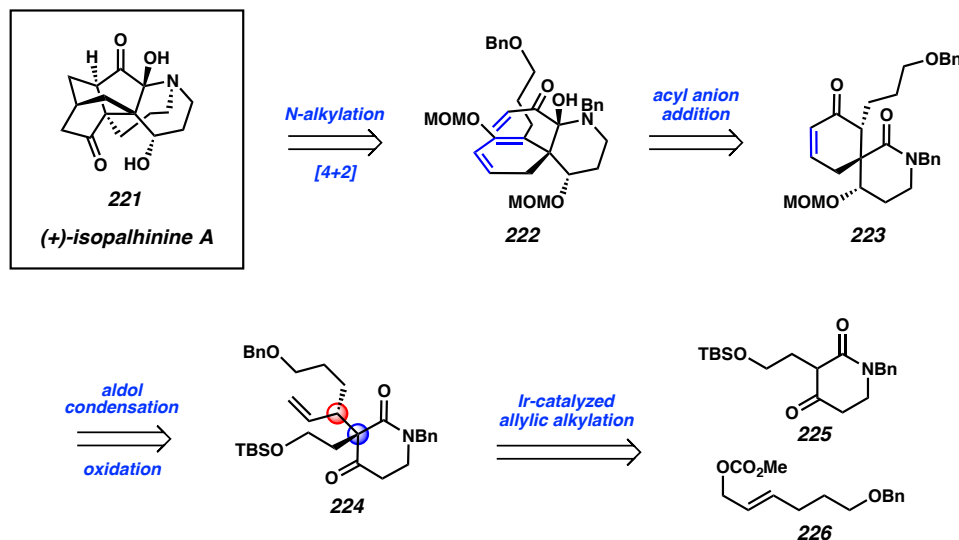
The *Lycopodium* alkaloids are family of complex, polycyclic, bioactive molecules that have been the subject of intense synthetic efforts over the past fifty years.¹ In 2013, a novel *Lycopodium* alkaloid, (+)-isopalhinine A (**221**, Scheme A13.1), was isolated containing an unprecedented (5/6/6/6/7) pentacyclic scaffold comprised of a densely functionalized isotwistane core containing vicinal all-carbon quaternary stereocenters appended to a 1-azabicyclo[4.3.1]decane moiety.² The complex architecture of (+)-isopalhinine A (**221**) has piqued the interest of the synthetic community, however, despite one report toward the isotwistane core,³ the natural product has yet to succumb to total synthesis. Herein, we detail our progress toward (+)-isopalhinine A (**221**) via a series of evolving strategies unified by the late-stage synthesis of the isotwistane core and the early construction of the functionalized nitrogen-containing heterocycle.

[†] Portions of this work were performed in collaboration with Dr. J. Caleb Hethcox.

A13.2 Iridium-Catalyzed Allylic Alkylation Route

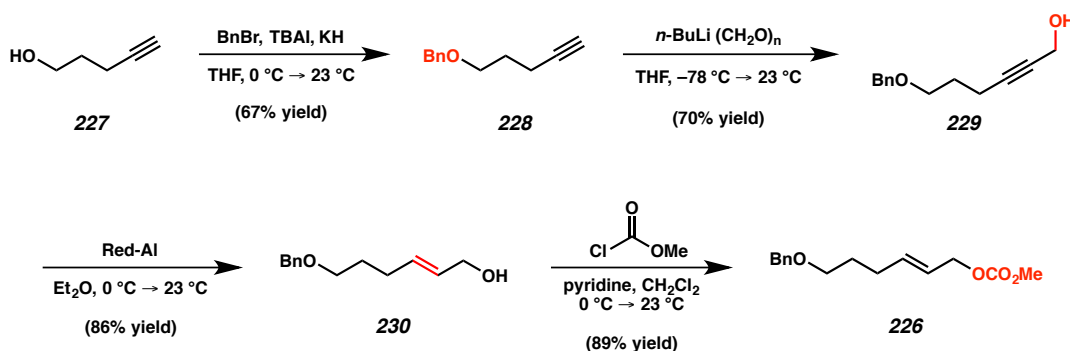
Our initial retrosynthetic analysis of (+)-isopalhinine A (**221**) began with disconnection of the caging architecture by C–N bond cleavage of the bridging propyl chain, followed by rupture of the central isotwistane core, which would be formed via an intramolecular Diels–Alder cycloaddition, to provide spirocycle **222** (Scheme A13.1). Spirocycle **222** would in turn be prepared by enolate formation and subsequent hemiaminal formation via the addition of an acyl anion equivalent into spirocyclic lactam **223**. Intramolecular aldol condensation and redox manipulation would then lead back to functionalized β -ketolactam **224**. Enantioenriched **224** would be generated from β -ketolactam **225** and allylic electrophile **226**, which would require the development of novel stereoselective iridium-catalyzed allylic alkylation technology as both the use of alkyl-substituted allylic electrophile **226** and endocyclic 1,3-dicarbonyl nucleophile **225** in iridium-catalyzed allylic alkylation chemistry is unprecedented in the literature. This synthetic strategy would enable rapid access to (+)-isopalhinine A (**221**) in as few as fourteen steps from **225** and **226**.

Scheme A13.1 Initial retrosynthetic analysis of (+)-isopalhinine A (**221**) via iridium-catalyzed allylic alkylation of endocyclic 1,3-dicarbonyl nucleophile **225**



We began our explorations into this initial synthetic plan with the synthesis of proposed iridium-catalyzed allylic alkylation substrates **225** and **226**. The preparation of allylic electrophile **226** proceeded via known allylic alcohol **230**, which was synthesized in three steps and 40% overall yield from commercially available 4-pentyn-1-ol (**227**, Scheme A13.2).^{4,5} Subsequent acylation with methyl chloroformate afforded requisite alkyl-substituted allylic electrophile **226** in 89% yield.⁶

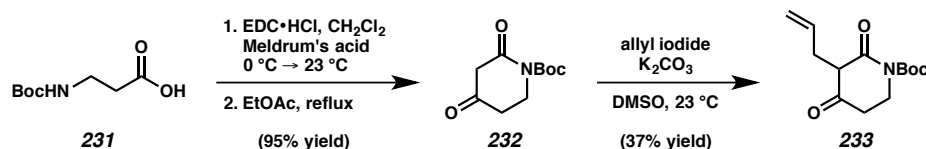
Scheme A13.2 Synthesis of alkyl-substituted electrophile **226**



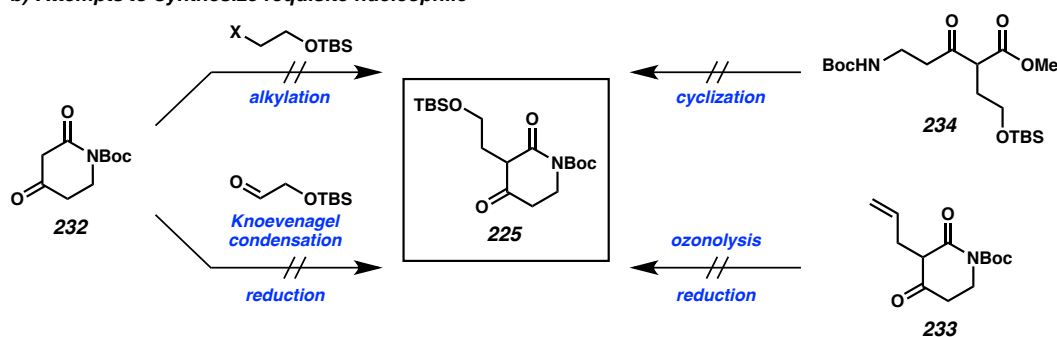
Synthesis of proposed endocyclic 1,3-dicarbonyl nucleophile **225** proved more challenging. While we were able to rapidly access allylated β -ketolactam **233** from Boc- β -alanine (**231**, Scheme A13.3a),⁷ we were unable to prepare desired alkyl-substituted nucleophile **225** (Scheme A13.3b). In our attempt to synthesize desired **225** we explored a variety of approaches including C-alkylation and Knoevenagel condensation/reduction sequences of β -ketolactam **232**, cyclization of β -ketoester **234**, as well as ozonolysis/reduction of allylated β -ketolactam **233**, but all routes were met with failure.

Scheme A13.3 Efforts to synthesize endocyclic 1,3-dicarbonyl nucleophiles

a) Synthesis of allylated nucleophile



b) Attempts to synthesize requisite nucleophile



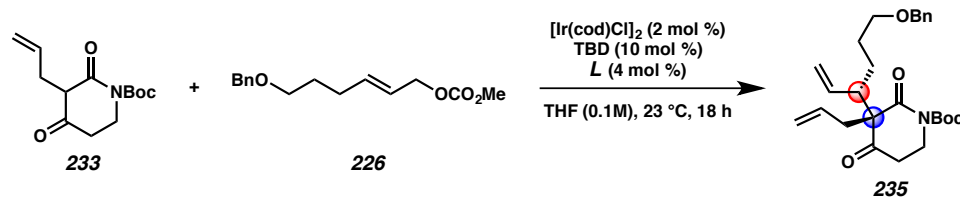
Unable to synthesize desired alkyl-substituted nucleophile **225**, we decided to instead explore the proposed iridium-catalyzed allylic alkylation reaction of alkyl-substituted electrophile **226** with allyl-substituted nucleophile **233**, postulating that we could subsequently perform redox manipulations on allylic alkylation product **235** in

order to intercept our original synthetic plan (Table A13.1). Our prior work on iridium-catalyzed allylic alkylation reactions with crotyl chloride primed us for the challenges involved in the use of alkyl-substituted electrophiles like **226**.⁸ Specifically, we anticipated poor regioselectivity in the allylic alkylation reaction as a result of the minimal stabilization of the allyl carbocation afforded by the alkyl substituent of **226**, in addition to poor reactivity due to the steric bulk of the alkyl group. Therefore, we hypothesized that we would need to explore novel ligand and additive combinations in the iridium-catalyzed allylic alkylation reaction in order to achieve both a selective and high yielding transformation.

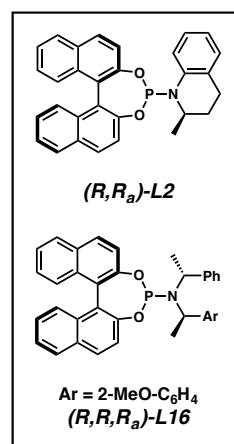
We began our studies employing our previously explored conditions for the iridium-catalyzed allylic alkylation of cinnamyl-derived electrophiles.⁹ Unsurprisingly, we observed that the reaction proceeded with poor branched selectivity, instead favoring the synthesis of the undesired linear product (Table A13.1, entry 1). Though base additives have been shown to play an important role in the selectivity of iridium-catalyzed allylic alkylations,^{8,9,10} an extensive investigation of bases proved unsuccessful in promoting branched selectivity in the reaction (entries 2–5). Turning our attention to the ligand, we found that the use of Alexakis ligand **L16**, instead of Me-THQphos (**L2**), in combination with LiBr or DABCO as additives, reversed the regioselectivity of the transformation to favor the synthesis of desired branched product **235** (entries 6 and 9). However, poor conversions (15% combined yield of branched and linear products, entry 9) and our inability to separate the branched and linear isomers by column chromatography led us to terminate our studies on endocyclic 1,3-dicarbonyl

nucleophiles in order to identify a more suitable nucleophile for the iridium-catalyzed allylic alkylation reaction.

Table A13.1 Optimization of the iridium-catalyzed allylic alkylation of endocyclic 1,3-dicarbonyl nucleophile **233**^a

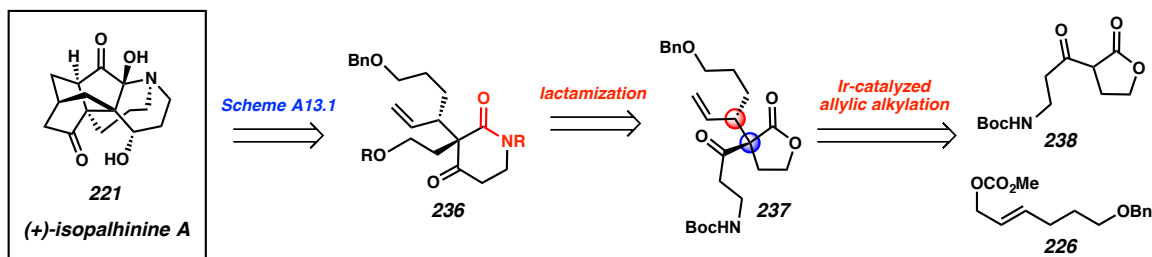


Entry	L	Additive (200 mol %)	b:l ^b
1	L2	LiBr	30:70
2	L2	LiO ^t Bu	27:73
3	L2	DABCO	39:61
4	L2	DMAP	12:88
5	L2	NEt ₃	28:72
6	L16	LiBr	64:36
7	L16	LiO ^t Bu	34:66
8	L16	Cs ₂ CO ₃	27:73
9	L16	DABCO	63:37
10	L16	DMAP	25:75
11	L16	NEt ₃	29:71

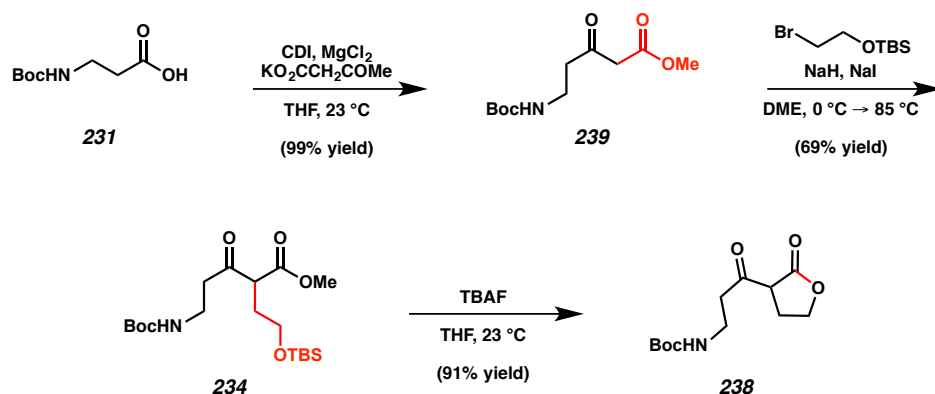


[a] Reactions performed on 0.2 mmol scale with 2:1 nucleophile/electrophile. [b] Determined by TOF LCMS analysis of the crude reaction mixture. [c] TBD = 1,3,5-triazabicyclo[4.4.0]dec-5-ene.

In a revised retrosynthetic analysis of (+)-isopalhinine A (**221**), we envisioned that we could employ lactone nucleophile **238**, in place of β -ketolactam **225**, in the proposed iridium-catalyzed allylic alkylation reaction of alkyl-substituted electrophile **226** (Scheme A13.4). Preserving our endgame strategy, allylic alkylation product **237** would then undergo lactamization to intercept key intermediate **236** from our original retrosynthesis (Scheme A13.1). We hypothesized that the similarity between lactone **238** and our group's previously explored β -ketoester nucleophiles^{9,11} would allow for a more facile optimization of the iridium-catalyzed allylic alkylation reaction.

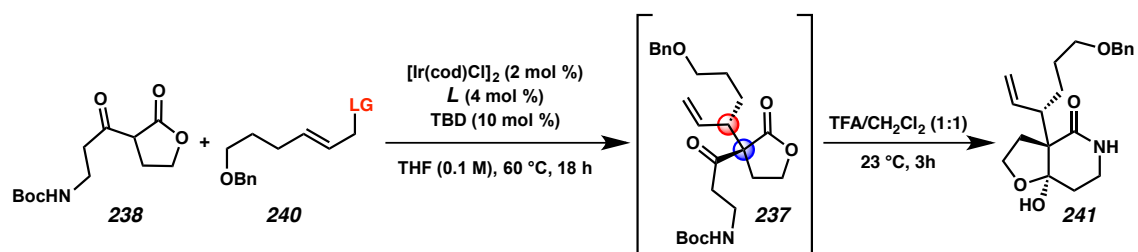
Scheme A13.4 Revised retrosynthetic analysis of (+)-isopalhinine A (**221**) via iridium-catalyzed allylic alkylation of lactone nucleophile **238**

To explore this idea, we synthesized lactone nucleophile **238** (Scheme A13.5). A Masamune-Claisen reaction of Boc- β -alanine (**231**) afforded β -ketoester **239** in 99% yield. Subsequent alkylation gave silyl ether **234**, which was then exposed to TBAF to effect deprotection and cyclization in order to provide lactone **238** in 91% yield.

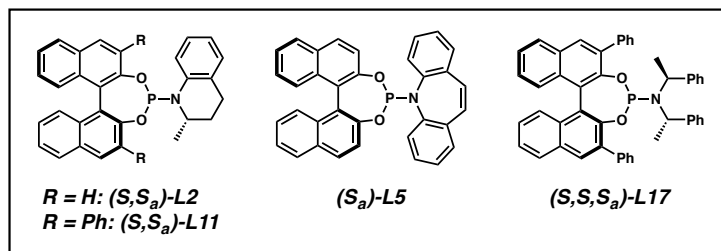
Scheme A13.5 Synthesis of lactone nucleophile **238**

With lactone nucleophile **238** in hand, we turned to explore its reactivity in the proposed iridium-catalyzed allylic alkylation reaction (Table A13.2). Due to early difficulties in isolating branched allylic alkylation product **237** in high purity, we were prompted to discover that γ -butyrolactone allylic alkylation product **237** could be elaborated to α -quaternary lactam derivative **241** in a one-pot fashion upon treatment with trifluoroacetic acid. Unlike lactone **237**, branched lactam **241** is separable from its linear isomer and is merely the hemiacetal of key intermediate **236** (Scheme A13.4).

With respect to the optimization of the allylic alkylation reaction, our group's previously reported conditions for the iridium-catalyzed allylic alkylation of crotyl chloride⁸ (Table A13.2, entry 1), poorly reactive allylic electrophiles¹² (entry 2), and β -ketoester nucleophiles⁹ (entry 3), all afforded poor selectivities when applied to our desired transformation. After extensive exploration of ligands and base additives, we found that the bulkier Feringa ligand **L17** in combination with DABCO gave desired lactam **241** in excellent yield, regio- and enantioselectivity, though poor diastereoselectivity (entry 5). We believe that the diastereoselectivity of this transformation can potentially be further improved by exploring dual catalytic systems.¹³ Of note, linear β -ketoester **234** (Scheme A13.5) was also explored in the iridium-catalyzed allylic alkylation reaction with electrophile **240**; however, the best results were observed using the same optimized conditions for lactam substrate **238** (Table A13.2, entry 5) and while the regioselectivity and yields were high (91:9 b:l, 94% yield), the diastereoselectivity was poor (1.2:1 dr) and all isomers were inseparable by column chromatography.

Table A13.2 Optimization of the iridium-catalyzed allylic alkylation of lactone **238**^a

Entry ^a	L	Base (200 mol %)	Additive (mol %)	LG	Yield (%) ^b	b:l ^c	dr ^c	ee (%) ^d
1	L11	proton sponge	LiCl (400)	Cl	87	87:13	1.4:1	68
2	L5	–	BEt ₃ (200)	OCO ₂ Me	49	31:69	1.2:1	–
3	L2	–	LiBr (200)	OCO ₂ Me	11	13:87	1.1:1	–
4	L17	–	LiBr (200)	OCO ₂ Me	50	57:43	1.0:1	–
5	L17	DABCO	–	OCO ₂ Me	79	99:1	1.5:1	96

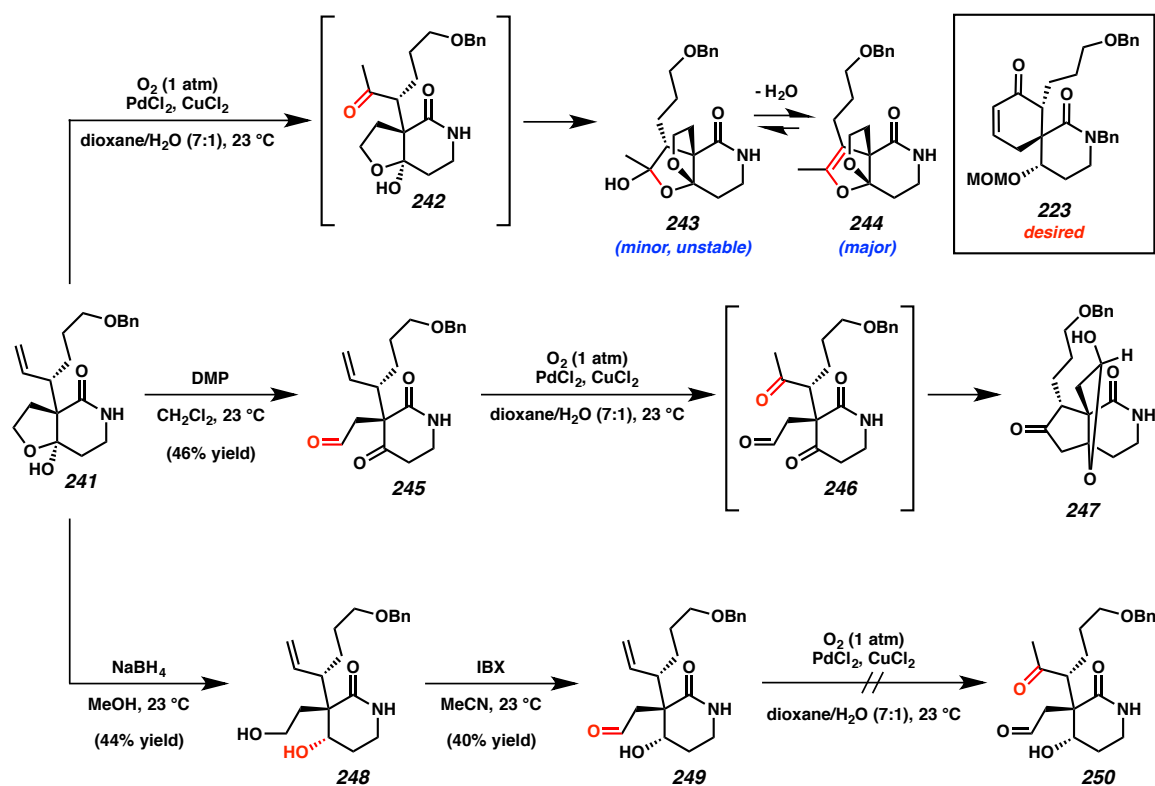


[a] Reactions performed on 0.1 mmol scale with 2:1 nucleophile/electrophile. [b] ¹H NMR yield based on internal standard. [c] Determined by ¹H NMR analysis of the crude reaction mixture. [d] Determined via chiral HPLC. [e] TBD = 1,3,5-triazabicyclo[4.4.0]dec-5-ene.

We next turned our attention to the advancement of bicyclic hemiacetal **241** to spirocyclic enone **223** (Scheme A13.6), which would set the stage for the pivotal acyl anion addition. Toward this end, we performed a Wacker oxidation of pendant olefin **241** (Scheme A13.6, top). However, despite a variety of conditions, we observed cyclization of the hemiacetal moiety into the nascent ketone of **242** forming new unstable hemiacetal **243**, which readily dehydrated to dihydrofuran **244**. In an effort to circumvent this undesired reactivity, we instead oxidized hemiacetal **241** to aldehyde **245** using Dess–Martin periodinane prior to the Wacker oxidation (Scheme A13.6, middle). Unfortunately, Wacker product **246** suffered an undesirable intramolecular aldol reaction in situ, delivering undesired 5-membered aldol product **247**. Lastly, we discovered that

we could perform a directed reduction of hemiacetal **241** using the hydroxyethyl group of the opened hemiacetal to access diol **248** (Scheme A13.6, bottom). Subsequent selective oxidation of the primary alcohol afforded aldehyde **249**. To our disappointment, attempts to perform a Wacker oxidation on aldehyde **250** proved unsuccessful. It is likely that protection of the primary alcohol and/or amide is required for the Wacker oxidation to proceed.

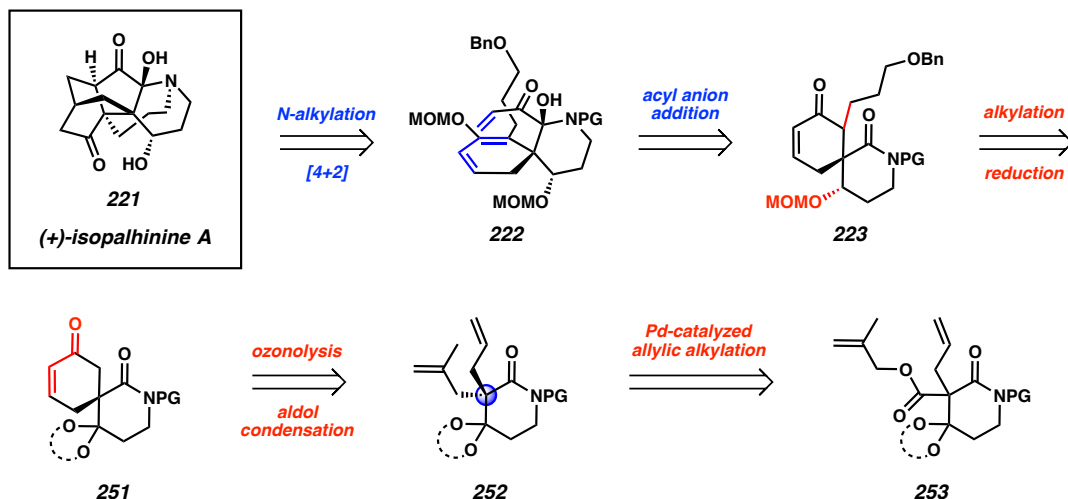
Scheme A13.6 Attempts to advance bicycle **241** to key spirocyclic intermediate **223**



A13.3 PALLADIUM-CATALYZED ALLYLIC ALKYLATION ROUTE USING A MASKED STABILIZED LACTAM ENOLATE

Concurrent with our efforts to develop an iridium-catalyzed allylic alkylation approach to (+)-isopalhinine A (**221**), an alternate route to the natural product relying on a palladium-catalyzed allylic alkylation was explored (Scheme A13.7). Maintaining the endgame strategy from the iridium-catalyzed allylic alkylation route (Scheme A13.1), this alternate retrosynthetic analysis leads through the same disconnects to spirocyclic intermediate **223**, which in this approach would be synthesized via an α -alkylation and diastereoselective reduction of the corresponding ketone of acetal **251**. Cyclic enone **251** would then arise from the ozonolysis and aldol condensation enantioenriched lactam **252**, which in turn would result from an enantioselective palladium-catalyzed decarboxylative allylic alkylation of substrate **253**. The key advantage to this alternate route is the elimination of the need to control diastereoselectivity in the allylic alkylation reaction, which was the main challenge in the aforementioned iridium-catalyzed allylic alkylation route. Moreover, the tertiary stereocenter of the vicinal tertiary and quaternary stereocenter set in the iridium-catalyzed allylic alkylation pathway was to be ablated later in the synthesis in the formation of cyclohexadiene **222** (Scheme A13.1 and Scheme A13.7), and therefore our efforts to achieve a diastereoselective reaction were ultimately unnecessary.

Scheme A13.7 Retrosynthetic analysis of (+)-isopalhinine A (**221**) via palladium-catalyzed allylic alkylation of masked stabilized lactam enolate **253**

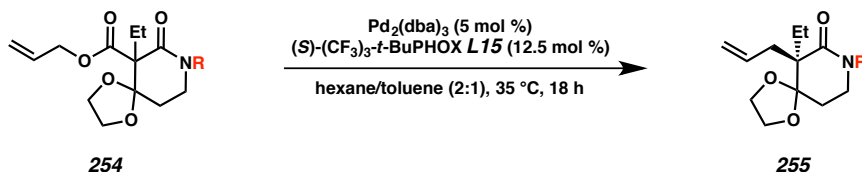


At the time we began our studies into this palladium-catalyzed route, the Stoltz group had previously examined the palladium-catalyzed decarboxylative alkylation of enolate-stabilized enol carbonates for the synthesis of all-carbon quaternary stereocenters¹⁴ as well as developed the asymmetric palladium-catalyzed decarboxylative allylic alkylation of lactams to reach quaternary *N*-heterocycles, specifically lactams, in high enantioselectivities.¹⁵ However, enolate-stabilized lactams such as **253** had yet to be explored in our palladium-catalyzed allylic alkylation chemistry. As such, we utilized easy-to-access model substrate **254** in order to explore the effects of protecting groups on yield and selectivity in our desired allylic alkylation reaction (Table A13.3). Through a series of optimization studies, we found that the nature of both the nitrogen (Table A13.3a) and ketone (Table A13.3b) protecting groups play pivotal roles on the enantioselectivity of the palladium-catalyzed decarboxylative alkylation of enolate-stabilized lactam **253**. Ultimately, we determined that protecting the amide nitrogen of model lactam **256** with a *para*-methoxy-benzoyl group (pMBz) and the ketone

functionality as a gem-dimethyl-dioxane moiety allowed us to access corresponding product **257** in the highest enantioselectivity (93% ee) and a moderate 46% yield.

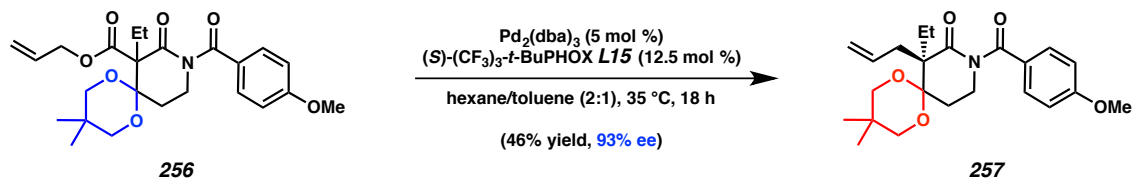
Table A13.3 Optimization of protecting groups for the palladium-catalyzed allylic alkylation reaction

a) Optimization of Lactam Protecting Group



Entry	R	Conversion (%)	ee (%)
1	Bz	42	48
2 ^a	Bn	7	29
3	4-MeO-Bz	75	62
4	3,4,5-triMeO-Bz	86	61
5	4-MeO-benzenesulfonyl	79	63
6	Boc	87	53

b) Optimization of Ketone Protecting Group

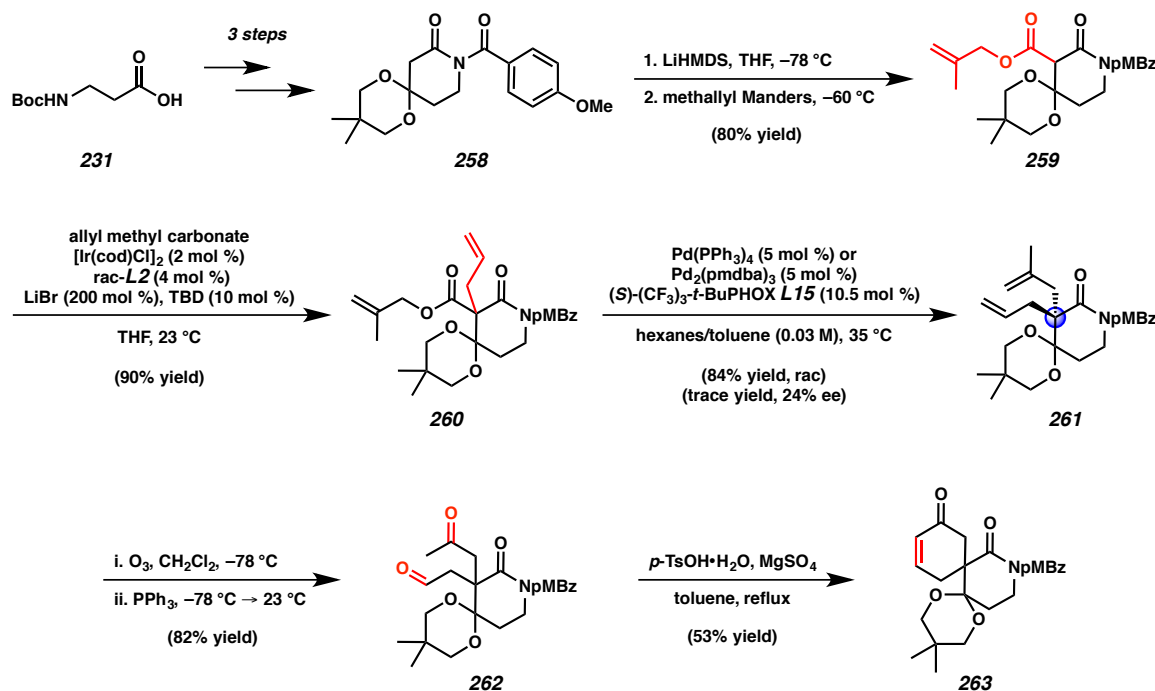


[a] Reaction performed in cyclohexane.

Having completed these optimization efforts, we moved to pursue the preparation of synthetically relevant substrate **260** for the proposed palladium-catalyzed allylic alkylation reaction (Scheme A13.8). Protected lactam **258** can be accessed in three steps from Boc-β-alanine (**231**). Subsequent acylation and allylation provided desired allylic alkylation substrate **260**. Of note, iridium-catalyzed allylic alkylation was required for the allylation of **259**, as we found that all attempts to allylate extremely sterically demanding **259** using standard methods resulted in returned starting material or deprotection of the starting material. Treatment of **260** with $\text{Pd}(\text{PPh}_3)_4$ afforded racemic product *rac*-**261** in a

high 84% yield. Unfortunately, attempts to render the allylic alkylation reaction enantioselective utilizing our optimization conditions from model system **257** (Table A13.3) resulted in only modest enantioselectivities and yields, likely due to the now increased steric bulk around the reactive site. Additional studies into alternate palladium-catalyzed allylic alkylation systems, specifically those utilizing Trost ligands known to tolerate more sterically encumbered substrates,¹⁶ also showed poor reactivity. Nonetheless, we were pleased to find that we could advance *rac*-**261** through an ozonolysis and an acid-catalyzed aldol reaction to provide desired spirocyclic enone **263**.

Scheme A13.8 Synthesis of spirocyclic intermediate **263** via palladium-catalyzed allylic alkylation^a

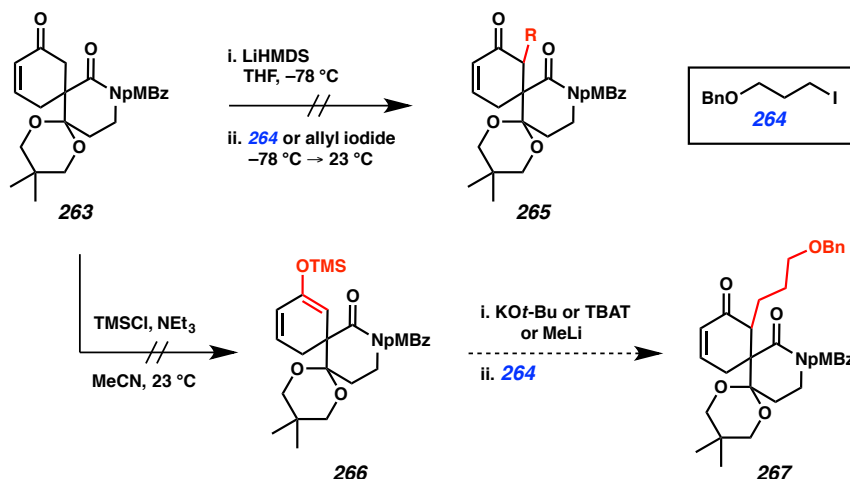


[a] pMBz = 4-MeO-Bz

We next attempted to alkylate spirocyclic enone **263** in order to obtain α'-alkylated intermediate **267** (Scheme A13.9). To our dismay, early efforts to directly alkylate or allylate **263** proved unsuccessful, likely due to the sterically hindered

neopentyl nature of the intermediate enolate, as well as the possibility of competitive γ -functionalization. We also found that forming silyl enol ether **266** was not fruitful, and were thus unable to explore alternate alkylation strategies.

Scheme A13.9 Attempted alkylations of spirocyclic enone **263**

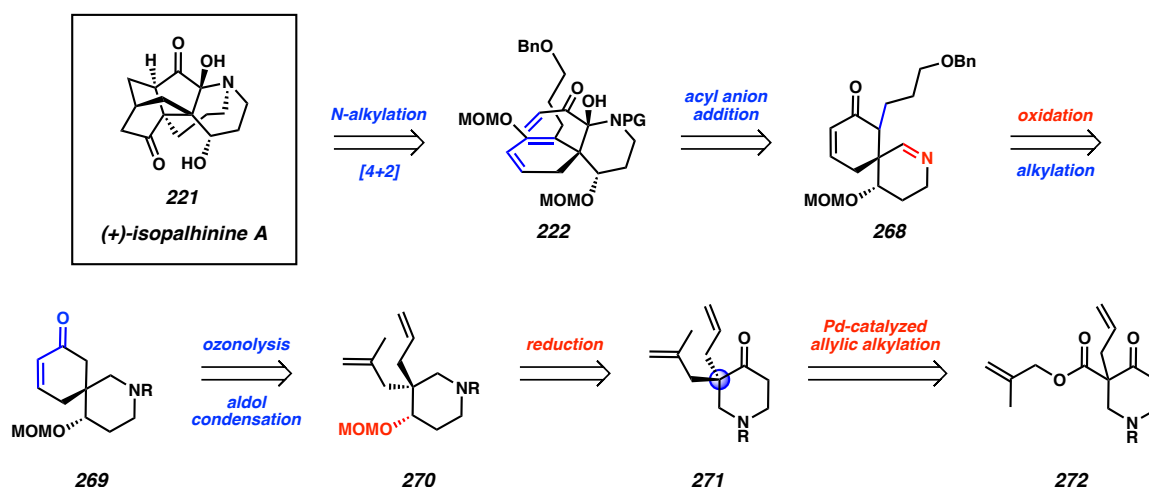


A13.4 PIPERIDONE PALLADIUM-CATALYZED ALLYLIC ALKYLATION ROUTE

In light of our inability to achieve a highly enantioselective palladium-catalyzed allylic alkylation using enolate-stabilized lactam substrate **253** (Section A13.3), we chose to investigate a modified palladium-catalyzed allylic alkylation route that employed a class of substrates already known to be successful in our group's methodology: piperidones (Scheme A13.10).¹⁷ In this revised retrosynthetic analysis of (+)-isopalhinine A (**221**), the *N*-alkylation and intramolecular Diels–Alder disconnects of the previous routes remain, however [4+2] substrate **222** is now the result of an acyl anion addition into imine **268**, which would arise from a late-stage oxidation of piperidine **269**. Similar to the previous palladium-catalyzed allylic alkylation route, enone **269** would be formed

via ozonolysis and aldol condensation of diene **270**. We envisioned that ether **270** would be prepared by diastereoselective reduction of enantioenriched piperidone **271**, which would be formed via enantioselective palladium-catalyzed decarboxylative allylic alkylation of substrate **272**.

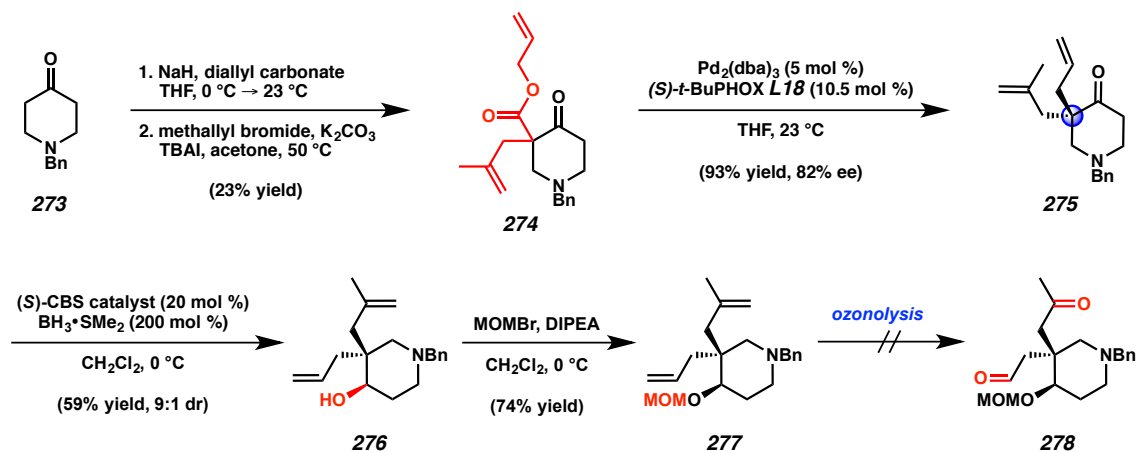
Scheme A13.10 Retrosynthetic analysis of (+)-isopalhinine A (**221**) via palladium-catalyzed allylic alkylation of piperidone **272**



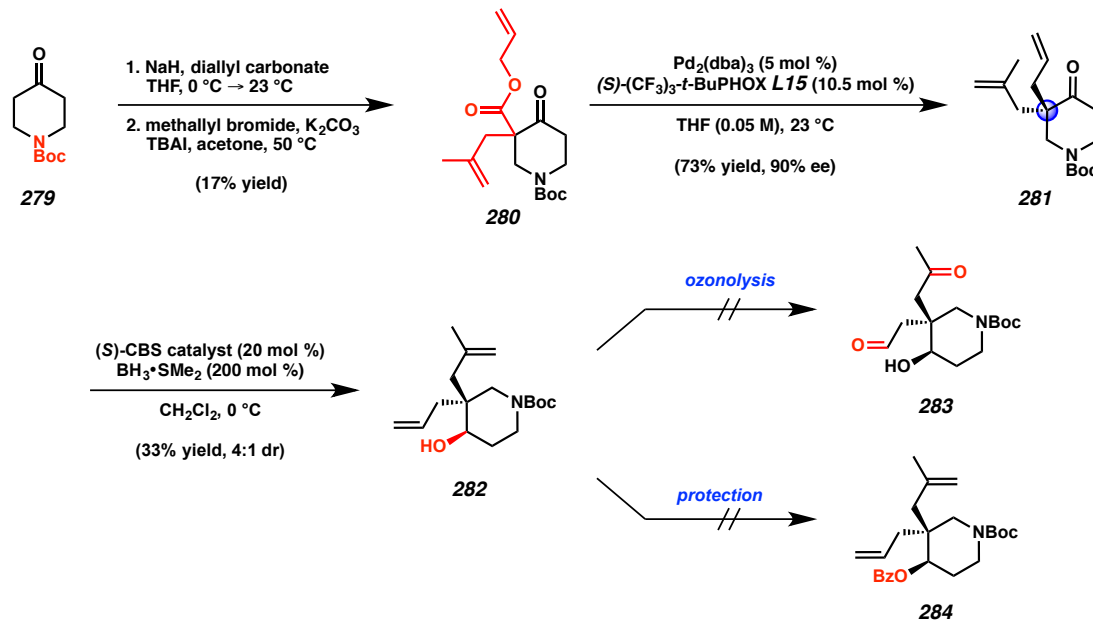
We first explored the feasibility of this revised plan by investigating the reactivity of benzyl-protected piperidone **273** (Scheme A13.11). Acylation and alkylation afforded allylic alkylation substrate **274**, which we were pleased to find smoothly underwent the proposed palladium-catalyzed decarboxylative allylic alkylation to afford corresponding product **275** in excellent 93% yield and good 82% ee. Of note, product **275** is the incorrect enantiomer to access (+)-isopalhinine A (**221**), however, the challenges of preparing the requisite (*R*)-**L15** led us to explore the early chemistry of this route using the easy-to-access **275**. Subsequent diastereoselective reduction of ketone **275** using CBS catalyst delivered alcohol **276** in a 9:1 dr. We found that while we were able to protect the hydroxyl group to give **277**, we were unable reveal the masked bis-carbonyl motif via

ozonolysis of diene **277**. Realizing that the basic nitrogen of **277** was likely problematic in the ozonolysis reaction, we directed efforts toward investigating alternative protecting groups for piperidone **273**, ultimately selecting a Boc group.

Scheme A13.11 Attempts to advance benzyl-protected piperidone **273**

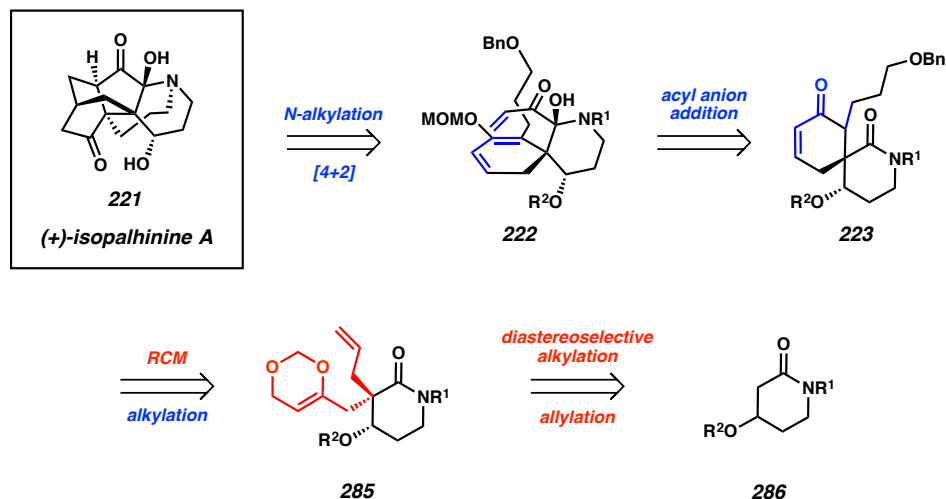


Boc-protected piperidone **279** performed similarly to benzyl-protected analogue **273** in the palladium-catalyzed decarboxylative allylic alkylation reaction, providing product **281** in 73% yield and 90% ee (Scheme A13.12). However, the CBS reduction of ketone **281** to give hydroxy **282** proceeded in significantly diminished yields and a now moderate 4:1 dr. Moreover, despite exploring a variety of conditions, efforts to either protect alcohol **282** or perform an ozonolysis were not successful. Given these difficulties and our concern with successfully performing the proposed selective late-stage oxidation to access imine **262** (Scheme A13.10), we elected to conclude explorations into this route.

Scheme A13.12 Attempts to advance Boc-protected piperidone **279****A13.5 DIASTEREOSELECTIVE ROUTE**

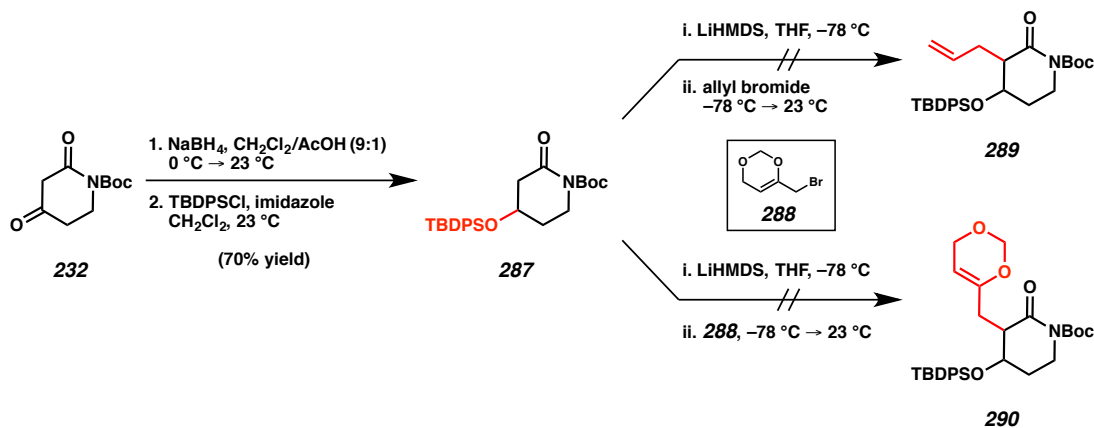
While working to develop an enantioselective route to key spirocyclic intermediate **223**, we wondered whether we could carry out a rapid, diastereoselective synthesis of **223** that would enable the preparation of large quantities of the compound for the purposes of exploring the proposed late-stage chemistry (Scheme A13.13). Toward this end, we envisioned that spirocyclic intermediate **223** could arise from an alkylation and ring closing metathesis of unmasked dioxin **285**,¹⁸ which would now be the result of a diastereoselective alkylation/allylation sequence of hydroxy lactam **286**.

Scheme A13.13 Retrosynthetic analysis of (+)-isopalhinine A (**221**) via diastereoselective alkylation/allylation sequence



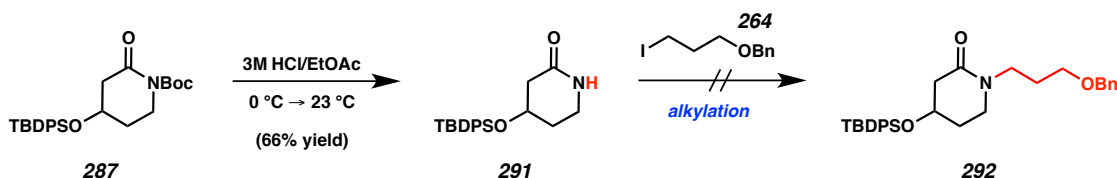
In the forward direction, we began our studies with known β -ketolactam **232** (Scheme A13.14). Reduction of the ketone functionality with sodium borohydride followed by protection of the resultant hydroxyl group gave silyl ether **287** in 70% yield. Disappointingly, attempts to allylate or alkylate lactam **287** returned only deprotected starting material.

Scheme A13.14 Attempts at diastereoselective functionalization

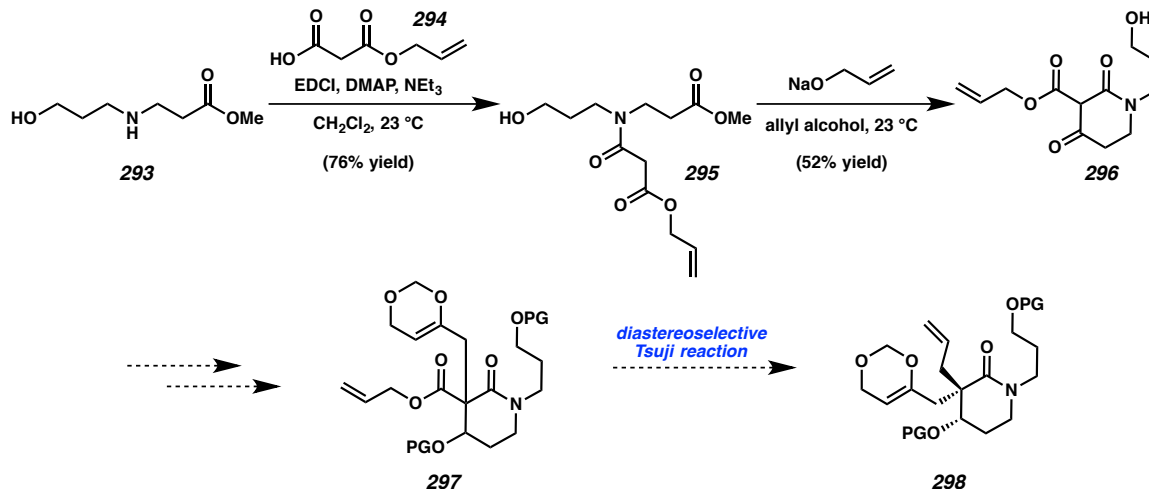


Realizing that we would need to replace the Boc group of lactam **287** with a base-stable protecting group in order to promote functionalization, we considered alkylating lactam **291** with the requisite hydroxypropyl tether required for the proposed late-stage *N*-alkylation event (Scheme A13.13). Unfortunately, despite significant efforts to *N*-alkylate lactam **291**, we observed only elimination of the iodide on the alkylating reagent or elimination of the silyl ether of **291** to form an enamide (Scheme A13.15).

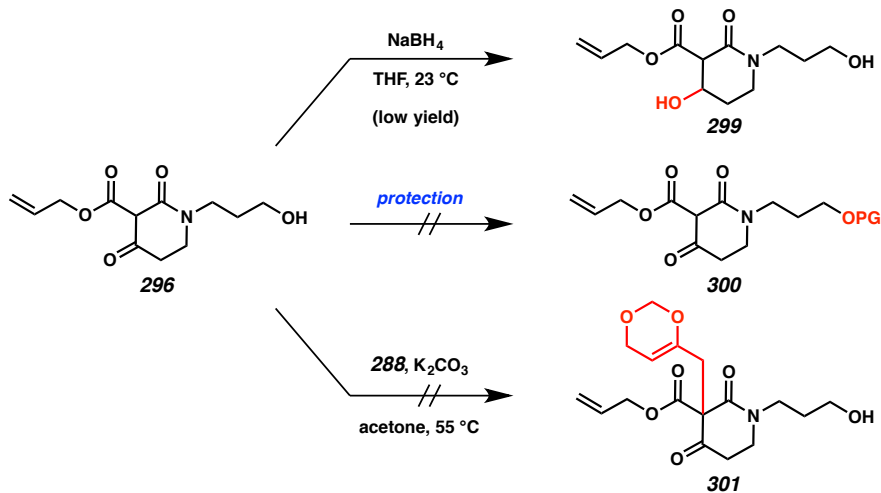
Scheme A13.15 Requisite propyl chain as a nitrogen protecting group



To circumvent the issues we were observing with functionalizing lactam **287**, we explored an alternative route to RCM precursor **298** that did not require the use of strong base, but would instead rely on a diastereoselective Tsuji reaction^{18a} (Scheme A13.16). In this synthetic sequence, secondary amine **293** is acylated with **294** to give amide **295** in 76% yield. Subsequent Dieckmann condensation delivered functionalized β -ketolactam **296** in a moderate 50% yield.

Scheme A13.16 Non-strong base route to RCM precursor **298**

We were disappointed to find that attempts to advance β -ketolactam **296** to Tsuji substrate **297** were unsuccessful (Scheme A13.17). Specifically, we found that we could only reduce ketone **296** in low yields using sodium borohydride (Scheme A13.17, top). Efforts to protect the resultant hydroxy group resulted in retro Dieckmann products of **296** (Scheme A13.17, middle), as did attempts to alkylate **296** with dioxin **288**¹⁸ (Scheme A13.7, bottom).

Scheme A13.17 Attempts to advance β -ketolactam **296**

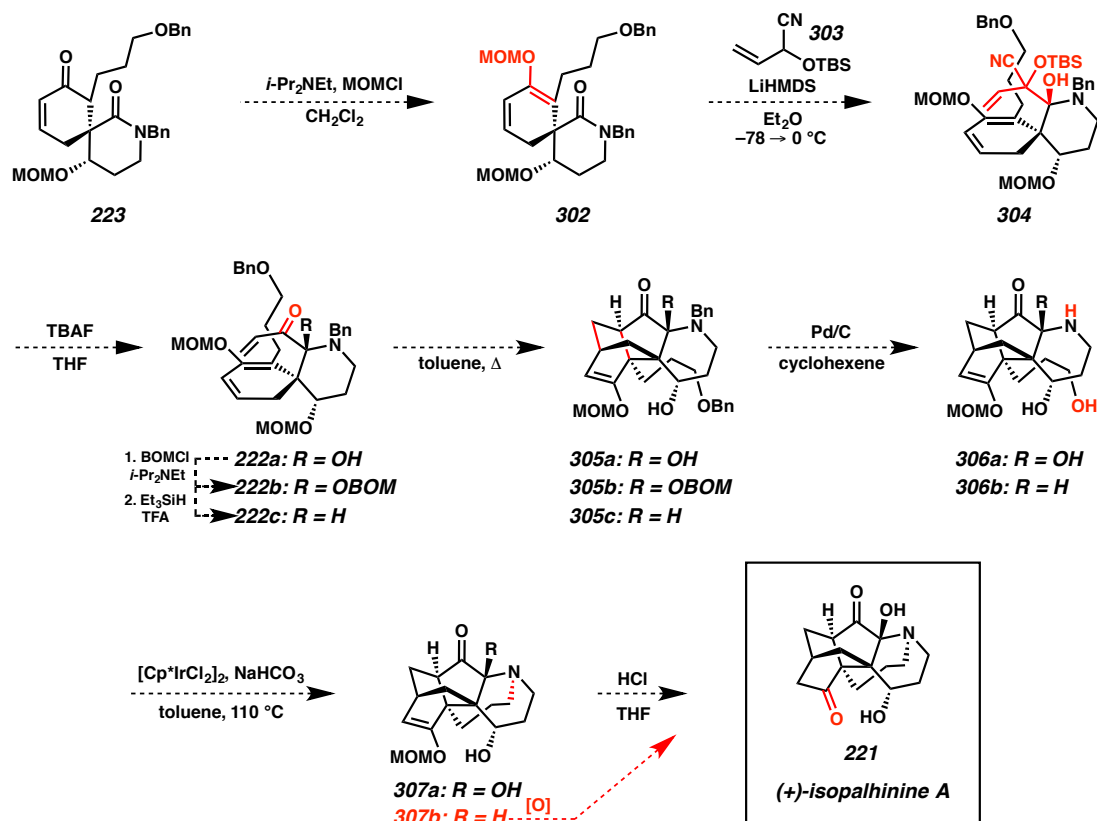
A13.6 FUTURE DIRECTIONS AND PROPOSED LATE-STAGE CHEMISTRY TO ACCESS (+)-ISOPALHININE A

Should additional efforts enable access to key spirocyclic intermediate **223** via any of the aforementioned routes, the proposed late-stage chemistry to synthesize (+)-isopalhinine A (**221**) is detailed in Scheme A13.18. Enone **223** will be converted to desired cyclohexadiene **302** by enolization and trapping with chloromethyl methyl ether. Diastereoselective addition of an acrolein-derived acyl anion equivalent (e.g., **303**) to the amide functionality of **302** by approach of the anion over the olefinic group (i.e., α -face attack) will then provide Diels–Alder substrate **304** upon revealing the carbonyl group by desilylation and cyanide extrusion. Such masked acyl-anion additions to lactams have ample precedent in the literature,¹⁹ and we anticipate that the keto aminal (e.g., **222a**) will likely be stable to subsequent manipulation, potentially as the free hydroxyl.²⁰ If the need arises, we anticipate protecting hemiaminal **222a** as a BOM ether (**222b**), or alternatively, reducing to the α -amidocarbonyl system (i.e., **222c**).

From spirocycle **222**, an intramolecular diastereoselective [4+2] Diels–Alder cycloaddition will furnish the isotwistane core of (+)-isopalhinine A (**221**) to yield **305**.²¹ The diastereoselectivity of the IMDA is controlled by the tethering of the dienophile to the top face of the spirocycle. Cleavage of the benzyl residues will occur via transfer hydrogenolysis (note: BOM cleavage would occur here if **305b** is employed) to yield aminoalcohol **306**.²² Subsequent *N*-alkylation via an iridium-catalyzed “borrowing hydrogen”-type alkylation will install the final ring.²³ Finally, removal of remaining MOM group with acid will deliver (+)-isopalhinine A (**221**). If we are confronted with stability issues that require the use of ketone **307b**, a late-stage oxidation (e.g., with

$\text{K}_2\text{Fe}(\text{CN})_6/\text{NaHCO}_3/\text{H}_2\text{O}$,²⁴ $\text{O}_2/\text{SiO}_2/\text{H}_2\text{O}$,²⁵ MnO_2 ,²⁶ $\text{NaOMe}/\text{O}_2/\text{H}_2\text{O}$ ²⁷) will be employed to install the aminal group and reach (+)-isopalhinine A (**221**).

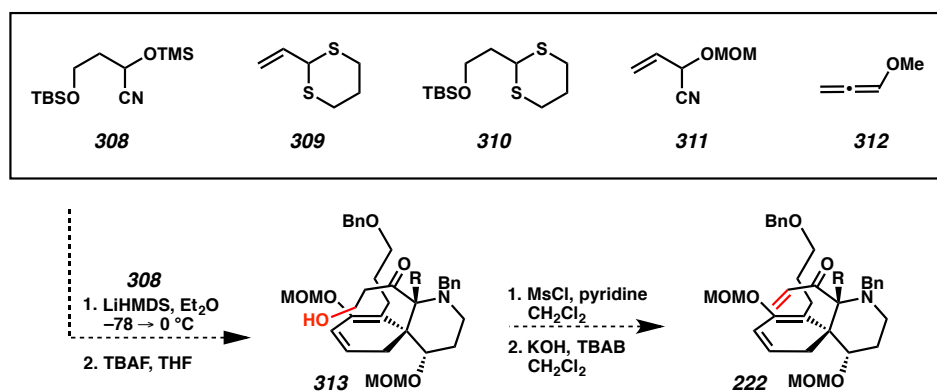
Scheme A13.18 Proposed route to (+)-isopalhinine A (**221**) from alkylated spirocycle **223**



Preliminary studies have been undertaken to investigate the proposed acyl anion addition chemistry in model systems. While the addition of aryl-functionalized silyl cyanohydrins into lactams is known,¹⁹ acrolein-derived silyl cyanohydrin, such as **303**, additions have yet to be explored. Our early studies indicated that γ -addition of acrolein equivalent **303** is a competitive pathway. As such, we anticipate that future studies into this addition chemistry will involve alternative silyl cyanohydrins, especially those with masked olefins²⁸ (e.g., **308** or **310**) or electronic biases for α -addition (e.g., **312**²⁹), that

will preclude γ -addition (Scheme A13.19). In the case of masked olefin equivalents, following addition, the olefin functionality of **222** can then be exposed by mesylation and elimination of the primary alcohol in addition product **313**.³⁰

Scheme A13.19 Alternative acyl anion equivalents



A13.7 CONCLUSIONS

In summary, we have detailed our efforts toward the total synthesis of (+)-isopalhinine A (**221**) including routes featuring an iridium-catalyzed allylic alkylation of an alkyl-substituted electrophile, a palladium-catalyzed allylic alkylation of an enolate-stabilized lactam, a palladium-catalyzed allylic alkylation of a piperidone, and a diastereoselective alkylation/allylation sequence. Each of these routes to (+)-isopalhinine A (**221**) preserve the endgame strategy discussed in Section A13.6, wherein variants of key spirocycle **223** is imagined to be advanced to the natural product. Future studies may include further optimization of the iridium-catalyzed allylic alkylation reaction of Section A13.2 using dual metal catalysis and alternative alkylation methods of palladium-catalyzed allylic alkylation intermediate **263** of Section A13.3. The successful completion of this work would represent the first total synthesis of (+)-isopalhinine A (**221**).

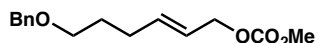
A13.8 EXPERIMENTAL SECTION**A13.8.1 MATERIALS AND METHODS**

Unless otherwise stated, reactions were performed in flame-dried glassware under an argon or nitrogen atmosphere using dry, deoxygenated solvents. Solvents were dried by passage through an activated alumina column under argon. Commercially obtained reagents were used as received. Chemicals were purchased from Sigma Aldrich/Strem/Alfa Aesar/Oakwood Chemicals and used as received. Reaction temperatures were controlled by an IKA Mag temperature modulator. Glove box manipulations were performed under a nitrogen atmosphere. Thin-layer chromatography (TLC) and preparatory TLC was performed using E. Merck silica gel 60 F254 precoated plates (0.25 mm) and visualized by UV fluorescence quenching, KMnO_4 , or *p*-anisaldehyde staining. SiliaFlash P60 Academic Silica gel (particle size 0.040–0.063 mm) was used for flash chromatography. Analytical chiral HPLC was performed with an Agilent 1100 Series HPLC utilizing a Chiralpak AD-H column (4.6 mm x 25 cm), Chiralpak AD column (4.6 mm x 25 cm), or a Chiralpak OJ column (4.6 mm x 25 cm), all obtained from Daicel Chemical Industries, Ltd. with visualization at 210 nm. Analytical SFC was performed with a Mettler SFC supercritical CO_2 analytical chromatography system utilizing a Chiralpak OJ-H column (4.6 mm x 25 cm) or Chiralpak AS-H column (4.6 mm x 25 cm) obtained from Daicel Chemical Industries, Ltd. with visualization at 210 nm. ^1H NMR spectra were recorded on a Bruker Avance HD 400 MHz spectrometer or a Varian Inova 500 MHz spectrometer and are reported relative to residual CHCl_3 (δ 7.26 ppm). ^{13}C NMR spectra were recorded on a Bruker Avance HD 400 MHz spectrometer or a Varian Inova 500 MHz spectrometer and are

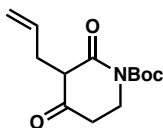
reported relative to residual CDCl_3 (δ 77.16 ppm). Data for ^1H NMR are reported as follows: s = singlet, d = doublet, t = triplet, q = quartet, p = pentet, sept = septuplet, m = multiplet, br s = broad singlet. Data for ^{13}C NMR are reported in terms of chemical shifts (δ ppm). Some reported spectra include minor solvent impurities of benzene (δ 7.36 ppm), water (δ 1.56 ppm), ethyl acetate (δ 4.12, 2.05, 1.26 ppm), methylene chloride (δ 5.30 ppm), grease (δ 1.26, 0.86 ppm), and/or silicon grease (δ 0.07 ppm), which do not impact product assignments. IR spectra were obtained using a Perkin Elmer Paragon 1000 spectrometer using thin films deposited on NaCl plates and reported in frequency of absorption (cm^{-1}).

A13.8.1.1 Preparation of Known Compounds

Previously reported methods were used to prepare ligands (*R,R,R_a*)-**L16**³¹ and (*S,S,S_a*)-**L17**.³² (*S*)-**L18** was purchased from Sigma Aldrich. For the preparation of ligands **L2**, **L5**, **L11**, and **L15**, see chapter or appendix where initially disclosed. Literature procedures were used to prepare known compounds **228–230**,^{4,5} **232**,⁷ **239**,³³ **264**,³⁴ **287**,³⁵ **293**.³⁶

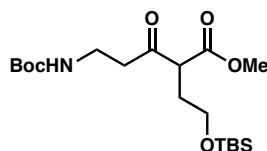
A13.8.2 EXPERIMENTAL PROCEDURES AND SPECTROSCOPIC DATA**A13.8.2.1 Experimental Procedures and Spectroscopic Data for the Synthesis of Synthetic Intermediates in Section A13.2**

(E)-6-(Benzyloxy)hex-2-en-1-yl methyl carbonate (226). Pyridine (2.8 mL, 34 mmol, 3.0 equiv) was added to a solution of alcohol **230**^{4,5} (2.4 g, 11 mmol, 1.0 equiv) in CH₂Cl₂ (100 mL) at 0 °C, followed by addition of methyl chloroformate (1.3 mL, 17 mmol, 1.5 equiv) dropwise. The resulting solution was allowed to warm to ambient temperature and was stirred for 18 h. The reaction was quenched with the addition of 1 M HCl (20 mL) and the aqueous layer was extracted with CH₂Cl₂ (3 x 30 mL). The combined organic layers were washed with brine (20 mL), dried over Na₂SO₄, and concentrated under reduced pressure. The crude product was purified by silica gel flash column chromatography (10% EtOAc/hexanes) to give carbonate **226** as a colorless oil (2.7 g, 89% yield): ¹H NMR (400 MHz, CDCl₃) δ 7.43 – 7.28 (m, 5H), 5.91 – 5.72 (m, 1H), 5.60 (dtt, *J* = 15.5, 6.5, 1.4 Hz, 1H), 4.56 (dq, *J* = 6.4, 1.0 Hz, 2H), 4.49 (s, 2H), 3.78 (s, 3H), 3.47 (t, *J* = 6.4 Hz, 2H), 2.17 (q, *J* = 7.1 Hz, 2H), 1.71 (dq, *J* = 8.3, 6.5 Hz, 2H).

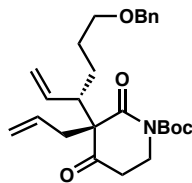


Tert-butyl 3-allyl-2,4-dioxopiperidine-1-carboxylate (233). To a solution of β-ketolactam **232**⁷ in DMSO (50 mL) was added potassium carbonate (2.6 g, 19 mmol, 1.0

equiv) followed by allyl iodide (1.6 mL, 17 mmol, 0.9 equiv). The resulting solution was stirred for 18 h at ambient temperature, whereupon the reaction mixture was directly purified by silica gel flash column chromatography (30–50% EtOAc/hexanes) to give allyl **233** as a tan oil (1.8 g, 37% yield): ^1H NMR (400 MHz, CDCl_3) δ 5.90 (ddtd, J = 17.1, 10.2, 7.0, 1.0 Hz, 1H), 5.23 – 4.96 (m, 2H), 4.62 – 4.39 (m, 1H), 3.88 – 3.68 (m, 1H), 3.61 – 3.42 (m, 1H), 2.80 – 2.41 (m, 4H), 1.55 (s, 9H); ^{13}C NMR (101 MHz, CDCl_3) δ 202.5, 166.6, 151.6, 135.5, 117.3, 84.4, 60.7, 39.7, 38.1, 28.1, 27.56.

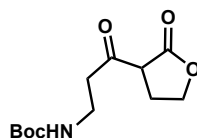


Methyl 5-(((tert-butoxycarbonyl)amino)-2-(2-(((tert-butyldimethylsilyl)oxy)ethyl)-3-oxopentanoate (234). To a suspension of NaH (2.8 g, 82 mmol, 1.2 equiv, 60% in mineral oil) in DME (300 mL) was added a solution of β -ketoester **239**³³ (17 g, 71 mmol, 1.0 equiv) in DME (100 mL) followed by a solution of (2-bromoethoxy)(*tert*-butyl)dimethylsilane (19 g, 78 mmol, 1.1 equiv) and sodium iodide (5.4 g, 36 mmol, 0.5 equiv) in DME (50 mL). The resulting solution was heated under reflux for 18 h, then cooled to ambient temperature, filtered through a pad of silica, rinsing with EtOAc, and concentrated under reduced pressure. The crude product was purified by silica gel flash column chromatography (20–80% EtOAc/hexanes) to give silyl ether **234** as a pale orange oil (20 g, 69% yield): ^1H NMR (400 MHz, CDCl_3) δ 4.97 (s, 1H), 3.78 – 3.67 (m, 4H), 3.61 (td, J = 6.0, 1.7 Hz, 2H), 3.37 (q, J = 5.9 Hz, 2H), 2.93 – 2.64 (m, 2H), 2.13 – 1.99 (m, 2H), 1.42 (s, 9H), 0.87 (s, 9H), 0.02 (s, 6H); ^{13}C NMR (101 MHz, CDCl_3) δ 205.3, 170.1, 155.9, 79.4, 60.5, 55.5, 52.6, 42.4, 35.2, 31.1, 28.5, 26.0, 18.4, -5.3.

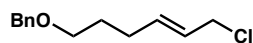


Tert-butyl (S)-3-allyl-3-((S)-6-(benzyloxy)hex-1-en-3-yl)-2,4-dioxopiperidine-1-carboxylate (235). *Please note* Absolute and relative stereochemistry were not determined, and the structure is drawn by analogy to previous work.⁹ A general procedure for the optimization reactions (Table A13.1) is as follows. In a nitrogen-filled glove box, to a 1 dram vial (vial A) equipped with a stir bar was added [Ir(cod)Cl]₂ (2.7 mg, 0.0040 mmol, 2 mol %), ligand (0.0080 mmol, 4 mol %), TBD (2.8 mg, 0.020 mmol, 10 mol%), and THF (1 mL). Vial A was stirred at 25 °C (ca. 10 min) while another 1 dram vial (vial B) was charged with additive (0.40 mmol, 200 mol %), nucleophile **233** (103 mg, 0.40 mmol, 2.0 equiv), and THF (1 mL). The pre-formed catalyst solution (vial A) was then transferred to vial B followed by carbonate **226** (53 mg, 0.20 mmol, 1.0 equiv). The vial was sealed and stirred at 23 °C. After 18, the vial was removed from the glove box and filtered through a pad of silica, rinsing with EtOAc, and concentrated under reduced pressure. The regioselectivity was determined by TOF LCMS (PMM_10min_50-80 ACN-AcOH). The crude mixture was purified by silica gel flash column chromatography (5–20% EtOAc/hexanes) to give allylic alkylation product **235** as a colorless oil and an inseparable mixture of branched and linear isomers: ¹H NMR (400 MHz, CDCl₃) δ 7.45 – 7.05 (m, 5H), 5.74 – 5.41 (m, 2H), 5.36 – 4.91 (m, 4H), 4.46 (d, *J* = 4.7 Hz, 2H), 3.93 – 3.62 (m, 2H), 3.49 – 3.33 (m, 2H), 2.70 – 2.44 (m, 6H), 2.03 (q, *J* = 7.3 Hz, 1H), 1.62 (dt, *J* = 8.7, 6.6 Hz, 2H), 1.54 (s, 9H); ¹³C NMR (101 MHz,

CDCl₃) δ 207.9, 207.6, 207.3, 172.0, 152.1, 138.7, 135.5, 132.2, 128.5, 127.7, 123.7, 119.8, 83.8, 73.0, 69.7, 64.2, 42.0, 41.3, 40.4, 39.3, 29.4, 29.3, 28.1.

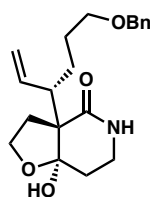


Tert-butyl (3-oxo-3-(2-oxotetrahydrofuran-3-yl)propyl)carbamate (238). To a solution of silyl ether **234** (7.6 g, 19 mmol, 1.0 equiv) in THF (200 mL) was added TBAF (25 mL, 25 mmol, 1.3 equiv). The resulting solution was stirred at ambient temperature for 7 h, whereupon the reaction mixture was concentrated onto silica gel under reduced pressure and purified by silica gel flash column chromatography (50–70% EtOAc/hexanes) to give lactone **238** as a pale pink oil (4.4 g, 91% yield): ¹H NMR (400 MHz, CDCl₃) δ 4.92 (s, 1H), 4.46 – 4.24 (m, 2H), 3.80 – 3.66 (m, 1H), 3.52 – 3.27 (m, 2H), 3.27 – 3.09 (m, 1H), 2.95 – 2.69 (m, 2H), 2.32 (dddd, J = 13.3, 9.3, 7.9, 5.7 Hz, 1H), 1.42 (s, 9H); ¹³C NMR (101 MHz, CDCl₃) δ 201.9, 172.5, 155.8, 79.5, 67.5, 52.2, 42.7, 35.1, 28.4, 23.8.



(E)-(((6-chlorohex-4-en-1-yl)oxy)methyl)benzene (240, LG = Cl). To a solution of *N*-chlorosuccinimide (1.9 g, 14 mmol, 1.5 equiv) in CH₂Cl₂ (40 mL) at 0 °C was added dimethyl sulfide (1.3 mL, 17 mmol, 1.9 equiv) dropwise over 5 min. A solution of alcohol **230**^{4,5} (1.9 g, 9.3 mmol, 1.0 equiv) in CH₂Cl₂ (10 mL) was then added and the resulting solution was stirred at 0 °C for 2 h, whereupon the mixture was allowed to warm to ambient temperature and was stirred for 18 h. The reaction was quenched with

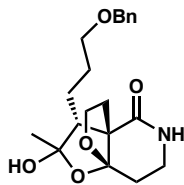
the addition of H₂O (20 mL), and the aqueous layer was extracted with Et₂O (3 x 20 mL). The combined organic layers were washed with brine (20 mL), dried over Na₂SO₄, and concentrated under reduced pressure. The crude residue was purified by silica gel flash column chromatography (5% EtOAc/hexanes) to provide chloride **240** as a pale yellow oil (1.7 g, 83% yield): ¹H NMR (400 MHz, CDCl₃) δ 7.38 – 7.26 (m, 5H), 5.82 – 5.72 (m, 1H), 5.66 – 5.58 (m, 1H), 4.50 (s, 2H), 4.02 (dd, *J* = 7.1, 1.0 Hz, 2H), 3.48 (t, *J* = 6.4 Hz, 2H), 2.25 – 2.07 (m, 2H), 1.81 – 1.61 (m, 2H); ¹³C NMR (101 MHz, CDCl₃) δ 138.6, 135.5, 128.5, 127.8, 127.7, 126.5, 73.1, 69.6, 45.5, 29.0, 28.9.



(3a*S*,7a*R*)-3a-((*S*)-6-(Benzyloxy)hex-1-en-3-yl)-7a-hydroxyhexahydrofuro[3,2-*c*]pyridin-4(2*H*)-one (241). *Please note* Absolute and relative stereochemistry were not determined, and the structure is drawn by analogy to previous work.⁹ A general procedure for the optimization reactions (Table A13.2) is as follows. In a nitrogen-filled glove box, to a 1 dram vial (vial A) equipped with a stir bar was added [Ir(cod)Cl]₂ (1.3 mg, 0.0020 mmol, 2 mol %), ligand (0.0040 mmol, 4 mol %), TBD (1.4 mg, 0.010 mmol, 10 mol %), and THF (0.5 mL). Vial A was stirred at 25 °C (ca. 10 min) while another 1 dram vial (vial B) was charged with additive (0.20 or 0.40 mmol, 200 or 400 mol %), lactone nucleophile **238** (52 mg, 0.20 mmol, 2.0 equiv), and THF (0.5 mL). The pre-formed catalyst solution (vial A) was then transferred to vial B followed by electrophile **240** (0.10 mmol, 1.0 equiv). The vial was sealed and stirred at 60 °C. After 18 h, the vial was

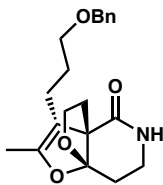
removed from the glove box and concentrated under reduced pressure to give lactone allylic alkylation product **237**.

To crude **237** was added TFA/CH₂Cl₂ (1:1, 1 mL) and the resulting solution was stirred for 3 h, whereupon NEt₃/CH₂Cl₂ (1:1, 1 mL) was added. The resulting solution was stirred for 18 h, whereupon brine (1 mL) was added. The aqueous layer was extracted with CH₂Cl₂ (3 x 5 mL). The combined organic layers were dried over Na₂SO₄, concentrated under reduced pressure and 1,2,4,5-tetrachloro-3-nitrobenzene (0.10 mmol in 0.5 mL CDCl₃) was added. The NMR yield (measured in reference to 1,2,4,5-tetrachloro-3-nitrobenzene δ 7.74 ppm (s, 1H)) was determined by ¹H NMR analysis of the crude mixture. The residue was purified by preparatory TLC (50% acetone/hexanes) to afford hemiacetal **241** as an inseparable mixture of diastereomers. The major diastereomer was isolated by preparatory HPLC (reverse phase, MeCN/H₂O, C18 column): 96% ee; ¹H NMR (400 MHz, CDCl₃) δ 7.36 – 7.27 (m, 5H), 5.75 – 5.49 (m, 2H), 5.21 – 4.91 (m, 2H), 4.48 (s, 2H), 4.04 – 3.94 (m, 1H), 3.70 (dddd, J = 16.7, 9.9, 8.3, 7.1 Hz, 1H), 3.53 – 3.28 (m, 3H), 3.22 – 3.07 (m, 1H), 2.69 – 2.41 (m, 3H), 2.39 – 2.11 (m, 3H), 1.89 (dd, J = 13.6, 4.9 Hz, 1H), 1.67 (tdd, J = 10.6, 7.1, 4.2 Hz, 2H), 1.51 – 1.38 (m, 1H), 1.24 (ddt, J = 17.0, 8.8, 4.4 Hz, 1H); ¹³C NMR (101 MHz, CDCl₃) δ 174.4, 173.9, 140.2, 139.4, 138.8, 138.7, 128.5, 128.5, 127.9, 127.8, 127.7, 127.6, 118.3, 116.4, 103.4, 103.3, 73.1, 72.9, 70.4, 69.8, 65.6, 65.1, 59.4, 58.9, 48.2, 47.2, 38.3, 38.3, 35.7, 33.9, 32.0, 30.6, 28.4, 27.6, 27.6, 26.5; HPLC conditions: 8% IPA, 1.0 mL/min, Chiralpak AD–H column, λ = 210 nm, t_R (min): major = 21.087, minor = 21.876.



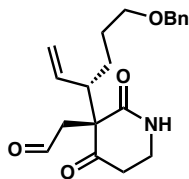
(3*R*,3*aS*,7*aS*)-3-(3-(Benzyloxy)propyl)-2-hydroxy-2-methyltetrahydro-7*a*,3*a*-

(epoxyethano)furo[3,2-*c*]pyridin-4(5*H*)-one (243). To a solution of hemiacetal **241** (13 mg, 0.036 mmol, 1.0 equiv) in dioxane/H₂O (7:1, 0.5 mL) was added PdCl₂ (1.0 mg, 0.0056 mmol, 0.16 equiv) and copper(I) chloride (3.6 mg, 0.036 mmol, 1.0 equiv). The resulting solution was sparged with oxygen (balloon) and stirred under an oxygen atmosphere for 4 h, whereupon the reaction mixture was filtered through a pad of silica, rinsing with EtOAc, and concentrated under reduced pressure. The crude residue was purified by silica gel flash column chromatography (30% acetone/hexanes) to provide **243** as a colorless oil: ¹H NMR (400 MHz, CDCl₃) δ 7.41 – 7.28 (m, 5H), 6.03 (s, 1H), 4.49 (d, *J* = 2.4 Hz, 2H), 4.25 (td, *J* = 8.6, 6.8 Hz, 1H), 3.86 (td, *J* = 8.3, 3.8 Hz, 1H), 3.57 – 3.40 (m, 2H), 3.21 (dp, *J* = 6.8, 2.9 Hz, 2H), 2.95 (s, 1H), 2.45 (ddd, *J* = 13.5, 6.7, 3.9 Hz, 1H), 2.23 (dt, *J* = 13.4, 8.5 Hz, 1H), 2.17 (s, 1H), 2.16 – 2.07 (m, 2H), 1.96 (ddd, *J* = 13.5, 8.2, 5.4 Hz, 2H), 1.78 (dq, *J* = 8.6, 3.4, 2.1 Hz, 5H), 1.53 (s, 3H); ¹³C NMR (101 MHz, CDCl₃) δ 176.4, 138.7, 128.5, 127.9, 127.6, 115.1, 104.8, 73.1, 70.6, 67.2, 54.9, 53.5, 37.9, 35.3, 31.1, 30.7, 29.9, 28.7, 28.2, 23.6.



(3a*S*,7a*S*)-3-(3-(benzyloxy)propyl)-2-methyl-6,7-dihydro-7a,3a-

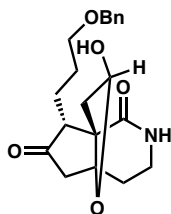
(epoxyethano)furo[3,2-*c*]pyridin-4(5*H*)-one (244). Olefin **244** was isolated as a byproduct in the synthesis and/or purification of **243**. The amount of olefin **244** was found to increase when the crude reaction mixture of **243** was subjected to reduced pressure: ^1H NMR (400 MHz, CDCl_3) δ 7.43 – 7.27 (m, 5H), 6.06 (d, $J = 5.4$ Hz, 1H), 4.47 (s, 2H), 4.01 (ddd, $J = 8.4, 5.3, 2.9$ Hz, 1H), 3.78 – 3.67 (m, 1H), 3.42 (t, $J = 6.4$ Hz, 2H), 3.31 – 3.12 (m, 2H), 2.34 (dt, $J = 13.5, 2.9$ Hz, 1H), 2.26 – 2.19 (m, 3H), 1.83 (s, 3H), 1.71 (td, $J = 8.4, 4.5$ Hz, 4H), 0.99 – 0.69 (m, 1H); ^{13}C NMR (101 MHz, CDCl_3) δ 207.2, 173.8, 152.8, 138.6, 128.5, 127.8, 114.7, 106.2, 73.0, 69.8, 66.9, 64.5, 37.9, 34.46, 31.1, 29.5, 20.7, 11.6.



2-((*S*)-3-((*S*)-6-(Benzyloxy)hex-1-en-3-yl)-2,4-dioxopiperidin-3-yl)acetaldehyde (245).

To a solution of hemiacetal **241** (56 mg, 0.16 mmol, 1.0 equiv) in CH_2Cl_2 (5 mL) was added Dess–Martin periodinane (83 g, 0.20 mmol, 1.2 equiv). The resulting solution was heated in a sealed vial to 50 °C for 2.5 h, whereupon the reaction mixture was cooled to ambient temperature, diluted with Et_2O , sequentially washed with 10% aqueous $\text{Na}_2\text{S}_2\text{O}_3$ /saturated aqueous NaHCO_3 mixture (1:1, 10 mL) and brine (20 mL), dried over

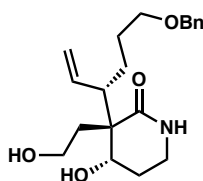
Na₂SO₄, and concentrated under reduced pressure. The crude residue was purified by silica gel flash column chromatography (50% EtOAc/hexanes then 50% acetone/hexanes) to provide **245** as a colorless oil (26 mg, 46% yield): ¹H NMR (400 MHz, CDCl₃) δ 9.52 (s, 1H), 7.36 – 7.27 (m, 5H), 6.45 (d, *J* = 14.5 Hz, 1H), 5.49 (ddt, *J* = 43.8, 16.9, 10.0 Hz, 1H), 5.19 (td, *J* = 10.3, 1.7 Hz, 1H), 5.10 – 5.02 (m, 1H), 4.46 (s, 3H), 3.74 (dtd, *J* = 12.0, 5.5, 2.6 Hz, 1H), 3.63 (dtd, *J* = 14.2, 6.4, 3.6 Hz, 1H), 3.57 – 3.47 (m, 1H), 3.42 (dddd, *J* = 8.7, 7.3, 3.5, 2.2 Hz, 3H), 3.37 – 3.15 (m, 2H), 3.01 – 2.81 (m, 1H), 2.74 – 2.59 (m, 1H), 2.46 (ddd, *J* = 12.2, 10.0, 2.3 Hz, 1H), 1.75 – 1.60 (m, 3H), 1.45 – 1.16 (m, 3H); ¹³C NMR (126 MHz, CDCl₃) δ 207.6, 207.2, 199.9, 173.8, 173.1, 138.5, 136.6, 136.4, 128.5, 127.8, 127.7, 119.9, 119.2, 89.5, 73.0, 72.9, 69.7, 59.9, 59.3, 50.6, 50.4, 49.2, 38.9, 37.9, 36.7, 36.5, 28.0, 27.9, 26.9, 25.9.



(7*R*,7*aS*)-7-(3-(Benzyloxy)propyl)-9-hydroxydihydro-5*H*-4*a*,7*a*-

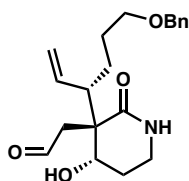
(epoxyethano)cyclopenta[*c*]pyridine-1,6(2*H*,7*H*)-dione (247). To a solution of aldehyde **245** (39 mg, 0.11 mmol, 1.0 equiv) in dioxane/H₂O (7:1, 1.5 mL) was added PdCl₂ (2.0 mg, 0.011 mmol, 0.1 equiv) and copper(I) chloride (11 mg, 0.11 mmol, 1.0 equiv). The resulting solution was sparged with oxygen (balloon) and stirred under an oxygen atmosphere for 18 h, whereupon the reaction mixture was filtered through a pad of silica, rinsing with EtOAc, and concentrated under reduced pressure. The crude residue was purified by silica gel flash column chromatography (75% acetone/hexanes)

to provide **247** as a colorless oil: ^1H NMR (400 MHz, CDCl_3) δ 7.33 (d, $J = 0.9$ Hz, 5H), 5.55 (d, $J = 6.1$ Hz, 1H), 4.53 – 4.45 (m, 4H), 3.55 – 3.40 (m, 4H), 3.20 (dt, $J = 7.7$, 4.0 Hz, 3H), 2.88 – 2.75 (m, 1H), 2.66 – 2.41 (m, 3H), 2.33 (t, $J = 6.7$ Hz, 1H), 2.22 – 2.07 (m, 2H), 1.92 (ddd, $J = 13.8$, 8.8, 5.4 Hz, 1H), 1.88 – 1.70 (m, 6H); ^{13}C NMR (101 MHz, CDCl_3) δ 175.8, 138.5, 128.4, 127.8, 127.6, 116.1, 107.0, 99.8, 72.9, 70.4, 55.0, 38.2, 37.8, 35.8, 28.5, 27.9, 27.6, 24.7.



(3*S*,4*S*)-3-((*S*)-6-(Benzyloxy)hex-1-en-3-yl)-4-hydroxy-3-(2-hydroxyethyl)piperidin-2-one (248). *Please note* Relative stereochemistry was not confirmed. To a solution of hemiacetal **241** (25 mg, 0.072 mmol, 1.0 equiv) in MeOH (1 mL) was added NaBH_4 (8.0 mg, 0.22 mmol, 3.0 equiv). The resulting solution was stirred for 18 h, whereupon the reaction was quenched with a saturated aqueous solution of sodium citrate (1 mL) and extracted with EtOAc (3 x 5 mL), washed with brine (5 mL), dried over Na_2SO_4 , and concentrated under reduced pressure. The crude residue was purified by preparatory TLC (33% acetone/hexanes) to provide hydroxy **248** as a colorless oil (11 mg, 44% yield): ^1H NMR (400 MHz, CDCl_3) δ 7.39 – 7.26 (m, 5H), 5.99 (ddd, $J = 17.3$, 8.6, 2.6 Hz, 1H), 5.85 – 5.67 (m, 1H), 5.27 – 5.04 (m, 2H), 4.48 (d, $J = 3.0$ Hz, 2H), 4.03 (ddd, $J = 23.5$, 7.0, 4.3 Hz, 1H), 3.94 – 3.64 (m, 2H), 3.58 – 3.39 (m, 3H), 3.26 (dddd, $J = 14.5$, 11.7, 6.9, 4.0 Hz, 1H), 2.70 (dtd, $J = 9.4$, 6.0, 2.6 Hz, 1H), 2.16 – 1.98 (m, 3H), 1.94 – 1.82 (m, 1H), 1.81 – 1.65 (m, 2H), 1.44 (ddt, $J = 13.8$, 10.5, 7.7 Hz, 2H); ^{13}C NMR (101 MHz,

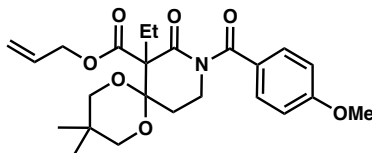
CDCl₃) δ 176.4, 176.3, 140.5, 138.7, 138.7, 138.6, 128.5, 128.5, 128.4, 127.9, 127.8, 127.7, 127.6, 118.3, 117.6, 73.0, 72.9, 71.4, 70.9, 70.4, 70.3, 59.5, 59.4, 52.5, 52.1, 47.7, 46.4, 38.0, 37.8, 37.3, 33.9, 28.9, 27.9, 27.8, 26.7, 26.1, 24.9.



2-((3*S*,4*S*)-3-((*S*)-6-(Benzyloxy)hex-1-en-3-yl)-4-hydroxy-2-oxopiperidin-3-

yl)acetaldehyde (249). To solution of alcohol **248** (10 mg, 0.029 mmol, 1.0 equiv) in MeCN (1 mL) was added IBX (25 mg, 0.089 mmol, 3.0 equiv). The resulting solution was stirred for 18 h, whereupon the reaction mixture was filtered through celite, rinsing with EtOAc, and concentrated under reduced pressure. The crude residue was purified by preparatory TLC (44% acetone/hexanes) to provide aldehyde **249** as a colorless oil (4.0 mg, 40% yield): ¹H NMR (400 MHz, CDCl₃) δ 9.52 (s, 1H), 7.36 – 7.28 (m, 5H), 5.45 (dt, *J* = 16.9, 10.1 Hz, 1H), 5.20 (ddd, *J* = 11.4, 10.1, 1.8 Hz, 1H), 5.07 (dddd, *J* = 17.0, 12.4, 1.8, 0.6 Hz, 1H), 4.47 (s, 3H), 3.83 – 3.72 (m, 1H), 3.66 (ddd, *J* = 6.2, 4.6, 2.5 Hz, 1H), 3.61 – 3.48 (m, 1H), 3.48 – 3.37 (m, 3H), 3.33 (dd, *J* = 18.9, 5.4 Hz, 1H), 3.02 – 2.83 (m, 1H), 2.75 – 2.61 (m, 1H), 2.51 – 2.40 (m, 1H), 1.75 – 1.63 (m, 2H), 1.54 – 1.14 (m, 3H); ¹³C NMR (101 MHz, CDCl₃) δ 207.5, 206.9, 199.9, 199.8, 173.7, 172.9, 138.6, 136.6, 136.4, 128.5, 127.9, 127.8, 127.72, 127.71, 119.9, 119.2, 73.0, 72.9, 69.8, 69.7, 60.0, 59.4, 50.7, 50.6, 50.5, 49.4, 38.9, 38.0, 36.8, 36.6, 28.0, 27.9, 27.0, 26.0.

A13.8.2.2 Experimental Procedures and Spectroscopic Data for the Synthesis of Synthetic Intermediates in Section A13.3

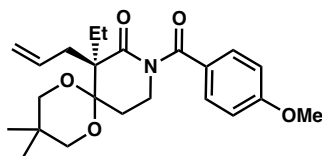


Allyl 7-ethyl-9-(4-methoxybenzoyl)-3,3-dimethyl-8-oxo-1,5-dioxo-9-

azaspiro[5.5]undecane-7-carboxylate (256). To a solution of LiHMDS (0.89 g, 5.4 mmol, 1.1 equiv) in THF (20 mL) at -78°C was added a solution of protected lactam **295** (1.6 g, 4.9 mmol, 1.0 equiv) in THF (20 mL). The resulting mixture was stirred for 2 h at -78°C , whereupon allyl chloroformate (0.59 g, 5.4 mmol, 1.1 equiv) was added dropwise. The reaction mixture was stirred for 3 h at -78°C followed by an additional 18 h at -50°C . The reaction was quenched with the addition of brine (20 mL) and the aqueous layer was extracted with CH_2Cl_2 (3 x 20 mL), washed with brine (5 mL), dried over Na_2SO_4 , and concentrated under reduced pressure. The crude residue was purified by silica gel flash column chromatography (35% EtOAc/hexanes) to provide **acylated-295** as a colorless oil (0.70 g, 34% yield).

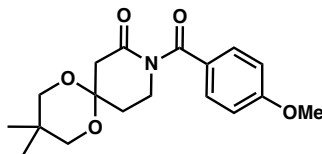
To a solution of **acylated-295** (0.20 g, 0.48 mmol, 1.0 equiv) in acetone (5 mL) was added potassium carbonate (0.33 g, 2.4 mmol, 5.0 equiv) and ethyl iodide (0.39 mL, 4.8 mmol, 10.0 equiv). The resulting solution was stirred for 18 h at ambient temperature, whereupon the mixture was filtered through a pad of silica, rinsing with EtOAc, and concentrated under reduced pressure. The crude residue was purified by preparatory TLC (50% EtOAc/hexanes) to provide ethyl **256** as a colorless oil (36 mg, 17% yield): ^1H NMR (400 MHz, CDCl_3) δ 7.85 – 7.71 (m, 2H), 6.95 – 6.75 (m, 2H), 6.09 – 5.82 (m,

1H), 5.51 – 5.19 (m, 2H), 4.86 – 4.60 (m, 2H), 3.82 (s, 4H), 3.79 – 3.40 (m, 6H), 2.74 (dt, $J = 14.6, 5.2$ Hz, 1H), 2.46 – 2.08 (m, 3H), 1.20 (s, 3H), 1.02 (t, $J = 7.4$ Hz, 3H), 0.76 (s, 3H).



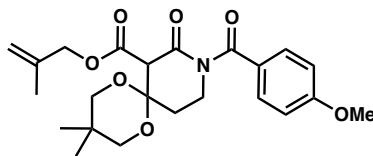
(*R*)-7-Allyl-7-ethyl-9-(4-methoxybenzoyl)-3,3-dimethyl-1,5-dioxaspiro[5.5]undecan-8-one (257).

azaspiro[5.5]undecan-8-one (257). In a nitrogen-filled glove box, to a 1 dram vial equipped with a stir bar was added $\text{Pd}_2(\text{dba})_3$ (3.7 mg, 0.0040 mmol, 5 mol %), (*S*)-**L15** (5.2 mg, 0.010 mmol, 12.5 mol %), and hexanes/toluene (2:1, 2.7 mL). The resulting solution was stirred at 25 °C for 10 min, whereupon substrate **256** (36 mg, 0.081 mmol, 1.0 equiv) was added. The vial was sealed and stirred at 35 °C for 18 h, whereupon the vial was removed from the glove box and filtered through a pad of silica, rinsing with EtOAc, and concentrated under reduced pressure. The crude residue was purified by preparatory TLC (30% EtOAc/hexanes) to provide allylic alkylation product **257** as a colorless solid (7.4 mg, 46% yield): 93% ee; ^1H NMR (400 MHz, CDCl_3) δ 7.52 (d, $J = 8.9$ Hz, 2H), 6.86 (d, $J = 8.8$ Hz, 2H), 6.23 – 6.00 (m, 1H), 5.18 – 4.93 (m, 2H), 3.83 (s, 3H), 3.77 – 3.56 (m, 4H), 3.43 (ddd, $J = 11.7, 5.2, 2.6$ Hz, 2H), 2.91 – 2.59 (m, 3H), 2.30 (ddd, $J = 14.5, 8.5, 7.3$ Hz, 1H), 2.15 – 1.98 (m, 1H), 1.93 (dt, $J = 14.4, 7.4$ Hz, 1H), 1.20 (s, 3H), 0.99 (t, $J = 7.5$ Hz, 3H), 0.77 (s, 3H); ^{13}C NMR (101 MHz, CDCl_3) δ 176.8, 175.3, 162.4, 136.5, 130.1, 128.9, 116.5, 113.6, 100.3, 70.4, 56.8, 55.5, 41.5, 33.2, 29.9, 25.2, 23.7, 22.5, 20.1, 9.1; SFC conditions: 3% MeOH, 3.0 mL/min, Chiralpak OJ-H column, $\lambda = 210$ nm, t_R (min): major = 18.627, minor = 4.817.

**9-(4-Methoxybenzoyl)-3,3-dimethyl-1,5-dioxaspiro[5.5]undecan-8-one (258).**

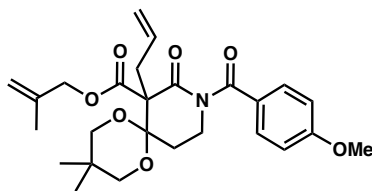
To a solution of **232**⁷ (45 g, 210 mmol, 1.0 equiv) in toluene (300 mL) was added *para*-toluenesulfonic acid (2.0 g, 11 mmol, 0.05 equiv) and 2,2-dimethyl-1,3-propanediol (33 g, 320 mmol, 1.5 equiv). The resulting solution was heated under reflux for 18 h with azeotropic removal of water via Dean–Stark trap, whereupon the mixture was cooled to ambient temperature and concentrated under reduced pressure. The crude residue was purified by recrystallization from boiling EtOAc to give the **protected ketone-232** (23 g, 54% yield).

To a solution of **protected ketone-232** (1.5 g, 7.5 mmol, 1.0 equiv) in THF (25 mL) was added NEt₃ (1.6 mL, 11.3 mmol, 1.5 equiv), 4-dimethylaminopyridine (0.91 g, 0.75 mmol, 0.1 equiv), and *para*-anisoyl chloride (1.3 mL, 9.8 mmol, 1.3 equiv). The resulting solution was stirred at ambient temperature for 18 h, whereupon the mixture was filtered through celite, rinsing CH₂Cl₂, and concentrated under reduced pressure. The crude residue was purified by silica gel flash column chromatography (20% acetone/hexanes) to afford protected lactam **258** as a white solid (1.3 g, 54% yield): ¹H NMR (400 MHz, CDCl₃) δ 7.59 (d, *J* = 8.9 Hz, 2H), 6.88 (d, *J* = 8.9 Hz, 2H), 3.84 (s, 3H), 3.82 – 3.75 (m, 2H), 3.55 (s, 4H), 2.92 (t, *J* = 1.0 Hz, 2H), 2.35 – 2.21 (m, 2H), 1.00 (d, *J* = 6.4 Hz, 6H); ¹³C NMR (101 MHz, CDCl₃) δ 173.6, 170.6, 162.9, 130.9, 127.6, 113.6, 96.4, 70.8, 55.5, 43.3, 41.9, 30.3, 30.2, 22.6, 22.6.

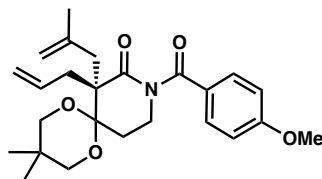


2-Methylallyl 9-(4-methoxybenzoyl)-3,3-dimethyl-8-oxo-1,5-dioxaspiro[5.5]undecane-7-carboxylate (259).

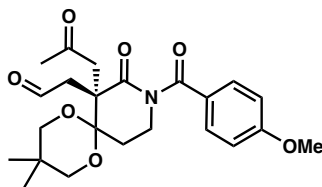
To a solution of LiHMDS (1.1 g, 6.6 mmol, 1.1 equiv) in THF (40 mL) at -78°C was added a solution of protected lactam **258** (2.0 g, 6.0 mmol, 1.0 equiv) in THF (40 mL). The resulting mixture was stirred for 2 h at -78°C , whereupon methallyl chloroformate (0.83 g, 6.6 mmol, 1.1 equiv) was added dropwise. The reaction mixture was stirred for 2 h at -78°C followed by an additional 18 h at -60°C . The reaction was quenched with the addition of brine (20 mL) and the aqueous layer was extracted with CH_2Cl_2 (3 x 40 mL), washed with brine (5 mL), dried over Na_2SO_4 , and concentrated under reduced pressure. The crude residue was purified by silica gel flash column chromatography (20–40% EtOAc/hexanes) to provide acylated **259** as a colorless foam (2.1 g, 80% yield): ^1H NMR (400 MHz, CDCl_3) δ 7.71 (d, $J = 8.9$ Hz, 2H), 6.85 (d, $J = 8.9$ Hz, 2H), 5.12 – 4.92 (m, 2H), 4.77 – 4.55 (m, 2H), 4.27 (d, $J = 2.2$ Hz, 1H), 4.12 (q, $J = 7.2$ Hz, 1H), 3.83 (s, 4H), 3.81 – 3.67 (m, 2H), 3.63 – 3.43 (m, 3H), 2.55 (ddd, $J = 13.8, 12.5, 5.9$ Hz, 1H), 2.28 (ddt, $J = 13.8, 4.5, 2.4$ Hz, 1H), 1.79 (d, $J = 0.6$ Hz, 3H), 1.07 (s, 3H), 0.93 (s, 3H).



2-Methylallyl 7-allyl-9-(4-methoxybenzoyl)-3,3-dimethyl-8-oxo-1,5-dioxo-9-azaspiro[5.5]undecane-7-carboxylate (260). In a nitrogen-filled glove box, to a 2 dram vial (vial A) equipped with a stir bar was added $[\text{Ir}(\text{cod})\text{Cl}]_2$ (31 mg, 0.046 mmol, 2 mol %), *rac*-**L2** (42 mg, 0.093 mmol, 4 mol %), TBD (32 mg, 0.23 mmol, 10 mol %), and THF (5 mL). Vial A was stirred at 25 °C (ca. 10 min) while another a 100 mL round bottom flask was charged with β -ketoamide **259** (1.0 g, 2.3 mmol, 1.0 equiv), LiBr (0.40 g, 4.6 mmol, 2.0 equiv), and THF (15 mL). The pre-formed catalyst solution (vial A) was then transferred to the round bottom flask followed by allyl methyl carbonate (0.40 g, 3.5 mmol, 1.5 equiv). The flask was removed from the glove box, placed under an argon atmosphere, and stirred at ambient temperature for 3.5 h, whereupon the reaction mixture was filtered through a pad of silica, rinsing with EtOAc, and concentrated under reduced pressure. The crude residue was purified by silica gel flash column chromatography (10% EtOAc/hexanes) to afford allylated **260** (0.98 g, 90% yield): ^1H NMR (400 MHz, CDCl_3) δ 7.81 – 7.71 (m, 2H), 6.89 – 6.78 (m, 2H), 6.00 (dddd, J = 16.8, 10.1, 7.7, 6.5 Hz, 1H), 5.14 – 5.02 (m, 2H), 4.97 (td, J = 4.3, 3.6, 2.2 Hz, 2H), 4.69 – 4.50 (m, 2H), 3.80 (s, 3H), 3.79 – 3.68 (m, 2H), 3.68 – 3.56 (m, 2H), 3.48 (ddd, J = 21.8, 11.4, 2.6 Hz, 2H), 3.06 – 2.90 (m, 2H), 2.78 (dt, J = 14.6, 4.9 Hz, 1H), 2.24 (ddd, J = 14.6, 10.3, 5.8 Hz, 1H), 1.76 (s, 3H), 1.20 (s, 3H), 0.76 (s, 3H).

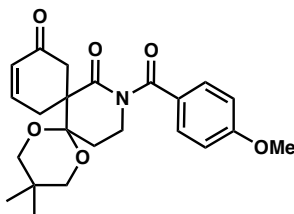


(R)-7-Allyl-9-(4-methoxybenzoyl)-3,3-dimethyl-7-(3-methylbut-3-en-1-yl)-1,5-dioxo-9-azaspiro[5.5]undecan-8-one (*rac*-261). In a nitrogen-filled glove box, to a 100 mL round bottom flask equipped with a stir bar was added Pd(PPh₃)₄ (46 mg, 0.040 mmol, 0.05 equiv), substrate **260** (0.37 g, 0.79 mmol, 1.0 equiv), and toluene (20 mL). The flask was removed from the glove box, placed under an argon atmosphere, and stirred at 35 °C for 18 h, whereupon the reaction mixture was filtered through a pad of silica, rinsing with EtOAc, and concentrated under reduced pressure. The crude residue was purified by silica gel flash column chromatography (10% EtOAc/hexanes) to afford allylic alkylation product ***rac*-261** (0.29 g, 84% yield): 24% ee; ¹H NMR (400 MHz, CDCl₃) δ 7.66 – 7.52 (m, 2H), 6.90 – 6.78 (m, 2H), 6.12 (ddt, *J* = 17.1, 10.1, 7.0 Hz, 1H), 5.11 – 4.94 (m, 2H), 4.83 (ddd, *J* = 10.4, 2.4, 1.3 Hz, 2H), 3.83 (s, 4H), 3.70 (dd, *J* = 18.9, 11.6 Hz, 2H), 3.55 (ddd, *J* = 12.6, 10.3, 6.0 Hz, 1H), 3.46 (ddd, *J* = 11.7, 3.9, 2.5 Hz, 2H), 2.92 – 2.69 (m, 3H), 2.69 – 2.49 (m, 2H), 2.21 (ddd, *J* = 14.6, 10.2, 6.5 Hz, 1H), 1.72 (d, *J* = 0.6 Hz, 3H), 1.23 (s, 3H), 0.78 (s, 3H); ¹³C NMR (101 MHz, CDCl₃) δ 175.9, 174.7, 162.5, 143.1, 136.8, 130.7, 128.4, 116.6, 115.9, 113.5, 99.6, 70.4, 56.9, 55.5, 41.4, 41.0, 36.8, 29.9, 24.7, 23.9, 22.6, 20.2; SFC conditions: 3% MeOH, 3.0 mL/min, Chiralpak AS-H column, λ = 210 nm, *t*_R (min): major = 11.875, minor = 10.765.



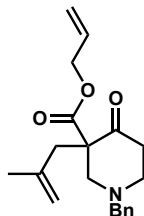
(R)-2-(9-(4-Methoxybenzoyl)-3,3-dimethyl-8-oxo-7-(3-oxobutyl)-1,5-dioxaspiro[5.5]undecan-7-yl)acetaldehyde (262).

A solution of olefin **261** (20 mg, 0.047 mmol, 1.0 equiv) in CH_2Cl_2 (5 mL) was cooled to $-78\text{ }^\circ\text{C}$. Ozone was bubbled through the reaction mixture for 0.5 h, whereupon the reaction mixture was sparged with N_2 and triphenylphosphine (25 mg, 0.094 mmol, 2.0 equiv) was added. The cooling bath was then removed and the reaction was stirred for 1.5 h at ambient temperature. The reaction mixture was concentrated under reduced pressure and the crude residue was purified by silica gel flash column chromatography (40% EtOAc/hexanes) to afford aldehyde **262** as a colorless oil (17 mg, 82% yield): ^1H NMR (400 MHz, CDCl_3) δ 9.59 (s, 1H), 7.67 (d, $J = 8.9$ Hz, 2H), 6.88 (d, $J = 8.9$ Hz, 3H), 3.83 (s, 4H), 3.78 – 3.61 (m, 5H), 3.42 (ddd, $J = 11.9, 7.3, 2.6$ Hz, 2H), 3.20 (d, $J = 15.8$ Hz, 1H), 3.11 (dd, $J = 16.0, 2.6$ Hz, 1H), 2.96 (d, $J = 15.9$ Hz, 1H), 2.81 (dd, $J = 16.1, 2.1$ Hz, 1H), 2.48 (qdd, $J = 14.6, 6.9, 5.6$ Hz, 2H), 2.21 (s, 3H), 1.16 (s, 3H), 0.77 (s, 3H); ^{13}C NMR (101 MHz, CDCl_3) δ 206.4, 199.1, 174.2, 173.9, 162.8, 130.8, 127.6, 113.5, 98.4, 70.4, 56.2, 55.4, 46.3, 45.1, 41.2, 31.8, 29.6, 23.4.



14-(4-Methoxybenzoyl)-3,3-dimethyl-1,5-dioxaspiro[5.0.5^{7,4}]hexadec-10-ene-9,13-dione (263). To a solution of bis-carbonyl **262** (20 mg, 0.046 mmol, 1.0 equiv) in toluene (2 mL) was added *para*-toluenesulfonic acid monohydrate (1 mg, 0.0046 mmol, 0.1 equiv) and MgSO₄ (20 mg, 100 wt %). The resulting slurry was heated to 100 °C for 0.5 h, whereupon the mixture was cooled to ambient temperature, filtered through a pad of silica, rinsing with EtOAc, and concentrated under reduced pressure. The crude residue was purified by preparatory TLC (40% acetone/hexanes) to afford enone **263** as a colorless oil (10 mg, 53% yield): ¹H NMR (400 MHz, CDCl₃) δ 7.45 – 7.36 (m, 2H), 6.89 (ddd, *J* = 10.2, 5.8, 2.5 Hz, 1H), 6.84 – 6.76 (m, 2H), 6.08 – 5.98 (m, 1H), 3.81 (s, 3H), 3.77 – 3.54 (m, 4H), 3.45 (ddd, *J* = 11.7, 4.1, 2.5 Hz, 2H), 3.12 – 2.76 (m, 4H), 2.58 (dt, *J* = 14.7, 5.9 Hz, 1H), 2.35 (ddd, *J* = 14.6, 8.3, 6.1 Hz, 1H), 1.18 (s, 3H), 0.78 (s, 3H); ¹³C NMR (101 MHz, CDCl₃) δ 197.0, 175.9, 174.2, 162.8, 145.5, 130.3, 129.1, 127.4, 113.7, 98.5, 70.8, 70.7, 56.5, 55.5, 41.6, 39.6, 30.1, 29.4, 23.3, 22.2, 20.0.

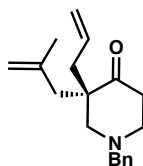
A13.8.2.3 Experimental Procedures and Spectroscopic Data for the Synthesis of Synthetic Intermediates in Section A13.4



Allyl 1-benzyl-3-(2-methylallyl)-4-oxopiperidine-3-carboxylate (274). To a solution of NaH (2.2 g, 66 mmol, 2.5 equiv, 60% in mineral oil) in THF (24 mL) at 0 °C was added a solution of 1-benzyl-4-piperidone (5 g, 26 mmol, 1.9 equiv) in THF (10 mL) over 15 min. The resulting mixture was warmed to ambient temperature, diallyl carbonate (5.7 mL, 40 mmol, 1.5 equiv) was added, and the solution was stirred for an additional 18 h. The reaction was quenched with a saturated aqueous solution of NH₄Cl (10 mL) and acidified (pH = 4) with 1 M HCl. The aqueous layer was extracted with EtOAc (3 x 40 mL), washed with brine (40 mL), dried over Na₂SO₄, and concentrated under reduced pressure. The crude residue was purified by silica gel flash column chromatography (20% EtOAc/hexanes) to provide **acylated-274** as a colorless oil (2.5 g, 35% yield).

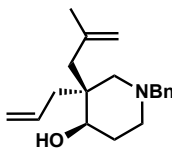
To a solution of **acylated-274** (0.10 g, 0.37 mmol, 1.0 equiv) in acetone (5 mL) was added potassium carbonate (0.10 g, 0.73 mmol, 2.0 equiv), tetrabutylammonium iodide (14 mg, 0.037 mmol, 0.1 equiv), and methallyl bromide (0.074 mL, 0.73 mmol, 2.0 equiv). The resulting solution was heated to 50 °C for 18 h, whereupon the reaction mixture was cooled to ambient temperature, filtered through a pad of silica, rinsing with EtOAc, and concentrated under reduced pressure. The crude residue was purified by silica gel flash column chromatography (10% EtOAc/hexanes) to afford functionalized

piperidone **274** as a colorless oil (78 mg, 65% yield): ^1H NMR (400 MHz, CDCl_3) δ 7.41 – 7.18 (m, 6H), 5.89 (ddt, $J = 17.3, 10.4, 5.8$ Hz, 1H), 5.44 – 5.16 (m, 2H), 4.80 (s, 1H), 4.71 – 4.56 (m, 3H), 3.72 – 3.54 (m, 2H), 3.49 (dd, $J = 11.6, 2.7$ Hz, 1H), 3.09 – 2.91 (m, 1H), 2.84 (ddd, $J = 15.3, 11.8, 6.6$ Hz, 1H), 2.64 (dd, $J = 13.9, 0.9$ Hz, 1H), 2.46 – 2.34 (m, 3H), 2.29 (d, $J = 11.6$ Hz, 1H), 1.66 (t, $J = 1.1$ Hz, 3H).

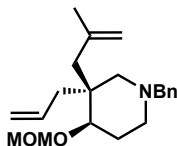


(S)-3-Allyl-1-benzyl-3-(2-methylallyl)piperidin-4-one (275). In a nitrogen-filled glove box, to a 250 mL round bottom flask equipped with a stir bar was added $\text{Pd}_2(\text{dba})_3$ (81 mg, 0.088 mmol, 2.5 mol %), (*S*)-**L18** (85 mg, 0.22 mmol, 6.25 mol %), and THF (110 mL). The resulting solution was stirred at 25 °C for 10 min, whereupon substrate **274** (1.2 g, 3.5 mmol, 1.0 equiv) was added. The flask was sealed and stirred at ambient temperature. After 18, the flask was removed from the glove box and filtered through a pad of silica, rinsing with EtOAc, and concentrated under reduced pressure. The crude residue was purified by silica gel flash column chromatography (8% EtOAc/hexanes) to provide allylic alkylation product **275** as a colorless oil (7.4 mg, 46% yield): 82% ee; ^1H NMR (400 MHz, CDCl_3) δ 7.46 – 7.21 (m, 5H), 5.75 – 5.58 (m, 1H), 5.12 – 4.95 (m, 2H), 4.84 (dq, $J = 2.9, 1.5$ Hz, 1H), 4.68 (dq, $J = 2.0, 0.9$ Hz, 1H), 3.68 – 3.47 (m, 2H), 2.78 (dddd, $J = 8.4, 6.4, 3.1, 1.5$ Hz, 1H), 2.69 – 2.56 (m, 4H), 2.53 – 2.45 (m, 2H), 2.46 – 2.36 (m, 2H), 1.68 (t, $J = 1.0$ Hz, 3H); ^{13}C NMR (101 MHz, CDCl_3) δ 212.3, 142.1, 138.7, 133.9, 128.9, 128.5, 127.4, 118.3, 115.3, 62.4, 62.3, 53.5, 52.3, 42.3, 39.54, 38.9,

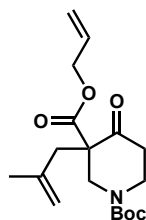
24.6; HPLC conditions: 1% EtOH, 1.0 mL/min, Chiralpak OJ column, λ = 210 nm, t_R (min): major = 10.113, minor = 8.486.



(3*S*,4*R*)-3-Allyl-1-benzyl-3-(2-methylallyl)piperidin-4-ol (276). *Please note* Relative stereochemistry was not confirmed. To a solution of ketone **275** (0.50 g, 1.8 mmol, 1.0 equiv) in CH₂Cl₂ (20 mL) at 0 °C was added (*S*)-CBS (1 M, 0.35 mL, 0.35 mmol, 0.2 equiv) followed by BH₃•DMS (2 M, 1.8 mL, 3.5 mmol, 2.0 equiv). The resulting solution was stirred for 1.5 h, whereupon the reaction was quenched with MeOH (5 mL) and a saturated aqueous sodium citrate solution (10 mL) then warmed to ambient temperature and stirred for an additional 15 min. The aqueous layer was extracted with Et₂O (3 x 30 mL), dried over MgSO₄, and concentrated under reduced pressure. The crude residue was purified by silica gel flash column chromatography (20% EtOAc/hexanes) to afford alcohol **276** as an inseparable mixture (9:1) of diastereomers and a colorless oil (0.50 g, 59% yield): ¹H NMR (400 MHz, CDCl₃) δ 7.36 – 7.31 (m, 5H), 5.98 (ddt, J = 17.4, 9.8, 7.5 Hz, 1H), 5.19 – 5.07 (m, 2H), 4.90 (dd, J = 2.6, 1.4 Hz, 1H), 4.80 (dd, J = 2.6, 1.1 Hz, 1H), 3.62 (t, J = 6.9 Hz, 1H), 3.53 (d, J = 13.0 Hz, 1H), 3.34 (d, J = 13.1 Hz, 1H), 2.63 – 2.42 (m, 2H), 2.42 – 2.32 (m, 1H), 2.29 (d, J = 13.3 Hz, 1H), 2.21 – 2.00 (m, 2H), 1.82 (t, J = 1.1 Hz, 3H), 1.80 – 1.69 (m, 3H); ¹³C NMR (101 MHz, CDCl₃) δ 144.1, 139.1, 135.6, 133.4, 132.8, 129.2, 128.7, 128.6, 128.3, 127.1, 126.7, 117.9, 115.2, 62.9, 42.7, 30.1, 26.0, 25.7.



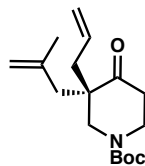
(3*S*,4*R*)-3-Allyl-1-benzyl-4-(methoxymethoxy)-3-(2-methylallyl)piperidine (277). To a solution of alcohol **276** (70 mg, 0.25 mmol, 1.0 equiv) in CH₂Cl₂ (10 mL) at 0°C was added DIPEA (0.065 mL, 0.38 mmol, 1.5 equiv) and bromomethyl methyl ether (0.040 mL, 0.49 mmol, 2.0 equiv). The resulting mixture was stirred for 3 h, whereupon the reaction was quenched with a saturated aqueous NaHCO₃ solution (5 mL) and the aqueous layer was extracted with EtOAc (3 x 10 mL), dried over Na₂SO₄, and concentrated under reduced pressure. The crude residue was purified by silica gel flash column chromatography (10% EtOAc/hexanes) to afford ether **277** as a colorless oil (61 mg, 74% yield): ¹H NMR (400 MHz, CDCl₃) δ 7.49 – 7.13 (m, 5H), 5.88 (dddt, *J* = 27.1, 17.3, 10.1, 7.4 Hz, 1H), 5.15 – 4.99 (m, 2H), 4.97 – 4.84 (m, 1H), 4.78 – 4.68 (m, 2H), 4.65 (dd, *J* = 7.7, 6.9 Hz, 1H), 3.59 – 3.41 (m, 2H), 3.39 (d, *J* = 1.1 Hz, 4H), 2.75 – 2.30 (m, 4H), 2.30 – 1.89 (m, 5H).



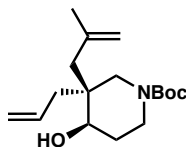
3-Allyl 1-(*tert*-butyl) 3-(2-methylallyl)-4-oxopiperidine-1,3-dicarboxylate (280). To a solution of NaH (4.2 g, 130 mmol, 2.5 equiv, 60% in mineral oil) in THF (45 mL) at 0 °C was added a solution of 1-Boc-4-piperidone (10.0 g, 50.2 mmol, 1.0 equiv) in THF (20 mL) over 15 min. The resulting mixture was warmed to ambient temperature, diallyl

carbonate (11 mL, 75 mmol, 1.5 equiv) was added, and the solution was stirred for an additional 18 h. The reaction was quenched with a saturated aqueous solution of NH_4Cl (30 mL) and acidified ($\text{pH} = 4$) with 1 M HCl . The aqueous layer was extracted with EtOAc (3 x 60 mL), washed with brine (60 mL), dried over Na_2SO_4 , and concentrated under reduced pressure.

To a solution of the crude residue in acetone (60 mL) was added potassium carbonate (14 g, 104 mmol, 2.0 equiv), tetrabutylammonium iodide (0.96 g, 2.6 mmol, 0.1 equiv), and methallyl chloride (10.0 mL, 104 mmol, 2.0 equiv). The resulting solution was heated to 45 °C for 18 h, whereupon the reaction mixture was cooled to ambient temperature, filtered through a pad of silica, rinsing with acetone, and concentrated under reduced pressure. The crude residue was purified by silica gel flash column chromatography (10–20% EtOAc /hexanes) to afford functionalized piperidone **280** as a colorless oil (2.9 g, 17% yield over 2 steps): ^1H NMR (400 MHz, CDCl_3) δ 5.90 (ddt, $J = 17.2, 10.3, 5.9$ Hz, 1H), 5.39 – 5.20 (m, 2H), 4.88 (t, $J = 1.7$ Hz, 1H), 4.74 (dp, $J = 2.9, 1.0$ Hz, 1H), 4.68 – 4.57 (m, 3H), 4.32 – 4.06 (m, 1H), 3.34 – 3.18 (m, 1H), 3.09 (d, $J = 13.7$ Hz, 1H), 2.78 – 2.67 (m, 2H), 2.55 – 2.41 (m, 2H), 1.75 (t, $J = 1.1$ Hz, 1H), 1.71 (t, $J = 1.1$ Hz, 3H), 1.51 (d, $J = 2.1$ Hz, 9H); ^{13}C NMR (101 MHz, CDCl_3) δ 208.8, 203.8, 169.6, 154.4, 141.8, 140.2, 131.2, 119.1, 115.7, 80.3, 66.1, 60.8, 51.6, 38.9, 28.3, 23.7.



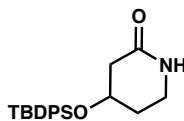
Tert-butyl (S)-3-allyl-3-(2-methylallyl)-4-oxopiperidine-1-carboxylate (281). In a nitrogen-filled glove box, to 1 dram vial equipped with a stir bar was added $\text{Pd}_2(\text{dba})_3$ (12 mg, 0.013 mmol, 2.5 mol %), (*S*)-**L15** (17 mg, 0.033 mmol, 6.25 mol %), and THF (10 mL). The resulting solution was stirred at 25 °C for 10 min, whereupon substrate **280** (0.18 g, 0.52 mmol, 1.0 equiv) was added. The flask was sealed and stirred at ambient temperature for 18 h, whereupon the flask was removed from the glove box and concentrated under reduced pressure. The crude residue was purified by silica gel flash column chromatography (8% EtOAc/hexanes) to provide allylic alkylation product **81** as a colorless oil (0.11 g, 73% yield): 90% ee; ^1H NMR (400 MHz, CDCl_3) δ 5.68 (dddd, J = 17.0, 10.3, 7.9, 6.8 Hz, 1H), 5.19 – 4.95 (m, 2H), 4.86 (s, 1H), 4.70 (d, J = 1.0 Hz, 1H), 3.95 – 3.35 (m, 4H), 2.71 – 2.19 (m, 6H), 1.66 (d, J = 0.7 Hz, 3H), 1.49 (s, 9H); ^{13}C NMR (101 MHz, CDCl_3) δ 154.9, 141.2, 132.9, 119.1, 115.8, 80.5, 52.9, 41.3, 39.1, 38.3, 31.7, 28.5, 24.5, 22.8, 14.3; HPLC conditions: 0.9% EtOH, 1.0 mL/min, Chiralpak AD & AD–H columns in series, λ = 210 nm, t_{R} (min): major = 11.319, minor = 11.808.



Tert-butyl (3*S*,4*R*)-3-allyl-4-hydroxy-3-(2-methylallyl)piperidine-1-carboxylate (282). *Please note* Relative stereochemistry was not confirmed. To a solution of ketone **281** (83 mg, 0.28 mmol, 1.0 equiv) in CH_2Cl_2 (10 mL) at 0 °C was added (*S*)-CBS (1 M,

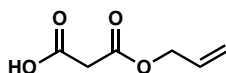
0.057 mL, 0.057 mmol, 0.2 equiv) followed by $\text{BH}_3\cdot\text{DMS}$ (2 M, 0.35 mL, 0.70 mmol, 2.0 equiv). The resulting solution was stirred for 7 h, whereupon a second aliquot of $\text{BH}_3\cdot\text{DMS}$ (2 M, 0.10 mL, 0.20 mmol, 0.7 equiv) was added. The reaction was stirred for an additional 3.5 h, quenched with MeOH (5 mL) and a saturated aqueous sodium citrate solution (10 mL), then warmed to ambient temperature and stirred for an additional 15 min. The aqueous layer was extracted with Et_2O (3 x 10 mL), dried over Mg_2SO_4 , and concentrated under reduced pressure. The crude residue was purified by silica gel flash column chromatography (30% EtOAc/hexanes) to afford alcohol **282** as an inseparable mixture (4:1) of diastereomers and a colorless oil (83 mg, 33% yield): ^1H NMR (400 MHz, CDCl_3) δ 6.20 – 5.85 (m, 1H), 5.23 – 5.06 (m, 2H), 5.03 – 4.94 (m, 1H), 4.86 (s, 1H), 4.04 – 3.13 (m, 2H), 3.01 – 2.84 (m, 2H), 2.43 – 2.19 (m, 3H), 2.01 (d, J = 13.7 Hz, 1H), 1.89 – 1.79 (m, 3H), 1.56 (q, J = 2.3, 1.8 Hz, 11H); ^{13}C NMR (101 MHz, CDCl_3) δ 155.2, 143.4, 134.3, 118.4, 118.2, 115.8, 115.6, 42.4, 41.9, 37.5, 29.7, 28.8, 28.4, 25.4, 25.4.

A13.8.2.4 Experimental Procedures and Spectroscopic Data for the Synthesis of Synthetic Intermediates in Section A13.5

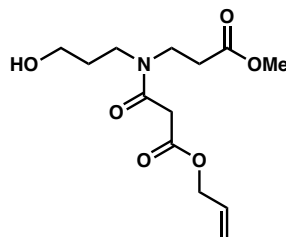


4-((*Tert*-butyldiphenylsilyl)oxy)piperidin-2-one (291). To a solution of 3 M HCl/EtOAc (0.5 mL) at 0 °C was added **287**³⁵ (0.10 g, 0.22 mmol, 1.0 equiv). The resulting mixture was stirred for 1 h, whereupon the reaction was concentrated under reduced pressure. The crude residue was purified by silica gel flash chromatography (35–

100% acetone/hexanes) to afford deprotected lactam **291** as a colorless solid (51 mg, 66% yield): ^1H NMR (400 MHz, CDCl_3) δ 7.78 – 7.32 (m, 10H), 7.17 (s, 1H), 4.15 (p, $J = 4.9$ Hz, 1H), 3.69 – 3.42 (m, 1H), 3.27 – 2.99 (m, 1H), 2.41 (dd, $J = 4.8, 1.6$ Hz, 2H), 1.74 (q, $J = 5.7$ Hz, 2H), 1.07 (s, 9H); ^{13}C NMR (101 MHz, CDCl_3) δ 171.9, 135.7, 135.7, 133.7, 133.4, 129.9, 129.9, 127.8, 127.8, 65.8, 40.5, 37.8, 29.9, 26.9, 19.1.



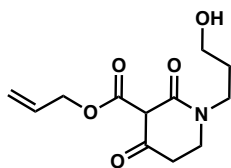
3-(Allyloxy)-3-oxopropanoic acid (294). A solution of Meldrum's acid (20.0 g, 0.14 mmol, 1.0 equiv) in allyl alcohol (40 mL) was heated under reflux for 18 h, whereupon the reaction was cooled to ambient temperature and concentrated under reduced pressure. The crude residue was dissolved in MeOH (60 mL), aqueous ammonia (50%, 7 mL) was added, the resulting solution was stirred for 15 min, and then concentrated under reduced pressure. The crude residue was washed with hexanes/ Et_2O (1:1, 2 x 15 mL), dissolved in H_2O (20 mL) and acidified with 1 M HCl. The aqueous layer was extracted with Et_2O (3 x 30 mL), washed with brine, dried over Na_2SO_4 , and concentrated under reduced pressure to give acid **294** as a colorless solid (13.0 g, 65% yield).



Allyl 3-((3-hydroxypropyl)(3-methoxy-3-oxopropyl)amino)-3-oxopropanoate (295).

To a solution of amino alcohol **293**³⁶ (2.0 g, 12 mmol, 1.0 equiv), 4-

dimethylaminopyridine (0.15 g, 1.2 mmol, 0.1 equiv), NEt₃ (4.5 mL, 32 mmol, 2.6 equiv) in CH₂Cl₂ (24 mL) at 0 °C was added acid **294** (2.3 g, 16 mmol, 1.3 equiv) followed by EDCI•HCl (3.1 g, 16 mmol, 1.3 equiv) portionwise. The resulting solution was stirred for 18 h, whereupon the reaction was quenched with 1 M HCl (pH < 7), extracted with CH₂Cl₂ (3 x 20 mL), washed with brine, dried over Na₂SO₄, and concentrated under reduced pressure to afford β-ketoamide **295** as a colorless oil (2.7 g, 76% yield): ¹H NMR (400 MHz, CDCl₃) δ 6.02 – 5.76 (m, 1H), 5.47 – 5.13 (m, 2H), 4.63 (ddtt, *J* = 4.8, 3.8, 2.5, 1.2 Hz, 2H), 3.89 – 3.18 (m, 7H), 2.64 (td, *J* = 7.1, 4.4 Hz, 1H), 2.06 – 1.44 (m, 1H); ¹³C NMR (101 MHz, CDCl₃) δ 172.6, 171.3, 167.7, 131.5, 119.2, 118.9, 66.3, 66.2, 66.1, 58.2, 52.3, 45.8, 43.9, 42.1, 41.4, 40.9, 33.2, 32.3, 31.1, 30.2.



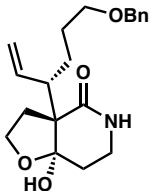
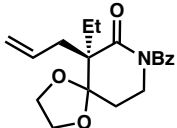
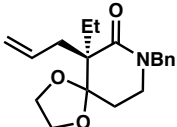
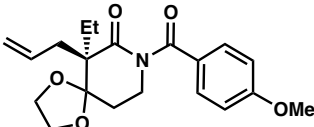
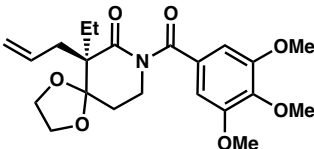
Allyl 1-(3-hydroxypropyl)-2,4-dioxopiperidine-3-carboxylate (296). To allyl alcohol (35 mL) was added Na metal (0.67 g, 29 mmol, 2.1 equiv) followed by β-ketoamide **295** (4.0 g, 14 mmol, 1.0 equiv). The resulting solution was heated under reflux for 18 h, whereupon the reaction was cooled to ambient temperature and concentrated under reduced pressure. The crude residue was dissolved in H₂O (30 mL) and the aqueous layer was extracted with EtOAc (3 x 30 mL). The aqueous layer was then acidified with 6 M HCl and extracted with 10% isopropanol/CH₂Cl₂ (3 x 30 mL). The combined organics were dried over Na₂SO₄ and concentrated under reduced pressure. The crude residue was purified by silica gel flash column chromatography to afford β-ketolactam **296** as a

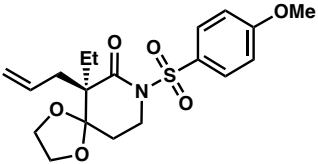
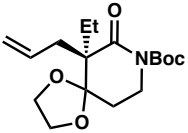
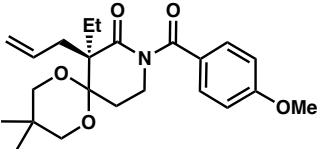
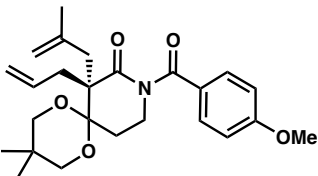
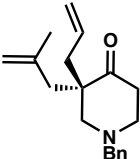
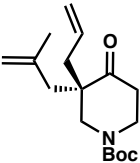
yellow oil (1.9 g, 52% yield): ^1H NMR (400 MHz, CDCl_3) δ 5.99 (ddt, $J = 17.2, 10.5, 5.5$ Hz, 1H), 5.50 – 5.41 (m, 1H), 5.28 (dt, $J = 10.5, 1.4$ Hz, 1H), 4.81 (dt, $J = 5.5, 1.5$ Hz, 2H), 4.03 (p, $J = 6.1$ Hz, 3H), 3.57 (q, $J = 6.0, 5.6$ Hz, 4H), 3.46 – 3.37 (m, 2H), 2.67 (t, $J = 6.9$ Hz, 2H).

A13.8.2.5 Determination of Enantiomeric Excess

Please note racemic products for palladium-catalyzed allylic alkylations were synthesized using $\text{Pd}(\text{PPh}_3)_4$. Racemic products for iridium-catalyzed allylic alkylations were synthesized using racemic **L2**.

Table A13.4 Determination of enantiomeric excess

Entry	Product	Assay Conditions	Retention time of major isomer (min)	Retention time of minor isomer (min)	%ee
1		HPLC Chiralpak AD-H 8% IPA isocratic, 1.0 mL/min	21.087	21.876	96%
2		SFC Chiralpak OJ-H 3% MeOH isocratic, 3.0 mL/min	19.747	22.731	48%
3		SFC Chiralpak OJ-H 5% MeOH isocratic, 3.0 mL/min	7.012	5.589	29%
4		SFC Chiralpak OJ-H 3% MeOH isocratic, 3.0 mL/min	20.272	24.437	62%
5		SFC Chiralpak OJ-H 1% MeOH isocratic, 3.0 mL/min	27.715	25.961	61%

Entry	Product	Assay Conditions	Retention time of major isomer (min)	Retention time of minor isomer (min)	%ee
6		SFC Chiralpak OJ-H 5% MeOH isocratic, 3.0 mL/min	15.378	17.679	63%
7		SFC Chiralpak OJ-H 1% MeOH isocratic, 3.0 mL/min	3.062	4.057	53%
8		SFC Chiralpak OJ-H 3% MeOH isocratic, 3.0 mL/min	18.627	4.817	93%
9		SFC AS-H 3% MeOH isocratic, 3.0 mL/min	11.875	10.765	24%
10		HPLC Chiralpak OJ 1% EtOH isocratic, 1.0 mL/min	10.113	8.486	82%
11		HPLC Chiralpak AD & AD-H in series 0.9% EtOH isocratic, 1.0 mL/min	11.319	11.808	90%

A13.9 REFERENCES AND NOTES

- (1) (a) Ma, X.; Gang, D. R. *Nat. Prod. Rep.* **2004**, *21*, 752–772; (b) Hirasawa, Y.; Kobayashi, J.; Morita, H. **2009**, *77*, 679–729; (c) Kitajima, M.; Takayama, H. *Top. Curr. Chem.* **2012**, *309*, 1–31.
- (2) Dong, L.-B.; Gao, X.; Liu, F.; He, J.; Wu, X.-D.; Li, Y.; Zhao, Q.-S. *Org. Lett.* **2013**, *15*, 3570–3573.
- (3) Sizemore, N.; Rychnovsky, S. D. *Org. Lett.* **2014**, *16*, 688–691.
- (4) Slack, E. D.; Gabriel, C. M.; Lipshutz, B. H. *Angew. Chem. Int. Ed.* **2014**, *53*, 14051–14054.
- (5) Marshall, J. A.; DeHoff, B. S. *J. Org. Chem.* **1986**, *51*, 863–872.
- (6) Dindaroğlu, M.; Dinçer, S. A.; Schmalz, H.-G. *Eur. J. Org. Chem.* **2014**, 4315–4326.
- (7) Butler, J. D.; Coffman, K. C.; Ziebart, K. T.; Toney, M. D.; Kurth, M. J. *Chem. Eur. J.* **2010**, *16*, 9002–9005.
- (8) Hethcox, J. C.; Shockley, S. E.; Stoltz, B. M. *Angew. Chem. Int. Ed.* **2016**, *55*, 16092–16095.
- (9) Liu, W.-B.; Reeves, C. M.; Virgil, S. C.; Stoltz, B. M. *J. Am. Chem. Soc.* **2013**, *135*, 10626–10629.
- (10) For select examples, see: (a) Kanayama, T.; Yoshida, K.; Miyabe, H.; Takemoto, Y. *Angew. Chem. Int. Ed.* **2003**, *42*, 2054–2056; (b) Jiang, X.; Chen, W.; Hartwig, J. F. *Angew. Chem. Int. Ed.* **2016**, *55*, 5819–5823; (c) Huo, X.; He, R.; Zhang, X.; Zhang, W. *J. Am. Chem. Soc.* **2016**, *138*, 11093–11096; (d) Chen, W.; Hartwig, J.

- F. *J. Am. Chem. Soc.* **2013**, *135*, 2068–2071; (e) Chen, W.; Hartwig, J. F. *J. Am. Chem. Soc.* **2014**, *136*, 377–382; (f) Krautwald, S.; Schafroth, M. A.; Sarlah, D.; Carreira, E. M. *J. Am. Chem. Soc.* **2014**, *136*, 3020–3023; (g) Sandmeier, T.; Krautwald, S.; Zipfel, Carreira, E. M. *Angew. Chem. Int. Ed.* **2015**, *54*, 14363–14367.
- (11) Liu, W.-B.; Reeves, C. M.; Stoltz, B. M. *J. Am. Chem. Soc.* **2013**, *135*, 17298–17301.
- (12) Shockley, S. E.; Hethcox, J. C.; Stoltz, B. M. *Angew. Chem. Int. Ed.* **2017**, *56*, 11545–11548.
- (13) For an example of a bimetallic dual catalytic system used in a diastereoselective iridium-catalyzed allylic alkylation, see: Huo, X.; He, R.; Zhang, W. *J. Am. Chem. Soc.* **2016**, *138*, 11093–11096.
- (14) McDougal, N. T.; Virgil, S. C.; Stoltz, B. M. *Synlett* **2010**, 1712–1716.
- (15) Behenna, D. C.; Liu, Y.; Yurino, T.; Kim, J.; White, D. E.; Virgil, S. C.; Stoltz, B. M. *Nature Chem.* **2012**, *4*, 130–133.
- (16) Trost, B. M. *Tetrahedron* **2015**, *71*, 5708–5733.
- (17) Behenna, D. C.; Mohr, J. T.; Sherden, N. H.; Marinescu, S. C.; Harned, A. M.; Tani, K.; Seto, M.; Ma, S.; Novák, Z.; Krout, M. R.; McFadden, R. M.; Roizen, J. L.; Enquist, J. A., Jr.; White, D. E.; Levine, S. R.; Petrova, K. V.; Iwashita, A.; Virgil, S. C.; Stoltz, B. M. *Chem. Eur. J.* **2011**, *17*, 14199–14223.
- (18) (a) Shockley, S. E.; Hethcox, J. C.; Stoltz, B. M. *Tetrahedron Lett.* **2017**, *58*, 3341–3343; (b) Greshock, T. J.; Funk, R. L. *J. Am. Chem. Soc.* **2002**, *124*, 754–755.

- (19) (a) Hünig, S.; Schäfer, M.; Schweeberg, W. *Chem. Ber.* **1993**, *126*, 191–204; (b) Wiedner, S. D.; Vedejs, E. *Org. Lett.* **2010**, *12*, 4030–4033.
- (20) Mupparapu, N.; Khan, S.; Battula, S.; Kushwaha, M.; Gupta, A. P.; Ahmed, Q. N.; Vishwakarma, R. A. *Org. Lett.* **2014**, *16*, 1152–1155.
- (21) For select examples of *exo*-selective IMDA reactions, see: (a) Crimmins, M. T.; Brown, B. H.; Plake, H. R. *J. Am. Chem. Soc.* **2006**, *128*, 1371–1378; (b) Pearson, E. L.; Kanizaj, N.; Willis, A. C.; Paddon-Row, M. N.; Sherburn, M. S. *Chem. Eur. J.* **2010**, *16*, 8280–8284.
- (22) (a) Izumi, M.; Wada, K.; Yuasa, H.; Hashimoto, H. *J. Org. Chem.* **2005**, *70*, 8817–8824; (b) Smith, A. B. III; Doughty, V. A.; Lin, Q.; Zhuang, L.; McBriar, M. D.; Boldi, A. M.; Moser, W. H.; Murase, N. M.; Nakayama, K.; Sobukawa, M. *Angew. Chem. Int. Ed.* **2001**, *40*, 191–195; (c) Myers, A. G.; Gin, D. Y.; Rogers, D. H. *J. Am. Chem. Soc.* **1994**, *116*, 4697–4718.
- (23) (a) Fujita, K.; Enoki, Y.; Yamaguchi, R; (b) Bähn, S.; Imm, S.; Neubert, L.; Zhang, M.; Neumann, H.; Beller, M. *ChemCatChem* **2011**, *3*, 1853–1864; (c) Dobereiner, G. E.; Crabtree, R. H. *Chem. Rev.* **2010**, *110*, 681–703; (d) Guillena, G.; Ramón, D. J.; Yus, M. *Chem. Rev.* **2010**, *110*, 1611–1641; (e) Hamid, M. H. S. A.; Slatford, P. A.; Williams, J. M. J. *Adv. Synth. Catal.* **2007**, *349*, 1555–1575; (f) Nixon, T. D.; Whittlesey, M. K.; Williams, J. M. J. *Dalton Trans.* **2009**, 753–762.
- (24) (a) He, F.; Bo, Y.; Altom, J. D.; Corey, E. J. *J. Am. Chem. Soc.* **1999**, *121*, 6771–6772; (b) Sumi, S.; Matsumoto, K.; Tokuyama, H.; Fukuyama, T. *Org. Lett.* **2003**,

- 5, 1891–1893; (c) Sumi, S.; Matsumoto, K.; Tokuyama, H.; Fukuyama, T. *Tetrahedron* **2003**, *59*, 8571–8587.
- (25) Wojaczyńska, E; Turowska-Tyrk, I. *Tetrahedron: Asymmetry* **2013**, *24*, 1247–1251.
- (26) Adam, G.; Huong, H. T. *Tetrahedron Lett.* **1980**, *21*, 1931–1932.
- (27) Bourry, A.; Couturier, D.; Sanz, G.; Van Hijfte, L.; Hénichart, J.-P.; Rigo, B. *Tetrahedron* **2006**, *62*, 4400–4407.
- (28) For an example of an alkyl-substituted silyl cyanohydrin addition, see: Kraus, G. A.; Wan, Z. *Tetrahedron Lett.* **1997**, *38*, 6509–6512.
- (29) Zhao, N.; Yin, S.; Xie, S.; Yan, H.; Ren, P.; Chen, G.; Chen, F.; Xu, J. *Angew. Chem. Int. Ed.* **2018**, *57*, 3386–3390.
- (30) Dai, W.-M.; Zhuo, W.-S. *Tetrahedron* **1985**, *41*, 4475–4482.
- (31) Polet, D.; Alexakis, A. *Org. Lett.* **2005**, *7*, 1621–1624.
- (32) Mercier, A.; Urbaneja, X.; Yeo, W. C.; Chaudhuri, P. D.; Cumming, G. R.; House, D.; Bernardinelli, G.; Kündig, E. P. *Chem. Eur. J.* **2010**, *16*, 6285–6299.
- (33) Kong, C.; Jana, N.; Jones, C.; Driver, T. G. *J. Am. Chem. Soc.* **2016**, *138*, 13271–13280.
- (34) Barbe, G.; St-Onge, M.; Charette, A. B. *Org. Lett.* **2008**, *10*, 5497–5499.
- (35) Adams, C.; Capparelli, M. P.; Ehara, T.; Karki, R. G.; Mainolfi, N.; Chun, Z. U.S. Patent WO2015009616 A1, Jan. 22, 2015.
- (36) Fabbrizzi, P.; Bianchini, F.; Menchi, G.; Raspanti, S.; Trabocchi, A. *Tetrahedron* **2014**, *70*, 5439–5449.

APPENDIX 14

Spectra Relevant to Appendix 13:

Progress Toward the Synthesis of (+)-Isopalhinine A

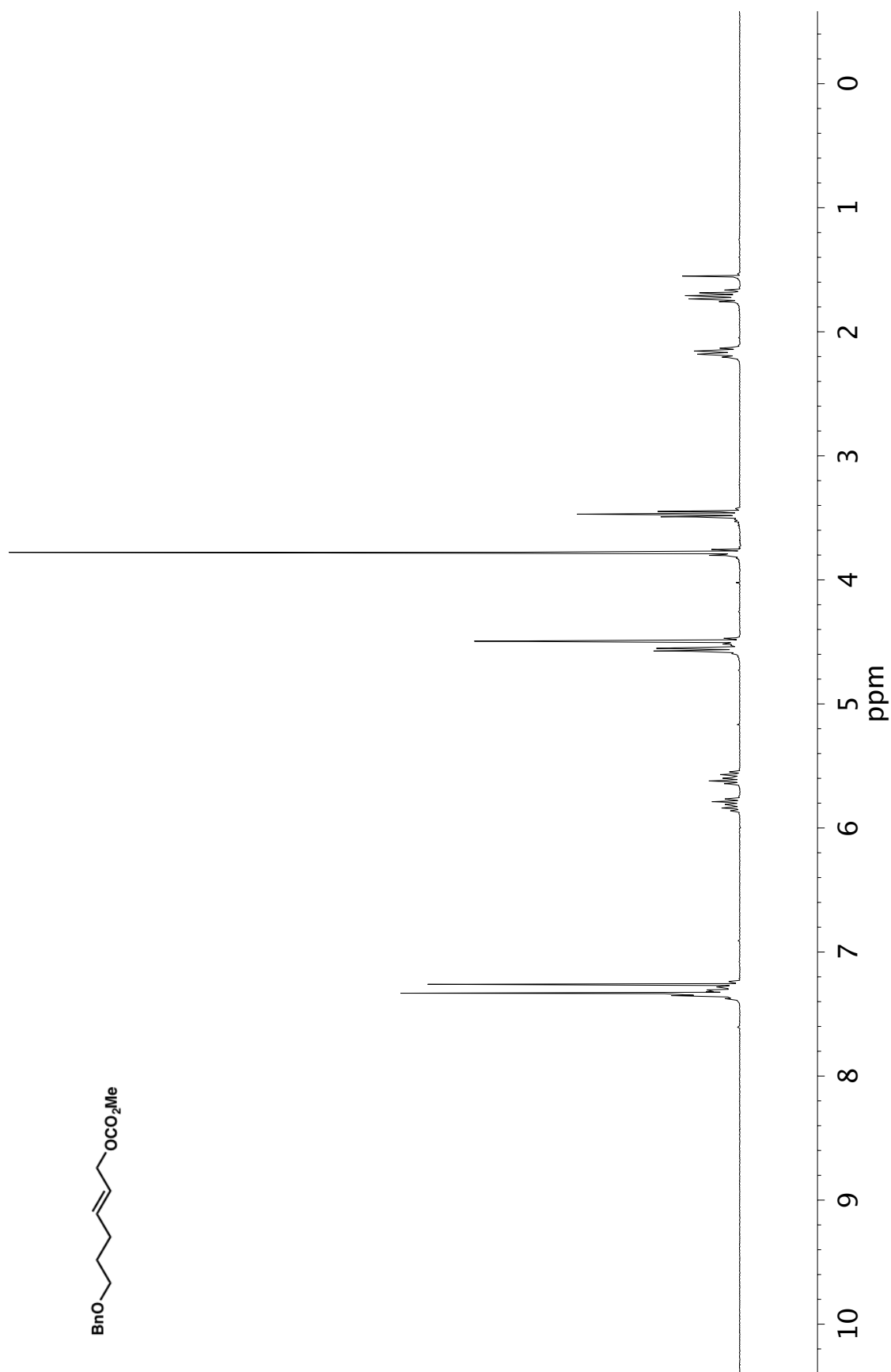


Figure A14.1 ^1H NMR (400 MHz, CDCl_3) of compound **226**

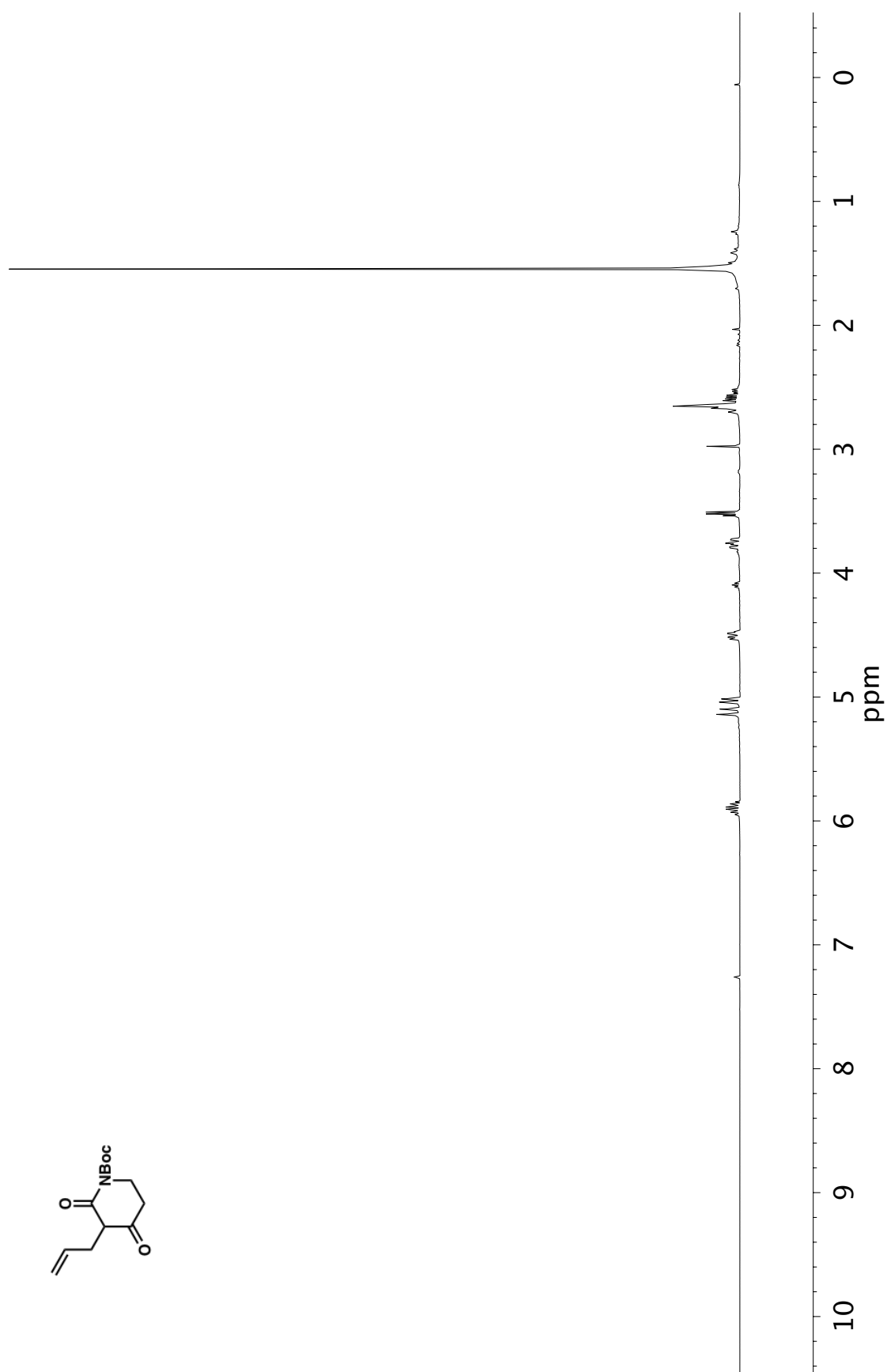


Figure A14.2 ¹H NMR (400 MHz, CDCl₃) of compound 233

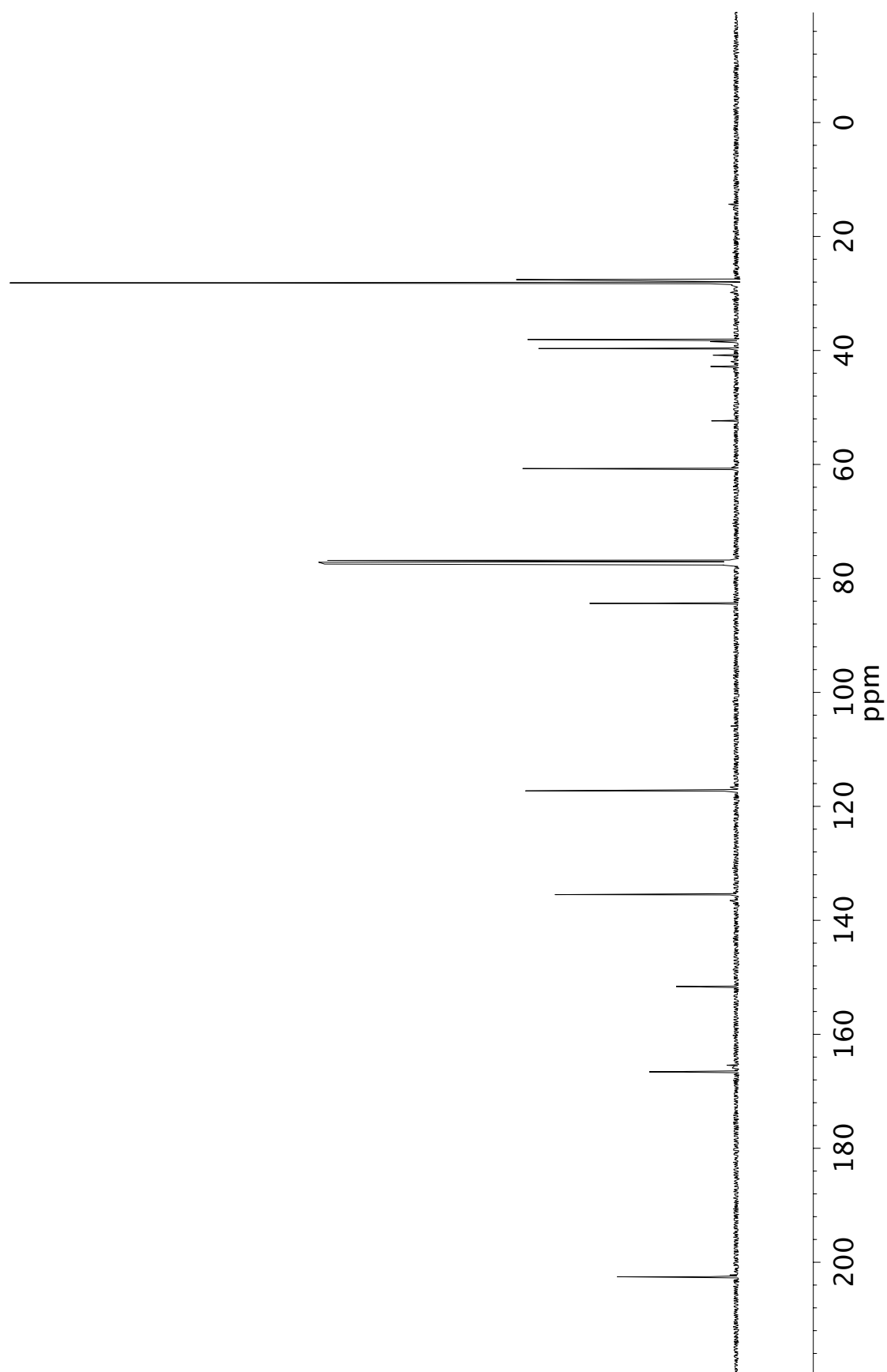
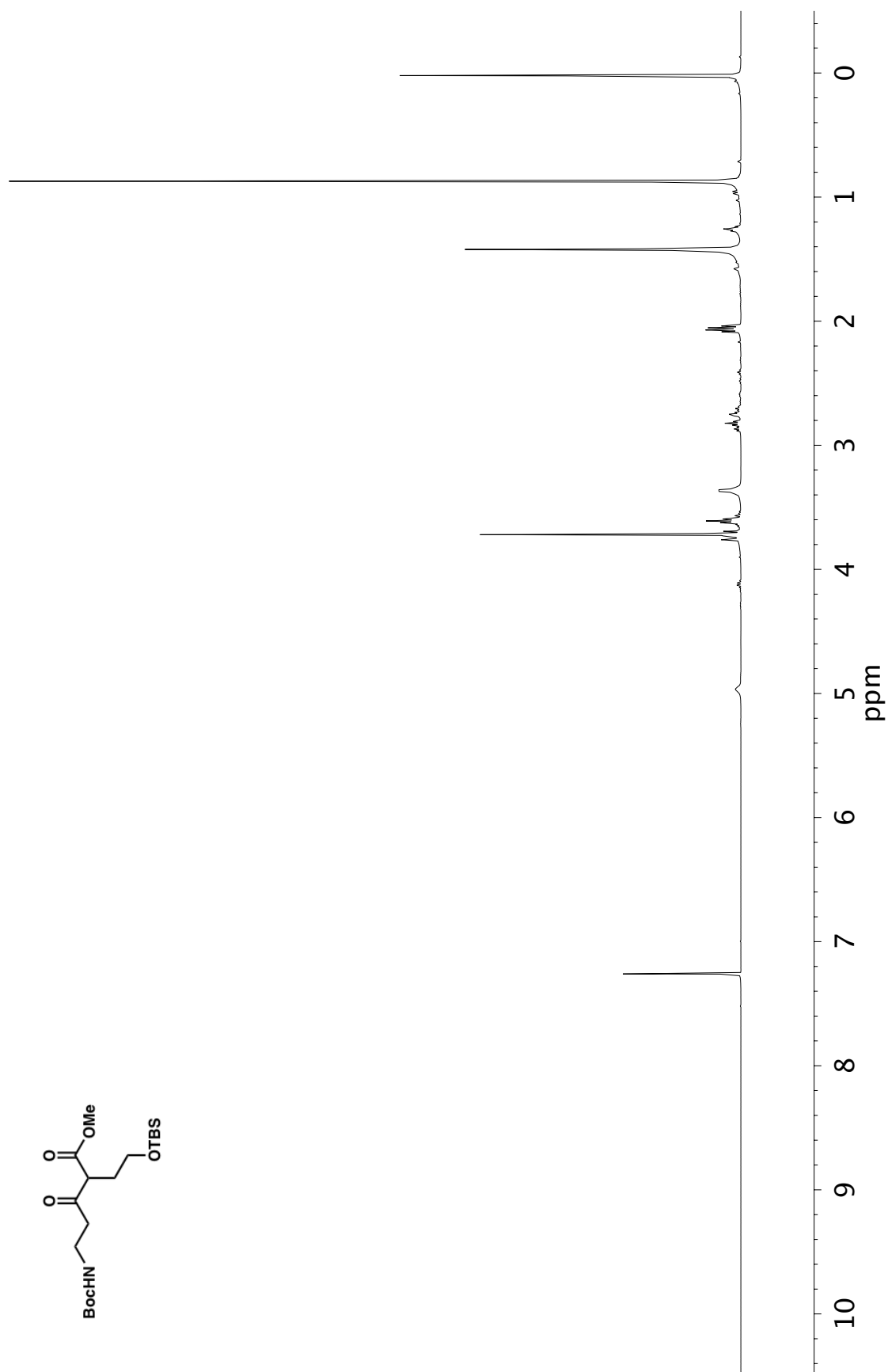


Figure A14.3 ^{13}C NMR (101 MHz, CDCl_3) of compound 233

**Figure A14.4** ¹H NMR (400 MHz, CDCl₃) of compound 234

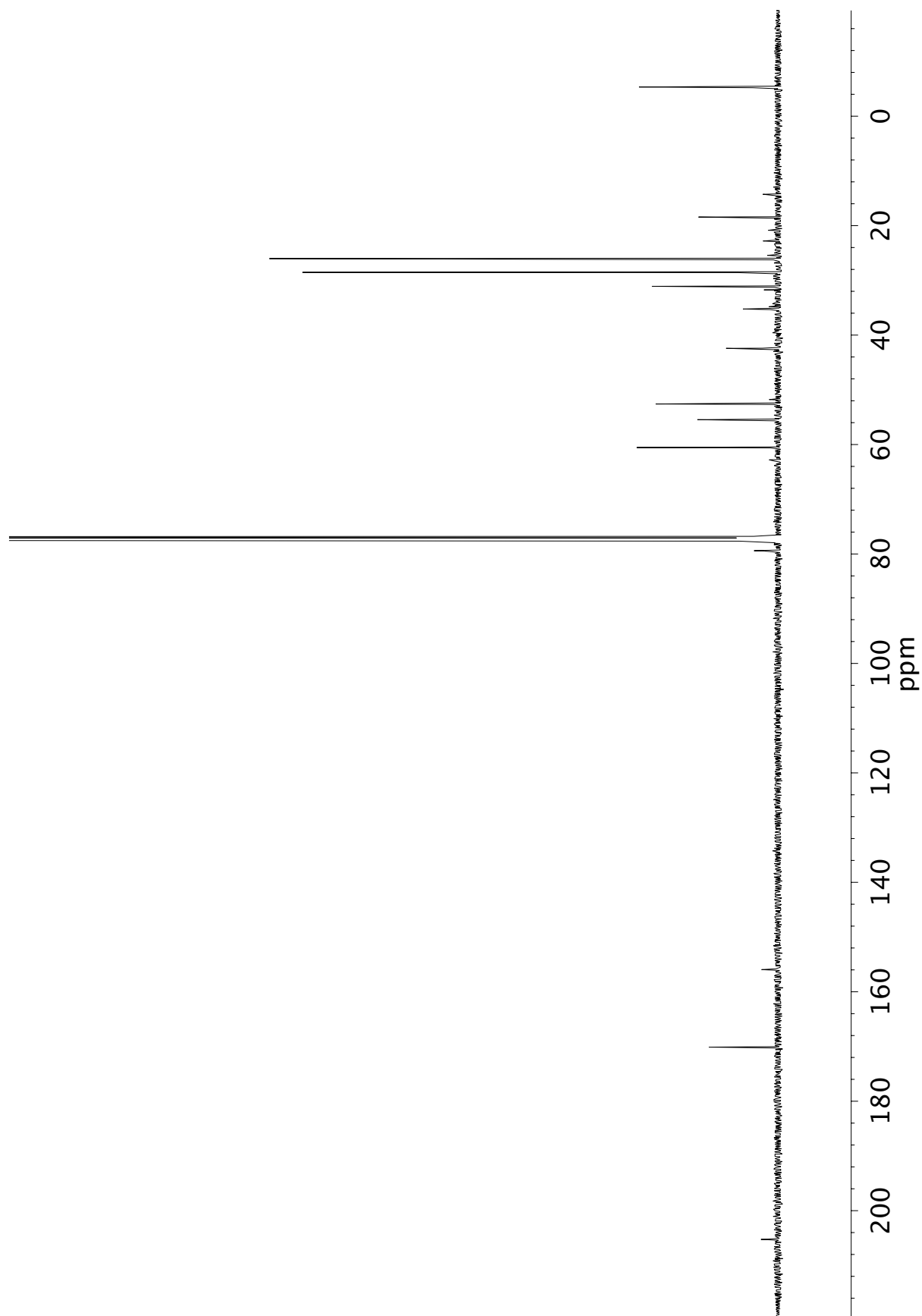


Figure A14.5 ¹³C NMR (101 MHz, CDCl₃) of compound 234

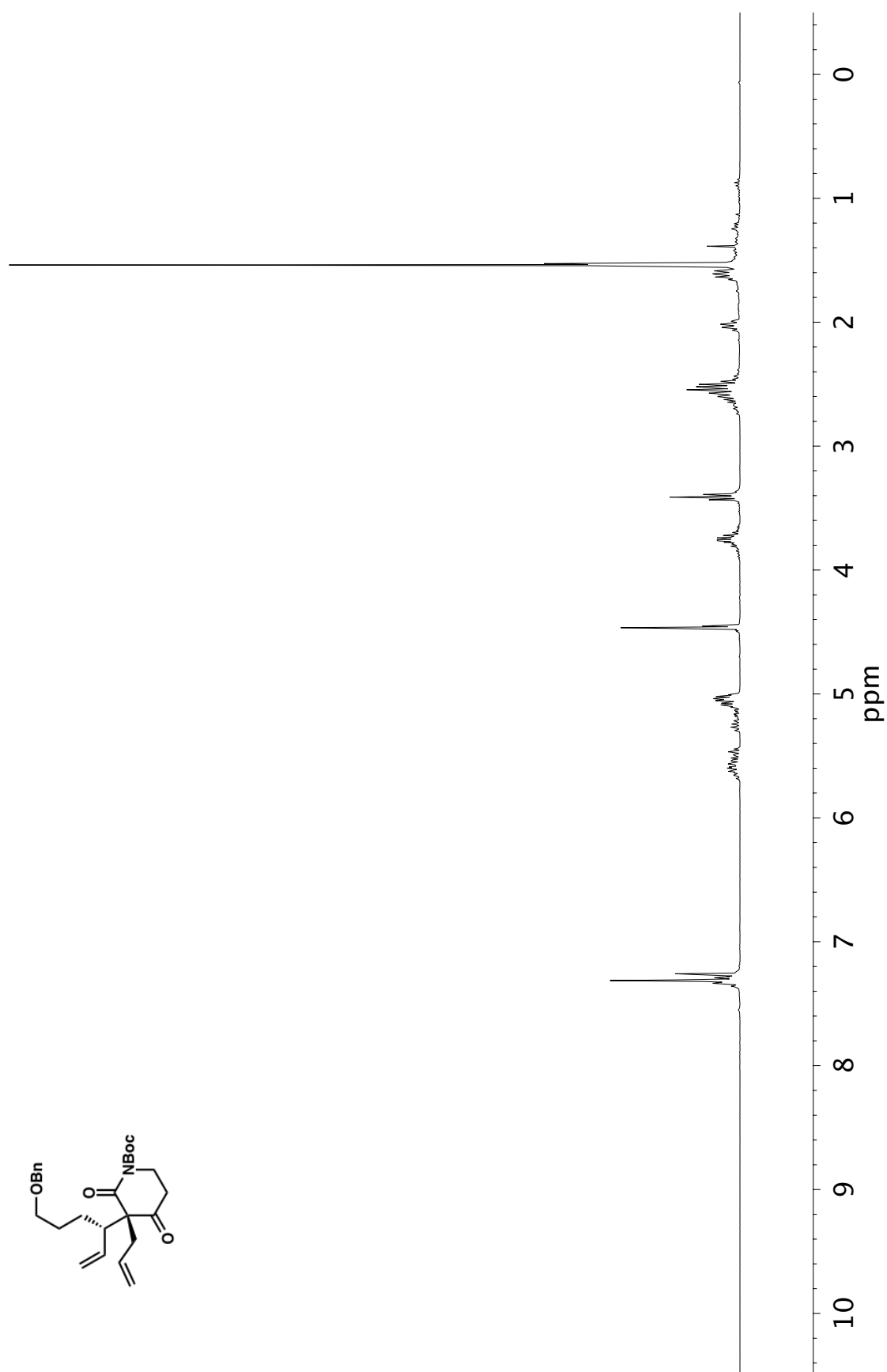


Figure A14.6 ¹H NMR (400 MHz, CDCl₃) of compound 235

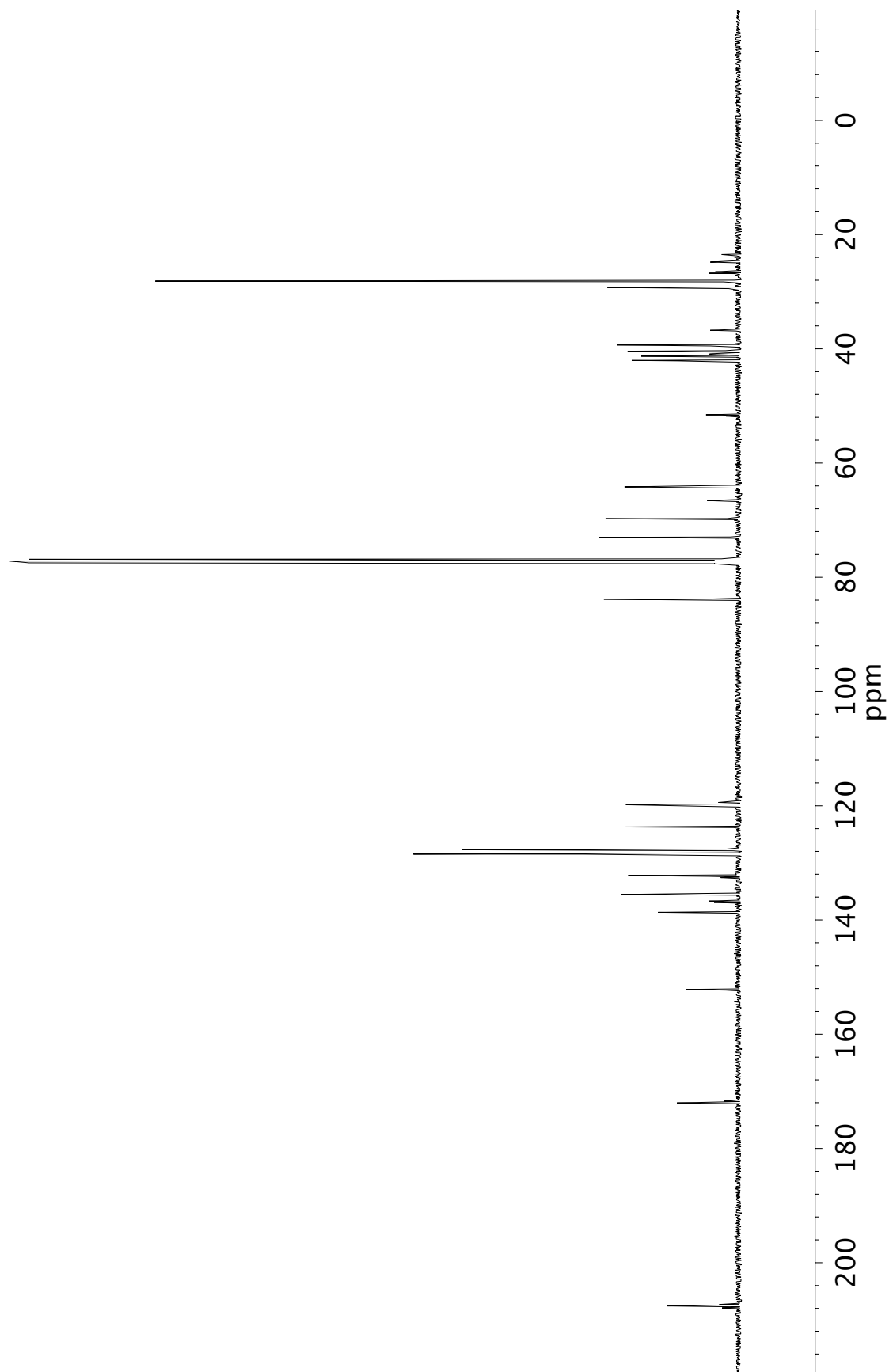


Figure A14.7 ^{13}C NMR (101 MHz, CDCl_3) of compound 235

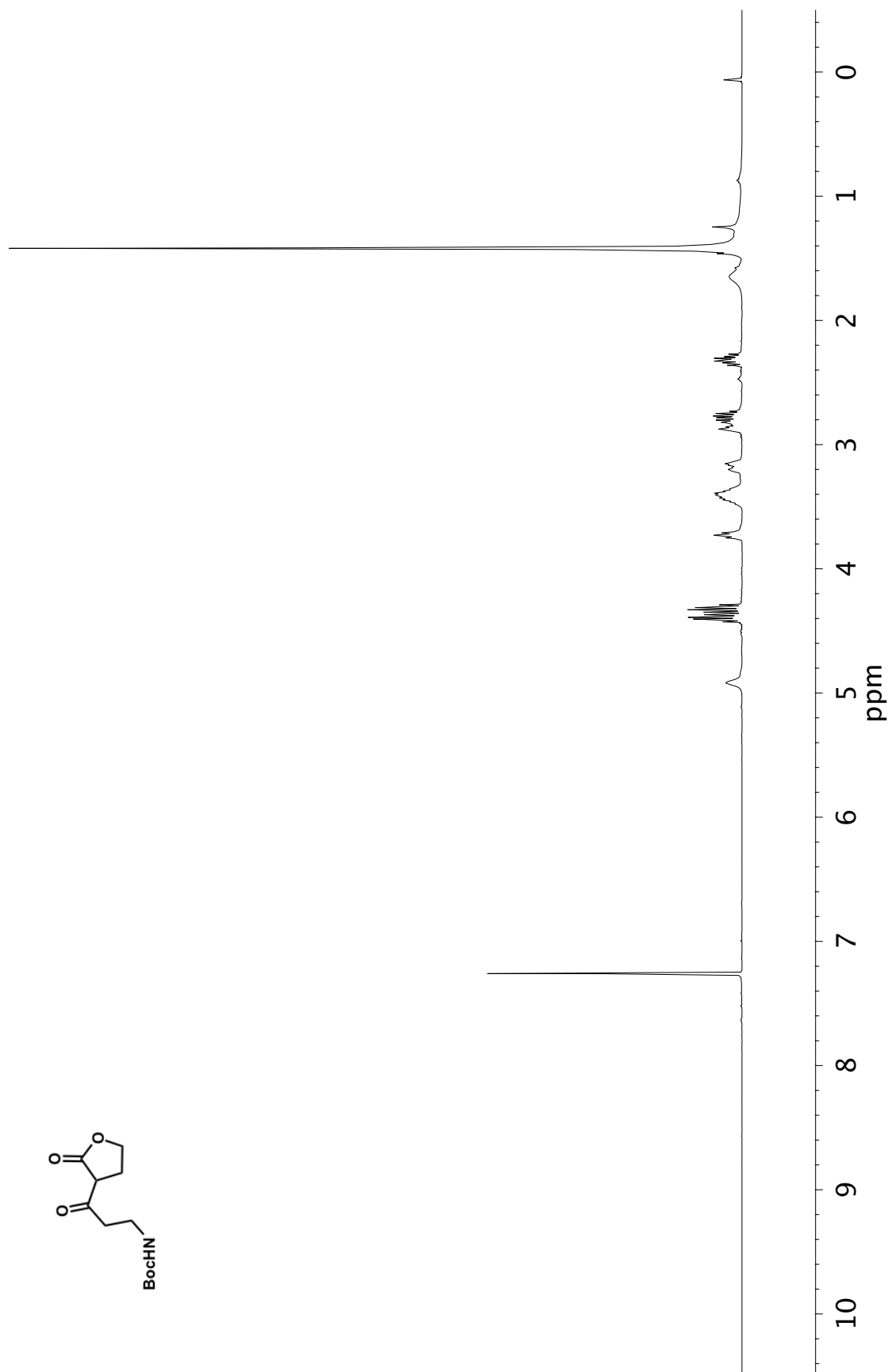


Figure A14.8 ^1H NMR (400 MHz, CDCl_3) of compound **238**

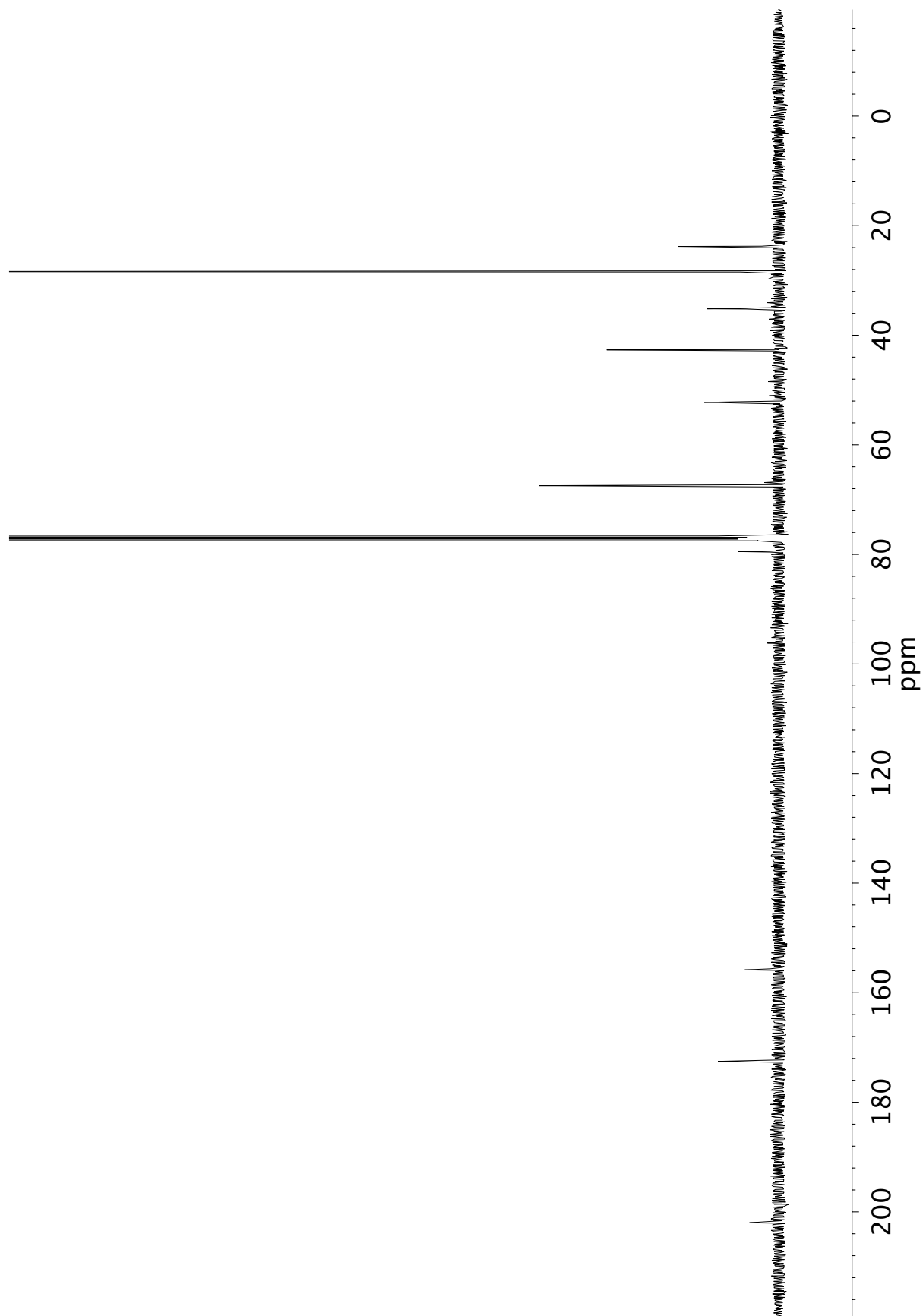


Figure A14.9 ^{13}C NMR (101 MHz, CDCl_3) of compound 238

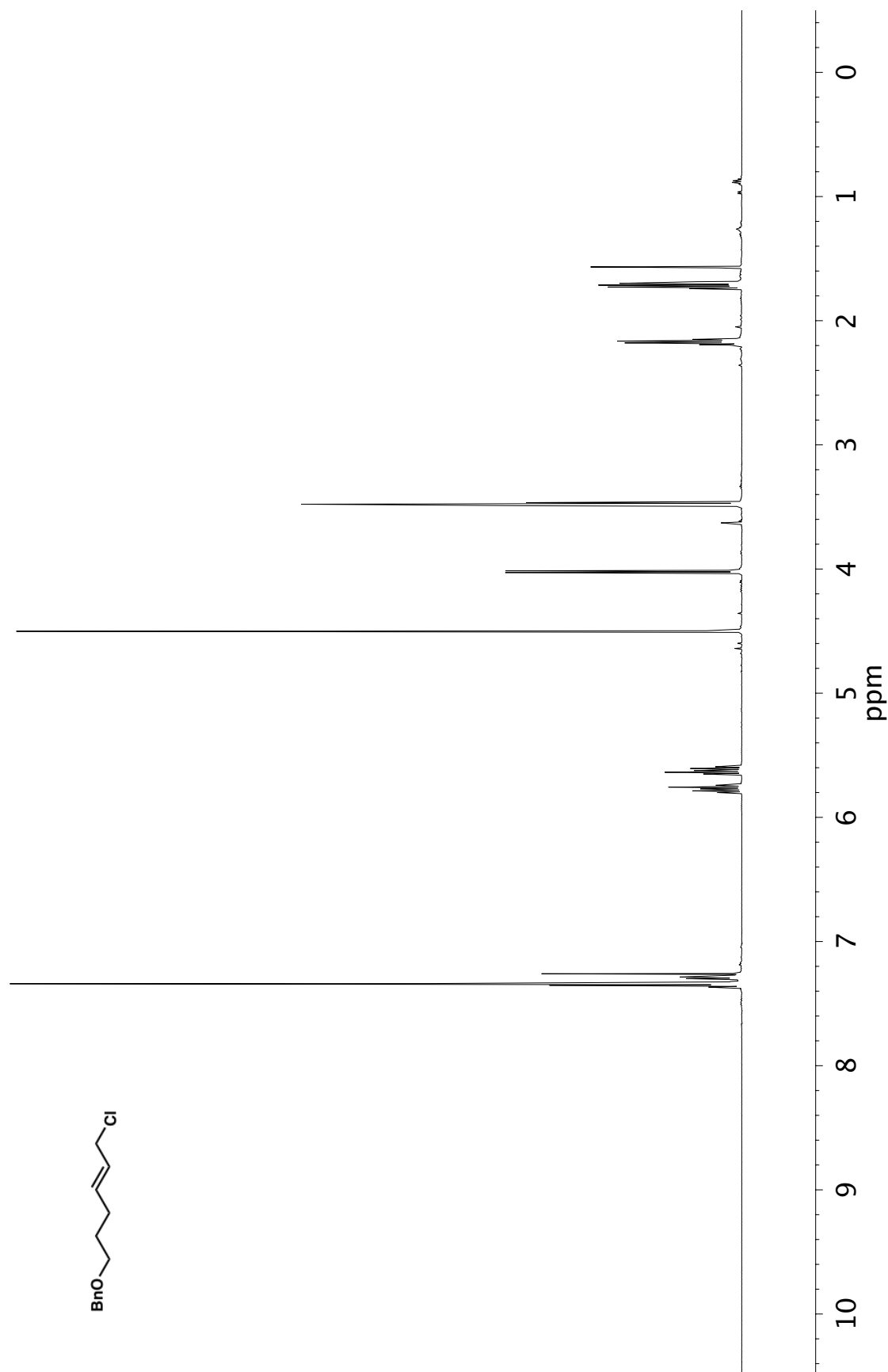


Figure A14.10 ^1H NMR (400 MHz, CDCl_3) of compound 240

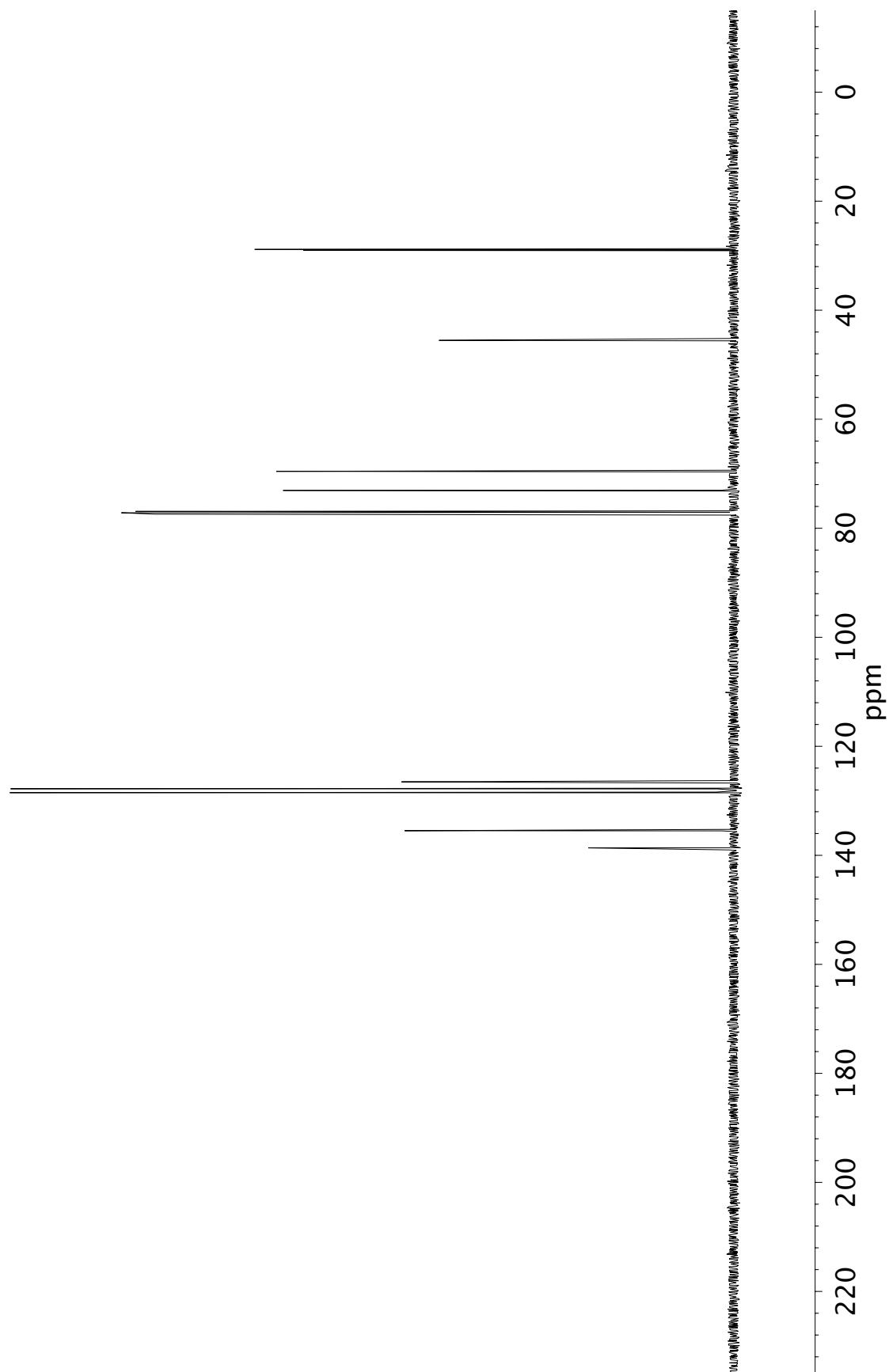


Figure A14.11 ^{13}C NMR (101 MHz, CDCl_3) of compound 240

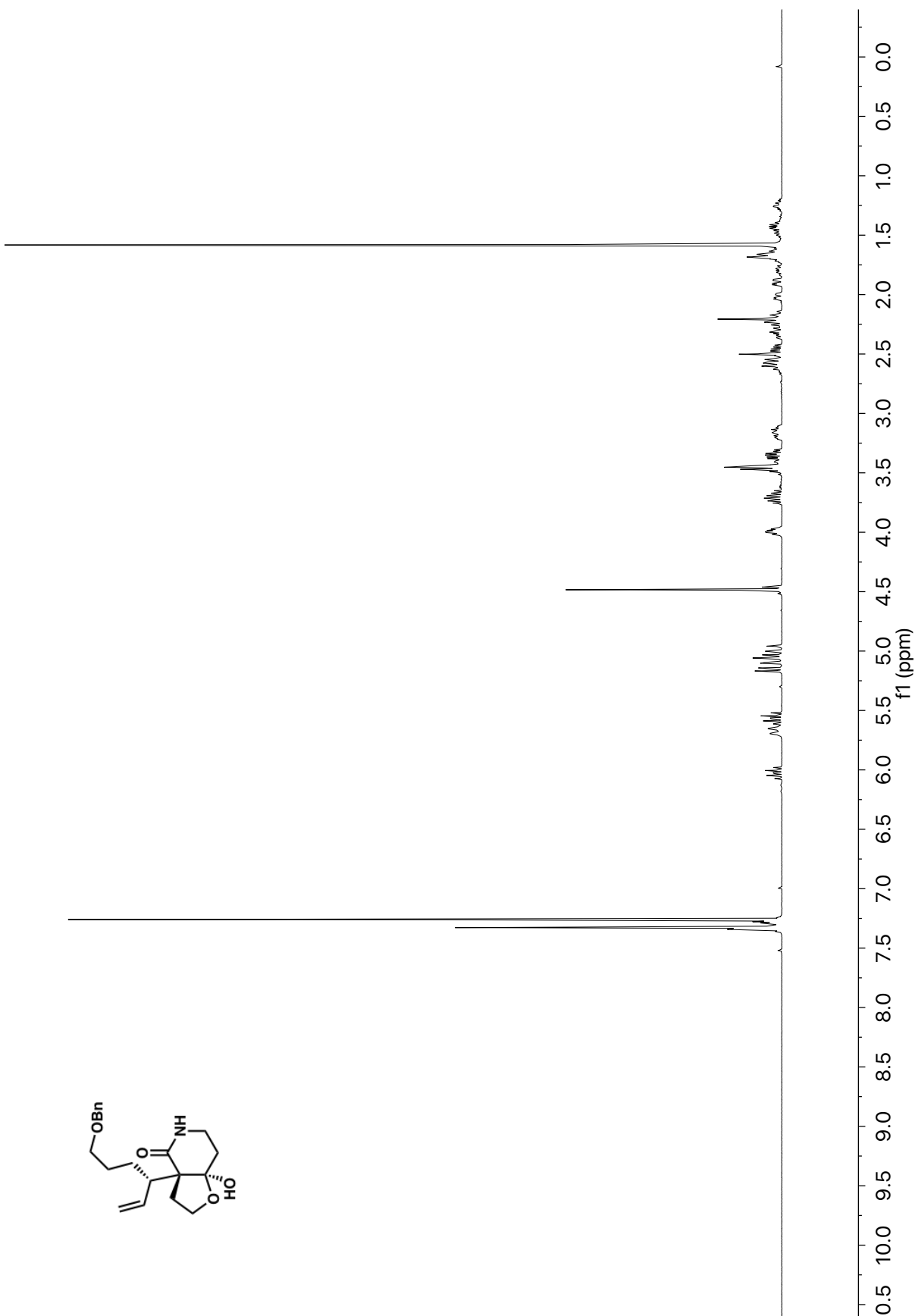


Figure A14.12 ¹H NMR (400 MHz, CDCl₃) of compound **241**

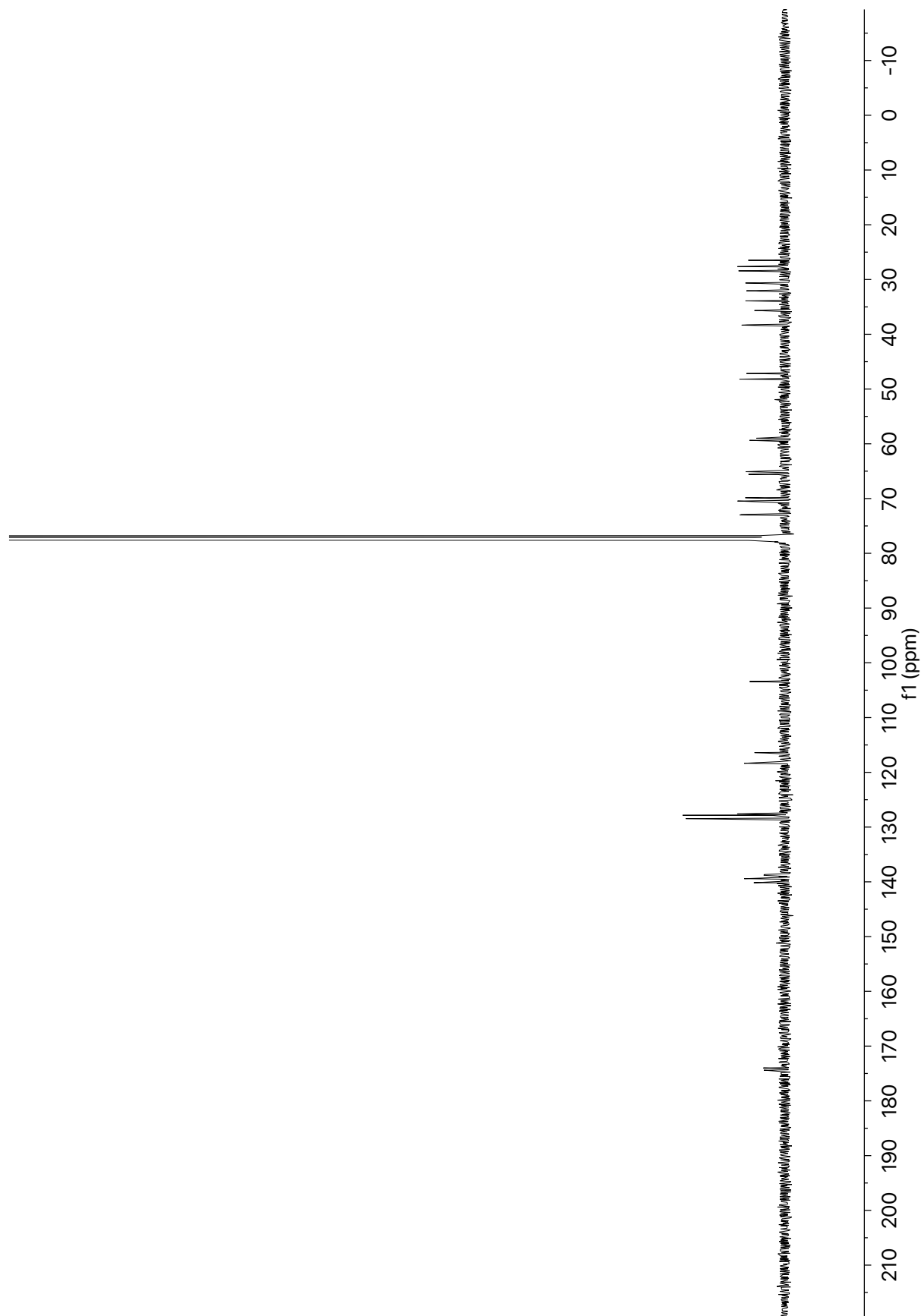


Figure A14.13 ^{13}C NMR (101 MHz, CDCl_3) of compound 241

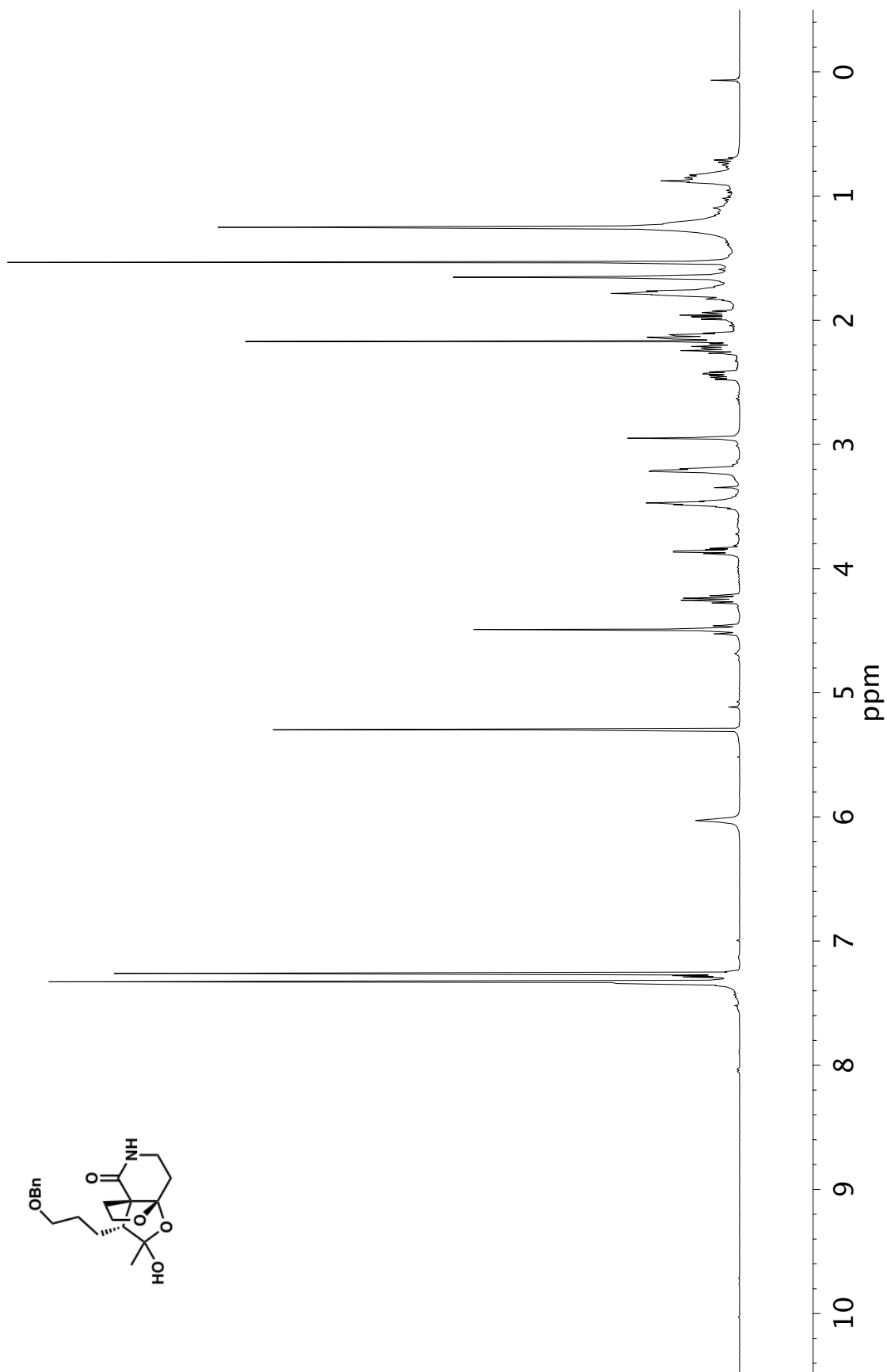


Figure A14.14 ^1H NMR (400 MHz, CDCl_3) of compound 243

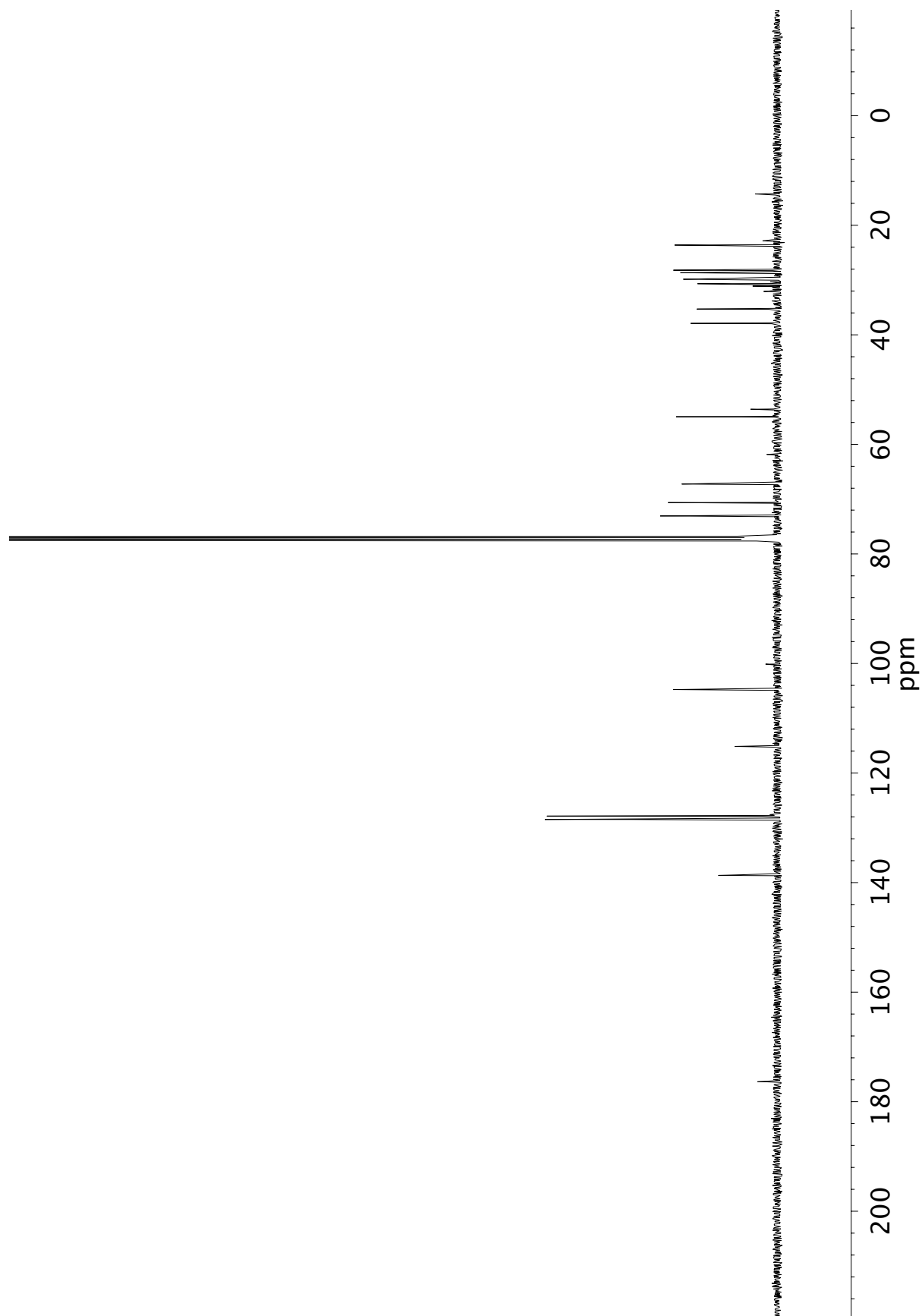


Figure A14.15 ^{13}C NMR (101 MHz, CDCl_3) of compound 243

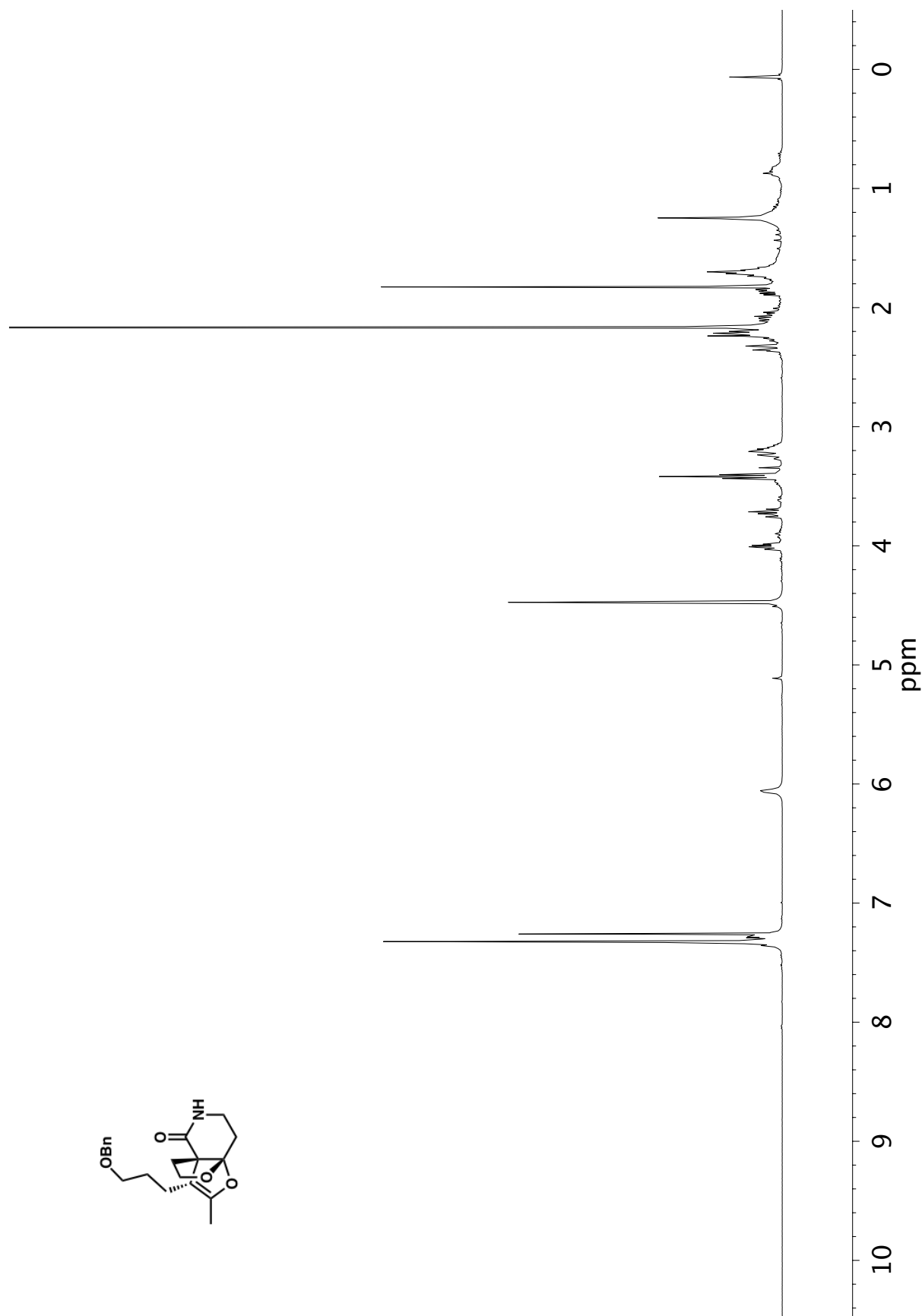


Figure A14.16 ^1H NMR (400 MHz, CDCl_3) of compound **244**

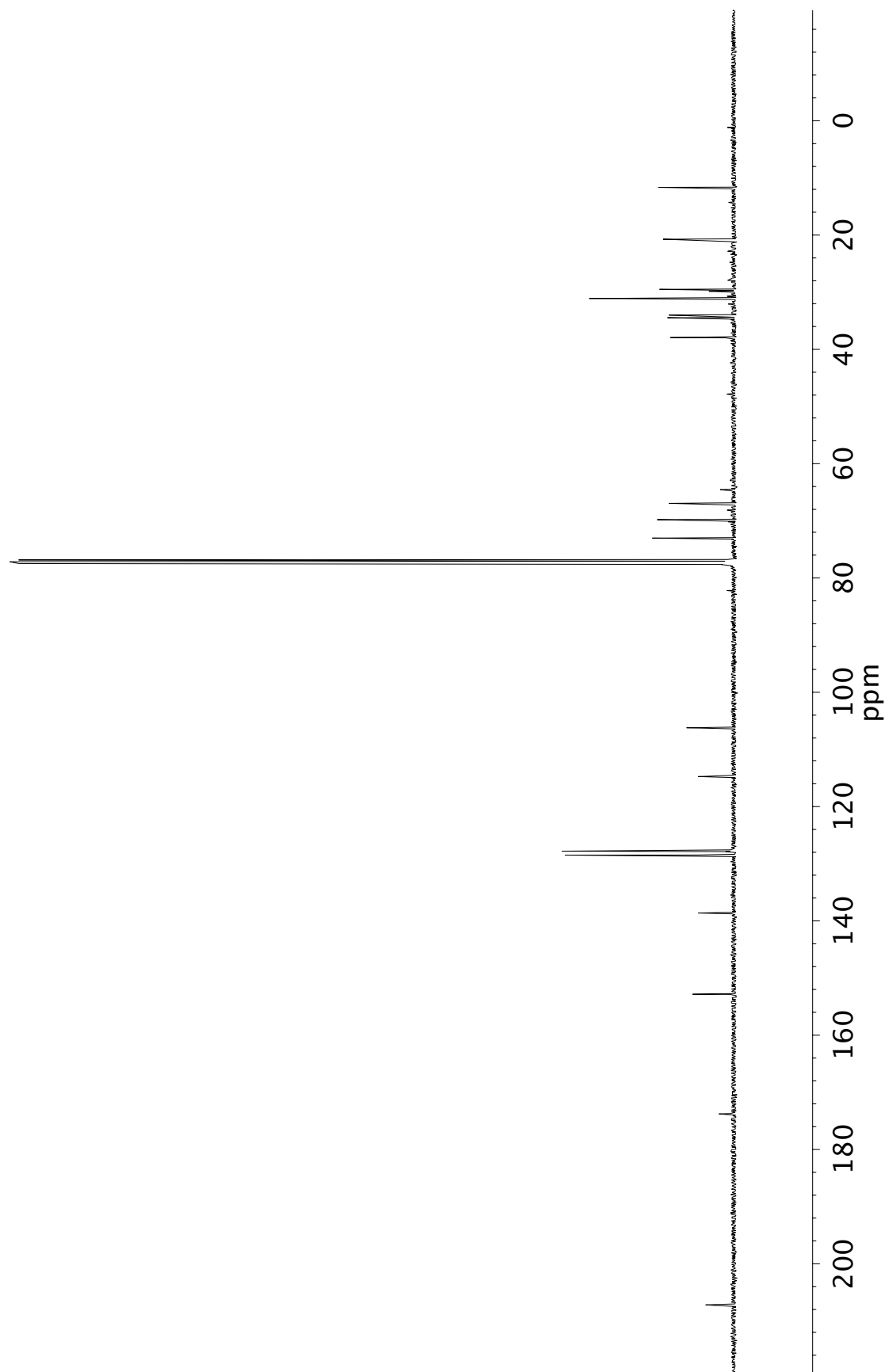


Figure A14.17 ^{13}C NMR (101 MHz, CDCl_3) of compound 244

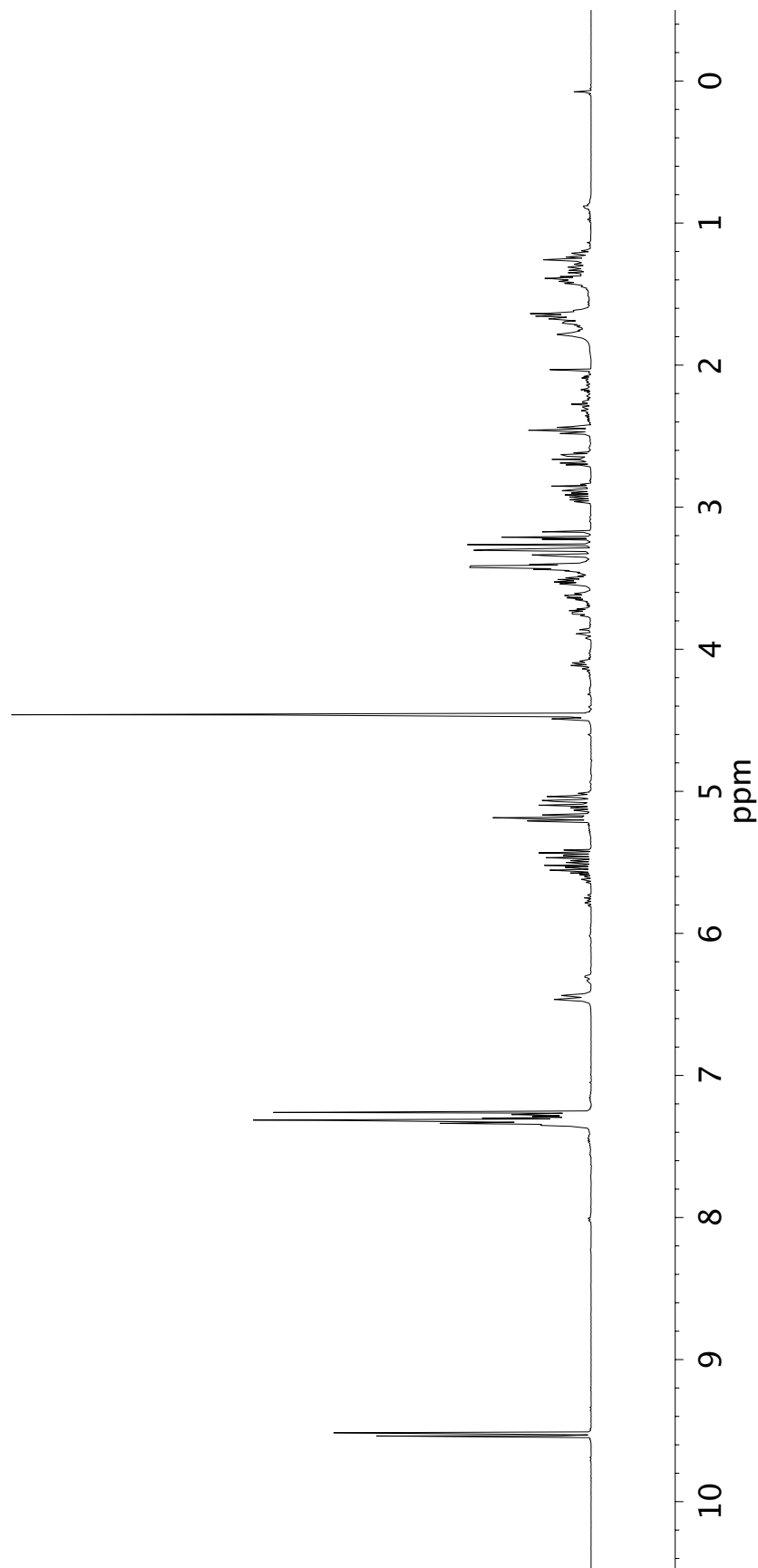
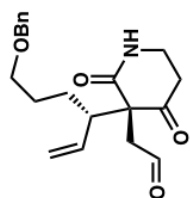


Figure A14.18 ^1H NMR (400 MHz, CDCl_3) of compound 245

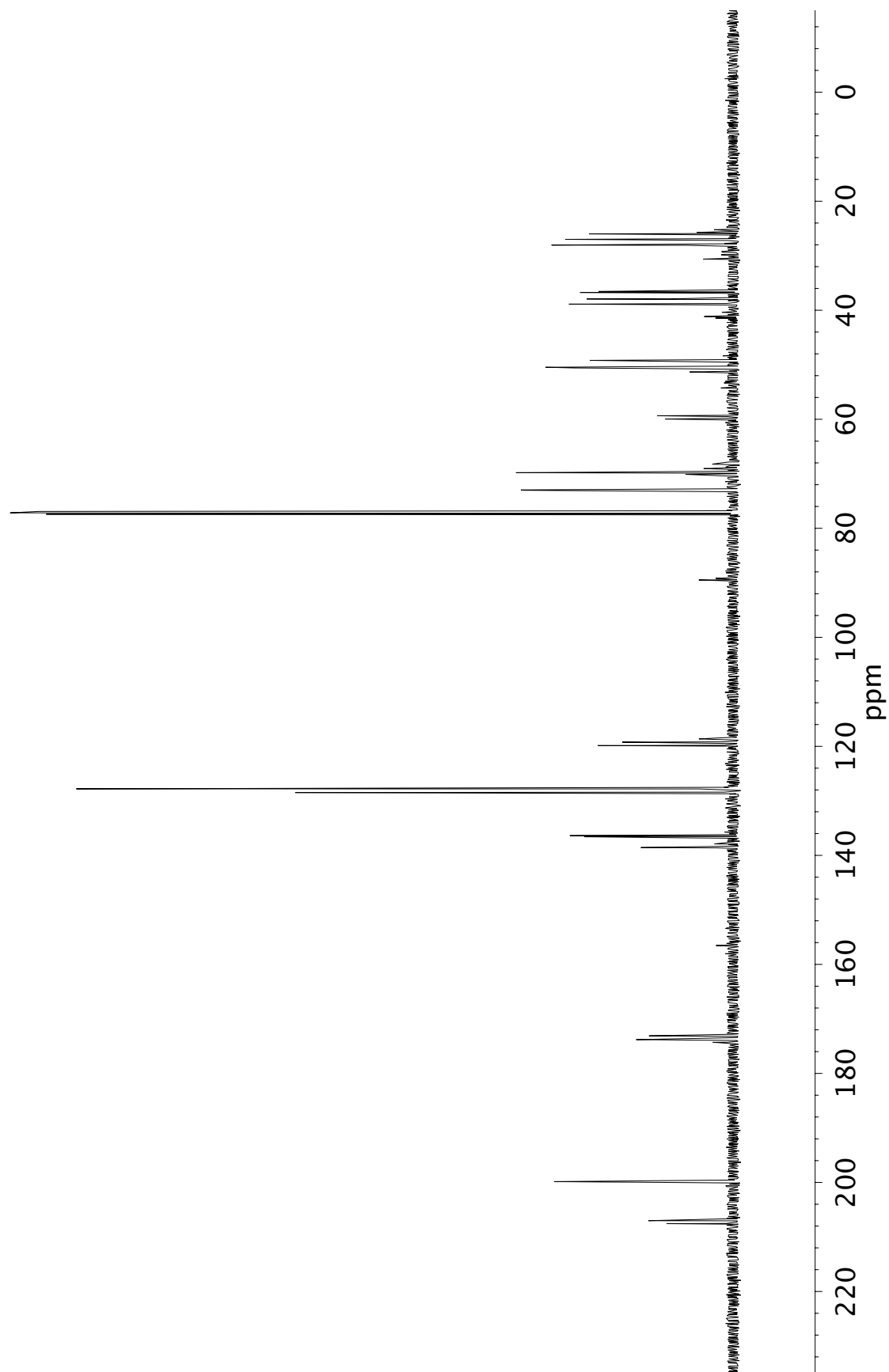


Figure A14.19 ^{13}C NMR (101 MHz, CDCl_3) of compound 245

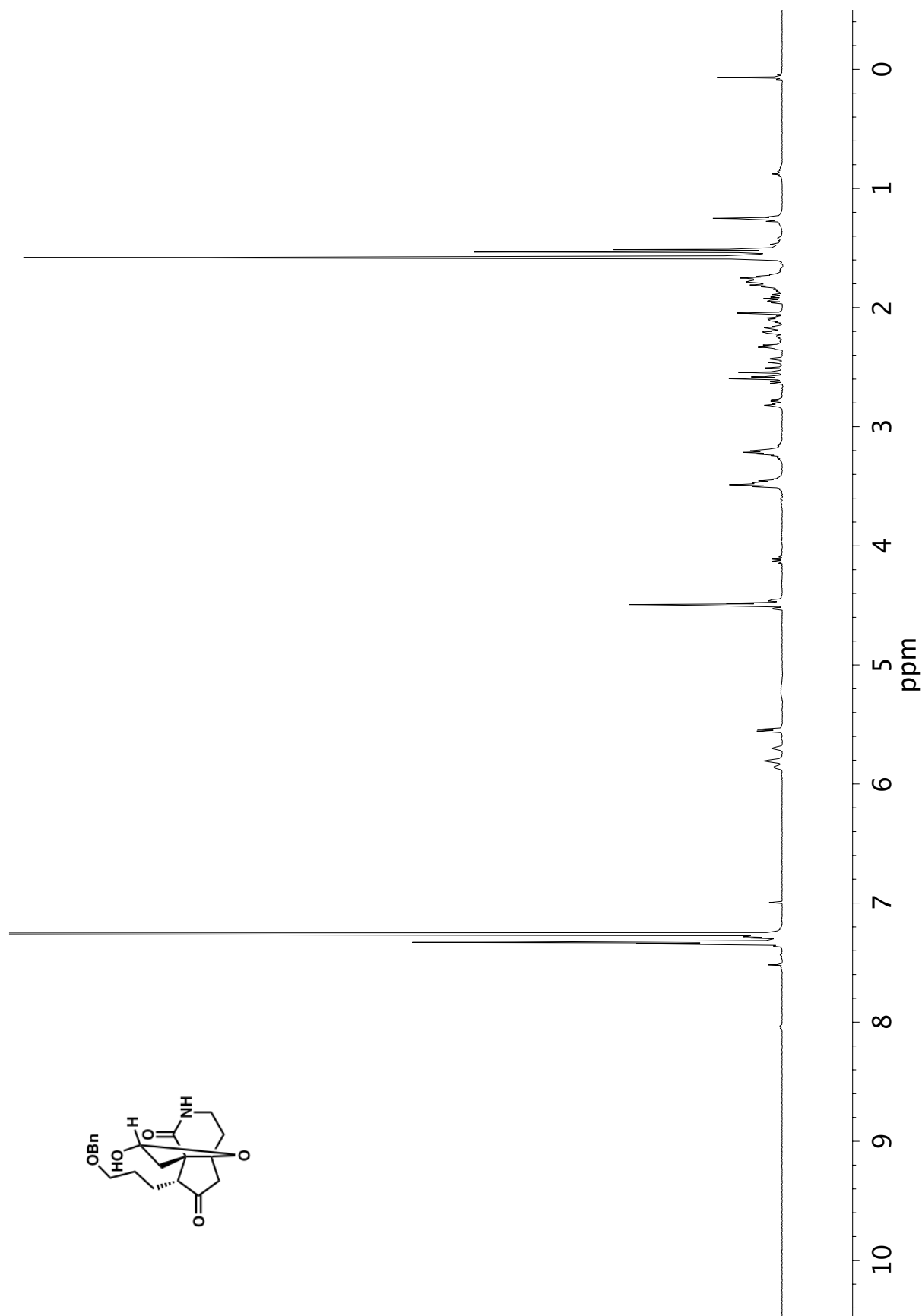


Figure A14.20 ^1H NMR (400 MHz, CDCl_3) of compound 247

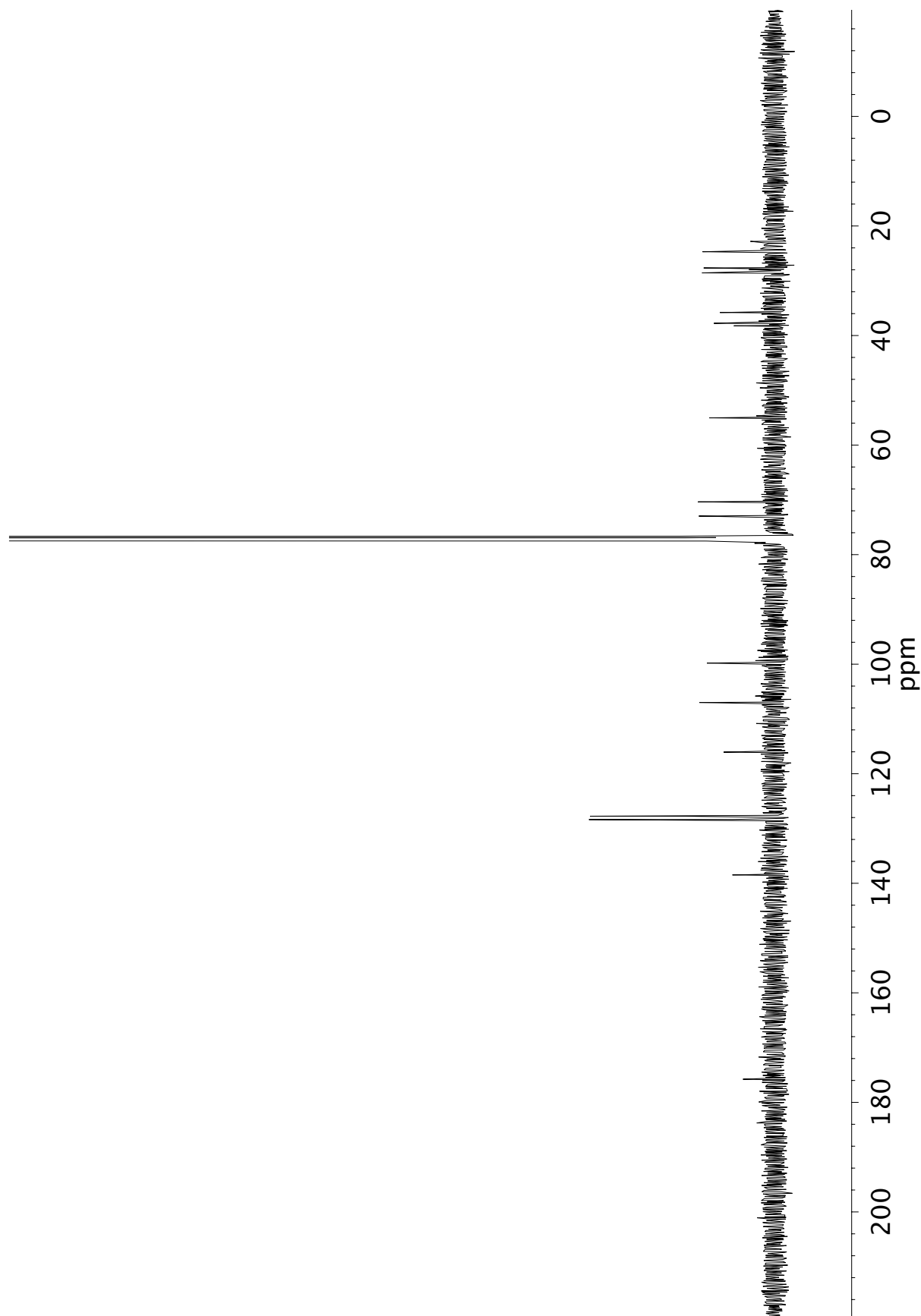


Figure A14.21 ^{13}C NMR (101 MHz, CDCl_3) of compound 247

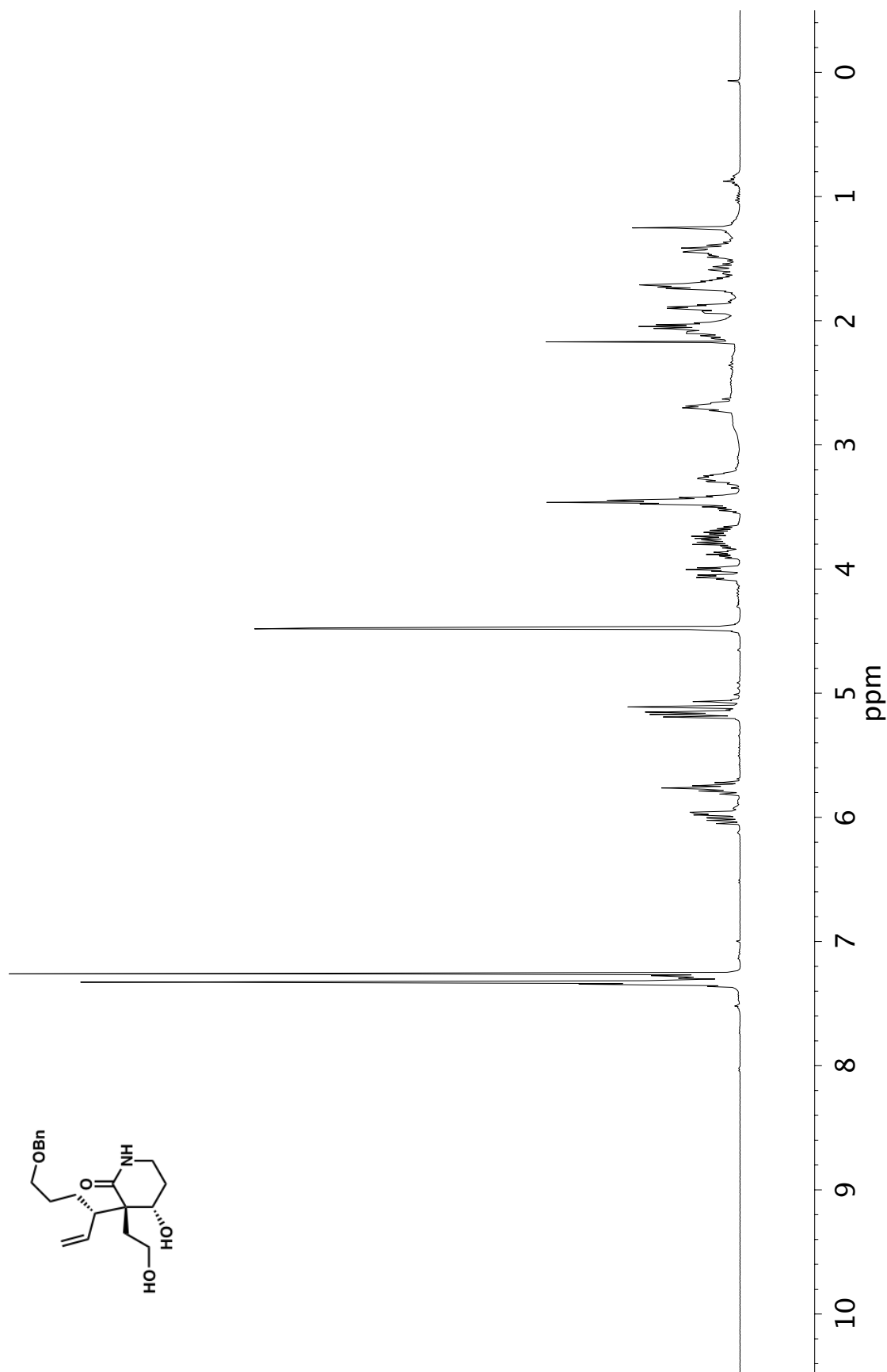


Figure A14.22 ¹H NMR (400 MHz, CDCl₃) of compound 248

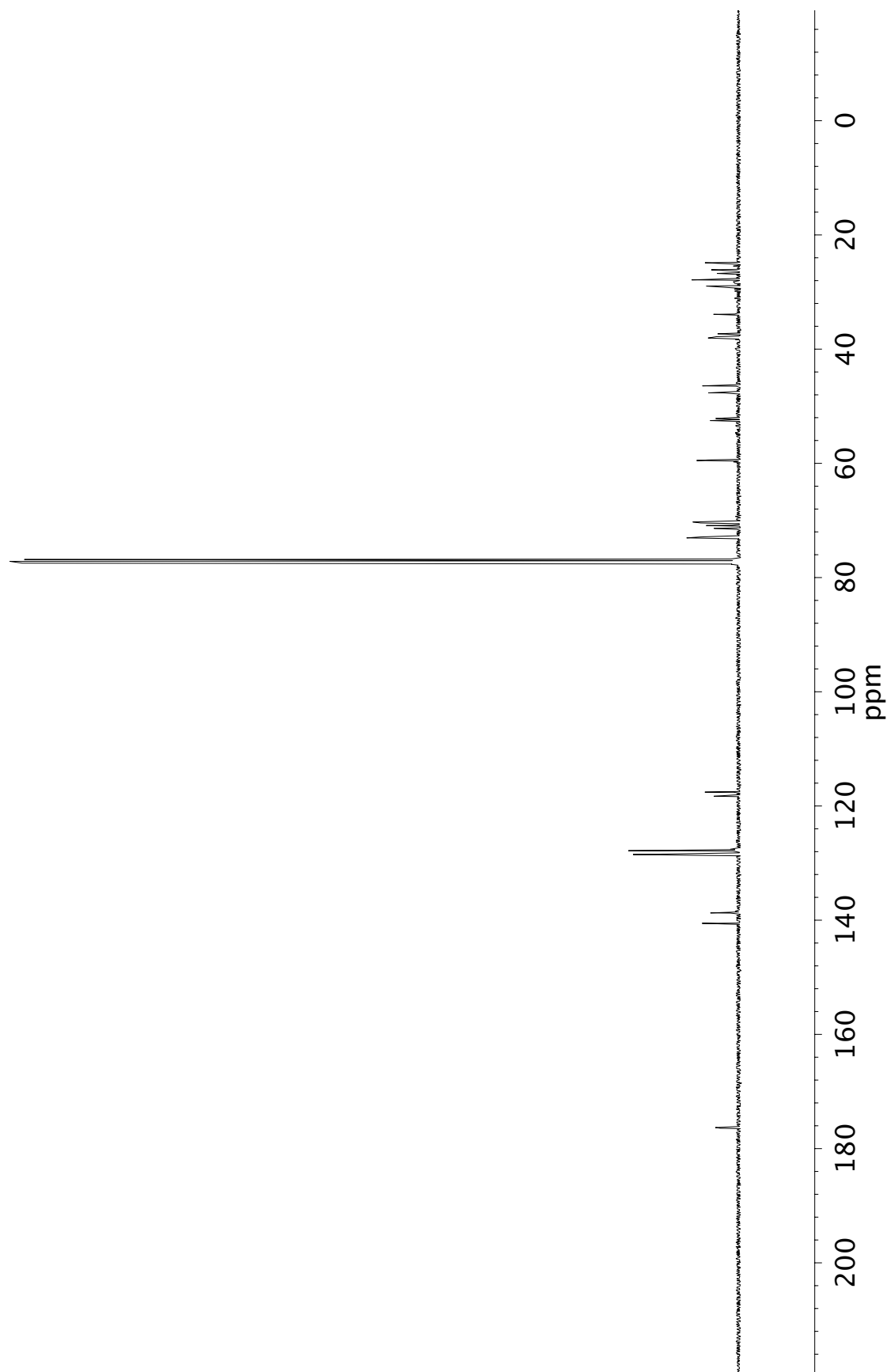
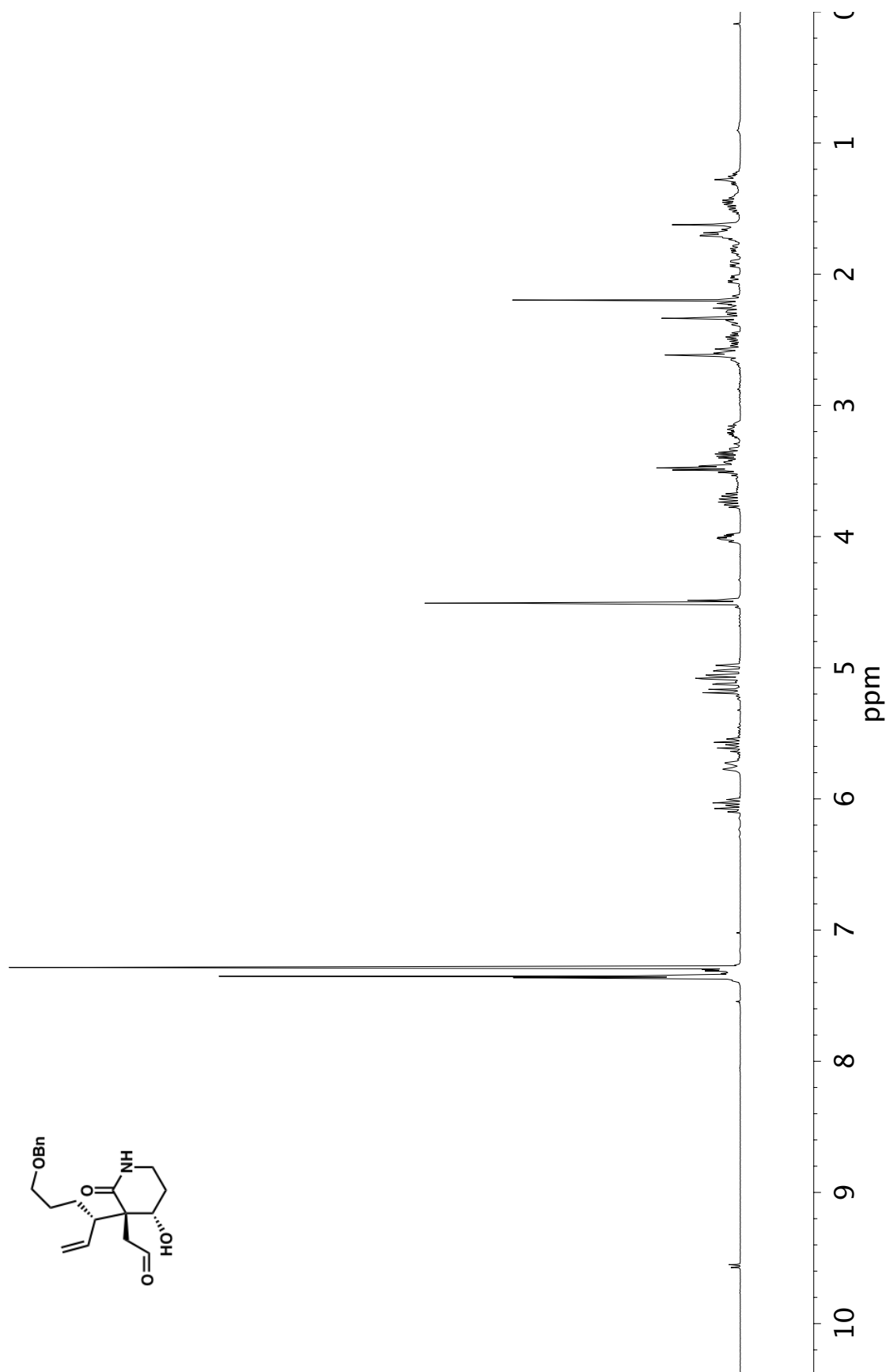


Figure A14.23 ^{13}C NMR (101 MHz, CDCl_3) of compound 248

Figure A14.24 ¹H NMR (400 MHz, CDCl₃) of compound 249

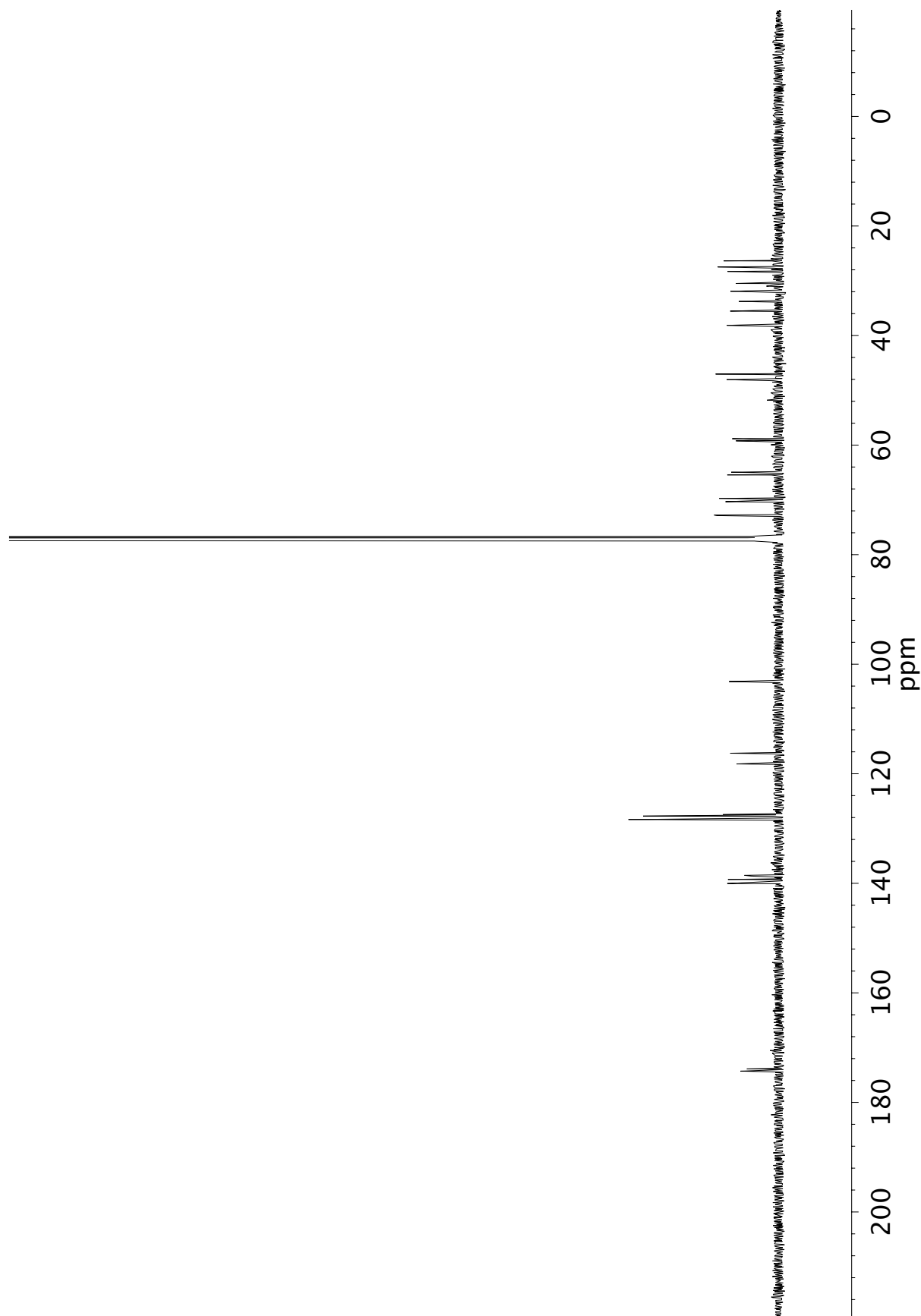


Figure A14.25 ^{13}C NMR (101 MHz, CDCl_3) of compound 249

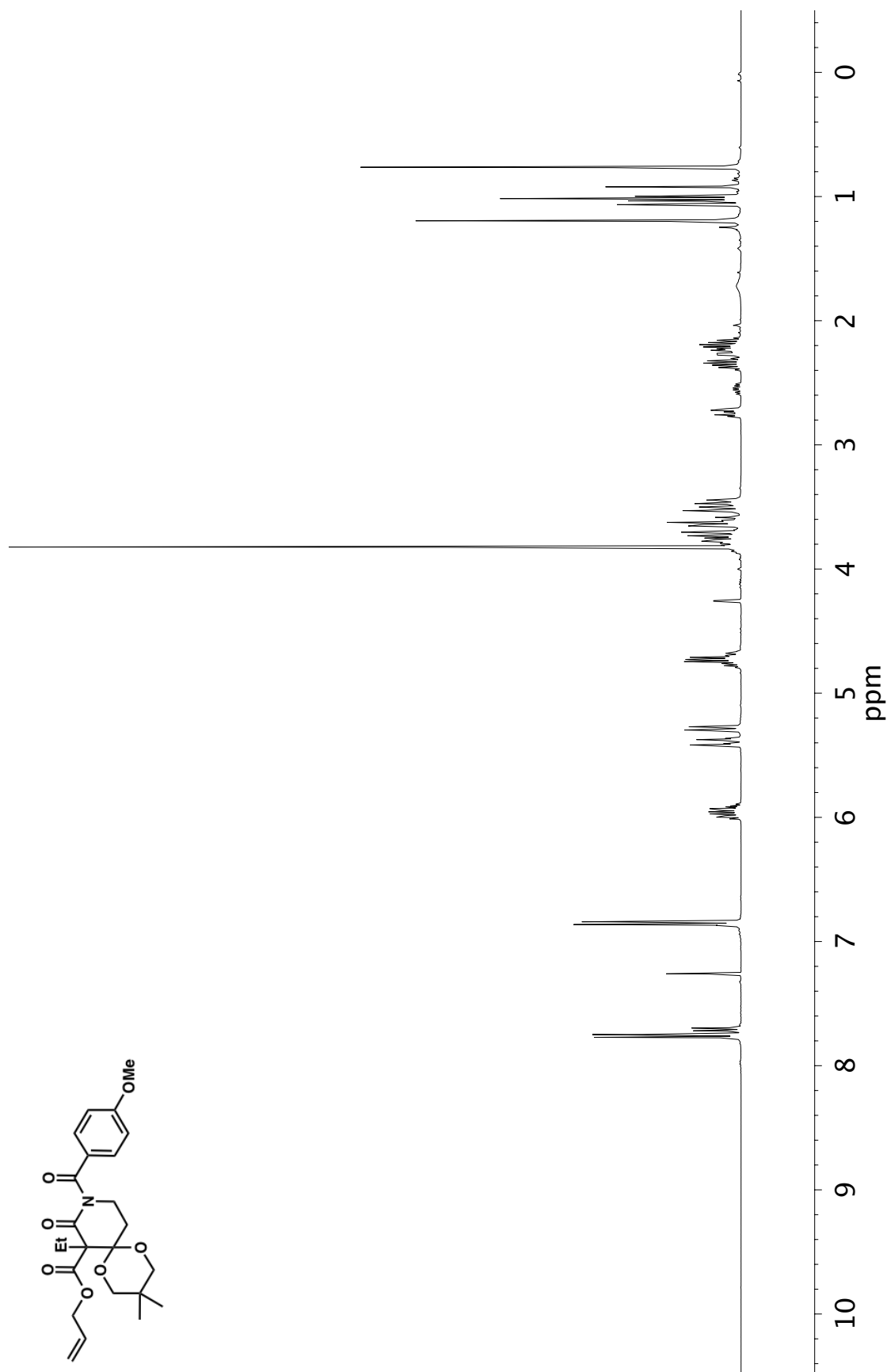


Figure A14.26 ¹H NMR (400 MHz, CDCl₃) of compound 256

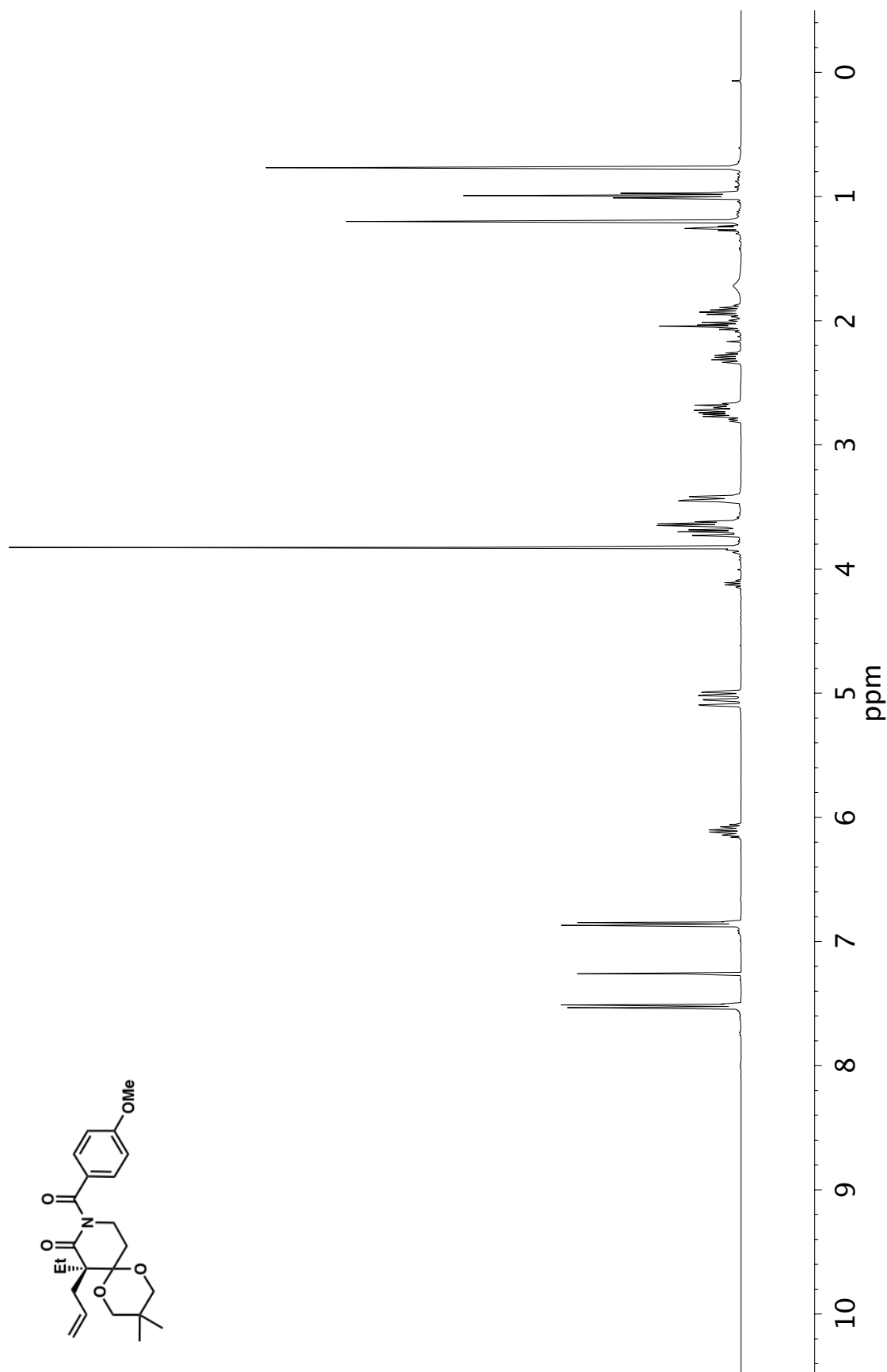


Figure A14.27 ¹H NMR (400 MHz, CDCl₃) of compound 257

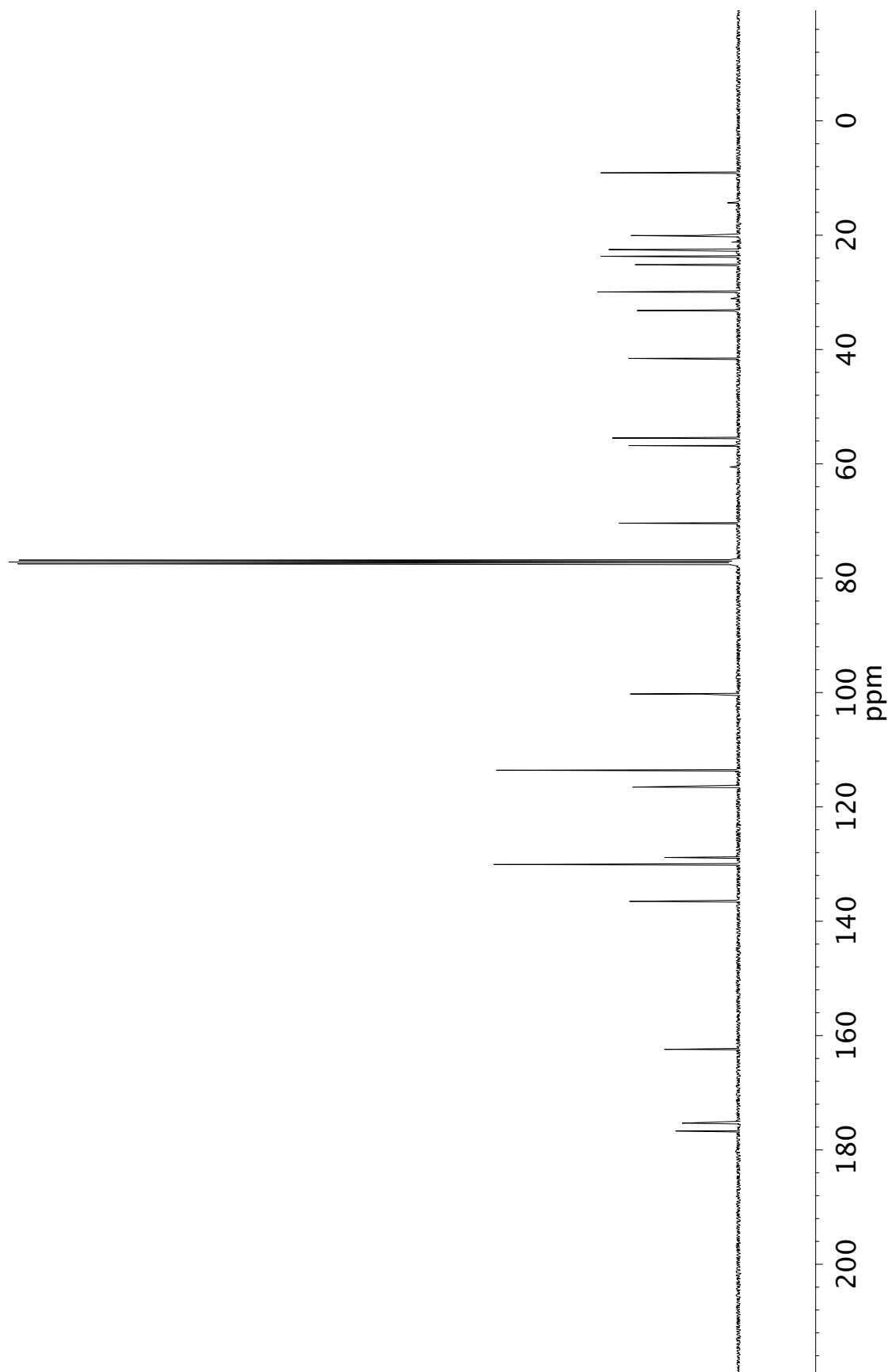


Figure A14.28 ^{13}C NMR (101 MHz, CDCl_3) of compound 257

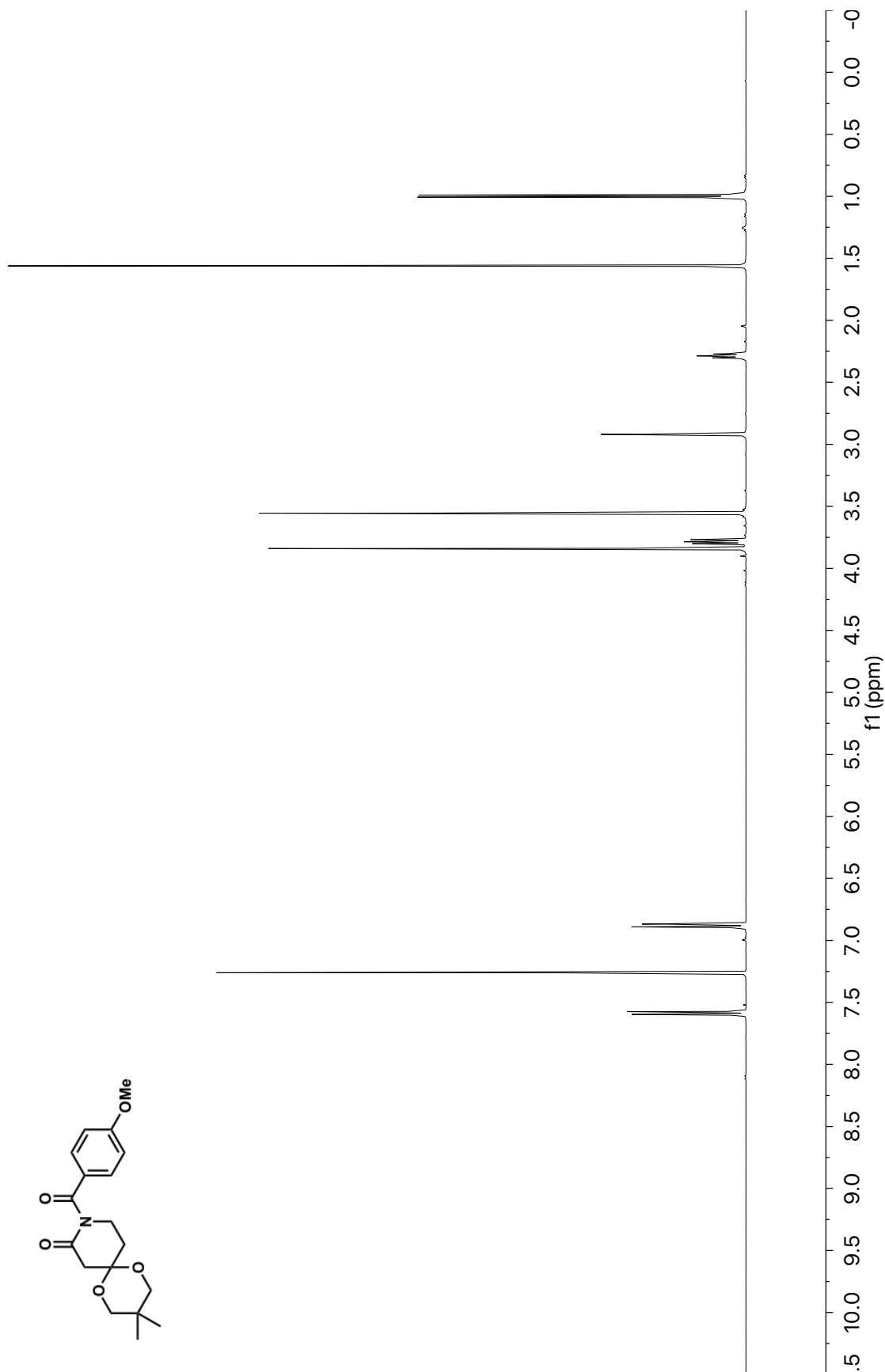


Figure A14.29 ¹H NMR (400 MHz, CDCl₃) of compound 258

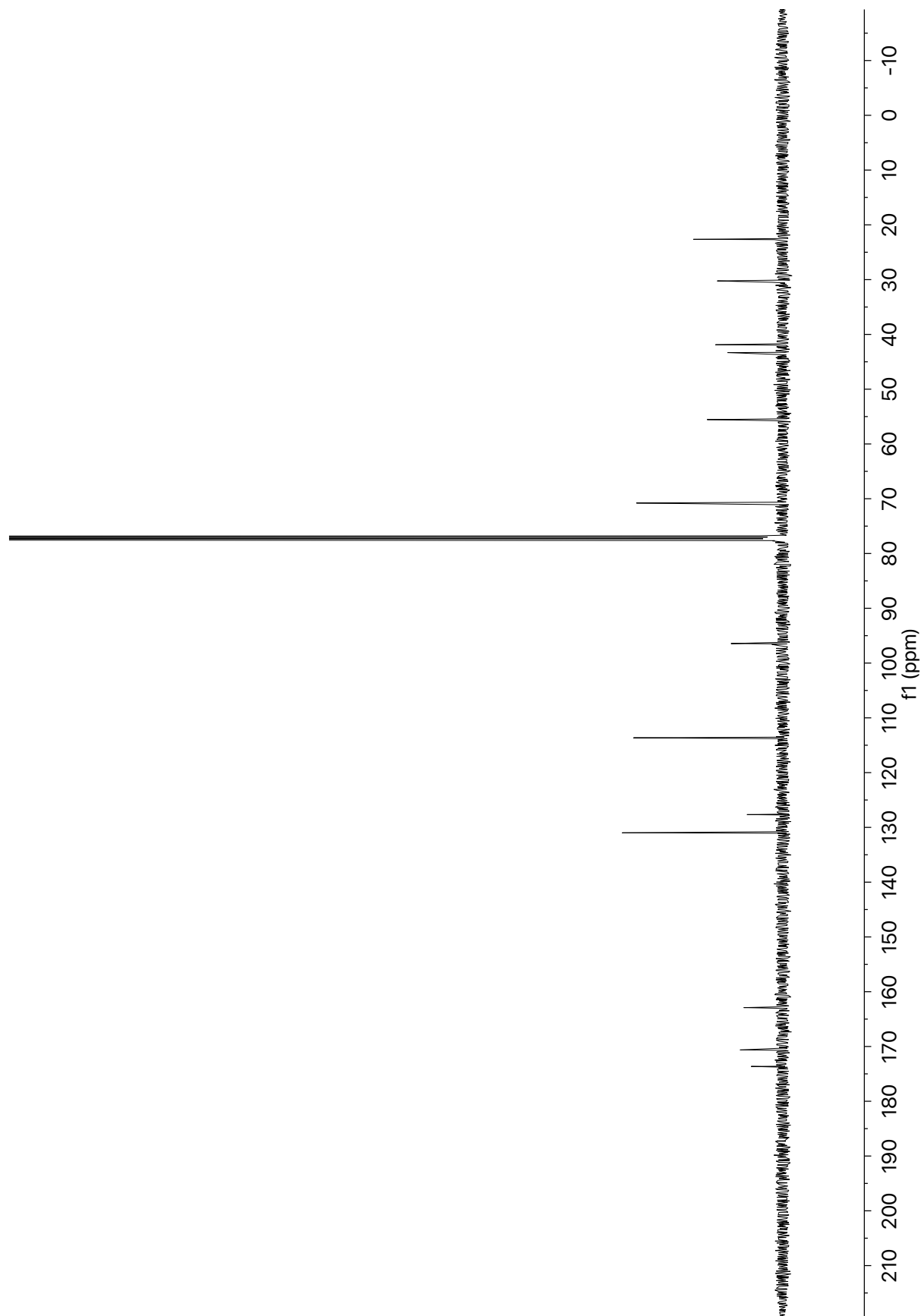


Figure A14.30 ^{13}C NMR (101 MHz, CDCl_3) of compound 258

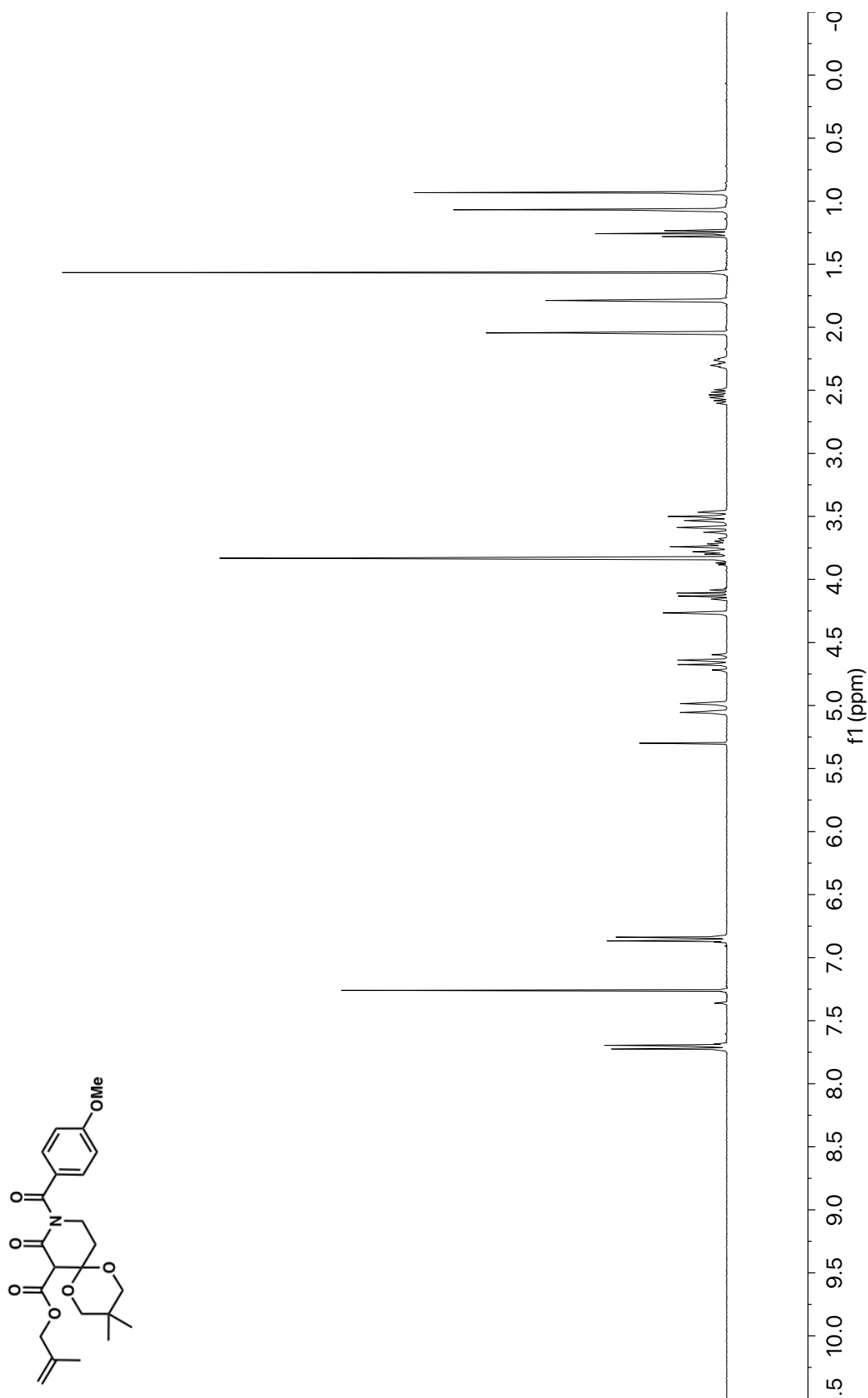


Figure A14.31 ¹H NMR (400 MHz, CDCl₃) of compound 259



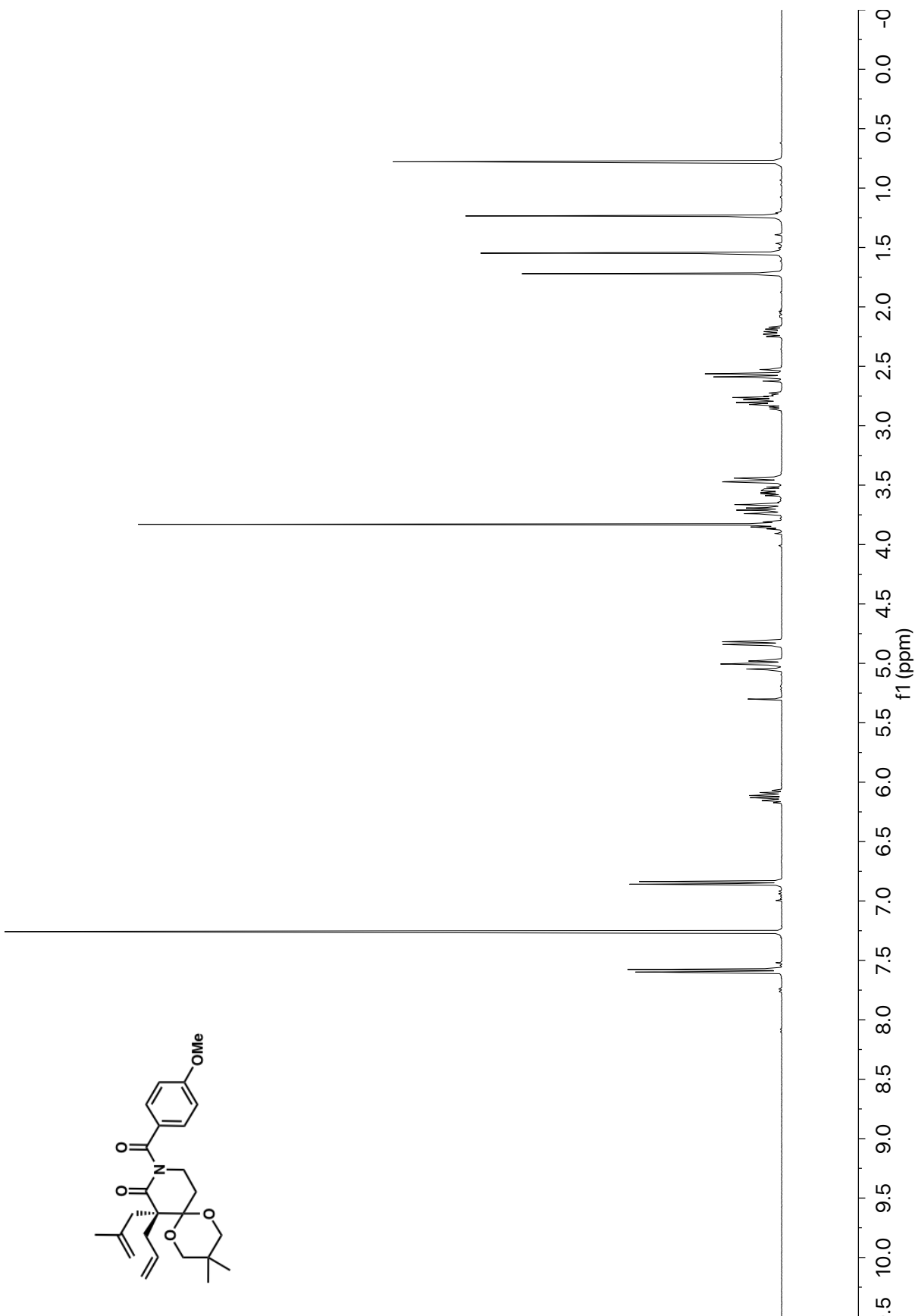
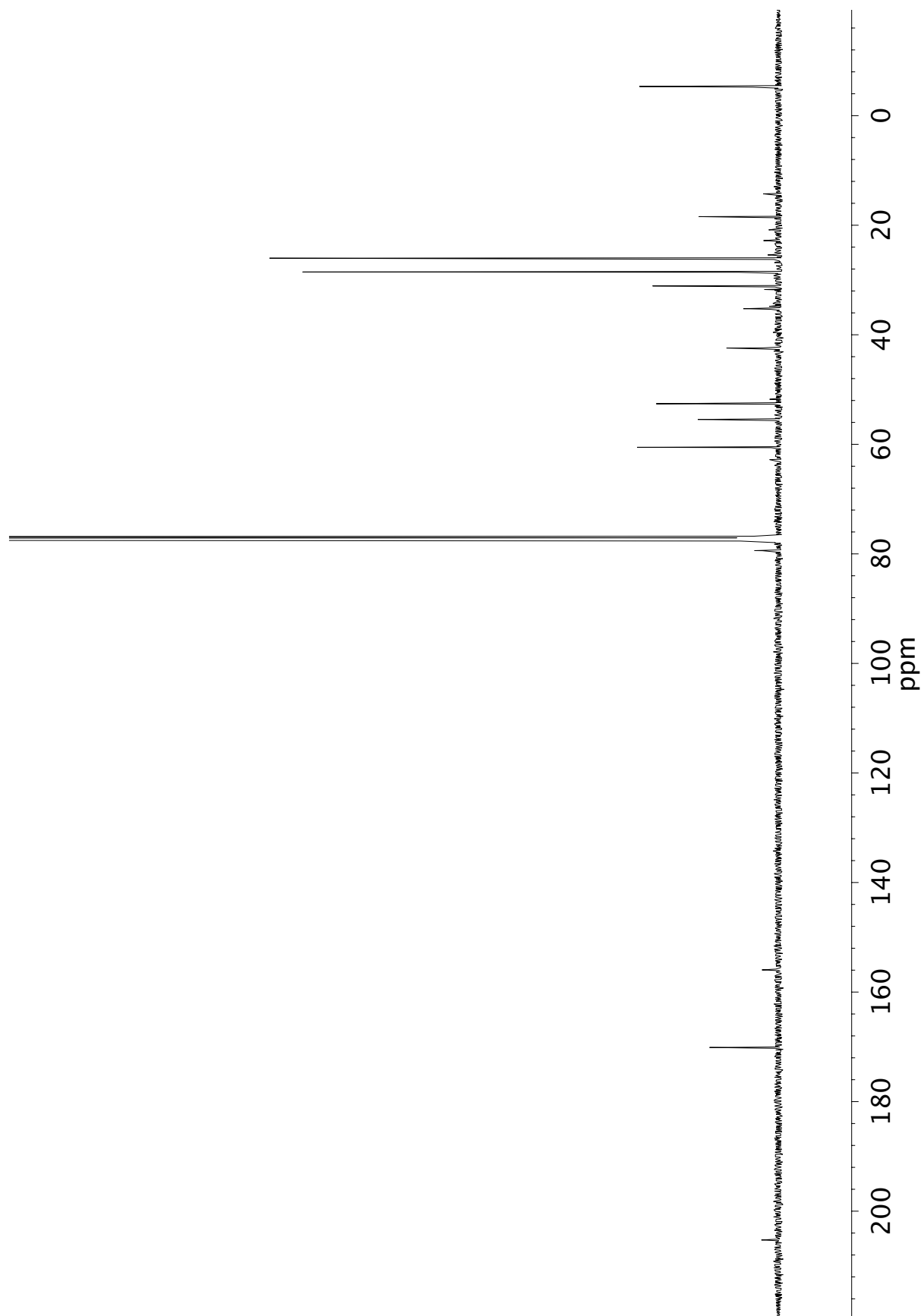


Figure A14.33 ¹H NMR (400 MHz, CDCl₃) of compound 261

**Figure A14.34** ^{13}C NMR (101 MHz, CDCl_3) of compound **261**

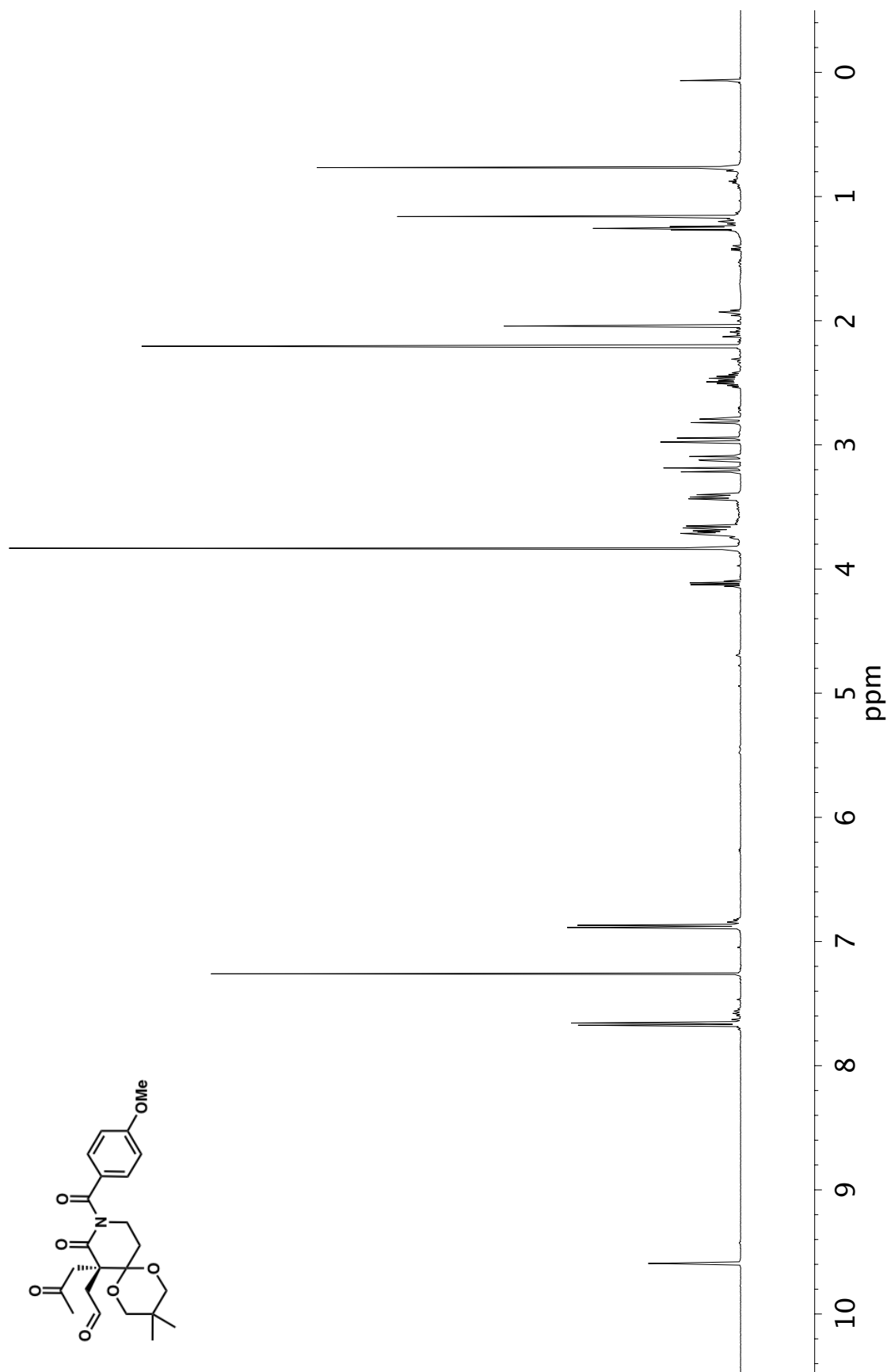


Figure A14.35 ¹H NMR (400 MHz, CDCl₃) of compound 262

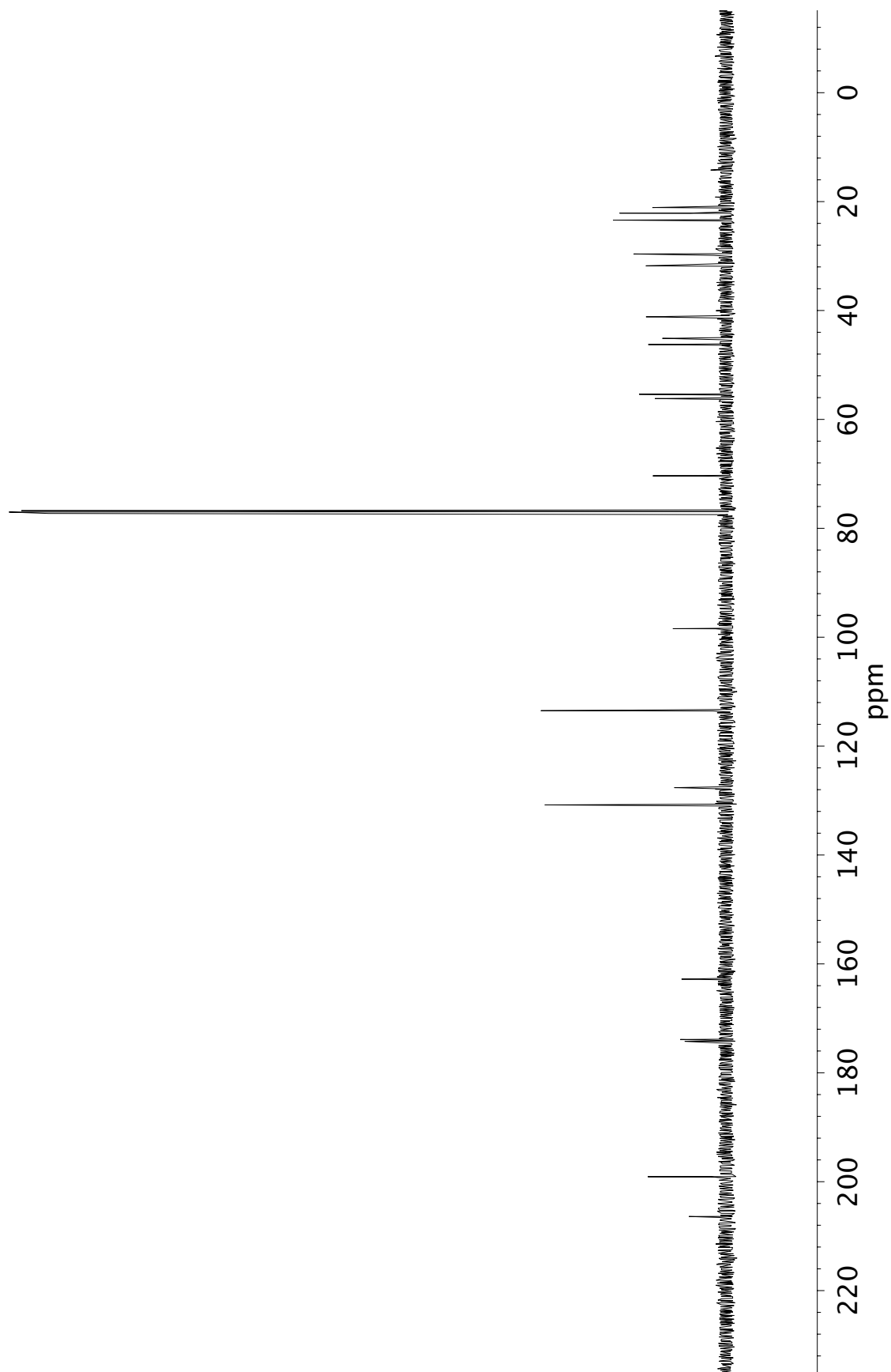


Figure A14.36 ^{13}C NMR (101 MHz, CDCl_3) of compound 262

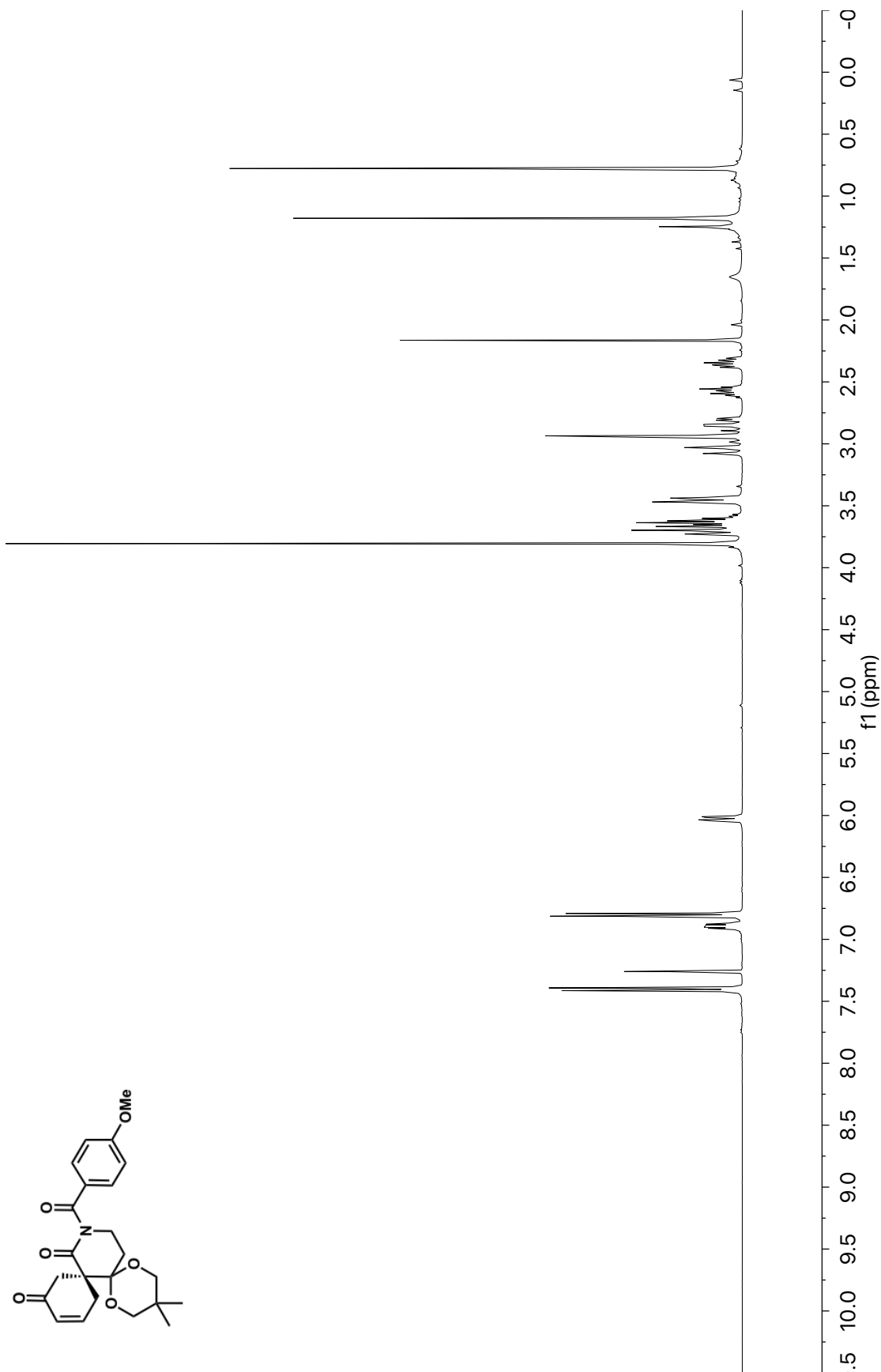


Figure A14.37 ¹H NMR (400 MHz, CDCl₃) of compound 263

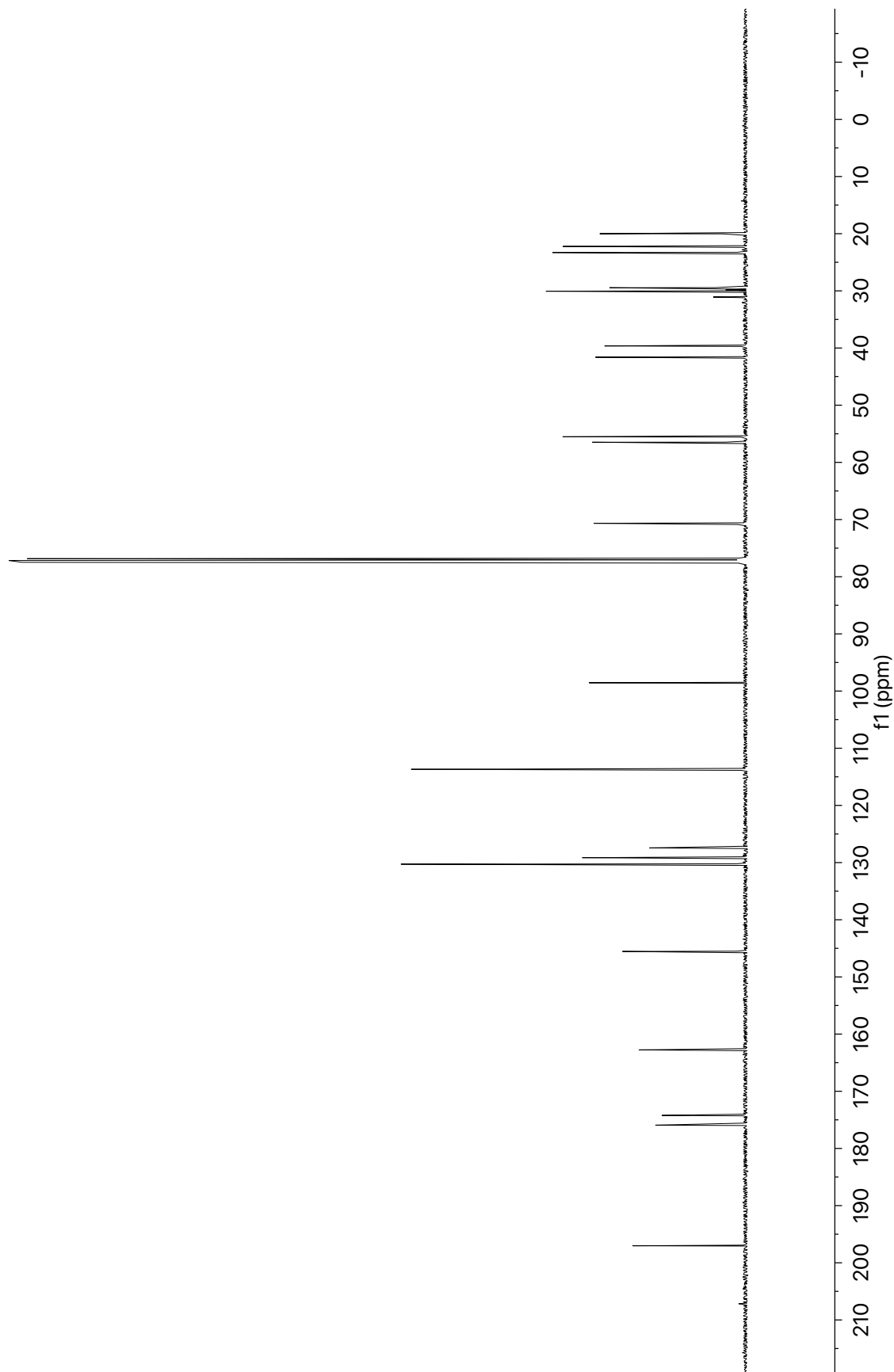


Figure A14.38 ^{13}C NMR (101 MHz, CDCl_3) of compound 263

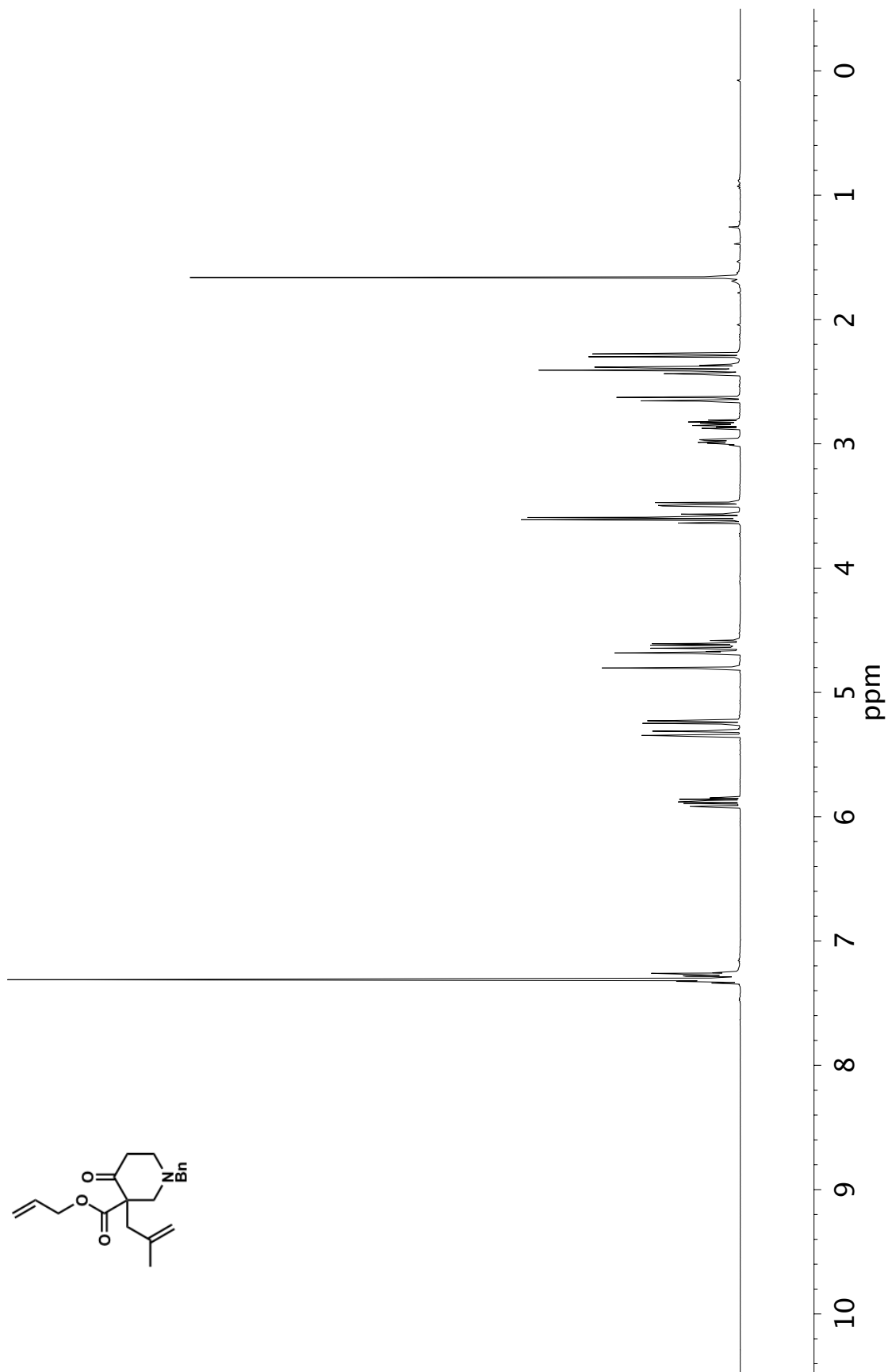


Figure A14.39 ¹H NMR (400 MHz, CDCl₃) of compound 274

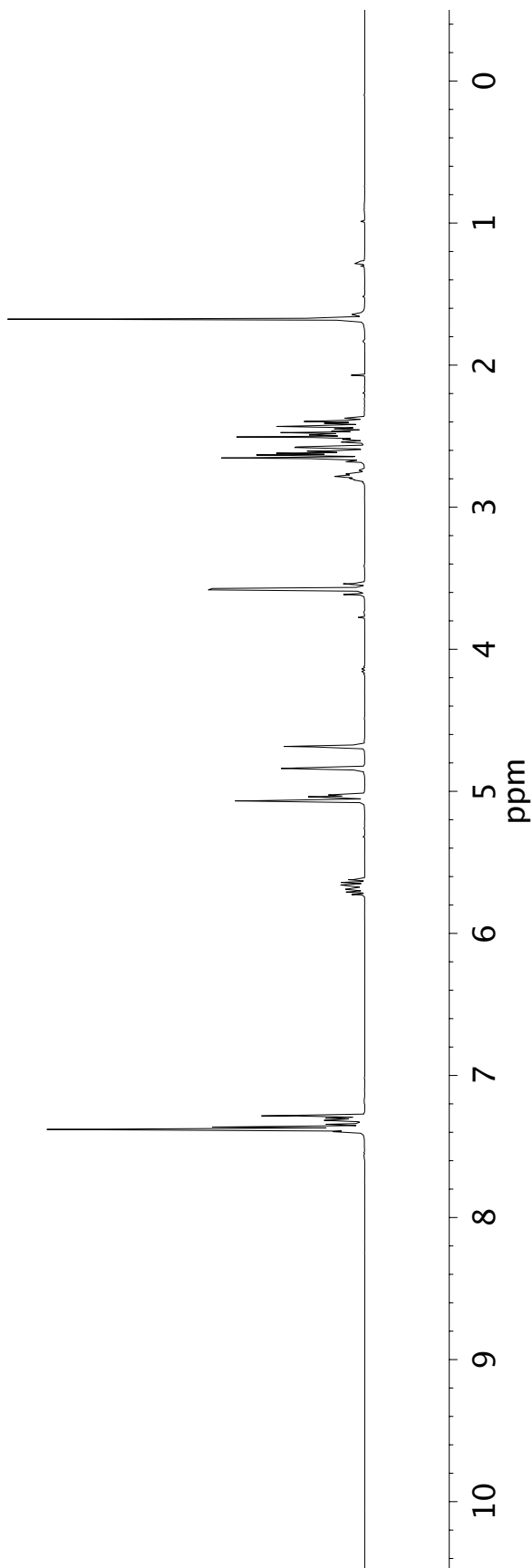
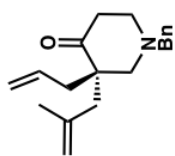


Figure A14.40 ¹H NMR (400 MHz, CDCl₃) of compound 275

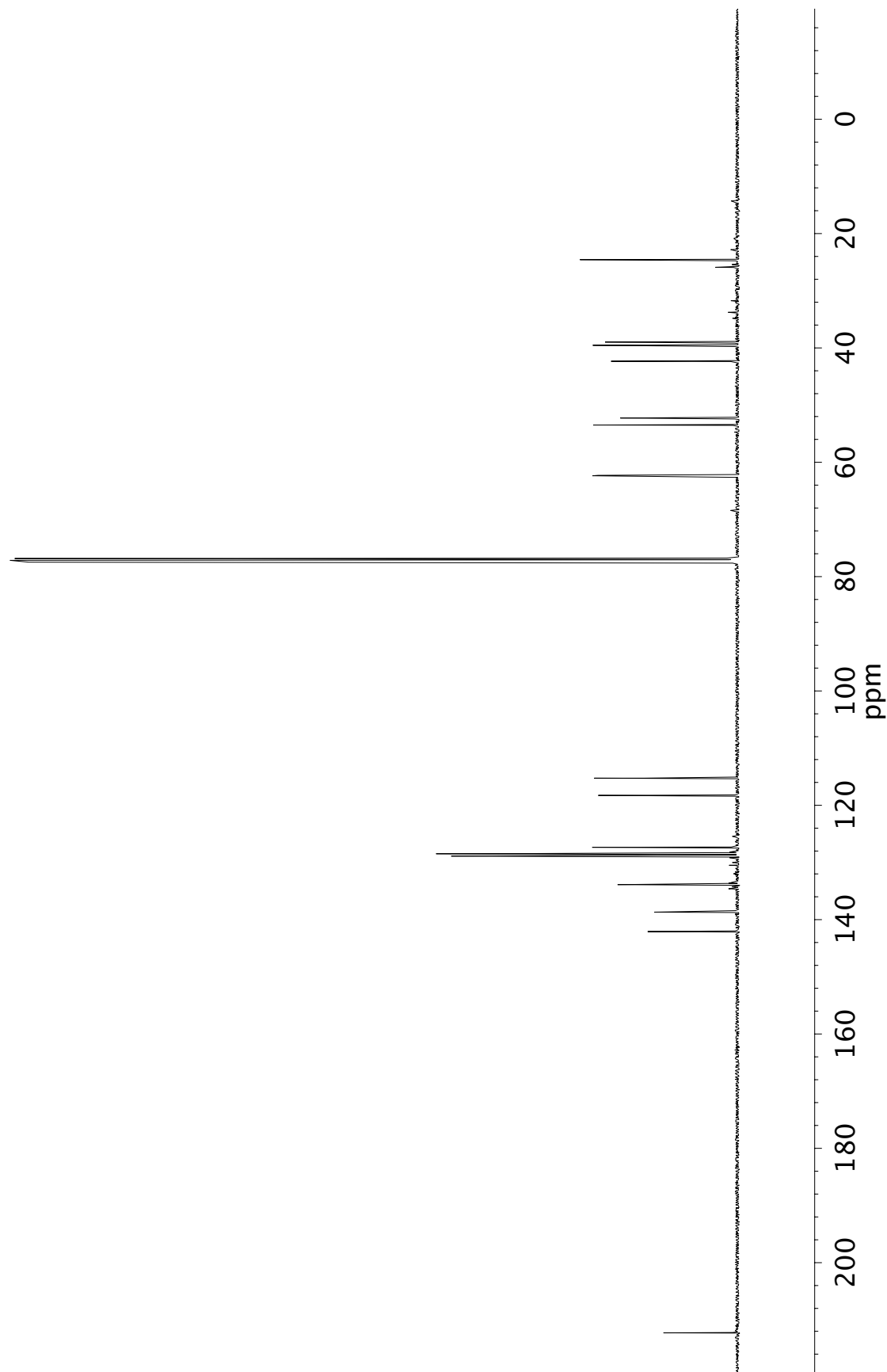


Figure A14.41 ^{13}C NMR (101 MHz, CDCl_3) of compound 275

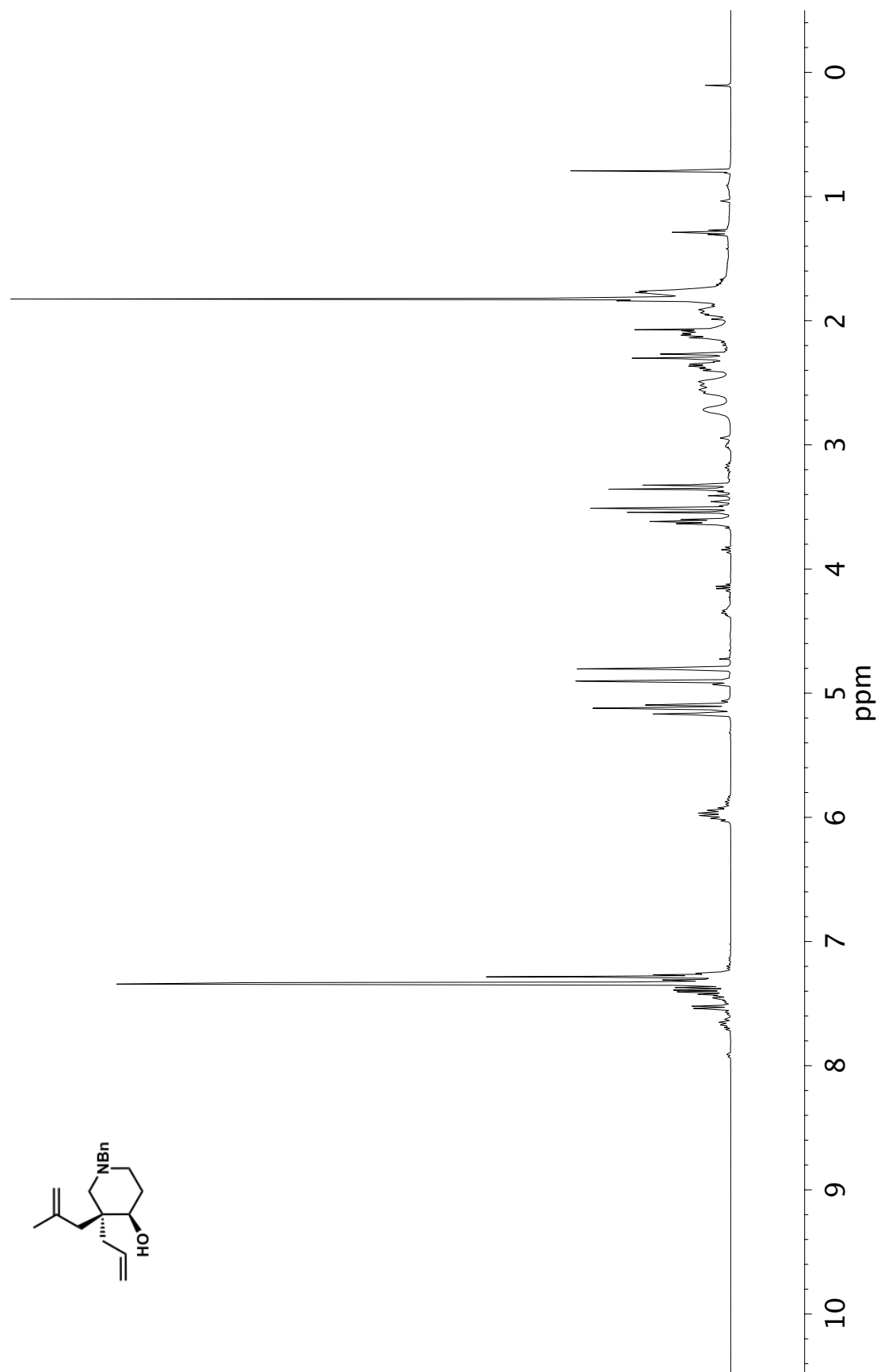


Figure A14.42 ¹H NMR (400 MHz, CDCl₃) of compound 276

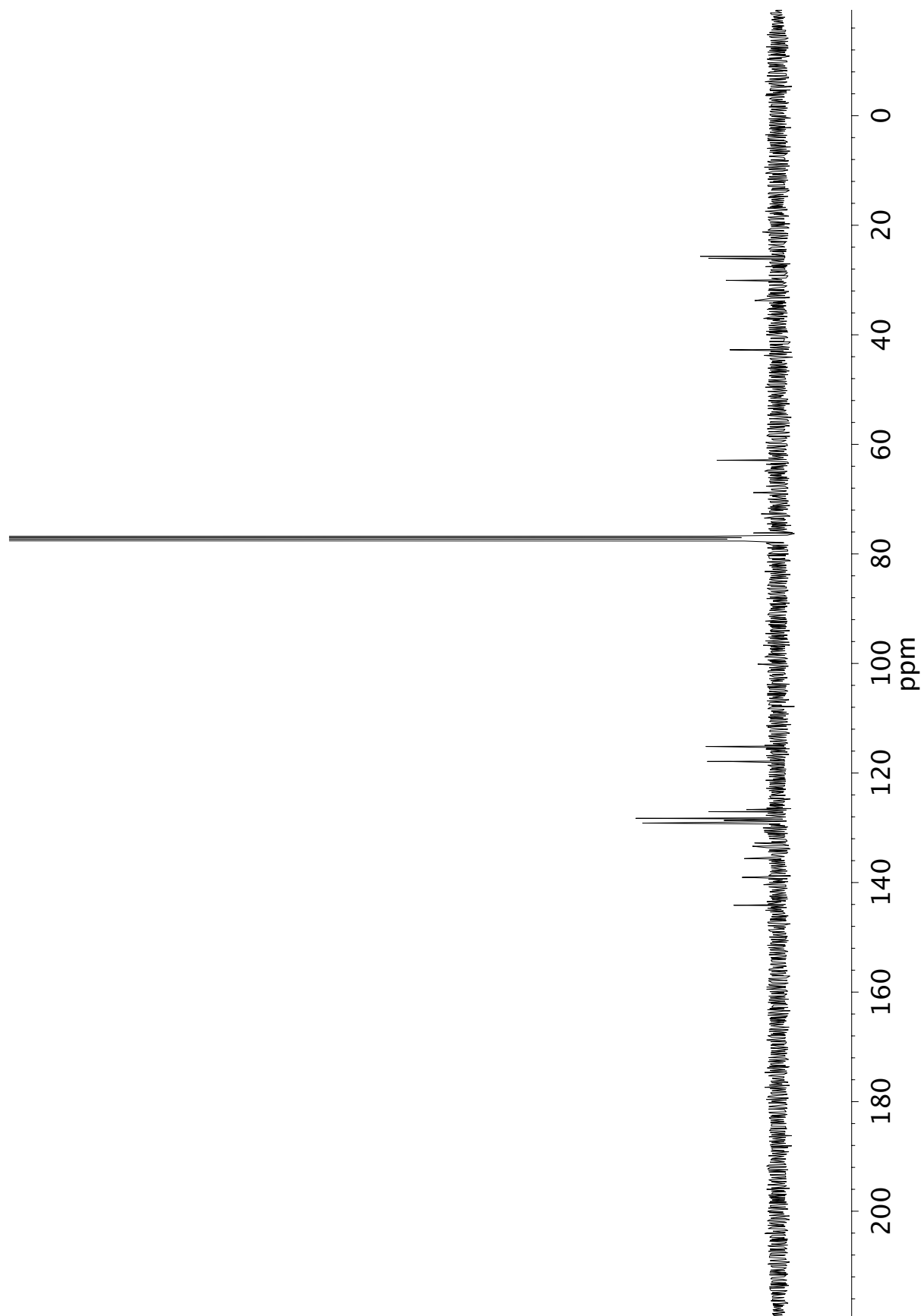


Figure A14.43 ^{13}C NMR (101 MHz, CDCl_3) of compound 276

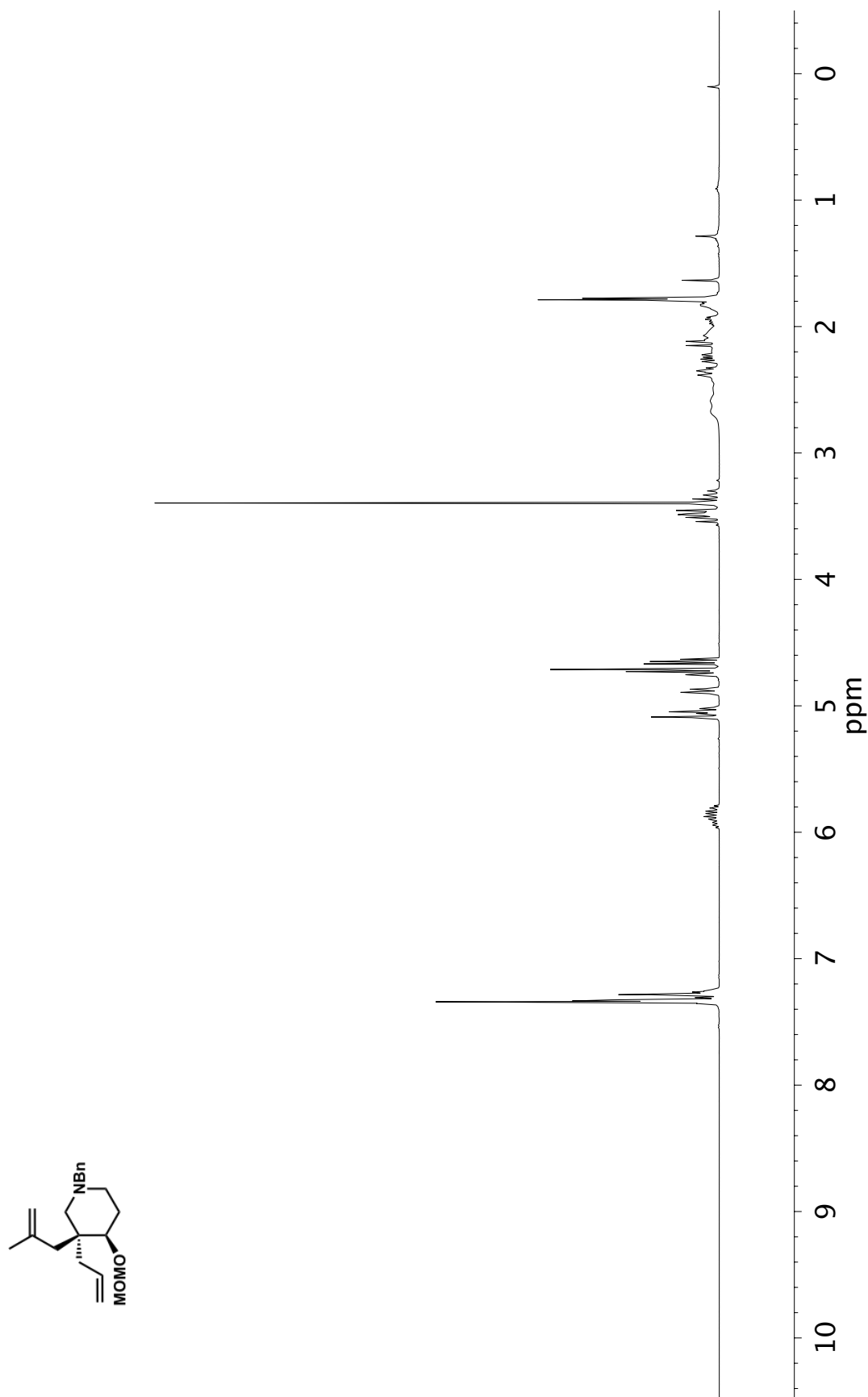


Figure A14.44 ¹H NMR (400 MHz, CDCl₃) of compound 277

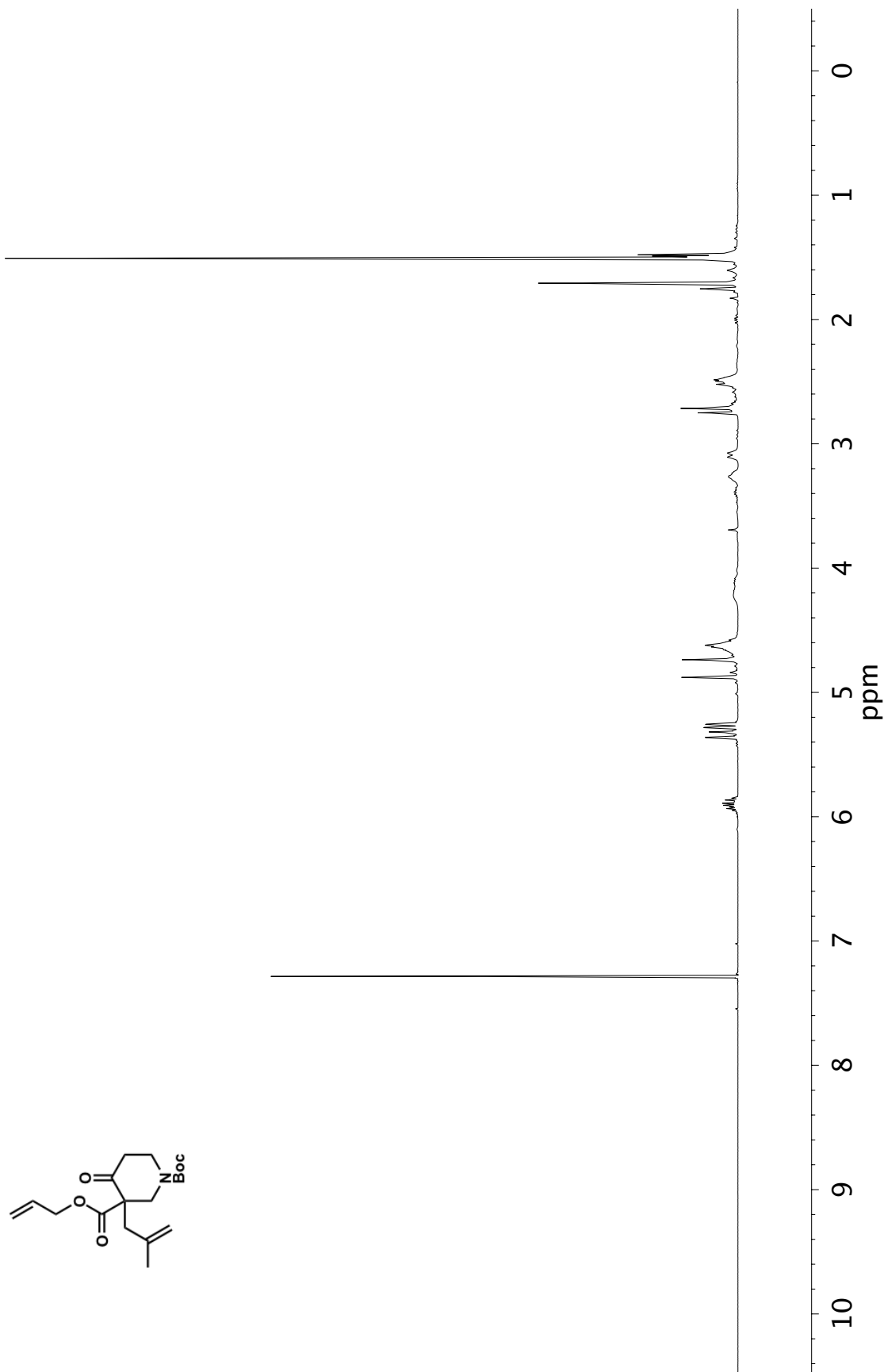


Figure A14.45 ¹H NMR (400 MHz, CDCl₃) of compound 280

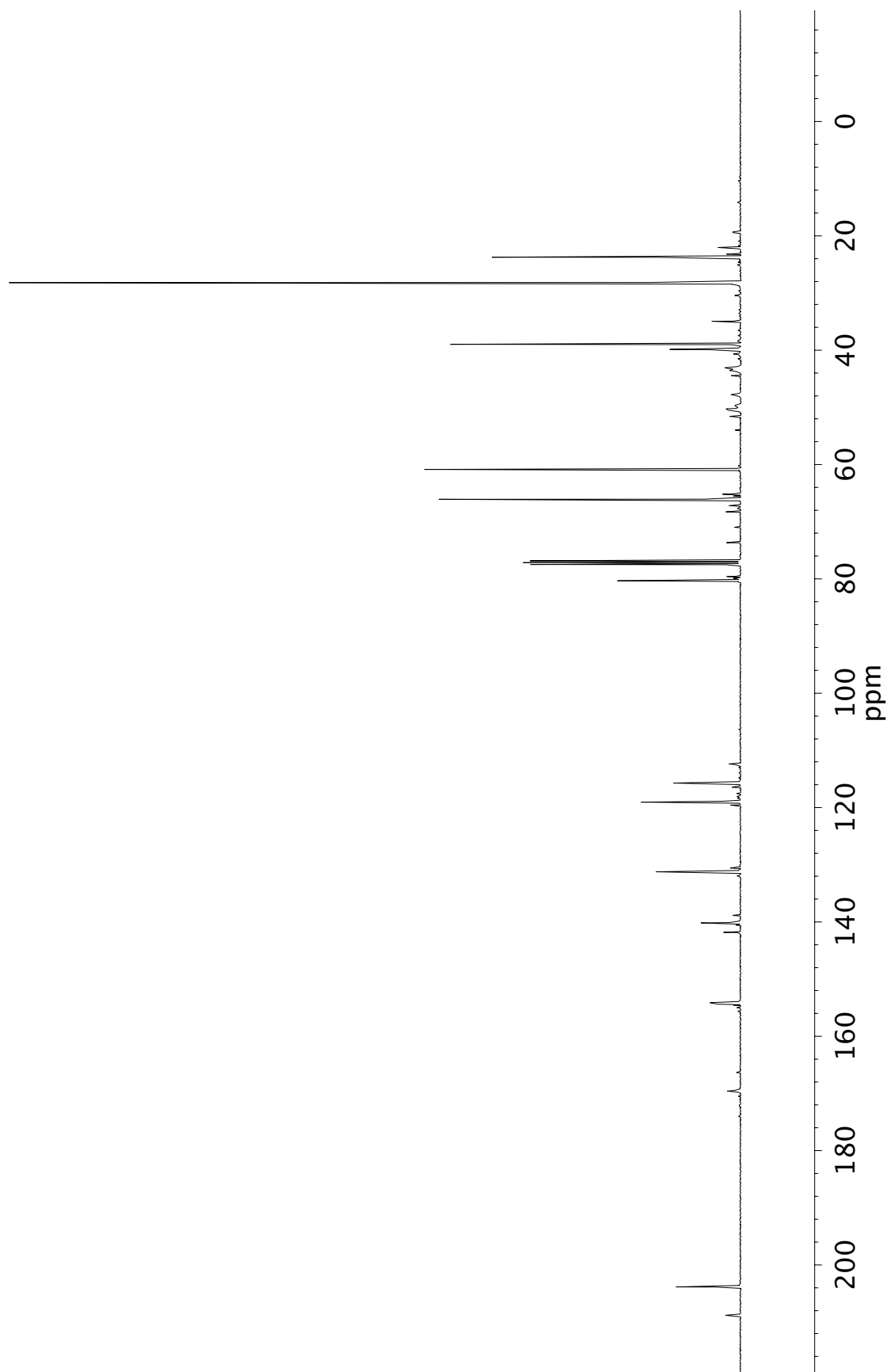


Figure A14.46 ¹³C NMR (101 MHz, CDCl₃) of compound 280

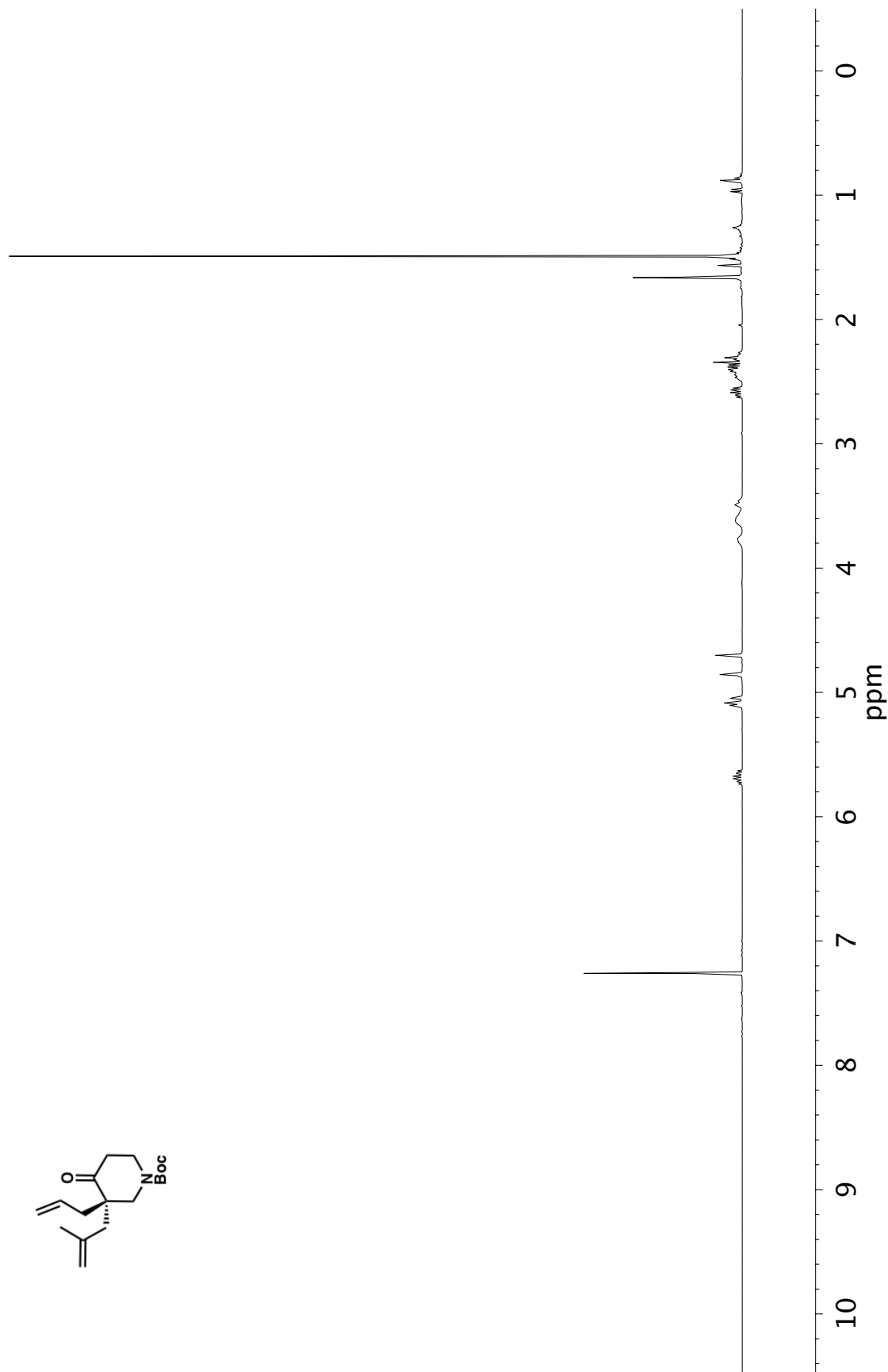


Figure A14.47 ¹H NMR (400 MHz, CDCl₃) of compound 281

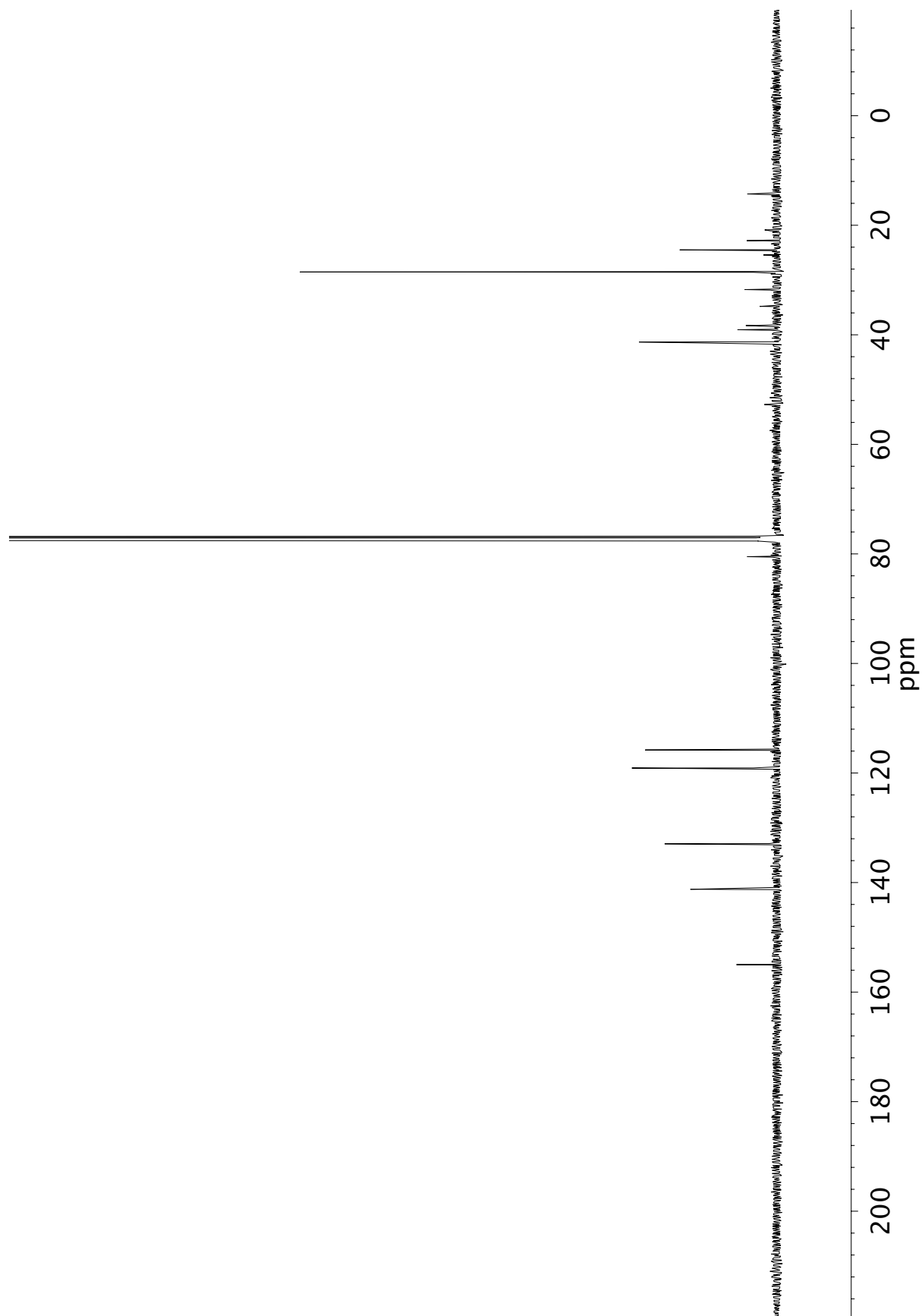
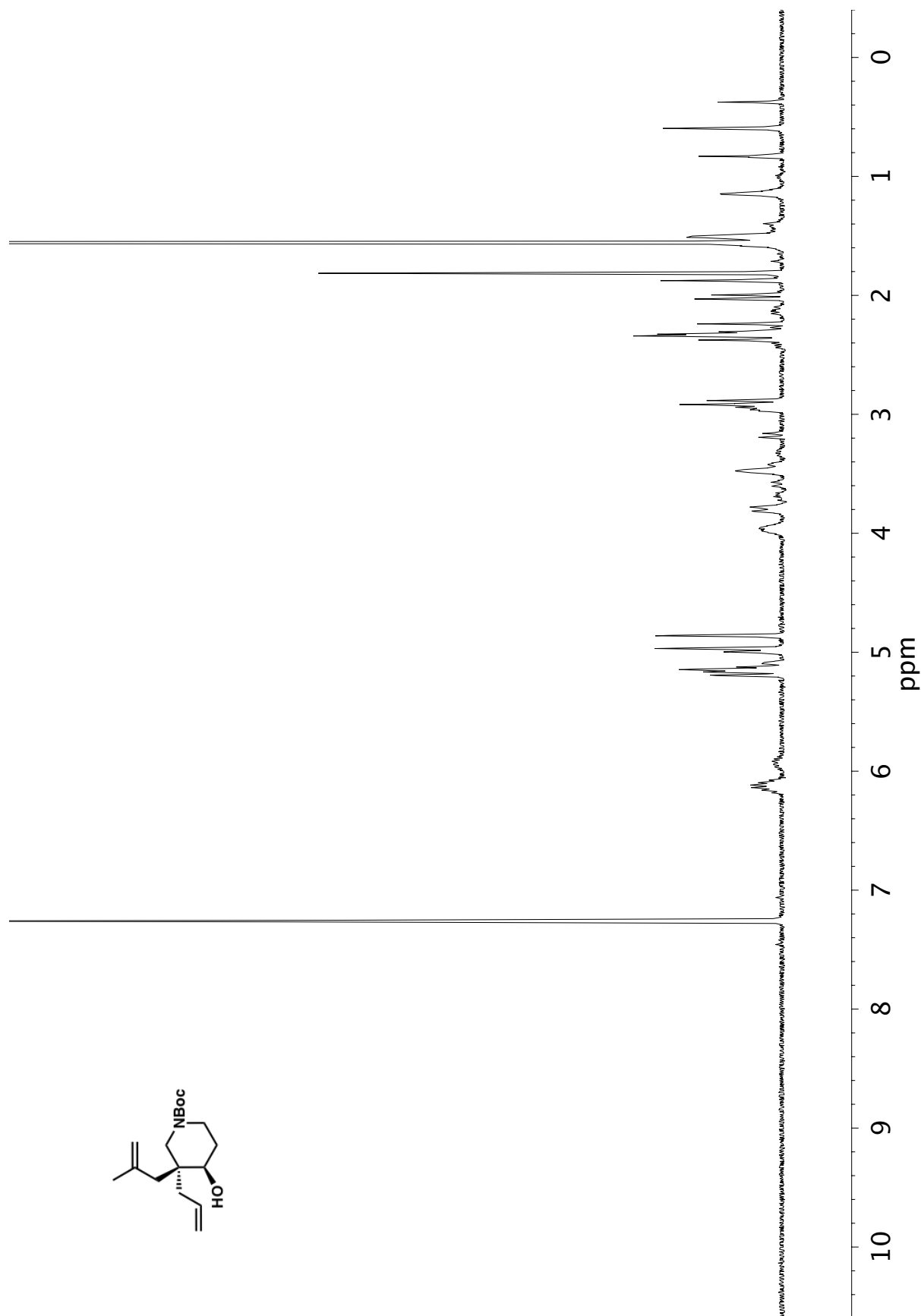


Figure A14.48 ^{13}C NMR (101 MHz, CDCl_3) of compound 281

Figure A14.49 ¹H NMR (400 MHz, CDCl₃) of compound 282

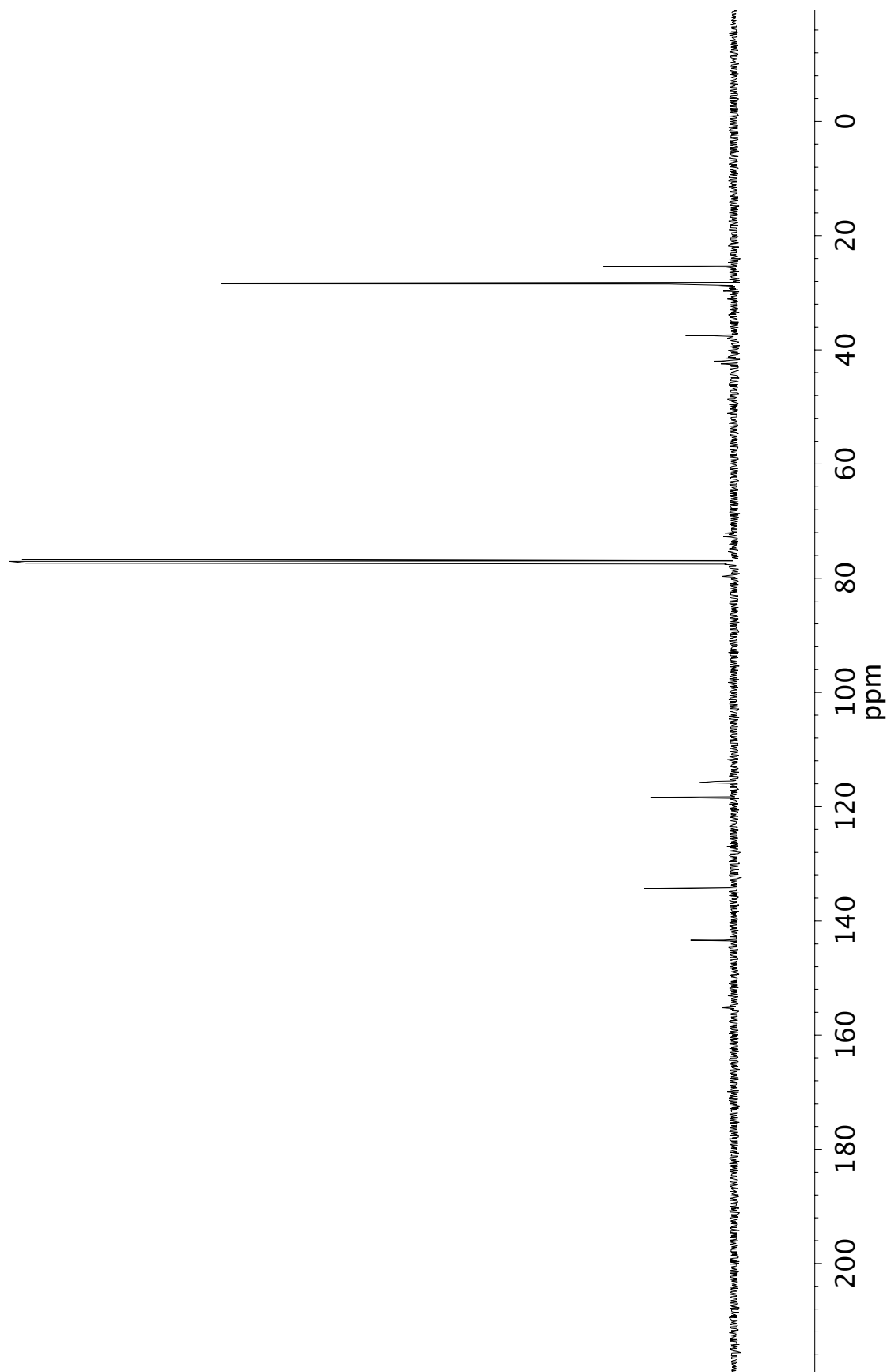


Figure A14.50 ^{13}C NMR (101 MHz, CDCl_3) of compound 282

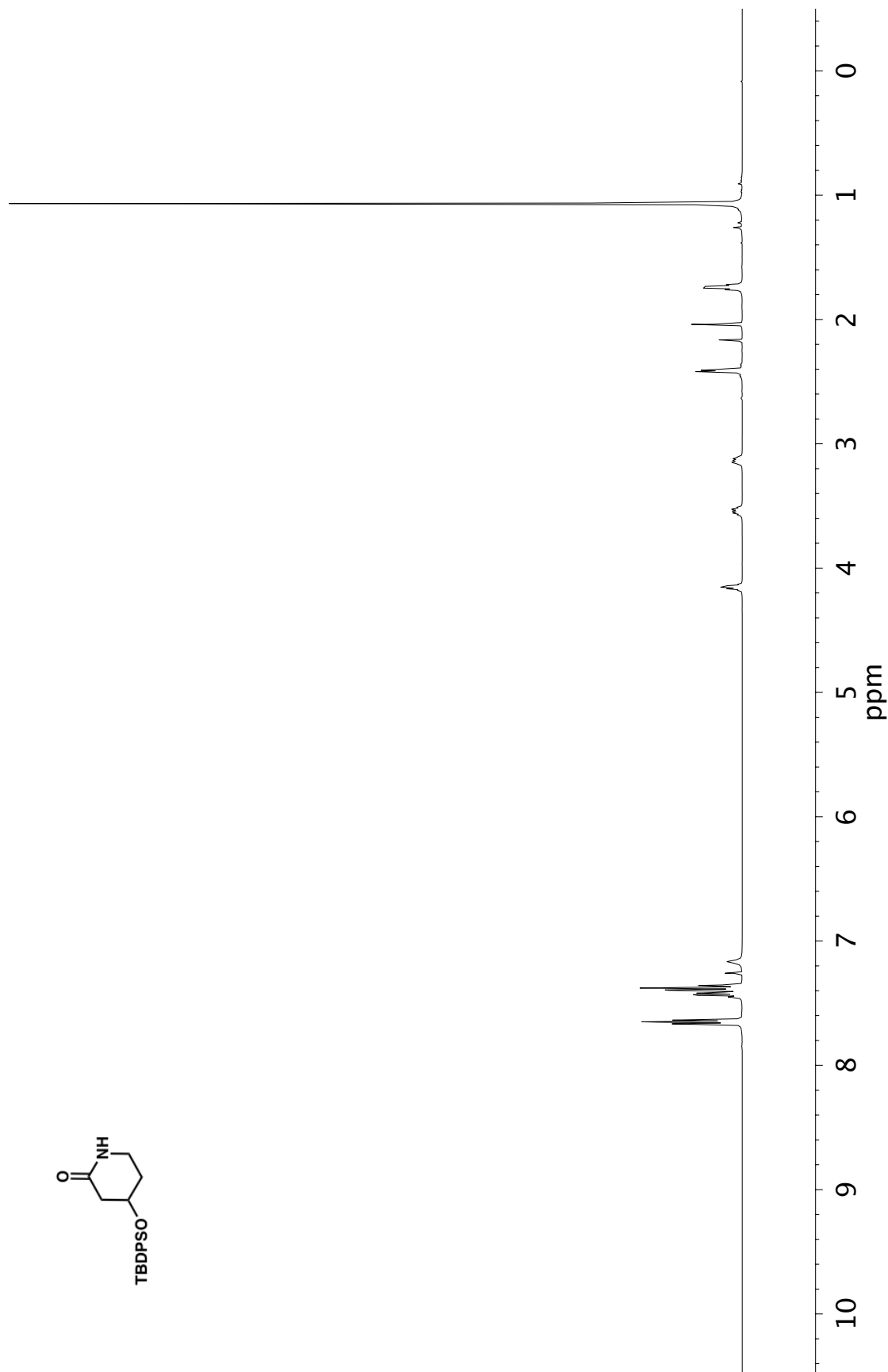


Figure A14.51 ¹H NMR (400 MHz, CDCl₃) of compound 291

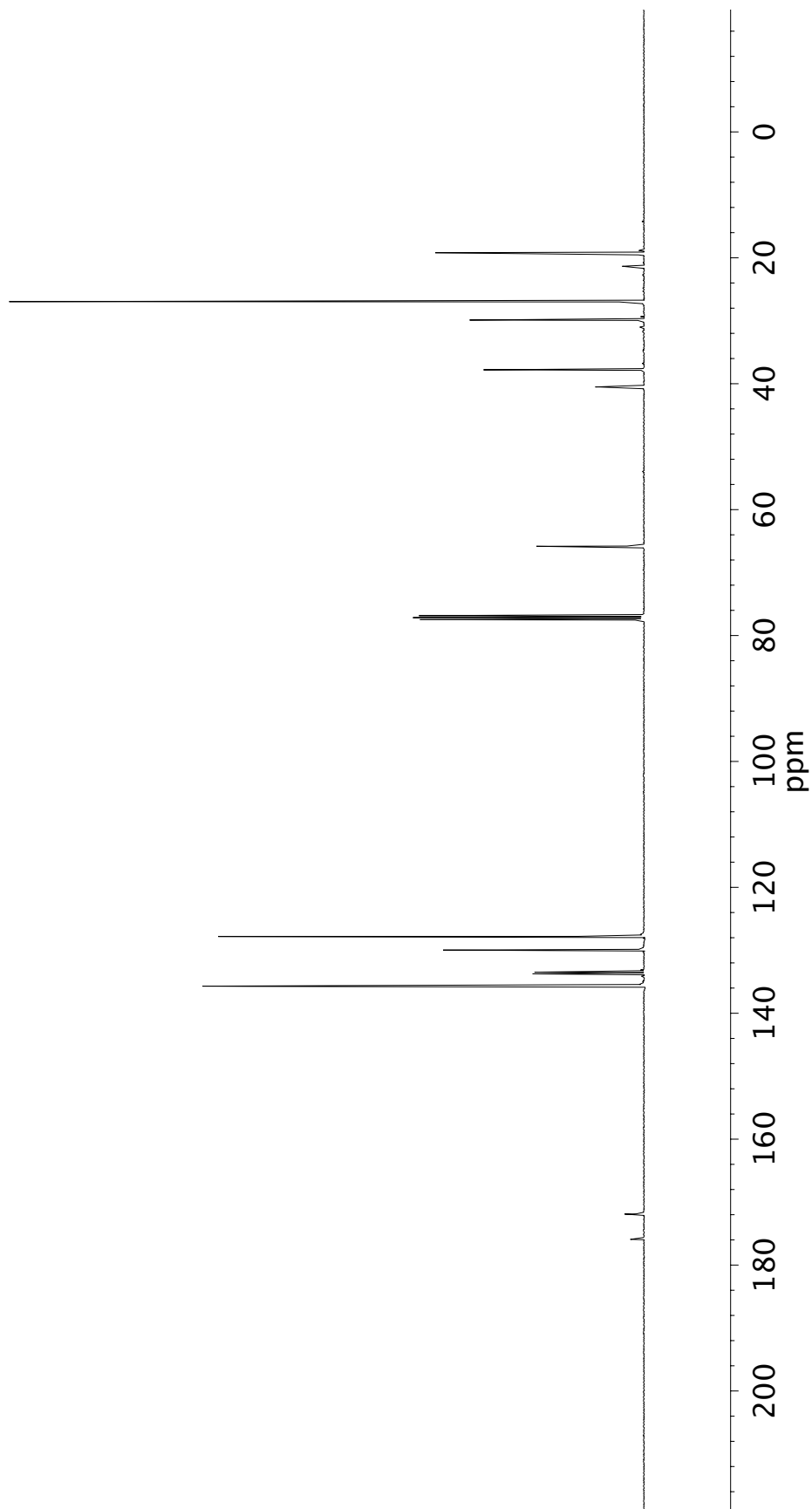


Figure A14.52 ^{13}C NMR (101 MHz, CDCl_3) of compound 291

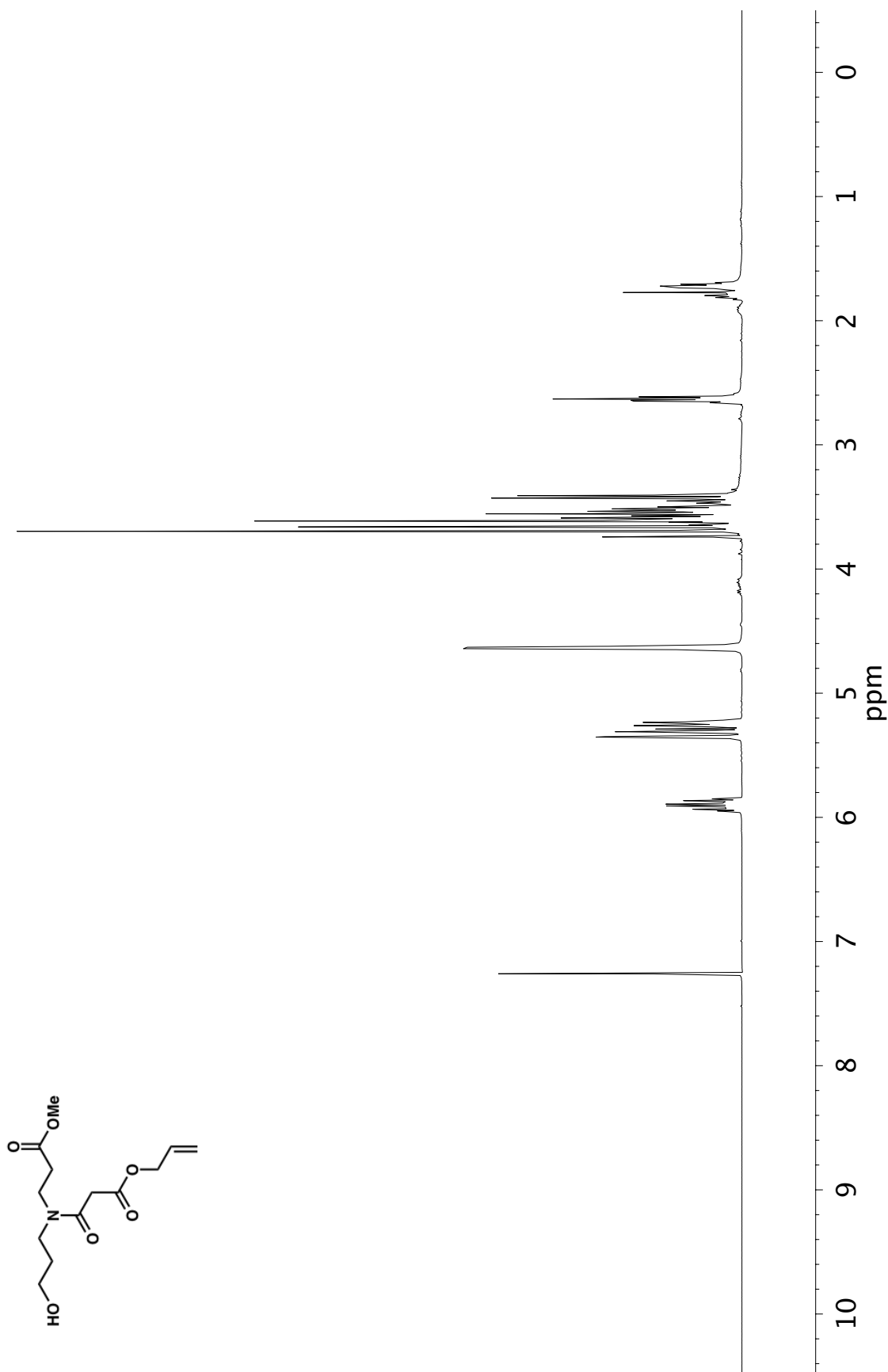


Figure A14.53 ¹H NMR (400 MHz, CDCl₃) of compound 295

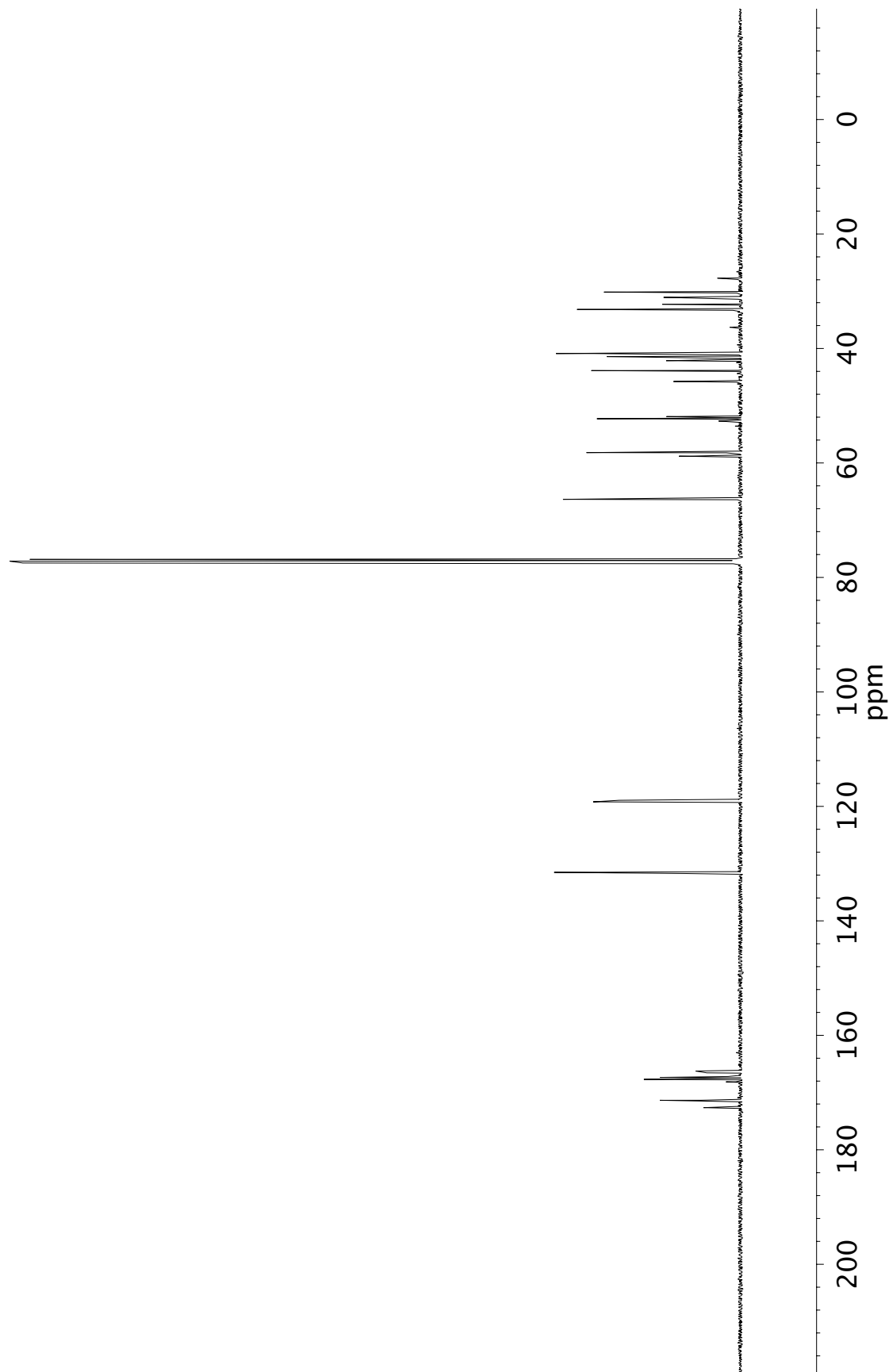


Figure A14.54 ^{13}C NMR (101 MHz, CDCl_3) of compound 295

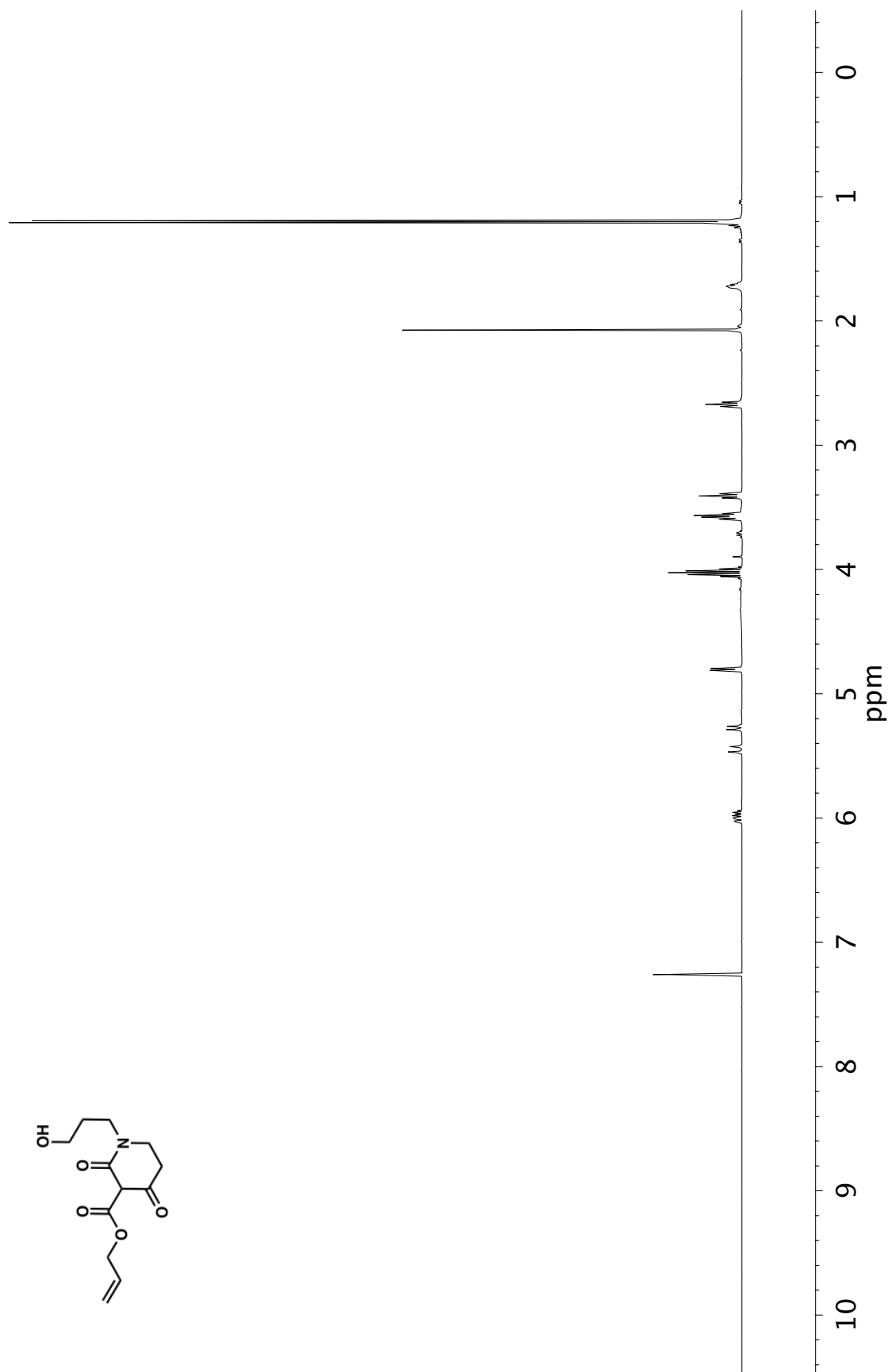


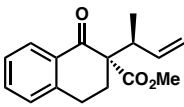
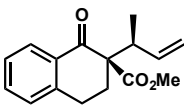
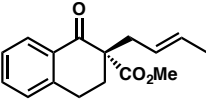
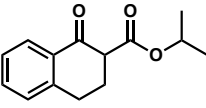
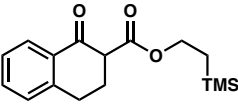
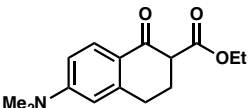
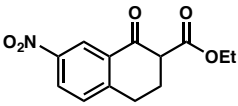
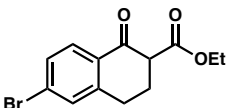
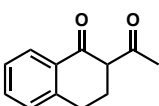
Figure A14.55 ¹H NMR (400 MHz, CDCl₃) of compound 296

APPENDIX 15

Notebook Cross-Reference for New Compounds

The following notebook cross-reference provides the file name for all original spectroscopic data obtained for new compounds presented within this thesis. The information is organized by chapter or appendix and sequentially by compound number. All ^1H NMR, ^{13}C NMR, as well as ^{19}F NMR and any two-dimensional NMR data, if applicable, are electronically stored on the Caltech NMR laboratory server (mangia.caltech.edu, most typically under the usernames 'sshockle', 'chethcox', or 'jholder') and on the Stoltz group server. Electronic copies of all IR spectra can also be found on the Stoltz group server. All laboratory notebooks are stored in the Stoltz group archive.

Table A15.1 Notebook cross-reference for compounds in Chapter 1

Compound	Chemical Structure	¹ H NMR	¹³ C NMR	IR
54		JCH-III-163B- pHPLC-fract2	JCH-III-163B- pHPLC-fract2	JCH-III-155A- pHPLC-fract3 (major-diaist)
epi-54		SES-IX-Me_ester_ minor_dr	SES-IX-Me_ester_ minor_dr	SES-IX-Me_Ester- minor-dr
55		JCH-III-163B- pHPLC-fract3	JCH-III-163B- pHPLC-fract3	JCH-III-155A- pHPLC-fract3 (linear)
56b		SES-VIII-235 -pTLC	SES-VIII-235 -pTLC	SES-VIII-235 -pTLC
56c		SES-IX-199-isco2 -fract3	SES-IX-199-isco2 -fract3	SES-IX-199
56e		SES-IX-233B -fract1-redo	SES-IX-233B -fract1-redo	SES-IX-233B -fract1
56g		SES-IX-237A -fract1	SES-IX-237A -fract1	SES-IX-237A -fract1
56h		SES-IX-237B -repurified	SES-IX-237B -repurified	SES-IX-237B -fract1
56k		JCH-III-131 -p_2	JCH-III-131 -p_2	ch3131p

Compound	Chemical Structure	¹ H NMR	¹³ C NMR	IR
58a		SES-IX-197A-d1	SES-IX-197A-d1	SES-IX-229B
58b		SES-IX-243A-d1	SES-IX-243A-d1	SES-IX-245
58c		SES-IX-239D-d1	SES-IX-239D-d1	SES-IX-239D
58d		JCH-III-217B-d1 -dry-real	JCH-III-217B-d1 -dry-real	SES-IX-239F-d1
58e		SES-IX-239G-d1	SES-IX-239G-d1	SES-IX-239G
58f		JCH-III-217A-d1	JCH-III-217A-d1	JCH-III-217A-d1
58g		SES-IX-239J -HPLC-1	SES-IX-239J -HPLC-1	SES-IX-239J
58h		SES-IX-239I-d1	SES-IX-239I-d1	SES-IX-239I
58i		JCH-III-217D-d1-dry	JCH-III-217D-d1-dry	SES-IX-239H-d1

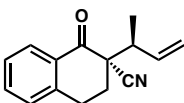
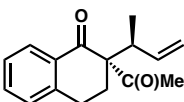
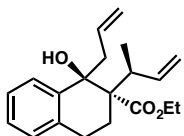
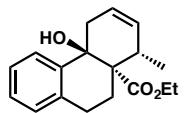
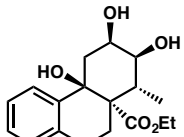
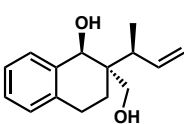
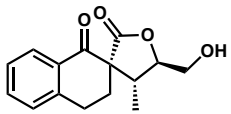
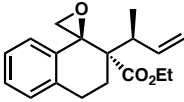
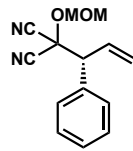
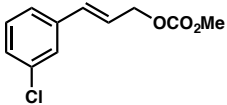
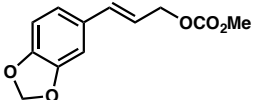
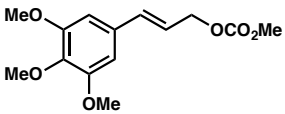
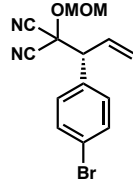
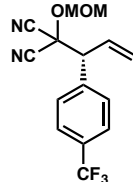
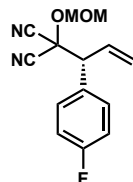
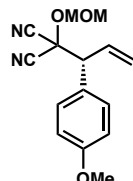
Compound	Chemical Structure	¹ H NMR	¹³ C NMR	IR
58j		SES-IX-239K-d1	SES-IX-239K-d1	SES-IX-239K-d1
58k		JCH-III-173F-2&3	JCH-III-173F-2&3	JCH-III-173F
61		JCH-III-249	JCH-III-249	JCH-III-249
62		JCH-III-253	JCH-III-253	JCH-III-253
63		JCH-III-267-fract1	JCH-III-267-fract1	JCH-III-267
64		JCH-III-255	JCH-III-255	JCH-III-255
65		JCH-III-243p	JCH-III-243p	JCH-III-243
66		SES-IX-269 -repurified	SES-IX-269 -repurified	SES-IX-269

Table A15.2 Notebook cross-reference for compounds in Chapter 2

Compound	Chemical Structure	¹ H NMR	¹³ C NMR	IR
69c		SES-IX-275-fract1	SES-IX-275-fract1	JCH-IV-139
70e		SES-X-179A-fract1	SES-X-179A-fract1	SES-X-179A
70f		SES-X-179C-fract1	SES-X-179C-fract1	SES-X-179C
70g		SES-X-183B	SES-X-183B-fract1	SES-X-183B
71a		JCH-IV-189A	JCH-IV-189A	JCH-IV-163B
71b		JCH-IV-197B -fract3	JCH-IV-197B -fract3	JCH-IV-163C
71c		JCH-IV-217A	JCH-IV-217A	JCH-IV-217A
71d		SES-X-185C-fract1	JCH-IV-163A	JCH-IV-163A

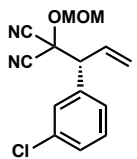
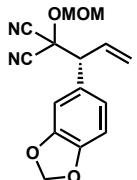
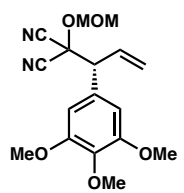
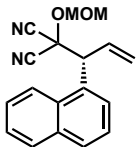
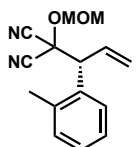
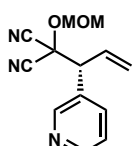
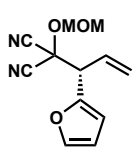
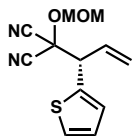
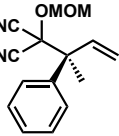
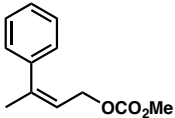
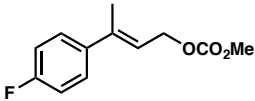
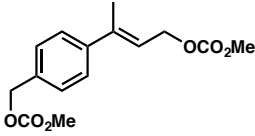
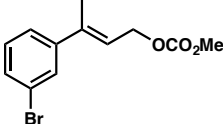
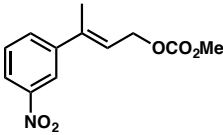
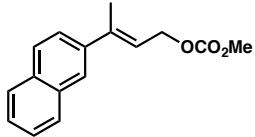
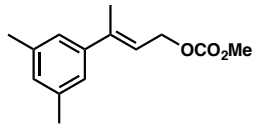
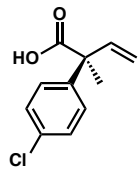
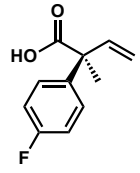
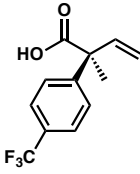
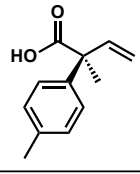
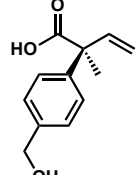
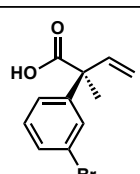
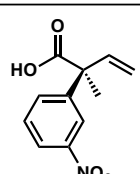
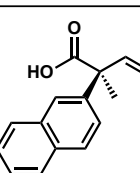
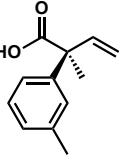
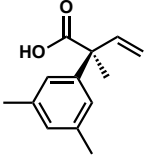
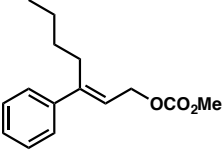
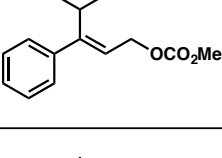
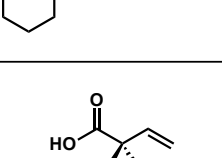
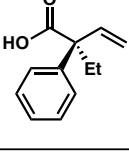
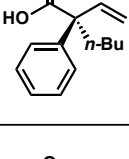
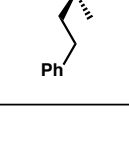
Compound	Chemical Structure	¹ H NMR	¹³ C NMR	IR
71e		JCH-IV-189B	JCH-IV-189B	JCH-IV-189B
71f		JCH-IV-189D	JCH-IV-189D	JCH-IV-189D
71g		JCH-IV-189C	JCH-IV-189C	JCH-IV-189C
71h		JCH-IV-217B	JCH-IV-217B	JCH-IV-217B
71i		JCH-IV-189E	JCH-IV-189E	JCH-IV-163D
71j		SES-X-169H -fract2	SES-X-169H -fract2	SES-X-169H
71k		JCH-IV-131B	JCH-IV-131B	JCH-IV-131B
71l		SES-X-169G	SES-X-169G	SES-X-169G

Table A15.3 Notebook cross-reference for compounds in Chapter 3

Compound	Chemical Structure	¹ H NMR	¹³ C NMR	IR
73		JCH-VI-35-prepHPLC	JCH-VI-35-prepHPLC	JCH-V-131A
74		JCH-V-93-fract1	JCH-V-93-fract1	JCH-V-93
76c		SES-XI-131B	SES-XI-131B	SES-XI-131B
76f		SES-XI-67C-fract1	SES-XI-67C-fract1	SES-XI-67C
76g		SES-XI-109I-fract1	SES-XI-109I-fract1	SES-XI-109I
76h		SES-XI-59A-fract1	SES-XI-59A-fract1	SES-XI-59A
76i		JCH-V-185B	JCH-V-185B	JCH-V-185B
76k		SES-XI-109G-fract1	SES-XI-109G-fract1	SES-XI-109G

Compound	Chemical Structure	¹ H NMR	¹³ C NMR	IR
77b		JCH-V-155B	JCH-V-155B	JCH-V-155B
77c		JCH-V-155C	JCH-V-155C	JCH-V-155C
77d		SES-XI-103BA	SES-XI-103BA	SES-XI-103B
77e		JCH-V-175D	JCH-V-175D	JCH-V-175D
77f		SES-XI-197AA-top	SES-XI-197AA-top	SES-XI-197A
77g		SES-XI-115C	SES-XI-115C	SES-XI-115C
77h		JCH-V-155E	JCH-V-155E	JCH-V-155E
77i		SES-XI-155GA	SES-XI-155GA	SES-XI-155H

Compound	Chemical Structure	¹ H NMR	¹³ C NMR	IR
77j		JCH-V-155D	JCH-V-155D	JCH-V-155D
77k		SES-XI-155A-fract1-conc	SES-XI-155A-fract1-conc	SES-XI-155A-fract1
78b		SES-XI-71B-fract1	SES-XI-71B-fract1	SES-XI-71B
78c		JCH-VI-35-fract1-bottom	JCH-VI-35-fract1-bottom	JCH-VI-35
78e		JCH-V-263-fract1	JCH-V-263-fract1	JCH-V-263
79a		SES-XI-155D-fract1	SES-XI-155D-fract1	JCH-V-155J
79b		SES-XI-179C-fract2	SES-XI-179C-fract2	JCH-V-155K
79f		SES-XI-119J-fract1	SES-XI-119J-fract1	JCH-V-155O

Compound	Chemical Structure	¹ H NMR	¹³ C NMR	IR
82		SES-XI-149-fract2	SES-XI-149-fract2	SES-XI-149-fract2
83		JCH-V-297-2-fract4	JCH-V-297-2-fract4	JCH-V-297
84		SES-XI-147-fract4	SES-XI-147-fract4	SES-XI-147-fract4
85		JCH-V-299-2-fract1	JCH-V-299-2-fract1	JCH-V-299
86		JCH-V-255	JCH-V-255	JCH-V-255
88		JCH-VI-19-fract2-dry	JCH-VI-19-fract2-dry	JCH-VI-19
89		JCH-VI-27-fract2	JCH-VI-27-fract2	JCH-VI-27
90		SES-XI-61D-fract1	SES-XI-61D-fract1	SES-XI-61D
91		SES-XI-105I-fract1	SES-XI-105I-fract1	SES-XI-105I

Table A15.4 Notebook cross-reference for compounds in Chapter 4

Compound	Chemical Structure	¹ H NMR	¹³ C NMR	IR
93		SES-XII-43A	SES-XII-43A	JCH-VI-179-fract1
95a		SES-XII-193C	SES-XII-95B-fract1	SES-XII-83A-fract2
95b		SES-XII-95D-fract1	SES-XII-95D-fract1	SES-XII-83B-fract1
95d		SES-XII-153B-fract1	SES-XII-153B-fract1	SES-XII-151C
95e		JCH-VI-183B-fract1	JCH-VI-183B-fract1	JCH-VI-183B
95f		SES-XII-95C-fract1	SES-XII-95C-fract1	SES-XII-83C-fract2
95g		SES-XII-185A-fract1	SES-XII-185A-fract1	SES-XII-185A
96b		JCH-VII-33A-fract1	JCH-VII-33A-fract1	JCH-VII-33A

Compound	Chemical Structure	¹ H NMR	¹³ C NMR	IR
96c		JCH-VII-33B-fract1	JCH-VII-33B-fract1	JCH-VII-33B
96f		JCH-VI-293C-fract1	JCH-VI-293C-fract1	JCH-VI-293C
97a		SES-XII-167B-fract1	SES-XII-167B-fract1	JCH-VI-279E
97b		SES-XII-191B-fract1-redo	SES-XII-191B-fract1-redo	SES-XII-191B-redo
97c		SES-XII-191A-fract1	SES-XII-191A-fract1	SES-XII-191A
97d		JCH-VI-277F-fract1	JCH-VI-277F-fract1	JCH-VI-275H
97e		SES-XII-97C-fract1	SES-XII-97C-fract1	SES-XII-97C-fract1
97f		SES-XII-187D-fract1	SES-XII-187D-fract1	SES-XII-187D
97g		SES-XII-157A-fract1	SES-XII-157A-fract1	SES-XII-155A

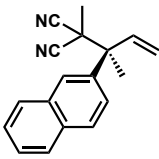
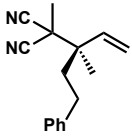
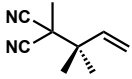
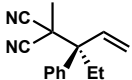
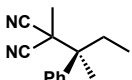
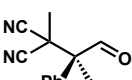
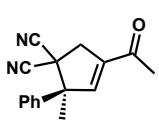
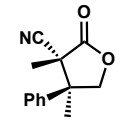
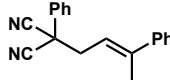
Compound	Chemical Structure	¹ H NMR	¹³ C NMR	IR
97h		SES-XII-97D-fract1	SES-XII-97D-fract1	SES-XII-97D-fract1
97j		SES-XII-193B-fract1	SES-XII-193B-fract1	SES-XII-195A
97k		SES-XII-193A-fract1	SES-XII-193A-fract1	SES-XII-193A-air
97l		SES-XII-97G-fract1	SES-XII-97G-fract1	SES-XII-97G-fract1
101		SES-XII-197-fract1	SES-XII-197-fract1	SES-XII-197
102		JCH-VII-61	JCH-VII-61	JCH-VII-61
103		JCH-VII-75-fract1	JCH-VII-75-fract1	JCH-VII-75
104		JCH-VI-215-top	JCH-VI-215-top	JCH-VI-115-fract2
105		JCH-VII-37-fract1	JCH-VII-37-fract1	JCH-VII-37

Table A15.5 Notebook cross-reference for compounds in Appendix 8

Compound	Chemical Structure	¹ H NMR	¹³ C NMR	IR
169b		JCH-X-167	JCH-X-167	JCH-X-167
169c		SES-III-85-fract2	SES-III-85-fract2	SES-Piv Iodo CA
169d		SES-II-119-fract2 & SES-II-143-fract1	SES-II-119-fract2 & SES-II-143-fract1	SES-BromoPiv CA
169e		SES-1-119 chiralcharc	SES-1-119 chiralcharc	SES-chloro Piv CA
169f		SES-III-129- fract1	SES-III-129- fract1/2	SES-Qins Intermediate
197		JCH-V-125 & JCH-X-bispiv_13C	JCH-V-125 & JCH-X-bispiv_13C	JCH-V-125 & JCH-X-bispiv_13C
198		JCH-X-165Bpin	JCH-X-165Bpin	JCH-X-165Bpin
199		JCH-Acyl B(OH)2 & JCH-X-167	JCH-Acyl B(OH)2 & JCH-X-167	JCH-Acyl B(OH)2 & JCH-X-167

Compound	Chemical Structure	¹ H NMR	¹³ C NMR	IR
202		JCH-X-189A	JCH-X-189A	JCH-X-189A
203		JCH-tricycle & JCH-X-215-A	JCH-tricycle & JCH-X-215-A	JCH-tricycle & JCH-X-215-A
205		SES-II-125	SES-II-125	SES-Bromo Piv
206		SES-II-127-crystals	SES-II-127-crystals	SES-Bromo PivBPin
207		SES-III-65	SES-III-65	SES-Bromo PivB(OH) ₂
208		SES-II-17-fract2	SES-II-17-fract2	SES-isopropenyl MonoPiv
209		SES-III-109 -fract1	SES-III-109 -fract1/2	SES-Nf Piv isopropenyl
210		SES-III-127B -fract1	SES-III-127B -fract1	SES-monopiv isopropyl

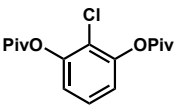
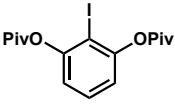
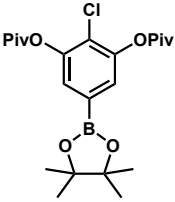
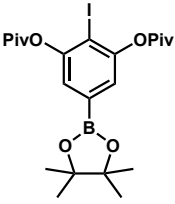
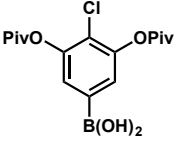
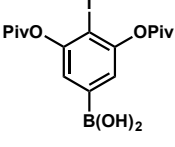
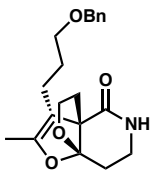
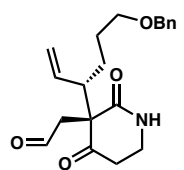
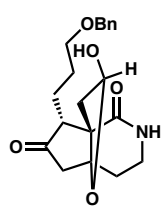
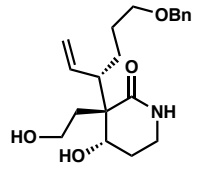
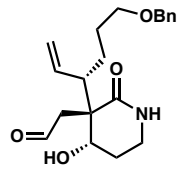
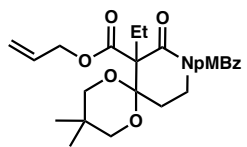
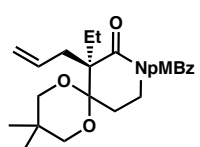
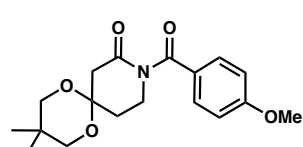
Compound	Chemical Structure	¹ H NMR	¹³ C NMR	IR
211		SES-1-137	SES-1-137	SES-chloroPiv
212		SES-1-203	SES-1-203	SES-Piv Iodo
213		SES-II-91	SES-II-91	SES-Piv Chloro BPin
214		SES-1-205	SES-1-205	SES-Piv Iodo BPin
215		SES-II-79	SES-II-79	SES-ChloroPiv B(OH) ₂
216		SES-1-207Bsolid	SES-1-207Bsolid	SES-Piv Iodo B(OH) ₂

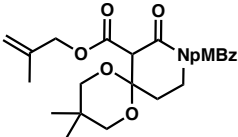
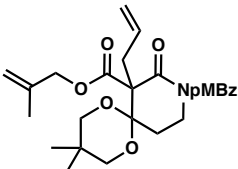
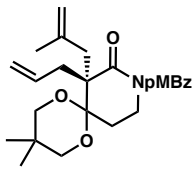
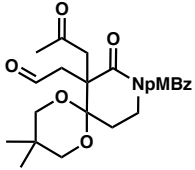
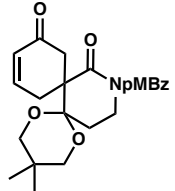
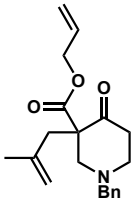
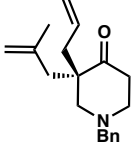
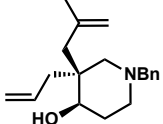
Table A15.6 Notebook cross-reference for compounds in Appendix 11

Compound	Chemical Structure	¹ H NMR	¹³ C NMR	IR
218a		SES-XI-207-fract2	SES-XI-207-fract2	SES-XI-207
218b		SES-XI-213-pTLC	SES-XI-213-pTLC	JCH-VI-39A (misabeled)
218c		JCH-VI-41-pTLC	JCH-VI-41-pTLC	JCH-VI-41
219a		SES-XI-215A	SES-XI-215A	SES-XI-215A
219b		SES-XI-215B	SES-XI-215B	SES-XI-215B
219c		SES-XI-217C	SES-XI-217C	SES-XI-217C
220a		JCH-VI-45A-fract1	JCH-VI-45A-fract1	JCH-VI-45A
220b		JCH-VI-43B	JCH-VI-43B	JCH-VI-43B
220c		JCH-VI-45C-fract1	JCH-VI-45C-fract1	JCH-VI-45C

Table A15.7 Notebook cross-reference for compounds in Appendix 13

Compound	Chemical Structure	¹ H NMR	¹³ C NMR	IR
226		SES-III-287-fract1	–	–
233		SES-III-293-fract1	SES-III-293-fract1	–
234		SES-V-153-fract1	SES-V-153-fract1	–
235		SES-V-41-fract3	SES-V-41-fract3	–
237		SES-V-275-fract1-redo	SES-V-275-fract1-redo	–
238		SES-V-251-fract1	SES-V-251-fract1	–
240 LG = Cl		SES-VIII-129-fract1	SES-VIII-129-fract1	–
241		SES-XI-249F-prepHPLC-fract2	SES-XI-249F-prepHPLC-fract2	–
243		SES-VI-131-135-fract2	SES-VI-131-135-fract2	–

Compound	Chemical Structure	¹ H NMR	¹³ C NMR	IR
244		SES-VI-121 -fract1	SES-VI-121 -fract1	–
245		SES-VI-219 -fract3	SES-VI-219 -fract3	–
247		SES-VI-215 -prepB	SES-VI-215 -prepB	–
248		JCH-V-35-fract3	JCH-V-35-fract3	SES-XI-15 -bottom
249		SES-XI-239 -fract1 & SES-XI-21-fract2	SES-XI-21 -fract2	–
256		SES-VII-209 -pTLC-middle	–	–
257		SES-VII-223 -rac-fract1	SES-VII-223 -rac-fract1	–
258		SES-XI-255 -fract2 & JCH-VI-91	SES-XI-255 -fract2 & JCH-VI-91	JCH-VI-91

Compound	Chemical Structure	¹ H NMR	¹³ C NMR	IR
259		SES-XI-257 -fract1	–	–
260		SES-VII-263 -redo-fract2	–	–
261		SES-XI-283 -fract1	SES-XI-283 -fract1	SES-XI-283
262		SES-VII-289 -fract1	SES-VII-289 -fract1	–
263		SES-XI-273 -fract1	SES-XI-273 -fract1	SES-XI-271
274		SES-IX-11B -fract1	–	–
275		SES-IX-17B -fract1	SES-IX-19 -fract1	–
276		SES-IX-37 -fract1	SES-IX-25 -fract2	–

COMPREHENSIVE BIBLIOGRAPHY

Adam, G.; Huong, H. T. *Tetrahedron Lett.* **1980**, *21*, 1931–1932.

Adams, C.; Capparelli, M. P.; Ehara, T.; Karki, R. G.; Mainolfi, N.; Chun, Z. U.S. Patent WO2015009616 A1, Jan. 22, 2015.

Alexakis, A.; Polet, D. *Org. Lett.* **2004**, *6*, 3529–3532.

Allen, A. E.; MacMillan, D. W. C. *Chem. Sci.* **2012**, *3*, 633–658.

Alvarez-Manzaneda, E.; Chahboun, R.; Alvarez, E.; Tapia, R.; Alvarez-Manzaneda, R. *Chem. Commun.* **2010**, *46*, 9244–9246.

Alvarez-Manzaneda, E.; Chahboun, R.; Cabrera, E.; Alvarex, E.; Haidour, A.; Ramos, J. M.; Alvarez-Manzaneda, R.; Hmamouchi, M.; Es-Samti, H. *Chem. Commun.* **2009**, 592–594.

Alvarez-Manzaneda, E.; Chahboun, R.; Cabrera, E.; Alvarez, E.; Alvarez-Manzaneda, R.; Meneses, R.; Es-Samti, H.; Fernández, A. *J. Org. Chem.* **2009**, *74*, 3384–3388.

Alvarez-Manzaneda, E.; Chahboun, R.; Cabrera, E.; Alvarez, E.; Haidour, A.; Ramos, J. M.; Alvarez-Manzaneda, R.; Charrah, Y.; Es-Samti, H. *Org. Biomol. Chem.* **2009**, *7*, 5146–5155.

Ankner, T.; Fridén-Saxin, M.; Pemberton, N.; Seifert, T.; Grøtli, M.; Luthman, K.; Hilmersson, G. *Org. Lett.* **2010**, *12*, 2210–2213.

Aoyama, T.; Nakano, T.; Marumo, K.; Uno, Y.; Shiori, T. *Synthesis* **1991**, 1163–1167.

Arason, K. M.; Bergmeier, S. C. *Org. Prep. Proced. Int.* **2002**, *34*, 337–366.

Ardolino, M. J.; Morken, J. P. *J. Am. Chem. Soc.* **2014**, *136*, 7092–7100.

B. P. Bondzic, A. Farwick, J. Liebich, P. Eilbracht, *Org. Biomol. Chem.* **2008**, *6*, 3723–3731.

Ball-Jones, N. R.; Badillo, J. J.; Franz, A. K. *Org. Biomol. Chem.* **2012**, *10*, 5165–5181.

Bähn, S.; Imm, S.; Neubert, L.; Zhang, M.; Neumann, H.; Beller, M. *ChemCatChem* **2011**, *3*, 1853–1864.

Banerjee, M.; Mukhopadhyay, R.; Achari, B.; Banerjee, A. K. *J. Org. Chem.* **2006**, *71*, 2787–2796.

Banerjee, M.; Mukhopadhyay, R.; Achari, B.; Banerjee, A. K. *Org. Lett.* **2003**, *5*, 3931–3933.

Barbe, G.; St-Onge, M.; Charette, A. B. *Org. Lett.* **2008**, *10*, 5497–5499.

Bartels, B.; Helmchen, G. *Chem. Commun.* **1999**, 741–742.

Behenna, D. C.; Liu, Y.; Yurino, T.; Kim, J.; White, D. E.; Virgil, S. C.; Stoltz, B. M. *Nat. Chem.* **2012**, *4*, 130–133.

Behenna, D. C.; Mohr, J. T.; Sherden, N. H.; Marinescu, S. C.; Harned, A. M.; Tani, K.; Seto, M.; Ma, S.; Novák, Z.; Krout, M. R.; McFadden, R. M.; Roizen, J. L.; Enquist, J. A., Jr.; White, D. E.; Levine, S. R.; Petrova, K. V.; Iwashita, A.; Virgil, S. C.; Stoltz, B. M. *Chem. Eur. J.* **2011**, *17*, 14199–14223.

Behenna, D. C.; Stoltz, B. M. *J. Am. Chem. Soc.* **2004**, *126*, 15044–15045.

- Benati, L.; Bencivenni, G.; Leardini, R.; Minozzi, M.; Nanni, D.; Scialpi, R.; Spagnolo, P.; Zanardi, G.; Rizzoli, C. *Org. Lett.* **2004**, *6*, 417–420.
- Bennett, N. B.; Duquette, D. C.; Kim, J.; Liu, W.-B.; Marziale, A. N.; Behenna, D. C.; Virgil, S. C.; Stoltz, B. M. *Chem. Eur. J.* **2013**, *19*, 4414–4418.
- Bensel, N.; Höhn, J.; Marschall, H.; Weyerstahl, P. *Eur. J. Inorg. Chem.* **1979**, *112*, 2256–2277.
- Bernasconi, M.; Ramella, V.; Tosatti, P.; Pfaltz, A. *Chem. Eur. J.* **2014**, *20*, 2440–2444.
- Boeser, C. L.; Holder, J. C.; Taylor, B. L. H.; Houk, K. N.; Stoltz, B. M.; Zare, R. N. *Chem. Sci.* **2015**, *6*, 1917–1922.
- Bondzic, B. P.; Farwick, A.; Liebich, J.; Eilbracht, P. *Org. Biomol. Chem.* **2008**, *6*, 3723–3731.
- Bourry, A.; Couturier, D.; Sanz, G.; Van Hijfte, L.; Hénichart, J.-P.; Rigo, B. *Tetrahedron* **2006**, *62*, 4400–4407.
- Breitenlechner, S.; Bach, T. *Angew. Chem. Int. Ed.* **2008**, *47*, 7957–7959.
- Breitler, S.; Carreira, E. M. *J. Am. Chem. Soc.* **2015**, *137*, 5296–5299.
- Brown, B.; Hegedus, L. S. *J. Org. Chem.* **2000**, *65*, 1865–1872.
- Brown, M. K.; May, T. L.; Baxter, C. A.; Hoveyda, A. H. *Angew. Chem. Int. Ed.* **2007**, *46*, 1097–1100.
- Brunner, H.; Obermann, U. *Chem. Ber.* **1989**, *122*, 499–507.

- Buter, J.; Moezelaar, R.; Minnaard, A. J. *Org. Biomol. Chem.* **2014**, *12*, 5883–5890.
- Butler, J. D.; Coffman, K. C.; Ziebart, K. T.; Toney, M. D.; Kurth, M. J. *Chem. Eur. J.* **2010**, *16*, 9002–9005.
- Cao, W.; Liu, X.; Peng, R.; He, P.; Lin, L.; Feng, X. *Chem. Commun.* **2013**, *49*, 3470–3472.
- Cao, Z.-Y.; Wang, X.; Tan, C.; Zhao, X.-L.; Zhou, J.; Ding, K. *J. Am. Chem. Soc.* **2013**, *135*, 8197–8200.
- Carrow, B. P.; Hartwig, J. F. *J. Am. Chem. Soc.* **2011**, *133*, 2116–2119.
- Castro, A. M. M. *Chem. Rev.* **2004**, *104*, 2939–3002.
- Chang, C. -I.; Chien, S.-C.; Lee, S.-M.; Kuo, Y.-H. *Chem. Pharm. Bull.* **2003**, *51*, 1420–1422.
- Chang, C.-I.; Chang, J.-Y.; Kuo, C.-C.; Pan, W.-Y.; Kuo, Y.-H. *Planta Med.* **2005**, *71*, 72–76.
- Chen, J.-P.; Ding, C.-H.; Liu, W.; Hou, X.-L.; Dai, L.-X. *J. Am. Chem. Soc.* **2010**, *132*, 15493–15495.
- Chen, J.; Chen, J.; Lang, F.; Zhang, X.; Cun, L.; Zhu, J.; Deng, J.; Liao, J. *J. Am. Chem. Soc.* **2010**, *132*, 4552–4553.
- Chen, M.; Hartwig, J. F. *Angew. Chem. Int. Ed.* **2016**, *55*, 11651–11655.
- Chen, W.; Chen, M.; Hartwig, J. F. *J. Am. Chem. Soc.* **2014**, *136*, 15825–15828.

- Chen, W.; Hartwig, J. F. *J. Am. Chem. Soc.* **2013**, *135*, 2068–2071.
- Chen, W.; Hartwig, J. F. *J. Am. Chem. Soc.* **2014**, *136* 377–382.
- Cheng, D.; Ishihara, Y.; Tan, B.; Barbas, C. F., III. *ACS Catal.* **2014**, *4*, 743–762.
- Cheng, Q.; Wang, Y.; You, S.-L. *Angew. Chem. Int. Ed.* **2016**, *55*, 3496–3499.
- Cherney, A. H.; Kadunce, N. T.; Reisman, S. E. *J. Am. Chem. Soc.* **2013**, *135*, 7442–7445.
- Christoffers, J.; Koripelly, G.; Rosiak, A.; Rössle M. *Synthesis* **2007**, 1279–1300.
- Christoffers, J.; Mann, A. *Angew. Chem. Int. Ed.* **2001**, *40*, 4591–4597.
- Cordova, A. *Catalytic Asymmetric Conjugate Reactions*, Wiley & Sons: Weinheim, 2010.
- Corey, E. J.; Guzman-Perez, A. *Angew. Chem. Int. Ed.* **1998**, *37*, 388–401.
- Craig, R. A., II; Loskot, S. A.; Mohr, J. T.; Behenna, D. C.; Harned, A. M.; Stoltz, B. M. *Org. Lett.* **2015**, *17*, 5160–5163.
- Crimmins, M. T.; Brown, B. H.; Plake, H. R. *J. Am. Chem. Soc.* **2006**, *128*, 1371–1378.
- Cui, L.-Q.; Dong, Z.-L.; Liu, K.; Zhang, C. *Org. Lett.* **2011**, *13*, 6488–6491.
- d’Augustin, M.; Palais, L.; Alexakis, A. *Angew. Chem. Int. Ed.* **2005**, *44*, 1376–1378.
- D’yakonov, V. A.; Trapeznikova, O. A.; de Meijere, A.; Dzhemilev, U. M. *Chem. Rev.* **2014**, *114*, 5775–5814.
- Dai, W.-M.; Zhuo, W.-S. *Tetrahedron* **1985**, *41*, 4475–4482.

Das, J. P.; Marek, I. *Chem. Commun.* **2011**, 47, 4593–4623.

DeAngelis, A.; Dmitrenko, O.; Yap, G. P. A.; Fox, J. M. *J. Am. Chem. Soc.* **2009**, 131, 7230–7231.

Defieber, C.; Ariger, M. A.; Moriel, P.; Carreira, E. M. *Angew. Chem. Int. Ed.* **2007**, 46, 3139–3143.

DeMartino, M. P.; Chen, K.; Baran, P. S. *J. Am. Chem. Soc.* **2008**, 130, 11546–11560.

Deng, J.; Li, R.; Luo, Y.; Li, J.; Zhou, S.; Li, Y.; Hu, J.; Li, A. *Org. Lett.* **2013**, 15, 2022–2025.

Denissova, I.; Barriault, L. *Tetrahedron* **2003**, 59, 10105–10146.

Denmark, S. E.; Wilson, T. W.; Burk, M. T. *Chem. Eur. J.* **2014**, 20, 9268–9279.

Díez-Barra, E.; de la Hoz, A.; Moreno, A.; Sánchez-Verdú, P. *J. Chem. Soc., Perkin Trans. I* **1991**, 0, 2589–2592.

Dindaroğlu, M.; Dinçer, S. A.; Schmalz, H.-G. *Eur. J. Org. Chem.* **2014**, 4315–4326.

Dobereiner, G. E.; Crabtree, R. H. *Chem. Rev.* **2010**, 110, 681–703.

Dong, L.-B.; Gao, X.; Liu, F.; He, J.; Wu, X.-D.; Li, Y.; Zhao, Q.-S. *Org. Lett.* **2013**, 15, 3570–3573.

Douglas, C. J.; Overman, L. E. *Proc. Natl. Acad. Sci. USA* **2004**, 101, 5363–5367.

- Duan, W.-L.; Iwamura, H.; Shintani, R.; Hayashi, T. *J. Am. Chem. Soc.* **2007**, *129*, 2130–2138.
- Duan, Z.-C.; Hu, X.-P.; Zhang, C.; Zheng, Z. *J. Org. Chem.* **2010**, *75*, 8319–8321.
- Dumas, A. M.; Fillion, E. *Acc. Chem. Res.* **2010**, *43*, 440–454.
- Duong, H. A.; Huleatt, P. B.; Tan, Q.-W.; Shuying, E. L. *Org. Lett.* **2013**, *15*, 4034–4037.
- Enders, D.; Knopp, M.; Runsink, J.; Raabe, G. *Angew. Chem. Int. Ed.* **1995**, *34*, 2278–2280.
- Enquist, J. A., Jr.; Stoltz, B. M. *Nature* **2008**, *453*, 1228–1231.
- Evans, P. A.; Oliver, S.; Chae, J. *J. Am. Chem. Soc.* **2012**, *134*, 19314–19317.
- Fabrizzi, P.; Bianchini, F.; Menchi, G.; Raspanti, S.; Trabocchi, A. *Tetrahedron* **2014**, *70*, 5439–5449.
- Falciola, C. A.; Alexakis, A. *Chem. Eur. J.* **2008**, *14*, 10615–10627.
- Fang, P.; Ding, C.-H.; Hou, X.-L.; Dai, L.-X. *Tetrahedron: Asymmetry* **2010**, *21*, 1176–1178.
- Feringa, B. L. *Acc. Chem. Res.* **2000**, *33*, 346–353.
- Fernández-Mateos, A.; Teijón, P. H.; Burón, L. M.; Clemente, R. R.; González, R. R. *J. Org. Chem.* **2007**, *72*, 9973–9982.
- Fillion, E.; Fishlock, D. *J. Am. Chem. Soc.* **2005**, *127*, 13144–13145.

- Fillion, E.; Wilsily, A. *J. Am. Chem. Soc.* **2006**, *128*, 2774–2775.
- Fiorito, D.; Folliet, S.; Liu, Y.; Mazet, C. *ACS Catal.* **2018**, *8*, 1392–1398.
- Fischer, C.; Defieber, C.; Suzuki, T.; Carreira, E. M. *J. Am. Chem. Soc.* **2004**, *126*, 1628–1629.
- Förster, S.; Tverskoy, O.; Helmchen, G. *Synlett* **2008**, *18*, 2803–2806.
- Franke, A.; Mattern, G.; Traber, W. *Helv. Chim. Acta* **1975**, *58*, 268–278.
- Franz, A. K.; Hanhan, N. V.; Ball-Jones, N. R. *ACS Catal.* **2013**, *3*, 540–553.
- Frisch, M. J.; et al. *Gaussian 03*, Revision C.02; Gaussian, Inc.: Wallingford, CT, 2004.
- Fuchs, N.; d'Augustin, M.; Humam, M.; Alexakis, A.; Taras, R.; Gladiali, S. *Tetrahedron: Asymmetry* **2005**, *16*, 3143–3146.
- Gao, C.; Tao, X.; Qian, Y.; Huang, J. *Synlett* **2003**, *11*, 1716–1718.
- Gao, F.; Lee, Y.; Mandai, K.; Hoveyda, A. H. *Angew. Chem. Int. Ed.* **2010**, *49*, 8370–8374.
- Gao, L.; Hwang, G.-S.; Ryu, D. H. *J. Am. Chem. Soc.* **2011**, *133*, 20708–20711.
- Ghorai, M. K.; Talukdar, R.; Tiwari, D. P. *Org. Lett.* **2014**, *16*, 2204–2207.
- Ghosh, S.; Bhunia, S.; Kakde, B. N.; De, S.; Bisai, A. *Chem. Commun.* **2014**, *50*, 2434–2437.
- Ghosh, S.; Chaudhuri, S.; Bisai, A. *Org. Lett.* **2015**, *17*, 1373–1376.

- Gini, F.; Hessen, B.; Feringa, B. L.; Minnaard, A. J. *Chem. Commun.* **2007**, 710–712.
- Gottumukkala, A. L.; Matcha, K.; Lutz, M.; de Vries, J. G.; Minnaard, A. J. *Chem.–Eur. J.* **2012**, *18*, 6907–6914.
- Greshock, T. J.; Funk, R. L. *J. Am. Chem. Soc.* **2002**, *124*, 754–755.
- Guduguntla, S.; Gualtierotti, J.-B.; Goh, S. S.; Feringa, B. L. *ACS Catal.* **2016**, *6*, 6591–6595.
- Guillaneux, D.; Zheo, S.-H.; Samuel, O.; Rainford, D.; Kagan, H. B. *J. Am. Chem. Soc.* **1994**, *116*, 9430–9439.
- Guillena, G.; Ramón, D. J.; Yus, M. *Chem. Rev.* **2010**, *110*, 1611–1641.
- Gunes, Y.; Arcelik, N.; Sahin, E.; Fleming, F. F.; Altundas, R. *Eur. J. Org. Chem.* **2015**, 6679–6686.
- Gürtler, C.; Buchwald, S. L. *Chem. Eur. J.* **1999**, *5*, 3107–3112.
- Gutnov, A. *Eur. J. Org. Chem.* **2008**, 4547–4554.
- Guzman-Martinez, A.; Hoveyda, A. H. *J. Am. Chem. Soc.* **2010**, *132*, 10634–10637.
- Hahn, B. T.; Tewes, F.; Fröhlich, R.; Glorius, F. *Angew Chem. Int. Ed.* **2010**, *49*, 1143–1146.
- Hamid, M. H. S. A.; Slatford, P. A.; Williams, J. M. J. *Adv. Synth. Catal.* **2007**, *349*, 1555–1575.
- Hamilton, J. Y.; Sarlah, D.; Carreira, E. M. *Org. Synth.* **2015**, *92*, 1–12.

Han, C.; Buchwald, S. L. *J. Am. Chem. Soc.* **2009**, *131*, 7532–7533.

Han, F.; Chen, G.; Zhang, X.; Liao, J. *Eur. J. Org. Chem.* **2011**, 2928–2931.

Hansch, C.; Leo, A.; Taft, R. W. *Chem. Rev.* **1991**, *91*, 165–195.

Hartwig, J. F.; Pouy, M. J. *Top. Organomet. Chem.* **2011**, *34*, 169–208.

Hawner, C.; Alexakis, A. *Chem. Commun.* **2010**, 7295–7306.

Hawner, C.; Li, K.; Cirriez, V.; Alexakis, A. *Angew. Chem. Int. Ed.* **2008**, *47*, 8211–8214.

Hawner, C.; Müller, D.; Gremaud, L.; Felouat, A.; Woodward, S.; Alexakis, A. *Angew. Chem. Int. Ed.* **2010**, *49*, 7769–7772.

Hayashi, T.; Kawatsura, M.; Uozumi, Y. *J. Am. Chem. Soc.* **1998**, *120*, 1681–1687.

Hayashi, T.; Ueyama, K.; Tokunaga, N.; Yoshida, K. *J. Am. Chem. Soc.* **2003**, *125*, 11508–11509.

Hayashi, T.; Yamasaki, K. *Chem. Rev.* **2003**, *103*, 2829–2844.

He, F.; Bo, Y.; Altom, J. D.; Corey, E. J. *J. Am. Chem. Soc.* **1999**, *121*, 6771–6772.

He, H.; Zheng, Z.-J.; Li, Y.; Dai, L.-X.; You, S.-L. *Org. Lett.* **2007**, *9*, 4339–4341.

He, Q.; So, C. M.; Bian, Z.; Hayashi, T.; Wang, J. *Chem. Asian J.* **2015**, *10*, 540–543.

Helmchen, G.; Dahnz, A.; Dübon, P.; Schelwies, M.; Weihofen, R. *Chem. Commun.* **2007**, 675–691.

Hénon, H.; Mauduit, M.; Alexakis, A. *Angew. Chem. Int. Ed.* **2008**, *47*, 9122–9124.

Hethcox, J. C.; Shockley, S. E.; Stoltz, B. M. *ACS Catal.* **2016**, *6*, 6207–6213.

Hethcox, J. C.; Shockley, S. E.; Stoltz, B. M. *Angew. Chem. Int. Ed.* **2018**, doi: 10.1002/anie.201804820.

Hethcox, J. C.; Shockley, S. E.; Stoltz, B. M. *Angew. Chem. Int. Ed.* **2016**, *55*, 16092–16095.

Hethcox, J. C.; Shockley, S. E.; Stoltz, B. M. *Org. Lett.* **2017**, *19*, 1527–1529.

Hirasawa, Y.; Kobayashi, J.; Morita, H. **2009**, *77*, 679–729.

Hird, A. W.; Hoveyda, A. H. *J. Am. Chem. Soc.* **2005**, *127*, 14988–14989.

Ho Oh, C.; Jung, H. H.; Kim, K. S.; Kim, N. *Angew. Chem. Int. Ed.* **2003**, *42*, 805–808.

Hojoh, K.; Ohmiya, H.; Sawamura, M. *J. Am. Chem. Soc.* **2017**, *139*, 2184–2187.

Holder, J. C.; Marziale, A. N.; Gatti, M.; Mao, B.; Stoltz, B. M. *Chem.–Eur. J.* **2013**, *19*, 74–77.

Holder, J. C.; Shockley, S. E.; Wiesenfeldt, M. P.; Shimizu, H.; Stoltz, B. M. *Org. Synth.* **2015**, *92*, 247–266.

Holder, J. C.; Zou, L.; Marziale, A. N.; Liu, P.; Lan, Y.; Gatti, M.; Kikushima, K.; Houk, K. N.; Stoltz, B. M. *J. Am. Chem. Soc.* **2013**, *135*, 14996–15007.

Hou, X.-L.; Sun, N. *Org. Lett.* **2004**, *6*, 4399–4401.

- Hu, X.; Xu, S.; Maimone, T. J. *Angew. Chem. Int. Ed.* **2017**, *56*, 1624–1628.
- Huang, S.-H.; Wu, T.-M.; Tsai, F.-Y. *Appl. Organomet. Chem.* **2010**, *24*, 619–624.
- Huang, X.; Wu, S.; Wu, W.; Li, P.; Fu, C.; Ma, S. *Nat. Commun.* **2016** doi: 10.1038/ncomms12382.
- Hünig, S.; Schäfer, M.; Schweenberg, W. *Chem. Ber.* **1993**, *126*, 191–204.
- Huo, X.; He, R.; Zhang, W. *J. Am. Chem. Soc.* **2016**, *138*, 11093–11096.
- Huo, X.; He, R.; Zhang, X.; Zhang, W. *J. Am. Chem. Soc.* **2016**, *138*, 11093–11096.
- Ilardi, E. A.; Stivala, C. E.; Zakarian, A. *Chem. Soc. Rev.* **2009**, *38*, 3133–3148.
- Ishiyama, T.; Takagi, J.; Ishida, K.; Miyaura, N.; Anastasi, N. R.; Hartwig, J. F. *J. Am. Chem. Soc.* **2002**, *124*, 390–391.
- Ito, H.; Taguchi, T. *Chem. Soc. Rev.* **1999**, *28*, 43–50.
- Iwamoto, M.; Ohtsu, H.; Tokuda, H.; Nishino, H.; Matsunaga, S.; Tanaka, R. *Bioorg. Med. Chem.* **2001**, *9*, 1911–1921.
- Izumi, M.; Wada, K.; Yuasa, H.; Hashimoto, H. *J. Org. Chem.* **2005**, *70*, 8817–8824.
- Jana, C. K.; Scopelliti, R.; Gademann, K. *Chem.–Eur. J.* **2010**, *16*, 7692–7695.
- Jana, C. K.; Scopelliti, R.; Gademann, K. *Synthesis* **2010**, 2223–2232.
- Janssen, J. P.; Helmchen, G. *Tetrahedron Lett.* **1997**, *38*, 8025–8026.

Jiang, X.; Beiger, J. J.; Hartwig, J. F. *J. Am. Chem. Soc.* **2017**, *139*, 87–90.

Jiang, X.; Chen, W.; Hartwig, J. F. *Angew. Chem. Int. Ed.* **2016**, *55*, 5819–5823.

Johnston, M. D.; Shapiro, B. L.; Shapiro, M. J.; Proulx, T. W.; Godwin, A. D.; Pearce, H. L. *J. Am. Chem. Soc.* **1975**, *97*, 542–554.

Jolit, A.; Walleser, P. M.; Yap, G. P. A.; Tius, M. A. *Angew. Chem. Int. Ed.* **2014**, *53*, 6180–6183.

Kadam, A. A.; Ellern, A.; Stanley, L. M. *Org. Lett.* **2017**, *15*, 4062–4065.

Kagawa, N.; Nibbs, A. E.; Rawal, V. H. *Org. Lett.* **2016**, *18*, 2363–2366.

Kanayama, T.; Yoshida, K.; Miyabe, H.; Takemoto, K. *Angew. Chem. Int. Ed.* **2003**, *42*, 2054–2056.

Katoh, T.; Akagi, T.; Noguchi, C.; Kajimoto, T.; Node, M.; Tanaka, R.; Nishizawa, M.; Ohtsu, H.; Suzuki, N.; Saito, K. *Bioorg. Med. Chem.* **2007**, *15*, 2736–2748.

Kawatsura, M.; Sato, M.; Tsuji, H.; Ata, F.; Itoh, T. *J. Org. Chem.* **2011**, *76*, 5485–5488.

Kawazoe, K.; Yamamoto, M.; Takaishi, Y.; Honda, G.; Fujita, T.; Sezik, E.; Yesilada, E. *Phytochemistry* **1999**, *50*, 493–497.

Kehrli, S.; Martin, D.; Rix, D.; Mauduit, M.; Alexakis, A. *Chem.—Eur. J.* **2010**, *16*, 9890–9904.

Khan, A.; Yang, L.; Xu, J.; Jin, L. Y.; Zhang, Y. J. *Angew. Chem. Int. Ed.* **2014**, *53*, 11257–11260.

- Kikushima, K.; Holder, J. C.; Gatti, M.; Stoltz, B. M. *J. Am. Chem. Soc.* **2011**, *133*, 6902–6905.
- Kim, D.; Reddy, S.; Singh, O. V.; Lee, J. S.; Kong, S. B.; Han, H. *Org. Lett.* **2013**, *15*, 512–515.
- Kitajima, M.; Takayama, H. *Top. Curr. Chem.* **2012**, *309*, 1–31.
- Kociólek, K.; Leplawy, M. T. *Synthesis* **1977**, 778–780.
- Kong, C.; Jana, N.; Jones, C.; Driver, T. G. *J. Am. Chem. Soc.* **2016**, *138*, 13271–13280.
- Korch, K. M.; Eidamshaus, C.; Behenna, D. C.; Nam, S.; Horne, D.; Stoltz, B. M. *Angew. Chem. Int. Ed.* **2015**, *54*, 179–183.
- Korenaga, T.; Hayashi, K.; Akaki, Y.; Maenishi, R.; Sakai, T. *Org. Lett.* **2011**, *13*, 2022–2025.
- Kotha, S.; Deb, A. C.; Lahiri, K.; Manivannan, E. *Synthesis* **2009**, 165–193.
- Krapcho A. P. *Synthesis* **1974**, 383–419.
- Kraus, G. A.; Wan, Z. *Tetrahedron Lett.* **1997**, *38*, 6509–6512.
- Krause, N.; Hoffman-Röder, A. *Synthesis* **2001**, 171–196.
- Krautwald, S.; Sarlah, D.; Schafroth, M. A.; Carreira, E. M. *Science* **2013**, *340*, 1065–1068.
- Krautwald, S.; Schafroth, M. A.; Sarlah, D.; Carreira, E. M. *J. Am. Chem. Soc.* **2014**, *136*, 3020–3023.
- Kubota, Y.; Nemoto, H.; Yamamoto, Y. *J. Org. Chem.* **1991**, *56*, 7195–7196.

Ladjel, C.; Fuchs, N.; Zhao, J.; Bernardinelli, G.; Alexakis, A. *Eur. J. Org. Chem.* **2009**, 4949–4955.

Lantaño, B.; Aguirre, J. M.; Ugliarolo, E. A.; Torviso, R.; Pomilio, N.; Moltrasio, G. Y. *Tetrahedron*, **2012**, 68, 913–921.

Lee, K.-S.; Brown, M. K.; Hird, A. W.; Hoveyda, A. H. *J. Am. Chem. Soc.* **2006**, 128, 7182–7184.

Lee, Y.; Hoveyda, A. H. *J. Am. Chem. Soc.* **2006**, 128, 15604–15605.

Leitner, A.; Shu, C.; Hartwig, J. F. *Org. Lett.* **2005**, 7, 1093–1096.

Li, L.-Q.; Li, M.-M.; Chen, D.; Liu, H.-M.; Geng, H.-C.; Lin, J.; Qin, H.-B. *Tetrahedron Lett.* **2014**, 55, 5960–5962.

Li, S.; Chiu, P. *Tetrahedron Lett.* **2008**, 49, 1741–1744.

Li, W.; Wang, J.; Hu, X.; Shen, K.; Wang, W.; Chu, Y.; Lin, L. Liu, X.; Feng, X. *J. Am. Chem. Soc.* **2010**, 132, 8532–8533.

Liang, G.; Xu, Y.; Seiple, I. B.; Trauner, D. *J. Am. Chem. Soc.* **2006**, 128, 11022–11023.

Liao, X.; Stanley, L. M.; Hartwig, J. F. *J. Am. Chem. Soc.* **2011**, 133, 2088–2091.

Lin, S.; Lu, X. *Org. Lett.* **2010**, 12, 2536–2539.

Lin, S.; Lu, X. *Tetrahedron Lett.* **2006**, 47, 7167–7170.

Lin, W.-H.; Fang, J.-M.; Cheng, Y.-S. *Phytochemistry* **1996**, 42, 1657–1663.

Ling, T.; Rivas, F. *Tetrahedron* **2016**, *72*, 6729–6777.

Liu, W.-B.; He, H.; Dai, L.-X.; You, S.-L. *Synthesis* **2009**, 2076–2082.

Liu, W.-B.; Okamoto, N.; Alexy, E. J.; Hong, A. J.; Tran, K.; Stoltz, B. M. *J. Am. Chem. Soc.* **2016**, *138*, 5234–5237.

Liu, W.-B.; Reeves, C. M.; Stoltz, B. M. *J. Am. Chem. Soc.* **2013**, *135*, 17298–17301.

Liu, W.-B.; Reeves, C. M.; Virgil, S. C.; Stoltz, B. M. *J. Am. Chem. Soc.* **2013**, *135*, 10626–10629.

Liu, W.-B.; Xia, J. B.; You, S.-L. *Top. Organomet. Chem.* **2011**, *38*, 155–208.

Liu, W.-B.; Zheng, C.; Zhuo, C.-X.; Dai, L.-X.; You, S.-L. *J. Am. Chem. Soc.* **2012**, *134*, 4812–4821.

Liu, W.; Chen, D.; Zhu, X.-Z.; Wan, X.-L.; Hou, X.-L. *J. Am. Chem. Soc.* **2009**, *131*, 8734–8735.

Liu, Y.; Han, S.-J.; Liu, W.-B.; Stoltz, B. M. *Acc. Chem. Res.* **2015**, *48*, 740–751.

Liu, Y.; Virgil, S. C.; Grubbs, R. H.; Stoltz, B. M. *Angew. Chem. Int. Ed.* **2015**, *54*, 11800–11803.

Long, R.; Huang, J.; Gong, J.; Yang, Z. *Nat. Prod. Rep.* **2015**, *32*, 1584–1601.

Lou, S.; Fu, G. C. *J. Am. Chem. Soc.* **2010**, *132*, 1264–1266.

Lu, X.; Lin, S. *J. Org. Chem.* **2005**, *70*, 9651–9653.

- Lu, Z.; Ma, S. *Angew. Chem. Int. Ed.* **2008**, *47*, 258–297.
- Lundin, P. M.; Esquivias, J.; Fu, G. C. *Angew. Chem. Int. Ed.* **2009**, *48*, 154–156.
- Ma, X.; Gang, D. R. *Nat. Prod. Rep.* **2004**, *21*, 752–772.
- Madrahimov, S. T.; Hartwig, J. F. *J. Am. Chem. Soc.* **2012**, *134*, 8136–8147.
- Madrahimov, S. T.; Li, Q.; Sharma, A.; Hartwig, J. F. *J. Am. Chem. Soc.* **2015**, *137*, 14968–14981.
- Majetich, G.; Shimkus, J. M. *J. Nat. Prod.* **2010**, *73*, 284–298.
- Majetich, G.; Shimkus, J. M. *Tetrahedron Lett.* **2009**, *50*, 3311–3313.
- Manitto, P.; Monti, D.; Zanzola, S.; Speranza, G. *J. Org. Chem.* **1997**, *62*, 6658–6665.
- Marshall, J. A.; DeHoff, B. S. *J. Org. Chem.* **1986**, *51*, 863–872.
- Martin, D.; Kehrli, S.; d'Augustin, M.; Clavier, H.; Mauduit, M.; Alexakis, A. *J. Am. Chem. Soc.* **2006**, *128*, 8416–8417.
- Matsubara, R.; Jamison, T. F. *J. Am. Chem. Soc.* **2010**, *132*, 6880–6881.
- Matsumoto, Y.; Yamada, K.-I.; Tomioka, K. *J. Org. Chem.* **2008**, *73*, 4578–4581.
- Mauleón, P.; Carretero, J. C. *Chem. Commun.* **2005**, 4961–4963.
- May, T. L.; Brown, M. K.; Hoveyda, A. H. *Angew. Chem. Int. Ed.* **2008**, *47*, 7358–7362.

McDougal, N. T.; Streuff, J.; Mukherjee, H.; Virgil, S. C.; Stoltz, B. M. *Tetrahedron Lett.* **2010**, *51*, 5550–5554.

McDougal, N. T.; Virgil, S. C.; Stoltz, B. M. *Synlett* **2010**, 1712–1716.

McFadden, R. M.; Stoltz, B. M. *J. Am. Chem. Soc.* **2006**, *128*, 7738–7739.

Mercier, A.; Urbaneja, X.; Yeo, W. C.; Chaudhuri, P. D.; Cumming, G. R.; House, D.; Bernardinelli, G.; Kündig, E. P. *Chem. Eur. J.* **2010**, *16*, 6285–6299.

Milhau, L.; Guiry, P. J. *Top. Organomet. Chem.* **2012**, *38*, 95–154.

Minami, T.; Iwamoto, M.; Ohtsu, H.; Ohishi, H.; Tanaka, R.; Yoshitake, A. *Planta Med.* **2002**, *68*, 742–745.

Mohr, J. T.; Behenna, D. C.; Harned, A. M.; Stoltz, B. M. *Angew. Chem. Int. Ed.* **2005**, *44*, 6924–6927.

Molander, G. A.; Rivero, M. R. *Org. Lett.* **2002**, *4*, 107–109.

Moss, T. A.; Alba, A.; Hepworth, D.; Dixon, D. J. *Chem. Commun.* **2008**, 2474–2476.

Müller, D.; Hawner, C.; Tissot, M.; Palais, L.; Alexakis, A. *Synlett* **2010**, 1694–1698.

Müller, J. M.; Stark, C. B. W. *Angew. Chem. Int. Ed.* **2016**, *55*, 4798–4802.

Müller, P. *Crystallography Reviews* **2009**, *15*, 57–83.

Mupparapu, N.; Khan, S.; Battula, S.; Kushwaha, M.; Gupta, A. P.; Ahmed, Q. N.; Vishwakarma, R. A. *Org. Lett.* **2014**, *16*, 1152–1155.

- Murphy, K. E.; Hoveyda, A. H. *J. Am. Chem. Soc.* **2003**, *125*, 4690–4691.
- Murphy, K. E.; Hoveyda, A. H. *Org. Lett.* **2005**, *7*, 1255–1258.
- Myers, A. G.; Gin, D. Y.; Rogers, D. H. *J. Am. Chem. Soc.* **1994**, *116*, 4697–4718.
- Nakatsuji, H.; Ueno, K.; Misaki, T.; Tanabe, Y. *Org. Lett.* **2008**, *10*, 2131–2134.
- Nemoto, H.; Kawamura, T.; Kitasaki, K.; Yatsuzuka, K.; Kamiya, M.; Yoshioka, Y. *Synthesis* **2009**, 1694–1702.
- Nemoto, H.; Kawamura, T.; Miyoshi, N. *J. Am. Chem. Soc.* **2005**, *127*, 14546–14547.
- Nemoto, H.; Kubota, Y.; Yamamoto, Y. *J. Org. Chem.* **1990**, *55*, 4515–4516.
- Nemoto, H.; Li, X.; Ma, R.; Suzuki, I.; Shibuya, M. *Tetrahedron Lett.* **2003**, *44*, 73–75.
- Nemoto, H.; Ma, R.; Ibaragi, T.; Suzuki, I.; Shibuya, M. *Tetrahedron* **2000**, *56*, 1463–1468.
- Nemoto, H.; Ma, R.; Kawamura, T.; Kamiya, M.; Shibuya, M. *J. Org. Chem.* **2006**, *71*, 6038–6043.
- Ngai, M.-Y.; Skucas, E.; Krische, M. J. *Org. Lett.* **2008**, *10*, 2705–2708.
- Nguyen, B. H.; Perkins, R. J.; Smith, J. A.; Moeller, K. D. *J. Org. Chem.* **2015**, *80*, 11953–11962.
- Nishitaka, T.; Yamamoto, Y.; Miyaura, N. *Organometallics* **2004**, *23*, 4317–4324.
- Nixon, T. D.; Whittlesey, M. K.; Williams, J. M. J. *Dalton Trans.* **2009**, 753–762.

Node, M.; Ozeki, M.; Planas, L.; Nakano, M.; Takita, H.; Mori, D.; Tamatani, S.; Kajimoto, T. *J. Org. Chem.* **2010**, *75*, 190–196.

Noole, A.; Sucman, N. S.; Kabeshov, M. A.; Kanger, T.; Macaev, F. Z.; Malkov, A. V. *Chem. Eur. J.* **2012**, *18*, 14929–14933.

Numajiri, Y.; Jiménez-Osés, G.; Wang, B.; Houk, K. N.; Stoltz, B. M. *Org. Lett.* **2015**, *17*, 1082–1085.

Numajiri, Y.; Pritchett, B. P.; Chiyoda, K.; Stoltz, B. M. *J. Am. Chem. Soc.* **2015**, *137*, 1040–1043.

Ohmatsu, K.; Ando, Y.; Ooi, T. *J. Am. Chem. Soc.* **2013**, *135*, 18706–18709.

Ohmatsu, K.; Imagawa, N.; Ooi, T. *Nat. Chem.* **2014**, *6*, 47–51.

Ohmura, T.; Hartwig, J. F. *J. Am. Chem. Soc.* **2002**, *124*, 15164–15165.

Okada, S.; Oohira, D.; Otaka, K. Patent WO2004020399 (A1), March 11, 2004.

Onodera, G.; Watabe, K.; Matsubara, M.; Oda, K.; Kezuka, S.; Takeuchi, R. *Adv. Synth. Catal.* **2008**, *350*, 2725–2732.

Otomaru, Y.; Okamoto, K.; Shintani, R.; Hayashi, T. *J. Org. Chem.* **2005**, *70*, 2503–2508.

Paganelli, S.; Sehionato, A.; Botteghi, C. *Tetrahedron Lett.* **1991**, *32*, 2807–2810.

Palais, L.; Alexakis, A. *Chem.—Eur. J.* **2009**, *15*, 10473–10485.

Palais, L.; Mikhel, I. S.; Bournaud, C.; Micouin, L.; Falciola, C. A.; Vuagnoux-d'Augustin, M.; Rosset, S.; Bernardinelli, G.; Alexakis, A. *Angew. Chem. Int. Ed.* **2007**, *46*, 7462–7465.

Paolo, B.; Diego, V.; Giampietro, B.; Roberto, S. U.S. Patent, 166800 A1, Sept. 4, 2003.

Paquin, J.-F.; Defieber, C.; Stephenson, C. R. J.; Carreira, E. M. *J. Am. Chem. Soc.* **2005**, *127*, 10850–10851.

Payette, J. N.; Yamamoto, H. *J. Am. Chem. Soc.* **2007**, *129*, 9536–9537.

Pearson, E. L.; Kanizaj, N.; Willis, A. C.; Paddon-Row, M. N.; Sherburn, M. S. *Chem. Eur. J.* **2010**, *16*, 8280–8284.

Perlmutter, P. *Conjugate Addition Reactions in Organic Synthesis*, Tetrahedron Organic Chemistry Series 9; Pergamon: Oxford, 1992.

Peterson, E. A.; Overman, L. E. *Proc. Natl. Acad. Sci. USA* **2004**, *101*, 11943–11948.

Planas, L.; Mogi, M.; Takita, H.; Kajimoto, T.; Node, M. *J. Org. Chem.* **2006**, *71*, 2896–2898.

Polet, D.; Alexakis, A. *Org. Lett.* **2005**, *7*, 1621–1624.

Polet, D.; Alexakis, A.; Tissot-Croset, K.; Corminboeuf, C.; Ditrich, K. *Chem. Eur. J.* **2006**, *12*, 3596–3609.

Poremba, K. E.; Lee, V. A.; Sculimbrene, B. R. *Tetrahedron* **2014**, *70*, 5463–5467.

Pouy, M. J.; Leitner, A.; Weix, D. J.; Ueno, S.; Hartwig, J. F. *Org. Lett.* **2007**, *9*, 3949–3952.

Pradhan, R.; Patra, M.; Behera, A. K.; Mishra, B. K.; Behera, R. K.; *Tetrahedron* **2006**, *62*, 779–828.

Prétôt, R.; Pfaltz, A. *Angew. Chem. Int. Ed.* **1998**, *37*, 323–325.

Quasdorf, K. W.; Overman, L. E. *Nature* **2014**, *516*, 181–191.

Ramachary, D. B.; Reddy, P. S.; Shruthi, K. S.; Madhavachary, R.; Reddy, P. V. G. *Eur. J. Org. Chem.* **2016**, 5220–5226.

Reetz, M. T.; Westermann, J.; Steinbach, R. *J. Chem. Soc. Chem. Commun.* **1981**, 237–239.

Reeves, C. M.; Behenna, D. C.; Stoltz, B. M. *Org. Lett.* **2014**, *16*, 2314–2317.

Reeves, C. M.; Eidamshaus, C.; Kim, J.; Stoltz, B. M. *Angew. Chem. Int. Ed.* **2013**, *52*, 6718–6721.

Rios, R. *Chem. Soc. Rev.* **2012**, *41*, 1060–1074.

Rossi, D.; Baraglia, A. C.; Serra, M.; Azzolina, O.; Collina, S. *Molecules* **2010**, *15*, 5928–5942.

Rossiter, B. E.; Swingle, N. M. *Chem. Rev.* **1992**, *92*, 771–806.

Rössler, S. L.; Krautwald, S.; Carreira, E. M. *J. Am. Chem. Soc.* **2017**, *139*, 3603–3606.

Ruan, J.; Li, X.; Saidi, O.; Xiao, J. *J. Am. Chem. Soc.* **2008**, *130*, 2424–2425.

Ruchti, J.; Carreira, E. M. *J. Am. Chem. Soc.* **2014**, *136*, 16756–16759.

- Saá, J. M.; Dopico, M.; Martorell, G.; García-Raso, A. *J. Org. Chem.* **1990**, *55*, 991–995.
- Sandmeier, T.; Krautwald, S.; Zipfel, Carreira, E. M. *Angew. Chem. Int. Ed.* **2015**, *54*, 14363–14367.
- Sannigrahi, M. *Tetrahedron* **1999**, *55*, 9007–9071.
- Sano, S.; Yokoyama, K.; Shiro, M.; Nagao, Y. *Chem. Pharm. Bull.* **2002**, *50*, 706–709.
- Sawamura, M.; Hamashima, H.; Ito, Y. *J. Am. Chem. Soc.* **1992**, *114*, 8295–8296.
- Schnermann, M. J.; Overman, L. E. *Angew. Chem. Int. Ed.* **2012**, *51*, 9576–9580.
- Schurig, V. *Inorg. Chem.* **1986**, *25*, 945–949.
- Seehafer, K.; Malakar, C. C.; Bender, M.; Qu, J.; Liang, C.; Helmchen, G. *Eur. J. Org. Chem.* **2016**, 493–501.
- Seitz, M.; Reiser, O. *Curr. Opin. Chem. Biol.* **2005**, *9*, 285–292.
- Sharma, S.; Kumar, S.; Shil, A. K.; Guha, N. R.; Bandna; Das, P. *Tetrahedron Lett.* **2012**, *53*, 7044–7051.
- Sheldrick, G. M. *Acta Cryst.* **1990**, A46, 467–473.
- Sheldrick, G. M. *Acta Cryst.* **2015**, C71, 3–8.
- Shimizu, H.; Holder, J. C.; Stoltz, B. M. *Beilstein J. Org. Chem.* **2013**, *9*, 1637–1642.
- Shintani, R.; Duan, W.-L.; Hayashi, T. *J. Am. Chem. Soc.* **2006**, *128*, 5628–5629.

Shintani, R.; Hayashi, T. *Org. Lett.* **2011**, *13*, 350–352.

Shintani, R.; Ueyama, K.; Yamada, I.; Hayashi, T. *Org. Lett.* **2004**, *6*, 3425–3427.

Shintani, R.; Yamagami, T.; Kimura, T.; Hayashi, T. *Org. Lett.* **2005**, *7*, 5317–5319.

Shockley, S. E.; Hethcox, J. C.; Stoltz, B. M. *Angew. Chem. Int. Ed.* **2017**, *56*, 11545–11548.

Shockley, S. E.; Hethcox, J. C.; Stoltz, B. M. *Tetrahedron Lett.* **2017**, *58*, 3341–3343.

Shockley, S. E.; Holder, J. C.; Stoltz, B. M. *Org. Lett.* **2014**, *16*, 6362–6365.

Shockley, S. E.; Hethcox, J. C.; Stoltz, B. M. *Manuscript submitted*.

Sibi, M. P.; Manyem, S. *Tetrahedron* **2000**, *56*, 8033–8061.

Singh, O. V.; Han, H. *J. Am. Chem. Soc.* **2007**, *129*, 774–775.

Sisak, A.; Ungvary, F.; Marko, L. *J. Org. Chem.* **1990**, *55*, 2508–2513.

Sizemore, N.; Rychnovsky, S. D. *Org. Lett.* **2014**, *16*, 688–691.

Slack, E. D.; Gabriel, C. M.; Lipshutz, B. H. *Angew. Chem. Int. Ed.* **2014**, *53*, 14051–14054.

Smith, A. B. III; Doughty, V. A.; Lin, Q.; Zhuang, L.; McBriar, M. D.; Boldi, A. M.; Moser, W. H.; Murase, N. M.; Nakayama, K.; Sobukawa, M. *Angew. Chem. Int. Ed.* **2001**, *40*, 191–195.

Smith, L. K.; Baxendale, I. R. *Org. Biomol. Chem.* **2015**, *13*, 9907–9933.

- Streuff, J.; White, D. E.; Virgil, S. C.; Stoltz, B. M. *Nat. Chem.* **2010**, *2*, 192–196.
- Su, Y.-L.; Li, Y.-H.; Chen, Y.-G.; Han, Z.-Y. *Chem. Commun.* **2017**, *53*, 1985–1988.
- Sumi, S.; Matsumoto, K.; Tokuyama, H.; Fukuyama, T. *Org. Lett.* **2003**, *5*, 1891–1893.
- Sumi, S.; Matsumoto, K.; Tokuyama, H.; Fukuyama, T. *Tetrahedron* **2003**, *59*, 8571–8587.
- Sun, J.; Perfetti, M. T.; Santos, W. L. *J. Org. Chem.* **2011**, *76*, 3571–3575.
- Suzuki, M.; Yanagisawa, A.; Noyori, R. *J. Am. Chem. Soc.* **1988**, *110*, 4718–4726.
- Takaya, J.; Iwasawa, N. *J. Am. Chem. Soc.* **2008**, *130*, 15254–15255.
- Takaya, Y.; Ogasawara, M.; Hayashi, T.; Sakai, M.; Miyaura, N. *J. Am. Chem. Soc.* **1998**, *120*, 5579–5580.
- Takeda, M.; Inoue, H.; Noguchi, K.; Honma, Y.; Kawamori, M.; Tsukamoto, G.; Yamawaki, Y.; Saito, S. *Chem. Pharm. Bull.* **1976**, *24*, 1514–1526.
- Takeuchi, R.; Kashio, M. *Angew. Chem. Int. Ed.* **1997**, *36*, 263–265.
- Tang, S.; Xu, Y.; He, J.; He, Y.; Zheng, J.; Pan, X.; She, X. *Org. Lett.* **2008**, *10*, 1855–1858.
- Tapia, R.; Guardia, J. J.; Alvarez, E.; Haidöur, A.; Ramos, J. M.; Alvarez-Manzaneda, R.; Chahboun, R.; Alvarez-Manzaneda, E. *J. Org. Chem.* **2012**, *77*, 573–584.
- Tomioka, K.; Nagaoka, Y., In *Comprehensive Asymmetric Catalysis*, Vol. 3; Jacobsen, E. N., Pfaltz, A., Yamamoto, H. Eds.; Springer-Verlag; New York, 1999; Chapter 31.

Trost B. M.; Osipov, M. *Angew. Chem. Int. Ed.* **2013**, *52*, 9176–9181.

Trost, B. M. *Tetrahedron* **2015**, *71*, 5708–5733.

Trost, B. M.; Brennan, M. K. *Synthesis* **2009**, 3003–3025.

Trost, B. M.; Chan, W. H.; Malhotra, S. *Chem. Eur. J.* **2017**, *23*, 4405–4414.

Trost, B. M.; Cramer, N.; Silverman, S. M. *J. Am. Chem. Soc.* **2007**, *129*, 12396–12397.

Trost, B. M.; Crawley, M. L. *Chem. Rev.* **2003**, *103*, 2921–2944.

Trost, B. M.; Jiang, C. *J. Am. Chem. Soc.* **2001**, *123*, 12907–12908.

Trost, B. M.; Jiang, C. *Synthesis* **2006**, 369–396.

Trost, B. M.; Malhotra, S.; Chan, W. H. *J. Am. Chem. Soc.* **2011**, *133*, 7328–7331.

Trost, B. M.; Miller, J. R.; Hoffman, C. M. Jr. *J. Am. Chem. Soc.* **2011**, *133*, 8165–8167.

Trost, B. M.; Osipov, M. *Angew. Chem. Int. Ed.* **2013**, *52*, 9176–9181.

Trost, B. M.; Ryan, M. C. *J. Am. Chem. Soc.* **2016**, *138*, 2981–2984.

Trost, B. M.; Silverman, S. M.; Stambuli, J. P. *J. Am. Chem. Soc.* **2011**, *133*, 19483–19497.

Trost, B. M.; Van Vranken, D. L. *Chem. Rev.* **1996**, *96*, 395–422.

Trost, B. M.; Xu, J. *J. Am. Chem. Soc.* **2005**, *127*, 17180–17181.

Trost, B. M.; Xu, J.; Schmidt, T. *J. Am. Chem. Soc.* **2009**, *131*, 18343–18357.

- Tsuji, J.; Takahashi, H.; Morikawa, M. *Tetrahedron Lett.* **1965**, *6*, 4387–4388.
- Turnbull, B. W. H.; Evans, P. A. *J. Am. Chem. Soc.* **2015**, *137*, 6156–6159.
- Ueda, M.; Hartwig, J. F. *Org. Lett.* **2010**, *12*, 92–94.
- Uyeda, C.; Rötheli, A. R.; Jacobsen, E. N. *Angew. Chem. Int. Ed.* **2010**, *49*, 9753–9756.
- Vita, M. V.; Waser, J. *Org. Lett.* **2013**, *15*, 3246–3249.
- Vuagnoux-d'Augustin, M.; Alexakis, A. *Chem.—Eur. J.* **2007**, *13*, 9647–9662.
- Vuagnoux-d'Augustin, M.; Kehrli, S.; Alexakis, A. *Synlett* **2007**, 2057–2060.
- Welter, C.; Moreno, R. M.; Streiff, S.; Helmchen, G. *Org. Biomol. Chem.* **2005**, *3*, 3266–3268.
- Wiedner, S. D.; Vedejs, E. *Org. Lett.* **2010**, *12*, 4030–4033.
- Willand-Charnley, R.; Fisher, T. J.; Johnson, B. M.; Dussault, P. H. *Org. Lett.* **2012**, *14*, 2242–2245.
- Wilsily, A.; Fillion, E. *J. Org. Chem.* **2009**, *74*, 8583–8594.
- Wilsily, A.; Fillion, E. *Org. Lett.* **2008**, *10*, 2801–2804.
- Wojaczyńska, E.; Turowska-Tyrk, I. *Tetrahedron: Asymmetry* **2013**, *24*, 1247–1251.
- Wong, K. C.; Ng, E.; Wong, W.-T.; Chiu, P. *Chem. Eur. J.* **2016**, *22*, 3709–3712.
- Wu, J.; Mampreian, D. M.; Hoveyda, A. H. *J. Am. Chem. Soc.* **2005**, *127*, 4584–4585.

Xiong, Y.; Zhang, G. *Org. Lett.* **2016**, *18*, 5094–5097.

Xu, C.; Xu, J. *Org. Biomol. Chem.* **2017**, *15*, 6375–6383.

Xu, Z.; Wang, Q.; Zhu, J. *J. Am. Chem. Soc.* **2013**, *135*, 19127–19130.

Yamashita, Y.; Gopalarathnam, A.; Hartwig J. F. *J. Am. Chem. Soc.* **2007**, *129*, 7508–7509.

Yamatsugu, K.; Kanai, M.; Shibasaki, M. *Tetrahedron* **2009**, *65*, 6017–6024.

Yan, S.-S.; Liang, C.-G.; Zhang, Y.; Hong, W.; Cao, B.-X.; Dai, L.-X.; Hou, X.-L. *Angew. Chem. Int. Ed.* **2005**, *44*, 6544–6546.

Yang, K. S.; Nibbs, A. E.; Türkmen, Y. E.; Rawal, V. H. *J. Am. Chem. Soc.* **2013**, *135*, 16050–16053.

Yang, K. S.; Rawal, V. H. *J. Am. Chem. Soc.* **2014**, *136*, 16148–16151.

Yang, W.; Du, D.-M. *Org. Lett.* **2010**, *12*, 5450–5453.

You, S.-L.; Zhu, X.-Z.; Luo, Y.-M.; Hou, X.-L.; Dai, L.-X. *J. Am. Chem. Soc.* **2001**, *123*, 7471–7472.

Zhang, A.; RajanBabu, T. V. *J. Am. Chem. Soc.* **2006**, *128*, 5620–5621.

Zhang, H.; Hong, L.; Kang, H.; Wang, R. *J. Am. Chem. Soc.* **2013**, *135*, 14098–14101.

Zhang, P.; Le, H.; Kyne, R. E.; Morken, J. P. *J. Am. Chem. Soc.* **2011**, *133*, 9716–9719.

Zhang, T.; Jiang, J.; Yao, L.; Geng, H.; Zhang, X. *Chem. Commun.* **2017**, *53*, 9258–9261.

Zhang, X.; Chen, J.; Han, F.; Cun, L. Liao, J. *Eur. J. Org. Chem.* **2011**, 1443–1446.

Zhang, X.; Liu, W.-B.; Cheng, Q.; You, S.-L. *Organometallics* **2016**, 35, 2467–2472.

Zhao, J.; Fang, B.; Luo, W.; Hao, X.; Liu, X.; Lin, L.; Feng, X. *Angew. Chem. Int. Ed.* **2015**, 54, 241–244.

Zhao, N.; Yin, S.; Xie, S.; Yan, H.; Ren, P.; Chen, G.; Chen, F.; Xu, J. *Angew. Chem. Int. Ed.* **2018**, 57, 3386–3390.

Zheng, J.; Lin, L.; Dai, L.; Tang, Q.; Liu, X.; Feng, X. *Angew. Chem. Int. Ed.* **2017**, 56, 13107–13111.

Zheng, W.-H.; Sun, N.; Hou, X.-L. *Org. Lett.* **2005**, 7, 5151–5154.

Zheng, W.-H.; Zheng, B.-H.; Zhang, Y.; Hou, X.-L. *J. Am. Chem. Soc.* **2007**, 129, 7718–7719.

Zhuo, C.-X.; Zheng, C.; You, S.-L. *Acc. Chem. Res.* **2014**, 47, 2558–2573.

INDEX

γ

γ -butyrolactone26, 211, 464, 632

π

π -allyl.....3, 19, 140, 141, 164, 328, 366, 450, 454, 458, 463

A

acyclic..... 7–11, 201, 202, 326, 327, 335, 449, 450, 457, 460–426, 465

aldol.....16, 334, 464, 472, 489, 493, 497, 627, 628, 634, 636, 637, 639, 641

alkyne24, 145, 332

C

carbocation 19, 447, 450, 630

carbon monoxide 141, 146, 455

carboxylic acid..... 201, 202, 206, 210, 223, 224, 233, 249, 318, 319, 455, 456, 460–462

CBS 641–643, 673, 676

chelation/chelating.....9, 10

cocatalyst 16, 17, 458, 465

Cope448

Corey–Chaykovsky26

counterion.....11, 27, 481

cyanohydrin648, 686

cyclopentene.....334, 464

D

DABCO.....9, 328, 330, 331, 333, 335, 341, 366, 463, 470, 630, 631, 633, 634

decarboxylative636, 637, 641, 642

Dieckmann.....645, 646

Diels–Alder627, 640, 647

dihydroxylation26, 210

E

enolate	1, 2, 7–10, 12–15, 140, 165, 445, 446, 449, 450, 452, 454, 627, 636, 637, 640, 649
epoxidation	26

G

Grignard	26
----------------	----

H

hemiacetal	632, 634, 635, 657, 658, 659, 661
heteroaryl/heteroaromatic	9–13, 15, 146, 208, 447, 449, 456
hydrogenation	210, 334, 496
hydrolysis	206–208, 460, 491

I

iridicycle	204, 205, 460, 470
------------------	--------------------

K

Knoevenagel	629
-------------------	-----

L

lactam	24, 592, 627, 632, 633, 636–638, 640, 643–645, 647–649, 663, 665, 666, 678
lactamization	631, 632
lactonization	26, 211
Lewis acid	203, 222, 458, 459, 465, 483

M

methyl vinyl ketone	592, 593
Michael	479, 590

O

one-pot	210, 211, 233, 460, 461, 593, 594, 632
---------------	----------------------------------------

ozonolysis211, 334, 464, 629, 636, 637, 639, 641–643

P

palladium1, 17, 18, 22, 325, 326, 334, 441–443, 467, 472–477, 479–481, 483–490,
493, 494, 498, 508, 528, 590–593, 599, 600, 636–642, 649, 681

piperidine36, 640

piperidone24, 640–643, 649, 671, 672, 674, 675

poison24, 482, 484

preparatory scale146, 153

prochiral2, 7–10, 12, 27, 212, 326, 442, 443, 445, 452

propargyl9, 24, 145, 209

proton sponge20, 21, 23, 25, 27, 36, 38, 451–453, 634

R

rhodium474, 475, 487

ring-closing metathesis/RCM26, 590, 591, 593, 594, 644–646

S

silver11, 12

steric/sterically3, 5, 11, 16, 144, 205, 206, 208, 327, 329, 332, 334, 445, 452,
456, 462, 464, 465, 485, 491, 495, 496, 593, 630, 638, 639

T

triethylborane203, 211, 335, 459

W

Wacker472, 634, 635

ABOUT THE AUTHOR

Samantha Elizabeth Shockley was born in Birmingham, Alabama on February 6th, 1990 to Susan and Edward Shockley. Sam grew up in Gainesville, Florida with her older brother Matthew Shockley.

In the fall of 2008, Sam moved to Chicago, Illinois to attend the University of Chicago. Despite her initial intention to study Egyptology, she graduated with B.S. degrees in chemistry and biochemistry and a B.A. in biology. While in college, she performed undergraduate research on zirconocene-catalyzed C–H functionalization under the guidance of Professor Richard Jordan.

Following her undergraduate education, Sam moved to Canberra, Australia to conduct a yearlong U.S. Fulbright research grant at the Australian National University in the laboratory of Professor Martin Banwell. During this time, she investigated the design and synthesis of lipophilic analogues of lamellarin W.

Upon returning to the States, Sam moved to Pasadena, California to pursue her doctoral studies at the California Institute of Technology with Professor Brian Stoltz. Her graduate work has focused on the development of enantioselective transition metal catalysis and natural product total synthesis. Upon completion of her doctoral research in May 2018, Sam will begin her professional career as a medicinal chemist at Merck, South San Francisco.